

MATERIALS SCIENCE AND TECHNOLOGIES

Textiles

Types, Uses and Production Methods

Ahmed El Nemr

Editor

NOVA

MATERIALS SCIENCE AND TECHNOLOGIES

TEXTILES: TYPES, USES AND PRODUCTION METHODS

No part of this digital document may be reproduced, stored in a retrieval system or transmitted in any form or by any means. The publisher has taken reasonable care in the preparation of this digital document, but makes no expressed or implied warranty of any kind and assumes no responsibility for any errors or omissions. No liability is assumed for incidental or consequential damages in connection with or arising out of information contained herein. This digital document is sold with the clear understanding that the publisher is not engaged in rendering legal, medical or any other professional services.

MATERIALS SCIENCE AND TECHNOLOGIES

Additional books in this series can be found on Nova's website
under the Series tab.

Additional E-books in this series can be found on Nova's website
under the E-book tab.

MATERIALS SCIENCE AND TECHNOLOGIES

TEXTILES: TYPES, USES AND PRODUCTION METHODS

AHMED EL NEMR
EDITOR



Nova Science Publishers, Inc.

New York

Copyright © 2012 by Nova Science Publishers, Inc.

All rights reserved. No part of this book may be reproduced, stored in a retrieval system or transmitted in any form or by any means: electronic, electrostatic, magnetic, tape, mechanical photocopying, recording or otherwise without the written permission of the Publisher.

For permission to use material from this book please contact us:

Telephone 631-231-7269; Fax 631-231-8175

Web Site: <http://www.novapublishers.com>

NOTICE TO THE READER

The Publisher has taken reasonable care in the preparation of this book, but makes no expressed or implied warranty of any kind and assumes no responsibility for any errors or omissions. No liability is assumed for incidental or consequential damages in connection with or arising out of information contained in this book. The Publisher shall not be liable for any special, consequential, or exemplary damages resulting, in whole or in part, from the readers' use of, or reliance upon, this material. Any parts of this book based on government reports are so indicated and copyright is claimed for those parts to the extent applicable to compilations of such works.

Independent verification should be sought for any data, advice or recommendations contained in this book. In addition, no responsibility is assumed by the publisher for any injury and/or damage to persons or property arising from any methods, products, instructions, ideas or otherwise contained in this publication.

This publication is designed to provide accurate and authoritative information with regard to the subject matter covered herein. It is sold with the clear understanding that the Publisher is not engaged in rendering legal or any other professional services. If legal or any other expert assistance is required, the services of a competent person should be sought. FROM A DECLARATION OF PARTICIPANTS JOINTLY ADOPTED BY A COMMITTEE OF THE AMERICAN BAR ASSOCIATION AND A COMMITTEE OF PUBLISHERS.

Additional color graphics may be available in the e-book version of this book.

LIBRARY OF CONGRESS CATALOGING-IN-PUBLICATION DATA

Textiles : types, uses, and production methods / [edited by] Ahmed El Nemr.

p. cm.

Includes index.

ISBN : 9: /3/84322/4: 6/2 (eBook)

1. Textile fibers. 2. Textile fabrics. 3. Textile research. 4. Textile industry. I. EL Nemr, Ahmed.

TS1765.T42 2011

677--dc23

Published by Nova Science Publishers, Inc. + New York

CONTENTS

Preface		vii
Chapter 1	From Natural to Synthetic Fibers <i>Ahmed El Nemr</i>	1
Chapter 2	Non-Destructive Instrumental Analysis of Excavated Textiles <i>Christina Margariti</i>	153
Chapter 3	Kinetics Study of Forced Textile Dyeing Process <i>Erasmus Mancusi, Antônio Augusto Ulson de Souza and Selene Maria de Arruda Guelli Ulson de Souza</i>	165
Chapter 4	Nanofibers, Nanoscience and Nanotechnology in Textile and Apparel Industry <i>Subramaniam Sadhasivam</i>	191
Chapter 5	Nanofibers from Natural Biopolymers in Regenerative Medicine <i>Georgios Toskas, Rolf-Dieter Hund, Ezzedine Laourine and Chokri Cherif</i>	203
Chapter 6	Development of Textiles Customized as Reinforcement to Cementitious Matrices <i>S. W. Mumenya</i>	223
Chapter 7	A Review on Thermal Engineering Design of Clothing <i>Luo Jie, Mao Aihua and Li Yi</i>	273
Chapter 8	Surface Modification of Textiles with Non-Thermal Plasmas <i>Nathalie De Geyter and Rino Morent</i>	297
Chapter 9	Technical Textile Yarns Containing Metal Filaments/Wires <i>Ayse (Celik) Bedeloglu and Yalcin Bozkurt</i>	317
Chapter 10	Mesoscopic Models of Woven Textiles <i>Jean-François Ganghoffer</i>	331
Chapter 11	A Novel Method for Antimicrobial Finishing of Textile with Inorganic Nanoparticles by Sonochemistry <i>Ilana Perelshtein, Nina Perkash, Guy Applerot and Aharon Gedanken</i>	369

Chapter 12	Advanced Textiles for Medical Uses <i>Anicuta Stoica-Guzun</i>	399
Chapter 13	Solvothermally Prepared Copper Modified TiO ₂ Composite Sols - A Coating Agent for Textiles to Realize Photocatalytic Active and Antimicrobial Fabrics <i>Frank Schmidt, Anja Fischer, Helfried Haufe, Tilmann Leisegang and Boris Mahltig</i>	439
Chapter 14	Functional Cellulose Fibres for Hygienic and Medical Applications <i>Lidija Fras Zemljic, Tatjana Kreze, Simona Strnad, Olivera Šauperl and Alenka Vesel</i>	467
Chapter 15	Skin Problems Associated with Textiles <i>Araceli Sánchez-Gilo, Enrique Gómez de la Fuente, Marta Andreu Barasoain and Jose Luis López Estebaran</i>	489
Chapter 16	Application of Layer-by-Layer Method for Textiles <i>Dawid Stawski</i>	507
Chapter 17	Challenges in the Preservation of Contemporary Couture – Consolidation and Protection of Textiles with Sol-Gel Silica Coatings <i>Marta Vieira, Márcia G. Ventura, Rita Macedo, Micaela M. Sousa, A. Jorge Parola and B. Coutinho</i>	519
Chapter 18	Development of Polymer-Derived SiC Fibers and their Applications <i>Guohua Jiang</i>	539
Chapter 19	Plasma-Assisted Modification of Textile Yarns in Liquid Environment <i>Sergey M. Kuzmin, Natalya P. Prorokova and Aleksey V. Khorev</i>	557
Chapter 20	Application of Ultrasonic Energy for Washing Textiles <i>Juan A. Gallego-Juarez</i>	579
Index		593

PREFACE

Fiber is a class of materials that are continuous filaments or are in discrete elongated pieces, similar to lengths of thread. Fibers are very important in the biology of both plants and animals, for holding tissues together. Plants yielding fibers have been only second to food plants in their usefulness to humans and their influence on the furthering of civilization. Primitive humans in their attempts to obtain the three most important necessities for life (food, clothing and shelter) focused on plants. Even though animal products were available, some forms of clothing were needed that were lighter and cooler than hides. It was easier to obtain from plants such items as nets, snares, etc. Also plant products were available from the leaves, stems and roots of many plants to construct human's shelter. Therefore, mankind was utilized the natural fibers significantly earlier than metals, alloys, and ceramics and it can be supposed that the natural fibers were used by humans long before recorded history.

Textiles stand next to agriculture as an income generation activity for most of the rural population. The structure of the fabric is as much a determining factor in its functions, as it is the choice of raw material. Some structures of the fabric lend themselves to any specific end use where as many other structures are versatile lending them to a variety of functions and end users. Good understandings of simple woven structures make it possible to apply them in the woven cloth in a variety of ways. This review book designed to cover the recent research in different branches of textile research. Chapter 1 shows the most known natural fibers and the way to synthetic fibers. It also reported the history of fiber production and uses as well as the modifications made to natural fibers to produce more comfortable fibers. Textile products, which incorporate with different sciences, are taking part in different application areas including industry, military, space, medical to perform needing for health, protection, defense, communication and automation.

Excavated textiles are generally characterized by a poor condition, as a result of the effects of burial on their physical and chemical properties. Knowledge of the new physical and chemical properties, by the application of instrumental analysis, is necessary for material identification and conservation. However, more often than not, only minute fragments have been preserved. This makes the selection of non-destructive methods of analysis a prerequisite for excavated textiles. Chapter 2 presents guidelines for the non-destructive analysis of textiles, based on a study of four textile finds excavated in Greece.

The use of computational methods to simulate the textile dyeing process provides a powerful tool to allow an understanding of the mass transfer kinetics in aqueous solutions during the dyeing process. Moreover, analysis of the time scales associated with the main

phenomena can lead to a precise knowledge of the dyeing kinetics during the process, which in turn can be used to improve the process control, reliability and, perhaps most importantly, the environmental impact of the dyeing process. Traditionally, dyeing techniques are carried out in a batch process. The bobbins of thread are fixed to perforated supports and receive dye from the liquid passing across the bobbins and re-circulating to a mixing tank. Inside the bobbins dye has to be transported by convection and dispersion to the inner core of the threads. Under normal operating conditions the dye is added at the beginning of a dyeing cycle in the mixing bath and the process runs under batch conditions, that is, without changing the amount of dye in the system. In general, dye distribution factor (DDF) and dye uptake (CDEP) benefit from high recirculation flux values and low dispersion resistances. In order to investigate possible improvements to the traditional dyeing process, the effect of periodic variations in the boundary conditions (reverse flow operation) on the bobbin thread dyeing process was studied in Chapter 3. The system is operated by periodically reversing the conditions of the dyeing bath fluid external to the thread bobbins and inside the bobbins. The periodic forcing is modeled by an *ad hoc* discontinuous periodic function and a partial differential equations mathematical model that takes this function into account is developed. A comparison between the forced and unforced processes was conducted by analyzing the dye distribution factor and the total amount of dye adsorbed during the transient regime for the two processes.

Technological advances during the past decade have opened many new doors for the Textile and Apparel industries, especially in the area of rapid prototyping and related activities. Chapter 4 reported the recent developments in the textile industry include designing entirely new fibrous materials incorporating carbon nanotubes, composites, biocompatible textile scaffolds, conducting polymers and electrospun nanofibres. High strength, elasticity, conductivity, controlled porosity and giant surface areas can be combined to provide new materials with revolutionary properties. The future success of nanotechnology in textile applications lies in areas where new functionalities are combined into durable, multifunctional textile systems without comprising the inherent favorable textile properties, including process-ability, flexibility, wash-ability and softness.

Recently, medical textile constructs for tissue replacement or release of drugs and faster healing of wounds are of increasing interest. They belong to the smart textiles concept, derived from material design, textile engineering and chemical finishing. Advances in electrospinning techniques have permitted the generation of continuous fibers at the nanometer scale with a high surface area to volume ratio. Nanofiber matrices have been found a large number of applications in the industrial sector and also in biomedical field. Natural polymers possess proven tissue compatibility and usually contain domains that can send important signals to guide cells at various stages of their development. The most used sources of natural derived polymers include proteins, especially from extracellular matrices (ECM) (e.g. collagen), polypeptides, and polysaccharides (including chitosan, cellulose, starch, hyaluronic acid, heparin and alginate). It has been shown that nanofibrous matrices can better mimic the target tissues than their bulk equivalents, as cells attach and proliferate well in micro and nanostructured materials and there is also the ability to modify the structure, composition and the chemistry at the nanoscale. Chapter 5 examines briefly the use of nanofibrous mats in regenerative medicine from the textile materials point of view, having as scope to introduce the reader to this constantly emerging sector. The nanofiber production of the main natural derived polymers, which have been used or have the potential to be used in

regenerative medicine, is reviewed in relation to their structure and correlated to the application possibilities, according to the type of engineered tissue.

During the ancient Roman civilization, discrete fibers were used to reinforce brittle matrices such as mortar and clay in order to improve the tensile load carrying capacity of the brittle matrices. Natural fibers such as: horse hair, sisal, and grass were employed in their natural form. The development of fiber reinforced cementitious composites can be traced back to the 1960's when straight short discrete steel fibers were mixed into mortar and concrete for construction of slabs on grade. Later, other fiber types were accepted for use in cementitious matrices. This insight was the driving force in innovations that occurred in mid 1970's involving new techniques of production of polypropylene fibers. Since 1990's, the manufacture and processing of different fiber types has been customized for cement-based applications. Among these fibers are steel, Alkali Resistant (AR) glass, carbon, polymeric fibers, as well as naturally occurring fibers. Similarly, for textiles, the innovations in the individual fibers has led to new processing and manufacturing techniques aimed at making the textiles adaptable to cementitious composites. To date, the use of fibers and textiles in cementitious composites have been adopted in many countries, for example, South Africa, India, United States of America, Germany, as well as in Kenya and other East African countries. Chapter 6 describes the development of the unique technology of manufacture of firstly the basic fibers, and secondly, textiles woven from the fibers for application in cementitious matrices. Chapter 6 is dealt with the advantages of treated sisal fibers and also discussed the manufacturing techniques of the fibers and textiles for adaptation in cementitious matrices.

Clothing thermal engineering design is an effective and economical solution of designing clothing with superior thermal performance for people to live in various environments with a feeling of comfort. To achieve desirable thermal functions, the clothing design process is not traditional trial and error but a functional engineering process which involves multi-disciplinary knowledge and computer-aided design (CAD) technologies to investigate, simulate and preview the physical thermal behaviors in the clothing. Clothing designers can thus scientifically evaluate with computer before the produce of real products that if their design concepts are achieved and suitable for the expected wearing environment. Chapter 7 gives a systematical review on the related research and methods in clothing thermal engineering design. The accomplishment of clothing thermal engineering design is on the fundaments of the computational simulation of the thermal behaviors and CAD technologies.

Chapter 8 attempts to give an introduction on surface modifications of textiles with non-thermal plasmas. A non-thermal (or cold or low temperature) plasma is a partially ionized gas with electron temperatures much higher than ion temperatures. The high-energy electrons and low-energy molecular species can initiate reactions in the plasma volume without excessive heat causing substrate degradation. Non-thermal plasmas are particularly suited to apply to textile processing because most textile materials are heat sensitive polymers. In addition, it is a versatile technique, where a large variety of chemically active functional groups can be incorporated into the textile surface. Possible aims are improved wettability, adhesion of coatings, printability, induced hydro-and/or oleophobic properties, changing physical and/or electrical properties, cleaning or disinfection of fiber surfaces etc. Moreover, non-thermal plasma surface modifications can be achieved over large textile areas. Chapter 8 starts after general introduction with a short overview of different plasma sources used for surface

modification of textiles. Thereafter, different effects that can be induced on a textile product by a plasma treatment and ways to obtain these effects are reviewed.

Conductive textiles also have interesting application areas due to their excellent properties that are provided by smart materials and a variety of manufacturing techniques. Conductive textile materials have a big role in production of sensors, electromechanical shielding, monitoring, static dissipation, anti-dust and anti-bacterial applications, data transfer and so on. Researchers focus on novel products, which have such smart and intelligent properties in applications for different requirements of humankind, over the last several years. Conductive fibers can be inherently conductive or gain conductive properties after some applications. Metal fibers can be obtained from metal plates or strips. Conductive yarns can be obtained from conductive filaments or wires, staple metal fibers or spinning traditional textile fibers with conductive filaments/wires. Metal filaments or wires also can be wrapped around the traditional textile yarns to develop conductive technical yarns. Chapter 9 aims to present novel designs, techniques and materials used for developing technical textile yarns containing metal filaments for smart textile applications. The review is organized as follows: In the first section, an overview of metal fibers, production methods and usage fields will be presented. In the second section, a general introduction to yarns containing metal filaments/wires and their features in terms of materials and manufacturing techniques used will be given. In addition, advancements and application areas with recent studies will be recounted. Finally, suggestions on future studies and the conclusions will be given.

Micromechanical schemes are elaborated for analyzing the mechanical behavior of woven structures at the scale of the weave pattern, which defines the repetitive unit cell for a quasi periodical textile at a mesoscopic scale. The mechanical behavior of the dry fabric before impregnation by the resin is the object of those analysis, with the general objective of calculating the overall effective mechanical properties versus the unit cell geometry and the mechanical properties of the micro-constituents, namely the weft and warp yarns. Micromechanical analyses further provide a quantitative understanding of the deformation mechanisms of woven, allowing relating the macroscopic overall response to the underlying microscopic behavior. Two parallel strategies are exposed in Chapter 10, the first one basing on the minimization of the total potential energy of the woven structure, and the second one relying on discrete homogenization techniques specific to architected materials. Simulations of the overall tensile response of serge and fabric highlight the effect of geometrical nonlinearities for fabric, due to the crimp changes, leading to a J-shape tensile response; by contrast, serge exhibits a quasi linear response, as the initial yarn profile is flatter. The impact of the yarn mechanical properties on the overall mechanical behavior is assessed; especially, the Poisson's ratio of fabric is evaluated versus the applied load and the respective properties of both sets of yarns. Discrete homogenization techniques are developed in the last part of Chapter 10, basing on an analysis of a repetitive unit cell, representing the pattern in the case of textile. The equivalent behavior of a Cauchy or Cosserat type continuum is obtained in algorithmic format as an outcome. The simulation of the tensile response of the crimp changes of fabric by a perturbative approach reproduces the J-shape curve measured behavior. Those micromechanical analyses provide overall a guideline for the design and optimization of woven structures.

Chapter 11 reviews the research that has been done for the functionalization of textile with inorganic nanoparticles by sonochemical method. Sonochemistry is one of the most efficient techniques for creation of nanosized compounds. Ultrasonic waves in the frequency

range of 20 kHz - 1 MHz are the driving force for chemical reaction. The sonochemical reaction is dependent on the acoustic cavitation, which means creation, growing and explosion collapse of a bubble in the solution. Extreme conditions are developed when this bubble collapses, and that is the reason of break and formation of chemical bonds. The nanoparticles have been deposited on the surface of various fabrics (cotton, nylon, polyester) using ultrasound irradiation. This process produces a uniform coating of nanoparticles on surfaces with different functional groups. The coating can be performed by an in-situ process where the nanoparticles are formed and immediately thrown to the surface of the fabrics. This approach was used for Ag, ZnO and CuO. In addition, the sonochemical process can be used as a "throwing stone" technique, namely, previously synthesized nanoparticles will be placed in the sonication bath and sonicated in the presence of the fabric. This process has been shown with MgO and Al₂O₃ nanoparticles. The nanoparticles are thrown to the surface by the microjets and strongly adhered to the textile. This phenomenon was explained because of the local melting of the substrate due to the high rate and temperature of nanoparticles thrown at the solid surface by sonochemical microjets. The antibacterial activities of the nanocoated fabric composites were tested against Gram negative and Gram positive cultures. A significant bactericidal effect, even with low concentration of the nanoparticles, less than 1wt%, was demonstrated.

The use of textiles in medicine has a long tradition. Because there are a huge number of diverse applications of medical textiles, in Chapter 12 only the new trends in this field are attaining. The attention focused on biopolymers as alginate, collagen, chitin, chitosan, cellulose and bacterial cellulose, gelatine and others which have already their place in advanced biomedical applications. The use of fibers and textiles in medicine has increased exponentially as new types of fibers, new innovative structures and new therapies have been developed. Also, the progress accomplished in the new emerging technologies like nanotechnology, electrospinning and biotechnology are underlined. Chapter 12 also presented the progress achieved in the advanced materials for regenerative medicine, wound healing and drug delivery. The development of wound dressing has changed from passive to actives types, having some specific functions in order to enhance wound healing without trauma for the patient. Textile structures for wound dressing can contain specialized additives with various properties, such as antibacterial properties. Among these, silver in different forms is the most well known, being used in medical applications.

Anatase containing TiO₂ sols are prepared by a solvothermal process and used as liquid coating agents for textiles. This solvothermal process is driven at temperatures of 140°C and 180°C, which are adequate process conditions for the formation of the crystalline TiO₂ species anatase out of an amorphous TiO₂ pre-compound. By using this liquid coating agent for textile treatment, functionalized textiles with photoactive and antimicrobial properties are realized. For these materials different potential applications are thinkable as for example the wastewater treatment in a process with photoactive functionalized textiles or medical applications with antimicrobial functionalized textiles. In Chapter 13, the pure TiO₂ sol is modified by copper doping. To perform this modification, a copper containing precursor was added to the sol before the solvothermal process. Under the chosen solvothermal conditions the copper precursor is proposed to be transformed to antimicrobial active copper containing compounds, probably a Cu-Ti crystalline phase. The formation of the crystalline TiO₂ type anatase is clearly determined by XRD. Also by XRD at least one unidentified copper containing phase is determined which could be probably an intermetallic phase of Cu:Ti as

oxide, nitride or carbide. Additional hints for the formation of those species are also found by UV/VIS-spectroscopy. The modified TiO₂-sols are applied as coating agent onto textile fabrics. The photoactivity of coated textile is determined by degradation of the organic dye stuff Acid Orange 7. The effect of photocatalytic dye degradation is also investigated in presence of H₂O₂. The antimicrobial property of the coated textiles can be clearly verified and is mainly the result of the metal component added to the TiO₂ coating. The high photoactivity observed in presence of H₂O₂ could be of high interest for applications in oxidative wastewater treatment. The developed high antimicrobial active textiles should also be of great relevance for the application in the medical sector to avoid the spreading of harmful germs.

The presented research thematic focuses on cellulose fibers' functionalization by means of introducing new, naturally alternative polysaccharides as coatings for natural cellulose material. In this way, new advanced sanitary and medical cellulose materials could be developed *with significant absorption*, antiviral, and antimicrobial properties. Chapter 14 covers the physico-chemical and structural properties of cellulose fibers (natural and regenerated) and the influence of both properties on the adsorption of polysaccharides, in order to introduce new bioactive functionalities. It examines which properties predominately influence specific fiber functionality. Moreover, relevant methods are presented for revealing the structural and physico-chemical properties (with an emphasis on the charge determination) of non-functionalized, as well as functionalized, cellulose fibers (natural and regenerated). Finally, the applicability of these new materials for different hygiene and health care segments (skin and hygiene care, skin and gynecological infections, wound treatment, etc.) are discussed.

Clothing is composed by textile fibers, coupling and fixer agents, finish products, dyes and complements. Contact dermatitis is produced by the contact between these clothing components and the skin. Chapter 15 shows that two types of textile contact dermatitis have been reported; irritant and allergic, being irritant contact dermatitis more frequent than allergic. Dyes are the main cause of allergic contact dermatitis. Disperse dyes are the most frequent sensitizers among textile dyes, followed by the reactive dyes. Acid, direct and basic dyes are less common sensitizers. The use of the different dyes depends on the kind of fiber used in the fabric. Disperse dyes are more common in industrialized countries, because people from these countries usually wear clothes with nylon and polyester/cotton fibers. Finish products are the second most common textile sensitizers; they are used in natural and mixed fibers. Resins belong to this group, being Kaurit and Fix the most allergenic formaldehyde resins. Exact incidence of textile dermatitis is unknown because of the lack of controlled epidemiological studies. Textile dye sensitization has an estimated incidence rate from 1.4% to 5.8%. Women have a greater prevalence of allergic reactions to textile dyes and resins than men; this may be due to the use of tighter fitting synthetic and dark-colored clothing. Contact textile dermatitis is increasing, probably as a result of the wide use of new dyes in clothes production. Many clinical manifestations of textile dermatitis have been described. Usually, patients are affected by an acute or chronic dermatitis, of localized or generalized distribution of lesions. Unusual forms can also be seen: purpuric lesions, hyperpigmented patches, papular rash, papulopustular lesions, urticaria, erythema multiforme-like lesions, nummular-like lesions, lichenification and erythroderma. Topical or systemic corticosteroids can be used in the treatment of textile contact dermatitis. In addition, the patient should avoid the offending allergen or irritant source, wearing 100% natural based fabrics, use loose fitting clothing, and avoid synthetic spandex, lycra, acetate, polyester fibers

and nylon. It is recommended washing clothes three times before wearing them the first time. Contact textile dermatitis may be undiagnosed because the atypical clinical manifestations do not give rise to suspicion of textile dermatitis. Clinical history, clinical findings and patch test are the best elements in the diagnosis. Therefore, the physician should suspect a contact dermatitis in patients showing suggestive clinical signs, which might lead to an early diagnosis and appropriate treatment.

Textile materials have many advantages which make them useful for clothing and technical applications. They can be used in different forms, be permeable to air or fluids if needed, and additionally textiles have good mechanical parameters. They have a large surface in comparison to their mass. In many cases they offer a solution to problems, which are beneficial in terms of price and given application parameters. That is why surface modification, significantly increasing the range of textiles' applications, is an important research topic in textiles materials. Systematically grows a need to produce new materials or products with improved characteristics. In Chapter 16 the latest methods which improve surface properties in a more effective way than conventional were described. One of the newest methods of textile surface modification is the layer-by-layer method. Initially this method has been used for different materials than textiles; however it is currently implemented in the textile industry. The use of multilayered polymeric films offers the possibility of creating new type of materials with great levels of reproducibility and controlled architectures. Fundamental and representative methods used for textile surface modification on the basis of layer-by-layer method were characterized. Theoretical assumptions, textile characteristic and practical conditions were discussed. Methods for specific applications were analyzed as far as application and difficulties in their usage are concerned.

Several haute couture contemporary textiles from museum collections exhibit serious conservation problems due to the high complexity of materials and production methods used in their conception. Conservation of contemporary textiles with new materials and production methods requires scientific research into the identification of materials and new conservation techniques. This was the case of the spectacular golden coat made by the French fashion designer Jean-Paul Gaultier, currently in MUDE (Museum of Fashion and Design), in Lisbon. The coat is an excellent example of Gaultier's eclectic selection of materials and technical versatility. It was created with a golden combined textile, with several attached golden polymeric and glass materials. Despite the importance of this piece, little information was available in the archives of Maison Gaultier. In order to understand the creative processes and identify the coat's materials that could provide important information for the stabilization and treatment of the piece, an interdisciplinary research was carried out. Chapter 17 reviews the Characterization of the coat's materials with several analytical techniques, which *revealed that the golden combined textile was a poly(ethylene terephthalate) canvas covered with apoly(dimethylsiloxane) (PDMS) layer and a yellow brass pigment hand-stitched to a yellow silk lining*. The golden coat exhibits several pathologies, namely oxidation of the brass pigment and a significant deterioration of the PDMS layer due to humidity action. Indeed, the cohesion and adhesion properties of the PDMS layer are fragile inducing considerable material loss of the attached materials. The consolidation of the PDMS layer as well as its protection from a humidity environment was considered fundamental to stabilize the degradation of the golden coat. With a similar PDMS chemical nature, sol-gel silica was considered a potential candidate for a coating application in order to enhance the PDMS

properties. Silica sols were prepared by the sol-gel method with tetraethoxysilane using ethanol, water and an acid and/or a base as catalyzers. Different additives were used to improve the PDMS properties such as hydrophobicity, flexibility and adherence. The films containing SiO₂ were applied to test samples. Homogeneous thin films with few micro-cracks were obtained using spin coating and vapor-spraying on the film deposition. Moreover, minimal differences in pH and color were observed. The contact angle value improved slightly, indicating that the films exert in some extent a protection against the humidity.

The polymer-derived SiC fiber is one of the most important reinforcing materials for high performance ceramic matrix composites (CMC). Three generation of SiC fibers have been developed over the past thirty years. The first generation fiber produced was an amorphous SiC fiber, next was a low-oxygen content SiC fiber, and nearly stoichiometric SiC fiber was developed. In Chapter 18, the preparation method, microstructure, and performance of three generation fibers are described. The representative properties of these fibrous materials and their expected applications are also described.

Chapter 19 explores ways to improve the properties of polyester material in the processing of its surface temperature plasma at atmospheric pressure. The plasma discharge was generated in a sodium hydroxide solution. During the modification process, a fiber was extending through the diaphragm which placed into electrolyte solution. Electric current was passed through the diaphragm which caused the appearance of the gas-vapor bubble. If the voltage applied to the diaphragm was 0.5 – 1.5 kV, a breakdown of the gas-vapor case is generated and discharge is allowed. The method of surface modification of polymers requires relatively low voltage, and allows concentrating zone of plasma near the surface of the sample. It is shown that plasma in the liquid environment is non-equilibrium and contains the components from the liquid substance. The influence of diaphragm size and broaching speed of polyester fiber through the plant for the plasma-chemical modification to the physical-mechanical characteristics of the finished polyester fibers was studied. The main criterion for successful modification of polyethylene terephthalate material was considered to be a formation the maximum possible number of active groups on its surface with the maximum preservation of strength parameters. It is shown that the use of such method of modification provides a formation of active hydroxyl and carboxyl groups on the surface of the polymeric material which are required for fixation of functional products. Their application on the surface of fibrous material can give it some new properties (hydrophobic, antimicrobial, deodorizing, etc.).

Cleaning of solid rigid materials is one of the older applications of high-intensity ultrasound. Nevertheless the use of ultrasonic energy for washing textiles was explored over several years without achieving successful development. Besides the specific problems related with softness of the fabric material, the strategies for ultrasonic washing of textiles were generally directed towards the production of washing machines to wash laundry by generating high-intensity ultrasonic waves in the entire volume of the basket containing the fabrics to be washed. Such strategies offer significant inconveniences because of the practical difficulties to achieve a homogeneous distribution of the ultrasonic energy in the entire washing volume. Then in the areas of low acoustic energy the cleaning effect is not reached and it causes the washing to be irregular. During the last twenty years the use of ultrasonic technologies for cleaning textiles in domestic and industrial washing machines has been reinvestigated and new important advances in this area has been achieved. In fact, it has been found out that by diminishing the amount of dissolved air or removing the big bubbles in the

wash liquor the application of ultrasonic energy improved wash results in comparison to conventional methods. It has been also shown that a high proportion of water with respect to the wash load is required to assure efficiency and homogeneity in the wash performance. The application of such requirements in domestic washing machines or even in large scale machines similar in design to them doesn't seem a realistic and economically viable option. However for specific industrial applications a new ultrasonic process has been developed in which the textiles are exposed to the ultrasonic field in flat format and within a thin layer of liquid by applying specific ultrasonic plate transducers. Such process has been implemented at laboratory and semi-industrial stage. Chapter 20 deals with the progressive advances in the use of the ultrasonic energy for washing textiles and in particular with the new process and the structure and performance of the systems developed for its implementation.

Chapter 1

FROM NATURAL TO SYNTHETIC FIBERS

*Ahmed El Nemr**

Environmental Division, National Institute of Oceanography and Fisheries,
Kayet Bey, El Anfoushy, Alexandria, Egypt

1. INTRODUCTION

Fiber is a class of materials that are continuous filaments or are in discrete elongated pieces, similar to lengths of thread. Fibers are very important in the biology of both plants and animals, for holding tissues together. Plants yielding fibers have been only second to food plants in their usefulness to humans and their influence on the furthering of civilization. Primitive humans in their attempts to obtain the three most important necessities for life (food, clothing and shelter) focused on plants. Even though animal products were available, some forms of clothing were needed that were lighter and cooler than hides. It was easier to obtain from plants such items as nets, snares, etc. Also plant products used to construct human's shelter were available from the leaves, stems and roots of many plants. Therefore, mankind was utilized the natural fibers significantly earlier than metals, alloys, and ceramics and it can be supposed that the natural fibers were used by humans long before recorded history. The cultivation of flax, for example, dates back to the Stone Age of Europe, as discovered in the remains of the Swiss Lake Dwellers. Linen was used in Ancient Egypt and cotton was the ancient national textile of India, being used by all the aboriginal peoples of the New World as well. Ramie or China grass has been grown in the orient many thousands of years. Fibers from natural sources, twisted by hand into yarns, and then woven into textile fabrics, constitute a materials technology which dates back over 10000 years [1, 2]. However, the utilization of history of fibers is much harder to trace than that of metals and ceramics due to deterioration of fibers through rot, mildew, and bacterial action and only a few specimens of early fibers have been found so far. Some animals produce fibers whereas others collect them from different sources for their needs. They use fibers when building nests such as birds and some mammals, webs such as spiders, for protection during reproduction such as caterpillars and silkworms, or for retrieving insects out of narrow holes such as chimpanzees.

* E-mail: ahmedmoustafaelnemr@yahoo.com; ahmed.m.elnemr@gmail.com

Still, up today, more than one-half of the world's fibers stem from natural sources, among which cotton constitutes the most important part (Figure 1).

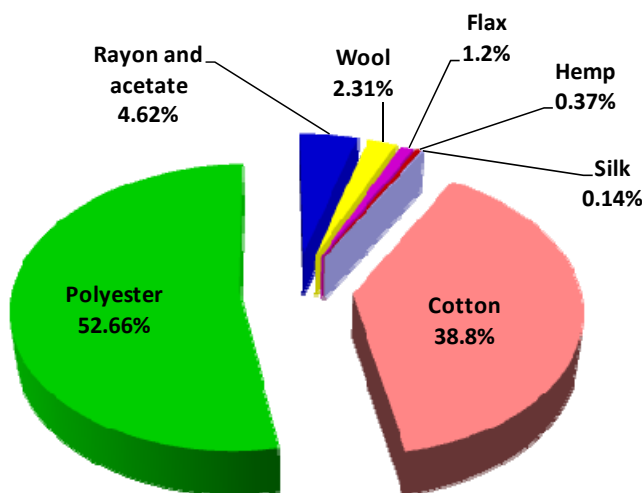


Figure 1. World textile fiber average production % in 2000-2008.

Apart from hand-tools, the yarns, woven and textile technology changed little until the industrial revolution, with the invention of power machines concentrated in 1775 - 1825. The available fibers, namely cotton, some fibers extracted from the stems or leaves of plants, wool, other hairs, and silk, remained unchanged for another 100 years. All except silk were short fibers, with staple lengths of about 1-10 cm. These fibers had to be twisted into yarns. Even silk filaments were of finite length and had to be "thrown" together into longer yarns, which were smooth and lustrous in contrast to the hairy staple-fiber yarns. Advances in chemistry led to solutions of cellulose derivatives, which could be extruded through multiple holes, coagulated, and regenerated as continuous filament yarns of effectively infinite length, which, for a time, were known as *artificial silk* such as *viscose rayon*, which was commercially first produced in 1905. The recognition of the idea of macromolecules in the 1920s led to manufactured, synthetic yarns of several vinyl polymers, but the major invention was nylon, which became commercial in 1938 and polyester was followed 10 years later. The two other major synthetic fibers of this first generation were acrylics and polypropylene. A second generation of high-performance fibers started with *Kevlar*, followed by high-modulus polyethylene. Elastomeric fibers, such as *Lycra*, were another development [3-12].

Natural fibers are generally classified by their origin [1]. They include those produced by plants, animals, and geological processes. They are biodegradable over time. They can be classified according to their origin as followed:

- I. Animal fibers are composed mostly of proteins, which are highly complex substances consist of long chains of alpha amino acids involving carbon, hydrogen, oxygen, nitrogen, and sulfur. Instances are spider silk, sinew, catgut, wool and hair such as cashmere, mohair and angora, fur such as sheepskin, rabbit, mink, fox, beaver, etc. The wool fibers from domestic sheep and silk are used most commonly both in the

manufacturing world as well as by the hand spinners. Also very popular are alpaca fiber and mohair from Angora goats. Unusual fibers such as Angora wool from rabbits [13-16] and *Chiengora* from dogs also exist, but are rarely used for mass production (*Chiengora*, pronounced “she-an-gora”, refers to yarn spun from dog hair. *Chien* is the French word for dog, and *gora* is derived from “angora”, which is the soft fur of a rabbit. The spinning of dog hair is an ancient art form dating back to pre-historic Scandinavia. It was the main fiber spun on the North American continent before the Spaniards introduced sheep wool. *Chiengora* is up to 1.8 warmer than wool and sheds water well. Its fiber is not elastic like wool, and is characterized by its fluffiness, known as a halo effect. It has a similar appearance to angora and is luxuriously soft) (<http://chiengorafibers.com/>). Not all animal fibers have the same properties even within same species. Merino is very soft and fine wool, while Cotswold is coarser, and yet both merino and Cotswold are types of sheep. This comparison can be continued on the microscopic level, comparing the diameter and structure of the fiber. With animal fibers, and natural fibers in general, the individual fibers look different, whereas all synthetic fibers look the same. This provides an easy way to differentiate between natural and synthetic fibers under a microscope. All animal fibers do not contain cellulose and are therefore more vulnerable to chemical damage and unfavorable environmental conditions than cellulose. After extraction of the fibers, the individual fibers are arranged in parallel to overlap each other, yielding a ribbon. These ribbons are then softened with mineral oil, lubricated, and eventually drawn down to the desired sizes and twisted for securing the position of the fibers and the yarn is eventually woven into fabrics.

- II. Vegetable fibers - generally based on arrangements of cellulose, often with lignin - examples include cotton, hemp, jute, flax, kenaf, roselle, coir, henequen, abaca, fique, phormium, ramie, and sisal. Plant fibers are employed in the manufacture of paper and textile (cloth), and dietary fiber is an important component of human nutrition. Indeed, it is estimated that in the Western Hemisphere alone, more than 1000 species of plants or parts of plants are utilized in one way or another to create utilitarian products. Most of them, however, are consumed locally or in such small quantities.
- III. Wood fiber - distinguished from vegetable fiber - is from tree sources. Forms include ground-wood, thermo-mechanical pulp (TMP) and bleached or unbleached Kraft or sulfite pulps. Kraft and sulfite refer to the type of pulping process used to remove the lignin bonding the original wood structure, thus freeing the fibers for use in paper and engineered wood products such as fiberboard.
- IV. Mineral fibers comprise asbestos. Asbestos is the only naturally occurring long mineral fiber. Short, fiber-like minerals include wollastonite [CaSiO_3 , which may contain small amounts of iron, magnesium, and manganese substituting for calcium and it is usually white, colorless or gray and it is formed when impure limestone or dolostone is subjected to high temperature and pressure in the presence of silica-bearing fluids as in skarns or contact metamorphic rocks. Associated minerals include garnets, vesuvianite, diopside, tremolite, epidote, plagioclase feldspar, pyroxene and calcite. It is named after the English chemist and mineralogist W.H. Wollaston (1766–1828)] [17-21], attapulgite (magnesium aluminium phyllosilicate with formula “ $(\text{Mg}, \text{Al})_2\text{Si}_4\text{O}_{10}(\text{OH}) \cdot 4(\text{H}_2\text{O})$ ” which occurs in a type of clay soil

common to the Southeastern United States) [22, 23] and halloysite (a 1:1 aluminosilicate clay mineral with the empirical formula $\text{Al}_2\text{Si}_2\text{O}_5(\text{OH})_4$. Its main constituents are aluminum (20.90%), silicon (21.76%), and hydrogen (1.56%). It is typically forms by hydrothermal alteration of alumino-silicate minerals. It can occur intermixed with dickite, kaolinite, montmorillonite and other clay minerals) [24-31]. Mineral fibers can be particular strong because they are formed with a low number of surface defects.

Table 1. Major sources of natural fibers, usage, and raw

Fiber	Usage	Principal growing countries
Flax/linen raw, retted	Fine textiles, cordage, yarn	Belgium, Netherlands, Russia, France, China
Ramie	Garment blend with cotton	China, Taiwan, Korea, Philippines, Brazil
Cotton	Garments, paper, explosives, oil, padding	China, USA, Pakistan, India, Uzbekistan, Brazil
Wool 7.5 cm and up	Knitting yarn, tweeds, flannels, carpets, blankets, upholstery, felts	Australia, New Zealand, China, South Africa, Russia, Argentina

Source: Department of Commerce, U.S. Census Bureau, Foreign Trade Statistics.

Textile fibers must be long and possess a high tensile strength and cohesiveness with pliability. They must have a fine, uniform, lustrous staple and must be durable and abundantly available. Only a small number of the different kinds of fibers possess these traits and are thus of commercial importance. The principal textile fibers are grouped into three classes: surface fibers, soft fibers and hard fibers, with the last two often referred to as long fibers. Surface or short fibers include the so-called cottons. The soft fibers are the bast fibers that are found mainly in the pericycle or secondary phloem of dicotyledon stems. Bast fibers are capable of subdivision into very fine flexible strands and are used for the best grades of cordage and fabrics. Included are hemp, jute, flax and ramie. Hard or mixed fibers are structural elements found mainly in the leaves of many tropical monocots, although they may be found in fruits and stems. They are used for the more coarse textiles. Sisal, abaca, henequen, agaves, coconut and pineapple are examples of plants with hard fibers.

Synthetic or man-made fibers generally come from synthetic materials such as petrochemicals. But some types of synthetic fibers are manufactured from natural cellulose; including rayon, modal, and the more recently developed *Lyocell* (a regenerated cellulose fiber made from dissolving pulp (bleached wood pulp). It was first manufactured in 1987 by Courtaulds Fibres UK and first went on public sale as a type of rayon in 1991. It is also manufactured by Lenzing AG of Lenzing, Austria in 2010, under the brand name "Lyocell by Lenzing", and under the brand name Tencel by the Tencel group, now owned by Lenzing AG) [32-36]. Cellulose-based fibers are of two types, regenerated or pure cellulose such as from the cupro-ammonium process and modified cellulose such as the cellulose acetates [37-40]. Cellulose fibers are a subset of man-made fibers, regenerated from natural cellulose, which comes from various sources. Modal is made from beech trees, bamboo fiber is a cellulose fiber made from bamboo, seacell is made from seaweed, etc. Synthetic fibers can often be produced very cheaply and in large amounts compared to natural fibers, but for

clothing natural fibers can give some benefits, such as comfort, over their man-made counterparts.

Fiberglass, made from specific glass, and optical fiber, made from purified natural quartz, are also man-made fibers that come from natural raw materials, silica fiber, made from sodium silicate (water glass) and basalt fiber made from melted basalt. Metallic fibers can be drawn from ductile metals such as copper, gold or silver and extruded or deposited from more brittle ones, such as nickel, aluminum or iron. Carbon fibers are often based on oxidized and carbonized polymers, but the end product is almost pure carbon.

The uses of textile fibers contain three categories; the first and second categories are *clothing* and *furnishing fabrics*. They are somewhat unusual in materials technology, since color and the other esthetic features of pattern and feel, which are determined by the fiber and textile structures, are as important as the functional requirements for cover, protection, warmth, and durability. The third category of *technical textiles* includes some old and simple uses, ranging from ropes to wiping cloths, but is becoming of increasing importance in demanding engineering and medical applications. The global textile fiber consumption is reported in Figure 2 [4].

The history of communication via fiber optics is also reported via the relatively recent advancement within the context of communication through history and the reported review article also offers projections of where this continuing advancement in communication technology may lead us over the next half century [41, 42].

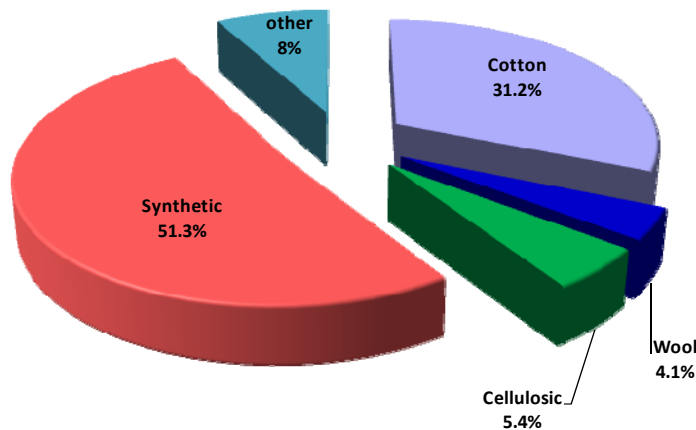


Figure 2. The global textile fibers average consumption.

2. WOOL

Wool probably was the first raw material turned by humane into fabrics, which suppose to be during the Old Stone Age, about 2 million years ago. Fabric from wool may have been produced by *felting*, a process that yields a nonwoven mat by the application of heat, moisture, and mechanical action to some animal fibers. That there was trade in wool dating back to 4200 B.C, which proved by documents and seals found in Tall Al-Asmar (Iraq) [1]. Breeding sheep producing-wool obviously started in Central Asia and extends from there to

other areas of the world, which come from the fact that sheep easily adapt to different climates. For example, it is reported that the Phoenicians brought the Merino sheep ancestors from Asia Minor to Spain several millennia ago. Now, Merino sheep are raised essentially on all of the continents, for example, New Zealand, with a population of only 4.0 million people, hosts more than 50 million sheep of various breeds, whose were introduced there by British settlers about 150 years ago. Wild sheep have long, coarse hairs and a softer undercoat of short and fine hairs which provides thermal insulation. The Merino sheep has been bred to eliminate the outer coat and the annual shedding, allowing instead a continuously growing fine and soft fleece which can be shorn off repeatedly [1].

2.1. Wool fibers

Wool is protein-based fiber obtained mostly from sheep and other animals such as *mohair* from the fleece of the Angora goat (named after the ancient province of Angora, today's Ankara, in Turkey), *cashmere wool* (stemming from the fine and soft undercoat of Kashmir goats which live in the mountains of Asia), and *camel hair* (which is collected during molting). In order for a natural goat fiber to be considered Cashmere, it must be under 18.5 μm in diameter and be at least 3.175 cm long. Cashmere is characterized by its luxuriously soft fibers, with high napability, loft, and it is noted as providing natural light-weight insulation without bulk. Cashmere fibers are highly adaptable and are easily constructed into fine or thick yarns, and light to heavy-weight fabrics [43-46]. Other specialty animal fibers stem from the *llama* and the *alpaca*, which are close relatives of the camel and live predominantly in the high grasslands of the Andes in South America. Further, one uses hair from *horses*, *cows*, and *angora rabbits*. There are many types of Angora rabbits - English, French, German and Giant. Angora is prized for its softness, thin fibers of around 12-16 μm for quality fiber, and what knitters refer to as a halo (fluffiness). The fiber felts very easily. Angora fiber comes in white, black, and various shades of brown.

Bison down is the soft wool undercoat of the American Bison, which contains two different types of fiber. The main Bison coat is made up of coarse fibers ($\sim 59 \mu\text{m}$) called guard hairs, and the downy undercoat ($\sim 18.5 \mu\text{m}$). This undercoat is shed annually and consists of fine, soft fibers which are very warm and protect the animal from severe winter conditions [9].

Alpaca fiber is that of an alpaca. It is warmer than sheep's wool and lighter in weight. It is soft, fine, glossy, and luxurious. The thickness of quality fiber is between 12-29 μm . Most alpaca fiber is white, but it also comes in various shades of brown and black [47-49].

Mohair is a silk-like fabric or yarn made from the hair of the Angora goat. Mohair is both durable, resilient and high luster and sheen, and is often used in fiber blends to add these qualities to a textile. Mohair also takes dye exceptionally well.

Qiviut is the fine underwool of the muskox and is 5 to 8 cm long, between 15 and 20 μm in diameter, and relatively smooth. It is approximately eight times warmer than sheep's wool and does not felt or shrink [50, 51].

The animal protein *keratin*, which is common in the outermost layers of the skin, nails, hooves, feathers, and hair, is the main component of wool. *Keratin* is completely insoluble in cold or hot water and is not attacked by proteolytic-enzymes that break proteins. *Keratin* in wool is composed of a mixture of peptides [52-54]. When wool is heated in water to about

90°C, it shrinks irreversibly, which is attributed to the breakage of hydrogen bonds and other non-covalent bonds [7, 8, 55].

Wool fibers range in diameter between 15 and 60 μm and are coarser than those of silk, rayon, cotton, or linen, and depending on their lengths. Fine wool fibers are 4.0–7.5 cm long, whereas coarse fibers measure up to 35 cm. Unlike vegetable fibers, wool has a lower breaking point when wet and the fibers are elastic to a certain extent, that is, they return to their original length after stretching or compression and thus resist wrinkling in garments. The low density of wool results in light-weight fabrics and wool can retain up to 18% of its weight in moisture. Still, wool has slow water absorption and release that allows the wool wearer not to feel damp or chilled [7, 8, 55]. Wool is essentially mildew-resistant and is little deteriorated when properly stored. However, clothes moths and carpet beetles feed on wool fibers, and extensive exposure to sunlight may cause decomposition. Further, wool deteriorates in strong alkali solutions and chars at 300°C [7, 8, 55].

Subjection of wet and hot wool to mechanical action leads to *Felting shrinkage*. Therefore, washing of wool in hot water with extensive mechanical action is harmful. On the other hand, felting produces a nonwoven fabric that is possible due to the fact that animal fibers (except silk) are covered with an outer layer of unidirectional overlapping scales, as depicted in Figure 3.

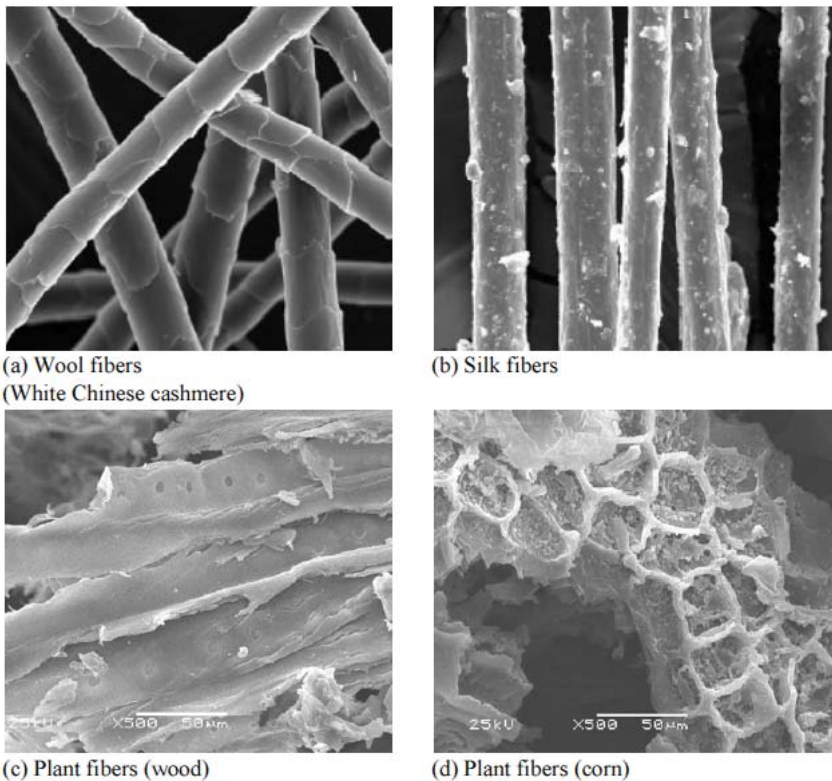


Figure 3. Scanning electron micrographs of (a) wool fiber, (b) silk fibers, (c) Wood fiber, and (d) Corn fiber.

2.2. Production of Wool

Global wool production is approximately 1.3 million tons per year, of which 60% goes into apparel. Australia is the leading producer of wool which is mostly from Merino sheep [56-58]. New Zealand is the second-largest producer of wool, and the largest producer of crossbred wool. China is the third-largest producer of wool. Sheep breeds such as *Lincoln*, *Romney*, *Tukidale*, *Drysdale* and *Elliotdale* produce coarser fibers, and wool from these sheep is usually used for making carpets. In the United States, Texas, New Mexico and Colorado have large commercial sheep flocks and their mainstay is the *Rambouillet* (or French Merino) (Figure 4) [59-61]. There is also a thriving home-flock contingent of small-scale farmers who raise small hobby flocks of specialty sheep for the hand spinning market. These small-scale farmers offer a wide selection of fleece.

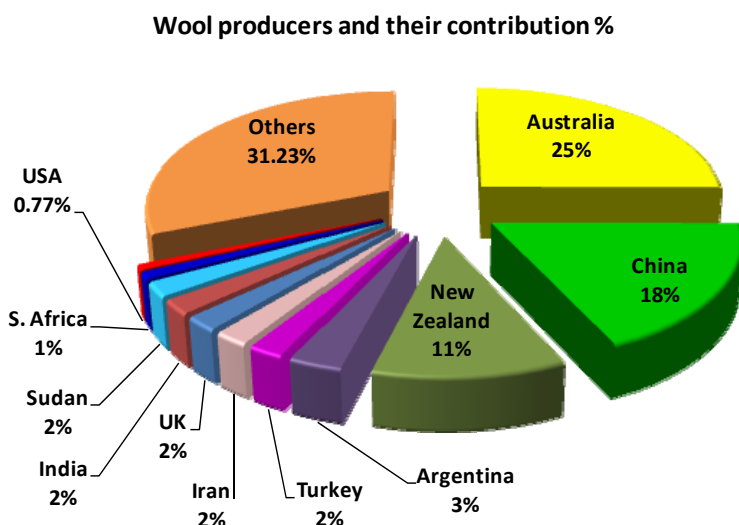


Figure 4. Global wool production (Source: <http://en.wikipedia.org/wiki/Wool>).

Organic wool (-wool that is from sheep that have not been exposed to chemicals like pesticides and are kept in humane and good farm conditions) is becoming more and more popular. This wool is very limited in supply and much of it comes from New Zealand and Australia. It is becoming easier to find in clothing and other products, but these products often carry a higher price. Wool is environmentally preferable (as compared to petroleum-based Nylon or Polypropylene) as a material for carpets as well, in particular when combined with a natural binding and the use of formaldehyde-free glues.

2.3. Quality of Wool

The quality of wool is determined by the following factors, fiber diameter, crimp, yield, color, and staple strength. Fiber diameter is the single most important wool characteristic determining quality and price. Merino wool is typically 7.5-12.5 μm in length and is very fine (between 12-24 μm) (<http://web.archive.org/web/20061105005633/> <http://www.>

merinos.com.au/history.asp). The finest and most valuable wool comes from Merino hogget. Wool taken from sheep produced for meat is typically coarser, and has fibers that are 3.5 to 15 cm in length. Damage or breaks in the wool can occur if the sheep is stressed while it is growing its fleece, resulting in a thin spot where the fleece is likely to break (<http://www.midstateswoolgrowers.com/management.htm>). Wool is also separated into grades based on the measurement of the wool's diameter in microns and also its style (Table 2) [62]. These grades may vary depending on the breed or purpose of the wool.

Table 2. Wool grades identification

Wool grades	Diameter (μm)
Ultrafine Merino	15.5
Superfine Merino	15.6-18.5
Fine Merino	18.6-20
Medium Merino	20.1-23
Strong Merino	>23
Comeback	21-26 white, 90–180 mm long
Fine crossbred	27-31
Medium crossbred	32–35
Downs	23-34, typically lacks luster and brightness (e.g. Aussiedown, Dorset Horn, Suffolk)
Coarse crossbred	36
Carpet wools	35-45

Source: <http://en.wikipedia.org/wiki/Wool>; Australian Wool Exchange (AWEX), 2010.

Wool diameter finer than 25 μm are used for garments, while coarser grades are used for outerwear or rugs. The finer the wool, the softer it is, while coarser grades are more durable and less prone to pilling. The finest Australian and New Zealand Merino wools are known as 1PP which is the industry benchmark of excellence for Merino wool that is 16.9 μm and finer. This style represents the top level of fineness, character, color, and style as determined on the basis of a series of parameters in accordance with the original dictates of British Wool as applied today by the Australian Wool Exchange (AWEX) Council. Only a few dozen of the millions of bales auctioned every year can be classified and marked 1PP (<http://www.awex.com.au/scripts>).

2.4. Uses of Wool

In addition to clothing, wool has been used for blankets, horse rugs, saddle cloths, carpeting, felt, wool insulation and upholstery. Wool felt covers piano hammers, and it is used to absorb odors and noise in heavy machinery and stereo speakers. Ancient Greeks lined their helmets with felt, and Roman legionnaires used breastplates made of wool felt. Wool has also been traditionally used to cover cloth diapers. Wool fiber exteriors are hydrophobic (repel water) and the interior of the wool fiber is hygroscopic (attracts water); this makes a wool garment able to cover a wet diaper while inhibiting wicking, so outer garments remain dry. Wool felted and treated with lanolin is water resistant, air permeable, and slightly antibacterial, so it resists the buildup of odor. Some modern cloth diapers use felted wool

fabric for covers, and there are several modern commercial knitting patterns for wool diaper covers. Initial studies of woolen underwear have found it prevented heat and sweat rashes because it more readily absorbs the moisture than other fibers. Merino wool has been used in baby sleep products such as swaddle baby wrap blankets and infant sleeping bags. As wool is an animal protein so it can be used as a soil fertilizer, being a slow release source of nitrogen and readymade amino acids [63, 64].

3. SILK

Silk is a "natural" protein fiber obtained from some insects; some forms of silk can be woven into textiles. The cultivation of the larva of *Bombyx mori* (commonly called mulberry *silkworm*), which produce of the silk, is attributed to the Chinese empress, Hsi-ling Shih, who, in 2640 B.C., discovered that the silk filament from a cocoon could be unwound. There is another sources claim that Japan was the first country in which silkworms were domesticated at about 3,000 B.C. The technique of silk-making (called *sericulture*) was kept a secret by the Chinese for about 3,000 years but eventually transferred to Japan, Persia, and India. Legend has it that two Persian monks smuggled some silkworm eggs and seeds of the mulberry tree (on whose leaves the larva feed) out of China. This triggered a silk industry in Byzantium during the reign of emperor Justinian (A.D. 527–565) and in Arabic countries beginning with the eighth century A.D. Eventually, the art of sericulture spread in the twelfth century to Italy and thus to Europe. Silk was and is still regarded even today as a highly esteemed, luxury fabric because it is the finest of all natural fibers and its production is cumbersome. The highest regarded animal fiber, however, is *silk*, which is spun by a caterpillar [1].

Chinese silk textiles manufactured during the Han dynasty (206 B.C. – 220 A.D.) have been found in graves located in northern Mongolia, Chinese Turkistan and Egypt. In the eighteenth and nineteenth centuries, during the industrial revolution years, a number of machines were invented and put into service which transferred spinning, weaving, and other fiber-processing techniques from individual homes to centralized factories with consequential economic hardships for some people and concomitant social upheavals. These machines which produced relatively inexpensive fabrics triggered lead to an increase in fiber demand and production.

Silks are produced by several other insects, but only the silk of moth caterpillars has been used for textile manufacturing [65-67]. There are some researchs into other silks, which differ at the molecular level. Silks are mainly produced by the larvae of insects undergoing complete metamorphosis, but also by some adult insects such as web-spinners [68]. Silk production is especially common in the Hymenoptera (bees, wasps, and ants), and is sometimes used in nest construction. Other types of arthropod produce silk, most notably various arachnids such as spiders [67, 69-71].

3.1. Silk Fibers

Silk is a continuous fiber has no cellular structure and its proteins contain about 80% fibroin (which makes up the filament) and about 20% sericin or silk gum, which holds the filaments together and a minor percentage of waxes, fats, salts, and ash. Fibroin is the structural center of the silk and sericin is the sticky material surrounding it. Fibroin is made up of the amino acids Gly-Ser-Gly-Ala-Gly-Ala and forms beta pleated sheets [72-74].

The best-known type of silk is obtained from cocoons made by the larvae of the silkworm *Bombyx mori* reared in captivity (sericulture). Degummed fibers from *B. mori* are 5-10 μm in diameter. The life cycle of *Bombyx mori* includes hatching of the disk-shaped eggs in an incubator at 27°C, which requires about 10 days. The “silkworm,” 3 mm long and 3 mg in mass, eventually grows into a 90 mm long caterpillar which needs five daily feedings of chopped, young mulberry leaves. After about 6 weeks and four moltings, it stops eating, shrinks somewhat, and its head makes restless rearing movements, indicating a readiness to spin the cocoon. The silkworm is then transferred into a compartmentalized tray or is given twigs. There it spins at first a net in whose center the cocoon is spun around the silkworm. After 3 days, during which time the filament is wound in a figure-eight pattern, the completed cocoon has the shape and size of a peanut shell [72-74].

The silk substance is produced by two glands and is discharged through a spinneret, a small opening below the jaws. The spinneret is made up of several chitin plates which press and form the filament. The filament (called *bave*) actually consists of two strands (called *brins*) that are glued together and coated by silk gum (*sericin*), which is excreted by two other glands in the head of the silkworm. The liquid substance hardens immediately due to the combined action of air exposure, the stretch and pressure applied by the spinneret, and to acid that is secreted from still another gland. Under normal circumstances, the chrysalis inside the cocoon would develop into a moth within 2 weeks and would break through the top by excreting an alkaline liquid that dissolves the filament. Male and female moths would then mate within 3 days and the female would lay 400–500 eggs, after which time the moths would die. The life cycle is, however, generally interrupted after the cocoon is spun by applying hot air or boiling water (called *stoving* or *stifling*) except in limited cases when egg production is desired. The filament of 2–7 cocoons are then unwound (called *reeling*) in staggered sequence to obtain homogeneous thread strength. The length of the silk fiber depends on how it has been prepared. Since the cocoon is made of one strand, if the cocoon is unwound carefully the fibers can be very long. The usable length of the continuous filament is between 600 and 900 meters. It takes 35,000 cocoons to yield 1 kg of silk. The electron microscope (SEM) of silk fibers is depicted in Figure 3b.

The raw silk is usually degummed to improve luster and softness by boiling it in soap and water, which reduces its weight by as much as 30% (*Sericin* is soluble in water whereas fibroin is not). The silk is subsequently treated with metallic salt solutions (e.g., stannic chloride), called weighing, which increases the mass (and profit) by about 11% and adds density. Excessive weighing beyond 11% causes the silk to discolor and decompose. Likewise, dying adds about 10% weight. Silk fabric treated with polyurethane possesses excellent wet wrinkle recovery and dimensional stability during washing [75-77]. Silk is more heat-resistant than wool (it decomposes at about 170°C); it is rarely attacked by mildew but degrades while exposed extensively to sunlight. Silk is also the strongest natural fiber known. The shimmering appearance for which silk is prized comes from the fibers' triangular prism-

like cross-sectional structure which allows silk cloth to refract incoming light at different angles. Silk can adsorb large quantities of salts, for example during perspiration. These salts, however, eventually weaken the silk and destroy it.

3.2. Properties of Silk

Silk fibers from the *Bombyx mori* silkworm have a triangular cross section with rounded corners, 5-10 μm wide. The fibroin-heavy chain is composed mostly of beta-sheets, due to a 59 mer amino acid repeat sequence with some variations [78]. The flat surfaces of the fibrils reflect light at many angles, giving silk a natural shine. The cross-section from other silkworms can vary in shape and diameter: crescent-like for *Anaphe* and elongated wedge for tussah. *Bave* diameters for tussah silk can reach 65 μm [79]. Silk has a smooth, soft texture that is not slippery, unlike many synthetic fibers.

Silk is one of the strongest natural fibers but loses up to 20% of its strength when wet. It has a good moisture regain of 11%. Its elasticity is moderate to poor: if elongated even a small amount, it remains stretched. It can be weakened if exposed to too much sunlight. It may also be attacked by insects, especially if left dirty. Silk is a poor conductor of electricity and thus susceptible to static cling. Unwashed silk chiffon may shrink up to 8% due to a relaxation of the fiber macrostructure. So silk should either be pre-washed prior to garment construction, or submitted to dry cleaner, but dry cleaning may still shrink the chiffon up to 4%. Occasionally, this shrinkage can be reversed by a gentle steaming with a press cloth. There is almost no gradual shrinkage or shrinkage due to molecular-level deformation. Natural and synthetic silk is known to manifest piezoelectric properties in proteins, probably due to its molecular structure. Silkworm silk was used as the standard for the denier, which is the measurement of linear density in fibers. Therefore the silkworm silk has a linear density of approximately 1 denier (1 den), or 1.1 dtex.

Hydrogen bonds form between chains, and side chains form above and below the plane of the hydrogen bond network. The high proportion (50%) of glycine, which is a small amino acid, allows tight packing and the fibers are strong and resistant to stretching. The tensile strength is due to the many interceded hydrogen bonds. Since the protein forms a beta sheet, when stretched the force is applied to these strong bonds and they do not break. Silk is resistant to most mineral acids, except for sulfuric acid, which dissolves it. It is yellowed by perspiration.

3.3. Uses of Silk

The absorbency of silk fibers makes it comfortable to wear in warm weather and during activities. While the low conductivity of silk fibers may keeps warm air close to the skin during the cold weather [80]. It is often used for clothing such as shirts, ties, blouses, formal dresses, high fashion clothes, lingerie, pajamas, robes, dress suits, sun dresses and kimonos.

Silk's attractive luster and drape makes it suitable for many furnishing applications. It is used for upholstery, wall coverings, window treatments (if blended with another fiber), rugs, bedding and wall hangings.

While on the decline now, due to artificial fibers, silk has many industrial and commercial uses; parachutes, bicycle tires, comforter filling and artillery gunpowder bags.

A special manufacturing process removes the outer irritant sericin coating of the silk, which makes it suitable as non-absorbable surgical sutures. This process has led to the introduction of specialist silk underclothing for children and adults with eczema where it can significantly reduce itch [81-83].

3.4. Production and Cultivation of Silk

Over 30 countries are cultivated silk “*sericulture*”, the major ones are China (54%) and India (14%) of 541000 tons per year (Figure 5) [84]. To produce 1 kg of silk, 104 kg of mulberry leaves must be eaten by 3000 silkworms. It takes about 5000 silkworms to make a pure silk kimono [85].

Silk moths lay eggs on specially prepared paper. The eggs hatch and the caterpillars (silkworms) are fed on fresh mulberry leaves. After about 35 days and 4 moltings, the caterpillars are 10,000 times heavier than when hatched and are ready to begin spinning a cocoon. A straw frame is placed over the tray of caterpillars, and each caterpillar begins spinning a cocoon. Two glands produce liquid silk and force it through openings in the head called spinnerets. Liquid silk is coated in sericin, a water-soluble protective gum, and solidifies on contact with the air. Within 2–3 days, the caterpillar spins about 1 mile of filament and is completely encased in a cocoon. The silk farmers then kill most caterpillars by heat, leaving some to metamorphose into moths to breed the next generation of caterpillars. Harvested cocoons are then soaked in boiling water to soften the sericin holding the silk fibers together in a cocoon shape. The fibers are then unwound to produce a continuous thread. Since a single thread is too fine and fragile for commercial use, anywhere from three to ten strands are spun together to form a single thread of silk.

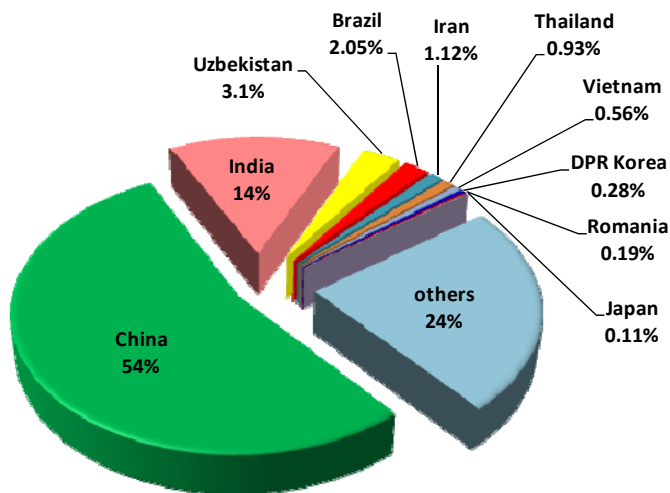


Figure 5. World Silk production [84].

4. COTTON

The English name of cotton derives from the Arabic *al-qutn* (قطن), which began to be used circa 1400 A.D. The cotton plant has always thrived in the wild and is member of Malvaceae, the marsh mallow family. There are about 40 species of wild cotton plants. By contrast, the historical origin of its commercial exploitation, particularly with regard to textile uses, is fuzzier. Relevant literary references point to two distinct geographical origins of cultivated cotton, namely; Asia and pre-Columbian America. In India, cotton was spun as early as 3200 B.C. as revealed by fragments of cloth found at the Mohenjo-Daro archaeological site on the banks of the River Indus and also as indicated by some finds in tombs and there is a Hindu hymn written around 1400 B.C. describes the fabrication of cotton yarn and the weaving of cotton cloth. From India, cotton textiles probably passed to Mesopotamia, where the trade started around 600 years B.C. [86, 87].

Cotton has been spun, woven, and dyed since prehistoric times. It clothed the people of ancient India, Egypt, and China. Hundreds of years before the Christian era, cotton textiles were woven in India with matchless skill, and their use spread to the Mediterranean countries. In the first century, Arab traders brought fine muslin and calico to Italy and Spain. The Moors introduced the cultivation of cotton into Spain in the 9th century. Fustians and dimities were woven there and in the 14th century in Venice and Milan, at first with a linen warp. Before the 15th century, little cotton cloth was imported to England, although small amounts were obtained chiefly for candlewicks. By the 17th century, the East India Company was bringing rare fabrics from India. Native Americans skillfully spun and wove cotton into fine garments and dyed tapestries. Cotton fabrics found in Peruvian tombs are said to belong to a pre-Inca culture.

There is evidence to suggest that trade in cotton started around Rome at the time of Alexander the Great, in the 4th century B.C. On the other hand, the Egyptians have started the cultivation of cotton at about 600–700 A.D. and from Egypt cotton spread to the Greek mainland and to the Romans. The trade flourished after the discovery of the maritime route passing by the Cape of Good Hope and the establishment of trading posts in India. Portuguese trading prominence in this part of the world had been challenged by other European countries (notably, France and England) since 1698. In England, the first cotton-spinning factory opened its doors in Manchester in 1641 (Table 3) [88]. Today, cotton fibers are used to make clothing, bed-sheets, towels, yarn, fishnets, tents, and innumerable other items, and the seed is used to produce cottonseed oil.

The advent of the Industrial Revolution in Britain provided a great boost to cotton manufacture, as textiles emerged as Britain's leading export. In 1738, Lewis Paul and John Wyatt, of Birmingham, England, patented the roller spinning machine, and the flyer-and-bobbin system for drawing cotton to a more even thickness using two sets of rollers that traveled at different speeds. Later, the invention of the spinning jenny in 1764 and Richard Arkwright's spinning frame (based on the roller spinning machine) in 1769 enabled British weavers to produce cotton yarn and cloth at much higher rates. From the late 18th century onwards, the British city of Manchester acquired the nickname "Cottonopolis" due to the cotton industry's omnipresence within the city, and Manchester's role as the heart of the global cotton trade. Production capacity in Britain and the United States was further improved by the invention of the cotton gin by the American Eli Whitney in 1793. Improving

technology and increasing control of world markets allowed British traders to develop a commercial chain in which raw cotton fibers were (at first) purchased from colonial plantations, processed into cotton cloth in the mills of Lancashire, and then exported on British ships to captive colonial markets in West Africa, India, and China (via Shanghai and Hong Kong) [1, 89-95].

Table 3. History of old cotton-spinning

Invented	Date	Inventor, Country
First cotton-spinning factory	1641	England
First flying shuttle	1733	Kay
Patented the roller spinning machine	1738	Paul and Wyatt, UK
First spinning wheel operating several spindles (spinning-Jenny)	1764	Hargreaves
Water-powered machine to draw out and turn the cotton thread (water-frame)	1767	Arkwright
Enabled British weavers to produce cotton yarn and cloth at much higher rates	1769	England
Invention of the cotton gin	1793	Eli Whitney, USA
Automatic weaving loom endowed with a chain of cards with holes punched in. The loom could weave several patterns	1805	Jacquard

4.1. Cotton Plant Species and Cottonseed Composition

Cotton is a natural fiber of vegetable origin, like linen, jute or hemp and mostly composed of 95 % cellulose (a carbohydrate plant substance, Figure 6). Cotton formed by twisted, ribbon-like shaped fibers and it is the fruit of a shrubby plant commonly referred to as the "cotton plant". The cotton plant, a variety of plants of the genus *Gossypium*, belongs to the Malvaceae family, which approximately comprises 1,500 species, also including the baobab tree, the *bombax* or the mallow. The plant, growing up to 10 m high in the wild, has been domesticated to range between 1 to 2 m under commercial cultivation in order to facilitate picking. Either herbaceous or ligneous, it thrives in dry tropical and subtropical areas. Whereas by nature the plant is a perennial tree (lasting about 10 years), under extensive cultivation it is mostly grown as an annual shrub. The cotton flower has five large petals (showy, white, white-creamy, or even rose in color), which soon fall off, leaving capsules, or "cotton bolls", having a thick and rigid external layer. The capsule bursts open upon maturity, revealing the seeds and masses of white-creamy and downy fibers. Cotton fibers of the *Gossypium hirsutum* species range from about 2 to 3 cm in length, whereas *Gossypium barbadense* cotton produces long-staple fibers up to 5 cm length. Their surface is finely indented, and they become kinked together and interlocked. The cotton plant is almost exclusively cultivated for its oleaginous seeds and for the seminal fibers growing from them (i.e. cotton, strictly speaking). In ordinary usage, the term "cotton" also makes reference to fibers that are made into fabric wires suitable for use in the textile industry [1, 96].

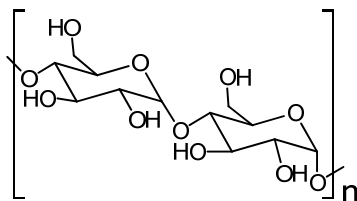


Figure 6. Cellulose structure.

Cotton plants have about 50 species in general (included 40 species of wild cotton) and only four species are domestically cultivated for their fibers. The most commonly cultivated species of cotton in the world include *Gossypium barbadense* of Peruvian origin, *Gossypium arboreum* (which originated in the Indo-Pakistan subcontinent), *Gossypium herbaceum* (from southern Africa) and *Gossypium hirsutum* originated in Mexico. The later species is the most important agricultural cotton, accounting for more than 90% of world fiber production, while *Gossypium barbadense* accounts for about 5% of world fiber. It includes cotton fibers of the highest quality, such as the Jumel variety (from the Barbados), among the finest cotton in terms of quality and fiber length. The remaining two species of cotton have short staple-length fiber with no commercial value per second (only 5% of world production all-together) [97-101].

4.2. Cultivation of Cotton

Cotton is a warm climate crop primarily grown at temperatures between 11 and 25°C in dry tropical and subtropical climates, and threatened by heat or freezing temperatures (below 5°C or above 25°C), although its resistance varies from species to species. Excessive exposure to dryness or moisture at latest two months from the plant growing may be harmful to cotton quality and yields, and in some cases might also kill the plant. The cotton seeds should be planted in well-prepared moist soil with high nutrient supplying capacity. Certainly, the cotton plant is particularly weak and its moisture and nutrient uptake is significant [102, 103]. Cotton production tends to weaken the soil, which may require some soil management practices typically by means of physical adjustments, fertilization, and crop rotation such as culture of leguminous plant and one of cereal. Furthermore, the root system of the cotton plant is particularly developed and penetrates downward deeply which sometimes led to double the height of its stem. Therefore, cotton should be planted in rich seedbeds that are muddy or argillaceous-sandy, where the taproot would grow downward deeply and develop under favorable conditions. Seedling appearance can occur between one to four weeks after planting. During germination, appearance and seedling growth of cotton plant, it needs warm temperature and 7,000 to 9,000 m³/ha water supplied by nature or by means of irrigation [102, 104]. Cotton leaves length and width are about 12-15 cm and develop along the main stem in a spiral arrangement. Each new leaf commonly develops 5 to 8 cm above the preceding leaf. Cotton flowering generally starts six to eight weeks after the crop is planted and continues regularly for several weeks, even months, depending on growing conditions. After flowering, the inner part of the bloom gradually develops into a fruit (cotton's boll), which keep growing until full size (2 to 3 cm width). It is required about

two months after first flower blooming to reach the first opening of the bolls. Cotton bolls burst open upon maturity, revealing soft masses of fibers [105, 106]. Cotton harvesting is then possible, the relevant timeframe is detailed in the Table 4 [88].

The cotton soft masses of fibers are picked either manually or mechanically. Manual picking is time-consuming task, a very labor intensive and may be rather expensive but it generally produces quality lint with limited amount of trash. Cotton is harvested mechanically by cotton pickers or strippers, which remove all the cotton bolls and are generally used after application of a defoliant. Mechanical harvesting is faster than the manual picking of cotton but it collected unwanted leaves and twigs with the cotton soft fibers. Therefore, cotton picked by a stripper might thus need sorting of the trash in order to obtain quality lint. After the cotton is picked it is transported to a cotton gin to separate the cotton fibers (lint) from the cottonseeds and the cotton lint is then compacted in bales and stored. Although irrigated cotton farming tends to be more expensive than "dry land" cotton (which relies on rainfall), it generally produces higher quality lint with greater uniformity and yield potential. Furthermore, the maturation period tends to be shorter than for dry land cotton [107-109].

Although the cotton plant is native to tropical countries, cotton production is not limited to the tropics. Indeed, the emergence of new varieties, as well as advances in cultivation techniques led to the expansion of its culture within an area straddling from approximately 47 degrees North latitude (Ukraine) to 32 degrees South (Australia). Although cotton is widely planted in both hemispheres, it remains a sun-loving plant highly vulnerable to freezing temperatures. Cotton is crucially important to several developing countries. Out of the 65 cotton-producing countries in 2007/08, 52 were developing countries, 21 of which were indexed by the United Nations among the least developed countries (LDCs) (Table 5) [88].

Cotton is of utmost importance for developing countries, particularly in West and Central Africa, where around 10 million people depend on the sector for their revenues. Besides being a major natural fiber crop, cotton also provides edible oil and seed by-products for livestock food. Cottonseed oil is a vegetable oil countering of about 4% of world consumption of vegetable oil and ranking fifth in world use among edible oils. The cottonseed meal is usually used as roughage in the diet of cattle for its high energetic and proteinic value.

4.3. Genetically Modified Cotton

Genetically modified cotton (GMC) was developed to reduce the heavy reliance on pesticides. The bacterium *Bacillus thuringiensis* naturally produces a chemical harmful only to a small fraction of insects, most notably the larvae of moths and butterflies, beetles, and flies, and harmless to other forms of life. Inserting the gene coding of *B. thuringiensis* toxin into cotton seeds led cotton plant to produce the above natural insecticide in its tissues. In many regions, the main pests in commercial cotton are lepidopteran larvae, which are killed by the *B. thuringiensis* protein in the transgenic cotton they eat. This reduces the need to use large amounts of broad-spectrum insecticides to kill lepidopteran pests. This releases natural insect predators in the farm ecology and further contributes to non-insecticide pest management. However, *B. thuringiensis* cotton is ineffective against many cotton pests, such as plant bugs, stink bugs, and aphides; depending on circumstances it may still be desirable to use insecticides against these [110-116].

Table 4. Planting and harvesting times for cotton, by producing country

[illegible]

	Jan	Feb	Mar	Apr	May	Jun	Jul	Aug	Sept	Oct	Nov	Dec
Brazil Center												
Brazil North East												
Paraguay												
United States												
Europe and other Countries												
Greece												
Turkey												
Australia												
	Planting period											
	Harvest time											

Table 5. Cotton-growing countries by geographical area

Geographical area	Developed countries	Developing countries			Total
		LDCs	Transition	Other	
Africa		18		9	27
North and Central America	1			1	2
South America				8	8
Caribbean				1	1
Asia	1	3	6	12	22
Europe	3		1		4
Oceania	1				1
Total	6	21	7	31	65

A study done by Chinese researchers at the Center for Chinese Agricultural Policy and the Chinese Academy of Science in 2006 on *B. thuringiensis* cotton farming in China found that after seven years these secondary pests that were normally controlled by pesticide had increased, necessitating the use of pesticides at similar levels to non *B. thuringiensis* cotton and causing less profit for farmers because of the extra expense of GM seeds. However a more recent study in 2009 by the Chinese Academy of Sciences, Stanford University and Rutgers University refutes this. They concluded that the GM cotton effectively controlled bollworm. The secondary pests were mostly plant bugs (miridae) whose increase was related to local temperature and rainfall and only continued to increase in half of the studied villages. Furthermore, the increase in insecticide use for the control of these secondary insects was far smaller than the reduction in total insecticide use due to *B. thuringiensis* cotton adoption [117-119].

Cotton has also been genetically modified for resistance to glyphosate (marketed as Roundup in North America), an inexpensive and highly effective, but broad-spectrum herbicide. Originally, it was only possible to achieve glyphosate resistance when the plant was young, but with the development of Roundup Ready Flex, it is possible to achieve glyphosate resistance much later in the growing season [120-122].

GMC is widely used throughout the world, with claims of requiring up to 80% less pesticide than ordinary cotton. The International Service for the Acquisition of Agri-biotech Applications (ISAAA) said that, worldwide, GMC was planted on an area of 16 million hectares in 2009 (<http://www.isaaa.org/>). This was 49% of the worldwide total area planted in cotton. The U.S.A. cotton crop was 93% GMC in 2010 and the Chinese cotton crop was 68% GMC in 2009. The initial introduction of GMC proved to be a huge success in Australia - the yields were equivalent to the no transgenic varieties and the crop used much less pesticide to produce (85% reduction). The subsequent introduction of a second variety of GMC led to increases in GMC production until 95% of the Australian cotton crop was GMC in 2009.

In India, GMC cultivation continues to grow at a rapid rate, increasing from 50,000 hectares in 2002 to 8.4 million hectares in 2009. The total cotton area in India was 9.6 million hectares (the largest in the world or, about 35% of world cotton area), so GMC was grown on 87% of the cotton area in 2009. This makes India the country with the largest area of GMC in the world, surpassing China (3.7 million hectares in 2009). The major reasons for this increase are a combination of increased farm income and a reduction in pesticide use to control the cotton bollworm. Cotton has gossypol, a toxin that makes it inedible. However,

scientists have silenced the gene that produces the toxin, making it a potential food crop [113, 114, 123].

4.4. Organic Cotton

Organic cotton is generally understood as cotton, from plants not genetically modified, that is certified to be grown without the use of any synthetic agricultural chemicals, such as fertilizers or pesticides. Its production also promotes and enhances biodiversity and biological cycles. Organic cotton is used to manufacture everything from handkerchiefs to kimono robes. Different levels of certification exist, but at a minimum, a crop must be grown in soil that has been chemical-free for at least three years [124-126].

United States cotton plantations are required to enforce the National Organic Program (NOP). This institution determines the allowed practices for pest control, growing, fertilizing, and handling of organic crops. As of 2007, 265,517 bales of organic cotton were produced in 24 countries, and worldwide production was growing at a rate of more than 50% per year.

In 2003, Ibrahim Abouleisch and the SEKEM (the most important grower of organic cotton in Egypt) initiative were awarded the alternative Nobel Prize for their activities in sustainable development. The prize was awarded in recognition of their development of organic cultivation methods. Apart from eco-textiles made from Egyptian cotton, SEKEM also produces herbal teas and organic foodstuffs. The initiative was particularly praised for its work in the field of fair trade, the income from which is used to finance Kindergarten, Waldorf Schools and soon, a free University (<http://www.pan-germany.org/download/africaprojects.pdf>).

4.5. Production of Cotton

Cotton remained a fairly minor crop until the invention of the cotton gin in 1793 by American inventor Eli Whitney. The cotton gin was a simple machine that removed the cotton fiber from the seeds so that part of the work no longer had to be done by hand. This led to a great reduction in the amount of labor and therefore the cost of producing cotton. About the same time new machines were being developed, especially in England, which likewise reduced the cost of spinning the fiber into thread and weaving it into cloth. This led to a tremendous increase in the amount of land used for cotton cultivation in the American South [127]. In 1850, cotton accounted for just over half the value of all goods exported from the United States [128]. From 1850 to 1860, the value of the American cotton crop doubled and was ten times the value of the tobacco crop, which had been the main cash crop of the South in the century before [128].

Since the early 1960s, the world annual yield production of cotton seed has increased in a constant manner with an annual average 2.2%. Therefore the seed cotton yields were rose from 0.86 t/ha in 1960 to 2.14 t/ha in 2007. During the 1960-1980, however, seed cotton yields in developed countries were on average 2.5 times more than those of developing countries. In 2005, the gap between developed and developing countries in seed cotton yields has been narrowed to a ratio of 1.4 times, which can be attributed to improved yields in China, mainly as a result of investment in research and innovation. Cotton fiber yields have

also followed the same path of seed cotton yields. Over 1960-2007 period, world average of fiber output per hectare was grown from 0.3 to 0.8 tons and a world average around 0.86 t/ha is forecasted for 2012/13 by International Cotton Advisory Committee (ICAC). In the period 1990-2006, the five largest producers by order of importance were China, USA, India, Pakistan and Uzbekistan. Since the beginning of the 2000s, China recorded higher yields per hectare compared to the other countries with an average of 3.5 tons per hectare for seed cotton (almost 2.5 times of the American yield over the period) and 1.1 t/ha for cotton fiber compared to 0.82 t/ha for the United States) [1].

Indian cotton seed yields have dramatically increased since 2002, the average yield from 2003 to 2007 jumped by more than 50% compared to its level over the previous period (1990-2002). Indian ginning output is particularly high compared to other major producing countries (Table 6). In regard to United States, second world producing country with 11.1 million tons of cottonseed since the beginning of the 2000s, productivity rate is far above world average yields (+16% above the world yield since the beginning of the decade). Despite this pretty high level, American yields per hectare are remaining far below the ones recorded by China (-14%) or Uzbekistan (-32%) for instance [1].

While a large number of African countries remain heavily dependent on cotton, cotton production in Africa is not significant on a global scale. For example, cotton accounts for 60% of foreign exchange earnings in Benin. West African countries reported approximately 1.1 t/ha cotton yield during the period between 1990 and 2007. Recently the cotton yield production in African countries have been improved by about +15% in 2000s compared to the average of the 1990s years, but globally remain below the ones of other producing countries. However, cotton production and productivity levels vary considerably among African countries, for example yield in Chad is 0.6 t/ha compared to 1.95 t/ha in Niger and 2.4 t/ha in Egypt, which deserves special consideration that is to say, Egypt produced per hectare more than double the cotton of the average West African countries. Indeed, production and productivity levels were remarkably higher in Egypt than in any other African cotton producing country. Egypt produces nearly 740,000 tons of cotton over the period 1990-2007 that about a fifth of the African production. This performance originates in the fact that cotton is grown under irrigation in Egypt, a way of cultivation that is generally not used in West Africa [1].

4.6. Competition between Cotton and Synthetic Fibers

In the 1890s, the manufactured fibers era started with the development of rayon in France. Rayon is derived from natural cellulose by extensive processing in a manufacturing process, which produces the less expensive replacement of more naturally derived materials. Acetate in fiber form was developed in 1924. A succession of new synthetic fibers was introduced by the chemicals industry in the following decades. The first fiber synthesized entirely from petrochemicals was Nylon, which introduced as a sewing thread by DuPont in 1936 and followed in 1944 by DuPont's acrylic [129]. Some clothes were created from Nylon and acrylic fibers, such as women's hosiery from nylon, but it was not effective on the cotton marketplace until the introduction of polyester into the fiber marketplace in the early 1950s, which strongly affected the cotton marketplace. The rapid uses of polyester clothes in the 1960s caused economic hardship in cotton-exporting economies between 1950 and 1965.

Cotton production recovered in the 1970s, but crashed to pre-1960 levels in the early 1990s. Beginning as a self-help program in the mid-1960s, the Cotton Research and Promotion Program (CRPP) was organized by U.S. cotton producers in response to cotton's steady decline in market share. At that time, producers voted to set up a per-bale assessment system to fund the program, with built-in safeguards to protect their investments. With the passage of the Cotton Research and Promotion Act of 1966, the program joined forces and began battling synthetic competitors and re-establishing markets for cotton. Today, the success of this program has made cotton the best-selling fiber in the U.S. and one of the best-selling fibers in the world [8, 130].

Table 6. Cotton yield in some countries during 1990-2007

Year	1990-2000			2000-2006			2007		
Country	SCY (t/ha)	CFY (t/ha)	GO (%)	SCY (t/ha)	CFY (t/ha)	GO (%)	SCY (t/ha)	CFY (t/ha)	GO (%)
China	2.61	0.84	32	3.95	1.28	32	4.21	1.29	31
Uzbekistan	2.41	0.79	33	2.61	0.85	33	2.28	0.82	36
India	0.71	0.30	42	0.99	0.43	44	1.02	0.52	51
United States	1.88	0.72	39	2.50	0.93	37	2.82	0.91	32
Pakistan	1.73	0.57	33	2.22	0.73	33	1.99	0.67	34
Africa	1.03	0.41	40	1.19	0.39	33	0.99	0.35	35
World	1.63	0.57	35	1.93	0.69	36	1.73	0.62	36

SCY: Seed cotton yields; CFY: Cotton fiber yields; GO%: Ginning output (%); t: tons; ha: hectare.

The African data analysis draws on figures for nine francophone African countries: Benin, Burkina Faso Cameroon, Centrafrican republic, Chad, Côte d'Ivoire, Mali, Senegal, Togo, Madagascar, and Niger.

4.7. Uses of Cotton

The cotton fiber is made primarily into yarns and threads for use in the textile and apparel sectors. The major end uses for cotton fiber include wearing apparel (approximately 60% of cotton consumption), home furnishings such as draperies (eventually the third major end use) or professional garments (about 5% of cotton fiber demand), and other industrial uses such as medical supplies and hygienic uses. Most notably, the fiber is used to manufacture hydrophile cotton (cotton wool), compress, gauze bandages, tampons or sanitary towels, and cotton swabs. The first medical use of cotton wool was by Dr. J. S. Gamgee at the Queen's Hospital (later the General Hospital) in Birmingham, England. In this field, the most suitable cotton variety is the species *Gossypium herbaceum* with short-staple thick fibers. Cotton is used to make a number of textile products. These include terrycloth for highly absorbent bath towels and robes; denim for blue jeans; chambray, popularly used in the manufacture of blue work shirts (from which we get the term "bluecollar"); and corduroy, seersucker, and cotton twill. Socks, underwear, and most T-shirts are made from cotton. Bed sheets often are made from cotton. Cotton also is used to make yarn used in crochet and knitting. Fabric also can be made from recycled or recovered cotton that otherwise would be

thrown away during the spinning, weaving, or cutting process. While many fabrics are made completely of cotton, some materials blend cotton with other fibers, including rayon and synthetic fibers such as polyester (Figure 7 and 8). It can either be used in knitted or woven fabrics, as it can be blended with elastane to make a stretchier thread for knitted fabrics, and apparel such as stretch jeans [131].

Besides traditional uses and as a result of different finishing processes that have been applied to the cotton fiber, cotton is made into specialty materials suitable for a great variety of uses. Cotton fabrics with specialty applications such as flame resistant apparel (chemical treated cotton), which is suitable for professional uses and provides effective protection against potential risks associated with high temperature and particularly flashover. Cotton without chemical treatment would burn up releasing very strong heat, just like the major part of synthetic fibers, which melt when they are exposed to high temperatures. Fire hoses were once made of cotton [132-138]. In addition to the textile industry, cotton is used in fishnets, coffee filters, tents, gunpowder (see nitrocellulose), cotton paper, and in bookbinding. The first Chinese paper was made of cotton fiber [1].

The cottonseed which remains after the cotton is ginned is used to produce cottonseed oil, which, after refining, can be consumed by humans like any other vegetable oil (Table 7). The cottonseed meal that is left generally is fed to ruminant livestock; the gossypol remaining in the meal is toxic to monogastric animals. Cottonseed hulls can be added to dairy cattle rations for roughage. During the American slavery period, cotton root bark was used in folk remedies as an abortifacient, that is, to induce a miscarriage [139-143].

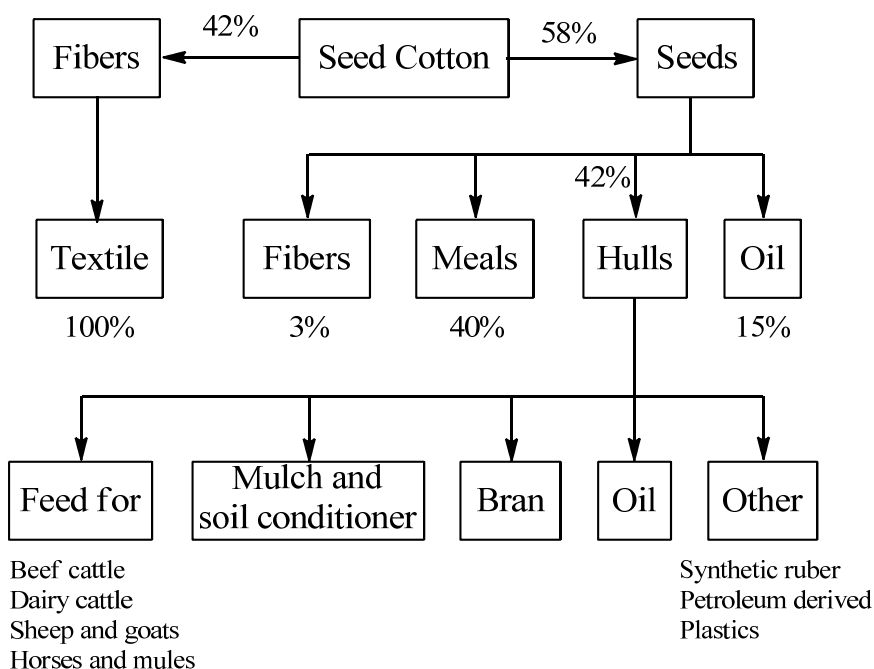


Figure 7. Products derived from seed cotton.

Table 7. Cottonseed composition

Content	Whole seed	Oil-meal (deoiled and partially peeled)	Oilcake expeller (partially peeled)	Hull
Dry matter (%)	92	90	93	92
Proteins (%) MS	22 (19-25)	42 (35-53)	40 (28-49)	5 (3-7)
Rough cellulose (%) MS	28 (23-37)	18 (11-23)	15 (11-23)	53 (49-62)
Fatty matter (%) MS	20 (10-28)	3 (0.4-6)	7 (4-11)	3 (0.6-5)
Ashes (%) MS	4	7	7	3
Calcium (%) MS	0.2	0.3	0.2	0.15
Phosphorus (%) MS	0.6	1.3	1.2	0.19

Cotton linters are fine, silky fibers which adhere to the seeds of the cotton plant after ginning. These curly fibers typically are less than 1/8 in (3 mm) long. The term also may apply to the longer textile fiber staple lint as well as the shorter fuzzy fibers from some upland species. Linters are traditionally used in the manufacture of paper and as a raw material in the manufacture of cellulose. In the UK, linters are referred to as "cotton wool". This can also be a refined product (absorbent cotton in U.S. usage) which has medical, cosmetic and many other practical uses (Figure 8) [1].

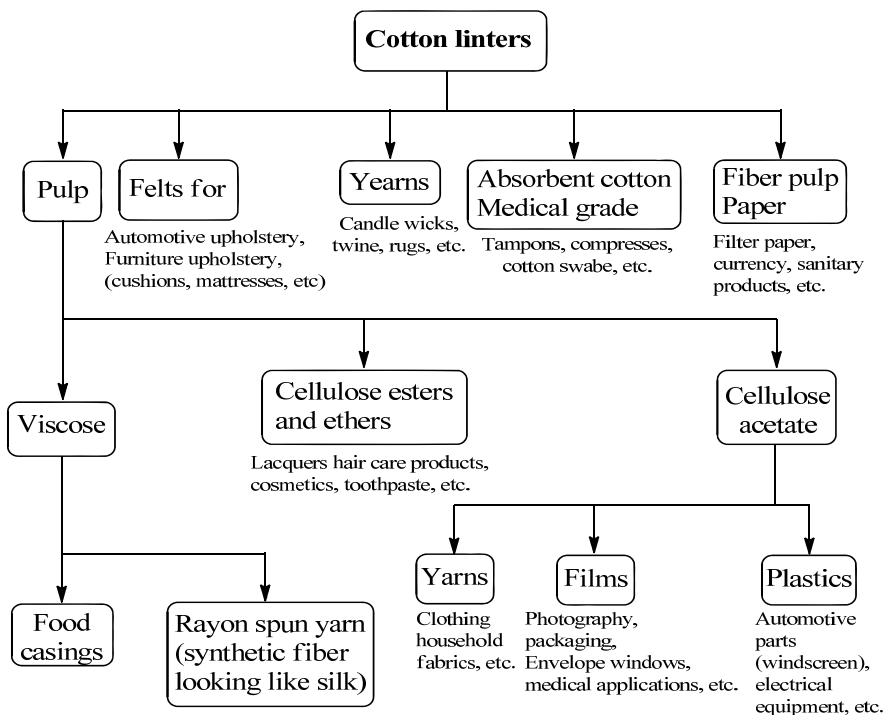


Figure 8. Major uses of cotton linters.

Shiny cotton is a processed version of the fiber that can be made into cloth resembling satin for shirts and suits. However, it is hydrophobic (does not absorb water easily), which makes it unfit for use in bath and dish towels.

The term “Egyptian cotton” refers to the extra long staple cotton grown in Egypt and favored for the luxury and up-market brands worldwide. During the U.S. Civil War, with heavy European investments, Egyptian-grown cotton became a major alternate source for British textile mills. Egyptian cotton is more durable and softer than American Pima cotton (that is grown in the southwestern states of the U.S.A.), which is why it is more expensive.

4.8. Cotton Pests and Diseases

The principal cause of cotton yield losses, which is about 15% of world annual production, is cotton insects [144-146]. More than 1300 different species of insect pests attack the crop. Among the most common and endogenous species found in cotton fields are:

- I. The pink bollworm (*Pectinophora gossypiella*) was first described in 1843 by W.W. Saunders as *Depressaria gossypiella*, from specimens found to be damaged cotton in India in 1842. The pink worm withdraws nutrients from the inside of the cottonseed and may cause serious yield losses. Although the most severe infestations have occurred in Africa and India, the pink bollworm has been recorded in nearly all cotton-producing countries and is a key pest in many of these areas. Infestations may be reduced by the heating of cottonseeds at about 55°C, as well as by other management tactics, including plantation treatment and destruction of the infested crop [147-151].
- II. The boll weevil (*Anthonomus grandis*), also known as bollworm, is most common in American cotton plantations [152-155].
- III. The Egyptian (spiny) bollworm (*Earias insulana*) and the red bollworm (*Diparopsis castanea*) feed on the developing cotton bolls [156-158].
- IV. Cotton stainers (*Dysdercus superstitionis*) attack maturing cotton bolls and seeds. They may cause the staining of the lint. In addition, feeding wounds may allow the entry to the boll of saprophytic fungi (organisms which draw nutrients from the host, but do not harm it, contrary to parasites) [159, 160].
- V. Other insect pests of cotton, such as the white flies (*Bemisia tabaci*), may adversely affect lint quality and yield potential [161, 162]. They suck sap from leaves and pose the most serious threat in India and Africa.
- VI. The cotton aphid (*Aphis gossypii*), also known as the melon aphid, infests the cotton seedlings. Cotton aphids are among the most injuring insects found in cotton. They suck sap from leaves and secrete honeydew (Liquid excretions of Homoptera, consisting largely of sugars and amino acids. Honeydew causes a scorching of leaves, the photosynthetic activity of which is reduced by the presence of sooty moulds) on the undersides of leaves. Honeydew secretions may burn the leaves and interfere with photosynthesis. In addition, aphid is a vector of viruses and a carrier of other insects. In Africa, aphid infestations are among the most injuring insect pests in terms of economic yield lost [163-166].

VII. Nematodes: There are approximately 128 species of nematodes associated with cotton. Five parasitic forms pose the most serious threat to the crop, including the *Meloidogyne incognita* (or root knot nematode) and the *Rotylenchulus reniformis* (or reniform nematode) [167]. These two species can become serious pests (in the United States, particularly in the State of Virginia, they accounted for 99% of the damage caused by cotton parasitic nematodes). These parasites live in the soil (the root knot nematode favors rough and Sandy “arenaceous” soil) and withdraw nutrients from the plant roots. Symptom patterns associated with nematodes include stunting, potassic deficiency or early maturity. Nematodes can reduce yields (in Alabama, United States, yield losses are estimated to average 10% or 20%, but can peak to 50% in arenaceous dry soil). Also, depending upon the stage of development of the infested crop, they can hamper the quality of cotton. Root knot nematodes do produce plant damage symptoms that are rather easy to recognize, such as the yellowing or whitening of normally green plant tissue because of a decreased amount of chlorophyll. Damage symptoms caused by other kinds of nematodes (for example, the reniform nematode) are more difficult to detect, since they are generally small and sparse. Besides the direct damage, nematodes are also an important factor in the incidence of Fusarium and other wilts of cotton. Nematodes may be controlled by cultural practices, such as crop rotations, soil tilling, and use of resistant varieties, or by chemical treatment through nematicides. The two types of nematodes seldom coexist in the same fields [164, 168].

4.9. Most Common Diseases in the Cotton Plant

- I. Bacterial blight of cotton, also called angular leaf spot (*Xanthomonas malvacearum*) is favored by wet weather (temp. >25°C and humidity >85%). Disease incidence is higher in plants with injured tissues (due to insect pests or cold temperatures). The disease causes stunting and yellowing of the leaves (mainly lower leaves). As diseases progresses, it may result in defoliation. Affected bolls are smaller than normal and exhibit small black spots on their surface. Bolls may fail to open or produce bad quality lint [169-171].
- II. Boll rot (*Diplodia gossyina*, *Colletotrichum* spp., *Fusarium* spp.) attacks lower bolls near maturity. Warm, humid conditions favor the disease. Affected bolls are dark brown, with a white to salmon-pink overgrowth. The fungus is capable of giving a brownish tint to the lint. This disease is a stress-related one, in the sense that it infects plants that have been previously damaged by insect pests. Management practices include seed treatment, as well as the use of resistant varieties [172].
- III. The *Verticillium dahliae*, a common soil inhabitant, penetrates through roots and grow up along the stem tissue. The fungus is favored by cooler temperatures, excessive soil moisture and excessive soil nitrogen levels. Symptoms first appear on the lower leaves, which turn yellow. Larger plants are stunted (as diseases progresses, defoliation may occur), whereas younger seedlings may die. Management strategies include proper management of irrigation and the selection of resistant varieties. Under conditions favorable to the development of the disease, yield reductions of up to 30% are possible [173-175].

- IV. Seedling diseases (fungi *Rhizoctonia solani*, *Pythium* spp.) cause seed and root rotting. In the case of *Rhizoctonia solani*, girdling of the stem at ground level is observed. *Pythium* spp. is characterized by the similar symptom patterns, with a water soaked lesion at the soil line [176-179].
- V. *Fusarium* wilt (*Fusarium oxysporum*, *F. vasinfectum*) was first discovered in the United States in 1892, in Egypt ten years later. Wet weather conditions (temperature above 23°C and relative humidity exceeding 85%) are particularly conducive to disease development. Disease incidence can be higher in plants with injured tissues (for example, plants damaged by nematodes). Plants can be affected by the disease at any stage during the season. The vascular tissue of infected plants exhibits a brown/chocolate discoloration through the main stem. Infected water-conducting stem tissues become inactive, causing wilted foliage. Plant death, wilting, yellowing and defoliation are typical of disease symptoms. Leaves turn yellow between veins and eventually shed to leave bare stems. Once the fungus has colonized the plant (diagnosis is confirmed by splitting the stem to reveal dark brown), it most likely causes the death of the host. There is no commercially viable way to eradicate the disease once established (apart from soil fumigation, which is excessively expensive). The impact of the disease may nonetheless be reduced by the use of varieties with high levels of resistance to *Fusarium* wilt, or by avoiding crop stresses such as over-irrigation and over-application of nitrogen. *Fusarium* wilt is now an important constraint to sustainable cotton production, especially in Australia [180-185].
- VI. Of all diseases known to occur in cotton, cotton root rot (*Phymatotrichum omnivorum*) is one of the most destructive and difficult to control. The fungus lives in alkaline soils low in organic matter. It occurs only at elevations below 1500 m. The fungus has unique biological characteristics that contribute to management difficulties. First of all, *Phymatotrichum omnivorum* has a remarkably wide host range (infecting over 2300 species alongside cotton), although it attacks only mature plants and does not easily spread from field to field. Second, the fungus survives for long periods of time in the soil (much of the fungus is found as deep as 60 cm to 2 m in soils). This explains why fungicides are not effective treatment. The fungus is only active when air and soil temperatures are high (respectively above 40 and 27°C). When environmental conditions are conducive to its development, the fungus invades the plants through their root system. Infected plants can die in two weeks. The first disease symptom is slight yellowing of the leaves, which then quickly turn to a bronze color and begin to wilt [186-188].

4.10. Consumption of Cotton

World cotton consumption has an average annual growth rate of about 2% since the beginning of the 1940s. The demand growth for cotton was comparatively higher in the 1950s and 1980s, with an average growth rate of 4.6% a year during the 1950s and 3% in the 1980s. Since the end of the Second World War, the developing countries have absorbed much of global cotton output and their share in global consumption has become even more significant since the beginning of 2000s. They accounted for approximately 78% of global cotton

consumption between 1981 and 1999; their ratio has been above 80% since 2000 and the International Cotton Advisory Committee (ICAC) projection figures expected more increase in their consumption to reach 94% in 2012, therefore, they would absorb almost of global cotton output. Cotton consumption has shifted to developing countries mainly as a reflection of rising wage levels in developed countries [189].

In the textile sector, labor accounts for about sixth of production costs. This means that raising labor costs eroded the competitive edge of developed countries, and contributed to the shifting of cotton processing to low-cost economies. Following specialization, certain countries were able to forge new patterns of comparative advantages out of competitive differences in quality. These countries built on the competitiveness and dynamism of the textile sector, which became the foundation stone of their development. Other exogenous factors (such as the development of new technologies and improved infrastructures) favored delocalization of production by multinational companies based in developed countries. The main cotton producing economies also account for a large part of consumption. According to ICAC data, China, the United States, India, and Pakistan as a whole have accounted for approximately more than 55% of global cotton consumption over the period 1980 to 2008. Their overall consumption has risen considerably in volume. For example, consumption in China and India was multiplied by 3 and more than 3, respectively. Pakistan has had the largest increase 6 times in volume between 1980 and 2008 in order to respond to export-driven demand for textiles [189].

5. BAST PLANTS AS A FIBER RESOURCE

Bast fibers or skin fibers have been grown for centuries throughout the world. They are plant fibers collected from the phloem (the "inner bark" or the skin) or bast surrounding the stem of certain plants. They support the conductive cells of the phloem and provide strength to the stem. Bast plants are characterized by long, strong fiber bundles that comprise the outer portion of the stalk [190-193]. The word "*bast*" refers to the outer portion of the stem of these plants. Bast fibers are taken from tall reed like the plants stems. This stringy, vascular portion comprises 10 - 40% of the mass of the stem depending upon the species of bast plant, as well as the particular variety, or cultivar, within a bast plant. The remainder of the stem inside this bast layer is a different type of fibrous material, which has different names depending upon the species selected. This inner material is known as *shives* when referring to flax and sometimes hemp, as *hurd* in the context of hemp, and as *core* when from kenaf. The fibers are cemented together by gums and need to be separated by a decomposing process called *retting*, which can be achieved by water retting (soaking the plants in water) or by dew retting (spreading them out and thus exposing them to the weather) or by chemicals (for instance high pH and chelating agents) or by pectinolytic enzymes. These two methods lead to eventually broken down the gummy substance by microbiological agents, which allow separating the fibers within one to five weeks. Subsequent vigorous mechanical action splits the fibers further apart into even finer *fibrils*, which are soft and fine, that is, hair-like. The longer ones are called *line fibers*. They are particularly suitable for processing into yarns, textiles, and cordage. The shorter pieces are called *tow*. The fibrils of bast consist of a large number of elongated cells whose ends are cemented together.

Most of the technically important bast fibers are obtained from herbs cultivated in agriculture, as for instance flax, hemp, or ramie, but also bast fibers from wild plants, as stinging nettle, and trees such as the *Tilia*, have been used to some extent. Examples for fibers from plants are jute, hemp, flax (linen), ramie, kenaf, kudzu, nettle, okra, paper mulberry, roselle hemp, rattan, and wisteria [190-193]. Since the valuable fibers are located in the phloem, they must often be separated from the xylem material (woody core), and sometimes also from epidermis. Often bast fibers have higher tensile strength than other kinds. Bast fibers are processed for use in rope, paper, burlap, high-quality textiles, carpet yarn, traditional carpets, geotextile (netting or matting), hessian or burlap, paper, sacks, etc. Bast fibers are also used in the non-woven, molding, and composite technology industries for the manufacturing of non-woven mats and carpets, composite boards as furniture materials, automobile door panels and headliners, etc. A special property of bast fibers is that they contain a special structure, the fiber node, which represents a weak point, while seed hairs, such as cotton, do not have nodes (Figure 9). From prehistoric times through at least the early 20th century, bast shoes were woven from bast strips in the forest areas of Eastern Europe. Table 8 compares the chemical composition of these bast plants with that of wood [1, 194-198].



Figure 9. Photo of bast fibers.

Table 8. Comparative chemical composition of some bast fibers

Fibrous material	cellulose	hemi-cellulose	lignin	extractives	ash
Coniferous	48.0	15.0	25.3	11.5	0.2
Deciduous	52.8	21.8	22.3	2.7	0.4
Flax	78.5	9.2	8.5	2.3	1.5
Hemp	68.1	15.1	10.6	3.6	2.5
Kenaf (bast)	60.8	20.3	11.0	3.2	4.7

Bast plants possess the following overall advantages:

- I. High tensile strength in bast portions, especially in fiber varieties,

- II. Bast plants have a relatively low specific gravity of 0.28-0.62, yielding an especially high specific strength, i.e. strength to weight ratio,
- III. Generally high fiber productivity rates, rivaling and even surpassing that of the most commercial tree Species, and
- IV. Potential for even greater productivity, bast portions, and mechanical properties through focused genetic breeding.

Bast plants also have the following overall limitations:

- I. Rotations at least every other year generally required,
- II. Limited research for composite applications in North America,
- III. Lack of related agricultural infrastructure in North America,
- IV. Relatively high absorption of moisture in core portion,
- V. Diminished board properties when using core for particleboard,
- VI. Difficulty in handling long fiber bundle lengths for processing, and
- VII. Difficulty in applying binder to long fiber bundle lengths.

Bast fibers Applications:

- I. Reinforcing fibers to other materials such as concrete, wood, or straw,
- II. Pultrusion products,
- III. Reinforcements for thermoplastics,
- IV. Insulation, and
- V. Additional proprietary pursuits.

Nevertheless, certain potential applications of the core material are possible. These include:

- I. Low-density insulation boards,
- II. Ceiling tiles,
- III. Substrate for lightweight furniture,
- IV. Components in manufactured housing,
- V. Office partitions,
- VI. Core materials for doors, and
- VII. Possibly particleboard and MDF.

5.1. Hemp

Hemp (from Old English *hænep*) is the name of the soft, durable fiber that is cultivated from plants of the *Cannabis* genus. Hemp is also a name for the *Cannabis* plant. Fibers retrieved from hemp plants likewise played an important role in early civilizations because of their usefulness for clothing, cordage, storage and shelter (e.g., tents). Hemp was first grown in Southeast Asia and in approximately 4500 B.C. transferred to China. There are some records indicate that hemp was presumably the oldest cultivated plant for fiber applications

purpose. It was originally grown for its fiber, and then around 900 BC also became known for its narcotic qualities. Hemp is a notable bast fiber crop has typically about 14% bast portion. In modern times, hemp has been used for industrial purposes including paper, textiles, biodegradable plastics, construction, health food, fuel, and medical purposes with modest commercial success. Hemp is a strong, durable, though harsh bast or phloem fiber, having a core which is characteristic of hardwood fiber. Hemp is an annual plant which at maturity develops a rigid, woody stem ranging in height from 1.2 – 5.0 m, and having a diameter from 4 to 20 mm [199, 200]. Production of hemp is restricted in some countries, where the plant is confused with marijuana. Optimum yield of hemp fiber is more than 2 t/ha, while average yields are around 650 kg/ha.

Cannabis sativa L. subsp. *sativa* var. *sativa* is the variety grown for industrial use, while *C. sativa* subsp. *indica* generally has poor fiber quality and is primarily used for production of recreational and medicinal drugs. The major difference between the two types of plants is the appearance and the amount of Δ^9 -tetrahydrocannabinol (THC) secreted in a resinous mixture by epidermal hairs called glandular trichomes, although they can also be distinguished genetically [201]. Oilseed and fiber varieties of *Cannabis* approved for industrial hemp production produce only minute amounts of this psychoactive drug, not enough for any physical or psychological effects. Typically, hemp contains below 0.3% THC, while cultivars of *Cannabis* grown for marijuana can contain anywhere from 6 to over 20% THC [202].

China is the world leading producer of hemp with smaller production in Europe, Chile and the Democratic People's Republic of Korea [203]. While more hemp is exported to the United States than to any other country, the United States Government does not consistently distinguish between marijuana and the non-psychoactive *Cannabis* used for industrial and commercial purposes [202].

Effectively all of Western Europe, including The United Kingdom, France, The Netherlands, and Germany, as well as Australia, have legalized low THC varieties of hemp to be grown for industrial purposes. THC is the drug producing substance found in traditional varieties of hemp. Beginning in 1998, Canada has now legalized the growth of hemp for commercial production and processing. The legalization of the production of industrial hemp is proceeding in several state legislatures in the United States at this time. Industrial hemp that contains only non-leafy material is currently allowed in all of the states for industrial processing.

Data suggests that hemp once had higher yields than those common today. Hemp is a vital part of the cordage industry throughout the world over a century ago. In recent decades, the United States and Canada are well noted for their ability to develop high levels of production of agricultural crops relative to the rest of the world. Limited energies by genetic agricultural research organizations in North America have thus far been applied to enhancing the productivity of hemp. With a concerted effort from the North American agricultural research community, it is reasonable to conclude yields substantially greater than those present in Hungary can be achieved in 4 - 10 years of genetic development. Hemp shows the following strengths:

- I. Hemp requires lesser moisture to grow than kenaf.
- II. Hemp's fiber-bundles are stronger and tougher than those of kenaf, generally comparable to varieties of flax, and most other known fiber species.
- III. Hemp is generally pest resistant, drought resistant, and light frost resistant.

- IV. With proper leaf removal, hemp has low net nutrient requirements and requires minimal cultivation.
- V. Hemp provides greater fiber yields in areas generally north of the 40th latitude than most other fiber crops, generally surpassing flax by 10%.

Hemp also has the following weaknesses:

- I. Restrictions of its growth and cultivation in North America, especially in the United States.
- II. Lower fiber yields than kenaf and other tropical species in the warmer portions of the United States and more southerly regions.
- III. Lower bast fiber portions relative to kenaf and flax.

5.1.1. Hemp Fiber

The fiber is one of the most valuable parts of the hemp plant. It is commonly called bast, which refers to the fibers that grow on the outside of the woody interior of the plant's stalk, and under the outer most part (the bark). Bast fibers give the plants strength. Hemp fibers can be between approximately 0.91 and 4.6 m long, running the length of the plant. Depending on the processing used to remove the fiber from the stem, the hemp may naturally be creamy white, brown, gray, black or green. Hemp was a popular fiber before the industrial revolution because it is strong and grows quickly; it produces roughly 10% more fiber than cotton or flax when grown on the same land. Hemp has been used to make paper. It was often used to make sail *canvas*, and the word canvas derives from *Cannabis* [204]. Abaca, or "Manila hemp", a relative of the banana plant, replaced its use for rope. Burlap, made from jute, took over the sacking market. The paper industry began using wood pulp. The carpet industry switched over to wool, sisal, and jute, then nylon. Netting and webbing applications were taken over by cotton and synthetics.

5.1.2. Uses of Hemp

Hemp plant is used for a wide variety of purposes. It has been used for centuries to make rope, canvas and paper. Long hemp fibers can be spun and woven to make crisp, linen-like fabric used in clothing, home furnishing textiles and floor coverings. In China, hemp is de-gummed for processing on flax or cotton machinery. Blending with cotton, linen, silk and wool gives hemp a softer feel, while adding resistance and durability to the product. In Europe, hemp fibers are mainly used in the special paper industry - thanks to lower lignin content, it can be pulped using fewer chemicals than wood. Hemp fibers are also used to reinforce molded thermoplastics in the automobile industry. The short core fibers go into insulation products, fiberboard and erosion control mats, while the fibrous core can be blended with lime to make strong, lightweight concrete [203].

In the United States an estimated 50,000 products can be produced from hemp including the manufacture of cordage of varying tensile strength, everlasting clothing, and nutritional products. The bast fibers can be used in 100% hemp products, but are commonly blended with other organic fibers such as flax, cotton or silk, for apparel and furnishings, most commonly at a 55%/45% hemp/cotton blend. The inner two fibers of hemp are woodier, and are often more used in non-woven items and other industrial applications, such as mulch,

animal bedding and litter. The oil from the fruits ("seeds") oxidizes (commonly, though inaccurately, called "drying") to become solid on exposure to air, similar to linseed oil, and is sometimes used in the manufacture of oil-based paints, in creams as a moisturizing agent, for cooking, and in plastics. Hemp seeds have been used in bird seed mix as well [205]. Hempseed is also used as fishing bait [206, 207].

Hemp seeds contain all the essential amino acids and essential fatty acids necessary to Tables maintain healthy human life (Tables 9 and 10). The seeds can be eaten raw, ground into a meal, sprouted, made into hemp milk (akin to soy milk), prepared as tea, and used in baking. The fresh leaves can also be eaten in salads. Products include cereals, frozen waffles, hemp tofu, and nut butters, to name a few. A few companies produce value added hemp seed items that include the seed oils, whole hemp grain (which is sterilized by law), dehulled hemp seed (the whole seed without the mineral rich outer shell), hemp flour, hemp cake (a by-product of pressing the seed for oil) and hemp protein powder. Hemp Seed appears on the UK market as a legal food product, and cultivation licenses are available for this purpose. In North America, hemp seed food products are sold, typically in health food stores or through mail order [208-212].

Table 9. Typical nutritional analysis of shelled hempseed

Nutritional	Amount	Nutritional	Amount
Arachidic 20:0	0.28%	PeroxideValue	<2 meq/Kg
Ash	6.6%	Polyunsaturated fat	36.2%
Calcium	74 mg	Protein (Nx5.46)	30.6%
Calories/100 g	567 kcal	Pseudomonas	<10/ g
Carbohydrate	10.9%	Riboflavin (Vit B2)	0.33 mg/100 g
Coliforms	<10/g	Salmonella	neg in 25 g
Dietary fiber	6.0	Saturated fat	5.2%
Fat	47.2%	Sodium	9.0 mg/100 g
Fructose	0.47%	Standard Plate Count	4000/g
Linoleic 18:2 (Omega-6)	27.6%	Stearic 18:0	1.46%
Gamma-Linolenic 18:3 (Omega-6)	0.8	Sucrose	1.24%
Glucose	0.30%	Sugars	1.99%
Iron	4.7 mg/100 g	Tetrahyrocannabinol	neg in 60 mg
Lactose	<0.1%	Thiamine (Vit B1)	1.38 mg/100 g
Linolenic 18:3 (Omega-3)	8.68%	Total Dietary fiber	6.0%
Maltose	<0.1%	Vitamin A (B-Carotene)	4 IU/100 g
Monounsaturated fat	5.8%	Vitamin B6	0.12 mg/100 g
Moisture	4.7%	Vitamin C	1.0 mg /100 g
Oleic 18:1 (Omega-9)	5.8%	Vitamin D	2277.5 IU/100 g
Molds	30/g	Vitamin E (dl-A-Tocopherol)	8.96 IU/100 g
Palmitic 16:0	3.44%	Yeast	<10/g

Source: <http://www.wcranchohemp.com/info.php>.

Approximately 44% of the weight of hempseed is healthy edible oils (Figure 10), containing about 80% essential fatty acids (EFAs); i.e., linoleic acid, omega-6 (LA, 55%), alpha-linolenic acid, omega-3 (ALA, 22%), in addition to gamma-linolenic acid, omega-6 (GLA, 1–4%) and stearidonic acid, omega-3 (SDA, 0–2%). Protein is the other major component (33%), second only to soy (35%), but more easily digestible because it's primarily globular proteins, 33% albumin and 65% edestin (a Greek word meaning edible) (Tables 9 and 10). Its amino acid profile is close to complete when compared to more common sources of proteins such as meat, milk, eggs and soy. The proportions of linoleic acid and alpha-linolenic acid in one tablespoon (15 ml) per day of hemp oil easily provides human daily requirements for EFAs. Unlike flaxseed oil, hemp oil can be used continuously without developing a deficiency or other imbalance of EFAs. This has been demonstrated in a clinical study, where the daily ingestion of flaxseed oil decreased the endogenous production of GLA [213].

Hempseed is an adequate source of dietary fiber, calcium and iron, and contains antioxidants and chlorophyll. Whole hempseeds are also a good source of phosphorus, magnesium, zinc, copper and manganese. Hempseed is usually very safe for those unable to tolerate nuts, gluten, lactose, and sugar [210, 212].

Table 10. Amino acid assay of shelled hempseed

Amino acid	% amount	Amino acid	% amount
Alanine	1.22%	Proline	1.43%
Arginine	3.35%	Serine	1.60%
Aspartic acid	2.97%	Threonine	1.03%
Cystine/cysteine	0.39%	Tryptophan	0.39%
Glutamic acid	5.31%	Tyrosine	1.04%
Glycine	1.21%	Valine	1.42%
Histidine	0.90%	Meth + cys	0.96%
Isoleucine	1.14%	Phen + tyr	2.19%
Leucine	1.88%		
Lysine	0.91%	Protein Digestibility	0.93
Methionine	0.57%	PDCAAS	0.46
Phenylalanine	1.14%	PER	1.87

Source: <http://www.wcranchohemp.com/info.php>.

5.2. Flax

Flax (linseed) is a bast fiber that is an annual plant which grows in the north and south temperate zones where the soil is fertile and sandy, and the weather is cool and damp during the summer. Flax is any plant of the genus *Linum* in the family Linaceae, especially *L. usitatissimum*, a slender, erect, annual plant having narrow, lance-shaped leaves and blue flowers, cultivated for its fiber and seedmes. Flax, *Linum usitatissimum*, is one of the bast fibers grown in temperate regions. Flax plants range in height from 30 to 120 cm, and have shallow taproots, with slender stems and slender lanceolate glaucous green leaves, which have 20–40 mm long and 3 mm broad. The flowers are pure pale blue, 15–25 mm diameter,

with five petals; they can also be bright red. The fruit is a round, dry capsule 5–9 mm diameter, containing several glossy brown seeds shaped like an apple pip, 4–7 mm long. Flax fibers are amongst the oldest fiber crops in the world. The use of flax for the production of linen goes back at least to ancient Egyptian times. Dyed flax fibers found in a cave in Dzudzuana (prehistoric Georgia) have been dated to 30,000 years ago [214, 215]. Flax is native to the region extending from the eastern Mediterranean to India and was probably first domesticated in the Fertile Crescent. Flax was extensively cultivated in ancient Ethiopia and ancient Egypt [216]. Pictures on tombs and temple walls at Thebes depict flowering flax plants. The use of flax fiber in the manufacturing of cloth in northern Europe dates back to Neolithic times. In North America, flax was introduced by the Puritans. Currently most flax produced in the USA and Canada is seed flax types for the production of linseed oil or flax seeds for human nutrition.

New Zealand flax is not related to flax but was named after it, as both plants are used to produce fibers. Flax has been cultivated for nearly 8,000 B.C., and it was probably cultivated in Egypt before 3400 B.C., at which time the art of spinning and weaving linen was already well developed [217, 218]. Woven wool and flax fabrics were found at the sites of the “Swiss lake dwellers” dating back to the seventh and sixth centuries B.C., and was grown in North America as early as 1626 A.C. With the invention of the cotton gin in 1793 A.C., cotton became an inexpensive substitute, and largely displaced flax as a fiber source in the United States and Canada. Afterward, flax has been cultivated in North America primarily for its seed.

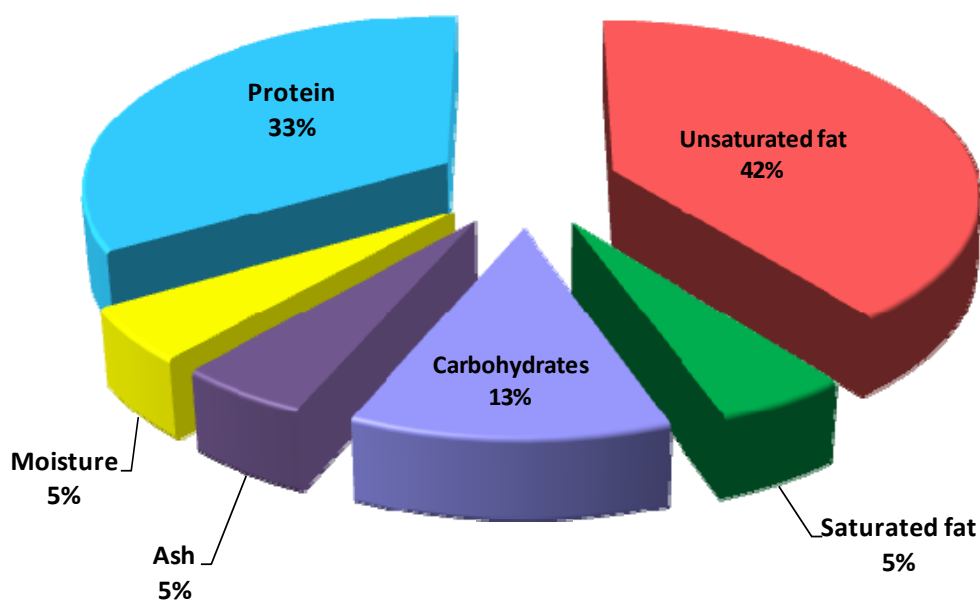


Figure 10. Typical Composition of hempseed.

5.2.1. Flax Fiber

Textile flax often has a relative high percentage of its stem that is bast fiber, up to 40%. Flax fiber is extracted from the bast or skin of the stem of the flax plant. Water retting (retting is the process of rotting away the inner stalk, leaving the outer fibers intact) yields the best linen (the fabric made from flax) and takes about 8–14 days, whereas dew retting (2–5 weeks) yields lesser qualities. The subsequent *scutching* mechanically crushes the retted stems into small pieces called *shives*, which are then beaten for separation. The long fibers (30–90 cm long and 0.05–0.5 mm in diameter) are used for fine textiles. The shorter pieces, which constitute one-third of the fiber yield, are used for coarse yarn, cordage, and shoe-stitching threads. Linen is characterized by high water absorption, pronounced swelling when wet, high strength, and low stretch. A new textile hybrid, *Heiya 8*, has been developed which has a stem yield of 6.5 t/ha and is drought resistant [219]. This indicates that certain varieties of flax when grown for textile can produce moderate yields. Decorticated textile bast fiber demonstrates exceptional mechanical properties including high tensile strength as well as a large proportion of bast material.

An estimated 12 million hectares grow textile flax, while 500,000 hectares are cultivated for the oil-seed variety [220]. This crop has a specific gravity of 0.32 - 0.68, somewhat greater than jute and hemp, but comparable to bagasse. In light of nutrient requirements, flax can only be grown once every five years on a particular acreage, [190]. Textile flax is primarily grown in Europe and the major flax-producing countries are western part of Belgium, The Netherlands, and Luxembourg. Virtually all the flax grown in North America is for seed-oil. Argentina, India, The Commonwealth of Independent States, and China also grow flax for oil-seed, [221]. Saskatchewan and Manitoba are the primary regions that grow flax in North America, although Alberta, North Dakota, and South Dakota grow flax as well. Over two million acres are grown in Canada, with lesser amounts grown in the United States. Of this 26% (65,000 tons) are used for pulp in specialty applications such as cigarette papers. Oil-seed flax is somewhat distinctive from the other temperate bast fibers, kenaf and hemp, on several different fronts. First, the diameter of the stalk of the oil seed flax is much less than kenaf or hemp, making the flax stalks much more slender. Secondly, the bast fiber yields per acre are also considerably lower than other bast varieties, generally reaching only 1,000 - 1,500 bone dry pounds per acre [220].

Flax fiber is soft, lustrous and flexible; bundles of fiber have the appearance of blonde hair, hence the description "flaxen". It is stronger than cotton fiber but less elastic. The best grades are used for linen fabrics such as damasks, lace and sheeting. Coarser grades are used for the manufacturing of twine and rope. Flax fiber is also a raw material for the high-quality paper industry for the use of printed banknotes and rolling paper for cigarettes and tea bags. Flax mills for spinning flaxen yarn were invented by John Kendrew and Thomas Porthouse of Darlington in 1787 [217].

5.2.2. Flax Seed

Flax seeds have two basic varieties, first are brown seeds and second are yellow or golden seeds, which are in most types, have similar nutritional characteristics and equal amounts of short-chain omega-3 fatty acids. Yellow flax seed called *solin* (trade name *Linola*) is the only exception type, which has a completely different oil profile and is very low in omega-3 fatty acids. Although brown seed can be consumed as readily as yellow seed, and has been for thousands of years, it is better known as an ingredient in paints, fiber and cattle

feed. Flax seeds produce a vegetable oil known as flaxseed or linseed oil, which is one of the oldest commercial oils, and solvent-processed flax seed oil has been used for centuries as a drying oil in painting and varnishing [206, 222-224].

One hundred grams of ground flax seed supplies about 450 kilocalories, 41 grams of fat, 28 grams of fiber, and 20 grams of protein. Flax seeds contain high levels of dietary fiber including lignans, an abundance of micronutrients and omega-3 fatty acids (Table 11). Flax seeds are chemically stable while whole and milled flax seed can be stored at least 4 months at room temperature with minimal or no changes in taste, smell, or chemical markers of rancidity, which can start with its seed coat becoming bitter.

Flax seeds may lower cholesterol levels, especially in women [225] and Initial studies suggest that flax seeds may benefit individuals with certain types of breast [226, 227] and prostate tumors [228]. Flax may also lessen the severity of diabetes by stabilizing blood-sugar levels [229].

Table 11. Nutritional in 100 g of flaxseed or linseed oil

Nutritional	Nutritional value per 100 g	Recommendations % of USA for adults
Energy	2234 kJ (534 kcal)	
Calcium	255 mg	26
Carbohydrates	28.88 g	
Dietary fiber	27.3 g	
Fat	42.16 g	
Iron	5.73 mg	46
Magnesium	392 mg	106
Niacin (Vit. B3)	3.08 mg	21
Pantothenic acid (B5)	0.985 mg	20
Phosphorus	642 mg	92
Potassium	813 mg	17
Protein	18.29 g	
Riboflavin (Vit. B2)	0.161 mg	11
Sugars	1.55 g	
Thiamine (Vit. B1)	1.644 mg	126
Vitamin B6	0.473 mg	36
Vitamin C	0.6 mg	1
Zinc	4.34 mg	43

Source: USDA Nutrient database (<http://www.nal.usda.gov/fnic/foodcomp/search/>).

5.2.3. Cultivation and Harvesting of Flax

The major flax producing countries are Canada (~34%), China (~25.5%), India (~9%), USA (~8%) and Ethiopia (~3.5%) and throughout Europe (Figure 11). Most of the United States crop is from the states of North Dakota, South Dakota, Minnesota, and Montana, where the soils are most suitable for flax, besides the alluvial kind, are deep loams, and containing a large proportion of organic matter. However, farming flax requires few fertilizers and pesticides. On the other hand, heavy clays as all soils of a gravelly or dry sandy nature are unsuitable for flax production. Flax plant will reach 10–15 cm in height within first 8 weeks

of sowing followed by growing several centimeters per day under its optimal growth conditions, reaching 70–80 cm within fifteen days. Flax may be harvested for fiber production after approximately 100 days of sowing, 30 days after the plant flowers or two weeks after the seed capsules form. The base of the plant will begin to turn yellow. If the plant is still green the seed will not be useful, and the fiber will be underdeveloped. The fiber degrades once the plant is brown [230-232].

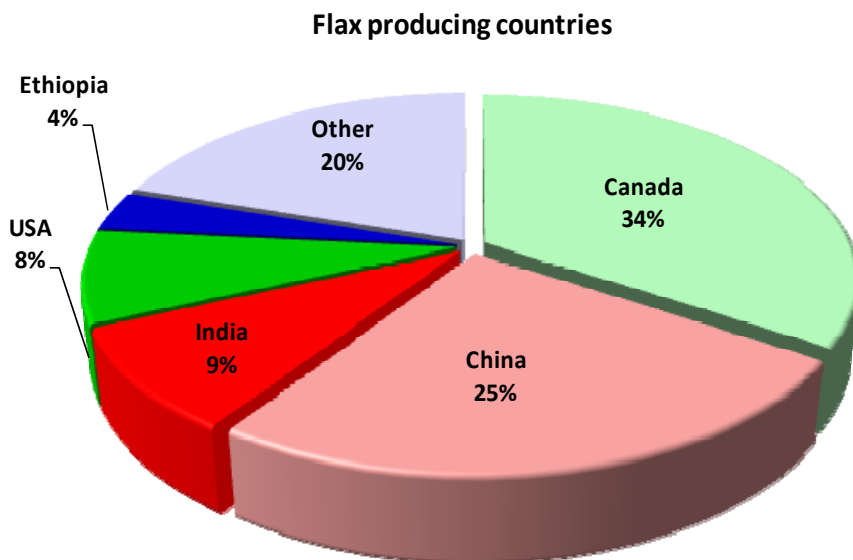


Figure 11. Flax producing countries.

5.2.4. Retting Flax

Flax is retted in a stream, pond, field or a tank. The retting is complete when the bundles of flax feel soft and slimy, and quite a few fibers are standing out from the stalks. When retted flax is wrapped around a finger the inner woody part springs away from the fibers. The fastest retting is pond retting and it consists of placing the flax in a pool of water. It generally takes place in a shallow pool, which will warm up dramatically in the sun; the process may take from a couple days to a couple weeks but it produced lower quality flax, possibly because the product can become dirty, and easily over-retted, damaging the fiber. Pond flax retting also produces quite an odor. Another retting is stream, which is similar to pool retting, but the flax is submerged in bundles in a stream or river. This generally takes two or three weeks longer than pond retting, but it produced less dirty flax and does not produce bad smell and it is less likely to be over-retted. However, both Pond and Stream retting were traditionally used less because they pollute the waters used for the process [233]. Field retting is laying the flax out in a large field, and allowing dew to collect on it, which is generally considered to provide the highest quality flax fibers and the least water pollution but it takes a month or more to complete retting. Retting can also be done any type of water tight container such as plastic, wood, concrete, or earthenware. However, metal containers cannot be used because the retting process produced acid, which would corrode the metal. The retting process takes 4 or 5 days when the water temperature is kept at 80°F. Currently 'enzymatic' retting of flax is being researched as a retting technique to engineer fibers with specific properties [234, 235].

5.2.5. Uses of Flax

Flax is grown both for its seeds and fibers since it has two general markets, first group grown for its textile, and a second group grown for its seed (Table 11). The use of flax for heavier grade purposes, such as canvas and towelling, has declined in recent times and its main use now is for finer fabric yarns including blending with wool and synthetic materials. Lower grades are also used in the paper industry such as cigarette paper manufacture; as well as in the automobile industry and for insulation purposes. Various parts of the plant have been used to make dye, medicines, fishing nets, hair gels, and soap. Flax seed is converted to linseed oil for paints and other industrial products, with a smaller but growing portion converted into linseed meal and oil as a health supplement [236-241]. The same species is used for both fiber and seed, with breeding of specialized cultivars for the two different products. The seed-producing varieties have shorter stems and are heavily branched. The fiber varieties pursue stem development resulting in a taller plant more sparsely branched. Flax is also grown as an ornamental plant in gardens.

The flax husks are often used as feed for chickens and other livestock. The seeds provide animals with much needed fiber and protein. Eggs from chickens that were fed flax seeds are often purported to be high in omega fatty acids and have added health benefits [242, 243].

5.3. Kenaf

Kenaf, *Hibiscus cannabinus* [244], originating from Africa, has traditionally been a source of bast fiber in India, China, The Commonwealth of Independent States, Iran, Nigeria, and Thailand. Kenaf is a member of the Malvaceae family, and may grow 2.4 to 6.0 m in height and is generally unbranched in thick stands. Kenaf is a newer crop to the United States that shows good potential as a raw material for use in composite products. In 1965, the areas of adaptation without supplementary water supply were low-elevations sections of North Carolina, South Carolina, Georgia, Florida, Alabama, Mississippi, Louisiana, and eastern Texas. Excellent yield potentials should exist in warm, dry areas with irrigation, [245]. Currently, around 4,300 acres of kenaf are cultivated in the United States; 2,000 acres are grown in Mississippi, 1,200 acres in Texas, 560 acres in California, with lesser amounts in Louisiana, New Mexico, and Georgia. Traditionally, kenaf has been known as a cordage crop or jute substitute. In 1957, research on kenaf was started in the United States and has continued occasionally since that time [190, 246]. The development in decortication equipments, which separates the core from the bast fiber, combined with fiber shortages has renewed recent interest in kenaf as a fiber source.

No known diseases or insect pests seriously injure kenaf and it is a fast-growing and competitive crop [247-249]. Kenaf chemical weed control is highly advisable in most production areas with exceptions being wide and bedded rows in Florida flat-wood soils. Nutrient requirements for kenaf cultivation are low, with no significant improvement in production yield at nitrogen levels above 33.5 pounds per acre. A growing period of 90 -150 days is needed, with fastest growth at temperatures of 20 - 22°C, and nearly 6000 m³ water per hectare. Growth becomes quite minimal when temperatures reach below 2°C, [245, 250-256].

Kenaf is grown these days as a minor fiber crop in some Asian countries, but also in the US and recently in Southern European countries such as Italy. In the US and Europe a

profitable outlet for the remaining woody core after fiber extraction is important for economical production of the crop. The use of kenaf core as animal bedding material is considered here as potential market outlet. An important aspect for this application is the moisture absorption capacity of the material [252, 256, 257].

The yield of extracted bast fibers is below 1/3 (26 - 35% of dry weight) of that of the kenaf stem weight [258]. Kenaf crop shows potential as a substitute for hardwood species as shortages may become more pronounced in various locales of the Southeast and Mid-South. Kenaf fibers average 2.5 mm in length, very similar to southern pine species, while the core, with lengths of 0.5 mm closely matches that of hardwoods. This composition provides a desirable blend for many pulp and paper applications, spurring continued interest and development, [259-264].

A limiting factor in the production of bast fiber from kenaf is retting, the process by which the fiber is freed from the non-fibrous tissue. A study was made to evaluate the variation in cell wall chemistry with maturity for different cultivars, particularly in relation to lignin and retting [194, 265, 266].

Kenaf possesses the following advantages:

- i. Excellent yields in southern regions. For example, 15 tons/acre were grown at College Station, Texas in research plots, [200]. Actual production yields of 7 -9 bone dry tons/acres can be expected in the warmer regions of Texas.
- ii. Low harvested whole stalk costs in favorable climatic regions such as southern Texas.
- iii. Genetic strains have been developed which yield 35% or greater bast portions. This is a relatively high proportion [267-269].
- iv. Considerable progress has been made in developing nematode resistance in the Texas growing region. Nematode susceptibility has long been an encumbrance to the viability of kenaf development [247, 248, 270].
- v. Is competitive showing favorable weeds control characteristics.
- vi. Is viewed favorably by the U.S. Department of Agriculture (USDA) as a prime candidate for alternative fiber development and has consequently received greater research funding.
- vii. Strong federal political support.

Kenaf also has the following limitations:

- i. Low productivity in cooler climates. Its growing season can be as short as 90 - 120 days, and consequently it will grow in almost any region of North America if sufficient moisture is available. The yields of kenaf in Rosemount, Minnesota, south of the Twin Cities, yielded only 2.5 tons/acre in a research plot, compared to the 15 ton/acre yield in College Station, Texas, [246, 250]. Actual production yields are roughly 60-70% of those in test plots.
- ii. High moisture requirements. 600 mm, (23.6 in) of water is preferable during its growing cycle of 120-150 days, [251, 254].

5.4. Ramie

Ramie (*Boehmeria nivea*) is a flowering plant in the nettle family Urticaceae native to eastern Asia (*Nettles* are between 30-45 species of flowering plants of the genus *Urtica* in the family Urticaceae, with a cosmopolitan though mainly temperate distribution [76, 271-274]. They are mostly herbaceous perennial plants, but some are annual and a few are shrubby. It can be harvested up to 6 times a year and it produces a large number of unbranched stems from underground rhizomes and has a crop life from 6 to 20 years. The bark contains gums and pectin causing the fibers to be useable only after chemical treatment. Most of the species have stinging hairs on the stems and leaves). Ramie is growing to 1–2.5 m tall and its leaves are heart-shaped with 7–15 cm long and 6–12 cm broad, and white on the underside with dense small hairs, which gives it a silvery appearance; unlike nettles, the hairs do not sting. White ramie is the Chinese cultivated plant also called the true ramie or China Grass. Green ramie (*Boehmeria nivea* var. *tenacissima*) is the second type also known as rhea and is believed to have originated in the Malay Peninsula. This type has smaller leaves which are green on the underside, and it appears to be better suited to tropical conditions. Ramie fiber is produced from the stalk of a plant and is processed like linen from flax.

Ramie is one of the oldest textile fibers. It was used in mummy cloths in Egypt during the period 5000 - 3000 B.C., and has been grown in China for many centuries. While ramie fiber has been relatively unknown for garments in the western part of the world, it was used for Chinese burial shrouds over 2000 years ago. Ramie fibers are very fine and silk-like, naturally white, and of high luster (Tables 12). Ramie is now often blended with cotton and resembles fine linen to coarse canvas. Ramie is resistant to bacteria, mildew, and insect attack. It is extremely absorbent, dyes easily, increases in strength when wet, does not shrink, and improves its luster with washing. However, ramie has a low elasticity, lacks resiliency, wrinkles easily, and is stiff and brittle and tends to break when a garment made of it is pressed too sharply [275, 276].

The main producers of ramie today are China, Brazil, Philippines, India, South Korea and Thailand. Only a small percentage of the ramie produced is available on the international market [277]. Japan, Germany, France and the UK are the main importers; the remaining supply is used domestically (in the country in which it is produced).

Ramie fiber is very durable, is pure white in color and has a silky luster. It is reported to have a tensile strength eight times that of cotton and seven times greater than silk. However, other reports claim that the tensile strengths of cotton, flax, hemp and ramie are similar. These discrepancies can be partly attributed to the effects of source of supply, method of processing, the test conditions, temperature and humidity, on the fiber strength. The ultimate fibers are exceptionally long and are claimed to be the longest of vegetable origin, with one report claiming the fibers range up to 580 mm, averaging about 125 mm. For the hand spinner, ramie is treated similar to flax in that it can be either wet or dry spun. A wet spun yarn will produce a smooth softer yarn with high luster, while a dry spun yarn will feel hairier; have lesser luster and a harsher handle. It can readily be blended with other fibers such as wool or silk, although the length of ramie can sometimes cause difficulties.

Table 12. Properties of selected fibers

Fiber	Fineness (den) ^a	Tenacity (g/den)	Tensile St. (MPa)	Elongation (strain) (%)	Color range
Bast Fibers					
Jute	20	3	39	1.5	Creamy white to brown
Flax (Linen)	5	5	66	1.5	White to brown
Hemp	6	4	52	2.0	Light to grayish brown
Ramie (China grass)	5	5	67	4.0	White to grayish brown
Leaf Fibers					
Sisal	290	4	51	3.0	Creamy white to yellowish
Henequen	370	3	39	5.0	Creamy white to reddish brown
Abaca (Manila hemp)	190	5	64	3.0	Creamy white to dark brown
Istle	360	2.5	32	5.0	White to reddish yellow
Seed Fiber					
Cotton	2	2.5	300	8.0	Creamy to grayish, white, brown, purple, blue, red
Animal Fibers					
Wool	4–20	1.5	150	40	Creamy white to brown
Silk	1.0	4	800	20–25	White
Synthetic Fibers					
Nylon	0.5–18	3–10	350–890	15–40	White-transparent
Polyester	0.1–10	3–9	500–1100	11–40	White-transparent

^a denier (den) is the mass in (g) of 9000 m of fiber. The finer the yarn is the smaller the number; St. Strength

The most suitable climate for ramie is one which is warm and humid, with an annual rainfall of at least 1000 mm. Well established plants can tolerate drought and frost, but grow better without. As ramie productivity is high it can rapidly deplete the soil of nutrients.

Ramie is most often blended (common is 55% ramie/45% cotton) with other fibers for its unique strength and absorbency, luster and dye-affinity. When blended with high-quality cotton it offers increased luster, strength and color. When ramie fiber is mixed with wool, it adds lightness and minimizes shrinkage to wool. When ramie fiber is blended with rayon, it offsets the low wet strength of rayon [274, 278-280].

5.4.1. Properties of Ramie Fiber

Ramie is one of the strongest natural fibers and exhibits even greater strength when wet. Ramie fiber has ability to hold shape, reduce wrinkling, and introduce a silky luster to the fabric appearance. Ramie fiber is usually used as a blend with other fibers such as cotton or wool because it is not as durable as other fibers. It is similar to flax in absorbency, density and microscopic appearance. However ramie fiber will not dyed as well as cotton. Ramie fiber is stiff and brittle and will break if folded repeatedly in the same place; it lacks resiliency and is low in elasticity and elongation potential due to its high molecular crystallinity (Figure 12)

[193, 281-283]. The advantages and disadvantages of ramie as a fabric are reported in Table 13.

Table 13. Properties of Ramie fiber

Advantages of Ramie as a Fabric	Disadvantages of Ramie as a Fabric
Resistant to bacteria, mildew, alkalis, rotting, light, insect attack	Low in elasticity
Extremely absorbent and therefore comfortable to wear, especially during warm weather	Low abrasion resistance
Has natural stain resisting ability with ease of stain/soil removal similar to that of linen (and this is better than cotton)	Wrinkles easily (but application of wrinkle-resistant finishes or blending with synthetic fibers can reduce the problem in woven fabrics)
Not harmed by mild acids	Stiff and brittle
Dyes fairly easily	The fiber is high cost which reduces its competitiveness against other textile fibers – this high cost is due to high labor requirement for production, harvesting and decortications
Good wet-fastness in laundering - though dark colors may lose their vibrancy over repeated launderings	There is a need to de-gum the fiber prior to processing
Increases in strength when wet	
Withstands high water temperatures during laundering	
Smooth lustrous appearance improves with washing	
Keeps its shape and does not shrink	
Can be bleached	

Source: <http://www.swicofil.com/products/007ramie.html>.

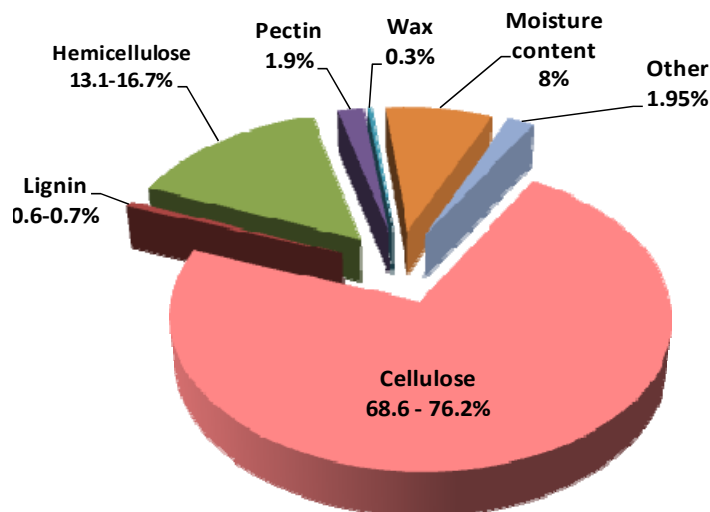


Figure 12. Ramie composition.

5.4.2. Cultivation and Harvesting of Ramie

Ramie is normally harvested two to three times a year but under good growing conditions can be harvested up to six times per year. Ramie requires chemical processing to degum the fiber unlike other bast crops. Harvesting is done just before or soon after the beginning of flowering because at this stage there is a decline in plant growth and the maximum fiber content is achieved. Stems are harvested by either cutting just above the lateral roots or else bending the stem, which enable the core to be broken and the cortex can be stripped from the plant in situ. After harvesting, stems are decorticated while the plants are fresh. If this is not done while the plants are still fresh the plants will dry out and the bark will be hard to remove. The bark ribbon is then dried as quickly as possible to prevent bacteria and fungi from attacking it. The dry weight of harvested stem ranges from 3.4 to 4.5 t/ha/year. 4.5 ton crop yields 1,600 kg/ha/year of dry non-de-gummed fiber, which produced about 1,200 kg of de-gummed fiber (25% loss during degum process) [284].

Ramie fiber is extracted in three stages: Firstly, decortications process, in which the cortex or bark removed either by hand or machine. The second stage involves scraping the cortex to remove most of the outer bark, the parenchyma in the bast layer and some of the gums and pectins. The third stage involves washing, drying and degumming of the residual cortex material to extract the spinnable fiber.

5.4.3. Uses of Ramie

Despite its strength, ramie has had limited acceptance for textile use. The fiber's extraction and cleaning are expensive, chiefly because of the several steps, which involving scraping, pounding, heating, washing, or exposure to chemicals. Some or all are needed to separate the raw fiber from the adhesive gums or resins in which it is unsheathed. Spinning the fiber is made difficult by its brittle quality and low elasticity; and weaving is complicated by the hairy surface of the yarn due to lack of cohesion between the fibers. The greater utilization of ramie depends upon the development of improved processing methods. Ramie fiber is used to make industrial sewing thread, packing materials, fishing nets, and filter cloths. Ramie fiber is also used for household furnishings such as upholstery and canvas and is used in clothing after blended with other textile fibers (for instance when used in admixture with wool, shrinkage is reported to be greatly reduced when compared with pure wool). Shorter ramie fibers and waste are used in paper manufacture. In 2010, Prius and Toyota started using a new range of plant-derived ecological bio-plastics made from the cellulose in wood or grass instead of petroleum. One of the two principal crops used is ramie. Ramie plant is also used as an ornamental plant in Eastern Asia.

5.5. Jute

Jute (*Corchorus capsularis* and *Corchorus olitorius*: the genus *Corchorus* has been classified in the family *Tiliaceae*, or more recently in *Malvaceae*) is vegetable bast fiber plants next to cotton in importance [285, 286]. Jute is one of the most affordable natural fibers and is second only to cotton in amount produced and variety of uses of vegetable fibers. Jute is a long, soft, shiny vegetable fiber that can be spun into coarse, strong threads. Jute fibers are composed primarily of the plant materials cellulose (major component of plant fiber) and

lignin (major components of wood fiber). It is thus a ligno-cellulosic fiber that is partially a textile fiber and partially wood (<http://en.wikipedia.org/wiki/Jute>).

White jute (*Corchorus capsularis*) and Tossa Jute (*Corchorus olitorius*) are usually the trade names of jute [287]. Jute fiber is often called hessian; jute fabrics are also called hessian cloth and jute sacks are called gunny bags in some European countries. The fabric made from jute is popularly known as burlap in North America. Jute fiber is finer and stronger than roselle, which make it better in quality. Depending on demand, price and climate, the production of jute and allied fibers in the world remains around 3 million tons annually. The jute fiber finds its use in the producing as well as in consuming countries in the agricultural, industrial, commercial and domestic fields. Sacking and Hessians (Burlap) constitute the bulk of the manufactured products. Sacking is commonly used as packaging material for various agricultural commodities such as rice, wheat, vegetables, corn, coffee beans etc. Sacking and Hessian Cloth are also used as packing materials in the cement and fertilizer manufacturing industries. Fine Hessian is used as carpet backing and often made into big bags for packaging other fibers such as cotton and wool [288, 289].

Structurally the Jute and Allied Fiber (JAF) stems are composed of epidermis, cortex, large phloem, cambium, wide xylem or wood and central pith tissues. The tissue, phloem, is most important as it is connected with fiber development. It forms a wide zone and is arranged in wedge shaped masses consisting of alternating bands of thick-walled fibers and thin walled tissues of sieve tubes, companion cells and phloem parenchyma. The thick walled fibers of phloem tissue are the fibers which are actually extracted after disintegration of the other associated tissues through retting for commercial use. Since the fibers originate from the phloem tissue, they are also known as phloem or bast fibers.

Jute has been an integral part of culture of Bengal for centuries, in the entire southwest of Bangladesh and some portions of West Bengal. Jute has been called the "Golden Fiber of Bangladesh". In the 19th and early 20th centuries, during the British Raj, much of the raw jute fiber of Bengal was carried off to the United Kingdom, where it was then processed in mills concentrated in Dundee. Initially, due to its texture, it could only be processed by hand until it was discovered in that city that treating it with whale oil, it could be treated by machine. The industry boomed ("jute weaver" was a recognized trade occupation in the 1901 UK census), but this trade had largely ceased by about 1970 due to the appearance of synthetic fibers.

A jute mill landowner in Dundee in the 1800s, Margaret Donnelly, set up the first jute mills in Bengal. In the 1950s and 1960s, when nylon and polythene were rarely used, one of the primary sources of foreign exchange earnings for the erstwhile United Pakistan was the export of jute products, based on jute grown in the East Bengal now Bangladesh. However, the jute industry in general experienced a decline due to increasing of the use of polythene and other synthetic materials as a substitute for jute. Many jute exporters diversified away from jute to other commodities. Jute-related organizations and government bodies were also forced to close, change or downsize. The long decline in demand forced the largest jute mill in the world (Adamjee Jute Mills) to close in Bangladesh [290-292]. Bangladesh's second largest mill, Latif Bawany Jute Mills, formerly owned by businessman, Yahya Bawany, was nationalized by the government (<http://www.bjmc.gov.bd/jutemills-latif.asp>). However, Bangladesh farmers have not completely ceased growing jute mainly due to demand in the internal market. Recently, the jute market recovered and the price of raw jute increased more than 500% between the years 2004-2010 because jute has entered many diverse sectors of industry, where natural fibers are gradually becoming better substitutes. Among these

industries are paper, celluloid products (films), non-woven textiles, composites (pseudo-wood), and geotextile.

5.5.1. Cultivation of Jute

Plain alluvial soil and standing water is needed for jute cultivation as well as warm and wet climate is required for growing jute, which is offered by the monsoon climate during the monsoon season. Temperatures from 20–40°C and relative humidity of 70–80% with 5–8 cm of rainfall weekly and more during the sowing period are favorable for successful jute cultivation [285, 293].

White jute (*Corchorus capsularis*): Several historical documents state that the poor villagers of India used to wear clothes made of jute. Simple handlooms and hand spinning wheels were used by the weavers, who used to spin cotton yarns as well. History also states that, especially Bengalis and some other Indians used ropes and twines made of white jute from ancient times for household and other uses.

Tossa jute (*Corchorus olitorius*) is an Afro-Arabian variety and it is quite popular for its leaves that are used as an ingredient in a mucilaginous potherb called *molokhiya* (ملوخية a word of uncertain etymology), popular in certain Arab countries. The Book of Job in the Hebrew Bible mentions this vegetable potherb as Jew's mallow. Tossa jute fiber is softer, silkier, and stronger than white jute. This variety astonishingly showed good sustainability in the climate of the Ganges Delta. Along with white jute, tossa jute has also been cultivated in the soil of Bengal where it is known as paat from the start of the 19th century. Currently, the Bengal region is the largest global producer of the tossa jute variety.

5.5.2. Production of Jute

India, Bangladesh, China, Thailand, Myanmar and Nepal are the major producing countries of Jute and Allied Fibers (JAF). Together they produce about 95% of the global production of JAF. India and Bangladesh produce mostly jute only about 10% kenaf and roselle in 500,000 hectares, China produces mostly kenaf and only about 10% jute in about 56,000 ha, while in Thailand JAF are cultivated in about 20,000 ha mainly kenaf and roselle. In Tarai belt of Eastern part of Nepal, Jute is grown in about 11000 ha. In India Jute and Kenaf are grown in about 1,000,000 ha. Most of the production comes from the States of West Bengal, Bihar, Assam, Orissa, Andhra Pradesh and Tripura. In Indonesia JAF are grown in 10,000-20,000 ha [290, 291].

Jute is a rain-fed crop with little need for fertilizer or pesticides. The production is concentrated in Bangladesh and some in India, mainly Bengal. The jute fiber comes from the stem and ribbon (outer skin) of the jute plant. The fibers are first extracted by retting. The retting process consists of bundling jute stems together and immersing them in low, running water. There are two types of retting: stem and ribbon. After the retting process, stripping begins. Women and children usually do this job. In the stripping process, non-fibrous matter is scraped off and then the workers dig in and grab the fibers from within the jute stem. India, Pakistan, China are the large buyers of local jute while Britain, Spain, Ivory Coast, Germany and Brazil also import raw jute from Bangladesh. India is the world's largest jute growing country (Figure 13).

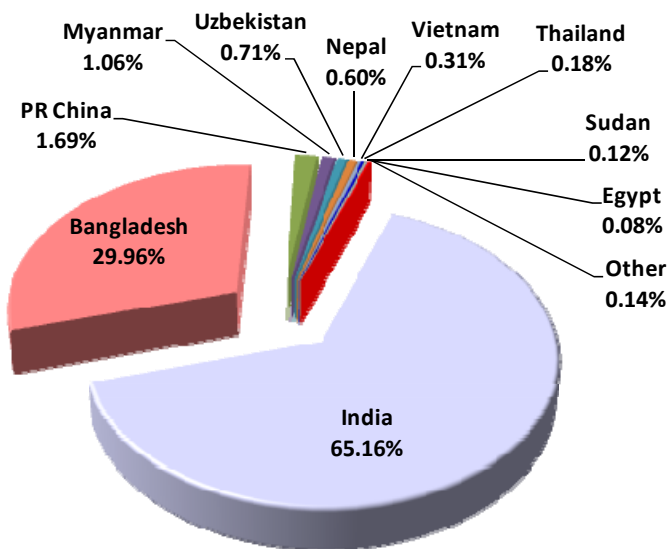


Figure 13. Jute producers in 2008.

5.5.3. Jute Fiber Retting

Retting has been used for a long time in case of extraction of fibers from jute and allied vegetable fiber plants (<http://www.youtube.com/watch?v=fW8NhCAUgLA>). Since the fibers are contained in the bark or the outer skins of stems, either stems or the outer skins called ribbons are retted for extracting the fibers. If the stems are retted, it is called stem retting. If ribbons are retted it is called ribbon retting. Retting is an important step in the production of good quality fiber [294-297].

In general, the practice of retting jute plants in the jute growing regions is to immerse the jute bundles in clear slow flowing water, in canals, rivulets, tanks, ponds or ditches. The minimum ratio of plant material to water in stagnant water should be 1:20. The important conditions for good retting are: *i*) The water should be non-saline and clear; *ii*) The volume of water should be enough to allow jute bundles to float; *iii*) Bundles, when immersed, should not touch the bottom; and *iv*) The same retting tank or ditch should not be used when water becomes dirtier.

5.5.4. Uses of Jute

5.5.4.1. Jute Fiber

Jute is the second most important vegetable fiber after cotton; not only for cultivation, but also for various uses. Jute has many advantages as a home textile, either replacing cotton or blending with it. It is a strong, durable, color and light-fast fiber. Its UV protection, sound and heat insulation, low thermal conduction and anti-static properties make it a wise choice in home décor. Also, fabrics made of jute fibers are carbon dioxide neutral and naturally decomposable. These properties are also why jute can be used in high performance technical textiles [298].

Moreover, jute can be grown in 4–6 months with a huge amount of cellulose being produced from the jute hurd (inner woody core or parenchyma of the jute stem) that can meet most of the wood needs of the world. Jute is the major crop among others that is able to

protect deforestation by industrialization. Thus, jute is the most environment-friendly fiber starting from the seed to expired fiber, as the expired fibers can be recycled more than once. Jute is also used to make ghillie suits, which are used as camouflage and resemble grasses or brush.

Jute is used chiefly to make cloth for wrapping bales of raw cotton, and to make sacks and coarse cloth. The fibers are also woven into curtains, chair coverings, carpets, area rugs, hessian cloth, and backing for linoleum. While jute is being replaced by synthetic materials in many of these uses, some uses take advantage of jute's biodegradable nature, where synthetics would be unsuitable such as containers for planting young trees, which can be planted directly with the container without disturbing the roots, and land restoration where jute cloth prevents erosion occurring while natural vegetation becomes established.

The jute fiber is used alone or blended with other types of fibers to make twine and rope. Jute rope has long been popular in Japan for use in bondage. Jute butts, the coarse ends of the plants, are used to make inexpensive cloth. Conversely, very fine threads of jute can be separated out and made into imitation silk. With increasing concern over forest destruction for the wood pulp used to make most paper, jute fiber is being used to make pulp and paper and the importance of jute for this purpose is increased.

Jute has a long history of use in the sackings, carpets, wrapping fabrics (cotton bale), and construction fabric manufacturing industry. Traditionally jute was used in traditional textile machineries as textile fibers having cellulose (vegetable fiber content) and lignin (wood fiber content). But, the major breakthrough came when the automobile, pulp and paper, and the furniture and bedding industries started to use jute and its allied fibers with their non-woven and composite technology to manufacture nonwovens, technical textiles, and composites. Therefore, jute has changed its textile fiber outlook and steadily heading towards its newer identity, i.e., wood fiber. As a textile fiber, jute has reached its peak from where there is no hope of progress, but as a wood fiber jute has many promising features. Jute can be used to create a number of fabrics such as Hessian cloth, sacking, scrim, carpet backing cloth (CBC), and canvas. Hessian, lighter than sacking, is used for bags, wrappers, wall-coverings, upholstery, and home furnishings. Sacking, a fabric made of heavy jute fibers, has its use in the name. CBC made of jute comes in two types. Primary CBC provides a tufting surface, while secondary CBC is bonded onto the primary backing for an overlay. Jute packaging is used as an eco-friendly substitute. Diversified jute products are becoming more and more valuable to the consumer today. Among these are espadrilles, floor coverings, home textiles, high performance technical textiles, Geotextile, composites, etc.

Jute floor coverings - They consist of woven and tufted and piled carpets. Jute Mats and mattings with 5/6 m width and of continuous length are easily being woven in Southern parts of India, in solid and fancy shades, and in different weaves like, Boucle, Panama, Herringbone, etc. Jute Mats and Rugs are made both through Power-loom and Hand-loom, in large volume from Kerala, India. The traditional Satranji mat is becoming very popular in home décor. Jute non-woven and composites can be used for underlay, linoleum substrate, etc.

Another diversified jute product is Geotextile, which made this agricultural commodity more popular in the agricultural sector [299, 300]. It is a lightly woven fabric made from natural fibers that is used for soil erosion control, seed protection, weed control, and many other agricultural and landscaping uses. The Geotextile can be used more than a year and the bio-degradable jute Geotextile left to rot on the ground keeps the ground cool and it is able to

make the land more fertile [301-306]. Methods such as this could be used to transfer the fertility of the Ganges Delta to the deserts of Sahara or Australia. On the other hand, jute has gained an advantage as being an eco-friendly option instead of poly and paper bags as poly-bag are made from petroleum and are non-biodegradable and manufacturing paper-bags requires large quantities of wood. Jute has none of these problems and is therefore being used widely for these purposes but higher cost is a setback for it. It is also used for making fashion and promotional bags.

5.5.4.2. Jute Leaves

Jute leaves (of Tossa jute: *Corchorus olitorius* L.) are consumed in various parts of the world (Table 14). The Yoruba of Nigeria call it "*ewedu*" and the Hausa people of Nigeria and their Fulbe neighbors call it "*rama*". They use it to produce soup "*taushe*" or boil the leaves and mix it with "*Kuli-kuli*" or groundnut cake and consume the mixture which they call "*kwado*" in Hausa. The Hausa peasant farmers cultivate it beside their corn-stalk constructed homesteads or among their main crops in their farms. There is commercial jute farmers in Northern and South Western Nigeria have a strong National Association registered by the authorities. In Northern Sudan Jute leaves are called "*Khudra*" meaning green in Sudanese Arabic. The Hausa and Fulbe peoples also use jute leaves to treat some diseases. And the Songhay of Mali calls it "*fakohoy*" whereas Tunisians call it *mulukhiyah*. It is made into a common mucilaginous (somewhat "slimy") soup or sauce in some West African cooking traditions, as well as in Egypt, where it is called *mulukhiyya*, Cypriots call it *molocha* - and that refers to food - in terms of fiber this would be unknown - and it is sometimes eaten as boiled vegetable with lemon and olive oil. It is also a popular dish in the northern provinces of the Philippines, where it is known as *saluyot*. Jute leaves are also consumed among the Luyhia people of Western Kenya, where it is commonly known as "*mrenda*" or "*murere*". It is eaten with "*ugali*", which is also a staple for most communities in Kenya. The leaves are rich in beta-carotene, iron, calcium, and Vitamin C. The plant has an antioxidant activity with a significant α -tocopherol equivalent Vitamin E. Diversified byproducts from jute can be used in cosmetics, medicine, paints, and other products [307-310].

Table 14. Jute leaves consumers countries and local name

Place	Local Name
Yoruba of Nigeria	<i>ewedu</i>
Hausa people of Nigeria and their Fulbe neighbors	<i>rama</i>
Northern Sudan	<i>Khudra</i>
Songhay of Mali	<i>fakohoy</i>
Tunisia, Egypt	<i>mulukhiyah</i>
Cypriots	<i>molocha</i>
Luyhia people of Western Kenya	<i>mrenda</i> or <i>murere</i>

5.5.5. Chemistry of Jute

Per 100 g, the leaves are reported to contain 43-58 calories, moisture (80.4-84.1%), protein (4.5-5.6%), fat (0.3%), total carbohydrate (7.6-12.4%), fiber (1.7-2.0%), ash (2.4%),

Ca (0.27-0.37%), phosphorus (97-122 mg), iron (7.2-7.7 mg), sodium (12 mg), potassium (444 mg), β -carotene equivalent (6,410-7,850 μ g), thiamine (0.13-0.15 mg), riboflavin (0.26-0.53 mg), niacin (1.1-1.2 mg), and ascorbic acid (53-80 mg). Leaves contain also oxydase and chlorogenic acid (Table 15). The folic acid content is substantially higher than that of other folacin-rich vegetables, ca 800 μ g per 100 g (ca 75% moisture) or ca 3200 μ g on a zero moisture basis [311]. The seeds contain 11.3-14.8% oil [312], reportedly estrogenic [197, 313], which contains palmitic acid (16.9%), stearic acid (3.7%), behenic acid (1.8%), lignoceic acid (1.1%), oleic acid (9.1%), linoleic acid (62.5%), and linolenic acids (0.9%) as well as large portions of B, Mn, Mo, and Zn (Figure 14).

Table 15. Contents of 100 g of fresh jute leaves
(*Corchorus olitorius* L.)

Reagent	100 g fresh jute leaves	Reagent	100 g fresh jute leaves
ash	2.40%	Phosphorous	0.097-0.122%
beta-carotene	6410-7850 μ g	protein	4.5-5.6%
Calcium	0.266-0.366%	Potassium	444 mg
Energy	43-58 calories	riboflavin	0.26-0.53 mg
fat	0.30%	Sodium	12 mg
fibers	1.7-2.0%	thiamine	0.13-0.15 mg
folic acid	800-3200 μ g	total carbohydrate	7.6-12.4%
Iron	7.2-7.7 mg	Vitamin C	53-80 mg
niacin	1.1-1.2 mg	water	80.4-84.1%

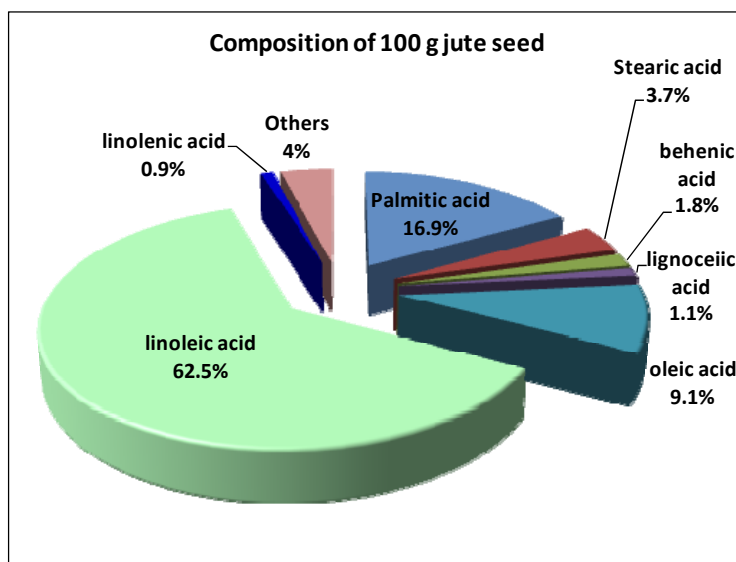


Figure 14. Composition of 100 g of jute seed.

5.5.6. Features of Jute

- i. Jute is the cheapest vegetable fiber procured from the bast or skin of the plant's stem.
- ii. Jute fiber is called The Golden Fiber because it is golden and silky shine natural fiber.
- iii. Jute fiber is environmentally friendly because it is 100% bio-degradable and recyclable.
- iv. Jute fiber is the second most important vegetable fiber after cotton, in terms of usage, global consumption, production, and availability.
- v. Jute fiber is very suitable in agricultural commodity bulk packaging because it has high tensile strength, low extensibility, and ensures better breathability of fabrics.
- vi. Jute fiber helps to make best quality industrial yarn, fabric, net, and sacks. It is one of the most versatile natural fibers that have been used in raw materials for packaging, textiles, non-textile, construction, and agricultural sectors. Bulking of yarn results in a reduced breaking tenacity and an increased breaking extensibility when blended as a ternary blend [314].
- vii. Bengal Delta Plain in the Ganges Delta (most of which is occupied by Bangladesh) is the best source of jute in the world.
- viii. Jute fiber has good insulating, antistatic properties and having low thermal conductivity and moderate moisture regain, as well as jute advantages include acoustic insulating properties and manufacture with no skin irritations.
- ix. Jute has the ability to be blended with other fibers, both synthetic and natural, and accepts cellulosic dye classes such as natural, basic, vat, sulfur, reactive, and pigment dyes [305, 315, 316]. As the demand for natural comfort fibers increases, the demand for jute and other natural fibers that can be blended with cotton will increase. To meet this demand, some manufactures in the natural fiber industry plan to modernize processing. The resulting jute/cotton yarns may produce fabrics with a reduced cost of wet processing treatments [317, 318].
- x. Treating jute fiber with caustic soda improve jute crimp, softness, pliability, and appearance, which aiding in its ability to be spun with wool.
- xi. Treatment of jute fiber with liquid ammonia gave a similar effect of caustic soda on jute fiber, as well as the added characteristic of improving flame resistance when treated with flame-proofing agents.
- xii. Poor durability, crease resistance, brittleness, fiber shedding and yellowing in sunlight are the noted disadvantages of jute fiber. However, preparation of fabrics with castor oil lubricants result in less yellowing and less fabric weight loss, as well as increased dyeing brilliance [319]. Jute fiber has a decreased strength when wet, and also becomes subject to microbial attack in humid climates. Jute can be processed with an enzyme in order to reduce some of its brittleness and stiffness [320]. Once treated with an enzyme, jute shows an affinity to readily accept natural dyes, which can be made from marigold flower extract [321]. In one attempt to dye jute fabric with this extract, bleached fabric was mordant with ferrous sulfate, increasing the fabric's dye uptake value [322]. This process is used for bright and fast colored value-added diversified products made from jute [323].

5.5.7. Effect of Jute on the Environment

In recent times they are found to be a valuable aid to sound environmental management. Because of jute fiber has environment-friendly characteristics, new opportunities on jute is likely to be provided by the worldwide awareness on environment and health. Jute and kenaf have been employed for centuries as packaging materials. The industry interests focus not only on the traditional uses of jute fiber, but also on the production of other value-added products such as, pulp and paper, geotextile, composites and home textiles etc [301, 302, 304, 306, 316].

Jute fiber is biodegradable and its products can be easily disposed without causing environmental hazards. The roots of jute plants play a vital role in increasing the fertility of the soil. By rotating with other crops like rice and potatoes, jute acts as a barrier to pest and diseases for others crops and provides also a substantial amount of nutrients to other crops in the form of organic matter and micronutrients. Jute and kenaf have ecological adaptability, and can be grown on a range of soil types. They have a good tolerance to salinity, water stress and water logging. Agronomically, jute and kenaf have advantages as regards their resistance to climatic extremes, pests and diseases.

Jute plants have high carbon dioxide (CO₂) assimilation rate and it clean the air by consuming large quantities of CO₂, which is the main cause of the greenhouse effect. Theoretically, one hectare of jute plants can consume about 15 tons of CO₂ from atmosphere and release about 11 tons of oxygen in the 100 days of the jute-growing season. Studies also show that the CO₂ assimilation rate of jute is several times higher than that of trees [324].

5.6. Roselle

In Australia, the roselle is known as the *rosella* or *rosella fruit*, which is close relative to *Hibiscus cannabinus*. Roselle, also called rosella, Jamaican sorrel, or java jute, (*Hibiscus sabdariffa*), plant of the hibiscus, or mallow, family (Malvaceae), and its fiber is one of the bast fiber groups. Table 16 reported the common names of roselle in different parts of the world. Roselle is probably native to West Africa and includes *H. sabdariffa* variety *altissima*, grown for fiber, and *H. sabdariffa* variety *sabdariffa* cultivated for the edible external portion of its flower (calyx). The plant, known in the West Indies early in the 16th century, was growing in Asia by the 17th century. Extensive cultivation in the Dutch East Indies (now Indonesia) began in the 1920s under a government-subsidized program established to obtain fiber for sugar-sack manufacture [325-329].

5.6.1. Cultivation of Roselle

Although a perennial, roselle is usually grown as an annual and propagated from seed. It grows best in loamy, well-drained soil, mainly in tropical climates, and requires rainfall averaging about 25 cm each month throughout the growing season. The roselle (*Hibiscus sabdariffa*) is a species of *Hibiscus* native to the Old World tropics, used for the production of bast fiber and as an infusion. It is an annual or perennial herb or woody-based subshrub, growing to 2.0–2.5 m tall. The leaves are deeply three- to five-lobed, 8–15 cm long, arranged alternately on the stems. Stalks and leaves range from dark green to reddish color. The flowers are 8–10 cm in diameter, creamy white to pale yellow with a dark red spot at the base of each petal, and have a stout fleshy calyx at the base, 1–2 cm wide, enlarging to 3–3.5 cm,

fleshy and bright red as the fruit matures. It takes about six months to mature. Plants for fruit crops, more widely spaced, are shorter and many-branched, and their calyxes are picked when plump and fleshy [330-332].

Table 16. Common names of roselle in different parts of the world

Countries	Common name
Australia	<i>rosella</i> or <i>rosella fruit</i>
Jamaica	<i>Rosella, Jamaican sorrel or java jute</i>
Indian subcontinent	<i>meṣṭa/meshta</i>
Assam	<i>Tengamora</i>
Telugu	<i>Gongura</i>
Kannada	<i>Pundi</i>
Mithila	<i>LalChatni</i> or <i>Kutrum</i>
Kerala	<i>Mathipuli</i>
Burma	<i>chin baung</i>
Thailand	<i>krajeab</i>
Senegal, Guinea Bissau, Mali, Burkina Faso, Ghana, Benin and Niger, the Congo and France	<i>bissap</i>
Mali	<i>dah</i> or <i>dah bleni</i>
Gambia	<i>wonjo</i>
western Nigeria	<i>zobo</i>
Yorubas in Nigeria	<i>Isapa</i>
Northern Nigeria	<i>Zoborodo</i>
Iran	<i>Chaye-Torosh</i>
Egypt, Saudi Arabia, and Sudan	<i>karkade</i> (كرکديه)
Namibia	<i>omutete</i>
Caribbean and in Latin America; In certain West Indian islands, Trinidad and Tobago	<i>sorrel</i>
Mexico	<i>'agua de flor de Jamaica</i>
Panama	<i>Saril</i>
Indonesia	<i>rosela</i>
Malaysia	<i>asam paya</i> or <i>asam susur</i>
China	<i>Luo Shen Hua</i> (洛神花)
Zambia	<i>Lumanda, katolo,</i>

For fiber crops, seeds are sown close together, producing plants 3 to 5 m high, with little branching. When buds appear, the stalks are cut and subjected to a retting process followed by stripped of bark or beaten to free the fiber. In some areas retting time is reduced by treating only the bark and its adhering fiber. Roselle fiber is lustrous and moderately strong with color ranging from creamy to silvery white. When grown for its fiber, it is planted closely to produce long stems with little foliage and weeding for the first month of planting is important. Fertilization practices vary widely. Roselle responds favorably to applications of nitrogen, and 45 kg/ha may be a safe level, applied in the form of compost or mineral fertilizer in conjunction with a small quantity of phosphate. Rotations are sometimes used, the

roselle, requiring several months to grow, making the land unavailable for other crops. The practice is recommended since the root-knot nematode, *Heterodera radiculicola*, is a pest. A sequence of a legume green-manure crop, then roselle and then corn is suggested. After germination, seedlings are thinned to stand 1 m apart. For larger plantings, seeds are sown in protected seedbeds and the seedlings transplanted to 1.3–2.6 m apart in rows 2–3.3 m apart. Applications of stable manure or commercial fertilizers are beneficial. Plants are subject to injury by root-knot nematodes and should not be planted on land infested with these pests [333-336].

5.6.2. Uses of Roselle

Primarily, roselle plant is cultivated for the production for fiber from its stem, which may be used as a substitute for jute in making burlap [337]. Roselle is considered to have antihypertensive and Antioxidative properties [338]. Roselle has been used in folk medicine as a diuretic, mild laxative, and treatment for cardiac and nerve diseases and cancer [339]. The red calyces of the plant are increasingly exported to America and Europe (Germany is the main importer), where they are used as food colorings. It can also be found in markets (as flowers or syrup) in some places such as France, where there are Senegalese immigrant communities. In many tropical areas, the red, somewhat acid calyxes of *H. sabdariffa* variety *altissima* are used locally for beverages, sauces, jellies, preserves, and chutneys; the leaves and stalks are consumed as salads or cooked vegetables and used to season curries; and in Africa the oil-containing seeds are eaten. The green leaves are used like a spicy version of spinach. They give flavor to the Senegalese fish and rice dish *thiéboudieune*. Proper records are not kept, but the Senegalese government estimates national production and consumption at 700 tons per year. Also in Myanmar their green leaves are the main ingredient in making chin *baung kyaw curry*. In East Africa, the calyx infusion, called "Sudan tea", is taken to relieve coughs. Roselle juice, with salt, pepper, asafetida and molasses, is taken as a remedy for biliousness. The dried flowers of roselle *Hibiscus cannabinus* can be found in every market.

Traditional medicine uses the heated leaves to cracks in the feet and on boils and ulcers to speed maturation. A lotion made from leaves is used on sores and wounds. The seeds are said to be diuretic and tonic in action and the brownish-yellow seed oil is claimed to heal sores on camels. In India, a decoction of the seeds is given to relieve dysuria, strangury and mild cases of dyspepsia. Brazilians attribute stomachic, emollient and resolute properties to the bitter roots [337].

Roselle *Hibiscus cannabinus* flowers are commonly used to make a sugary herbal tea that is commonly sold on the street in Africa, especially the Sahel. Roselle tea is also quite common in Italy where it spread during the first decades of the 20th century as a typical product of the Italian colonies.

The Carib Brewery Trinidad Limited, a Trinidad and Tobago brewery, produces a *Shandy Sorrel* in which the tea is combined with beer. In Thailand, Roselle is drunk as a tea, believed to also reduce cholesterol. It can also be made into a wine - *Hibiscus* flowers are commonly found in commercial herbal teas, especially teas advertised as berry flavored, as they give a bright red coloring to the drink. In the Caribbean sorrel drink is made from sepals of the roselle. In Malaysia, roselle calyces are harvested fresh to produce pro-health drink due to high contents of vitamin C and anthocyanins.

In Mexico, '*agua de Flor de Jamaica*' (water flavored with roselle) frequently called "*agua de Jamaica*" is most often homemade. Also, since many untrained consumers mistake the calyces of the plant to be dried flowers, it is widely, but erroneously, believed that the drink is made from the flowers of the non-existent "Jamaica plant". It is prepared by boiling dried calyces of the Flower of Jamaica plant in water for 8 to 10 minutes (or until the water turns red), then adding sugar. It is often served chilled. This is also done in Barbados, Jamaica and Trinidad and Tobago where it is called '*sorrel*'. The drink is common in Mexico and Central America, UK, Jamaica, Trinidad and Tobago, Mali, Senegal, The Gambia, Burkina Faso, Benin, Sudan, and Lebanon. This drink is particularly good for people who have a tendency, temporary or otherwise, toward water retention: it is a mild diuretic. The fresh calyces are imported mainly during December and January in order to make Christmas and New Year infusions, which are often made into cocktails with additional rum. They are very perishable, rapidly developing fungal rot, and need to be used soon after purchase – unlike the dried product, which has a long shelf-life.

In Australia, rosella jam has been made since Colonial times and is still sold regularly at community fetes and charity stalls. It is similar in flavor to plum jam, although more acidic. It differs from other jams in that the pectin is obtained from boiling the interior buds of the rosella flowers. It is thus possible to make rosella jam with nothing but rosella buds and sugar.

Many parts of the plant are also claimed to have various medicinal values [340]. Roselle is associated with traditional medicine and is reported to be used as treatment for several diseases such as hypertension and urinary tract infections. There is currently insufficient evidence to demonstrate any beneficial effect of roselle on raised blood pressure [341] or on blood lipid lowering [342], although experimental results seem contradictory [343]. It may lower blood pressure in pre- and mildly hypertensive adults [344]. A recent clinical trial demonstrated important antihypertensive effectiveness [345]. Another trial on sixty diabetic patients with mild hypertension found that *Hibiscus sabdariffa* infusion had positive effects on BP in type II diabetic patients with mild hypertension [346].

The plants are rich in anthocyanins and protocatechuic and the dried calyces contain the flavonoids, gossypetin, hibiscetine and sabdaretine. The major pigment, formerly reported as hibiscin, has been identified as daphniphylline. Small amounts of myrtillin (delphinidin 3-monoglucoside), Chrysanthenin (cyanidin 3-monoglucoside), and delphinidin are also present. Roselle seeds are a good source of lipidsoluble antioxidants, particularly gamma-tocopherol [347].

5.6.3. Production of Roselle

China and Thailand are the largest producers and control much of the world supply. Thailand invested heavily in roselle production and their product is of superior quality, whereas China's product, with less stringent quality control practices, is less reliable and reputable. The world's best roselle comes from the Sudan, but the quantity is low and poor processing hampers quality. Mexico, Egypt, Senegal, Tanzania, Mali and Jamaica are also important suppliers but production is mostly used domestically [348].

In the Indian subcontinent (especially in the Ganges Delta region), roselle is cultivated for vegetable fibers. Most of its fibers are locally consumed and the fiber from the roselle plant has great demand in various natural fiber using industries.

In early 1990s roselle was introduced as new crop in Malaysia and its commercial planting was first promoted in 1993 by the Department of Agriculture in Terengganu, Malaysia [349-351]. The planted acreage was 12.8 ha in 1993, but had steadily increased to peak at 506 ha in 2000. The planted area is now less than 150 ha annually, planted with two main varieties. Despite the dwindling planting area over the past decade or so, roselle is becoming increasingly known to the general population as an important pro-health drink in the Malaysia [352, 353].

5.7. Coir Fiber

Coir is a natural fiber extracted from the husk of coconut and technically coir is the fibrous material found between the hard, internal shell and the outer coat of a coconut. The individual coir fiber cells are narrow and hollow, with thick walls made of cellulose. They are pale when immature but later become hardened and yellowed as a layer of lignin is deposited on their walls. Each cell is about 1 mm long and 10 to 20 μm in diameter. Fibers are typically 10 to 30 cm long. Coir fiber is used in products such as floor mats, doormats, brushes, mattresses etc. The coir fiber is relatively water-proof and is one of the few natural fibers resistant to damage by salt water. There are two varieties of coir fibers. First, brown coir made from fully ripened coconut and it is thick, strong and has high abrasion resistance. Mature brown coir fibers contain more lignin and less cellulose than fibers such as flax and cotton and so are stronger but less flexible. It is typically used in upholstery padding, mats, brushes, sacking and horticulture. Second, White coir fibers are harvested from unripe coconuts. These fibers are white or light brown in color and are smoother and finer, but also weaker. They are generally spun to make yarn that is used in mats or rope and is also used for making finer brushes, string, and fishing nets. Fresh water is used to process brown coir, while sea water and fresh water are both used in the production of white coir [354, 355]. Figure 15 shows the coir fiber composition.

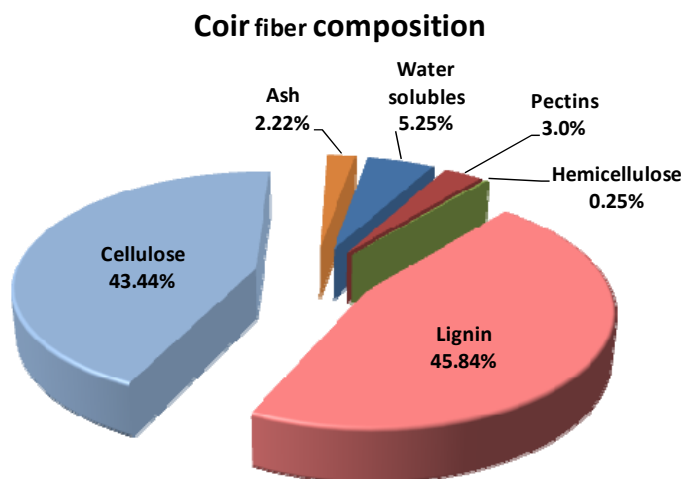


Figure 15. Coir fiber composition.

5.7.1. Harvesting of Coconuts

Coconuts are the seed of a species of palm trees, *Cocos nucifera*, which are flower on a monthly basis and the fruit takes 1 year to ripen. Therefore, a balls palm tree has fruit in every stage of maturity and can produce 50–100 coconuts per year. Coconuts can be harvested from the ground once they have ripened and fallen or they can be harvested while still on the tree. A human climber can harvest approximately 25 trees in a day, while a knife attached to a pole can up the number to 250 trees harvested in a day. Monkeys can also be trained to harvest the coconuts, but this practice is less efficient than other methods. Green coconuts, which contain pliable white fibers, are harvested after about six to twelve months on the plant. Brown fiber is obtained by harvesting fully mature coconuts when the nutritious layer surrounding the seed is ready to be processed into copra and desiccated coconut [356].

5.7.2. Processing of Coir Fibers

The fibrous layer of the fruit is manually separated from the hard shell by driving the fruit down onto a spike to split it (de-husking). 2,000 coconuts can manually separate per day by a well seasoned husker. Machines, which can process up to 2,000 coconuts per hour, are now available for crushing the whole fruit to give the loose fibers [357, 358].

The mass of the ground tissue of the husk is mainly constituted of hemicelluloses and pectin, which are behave as a spongy binding material to bind the prominent fiber cells united forming the husk. Chemically coir fiber is compiled of an extremely converted into wood form of cellulose (cellulose lignin complex), which bills for its harshness, color and proportional brittleness in comparability with perfect cellulose fiber. Coconut coir is generally in large demand not accounted of natural resilience, resistance to dampness, durability and other related properties. The rating of coir fiber is done based on its color, fiber length, resilience and cleanliness in relation to the large quantity of pith present. The two distinguished categories of coir fiber are brown coir and white coir, the differences are mainly due to the prevailing condition of the husk which is generally used and the methodology used in extraction, the physical properties and it addition in its uses [359].

5.7.2.1. Processing of Brown Coir Fiber

The coir fibrous husks are soaked in pits or in nets in a slow moving body of water to swell and soften the fibers. The long bristle fibers are separated from the shorter mattress fibers underneath the skin of the nut, a process known as wet-milling [360]. The mattress fibers are sifted to remove dirt and other rubbish, dried in the sun and packed into bales. Some mattress fibers are allowed to retain more moisture so that it retains its elasticity for twisted fiber production. The coir fiber is elastic enough to twist without breaking and it holds a curl as though permanently waved. Twisting is done by simply making a rope of the hank of fiber and twisting it using a machine or by hand. The longer bristle fiber is washed in clean water and then dried before being tied into bundles or hunks. It may then be cleaned and 'hackled' by steel combs to straighten the fibers and remove any shorter fiber pieces. Bristle Coir fibers can also be bleached and dyed to obtain hanks of different colors [361].

5.7.2.2. Processing of White Coir Fiber

The immature coir husks are retting by suspended in a river or water-filled pit for up to ten months, during which the microorganisms break down the plant tissues surrounding the fibers to loosen them. Segments of the husk are then beaten by hand to separate out the long

fibers which are subsequently dried and cleaned. Cleaned fiber is ready for spinning into yarn using a simple one-handed system or a spinning wheel. Recently, the technology uses enzymes to separate the fibers by converting plant compounds into soluble compounds and hence curbs the pollution of water-bodies caused by retting of coconut husks was developed [362-364].

5.7.3. Uses of Coir Fiber

Brown coir is used in floor mats and doormats, brushes, mattresses, floor tiles, sacking and a small amount is also made into twine as well as pads, which made by needle-felting (a machine technique that mats the fibers together). Brown coir fibers are also shaped and cut to fill mattresses and for use in erosion control on river banks and hillsides. Also brown coir pads are sprayed with rubber latex to bond the fibers together (rubberized coir) to be used as upholstery padding for the automobile industry in Europe. The brown coir fiber is also used for insulation and packaging. White coir fiber is used in rope manufacture and the mats of woven coir fiber are made from the finer grades of bristle and white fiber using hand or mechanical looms. Because of white coir fiber has strong resilience to salt water it is used to manufacture fishing nets. Coir fiber is a strongly recommended in horticulture to substitute the sphagnum moss because it is free of fungal spores and bacteria, as well as produces good results without the environmental damage caused by peat mining. Coir fiber is also useful to deter snails from delicate plantings and as a growing media in intensive glasshouse horticulture. Coir from Mexico has been found to contain large numbers of colonies of the beneficial fungus *Aspergillus terreus*, which acts as a biological control against plant pathogenic fungi. Coir fiber is an allergen and the latex and other materials are used frequently in the treatment of coir [362, 365-370].

5.7.4. Major Coir Producers

The coir fiber industry is particularly important in some areas of the developing world. Total world production of coir fiber is 617,000 tons/year. Mainly the coastal region of Kerala State of India produces 60% (50% of which mainly consumed in the countries of origin) of the total world supply of white coir fiber. Sri-Lanka produces 36% of the total world brown fiber output. Together India and Sri-Lanka produce 86% of the 617,000 tons of coir produced every year (Figure 16).

Recently, Mexico, Indonesia, Vietnam and certain Caribbean countries have started to supply coir fiber to the global market in large scale. Decompressing the imported coir blocks has presented problems for many commercial growers. Many companies have installed machinery to bust the coir blocks apart in a dry state. Other companies have tried hydrating the coir blocks with water; however coir buster type machines are usually best. Coir buster type machines decompress the coir blocks apart by rubbing them apart in a chamber that keeps the coir blocks (or bricks) tightly compressed together crumbling the material, then sifting through a screen with no fiber damage [371].

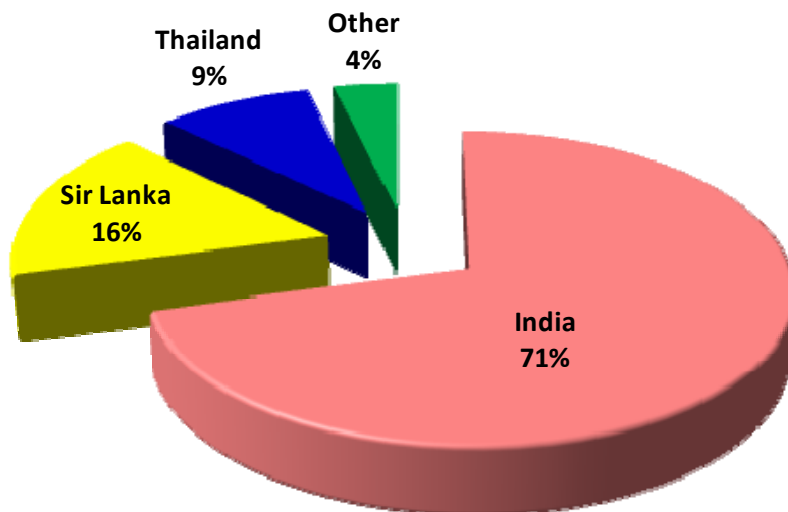


Figure 16. Coir fiber produces in 2008.

6. LEAF FIBERS

Leaf fibers usually extend along the entire length of a leaf to reinforce its structure and keep it rigid. The fibers are embedded in a pulpy tissue which needs to be removed by mechanical scraping, called *decortication*. Leaf fibers are generally hard and coarse compared to bast fibers (Table 12). Most leaf fibers are long and somewhat stiff.

The fibrils of leaf fibers consist of a large number of elongated cells whose ends are cemented together. The cell walls of leaf fibers are composed of *cellulose*, which is composed of linear carbohydrate and complex carbohydrate macromolecules that consists of hundreds or thousands of glucose units having the formula $C_6H_{10}O_5$. Cellulose is insoluble in water and is the most abundant of all naturally occurring organic compounds. The fibers are mostly crystalline and are separated by small amorphous regions. It is undigestible by humans but can be broken down by microorganisms, for example, in the stomachs of certain herbivorous animals such as cows, horses, and sheep.

Lignin is a complex macromolecule not based on carbohydrates and served as the cementing constituent between the cells of woody tissue. *Pectic substances*, which consist of an associated group of polysaccharides and contained in plant in small percentages, are capable of forming thick solutions. On the other hand, the plant parts extraction contains gums, fats, resins, waxes, sugars, oils, starches, alkaloids, tannins in various amounts. Extracted materials are nonstructural components that are deposited in cell walls or cell cavities. These materials may be extracted without changing the structure of wood. Further constituents of plant fibers are *minerals*, which remain as *ash* when a plant is incinerated. The compositions of some selected commercially important vegetable fibers are presented in Table 17.

Table 17. Composition of selected plant fibers

Fiber	Cellulose (%)	Moisture (%)	Ash (%)	Lignin and Pectin (%)	Extractives (%)
Bast Fibers					
Congo jute	75.3	7.7	1.8	13.5	1.4
Flax (linen)	76.0	9.0	1.0	10.5	3.5
Hemp	77.1	8.8	0.8	9.3	4.0
Ramie (China grass)	91.0			0.6	
Leaf Fibers					
Sisal	77.2	6.2	1.0	14.5	1.1
Henequen	77.6	4.6	1.1	13.1	3.6
Abaca (Manila hemp)	63.7	11.8	1	21.8	1.6
Istle ^a	73.5	5.6	1.6	17.4	1.9
Seed Fiber					
Cotton ^b	90.0	8.0	1.0	0.5	0.5

^a Istle: In ancient times there were several fibers used in Mexico under the names of Istle, Ixtle or Tampico Fiber. Three species of most importance are Jaumaveistle, *Agave funkiana*, Tula Istle, *A. lecheguilla*, and Palma Istle, *Samuela carnerosana*. Several species of *Yucca* were also grouped under the category of Istle. The fibers are obtained from immature leaves of wild plants. Although these fibers are shorter than those of sisal and henequén, they are very strong and durable. They were formerly used for brushes and as a cheap substitute for sisal and abacá to make bagging, twine and rope.

^b Note: “Easy care” or “no-iron” fibers are treated with formaldehyde resin that emits formaldehyde fumes. They have been observed to cause tiredness, headaches, coughing, watery eyes, or respiratory problems.

6.1. Piña Fiber

Piña fiber is a pineapple fiber made from the leaves of a pineapple plant and is commonly used in the Philippines. Piña's name comes from the Spanish word piña which literally means pineapple. Piña fiber is sometimes combined with silk or polyester to create a textile fabric. Since piña is from a leaf, the leaf has to be cut first from the plant and then the fiber is pulled or split away from the leaf. Each strand of the Piña fiber is hand scraped and is knotted one by one to form a continuous filament to be hand-woven and then made into a Piña cloth. Piña weaving is an age-old tradition which was recently revived in the past 20 years. Aklan Kalibo is the main and the oldest manufacturer-weaver of Piña cloth in the Philippines, which are being exported to various parts of the world most particularly North America, and Europe. History records suggest that Kalibo's Piña cloth was traded during the Pre-Hispanic times and reached as far as Greece and Egypt during its heyday. Kalibo is also known for other native products such as handbags made of buri leaves which are a favorite for Caucasian females visiting the town. Piña fabric is also used for table linens, bags, mats and some other clothing items, or anytime that a lightweight, but stiff and sheer fabric is needed. Pineapple silk is considered the queen of Philippine fabrics and is considered the fabric of choice of the

Philippine elite. A major use for piña fabric is in the creation of the Barong Tagalog and other formal wear that is common in the Philippines [372-375].

6.2. Sisal

Sisal (*Agave sisalana*) is an agave that yields a stiff fiber traditionally used in making twine, rope and also dartboards. Sisal may refer either to the plant or the fiber, depending on context. It is sometimes incorrectly referred to as sisal hemp because hemp was for centuries a major source for fiber, so other fibers were sometimes named after it. The sisal plant's origin is uncertain; while traditionally it was deemed to be a native of Yucatan; there are no records of botanical collections from there. In the 19th century, sisal cultivation spread to Florida, the Caribbean islands and Brazil, as well as to Tanzania and Kenya in Africa, as well as Asia. In Brazil, the first commercial plantings were made in the late 1930s and the first sisal fiber exports from there were made in 1948. Brazilian production of sisal fiber was accelerated and the first of many spinning mills was established after 1960s and today Brazil is the major world producer of sisal.

Sisal plants consist of a rosette of sword-shaped leaves about 1.5 to 2 m tall. Young sisal leaves may have a few minute teeth along their margins, but lose them as they mature. Sisals are sterile hybrids of uncertain origin; although shipped from the port of Sisal in Yucatán, they do not actually grow in Yucatán; the plantations there cultivate henequen (*Agave fourcroydes*) instead. Evidence of an indigenous cottage industry in Chiapas suggests it as the original location, possibly as a cross of *Agave angustifolia* and *Agave kewensis* [376-380].

6.2.1. Cultivation of Sisal

Sisal is considered a plant of the tropics and subtropics, since production benefits from temperatures above 25°C and sunshine. Propagation of sisal is generally by using bulbils produced from buds in the flower stalk or by suckers growing around the base of the plant, which are grown in nursery fields until large enough to be transplanted to their final position. These methods offer no potential for genetic improvement. Invitro multiplication of selected genetic material using Meristematic Tissue Culture (MST) offers considerable potential for the development of improved genetic material. The sisal plant has a 7-10 year life-span and typically produces 200-250 commercially usable leaves and each leaf contains an average of around 1000 fibers. Sisal fibers are accounted only for about 4% of the plant by weight [381-385].

6.2.2. Sisal Fiber Extracting

Decortication is the process used to extract sisal fiber, where leaves are crushed and beaten by a rotating wheel set with blunt knives, so that only fibers remain. In East Africa (superior quality of sisal fiber is found) where production is typically on large estates, the leaves are transported to a central decortications plant, where water is used to wash away the waste parts of the leaf. The sisal fiber is then dried, brushed and baled for export. Proper drying is important as sisal fiber quality depends largely on moisture content. Artificial drying has been found to result in generally better grades of fiber than sun drying, but is not feasible in the developing countries where sisal is produced. In north-east Brazil, where climate is drier, sisal is mainly grown by smallholders and the fiber is extracted by teams using portable raspadors which do not use water but fiber is subsequently cleaned by brushing. On the basis

of the in-field separation of leaves into size groups, the dry fibers are machine combed and sorted into various grades (<http://www.youtube.com/watch?v=fxKrJVEhMHA>; <http://www.youtube.com/watch?v=c0qNKgSXJ2EandNR=1>).

6.2.3. Sisal Environmental Impact

The decortication process effluent causes serious pollution when it is allowed to flow into watercourses. However, in Tanzania, there are plans to use the decortications waste as bio-fuel. Sisal farming initially caused environmental degradation, because sisal plantations replaced native forests but it is still considered less damaging than many types of farming. In sisal production, no chemical fertilizers are used and the impact of herbicides, which are occasionally used during plantation, may be eliminated since most weeding is done by hand.

In recent years sisal has been utilized as an environmentally friendly strengthening agent to replace asbestos and fiberglass in composite materials in various uses including the automobile industry (<http://www.filepie.us/?title=Sisal>).

6.2.4. Uses of Sisal Fiber

Traditionally, sisal has been the leading material for agricultural twine (binder twine and baler twine) because of its strength, durability, ability to stretch, affinity for certain dyestuffs, and resistance to deterioration in saltwater, but the importance of this traditional use is diminishing with competition from polypropylene and the development of other haymaking techniques, while new higher-valued sisal products have been developed. Apart from ropes, twines, and general cordage, sisal is used in low-cost and specialty paper, dartboards, buffing cloth, filters, geotextiles, mattresses, carpets, handicrafts, wire rope cores, and Macramé (<http://www.ropesandtwines.com/usesofsisal.asp>).

The higher-grade fiber after treatment is converted into yarns and used by the carpet industry. The medium-grade fiber is used in the cordage industry for making ropes, baler and binder twine. Ropes and twines are widely employed for marine, agricultural, and general industrial use. The lower-grade fiber is processed by the paper industry because of its high content of cellulose and hemicelluloses. Other products developed from sisal fiber include spa products, cat scratching posts, lumbar support belts, rugs, slippers, cloths, and disc buffers.

Sisal wall covering meets the abrasion and tearing resistance standards of the American Society for Testing and Materials and of the National Fire Protection Association. Despite the yarn durability sisal is known for, slight matting of sisal carpeting may occur in high-traffic areas. Sisal carpet does not build up static nor does it trap dust, so vacuuming is the only maintenance required. High-spill areas should be treated with a fiber sealer and for spot removal, a dry-cleaning powder is recommended. Depending on climatic conditions, sisal will absorb air humidity or release it, causing expansion or contraction.

Sisal is not recommended for areas that receive wet spills or rain or snow. Sisal is used by itself in carpets or in blends with wool and acrylic for a softer hand. As extraction of fiber uses only a small percentage of the plant, some attempts to improve economic viability have focused on utilizing the waste material for production of biogas, for stock-feed, or the extraction of pharmaceutical materials. Sisal is valuable forage for honey bees because of its long flowering period. It is particularly attractive to them during pollen shortage. The honey produced is however dark and has a strong and unpleasant flavor.

6.2.5. Production of Sisal

Global production of sisal fiber in 2007 amounted to 240,000 tons of which Brazil was the largest producing country, produced 113,000 tons [386]. Tanzania produced approximately 37,000 tons, Kenya produced 27,600 tons, Venezuela 10,500 tons and 9,000 tons were produced in Madagascar (Figure 17). China contributed by 40,000 tons in addition to smaller amounts coming from South Africa, Mozambique, Haiti, and Cuba. Sisal occupies 6th place among fiber plants, representing 2% of the world's production of plant fibers (plant fibers provide 65% of the world's fibers).

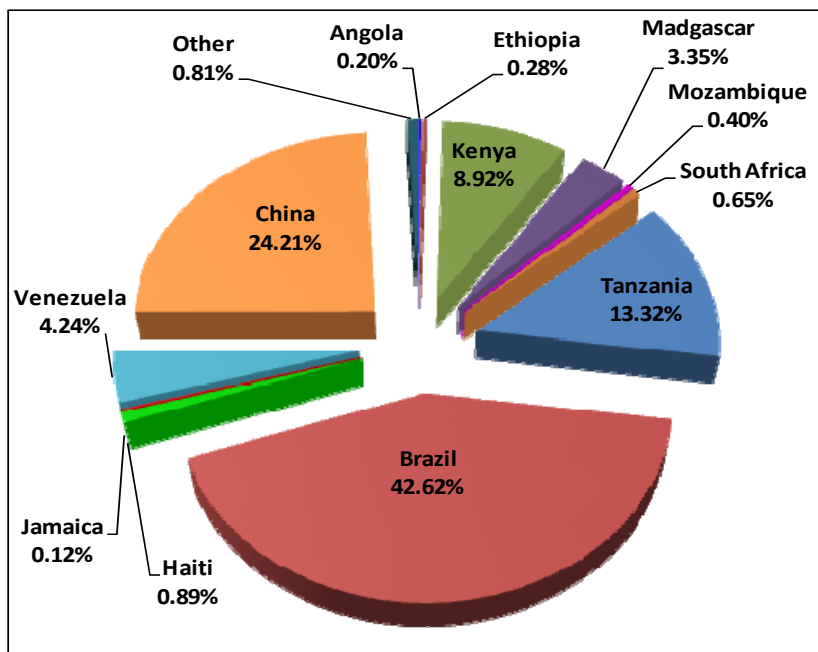


Figure 17. Sisal producing countries and their contribution % in the world production.

6.3. Henequen

Henequen is a fiber obtained from the leaves of plant *Agave fourcroydes* (Varieties of *A. fourcroydes* include *ixtli*, *longifolia*, *minima*, and *rigida*), of the family agave (Agavaceae). Henequen is the third importance fiber among the leaf fiber group. The henequen plant is native to Mexico and it is produced only in Mexico, Cuba and El Salvador, where it has been a source of textile fiber since pre-Columbian times [22, 23]. It is the major plantation fiber agave of eastern Mexico, being grown extensively in Yucatán, Veracruz, and southern Tamaulipas. In the 19th century, Henequen was introduced to Cuba and by the 1920s becoming the country's chief fiber crop. Henequen is sometimes incorrectly called sisal. The plant appears as a rosette of sword-shaped leaves 1.2 to 1.8 m long, growing out of a thick stem that may reach 1.7 m. The leaves have regularly-spaced teeth 3-6 mm long, and a terminal spine 2-3 cm long. Henequen is the major plantation fiber agave of eastern Mexico, being grown extensively in Yucatán, Veracruz, and southern Tamaulipas [387, 388].

The first to document the plant and its usefulness for ropes and other naval utensils was José María Lanz, a Mexican-born engineer in service of the Spanish Navy, who studied henequen in Yucatan in 1783 (<http://www.answers.com/topic/henequen>).

A. fourcroydes is a sterile hybrid and its ovaries never produce seeds like the sisal. The plant does produce bulbils that may be planted, but commercial growers prefer to use the frequent suckers, which develop more quickly. Henequen fiber is suitable for rope and twine, but not of as high a quality as sisal. It is also used to make a traditional Mexican alcoholic drink “*Licor del henequen*”. Figure 18 shows the world producer countries and their contribution percentage.

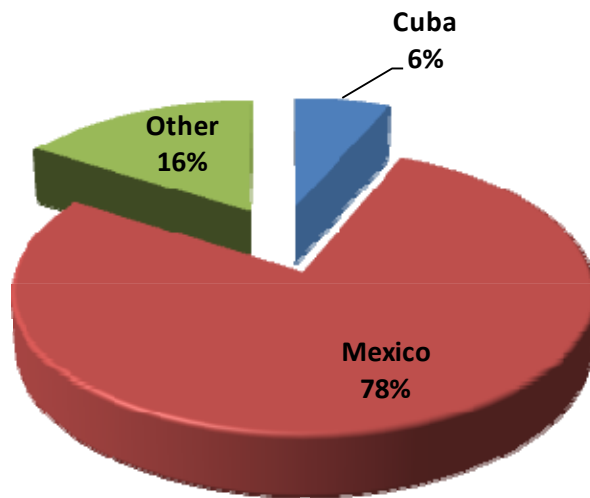


Figure 18. Henequen (*Agave fourcroydes*) world production in 2008.

6.3.1. Extracting Fiber from Henequen Plants

Traditional method: on the ground, the henequen-plant leaves are whacked to split the skin and loosen the fibers. The leaves are strapped to a flat board with twine (1-4 leaves at same time) and press using special rasping sticks to remove the liquid and mucilage (four scrapes are needed for one leaf, while more leaves tack more times). Bending over with the board pressing into their stomach, resting at 45 degrees angle, the man presses and pushes scraping along the leaf to remove the pulp and short fibers. Then the leaves are turned around and the process is repeated and the obtained fibers washed (<http://www.backyardnature.net/m/crafts/fiberout.htm>; <http://gorbman.com/2010/02/24/henequen-in-yucatan/>).

Mechanical Method: bundles of henequen leaves, tied with henequen twine, are loaded onto trucks deliver the leaves to the milling factory or desfibradora. The bundles are unloaded at the base of a vertical conveyor at the top of the conveyor, workers stand on raised benches; untie the bundles, placing the twine over a wooden bar to be reused. Leaves are conveyed down a large, shiny, brass chain to two drums that crush the leaves and beat the pulp while water is sprayed over them. Then the leaves are flipped over and crushed, beaten and sprayed again. The pulp residue, bagasso, falls through the pressing area into bins that look like little dump trucks; when they are full, little mules pull these bins out to fallow areas where it is dumped to dry. The wastes can be used as mulch. Below the beating area there are little

canals for carrying off the pulpy water, which has non-pleasant smell. When the remaining tough long fibers emerge from the other side, workers separate the fibers into hand-size bundles, slide them down either a pipe or smooth wooden beam where they are placed on trucks and then transferred to drying field. The fiber dries in only a few hours. In order to preserve its clean white color it should not get wet. The fiber is brought back to the factory storerooms where it is then pressed into huge bales held together with henequen twine (<http://www.backyardnature.net/m/crafts/fiberout.htm>).

6.4. Abaca

Abaca is a type of fiber obtained from the leaves of the plant abacá (*Musa textilis*), a relative of the banana belongs to the family of the banana plant (Musaceae) and is indigenous to the Philippines. The banana and abaca plants have a striking similarity in looks but the main difference is that the fruit of the abaca plant is inedible. Abaca is not hemp but since hemp was the main source of fibers for centuries, the abaca fiber was known as Manila hemp. It is mostly used for pulping for a range of uses, including specialty papers. Manila envelopes and Manila paper take their name from this fiber. It was once used mainly to make manila rope, but this is now of minor importance. Abaca has been cultivated in the Philippines since the 1500s and became known worldwide in the 1800s and it was mainly used as ropes in ship rigging. Philippines and Ecuador produce 97% of the world production of abaca fiber (Figure 19).

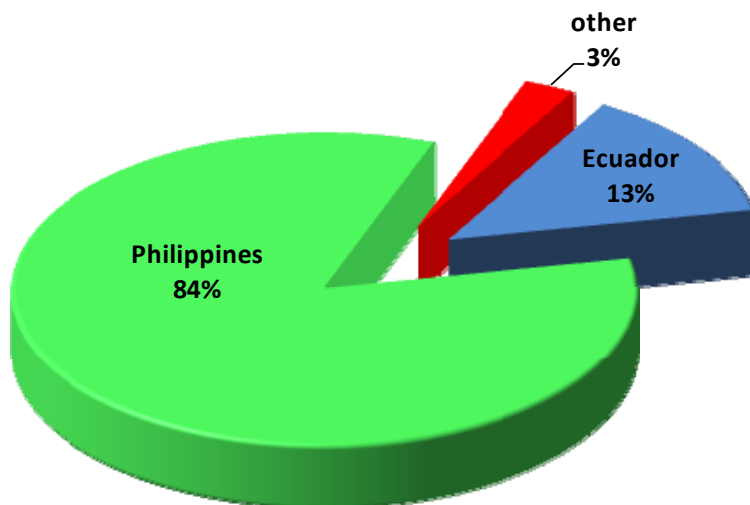


Figure 19. Abaca fiber producers in 2009.

The abaca plant grows up to twenty feet when mature and harvested 2 to 4 times per year by cutting down the trunk above the roots to harvest the fibers. New sprouts will grow from the roots soon after cutting. Leaf sheaths are then stripped and pulp is scrapped off to get the abaca fiber strands. To make ropes, the strands are twisted together. These strands are mainly composed of cellulose, pectin and lignin. Superior qualities of abaca fiber are extremely

strong, durable, resistant to salt water, and can be made into many hard-wearing products, relatively cheap to produce. It has a beautiful texture when made into hats and other products, as well as it is biodegradable and eco-friendly material [389-393].

6.4.1. Abaca Fiber and Its Uses

The stalk is the source of fibers which are extracted from the outermost portion of the leaf sheath using hand-stripping or a stripping machine. Abaca-Lupis is the third and fourth layer of the leaf-sheath, which producing the abaca fiber. Abaca-Lupis is brownish in nature and skinny on the other part of the stripped fiber. Abaca fibers are also used in *Sinamay* (*Sinamay* is of less gossamer tissue) weaving, but almost transparent and far more durable than the fabrics made from pineapple fiber. Abaca-Lupis can be used to make decorative accessories, fashion accessories, furniture, garments, textile, making gift boxes, packaging materials, footwear, wall covering, draperies, and playthings for pets, table-top accessories, sports paraphernalia and more. The abaca fibers are used in the production of handicraft products such as rope, abaca paper abaca rug, abaca furniture, abaca dye mat, abaca carpet, manila envelope and countless other products.

Abaca fibers are also used in pulp-making which are used as raw material in the production of currency and bank notes, tea bags, coffee filters, meat casings, coating for pills, surgical caps and masks, high capacitor papers, cable insulation papers, Bible paper, restoration and conservation of historical documents, adhesive tape paper, lens tissue, carbonizing tissue, abrasive base paper, mimeograph stencil base paper, weather-proof Bristol, maps, charts, as a strengthening material for napkins and tissue paper; insulation for computer chips, etc.

Abaca fibers also have several medical and industrial applications: such as for orthopedic materials (joint replacements and fracture healing implants); as material composites to replace glass fibers in the manufacturing of cars, planes, yachts. For building materials such as fiberboards, ceramic tiles, wall facades, plumbing fixtures, reinforced concrete and roofing, caulking, flooring, electricity poles, in the production of sporting goods, telephones, cleaners and paints and more [394-397].

6.4.2. Abaca Seeds and Corms

Abaca products are renewed for their versatility across the globe. Most people think of abaca by-products such as ropes, cordage, paper, cloth, furniture, fashion accessories and home decors as it has been used for many decades for such things. While, the abaca seed can be used for food; for cosmetics, skin-care products and for industrial uses such as paints and inks. Test results show that the biochemistry and nutritional analysis of the abaca seeds can have many beneficial uses and benefits. The full potential is yet to be realized in the form of the abaca seed oil. Remaining portion or wastes can be used in the production of starch for industrial purposes. Abaca corms can be used as planting materials (<http://www.abacaphilippines.com/abaca.php?go=aboutandshow=uses>).

6.4.3. Extracting Process of Abaca Fiber

The first step in the extracting process of the abaca fiber is to cut the round stalk of the abaca plant and sliced into quarters lengthwise. Then, the stalk is placed under a large knife look similar to that of a paper cutting board where the knife is pressed halfway down and is secured in that position and the stalk pulled through the knife scrapping off the none

filamented materials to produce the raw abaca fiber. The fiber will then be hung up to dry and brought in for inspection to classify into different grades of fibers. The final product is white, shiny and clean processed fiber. The abaca fiber is baled and every bale is then tied and packed with polyethylene plastic and covered with a sack (<http://www.peral.net/fiber.htm>).

6.5. Fique Fiber

Fique fiber grows in the leaves of the fique plant (*Furcraea andina*) Family Agavaceae, a xerophytic monocot native to Andean regions of Colombia and extended to Venezuela and the east coast of Brazil. The fique plant is often confused with the agave plant. The differences are that the agave leaves are yellowish and stiff with a strong spike in the tips, while the fique plant leaves are droopy and greenish without a spike. Fique fiber has common names: Fique, Cabuya, Pita, Penca, Maguey, Cabui, Chuchao or Coquiza.

The fique fibers are extracted by the pre-Columbian inhabitants and they used for several centuries before the arrival of Spanish conquerors, which was used fique fiber to make garments, ropes, hammocks and many other applications. Dutch colonists, in the 17th century, carried the plant from their Brazilian colonies in Pernambuco to the island of Mauritius. The native inhabitants of the Mauritius Island learned to use the fiber and called it *caraguata-acu*, *croata-acu* or *gravata-acu*. The fiber was also introduced to St. Helena, India, Sri Lanka, Algeria, Madagascar, East Africa, Mexico and Costa Rica.

Between 1970 and 1975, the fique industry suffered a crisis due to the development of polypropylene that costs less and is produced much faster. Nowadays, fique is considered the Colombian national fiber and is used in the fabrication of ethnic products, Colombian handicrafts and recently has been used for the heath protectors (handmade in Barichara) placed around the Colombian coffee (<http://www.mundomaterial.eu/2009/05/18/2009-international-year-of-natural-fibres-fique-in-colombia/?lang=en>).

6.5.1. Uses of Fique Fiber

The main use of the Colombian *cabuya* is for the fabrication of sacks and packages for agriculture. Used for flour and small grains packing such rice and for bigger grains such coffee and beans, as well as fruits, vegetables and panela. Also, fique fiber is used to make very resistant ropes and strings of different *calibres*, from threads to manilas one inch in diameter. Such ropes are used in the industries of transportation, construction, sailing and many others. Many of the elements used in the pack animals such as *enjalmas*, *cinchas*, *retrancas*, *lazos*, *pretales*, *tapa de enjalma*, and *cinchos* are handmade with fique. The mixed and crude *cabuya* is used in rugs and tapestry of different size and quality. The fibers can be stained with different organic materials such as avocado seed, achiote and eucalyptus cortex. Fique fiber are applied also in handicrafts, purses, bags, handbags, mattresses, curtains, shoes, umbrellas, baskets and many other products [398-401].

On the other hand, fique pulp is used to produce organic fertilizing and paper Leaves juice can be used for fabrication of soap, fungicides, alcoholic beverages (homemade tapetusa, organic fuel and animal food). The strong floral stem of the fique plant is used in the construction of houses and ladders. Also, the pickled terminal bulbs of the plant are edible. The peasants use the leaves in topic preparations for treatment of boils and the extract of leaves is used against the horse lice [402, 403].

6.5.2. Cultivation of Fique

Optimal conditions for the growing of the fique plant are: Soil: dry, rich in silicates; Temperature: 19 - 23°C Altitude: 1,300 m - 1,900 m; Annual rainfall: 1,000 - 1,600 mm; Sunlight: 5–6 hours/day. The plant is very adaptable to different ecological conditions. The fique crops bring nitrogen to the soil, improving its fertility. A fique plant can produce 1 to 6 kg of fibers each year (<http://www.chemeurope.com/en/encyclopedia/Fique.html>).

The fique can be obtained from several species of *Furcraea*, such as *F. macrophylla*, *cabuya Trel*, *andina Trel*, and *castilla*. Depending on the process of the fiber and the species used, many varieties of fique fibers can be obtained. Among others: Main varieties are *Ceniza* (ash-colored), *Espinosa* (rough texture), *Castilla* or Golden border, Sisal and secondary varieties are *Cabuya verde* (green), *Uña de águila* (eagle nail), *Negra común* (black common), *Chachagueña*, *Genoia*, *Tunosa común* (common spiked), *Jardineña*, *Espadilla*, *Rabo de chucha* (opossum tail).

6.5.3. Diseases of Fique

Llaga Macana or Rayadilla: a viral disease has no chemical control attacks all varieties of fique and all the parts of the plant, especially in crops over 1900 m altitude. This disease must be managed with preventive measures. Fungus *Corticium salmonicolor* causes Pink disease, which damages the leaves and disrupting the fibers. Treatment is undertaken with copper-based fungicides. Also, the peasants treat this disease by applying ashes to the base of the leaves. Parasitic insect (*Diaspis bromeliae*) causes Leaf Cochineal. Leaf Beetle: a beetle that perforates the base of the leaves [404-407]

6.6. Phormium Fiber

Phormium tenax was first collected on Captain Cook's second expedition to the South Pacific in 1773. It was probably one of the first plants noted upon landing as it can be found on the beach, in river mouths, on coastal cliffs and along alpine lakes. Later in 1848, *Phormium cookianum* was discovered and named by Auguste Francois Le Jolis. In 1864 the name *Phormium colensoi* was applied to what is now called properly called *Phormium cookianum* sp. *hookeri* [408, 409].

Phormium tenax and *Phormium cookianum*, an herbaceous perennial monocot, Family: Hemerocallidaceae, known by the Māori names *harakeke* and *wharariki*, respectively are common New Zealand perennial plants. They are quite distinct from the Northern Hemisphere plant known as flax (*Linum usitatissimum*), but the genus was given the common name 'flax' by Anglophone Europeans as it too could be used for its fibers. New Zealand flax produces long leaf fibers that have played an important role in the culture, history, and economy of New Zealand. While *Phormium cookianum* is endemic to New Zealand, the *Phormium tenax* occurs naturally in New Zealand and Norfolk Island. However, both species have been widely distributed to temperate regions of the world as economic fiber and ornamental plants [410-418].

In 1793, when French ships visited the far north of the North Island of New Zealand, the naturalist “Jacques Labillardière” collected indigenous flax plants because he had noted the many uses the plant. In 1803, it had the scientific name *Phormium*, meaning "basket" or "wickerwork", and *tenax* meaning "tenacity" or "holding fast".

Phormium tenax is found mainly in swamps or low lying areas but will grow just about anywhere and is also much propagated in gardens as an evergreen decorative plant, both in New Zealand and now worldwide. Recent classification systems have been found *Phormium tenax* to be closely related to daylilies (*Hemerocallis*). *Phormium tenax* formerly belonged to the family Agavaceae and many classification systems still place it there.

The tough, sword-shaped leaves grow up to 3 m long and up to 125 mm wide and they are usually darkish green but sometimes have colored edges and central ribs. Cultivated varieties range from light green through pink to deep russet bronze. There are numerous variegated cultivars with leaves marked by contrasting stripes in shades of green, red, bronze, pink and yellow. The rigid flower stalks can be up to 5 m long, projecting high above the foliage. In November (in New Zealand) they produce clumps of curving tube-like flowers which turn bright red when mature. These produce unusually large quantities of nectar to attract all nectar feeding birds. Each seedpod that develops after pollination contains hundreds of seeds which are later widely dispersed by the wind.

Leaves were cut near the base of the plant using a sharp mussel shell or specially shaped rocks, more often than not greenstone. The green fleshy substance of the leaf was stripped off, again using a mussel shell, right through to the fiber which went through several processes of washing, bleaching, fixing, softening, dyeing and drying.

6.6.1. Uses of *Phormium*

Plaiting and weaving the flax fibers into baskets were only the two great varieties of uses made of phormium by Māori who recognized nearly 60 varieties, and who carefully propagated their own phormium nurseries and plantations throughout the land [419]. The fibers of various strengths were used to fashion eel traps (*hinaki*), surprisingly large fishing nets (*kupenga*) and lines, bird snares, cordage for ropes, baskets (*kete*), bags, mats, clothing, sandals (*paraerae*), buckets, food baskets (*rourou*), and cooking utensils etc [420- 424].

The phormium fiber called *muka* is laboriously washed, pounded and hand wrung to make soft for the skin. Cords (*Muka whenu*) form the base-cloth for intricate cloak or garments (*kākahu*) such as the feather cloak (*kahu huruhuru*), a highly prized traditional garment. Cloaks adorned with colorful feathers from the native birds i.e. woodpigeon (*huia*, *kiwi*, *tui*, *kererū*) and parrot (*kākā*), will reference the main type used i.e. *Kahu Kiwi*, *Kahu Kākā*, etc.

The handmade phormium cording and ropes had such great tensile strength that they were used to successfully bind together sections of hollowed out logs to create huge ocean-going canoes (*waka*). It was also used to make rigging, sails and lengthy anchor warps, and roofs for housing. Frayed ends of flax leaves were fashioned into torches and lights for use at night. The dried flower stalks, which are extremely light, were bound together with flax twine to make river rafts called *mokihi*.

6.6.1. Medicinal Uses of *Phormium*

For centuries, Māori have drawn the abundant nectar from the flowers as a general sweetener. Myriad medicinal uses make the plant even more important to the everyday health of Māori. Boiled and crushed *harakeke* roots are applied externally as a poultice for boils, tumors and abscesses, as well as to varicose ulcers. Juice from the pounded roots can be generally used as a disinfectant, and taken internally to relieve constipation or expel worms. It has also been applied to bullet or bayonet wounds [425-428].

The gum-like sap produced by *harakeke* contains enzymes that give it blood clotting and antiseptic qualities to help healing processes. Māori are fully aware of its curative properties and that it is a mild anesthetic, and applies the sap to boils and various wounds, to aching teeth, to rheumatic and associated pains, ringworm and various skin irritations, and scalds and burns. Splints can be fashioned from flower stalks (korari) and leaves, and fine cords of muka fiber utilize the styptic properties of the gel before being used to stitch wounds. *Harakeke* leaves make excellent bandages and can secure broken bones much as plaster is used today. The pulp of pounded leaves can also be applied as dressings. Research into modern medicinal and cosmetic uses is still being carried out in New Zealand. Many organic compounds have been isolated from the different parts of phormium plant [418, 429-434].

In 1993, Oil from New Zealand phormium seed was first commercially produced by the Waihi Bush organic farm in the South Island. New Zealand phormium seed oil has high levels of Omega-3, and provides an alternative to take fish oil [435, 436].

7. WOOD

Wood is a major material for construction, tools, paper-making, fuel, weapons, and as a source for cellulose. Indeed, manuscripts have been found by Theophrastus Aristotle and other ancient writers who describe the properties of wood as it was known in those days. Goods made of wood, when left unpainted, are aesthetically pleasing and convey a feeling of warmth. Wood is one of the few natural resources that can be renewed when forests are managed properly. Moreover, forests are a necessity for water control, oxygen production, recreation, and for providing habitat to many animal species. Approximately one-third of the land mass of the earth (27%) is presently covered with forests. However, it is estimated that the world's forests decrease annually by about 0.9% [1].

Wood has a high strength in relation to its weight and it is an electrical and thermal insulator and has desirable acoustic properties. Wood can be easily shaped and finished and is inert to many chemicals. However, not all properties of wood are favorable, many types of wood decay through interaction with water and wood-destroying organisms [437]. Wood may burn, it is hygroscopic, and changes its size when the humidity fluctuates. Moreover, the physical properties of wood vary in different directions due to its fibrous nature (anisotropy), as shown in Table 18. Finally, cut lumber may have imperfections from knots, etc., which decrease its strength. In short, wood is not a homogeneous and static material as are many metals and ceramics [1].

Lumber (wood) is generally classified into *softwood* and *hardwood* (even though some “hardwoods” are actually softer than some “softwoods”). Major growth areas for softwoods are located in the temperate climate zone whereas the home of hardwood is predominantly in the tropical forests of Africa and the Amazonas region.

Wood is a naturally occurring *composite material* and the structural components of wood consist of elongated plant cells that are made from cellulose compound which are held together by lignin. Two general types of cells exist: first one is the food-storing elements which are called *parenchyma* and they normally remain alive for more than one year. Second one is the cells that provide the support of the tree and serve for the conduction of the protoplasm are known by the name *prosenchyma* and they lose their function in the same year

they were formed. The food-conducting tissue located at the outer part of the *prosenchyma* is called the *phloem*. In these specialized cells, the *phloem* sap that carries the products of photosynthesis streams downward from the leaves to the root. On the other hand, the water and minerals stream upward in the cells located toward the inside, called the *xylem* (Figure 3). Botanists subdivide both the *phloem* and *xylem* into primary and secondary parts. The secondary *phloem* contributes to the formation of bark, and the secondary *xylem* contributes to the formation of wood. The new wood in the secondary *xylem* is called *sapwood*. Eventually, over a period of years, the older *sapwood* dies and becomes more rigid; it is then called *heartwood*. The heartwood is the strong part of the tree at the center and provides strength and support. The heartwood is the principle source for wood and pulp. The *xylem* and *phloem* areas instead supply the chemicals such as wood distillates, latex (for rubber), and fuel [1].

Table 18. Properties of some wood species (12% Moisture)

	Tensile strength σT [MPa]		Compressive strength [MPa]		Density [g/cm ³]	Modulus of elasticity to grain [GPa]
Material	to grain	⊥to grain	to grain	⊥to grain		
Soft Wood						
Douglas fir	78	2.7	37.6	4.2	0.45	13.5
Ponderosa pine	73	2.1	33.1	3.0	0.38	8.5
White spruce	60	2.5	38.7	4.0	0.35	9.2
Red cedar	45.5	2.2	41.5	6.3	0.3	7.7
Hard Wood						
American elm	121	4.5	38	4.7	0.46	9.2
Sugar maple	108	7.6	54	10.1	0.56	12.6
Beech	86.2	7	50.3	7	0.62	
Oaks	78	6.5	42.7	5.6	0.51–0.64	12.3

The growth in diameter of a tree takes place in a single row of cells between the *phloem* and the *xylem*, which is called the *cambium*. As cell division proceeds, about 6–8 *xylem* cells are formed for every *phloem* cell. In other words, the increase in thickness of the wood is greater than that of the bark. As a consequence, the larger formation of the secondary *xylem* cells forces the *cambium* outward and the diameter of the stem increases.

The *phloem* in turn is surrounded by the *cortex* and the *epidermis*, which protect the underlying tissue from mechanical injury (Figure 20). As the plant grows, the *epidermis* is ruptured and one or more protection layers called *periderms* are formed. When rapid growth occurs, cell division in the *cambium* is larger during spring. This leads to the formation of *spring wood* (early wood), which is somewhat different in chemical composition, color, and physical structure than *summer wood* (late wood). The age of a tree can be estimated by counting these *annual rings*. However, in some years, for reasons not well understood,

additional rings or no rings at all form. The term *growth rings* instead of annual rings are therefore preferred.

Many cross-sectional cuts of trees show *rays*, that is, bands of tissue that radiate from the center (called *pith*) to the *phloem* and they are essentially *parenchyma* (food-storing) cells and they add to the liveliness of wood.

Table 18 presents some physical properties of some common wood species. The wood density is commonly given for a moisture content of 12%, compared to green wood, which is characteristic for 65% environmental humidity. It is reported that the *softwood* density is generally lower than that of *hardwood* because *softwood* contains more void spaces. The hollow interior of the cells is called the *lumen*, which is containing the water is held in the cavities of the cells (*lumen*) from where it can escape relatively effortlessly, or in the cell walls of the cellulose where it is more firmly held. Balsa, which is the lightest wood of commercial importance, has a density of only 0.11 g cm^{-3} , is lighter than cork (0.24 g cm^{-3}), whereas black ironwood of South Florida has a density of 1.42 g cm^{-3} and therefore does not float in water. Heartwood generally has a higher density than sapwood owing to the deposition of extraneous materials.

The tensile strengths (σ_T) of some representative types of wood are reported in Table 18. The σ_T is considerably larger when wood is stretched parallel to its fibers compared to when it is stretched in its radial direction. This can be understood when knowing that the bonds between the individual cellulose fibers are much weaker compared to those within the crystalline fibrils. Moreover, the tensile strength in compression parallel to the fibers is lower than that in tension since the fibers tend to buckle in compression. This anisotropic behavior is reduced in particle board and plywood, in which small wood chips of random orientations or thin layers of wood (plies) having mutual orientations of 90° are glued together.

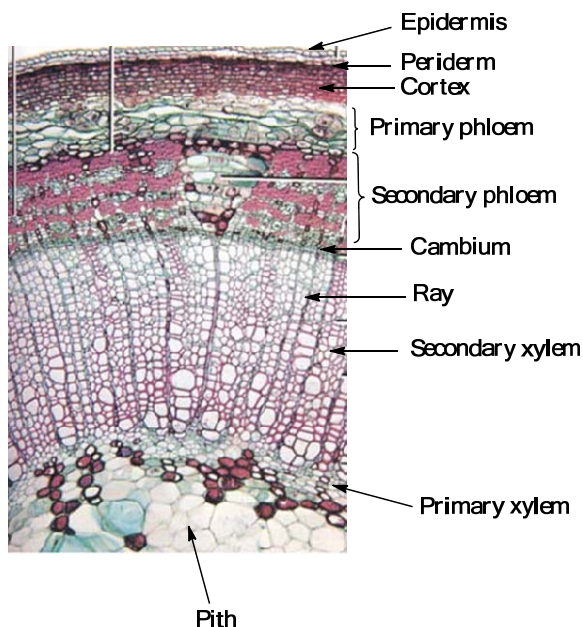


Figure 20. Schematic representation of a cross section of one year wood stems showing *xylem*, *cambium*, *phloem*, *cortex*, and *epidermis*.

The modulus of elasticity for wood is fairly small compared to metals and ceramics, which underscores the well-known elastic properties of wood. The moduli of elasticity in tension, compression, and bending are approximately equal, but the elastic limit is considerably lower for compression than that for tension.

When wood is completely saturated with water is slowly and uniformly dried, the water in the wood evaporates and the wood does not change its dimensions. As a result, no change in the stiffness or strength is observed and further drying to less than about 30% of water content leads to loss some water from the cell walls. At this point the wood shrinks due to the reduced distance between the cells. As a consequence, the densities as well as the bonding between the fibers and thus the strength increase. Therefore, completely dry wood is stronger than green wood but less elastic [1].

8. PAPER

The word “paper” is derived from a reed plant named *Cyperus papyrus*, which was utilized by the Egyptians to make a paper-like material. The Egyptians procedure was as followed, the fibrous layers of the *Cyperus papyrus* stem were placed side by side and crossed at right angles with another identical layer, which were subsequently dampened and pressed. The art of paper-making was invented at about 105 A.D. in China by Ts'ai Lun, who utilized fibers from flax, hemp, and mulberry tree bark. His technique transferred in time to central Asia, Persia, Egypt, Morocco, and eventually, to Europe during the second millennium A.D. There are written documents recorded before that time on *parchment*, which is processed-skin of certain animals such as sheep, goats, and calves. The name “*parchment*” is supposedly derived from the city of Pergamum (today Bergama, Turkey) where *parchment* is said to have originated in the second century B.C. Skins for writing materials were used still earlier, but the *parchment* technique involving better cleaning, stretching, and scraping allowed the utilization of both sides of the skin and thus facilitated books rather than resorting to a rolled manuscript. Particularly fine *parchment*, made from stillborn or newly born calves or lambs, is called *vellum*. However, the *parchment* name is now broadened to include fine paper made from wood and rag pulp.

Now, the most utilized raw material for paper production is wood pulp in addition to other different materials such as flax, cotton scrap (rags), cereal straw, hemp, jute, esparto, inorganic fibers (glass), and synthetic polymer fibers (nylon and polyolefins), which are used for fine or specialty products. Fibers from recycled waste paper are used to produce low-grade paper, paper board, and wrapping paper. Waste paper utilization ranges from 48% (USA) to 3% (Finland) [1].

Paper-making commences with *pulping*, that is, with separating the fibers of wood, etc., either by mechanical means (ground wood pulp) or by chemical solutions which dissolve and remove the lignin and other wood components leaving only cellulose behind. Ground wood pulp is made by involving either a grinder or by passing wood chips through a mill causing a required degree of fragmentation. Therefore, ground wood pulp will contain *all* wood components and is thus not suitable for papers in which high whiteness and permanence are required, while it is highly absorbent and is therefore used for printing and wallpaper. *Chemical wood pulp* is obtained by cooking wood chips in chemical solutions at high

pressures. It is employed when high brightness, strength, and permanence are desired. An optional but environmentally objectionable is *bleaching* process with chlorine whitens the pulp even further, which named alpha or dissolving pulp. Lignin is dissolved in caustic soda [NaOH] + sodium sulfide [Na₂S] (called kraft process), or calcium bisulfate [Ca(SO₃OH)₂] + sulfurous acid [SO₃H₂] [1].

Beating or *refining* is the second step in paper-making, during which the cellulose fibers which are dispersed in aqueous slurry (slush) are mechanically squeezed and pounded. This reduces the size of the fibrils, compact fibrils, makes fibrils flexible, causes fibrils to swell, and makes fibrils slimy. *Beating* also reduces the rate of water drainage and increases the ability of the fibers to bond together when dried. Beating for one hour or more eventually produces a dense paper of high tensile strength, low porosity, and high stiffness. Instead, a sheet from unbeaten pulp is light, fluffy, porous, and weak. Industry predominantly uses the *Hollander beater*, developed in 1690 and it consists of an oval tank in which a heavy roll revolves against a bedplate.

The third step, called *filling* or *loading* mineral pigments, in particular, Kaolin, but also occasionally titanium dioxide (TiO₂) or zinc sulfide (ZnS) are added to improve brightness, opacity, softness, smoothness, and ink receptivity. Fillers are essentially insoluble in water and have, in most cases, no affinity to fibers and therefore, an agent such as alum is added to hold the filler in the future sheet. The amount of filler varies from 1 to 10% of the fiber. Paper that contains only cellulose absorbs substantial quantities of water. This causes water-based ink to readily spread in it. If, however, the paper is impregnated with appropriate substances (called *sizing*), the wetting is prevented. Agents for sizing are starch, glue, casein, resin (from pine tree stumps), waxes, asphalt emulsions, or synthetic resins, to mention a few. Unsized papers are used for facial tissue, paper towels, and blotting paper. Further additives to paper-making include *colorants*, pH controller (acidic paper deteriorates with time), and addition of polymers from the urea-formaldehyde family to provide wet strength to the finished paper.

Sheet forming and *drying* are the last major steps involve in paper-making, which has been done by hand for many centuries. A fine screen contained in a wooden frame is dipped into the fibrous suspension followed by drain of the water through the screen leaving a thin mat of fibers which is removed, squeezed, and dried. Similar principle is used in the modern machines.

The waste water may also be poisonous or have a biochemical oxygen demand which is hazardous to aquatic life. The major problem during large-scale paper production is the waste water which may contain inert solids (slime) that finally settles on the bottoms of rivers or lakes. Recycling of waste water employing filtration, flotation, and sedimentation should therefore be the rule.

The physical properties of papers are classified by basis weight (g m⁻²), thickness (caliper), stretch, tensile strength, tearing strength, bursting strength, folding endurance, stiffness, water resistance, moisture content, color, brightness, gloss, opacity, and transparency. Food and Drug Administration regulate the papers that come in contact with food (packaging). Bank notes papers required specialty maximum strength, durability, color, texture, and feel, while high grade stationary paper is required for papers for Bibles, cigarettes, legal documents, security certificates, and so on. These types of papers are mostly made of cotton or linen fibers that are derived from scraps obtained from the textile industry.

9. VISCOSE OR RAYON (CELLULOSE)

Viscose is a viscous organic liquid used to make art silk, cellophane, rayon (rayon is known by the names *viscose rayon* and art silk in the textile industry [438-443]. It usually has a high luster quality giving it a bright sheen), modal and synthetic velvet. Viscose is becoming synonymous with rayon, a soft material commonly used in shirts, shorts, coats, jackets, and other outer wear. In the 1880s, cellulose was obtained from soft wood and to extrude the resulting substance through narrow nozzles to form regenerated cellulose fibers such as artificial silk, which was later called viscose or rayon. French scientist Hilaire de Chardonnet (1838-1924) invented the first artificial textile fiber and artificial silk (viscose) in Échirolles in 1891. Three British scientists, Charles Frederick Cross, Edward John Bevan, and Clayton Beadle patented the process in 1902 [444]. In France, viscose was called “mother-in-law silk” because of its extremely high flammability. Actually, the first artificial silk have been made in 1879 by J.W. Swan in England for filaments of light bulbs even before Edison made his light lamp version (German H. Goebel, in 1854, was invented the first useful light bulb by the insert of a carbonized bamboo fiber into an evacuated glass flask exactly as Edison made 25 years later). The first rayon stockings for women were manufactured in Germany in 1910. The plant or vegetable fibers are mostly cellulose-based, which are consisted of polymers derived from carbohydrates ($C_nH_{2n}O_n$) which are manufactured by the plant through photosynthesis from water and CO_2 . They include *bast fibers* from stems of plants (jute, flax, hemp, ramie and sunn), *leaf fibers* (abaca, henequen, istle, New Zealand flax and sisal), *palm-type and brush fibers* (coir, raffia, palmyra and piassava), *seed and fruit-hair fibers* (cotton and kapok), and, of course, *wood* from trees [445]. Table 1 contains usage, price, and origin of some of these fibers [1].

9.1. Synthesis of Viscose

Viscose are manufactured from wood by dissolving of wood pulp in caustic soda followed by steeping it for a specified period of time and then shredded and allowed to age (Figure 21). Ageing contributes to viscosity of viscose. The longer the ageing time the more viscosity it will have. The aged pulp is then treated with carbon disulphide to form a yellow-colored cellulose xanthate, which is dissolved in caustic soda again, but of a lower concentration. This is the starting stage of viscose formation. During the process an acetate dope is added to alkali cellulose which is necessary for the yarn luster [446-458].

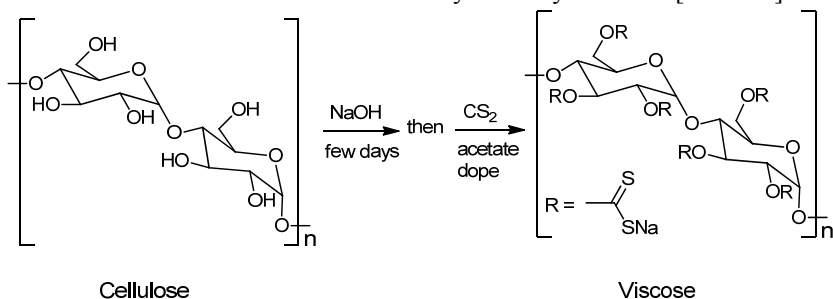


Figure 21. Synthesis of viscose from cellulose of wood pulp.

The U.S. Federal Trade Commission, in early 2010, warned several retailers that six major manufacturers were falsely labeling rayon products as "bamboo", in order to appeal to environmentally conscious consumers. While rayon may be produced with bamboo as a raw material, and the two may be used for similar fabrics (though natural bamboo is not as smooth), rayon is so far removed from bamboo by chemical processing that the two are entirely separate. [443, 459, 460].

Because of the polluting effects of carbon disulfide and other by-products of the viscose producing process, it becomes currently less common and forcing some factories to stop producing viscose [461-464]. Installing a wet sulfuric acid process unit to recover emitted sulfur compounds to sulfuric acid is one way to comply with sulphur emission standards. Another method is to use the Lyocell process which uses *N*-Methylmorpholine *N*-oxide as solvent [457, 465].

10. RUBBER

10.1. Natural Rubber

Natural rubber (an elastic hydrocarbon polymer) is probably the most fascinating natural material known by the Maya name *caoutchouc* [*Caa* = wood and *o-chu* = weeping, i.e., weeping wood]. The purified form of natural rubber is the chemical polyisoprene, which can also be produced synthetically, producing what is sometimes referred to as "synthetic natural rubber". (Figure 22). Latex is a natural polymer of isoprene (most often *cis*-1,4-polyisoprene), with a molecular weight of 100,000 to 1,000,000. Typically, a small percentage (up to 5% of dry mass) of other materials, such as proteins, fatty acids, resins and inorganic materials (salts) are found in natural rubber. Some natural rubber sources called gutta-percha are composed of *trans*-1,4-polyisoprene, a structural isomer which has similar, but not identical, properties [466-469].

Natural rubber is used extensively in many applications and products, as is synthetic rubber. Knowledge of the elastic properties of rubber was brought from Haiti to Europe by Christopher Columbus in 1496, who observed Haiti inhabitants playing with bouncing balls. Later, in 1615, an explorer from Spain reported how "milk" (*latex* [*Latex* (Latin) = fluid]) gathered from incisions made on specific tropical trees was brushed on cloaks, rendering them waterproof after drying, or on earthen, bottle-shaped molds to produce containers. In 1735, a French geographical expedition identified *caoutchouc* as the condensed sap of the *rubber tree* (*Hevea brasiliensis* tree), because rubber has the capability to erase (rub off) pencil marks. *Rubber* trees grow only in a tropical climate that is about ten degrees north or south of the equator and need heavy annual rainfalls of about 250 cm. The rubber tree is cultivated in Malaysia, Ceylon, Southeast Asia, and West Africa, while, wild rubber is still harvested in South America (Brazil and Peru).

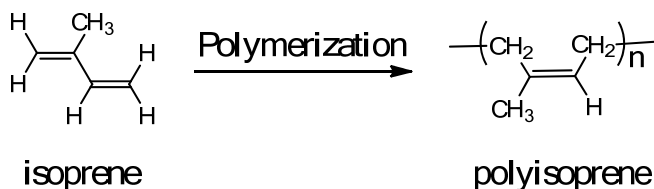


Figure 22. Structure of polyisoprene (natural rubber).

Other plants containing latex include gutta-percha (*Palaquium gutta*) [470-472], rubber fig (*Ficus elastica*) [473-475], Panama rubber tree (*Castilla elastica*) [476], spurges (*Euphorbia* spp.) [477-480], lettuce, common dandelion (*Taraxacum officinale*), Russian dandelion (*Taraxacum kok-saghyz*) [470, 481, 482], Scorzoneria (*tau-saghyz*) [483], and guayule (*Parthenium argentatum*) [472, 484-490]. Although these have not been major sources of rubber, Germany attempted to use some of these during Second World War when it was cut off from rubber supplies. These attempts were later supplanted by the development of synthetic rubbers. To distinguish the tree-obtained version of natural rubber from the synthetic version, the term gum rubber is sometimes used [491, 492].

Because the Latex is only workable when freshly tapped from the rubber tree, Europeans struggled considerably to find solvents for *caoutchouc* to make it spreadable after it arrived in Europe in its “dried” (solid) state. Efforts utilizing turpentine, ether, or naphtha were only partially successful since the waterproofed items, produced from rubber, remained sticky particularly when warm, and turned to dust in hot summers. Moreover, these rubber items were odorous, perishable, and became brittle and even cracked upon the slightest use during extremely cold winters. In the early 1800s, a large number of products were manufactured from rubber such as air mattresses, waterproof mailbags, boots, portable bath tubs, and mackintoshes, which consisted of a mixture of naphtha and rubber sandwiched between double layers of cloth. In England, Thomas Hancock in the 1820s applied a different (nonchemical) approach by built a machine that rapidly cuts rubber into small pieces which generated heat and thus facilitated the fusing of rubber scraps into blocks. This process is called *mastication* [*Mastikhan* (Greek) = to grind the teeth] and is still used in the rubber industry. In the cold winter of 1839, Charles Goodyear of Boston (USA) after considerable experimentation, accidentally dropped a piece of rubber coated with sulfur and lead [other sources say zinc] onto a hot stove. The new substance did not melt as untreated rubber would do and it was durable and retained its elasticity when cold and this technique of *vulcanization* is still used today with very little modification. However, Goodyear’s discovery was made at a time when rubber had a bad reputation because many rubber products had failed in extreme weather. As a consequence, potential investors were reluctant to risk money for the support of additional experimentation. Further, Goodyear was imprisoned for debt more than once, which required him to sell even his children’s school books at one point. Nevertheless, in 1842, Goodyear received a U.S. patent which became probably the most litigated one in history (about 150 suits were filed in the first 12 years). Goodyear received a gold medal for excellence at the international exhibitions in London and Paris in the 1850s, at which he displayed his entire vision about the future of rubber products, including “hard rubber,” which he and his brother Nelson created by extending the heating and sulfurization of *caoutchouc*. Goodyear died in 1860 and left his widow and six children with \$200,000 in debts [1].

In 1888, a British veterinarian, John B. Dunlop, fared much better after he patented and developed the pneumatic rubber tire based on Goodyear's invention, which eventually made the bicycle popular and had an impact on the automobile industry several decades later. High-performance tires such as for trucks are still produced from this exceptional material.

The demand for natural *caoutchouc* has not decreased in this century despite fierce competition from synthetic rubber such as Buna, neoprene, and methyl rubber, which was already produced in Germany in the 1910s.

Natural rubber is an elastomer and a thermoplastic, however, it should be noted that once the rubber is vulcanized, it will turn into a thermoset. Most rubber in everyday use is vulcanized to a point where it shares properties of both; i.e., if it is heated and cooled, it is degraded but not destroyed [493-499].

10.1.1. Elasticity of Rubber

In most elastic materials, such as metals used in springs, the elastic behavior is caused by bond distortions. When force is applied, bond lengths deviate from the (minimum energy) equilibrium and strain energy is stored electrostatically. Rubber is often assumed to behave in the same way, but it turns out this is a poor description. Rubber is a curious material because, unlike metals, strain energy is stored thermally. Also, natural rubber is so elastic that when force is applied, on natural rubber when it is on a surface similar to carpet, it may be difficult to 'pull' across the surface and it will stick. In its relaxed state, rubber consists of long, coiled-up polymer chains that are interlinked at a few points (Figure 22). Between a pair of links, each monomer can rotate freely about its neighbor, thus giving each section of chain leeway to assume a large number of geometries, like a very loose rope attached to a pair of fixed points. At room temperature, rubber stores enough kinetic energy so that each section of chain oscillates chaotically, like the above piece of rope being shaken violently. The entropy model of rubber was developed in 1934 by Werner Kuhn. When rubber is stretched, the "loose pieces of rope" are taut and thus no longer able to oscillate. Their kinetic energy is given off as excess heat. Therefore, the entropy decreases when going from the relaxed to the stretched state, and it increases during relaxation. This change in entropy can also be explained by the fact that a tight section of chain can fold in fewer ways (W) than a loose section of chain, at a given temperature (entropy is defined as $S=k\ln(W)$). Relaxation of a stretched rubber band is thus driven by an increase in entropy, and the force experienced is not electrostatic, rather it is a result of the thermal energy of the material being converted to kinetic energy. Rubber relaxation is endothermic, and for this reason the force exerted by a stretched piece of rubber increases with temperature. (Metals, for example, become softer as temperature increases). The material undergoes adiabatic cooling during contraction. This property of rubber can easily be verified by holding a stretched rubber band to your lips and relaxing it. Stretching of a rubber band is in some ways equivalent to the compression of an ideal gas, and relaxation is equivalent to its expansion. Note that a compressed gas also exhibits "elastic" properties, for instance inside an inflated car tire. The fact that stretching is equivalent to compression may seem somewhat counterintuitive, but it makes sense if rubber is viewed as a one-dimensional gas. Stretching reduces the "space" available to each section of chain.

Natural rubber is often vulcanized, a process by which the rubber is heated and sulfur, peroxide or bisphenol are added to improve resilience and elasticity, and to prevent it from perishing. The development of vulcanization is most closely associated with Charles Goodyear in 1839 [500]. Carbon black is often used as an additive to rubber to improve its

strength, especially in vehicle tires. Vulcanization of rubber creates more disulfide bonds between chains, so it shortens each free section of chain [493-499]. The result is that the chains tighten more quickly for a given length of strain, thereby increasing the elastic force constant and making rubber harder and less extensible. When cooled below the glass transition temperature, the quasi-fluid chain segments "freeze" into fixed geometries and the rubber abruptly loses its elastic properties, although the process is reversible. This is a property it shares with most elastomers (An elastomer is a material with the mechanical or material property that it can undergo much more elastic deformation under stress than most materials and still return to its previous size without permanent deformation). At very low temperatures, rubber is rather brittle; it will break into shards when struck or stretched. This critical temperature is the reason winter tires use a softer version of rubber than normal tires. The failing rubber o-ring seals that contributed to the cause of the Challenger disaster were thought to have cooled below their critical temperature [1].

10.1.2. Natural Rubber Sources and Cultivation

Commercially, natural rubber is obtained almost exclusively from *Hevea brasiliensis* (genus *Hevea*, family Euphorbiaceae), a tall softwood tree indigenous to Brazil. Industry botanists have concentrated their efforts mostly on this species. Among other shrub species, which have received commercial attention are the *Ficus elastic* (Moraceae family), the guayule bush (of the family Asteraceae), and the Russian dandelion (Asteraceae, *alt.* Compositae). Guayule (*Parthenium argentatum*), a rubber-containing desert shrub of the family Asteraceae, native to the north-central plateau of Mexico and the Big Bend area of Texas, is the only other plant under cultivation as a commercial rubber source. In recent years, these and other species have attracted increasing attention, because of diminishing acreage of *Hevea* plantations, increasing demand for high quality rubber with specialty applications, and severe allergic response to the latex based products of the *Hevea*. Guayule has attracted increasing interest as a commercial alternative for hypoallergenic latex. In a number of Latin American countries, hybridization between *Hevea benthamiana* and *Hevea brasiliensis* has provided relatively SALB-free sources of rubber. The molecular mechanism of rubber biosynthesis in other plants (for example, in the fig tree *Ficus carica*) is being investigated with a view to developing alternative rubber crops [309, 501-508].

Hevea brasiliensis and most of the other rubber-yielding species only grow within a well defined area of the tropical and sub-tropical countries, though there are also some rubber-bearing species whose distributional range includes temperate areas (e.g., *Taraxacum kok-saghyz*, native to the Soviet Middle Asia, i.e. Kazakhstan and Kyrgyzstan, and China, as well as other species of the family Compositae) [502, 509-512].

For statistical purpose, rubbery materials extracted from species other than *Hevea Brasiliensis*, including guayule (*Parthenium argentatum*) and gutta-percha (*Palachium gutta*), are conventionally referred to as "Natural Gums" [509-512].

The economic life period of rubber trees in plantations is around 32 years – 7 years of immature phase and about 25 years of productive phase. The soil requirement of the plant is generally well-drained weathered soil consisting of laterite, lateritic types, sedimentary types, non-lateritic red or alluvial soils [506]. The climatic conditions for optimum growth of rubber trees consist of (i) rainfall of around 250 cm evenly distributed without any marked dry season and with at least 100 rainy days per year; (ii) temperature range of about 20 to 34°C with a monthly mean of 25 to 28°C; (iii) high atmospheric humidity of around 80%; (iv)

bright sunshine amounting to about 2000 hours per year at the rate of 6 hours per day throughout the year, and (v) absence of strong winds. Many high-yielding clones have been developed for commercial planting. These clones yield more than 2 tons/ha/year of dry rubber, when grown under ideal conditions.

The first use of rubber was by the Olmecs, who centuries later passed on the knowledge of natural latex from the *Hevea* tree in 1600 BC to the ancient Mayans. They boiled the harvested latex to make a ball for a sport [513-517].

Table 19. Selected rubber-yielding tree common name and species

Common name	Scientific name	Distributional range
Panama rubber tree	<i>Castilla elastica</i> <i>Sessé</i>	America (Mexico; Central America; Western South America) widely naturalized in tropics
West African rubber tree	<i>Ficus vogelii</i> (Miq.) Miq.	Africa (Micronesia; Northeast Tropical Africa; East Tropical Africa; West-Central Tropical Africa; West Tropical Africa; South Tropical Africa; South Africa; Western Indian Ocean)
Lagos silk rubber tree	<i>Funtumia africana</i> (Benth.) Stapf	Africa (East Tropical Africa; West-Central Tropical Africa; West Tropical Africa; South Tropical Africa)
Rubber tree	<i>Hevea brasiliensis</i> (Willd. ex Adr. Juss.) Muell. Arg.	SOUTHERN AMERICA (Brazil; Bolivia; Colombia ; Peru) also cultivated and naturalized elsewhere
False rubber tree	<i>Holarrhena floribunda</i> (G. Don) Durand and Schinz	Africa (West-Central Tropical Africa; West Tropical Africa)
	<i>Funtumia elastica</i>	Africa (Northeast Tropical Africa; East Tropical Africa; West-Central Tropical Africa; West Tropical Africa) also cultivated elsewhere
Indian rubber plant	<i>Ficus elastica</i>	Asia-Tropical (India; China; Malaysia) widely cultivated elsewhere
Guayule	<i>Parthenium argentatum</i>	Northern America (South-Central U.S.A.; Mexico)
Russian	<i>Taraxacum</i>	Asia-Temperate
Dandelion	<i>koksahgyz</i>	Former Soviet Union; China

Source: UNCTAD secretariat (Links: USDA, NRCS. 2005. The Plants Database, Version 3.5. Data compiled from various sources by Mark W. Skinner. National Plant Data Center, Baton Rouge, LA 70874-4490 USA).

10.1.3. Production of Natural Rubber

The supply of natural rubber hinges upon the interplay among several factors, including production capacity, underlying technological change, input and processing costs as well as price differential with synthetic rubber. By the early 1960s synthetic rubbers had overtaken natural rubber in volume. However, natural rubber production grew on average 3.4% a year during 1961-2005 (Rubber World Magazine: http://www.rubberworld.com/RWmarket_report.asp?id=333).

In 2005, the six leading producers -Thailand, Indonesia, Malaysia, India, China and Vietnam - accounted for roughly 89% of world natural rubber production. Combined output in Thailand, Indonesia and Malaysia alone represented around 70% of the global output (Figure 23). Despite the substitution effect with synthetic rubber, world natural rubber production increased from roughly 2.1 million tons in 1961 to over 9.1 million tons in 2005. According to International Rubber Study Group (IRSG) predictions for 2009, the world's production rise for natural rubber should not overcome 3.6% and 3.5% for synthetic rubber. As more, Indonesia should stay the most dynamic market with a rise of 6.8% (IRSG: <http://www.rubberstudy.com/news-article.aspx?id=5020&db=default.aspx>).

Production in Thailand has been increased steadily during 1961-2005, from a reported 186,100 tons in 1961 to over 3 million tons in 2009 (at an average rate of 6.5% per year over the period). It has tended to stabilize for the last two years due to bad weather conditions (heavy rains). Thailand nevertheless remains the world leading natural rubber producing country. Its share of world output has also increased over the years, from as low as 8.8% in 1961 to over 34% in 2009 [518].

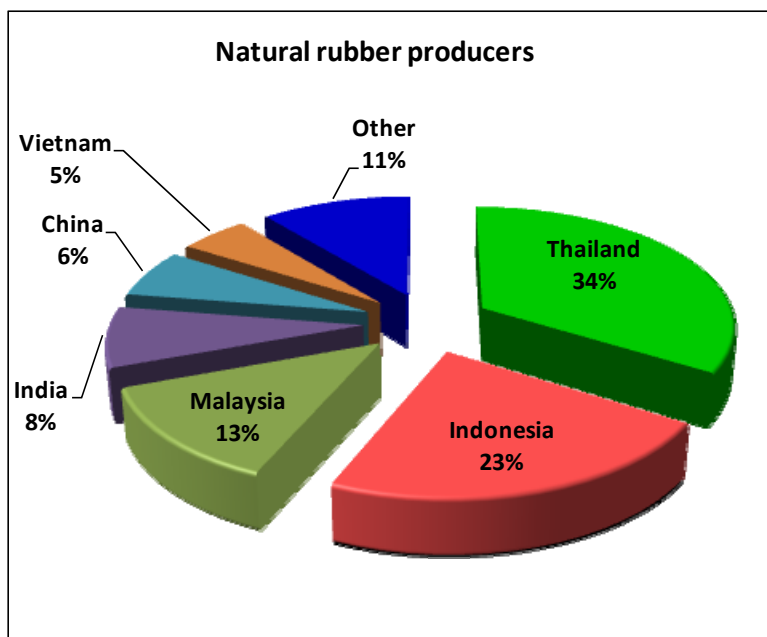


Figure 23. Percentage of natural rubber production by major producing countries.

10.1.4. Consumption of Natural Rubber

Rubbers are intermediate goods used in producing final consumer goods (notably tires). In this respect, demand for a specific type and grade of rubber is derived, since it depends on demand for determined final goods, of which rubbers are only one component. General income, expected price of a specific type and grade of natural rubber and of its substitutes, expected price of final goods, as well as relative processing costs for natural rubber and synthetic rubber can all be regarded as having an impact on natural rubber consumption.

The five largest natural rubber consuming countries are China, the United States of America (USA), Japan, India, and Malaysia. World rubber's consumption was of approximately 21 millions of tons in 2005 (+3.1% growth). The growth is less significant compare to the last four years (especially 2003 with a peak of 6% growth).

China overtook the USA to become the world's top natural rubber consuming country. According to figures from the International Rubber Study Group (IRSG), natural rubber consumption in China grew quite sharply by an average 12% a year throughout 1998-2005 to reach over 1.8 million tons in 2005 (Figure 24). High demand for motor vehicles, and hence for tires, stimulated by the stronger economic growth, together with the spike of oil prices which resulted in higher price for synthetic rubber, contributed to the relatively sharp rise in natural rubber consumption in China.

The USA relinquished its top position in natural rubber consumption since 2001, with continued sharp growth in Chinese rubber consumption and a decline in US consumption (over the 1998-2001 period, -6% per year according to IRSG). As for the other largest consumers, most rubber goes to the tire sector. In the USA, synthetic rubber has traditionally been the major type of rubber consumed.

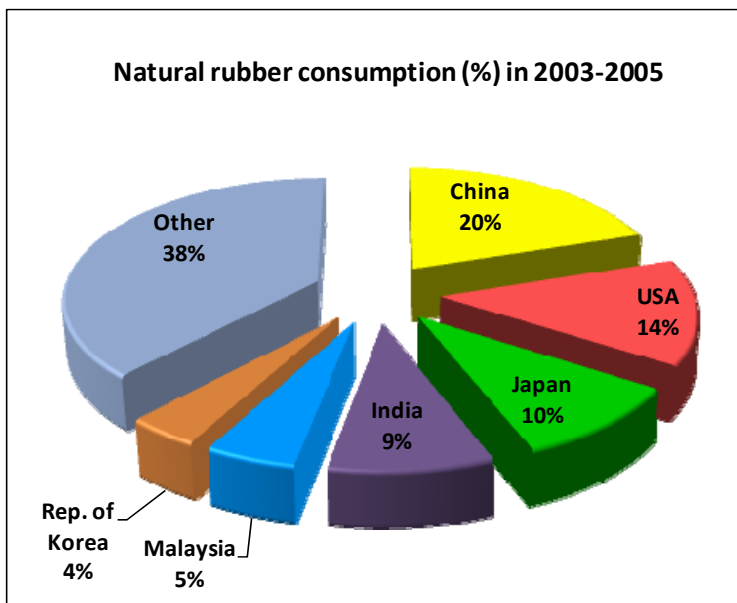


Figure 24. Breakdown of natural rubber consumption by top six consuming countries (%), average 2003-2005.

In Japan, Breakdown consumption allegedly grew during 1998-2005 at the relatively modest rate of 2.8% a year. The decline in the ranking of Japan's rubber consumption was not only a result of the rapid growth of China's rubber industry, but also because of Japanese rubber manufacturers relocating elsewhere.

10.1.5. Uses of Natural Rubber

The use of rubber is widespread, ranging from household to industrial products, entering the production stream at the intermediate stage or as final products. Tires and tubes are the

largest consumers of rubber. The remaining is taken up by the general rubber goods (GRG) sector, which includes all products except tires and tubes.

Other significant uses of rubber are door and window profiles, hoses, belts, matting, flooring and dampeners (anti-vibration mounts) for the automotive industry in what is known as the "under the bonnet" products. Gloves (medical, household and industrial) and toy balloons are also large consumers of rubber, although the type of rubber used is that of the concentrated latex. Significant tonnage of rubber is used as adhesives in many manufacturing industries and products, although the two most noticeable are the paper and the carpet industries (Figure 25). Rubber is also commonly used to make rubber bands and pencil erasers. Many aircraft tires and inner tubes are still made of natural rubber due to the high cost of certification for aircraft use of synthetic replacements.

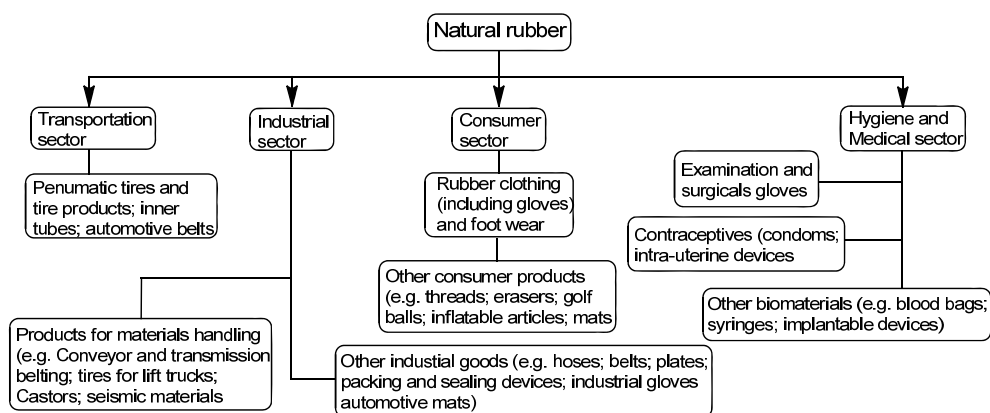


Figure 25. Uses of Natural rubber in different life sectors.

Additionally, rubber produced as a fiber sometimes called *elastic*, has significant value for use in the textile industry because of its excellent elongation and recovery properties. For these purposes, manufactured rubber fiber is made as either an extruded round fiber or rectangular fibers that are cut into strips from extruded film. Because of its low dye acceptance, feel and appearance, the rubber fiber is either covered by yarn of another fiber or directly woven with other yarns into the fabric. For example, in the early 1900s, rubber yarns were used in foundation garments. While rubber is still used in textile manufacturing, its low tenacity limits its use in lightweight garments because latex lacks resistance to oxidizing agents and is damaged by aging, sunlight, oil, and perspiration. Seeking a way to address these shortcomings, the textile industry has turned to Neoprene (polymer form of Chloroprene) (Figure 26), a type of synthetic rubber as well as another more commonly used elastomer fiber, spandex (also known as elastane), because of their superiority to rubber in both strength and durability.

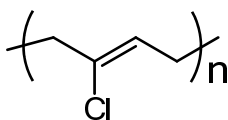


Figure 26. Structure of neoprene rubber (polymer form of Chloroprene).

Despite the competition of synthetic compounds, natural rubber continues to hold an important place in tire consumption. In particular, its superior tear strength and excellent resistance to heat up makes it better suited for high-performance tires used on racing cars, trucks and buses, and aircraft. In these applications, the potential for switching from natural to synthetic rubber is quite limited, given the clear-cut technological advantages to natural rubber. Rubber tires are of two types: solid (or cushion) tires, in which the rubber portion functions to carry the load and absorb shocks; and pneumatic tires, with compressed air that fills the tire. The former are used on industrial machinery and on military vehicles; pneumatic tires are used for almost all free-moving vehicles (i.e., other than railroad cars). Pneumatic tires include tires for automobiles, trucks and buses, (motor) bicycles and airplanes and "off-the-road" tires for special vehicles (such as construction vehicles and agricultural machinery). The distribution channel for pneumatic and solid tires is two-tired, consisting of original equipment manufacturers (OEMs) and the replacement market. Generally, the larger the tire is the greater the share of natural rubber. Figures 27 and 28 refer to relatively small-size truck tires.

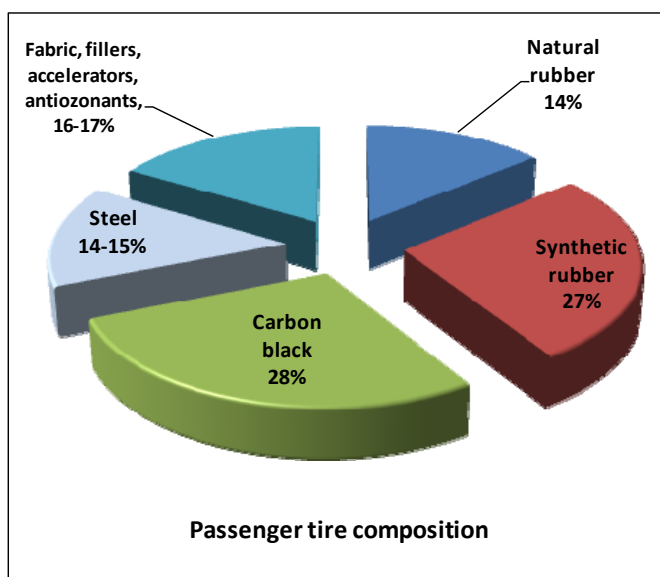


Figure 27. Passenger tire composition.

As for high-performance tires, technical factors (performance needs of the products and process technology) also constrain the ease of substituting synthetic rubber for natural rubber in the latex product market [519]. For example, because it is waterproof (whereas some synthetics absorb water), natural rubber latex is best suited for use in surgical and medical examination gloves and in condoms (Figure 25). Natural rubber latex is possibly the best protection against pathogens such as HIV. Latex products include, inter alia, condoms, gloves, threads, adhesives, and molded foams. They found applications, including specialty applications, in different sectors, among which is the medical and hygiene sector. Overall, the competitive relation between natural and synthetic rubbers hinges upon a variety of related factors, which include technical factors (technical properties of the rubber, performance needs of the product, process technology), economic factors (relative input prices and processing

costs), and relative efficiency of marketing channels. As in the case of contraceptives and high-performance tires, the extent to which substitution from natural rubber to synthetic rubber may take place on the basis of price is limited. It is mostly dependent on technical factors, which also determine the category and grade of elastomers used. Natural rubber is processed in different types and grade with characteristic applications. For example, latex concentrate is the basic constituent of contraceptives, surgical dipped goods, and rubber threads. Ribbed smoked sheets are used in the industrial sector when extra tough rubber is needed (for example, for tank liners). Pale Crepe is valuable for medical sundries, footwear, cements and adhesives. Rubber producers increasingly produced custom-make a wide range of special rubbers that meet customers' specifications. These rubbers are often made by means of compounding natural rubber and synthetics, which also tends to complicate the distinction between natural rubber and synthetic rubber.

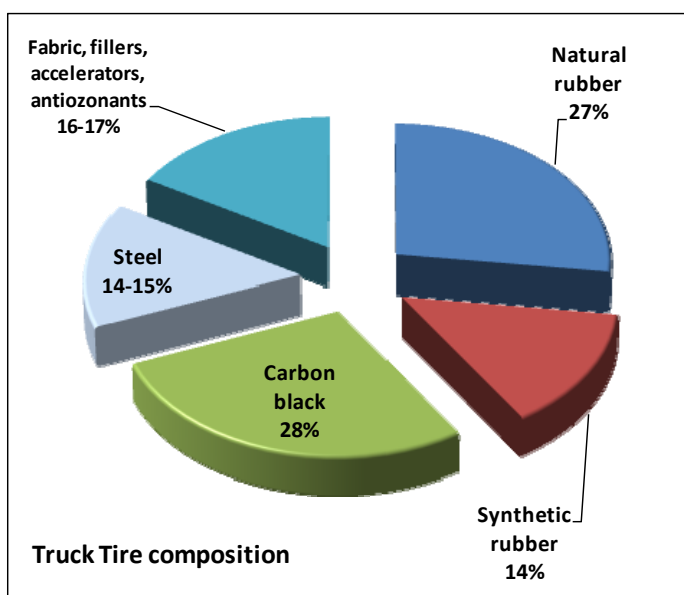


Figure 28. Truck tire composition.

10.2. Synthetic Rubber

Synthetic rubber is any type of artificial elastomer, invariably a polymer. Synthetic rubber serves as a substitute for natural rubber in many cases, especially when improved material properties are required. Nowadays synthetic rubber is used a great deal in printing textile, which is called rubber paste. In most cases titanium dioxide is used with copolymerization and volatile matter in producing such synthetic rubber for textile use. Moreover this kind of preparation can be considered to be the pigment preparation based on titanium dioxide.

Synthetic rubber can be made from the polymerization of a variety of monomers including isoprene (2-methyl-1,3-butadiene produce polyisoprene, Figure 22), 1,3-butadiene (produce polybutadiene), chloroprene (2-chloro-1,3-butadiene; produce neoprene rubber,

Figure 26), and isobutylene (methylpropene) with a small percentage of isoprene for cross-linking (Figure 29). These and other monomers can be mixed in various desirable proportions to be copolymerized for a wide range of physical, mechanical, and chemical properties. The monomers can be produced pure and the addition of impurities or additives can be controlled by design to give optimal properties. Polymerization of pure monomers can be better controlled to give a desired proportion of *cis* and *trans* double bonds.

Bouchardt, in 1879, created one form of synthetic rubber, producing a polymer of isoprene in a laboratory. The expanded use of motor vehicles, and particularly motor vehicle tires, starting in the 1890s, created increased demand for rubber. A team headed by Fritz Hofmann, in 1909, working at the Bayer laboratory in Elberfeld, Germany, also succeeded in polymerizing methyl isoprene, the first synthetic rubber [520, 521]. Scientists in England and Germany developed alternative methods for creating isoprene polymers from 1910–1912.

In 1910, the Russian scientist Sergei Vasiljevich Lebedev created the first rubber polymer synthesized from butadiene, which form of synthetic rubber provided the basis for the first large-scale commercial production, which occurred during First World War as a result of shortages of natural rubber. This early form of synthetic rubber was again replaced with natural rubber after the war ended, but investigations of synthetic rubber continued. Russian American Ivan Ostromislensky did significant early research on synthetic rubber and a couple of monomers in the earlier 1900s. Political problems that resulted from great fluctuations in the cost of natural rubber led to the enactment of the Stevenson Act in 1921. This act essentially created a cartel which supported rubber prices by regulating production, but insufficient supply, especially due to wartime shortages, also led to a search for alternative forms of synthetic rubber. By 1925 the price of natural rubber had increased to the point that many companies were exploring methods of producing synthetic rubber to compete with natural rubber.

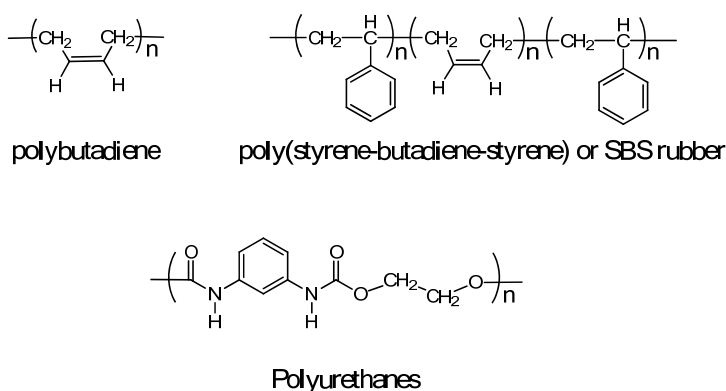


Figure 29. Chemical structure of some synthetic rubber.

In the United States, the investigation focused on different materials than in Europe, building on the early laboratory work of Nieuwland. Studies published in 1930 written independently by Lebedev, the American Wallace Carothers and the German scientist Hermann Staudinger led in 1931 to one of the first successful synthetic rubbers, known as neoprene (Figure 26), which was developed at DuPont under the direction of E.K. Bolton [129]. Neoprene is highly resistant to heat and chemicals such as oil and gasoline, and is used

in fuel hoses and as an insulating material in machinery. The company Thiokol applied their name to a competing type of rubber based on ethylene dichloride which was commercially available in 1930. In 1935, German chemists synthesized the first of a series of synthetic rubbers known as Buna rubbers. These were copolymers, meaning the polymers were made up from two monomers in alternating sequence. The rubber designated GRS (Government Rubber Styrene), a copolymer of butadiene and styrene, was the basis for U.S. synthetic rubber production during Second World War. It still represents about half of total world production. Other brands included Koroseal, which Waldo Semon developed in 1935, and Sovprene, which Russian researchers created in 1940 [522].

Waldo Semon scientist of B.F. Goodrich Company was developed a new and cheaper version of synthetic rubber known as Ameripol in 1940, which made synthetic rubber production much more cost effective, helping to meet the country's needs during Second World War. By 1944, a total of 50 factories were manufacturing it, pouring out a volume of the material twice that of the world's natural rubber production before the beginning of the war [523-525]. Table 20 reports different synthetic rubbers and their common names and ISO standard code.

Table 20. Common synthetic rubbers

Technical Name	Common Names	ISO Standard Code
Acrylonitrile Butadiene	NBR, Nitrile rubber, Perbunan, Buna-N	NBR
Acrylonitrile Butadiene Carboxy Monomer	XNBR, Carboxylated Nitrile	XNBR
Bromo Isobutylene Isoprene	Bromobutyl	BIIR
Chloro Isobutylene Isoprene	Chlorobutyl, Butyl	CIIR
Chlorosulphonated Polyethylene	Hypalon	CSM
Epichlorohydrin	ECO, Epichlorohydrin, Epichlore, Epichloridrine, Herclor, Hydrin	ECO
Ethylene Propylene	Ethylene Propylene	EP
Ethylene Propylene Diene Monomer	EPDM, Nordel	EPDM
Fluorinated Hydrocarbon	Viton, Kalrez, Fluorel, Chemraz	FKM
Fluoro Silicone	FVQM	FVQM
Hydrogenated Nitrile Butadiene	HNBR	HNBR
Isobutylene Isoprene Butyl	Butyl	IIR
Methyl Vinyl Silicone	Silicone Rubber	MVQ
Polybutadiene	Buna CB	BR
Polychloroprene	Chloroprene, Neoprene	CR
Polyisoprene	(Synthetic) Natural Rubber	IR
Polysiloxane	Silicone Rubber	SI
Polyurethane	PU, Polyurethane	PU
Styrene Butadiene	SBR, Buna-S, GRS, Buna VSL, Buna SE	SBR
Styrene Ethylene/Butylene Styrene	SEBS Rubber	SEBS

Synthetic rubbers overtook natural rubber in production and consumption volume since the 1960s. Growth in natural rubber usage has been stronger than that of synthetic rubber for 1998-2005 (a growth rate of 4% -annual average- as compared to 3% for SR). Sharply rising

oil prices, which may add significantly to the costs of major synthetic rubbers producers, and developments in natural rubber pricing relative to synthetic rubbers (the relative natural rubber/ synthetic rubbers % price ratio rose from around 80% to 120% between the start and finish of 2005) have intensified the debate surrounding possibilities for substitution..

In China (the largest single consumer of natural rubber), synthetic rubber consumption increased at an estimated 14% a year over 1998-2005 to reach 2.6 million tons by 2005 (up from 1 million tons in 1998).

11. CORK

Cork is natural material - not fibers - have been used by mankind over the millennia. Cork is harvested from cork oaks (*quercus suber*, which is endemic to southwest Europe and northwest Africa) by stripping their bark, boiling it, and scraping off the outer layer [526-533]. The cork oak is native to the Mediterranean area and is cultivated in Italy, Spain, and Portugal, as well as India [534-539]. The cork oaks trees need to be at least 20 years old but can be stripped again at 8–10-year intervals [540-544].

11.1. Uses of Cork

The Romans as early as 400 B.C. was utilized Cork for sandals, float anchors, and fishing nets. Cork is composed of suberin, a hydrophobic substance, and because of its impermeability, buoyancy, elasticity, and fire resistance, it is used in a variety of products; in the 17th century, cork was used for production of bottle stoppers. Today, cork is used for heat-and-sound insulation, gasket seals, buoys, household goods and linoleum that prepared by mixing cork powder with linseed oil and spreading it over burlap. Cork stoppers represent about 60% of all cork based production. Granules of cork can also be mixed into concrete. The composites made by mixing cork granules and cement have lower thermal conductivity, lower density and good energy absorption [545-547]. Some of the property ranges of the composites are density (400–1500 kg/m³), compressive strength (1–26 MPa) and flexural strength (0.5–4.0 MPa) [526, 548-550]. Figure 30 shows the untreated cork panel.



Figure 30. Untreated cork panel.

Also, cork is used in musical instruments, particularly woodwind instruments, where it is used to fasten together segments of the instrument, making the seams airtight. Conducting baton handles and spacecraft heat shields are also often made out of cork. Cork can be used as bricks for the outer walls of houses and as a core material in sandwich composite construction. Cork is used as the core of both baseballs and cricket balls and inside footwear to improve climate control and comfort. Cork can be used as the friction lining material of an automatic transmission clutch, as designed in certain mopeds [551].

11.2. Production of Cork

There are about 2,200,000 hectares of cork forest worldwide; 32.4% in Portugal, and 22.2% in Spain. Annual production is about 300,000 tons; 52.5% from Portugal, 29.5% from Spain, 5.5% Italy [532, 533]. Once the trees are about 25 years old the cork is stripped from the trunks every ten years. The trees live for about 200 years. The first two harvests produce poorer quality cork (Figure 31).

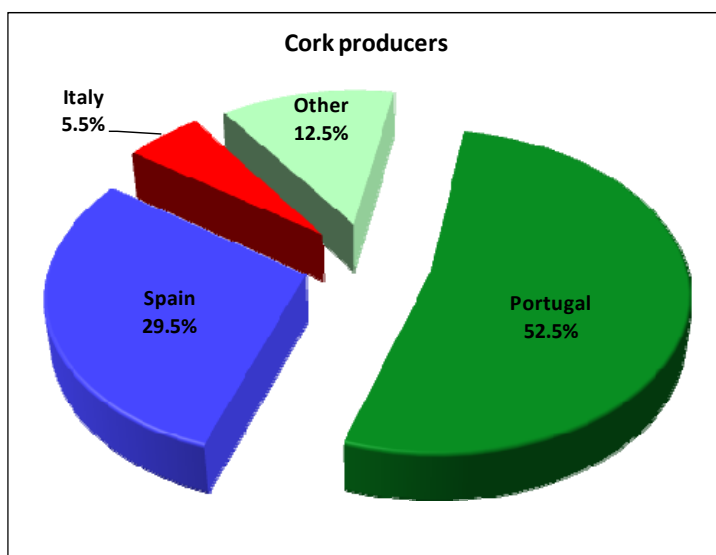


Figure 31. Cork producer countries and their contribution % [552].

12. SPONGES

Sponges are animals of the phylum Porifera (meaning "pore bearers") whose bodies are consisted of jelly-like mesohyl sandwiched between two thin layers of cells and it do not have nervous, digestive or circulatory systems. Instead, most rely on maintaining a constant water flow through their bodies to obtain food and oxygen and to remove wastes, and the shapes of their bodies are adapted to maximize the efficiency of the water flow. While all animals have unspecialized cells that can transform into specialized cells, sponges are unique in having some specialized cells that can transform into other types, often migrating between the main

cell layers and the mesohyl in the process. All sponges are sessile aquatic animals and, although there are freshwater species, the great majorities are marine (salt water) species, ranging from tidal zones to depths exceeding 8,800 m [553, 554].

A few species of sponge that live in food-poor environments have become carnivores that prey mainly on small crustaceans. While most of the known species (approximately 10,000 species) feed on bacteria and other food particles in the water, some host photosynthesizing micro-organisms as endosymbionts and these alliances often produce more food and oxygen than they consume [553, 554].

Most sponge species use sexual reproduction, releasing sperm cells into the water and meeting ova that in species are released and others are retained the "mother". The fertilized eggs form larvae which swim off in search of places to settle. Sponges are known for regenerating from fragments that are broken off, although this only works if the fragments include the right types of cells. A few species reproduce by budding. When conditions deteriorate, for example as temperatures drop, many freshwater species and a few marine ones produce survival pods "gemmules" of unspecialized cells that remain dormant until conditions improve and then either form completely new sponges or re-colonize the skeletons of their parents.

The mesohyl functions as an endoskeleton in most sponges, and is the only skeleton in soft sponges that encrust hard surfaces such as rocks. More commonly the mesohyl is stiffened by mineral spicules, by spongin fibers or both. Demosponges use spongin, and in many species silica spicules and in some species calcium carbonate exoskeletons. Demosponges constitute about 90% of all known sponge species, including all freshwater ones, and have the widest range of habitats. Calcareous sponges, which have calcium carbonate spicules and in some species calcium carbonate exoskeletons are restricted to relatively shallow marine waters where production of calcium carbonate is easiest. The fragile glass sponges, with "scaffolding" of silica spicules, are restricted to Polar Regions and the ocean depths where predators are rare. Fossils of all of these types have been found in rocks dated from 580 million years ago. In addition Archaeocyathids, whose fossils are common in rocks from 530 to 490 million years ago, are now regarded as a type of sponge [553, 554].

It is generally thought that the sponge's closest single-celled relatives are choanoflagellates, which strongly resemble the cells that sponges use to drive their water flow systems and capture most of their food. It is also generally agreed that sponges do not form a monophyletic group, in other words do not include all and only the descendants of a common ancestor, because it is thought that Eumetazoa (more complex animals) are descendants of a sub-group of sponges. However it is uncertain which group of sponges is closest to Eumetazoa, as both calcareous sponges and a sub-group of demosponges called Homoscleromorpha have been nominated by different researchers. In addition a study in 2008 suggested that the earliest animals may have been similar to modern comb jellies.

The few species of demosponge that have entirely soft fibrous skeletons with no hard elements have been used by humans over thousands of years for several purposes, including as padding and as cleaning tools. However by the 1950s these had been over-fished so heavily that the industry almost collapsed, and most sponge-like materials are now synthetic. Sponges and their microscopic endosymbionts are now being researched as possible sources of medicines for treating a wide range of diseases [553, 554].

Sponges are removed by skin divers from tidal levels to depths of about 70 meters, particularly in the Eastern Mediterranean area and on the West coast of Florida [555].

12.1. Uses of Sponge

The ancient Greeks and Romans have been utilized sponges for applying paint, as mops, and as substitutes for drinking vessels. The calcium carbonate or silica spicules of most sponge genera make them too rough for most uses, but two genera, *Hippospongia* and *Spongia*, have soft, entirely fibrous skeletons.

Early Europeans used soft sponges for many purposes, including padding for helmets, portable drinking utensils and municipal water filters. Until the invention of synthetic sponges, they were used as cleaning tools, applicators for paints and ceramic glazes and discreet contraceptives. However by the mid-20th century, over-fishing brought both the animals and the industry close to extinction [556]. Many objects with sponge-like textures are now made of substances not derived from poriferans. Synthetic sponges include personal and household cleaning tools, breast implants [557], and contraceptive sponges [558]. Typical materials used are cellulose foam, polyurethane foam, and less frequently, silicone foam. The luffa "sponge", also spelled loofah, which is commonly sold for use in the kitchen or the shower, is not derived from an animal but from the fibrous "skeleton" of a gourd (*Cucurbitaceae*) [559].

A report in 1997 described use of sponges as a tool by bottlenose dolphins in Shark Bay. A dolphin will attach a marine sponge to its rostrum, which is presumably then used to protect it when searching for food in the sandy sea bottom [560]. The behavior, known as sponging, has only been observed in this bay, and is almost exclusively shown by females. A study in 2005 concluded that mothers teach the behavior to their daughters, and that all the sponge-users are closely related, suggesting that it is a fairly recent innovation [561].

In the Middle Ages, burned sponges were used as medicine. Sponges have medicinal potential due to the presence in sponges themselves or their microbial symbionts of chemicals that may be used to control viruses, bacteria, tumors and fungi [562-564].

13. ASBESTOS

The term "*asbestos*" has been given to six naturally occurring mineral fibers that have been used for commercial purposes. *Asbestos* [*Asbestos* (Greek) = indestructible] is the major member of the natural mineral fibers group of about 30 crystalline magnesium silicates (MgSiO_3) (Figure 32). Asbestos can be found in hundreds of countries on just about every continent. These fibers belong to two separate mineral groups, known as *serpentine* (usually of a curly form, contains only one asbesti-form variety, referred to as *chrysotile*) and *amphibole* (it is straight and needle-like, contains five asbesti-form varieties: *anthophyllite*, *grunerite* (*amosite*), *riebeckite* (*crocidolite*), *tremolite*, and *actinolite*) [565-567].

Asbestos has been commonly used in a variety of building construction materials for insulation, high electrical resistance and as a fire-retardant. Because of its fiber strength and heat resistant properties, asbestos has been used for a wide range of manufactured goods, mostly in building materials (roofing shingles, ceiling and floor tiles, paper products, and asbestos cement products), friction products (automobile clutch, brake, and transmission parts), heat-resistant fabrics, packaging, gaskets, and coatings. The fire-resistant property of asbestos was known to the Greeks as was documented during the first century A.D. by a

Roman historian. Also, Marco Polo reported that the Chinese knew about asbestos in the thirteenth century A.D.

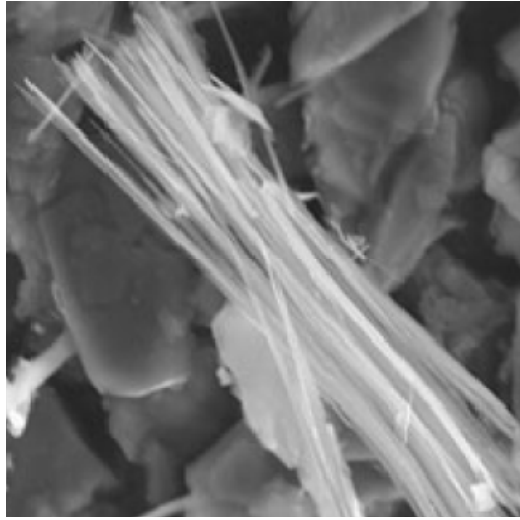


Figure 32. Asbestos.

The mineral's innate resistance to heat, fire and conduct electricity is what has made asbestos so important in both industrial and domestic products. The asbestos fibers are fine, flexible and can be spun into thread and woven into cloth that is flame-proof, difficult to tear, and carries excellent insulation properties. It is virtually indestructible by heat, salt water, corrosive chemicals (especially alkalis), and any chemical or biological process. The fibers mix well into other materials, such as asphalt or cement, and make such products stronger, more flexible, and fire-retardant. They do not dissolve or evaporate with water, which makes the light fibers easy to mix [565].

There are six recognized asbestos minerals, which are considered silicates include:

- I. *Chrysotile* - (Also known as white or green asbestos, from the Greek word meaning "fine, silky hair") Appears as curly, whitish fibers and constitutes 95% of the world production. Scientists believe this to be the least toxic of all asbestos forms. *Chrysotile* is mined throughout the world, but most of the United State's *chrysotile* supply comes from Canada, Africa, and former USSR.
- II. *Crocidolite* - (Also known as *riebeckite* or blue asbestos) Composed of straight fibers, most *crocidolite* comes from southern Africa and Australia. It is believed to be the most toxic form of all asbestos minerals.
- III. *Amosite* - (Also known as *cummingtonite-grunerite* or brown asbestos) The trade name "*amosite*" is an acronym for Asbestos Mines of South Africa, after the Amosa mines. *Amosite* is also straight in shape, but brittle in structure and excellent for use in heat insulation.
- IV. *Anthophyllite* - This form of asbestos is brittle, white, and contains various forms of iron. It has been found to have excellent resistance to chemicals and heat.

- V. *Tremolite* - In rough form, *tremolite* appears white and chalky. *Tremolite* can also be naturally found in other mineral forms aside from asbesti-form. It has been the major ingredient in industrial and commercial talc.
- VI. *Actinolite* – It typically prismatic, flat in structure, and elongated. *Actinolite* also comes in forms other than asbesti-form and has poor resistance to chemicals.

The last five amphibole (which translates to "ambiguous" in Greek) types have a slightly more complex crystal structure than *chrysotile* and are not used as extensively in commercial products as *chrysotile*. Due to their structure, amphiboles tend to stay in the lungs longer than *chrysotile* and are more likely to cause illness because of this factor. Some hypothesize very small contaminations of amphibole fibers within *chrysotile* are most to blame for cancer deaths caused by asbestos exposure.

Now, *Asbestos* is no longer utilized for general applications because of its health hazards to the lungs [565, 568-572]. Worldwide, 60 countries (including those in the European Union) have banned the use of asbestos, in whole or in part. The problem with asbestos arises when the fibers become airborne and are inhaled. Because of the size of the fibers, the lungs cannot expel them. They are also sharp and penetrate tissues. Health problems attributed to asbestos include the following:

- I. *Asbestosis* - A lung disease first found in textile workers, asbestosis is a scarring of the lung tissue from an acid produced by the body's attempt to dissolve the fibers. The scarring may eventually become so severe that the lungs can no longer function. The latency period (meaning the time it takes for the disease to develop) is often 10–20 years.
- II. *Mesothelioma* - A cancer of the mesothelial lining of the lungs and the chest cavity, the peritoneum (abdominal cavity) or the pericardium (a sac surrounding the heart). Unlike lung cancer, *mesothelioma* has no association with smoking. The only established causal factor is exposure to asbestos or similar fibers. The latency period for *mesothelioma* may be 20–50 years. The prognosis for *mesothelioma* is grim, with most patients dying within 12 months of diagnosis [573].
- III. *Cancer* - Cancer of the lung, gastrointestinal tract, kidney and larynx have been linked to asbestos. The latency period for cancer is often 15–30 years [574].
- IV. *Diffuse pleural thickening* and also asbestos exposure increases the risk of gastrointestinal, colorectal, throat, kidney, esophageal, and gallbladder cancer. Those who suspect they may have been exposed to asbestos should speak with a doctor to be medically assessed for asbestos exposure.

14. NYLON

Nylon is a synthetic polymer made of repeating units linked by amide bonds and is frequently referred to as polyamide has thermoplastic silky properties. It was first produced on February 28, 1935 at the DuPont Experimental Station. It was followed the manufactured of rayon and it can be created from coal or oil. These new products challenged the monopoly of natural fibers for textile and industrial uses [1, 129].

Nylon was first used commercially in a nylon-bristled toothbrush (1938), followed more famously by women's stockings ("nylons"; 1940). Nylon was the first commercially successful synthetic polymer. There are two common methods of making nylon for fiber applications. Nylon was intended to be a synthetic replacement for silk and substituted for it in many different products after silk became scarce during Second World War. It replaced silk in military applications such as parachutes and flak vests, and was used in many types of vehicle tires.

14.1. Uses of nylon

Nylon fibers are used in many applications, including fabrics, bridal veils, carpets, musical strings, and rope. It was also used to make tires, tents, ropes, ponchos, and other supplies for the military. It was even used in the production of a high-grade paper for U.S. currency. Solid nylon is used for mechanical parts such as machine screws, gears and other low- to medium-stress components previously cast in metal. Engineering-grade nylon is processed by extrusion, casting, and injection molding. Solid nylon is used in hair combs. Type 6,6 Nylon 101 is the most common commercial grade of nylon, and Nylon 6 is the most common commercial grade of molded nylon. Nylon is available in glass-filled variants which increase structural and impact strength and rigidity, and molybdenum sulfide-filled variants which increase lubricity [575].

Now, various types of nylons are being manufactured in the form of fiber, sheets, and molded plastics. They are being used to make a wide range of products, such as clothing, pantyhose, parachutes, toothbrush bristles, fishing lines, nets, carpet fiber, airbag fiber, slings, rope for climbing gear, automobile parts, including manifolds and gasoline tanks, machine parts, such as gears and bearings, metalized balloons, classical and flamenco guitar strings, paintball marker bolts, racquetball, squash, and tennis racquet strings.

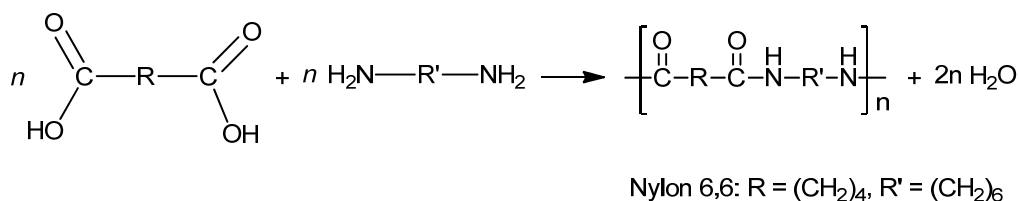
14.2. Synthesis of Nylon

Nylons are formed by reaction of equal parts of a diamine and a dicarboxylic acid, so that amides are formed at both ends of each monomer in a process analogous to polypeptide biopolymers. Chemical elements included are carbon, hydrogen, nitrogen, and oxygen. The numerical suffix specifies the numbers of carbons donated by the monomers; the diamine first and the diacid second. The most common variant is nylon 6,6 which refers to the fact that the diamine (1,6-diaminohexane) and the diacid (adipic acid, hexane-1,6-dicarboxylic acid) each donate 6 carbons to the polymer chain (Figure 33). As with other regular copolymers like polyesters and polyurethanes, the "repeating unit" consists of one of each monomer, so that they alternate in the chain. Since each monomer in this copolymer has the same reactive group on both ends, the direction of the amide bond reverses between each monomer, unlike natural polyamide proteins which have overall directionality: C terminal → N terminal. In the laboratory, nylon 6-6 can also be made using adipoyl chloride instead of adipic acid.

It is difficult to get the proportions exactly correct, and deviations can lead to chain termination at molecular weights less than a desirable 10,000 daltons. To overcome this problem, a crystalline, solid "nylon salt" can be formed at room temperature, using an exact

1:1 ratio of the acid and the base to neutralize each other followed by heating the reaction mixture to 285°C to complete the salt reaction to form nylon polymer [576-578]. It is impossible to spin the nylon chains above 20,000 daltons into yarn. To combat this problem; some acetic acid is added to react with a free amine end group during polymer elongation to limit the molecular weight. In practice, and especially for 6,6, the monomers are often combined in a water solution. The water used to make the solution is evaporated under controlled conditions, and the increasing concentration of "salt" is polymerized to the final molecular weight.

First approach



Second approach

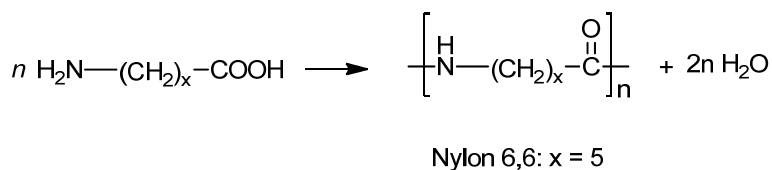


Figure 33. The two approach for synthesis of nylon.

DuPont patented [579] nylon 6,6, so in order to compete, other companies (particularly the German BASF) developed the homopolymer nylon 6 (polycaprolactam), which is not a condensation polymer, but formed by a ring-opening polymerization [129]. The peptide bond within the caprolactam is broken with the exposed active groups on each side being incorporated into two new bonds as the monomer becomes part of the polymer backbone. In this case, all amide bonds lie in the same direction, but the properties of nylon 6 are sometimes indistinguishable from those of nylon 6,6; except for melt temperature and some fiber properties in products like carpets and textiles. There is also nylon 9. The 220 °C melting point of nylon 6 is lower than the 265°C melting point of nylon 6,6. Nylon 5,10, made from pentamethylene diamine and sebacic acid, was studied by Carothers even before nylon 6,6 and has superior properties, but is more expensive to make. In keeping with this naming convention, "nylon 6,12" (N-6,12) or "PA-6,12" is a copolymer of a 6 C diamine and a 12 C diacid. Similarly for N-5,10 N-6,11; N-10,12, etc. Other nylons include copolymerized dicarboxylic acid/diamine products that are not based upon the monomers listed above. For example, some aromatic nylons are polymerized with the addition of diacids like terephthalic acid (→ Kevlar Twaron) or isophthalic acid (→ Nomex), more commonly associated with polyesters. There are copolymers of N-6,6/N6; copolymers of N-6,6/N-6/N-12; and others. Because of the way polyamides are formed, nylon would seem to be limited to unbranched, straight chains. But "star" branched nylon can be produced by the condensation of

dicarboxylic acids with polyamines having three or more amino groups. A molecule of water is given off and the nylon is formed. Its properties are determined by the R and R' groups in the monomers. In nylon 6,6, R = 4 C and R' = 6 C alkanes, but one also has to include the two carboxyl carbons in the diacid to get the number it donates to the chain. In Kevlar, both R and R' are benzene rings (Figure 33).

15. PLASTICS

A *plastic* material is any of a wide range of synthetic or semi-synthetic organic solids used in the manufacture of industrial products. Plastics are typically polymers of high molecular mass, and may contain other substances to improve performance and/or reduce costs. Monomers of plastic are either natural or synthetic organic compounds [1].

There are two types of plastics: thermoplastics and thermosetting polymers [580-584]. Thermoplastics are the plastics that don't undergo chemical change in their composition when heated and can be molded again and again; examples are polyethylene, polystyrene, polyvinyl chloride and polytetrafluoroethylene. Thermosets can melt and take shape once; after they have solidified, they stay solid (Table 21).

In 1846, plastics start by Professor Schönbein, a German chemist who taught at the University of Basel (Switzerland), when he spilled an aggressive mixture of sulfuric acid and nitric acid in his wife's kitchen for quick mopped it up. His wife's cotton apron contacted with these two strong acids was immediately rinsed the apron in running water and hung it up to dry near the stove. Soon afterwards the cotton apron ignited and burned to dust, which was the birth of smokeless *gun cotton* and more importantly, it was the birth of man-made plastics. A transformation took place to convert relatively inert cellulose into reactive *cellulose nitrate*. Specifically, a new compound was formed in which some of the hydroxyl groups (-OH) of the cellulose polymer converted into oxygen nitrate groups (-O-NO₂), whereby the sulfuric acid served as a catalyst. In short, Schönbein's discovery opened the door to a completely new world, namely, that of synthetic (or semi-synthetic) polymeric materials called *plastics* [1, 585, 586].

Interestingly enough, some important differences between various cellulose nitrates are existed. Completely nitrated cellulose is explosive modification form and is called *trinitrate* of cellulose. On the other hand, the lesser nitrated (dinitrate, which contains many residual hydrogen bonds), is no longer explosive, but still highly flammable. The flammability can be reduced by decreasing the nitrate number via denitration using sodium bisulfate or other substances [1, 586, 587].

Cellulose nitrate, in contrast to cellulose, can be dissolved in a number of organic liquids such as in 1:1 mixture of ether and alcohol. Moreover, *nitrocellulose* is pliable at elevated temperatures and thus can be molded into objects that retain their form and are hard after cooling. Nitrocellulose is called a thermoplastic [*Thermos* (Greek) = warm; *plasticos* (Greek) = to shape, to form] material because it can be reshaped as often as desired by renewed heating. For this reason, the applications have been manifold, for example, artificial silk can be spun from cellulose nitrate solutions, which was accomplished in 1884 by the French Count de Chardonnet. Somewhat before that time, i.e., in 1879, J.W. Swan experimented with filaments for electric light bulbs made of artificial silk. The early movie industry would not

have been possible without thin cellulose nitrate layers, called *films*, on which a light-sensitive emulsion was cast. However, because of their flammability, cellulose nitrate films now have been replaced by other substances [588-590].

In 1863, the New England firm of Phelan and Collander, which manufactured billiard balls made of ivory, became concerned about the ever increasing slaughter of elephants whose tusks provided the raw material for their products. Their demand was in direct competition with that of other companies which utilized ivory for jewelry, piano keys, ornaments, and knife handles. In the 1860s, about 100,000 elephants per year had to give their lives by a large number of hunters to satisfy the demand of the world's ivory industry. No wonder that the above-mentioned manufacturers were worried about a possible extinction of the elephant raw material and they offered \$10,000 (in gold) handsome price to the person who would be able to produce a suitable synthetic substitute. The American journeyman printer John Hyatt found that collodion (a solution of nitrocellulose in ether and alcohol, which printers use to coat their fingertips to keep them from getting scorched by hot lead) when spilled out and had turned into a tough, flexible, solid layer. This gave Hyatt the idea to try collodion as a material for billiard balls making, but there was one big drawback of these billiard balls: each time they collided with force; they exploded and caused every man in a saloon to pull his gun. Experimental done by Hyatt led to add some of camphor compound (obtained from tree) to nitrocellulose to decrease its degree of nitrification that resulted in a thermoplastic material, originally called *artificial ivory* but later named *celluloid*. Billiard balls made of celluloid was found to be somewhat too brittle, while other products made from celluloid such as combs, ping-pong balls, films, photographic and dental plates were quite successful. The only shortfall of celluloid is still inflames quite readily [1, 586].

Cellulose nitrate, celluloid, and galalith [*Gala* (Greek) = milk; *lithos* (Greek) = stone. A product developed by Krische and Spitteler of Germany in 1897 from milk casein, kaolin, and Formaldehyde] are made of natural materials that are chemically converted into new compounds. These products showed no creation of new polymer but a modification of natural polymers is performed and therefore it classified as semi-synthetics [1, 586].

On the other hand, Amero-Belgian L.H. Baekeland in 1906 invented a *fully synthetic* organic polymer (resin) was made of various phenols (C_6H_5OH) by heating with formaldehyde (CH_2O) under pressure that yielded an insoluble and hard plastic. *Bakelite*, as it was called, is inert against solvents and is a good electrical and heat insulator. Bakelite and other phenolic resins are *retained* their shape upon heating and are therefore called *thermosets* such as epoxies, polyesters, and phenolic resins. Consequently, they have a good dimensional stability. The third category of plastics is called *elastomers*. Natural rubber and vulcanized rubber are belonging to this family of materials. Table 21 reported some of the common and special purpose plastics and their uses. Also there are many other types of plastics such as conductive polymer, corn construction, Molding (process: flexible mold and injection molding), films, light activated resin, nurdle, organic light emitting diode, plastics engineering, plastics extrusion, plasticulture, progressive bag alliance, roll-to-roll processing, self-healing plastic, thermoforming, timeline of materials technology [1, 586].

The biggest threat to the conventional plastics industry is most likely to be environmental concerns, including the release of toxic pollutants, greenhouse gas, litter, biodegradable and non-biodegradable landfill impact as a result of the production and disposal of petroleum and petroleum-based plastics. Of particular concern has been the recent accumulation of enormous quantities of plastic trash in ocean gyres [591-595]. For decades one of the great

appeals of plastics has been their low price. Yet in recent years the cost of plastics has been rising dramatically. A major cause is the sharply rising cost of petroleum, the raw material that is chemically altered to form commercial plastics. With some observers suggesting that future oil reserves are uncertain, the price of petroleum may increase further. Therefore, alternatives are being sought. Oil shale and tar oil are alternatives for plastic production but are expensive. Companies and research organizations around the world are experimenting with plant-based plastics in a bid to lower carbon dioxide emissions and reduce the use of petroleum as oil stocks decline. Now researchers led by chemical engineer James Dumesic at the University of Wisconsin, Madison, have developed an efficient way to convert fructose into a polymer precursor [596].

Table 21. Common and special purpose plastics their uses

Plastic Name	Acronym	Uses
Polyester	PES	Fibers, textiles.
Polyethylene terephthalate	PET	Carbonated drinks bottles, peanut butter jars, plastic film, microwavable packaging.
Polyethylene	PE	Wide range of inexpensive uses including supermarket bags, plastic bottles.
High-density polyethylene	HDPE	Detergent bottles and milk jugs.
Polyvinyl chloride	PVC	Plumbing pipes and guttering, shower curtains, window frames, flooring.
Polyvinylidene chloride	PVDC (Saran)	Food packaging.
Low-density polyethylene	LDPE	Outdoor furniture, siding, floor tiles, shower curtains, clamshell packaging.
Polypropylene	PP	Bottle caps, drinking straws, yogurt containers, appliances, car fenders (bumpers), plastic pressure pipe systems.
Polystyrene	PS	Packaging foam/"peanuts", food containers, plastic tableware, disposable cups, plates, cutlery, CD and cassette boxes.
High impact polystyrene	HIPS	Refrigerator liners, food packaging, and vending cups.
Polyamides	PA (Nylons)	Fibers, toothbrush bristles, fishing line, under-the-hood car engine moldings.
Acrylonitrile butadiene styrene	ABS	Electronic equipment cases (e.g., computer monitors, printers, keyboards), drainage pipe.
Polycarbonate	PC	Compact discs, eyeglasses, riot shields, security windows, traffic lights, lenses.
Polycarbonate/Acrylonitrile Butadiene Styrene	PC/ABS	A blend of PC and ABS that creates a stronger plastic. Used in car interior and exterior parts, and mobile phone bodies.
Polyurethanes	PU	Cushioning foams, thermal insulation foams, surface coatings, printing rollers (Currently 6th or 7 th most commonly used plastic material, for instance the most commonly used plastic found in cars).
Melamine formaldehyde	MF	One of the aminoplasts, and used as a multi-colorable alternative to phenolics, for instance in moldings (e.g., break-resistance alternatives to ceramic cups, plates and bowls for children) and the decorated top surface layer of the paper laminates (e.g., Formica).

Table 21. Continued

Plastic Name	Acronym	Uses
Plastarch material	PM	Biodegradable and heat resistant, thermoplastic composed of modified corn starch.
Phenolics or phenol formaldehydes	PF	High modulus, relatively heat resistant, and excellent fire resistant polymer. Used for insulating parts in electrical fixtures, paper laminated products (e.g., Formica), thermally insulation foams. It is a thermosetting plastic, with the familiar trade name Bakelite, that can be molded by heat and pressure when mixed with a filler-like wood flour or can be cast in its unfilled liquid form or cast as foam (e.g., Oasis). Problems include the probability of moldings naturally being dark colors (red, green, brown), and as thermoset it is difficult to recycle.
Polyetheretherketone	PEEK	Strong, chemical- and heat-resistant thermoplastic, biocompatibility allows for use in medical implant applications, aerospace moldings. One of the most expensive commercial polymers.
Polyetherimide	PEI (Utem)	A high temperature, chemically stable polymer that does not crystallize.
Polylactic acid	PLA	A biodegradable, thermoplastic found converted into a variety of aliphatic polyesters derived from lactic acid which in turn can be made by fermentation of various agricultural products such as corn starch, once made from dairy products.
Polymethyl methacrylate	PMMA	Contact lenses, glazing (best known in this form by its various trade names around the world; e.g., Perspex, Oroglass, Plexiglas), aglets, fluorescent light diffusers, rear light covers for vehicles. It forms the basis of artistic and commercial acrylic paints when suspended in water with the use of other agents.
Polytetrafluoroethylene	PTFE	Heat-resistant, low-friction coatings, used in things like non-stick surfaces for frying pans, plumber's tape and water slides. It is more commonly known as Teflon.
Urea-formaldehyde	UF	One of the aminoplasts and used as a multi-colorable alternative to phenolics. Used as a wood adhesive (for plywood, chipboard, hardboard) and electrical switch housings.

(<http://dwb.unl.edu/Teacher/NSF/C06/C06Links/qlink.queensu.ca/~6jrt/chem210/Page3.html>).

15.1. Biodegradable Plastics

Research has been done on biodegradable plastics that break down with exposure to sunlight (e.g., ultraviolet radiation), water or dampness, bacteria, enzymes, wind abrasion and some instances rodent pest or insect attack are also included as forms of biodegradation or environmental degradation [597-600]. It is clear some of these modes of degradation will only work if the plastic is exposed at the surface, while other modes will only be effective if certain conditions exist in landfill or composting systems. Starch powder has been mixed with plastic as a filler to allow it to degrade more easily, but it still does not lead to complete

breakdown of the plastic. Some researchers have actually genetically engineered bacteria that synthesize a completely biodegradable plastic, but this material, such as Biopol, is expensive at present. The German chemical company BASF makes Ecoflex, fully biodegradable polyester for food packaging applications [601].

Oxo-biodegradable (OBD) plastic is polyolefin plastic to which has been added very small (catalytic) amounts of metal salts [602-604]. As long as the plastic has access to oxygen (as in a littered state), these additives catalyze the natural degradation process to speed it up so that the OBD plastic will degrade when subject to environmental conditions. Once degraded to a small enough particle they can interact with biological processes to produce to water, carbon dioxide and biomass. The process is shortened from hundreds of years to months for degradation and thereafter biodegradation depends on the micro-organisms in the environment. Typically this process is not fast enough to meet Standard Specification for Compostable Plastics (ASTM D6400) standards for definition as compostable plastics [605]. The ASTM D6400 standard requires 60% biodegradation within 180 days. This requirement is similar to the requirements of ISO 14855 and DIN V49000, but differs from the stricter EN 13432 standards, which requires 90% biodegradation in that time. The ASTM D6400 standard provides two separate definitions:

(i) Biodegradable Plastic: the degradation results from the action of naturally occurring microorganisms such as bacteria, fungi and algae. (ii) Compostable Plastic: a plastic that undergoes degradation by biological processes during composting to yield CO₂, water, inorganic compounds and biomass at a rate consistent with other compostable materials and leaves no visible, distinguishable or toxic residue [606, 607].

15.2. Polymerization

Eduard Simon, in 1839, found that when he heated an organic liquid called *styrene*, obtained from an Asian tree having the botanical name *Liquambar orientalis* and whose sap was used 3000 years ago by Egyptians for embalming bodies, to 200°C did not yield a gas as observed for other substances known at that time, but instead produced a gelatinous solid. The analysis by Blyth and Hofman six years later revealed that the chemical composition of the liquid and the solid form of styrene were identical, that is, styrene and *metastyrene* [*meta* (Greek) = after, between] both had a ratio of 8 carbon atoms to 8 hydrogen atoms. This disproved an earlier hypothesis which postulated that a reaction between styrene and oxygen may have taken place. Actually, what happened was that several styrene molecules (called styrene *monomers*) united via covalent bonds with other styrene molecules without changing the ratio of the atoms, which is called polymerization process [*Poly* (Greek) = many; *meros* (Greek) = part, particle.]. The chemical equation for this reaction is commonly written as Figure 34.

Where n in Figure 34 is an integer and the lines between the carbon and hydrogen atoms symbolize, as usual, the covalent single (–) or double (=) bonds (Figure 35c) [1]. The reaction in Figure 34 essentially expresses that n individual styrene molecules combine to form a polymeric chain (called here a *linear polymer*) having n members called *mers* or *repeat units*. The wavy lines to the left and right of *metastyrene* (or *polystyrene* as it is called today) indicate a multiple continuation of the same repeat unit until eventually the chain is terminated by an *end-group* [608, 609].

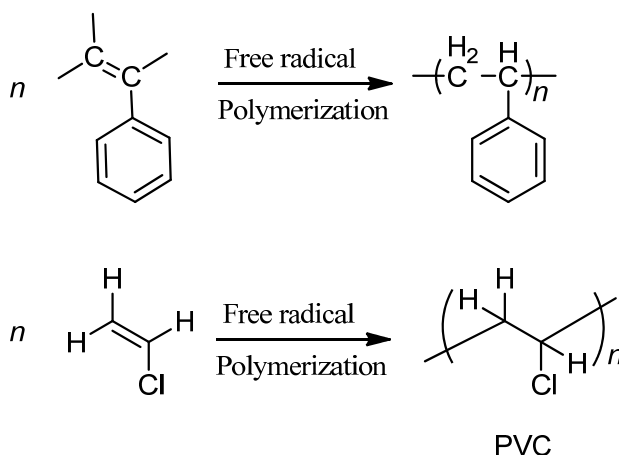


Figure 34. Polymerization process.

The study of the shape of these polymers was vigorously debated during the end of the 19th and the beginning of the 20th century's, and in the early 1930s, Staudinger, (H. Staudinger, German chemistry professor, taught at the Technical University of Zürich, Switzerland. He received the Nobel Prize for Chemistry in 1953 for the above-mentioned work), reported that the polymer compounds involving essentially long chains and having occasionally side branches, or rings are generally accepted. The question then arises, how long are these “super-molecules”? This information can be obtained by knowing the molar mass (Formerly called “molecular weight”) of the polymeric chains. T. Svedberg, Swedish professor, made extensive studies during 1924–1927 utilizing viscosity measurements and particularly the ultracentrifuge eventually which led to the conclusion that molar masses of 100,000 g/mol, for examples natural rubber, nitrocellulose, starch, etc., as well as, a specific deoxyribonucleic acid has a molar mass of 6.9×10^{13} g/mol. In other words, these molecules must have an enormous amount of repeat units. The word *macromolecule* [*Macros* (Greek) = big] is therefore appropriate name and macromolecules may have lengths of up to several meters but diameters that are merely in the nanometer range. Polymers solidify in amorphous or crystalline structures, or in a mixture of both. Randomly arranged macromolecules are amorphous or “glass like” and crystalline macromolecules are organized by folding of the chains back and forth. Actually, chain folding was discovered at a relatively late date, namely in 1957. Before that time, a coil-shaped macromolecule was the more preferred model [1, 608, 609].

The graphic representation of polymers has several possibilities exist, among them; the three-dimensional model gives a vivid impression of the special arrangement of the atoms. For example, in Figure 35(a) a *backbone* of carbon atoms that twists and turns through space. Each carbon atom in the present case is additionally bonded to two hydrogen atoms. The angle between the bond axes is 109.5° [1].

Two-dimensional representation is shown with the tacit understanding that the special arrangement has been neglected (Figures 35b and 35c). In still other cases, a short-hand chain formula is used, as was presented in the reaction Figure 34. The important question is how single monomers can be induced to form polymers. The answer is: there is more than one method to do this, and the techniques in modern days have become increasingly complex [1].

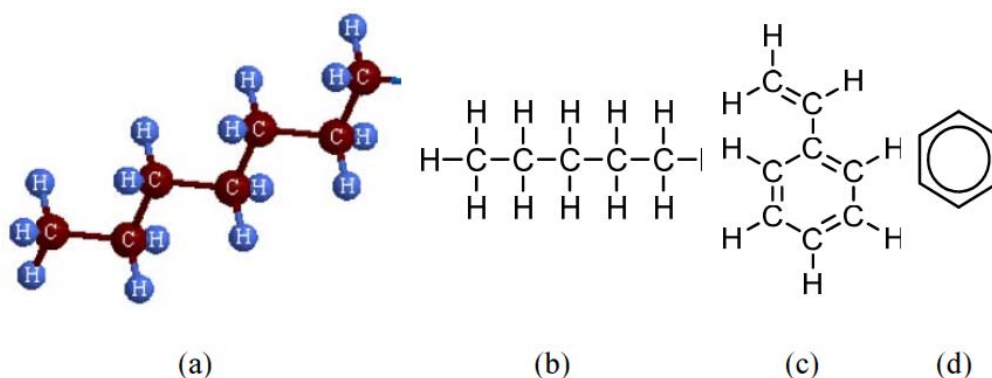


Figure 35. Schematic representation of the structure of some polymers. (a) Three-dimensional display of polyethylene. Note that each carbon atom can be positioned on a circle of a cone which has an angle of 109.5° between the bond axes. (b) Two-dimensional display of polyethylene. (c) Two-dimensional display of styrene which contains a benzene ring structure [compare to Eq. (1)]. (d) The ring is often abbreviated by a hexagon with an inscribed circle].

The principles of polymerization can be described briefly as follows: the techniques, called addition polymerization (or chain reaction polymerization) shall be explained first using polyethylene as an example. The ethylene monomer ($\text{H}_2\text{C}=\text{CH}_2$) consists of two carbon atoms and four hydrogen atoms that are covalently bonded, as shown in Figure 36a. The two carbon atoms are joined by a double bond called an *unsaturated bond*. The latter term implies that, under certain conditions of heat, UV light, pressure, or catalytic action, one of the comparatively weak double bonds can be broken. This renders the molecule reactive, i.e., it may join other reactive molecules. As an example, we consider in Figure 36b the reaction of ethylene with hydrogen peroxide (H_2O_2), which is called in the present context an *initiator*.

H_2O_2 splits under the influence of slight heat into two HO^\bullet groups whereby the dot symbolizes an unpaired electron, termed here a *free radical*. This HO radical breaks the double bond in ethylene ($\text{H}_2\text{C}=\text{CH}_2$) and then attaches to one of its ends, creating a free radical on the other end of ethylene, as depicted in Figure 36b. In the present case, two sides of the ethylene molecule may react and the system is therefore called *bifunctional*. In other words, reaction of an initiator with a monomer leaves a free radical at one end of this monomer which is then available for chain building. Effectively, once a free radical has been formed, the addition of other repeat units to the chain (propagation) progresses with substantial speed. The reaction is driven by an energy difference between the monomer and the polymer. Specifically, the polymer has a lower energy than the monomer. Thus, energy is set free (in the form of heat) during polymerization. This process eventually slows down, however, when the remaining monomers need to diffuse a comparatively long distance until they find a reaction partner. During maximal growth periods, about 10^5 – 10^6 mer units per second are added to a chain.

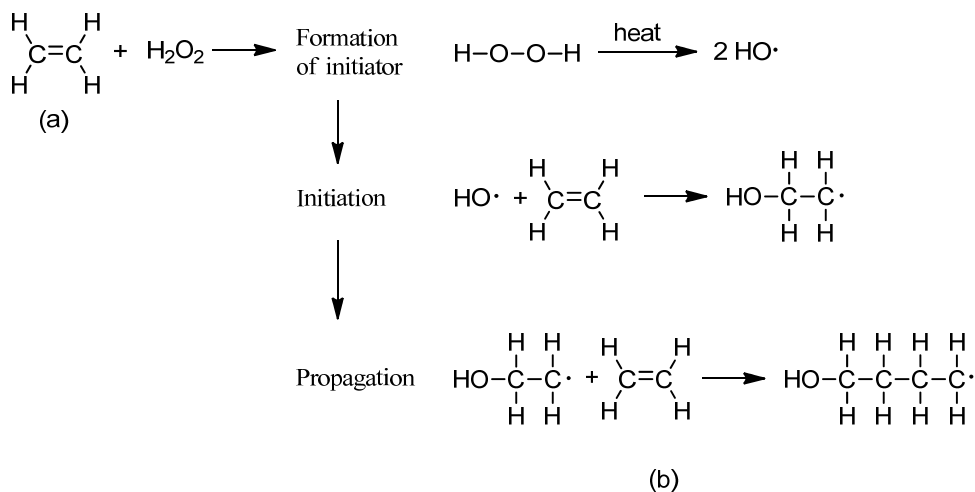


Figure 36. (a) Ethylene monomer, (b) Reaction of an initiator for addition polymerization (here H_2O_2) to an ethylene monomer which initiates polyethylene to form.

Each chain must eventually have an end, which may take place in several ways as follows: (i) the active ends of two chains may link together to form a larger, but nonreactive macromolecule that stops further growth and is called termination by *combination*; (ii) the active end of a chain may react with an initiator or another constituent that has a free radical, thus forming an end group; (iii) a hydrogen atom from one chain may be removed by an active end of another chain, thus causing a double carbon bond to be formed, which called *disproportionation* (simultaneously ends two chains, one from which the hydrogen atom was removed and one to which it was attached). Since termination is essentially a random process, a distribution of chain lengths and therefore of molar masses is encountered. In order to arrive at an average molar mass, one group the chain lengths in a series of ranges and then determines the number fraction of chains within each group. This leads to the number-average molar mass:

$$\overline{M}_n = \sum n_i M_i \quad (1)$$

where M_i is the mean molar mass of size range i and n_i is the fraction of the chains that have this mean molar mass. Frequently, an alternative parameter is defined called the *mass average molar mass*, (\overline{M}_w), which is based on the mass fraction of molecules within various size ranges. The degree of polymerization, n_n , is defined as:

$$n_n = \frac{\overline{M}_n}{\overline{m}} \quad (2)$$

where \overline{m} is the molar mass of the involved mer.

The length of a chain can be influenced to a certain degree by controlling the amount of initiator: A large quantity of initiator produces more and therefore shorter chains, and also terminates the chains more readily. Among the polymers that are synthesized by the addition mechanism are polyethylene, polypropylene, polystyrene, and polyvinyl chloride (PVC).

Another mechanism by which polymerization can be achieved is called condensation (or *step-growth reaction*). It involves more than one monomer species which react and combine. During the reaction, they release a by-product of low molar mass such as water or alcohol. This by-product is discarded. Condensation polymerization is used to make *thermosetting polymers* as well as *thermoplastic polymers* [580-584]. For example the formation of an ester by the reaction between ethylene glycol and adipic acid give water as the by-product (Figure 37). Both of the monomers in the given example are *bifunctional*. Thus, condensation polymerization yields in the present case a linear polymeric chain. However, if *trifunctional* monomers are involved, cross-linking yields network polymers. These network polymers are referred to as *thermosets* as stated earlier. Examples for condensation polymers are the nylons, phenol-formaldehyde, the polycarbonates, and polyesters.

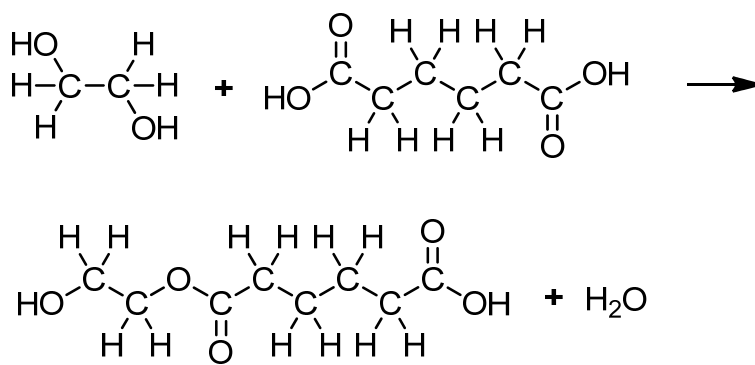


Figure 37. Reaction between ethylene glycol and adipic acid.

15.2.1. History of Polymer Science

The beauty of polymer science is that its history is less than 200 years old, in contrast to the history of most other materials. Thus, it is quite possible today to follow from the literature how scientists and inventors slowly and painstakingly came to grips with the nature of synthetic and naturally occurring polymers. It took a substantial amount of time to transfer from the discovery of a polymer to its industrial production. Table 22 lists the history of polymer discoveries, applications, and inventors. Present-day researchers receive new technology from other scientists who live and work all over the world, in contrast to antiquity where developments often occurred locally with very little and time-delayed interaction between various scientists. A gap of information exchange occurred, however, during Second World War, at which time separate and secret developments took place in both camps. Attempts were made to bridge this gap by a group of American polymer specialists who swarmed all over Germany right after the war in order to find out what progress had been made over there. It is amazing to read a 550-page book entitled, *German Plastics Practice* which is based on "Quartermaster Reports" and which was published in 1946 under the auspices of the U.S. Department of Commerce. This document provides a detailed account of the accomplishments of that time, listing hitherto known polymer materials, know-how, production facilities, production figures, and the men and women who made it possible. Times have changed and current progress is now essentially available in the open literature [513, 610-613].

Table 22. History of polymer discoveries, applications, and inventors

Polymer	Discover y	Producti on	Typical applications	Inventor
Derivatives of Natural Polymers (Semi-Synthetics)				
Vulcanized natural rubber	1839	1850	Tires, rain gear, shoes	Goodyear
Cellulose nitrate	1846	1869	Tool handles, frames for eyeglasses, films, gun cotton	Schönbein
Cellulose acetate	1865	1927	Photographic films, packaging, fibers, audio and video tapes	
Celluloid	1869	1870	Combs, films, collars, ping-pong balls	Hyatt
Nitrocellulose fiber	1884	1891	Artificial silk (rayon)	de Chardonnet
Casein/formaldehyde thermoset	1897	1904	Accessories	Krische and Spitteler
Cellophane	1908	1911	Packaging	Brandenberger
Fully Synthetic Thermoplastics				
Polyvinyl chloride	1838	1914	Shopping bags, window frames, floor tiles	Regnault
Polyvinylidene chloride	1838	1939	Packaging films	
Polystyrene	1839	1930	Small containers, foam, toys	Simon, Blyth, Hofman
Polymethyl methacrylate	1880	1928	Lamp casings, advertising signs	
Polyethylene	1932	1939	Garbage bags, milk bottles	
Fully Synthetic Thermosets				
Alkyd resins	1901	1926	Coatings	Röhm
Phenol/formaldehyde (Bakelite)	1906	1909	Electrical insulators	Baekeland
Synthetic Rubbers				
Polyisoprene	1879	1955	Tires	
Polybutadiene	1911	1929	Tires, gaskets	

15.3. Properties of Synthetic Polymers

The properties and the structure of polymers are substantially interrelated. Figure 38 schematically depicts the chain structures of the above mentioned three principal types of

polymers. Figure 38a represents the thermosetting polymers which composed of long molecular chains that are rigidly *cross-linked* and thus form a three-dimensional network and hence, they belong to the group of *network polymers*. Usually the cross-linked polymers have 10 to 50% mer units. As a consequence, thermosetting polymers are strong to the extent of brittleness (Table 23). In some thermosetting polymers, such as the *epoxy glues*, the “hardener” irreversibly initiates the cross-linking in the resin, and therefore, *cross-linked thermosets* cannot be reshaped by heating. On the other hand, heating at high temperatures led to cross-links break and destruction of the *cross-linked thermoset* materials and therefore the recyclability of *cross-linked thermosets* is limited [1, 609].

Figure 38b shows that, the polymeric chains in *thermoplastic* materials are belonging to the group of *linear polymers* and not chemically interconnected and they are comparable to spaghetti in a bowl. Thermoplastics are held together by weak forces such as van der Waals forces and mechanical entanglement. At certain high temperatures, *linear polymer thermoplastics* are soft and ductile and they can be easily recycled by reheating and remolding them into a new product. In specific cases, some of the macromolecules are folded back and forth over small distances forming platelets or lamellae about 100 atomic layers thick and on the order of 10 μm in diameter, which depicts the folded chain model (Figures 38b and 38d). The platelets represent crystallites due to the periodic arrangement of the chains. Several of these crystallites are stacked on top of each other and thus form multilayered structures. Crystallization of polymers from dilute solutions possesses such folded chain morphology within a single crystal. When the crystallites emerge from a melt, several lamellae or chain folded ribbons combine and form star-like three-dimensional structures which are called *spherulites*. The spaces between the crystalline areas are amorphous and these polymers type are therefore termed *semicrystalline*. Heavily crystallized polymers have an increased density and they are effectively resistant to chemical attack, as well as, they retain their mechanical properties even at elevated temperatures. However, not all thermoplastics have a crystalline structure [1].

Finally, *elastomer* polymers have a structure somewhat in between the *cross-linked* and *linear polymer thermoplastics* and thus, they are slightly, but not rigidly, cross-linked (Figure 38c). Vulcanization at processing temperatures between 120 and 180°C, for example, produces cross-links containing sulfur atoms. Low sulfur content (~0.5%) causes the rubber to be soft and flexible (for example: rubber bands), whereas sulfur contents from 1 to 5% make the rubber stiffer and harder. This material is used to dampen vibrations of machines. Elastomers are generally amorphous and their molecular chains are substantially coiled, twisted, and kinked. Applying tensile force to elastomers causes the chains to straighten out, which results in an elongation of the material and a rather ordered state. However, once the stress on rubber is released, the chains instantly revert back into their former condition. The temperature of natural rubber rises during stretching due to crystallization [1].

15.4. Mechanical Properties of Polymers

Understanding of the mechanical properties of polymers can be gained by inspecting their stress–strain diagrams. Their behavior is similar to that found in ceramics, refractory metals, diamond, etc. It is reported that, only little ductile behavior is encountered, the strength is high, and the elastic modulus is large (Table 23). This can be understood by knowing that

chemically *cross-linked* chains are strongly tied together and thus sustain a rigid network. In contrast to this, *elastomeric polymers*, which they have a large nonlinear elastic region, allow considerable deformation under little stress (Figure 38c). The elastic modulus and the tensile strength are small. This can be interpreted by considering the individual chains in *elastomers* initially uncoil and straighten due to the applied stress and thus, they slide easily past each other. Once the chains have been completely straightened, further stressing leads to a stretching of the bonds and to an increase in the elastic modulus [614-616].

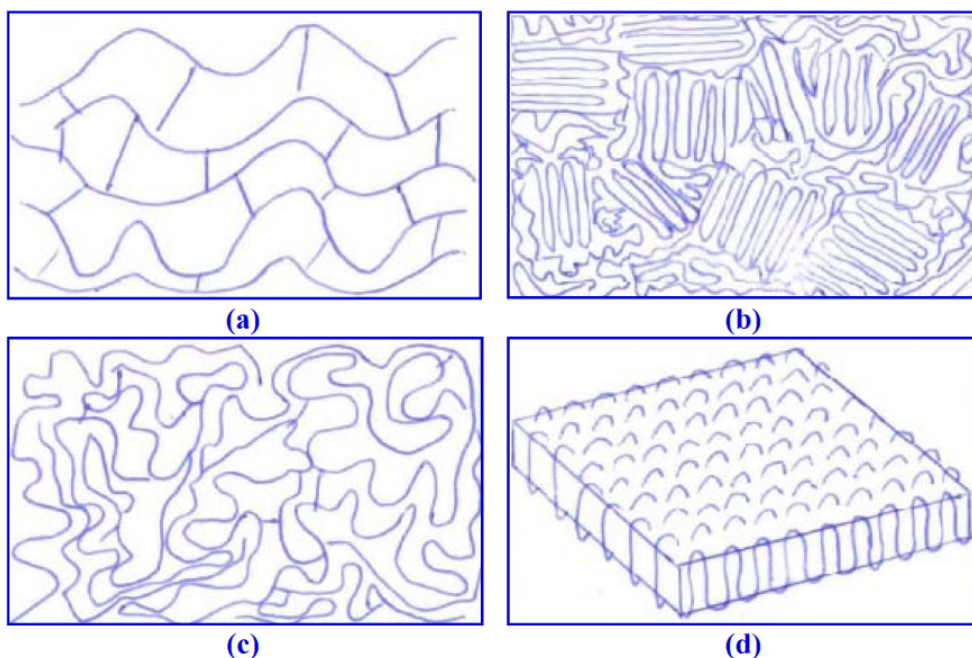


Figure 38. Schematic representations of some polymeric structures: (a) Thermosetting polymers (strong covalent bridges between individual chains exist). (b) Semicrystalline thermoplastic polymer (folded chain model). The crystallites are regularly shaped, thin platelets or lamellae which are about 100 atomic layers thick and on the order of 10 μm in diameter. The space between the crystalline areas is amorphous. (c) Elastomers polymers; some cross-linking takes place. (d) Three-dimensional representation of a folded chain crystalline platelet of thermoplastic polymers.

The stress–strain diagrams for *thermoplastic* materials are instead more involved. Similar to most metals, at low applied stresses the material behaves elastically because of the covalent bonds within the chains stretch and reverts back almost instantly into their original positions upon release of a force (linear elastic deformation). While, at higher applied stresses thermoplastics behave in a non-elastic, viscous manner. In this *nonlinear elastic range*, entire segments of the polymeric chains are distorted and this behavior is only observed if the stress is applied slowly or when the temperature is high. The nonlinear elastic behavior is linked to the viscosity of the material. However, if the force is applied quickly or the temperature is low, a brittle fracture is encountered. It can be said that the stress–strain diagrams vary with temperature and rate of deformation [609, 615, 616].

Once the stress eventually exceeds the yield strength σ_y , plastic deformation sets in. It occurs when the individual polymeric chains slide past each other, and when the

entanglement of the chains is straightened out. (This mechanism is in sharp contrast to that encountered in metals, where dislocation movement is the prime cause for plastic deformation, as discussed in Section 3.4.) As in metals, necking eventually sets in, allowing chain sliding at a lower nominal stress until finally the chains become almost parallel to each other. At this point, van der Waals forces hold the chains together, thus causing an increase in required stress upon further straining [614-617].

Table 23. Some mechanical properties of polymers at room temperature compared to metals and spider drag lines

Material	Modulus of elasticity E [GPa]	Tensile strength σ_T [MPa]	Ductility, i.e., elongation at break [%]
Thermosets <i>Example: Epoxy</i>	2.8–4.1	50–100	30–300
Thermoplastics <i>Example: Polyethylene</i>	0.17–1.1	8.3–31	100–1200
Elastomers <i>Example: Rubbers</i>	0.01–0.1	5–30	300–2000
Metals (see Table 2.1)	10–400	10–1500	<50
Spider drag line (single strand)	2.8–4.7	870–1420	30

Table 23 compares the mechanical properties of synthetic polymers with those of metals and spider drag lines. The spider drag line remarkable tensile strength is comparable to that of steel. The mechanical properties of many polymers are quite temperature-dependent, which occurs already around room temperature, contrary to the much higher temperatures needed for metals and ceramics. At low temperatures near 0°C, acrylics are brittle and comparatively strong, having a high elastic modulus and a high tensile strength. The elastic modulus and the tensile strength of acrylics decrease upon moderately increasing the temperature, and the material becomes ductile and soft [609, 615, 616, 618].

Characteristic transformations of polymers occurred at specific temperatures or temperature ranges. Similar observations are also known for ceramics, glasses, and metals. For comparison we display the temperature dependence of the specific volume, V_s (that is, the volume per unit mass). The *crystalline* polymers possess a sharp discontinuity in V_s at the melting temperature, T_m . (Note, the completely crystalline polymers are never found, but amorphous transition regions between the crystallites are always encountered). In comparison to this, *amorphous* polymers do not possess a kink of V_s at T_m . Alternatively, when the liquid state is cooled; they pass through various stages called *viscous*, *rubbery*, *leathery*, and *glassy*. These descriptive terms vividly refer to the degree of viscosity in each state. However, a slight change in the slope of V_s occurs at the *glass transition temperature*, T_g , below which the material is called glassy amorphous solid [609, 615, 616, 618].

Finally, *semicrystalline* polymers display discontinuities of V_s at T_g as well as at T_m upon cooling, hence having the characteristics of the crystalline as well as the amorphous phases.

Generally, T_g is about two-thirds of T_m (where T is the absolute temperature), i.e., T_g/T_m is about 0.67. Characteristic melting temperatures for polymers are between 100 and 350°C, whereas glass transition temperatures range between -150 and +300°C. Some important polymers such as polyvinyl chloride and polystyrene have a T_g above room temperature. The *degradation* or *decomposition temperature*, T_d , an additional characteristic temperature is often defined as the temperature that above it the polymer burns or chars [614-616, 619-621].

15.5. Properties due to Production Procedures

The polymers properties are affected by a large number of production procedures, for example, the strength of polymers can be increased by enhancing the molar mass, which may be accomplished by decreasing the amount of initiators. Further, the strength can be improved if the polymers are pre-deformed. This procedure leading to a highly oriented structure due to aligns the crystalline lamellae in the direction of the tensile force. The defects in polymers properties have been reported [618, 622, 623].

15.6. Properties Enhancement by Additives

The abrasion resistance and strength of polymers are often enhanced by adding fillers such as carbon black (for tires), sand, saw dust, talc, clay, or glass. The respective particles have sizes from 10 nm upward. The deterioration of some polymers that is caused by ultraviolet light or oxidation can be counteracted by addition of a *stabilizer*. Specifically, UV radiation on the polymers may produce enough energy to break some of its covalent bonds, which led to shortening its molecular chains. As a result, substantial cross-linking and, thus, embrittlement may take place. Plasticizers (liquids that possess a low vapor pressure and a small molar mass) are added to brittle polymers (such as polyvinylchloride) to increase the distances between chains and thus reduce T_g , which makes the polymer more pliable but also decreases its hardness and stiffness. When add flame retardants to polymers, it interferes with the combustion process by releasing a suffocating gas or by cooling the burning region through a chemical reaction. Addition of antistatic agents to the polymers is important because polymers are generally poor electrical conductors and therefore retain static electricity. Antistatic agents can attract moisture from the air, which may lead to increase the surface conductivity [609, 624].

The properties can also be altered by joining two or more different linear addition polymers, thus forming a so-called copolymer. Various types of copolymers are synthesized such as by alternating the sequence of the involved monomers either periodically or randomly or by grafting (adding side branches to the main chain). Copolymers usually have excellent combinations of toughness, rigidity, and strength. Finally, mixing *elastomers* with *thermoplastics* produces two-phase polymers. This improves the toughness by absorbing the impact of a sudden blow, and the possibilities for variations seem to be virtually unlimited. Controlling the synthesis of polymers, however, are still at a very primitive stage. A mixture of chain lengths with usually only one or two types of mers is currently produced. On the contrary, the human skin is composed of collagen, which has units containing about ten

different mers that are arranged in an exact order whereby each chain is exactly 1056 mers long.

Some polymers have quite interesting and commercially exploitable electrical, optical, and thermal properties, for examples, lenses for cameras, conducting polymers, superconductors, magnetic films, light-emitting polymers, and applications in the computer-chip industry.

16. COMPOSITE SUBSTANCES

Composites are solid materials that are produced by structurally joining two or more substances to obtain new properties that should not be acquired by any of the original materials alone. The origins of composite materials, in the widest definition of this term, occurred long before recorded history and may be traced through examples of clay reinforced with wood and other natural fibers, the *papier mâché* of the ancient Egyptians and numerous combinations of wood with leather or metal. As examples the insertion of straw fibers into clay bricks (ancient Egypt) and concrete without iron-rod reinforcements [625-627]. Also, wood is a naturally occurring composite that consists of elongated plant cells (cellulose) that are jointed together by soft lignin. The technology behind some of these materials and their applications was no less ingenious than that for today's high performance structural composites, the origins of which can be pin-pointed with accuracy to the concepts and work of N.A. de Bruyne and J.E. Gordon in the late 1930s [131, 628].

Recently, synthetic composite materials have seen good upswing in development and application due to improved their strength and stiffness, which are caused by the strong ionic and covalent bonds of the involved fibers and their lack of flaws that, if present, would propagate cracks through the material. For example, brittle materials such as glass, porcelain, ceramics, etc., and soft materials, such as plastics, can be reinforced considerably by incorporating fibers into them. Composites are often light and corrosion resistant toward oil, gasoline, or other organic fluids. Composite materials are used in the automotive sector because they are mechanically safer in cases of accidents compared to metals due to their improved energy-absorbing properties. Also, some composite materials are high thermal conductivity, which stems from the fact that they are good phonon- as well as electron conductors. Since phonons are easily propagate in a stiff lattice of light atoms, particularly if they are in fibrous form (having a low level of structural defects), composite materials produced from boron, carbon, or silicon carbide are excellent thermal conductors. Furthermore, composite materials that their atoms are held together by strong ionic and covalent bonds are good insulators. The manufacturing of a composite often takes place concomitantly with the shaping of a commercial product. One of the most important types of composite materials involves polymers as a matrix (such as epoxy resins or polyester) in which fibers of glass, carbon, Al_2O_3 , polyethylene, boron, beryllium, or ZrO_2 are inserted before polymerization has taken place (fiber-reinforced composites) [2, 628-630].

The most visible application is pavement in roadways in the form of either steel and aggregate reinforced Portland cement or asphalt concrete [5, 365, 401, 433, 377, 545-547]. Those composites closest to our personal hygiene form our shower stalls and bathtubs made of fiberglass. Imitation granite and cultured marble sinks and countertops are widely used.

The disadvantages of composite materials are encountered higher cost of production, a lower wear resistance in the case of polymer-based composites, some degradation at temperatures above 200°C, and difficulty in recycling discarded products.

New types of fibers are contemplated consisting of diamond strands or carbon *nanotubes*, the latter of which are molecular-scale structures like *Bucky balls*, made up of one or more of cylindrical graphite basal-plane layers [631-633]. They have strengths and stiffnesses more than those known for conventional carbon fibers. Whiskers that are tiny single crystals are utilized and the matrix does not need to be a polymer. For example, high-performance automotive brakes are made of a carbon matrix in which carbon fibers are incorporated [634, 635].

Recently, due to low electrical conductivity for some polymer-based composites combined with oxide fibers and their ability to evade radar detection they are used for stealth aircrafts [636]. Other fibers used for this purpose are consisted of *aramid* (a polyamide fiber similar to nylon), which is chopped into small pieces to particles size equal to one quarter of the wavelength of the incoming radiation, which lead to absorption of the endangering signal. There is commercial interest in metallic matrices (such as aluminum) because metals are stronger, stiffer, tougher, and more heat resistant than polymers, but their utilization is in its early years. This is mainly due to the fact that highly hot metals may damage specific fibers. Further, some of the advantageous properties of metals may be compromised by some fibers. Still, brake disks for sports cars are made from aluminum that is reinforced by silicon carbide particles (Al-SiC), which have a wear resistance beyond that of pure aluminum, a good thermal conduction (which prevents overheating), a smaller thermal expansion coefficient, and are much lighter than the traditional cast-iron disks. For obtaining extremely hard cutting tools, hard ceramic particles, such as tungsten carbide are dispersed in a metallic matrix consisting, for example, of cobalt, which is used to lighten the brittleness of the tungsten carbide and to increase the impact resistance. These composites are called *cermets* (or cemented carbides). For industrializing, the pressed powder of the components is heated above the cobalt melting point, which make the Co surrounds the carbide particles after solidification and thus acts fundamentally as a ductile binder. Also, reinforce of the good-conducting silver by hard tungsten yielding electrical contacts that are wear resistant under arcing as needed in automobile distributors [1, 637].

Fibers are usually packed densely parallel to one another that cause the resulting sheets to be mechanically anisotropic (the sheets are strong in its length direction and weak sideways) just as is known for wood. To reduce this deficiency, sheets in which the fibers are lying in different directions are stacked on top of one another and then bonded, as in plywood. This technique is often used to produce sporting goods (tennis rackets, golf clubs) or the airplanes wings. Also, the modern automobile tire is made of layers of rubber, fiber bundles (made of nylon, rayon, glass, polyaramid), and metal sheets (steel) that interleaved to withstand multiple flexing loads (laminar composites) [638].

17. ADVANCED FABRICS

The search for new fibrous materials for technical textile applications is still continues and produced materials are either already on the market or are still in development. These

advanced materials often have *smart* properties such as sense and respond to chemical or biological substances or react to physical stimuli such as blood pressure, body temperature, or blood oxygen levels. It has also been proposed that computers or other electronic systems be integrated into textiles (“*wearable mother boards*”), among them are photovoltaics, energy conversion systems (mechanical to electrical), switches, or storage elements [639-641].

For the automobile or home, advanced filters that hold back pollen down to nanometer sizes and even remove odors have been developed. In the medical field, antimicrobial, thrombotic, and super-absorbing textiles are used or under development [640, 641].

Bulletproof vests are other important textiles for protection against impact made from high-strength fibers (Kevlar, carbon strands, nylon, M5). They possess a high stiffness in order to transfer the impact stress along the fibers such as cellulose fibers possess an elastic modulus of 90–140 GPa, whereas polyacrylonitrile-based carbon has a modulus of 900–1100 GPa, mainly because of its covalent bonds between adjacent carbon planes. Somewhere in between is the so-called M5 (or PIPD) fiber whose tensile modulus is 550 GPa but whose specific strength (tenacity) is 5 GPa compared to 3.5 GPa for the high-strength carbon fiber [642, 643].

Suits consist of barrier laminates that are completely impermeable, such as Tyvek-reinforced polypropylene films with a rugged outer-shell fabric such as aluminized Kevlar and polybenzobisoxazole (PBO). There is also a strong interest in protective suits or overgarments that shield humans from biological contaminants or fire resistant. They should be lightweight and provide comfort over long time periods, which are accomplished by utilizing semi-permeable adsorptive carbon liners within the garment. Concurrently, carbon layers adsorb vapors that may pass into the clothing, thus providing protection. Recently, membranes that permit the penetration of water vapor molecules to allow transpiration and cooling, but are impermeable for larger molecules have been developed. These “*perm-selective*” membranes have been used for water purification by reverse osmosis and are made of polyvinyl alcohol, cellulose acetate, cellulosic cotton, or polyallylamine. Developments of new fabrics are self-decontaminating and kill dangerous airborne microorganisms that attach to the protecting garment. These antimicrobial substances consist, among others, of silver or silver salts [640].

A particularly interesting fiber is capable of changing its color upon an electrical or biological stimulus from a bright orange to a camouflaging dark green. This “*chameleon fiber*” may be of interest to hunters. Among these smart materials are conducting polymers made from polypyrrole or polyaniline, which are coated on woven fabrics made of polyethylene terephthalate [644].

ACKNOWLEDGMENTS

I would like to thanks Professor Sawsan Mohamed Aboul Ezz of our Institute for reading this manuscript.

REFERENCES

- [1] Hummel, E. (2005). From Natural Fibers to Man-Made Plastics. In *Understanding Materials Science Part III*, 326-365, DOI: 10.1007/0-387-26691-7_16.
- [2] Kelly, A. (2005). Very stiff fibers woven into history – very personal recollections of some of the British scene. *Composites Science and Technology*, 65(15-16): 2285-2294.
- [3] Gracies, J.-M., Fitzpatrick, R., Wilson, L., Burke, D., and Gandevia, S.C. (1997). Lycra garments designed for patients with upper limb spasticity: Mechanical effects in normal subjects. *Archives of Physical Medicine and Rehabilitation*, 78(10): 1066-1071.
- [4] Karmakar, S.R. (1999). Chemical technology in the pre-treatment processes of textile. In *Textile Science and Technology*, 12: 1-48. Publisher: Elsevier Science and Technology, ISBN: 9780444500601.
- [5] Lin, T.K., Wu, S.J., Lai, J.G., and Shyu, S.S. (2000). The Effect of chemical treatment on reinforcement/matrix interaction in Kevlar-fiber/bismaleimide composites. *Composites Science and Technology*, 60(9): 1873-1878.
- [6] Ran, S., Fang, D., Zong, X., Hsiao, B.S., Chu, B., and Cuniff, P.M. (2001). Structural changes during deformation of Kevlar fibers via on-line synchrotron SAXS/WAXD techniques. *Polymer*, 42(4): 1601-1612.
- [7] Hearle, J.W.S. (2001). Textile fibers: A comparative overview. *Encyclopedia of materials: Science and Technology*. Pages 9100-9116.
- [8] Hearle, J.W.S. (2008). Textile Fibers: A Comparative Overview. *Encyclopedia of Materials: Science and Technology* 9100-9116.
- [9] Hart, B.L., and Pryor, P.A. (2004). Developmental and hair-coat determinants of grooming behavior in goats and sheep. *Animal Behavior*, 67(1): 11-19.
- [10] Merdan, N., Akalin, M., Kocak, D., and Usta, I. (2004). Effects of ultrasonic energy on dyeing of polyamide (microfibre)/Lycra blends. *Ultrasonics*, 42(1-9): 165-168.
- [11] Wu, J., Zhou, D., Too, C.O., and Wallace, G.G. (2005). Conducting polymer coated Lycra. *Synthetic Metals*, 155(3): 698-701.
- [12] Su, M., Gu, A., Liang, G., and Yuan, L. (2011). The effect of oxygen-plasma treatment on Kevlar fibers and the properties of Kevlar fibers/bismaleimide composites. *Applied Surface Science*, 257(8): 3158-3167.
- [13] Danish, N., Garg, M.K., Rane, R.S., Jhala, P.B., and Nema, S.K. (2007). Surface modification of Angora rabbit fibers using dielectric barrier discharge. *Applied Surface Science*, 253(16): 6915-6921.
- [14] Rafat, S.A., Allain, D., Thébault, R.G., and de Rochambeau, H. (2007). Divergent selection for fleece weight in French Angora rabbits: Non-genetic effects, genetic parameters and response to selection. *Livestock Science*, 106(2-3): 169-175.
- [15] Rafat, S.A., de Rochambeau, H., Thébault, R.G., David, I., Deretz, S., Bonnet, M., Pena-Arnaud, B., and Allain, D. (2008). Divergent selection for total fleece weight in Angora rabbits: Correlated responses in wool characteristics. *Livestock Science*, 113(1): 8-13.
- [16] Perincek, S., Bahtiyari, M.İ., Körlü, A.E., and Duran, K. (2008). Ozone treatment of Angora rabbit fiber. *Journal of Cleaner Production*, 16(17): 1900-1906.
- [17] Buerger, M.J.; Prewitt, C.T. (1961). The crystal structures of wollastonite and pectolite. *Proceedings of the National Academy of Sciences, U.S.A.*, 47, 1884-1888.

-
- [18] Tong, J., Ma, Y., Arnell, R.D., and Ren, L. (2006). Free abrasive wear behavior of UHMWPE composites filled with wollastonite fibers Composites Part A. *Applied Science and Manufacturing*, 37(1): 38-45.
- [19] Krupa, I., Cecen, V., Tlili, R., Boudenne, A., and Ibos, L. (2008). Thermophysical properties of ethylene–vinylacetate copolymer (EVA) filled with wollastonite fibers coated by silver. *European Polymer Journal*, 44(11): 3817-3826.
- [20] Ptáček, P., Nosková, M., Brandštetr, J., Šoukal, F., and Opravil, T. (2011). Mechanism and kinetics of wollastonite fibre dissolution in the aqueous solution of acetic acid. *Powder Technology*, 206(3): 338-344.
- [21] Howie, D. (1997). Rock Forming Minerals; Single Chain Silicates, *The geological society* Vol. 2A, Second Edition, London.
- [22] Arnold, D.E. and Bohor, B.F. (1975). Attapulgit and Maya Blue: an Ancient Mine Comes to Light. *Archaeology*, 28(1): 23–29.
- [23] Arnold, D.E. (2005). Maya Blue and Palygorskite: A second possible pre-Columbian source. *Ancient Mesoamerica*, 16: 51–62.
- [24] Kerr, P.F. (1952). Formation and occurrence of clay minerals. *Clays and Clay Minerals*, 1: 19–32.
- [25] Brindley, G.W. (1952). Structural mineralogy of clays. *Clays and Clay Minerals*, 1: 33–43.
- [26] Carroll, D. (1959). Ion exchange in clays and other minerals. *Geological Society of America Bulletin*, 70(6): 749-780.
- [27] Papke, K.G. (1971). Halloysite Deposits in the terraced Hills Washoe County, Nevada. *Clays and Clay Minerals*, 19(2): 71–74.
- [28] Wilson, M.J. (1999). The Origin and Formation of Clay Minerals in Soils: Past Present and Future Perspectives. *Clay Minerals*, 34. No. 1.
- [29] Singer, A., Zarei, M., Lange, F.M., and Stahr, K. (2004). Halloysite characteristics and formation in the northern Golan Heights. *Geoderma*, 123(3-4): 279-295.
- [30] Marney, D.C.O., Russell, L.J., Wu, D.Y., Nguyen, T., Cramm, D., Rigopoulos, N., Wright, N., and Greaves, M. (2008). The suitability of halloysite nanotubes as a fire retardant for nylon 6. *Polymer Degradation and Stability*, 93(10): 1971-1978.
- [31] Etame, J., Gerard, M., Suh, C.E., and Bilong, P. (2009). Halloysite neoformation during the weathering of nephelinitic rocks under humid tropical conditions at Mt Etinde, Cameroon. *Geoderma*, 154(1-2): 59-68.
- [32] Grieve, M.C. (1996). New man-made fibers under the microscope – Lyocell fibers and Nylon 6 block co-polymers. *Science and Justice*, 36(2): 71-80.
- [33] Coyle, T.J., Robson, R., and Bauer, P. (2002). Identification of Lyocell using dispersion staining. *Science and Justice*, 42(2): 75-79.
- [34] Rosenau, T., Potthast, A., Sixta, H., and Kosma, P. (2001). The chemistry of side reactions and byproduct formation in the system NMMO/cellulose (Lyocell process). *Progress in Polymer Science*, 26(9):1763-1837.
- [35] Manian, A.P., Ruef, H., Bechtold, T. (2007). Spun-dyed lyocell, *Dyes and Pigments*, 74(3): 519-524.
- [36] Manian, A.P., Abu-Rous, M., Lenninger, M., Roeder, T., Schuster, K.C., and Bechtold, T. (2008). The influence of alkali pretreatments in lyocell resin finishing – Fiber structure. *Carbohydrate Polymers*, 71(4): 664-671.

-
- [37] Tsunoda, Y. (1954). Process for making cupro-ammonium rayon spinning solution. Nobeoka-Shi, Japan, assignor to Asahi Kasei Kogyo Kabushiki-Kaisha, Osaka-Shi, Japan. US Patent, Mar. 30, 2673811.
 - [38] Morita, R., Khan, F.Z., Sakaguchi, T., Shiotsuki, M., Nishio, Y., and Masuda, T. (2007). Synthesis, characterization, and gas permeation properties of the silyl derivatives of cellulose acetate. *Journal of Membrane Science*, 305(1-2): 136-145.
 - [39] Shaikh, H.M., Pandare, K.V., Nair, G., Varma, A.J. (2009). Utilization of sugarcane bagasse cellulose for producing cellulose acetates: Novel use of residual hemicellulose as plasticizer. *Carbohydrate Polymers*, 76(1): 23-29.
 - [40] Cheng, H.N., Dowd, M.K., Selling, G.W., and Biswas, A. (2010). Synthesis of cellulose acetate from cotton byproducts. *Carbohydrate Polymers*, 80(2): 449-452.
 - [41] Montgomery, J.D. (2002). Chapter 1 - History of Fiber Optics” in *Fiber Optic Data Communication*, 3-31.
 - [42] Tricker, R. (2002). The history of fiber optics, *Optoelectronics and Fiber Optic Technology*, 1-35.
 - [43] Yalejean, M.Y. (1995). Application of wild goats in cashmere breeding. *Small Ruminant Research*, 15(3): 287-291.
 - [44] McGregor, B.A. (2009). A review of cashmere nutrition experiments with suggestions for improving their design and conduct. *Small Ruminant Research*, 82(2-3): 71-83.
 - [45] McGregor, B.A., and Butler, K.L. (2008). Determinants of cashmere production: The contribution of fleece measurements and animal growth on farms. *Small Ruminant Research*, 78(1-3): 96-105.
 - [46] Ji, W., Bai, L., Ji, M., and Yang, X. (2010). A method for quantifying mixed goat cashmere and sheep wool. *Forensic Science International*, In Press. doi:10.1016/j.forsciint.2010.11.017.
 - [47] Wuliji, T., Davis, G.H., Dodds, K.G., Turner, P.R., Andrews, R.N., and Bruce, G.D. (2000). Production performance, repeatability and heritability estimates for live weight, fleece weight and fiber characteristics of alpacas in New Zealand. *Small Ruminant Research*, 37(3): 189-201.
 - [48] Lupton, C.J., McColl, A., and Stobart, R.H. (2006). Fiber characteristics of the Huacaya Alpaca. *Small Ruminant Research*, 64(3): 211-224.
 - [49] Braga, W., Leyva, V., and Cochran, R. (2007). The effect of altitude on alpaca (*Lama pacos*) fiber production. *Small Ruminant Research*, 68(3): 323-328.
 - [50] Rowell, J.E., Lupton, C.J., Robertson, M.A., Pfeiffer, F.A., Nagy, J.A., and White, R.G. (2001). Fiber characteristics of qiviut and guard hair from wild muskoxen (*Ovibos moschatus*). *Journal of Animal Science*, 79: 1670-1674.
 - [51] Munn, A.J., and Barboza, P.S. (2008). Could a big gut be too costly for muskoxen (*Ovibos moschatus*) in their first winter?. *Zoology*, 111(5): 350-362.
 - [52] Yang, X., Zhang, H., Yuan, X., and Cui, S. (2009). Wool keratin: A novel building block for layer-by-layer self-assembly. *Journal of Colloid and Interface Science*, 336(2): 756-760.
 - [53] Zoccola, M., Aluigi, A., and Tonin, C. (2009). Characterisation of keratin biomass from butchery and wool industry wastes. *Journal of Molecular Structure*, 938(1-3) 35-40.
 - [54] Cardamone, J.M. (2010). Investigating the microstructure of keratin extracted from wool: Peptide sequence (MALDI-TOF/TOF) and protein conformation (FTIR). *Journal of Molecular Structure*, 969(1-3): 97-105.

-
- [55] Hearle, J.W.S. (2000). A critical review of the structural mechanics of wool and hair fibers. *International Journal of Biological Macromolecules*, 27(2): 123-138.
- [56] Harle, K.J., Howden, S.M., Hunt, L.P., and Dunlop, M. (2007). The potential impact of climate change on the Australian wool industry by 2030. *Agricultural Systems*, 93(1-3): 61-89.
- [57] Verikios, G. (2009). Modelling the world wool market: A hybrid approach. *Economic Modelling*, 26(2): 418-431.
- [58] Biswas, W.K., Graham, J., Kelly, K., and John, M.B. (2010). Global warming contributions from wheat, sheep meat and wool production in Victoria, Australia – a life cycle assessment. *Journal of Cleaner Production*, 18(14): 1386-1392.
- [59] Prod'Homme, P., and Lauvergne, J.J. (1993). The Merino Rambouillet flock in the National Sheep Fold in France. *Small Ruminant Research*, 10(4): 303-315.
- [60] Curry, K.C., Berardinelli, J.G., Burfening, P.J., and Adair, R. (1993). Selection for reproductive rate in females and feeding regimen on testicular traits and epididymal sperm reserves in Rambouillet rams. *Small Ruminant Research*, 11(3): 257-265.
- [61] Amarante, A.F.T., Craig, T.M., Ramsey, W.S., El-Sayed, N.M., Desouki, A.Y., and Bazer, F.W. (1999). Comparison of naturally acquired parasite burdens among Florida Native, Rambouillet and crossbreed ewes. *Veterinary Parasitology*, 85(1): 61-69.
- [62] D'Arcy, J.B. (1986). *Sheep Management and Wool Technology*, NSW University Press, ISBN 0 86840 106 4.
- [63] McNeil, S.J., Sunderland, M.R., and Zaitseva, L.I. (2007). Closed-loop wool carpet recycling. *Resources, Conservation and Recycling*, 51(1): 220-224.
- [64] Zheljaskov, V.D., Stratton, G.W., Pincock, J., Butler, S., Jeliaskova, E.A., Nedkov, N.K., and Gerard, P.D. (2009). Wool-waste as organic nutrient source for container-grown plants. *Waste Management*, 29(7): 2160-2164.
- [65] Kenchington, W. (1983). The larval silk of *Hypera* spp. (*Coleoptera: Curculionidae*). A new example of the cross- β protein conformation in an insect silk. *Journal of Insect Physiology*, 29(4): 355-361.
- [66] Craig, C.L., Hsu, M., Kaplan, D., and Pierce, N.E. (1999). A comparison of the composition of silk proteins produced by spiders and insects. *International Journal of Biological Macromolecules*, 24(2-3): 109-118.
- [67] Craig, C.L., and Riekel, C. (2002). Comparative architecture of silks, fibrous proteins and their encoding genes in insects and spiders. *Comparative Biochemistry and Physiology Part B: Biochemistry and Molecular Biology*, 133(4): 493-507.
- [68] Okada, S., Weisman, S., Trueman, H.E., Mudie, S.T., Haritos, V.S., and Sutherland, T.D. (2008). An Australian webspinner species makes the finest known insect silk fibers. *International Journal of Biological Macromolecules*, 43(3): 271-275.
- [69] Sehnael, F., and Akai, H. (1990). Insect silk glands: their types, development and function, and effects of environmental factors and morphogenetic hormones on them. *International Journal of Insect Morphology and Embryology*, 19(2): 79-132.
- [70] Bini, E., Knight, D.P., and Kaplan, D.L. (2004). Mapping Domain Structures in Silks from Insects and Spiders Related to Protein Assembly. *Journal of Molecular Biology*, 335(1): 27-40.
- [71] Reddy, N., and Yang, Y. (2010). Morphology and tensile properties of silk fibers produced by uncommon *Saturniidae*. *International Journal of Biological Macromolecules*, 46(4): 419-424.

-
- [72] Asakura, T., Ashida, J., Yamane, T., Kameda, T., Nakazawa, Y., Ohgo, K., and Komatsu, K. (2001). A repeated β -turn structure in Poly(Ala-Gly) as a model for silk I of *Bombyx mori* silk fibroin studied with two-dimensional spin-diffusion NMR under off magic angle spinning and rotational echo double resonance. *Journal of Molecular Biology*, 306(2): 291-305.
 - [73] Takasu, Y., Yamada, H., Tamura, T., Sezutsu, H., Mita, K., and Tsubouchi, K. (2007). Identification and characterization of a novel sericin gene expressed in the anterior middle silk gland of the silkworm *Bombyx mori*. *Insect Biochemistry and Molecular Biology*, 37(11): 1234-1240.
 - [74] Takasu, Y., Hata, T., Uchino, K., and Zhang, Q. (2010). Identification of Ser2 proteins as major sericin components in the non-cocoon silk of *Bombyx mori*. *Insect Biochemistry and Molecular Biology*, Volume 40, Issue 4, April 2010, Pages 339-344.
 - [75] Vepari, C., and Kaplan, D.L. (2007). Silk as a biomaterial. *Progress in Polymer Science*, 32(8-9): 991-1007.
 - [76] Liu, H., Xu, W., Zou, H., Ke, G., Li, W., and Ouyang, C. (2008). Feasibility of wet spinning of silk-inspired polyurethane elastic biofiber. *Materials Letters*, 62(12-13): 1949-1952.
 - [77] Hardy, J.G., and Scheibel, T.R. (2010). Composite materials based on silk proteins. *Progress in Polymer Science*, 35(9): 1093-1115.
 - [78] Menachem, L., (Editor, 3rd ed) (2006), Handbook of Fiber Chemistry, CRC press, ISBN 0-8247-2565-4.
 - [79] Menachem, L., (Editor, 2nd ed) (1998), Handbook of Fiber Chemistry, Marcel Dekker, pp. 438-441, ISBN 0-8247-9471-0.
 - [80] Murphy, E.J. (1960). The dependence of the conductivity of cellulose, silk and wool on their water content. *Journal of Physics and Chemistry of Solids*, 16(1-2): 115-122.
 - [81] Figley, K.D., and Parkhurst, H.J. (1933). Silk sensitivity : With especial reference to its rôle in atopic eczema. *Journal of Allergy*, 5(1): 60-69.
 - [82] Parlato, S.J., and Swarthout, G. (1934). A study of the silk allergen. *Journal of Allergy*, 5(5): 505-514.
 - [83] Gelmetti, C., Frasin, A., and Restano, L. (2010). Innovative Therapeutics in Pediatric Dermatology. *Dermatologic Clinics*, 28(3):619-629.
 - [84] FAO (2005). Food And Agricultural Organization of United Nations: Economic And Social Department: The Statistical Division
 - [85] (<http://www.fao.org/es/ess/top/commodity.html?lang=en&item=1185&year=2005>).
 - [86] So, A.Y. (1986). The South China Silk District, State University of New York Press, Albany, NY (1986).
 - [87] Iziko Museums of Cape Town (2006). Gossypium (Cotton). (<http://www.museums.org.za/bio/plants/malvaceae/gossypium.htm>).
 - [88] Wolpert, S. (1991). India. Berkeley, CA: University of California Press. ISBN 0520072170.
 - [89] UNCTAD (2009). <http://www.unctad.org/infocomm/anglais/cotton/characteristics.htm>
 - [90] Richmond, T.R., 1951. Procedures and Methods of Cotton Breeding with Special Reference to American Cultivated Species. *Advances in Genetics*, 4: 213-245.
 - [91] Kenny, S. (1982). Sub-regional specialization in the Lancashire cotton industry, 1884–1914: a study in organizational and locational change. *Journal of Historical Geography*, 8(1): 41-63.

-
- [92] Huberman, M. (1991). How did labor markets work in Lancashire? more evidence on prices and quantities in cotton spinning, 1822–1852. *Explorations in Economic History*, 28(1): 87-120.
- [93] Toms, J.S. (1998). The supply of and demand for accounting information in an unregulated market: Examples from the Lancashire cotton mills, 1855–1914. *Accounting, Organizations and Society*, 23(2): 217-238.
- [94] Toms, J.S. (2002). The rise of modern accounting and the fall of the public company: the Lancashire cotton mills 1870–1914. *Accounting, Organizations and Society*, 27(1-2): 61-84.
- [95] Toms, S. (2005). Financial control, managerial control and accountability: evidence from the British Cotton Industry, 1700–2000. *Accounting, Organizations and Society*, 30(7-8): 627-653.
- [96] Ciliberto, F. (2010). Were British cotton entrepreneurs technologically backward? Firm-level evidence on the adoption of ring spinning. *Explorations in Economic History*, 47(4): 487-504.
- [97] Small, R.L., Ryburn, J.A., Cronn, R.C., Seelanan, T., and Wendel, J.F. (1998). The Tortoise and the Hare: Choosing between *Noncoding Plastome* and Nuclear Adh Sequences for Phylogeny Reconstruction in a Recently Diverged Plant Group". *American Journal of Botany (Botanical Society of America)* 85(9): 1301.
- [98] Endrizzi, J.E., Turcotte, E.L., and Kohel, R.J. (1985). Genetics, Cytology, and Evolution of *Gossypium*. *Advances in Genetics*, 23: 271-375.
- [99] Wise, R.R., Sassenrath-Cole, G.F., and Percy, R.G. (2000). A Comparison of Leaf Anatomy in Field-grown *Gossypium hirsutum* and *G. barbadense*. *Annals of Botany*, 86(4): 731-738.
- [100] Zi-hong, Y.E., Yong-jun, M.E.I., Ke-qin, Z.O.U., Xian-shu, F.U., Lin-shu, J.I.A.N.G. (2008). Genetic Dissection of Net Effects Between Yield and Its Components in Sea Island Cotton (*Gossypium barbadense* L.). *Agricultural Sciences in China*, 7(9): 1052-1060.
- [101] Zhang, P.-P., Wang, X.-Q., Yu, Y., Yu, Y., Lin, Z.-X., and Zhang, X.-L. (2009). Isolation, Characterization, and Mapping of Genomic Microsatellite Markers in Sea-Island Cotton (*Gossypium barbadense*). *Acta Agronomica Sinica*, 35(6): 1013-1020.
- [102] Bolek, Y. (2010). Genetic variability among cotton genotypes for cold tolerance. *Field Crops Research*, 119(1): 59-67.
- [103] Chapagain, A.K., Hoekstra, A.Y., Savenije, H.H.G., and Gautam, R. (2006). The water footprint of cotton consumption: An assessment of the impact of worldwide consumption of cotton products on the water resources in the cotton producing countries. *Ecological Economics*, 60(1), 186-203.
- [104] Kaminski, J., Headey, D., and Bernard, T. (2011). The Burkina Faso Cotton Story 1992–2007: Sustainable Success or Sub-Saharan Mirage?. *World Development*, In Press, doi:10.1016/j.worlddev.2010.12.003.
- [105] Tennakoon, S. B., and Milroy, S.P. (2003). Crop water use and water use efficiency on irrigated cotton farms in Australia *Agricultural Water Management*, 61(3): 179-194.
- [106] Prentice, A.N. (1972). Cotton with Special Reference to Africa: chapter 10 – the physical environment: climate and soil.

-
- [107] Lacape, M.J., Wery, J., and Annerose, D.J.M. (1998). Relationships between plant and soil water status in five field-grown cotton (*Gossypium hirsutum* L.) cultivars. *Field Crops Research*, 57(1): 29-43.
 - [108] Golenko-Ginzburg, D., Sinuany-Stern, Z., and Kats, V. (1996). A multilevel decision-making system with multiple resources for controlling cotton harvesting. *International Journal of Production Economics*, 46-47: 55-63.
 - [109] Gemtos, T.A., and Tsiricoglou, Th. (1999). Harvesting of cotton residue for energy production. *Biomass and Bioenergy*, 16(1): 51-59.
 - [110] McLaughlin, J.W., Gale, M.R., Jurgensen, M.F., and Trettin, C.C. (2000). Soil organic matter and nitrogen cycling in response to harvesting, mechanical site preparation, and fertilization in a wetland with a mineral substrate. *Forest Ecology and Management*, 129(1-3): 7-23.
 - [111] Sun, X., Chen, X., Zhang, Z., Wang, H., Bianchi, F.J.J.A., Peng, H., Vlak, J.M., and Hu, Z. (2002). Bollworm responses to release of genetically modified *Helicoverpa armigera* nucleopolyhedroviruses in cotton. *Journal of Invertebrate Pathology*, 81(2): 63-69.
 - [112] Sun, X., van der Werf, W., Bianchi, F.J.J.A., Hu, Z., and Vlak, J.M. (2006). Modelling biological control with wild-type and genetically modified baculoviruses in the *Helicoverpa armigera*–cotton system. *Ecological Modelling*, 198(3-4): 387-398.
 - [113] Chen, D., Ye, G., Yang, C., Chen, Y., and Wu, Y. (2005). The effect of high temperature on the insecticidal properties of Bt Cotton. *Environmental and Experimental Botany*, 53(3): 333-342.
 - [114] Morse, S., Bennett, R.M., and Ismael, Y. (2005). Genetically modified insect resistance in cotton: some farm level economic impacts in India. *Crop Protection*, 24(5): 433-440.
 - [115] Morse, S., Bennett, R.M., and Ismael, Y. (2006). Environmental impact of genetically modified cotton in South Africa. *Agriculture, Ecosystems and Environment*, 117(4): 277-289.
 - [116] Lu, Y.H., Qiu, F., Feng, H.Q., Li, H.B., Yang, Z.C., Wyckhuys, K.A.G., and Wu, K.M. (2008). Species composition and seasonal abundance of pestiferous plant bugs (Hemiptera: Miridae) on Bt Cotton in China. *Crop Protection*, 27(3-5): 465-472.
 - [117] Sacks, E.J., and Robinson, A.F. (2009). Introgression of resistance to reniform nematode (*Rotylenchulus reniformis*) into upland cotton (*Gossypium hirsutum*) from *Gossypium arboreum* and a *G. hirsutum*/*Gossypium aridum* bridging line. *Field Crops Research*, 112(1): 1-6.
 - [118] Toenniessen, G.H., O'Toole, J.C., and DeVries, J. (2003). Advances in plant biotechnology and its adoption in developing countries. *Current Opinion in Plant Biology*, 6(2): 191-198.
 - [119] Frisvold, G.B., and Reeves, J.M. (2008). The costs and benefits of refuge requirements: The case of Bt cotton. *Ecological Economics*, 65(1): 87-97.
 - [120] Marzban, R., He, Q., Liu, X., and Zhang, Q. (2009). Effects of *Bacillus thuringiensis* toxin Cry1Ac and cytoplasmic polyhedrosis virus of *Helicoverpa armigera* (Hübner) (HaCPV) on cotton bollworm (Lepidoptera: Noctuidae). *Journal of Invertebrate Pathology*, 101(1): 71-76.
 - [121] Llewellyn, D., Tyson, C., Constable, G., Duggan, B., Beale, S., and Steel, P. (2007). Containment of regulated genetically modified cotton in the field. *Agriculture, Ecosystems and Environment*, 121(4): 419-429.

-
- [122] Knox, O.G.G., Nehl, D.B., Mor, T., Roberts, G.N., and Gupta, V.V.S.R. (2008). Genetically modified cotton has no effect on arbuscular mycorrhizal colonisation of roots. *Field Crops Research*, 109(1-3): 57-60.
- [123] Johnson, W.G., Davis, V.M., Kruger, G.R., and Weller, S.C. (2009). Influence of glyphosate-resistant cropping systems on weed species shifts and glyphosate-resistant weed populations. *European Journal of Agronomy*, 31(3): 162-172.
- [124] Subramanian, A., and Qaim, M. (2009). Village-wide Effects of Agricultural Biotechnology: The Case of Bt Cotton in India. *World Development*, 37(1): 256-267.
- [125] John, J., Diallo, G. (2005). Organic cotton at Koussanar, Eastern Senegal in: Baier A., Hammer J. (2005): Proceedings – Back to the roots: The farmers' perspective on organic cotton production and Marketing, PAN Germany, Hamburg.
- [126] EJF (2007). The deadly chemicals in cotton. Environmental Justice Foundation in collaboration with Pesticide Action Network UK: London, UK. ISBN No. 1-904523-10-2.
- [127] Rieple, A., and Singh, R. (2010). A value chain analysis of the organic cotton industry: The case of UK retailers and Indian suppliers. *Ecological Economics*, 69(11): 2292-2302.
- [128] Cooper, J. C., and Terrill, T.E. (1991). The American South. New York: Alfred A. Knopf. ISBN 0394589483.
- [129] Dodd, W.v.E. (1920). The Cotton Kingdom: A Chronicle of the Old South. New Haven, CT: Yale University Press.
- [130] Moch, Jr. I. (1989). A twenty year case history: B-9 Hollow fiber permeator, *Desalination*, 74: 171-181.
- [131] Zhang, P., Fletcher, S.M., and Ethridge, D.E. (1994). Interfiber Competition in Textile Mills Over Time. *Journal of Agriculture and Applied Economy*, 26(1): 173-182.
- [132] Ramakrishna, S., Mayer, J., Wintermantel, E., and Leong, K.W. (2001). Biomedical applications of polymer-composite materials: a review. *Composites Science and Technology*, 61(9): 1189-1224.
- [133] Horrocks, A.R., Kandola, B.K., Davies, P.J., Zhang, S., Padbury, S.A. (2005). Developments in flame retardant textiles – a review. *Polymer Degradation and Stability*, 88(1): 3-12.
- [134] Giraud, S., Bourbigot, S., Rochery, M., Vroman, I., Tighzert, L., Delobel, R., and Poutch, F. (2005). Flame retarded polyurea with microencapsulated ammonium phosphate for textile coating. *Polymer Degradation and Stability*, 88(1): 106-113.
- [135] Yang, H., and Yang, C.Q. (2005). Durable flame retardant finishing of the nylon/cotton blend fabric using a hydroxyl-functional organophosphorus oligomer. *Polymer Degradation and Stability*, 88(3): 363-370.
- [136] Siriviriyun, A., O'Rear, E.A., and Yanumet, N. (2009). The effect of phosphorus content on the thermal and the burning properties of cotton fabric coated with an ultrathin film of a phosphorus-containing polymer. *Polymer Degradation and Stability*, 94(4): 558-565.
- [137] Delhom, C.D., White-Ghoorahoo, L.A., and Pang, S.S. (2010). Development and characterization of cellulose/clay nanocomposites. *Composites Part B: Engineering*, 41(6): 475-481.

-
- [138] Horrocks, A.R. (2011). Flame retardant challenges for textiles and fibers: New chemistry versus innovatory solutions. *Polymer Degradation and Stability*, 96(3): 377-392.
 - [139] Alongi, J., Ciobanu, M., and Malucelli, G. (2011). Novel flame retardant finishing systems for cotton fabrics based on phosphorus-containing compounds and silica derived from sol-gel processes. *Carbohydrate Polymers*, In Press, doi:10.1016/j.carbpol.2011.03.024.
 - [140] Adams, J.E. (1950). Cotton. *Advances in Agronomy*, 2: 1-80.
 - [141] El-Nockrashy, A.S., Simmons, J.G., and Frampton, V.L. (1969). A chemical survey of seeds of the genus *Gossypium*. *Phytochemistry*, 8(10): 1949-1958.
 - [142] Carter, F.L., Castillo, A.E., Frampton, V.L., Kerr, T. (1966). Chemical composition studies of seeds of the genus *Gossypium*. *Phytochemistry*, 5(6): 1103-1112
 - [143] Arieli, A. (1998). Whole cottonseed in dairy cattle feeding: a review. *Animal Feed Science and Technology*, 72(1-2): 97-110.
 - [144] Bertrand, J.A., Sudduth, T.Q., Condon, A., Jenkins, T.C., and Calhoun, M.C. (2005). Nutrient Content of Whole Cottonseed. *Journal of Dairy Science*, 88(4): 1470-1477.
 - [145] Cauquil, J. (1987). Cotton-pest control: a review of the introduction of ultra-low-volume (ULV) spraying in sub-Saharan French-speaking Africa. *Crop Protection*, 6(1): 38-42.
 - [146] Smith, C.W. (1992). History and Status of Host Plant Resistance in Cotton to Insects in the United States. *Advances in Agronomy*, 48: 251-296
 - [147] Summy, K.R., and King, E.G. (1992). Cultural control of cotton insect pests in the United States. *Crop Protection*, 11(4): 307-319.
 - [148] Henneberry, T.J., and Clayton, T.E. (1982). Pink bollworm of cotton (*Pectinophora gossypiella* (Saunders)): male moth catches in gossyplure-baited traps and relationships to oviposition, boll infestation and moth emergence. *Crop Protection*, 1(4): 497-504.
 - [149] Gouge, D.H., Lee, L.L., and Henneberry, T.J. (1999). Parasitism of diapausing pink bollworm *Pectinophora gossypiella* (Lepidoptera: *Gelechiidae*) larvae by entomopathogenic nematodes (Nematoda: *Steinernematidae*, *Heterorhabditidae*). *Crop Protection*, 18(8): 531-537.
 - [150] González-Cabrera, J., Escriche, B., Tabashnik, B.E., and Ferré, J. (2003). Binding of *Bacillus thuringiensis* toxins in resistant and susceptible strains of pink bollworm (*Pectinophora gossypiella*). *Insect Biochemistry and Molecular Biology*, 33(9): 929-935.
 - [151] Wan, P., Wu, K., Huang, M., and Wu, J. (2004). Seasonal pattern of infestation by pink bollworm *Pectinophora gossypiella* (Saunders) in field plots of Bt transgenic cotton in the Yangtze River valley of China. *Crop Protection*, 23(5): 463-467.
 - [152] Lykouressis, D., Perdakis, D., Samartzis, D., Fantinou, A., and Toutouzas, S. (2005). Management of the pink bollworm *Pectinophora gossypiella* (Saunders) (Lepidoptera: *Gelechiidae*) by mating disruption in cotton fields. *Crop Protection*, 24(2): 177-183.
 - [153] Rojas, R.R., Leggett, J.E., and Leopold, R.A. (1990). Dormancy in southwestern cotton boll weevils: A comparative physiological study of *Anthonomus grandis* in wild and domesticated cotton bolls. *Journal of Insect Physiology*, 36(8): 601-606.
 - [154] Summy, K.R., Greenberg, S.M., Morales-Ramos, J.A., and King, E.G. (1997). Suppression of Boll Weevil Infestations (Coleoptera: *Curculionidae*) Occurring on

- Fallow-Season Cotton in Southern Texas by Augmentative Releases of *Catolaccus grandis* (Hymenoptera: *Pteromalidae*). *Biological Control*, 9(3): 209-215.
- [155] Gomes, A.P.G., Dias, S.C., Bloch Jr., C., Melo, F.R., Furtado Jr., J.R., Monnerat, R.G., Grossi-de-Sá, M.F., and Franco, O.L. (2005). Toxicity to cotton boll weevil *Anthonomus grandis* of a trypsin inhibitor from chickpea seeds. *Comparative Biochemistry and Physiology Part B: Biochemistry and Molecular Biology*, 140(2): 313-319.
- [156] Martins, É.S., Monnerat, R.G., Queiroz, P.R., Dumas, V.F., Braz, S.V., Aguiar, R.W.S., Ana Cristina Menezes Mendes Gomes, Jorge Sánchez, Alejandra Bravo, and Bergmann Ribeiro, M. (2010). Midgut GPI-anchored proteins with alkaline phosphatase activity from the cotton boll weevil (*Anthonomus grandis*) are putative receptors for the Cry1B protein of *Bacillus thuringiensis*. *Insect Biochemistry and Molecular Biology*, 40(2): 138-145.
- [157] Horowitz, A.R., Klein, M., Yablonski, S., Ishaaya, I. (1992). Evaluation of benzoylphenyl ureas for controlling the spiny bollworm, *Earias insulana* (Boisd.), in cotton. *Crop Protection*, 11(5): 465-469.
- [158] Ibargutxi, M.A., Muñoz, D., Ruíz de Escudero, I., and Caballero, P. (2008). Interactions between Cry1Ac, Cry2Ab, and Cry1Fa *Bacillus thuringiensis* toxins in the cotton pests *Helicoverpa armigera* (Hübner) and *Earias insulana* (Boisduval). *Biological Control*, 47(1): 89-96.
- [159] Brévault, T., Oumarou, Y., Achaleke, J., Vaissayre, M., and Nibouche, S. (2009). Initial activity and persistence of insecticides for the control of bollworms (Lepidoptera: Noctuidae) in cotton crops. *Crop Protection*, 28(5): 401-406.
- [160] Farine, J.-P., Everaerts, C., Brossut, R., and Le Quère, J.-L. (1993). Defensive secretions of nymphs and adults of five species of *Pyrrhocoridae* (Insecta: *Heteroptera*). *Biochemical Systematics and Ecology*, 21(3): 363-371.
- [161] Okunade, A. L. (2002). *Ageratum conyzoides* L. (Asteraceae). *Fitoterapia*, 73(1): 1-16.
- [162] Butler Jr., G.D., Rimon, D., and Henneberry, T.J. (1988). *Bemisia tabaci* (Homoptera: *Aleyrodidae*): populations on different cotton varieties and cotton stickiness in Israel. *Crop Protection*, 7(1): 43-47.
- [163] Naranjo, S.E., Ellsworth, P.C., and Hagler, J.R. (2004). Conservation of natural enemies in cotton: role of insect growth regulators in management of *Bemisia tabaci*. *Biological Control*, 30(1): 52-72.
- [164] Steinkraus, D.C., Boys, G.O., and Rosenheim, J.A. (2002). Classical biological control of *Aphis gossypii* (Homoptera: Aphididae) with *Neozygites fresenii* (Entomophthorales: Neozygiteaceae) in California cotton. *Biological Control*, 25(3): 297-304.
- [165] Obrycki, J.J., Harwood, J.D., Kring, T.J., and O'Neil, R.J. (2009). Aphidophagy by Coccinellidae: Application of biological control in agroecosystems. *Biological Control*, 51(2): 244-254.
- [166] Kim, J.J., Goettel, M.S., and Gillespie, D.R. (2010). Evaluation of *Lecanicillium longisporum*, Vertalec against the cotton aphid, *Aphis gossypii*, and cucumber powdery mildew, *Sphaerotheca fuliginea* in a greenhouse environment. *Crop Protection*, 29(6): 540-544.
- [167] Dang, Q.L., Lee, G.Y., Choi, Y.H., Choi, G.J., Jang, K.S., Park, M.S., Soh, H.S., Han, Y.H., Lim, C.H., and Kim, J.-C. (2010). Insecticidal activities of crude extracts and

- phospholipids from *Chenopodium ficifolium* against melon and cotton aphid, *Aphis gossypii*. *Crop Protection*, 29(10): 1124-1129.
- [168] Barbosa, A.E.A.D., Fragoso, R.R., Souza, D.S.L., Freire, É., Neto, O.B.O., Viana, A.A.B., Togawa, R.C., Guimarães, L.M., Martins, N.F., Cia, E., Fernandez, D., Lima, L.M., Silva, M.C.M., Rocha, T.L., and Grossi-de-Sa, M.F. (2009). Differentially expressed genes in cotton plant genotypes infected with *Meloidogyne incognita*. *Plant Science*, 177(5): 492-497.
- [169] CIRAD (2010). <http://www.cirad.fr/fr/index.php>.
- [170] Essenberg, M., Cason Jr., E.T., Hamilton, B., Brinkerhoff, L.A., Gholson, R.K., and Richardson, P.E. (1979). Single cell colonies of *Xanthomonas malvacearum* in susceptible and immune cotton leaves and the local resistant response to colonies in immune leaves. *Physiological Plant Pathology*, 15(1): 53-58, IN16-IN19, 59-68.
- [171] Poswal, M.A.T., and Erinle, I.D. (1983). A survey of extent of infection and contamination of cotton-seed market and commercial gin samples by *Xanthomonas malvacearum* (E.F. Smith) Dowson in the Northern States of Nigeria. *Crop Protection*, 2(4): 473-481.
- [172] Poswal, M.A.T., and Erinle, I.D. (1984). Assessment of levels of resistance of cotton cultivars to isolates of *Xanthomonas malvacearum* (E.F. Smith) Dowson in Nigeria. *Crop Protection*, 3(1): 103-110.
- [173] Hopkins, J.C.F. (1931). *Alternaria gossypina* (Thüm.) comb. nov. causing a leaf spot and boll rot of cotton. *Transactions of the British Mycological Society*, 16(2-3): 136-144, IN4.
- [174] Fan, W.-w., Wang, L.-a., Ma, C.-h., Dong, W.-q. Li, Y.-c., Liu, Z.-h., Jia, Y.-s., Geng, J.-y., and Zhang, X.-y. (2007). The Influence of the *Verticillium dahliae* Kleb Infection on the Anti-Enzyme Inside the Body of the Cotton with Different Root Injured Degree. *Agricultural Sciences in China*, 6(7): 816-824
- [175] Kurt, S., Dervis, S., and Sahinler, S. (2003). Sensitivity of *Verticillium dahliae* to prochloraz and prochloraz–manganese complex and control of *Verticillium* wilt of cotton in the field. *Crop Protection*, 22(1): 51-55.
- [176] Göre, M.E., Caner, Ö.K., Altın, N., Aydın, M.H., Erdoğan, O., Filizer, F., and Büyükdöğerlioğlu, A. (2009). Evaluation of cotton cultivars for resistance to pathotypes of *Verticillium dahlia*. *Crop Protection*, 28(3): 215-219.
- [177] Bailey, B.A., and Bourland, F.M. (1986). The influence of seed quality on response of cotton seedlings to the preplant herbicide trifluralin. *Field Crops Research*, 13: 375-382.
- [178] Hillocks, R.J., Chinodya, R., Gunner, R. (1988). Evaluation of seed dressing and in-furrow treatments with fungicides for control of seedling disease in cotton caused by *Rhizoctonia solani*. *Crop Protection*, 7(5): 309-313.
- [179] Hancock, J.H., Wilkerson, J.B., Moody, F.H., Newman, M.A. (2004). Seed-specific placement of in-furrow fungicides for control of seedling disease in cotton. *Crop Protection*, Volume 23(9): 789-794.
- [180] Howell, C.R., and Puckhaber, L.S. (2005). A study of the characteristics of “P” and “Q” strains of *Trichoderma virens* to account for differences in biological control efficacy against cotton seedling diseases. *Biological Control*, 33(2): 217-222.
- [181] Rao, M.V., and Rao, A.S., 1966. *Fusarium* wilt of cotton in relation to inoculum potential. *Transactions of the British Mycological Society*, Volume 49(3):403-409.

- [182] Harrison, N.A., and Beckman, C.H. (1982). Time/space relationships of colonization and host response in wilt-resistant and wilt-susceptible cotton (*Gossypium*) cultivars inoculated with *Verticillium dahliae* and *Fusarium oxysporum* f. sp. *Vasinfestum*. *Physiological Plant Pathology*, 21(2): 193-207.
- [183] El-Abyad, M.S., Ismail, I.K., and Al-Meshhadani, S.A. (1983). Effects of some biocides on *Fusarium oxysporum* formae speciales causing cotton and tomato wilts in Egypt. *Transactions of the British Mycological Society*, 80(2): 283-287.
- [184] Shen, C.-Y. (1985). Integrated management of *Fusarium* and *Verticillium* wilts of cotton in China. *Crop Protection*, 4(3): 337-345.
- [185] Wang, P.-z., Shi, L.-f., Su, L., and Hu, B.-m. (2010). Quantitative Trait Loci for Resistance Against *Fusarium* Wilt Based on Three Cotton F2 Populations. *Agricultural Sciences in China*, 9(12): 1799-1806.
- [186] Hu, J.-L., Lin, X.-G., Wang, J.-H., Shen, W.-S., Wu, S., Peng, S.-P., and Mao, T.-T. (2010). Arbuscular Mycorrhizal Fungal Inoculation Enhances Suppression of Cucumber *Fusarium* Wilt in Greenhouse Soils. *Pedosphere*, 20(5): 586-593.
- [187] Gunasekaran, M., Hess, W.M., Weber, D.J. (1974). Lipids and ultrastructure of *Phymatotrichum omnivorum*. *Transactions of the British Mycological Society*, Volume 63, Issue 3, December 1974, Pages 519-525, IN22-IN24.
- [188] Kenerley, C.M., Jeger, M.J., Zuberer, D.A., Jones, R.W. (1987). Populations of fungi associated with sclerotia of *Phymatotrichum omnivorum* buried in Houston black clay. *Transactions of the British Mycological Society*, 89(4): 437-445.
- [189] Yang, C., Everitt, J.H., and Fernandez, C.J. (2010). Comparison of airborne multispectral and hyperspectral imagery for mapping cotton root rot. *Biosystems Engineering*, 107(2): 131-139.
- [190] ICAC (2011). International Cotton Advisory Committee. <http://www.icac.org/>
- [191] Lloyd, E.H., and Seber, D. (2000). "Bast fiber applications for composites" <http://www.fibrealternatives.com/bast.fiber.applacationforcomposite.htm> (last access 2/9/2011 2:13 PM).
- [192] Summerscales, J., Dissanayake, N., Virk, A., and Hall, W. (2010). A review of bast fibres and their composites. Part 2 – Composites. *Composites Part A: Applied Science and Manufacturing*, 41(10): 1336-1344.
- [193] Summerscales, J., Dissanayake, N.P.J., Virk, A.S., Hall, W. (2010). A review of bast fibres and their composites. Part 1 – Fibres as reinforcements. *Composites Part A: Applied Science and Manufacturing*, 41(10): 1329-1335.
- [194] Bergfjord, C., and Holst, B. (2010). A procedure for identifying textile bast fibres using microscopy: Flax, nettle/ramie, hemp and jute. *Ultramicroscopy*, 110(9): 1192-1197.
- [195] Morrison III, W.H., Akin, D.E., Archibald, D.D., Dodd, R.B., and Raymer, P.L. (1999). Chemical and instrumental characterization of maturing kenaf core and bast. *Industrial Crops and Products*, 10(1): 21-34.
- [196] Kuroda, K.-i., Nakagawa-izumi, A., Mazumder, B.B., Ohtani, Y., and Sameshima, K. (2005). Evaluation of chemical composition of the core and bast lignins of variety Chinpi-3 kenaf (*Hibiscus cannabinus* L.) by pyrolysis–gas chromatography/mass spectrometry and cupric oxide oxidation. *Industrial Crops and Products*, 22(3): 223-232.

-
- [197] Gurjanov, O.P., Ibragimova, N.N., Gnezdilov, O.I., and Gorshkova, T.A. (2008). Polysaccharides, tightly bound to cellulose in cell wall of flax bast fiber: Isolation and identification. *Carbohydrate Polymers*, 72(4): 719-729.
 - [198] del Río, J.C., Marques, G., Rodríguez, I.M., and Gutiérrez, A. (2009). Chemical composition of lipophilic extractives from jute (*Corchorus capsularis*) fibers used for manufacturing of high-quality paper pulps. *Industrial Crops and Products*, 30(2): 241-249.
 - [199] Khiari, R., Mhenni, M.F., Belgacem, M.N., and Mauret, E. (2010). Chemical composition and pulping of date palm rachis and *Posidonia oceanica* – A comparison with other wood and non-wood fiber sources. *Bioresource Technology*, 101(2): 775-780.
 - [200] Hayward, H.E. (1948). *The Structure of Economic Plants*, MacMillan.
 - [201] Berger, J. (1969). *The World's Major Fibre Crops*, Center d'Etude de l'Azote, Zurich.
 - [202] Datwyler, S.L., and Weiblen, G.D. (2006). Genetic Variation in Hemp and marijuana (*Cannabis sativa* L.) sativa plants are taller and less dense. Indica plants are shorter but a lot more dense than sativas. According to Amplified Fragment Length Polymorphisms. *J. Forensic Sci.* 51(2): 371-375.
 - [203] West, D.P. (1998). *Hemp and Marijuana: Myths and Realities*, 998 North American Industrial Hemp Council, INC.
 - [204] http://www.naihc.org/hemp_information/content/hemp.mj.html. Retrieved 2011-03-15.
 - [205] NF (2009). (<http://www.naturalfibres2009.org/en/fibres/hemp.html>).
 - [206] CRRH (2010). (<http://crrh.org/cannabis/>;
 - [207] <http://www.etymonline.com/index.php?term=canvas>).
 - [208] Schultes, R.E., Hofmann, A., and Rätsch, C. (2001). *Plants of the Gods: Their Sacred, Healing and Hallucinogenic Powers*. Inner Traditions Publishers, pp 208, ISBN: 0892819790. http://www.erowid.org/plants/cannabis/cannabis_culture2.shtml.
 - [209] Schwab, U., Callaway, J., Erkkilä, A., Gynther, J., Uusitupa, M., and Järvinen, T. (2006). Effects of hempseed and flaxseed oils on the profile of serum lipids, serum total and lipoprotein lipid concentrations and haemostatic. *European J. Nutrition*, 45(8): 470-7.
 - [210] Meints, J. (2007). *The Hemp Plant, Humankind's Savior “The Hemp Plant, Humankind's Savior - 50,000 Uses and Counting”*.
 - [211] <http://www.voteindustrialhemp.com/>. Retrieved 2011-03-15.
 - [212] Osburn, L. 1992. Hemp seed: the most nutritionally complete food source in the world. *Hemp Line J.*, 1(1): 114-15.
 - [213] USDA (1998). <http://www.ers.usda.gov/publications/ages001E/ages001Eh.pdf>. Retrieved 2011-03-15.
 - [214] Webster, C.D., Thompson, K.R., Morgan, A.M., Grisby, E.J., and Gannam, A.L. (2000). Use of hempseed meal, poultry by-product meal, and canola meal in practical diets without fish meal for sunshine bass (*Morone chrysops*×*M. saxatilis*). *Aquaculture*, 188(3-4): 299-309.
 - [215] Oomah, B.D., Busson, M., Godfrey, D.V., and Drover, J.C.G. (2002). Characteristics of hemp (*Cannabis sativa* L.) seed oil. *Food Chemistry*, 76(1): 33-43.
 - [216] Lu, R.-R., Qian, P., Sun, Z., Zhou, X.-H., Chen, T.-P., He, J.-F., Zhang, H., and Wu, J. (2010). Hempseed protein derived antioxidative peptides: Purification, identification

- and protection from hydrogen peroxide-induced apoptosis in PC12 cells *Original Research Article Food Chemistry*, 123(4): 1210-1218.
- [217] Callaway, J.C. (2004). Hempseed as a nutritional resource: an overview, *Euphytica* 140: 65-72.
- [218] Balter M. (2009). Clothes make the (Hu) Man. *Science*, 325(5946): 1329. doi:10.1126/science.325_1329a (http://dx.doi.org/10.1126%2Fscience.325_1329a).
- [219] Kvavadze, E; Bar-Yosef, O; Belfer-Cohen, A; Boaretto, E; Jakeli, N; Matskevich, Z; and Meshveliani, T., (2009). 30,000-Year-Old Wild Flax Fibers. *Science*, 325 (5946): 1359. doi:10.1126/science.1175404 (<http://dx.doi.org/10.1126%2Fscience.1175404>) Supporting Online Material
- [220] (<http://www.sciencemag.org/cgi/data/325/5946/1359/DC1/1>).
- [221] Westonaprice (2010). <http://www.westonaprice.org/Flaxseed-and-Flaxseed-Oils-for-Omega-3-Fatty-Acids.html>.
- [222] EW (2010). <http://en.wikipedia.org/wiki/Flax>.
- [223] Mo., A.H. (1969). "Flax article", Funk and Wagnalls New Encyclopedia, Vol. 10.
- [224] Gu, Z.F. (1994). "Study on the selection of new flax cultivar Heiya 8 and its cultivation," China's Fiber Crops. Academy of Agricultural Sciences, Hulan Country, Heilongjiang, China. No. 1, 6-7.
- [225] Wong, Al. (1990). "Bleached Flax Pulp Mill Prospectus", Arboken, Vancouver, British Columbia.
- [226] Wilkens, C. 1988. "Amazing Flax, Such a versatile Prairie crop", *Canadian Geographic*, Oct/Nov (1988).
- [227] G.F.S. (1927). On the change of refractive index of linseed oil in the process of drying and its effect on the deterioration of oil paintings: A. P. Laurie. *Proc. Roy. Soc., A* 760. *Journal of the Franklin Institute*, 203(2): 209-210.
- [228] Oldring, P.K.T. (2004). Coatings, Colorants, and Paints. *Encyclopedia of Physical Science and Technology*, 175-190.
- [229] Araujo, W.S., Margarit, I.C.P., Mattos, O.R., Fragata, F.L., and de Lima-Neto, P. (2010). Corrosion aspects of alkyd paints modified with linseed and soy oils. *Electrochimica Acta*, 55(21): 6204-6211.
- [230] Pan, A., Yu, D., Demark-Wahnefried, W., Franco, O.H., and Lin, X. (2009). Meta-analysis of the effects of flaxseed interventions on blood lipids, *Am. J. Clin. Nutr.* 90(2): 288-297.
- [231] Chen, J., Wang, L., and Thompson, L.U. (2006). Flaxseed and its components reduce metastasis after surgical excision of solid human breast tumor in nude mice, *Cancer Lett.* 234(2): 168-175.
- [232] Thompson, L.U., Chen, J.M.; Li, T., Strasser-Weippl, K., and Goss, P.E. (2005). Dietary flaxseed alters tumor biological markers in postmenopausal breast cancer. *Clin. Cancer Res.* 11(10): 3828-2835.
- [233] Science Daily (2007). Flaxseed Stunts The Growth Of Prostate Tumors" (<http://www.sciencedaily.com/releases/2007/06/070603215443.htm>).
- [234] Dahl, W.J.; Lockert, E.A.; Cammer, A.L.; and Whiting, S.J. (2005). Effects of Flax Fiber on Laxation and Glycemic Response in Healthy Volunteers, *Journal of Medicinal and Food*, 8(4): 508-511.
- [235] Shinn, J., 1886. The cultivation of flax in the United States. *Journal of the Franklin Institute*, 121(5): 362-373.

- [236] Culbertson, J.O. (1954). Seed-Flax Improvement. *Advances in Agronomy*, 6: 143-182.
- [237] Pals, J.P., and van Dierendonck, M.C. (1988). Between flax and fabric: Cultivation and processing of flax in a mediaeval peat reclamation settlement near midwoud (Prov. Noord Holland). *Journal of Archaeological Science*, 15(3): 237-251.
- [238] van der Werf, H.M.G., and Turunen, L. (2008). The environmental impacts of the production of hemp and flax textile yarn. *Industrial Crops and Products*, 27(1): 1-10.
- [239] Dodd, F.A. (2001). Processing techniques for improving enzyme-retting of flax, *International Crops and Production*, 13, 239-248.
- [240] Dodd, F.A. (2008). Pectinolytic enzymes and retting. *BioResources*, 3(1): 155-169.
- [241] Bell, J.M., and Keith, M.O. (1993). Nutritional evaluation of linseed meals from flax with yellow or brown hulls, using mice and pigs. *Animal Feed Science and Technology*, 43(1-2): 1-18.
- [242] Casa, R., Russell, G., Lo B., Cascio, Rossini, F. (1999). Environmental effects on linseed (*Linum usitatissimum* L.) yield and growth of flax at different stand densities. *European Journal of Agronomy*, 11(3-4): 267-278.
- [243] Gros, C., Lanoisellé, J.-L. and Vorobiev, E. (2003). Towards an Alternative Extraction Process for Linseed Oil. *Chemical Engineering Research and Design*, 81(9): 1059-1065.
- [244] Williams, D., Verghese, M., Walker, L.T., Boateng, J., Shackelford, L., and Chawan, C.B. (2007). Flax seed oil and flax seed meal reduce the formation of aberrant crypt foci (ACF) in azoxymethane-induced colon cancer in Fisher 344 male rats. *Food and Chemical Toxicology*, 45(1): 153-159.
- [245] Cämmerer, B., and Kroh, L.W. (2009). Shelf life of linseeds and peanuts in relation to roasting. *LWT- Food Science and Technology*, 42(2): 545-549.
- [246] Mueller, K., Eisner, P., and Kirchhoff, E. (2010). Simplified fractionation process for linseed meal by alkaline extraction – Functional properties of protein and fiber fractions. *Journal of Food Engineering*, 99(1): 49-54.
- [247] Beynen, A.C. (2004). Fatty acid composition of eggs produced by hens fed diets containing groundnut, soya bean or linseed. *NJAS - Wageningen Journal of Life Sciences*, 52(1): 3-10.
- [248] Peiretti, P.G. and Meineri, G. (2007). Fatty acids, chemical composition and organic matter digestibility of seeds and vegetative parts of false flax (*Camelina sativa* L.) after different lengths of growth. *Animal Feed Science and Technology*, 133(3-4): 341-350.
- [249] Webber-III, C.L., Whitworth, J., and Dole, J. (1999). Kenaf (*Hibiscus cannabinus* L.) core as a containerized growth medium component. *Industrial Crops and Products*, 10(2): 97-105.
- [250] US-DAARS (1970). U. S. Department of Agriculture, Agricultural Research Service. 1970. "Cultural and Harvesting Methods for Kenaf, an Annual Crop Source of Pulp in the Southeast." U. S. Department of Agriculture, Agricultural Research Service.
- [251] White, G.A., and Higgins, J.J. 1964. "Growing Kenaf for Paper". Second International Kenaf Conference Proceedings, Palm Beach, Florida, pp. 27-40.
- [252] Bergeson, G.B. (1972). Concepts of nematode - Fungus associations in plant disease complexes: A review. *Experimental Parasitology*, 32(2): 301-314.
- [253] Robinson, A.F., and Cook, C.G. (2001). Root-knot and reniform nematode reproduction on kenaf and sunn hemp compared with that on nematode resistant and susceptible cotton. *Industrial Crops and Products*, 13(3): 249-264.

-
- [254] Webber III, C.L., and Bledsoe, V.K. (2002). Plant maturity and kenaf yield components. *Industrial Crops and Products*, 16(2): 81-88.
- [255] LeMahieu, P.J., Oplinger E.S., and Putnam, D.H. (1991). Kenaf, in *Alternative Field Crops Manual*. Wisconsin Agricultural Extension Service. Madison, Wisconsin.
- [256] Vannini, L., and Venturi, G. (1992). "Aspetti tecnico-economici della coltivazione del kenaf", "Technical and economic aspects of growing kenaf". *Informatore-Agrario*. 48: 47, 33-39.
- [257] Ayerza (h), R., and Coates, W. (1996). Kenaf performance in northwestern Argentina. *Industrial Crops and Products*, 5(3): 223-228.
- [258] Ogbonnaya, C.I., Nwalozie, M.C., Roy-Macauley, H., and Annerose, D.J.M. (1998). Growth and water relations of Kenaf (*Hibiscus cannabinus* L.) under water deficit on a sandy soil. *Industrial Crops and Products*, 8(1): 65-76.
- [259] Angelini, L.G., Macchia, M., Ceccarini, L., and Bonari, E. (1998). Screening of kenaf (*Hibiscus cannabinus* L.) genotypes for low temperature requirements during germination and evaluation of feasibility of seed production in Italy. *Field Crops Research*, 59(1): 73-79.
- [260] Bañuelos, G.S., Bryla, D.R., and Cook, C.G. (2002). Vegetative production of kenaf and canola under irrigation in central California. *Industrial Crops and Products*, 15(3): 237-245.
- [261] Danalatos, N.G., and Archontoulis, S.V. (2010). Growth and biomass productivity of kenaf (*Hibiscus cannabinus*, L.) under different agricultural inputs and management practices in central Greece. *Industrial Crops and Products*, 32(3): 231-240.
- [262] Lips, S.J.J., Iñiguez de Heredia, G.M., Op den Kamp, R.G.M., and van Dam, J.E.G. (2009). Water absorption characteristics of kenaf core to use as animal bedding material. *Industrial Crops and Products*, 29(1): 73-79.
- [263] Sellers, T., Miller, G.D., and Fuller, M.J. (1993). "Kenaf core as a board raw material," *Forest Products Journal*. 1993, 43: 7-8, 69-71.
- [264] Schroeter, M.C. (1994). "Use of Kenaf for Linerboard Quality Enhancement," *Proceedings from 1994 Pulp Conference*. Herty Foundation Research and Development Center, Savannah, Georgia.
- [265] Petrini, C., Bazzocchi, R., and Montalti, P. (1994). Yield potential and adaptation of kenaf (*Hibiscus cannabinus*) in north-central Italy. *Industrial Crops and Products*, 3(1-2): 11-15.
- [266] Keshk, S., Suwinarti, W., and Sameshima, K. (2006). Physicochemical characterization of different treatment sequences on kenaf bast fiber. *Carbohydrate Polymers*, 65(2): 202-206.
- [267] Komiyama, H., Kato, A., Aimi, H., Ogihara, J., and Shimizu, K. (2008). Chemical structure of kenaf xylan. *Carbohydrate Polymers*, 72(4): 638-645.
- [268] Juhaida, M.F., Paridah, M.T., Mohd. M., Hilmi, Z., Sarani, H., Jalaluddin, A.R., Zaki, M. (2010). Liquefaction of kenaf (*Hibiscus cannabinus* L.) core for wood laminating adhesive. *Bioresource Technology*, 101(4): 1355-1360.
- [269] Abdul Khalil, H.P.S., Yusra, A.F.I., Bhat, A.H., and Jawaid, M. (2010). Cell wall ultrastructure, anatomy, lignin distribution, and chemical composition of Malaysian cultivated kenaf fiber. *Industrial Crops and Products*, 31(1): 113-121.

- [270] Nishimura, N., Izumi, A., and Kuroda, K.-i. (2002). Structural characterization of kenaf lignin: differences among kenaf varieties. *Industrial Crops and Products*, 15(2): 115-122.
- [271] Yu, H., and Yu, C. (2007). Study on microbe retting of kenaf fiber. *Enzyme and Microbial Technology*, 40(7): 1806-1809.
- [272] Srivatanakul, M., Park, S.H., Salas, M.G., and Smith, R.H. (2001). Transformation parameters enhancing T-DNA expression in kenaf (*Hibiscus cannabinus*). *Journal of Plant Physiology*, 158(2): 255-260.
- [273] Kojima, M., Shioiri, H., Nogawa, M., Nozue, M., Matsumoto, D., Wada, A., Saiki, Y., and Kiguchi, K. (2004). In planta transformation of kenaf plants (*Hibiscus cannabinus* var. aokawa No. 3) by *Agrobacterium tumefaciens*. *Journal of Bioscience and Bioengineering*, 98(2): 136-139.
- [274] Ruotolo, G., Toro, A.D., Chiaiese, P., and Filippone, E. (2011). Multiple buds are an alternative target to genetic manipulation of kenaf (*Hibiscus cannabinus* L.). *Industrial Crops and Products*, In Press.
- [275] Cook, C.G., Riggs, J.L., Smart, J.R., and Mullin-Schading, B.A. (1995). Evaluation of six kenaf cultivars for resistance to *Phymatotrichum omnivorum*. *Industrial Crops and Products*, 4(3): 229-232.
- [276] Angelini, L.G., Lazzeri, A., Levita, G., Fontanelli, D., and Bozzi, C. (2000). Ramie (*Boehmeria nivea* L.) Gaud. and Spanish Broom (*Spartium junceum* L.) fibers for composite materials: agronomical aspects, morphology and mechanical properties. *Industrial Crops and Products*, 11(2-3): 145-161.
- [277] Juvenet, J. (1889). Ramie. *Journal of the Franklin Institute*, 128(5): 371-376.
- [278] Liu, F., Liang, X., Zhang, N., Huang, Y., and Zhang, S. (2001). Effect of growth regulators on yield and fiber quality in ramie (*Boehmeria nivea* (L.) Gaud.), China grass. *Field Crops Research*, 69(1): 41-46.
- [279] Liu, Z.-T., Yang, Y., Zhang, L., Sun, P., Liu, Z.-W., Lu, J., Xiong, H., Peng, Y., and Tang, S. (2006). Study on the performance of ramie fiber modified with ethylenediamine. *Carbohydrate Polymers*, 71(1): 18-25.
- [280] Treitel, O. (1947). The submicroscopic structure of plant cell walls. *Journal of Colloid Science*, 2(2): 237-246.
- [281] Treitel, O. (1946). Elasticity, plasticity and fine structure of plant cell walls. *Journal of Colloid Science*, 1(4): 327-370.
- [282] Hester, S. B., and Yuen, M.L. (1989). Ramie: Patterns of World Production and Trade, *Journal of the Textile Institute*, 1754-2340, Vol. 80 (4): 493 – 505.
- [283] Hayashi, N., Sugiyama, J., Okano, T., and Ishihara, M. (1997). The enzymatic susceptibility of cellulose microfibrils of the algal-bacterial type and the cotton-ramie type. *Carbohydrate Research*, 305(2): 261-269.
- [284] Júnior, P., C.Z., de Carvalho, L.H., Fonseca, V.M., Monteiro, S.N., and d'Almeida, J.R.M. (2004). Analysis of the tensile strength of polyester/hybrid ramie-cotton fabric composites. *Polymer Testing*, 23(2): 131-135.
- [285] Cengiz, T.G., and Babalik, F.C. (2009). The effects of ramie blended car seat covers on thermal comfort during road trials. *International Journal of Industrial Ergonomics*, 39(2): 287-294.
- [286] Kadolph, S.J., Langford, A.L. (2001). Textiles (9th ed.). Upper Saddle River, NJ: Prentice Hall. ISBN 0-13-025443-6.

-
- [287] Mohanty, A. K., Misra, M., and Hinrichsen, G. (2000). "Biofibers, biodegradable polymers and biocomposites: An overview". *Macromol. Mater. Eng.* 276-277 (1): 1 – 24.
- [288] Brühlmann, F., Leupin, M., Erismann, K.H., Fiechter, A. (2000). Enzymatic degumming of ramie bast fibers. *Journal of Biotechnology*, 76(1): 43-50.
- [289] Baker IV, J.L. and Boots, V.A. (1997). Three-way harvester/decorticator for bast fiber crops with initial chemical processing in the field utilizing improved stapling technique. US patent number 5632135, 17 pages.
- [290] Rao, P.V. (1980). Determination of a growth - environment relationship in jute (*Corchorus olitorius* L.). *Agricultural Meteorology*, 22(1): 45-52.
- [291] WinklerPrins, A.M.G.A. (2006). Jute cultivation in the Lower Amazon, 1940–1990: an ethnographic account from Santarém, Pará, Brazil. *Journal of Historical Geography*, 32(4): 818-838.
- [292] Kozłowski, R., and Manys, S. (1999). Green Fibers. The Textile Institute. Textile Industry: Winning Strategies for the New Millennium-Papers Presented at the World Conference. Feb. 10–13 (1999): 29 (13p).
- [293] Srinivasan, J., Venkatachalam, A. and Radhakrishnan, P. (1999). Small-Scale Jute Spinning: An Analysis. *Textile Magazine*, 40(4): 29.
- [294] Jute (2011). <http://www.jute.org/plant.htm>.
- [295] Kibria, M.G., and Tisdell, C.A (1985). Operating capital and productivity patterns in jute weaving in Bangladesh. *Journal of Development Economics*, 18(1): 133-152.
- [296] Kibria, M.G., and Tisdell, C.A. (1985). Productivity, progress and learning: The case of jute spinning in Bangladesh. *World Development*, 13(10-11): 1151-1161.
- [297] Uddin, S., Hopper, T. (2003). Accounting For Privatisation In Bangladesh: Testing World Bank Claims. *Critical Perspectives on Accounting*, 14(7): 739-774.
- [298] Holm, L.G., Pancho, J.V., Herberger, J.P., and Plucknett, D.L. (1979). A geographical atlas of world weeds. John Wiley and Sons, New York.
- [299] Majumdar, S., Kundu, A.B., Dey, S., Ghosh, B.L. (1991). Enzymatic retting of jute ribbons. *International Biodeterioration*, 27(3): 223-235.
- [300] Banik, A., Sen, M., and Sen, S.P. (1993). Methane emission from jute-retting tanks. *Ecological Engineering*, 2(1): 73-79.
- [301] Banik, S., Basak, M.K., Paul, D., Nayak, P., Sardar, D., Sil, S.C., Sanpui, B.C., and Ghosh, A. (2003). Ribbon retting of jute-a prospective and eco-friendly method for improvement of fiber quality. *Industrial Crops and Products*, 17(3): 183-190.
- [302] Tanner, R.D., Prokop, A., and Bajpai, R.K. (1993). Removal of fiber from vines by solid state fermentation/enzymatic degradation: A comparison of flax and kudzu retting. *Biotechnology Advances*, 11(3): 635-643.
- [303] Gopal, M., and Mathew, M.D. (1986). The scope for utilizing jute wastes as raw materials in various industries: A review. *Agricultural Wastes*, 15(2): 149-158.
- [304] Ghosh, A., Ghosh, A., and Bera, A.K. (2005). Bearing capacity of square footing on pond ash reinforced with jute-geotextile. *Geotextiles and Geomembranes*, 23(2): 144-173.
- [305] Basu, G., Roy, A.N., Bhattacharyya, S.K., and Ghosh, S.K. (2009). Construction of unpaved rural road using jute–synthetic blended woven geotextile – A case study. *Geotextiles and Geomembranes*, 27(6): 506-512.

-
- [306] Tan, S.-A., Karunaratne, G.P., and Muhammad, N. (1993). The measurement of interface friction between a jute geotextile and a clay slurry. *Geotextiles and Geomembranes*, 12(4): 363-376.
 - [307] Tan, S.-A., Muhammad, N., and Karunaratne, G.-P. (1994). Forming a thin sand seam on a clay slurry with the aid of a jute geotextile. *Geotextiles and Geomembranes*, 13(3): 147-163.
 - [308] Ranganathan, S.R. (1994). Development and potential of jute geotextiles. *Geotextiles and Geomembranes*, 13(6-7): 421-433.
 - [309] Chattopadhyay, B.C., and Chakravarty, S. (2009). Application of jute geotextiles as facilitator in drainage. *Geotextiles and Geomembranes*, 27(2): 156-161.
 - [310] Chattopadhyay, S. N., Pan, N. C., and Day, A. (2004). A Novel Process of Dyeing of Jute Fabric Using Reactive Dye. *Textile Industry of India*, 42(9): 15-22.
 - [311] Boutron, O., Gouy, V., Touze-Foltz, N., Benoit, P., Chovelon, J.M., and Margoum, C. (2009). Geotextile fibers retention properties to prevent surface water nonpoint contamination by pesticides in agricultural areas. *Geotextiles and Geomembranes*, 27(4): 254-261.
 - [312] Nishiumi, S., Yabushita, Y., Fukuda, I., Mukai, R., Yoshida, K.-i., and Ashida, H. (2006). Molokhia (*Corchorus olitorius* L.) extract suppresses transformation of the aryl hydrocarbon receptor induced by dioxins. *Food and Chemical Toxicology*, 44(2): 250-260.
 - [313] Das, A.K., Dewanjee, S., Sahu, R., Dua, T.K., Gangopadhyay, M., and Sinha, M.K. (2010). Protective effect of *Corchorus olitorius* leaves against arsenic-induced oxidative stress in rat brain. *Environmental Toxicology and Pharmacology*, 29(1): 64-69.
 - [314] Das, H.P., and Stigter, C.J. (2010). Detection and Awareness of Increasing Climate Variability and the Elevating Climate Risk in Farming Systems with Non-Forest Trees. 2010, *Applied Agrometeorology*, Part 3, 707-709.
 - [315] Phuwapraisirisan, P., Puksasook, T., Kokpol, U., and Suwanborirux, K. (2009). *Corchorusides* A and B, new flavonol glycosides as α -glucosidase inhibitors from the leaves of *Corchorus olitorius*. *Tetrahedron Letters*, 50(42): 5864-5867.
 - [316] Chen, T.S., and Saad, S. (1981). Folic acid in Egyptian vegetables: The effect of drying method as storage on the folacin content of mulukhiyah (*Corchorus olitorius*). *Ecology of Food and Nutrition*, 10: 249-255.
 - [317] Watt, J.M., and Breyer-Brandwijk, M.G. (1962). The medicinal and poisonous plants of southern and eastern Africa. 2nd ed. E.andS. Livingstone, Ltd., Edinburgh and London.
 - [318] Sharaf, A., Kamel, S.H., Salama, A., and Arbid, M.S. (1979). Oestrogenicity of *Corchorus olitorius* L. seed oil. *Egyptian Journal of Veterinary Medicine*, 14(2):87-93.
 - [319] Pan, N.C., Day, A., and Mahalanabis, K.K. (2000). Properties of Jute. *Indian Textile Journal*, 110(5): 16.
 - [320] Doraiswamy, I., Basu, A., and Chellamani, K.P. (1998). Development of Fine Quality Jute Fibres. *Colourage*. Nov. 6-8: 1998, 2p.
 - [321] Madhu, T. (2002). Bio-Composites: An Overview. *Textile Magazine*. 43(8): 49 (2 pp).
 - [322] Maulik, S.R. (2001). Chemical Modification of Jute. *Asian Textile Journal*, 10(7): 99 (8 pp).
 - [323] Vijayakumar, K. A., and Raajendraa, P. R. (2005). A New Method to Determine the Proportion of Jute in a Jute/Cotton Blend. *Asian Textile Journal*, 14(5): 70-72.

-
- [324] Roy, T.K.G., Chatterjee, S.K., and Gupta, B.D. (2002). Comparative Studies on Bleaching and Dyeing of Jute after Processing with Mineral Oil in Water Emulsion vis-a-vis Self-Emulsifiable Castor Oil. *Colourage* 49(8): 27 (5 pp).
- [325] Shenai, V.A. (2003). Enzyme Treatment. *Indian Textile Journal*, 114(2): 112–113.
- [326] Pan, N.C., Chattopadhyay, S.N., and Day, A. (2004). Dyeing of Jute Fabric with Natural Dye Extracted from Marigold Flower. *Asian Textile Journal*, 13(7): 80–82.
- [327] Moses, J., and Ramasamy, M. (2004). Quality Improvement on Jute and Jute Cotton Materials Using Enzyme Treatment and Natural Dyeing. *Man-Made Textiles in India*. 47(7): 252–255.
- [328] Basu, G., Sinha, A.K., and Chattopadhyay, S.N. (2005). Properties of Jute Based Ternary Blended Bulked Yarns. *Man-Made Textiles in India*. Vol. 48(9): 350–353.
- [329] Buston, H.W., Moss, M.O., Tyrrell, D. (1966). The influence of carbon dioxide on growth and sporulation of *Chaetomium globosum*. *Transactions of the British Mycological Society*, 49(3): 387-396, IN4-IN6.
- [330] Chewonarin, T., Kinouchi, T., Kataoka, K., Arimochi, H., Kuwahara, T., Vinitketkumnuen, U., and Ohnishi, Y. (1999). Effects of Roselle (*Hibiscus sabdariffa* Linn.), a Thai Medicinal Plant, on the Mutagenicity of Various Known Mutagens in *Salmonella typhimurium* and on Formation of Aberrant Crypt Foci Induced by the Colon Carcinogens Azoxymethane and 2-Amino-1-methyl-6-phenylimidazo[4,5-b]pyridine in F344 rats. *Food and Chemical Toxicology*, 37(6): 591-601.
- [331] Sánchez-Mendoza, J., Domínguez-López, A., Navarro-Galindo, S., and López-Sandoval, J.A. (2008). Some physical properties of Roselle (*Hibiscus sabdariffa* L.) seeds as a function of moisture content. *Journal of Food Engineering*, 87(3): 391-397.
- [332] Hainida, K.I.E., Amin, I., Normah, H., and Mohd.-Esa, N. (2008). Nutritional and amino acid contents of differently treated Roselle (*Hibiscus sabdariffa* L.) seeds. *Food Chemistry*, 111(4): 906-911.
- [333] Mohd-Esa, N., Hern, F.S., Ismail, A., and Yee, C.L. (2010). Antioxidant activity in different parts of roselle (*Hibiscus sabdariffa* L.) extracts and potential exploitation of the seeds. *Food Chemistry*, 122(4): 1055-1060.
- [334] Britannica, (2011). <http://www.britannica.com/EBchecked/topic/509866/roselle>.
- [335] Gibson, T.A., and Waring, S.A. (1994). The soil fertility effects of leguminous ley pastures in north-east Thailand : I. Effects on the growth of roselle (*Hibiscus sabdariffa* c.v. *Altissima*) and cassava (*Manihot esculenta*). *Field Crops Research*, 39(2-3): 119-127.
- [336] Waring, S.A., Gibson, T.A., and Ila'Ava, V.P. (1994). The soil fertility effects of leguminous ley pastures in north-east Thailand III. Estimates of soil nitrogen availability. *Field Crops Research*, 39(2-3): 139-145.
- [337] Waring, S.A., and Gibson, T.A. (1994). The soil fertility effects of leguminous ley pastures in north-east Thailand : II. Effects on soil physical and chemical parameters. *Field Crops Research*, 39(2-3): 129-137.
- [338] Crane, J.C. (1949). Roselle - a potentially important plant fiber. *Economic Botany*, 3: 89–103.
- [339] Duke, J.A. (1979). Ecosystematic data on economic plants. *Quart. J. Crude Drug Res.* 17(3–4): 91–110.
- [340] Duke, J.A., and Atchley, A.A. (1984). *Proximate analysis*. In: Christie, B.R. (ed.), *The handbook of plant science in agriculture*. CRC Press, Inc., Boca Raton, FL.

- [341] El Tahir, B.A., Ahmed, D.M., Ardö, J., Gaafar, A.M., and Salih, A.A. (2009). Changes in soil properties following conversion of *Acacia senegal* plantation to other land management systems in North Kordofan State, Sudan. *Journal of Arid Environments*, 73(4-5): 499-505.
- [342] Hort.purdue (2011). http://www.hort.purdue.edu/newcrop/duke_energy/Hibiscus_sabdariffa.html.
- [343] Pau, L.T., Salmah, Y., and Suhaila, M. (2002). Antioxidative properties of roselle (*Hibiscus sabdariffa* L.) in linoleic acid model system. *Nutrition and Food Science*, 32(1): 17-20.
- [344] Drugs (2011). <http://www.drugs.com/npp/roselle.html>.
- [345] Chau, J. W.; Jin, M. W.; Wea, L. L.; Chia, Y. C.; Fen, P. C.; and Tsui, H. T. (2000). Protective effect of *Hibiscus* anthocyanins against tert-butyl hydroperoxide-induced hepatic toxicity in rats. *Food and Chemical Toxicology*, 38 (5): 411-416.
- [346] Cochrane (2011). <http://www.cochrane.org/reviews/en/ab007894.html>
- [347] Kuriyan, R., Kumar, D.R., and Kurpad, R.R. (2010). An evaluation of the hypolipidemic effect of an extract of *Hibiscus Sabdariffa* leaves in hyperlipidemic Indians: a double blind, placebo controlled trial. *BMC Complement Altern, Med.* 10:27.
- [348] Gurrola-Diaz, C.M., Garcia-Lopez, P.M., Sanchez-Enriquez, S., Troyo-Sanroman, R., Andrade-Gonzalez, I., and Gomez-Leyva, J.F. (2010). Effects of *Hibiscus sabdariffa* extract powder and preventive treatment (diet) on the lipid profiles of patients with metabolic syndrome (MeSy). *Phytomedicine*, 17(7): 500-505.
- [349] McKay, D.L., Chen, C.Y., Saltzman, E., and Blumberg, J.B. (2010). *Hibiscus sabdariffa* L. tea (tisane) lowers blood pressure in prehypertensive and mildly hypertensive adults. *J. Nutrition*, 140(2): 298-303.
- [350] Herrera-Arellano, A., Miranda-Sanchez, J., Avila-Castro, P., Herrera-Alvarez, S., Jimenez-Ferrer, J.E., Zamilpa, A., Roman-Ramos, R., Ponce-Monter, H., and Tortoriello, J. (2007). Clinical effects produced by a standardized herbal medicinal product of *Hibiscus sabdariffa* on patients with hypertension. A randomized, double-blind, lisinopril-controlled clinical trial. *Planta Medica*, 73(1): 6-12.
- [351] Mozaffari-Khosravi, H., Jalali-Khanabadi, B.A., Afkhami-Ardekani, M., Fatehi, F., and Noori-Shadkam, M. (2009). The effects of sour tea (*Hibiscus sabdariffa*) on hypertension in patients with type II diabetes. *J. Human Hypertension*, 23(1): 48-54.
- [352] Mohamed, R., Fernandez, J., Pineda, M., and Aguilar, M. (2007). Roselle (*Hibiscus sabdariffa*) seed oil is a rich source of gamma-tocopherol." *J. Food Sci.* 72(3): S207-211.
- [353] FAO (2011). <http://www.fao.org/inpho/content/compend/text/ch28/ch28.htm>.
- [354] Mohamad, O., Mohd. Nazir, B., Abdul Rahman, M., and Herman, S. (2002). Roselle: A new crop in Malaysia. Buletin PGM Dec 2002, p. 12-13.
- [355] Mohamad, O., Mohd. Nazir, B., Azhar, M., Gandhi, R., Shamsudin, S., Arbayana, A., Mohammad Feroz, K., Liew, S.K., Sam, C.W., Nooreliza, C.E., and Herman, S. (2002). Roselle improvement through conventional and mutation breeding. *Proc. Intern. Nuclear Conf.* 2002, 15-18 Oct 2002, Kuala Lumpur. 19 pp.
- [356] Mohamad, O., Ramadan, G., Herman, S., Halimaton Saadiah, O., Noor Baiti, A. A., Ahmad Bachtiar, B., Aminah, A., Mamot, S., and Jalifah, A.L. (2008). A promising mutant line for roselle industry in Malaysia. FAO Plant Breeding News, Edition 195. Available at <http://www.fao.org/ag/AGp/agpc/doc/services/pbn/pbn-195.htm>.

-
- [357] Fnca (2005). http://www.fnca.mext.go.jp/english/mb/e_ws_2005.html.
- [358] Vaidya, K.R. (2000). Natural cross-pollination in roselle, *Hibiscus sabdariffa* L. (Malvaceae). *Genetics and Molecular Biology*, 23(3): 667–669.
- [359] Hyder, N., Sims, J.J., and Wegulo, S.N. (2008). In Vitro Suppression of Soilborne Plant Pathogens by Coir. Department of Plant Pathology, University of Nebraska, 448 Plant Science Hall, Lincoln, NE 68583. 2008-11-19. URL:<http://www.agrococo.com>
- [360] Madehow (2011). <http://www.madehow.com/Volume-6/Coir.html>.
- [361] TWR (1967). Training without Reward: Traditional Training of Pig-tailed Macaques as Coconut Harvesters, Mireille Bertrand, *Science*, 155 (3761): 484-486.
- [362] Javadi, A., Srithep, Y., Pilla, S., Lee, J., Gong, S., and Turng, L.-S. (2010). Processing and characterization of solid and microcellular PHBV/coir fiber composites. *Materials Science and Engineering: C*, 30(5): 749-757.
- [363] Ezekiel, N., Ndazi B., Nyahumwa, C., and Karlsson, S. (2011). Effect of temperature and durations of heating on coir fibers. *Industrial Crops and Products*, 33(3): 638-643.
- [364] Saw, S.K., Sarkhel, G., and Choudhury, A. (2011). Surface modification of coir fibre involving oxidation of lignins followed by reaction with furfuryl alcohol: Characterization and stability. *Applied Surface Science*, 257(8): 3763-3769.
- [365] van Dam, J.E.G., van den Oever, M.J.A., and Keijzers, E.R.P. (2004). Production process for high density high performance binderless boards from whole coconut husk. *Industrial Crops and Products*, 20(1 97-101.
- [366] Varma, D.S., Varma, M., and Varma, I.K. (1986). Thermal behaviour of coir fibers. *Thermochimica Acta*, 108: 199-210.
- [367] Basak, M.K., Bhaduri, S.K., and Paul, N.B. (1983). Nature of the microbiologically extracted coir fibre from green coconut husks - An agro-waste. *Agricultural Wastes*, 5(1): 51-58.
- [368] Nazareth, S., and Mavinkurve, S. (1987). Labotory studies on retting of coconut husk. *International Biodeterioration*, 23(6): 343-355.
- [369] Tomczak, F., Sydenstricker, T.H.D., and Satyanarayana, K.G. (2007). Studies on lignocellulosic fibers of Brazil. Part II: Morphology and properties of Brazilian coconut fibers. Composites Part A: *Applied Science and Manufacturing*, 38(7): 1710-1721.
- [370] Aggarwal, L.K. (1992). Studies on cement-bonded coir fiber boards. *Cement and Concrete Composites*, 14(1): 63-69.
- [371] Rahman, M.M., and Khan, M.A. (2007). Surface treatment of coir (*Cocos nucifera*) fibers and its influence on the fibers' physico-mechanical properties. *Composites Science and Technology*, 67(11-12): 2369-2376.
- [372] Pramanik, P. (2010). Changes in microbial properties and nutrient dynamics in bagasse and coir during vermicomposting: Quantification of fungal biomass through ergosterol estimation in vermicompost. *Waste Management*, 30(5): 787-791.
- [373] Tran, L.Q.N., Fuentes, C.A., Dupont-Gillain, C., Van Vuure, A.W., and Verpoest, I. (2011). Wetting analysis and surface characterisation of coir fibers used as reinforcement for composites. *Colloids and Surfaces A: Physicochemical and Engineering Aspects*, 377(1-3): 251-260.
- [374] Fouladi, M.H., Ayub, Md., and Nor, M.J.M. (2011). Analysis of coir fiber acoustical characteristics. *Applied Acoustics*, 72(1): 35-42.

-
- [375] Yousif, B.F., and Ku, H. (2011). Suitability of using coir fiber/polymeric composite for the design of liquid storage tanks. *Materials and Design*, In Press, doi:10.1016/j.matdes.2011.01.063.
- [376] Woolley, T., Kimmins, S., Harrison, P., and Harrison, R. (1997). *Green Building Handbook Volume 1: A guide to building products and their impact on the environment*. Green Building Digest. Spon Press. 1997. ISBN 0-419-22690-7.
- [377] Sharma, U. (1981). Investigations on the fibers of pineapple [*Ananas comosus* (L). Merr.] leaves. *Carbohydrate Research*, 97(2): 323-329.
- [378] George, J., Janardhan, R., Anand, J.S., Bhagawan, S.S., and Thomas, S. (1996). Melt rheological behaviour of short pineapple fibre reinforced low density polyethylene composites. *Polymer*, 37(24): 5421-5431.
- [379] Arib, R.M.N., Sapuan, S.M., Ahmad, M.M.H.M., Paridah, M.T., and Zaman, H.M.D.K. (2006). Mechanical properties of pineapple leaf fiber reinforced polypropylene composites. *Materials and Design*, 27(5): 391-396.
- [380] Cherian, B.M., Leão, A.L., Ferreira de Souza, S., Thomas, S., Pothan, L.A., and Kottaisamy, M. (2010). Isolation of nanocellulose from pineapple leaf fibres by steam explosion. *Carbohydrate Polymers*, 81(3): 720-725.
- [381] Stewart, D., Azzini, A., Hall, A.T., and Morrison, I.M. (1997). Sisal fibers and their constituent non-cellulosic polymers. *Industrial Crops and Products*, 6(1): 17-26.
- [382] Savastano Jr., H., Warden, P.G., and Coutts, R.S.P. (2003). Mechanically pulped sisal as reinforcement in cementitious matrices. *Cement and Concrete Composites*, 25(3): 311-319.
- [383] Gutiérrez, A., Rodríguez, I.M., and del Río, J.C. (2008). Chemical composition of lipophilic extractives from sisal (*Agave sisalana*) fibers. *Industrial Crops and Products*, 28(1): 81-87.
- [384] Bessadok, A., Marais, S., Roudesli, S., Lixon, C., and Métayer, M. (2008). Influence of chemical modifications on water-sorption and mechanical properties of Agave fibers. *Composites Part A: Applied Science and Manufacturing*, 39(1): 29-45.
- [385] Barreto, A.C.H., Rosa, D.S., Fachine, P.B.A., and Mazzetto, S.E. (2011). Properties of sisal fibers treated by alkali solution and their application into cardanol-based biocomposites. *Composites Part A: Applied Science and Manufacturing*, 42(5): 492-500.
- [386] Tomlinson, P.B. (1970). Monocotyledons - Towards an Understanding of their Morphology and Anatomy. *Advances in Botanical Research*, 3: 207-292.
- [387] Dey, P.M., and Brinson, K. (1984). Plant Cell-Walls. *Advances in Carbohydrate Chemistry and Biochemistry*, 42: 265-382.
- [388] Hartemink, A.E. (1997). Soil fertility decline in some Major Soil Groupings under permanent cropping in Tanga region, Tanzania. *Geoderma*, 75(3-4): 215-229.
- [389] González-Iturbe, J.A., Olmsted, I., and Tun-Dzul, F. (2002). Tropical dry forest recovery after long term Henequen (sisal, *Agave fourcroydes* Lem.) plantation in northern Yucatan, Mexico. *Forest Ecology and Management*, 167(1-3): 67-82.
- [390] Strosse, H., Schoofs, H., Panis, B., Andre, E., Reyniers, K., and Swennen, R. (2006). Development of embryogenic cell suspensions from shoot meristematic tissue in bananas and plantains (*Musa* spp.). *Plant Science*, 170(1): 104-112.
- [391] FAO (2007). *Fibers Statistical Bulletin*:
- [392] http://www.fao.org/es/ESC/en/15/320/highlight_323.html.

-
- [393] Valadez-Gonzalez, A., Cervantes-Uc, J.M., Olayo, R., and Herrera-Franco, P.J. (1999). Chemical modification of henequén fibers with an organosilane coupling agent. *Composites Part B: Engineering*, 30(3): 321-331.
- [394] Han, S.O., and Jung, Y.M. (2008). Characterization of henequen natural fiber by using two-dimensional correlation spectroscopy. *Journal of Molecular Structure*, 883-884: 142-148.
- [395] Army and navy note, 1945. Abacá. *Journal of the Franklin Institute*, 240(1): 67-68.
- [396] Sun, R.C., Fang, J.M., Goodwin, A., Lawther, J.M., and Bolton, A.J. (1998). Fractionation and characterization of polysaccharides from abaca fiber. *Carbohydrate Polymers*, 37(4): 351-359.
- [397] del Río, J.C., Gutiérrez, A., Rodríguez, I.M., Ibarra, D., and Martínez, Á.T. (2007). Composition of non-woody plant lignins and cinnamic acids by Py-GC/MS, Py/TMAH and FT-IR. *Journal of Analytical and Applied Pyrolysis*, 79(1-2): 39-46.
- [398] Armecin, R.B., and Gabon, F.M. (2008). Biomass, organic carbon and mineral matter contents of abaca (*Musa textilis* Nee) at different stages of growth. *Industrial Crops and Products*, 28(3): 340-345.
- [399] Jiménez, L., Ramos, E., De la Torre, M.J., Pérez, I., and Ferrer, J.L. (2008). Bleaching of soda pulp of fibres of *Musa textilis* nee (abaca) with peracetic acid. *Bioresource Technology*, 99(5): 1474-1480.
- [400] Coutts, R.S.P., and Warden, P.G. (1987). Air-cured abaca reinforced cement composites. *International Journal of Cement Composites and Lightweight Concrete*, 9(2): 69-73.
- [401] Rahman, Md.R., Huque, Md.M., Islam, Md.N., and Hasan, M. (2009). Mechanical properties of polypropylene composites reinforced with chemically treated abaca. *Composites Part A: Applied Science and Manufacturing*, 40(4): 511-517.
- [402] Vilaseca, F., Valadez-Gonzalez, A., Herrera-Franco, P.J., Àngels Pèlach, M., López, J.P., and Mutjé, P. (2010). Biocomposites from abaca strands and polypropylene. Part I: Evaluation of the tensile properties. *Bioresource Technology*, 101(1): 387-395.
- [403] Bledzki, A.K., Mamun, A.A., Jazskiewicz, A., and Erdmann, K. (2010). Polypropylene composites with enzyme modified abaca fiber. *Composites Science and Technology*, 70(5): 854-860.
- [404] Gañán, P., and Mondragon, I. (2004). Fique fiber-reinforced polyester composites: Effects of fiber surface treatments on mechanical behavior. *Journal of Materials Science* (2004), Volume 39, Number 9, Pages 3121-3128.
- [405] Gañán P., and Mondragon, I. (2003). Thermal and degradation behavior of fique fiber reinforced thermoplastic matrix composites. *Journal of Thermal Analysis and Calorimetry*, 73(3): 783-795.
- [406] Delvasto, S., Toro, E.F., Perdomo, F., and Mejía de Gutiérrez, R. (2010). An appropriate vacuum technology for manufacture of corrugated fique fiber reinforced cementitious sheets. *Construction and Building Materials*, 24(2): 187-192.
- [407] Tonoli, G.H.D., Santos, S.F., Savastano Jr., H., Delvasto, S., Mejía de Gutiérrez, R., Lopez de and Murphy, Md.M. (2011). Effects of natural weathering on microstructure and mineral composition of cementitious roofing tiles reinforced with fique fiber. *Cement and Concrete Composites*, 33(2): 225-232.

- [408] Rondon, X.J., Banack S.A., and Diaz-Huamanchumo, W. (2003). Ethnobotanical investigation of *Caballitos* (*Schoenoplectus californicus*: cyperaceae) in Huanchaco, Peru. *Economic Botany*, 57(1): 35-47.
- [409] De-la-Cruz, H., Vilcapoma, G., and Zevallos, P.A. (2007). Ethnobotanical study of medicinal plants used by the Andean people of Canta, Lima, Peru. *Journal of Ethnopharmacology*, 111(2): 284-294.
- [410] Wingfield M.J., and Robison, D.J. (2004). Diseases and insect pests of *Gmelina arborea*: real threats and real opportunities. *New Forests*, 28(2-3): 227-243.
- [411] Hill, D.S. (2008). Major tropical crops and their pest spectra. In *Pests of Crops in Warmer Climates and Their Control*. Springer Science Publishers, ISBN: 978-1-4020-6737-2. 2008, 511-658, DOI: 10.1007/978-1-4020-6738-9_10.
- [412] DAISIE (2009). List of Species Alien in Europe and to Europe. Handbook of Alien Species in Europe. *Invading Nature - Springer Series in Invasion Ecology*, 3: 133-263, DOI: 10.1007/978-1-4020-8280-1_11.
- [413] <http://www.chemeurope.com/en/encyclopedia/Fique.html>
- [414] Baldwin, R., and Growers, S.M. (1998). The New Cultivars of New Zealand Flax. *International Plant Propagators Society Western Meeting*. Ontario, CA. (http://search.yahoo.com/r/_ylt=A0oG7lj9G5xNBX8AetlXNyoA;_ylu=X3oDMTE1ZjM0MmI4BHNIYwNzcGRwb3MDMGRjb2xvA2FjMGR2dGlkA0FDQlkwMI8xNDQ-/SIG=11vuji526/EXP=1302098013/**http%3a/www.smgrowers.com/info/NewNZFlax.pdf).
- [415] <http://www.smgrowers.com/>
- [416] Critchfield, H.J. (1951). *Phormium tenax* - New Zealand's native hard fiber. *Economic Botany*, 5(2): 172-184.
- [417] Jarvis L.R., and Wardrop, A.B. (1974). The development of the cuticle in *Phormium tenax*. *Planta*, 119(2): 101-112.
- [418] McIvor, E.G. (1980). *Phormium tenax*- a proving. *British Homoeopathic journal*, 69(1): 26-32.
- [419] Haase, P. (1990). Potential plant genetic resources of the New Zealand flora. *Economic Botany*, 44(4): 503-515.
- [420] Liefing, L.W., Beever, R.E., Winksc, C.J., Pearson M.N., and Forster, R.L.S. (1997). Planthopper transmission of *Phormium* yellow leaf phytoplasma. *Australasian Plant Pathology*, 26(3): 148-154.
- [421] Liefing, L.W., Padovan, A.C., Gibb, K.S., Beever, R.E., and Andersen, M.T., *et al.* (1998). 'Candidatus Phytoplasma australiense' is the phytoplasma associated with Australian grapevine yellows, papaya dieback and *Phormium* yellow leaf diseases. *European Journal of Plant Pathology*, 104(6): 619-623.
- [422] Pearson, M.N., Clover, G.R.G., Guy, P.L., Fletcher J.D., and Beever, R.E. (2006). A review of the plant virus, viroid and mollicute records for New Zealand. *Australasian Plant Pathology*, 35(2): 217-252.
- [423] Horst, R.K. (2008). NEW ZEALAND Flax (*Phormium tenax*) in *Westcott's Plant Disease Handbook*. 7th Ed., Springer Science Publishers, ISBN: 978-1-4020-4585-1. 2008, 4, Part 54, 979, DOI: 10.1007/978-1-4020-4585-1_2312.
- [424] Harris, J.C., Song, J., Jameson, P.E., and Clemens, J. (2009). Autonomous, environmental and exogenous gibberellin regulation of floral development and isolation

- of a putative partial FLORICAULA/LEAFY homologue in *Phormium cookianum* (Agavaceae). *Plant Growth Regulation*, 58(2): 191-199.
- [425] Gillow, J., and Sentance, B. (2004). *World Textiles: A Visual Guide to Traditional Techniques*, London: Thames and Hudson, 220, 64.
- [426] Newman, R.H., Clauss, E.C., Carpenter, J.E.P., and Thumm, A. (2007). Epoxy composites reinforced with deacetylated *Phormium tenax* leaf fibers. *Composites Part A: Applied Science and Manufacturing*, 38(10): 2164-2170.
- [427] Newman, R.H., Le Guen, M.J., Battley, M.A., and Carpenter, J.E.P. (2010). Failure mechanisms in composites reinforced with unidirectional *Phormium* leaf fiber. *Composites Part A: Applied Science and Manufacturing*, 41(3): 353-359.
- [428] Le Guen, M.J., and Newman, R.H. (2007). Pulped *Phormium tenax* leaf fibers as reinforcement for epoxy composites. *Composites Part A: Applied Science and Manufacturing*, 38(10): 2109-2115.
- [429] Jayaraman, K., and Halliwell, R. (2009). Harakeke (*phormium tenax*) fiber-waste plastics blend composites processed by screwless extrusion. *Composites Part B: Engineering*, 40(7): 645-649.
- [430] de Rosa, I.M., Santulli, C., and Sarasini, F. (2010). Mechanical and thermal characterization of epoxy composites reinforced with random and quasi-unidirectional untreated *Phormium tenax* leaf fibers. *Materials and Design*, 31(5): 2397-2405.
- [431] Vitrebert, E. (1876). Zur Unterscheidung der Faser des neuseeländischen Flachses (*Phormium tenax*) von der des Flachses, Hanfs etc. *Fresenius' Journal of Analytical Chemistry*, 15(1): 492-493.
- [432] Kupchan, S.M., Meshulam, H., and Sneden, A.T. (1978). New cucurbitacins from *Phormium tenax* and *Marah oreganus*. *Phytochemistry*, 17(4): 767-769.
- [433] Craig, J.L. (1989). Seed set in *Phormium*: interactive effects of pollinator behavior, pollen carryover and pollen source. *Oecologia*, 81(1): 1-5.
- [434] Golzar, H., and Wang, C. (2010). First report of *Colletotrichum phormii* the cause of anthracnose on *Phormium tenax* in Australia. *Australasian Plant Disease Notes*, 5(1): 110-112.
- [435] Palm, M.E. (1996). *Kirramyces phormii* comb. nov. from leaves of *Phormium*. *Mycological Research*, 100(3): 373-376.
- [436] Sims, I.M. (2003). Structural diversity of fructans from members of the order Asparagales in New Zealand. *Phytochemistry*, 63(3): 351-359.
- [437] Sims, I.M., Cairns, A.J., and Furneaux, R.H. (2001). Structure of fructans from excised leaves of New Zealand flax. *Phytochemistry*, 57(5): 661-668.
- [438] Sims, I.M., and Newman, R.H. (2006). Structural studies of acidic xylans exuded from leaves of the monocotyledonous plants *Phormium tenax* and *Phormium cookianum*. *Carbohydrate Polymers*, 63(3): 379-384.
- [439] Segetin, M., Jayaraman, K., and Xu, X. (2007). Harakeke reinforcement of soil-cement building materials: Manufacturability and properties. *Building and Environment*, 42(8): 3066-3079.
- [440] Earl, E.A., Altaf, M., Murikoli, R.V., Swift S., and O'Toole, R. (2010). Native New Zealand plants with inhibitory activity towards *Mycobacterium tuberculosis*. *BMC Complementary and Alternative Medicine*, 10(1): 25.
- [441] Morice, I.M. (1970). Seed fats of some New Zealand and Australian monocotyledons. *Phytochemistry*, 8: 1829-1833.

- [442] Tolkachev, O.N., and Zhuchenko, A.A. (2000). Biologically Active Substances of Flax: Medicinal and Nutritional Properties (A Review). *Pharmaceutical Chemistry Journal*, 34(7): 360-367.
- [443] Baker, G.E., and Yeager, L.D. (1974). Wood Technology, Howard W. Sams, Indianapolis (1974).
- [444] Kipershlak, É.Z., and Pakshver, A.B. (1977). New developments in viscose research - a review. *Fibre Chemistry*, 9(5): 458-467.
- [445] Virezub, A.I., and Pakshver, A.B. (1978). Viscose filtration (review). *Fibre Chemistry*, 10(3): 246-254.
- [446] Budnitskii, G.A., Matveev, V.S., Kazakov, M.E. (1993). Carbon fibers and materials based on viscose fibers (review). *Fibre Chemistry*, 25(5): 360-364.
- [447] Serebryakova, Z.G., and Tokareva, L.G. (1996). Surfactants and modifiers in production of viscose fibers (review). *Fibre Chemistry*, 28(2): 91-94.
- [448] Perepelkin, K.E. (2003). Trends and Changes in World Chemical Fiber Production. An Analytical Review. Part 2. Trends in the Development of Traditional and Promising Kinds of Chemical Fibers. *Fibre Chemistry*, 35(4): 241-249.
- [449] Sarkar, A.K., and Appidi, S. (2009). Single bath process for imparting antimicrobial activity and ultraviolet protective property to bamboo viscose fabric. *Cellulose*, 16(5): 923-928.
- [450] En.Wikipedia (2011). <http://en.wikipedia.org/wiki/Viscose>.
- [451] Eichhorn, S.J., Baillie, C.A., Zafeiropoulos, N., Mwaikambo, L.Y., Ansell, M.P., *et al.* (2001). Review: Current international research into cellulosic fibers and composites. *Journal of Materials Science*, 36(9): 2107-2131.
- [452] Butkova, N.T., Petrova, N.I., Tokareva, T.I., Malyugin, Y.Y., and Pakshver, A.B. (1978). Textile yarn from viscose with a lower NaOH/ α -cellulose ratio due to a decrease in the carbon disulfide content. *Fibre Chemistry*, 10(3): 258-261.
- [453] Butyagin, P.A., Butkova, N.T., Baksheev, I.P., Malyugin, Y.Y., and Sokolovskii, B.M. (1988). Promising technology in the preparation of viscose textile yarn. *Fibre Chemistry*, 20(3): 155-158.
- [454] Tomlinson, J.B., Freeman, J.J., and Theocharis, C.R. (1993). The preparation and adsorptive properties of ammonia-activated viscose rayon chars. *Carbon*, 31(1): 13-20.
- [455] Serebryakova, Z.G. (1996). Textile-auxiliary substances in production of viscose fibers (review). *Fibre Chemistry*, 28(2): 85-90.
- [456] Irklei, V.M., Kliner, Y.Y., Vavrinyuk, O.S., and Skoratski, É. (1997). Practical implementation of cellulose material production technologies with low consumption of carbon disulfide. *Fibre Chemistry*, 29(4): 244-246.
- [457] Stepanik, T.M., Ewing, D.E., and Whitehouse, R. (2000). Electron treatment of wood pulp for the viscose process. *Radiation Physics and Chemistry*, 57(3-6): 377-379.
- [458] Stepanik, T.M., Rajagopal, S., Ewing, D., and Whitehouse, R. (1998). Electron-processing technology: A promising application for the viscose industry. *Radiation Physics and Chemistry*, 52(1-6): 505-509.
- [459] Polyutov, A.A., Kleiner, Y.Y., Irklei V.M., and Gal'braikh, L.S. (2000). Study of the possibility of processing cotton cellulose in bulk for fabrication of viscose fiber. *Fibre Chemistry*, 32(5): 353-355.
- [460] Colom, X., and Carrillo, F. (2002). Crystallinity changes in lyocell and viscose-type fibers by caustic treatment. *European Polymer Journal*, 38(11): 2225-2230.

-
- [461] Kazakovtsev, Y.A. (2002). New Domestic Equipment for Continuous Production of Viscose Fiber. *Fibre Chemistry*, 34(3): 233-236.
- [462] Carrillo, F., Colom, X., López-Mesas, M., Lis, M.J., González, F., and Valldeperas, J. (2003). Cellulase processing of lyocell and viscose type fibers: kinetics parameters. *Process Biochemistry*, 39(2): 257-261.
- [463] Perepelkin, K.E. (2008). Ways of developing chemical fibers made of cellulose: Viscose fibers and their prospects. Part 2. Recycling and treating viscose production emissions. Current solutions. *Fibre Chemistry*, 40(2): 94-102
- [464] Vu-Manh, H., Öztürk, H.B., and Bechtold, T. (2010). Swelling and dissolution mechanism of regenerated cellulosic fibers in aqueous alkaline solution containing ferric tartaric acid complex: Part I. Viscose fibers. *Carbohydrate Polymers*, 82(3): 761-767.
- [465] Bamboo-zled, (2010). FTC says retailers fibbed about bamboo product claims (<http://www.walletpop.com/blog/2010/02/03/bamboo-zled-ftc-says-retailersfibbed-about-bamboo-product-clai/>).
- [466] Ibarra, D., Köpcke, V., and Ek, M. (2010). Behavior of different monocomponent endoglucanases on the accessibility and reactivity of dissolving-grade pulps for viscose process. *Enzyme and Microbial Technology*, 47(7): 355-362.
- [467] Davidson, M., and Feinleib, M. (1972). Carbon disulfide poisoning: A review. *American Heart Journal*, 83(1): 100-114.
- [468] Tan, X., Wang, F., Bi, Y., He, J., Su, Y., Braeckman, L., de Bacquer, D., and Vanhoorne, M. (2001). Carbon disulfide exposure assessment in a Chinese viscose filament plant. *International Journal of Hygiene and Environmental Health*, 203(5-6): 465-471.
- [469] Tan, X., Chen, G., Peng, X., Wang, F., Bi, Y., Tao, N., Wang, C., Yan, J., Ma, S., Cao, Z., He, J., Yi, P., Braeckman, L., and Vanhoorne, M. (2004). Cross-sectional study of cardiovascular effects of carbon disulfide among Chinese workers of a viscose factory. *International Journal of Hygiene and Environmental Health*, 207(3): 217-225.
- [470] Wang, C., Tan, X., Bi, Y., Su, Y., Yan, J., Ma, S., He, J., Braeckman, L., De Bacquer, D., Wang, F., and Vanhoorne, M. (2002). Cross-sectional study of the ophthalmological effects of carbon disulfide in Chinese viscose workers. *International Journal of Hygiene and Environmental Health*, 205(5): 367-372.
- [471] Shimko, I.G., Chinennaya, S.K., Zakirova, R.I., Minster, V.Sh., and Katushkin, V.P., *et al.* (1984). Clean-up of low-concentration ventilation discharge from viscose manufacturing plants from carbon disulfide and hydrogen sulfide. *Fibre Chemistry*, 16(6): 381-386.
- [472] Davies, C.K.L., and Long, O.E. (1977). Morphology of trans-1, 4-polyisoprene crystallized in thin films. *Journal of Materials Science*, 12(11): 2165-2183.
- [473] Chaturvedi, P.N. (1987). Certain unusual habits of trans-1,4-polyisoprene single crystals. *Journal of Materials Science Letters*, 6(3): 305-307.
- [474] Chaturvedi, P.N., Patel, M.J., Patel, K.C., and Patel, R.D. (1987). Morphology of solution crystallized trans-1,4-polyisoprene. *Colloid and Polymer Science*, 265(7): 592-596.
- [475] Gooch, J.W. (2011). Rubber, Natural. *Encyclopedic Dictionary of Polymers*. Part 18, 640, DOI: 10.1007/978-1-4419-6247-8_10194.

- [476] Williams, C.A., Goldstone, F., and Greenham, J. (1996). Flavonoids, cinnamic acids and coumarins from the different tissues and medicinal preparations of *Taraxacum officinale*. *Phytochemistry*, 42(1): 121-127.
- [477] Williams, L. (1963). Laticiferous plants of economic importance IV jelutong (*Dyera* spp.). *Economic Botany*, 17(2): 110-126.
- [478] Williams, L. (1964). Laticiferous plants of economic importance V. Resources of *gutta-percha- Palaquium* species (*Sapotaceae*). *Economic Botany*, 18(1): 5-26.
- [479] Cornish, K., and Brichta, J.L. (2002). Some Rheological Properties of Latex from *Parthenium argentatum* Gray Compared with Latex from *Hevea brasiliensis* and *Ficus elastica*. *Journal of Polymers and the Environment*, 10(1-2): 13-18.
- [480] Kol'chugina, I. B., and Markarova, E.N. (2009). Photoheterotrophic callus culture *Ficus elastica*. The formation of polyisoprene synthesis. *Moscow University Biological Sciences Bulletin*, 64(1): 28-31.
- [481] Augustus, G.D.P.S., and Seiler, G.J. (2011). *Ficus elastica* - The Indian rubber tree - An underutilized promising multi-use species. *Biomass and Bioenergy*, In Press, doi:10.1016/j.biombioe.2011.03.015.
- [482] Müller-Schwarze, N.K. 2006. Antes and Hoy Dña: Plant knowledge and categorization as adaptations to life in Panama in the Twenty-First Century. *Economic Botany*, (2006), Volume 60, Number 4, Pages 321-334.
- [483] Uzabakiliho, B., Largeau, C., Casadevall, E. (1987). Latex constituents of *Euphorbia candelabrum*, *E. grantii*, *E. tirucalli* and *Synadenium grantii*. *Phytochemistry*, 26(11): 3041-3045.
- [484] Koops, A.J., Baas, W.J., and Groeneveld, H.W. (1991). The composition of phytosterols, latex triterpenols and wax triterpenoids in the seedling of *Euphorbia lathyris* L. *Plant Science*, 74(2): 185-191.
- [485] Amani, M., Moosavi-Movahedi, A.A., Floris, G., Longu, S., and Mura, A. (2005). Comparative Study of the Conformational Lock, Dissociative Thermal Inactivation and Stability of *Euphorbia* Latex and Lentil Seedling Amine Oxidases. *The Protein Journal*, 24(3): 183-191.
- [486] Ma, G., Teixeira da Silva, J.A., Wu, G. (2011). Direct Adventitious Shoot Formation from Apical Shoot Explants of *Euphorbia tirucalli*. *Journal of Plant Growth Regulation*, 30(1): 114-116.
- [487] Akashi, T., Furuno, T., Takahashi, T., and Ayabe, S.-I. (1994). Biosynthesis of triterpenoids in cultured cells, and regenerated and wild plant organs of *Taraxacum officinale*. *Phytochemistry*, 36(2): 303-308.
- [488] Rudenskaya, G.N., Bogacheva, A.M., Preusser, A., Kuznetsova, A.V., Dunaevsky, Y.E., Golovkin, B.N., and Stepanov, V.M. (1998). *Taraxalisin* – a serine proteinase from dandelion *Taraxacum officinale* Webb s.l. *FEBS Letters*, 437(3): 237-240.
- [489] Wu, Q.-X., Su, Y.-B., and Zhu, Y. (2011). Triterpenes and steroids from the roots of *Scorzonera austriaca*. *Fitoterapia*, 82(3): 493-496.
- [490] Siler, D.J., Cornish, K., and Hamilton, R.G. (1996). Absence of cross-reactivity of IgE antibodies from subjects allergic to *Hevea brasiliensis* latex with a new source of natural rubber latex from guayule (*Parthenium argentatum*). *Journal of Allergy and Clinical Immunology*, 98(5): 895-902.

- [491] Dierig, D.A., Ray, D.T., Coffelt, T.A., Nakayama, F.S., Leake, G.S., and Lorenz, G. (2001). Heritability of height, width, resin, rubber, and latex in guayule (*Parthenium argentatum*). *Industrial Crops and Products*, 13(3): 229-238.
- [492] Cornish, K., and Wood, D.F. (2002). Visualization of the Malleability of the Rubber Core of Rubber Particles from *Parthenium argentatum* Gray and Other Rubber-Producing Species Under Extremely Cold Temperatures. *Journal of Polymers and the Environment*, 10(4): 155-162.
- [493] Sundar, D., Chaitanya, K.V., Jutur, P.P., and Reddy, A.R. (2004). Low temperature-induced changes in antioxidative metabolism in rubber-producing shrub, guayule (*Parthenium argentatum* Gray). *Plant Growth Regulation*, 44(2): 175-181.
- [494] Cornish, K., Whitehand, L.C., Fleet, J.E.V., Brichta, J.L., Chapman, M.H., and Knuckles, B.E. (2005). Latex yield and quality during storage of guayule (*Parthenium argentatum* Gray) homogenates. *Industrial Crops and Products*, 22(1): 75-85.
- [495] Coffelt, T.A., Ray, D.T., Nakayama, F.S., and Dierig, D.A. (2005). Genotypic and environmental effects on guayule (*Parthenium argentatum*) latex and growth. *Industrial Crops and Products*, 22(1): 95-99.
- [496] Kumar, S., Hahn, F.M., McMahan, C.M., Cornish, K., and Whalen, M.C. (2009). Comparative analysis of the complete sequence of the plastid genome of *Parthenium argentatum* and identification of DNA barcodes to differentiate *Parthenium* species and lines. *BMC Plant Biology*, 9(1): 131.
- [497] Costa, G.E., Johnson, J.D., and Hamilton, R.G. (2001). Cross-Reactivity Studies of Gutta-Percha, Gutta-Balata, and Natural Rubber Latex (*Hevea brasiliensis*). *Journal of Endodontics*, 27(9): 584-587.
- [498] Howell, C.J., Schwabe, K.A., and Abu Samah, A.H. (2010). Non-timber forest product dependence among the Jah Hut subgroup of Peninsular Malaysia's Orang Asli. *Environment, Development and Sustainability*, 12(1): 1-18.
- [499] Zhuravlev, V.M., Ryabis, A.A., and Antifeev, V.A. (1973). Optimization of the heating mode in the vulcanization of rubber products. *Journal of Engineering Physics and Thermophysics*, 24(2): 249-252.
- [500] Makuuchi, K., Yoshii, F., Ishigaki, I., Tsushima, K., Mogi, M., and Saito, T. (1990). Development of rubber gloves by radiation vulcanization. *International Journal of Radiation Applications and Instrumentation. Part C. Radiation Physics and Chemistry*, 35(1-3): 154-157.
- [501] Martin, D., Ighigeanu, D., Mateescu, E., Craciun, G., and Ighigeanu, A. (2002). Vulcanization of rubber mixtures by simultaneous electron beam and microwave irradiation. *Radiation Physics and Chemistry*, 65(1): 63-65.
- [502] Clemens, F. (2007). Thermoplastic Extrusion for Ceramic Bodies. In *Engineering Materials and Processes, Extrusion in Ceramics*, 295-311. DOI: 10.1007/978-3-540-27102-4_17.
- [503] Lin, X., Liu, Q., Chen, Z., and Wang, D. (2007). Study on Kinetics of Natural Rubber Vulcanization by S/La(DiPDP)3. *Journal of Rare Earths*, 25(4): 396-400.
- [504] Milani, G., and Milani, F. (2010). A new simple numerical model based on experimental scorch curve data fitting for the interpretation of sulphur vulcanization. *Journal of Mathematical Chemistry*, 48(3): 530-557.

-
- [505] Milani, G., and Milani, F. (2010). Optimal vulcanization of 2D–3D EPM/EPDM thick elements through peroxidic mixtures. *Journal of Mathematical Chemistry*, 47(1): 229-267.
 - [506] Slack, C. (2002). Noble Obsession: Charles Goodyear, Thomas Hancock, and the Race to Unlock the Greatest Industrial Secret of the Nineteenth Century. Hyperion [ISBN 9780786867899].
 - [507] Schultes, R.E. (1977). The odyssey of the cultivated rubber tree. *Endeavour*, 1(3-4): 133-138.
 - [508] Jiang, A. (1988). Climate and natural production of rubber (*Hevea brasiliensis*) in *Xishuangbanna*, southern part of Yunnan province, China. *International Journal of Biometeorology*, 32(4): 280-282.
 - [509] Barlow, C. (1997). Growth, structural change and plantation tree crops: The case of rubber. *World Development*, 25(10): 1589-1607.
 - [510] Suyanto, S., Tomich, T.P., and Otsuka, K. (2000). Land tenure and farm management efficiency: The case of smallholder rubber production in customary land areas of Sumatra. *Agroforestry Systems*, 50(2): 145-160.
 - [511] Rodrigo, V.H.L., Stirling, C.M., Naranpanawa, R.M.A.K.B., and Herath, P.H.M.U. (2001). Intercropping of immature rubber in Sri Lanka: present status and financial analysis of intercrops planted at three densities of banana. *Agroforestry Systems*, 51(1): 35-48.
 - [512] Dea, G.B., Assiri, A.A., Gabla, O.R., and Boa, D. (2001). Influence of soil preparation method on root and vegetative growth of rubber tree (*Hevea brasiliensis*) in the southwest Côte d'Ivoire. *Soil and Tillage Research*, 59(1-2): 3-11.
 - [513] Purnamasari, R., Cacho, O., and Simmons, P. (2002). Management strategies for Indonesian rubber production under yield and price uncertainty: a bioeconomic analysis. *Agroforestry Systems*, 54(2): 121-135.
 - [514] Priyadarshan, P.M., Gonçalves, P.S., and Omokhaye, K.O. (2009). Breeding Hevea Rubber. Breeding Plantation Tree Crops: *Tropical Species*, Part III, 469-522.
 - [515] Cornish, K., Myers, M.D., and Kelley, S.S. (2004). Latex quantification in homogenate and purified latex samples from various plant species using near infrared reflectance spectroscopy. *Industrial Crops and Products*, 19(3): 283-296.
 - [516] van Beilen, J.B., and Poirier, Y. (2007). Establishment of new crops for the production of natural rubber. *Trends in Biotechnology*, 25(11): 522-529.
 - [517] Schmidt, T., Lenders, M., Hillebrand, A., van Deenen, N., and Munt, O., *et al.* (2010). Characterization of rubber particles and rubber chain elongation in *Taraxacum koksaghyz*. *BMC Biochemistry*, 11(1): 11.
 - [518] Konno, K. (2011). Plant latex and other exudates as plant defense systems: Roles of various defense chemicals and proteins contained therein. *Phytochemistry*, In Press.
 - [519] Utracki, L.A. (2003). Introduction to Polymer Blends. *Polymer Blends Handbook*, 1-122. Springer Publishers. DOI: 10.1007/0-306-48244-4_1.
 - [520] Puskas, J.E., Gautriaud, E., Deffieux, A., and Kennedy, J.P. (2006). Natural rubber biosynthesis - A living carbocationic polymerization?. *Progress in Polymer Science*, 31(6): 533-548.
 - [521] Martinez, J.M.M. (2006). Natural rubber by a rubber man. *Materials Today*, 9(3): 55.
 - [522] Wendt, C.J., and Cyphers, A. (2008). How the Olmec used bitumen in ancient Mesoamerica. *Journal of Anthropological Archaeology*, 27(2): 175-191.

- [523] Pohl, M.D., and von Nagy, C. (2008). Americas, Central, The Olmec and Their Contemporaries. *Encyclopedia of Archaeology*, 217-230.
- [524] (http://search.yahoo.com/r/_ylt=A0oG7mdiYZxNbRsAtXJXNyoA;_ylu=X3oDMTE1cGQ4Yjl0BHNIYwNzcgRwb3MDNARjb2xvA2FjMgR2dGlkA0FDQlkwMl8xNDQ-/SIG=127jr5ql6/EXP=1302115778/**http%3a//www.boi.go.th/english/why/rubber_summary.pdf).
- [525] Genta, G., and Morello, L. (2009). Wheels and Tires. Mechanical Engineering Series, in *The Automotive Chassis*, I, Vol. 1: *Components Design*, 53-132. Springer Publishers. 0.1007/978-1-4020-8676-2.
- [526] LANXESS AG (2009). The Moving Powers of Rubber, Leverkusen, Germany: LANXESS AG: 20 (http://en.wikipedia.org/wiki/Synthetic_rubber).
- [527] LANXESS (2009). http://www.annualreport2009.lanxess.de/fileadmin/_09_GB/PDF_EN/LANXESS_AR09-English.pdf.
- [528] Current Biography, 1940, "SEMON, WALDO LONSBURY" pp723-724.
- [529] Williamson, C.C., Hughes, R.D., Cabell, C.P., Nazarro, J.J., Bender, F.P. and Crigglesworth, W.J. (5th March 1944), Plan for Completion of Combined Bomber Offensive (Appendices C and F), Dwight D. Eisenhower Presidential Library: SMITH, WALTER BEDELL: Collection of World War II Documents, 1941–1945; Box No.: 48: HQ, U.S.S.T.A.F, "DECLASSIFIED ... 4/24/74".
- [530] Stormont, J. W. (1946). AAFRH-19: The Combined Bomber Offensive; April through December 1943, Dwight D. Eisenhower Presidential Library: Collection of 20th Century Military Records, 1918–1950 Series I: Historical Studies Box 35: AAF Historical Office; Headquarters, Army Air Force, pp. 74–5, 81, "SECRET ... Classification Cancelled ... JUN 10 1959".
- [531] Gurney, G. (Major, USAF) (1962). The War in the Air: a pictorial history of World War II Air Forces in combat, New York: Bonanza Books, pp. 215.
- [532] Cookb, G.B. (1948). Cork and cork products. *Economic Botany*, 2(4): 393-402.
- [533] Fialho, C., Lopes, F., and Pereira, H. (2001). The effect of cork removal on the radial growth and phenology of young cork oak trees. *Forest Ecology and Management*, 141(3): 251-258.
- [534] Ribeiro, F., and Tomé, M. (2002). Cork weight prediction at tree level. *Forest Ecology and Management*, 171(3): 231-241.
- [535] Costa, A., Madeira, M., and Oliveira, Â.C. (2008). The relationship between cork oak growth patterns and soil, slope and drainage in a cork oak woodland in Southern Portugal. *Forest Ecology and Management*, 255(5-6): 1525-1535.
- [536] Costa, A., Pereira, H., and Oliveira, A. (2003). Variability of radial growth in cork oak adult trees under cork production. *Forest Ecology and Management*, 175(1-3): 239-246.
- [537] Sánchez-González, M., del Río, M., Cañellas, I., and Montero, G. (2006). Distance independent tree diameter growth model for cork oak stands. *Forest Ecology and Management*, 225(1-3): 262-270.
- [538] Pereira, H. (2007). The chemical composition of cork. *Cork*, 55-99.
- [539] Pereira, H. (2007). The cork oak. *Cork*, 103-125
- [540] Caritat, A., Molinas, M., and Gutierrez, E. (1996). Annual cork-ring width variability of *Quercus suber* L. in relation to temperature and precipitation (Extremadura, southwestern Spain). *Forest Ecology and Management*, 86(1-3): 113-120.

-
- [541] Cardillo, E., Bernal, C.J. (2006). Morphological response and growth of cork oak (*Quercus suber* L.) seedlings at different shade levels. *Forest Ecology and Management*, 222(1-3): 296-301.
- [542] Hidalgo, P.J., Marín, J.M., Quijada, J., and Moreira, J.M. (2008). A spatial distribution model of cork oak (*Quercus suber*) in southwestern Spain: A suitable tool for reforestation. *Forest Ecology and Management*, 255(1): 25-34.
- [543] Campos, P., Daly-Hassen, H., Oviedo, J.L., Ovando, P., and Chebil, A. (2008). Accounting for single and aggregated forest incomes: Application to public cork oak forests in Jerez (Spain) and Iteimia (Tunisia). *Ecological Economics*, 65(1): 76-86.
- [544] Chaar, H., Mechergui, T., Khouaja, A., and Abid, H. (2008). Effects of treeshelters and polyethylene mulch sheets on survival and growth of cork oak (*Quercus suber* L.) seedlings planted in northwestern Tunisia. *Forest Ecology and Management*, 256(4): 722-731.
- [545] Pizzurro, G.M., Maetzke, F., and La Mela Veca, D.S. (2010). Differences of raw cork quality in productive cork oak woods in Sicily in relation to stand density. *Forest Ecology and Management*, 260(5): 923-929.
- [546] Paulo, J.A., and Tomé, M. (2010). Predicting mature cork biomass with t years of growth from one measurement taken at any other age. *Forest Ecology and Management*, 259(10): 1993-2005.
- [547] Almeida, A.M., Tomé, J., and Tomé, M. (2010). Development of a system to predict the evolution of individual tree mature cork caliber over time. *Forest Ecology and Management*, 260(8): 1303-1314.
- [548] Leal, S., Nunes, E., and Pereira, H. (2008). Cork oak (*Quercus suber* L.) wood growth and vessel characteristics variations in relation to climate and cork harvesting. *European Journal of Forest Research*, 127(1): 33-41.
- [549] Leal, S., Sousa, V.B., Knapic, S., Louzada, J.L., and Pereira, H. (2011). Vessel size and number are contributors to define wood density in cork oak. *European Journal of Forest Research*, Online First, 14 February 2011.
- [550] Knapic, S., Seppä, I.P., Usenius, A., and Pereira, H. (2011). Stem modeling and simulation of conversion of cork oak stems for quality wood products. *European Journal of Forest Research*, In Press. DOI: 10.1007/s10342-010-0467-z.
- [551] Aziz, M.A., Murphy, C.K., and Ramaswamy, S.D. (1979). Lightweight concrete using cork granules. *International Journal of Cement Composites and Lightweight Concrete*, 1(1): 29-33.
- [552] Pereira, C., Jorge, F.C., Irle, M., and Ferreira, J.M. (2006)a. Characterizing the setting of cement when mixed with cork, blue gum, or maritime pine, grown in Portugal I: temperature profiles and compatibility indices. *Journal of Wood Science*, 52(4): 311-317.
- [553] Pereira, C., Jorge, F.C., Irle, M., and Ferreira, J.M. (2006)b. Characterizing the setting of cement when mixed with cork, blue gum, or maritime pine, grown in Portugal II: X-ray diffraction and differential thermal analyzes. *Journal of Wood Science*, 52(4): 318-324.
- [554] Hernández-Olivares, F., Bollati, M.R., del Rio, M., and Parga-Landa, B. (1999). Development of cork-gypsum composites for building applications. *Construction and Building Materials*, 13(4): 179-186.

-
- [555] Karade, S.R. (2003). An Investigation of Cork Cement Composites. PhD Thesis. 6. BCUC. Brunel University, UK.
- [556] Nóvoa, P.J.R.O., Ribeiro, M.C.S., Ferreira, A.J.M., and Marques, A.T. (2004). Mechanical characterization of lightweight polymer mortar modified with cork granulates. *Composites Science and Technology*, 64(13-14): 2197-2205.
- [557] Silvestre, A.J.D., Neto, C.P., and Gandini, A. (2008). Cork and Suberins: Major Sources, Properties and Applications. *Monomers, Polymers and Composites from Renewable Resources*, 305-320.
- [558] (<http://corkqc.com/production/production.htm>;
<http://www.corkfacts.com/natlerk11.htm>; [http://en.wikipedia.org/wiki/Cork_\(material\)](http://en.wikipedia.org/wiki/Cork_(material))).
- [559] Ng, W.T. (2004). The versatile laparoscopic sponge. *Surgical Endoscopy*, 18(6): 1002-1003.
- [560] Ehrlich, H. (2010). Spongin. In *Biological Materials of Marine Origin Biologically-Inspired Systems*, 1(4): 245-256, DOI: 10.1007/978-90-481-9130-7_13.
- [561] Hausmann, R., Vitello, M.P., Leitermann, F., and Syltatk, C. (2006). Advances in the production of sponge biomass *Aplysina aerophoba* - A model sponge for ex situ sponge biomass production. *Journal of Biotechnology*, 124(1): 117-127.
- [562] McClenachan, L. (2008). "Social conflict, Over-fishing and Disease in the Florida Sponge Fishery, 1849-1939"
- [563] (<http://books.google.com/?id=cGEeEffFegvECandpg=PA26anddq=sponge+fishing>). In Starkey, D. J.; Holm, P., and Barnard, M., *Oceans Past: Management Insights from the History of Marine Animal Populations*. Earthscan. pp. 25-27. ISBN 1844075273.
- [564] Jacobson, N. (2000). Cleavage. Rutgers University Press. p. 62. ISBN 0813527155. (http://books.google.com/?id=3Zlw_3Px4AECandpg=PA62anddq=sponge+synthetic).
- [565] CBAS, (2004). "Sponges" (<http://www.cervicalbarriers.org/information/sponges.cfm>). Cervical Barrier Advancement Society.
- [566] <http://www.cervicalbarriers.org/information/sponges.cfm>. Retrieved 2011-03-17.
- [567] Porterfield, W.M. (1955). "Loofah - The sponge gourd". *Economic Botany* 9 (3): 211-223.
- [568] Smolker, R., Richards, A., Connor, R., Mann J., and Berggren, P. (1997). Sponge-carrying by Indian Ocean bottlenose dolphins: Possible tool-use by a delphinid. *Ethology*, 103: 454-465.
- [569] Krutzen, M.; Mann, J.; Heithaus, M.R.; Connor, R.C.; Bejder, L.; and Sherwin, W.B. (2005). Cultural transmission of tool use in bottlenose dolphins. *Proceedings of the National Academy of Sciences* 102 (25): 8939-8943. (<http://www.pubmedcentral.nih.gov/articlerender.fcgi?tool=pmcentrezandartid=1157020>).
- [570] Belarbi, E.H., Gómez, A.C., Chisti, Y., Camacho, F.G., and Grima, E.M. (2003). Producing drugs from marine sponges. *Biotechnology Advances*, 21(7): 585-598.
- [571] Imhoff, J. F., and Stöhr, R. (2003). "Sponge-Associated Bacteria". In Müller, W. E. G., *Sponges (Porifera): Porifera*. Springer. pp. 43-44. ISBN 354000968X.
- [572] Teeyapant, R., Woerdenbag, H. J., Kreis, P., Hacker, J., Wray, V., Witte, L., and Proksch P. (1993). Antibiotic and cytotoxic activity of brominated compounds from the marine sponge *Verongia aerophoba*. *Zeitschrift für Naturforschung. C, Journal of biosciences*, 48: 939-945.

-
- [573] Lee, R.J., Strohmeier, B.R., Bunker, K.L., and Van Orden, D.R. (2008). Naturally occurring asbestos - A recurring public policy challenge. *Journal of Hazardous Materials*, 153(1-2): 1-21.
 - [574] Wagner, G.R., and Lemen, R. (2008). Asbestos. *International Encyclopedia of Public Health*, 238-245.
 - [575] Ross, M., Langer, A.M., Nord, G.L., Nolan, R.P., Lee, R.J., Van Orden, D., and Addison, J. (2008). The mineral nature of asbestos. *Regulatory Toxicology and Pharmacology*, 52(1): S26-S30.
 - [576] Yu II, J., Moon, Y.H., Sakai, K., Hisanaga, N., Park, J.D., and Takeuchi, Y. (1998). Asbestos and non-asbestos fiber content in lungs of Korean subjects with no known occupational asbestos exposure history. *Environment International*, 24(3): 293-300.
 - [577] Manning, C.B., Vallyathan, V., and Mossman, B.T. (2002). Diseases caused by asbestos: mechanisms of injury and disease development. *International Immunopharmacology*, 2(2-3): 191-200.
 - [578] Rudd, R. (2004). *Asbestos and the lung*. *Medicine*, 32(1): 111-113.
 - [579] Brody, A.R. (2006). Occupational diseases: Asbestos-Related Lung Disease. *Encyclopedia of Respiratory Medicine*, 216-226.
 - [580] Attanoos, R.L. (2010). Asbestos-Related Lung Disease. *Surgical Pathology Clinics*, 3(1): 109-127.
 - [581] McDonald, J.C., and McDonald, A. (2005). Mesothelioma and Asbestos Exposure. In *Malignant Mesothelioma*, Springer Publishers, Part Three, 267-292. DOI: 10.1007/0-387-28274-2_17.
 - [582] Conforti, P.M., Kanarek, M.S., Jackson, L.A., Cooper, R.C., and Murchio, J.C. (1981). Asbestos in drinking water and cancer in the San Francisco bay area: 1969-1974 incidence. *Journal of Chronic Diseases*, 34(5): 211-224.
 - [583] Allen, N.S., Ledward, M., and Follows, G.W. (1992). Photooxidation and stabilization of mixed acid dyed nylon 6,6 film and fibers: influence of thermal history, delustrant and relationship with luminescent species, *Polymer Degradation and Stability*, 38(2): 95-105.
 - [584] Papaspyrides, C.D. (1988). Solid-state polyamidation of nylon salts. *Polymer*, 29(1): 114-117.
 - [585] Papaspyrides, C.D. (1990). Solid-state polyamidation of unsaturated nylon salts: the role of polycondensation water. *Polymer*, 31(3): 496-500.
 - [586] Imai, Y. (1999). Rapid Synthesis of Polyimides from Nylon-Salt-Type Monomers in Advances in Polymer Science, *Progress in Polyimide Chemistry I*, 140: 1-22. Springer Publishers. DOI: 10.1007/3-540-49815-X_1.
 - [587] History of Nylon (2011). (<http://www.caimateriali.org/index.php?id=32>) US Patent 2,130,523 'Linear polyamides suitable for spinning into strong pliable fibers', U.S. Patent 2,130,947 'Diamine dicarboxylic acid salt' and U.S. Patent 2,130,948 'Synthetic fibers', all issued September 20, 1938.
 - [588] Stenzenberger, H.D. (1993). Recent developments of thermosetting polymers for advanced. *Composite Structures*, 24(3): 219-231.
 - [589] Kinloch, A.J., Yuen, M.L., and Jenkins, S.D. (1994). Thermoplastic-toughened epoxy polymers. *Journal of Materials Science*, 29(14): 3781-3790.

-
- [590] Wang, Y., Cheng, S., Li, W., Huang, C., and Li, F., *et al.* (2007). Synthesis and Properties of Thermosetting Modified Polyphenylene Ether. *Polymer Bulletin*, 59(3): 391-402.
- [591] Zhang, X., Yi, X., and Xu, Y. (2008). Phase separation time/temperature dependence of some thermoplastics-modified thermosetting systems. *Frontiers of Chemistry in China*, 3(4): 471-479.
- [592] Zarrelli, M., Skordos, A.A., and Partridge, I.K. (2008). Thermomechanical analysis of a toughened thermosetting system. *Mechanics of Composite Materials*, 44(2): 181-190.
- [593] Alper, J., and Nelson, G.L. (1989). *Polymeric Materials, Chemistry for the Future*, American Chemical Society, Washington, DC.
- [594] Coleman, M.M., and Painter, P.C. (2005). History of Polymers. *Encyclopedia of Condensed Matter Physics*, 386-391.
- [595] Syutkin, V.N., Lelinkov, O.S., Utevsii, L.Y., Slutsker, L.I., and Danilov, S.N. (1976). The physico-mechanical properties of cellulose nitrates with various degrees of substitution and orientation. *Polymer Science U.S.S.R.*, 18(8): 1982-1988.
- [596] Hilderbrand, D., Benton, E.V. (1980). The chemical etching behavior of cellulose nitrate. *Nuclear Tracks*, 4(2): 77-90.
- [597] Winkler, D.A. (1986). Molecular conformational studies of cellulose nitrate. *Polymer*, 27(5): 765-768.
- [598] Heinze, T., and Liebert, T. (2001). Unconventional methods in cellulose functionalization. *Progress in Polymer Science*, 26(9): 1689-1762.
- [599] Laist, D.W. (1987). Overview of the biological effects of lost and discarded plastic debris in the marine environment. *Marine Pollution Bulletin*, 18(6): 319-326.
- [600] Day, R.H., and Shaw, D.G. (1987). Patterns in the abundance of pelagic plastic and tar in the north pacific ocean, 1976–1985. *Marine Pollution Bulletin*, 18(6): 311-316.
- [601] Moore, C.J. (2008). Synthetic polymers in the marine environment: A rapidly increasing, long-term threat. *Environmental Research*, 108(2): 131-139.
- [602] vom Saal, F.S., Parmigiani, S., Palanza, P.L., Everett, L.G., and Ragaini, R. (2008). The plastic world: Sources, amounts, ecological impacts and effects on development, reproduction, brain and behavior in aquatic and terrestrial animals and humans. *Environmental Research*, 108(2): 127-130.
- [603] Doyle, M.J., Watson, W., Bowlin, N.M., and Sheavly, S.B. (2011). Plastic particles in coastal pelagic ecosystems of the Northeast Pacific ocean. *Marine Environmental Research*, 71(1): 41-52.
- [604] Sugar plastic (2006). <http://www.newscientist.com/article/dn9440-sugar-plasticcould-reduce-reliance-on-petroleum.html>
- [605] Chandra, R., and Rustgi, R. (1998). Biodegradable polymers. *Progress in Polymer Science*, 23(7): 1273-1335.
- [606] Ren, X. (2003). Biodegradable plastics: a solution or a challenge?. *Journal of Cleaner Production*, 11(1): 27-40.
- [607] Flieger, M., Kantorová, M., Prell, A., Řezanka, T., and Votruba, J. (2003). Biodegradable plastics from renewable sources. *Folia Microbiologica*, 48(1): 27-44.
- [608] Fang, J.M., Fowler, P.A., Escrig, C., Gonzalez, R., Costa, J.A., and Chamudis, L. (2005). Development of biodegradable laminate films derived from naturally occurring carbohydrate polymers. *Carbohydrate Polymers*, 60(1): 39-42.
- [609] (<http://www2.basf.us/PLASTICSWEB/displayanyfile?id=0901a5e1801359f9>).

- [610] Kyrikou, I., and Briassoulis, D. (2007). Biodegradation of Agricultural Plastic Films: A Critical Review. *Journal of Polymers and the Environment*, 15(2): 125-150.
- [611] Briassoulis, D., Dejean, C., and Picuno, P. (2010). Critical Review of Norms and Standards for Biodegradable Agricultural Plastics Part II: Composting. *Journal of Polymers and the Environment*, 18(3): 364-383.
- [612] Ammala, A., Bateman, S., Dean, K., Petinakis, E., Sangwan, P., Wong, S., Yuan, Q., Yu, L., Patrick, C., and Leong, K.H. (2010). An overview of degradable and biodegradable polyolefins. *Progress in Polymer Science*, In Press, doi:10.1016/j.progpolymsci.2010.12.002.
- [613] (http://greenplastics.com/reference/index.php?title=ASTM_D6400)
- [614] Yu, L. (2008). *Biodegradable Polymer Blends and Composites from Renewable Resources*. PP 488. Wiley Publishers. ISBN-10: 0470146834; ISBN-13: 978-0470146835.
- [615] Belgacem, M.N., and Gandini, A. (2008). *Monomers, Polymers and Composites from Renewable Resources*. Elsevier Science Publishers. PP 560. ISBN-10: 0080453163; ISBN-13: 978-0080453163.
- [616] Seymour, R.B., Carraher, Jr. C.E. (1992). *Polymer Chemistry*, 3rd Edition, Marcel Dekker, New York (1992).
- [617] Braun, D., Cherdron, H., Rehahn, M., Ritter, H., and Voit, B. (2010). *Polymer Synthesis: Theory and Practice: Fundamentals, Methods, Experiments*. PP 385. Springer Publishers. ISBN-10: 3642058612; ISBN-13: 978-3642058615.
- [618] Sperling, L.H. (2000). History and development of polymer blends and IPNS. *Applied Polymer Science*: 21st Century, 343-354.
- [619] Sawyer, L.C., Grubb, D.T., and Meyers, G.F. (2008). Introduction to Polymer Morphology. 2008, *Polymer Microscopy*, 3rd Ed., Springer Publishers, 1-25. DOI: 10.1007/978-0-387-72628-1_1.
- [620] Chum, P.S., and Swogger, K.W. (2008). Olefin polymer technologies - History and recent progress at The Dow Chemical Company. *Progress in Polymer Science*, 33(8): 797-819.
- [621] Elias, H.G. (1987). *Mega Molecules*, Springer-Verlag, Berlin, PP 202. ISBN-10: 0387175415; ISBN-13: 978-0387175416.
- [622] Nielsen, L.E., and Landel, R.F. (1993). *Mechanical Properties of Polymers and Composites (Dekker Mechanical Engineering)*. CRC press Publishers. PP 580. ISBN-10: 9780824789640; ISBN-13: 978-0824789640.
- [623] Meijer, H.E.H., and Govaert, L.E. (2005). Mechanical performance of polymer systems: The relation between structure and properties. *Progress in Polymer Science*, 30(8-9): 915-938.
- [624] Tjong, S.C. (2006). Structural and mechanical properties of polymer nanocomposites. *Materials Science and Engineering: R: Reports*, 53(3-4): 73-197.
- [625] Menczel, J.D., and Prime, R.B. (2009). *Thermal Analysis of Polymers, Fundamentals and Applications*. PP 609. Wiley Publishers. ISBN-10: 0471769170; ISBN-13: 978-0471769170.
- [626] Sperling, L.H. (2005). *Introduction to Physical Polymer Science*. Springer Publishers. PP 880. ISBN-10: 047170606X; ISBN-13: 978-0471706069.

-
- [627] ISO (2000). ISO 3146:2000. Plastics - Determination of melting behaviour (melting temperature or melting range) of semi-crystalline polymers by capillary tube and polarizing-microscope methods. ISO TC 61/SC 5/WG 8.
- [628] Janeschitz-Kriegl, H. (2009). *Crystallization Modalities in Polymer Melt Processing: Fundamental Aspects of Structure Formation*. Springer Publishers. PP 222. ISBN-10: 9783211876268; ISBN-13: 978-3211876268.
- [629] Reiter, G., and Sommer, J.-U., (Eds.) (2010). *Polymer Crystallization: Observations, Concepts and Interpretations (Lecture Notes in Physics)*. Springer Publishers. PP 386. ISBN-10: 3642079334; ISBN-13: 978-3642079337.
- [630] Martin, D.C., and Viney, C. (1995). Editors, Defects in Polymers, MRS Bulletin, dedicated issue, September 1995, Materials Research Society, Pittsburgh, PA.
- [631] Shaw, M.T., and MacKnight, W.J. (2005). *Introduction to Polymer Viscoelasticity, 3rd Edition*. Wiley-Interscience Publishers. PP 316. ISBN-10: 0471740454; ISBN-13: 978-0471740452.
- [632] Wool, R., and Sun, X.S. (2005). *Bio-Based Polymers and Composites. Academic Press Publishers*. PP 640. ISBN-10: 0127639527; ISBN-13: 978-0127639529.
- [633] McMullen, P. (1984). Fibre/resin composites for aircraft primary structures: a short history, 1936–1984, *Composites*, 15(3): 222-230.
- [634] Astrom, B.T. (1997). *Manufacturing of Polymer Composites*. CRC press Publishers. PP 469. ISBN-10: 0748770763; ISBN-13: 978-0748770762.
- [635] Dave, R.S., and Loos, A.C. (1999). *Processing of Composites (Progress in Polymer Processing)*. Hanser Gardner Publications. PP 480. ISBN-10: 9781569902264; ISBN-13: 978-1569902264.
- [636] Rotem, A., and Baruch, J. (1974). Determining the load time history of fibre composite materials by acoustic emission, *Journal of Materials Science*, 9(11): 1789–1798.
- [637] Barbaro, A.J. (1998). *Introduction to Composite Materials Design*, Teyler and Francis, London.
- [638] Kelly, T., and Clyne, B. (1999). Composite Materials—Reflections on the First Half Century, *Physics Today*, College Park, MD, 52, 37.
- [639] O'Connell, M.J. (2006). *Carbon Nanotubes: Properties and Applications. CRC Press Publishers*. PP 360. ISBN-10: 9780849327483; ISBN-13: 978-0849327483.
- [640] Jorio, A., Dresselhaus, G., and Dresselhaus, M.S. (2008). *Carbon Nanotubes: Advanced Topics in the Synthesis, Structure, Properties and Applications (Topics in Applied Physics)*. Springer Publishers. PP 720. ISBN-10: 9783540728641; ISBN-13: 978-3540728641.
- [641] Harris, P.J. F. (2011). *Carbon Nanotube Science: Synthesis, Properties and Applications*. Cambridge University Press. PP 314. ISBN-10: 0521535859; ISBN-13: 978-0521535854.
- [642] Mei, Z., and Chung, D.D.L. (2001). Thermal history of carbon-fiber polymer-matrix composite, evaluated by electrical resistance measurement, *Thermochimica Acta*, 369(1-2): 87-93.
- [643] Guldi, D.M., and Martín, N. (2010). *Carbon Nanotubes and Related Structures: Synthesis, Characterization, Functionalization, and Applications*. Wiley-VCH Publishers. PP 562. ISBN-10: 3527324062; ISBN-13: 978-3527324064.

-
- [644] Li, Y., Lu, D., and Wong, C.P. (2009). *Electrical Conductive Adhesives with Nanotechnologies*. Springer Publishers. PP 433. ISBN-10: 0387887822; ISBN-13: 978-0387887821.
- [645] Zhang, Q. (2008). Electrical conductivity and rheological behavior of multiphase polymer composites containing conducting carbon black. *Polymer Engineering and Science* (Magazine/Journal). Society of Plastics Engineers, Inc.: 48(11): 2090(8).
- [646] Educated, G.S. (1999). *Laminar Composites*. Butterworth-Heinemann. PP 328. ISBN-10: 9780750671248; ISBN-13: 978-0750671248.
- [647] Schreuder-Gibson, H.F., and Realff, M.L. (2003). Eds. Advanced Fabrics, MRS Bulletin 28 (2003) 558.
- [648] Langenhove, L.V. (2007). Smart Textiles for Medicine and Healthcare: Materials, Systems and Applications (Woodhead Publishing in Textiles). CRC Press Publishers. PP 312. ISBN-10: 1420044486; ISBN-13: 978-1420044485.
- [649] Vincenzini, P. (2009). *Smart Textiles (Advances in Science and Technology)*. Trans Tech Pubn. PP 190. ISBN-10: 3908158265; ISBN-13: 978-3908158264.
- [650] Chung, D. (1994). *Carbon Fiber Composites*. Butterworth-Heinemann Publishers. PP 215. ISBN-10: 9780750691697; ISBN-13: 978-0750691697.
- [651] Donnet, J.-B., Wang, T.K., Rebouillat, S., and Peng, J.C.M. (1998). *Carbon Fibers*, 3rd Ed. CRC Press Publishers. PP 584. ISBN-10: 9780824701727; ISBN-13: 978-0824701727.
- [652] Gupta, V.B., Radhakrishnan, J., and Sett, S.K. (1994). Effect of processing history on shrinkage stress in axially oriented poly(ethylene terephthalate) fibers and films, *Polymer*, 35(12), 2560-2567.

Chapter 2

NON-DESTRUCTIVE INSTRUMENTAL ANALYSIS OF EXCAVATED TEXTILES

Christina Margariti*

Textile Conservator, Directorate of Conservation of Ancient and Modern Monuments,
Hellenic Ministry of Culture, 81 Peiraios Avenue, 10553 Athens, Greece.

ABSTRACT

Excavated textiles are generally characterized by a poor condition, as a result of the effects of burial on their physical and chemical properties. Knowledge of the new physical and chemical properties, by the application of instrumental analysis, is necessary for material identification and conservation. However, more often than not, only minute fragments have been preserved. This makes the selection of non-destructive methods of analysis a prerequisite for excavated textiles. This paper presents guidelines for the non-destructive analysis of textiles, based on a study of four textile finds excavated in Greece.

1. INTRODUCTION

Knowledge of the physical and chemical properties of excavated textiles is necessary for various reasons. For example, in order to: (i) characterize or identify the constituent materials and to assess their condition; (ii) inform any intervention, such as remedial action to stabilize brittle material and thereby improve the condition of the find [1]; (iii) select the appropriate conditions and materials for the immediate and long-term storage and/or the display of the find; (iv) enable the technological and historical information revealed by the conservation process to be presented to the public [2,3]; (v) monitor the set standards of care, ensuring that they are remaining effective. Therefore, instrumental analysis seems to be one important way of addressing the challenge of excavated textiles [4-6]. This chapter presents guidelines for the non-destructive analysis of textiles, based on a study of textiles excavated in Greece.

* E-mail: chmargariti@culture.gr

1.1. The Case Studies

This chapter focuses on textiles excavated in Greece where four different types of preservation were identified: (i) in association with a metal (for the majority of the case studies this metal was copper); (ii) in association with a metal in combination with a deprived oxygen environment; (iii) in association with salts; and, (iv) incomplete burning. Therefore, the following four case studies were selected: (i) a sixth century BC find, preserved in a copper vessel; (ii) a fifth century BC find, preserved in a sealed copper vessel; (iii) a fifth century BC find, preserved on a ceramic vessel inside a marble urn, and; (iv) an eleventh century BC find, preserved by charring.

Table 1. Major instrumental analytical techniques applied to excavated textiles

Technique	ND/D/*	Sample size	Application
Stereo Microscopy	ND	Any	Weave and yarn analysis
Optical microscopy	ND	1-2 mm	Fiber identification and condition assessment
Scanning electron microscopy (SEM)	D	1-2 mm	Fiber identification and condition assessment
Environmental scanning electron microscopy (ESEM)	ND	1-2 mm	Fiber identification and condition assessment
Environmental / Scanning electron microscopy - Energy dispersive X-ray spectroscopy (E/SEM-EDX)	ND	1-2 mm	Elemental analysis of the fiber and other material (e.g. mordants, encrustations)
X-ray fluorescence (XRF)	ND	1-2 mm	Elemental analysis of the fiber and other material (e.g. mordants, encrustations)
X-ray diffraction (XRD)	?	2-3 mm	Fiber identification and condition assessment and detection of other material, e.g. pigments
Technique	ND/D/*	Sample size	Application
Staining tests	D	2-3 mm	Fiber identification
Fourier transform infrared spectroscopy (FTIR)	?	1-2 mm	Fiber identification, condition assessment, and dye analysis
Raman spectroscopy	?	1-2 mm	Fiber identification, condition assessment, and dye analysis
Fourier transform Raman spectroscopy (FT-RS)	?	1-2 mm	Fiber identification, condition assessment, and dye analysis
High performance liquid chromatography (HPLC)	D	0.1-1 mg	Dye and proteinaceous fiber identification

*ND = non-destructive, D = destructive, ? = fragile textile samples may be damaged.

2. SELECTING THE MOST APPROPRIATE ANALYTICAL TECHNIQUE(S)

The application of instrumental analysis is not straightforward because there are numerous techniques available, each one giving a different kind of information and each having its own advantages and limitations. Therefore, in order to select the most appropriate technique(s), it is necessary to be aware of their applicability, to form specific questions, and to know what kind of analysis is wanted and/or allowed (e.g. qualitative/quantitative, destructive/non-destructive).

2.1. Applicability

Numerous techniques have been applied to the conservation of excavated textiles, as listed in Table 1.

2.2. Forming Specific Questions

The ultimate goal when conserving an excavated textile is to preserve both the information ‘contained within’ the object and the physical existence of the object itself. The process is optimized by collaboration between the conservator, the archaeologist and the textile historian [1, 2, 7-9]. Therefore, when forming the specific questions to be answered, the information sought by all three professionals should be taken into consideration, to address the following questions:

- I. How was the material constructed? For example, in the case of woven material, how were the yarns constructed?
- II. What types of fibers (and other materials) were present?
- III. How have the fibers/yarn/textiles been preserved?
- IV. Are there organic remains still present within the fibers?

2.3. Knowing the Kind of Analysis Wanted and/or Allowed

As mentioned before, it was a fundamental prerequisite that the technique(s) chosen should be non-destructive, in the sense of the sample being removed but not being destroyed or coated. This was considered essential from an ethical viewpoint. According to Conservation Codes of Ethics any destruction or alteration even to minute parts of an object should be adequately justified and only chosen when other, non-destructive ways cannot answer the research questions [10-12].

2.4. The Techniques Selected

Accordingly, destructive techniques were immediately ruled out. For the same reason, scanning electron microscopy (SEM), which requires sample modification (coating), was also ruled out. Seven analytical methods were selected for this study. They can all be considered non-destructive, and require minimum to no sample preparation. The questions that each technique might address are listed below:

- Stereomicroscopy – question 1
- Optical microscopy – questions 2, 3
- Environmental scanning electron microscopy (ESEM) – questions 1, 2, 3
- Environmental scanning electron microscopy-Energy dispersive X-ray spectroscopy (ESEM-EDX) – question 3
- X-ray fluorescence (XRF) – question 3
- Fourier transform infrared microspectroscopy (FTIR) – questions 2, 3, 4
- Raman microspectroscopy – questions 2, 3, 4

3. NON-DESTRUCTIVE INSTRUMENTAL ANALYSIS OF EXCAVATED TEXTILES

Experience gained from the investigation of the selected case studies showed that there are four issues that are critical to the analysis of excavated textiles: collaboration between archaeologists, conservators and textile historians; sampling; choice of the most appropriate technique; and the sequence in which the techniques applied.

3.1. Collaboration between Archaeologists, Conservators and Textile Historians

Collaboration between the professionals involved was achieved at different levels in each case study. This affected the level of access to the find, the extent of the interpretation of the results and therefore, the quality of the analyses. More specifically, collaboration with the archaeologist was established in case studies 1 and 4 and access to the finds was unlimited; this enabled detailed and comprehensive analyses. In case study 2, collaboration with the archaeologist was established but access to the find was limited due to its location; this resulted in limited study of the construction of the textiles. The textile in case study 3 had already been studied by a textile historian, which meant that information on its construction was available but since no collaboration was established, it also meant that additional samples had to be removed to get information on the condition of the textile and its type of preservation.

The success of analysis and the welfare of the object both depend on effective collaboration between the archaeologist, the textile conservator and the textile historian. The knowledge and expertise each professional has is necessary to form the questions to be

answered by analysis and to interpret the analytical results. Moreover, one technique might answer more than one question, so saving the object from repeated sampling and analysis.

The archaeologist should allow unlimited access to the find and sampling. Collecting more than one sample of the same textile is necessary for the characterization of its condition, which in turn would be used to inform conservation decision-making. The archaeologist should be precise concerning the questions they might have about the object and its future role (e.g. whether it would be on display, or retained in storage or used as a study piece). The conservator should decide on which instrumental analytical techniques are appropriate in order to answer the questions about the object. S/he should study the object to identify and remove the most appropriate samples. S/he should handle and store the samples and ensure that all techniques used are non-destructive, so that all removed samples are returned to the object and are left fit for future analysis. Even if a textile historian is not currently collaborating with the team, the conservator should ensure that all information necessary for the technological analysis of the find has been recorded in detail and is accessible. The textile historian should be precise in collecting the information necessary for the technological study of the object. In cases where a conservator is not currently collaborating with the team it may be appropriate for the textile historian to ensure safe removal and storage of the sample(s) collected and the use of non-destructive methods of analysis, so that samples can be further analyzed and the results made accessible.

3.2. Sampling

In this study sampling of the finds proved to be a multifaceted task. Close examination of textiles in case study 1, revealed different coloration of fragments of the same textile (which corresponded to different types of preservation rather than evidence of dyeing). In addition, the fragments were embedded in soil and/or pulverized organic matter filled with bone and metal fragments, all of which were potential sources of contamination, and also information. The use of the stereomicroscope was vital in the sampling process. Small tubular shaped, green-colored fragments, which were initially thought to be metal beads, turned out to be tightly spun warp fragments impregnated by metal corrosion products. In case study 4, some of the fragments had been consolidated during lifting; this was taken into consideration when collecting samples. In case studies 1, 3 and 4 loose fragments of all different textiles were available, therefore the more uniform areas of the finds were not disturbed. However, in case study 2, samples had to be removed from the textiles and this was done with a scalpel rather than scissors, since the latter disturbs the cross-section of the fibers, as shown by experimenting on reference samples. Fragments rather than loose fibers proved to be the safest choice, since a loose yarn collected from case study 1 and studied at the ESEM gave rise to much confusion and repetitive analyses until it was realized it was not part of the object.

There are several issues that should be considered when sampling an excavated textile: whether it consists of one or more different textiles; whether samples are representative of any differences in the type of preservation and/or condition of the find; in the case of woven textiles, whether samples include both warp and weft fibers; to collect samples from any possible sources of contamination (such as metals, bones, soil or other foreign material); whether the object has been treated in the past (e.g. consolidation); whether a sample can be

removed; the amount of sample that can be removed; the area from which the sample could be removed; the size of sample necessary for the analysis to be performed. The use of a stereomicroscope, a thread-counter or other hand-held magnifying lens is necessary to determine answers to these questions.

The experience of this study suggests that loose fragments should be preferred. In cases where there are no loose fragments available, samples should be removed from an already disturbed area of the textile. A scalpel rather than a pair of scissors should be used to remove the sample from the textile. Loose fibers and/or yarns should not be chosen because they could be products of contamination and confuse the results. In general the instrumental analytical techniques included in these guidelines do not need a sample larger than 2-3 mm². Therefore, fragments of that size should be collected as samples. In cases where no such small fragments exist, then the smallest fragment available should be collected without attempting to cut it or otherwise reduce its size, since this action could destroy it.

Samples should be handled with spatulas and/or vacuum tweezers (such as the DA7c-Charles Austen Pumps) wearing nitrile or nitrile but not cotton gloves, as samples could get tangled and/or contaminated. Samples should be stored in sterilized, rigid plastic containers.

Photographs should be taken of the areas from which samples are collected.

3.3. Choice of the Most Appropriate Instrumental Analytical Technique

The following techniques were all non-destructive (in the sense that the sample analyzed was not consumed or altered in any way) and non-intrusive, in cases where loose fragments were collected as samples. As shown below, there was more than one technique providing similar information. When these results were combined the techniques were shown to provide complementary and/or confirmatory results. The same sample was used for all consequent analyses.

3.4. Construction and Yarn-Making - Stereomicroscopy

Stereomicroscopy revealed that the finds in case studies 1, 2 and 4 consisted of more than one textile. Unlimited access in case studies 1 and 4 meant that it was possible to record and measure technological characteristics, such as the weave type, selvages, starting edges and evidence of stitching. In contrast, limited access in case studies 2 and 3 was enabled recording and measurement only of the weave type, but no other technological characteristics, such as selvages or evidence of embroidery, which were identified by visual observation. Therefore, it is of crucial importance to be able to apply this technique to the whole of the find rather than to limit it to the samples chosen for further analysis.

When observing by eye, the magnification is the product of that afforded by the objective and eyepiece lenses. The overall magnification recorded through an attached digital camera may be somewhat different, and it is essential to calibrate the images, for example, by the use of a micrometer scale.

3.5. Fiber Identification – ESEM/-EDX, FTIR

In case studies 1 and 2, the combination of ESEM/-EDX and FTIR microspectroscopy provided information on fiber identification. In case study 1, both cellulosic and proteinaceous fibers seemed to be present. ESEM-EDX detected sulfur in the negative casts of possibly wool fibers (as indicated by the ESEM), which is a constituent of wool keratin, Figures 1 and 2. In case study 2, the application of ESEM and FTIR microspectroscopy showed that all three textiles were made of cellulosic bast fibers, Figures 3 and 4. In case study 4, ESEM analyses showed that both textiles were made of the same cellulosic bast fibers, possibly flax, Figure 5. ESEM-EDX and XRF analyses identified calcium, which is a constituent of plant fibers, the detectable amount of which seems to increase by charring [13]. In case study 3, none of the techniques applied provided any indication as to fiber type, since the fibers' morphological characteristics were masked and the chemical properties had altered to an unidentifiable extent, Figure 6.

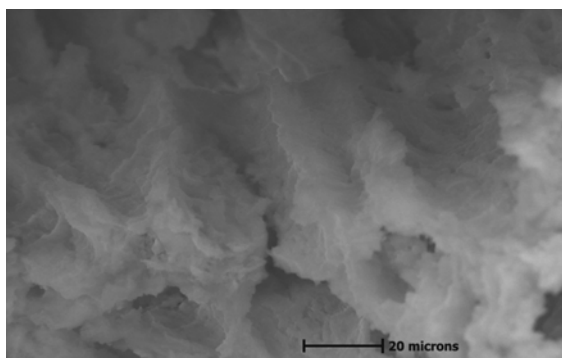


Figure 1. Scanning electron micrograph of the weft fibers of one of the three textiles. Negative casts of the fibers seemed to have been preserved, with a pattern indicative of the epithelial scales of wool fibers.

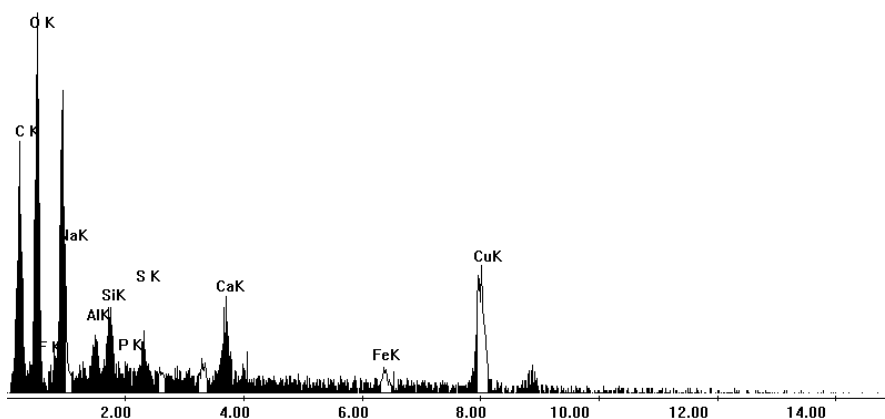


Figure 2. EDX spectrum of the weft fibers of one of the three textiles. In general, the same elements as in the warp fibers were present (copper, iron, carbon, oxygen, aluminum and silicon). However, sulphur was also detected, which could be indicative of wool fibers. The X-ray energy scale is in keV.

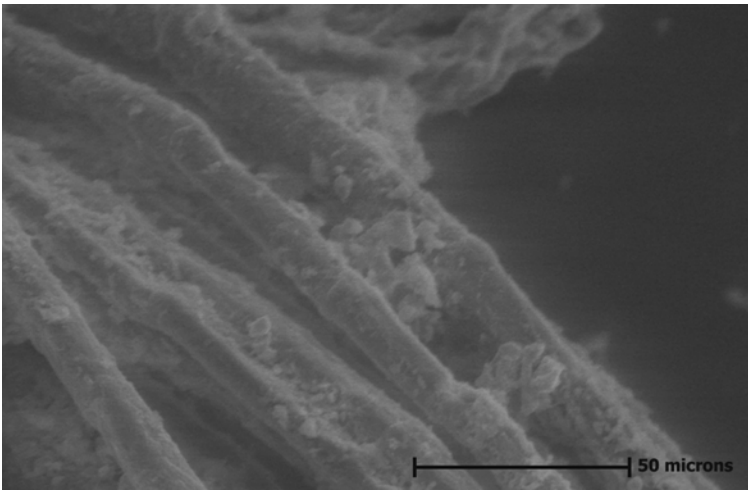


Figure 3. Scanning electron micrograph of the fibers of one of the three textiles. They have smooth surfaces, cylindrical shape and exhibit nodular thickening across their length, all of which are characteristics of cellulosic bast fibers.

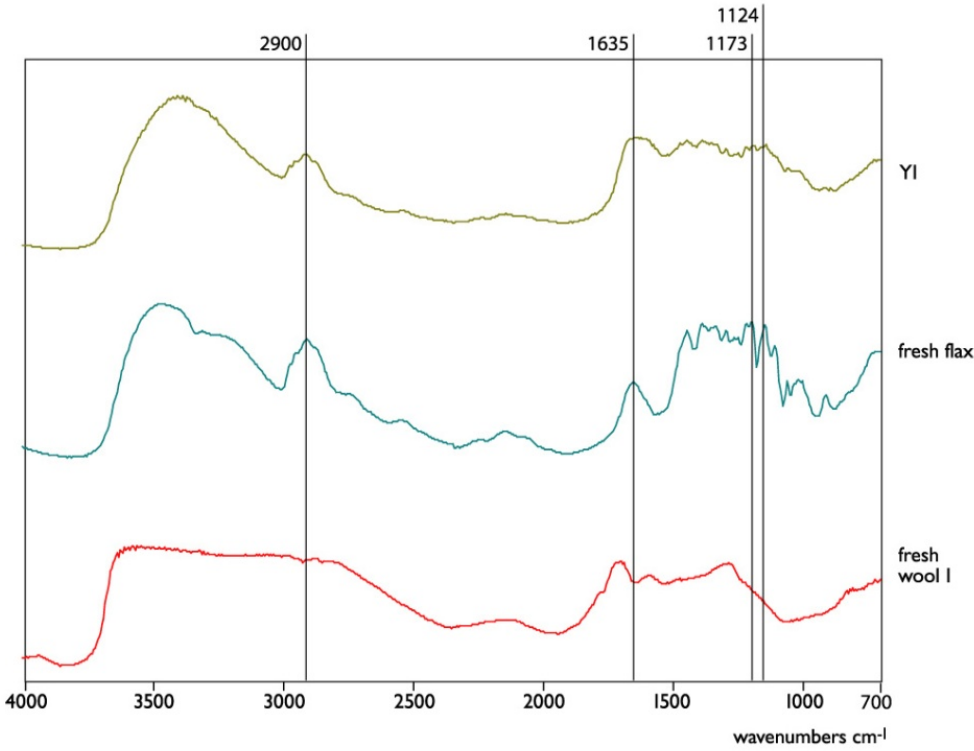


Figure 4. FTIR microscope reflectance spectra of one of the textiles (top), ‘fresh’ flax (middle) and ‘fresh’ wool 1 (bottom). The spectrum of the excavated textiles has the characteristic peaks of cellulose.

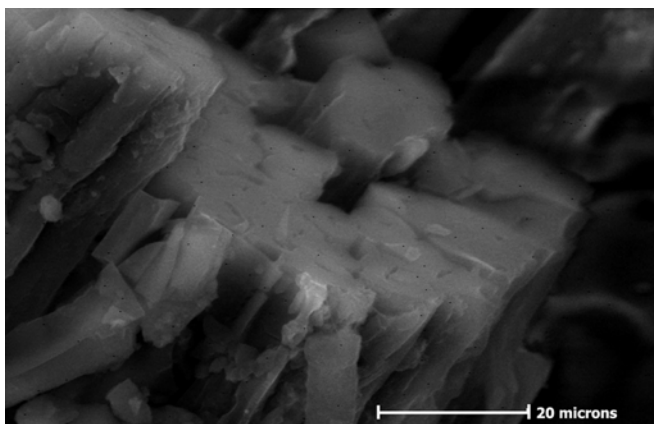


Figure 5. Fibers in cross-section imaged in the ESEM. The fibers appeared to occur in bundles, each with a polygonal cross-section, narrow lumen and thick cell walls, characteristic features of bast fibers, possibly flax.

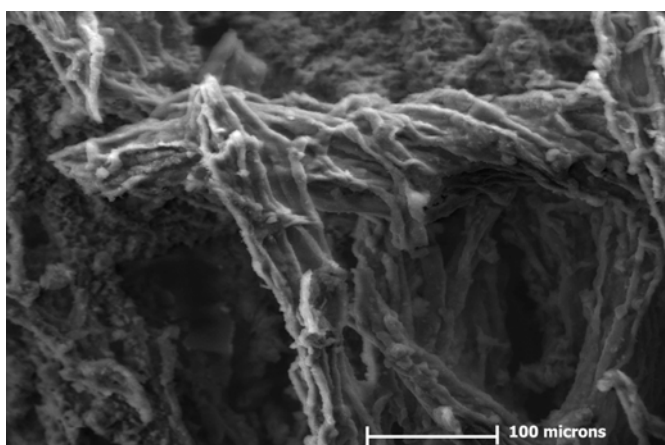


Figure 6. Scanning electron micrograph of the sample. The fibers have homogenised to a compact mass by the deposits and identification is not possible.

The experiments conducted in this study showed that an ESEM should be used because it allows non-conducting samples to be observed directly without the need for the application of a conductive surface coating, hence it is a non-destructive technique. The quality of the image produced is good enough, even at higher magnifications, to allow fiber identification, hence there is no reason to use a conventional SEM where coating of the sample is necessary. Similarly, no higher than a 15keV electron beam should be used, since it affords a good quality image and the energy is low enough not to damage the sample.

No attempt should be made to remove fibers and/or yarns from the samples as they may be destroyed. A small piece of double-sided adhesive tape should be placed on the centre of the microscope stub and the sample lightly adhered to the edge of it. This affords enough grips to secure the sample in the chamber and at the same time be loose enough to be safely removed from the stub.

The ESEM used should be equipped with an energy dispersive X-ray spectrometer. Since localized spot analysis is possible, it should always be recorded whether a fiber or other material, such as a foreign particle, was analyzed in order to avoid misinterpretation of the results.

An FTIR spectrometer attached to a microscope should be used in reflectance mode. No attempt should be made to prepare the samples by pressing as this would destroy them. Good quality spectra can be acquired by accumulating e.g. 32 scans with a resolution of 4 cm^{-1} over the range 4000 to 700 cm^{-1} . At least five different areas of each sample must be analysed to ensure consistency of the results. In the case of woven textiles, spectra of both the warps and wefts of each sample should be taken to detect any differences and/or similarities between them. Impurities likely to be present in excavated textiles may generate a number of peaks that might mask underlying characteristic peaks of the fibers, so spectra of soil and debris should be recorded.

3.6. Characterization of the Condition – ESEM/-EDX, FTIR

In case studies 1, 2, and 3, the application of ESEM/-EDX and FTIR microspectroscopy revealed information on the condition of the textiles. In case study 1, the fibers appeared to be heavily masked and/or impregnated by a significant amount of copper and a smaller amount of iron degradation products, calcium salts and debris (such as aluminosilicates). Wool fibers seemed to be mainly preserved in the form of negative casts. ESEM/-EDX and FTIR indicated that cellulosic (?) fibers were not totally masked and/or impregnated by degradation products and organic residues might still be present. In case study 2, the textile fibers were partially masked and/or impregnated by copper degradation products and debris. The applied techniques clearly showed that textile fibers were still organic. In case study 3, the textile fibers appeared to be heavily masked and/or impregnated by a significant amount of calcium products. The fact that these techniques are able to analyse up to a depth of a few microns meant that results were not conclusive as to whether there were organic residues preserved within the fibers. Similarly, in case study 4, results were indicative but not conclusive. It was not clear whether the condition (organic remains within the fibers) or the type of preservation (charring) was responsible for the carbon detected by ESEM-EDX.

3.7. Characterization of the Type of Preservation – ESEM/-EDX, XRF

In case studies 1, 2, and 3, the type of preservation was determined by the application of ESEM-EDX and XRF. More specifically: in case study 1, the textiles had been preserved in association with copper and iron degradation products; in case study 2, they had been preserved in association with copper degradation products; and, in case study 3, by impregnation and/or coating by calcium products. However, none of the techniques applied gave any conclusive results on the characterisation of the type of preservation of the textiles in case study 4. An indication of the type of preservation could be the increased calcium values detected by ESEM-EDX and XRF, which is detected in cellulosic fibers and its value increases by charring. A portable XRF is preferable, in case it is available, since it affords non-destructive and non-intrusive analysis of any area of the find *in situ*. Normalisation of the

data may be necessary. Optical microscopy and Raman microspectroscopy did not provide any useful results in this study.

3.8. Sequence of the Techniques Applied

In theory, the ideal sequence of the techniques applied would be from a macroscopic to a microscopic to a molecular and elemental analysis level. Experience from the current research suggests, however, that the following is the more practical:

- Stereomicroscopy should be applied first to the whole of the find before samples are removed. Stereomicroscope analysis should never be omitted.
- A portable XRF should then be used, so that sample removal is not necessary and analysis can be performed across the whole of the object.
- Reflectance FTIR microspectroscopy.
- ESEM/-EDX should be last, on account of possible destruction of the sample, since it may not be able to withstand removal from the microscope stub without destruction. In that case, it should remain on the stub and be returned to the object.

In cases where funding, time and/or accessibility limits the investigation to one technique only (other than the stereomicroscope) then ESEM/-EDX analysis should be preferred as it is the technique which can provide most information on the characterization of both the type of preservation and the condition of the find, and fiber identification.

CONCLUSION

This chapter has shown that the application of non-destructive instrumental can provide very important information on excavated textiles. Good collaboration between the conservator, archaeologist and textile historian is particularly helpful to the process of analysis. Experimenting with four textile finds, representative of different types of preservation of textiles excavated in Greece, showed that stereomicroscopy, XRF, FTIR and ESEM/-EDX are the most useful techniques and should be applied in this sequence. Nevertheless, it should always be kept in mind that the application of instrumental analysis might not provide any conclusive information, which makes the application of non-destructive techniques imperative.

ACKNOWLEDGEMENTS

The Textile Conservation Centre (TCC), UK, for FTIR and XRF access. Dr Dimitris Papageorgiou, Research Coordinator, Titan Cement Company SA, Greece, for access to the ESEM-EDX facilities.

REFERENCES

- [1] Cruickshank, P., Harrison, A. and Fields, J. (2002). From excavation to display: the conservation of archaeological textiles from an AD first-third century cemetery site in Jordan. *The Conservator*, 26: 44-55.
- [2] Brooks, M., Lister, A., Eastop, D. and Bennett, T. Artifact or information? Articulating the conflicts in conserving archaeological textiles. In: *Archaeological Conservation and its Consequences*, London: Oxbow Books, p. 16-21.
- [3] Hillyer, L. (1990). The cleaning of archaeological textiles. In: *Archaeological Textiles*, London: United Kingdom Institute for Conservation, p. 18-21.
- [4] Jakes, K. A., Sibley, L. R. and Yerkes, R. (1994). A comparative collection for the study of fibers used in prehistoric textiles from Eastern North America. *Journal of Archaeological Science*, 21 (5): 641-650.
- [5] Kouznetsov, D. A., Ivanov, A. and Veletsky, P. R. (1996). Analysis of cellulose chemical modification: a potentially promising technique for characterising cellulose archaeological textiles. *Journal of Archaeological Science*, 23 (1): 23-34.
- [6] Janaway, R. (1983). Textile fiber characteristics preserved by metal corrosion: the potential of SEM studies. *The Conservator*, 7: 48-52.
- [7] Rotroff, S. (2001). Archaeologists on conservation: how codes of archaeological ethics and professional standards treat conservation. *Journal of the American Institute for Conservation*, 40 (2): 137-146.
- [8] Boccia-Paterakis, A. (1996). Conservation: preservation versus analysis?. In: *Archaeological Conservation and its Consequences*, London: Oxbow Books, p. 143-148.
- [9] Wild, J. P. (1990). An introduction to archaeological textile studies. In: *Archaeological Textiles*, London: United Kingdom Institute for Conservation, p. 3-4.
- [10] The National Trust of Australia, Burra Charter: Guidelines for Cemetery Conservation [online] 2007 [13 February 2007]. Available from <http://www.nsw.nationaltrust.au/burracharter.html>
- [11] Canadian Association for Conservation-Canadian Association of Professional Conservators (2003-3rd edition) *Code of Ethics and Guidance for Practice*, Ontario: Canadian Association for Conservation-Canadian Association of Professional Conservators.
- [12] American Institute for Conservation, Code of Ethics [online] 2008 [22 November 2008]. Available from <http://aic.stanford.edu/pubs/ethics.html>
- [13] Sibley, L. R. and Jakes, K. A. (1986). Characterization of selected Prehistoric fabrics of Southeastern North America. In: *Historic Textiles and Paper Materials: Conservation and Characterisation, Advances in Chemistry Series 212*, Washington DC: ACS Publications, p. 253-275.

Chapter 3

KINETICS STUDY OF FORCED TEXTILE DYEING PROCESS

***Erasmio Mancusi^{a,b,*}, Antônio Augusto Ulson de Souza^b,
and Selene Maria de Arruda Guelli Ulson de Souza^b***

^a University of Sannio, Engineering Department, Piazza Roma, 82100, Benevento, Italy.

^b Chemical Engineering and Food Engineering Department, Federal University of Santa Catarina, PO Box 476, Florianopolis, SC 88040-900, Brazil.

ABSTRACT

The use of computational methods to simulate the textile dyeing process provides a powerful tool to allow an understanding of the mass transfer kinetics in aqueous solutions during the dyeing process. Moreover, analysis of the time scales associated with the main phenomena can lead to a precise knowledge of the dyeing kinetics during the process, which in turn can be used to improve the process control, reliability and, perhaps most importantly, the environmental impact of the dyeing process. Traditionally, dyeing techniques are carried out in a batch process.

The bobbins of thread are fixed to perforated supports and receive dye from the liquid passing across the bobbins and re-circulating to a mixing tank. Inside the bobbins dye has to be transported by convection and dispersion to the inner core of the threads. Under normal operating conditions the dye is added at the beginning of a dyeing cycle in the mixing bath and the process runs under batch conditions, that is, without changing the amount of dye in the system.

In general, dye distribution factor (DDF) and dye uptake (CDEP) benefit from high recirculation flux values and low dispersion resistances. In order to investigate possible improvements to the traditional dyeing process, the effect of periodic variations in the boundary conditions (reverse flow operation) on the bobbin thread dyeing process was studied. The system is operated by periodically reversing the conditions of the dyeing bath fluid external to the thread bobbins and inside the bobbins. The periodic forcing is modeled by an *ad hoc* discontinuous periodic function and a partial differential equations mathematical model that takes this function into account is developed. A comparison between the forced and unforced processes was conducted by analyzing the dye

* mancusi@unisannio.it

distribution factor and the total amount of dye adsorbed during the transient regime for the two processes. Due to the batch nature of the dyeing process under study there are no differences between the regime values for the forced and unforced processes. In other words, asymptotically (after more than three hours) the two processes reach the same dye distribution. On the other hand, the transient forced and unforced processes exhibit qualitative and quantitative differences. Finally, we demonstrate that to benefit from the reverse flow operation the switch time magnitude has to be comparable with the time scales of the main transport phenomena, the convection time being the most important transfer phenomenon.

NOMENCLATURE

C	liquid concentration of dye
C_M	mixing tank concentration
C_T	thread concentration
C_T^*	equilibrium thread concentration
D_A	dispersion coefficient
DDF	dye distribution factor
$g(t)$	forcing function defined in Eq. 8
H	height of the bobbins
K	integer number
k_t	global mass transfer coefficient
Q	flow rate
T	time
V	volume of dyeing bath in the mixing

Greek Letters

α	equilibrium constant
ε	bobbin void fraction
ρ	fiber density
v_r	interstitial fluid velocity in radial direction
τ	switch time

Subscripts and Superscripts

M	mixing tank
R _E	external bobbin radius.
R _I	internal bobbin radius.

1. INTRODUCTION

The textile industry is of great interest in terms of the Brazilian economy and, in particular, it constitutes one of the most important branches of the economy of the state of Santa Catarina (SC). In this state there are more than three hundred textile plants and the most important industrial textile poles are in Blumenau, Brusque, Joinville and Jaraguá do Sul.

The development of new dyes and textile fibers has led to an increase in new dyeing technologies which are the result of a large number of studies carried out in the area of textile dyeing. The main objectives of these technological advancements have been to increase the productivity of the process and the quality of the dyed product [1-4] and to reduce environmental pollution [5-12]. These studies are largely empirical in nature and provide a thorough analysis of the physical mechanisms responsible for the characteristics of the dyed product.

Analysis of the bobbin thread dyeing process is rather complicated [1, 13]. The dyeing process is intrinsically heterogeneous and many phenomena occur. Dye is transferred in the liquid phase by convection and dispersion and at the same time there are exchanges between the liquid and solid (thread) phases. Several scientists have defined various models to describe the dyeing process and/or relate the conditions during this process to the quality of the resulting dyed material. Some studies have focused on the on-line control of the dyeing process [14-17]. Others have focused on the physical chemistry of the dye adsorption and transport of dye into the threads through the comprehensive investigation of the effect of various process parameters on the dye distribution and dye uptake [18-23].

In standard dyeing equipment the bobbins of thread are fixed to perforated supports and receive dye from the liquid passing across the bobbins and re-circulating to a mixing tank [1]. Under traditional operating conditions the dye is added at the beginning of a dyeing cycle in the mixing bath and the process runs under batch conditions, that is, without changing the amount of dye in the system. Periodic forcing of chemical processes, as a means to obtain better average performance compared to unforced operation, has been widely studied for some time [24]. Burely *et al.* [25] analyzed the feasibility of a forced dyeing process implementing a flexible dyeing strategy which forces the process adding and/or removing dye during the process. Over the last few decades the analysis and design of periodically-forced continuous chemical processes has been an area of intense research and many forcing strategies have been studied [26]. It has been established that such periodic forcing may, under certain conditions, lead to the intensification of traditional processes, thus enhancing the arsenal for engineering better products with much greater efficiency. For example, periodically-forced tubular catalytic reactors have been successfully used for the reduction of volatile organic compound (VOC) concentrations in industrial exhaust gas [27-29] to improve equilibrium-limited exothermic reactions such as methanol synthesis [30, 31].

The most common configuration involves the reversal of the flow direction. Such reactors are called Reverse Flow Reactors [28]. The ability of the forcing operation to generate a significant driving force between two phases has also been investigated in the area of adsorption processes, such as pressure swing adsorption (PSA) [32-35]. PSA processes have been recommended as an energy-saving process and as an alternative to traditional separation, distillation, and absorption methods for bulk gas separations (air purification [36]; propane/propylene separation [37] and hydrogen purification [38]).

Herein, a cyclic reverse dyeing strategy is investigated. More specifically, without changing the overall amount of dye loaded we forced the flow direction inside the bobbins using a cyclic reverse flow. The transport of dye through the bobbins is described by a set of time-dependent partial differential equations, accounting for the convection, dispersion and adsorption of dye. The effect of periodic changes in the flow direction inside the bobbins is described by a discontinuous periodic function [39, 40]. A detailed mathematical model is obtained and numerically integrated. Numerical simulations are performed with the aim of facilitating an understanding of the process phenomena and evaluating the feasibility of the forcing strategy with respect to the classical unforced process. Spatial profiles and time series are presented for different values of operating parameters in order to elucidate the effect of the cyclic reversal of the flow direction on the quality of the dyed product. To evaluate the quality of the dyed product, the dye distribution throughout the bobbins and the total amount of adsorbed dye will be considered. The advantages of the forced process compared to the unforced process are outlined.

In this chapter, we will investigate the feasibility of the dyeing strategy based on a cyclic reversal of the flow direction inside the bobbins. To this aim, we develop a mathematical model capable of describing the evolution of the dyeing process operated under periodically-forced conditions and we will study the effect of the main operative parameters on the quality of the dyed product.

The chapter is organized as follows. In section 2, we firstly describe the mathematical model of the unforced dyeing of bobbins of thread, then the effect of the cyclic reversal of the flow direction is formalized by an *ad hoc* discontinuous function and the model for the forced dyeing process is derived. In section 3, the performances of the unforced and periodically-forced process are studied by comparing the spatial profiles, the evenness of the dye distribution throughout the bobbins and the total amount of adsorbed dye for forced and unforced operations. A final discussion ends this chapter.

2. MODELING

The apparatus used for the dying process was composed of a pressurized autoclave loaded with bobbins of thread fixed to perforated supports through which the dye bath contents is recycled by means of a pump. A simplified scheme of the equipment is given in Figure 1(a) where the squared region represents the bobbins of thread and is the calculation domain, while in Figure 1(b) a schematic representation of the bobbin of thread and the perforated support are shown.

Due to the natural symmetry of the problem only half of the bobbin is here considered. The western face is the bobbin support, with radius R_i ; the eastern face, with radius R_e , of the bobbin is in external contact with the dye bath fluid, which has a concentration of C_f , and H is the height of the bobbin [1]. For an explanation of all the symbols please see the Notation section.

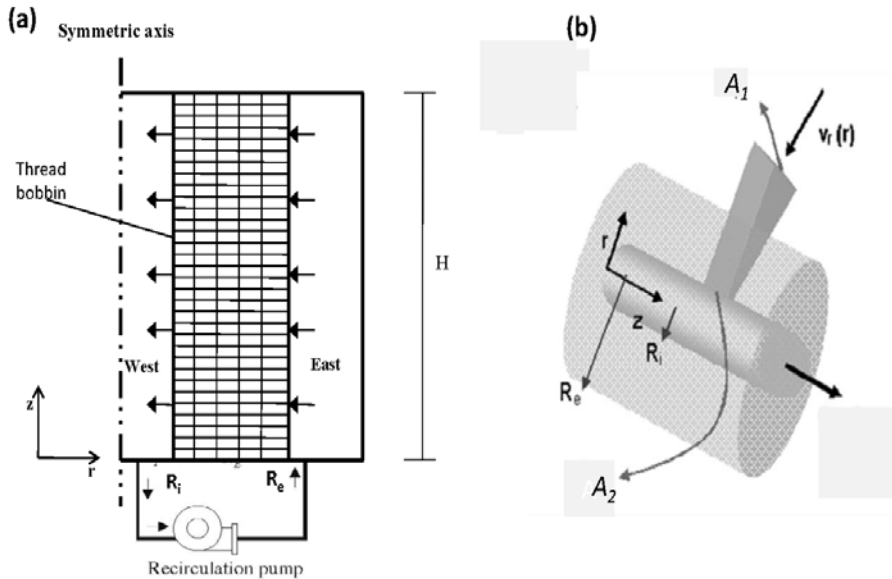


Figure 1. Simplified scheme of the equipment used for the dyeing process.

The process start-up can be summarized in the following step. Firstly, the bobbins are loaded, and then the water and the auxiliary products are added into the system at ambient temperature (20°C). The bath is heated quickly up to 70°C, when the basic dye is added to the dye bath. Starting from the addition of the dye the bath is heated (approximately of 0.3°C per minute) until reaching 102°C. This temperature is kept constant throughout the dyeing process [1]. The pump (Figure 1a) allows the recirculation from the dye bath to the perforated support where the liquid is collected and re-injected into the external bath.

It is worth noting that the most general approach to a dyeing process is from a micro-scale point of view (see for more details [1, 41, 42]). In order to take into account the forcing effect due to the cyclic permutation of flow direction inside the bobbins in this project a simplified approach is considered. Therefore, a macroscopic point of view is preliminarily adopted.

There are a number of macroscopic models for the dyeing process reported in the literature. The Langmuir model is one such model developed to explain the equilibrium behavior of the dyeing system. A previous study by Lu *et al.* [43] on adapting the equilibrium model to predict the kinetic behavior gave promising results. In addition, the Langmuir model is fairly simple and the parameters are easily identifiable. The Langmuir model assumes that the dyeing process is a combination of two simultaneous processes of absorption and desorption. The absorption rate is proportional to the concentration of dye in the solution and the concentration of available sites in the threads; the desorption rate is proportional to the concentration of dye in the threads.

In the modeling of mass-transfer in fluid systems a dispersion model is frequently used to represent the flow characteristics in packed beds. Dispersion is important in terms of mass transfer in a fluid system through porous materials such as bobbins of thread. This model is known to hold well in describing the flow behavior of real systems, which do not deviate significantly from plug flow. Thus, as an alternative to the Langmuir model, the dispersion

model can be considered. Moreover, the recirculation of the liquid induced by the external pump has to be taken into account by an appropriate convective flux across the bobbins, where a non-uniform interstitial velocity is considered due to the cylindrical section of the bobbins (see Figure 1b for more details).

The mathematical model was developed herein for the two phase system composed of a solid phase (threads on bobbins) and a liquid phase (dye bath) external to the bobbin represented in Figure 1. The mathematical model is composed of two mass balance equations, one for each phase. The most important assumptions are:

- a) The external dye bath is well mixed. Therefore, the liquid concentration inside the bobbins is assumed to be uniform with respect to the height coordinate;
- b) The process is isothermal;
- c) The bobbin porosity is constant;
- d) The dispersion and equilibrium constant are constant;
- e) A linear adsorption isotherm is considered to describe the adsorption process [44];
- f) The time delay inside the pipe is negligible.

Here we firstly report the mathematical model of the unforced dyeing process and afterwards discuss the periodic forcing and how it can be modeled. A detailed mathematical model that takes into account the periodic reversal of the flow direction inside the bobbins is presented and a discussion on the numerical technique used to reduce the partial differential equations to a set of ordinary differential equations closes the section.

2.1. Unforced Dyeing Process

The mass balance with respect to the radial coordinate for transport in the liquid phase based on a convection–dispersion–adsorption equation can be derived as shown in Eq. 1:

$$\frac{\partial C}{\partial t} = \frac{D_a}{r} \frac{\partial}{\partial r} \left(r \frac{\partial C}{\partial r} \right) + v_r \frac{\partial C}{\partial r} - \frac{(1-\varepsilon)}{\varepsilon} \frac{\partial C_T}{\partial t}. \quad (1)$$

A flow direction from the east to the west surface is assumed (Figure 1a). The concentration of dye in the circulating liquid will be referred to as the liquid concentration (C) while the amount of dye absorbed by the threads will be called the thread concentration (C_T).

The amount of dye in the liquid phase is low and therefore we can assume the total amount of the recirculated liquid (Q) to be constant. Following this simplification the interstitial velocity v_r in Eq. 1 is dependent only on the radial position and can be expressed as:

$$v_r(r) = \frac{Q}{2\pi H r} \quad (2)$$

For Eq. 1 the following boundary conditions are assumed:

$$r = R_I \Rightarrow \frac{\partial C}{\partial r} = 0, \quad (3)$$

$$r = R_E \Rightarrow C = C_M. \quad (4)$$

To accurately describe the dye distribution in the solid phase, the intra-fiber transport phenomenon should be, in principle, considered (e.g. Guelli U. Souza *et al.* [1]). However, since it can be computationally very time-consuming, we instead assume a uniform thread concentration profile. Under this assumption, the mass balance in the threads can be described by a space-independent expression for the adsorption rate. A common approach is that given by Linear Driving Force model [33]:

$$\frac{dC_T}{dt} = k_t (C_T^* - C_T). \quad (5)$$

where k_t is the effective mass transfer coefficient and C_T^* is the equilibrium thread concentration which is related to the liquid concentration phase by the so-called adsorption isotherm. Following the experimental results of Revello *et al.* [44], C_T^* can be expressed as follows:

$$C_T^* = \alpha C \quad (6)$$

A mass balance for the mixing tank is formulated under the assumption of vigorous agitation to capture the temporal evolution of C_M , as shown in the following equation:

$$\frac{dC_M}{dt} = \frac{Q}{V} (C|_{R_I} - C_M) \quad (7)$$

where Q is the recirculation flow rate, V is the total volume of the mixing tank and C_M is the inlet concentration of the mixing tank, namely the concentration of dye in the liquid stream leaving the bobbins (see Figure 1).

The solution of Eq. 7 provides the time dependence of C_M , which is required for the boundary condition of Eq. 4. The concentration in Eq. 7 is evaluated at the exit of the bobbins. The system of equations 1-7 describes the unforced bobbin thread dyeing process and the parameter values and the initial conditions used in this chapter are reported in Table 1.

Table 1 Parameter values and initial conditions [45, 46]

R_e	0.0975 m	R_i	0.0385 m
H	0.1475 m	V	15 l
D_a	$10^{-5} \text{ m}^2 \text{ min}^{-1}$	k_t	$2.9 \cdot 10^{-2} \text{ min}^{-1}$
ε	0.57	ρ	1170 kg m^{-3}
α	562.32	$C_M(0)$	0.15 g/l
$C(r,0)$	0.15 g/l	$C_T(r,0)$	0

2.2. Periodically-Forced Dyeing Process

The periodic inversion of the flow direction inside the bobbins is allowed by a system of coupled valves that are opened and/or closed pairwise at regular time intervals (Figure 2). We refer, from now on, to the switch time τ as the time after which the flow direction is reversed. In particular, during the interval $[k\tau, (k+1)\tau]$ the valves (B) are open while the other pair (A) are closed and the liquid flows from the east surface to the west surface. In the time interval $[(k+1)\tau, (k+2)\tau]$ the valves (B) are closed while the other pair (A) are open and the liquid flows from the west surface to the east surface.

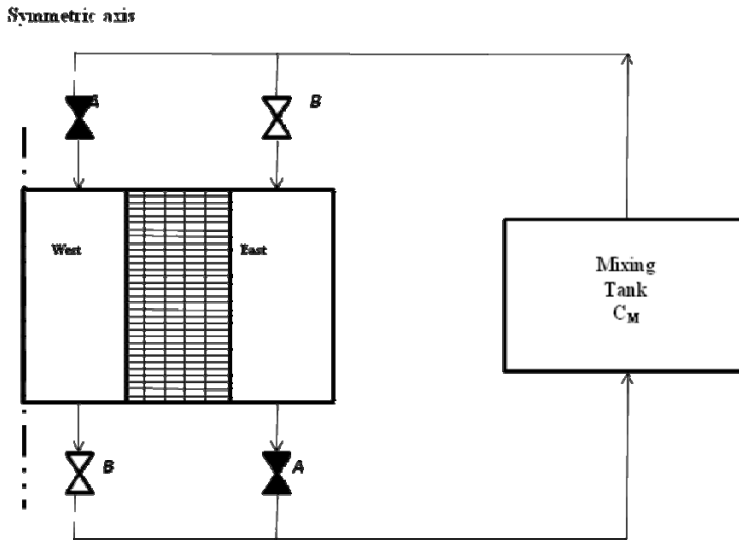


Figure 2. A simplified scheme of the equipment used for the periodically-forced dyeing process.

From a mathematical point of view, the reverse operation means that, according to the flow direction, the inlet concentration to the mixing tank is $C|_{R_i}$ when the liquid flows from west to east and is $C|_{R_E}$ when the flow direction is reversed (see Figure 2). In order to take into account the periodic reversal of the flow direction we here consider a discontinuous periodic function $g(t)$ [40]:

$$g(t) = \text{int}\left(\frac{t}{\tau}\right) - 2\text{int}\left(\frac{t}{2\tau}\right) \quad (8)$$

where $\text{int}(x)$ denotes the integer part of the variable x , $g(t)$ is a discontinuous rectangular wave-type function of unit amplitude and is periodic with a minimum period $T=2\tau$. A schematic representation of $g(t)$ is reported in Figure 3.

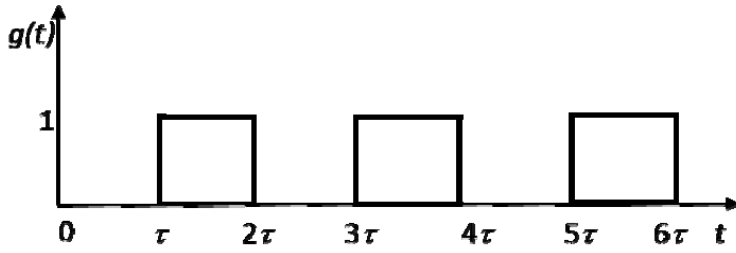


Figure 3. The forcing function $g(t)$.

According to the introduction of the periodic function $g(t)$ we can reformulate the mathematical model in order to take into account the cyclic reversal of the flow direction. A change in the flow direction inside the bobbins implies the reversal of the velocity direction and the mirror change of the boundary conditions at each switch time τ .

$$\frac{\partial C}{\partial t} = \frac{D_a}{r} \frac{\partial}{\partial r} \left(r \frac{\partial C}{\partial r} \right) + (1 - 2g(t))v_r \frac{\partial C}{\partial r} - \frac{(1 - \varepsilon)}{\varepsilon} \frac{\partial C_T}{\partial t}. \quad (9)$$

According to $g(t)$, the boundary conditions and the mass balance in the mixing tank can be recast as follows:

$$r = R_I \Rightarrow \frac{\partial C}{\partial r} (1 - g(t)) + (C|_{R_I} - C_M) g(t) = 0 \quad (10)$$

$$r = R_E \Rightarrow \frac{\partial C}{\partial r} g(t) + (C|_{R_E} - C_M) (1 - g(t)) = 0. \quad (11)$$

$$\frac{dC_M}{dt} = \frac{Q}{V} (C|_{R_E} g(t) + C|_{R_I} (1 - g(t)) - C_M) \quad (12)$$

Therefore, the liquid and solid mass balances (Eqs. 9 and 5), the boundary conditions (Eqs. 10-11) and the balance in the mixing tank (Eq. 12) describe the periodically-forced dyeing process under study herein.

2.3. Numerical Approach

Numerical simulations are used to elucidate transient behavior of the model for the dyeing process described in the previous section. The development and application of efficient numerical methods for numerical simulation of the periodic processes is not a simple task [24, 47, 48]). Even simple models will involve diffusion/convective equations which mathematically are represented by a large set of partial differential equations (PDEs). Moreover, since the process is periodic the concentration profiles will be characterized by sharp moving fronts inside the bobbins. In order to perform numerical time integration of the system described in the previous section, the first step is to discretize the space domain and

transform the set of PDEs into a set of ordinary differential equations (ODEs) in the time domain. Among the classical numerical approaches, finite difference methods are simple but require a relatively large number of ODEs to obtain an accurate approximation of the original PDE problem. Projection methods provide an interesting framework in that, through proper choice of the functional basis, one can reduce the number of ODEs necessary to accurately describe the dynamics of the original PDE model (see Canuto *et al.* [49] and references therein). The standard projection methods (Galerkin methods), based on generalized Fourier expansion constitute a particularly convenient way to handle polynomial nonlinearities either in the concentration field or in its gradient. An example of an alternative to the Galerkin methods is the application of a collocation method. In their standard formulation, however, such methods may not be accurate for the case of sharp moving fronts. To overcome this difficulty we developed a software simulator testing finite-element collocation method, where the space domain will be divided into subdomains in which standard collocation methods can be applied. This choice is also motivated by the need to overcome the intrinsic problems of classical polynomial collocation algorithms in order to handle a number of collocation points larger than 20 [50].

Further details on the collocation method are reported below (also see Villadsen and Michelsen [50]). The method of orthogonal collocation is a variation of the method of weighted residuals (MWR). In this method, the model is approximated by coupled, ordinary differential equations (ODEs) for the values of the dependent variable at the collocation points. The method is easy to apply and program for this problem and the solution at any point can be obtained from the values of the dependent variables at the collocation points. The method of orthogonal collocation is also superior to finite differences in terms of stability because it uses the information from all collocation points, instead of just neighboring points, to estimate the derivatives at each point. In this chapter, the method of orthogonal collocation on finite elements was employed to obtain the desired numerical solution. In orthogonal collocation on finite elements, the domain of the problem is divided into subdomains (called elements) and the method of orthogonal collocation is applied on each subdomain. This variation is particularly useful for problems with sharp variations in the distribution of states, as in our problem.

Suppose we have a linear differential operator L in the space derivative acting on a function $u(x)$:

$$\frac{du}{dt} + L(u) + p(x, t) = 0 \quad (13)$$

In the case under examination in this chapter the differential operator L is:

$$L \rightarrow \frac{1}{r} \frac{\partial}{\partial r} \left(r \frac{\partial}{\partial r} \right) + \frac{\partial}{\partial r} \quad (14)$$

The basic idea of MWR is to approximate u using a function \tilde{u} , which is a linear combination of basis functions chosen from a linearly independent set. That is:

$$u \cong \tilde{u} = \sum_{i=1}^N a_i(t) \varphi_i(x) \quad (15)$$

where $\varphi_i(x)$ are the known basis functions (e.g. trigonometric, Legendre, etc.), selected from a set of complete (perhaps orthonormal) basis functions, which satisfy the boundary conditions. Substituting the function \tilde{u} in the original equation (13) the result is not zero but is an error or *residual*:

$$E(x) = R(x) = \frac{d\tilde{u}}{dt} + L(\tilde{u}(x)) + p(x) \neq 0 \quad (16)$$

The notion in the MWR is to force the residual to zero in some average sense over the domain. To develop this idea we select N weighting functions $w_i(x)$, $i = 1, 2, \dots, N$, where the number of weighting functions is exactly equal to the number of unknown functions $a_i(t)$ in \tilde{u} . Introducing the spatial average (inner product or weighted integral):

$$(w, v) = \int_V w v dV \quad (17)$$

and setting the N weighted integrals of the equation residual $R(x)$ equal to zero:

$$(w_i(x), R(x)) = 0, \quad i = 1, 2, \dots, N \quad (18)$$

We obtain a set of N differential equations in the unknown function $a_i(t)$. It is worth noting that Eq. 18 implies that the residual error is required to be orthogonal to each of the weighting functions. There are (at least) five MWR sub-methods, according to the choices for the $w_i(x)$ and the basis function $\varphi_i(x)$. In the collocation method, the weighting functions are taken from the family of Dirac δ functions in the domain. That is, $w_i(x) = \delta(x - x_i)$ where:

$$\delta(x - x_i) = \begin{cases} 1 & x = x_i \\ 0 & \text{otherwise} \end{cases} \quad (19)$$

Hence the integration of the weighted residual statement results in the forcing of the residual to zero at specific points in the domain. That is, integration of Eq. 18 with $w_i(x) = \delta(x - x_i)$ results in:

$$R(x_i) = 0 \quad (20)$$

The x_i are chosen to be the zero of the Jacobi polynomials $P_n^{(\alpha,\beta)}$. Such polynomials are also selected as basis functions. The Jacobi polynomials $P_n^{(\alpha,\beta)}$, also known as hypergeometric polynomials, are the eigenfunctions of the singular Sturm–Liouville problem:

$$-\frac{d}{d\xi} \left((1-\xi^2) \omega^{\alpha,\beta} - \frac{dP(\xi)^{\alpha,\beta}}{d\xi} \right) = \lambda^{\alpha,\beta} \omega^{\alpha,\beta} P(\xi)^{\alpha,\beta} \quad (21)$$

$$\xi \in [-1, 1]$$

under suitable boundary conditions. The weighting function $\omega^{\alpha,\beta}$ and eigenvalues $\lambda^{\alpha,\beta}$ are given as:

$$\lambda^{\alpha,\beta} = n(n+1+\alpha+\beta) \quad (22)$$

$$\omega^{\alpha,\beta} = (1-\xi)^\alpha (1+\xi)^\beta$$

The Jacobi polynomial $P_n^{(\alpha,\beta)}$ of degree n is dependent on two parameters α, β ($\alpha, \beta > -1$). Moreover, the Jacobi polynomials satisfy the orthogonality property:

$$\int_{-1}^1 P_n^{(\alpha,\beta)}(x) P_m^{(\alpha,\beta)}(x) \omega^{\alpha,\beta}(x) dx = 0 \quad n \neq m \quad (23)$$

In this chapter, the space domain is divided into 6 subdomains and for each we have found that 5 collocation points are sufficient to capture efficiently the shape of the concentration profiles for the two phases. The PDE model (Eqs. 6, 8-10) reduced to a finite set of ordinary differential equation can then be written in abstract form as the following dynamical system:

$$\begin{cases} \dot{\mathbf{u}} = \mathbf{F}(\mathbf{u}, \boldsymbol{\lambda}, t) & \mathbf{F}(\mathbf{u}, \boldsymbol{\lambda}, t) = \mathbf{F}(\mathbf{u}, \boldsymbol{\lambda}, t + T) \\ \mathbf{u}(t_0) = \mathbf{u}_0 \end{cases} \quad (24)$$

where \mathbf{u} is the state vector of the system and $\boldsymbol{\lambda}$ is the parameter vector. This type of system lies within a particular class of non-autonomous dynamical systems. An n -order dynamical system (i.e. a system of n first-order ODEs) is non-autonomous if the vector field is explicitly dependent on time.

3. RESULTS

The unforced dyeing of bobbin threads is a process characterized by three different time scales. Namely, the time scales of the dispersion $t_D = (R_E - R_I)^2 / D_a$, of the convection $t_c = (R_E - R_I) / v_r$ and finally of the adsorption process described by $t_A = 1/k_t$. The adsorption time can be considered as a reaction time. In fact, the dyeing process is similar to many operations in chemical engineering and in this sense can be considered as the transformation of reactants into products. When a transformation includes both physical as well as chemical changes, the term 'reactants' is employed to describe the state of the materials of interest at the start of the process, while the terms 'products' describes their state after completion of the process [16]. The analysis of the time scales phenomenon can lead to a more in-depth understanding of the dyeing process.

The forced process of reverse flow operation is characterized by another time scale: the switch time τ , which can be considered as an operative parameter of the forced system. We will address the effect of the switch time variation on the performance of bobbin thread dyeing process.

In order to understand the effect of each phenomenon on the dye adsorption process we will firstly study an unforced problem characterized only by dispersion and adsorption, neglecting the convection effect. We will then neglect the dispersion phenomenon studying a simplified unforced convection-adsorption process. Finally, the full mathematical model describing the process of the forced dyeing of bobbin threads will be studied.

The effect of the cyclic reversal operation on the dyeing process performance was studied by comparing the dye distribution factor (DDF) throughout the volume, the total amount of adsorbed dye, and the rate of dye uptake. The dimensionless DDF is the ratio between the highest and the lowest thread concentration and it provides a measure of the level of dyeing of the threads. For the unforced dyeing process it is reasonable to assume that the DDF represents the ratio between the thread concentration values observed at the bobbin inlet and outlet flow points. In contrast, for the reverse flow operation the DDF is here evaluated as the ratio between the maximum and minimum thread concentrations. Due to the batch nature of dyeing process, the total amount of adsorbed dye can be approximated from data on the dye concentration at different times in the mixing tank. Finally, the rate of dye uptake can be estimated from the thread concentration vs. time profile, more precisely, the angle between the tangent line of the thread concentration vs. time curve and the time line coordinate represents the rate of dye uptake [51]. In the unforced process, the thread concentration is measured at the point where the flow leaves the bobbins [18]. Since for the forced process the feed and exit positions are periodically inverted, the rate of dye uptake is estimated from the time history of the thread concentration in the middle of the bobbins.

The spatial profiles and time series data are presented to elucidate the effect of different parameters on the dyeing process performance. In particular, different values were considered for the switch time (τ) and recirculation flow rate (Q). These two operating parameters are very important key parameters. Indeed, the switch time is an intrinsic parameter of the periodic forcing and it directly affects the efficiency of the periodic action, whereas the recirculation flow rate strongly affects the time required for the liquid to cross the bobbins.

Finally, it is important to stress, that all the results reported herein were obtained using the same uniform initial conditions. In particular, the initial dye concentration in the liquid phase was fixed at the same value as that for the external bath, while zero initial concentration was assumed for the solid phase (see Table 1).

In Figure 4 the time series data for the dye bath concentration is reported for the unforced system. The dye concentration in the bath quickly decreased and after approximately 30 min all the dye had been adsorbed by the threads.

Nevertheless, the dye distribution in the threads was still not uniform after 30 min. This can be observed in Figure 5 where the spatial evolution over time of the dye concentration in the liquid phase (a) and in the threads (b) is represented. For the chosen initial conditions, the driven force between the two phases is maximum at time zero and then quickly reduces as the dye is adsorbed by the threads. As a consequence of a greater driving force the dye concentration in the liquid rapidly reduces while the dye concentration in solid phase quickly increases. After the initial dye load present at time zero in liquid phase has been consumed, the bobbins are fed only by the recirculated dye and the liquid dye concentration reduces more slowly. Moreover, in Figure 5(b) it is possible to see that the spatial profile of the liquid concentration after a time of approximately 30 min exhibits a maximum traveling across the bobbin domain. This maximum can be explained considering that after a time of approximately 30 min the liquid phase does not receive “fresh dye” from the bath (see Figure 4).

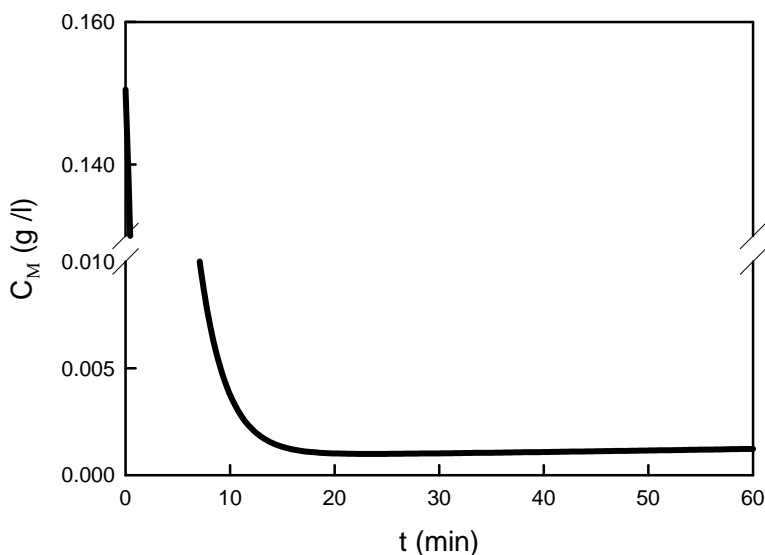


Figure 4. Dye bath concentration vs. time.

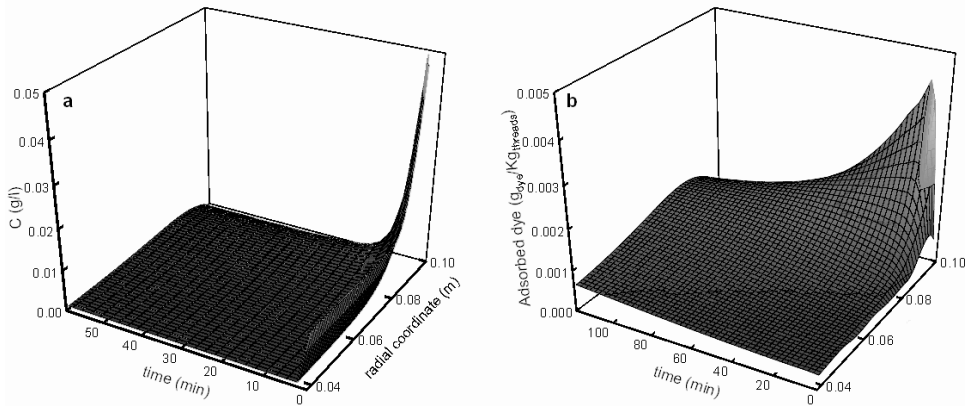


Figure 5. Spatial profiles of liquid (a) and thread (b) concentrations for recirculation flux $Q=1 \text{ l s}^{-1}$ while the other parameters are fixed at the values reported in Table 1.

Therefore, the concentration close to the external east surface (see Figure 1) is very low whereas on the other side the threads are enriched in dye and this produces mass transfer from the solid to liquid phase. In other words the external thread volume functions as the lungs of the dye. In the initial time interval this volume captures the dye initially present in the bath and subsequently, as with lungs, this volume releases the dye which is transferred to the more internal threads.

We note here (see Figure 5) that during the transient the bobbin volume can be divide into two parts: The first lies close to external bobbin surface and is where all the quantitative and qualitative changes in the concentrations of the two phases occur; the other part of the bobbin volume, the inner part, does not show a significant change in dye concentration. This observation indicates non efficient dye dispersion during the transient. This is supported by the results reported in Figure 6 where the dye distribution factor (DDF) for different values of dispersion coefficient (Figure 6(a)) and recirculation flux (Figure 6(b)) are represented.

The DDF reported in Figure 6 quickly increases at the beginning due to the high driving force between the two phases. Thus, the dye dispersion during the transient is not efficient, in fact the DDF value is considerably higher than 1. After reaching the maximum value the DDF start to decrease. While different dispersion coefficient values do not affect the maximum DDF, increasing the recirculation flux leads to a lower maximum DDF value. Moreover, in the latter case, this maximum is reached within a shorter time, as can be seen in Figure 6(b). This phenomenon can be easily explained by considering that the governing mass transport effect is convection rather than dispersion. Therefore, an increase in the recirculation flux clearly increases the convective velocity.

It is worth noting that in all cases reported in Figure 6, with the exception of the less realistic recirculation flux $Q = 10 \text{ l s}^{-1}$, the dye distribution factor is considerably lower than the ideal value of one and the uniform dyeing of the threads is only reached for a dyeing period of greater than 2 h.

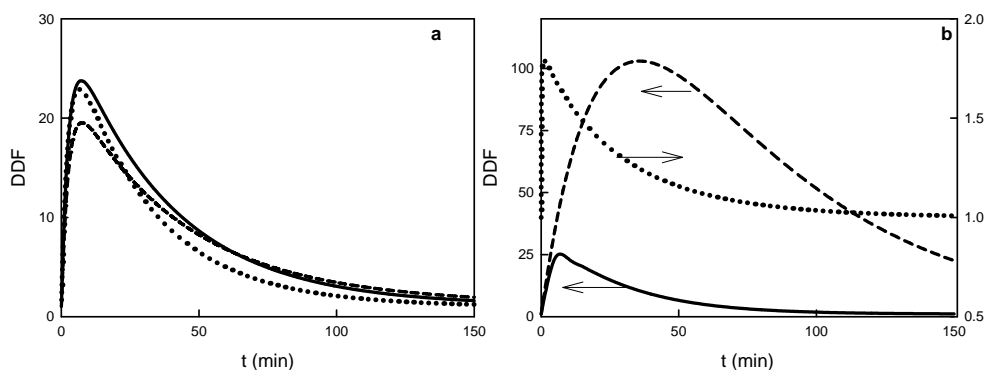


Figure 6. (a) Dye distribution factor (DDF) vs. time, when different dispersion coefficients are used. Solid line $D_a = 10^{-3} \text{ m}^2 \text{ min}^{-1}$, dashed line $D_a = 10^{-4} \text{ m}^2 \text{ min}^{-1}$ and dotted line $D_a = 10^{-5} \text{ m}^2 \text{ min}^{-1}$ for $Q = 1 \text{ l s}^{-1}$. (b) DDF vs. time, when different recirculation fluxes are used. Solid line $Q = 1 \text{ l s}^{-1}$, dashed line $Q = 0.1 \text{ l s}^{-1}$ and dotted line $Q = 10 \text{ l s}^{-1}$ for $D_a = 10^{-5} \text{ m}^2 \text{ min}^{-1}$. The right scale refers to the case of $Q = 10 \text{ l s}^{-1}$.

3.1. The Thermodynamic Equilibrium between the Phases: Regime Profiles

Before analyzing the differences between the forced and unforced process, it should once again be emphasized that for both processes the system is intrinsically batch. Therefore, we can observe a transient behavior until the two phases exchange dye. Then, when the equilibrium between the two phases is reached, flat concentration profiles are observed and no further change occurs. This regime is dependent only on the physics of the problem and the way the process is forced does not change the concentration profile reached after a prolonged period (regime). Therefore, the regime of the periodically-forced dyeing process will be the same as that of the unforced process. On the other hand, we show in this section that the reverse operation enables a more uniform dye distribution to be rapidly achieved. This is of great practical relevance, since the process is stopped before reaching thermodynamic equilibrium conditions.

Figure 7 shows the mixing tank concentration (C_M) history for different switch times. The dye concentration C_M decreases showing damped oscillations during the transient period and asymptotically tends toward the unforced behavior represented with a dotted line in Figure 7. The oscillating transient behavior is due to the reversal of the flow direction inside the bobbins and the period of damped oscillations is equal to the switch time τ . Independently of the switch time values, in Figure 3, in the first time interval ($\tau \sim [0.15 \text{ min}]$), the rapid decrease due to the adsorption of dye by the thread can be observed. After three hours (approximately) no further change in the mixing tank can be detected ($C_M \approx 10^{-3} \text{ g l}^{-1}$).

From the results reported in Figure 7 it is possible to argue that the total amount of dye adsorbed by the threads is invariably the same for the forced and unforced process. Therefore, the reverse operation does not affect the total amount of dye adsorbed by the threads with respect to the classical operation process.

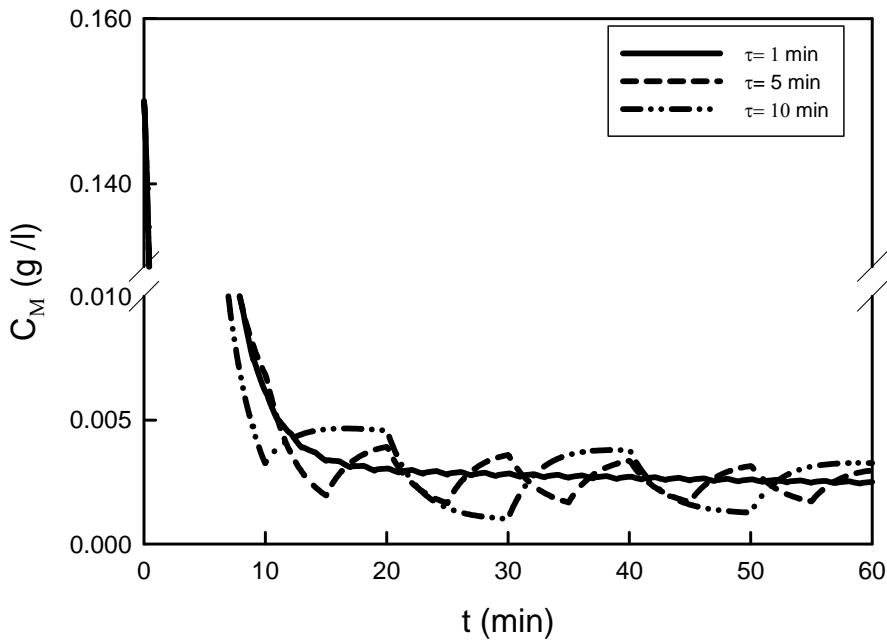


Figure 7. Time series of mixing tank concentration for different switch times. The recirculation flow rate used is $Q = 1 \text{ l s}^{-1}$ while the other parameters are fixed at the values reported in Table 1.

In all the case here discussed most of the dye was adsorbed in the first 15 min, however, there is no information on the dye distribution. This information is reported in Figure 8 where the DDF history for three different switch times for the unforced process is represented. During the first time interval, independently by the adopted switch time τ , the DDF quickly increases. In fact, at the beginning, the thread concentration close to the inlet flow surface increases rapidly due to the fact that this volume of thread receives dye directly from the mixing tank while the innermost threads receive dye transferred by convection/dispersion mass transport. The great discrepancies between the dye concentration close to the inlet flow and those close to the outlet give rise to a rapidly increasing DDF. As the process runs the adsorbed dye is dispersed along the entire bobbin thread and then the DDF decreases reaching asymptotically the unit value that corresponds to a perfect dye distribution. As is apparent in Figure 7, in the forced process, after the first switch the DDF starts to decrease and approaches the asymptotic value for a perfect distribution faster than in the unforced process. In fact, after each switch the bobbin surface that is fed by “fresh” dye changes. In other words, the internal thread receives liquid rich in dye prior to the onset of convective and dispersive mass transport. Therefore, the reverse flow operation allows a better distribution of the driving force between the two phases and a better thread concentration distribution is obtained. After 30 minutes the percent difference between the DDF for the unforced and forced processes is 52% for $\tau = 1 \text{ min}$, 34% for $\tau = 5 \text{ min}$, and 25% for $\tau = 10 \text{ min}$. After 1 hr, the percent difference becomes 35% for $\tau = 1 \text{ min}$, 23% for $\tau = 5 \text{ min}$, and 13% for $\tau = 10 \text{ min}$. The percent difference between the forced and unforced processes reaches less than 5% only after 90 min.

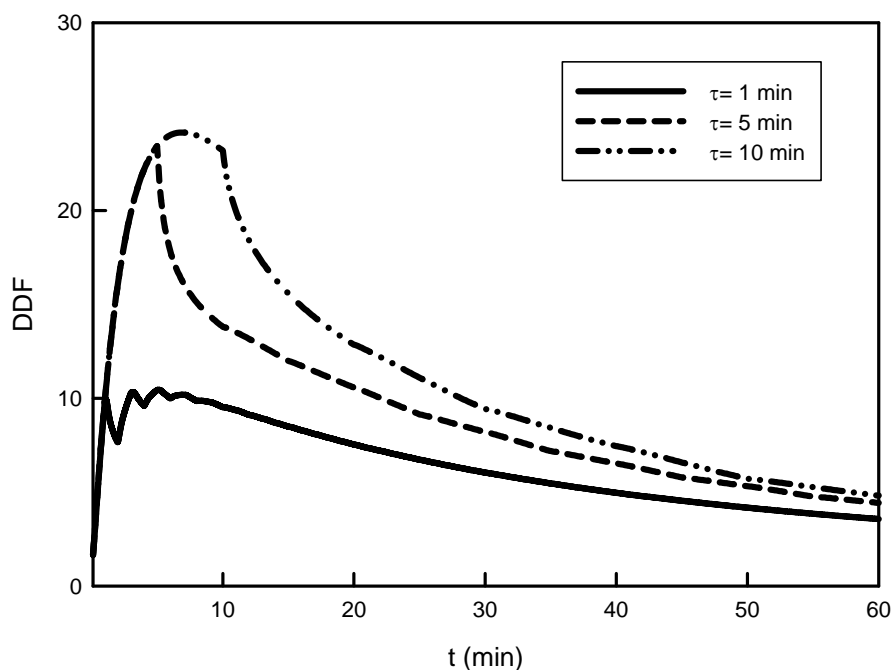


Figure 8. DDF vs. time for different switch times. The recirculation flow rate used is $Q = 1 \text{ l s}^{-1}$ while the other parameters are fixed at the values reported in Table 1.

The effect of the reverse flow operation is enhanced as the switch time approaches the characteristic recirculation time (approximately 1 min for the recirculation flux chosen). For large switch time values, the benefits of the cyclic reversal of the flow direction are lost in spite of the natural recirculation imposed by the process.

A better insight into the dye distribution can be obtained by analyzing the spatial profiles for the liquid and thread concentrations represented in Figure 9. In the case of the unforced process the liquid concentration rapidly decreases (see Figure 5(a)) and the cyclic reversal of the feed position means that both the internal and external surfaces receive periodically high dye concentrations. Thus, the reversal of the flow direction leads to a higher liquid concentration close to the internal surface of the bobbins. As a result the unadsorbed dye is globally better distributed across the bobbins as shown by the wavy shape of the spatial profile reported in Figure 9(b).

The thread concentration for the unforced process exhibits a maximum during the first time instants close to the feed surface of the bobbin (see Figure 5(a)). As the process runs this maximum decreases and moves toward the inner part of the bobbin. The dye is transferred to the internal threads only by convection/dispersion mass transport. Therefore, the thread concentration in the innermost threads slowly increases, as shown in Figure 9(a). In terms of the dye, the external thread volume functions analogously to lungs. In the first time interval this volume captures the dye initially present in the liquid, then, similarly to lungs, this volume releases the dye which is transferred by convection and dispersion to the innermost

threads. When the process is forced the internal threads periodically receive fresh dye and the thread concentration “symmetrically” increases, as represented in Figure 9(b).

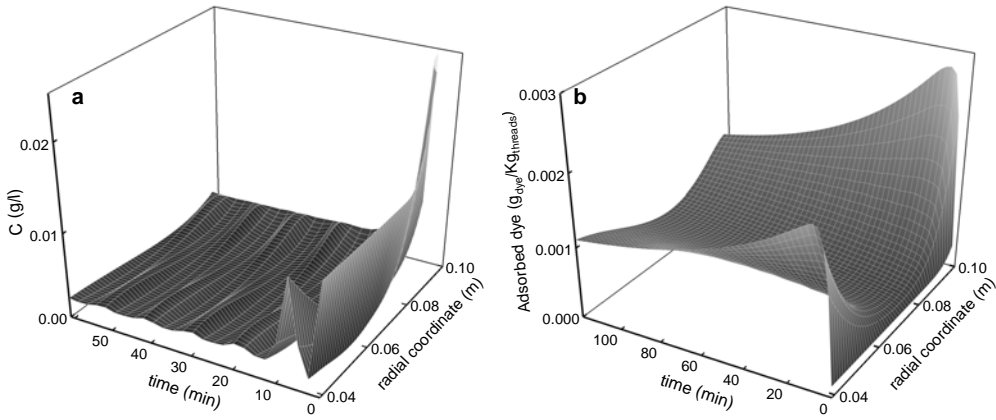


Figure 9. Spatial profiles for liquid (a) and thread (b) concentrations in the forced dyeing process for $\tau = 1 \text{ min}$ and $Q = 1 \text{ l s}^{-1}$ while the other parameters are fixed at the values reported in Table 1.

Finally, we report the spatial profiles for the mass flux between the two phases, which is proportional to the driving force of the global dyeing process. It is apparent from analysis of the results reported in Figure 10 that the reverse flow operation allows a greater mass flux between the liquid and solid phases. For the unforced process (Figure 10(a)) the mass flux rapidly decreases reaching an almost flat profile while the wavy shape (Figure 10(b)) for the forced process indicates a mass flux well distributed over the entire volume of the threads.

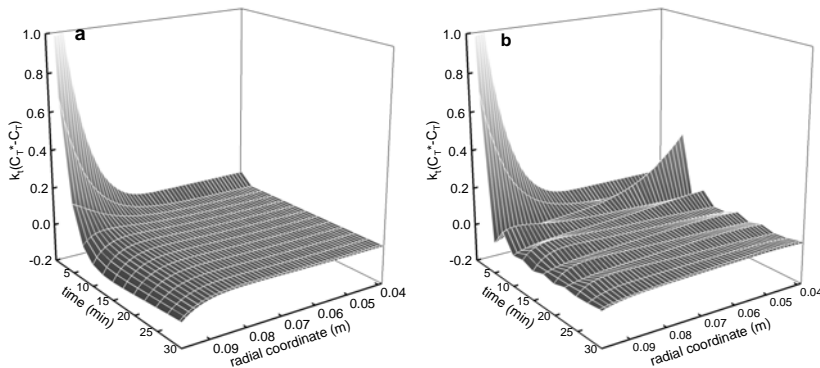


Figure 10. Spatial profiles for the driving force between the two phases, (a) unforced, (b) forced dyeing process for $\tau = 1 \text{ min}$ and $Q = 1 \text{ l s}^{-1}$ while the other parameters are fixed at the values reported in Table 1.

We observe that for the unforced process a parameter which can be used to evaluate the dyeing efficiency is the rate of dye uptake, which can be estimated from the thread concentration where the flow exits the bobbins over time (g dye/kg threads,). More precisely, the angle between the tangent line of the thread concentration vs. time curve and the time line

coordinate represents the rate of dye uptake [18, 51]. In the unforced process, the thread concentration is measured at the point where the flow exits from the bobbins because this is the last point reached by dye. For the unforced process the internal threads are reached by the dye only via convection/dispersion mass transport. This is not the case for the process with periodic reversal. In fact, periodic reversal of the flow direction dictates that the feed and exit position are periodically inverted. Therefore, after the first switch, the internal threads are immediately reached by fresh dye. For the periodically-forced operation the dye uptake rate can be estimated from the thread concentration in the center of the bobbin. In Fig. 11 the dye uptake is reported. A comparison between the forced and unforced processes is not possible in this case. However, it is important to stress that the dye uptake is not affected by the switch time.

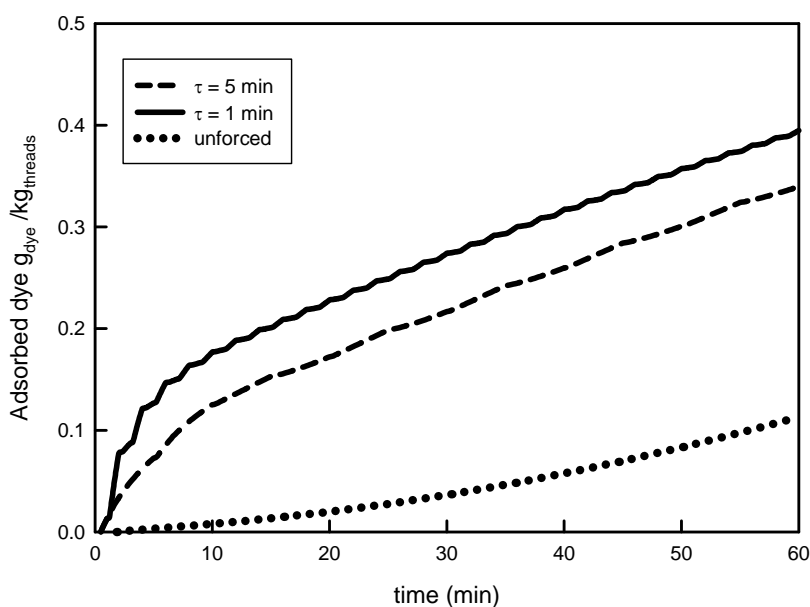


Figure 11. Dye uptake vs. time for different switch times and for $Q = 1 \text{ l s}^{-1}$ while the other parameters are fixed at the values reported in Table 1 [52].

In Figure 12 the dye distribution factor for a greater recirculation flux value is reported. On increasing the recirculation flux value the recirculation time decreases. Thus, the forced process has to be forced with a higher frequency in order to allow effective forcing. The DDF for a process forced with a switch time of 5 min or greater is very similar to that of an unforced process. On the other hand, with a reasonable switch time of 1 min the favorable effects of the cyclic reverse of the flow direction were still apparent (Figure 12). After 30 minutes the percent differences between the unforced and forced process were 30% for $\tau=30 \text{ s}$ and 10% and $\tau=1 \text{ min}$, and after 1 hr they were 10% for $\tau=30 \text{ s}$ and 7% and $\tau=1 \text{ min}$. The percent difference between the forced and unforced processes was less than 5% only after more than 1 hr.

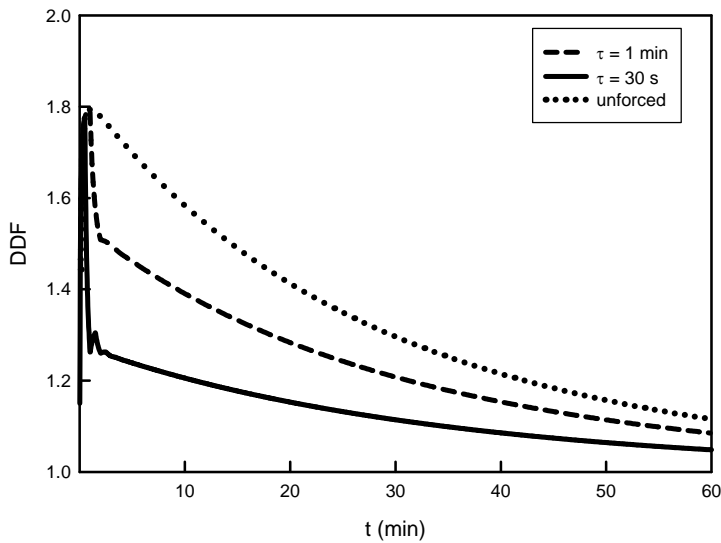


Figure 12. DDF vs. time for different switch times and for $Q = 10 \text{ l s}^{-1}$ while the other parameters are fixed to the values reported in Table 1 [30].

CONCLUSION

The numerical analysis technique provides a powerful tool to investigate the bobbin thread dyeing process. In this chapter, the transfer of dye through the bobbin was described by a set of time-dependent partial differential equations, which govern the convection, dispersion and adsorption of dyes in the dye bath and across the bobbin threads. A classical dyeing process was studied and improved by applying periodic forcing by periodically reversing the flow direction inside the bobbins.

The spatial concentration profiles for the periodically-forced dyeing process are characterized by sharp moving fronts. An accurate simulation of the periodically-forced system with a classical finite difference scheme requires a large number of internal nodes (and thus a large number of ODEs). In order to reduce the computational effort an *ad hoc* computer program based on an orthogonal collocation method on finite elements was developed to obtain an accurate approximation of the original PDE problem.

The regime profiles were not affected by the periodic change in the flow direction, however, the reverse operation plays an important role in the dye distribution during the transient behavior, allowing a better dye distribution. In the classical dyeing process dye has to be transported by convection and diffusion to the internal core of the threads, however, with the periodical reversal of the flow direction this problem was avoided. In order to gain the beneficial effects of reversing the flow the switch time needs to be comparable with the characteristic mass transfer time. This was investigated considering different recirculation fluxes. For a high recirculation flux value no difference between the forced and unforced processes was observed. On decreasing the recirculation flux the reverse of the flow allowed a better distribution of the dye at least in the initial moments.

On varying the dispersion coefficient within a physical range no difference in the reverse flow operation was apparent. This can be easily explained considering that for the parameter values used in this chapter the dispersion time is longer than the convection time and the dye inside the liquid is essentially transferred by convection.

REFERENCES

- [1] Guelli U. Souza, S.M.A., de Souza, D.P.; da Silva, A.A.B., and Ulson de Souza, A.A. (2007a). Modeling of the Dyeing Process of Packed Cotton Threads Using Reactive Dyes. *Transport in Porous Media*, 68: 341-363.
- [2] Broadbent, A.D., Mir, Y., Lhachimi, A., Billong, J.B., and Capistran, S. (2007). Continuous Dyeing of Cotton/Polyester and Polyester Fabrics with Reactive and Disperse Dyes Using Infrared Heat. *Industrial Engineering and Chemistry Research*, 46: 2710-2714.
- [3] Hauser, P.J., and Tabba, A.H. (2001). Improving the Environmental and Economic Aspects of Cotton Dyeing Using a Cationised Cotton. *Coloration Technology*, 5: 282-288.
- [4] Szpyrkowicz, L., Juzzolino, C., Kaul, S.N., Daniele, S., and De Faveri, M.D. (2000). Electrochemical Oxidation of Dyeing Baths Bearing Disperse Dyes. *Industrial Engineering and Chemistry Research*, 39: 3241-3248.
- [5] Guelli U. Souza, S.M.A., Santos, K.A., and Ulson de Souza, A.A. (2010). Removal of COD and Colour from Textile Effluents by Combined Ozonation and Biological Treatment. *Journal of Hazardous Materials*, 179: 35-42.
- [6] Furlan, F.R., Silva, L.G.M., Ulson de Souza, A.A., Morgado, A.F., and Guelli U. Souza, S.M.A., (2010). Removal of reactive dyes from aqueous solutions using combined coagulation/flocculation and adsorption on activated carbon. *Resources, Conservation and Recycling*, 54: 283-290.
- [7] Immich, A.P.S., Ulson de Souza, A.A., and Guelli U. Souza, S.M.A. (2009). Adsorption of Remazol Blue RR from textile effluents using *Azadirachta indica* leaf powder as an alternative adsorbent. *Adsorption Science and Technology*, 27: 461-478.
- [8] Guelli U. Souza, S.M.A., Forgiarini, E., and Ulson de Souza, A.A. (2007b). Toxicity of textile dyes and their degradation by the enzyme horseradish peroxidase (HRP). *Journal of Hazardous Materials*, 147: 1073-1078.
- [9] Stern, S.R., Szpyrkowicz, L., and Rodighiero, I. (2003). Anaerobic Treatment of Textile Dyeing Wastewater. *Water Science and Technology*, 47: 55-59.
- [10] Ulson de Souza, A.A., Melo, A.R., Pessoa, L.F.P., and Guelli U. Souza, S.M.A. (2010). The Modified Water Source Diagram Method applied to Reuse of Textile Industry Continuous Washing Water. *Resources, Conservation and Recycling*, 54: 1405-1411.
- [11] Vasques, A.R., Guelli U. Souza, S.M.A., Valle, J.A.B., and Ulson de Souza, A.A. (2009). Application of Ecological Adsorbent in the Removal of Reactive Dyes from Textile Effluents. *Journal of Chemical Technology and Biotechnology*, 84: 1146-1155.
- [12] Pearce, C.I., Lloyd, J.R., and Guthrie, J.T. (2003). The Removal of Colour from Textile Wastewater Using Whole Bacterial Cells: a Review. *Dyes and Pigments*, 58: 179-196.

-
- [13] Guelli U. Souza, S.M.A., Peruzzo, L.C., and Ulson de Souza, A.A. (2008). Numerical Study of the Adsorption of Dyes from Textile Effluents. *Applied Mathematical Modelling*, 32: 1711-1718.
- [14] Koksall, G., Smith, W.A., Fathi, Y., Lu, J.C.Y., and McGregor, R. (1998). A Case Study in Off-Line Quality Control: Characterization and Optimization of Batch Dyeing Process Design. *International Journal of Technology Management*, 16: 358-382.
- [15] Gilchrist, A., and Nobbs, J.H. (2000). Dyeing Machine Control Using In-Line Color Measurement. Part 3: Online Dyeing Quality Control. *Coloration Technology*, 116: 154-158.
- [16] Shamey, M.R., and Nobbs, J.H. (2000). The Application of Feed Forward Profiles in the Control of Dyeing Machinery. *Textile Chemist and Colorist and American Dyestuff Reporter*, 32: 47-52.
- [17] Smith, B. (2007). Dyebath Monitoring and Control: Past, Present, and Future. *AATCC Review*, 7: 36-41.
- [18] Zhao, X., Wardman, R.H., and Shamey, R. (2006). Theoretical Study of the Influence of Dispersion Factor on Dye Transport during the Dyeing Process. *Coloration Technology*, 122: 110-114.
- [19] Karst, D., Rapp, and W.A., Yang, Y. (2003). Theoretical Study on the Use of Collars and Outer Wrapping to Improve Liquor Flow in Fabric Beam Dyeing. *Coloration Technology*, 119: 354-358.
- [20] Reddy, M., Lee, G., Mc Gregor, R., and Jasper, W. (1995). Modeling of the Batch Dyeing Process. In *American Control Conference*. Seattle, WA, 3: 2180-2184.
- [21] Reddy, M., Jasper, W.J., Mc Gregor, R., and Lee, G. (1997). Effects of Temperature and Salt on Dye Mixtures in the Batch Dyeing Process. *Textile Research Journal*, 67: 109-117.
- [22] Burely, R., Wai, P., and Mc Guire, G.R. (1987). Process Engineering Approach to Dyeing Machinery - a Study of Package Dyeing Machine Dynamics. *Chemical Engineering Research and Design*, 65: 505-513.
- [23] Burely, R., and Flower, J.R. (1991). Dynamic Behavior of Dyeing Machinery and Computer Simulation: some Examples. *Journal of Society of Dyers Colourists*, 107: 434-441.
- [24] Mancusi, E., Russo, L., Brasiello, A., Crescitelli, S., and di Bernardo, M. (2007a). Hybrid modeling and dynamics of a controlled reverse flow reactor. *AIChE Journal*, 53: 2084-2096.
- [25] Burely, R., Wai, P., and McGuire, G.R. (1985). Numerical Simulation of an Axial Flow Package Dyeing Machine. *Applied Mathematical Modelling*, 9: 33-39.
- [26] Bailey, J.E. (1993). Periodic Operation of Chemical Reactors: a Review. *Chemical Engineering Communication*, 1: 111-124.
- [27] Eigenberger, G., and Nieken, U. (1998). Catalytic Combustion with Periodical Flow Reversal. *Chemical Engineering Science*, 43: 2109-2115.
- [28] Matros, Y. S. (1989). Catalytic process under unsteady state conditions, Elsevier: Amsterdam.
- [29] Matros, Y.S., and Bunimovich, G.A. (1996). Reverse Flow Operation in Fixed Bed Catalytic Reactors. *Catalysis Reviews, Science and Engineering*, 38: 1236-1252.

-
- [30] Mancusi, E., Guelli U. Souza, S.M.A., and Ulson de Souza, A.A. (2010b). Numerical analysis of a periodically forced dyeing process. *Industrial Engineering and Chemistry Research*, 49: 8568-8574.
- [31] Neophydes, S.G., and Froment, G.G. (1992). A Bench Scale Study of Reversed Flow Methanol Synthesis. *Industrial Engineering and Chemistry Research*, 31: 1583-1592.
- [32] Jasra, R.V., Choudary, N.V., and Bhat, S.G.T. (1991). Separation of Gases by Pressure Swing Adsorption. *Separation Science and Technology*, 26: 885-930.
- [33] Ruthven, D.M., Farooq, S., and Knaebel, K.S. (1994). *Pressure Swing Adsorption*, Wiley-VCH Publishers: New York, NY.
- [34] Ruthven, D.M. (2000). Past Progress and Future Challenges in Adsorption Research. *Industrial Engineering and Chemistry Research*, 39: 2127-2131.
- [35] Sircar, S. (2002). Pressure Swing Adsorption. *Industrial Engineering and Chemistry Research*, 41: 1389-1392.
- [36] Ritter, J.A., and Yang, R.T. (1991). Pressure Swing Adsorption: Experimental and Theoretical Study on Air Purification and Vapor Recovery. *Industrial Engineering and Chemistry Research*, 30: 1023-1044.
- [37] Rege, S.U., and Yang, R.T. (2002). Propane/Propylene Separation by Pressure Swing Adsorption: Sorbent Comparison and Multiplicity of Cyclic Steady States. *Chemical Engineering Science*, 57: 1139-1149.
- [38] Sircar, S., and Golden, T.C. (2000). Purification of Hydrogen by Pressure Swing Adsorption. *Separation Science and Technology*, 35: 667-687.
- [39] Żukowski, W., and Berezowski, M. (2000). Generation of Chaotic Oscillations in a System with Flow Reversal. *Chemical Engineering Science*, 55: 339-343.
- [40] Russo, L., Mancusi, E., Maffettone, P.L., and Crescitelli, S. (2002). Symmetry properties and bifurcation analysis of a class of periodically forced reactors. *Chemical Engineering Science*, 57: 5065-5082.
- [41] Guelli U. Souza, S.M.A., and Whitaker, S. (2003). Mass Transfer in Porous Media with Heterogeneous Chemical Reaction. *Brazilian Journal of Chemical Engineering*, 20: 191-199.
- [42] Ulson de Souza, A.A., and Whitaker, S. (2003). The Modelling of a Textile Dyeing Process Utilizing the Method of Volume Averaging. *Brazilian Journal of Chemical Engineering*, 20: 445-453.
- [43] Lu, J., Spiekerman, C., McGregor, R., and Smith, B.A. (1992). Novel Approach to Modeling and Controlling Dyeing Processes. In *AATCC International Dyeing Symposium*, 161-166.
- [44] Revello, J.H.P., Ulson de Souza, A.A., and Ulson de Souza, S.M.G. (2001). Modelagem e Simulação do Processo de Tingimento de Fios em Bobinas (Modeling and Simulation of the Process of Dyeing of Threads in Bobbins). In *22st Iberian Latin-American Congress on Computational Methods in Engineering*, Campinas, SP, Brazil.
- [45] Revello, J. H.P., Guelli U. Souza, S.M.A., Ulson de Souza, A.A. (2008). Modelo Matemático del Proceso de Tintura de Hilos en Bobinas. *Ingeniería Química*, 458: 229-232.
- [46] Revello, J.H.P. (2002). Tingimento de Fios Têxteis em Bobinas: Uma Abordagem Numérica e Experimental (Dyeing of Textile Threads in Bobbins: A Numerical and Experimental Approach). Ph. D. Thesis, Universidade Federal de Santa Catarina, Florianópolis, SC, Brazil.

-
- [47] Altimari, P., Mancusi, E., Russo L., Maffettone, P.L., and Crescitelli, S. (2006). Non-linear Dynamics of a VOC Combustion Loop Reactor. *AIChE Journal*, 52: 2812-2821.
 - [48] Mancusi, E., Russo, L., Altimari, P., Maffettone, P. L., and Crescitelli, S. (2007b). Effect of the switch strategy on the stability of reactor networks. *Industrial Engineering and Chemistry Research*, 46: 6510-6521.
 - [49] Villadsen, J., and Michelsen, M.L. (1978). *Solution of Differential Equation Models by Polynomial Approximation*, Prentice-Hall: Englewood Cliffs, NY.
 - [50] Canuto, C., Hussaini, M.Y., Quarteroni, A., and Zang, T.A. (1988). *Spectral Methods in Fluid Dynamics*; Springer Verlag: Berlin, 1988.
 - [51] Ferus-Comelo, M. (2006). Analysis of the factors influencing dye uptake on jet dyeing equipment. *Coloration Technology*, 122: 289-297.
 - [52] Mancusi, E., Russo, L., Altimari, P., Maffettone, and P.L., Crescitelli, S. (2010a). Temperature and conversion patterns in a network of catalytic reactors for methanol synthesis for different switch strategies. *Chemical Engineering Science*, 65: 4579-4590.

Chapter 4

NANOFIBERS, NANOSCIENCE AND NANOTECHNOLOGY IN TEXTILE AND APPAREL INDUSTRY

Subramaniam Sadhasivam*

Biomaterials Laboratory, Institute of Biomedical Engineering
National Taiwan University, Taipei, Taiwan R.O.C.

ABSTRACT

A textile is a collection of many disciplines that revolve around: the structure, properties and behavior of fibers, how fibers are assembled into fibrous structures and fabrics the making, analysis, sale and end uses of fibers and fabrics. Most textiles are produced by twisting fibers into yarns and then knitting or weaving the yarns into a fabric. Textiles have an assortment of uses, the most common of which are for clothing and the textiles used for industrial purposes are commonly referred to “technical textiles” which found its application in automotive, medical implants, geo textiles etc. Technological advances during the past decade have opened many new doors for the Textile and Apparel industries, especially in the area of rapid prototyping and related activities. Recent developments in the textile industry include designing entirely new fibrous materials incorporating carbon nanotubes, composites, biocompatible textile scaffolds, conducting polymers and electrospun nanofibres. High strength, elasticity, conductivity, controlled porosity and giant surface areas can be combined to provide new materials with revolutionary properties. The future success of nanotechnology in textile applications lies in areas where new functionalities are combined into durable, multifunctional textile systems without comprising the inherent favorable textile properties, including processability, flexibility, washability and softness.

* E-mail: rahulsbio@yahoo.co.in

1. INTRODUCTION

A textile is a cloth, which is either woven by hand or machine. "Textile" has traditionally meant, "a woven fabric". The term comes from the Latin word *texere*, meaning *to weave*. Fibers are the raw materials for all fabrics. Some fibers occur in nature as fine strands that can be twisted into yarns. Yarn is produced by spinning raw wool fibres, flax, cotton, or other material on a spinning wheel to produce long strands. For most of history, people had only natural fibers to use in making cloth. But modern science has learned how to produce fibers by chemical and technical means. Today, these manufactured fibers account for more than two-thirds of the fibers processed by U.S. textile mills. Textiles can be made from many materials. They are classified on the basis of their component fibers into, animal (wool, silk), plant (cotton, flax, jute), mineral (asbestos, glass fiber), and synthetic (nylon, polyester, acrylic). They are also classified as to their structure or weave, according to the manner in which warp and weft cross each other in the loom. Textiles are made in various strengths and degrees of durability, from the finest gossamer to the sturdiest canvas. The relative thickness of fibers in cloth is measured in deniers. Microfiber refers to fibers made of strands thinner than one denier.

2. TEXTILE TYPES

Textiles can be made from many materials. They are classified on the basis of their component fibers into, animal (wool, silk), plant (cotton, flax, jute), mineral (asbestos, glass fiber), and synthetic (nylon, polyester, acrylic). They are also classified as to their structure or weave, according to the manner in which warp and weft cross each other in the loom. Textiles are made in various strengths and degrees of durability, from the finest gossamer to the sturdiest canvas. The relative thickness of fibers in cloth is measured in deniers. Microfiber refers to fibers made of strands thinner than one denier.

2.1. Animal Textiles

The main animal fiber used for textiles is wool. Animal textiles are commonly made from hair or fur of animals. Silk is another animal fiber produces one of the most luxurious fabrics. Sheep supply most of the wool, but members of the camel family and some goats also furnish wool. Wool, commonly used for warm clothing, refers to the hair of the domestic goat or sheep and it is coated with an oil known as lanolin, which is water-proof and dirt-proof making a comfortable fabric for dresses, suits, and sweaters. The term woolen refers to raw wool, while *worsted* refers to the yarn spun from raw wool. Cashmere, the hair of the Indian Cashmere goat, and mohair, the hair of the North African Angora goat, are types of wool known for their softness. Other animal textiles made from hair or fur is alpaca wool, vicuña wool, llama wool, and camel hair. They are generally used in the production of coats, jackets, ponchos, blankets, and other warm coverings. Angora refers to the long, thick, soft hair of the Angora rabbit.

Silk is an animal textile made from the fibers of the cocoon of the Chinese silkworm. It is spun into a smooth, shiny fabric prized for its sleek texture. Silk comes from cocoons spun by silkworms. Workers unwind the cocoons to obtain long, natural filaments. Fabrics made from

silk fibers have great luster and softness and can be dyed brilliant colors. Silk is especially popular for saree, scarfs and neckties.

2.2. Plant Textiles

Plants provide more textile fibers than do animals or minerals. Cotton fibers produce soft, absorbent fabrics that are widely used for clothing, sheets, and towels. Fibers of the flax plant are made into linen. The strength and beauty of linen have made it a popular fabric for fine tablecloths, napkins, and handkerchiefs.

Grass, rush, hemp, and sisal are all used in making rope. In the first two cases, the entire plant is used for this purpose, while in the latter two; only fibers from the plant are utilized. Coir (coconut fiber) is used in making twine, floor mats, door mats, brushes, mattresses, floor tiles, and sacking. Straw and bamboo are both used to make hats. Straw, a dried form of grass, is also used for stuffing, as is kapok. Fibers from pulpwood trees, cotton, rice, hemp, and nettle are used in making paper. Cotton, flax, jute, and modal are all used in clothing. Piña (pineapple fiber) and ramie are also fibers used in clothing, generally with a blend of other fabrics such as cotton. Seaweed is sometimes used in the production of textiles. A water-soluble fiber known as *alginate* is produced and used as a holding fiber. When the cloth is finished, the alginate is dissolved, leaving an open area.

2.3. Mineral Textiles

Asbestos and basalt fiber are used for vinyl tiles, sheeting, and adhesives, "transite" panels and siding, acoustical ceilings, stage curtains, and fire blankets. Glass fiber is used in the production of spacesuits, ironing board and mattress covers, ropes and cables, reinforcement fiber for motorized vehicles, insect netting, flame-retardant and protective fabric, soundproof, fireproof, and insulating fibers. Metal fiber, metal foil, and metal wire have a variety of uses, including the production of "cloth-of-gold" and jewelry.

2.4. Synthetic Textiles

Most manufactured fibers are made from wood pulp, cotton linters, or petrochemicals. Petrochemicals are chemicals made from crude oil and natural gas. The chief fibers manufactured from petrochemicals include nylon, polyester, acrylic, and olefin. Nylon has exceptional strength, wears well, and is easy to launder. It is popular for hosiery and other clothing and for carpeting and upholstery. Such products as conveyor belts and fire hoses are also made of nylon. All synthetic textiles are used primarily in the production of clothing.

- Polyester fiber is used in all types of clothing, either alone or blended with fibers such as cotton.
- Acrylic is a fiber used to imitate wools, including cashmere, and is often used in place of them.

- Nylon is a fiber used to imitate silk and is tight-fitting; it is widely used in the production of pantyhose.
- Lycra, spandex, and tactel are fibers that stretch easily and are also tight-fitting. They are used to make active wear, bras, and swimsuits.
- Olefin (Polypropylene or Herculon) fiber is a thermal fiber used in active wear, linings, and warm clothing.
- Lurex is a metallic fiber used in clothing embellishment.
- Ingeo is a fiber blended with other fibers such as cotton and used in clothing. It is prized for its ability to wick away perspiration.

3. TEXTILE PRODUCTION

3.1. Production Methods

Most textiles are produced by twisting fibers into yarns and then knitting or weaving the yarns into a fabric. This method of making cloth has been used for thousands of years. But throughout most of that time, workers did the twisting, knitting, or weaving largely by hand. With today's modern machinery, textile mills can manufacture as much fabric in a few seconds as it once took workers weeks to produce by hand. The production of textiles are done by different methods and some of the common production methods are listed as follows: (i) *Weaving* (by machine as well as by hand) (ii) *Knitting* (iii) *Crochet* (iv) *Felt* (fibers are matted together to produce a cloth) (v) *Braiding* (vi) *Knotting*.

Weaving is a textile production method that involves interlacing a set of vertical threads (called the warp) with a set of horizontal threads (called the weft). This is done on a machine known as a loom, of which there are a number of types. Some weaving is still done by hand, but a mechanized process is used most often. Tapestry, sometimes classed as embroidery, is a modified form of plain cloth weaving.

Knitting and *crocheting* involve interlacing loops of yarn, which are formed either on a knitting needle or crochet hook, together in a line. The two processes differ in that the knitting needle has several active loops at one time waiting to interlock with another loop, while crocheting never has more than one active loop on the needle.

Other specially prepared fabrics not woven are *felt* and *bark* (or *tapa*) cloth, which are beaten or matted together, and a few in which a single thread is looped or plaited, as in crochet and netting work and various laces. *Braiding* or *plaiting* involves twisting threads together into cloth. Knotting involves tying threads together and is used in making macrame.

Most textiles are now produced in factories, with highly specialized power looms, but many of the finest velvets, brocades, and table linens are still made by hand. Lace is made by interlocking threads together independently, using a backing and any of the methods described above, to create a fine fabric with open holes in the work. Lace can be made by hand or machine. The weaving of carpet and rugs is a special branch of the textile industry. Carpets, rugs, velvet, velour, and velveteen are made by interlacing a secondary yarn through woven cloth, creating a tufted layer known as a nap or pile.

3.2. Production of Cotton Clothes

In the 1700s, English textile manufacturers developed machines that made it possible to spin thread and weave cloth into large quantities. Today, the United States, Russia, China and India are major producers of cotton. When cotton arrives at a textile mill, several blenders feed cotton into *cleaning machines*, which mix the cotton, break it into smaller pieces and remove trash. The cotton is sucked through a pipe into *picking machines*. Beaters in these machines strike the cotton repeatedly to knock out dirt and separate lumps of cotton into smaller pieces. Cotton then goes to the *carding machine*, where the fibers are separated. Trash and short fibers are removed. Some cotton goes through a *comber* that removes more short fibers and makes a stronger, more lustrous yarn. This is followed by spinning processes which do three jobs: *draft* the cotton, or reduce it to smaller structures, straighten and parallel the fibers and lastly, put twist into the yarn. The yarns are then made into cloth by weaving, knitting or other processes.

Some of the properties of cotton are discussed as follows; (i) soft and comfortable, (ii) wrinkles easily, (iii) absorbs perspiration quickly, (iv) good color retention and good to print on, and (v) strong and durable.

3.3. Production of Wool

The processing of wool involves four major steps. First comes shearing, followed by sorting and grading, making yarn and lastly, making fabric. This is followed by grading and sorting, where workers remove any stained, damaged or inferior wool from each fleece and sort the rest of the wool according to the quality of the fibers. Wool fibers are judged not only on the basis of their strength but also by their *fineness* (diameter), length, *crimp* (waviness) and color.

The wool is then scoured with detergents to remove the *yolk* and such impurities as sand and dust. After the wool dries, it is *carded*. The carding process involves passing the wool through rollers that have thin wire teeth. The teeth untangle the fibers and arrange them into a flat sheet called a *web*. The web is then formed into narrow ropes known as *silvers*. After carding, the processes used in making yarn vary slightly, depending on the length of the fibers. Carding length fibers are used to make woolen yarn. Combing length fibers and French combing length fibers are made into *worsted yarn*.

Woolen yarn, which feels soft, has a fuzzy surface and it is heavier than worsted. While worsted wool is lighter and highly twisted, it is also smoother, and is not as bulky, thus making it easier to carry or transport about. Making worsted wool requires a greater number of processes, during which the fibers are arranged parallel to each other. The smoother the hard-surface worsted yarns, the smoother the wool it produces, meaning, less fuzziness. Fine worsted wool can be used in the making of athletics attire, because it is not as hot as polyester, and the weave of the fabric allows wool to absorb perspiration, allowing the body to "breathe". Wool manufacturers knit or weave yarn into a variety of fabrics. Wool may also be dyed at various stages of the manufacturing process and undergo finishing processes to give them the desired look and feel.

The finishing of fabrics made of woolen yarn begins with *fulling*. This process involves wetting the fabric thoroughly with water and then passing it through the rollers. Fulling

makes the fibers interlock and mat together. It shrinks the material and gives it additional strength and thickness. Worsteds go through a process called *crabbing* in which the fabric passes through boiling water and then cold water. This procedure strengthens the fabric.

The exclusive features of cotton fabric are (i) hard wearing and absorbs moisture, (ii) does not burn over a flame but smoulders instead, (iii) lightweight and versatile, (iv) does not wrinkle easily, and (v) resistant to dirt and wear and tear.

3.4. Production of Silk

Silkworms are cultivated and fed with mulberry leaves. Some of these eggs are hatched by artificial means such as an incubator, and in the olden times, the people carried it close to their bodies so that it would remain warm. Silkworms that feed on smaller, domestic tree leaves produce the finer silk, while the coarser silk is produced by silkworms that have fed on oak leaves. From the time they hatch to the time they start to spin cocoons, they are very carefully tended to. Noise is believed to affect the process, thus the cultivators try not to startle the silkworms. Their cocoons are spun from the tops of loose straw. It will be completed in two to three days' time. The cultivators then gather the cocoons and the chrysales are killed by heating and drying the cocoons. In the olden days, they were packed with leaves and salt in a jar, and then buried in the ground, or else other insects might bite holes in it. Modern machines and modern methods can be used to produce silk but the old-fashioned hand-reels and looms can also produce equally beautiful silk.

The properties of cotton includes; (i) versatile and very comfortable, (ii) absorbs moisture, (iii) cool to wear in the summer yet warm to wear in winter, (v) easily dyed, (v) strongest natural fiber and is lustrous, and (vi) poor resistance to sunlight exposure.

3.5. Production of Nylon Materials

Nylon is made by forcing molten nylon through very small holes in a device called a spinneret. The streams of nylon harden into filament once they come in contact with air. They are then wound onto bobbins. These fibers are drawn (stretched) after they cool. Drawing involves unwinding the yarn or filaments and then winding it around another spool. Drawing makes the molecules in each filament fall into parallel lines. This gives the nylon fiber strength and elasticity. After the whole drawing process, the yarn may be twisted a few turns per yard or meters as it is wound onto spools. Further treatment to it can give it a different texture or bulk.

Properties of the nylon: (i) it is strong and elastic, (ii) it is easy to launder, (iii) it dries quickly, (iv) it retains its shape, and (v) it is resilient and responsive to heat setting.

3.6. Production of Polyester

Polyesters are made from chemical substances found mainly in petroleum. Polyesters are manufactured in three basic forms - *fibers*, *films* and *plastics*. Polyester fibers are used to make fabrics. Poly (ethylene terephthalate or simply PET) is the most common polyester used

for fiber purposes. This is the polymer used for making soft drink bottles. Recycling of PET by re-melting and extruding it as fiber may save much raw material as well as energy. PET is made by ethylene glycol with either terephthalic acid or its methyl ester in the presence of an antimony catalyst. In order to achieve high molecular weights needed to form useful fibers, the reaction has to be carried out at high temperature and in a vacuum.

4. TECHNOLOGICAL USES

Textile materials are materials for the daily use. Besides, textiles also play a vital role in fashion shows. Technically, they are applied in a variety of our life savers including safety belt, and the airbags in the cars, bullet-proof vests protect against weapons, used as implant material in medical applications [1]. Recently, polyurethane (PU) foams that can be combined with Plaiton thermoplastic polyurethane (TPU) films are used as excellent material for functional medical wound dressing which not only helps wounds to heal but also allows the wound to breathe by permeating the water-vapor.

4.1. Advancements in Textile Production

Technological advances during the past decade have opened many new doors for the Textile and Apparel industries, especially in the area of rapid prototyping and related activities. During the past decade, the textile and apparel complex has been scrambling to adjust to a rapidly changing business environment. Textiles and yarns have been around for thousands of years but in the last 50 years, progress in the technology has been most remarkable. The application of textiles and yarns has moved beyond clothing and fabrics and they are increasingly used in high value-added applications such as composites, filtration media, gas separation, sensors and biomedical engineering. With the emergence of nanotechnology, the users of textiles and yarns are switching their attention to the production of nanometer diameter fibers.

4.2. Body Scanning

The development of 3 dimensional body scanning technologies may have significant potential for use in the apparel industry, for a number of reasons. First, this technology has the potential of obtaining an unlimited number of linear and non-linear measurements of human bodies (in addition to other objects) in a matter of seconds. Because an image of the body is captured during the scanning process, the location and description of the measurements can be altered as needed in mere seconds, as well. Second, the measurements obtained using this technology have the potential of being more precise and reproducible than measurements obtained through the physical measurement process. Third, with the availability of an infinite number of linear and non-linear measurements the possibility exists for garments to be created to mold to the 3 dimensional shapes of unique human bodies. Finally, the scanning technology allows measurements to be obtained in a digital format that

could integrate automatically into apparel CAD systems without the human intervention that takes additional time and can introduce error.

4.3. Apparel CAD

Adoption of CAD/CAM technology over the past few decades has increased the speed and accuracy of developing new products, reducing the manpower required to complete the development process. Unfortunately, this technology has also encouraged manufacturers to simplify the design of garments, allowing a more efficient use of materials and making mass production much easier [2]. These systems initially only made an effort to adapt traditional manual methods instead of encouraging innovation in design or fit adaptations. Current developments in the area of information technology help build on the traditional CAD/CAM functions and offer a new way of looking at and using the systems for design and product development [3].

4.4. Nanofiber Fabrication

As with all new technologies, polymeric nanofibers have brought with it a new beginning to the understanding of polymeric fibers. One apparent advantage of nanofibers is the huge increase in the surface area to volume ratio. Given the huge potential of nanofibers, the key is to use a technique that is able to easily fabricate nanofibers out of most, if not all the different type of polymers. A number of processing techniques such as drawing [4], template synthesis [5], phase separation [6], self-assembly [7], electrospinning [8], etc. have been used to prepare polymer nanofibers in recent years. The drawing is a process similar to dry spinning in fiber industry, which can make one-by-one very long single nanofibers. The template synthesis, as the name suggests, uses a nanoporous membrane as a template to make nanofibers of solid (a fibril) or hollow (a tubule) shape. The phase separation consists of dissolution, gelation, and extraction using a different solvent, freezing, and drying resulting in nanoscale porous foam. The process takes relatively long period of time to transfer the solid polymer into the nano-porous foam. The self-assembly is a process in which individual, pre-existing components organize themselves into desired patterns and functions.

4.5. Electrospinning

Electrospinning is a process where continuous fibers with diameters in the sub-micron range are produced through the action of an applied electric field imposed on a polymer solution. Textiles made from these fibers have high surface area and small pore size, making them ideal materials for use in protective clothing. There are currently several applications of electrospinning that are being investigated, including: The fabrication of transparent composites reinforced with nanofibers. The effect of processing conditions on the morphology of polymers has been investigated. The scaling up of current production techniques is one of the main areas of research in which we have ongoing interest is the

development of polymer nanofibers for applications requiring a specific surface chemistry. Adhesives, Permselective membranes, Anti-fouling coatings, Active protective barriers against chemical and biological threats are few examples of nanofibers produced through electrospinning.

4.6. Textile Modification

Considering special advantages and high potentialities of the application of nano-structured materials in textile industry, especially for producing high performance textiles, here we reviewed the application of nano-structured materials for anti-bacterial modification of textile and polymeric materials. The modification of textile fibers is carried out by commonly used chemical or electro-chemical application methods. Many of the classical textile finishing techniques (e.g. hydrophobization, easy-care finishing) that are already used since decades are amongst these methods. Modification of textiles via producing polymeric nano-composites and also surface modification of textiles with metallic and inorganic nano-structured materials are developed due to their unique properties. Considering the fact that fiber and film processing are the most difficult procedures of molding polymeric materials, bulk modification of continuous multi-filament yarns is an extremely sensitive process. However, achieving optimum process conditions will present an economical technique.

Different methods have been used for surface modifications of textiles by using poly carboxylic acids as spacers for attaching TiO_2 nano-particles to the fabrics [9] and argon plasma grafting nano-particles on wool surface [10]. Plasma pre-treatment has been used for the generation of active groups on the surface to be combined with TiO_2 nano-particles [11]. The radical groups on the surface have also been generated using irradiation of the textile surfaces with UV light to bond the nano-particles [12]. Deposition of nano-particles from their metallic salt solution on the surface pretreated with RF-plasma and vacuum-UV [13].

Nanotechnology holds great potential in the textile and clothing industry offering enhanced performance of textile manufacturing machines and processes so as to overcome the limitations of conventional methods. Nanofibres have good properties such as high surface area, a small fiber diameter, good filtration properties and high permeability. Nanofibres can be obtained via electro-spinning application or bicomponent extrusion (islands in the sea technique). One of the interesting areas for the application of nanotechnology in the textile industry are coating and finishing processes of textiles which is done by the techniques like sol-gel [14] and plasma [15]. Nanotech enhanced textiles include sporting industry, skincare, space technology and clothing as well as material technology exhibiting better healthcare systems, protective clothing and integrated electronics. By using nanotechnology, textiles with self-cleaning surfaces have attracted much attention which is created by the lotus effect. In brief, nanoscaled structures similar to those of a lotus leaf create a surface that causes water and oil to be repelled, forming droplets, which will simply roll off the surface, taking any with them [16].

With the advent of nanoscience and technology, a new area has developed in the area of textile finishing called "Nanofinishing". Growing awareness of health and hygiene has increased the demand for bioactive or antimicrobial and UV-protecting textiles. Coating the

surface of textiles and clothing with nanoparticles is an approach to the production of highly active surfaces to have UV blocking, antimicrobial, flame retardant, water repellant and self-cleaning properties. The UV-blocking property of a fabric is enhanced when a dye, pigment, delustrant, or ultraviolet absorber finish is present that absorbs ultraviolet radiation and blocks its transmission through a fabric to the skin. Metal oxides like ZnO as UV-blocker are more stable when compared to organic UV-blocking agents. For antibacterial finishing, ZnO nanoparticles scores over nano-silver in cost-effectiveness, whiteness, and UV-blocking property [17].

CONCLUSION

The future success of nanotechnology in textile applications lies in areas where new functionalities are combined into durable, multifunctional textile systems without comprising the inherent favorable textile properties, including processability, flexibility, washability and softness. Nanotech enhanced textiles include sporting industry, skincare, space technology and clothing as well as material technology exhibiting better healthcare systems, protective clothing and integrated electronics.

REFERENCES

- [1] Mahltig, B. and Textor, T. (2008). Nanosols and Textiles. World scientific publishing pvt. Ltd, Germany, p. 236.
- [2] Bye, E. and LaBat, K. (1994). Technology: Shaping the Aesthetic Product. In: *Aesthetics of Textiles and Clothing: Advancing Multi-Disciplinary Perspectives*, Monograph #7 on Aesthetics. Monument, CO: International Textile and Apparel Association, 28-38.
- [3] Bye, E. (1999). The Influence of Technology on the Apparel Product. In: *Proceedings of the World Congress on Textiles in the Millennium*, July 6-7: 249-255.
- [4] Ondarcuhu, T., and Joachim, C. (1998). Drawing a single nanofibre over hundreds of microns. *Europhysics Letters*, 42: 215-220.
- [5] Feng, L., Li, S., Li, H., Zhai, J., Song, Y., Jiang, L., and Zhu, D. (2002). Super-Hydrophobic Surface of Aligned Polyacrylonitrile Nanofibers. *Angewandte Chemie International Edition*, 41:1221-1223.
- [6] Ma, P.X., and Zhang, R. (1999). Synthetic nano-scale fibrous extracellular matrix. *Journal of Biomedical Materials Research*, 46: 60-72.
- [7] Whitesides, G.M., and Grzybowski, B. (2002). Self-assembly at all scales. *Science*, 295: 2418-2421.
- [8] Deitzel, J.M., Kleinmeyer, J., Hirvonen, J.K., and Beck, T.N.C. (2001). Controlled deposition of electrospun poly(ethylene oxide) fibers. *Polymer*, 42: 8163-8170.
- [9] Meilert, K.T., Laubb, D., and Kiwi, J. (2005). Photocatalytic self-cleaning of modified cotton textiles by TiO₂ clusters attached by chemical spacers. *Journal of Molecular Catalysis A: Chemical*, 237: 101-108.

-
- [10] Wang, S., Hou, W., Wei, L., Jia, H., Liu, X., and Xu, B. (2007). Antibacterial activity of nano-SiO₂ antibacterial agent grafted on wool surface. *Surface and Coatings Technology*, 202: 460–465.
 - [11] Bozzi, A., Yuranova, T., and Kiwi, J. (2005). Self-cleaning of wool-polyamide and polyester textile by TiO₂-rutile modification under daylight irradiation at ambient temperature. *Journal of Photochemistry A: Chemistry*, 172: 27–43.
 - [12] Xu, B., Niu, M., Wei, L., Hou, W., and Liu, X. (2007). The structural analysis of biomacromolecule wool fiber with Ag-loading SiO₂ nano-antibacterial agent by UV radiation. *Journal of Photochemistry and Photobiology A: Chemistry*, 188: 98–105.
 - [13] Yuranova, T., Rincon, A.G., Bozzi, A., Parra, S., Pulgarin, C., Albers, P., and Kiwi, J. (2003). Antibacterial textiles prepared by RF-plasma and vacuum-UV mediated deposition of silver. *Journal of Photochemistry and Photobiology A: Chemistry*, 161: 27–34.
 - [14] Mahltig, B., Fiedler, D., Fischer, A., and Simon, P. (2010). During the past decade, the textile and apparel complex has been scrambling to adjust to a rapidly changing business environment. *Journal of Sol-Gel Science and Technology*, 55: 269-277.
 - [15] Mehta, R. (2010). "Plasma Treatment" in the textile industry. *Colourage*, 57: 45-48.
 - [16] De Schrijver, I., Eufinger, K., Heyse, P., Vanneste, M., and Ruys, L. (2009). Textiles of the future? Incorporation of nanotechnology in textile applications. *Unitex*, 2: 4-6.
 - [17] Vigneshwaran, N., Sampath Kumar, Kathe, A.A., Varadarajan, P.V., and Virendra Prasad. (2006). Functional finishing of cotton fabrics using zinc oxide-soluble starch nanocomposites. *Nanotechnology*, 17: 5087-5095.

Chapter 5

NANOFIBERS FROM NATURAL BIOPOLYMERS IN REGENERATIVE MEDICINE

***Georgios Toskas*, Rolf-Dieter Hund,
Ezzedine Laourine and Chokri Cherif***

Institute of Textile Machinery and High Performance Material Technology (ITM),
Technische Universität Dresden, Hohestr. 6, 01069 Dresden, Germany.

ABSTRACT

Medical textile constructs for tissue replacement or release of drugs and faster healing of wounds are of increasing interest recently. They belong to the smart textiles concept, derived from material design, textile engineering and chemical finishing. Advances in electrospinning techniques have permitted the generation of continuous fibers at the nanometer scale with a high surface area to volume ratio. Nanofiber matrices have been found a large number of applications in the industrial sector and also in biomedical field. Natural polymers possess proven tissue compatibility and usually contain domains that can send important signals to guide cells at various stages of their development. The most used sources of natural derived polymers include proteins, especially from extracellular matrices (ECM) (e.g. collagen), polypeptides, and polysaccharides (including chitosan, cellulose, starch, hyaluronic acid, heparin and alginate). It has been shown that nanofibrous matrices can better mimic the target tissues than their bulk equivalents, as cells attach and proliferate well in micro and nanostructured materials and there is also the ability to modify the structure, composition and the chemistry at the nanoscale. In this chapter, we examine briefly the use of nanofibrous mats in regenerative medicine from the textile materials point of view, having as scope to introduce the reader to this constantly emerging sector. The nanofiber production of the main natural derived polymers, which have been used or have the potential to be used in regenerative medicine, is reviewed in relation to their structure and correlated to the application possibilities, according to the type of engineered tissue.

* Corresponding author: Dr. Georgios Toskas, Associate Professor, Present address: Technological Education Institute of Piraeus, School of Engineering, Department of Textiles, P. Ralli & Thivon 250, 12244 Egaleo, Greece. Tel.: +30 210 5381171. Fax: +30 210 5381255. E-mails: georg.toskas@gmx.de; gtoskas@gmail.com

1. INTRODUCTION

It has been postulated that the smart textile concept, can lead to novel medical textile materials for tissue replacement, release of drugs and faster healing/recovery of wounds by moisture regulation. This is achieved by the development of new materials design derived from chemical finishing [1]. In addition, Peppas and Langer define biomedical engineering as an extension of chemical engineering towards biomaterials [2]. Tissue engineering (TE) combines the design principles of living organisms and modern engineering with the development of viable substitutes of human tissues such as skin, cartilage, bone, muscle and even cardiovascular and neuronal structures. Progress in this field is attained via scaffolds implementing a variety of bioactive molecules to balance cell proliferation and differentiation. TE skin equivalents have been in clinical use since 1997 and a fast-growing arsenal of replacement devices is in clinical trials or already approved as therapies for tissues including cartilage, bone, blood vessel and pancreas. A scaffold, in the context of regenerative medicine, is designed to functionally restore or repair diseased or lost tissue in the human body. It is usually made for a particular tissue type to stimulate or accelerate the tissue growth. This process is initiated by encouraging cell attachment, proliferation and differentiation. The cells populated in the scaffold then “secrete” the natural extracellular matrix (ECM) as the scaffold gradually degrades. The scaffold should have a highly porous structure with a proper pore size to help cell in growth and a degradation rate that matches that of tissue growth. An emerging philosophy in tissue engineering is that rather than attempting to recreate the complexity of living tissues *ex vivo*, we should aim to develop synthetic materials that establish key interactions with cells in ways that unlock the body’s innate powers of organization and self-repair [3].

In general, chemistry (materials and surfaces), biology, engineering (physical/mechanical properties) and healing and medicine (immunology) need to be considered simultaneously to design and develop composite scaffolds. Viable substitutes of human tissues such as skin, cartilage, bone, muscle and also cardiovascular and neuronal structures can be obtained by constructing biomimetic and bioactive artificial extracellular matrices (ECM). Tissue-engineering scaffolds can be designed to interact with cells by mimicking key molecular features of the ECM. Natural extracellular matrix separates different tissues, supports and fixes cells. ECM contains many macromolecules such as proteoglycans, collagens, laminins, and fibronectin and sequestered growth factors, and it is primarily this molecular information that confers its bioactivity.

The concept of biomimetic materials is based on the use of biopolymers, templates, matrix architectures or composites, bioactive molecules and living cells leading to novel routes in regenerative medicine. Considerable efforts in the bioengineering community consist on the investigation of biodegradable polymers serving as scaffolds suitable for tissue engineering applications [4]. Among the different classes of polymers, biodegradable biopolymers, obtained from natural wastes, are of great importance in regenerative medicine. The most used sources of natural derived polymers include proteins, especially from extracellular matrices (ECM) (e.g. collagen), polypeptides, and polysaccharides (including chitosan, cellulose, starch, hyaluronic acid, heparin and alginate) [5, 6].

Nanofiber matrices have been found a large number of applications in the industrial sector i.e. in filtration, membrane, textile coating and catalysis and also in biomedical field,

i.e. in wound healing, drug delivery systems and tissue engineering scaffolds. Two classes of extracellular macromolecules are mainly found in natural ECM: proteoglycans and fibrous proteins with fiber diameters ranging from 50 to 150 nm, depending on tissue type [7]. Additionally, it has been shown that nanofibrous matrices can better mimic the target tissues than their bulk equivalents, as cells attach and proliferate well in micro and nanostructured materials [8,9]. Therefore, nanofiber matrices originated from natural polymers have gotten increasing attention for their application in the biomedical sector [10-12].

Electrospinning process has become the most attractive method for the nanofibers production because it is cost-effective and applicable to a variety of polymers. The rapidly increasing number of research concerning nanofibers via electrospinning for biomedical applications renders a review unlimited. In this chapter, we review briefly the use of nanofibers of the main natural derived polymers in regenerative medicine, relating the application possibilities to the type of engineered tissue.

2. FABRICATION OF NANOFIBERS: BASICS IN ELECTROSPINNING PROCESS

Commercial fibers have diameters in the range of 10-500 μm and with conventional techniques it is difficult to obtain diameters smaller than 2 μm . Nanofibers with diameters less than 500 nm possess a high surface area to volume ratio, providing them the ability to manipulate the structure, composition and the chemistry at the nanoscale. As they have lengths of kilometers with diameters of a few nanometers, they can be seen as a connection of the macro- to the nanoscale domain.

A number of manufacturing processes have explored to fabricate micro or nanofibrous matrices, including drawing, self-assembly, template-directed synthesis, phase separation, and electrospinning. Among these techniques, electrospinning has been widely accepted as the simplest and least expensive means to fabricate ultra fine continuous fibers, with diameters from 5-500nm, from a variety of synthetic or natural polymers. It takes place when an electric field is applied between a nozzle (in most of the cases a needle capillary end or more recently a needleless type of stick or roller) and a target electrode (collector); surface charge is induced on a polymer fluid deforming a spherical pendant droplet to a conical shape (Taylor cone). High surface charge densities enhance a whipping mode, where bending of the jet produces highly stretched polymeric fiber with simultaneous rapid evaporation of the solvent [13]. A pioneering research group in this field investigated the detailed mechanism of electrospinning, including jet initiation, growth of bending instability, elongation of the jet and solidification of the jet into the nanofiber [14]. The electrospinning phenomenon itself involves basic and significant issues in polymer science for solution dynamics, in which viscoelastic parameters, surface free energy (surface tension) and electroconductivity are critical factors for the successful spinning of nanofibers. The solvent performs two crucial roles in electrospinning. First, to solvate the polymer molecules, ready to form the electrified jet. The second is to carry the solvated polymer molecules towards the collector, then to leave the polymer fibers by rapid vaporization of the solvent molecules. The appropriate selection of a solvent system is a prerequisite for successful electrospinning [15].

Some of the advantages of electrospinning are ease of processability, possibility of large-scale production, easy functionalization, and apparatus modifications. A versatile modification concerns the coaxial electrospinning which permits the fabrication of core-shell nanofibers. This technique is allowing the encapsulation of biomolecules as drugs and other nanocomposites [11]. Another technique is the Layer-by-layer (LbL) electrospinning, based on the equivalent layer-by-layer (LbL) assembly which consists in depositing alternately, polyelectrolytes that self-assemble and self-organize on a surface, leading to the formation of polyelectrolyte multilayer films (PEM) [16, 17]. Essentially, a polyelectrolyte is electrospun onto a surface of opposite charge. This leads to a reversal of the net surface charge, due to excess charged groups on the polymer chain, allowing the subsequent deposition of a second, oppositely charged polyelectrolyte. Multiple repetitions of this process lead to the build-up of a strong, coherent surface coating, generally with a thickness ranging from tens to hundreds of nanometers. The suitability of the LbL assemblies as host to a variety of biologically active molecules, such as drugs, enzymes, DNA or proteins, offers numerous opportunities for clinical applications [18]. Finally, another technique consists on the ability to align electrospun fibers which has interesting implications in tissue engineering, particularly for the development and remodeling of both native and engineered heart tissues. This is achieved through a rotating drum collector with a rotating speed of up to 3000 rpm.

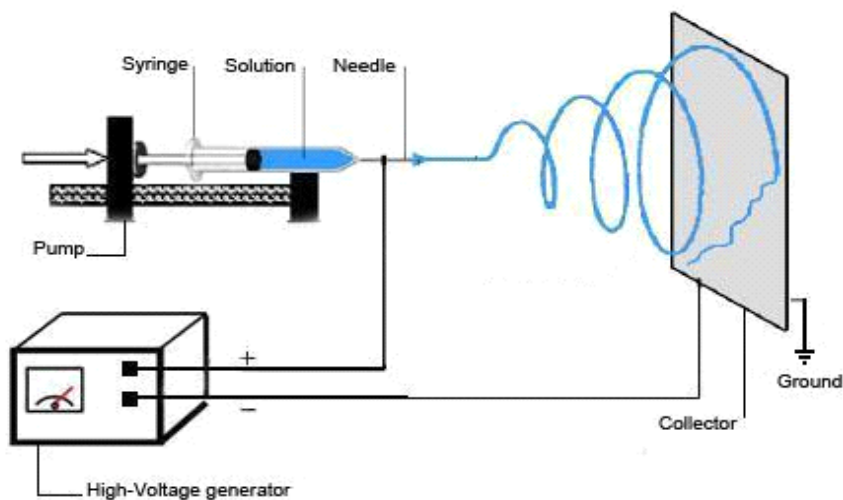


Figure 1. Horizontal electrospinning set-up.

Electrospinning set-up, as designed in Figure 1, can be performed horizontally or vertically. The electrospinning apparatus for the production of the electrospun natural biopolymers reported in this chapter could set up horizontally or vertically and the spinneret was mounted on an electrically insulated chamber. An in-house fabricated high-voltage DC power supply generator allowed voltages of up to 50 kV. The polymer solution was put into a 1 mL disposable syringe fitted with tip-ground-to-flat needles and fed with the help of a programmable KD scientific pump. The nanofibers were collected on a polypropylene non-

woven fabric or aluminum foil fitted on a stable circular collector at different distances from 5 to 15 cm. The electric potential, solution flow rates and the needle to collector distance were adjusted so that a stable jet was obtained. The flow rate is dependent on the viscosity of the solutions and had to be adjusted with the electric field.

3. NATURAL BIOPOLYMERS IN REGENERATIVE MEDICINE

The development of new resorbable materials for tissue replacement remains an important aim in regenerative medicine. The potential biomedical use of these materials is governed by the physical, chemical and biological compatibility and also by their biodegradability. Physical properties, such as tensile strength, deformation resistance and elasticity modulus have to match with that of the tissue to be replaced. Also, chemical reactions at the interface of implanted biomaterial influence biocompatibility.

The use of polymers for the development of biocompatible materials serving as scaffolds is manifold. Working backward from the end use, a series of design criteria are established where the site of implantation and expected performance define polymer selection. On the one hand, synthetic polymers can be tuned in terms of composition, rate of degradation, mechanical, and chemical properties. On the other hand, naturally derived polymers provide compositional uniqueness, such as stimulating a specific cellular response, which in many cases overrides the advantages of synthetic polymers. But as they show poor processability, they must be often modified in order to perform electrospinning. Sometimes, a crosslinking is required so that the nanofibers retain their form. Another method is the combination of natural polymers with synthetic polymers, thus gaining of the better mechanical properties of these late. Natural biopolymers are bearing good biofunctionality and are better suited for applications requiring flexibility and elasticity, as in soft tissue replacement and cardiovascular grafts [19].

For scaffolds development, high surface area and an open and interconnected 3D pore system are necessary. A minimum pore size is required for cell adherence and infiltration, permitting also the diffuse of cell nutrients. Electrospinning generates loosely connected 3D porous mats with high porosity and high surface area capable of absorbing proteins and providing enough binding sites to cell membrane receptors [20]. Also, as cells perform amoeboid movement to migrate through the pores, they push the surrounding fibers aside to expand the hole as the thin fibers offer little resistance to cell movement. This could presume that the pores with smaller diameters in this structure may not hinder cell migration and provide the cells with an opportunity to adjust optimally the pore diameter and grow into the scaffold [10]. The nanofibrous mats as a dynamic architecture, are therefore excellent candidates for use in TE. Nevertheless, round cells having diameters of about 10 μm cannot attach in nanofiber meshes with pores on the nanometer scale. These nanofiber meshes can be useful for barrier applications such as skin and vascular grafts [21].

In addition, drug release methods via nanofiber matrices are strictly related with tissue engineering, as the release of various therapeutic factors can increase the efficiency of regeneration. In the following sections, a focus on nanofibers from the main natural biopolymers and their potential applications in regenerative medicine will be introduced.

3.1. Proteins

3.1.1. Collagen

Collagen is distinguished by its abundance in the mammalian organism and its importance for the connective properties of tissues. Native blood vessel is a composite three layered tubular structure, each layer having different composition and arrangement of elastin and collagen nanofibers. In many native tissues, polymers of type I and type III collagen are the principal structural elements of the extracellular matrix. The underlying α chains that form these natural polymers are arranged into a repeating motif which forms a coiled coil structure. At the ultra structural level, this repeating motif exhibits a 67 nm interval that imparts a characteristic banding pattern to the collagen fibril. The specific complement of α subunits present within the fibril defines the material properties of the polymer. Type I collagen fibrils are composed of two α_1 chains and one α_2 chain. In native tissues, polymers of type I collagen are approximately 50 nm in diameter and very uniform in size [22].

Huang and coworkers were the first to electrospin collagen scaffolds for wound dressing [23, 24]. Shortly thereafter, Matthews *et al.* [25] described electrospinning of collagen and elastin fibers for preliminary vascular tissue engineering. Optimizing conditions for calfskin type I collagen, dissolved at various concentrations in 1,1,1,3,3,3 hexafluoro-2-propanol (HFP), produced a matrix composed of 100 nm fibers that exhibited the 67 nm banding pattern, characteristic of native collagen [25]. Zhong *et al.* described later the collagen electrospinning by the use of the high volatile 2,2,2-trifluoroethanol (TFE) [26]. Additionally, uniform collagen fibers were produced by adding sodium chloride at concentrations of 0.01-0.03 wt% and Triton® X-100 at 0.001-0.003 wt % [27]. However, the main problem of collagen electrospinning out of fluoroalcohols such as HFP and TFE is its denaturation to gelatin, as recently revealed by Zeugolis *et al.* [28]. Moreover, in a recent publication it was shown that 45% of collagen was apparently lost during electrospinning [29].

To overcome this problem, we have attempted in our laboratory to electrospin collagen in distilled water. Unpurified collagen at a concentration up to 1 wt% produced a nanofiber net interconnected by beads with fibers diameters between 30 and 160 nm. The electrospinnability of collagen in water was improved by blending with polyvinyl alcohol (PVA) at varying ratios. Uniform collagen/PVA nanofibers were produced with average diameters of 25 - 255 nm [30, 31].

In order to tailor the mechanical properties of native tissues, several collagen nanofiber blends with either other natural biopolymers as elastin or synthetic as poly(caprolactone) (PCL) have been reported [32, 33].

3.1.2. Other Proteins

A comparative study on various proteins including collagen, gelatin, α -elastin and recombinant human tropoelastin is given by Li *et al.* [34]. And more recently, Sell *et al.* [33] have reviewed the collagen/biopolymers electrospinning in regenerative medicine and cardiovascular tissue engineering applications.

Elastin is becoming more and more popular for tissue engineering applications as one of the main structural components of the vascular ECM. In vivo, elastin is a chemically inert, highly insoluble polymer composed of covalently cross-linked molecules of its precursor, tropoelastin, a soluble highly hydrophobic protein.

Li *et al.* [34] demonstrated that recombinant human tropoelastin could be electrospun to form both nanofibers and microfibers, depending on the delivery rate. In their study, both tropoelastin and solubilized α -elastin were electrospun and the cellular activity with human embryonic palatal mesenchymal (HEPM) cells was proved. It was determined that the elasticity of tropoelastin far exceeded that of soluble elastin, which could allow the creation of grafts with compliance matching native artery.

Gelatin is a derivative of collagen, acquired by denaturing the triple-helix structure. Gelatin nanofibers have been electrospun from the organic solvents HFP and trifluoroethanol (TFE), as well as formic acid, acetic acid, and water. The average diameter of electrospun gelatin and collagen fibers have been found similar, and could be scaled down to 200–500 nm [34, 35] (see Figure 2a). In addition to similar mechanical properties to collagen, gelatin exhibits excellent biodegradability, non-antigenicity, and cost efficiency.

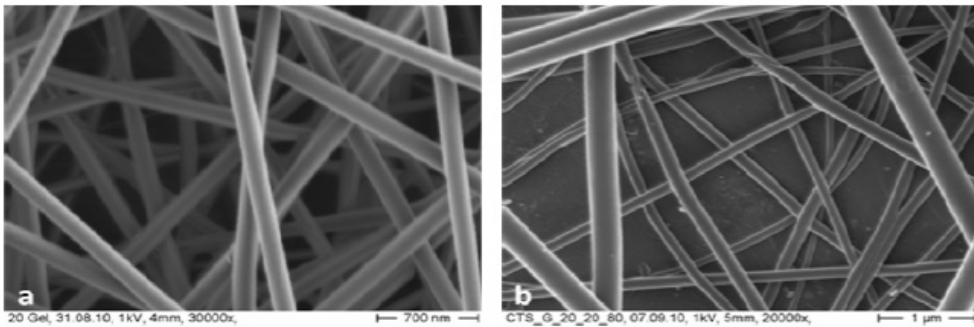


Figure 2. a. Gelatin nanofibers (magnification: x30000); b. Gelatin/chitosan (ratio 80:20 wt) nanofibers (magnification: x20000); Ref. [35].

Fibrinogen is a glycoprotein, synthesized by the liver and found freely circulating in the bloodstream, which plays a critical role in the coagulation of blood. Electrospinning of fibrinogen nanofibers was first published by Wnek *et al.*, and has since been demonstrated as a tissue engineering scaffold with great potential [36].

Silk is a challenging natural protein, used for centuries as a medical grade suture, which is gaining actually as a tissue engineering scaffold due to its unique blend of material characteristics and biocompatibility. It has been reported that natural silk fibers have tensile strength and yield at fracture values comparable to synthetic fibers such as Kevlar. The use of silk fibers in tissue engineering typically refers to the use of *silk fibroin* (SF). Tissue engineering with SF has been reserved mainly for ligament engineering applications, as both knitted constructs and as electrospun scaffolds of reconstituted SF. However, SF has also been recently utilized in the creation of electrospun bioresorbable vascular grafts with promising results. Zhang *et al.* successfully seeded electrospun SF with both human aortic endothelial cells (hAEC) and human coronary artery smooth muscle cells (hCASMC) [37].

Electrospinning was also used to fabricate non-woven nanofibrous tubular scaffolds from *Bombyx mori* silk fibroin using an all aqueous process. Human endothelial cells and smooth muscle cells were successfully cultured on the electrospun silk [32, 38].

3.1.3. Polypeptides

Peptides are short linear amino acid polymers linked by peptide bonds. They have the same peptide bonds as those in proteins, but are commonly shorter in length. *Self-assembling peptides* appear to have great promise in promoting regeneration of the myocardium. Heart failure after a *myocardial infarction* is often progressive. Cardiac muscle becomes terminally differentiated shortly after birth, causing these cells to lose their ability to divide. As a result, cardiac muscle will not regenerate after injury, such as that caused by myocardial infarction [39]. Polypeptides are found to form nanofibers upon injection, creating a microenvironment that is suitable for cell and vessel in growth. After injection of the peptides alone into the infarct, progenitor cells expressing endothelial cell markers and vascular smooth-muscle cells were recruited into the nanofibers. Analogously, a heparin-presenting injectable self-assembling peptide nanofiber network was used to bind and deliver *paracrine factors* derived from hypoxic conditioned stem cell media to mimic the stem cell paracrine effect. Bundling of these nanofibers produces a gel matrix consisting of fibrillar nanostructures of similar dimensions to natural extracellular matrix components. These self-assembled nanofibers immobilize and present heparin in a biomimetic fashion [40].

3.2. Polysaccharides

Polysaccharides are presented as the homopolymers or copolymers of monosaccharides. In nature, polysaccharides are found in many organisms from which can be extracted. We distinguish polysaccharides of algal origin (e.g. alginate, ulvan), plant origin (e.g. cellulose and starch), microbial origin (e.g. dextran), and animal origin (e.g. chitosan, hyaluronic acid and heparin).

3.2.1. Alginate

Alginate is a linear copolymer consisting of two sterically different repeating units, (1,4)- α -L-guluronate (G unit) and (1,4)- β -D-mannuronate (M unit) in different proportions [41]. It is an anionic polysaccharide derived from brown seaweed and can form hydrogels, porous sponges, and microfibers. Alginate has been thoroughly used in tissue engineering applications, such as skin, cartilage, bone, liver, and cardiac tissue regeneration [42-48]. It has excellent biocompatibility, low toxicity and non-immunogenicity. Rather than degrading, ionically cross-linked alginate gels can be dissolved into the surrounding media. Alginate nanofibers were recently successfully electrospun by using glycerol as a co-solvent. At a volume ratio of glycerol to water of 2, continuous fibers were obtained [49]. At that ratio, the chain entanglement concentration was enhanced, resulting to stable jet formation.

3.2.2. Cellulose

Cellulose consists of (1,4)-linked β -D-glucose units and has been of particular interest due to its abundance as a renewable resource, biodegradability, and biocompatibility. Cellulose-based materials have been extensively used in the pharmaceutical and biomedical fields, including applications as filters, artificial tissue/skin, and protective clothing. The processability of cellulose is extremely restricted by its limited solubility in common organic solvents and its inability to melt. In order to enhance the solubility of cellulose and improve its electrospinnability, *cellulose derivatives* have been developed. Cellulose derivatives can be

easily electrospun into fibers and then converted to cellulose by aqueous or ethanolic hydrolysis. Cellulose derivatives used for electrospinning include most commonly cellulose acetate (CA) [50-53], but cellulose triacetate (CTA), hydroxypropyl cellulose (HPC), ethyl cellulose (EC), methyl cellulose (MC), and ethyl-cyanoethyl cellulose (E-CE C) have been also investigated. Electrospun cellulose-based nanofiber matrices have been used as affinity or barrier membranes, antimicrobial membranes, three-dimensional structures resembling the urinary bladder matrix [54], membranes for enzyme immobilization, and membranes for drug delivery [55-58]. Nanofibers from cellulose and its derivatives have been functionalized by incorporating functional compounds (e.g. drug) into the spinning solution. Thus, vitamin-loaded CA matrices of electrospun nanofibers were successfully fabricated by electrospinning a 17 wt% CA solution in an acetone/DMAc (2/2, v/v) solvent mixture [55]. CA nanofibrous matrices containing four types of model drugs including naproxen (NAP), indomethacin (IND), ibuprofen (IBU), and sulidac (SUL) were also prepared by electrospinning [12].

3.2.3. Chitin and Chitosan

Chitin, the second most abundant natural polymer in the world derived from crustacean shells (e.g. from crabs and shrimps), is composed of (1,4)-linked *N*-acetyl- β -D-glucosamine. It is an analogue of cellulose with *N*-acetyl groups instead of hydroxyl groups in position 2. Chitin is converted to chitosan by alkaline treatment. Alkali splits most of the *N*-acetyl groups (75-95%), generating free amino groups that provide fungistatic and bacterostatic effects. This mild *antimicrobial activity* may be amplified by methylation of the amino groups to quaternary trimethylammonium structures. [1]. *Chitosan*, this partially (over 50 %) deacetylated form of chitin, is a high molecular weight polysaccharide composed of β -(1,4)-2-acetamido-2-deoxy-D-glucose and β -(1,4)-2-amino-2-deoxy-D-glucose units. This natural cationic polymer, offers unique properties; it is biologically renewable, biodegradable, biocompatible, non-antigenic, non-toxic, and biofunctional. It has been proved to have anti-bacterial, anti-fungal and haemostatic properties, while accelerating wound healing.

Chitin nanofibrous matrices (Chi-N) have been fabricated and their biodegradability and cellular behavior were compared with a commercially available chitin microfiber (Beschitin W®, Chi-M). Chi-N fibrous matrices are considered potentially useful for wound healing and regeneration of oral mucosa and skin [59].

Chitosan and collagen are the two naturally derived polymers that are most commonly used in tissue engineering [60]. But as chitosan has a polycationic backbone, its electrospinning is hindered by the high viscosities of acid solutions when increasing the polymer concentration, resulting in highly viscous gel.

In the first and up to now more succeeded fabrication of chitosan nanofibers via electrospinning, chitosan-10 (viscosity average molecular weight, $M_v = 2.1 \cdot 10^5$; degree of deacetylation, 0.78) and chitosan-100 ($M_v = 1.3 \cdot 10^6$; degree of deacetylation, 0.77) were used. Chitosan-10 was dissolved in neat TFA (trifluoroacetic acid) at 7 wt%. The addition of dichloromethane to the chitosan - TFA solution improved the homogeneity of the electrospun chitosan fibres [15]. However, two groups have fabricated chitosan nanofibers using a solvent system of 90% acetic acid. The first group, Geng *et al.* used 7 wt% concentration of chitosan (molecular weight of 106000 g/mol) but with a 54% degree of deacetylation (DD) [61]. The second group, De Vrieze *et al.* was able to fabricate fibers using only a 3 wt% solution of chitosan (molecular weight ranging from 190000 to 310000 g mol⁻¹) with a DD of 75-85% [62]. The second more usual method involves the use of poly(ethylene oxide), in order to

reduce the viscosity of chitosan solution so that the solution is spinnable at high polymer concentrations [9,63-66]. Chitosan from crab shells with 85% of deacetylation ($M_w = 190$ kDa) and poly(ethylene oxide) (PEO) ($M_w = 900$ kDa and High $M_w = 5\,000$ kDa) were used. Two percent (2%) chitosan solution and 3% PEO solution were first prepared separately by dissolving chitosan or PEO in 0.5M acetic acid. The chitosan and PEO solutions of different proportions were then mixed to obtain the mixtures with weight ratios of chitosan to PEO ranging from 60/40 to 90/10. In a more recent work surfactants like dodecyltrimethylammonium bromide (DTAB) are added to that system in order to lower surface tension [67].

In our experiments, 2.5 wt% of chitosan solution and 3.0% PEO solution in acetic acid were blended with variable weight ratios of chitosan to PEO [31]. The optima results were obtained at a chitosan/PEO ratio of 60:40 with 20 wt % total acetic acid concentration. The fibers produced, had diameters ranging from 47 to 177 nm. A membrane like cross-linked nanofiber mat was produced on the stationary collector, having an estimated by SEM porosity of 400 nm to 870 nm (Figure 3).

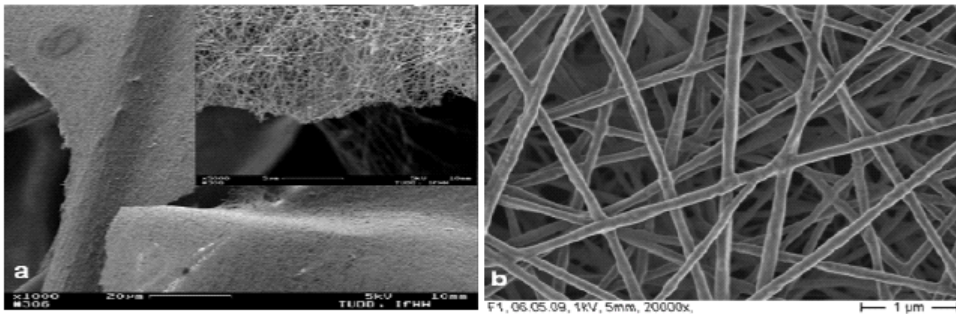


Figure 3. SEM images of 2 wt% chitosan/3 wt% PEO (60:40). (Magnification: a. x1000; insight photo: x5000; b. x20000).

On the contrary of out it was observed by Klossner *et al.* [64], our solutions prepared either with distilled or deionized water, stored at room temperature, were able to produce nanofibers even after six (6) months without need of NaCl addition. The cross-linked nanofiber membranes we have prepared can have possible in vivo applications i.e. in bone regeneration, if combined with other biomaterials in order to improve chitosan's mechanical properties and create structures with predictable pore sizes. In fact, chitosan scaffolds are osteoconductive and can enhance bone formation both in vitro and in vivo. But, in spite of its general acceptance as a tissue biocompatible material, chitosan itself is mechanically rather weak and unstable, and unable to maintain a predefined shape for transplantation as a result of swelling (good tensile strength, but poor bedding behavior).

Several chitosan-blended nanofibers have been fabricated [12], including synthetic polymers such as poly(ethylene oxide) PEO, poly(vinyl alcohol) PVA, poly(lactic acid) PLA and poly(ϵ -caprolactone) (PCL) as well as natural polymers such as collagen, silk fibroin and gelatin (Figure 2b; [35]). Chitosan nanofiber applications are extended to drug release systems and immobilization of enzymes. Jiang *et al.* [68] prepared ibuprofen loaded composite membranes composed of PLGA and PEG-g-chitosan by electrospinning and

Huang *et al.* [69] immobilized lipase in a nanofibrous chitosan/PVA membrane using glutaraldehyde as a coupling agent.

3.2.4. Dextran

Dextran is a bacterial polysaccharide synthesized from sucrose by *L. mesenteroides* and *S. mutans*. It consists of (1,6)-linked α -D glucopyranose structures with some α -1,4 linked branches. Dextran and its derivatives have been used as blood substitutes and drug delivery carriers. Uniform nanofibrous dextran membranes can be prepared by electrospinning using water, a DMSO/water mixture, or a DMSO/DMF mixture as solvents. Up to 10% of BSA or lysozyme can be directly incorporated into the dextran electrospun membrane by electrospinning of protein/dextran aqueous solution. In addition, electrospinning of PLGA/dextran solution in a DMSO/DMF mixture produced a hydrophobic/hydrophilic composite membrane [68]. The same group, Jiang *et al.* [70], prepared biodegradable core-shell structured fibers with poly(ϵ -caprolactone) as the shell and bovine serum albumin (BSA)-containing dextran as the core by coaxial electrospinning.

3.2.5. Heparin

Heparin, a highly-sulfated linear glycosaminoglycan which has the highest negative charge density of any known biological molecule, plays a critical role in regulating various biological activities [3, 40, 71] and has been widely used as an anticoagulant. The most common disaccharide unit of heparin is composed of a 2-*O*-sulfated iduronic acid and 6-*O*-sulfated, *N*-sulfated glucosamine units.

Creating a viable engineered vasculature represents one of the most fundamental challenges in tissue engineering. ECM macromolecules glycosaminoglycans (GAGs) share characteristic linear structures of repeating hexosamine-uronic acid disaccharide units. *Heparin*, and heparan-, chondroitin-, keratin- and dermatan-sulphate GAGs (HS, CS, KS, and DS, respectively) also have tightly regulated regiospecific sulphation patterns, which determine their specific interactions with proteins increasing their uptake. Heparin has been widely incorporated into TE scaffolds to offer a slow release mechanism and modulate the activity of cell-derived signaling factors. It is promising that the outcome of growth factor administration can be improved enormously with the use of technically simple slow-release schemes, such as delivery using polymers.

Degradable heparin loaded PCL or cellulose fiber matrices were successfully fabricated by electrospinning [71, 72]. A sustained release of heparin was achieved from the nanofiber over 14 days, indicating a potential delivery system for the localized administration of heparin to the site of vascular grafts [72].

3.2.6. Hyaluronic Acid

Hyaluronic acid (HA) is a main component of the ECM of connective tissues serving in various important biological functions. It is a linear polysaccharide consisting of alternating disaccharide units of (1,4)-linked α -D-gluconic acid and (1,3)-linked β -*N*-acetyl-D-glucosamine. HA and its derivatives have been extensively used in biomedical areas including wound dressings and implant materials. Because of the high viscosity and surface tension, the fabrication of HA nanofibrous membranes from aqueous solution was successfully carried out only after the development of blowing-assisted electrospinning (electro-blowing system) [73]. HA nanofibers were fabricated using a DMF/water mixture

(mean diameter=200 nm). HA has also been electrospun by blending it with gelatin, PEO, and zein, a major protein in corn. HA-based nanofibrous membranes, possessing excellent biocompatibility and biodegradability, have been extremely attractive as biomimetic tissue engineering scaffolds, wound healing materials, and drug delivery systems.

3.2.7. Starch

Starch, consisting of a large number of glucose units joined together by glycosidic bonds, is the major carbohydrate reserve in plants. It is composed of two types of molecules, amylose (normally 20–30%) and amylopectin (normally 70–80%). Amylose consists of a single linear chain of (1,4)-linked α -D-glucose units while amylopectin is formed by (1,6)-linked branching of the (1,4)-linked α -D-glucose structure. Starch-based nano- and microfiber combined scaffolds were fabricated from a starch/poly(ϵ - caprolactone) blend (30/70, w/w) by a fiber bonding process [74].

3.2.8. Ulvan

Ulvan is a complex acidic sulfated polysaccharide extracted from the cell-walls of the green sea weed *Ulva* (Chlorophyta). The generated and underexploited biomass from proliferating algae in eutrophicated coastal waters represents a low cost source of great potential in renewable polymers such as ulvan. The main disaccharide units that constitute the aldobiuronic acid blocks of ulvan, also reported as ulvanobiuronic acid 3-sulfate, are formed by a Type A_{3s} glucuronorhamnose and a Type B_{3s} iduronorhamnose, arranged in regular sequences within the heteropolymer chain (Figure 4).

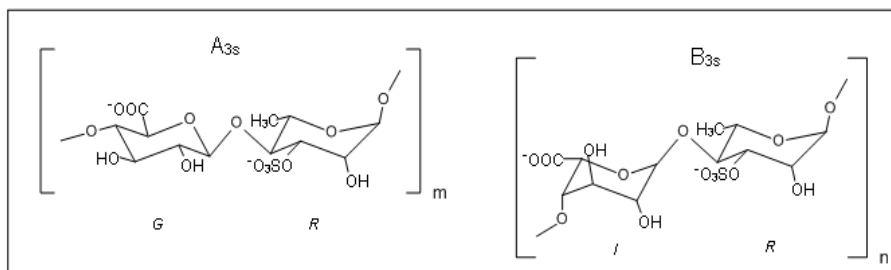


Figure 4. The structure of the main disaccharide units in *Ulva ulvan*: A_{3s} and B_{3s}; G: (1,4)-linked β -D-glucuronic acid; R: (1,4)-linked α -L-rhamnose- 3-sulfate; I: (1,4)-linked α -L-iduronic acid.

This chemical composition could, analogously to mammalian glycosaminoglycans (GAGs), provide this yet greatly unexplored polysaccharide with antithrombogenic properties such as that of *heparin* [75]. Interestingly enough, ulvan has shown several physico-chemical and biological properties that could have a potential impact in many applications. It has been reported as anticoagulant, antioxidant, antitumor and immune modulator, lowering the low-density lipoprotein cholesterol (LDL-cholesterol), thus reducing the atherogenic index, and binding heavy metals [76, 77].

The nanofiber ability of ulvan, originated from the low cost biomass of the alga *Ulva rigida*, has been achieved for the first time via electrospinning by Toskas *et al.* [78]. Ulvan-based uniform nanofibers were produced by being blended with poly(vinyl alcohol) (PVA) at

ratios up to 70:30 of ulvan/PVA. The nanofibers have an average diameter controllable down to 84 nm and present a highly ordered crystalline structure under transmission electron microscopy (TEM) (Figure 5).

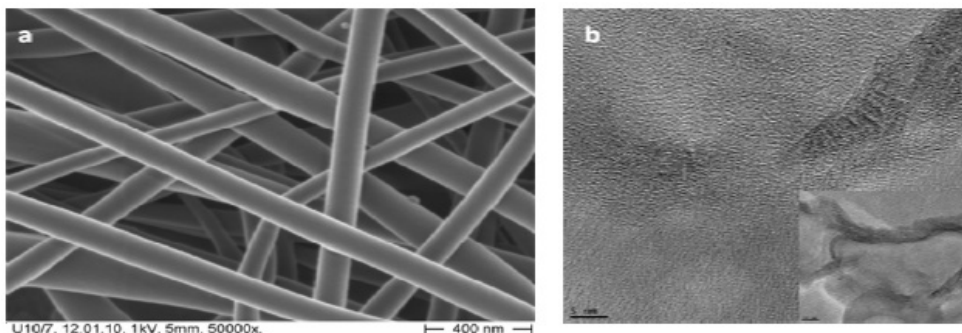


Figure 5. a. SEM image of (a) ulvan/PVA (50:50); (magnification: x50000). b. TEM image of ulvan/PVA (50:50) nanofiber revealing the layered structure: The image shows part of a single nanofiber, presented in the insight image (scale: 10 nm), at higher magnification (scale: 5 nm).

A new complex fiber is created, which results from ulvan and PVA ionic assembly and involves borate esters and divalent cations. The spinnability of this anionic sulfated polysaccharide in combination with its interesting biological and physicochemical properties can lead to new biomedical applications such as drug release systems. Finally, the biocompatibility and bioactivity, currently under investigation, of this promising biopolymer could unveil a potential biomaterial from cheap natural resources.

CONCLUSION

According to Langer, enormous challenges remain for the field of regenerative medicine and tissue engineering, even if over 20 different tissues have been yet engineered [79]. There are many cases such as liver failure and spinal cord repair that the disease treatment based on classical drugs or therapeutic methods cannot be medicated. Such situations can be handled with transplantation or better with regenerative medicine and living tissue replacement, reducing thereby the dependence on donor tissue and organs. Within the context of tissue engineering and regenerative medicine, there continues to be a clear and present need to develop advanced materials design and processing methods that can better replicate the exquisite architecture and functional properties of native tissues. Future generations of tissue engineering scaffolds are considered to provide tissue-like mechanical properties as well as micro-to-nanoscale structural features capable of modulating tissue regeneration at the cell level [80].

The use of natural polymers, for the development of biocompatible materials serving as scaffolds, provides many of the instructive cues which are required for the cells attachment and proliferation. This fact induces the biocompatible and biomimetic character of these naturally derived materials. Nanofibers derived from natural polymers and obtained mainly via electrospinning have shown a great potential in regenerative medicine. In this chapter, the

most recent and state-of-the art work on natural nanofibers applications in tissue engineering and other related fields as drug release have been briefly discussed.

Several material issues remain to be tackled, e.g. the problem of batch-to-batch quality variation, the limited solubility of many natural polymers such as cellulose and chitosan, the mechanical properties and the interaction with biological systems such as growth factors and cells. Future critical challenges include synthesis of new derivatives, hybrids of natural and synthetic polymers, fabrication of novel core-shell nanofibers, surface tailored chemistries and development of electrospinning engineering parameters such as blowing-assisted device and rotating collector supplying aligned nanofibers. Another issue concerns the density of nanofibers and subsequently the porosity of nanofibrous scaffolds. Nanoscale scaffolds deploy more binding sites to cell membrane receptors and have greater surface areas for protein absorption. This has a significant importance in tissue engineering of vascular grafts. However, small pores in nanofiber meshes are not advantageous for all applications. In a 3-dimensional scaffold, cells need sufficient space to infiltrate and migrate, and this requires pores of approximately 10 μm . The fabrication of micro/nanofiber composites has been proved advantageous in the only few cases tested [81, 82]. In this combination, one can benefit from both the strength provided by the knitted structure of the microfiber and the cell-seeding ability of the spun nanofiber mesh. The use of nanofibers from natural biopolymers in regenerative medicine will continue to expand towards clinical applications. Textile materials scientists and engineers could afford solutions on a real technical scale, e.g. by developing natural fibers with improved properties and constructing tailored knitted scaffolds for tissue replacement. Closer collaboration among scientists and clinicians could advance the in vivo studies and final applications of these textile scaffolds.

REFERENCES

- [1] Schindler, W.D. and Hauser, P.J. (2004). In: *Chemical finishing of textiles*. Cambridge: Woodhead Publishing Ltd and CRC Press LLC, p. 198-206 and 169-171.
- [2] Peppas, N. A. and Langer, R. (2004). Origins and development of biomedical engineering within chemical engineering. *AIChE Journal*, 50: 536-545.
- [3] Place E. S., Evans N. D., and Stevens M.M. (2009). Complexity in biomaterials for tissue engineering. *Nature Materials*, 8: 457-470.
- [4] Vacanti, J. P. and Vacanti, C. A. (1997). In: *Principles of Tissue Engineering*. Georgetown, TX: R. G. Landes Company, p.1.
- [5] Mano, J. F., and Reis, R. L. (2007). Osteochondral defects: present situation and tissue engineering approaches. *Journal of Tissue Engineering and Regeneration Medicine*, 1, 261-273.
- [6] Jagur-Grodzinski, (2006). Polymers for tissue engineering, medical devices and regenerative medicine. Concise general review of recent studies. *Polymers for Advanced Technologies*, 17: 395-418.
- [7] Kadler, K. (2004). Matrix loading: assembly of extracellular matrix collagen fibrils during embryogenesis. *Birth Defects Research Part C Embryo Today*, 72: 1-11.

-
- [8] Teixeira, A. I., Abrams, G. A., Bertics, P. J., Murphy, C. J., and Nealey, P. F. (2003). Epithelial contact guidance on well-defined micro-and nanostructured substrates. *Journal of Cell Science*, 116: 1881–1892.
- [9] Bhattarai, N., Edmondson, D., Veiseh, O., Matsen, F. A., and Zhang, M. (2005). Electrospun chitosan-based nanofibers and their cellular compatibility. *Biomaterials*, 26: 6176–6184.
- [10] Venugopal, J. and Ramakrishna, S. (2005). Applications of Polymer Nanofibers in Biomedicine and Biotechnology. *Applied Biochemistry and Biotechnology*, 125: 147–157.
- [11] Greiner, A. and Wendorf, J. H. (2007). Electrospinning: A fascinating method for the preparation of ultrathin fibers. *Angewandte Chemie*, 46 (30): 5670–5703.
- [12] Lee, K. Y., Jeong, L., Kang, Y. O., Lee, S. J., and Park, W. H. (2009). Electrospinning of polysaccharides for regenerative medicine. *Advanced Drug Delivery Reviews*, 61: 1020–1032.
- [13] Ramakrishna, S., Fujihara, K., Teo, W. E., Lim, T. C., and Ma, Z. (2005). In: *An Introduction to Electrospinning and Nanofibers*. Hackensack, NJ, London: World Scientific Publishing Co. Pte. Ltd., p. 22–86.
- [14] Reneker, D. H., Yarin, A. L., Fong, H., and Koombhongse, S. (2000). Bending instability of electrically charged liquid jets of polymer solutions in electrospinning. *Journal of Applied Physics*, 87: 4531–4547.
- [15] Ohkawa, K., Cha, D., Kim, H., Nishida, A., and Yamamoto, H. (2004). Electrospinning of Chitosan. *Macromolecular Rapid Communications*, 25 (18): 1600–1605.
- [16] Boudou, T., Crouzier, T., Ren, K., Blin, G., and Picart, C. (2009). Multiple Functionalities of Polyelectrolyte Multilayer Films: New Biomedical Applications. *Advanced Materials*, 21: 1–27.
- [17] Kidoaki, S., Kwon, I. K., and Matsuda, T. (2005). Mesoscopic spatial designs of nano- and microfiber meshes for tissue-engineering matrix and scaffold based on newly devised multilayering and mixing electrospinning techniques. *Biomaterials*, 26: 39–46.
- [18] Fukuda, J., Khademhosseini, A., Yeh, J., Eng, G., Cheng, J., Farokhzad, O. C., and Langer, R. (2006). Micropatterned cell co-cultures using layer-by-layer deposition of extracellular matrix components. *Biomaterials*, 27: 1479–1486.
- [19] Buschle-Diller, G., Hawkins, A., and Cooper, J. (2006). In: *Modified Fibers with Medical and Specialty Applications*. Netherlands: Springer, p. 67–80.
- [20] Agarwal, S., Wendorf, J. H., and Greiner, A. (2009). Progress in the Field of Electrospinning for Tissue Engineering Applications. *Advanced Materials*, 21: 3343–3351.
- [21] Sill, T.J. and von Recum, H.A. (2008). Electrospinning: Applications in drug delivery and tissue engineering. *Biomaterials*, 29: 1989–2006.
- [22] Parry, D. and Craig, A. (1988). In: *Collagen fibrils during development and maturation and their contribution to the mechanical attributes of connective tissue*. Boca Raton, FL: CRC Press, p 2.
- [23] Huang, L., Nagapudi, K., Apkarian, R. P., and Chaikof, E. L. (2001). Engineered collagen-PEO nanofibers and fabrics. *Journal of Biomaterials Science Polymer Ed.*, 12: 979–993.
- [24] Huang, L., Apkarian, R. P., and Chaikof, E. L. (2001). High-resolution analysis of engineered type I collagen nanofibers by electron microscopy. *Scanning*, 23: 372–375.

-
- [25] Matthews, J. A., Wnek, G. E., Simpson, D. G., and Bowlin G. L. (2002). Electrospinning of collagen nanofibers. *Biomacromolecules*, 3(2): 232–238.
- [26] Zhong, S., Teo, W. E., Zhu, X., Beuerman, R., Ramakrishna, S., and Yung, L. Y. (2005). Formation of collagen-glycosaminoglycan blended nanofibrous scaffolds and their biological properties. *Biomacromolecules*, 6: 2998–3004.
- [27] Buttafoco, L., Kolkman, N. G., Engbers-Buijtenhuijs, P., Poot, A. A., Dijkstra, P. J., Vermes, I., and Feijen, J. (2006). Electrospinning of collagen and elastin for tissue engineering applications. *Biomaterials*, 27: 724–734.
- [28] Zeugolis, D. I., Khew, S. T., Yew, E. S. Y., Ekaputra, A. K., Tong, Y. W., Yung, L. Y. L., Hutmacher, D. W., Sheppard, C., and Raghunath, M. (2008). Electro-spinning of pure collagen nano-fibers – Just an expensive way to make gelatin. *Biomaterials*, 29: 2293–2305.
- [29] Yang, L., Fitie, C. F. C., van der Werf, K. O., Bennink, M. L., Dijkstra, P. J., and Feijen, J. (2008). Mechanical properties of single electrospun collagen type I fibers. *Biomaterials*, 29: 955–962.
- [30] Kaeosomboon W. *Collagen/PVA nanofibers via electrospinning process*, Master Thesis, Nr. 1346, 2008, ITB/MW, Technische Universität Dresden, Germany.
- [31] Toskas, G., Laourine, E., Kaeosomboon, W., and Cherif, C. (2009). Electrospinning of collagen and chitosan in perspective of medical scaffolds applications. In: *International Conference on Latest Advancements in High Tech Textiles and Textile-based Materials*, Gent, Belgium.
- [32] Agarwal, S., Wendorf, J. H., and Greiner, A. (2008). Use of electrospinning technique for biomedical applications. *Polymer*, 49: 5603–5621.
- [33] Sell, S. A., McClure, M. J., Garg, K., Wolfe, P. S., and Bowlin, G. L. (2009). Electrospinning of collagen/biopolymers for regenerative medicine and cardiovascular tissue engineering. *Advanced Drug Delivery Reviews*, 61 (12): 1007–1019.
- [34] Li, M., Mondrinos, M. J., Gandhi, M. R., Ko, F. K., Weiss, A. S., and Lelkes, P. I. (2005). Electrospun protein fibers as matrices for tissue engineering. *Biomaterials*, 26: 5999–6008.
- [35] Toskas G. et al., *unpublished results*, ITM, Technische Universität Dresden, Germany.
- [36] Wnek, G. E., Carr, M., Simpson, D. G., and Bowlin, G. L. (2003). Electrospinning of nanofiber fibrinogen structures. *Nano Letters*, 3: 213–216.
- [37] Zhang, X., Baughman, C. B., and Kaplan, D. L. (2008). In vitro evaluation of silk fibroin scaffolds for vascular cell growth. *Biomaterials*, 29: 2217–2227.
- [38] Soffer, L., Wang, X., Zhang, X., Kluge, J., Dorfmann, L., Kaplan, D., and Leisk, G. (2008). Silk-based electrospun tubular scaffolds for tissue-engineered vascular grafts *Journal of Biomaterials Science Polymer Ed.*, 19(5): 653–664.
- [39] Christman, K. L. and Randall, L. (2006). Biomaterials for the Treatment of Myocardial Infarction. *Journal of the American College of Cardiology*, 48 (5): 907–913.
- [40] Weber, M. J., Han, X., Prasanna Murthy, S. N., Rajangam, K., Stupp, S. I., and Lomasney, J. W. (2010). Capturing the stem cell paracrine effect using heparin-presenting nanofibers to treat cardiovascular diseases. *Journal of Tissue Engineering and Regenerative Medicine*, 4 (8): 600–610.
- [41] Bhattarai, N. and Zhang, M. (2007). Controlled synthesis and structural stability of alginate based nanofibers. *Nanotechnology*, 18: 455–601.

-
- [42] Hashimoto, T., Suzuki, Y., Tanihara, M., Kakimaru, Y., and Suzuki, K. (2004). Development of alginate wound dressings linked with hybrid peptides derived from laminin and elastin. *Biomaterials*, 25: 1407–1414.
- [43] Li, Z. and Zhang, M. (2005). Chitosan-alginate as scaffolding material for cartilage tissue engineering. *Journal of Biomedical Materials Research*, 75A: 485–493.
- [44] Alsberg, E., Anderson, K. W., Albeiruto, A., Rowley, J. A., and Mooney, D. J. (2002). Engineering growing tissues *Proceedings National Academy of Science USA*, 99: 12025–12030.
- [45] Li, Z., Ramay, H. R., Hauch, K. D., Xiao, D., and Zhang, M. (2005). Chitosan-alginate hybrid scaffolds for bone tissue engineering. *Biomaterials*, 26: 3919–3928.
- [46] Yang, J., Chung, T. W., Nagaoka, M., Goto, M., Cho, C.S., and Akaike, T. (2001). Hepatocyte-specific porous polymer-scaffolds of alginate/galactosylated chitosan sponge for liver tissue engineering. *Biotechnology Letters*, 23: 1385–1389.
- [47] Chung, T. W., Yang, J., Akaike, T., Cho, K. Y., Nah, J. W., Kim, S. I., and Cho, C. S. (2002). Hepatocyte-specific porous polymer-scaffolds of alginate/galactosylated chitosan sponge for liver tissue engineering. *Biomaterials*, 23: 2827–2834.
- [48] Dar, A., Shachar, M., Leor, J., and Cohen, S. (2002). Cardiac tissue engineering-optimization of cardiac cell seeding and distribution in 3D porous alginate scaffolds. *Biotechnology and Bioengineering*, 80: 305–312.
- [49] Nie, H., He, A., Zheng, J., Xu, S., Li, J., and Han, C. C. (2008). Effects of Chain Conformation and Entanglement of Pure Alginate. *Biomacromolecules*, 9: 1362–1365.
- [50] Liu, H.; Hsieh, Y. (2003). Surface methacrylation and graft copolymerization of ultrafine cellulose fibers. *Journal of Polymer Science Part B Polymer Physics*, 41: 953–964.
- [51] Son, W. K., Youk, J. H., Lee, T. S., and Park, W. H. (2004). Electrospinning of ultrafine cellulose acetate fibers: studies of a new solvent system and deacetylation of ultrafine cellulose acetate fibers. *Journal of Polymer Science Part B Polymer Physics*, 42: 5–11.
- [52] Tungprapa, S., Puangparn, T., Weerasombut, M., Jangchud, I., Fakum, P., Semongkhon, S., Meechaisue, C., and Supaphol, P. (2007). Electrospun cellulose acetate fibers: effect of solvent system on morphology and fiber diameter. *Cellulose*, 14: 563–575.
- [53] Han, S. O., Youk, J. H., Min, K. D., Kang, Y. O., and Park, W. H. (2008). Electrospinning of cellulose acetate nanofibers using a mixed solvent of acetic acid/water: Effects of solvent composition on the fiber diameter. *Materials Letters*, 62: 759–762.
- [54] Stankus, J. J., Freytes, D. O., Badylak, S. F., and Wagner, W. R. (2008). Hybrid nanofibrous scaffolds from electrospinning of a synthetic biodegradable elastomer and urinary bladder matrix. *Journal of Biomaterials Science Polymer Ed.*, 19: 635–652.
- [55] Taepaiboon, P.; Rungsardthong, U., and Supaphol, P. (2007). Vitamin-loaded electrospun cellulose acetate nanofiber mats as transdermal and dermal therapeutic agents of vitamin A acid and vitamin E. *European Journal of Pharmaceutics and Biopharmaceutics*, 67: 387–397.
- [56] Tungprapa, S., Jangchud, I., and Supaphol, P. (2007). Release characteristics of four model drugs from drug-loaded electrospun cellulose acetate fiber mats. *Polymer*, 48: 5030–5041.

-
- [57] Suwanton, O., Opanasopit, P., Ruktanonchai, U., and Supaphol, P. (2007). Electrospun cellulose acetate fiber mats containing curcumin and release characteristic of the herbal substance *Polymer*, 48: 7546–7557.
- [58] Suwanton, O., Ruktanonchai, U., and Supaphol, P. (2008). Electrospun cellulose acetate fiber mats containing asiaticoside or Centella asiatica crude extract and the release characteristics of asiaticoside. *Polymer*, 49: 4239–4247.
- [59] Noh, H. K., Lee, S. W., Kim, J. M., Oh, J. E., Kim, K. W., Chung, C. P., Choi, S. C., Park, W. H., and Min, B. (2006). Electrospinning of chitin nanofibers: degradation behavior and cellular response to normal human keratinocytes and fibroblasts. *Biomaterials*, 27: 3934–3944.
- [60] Kumar, M. N. V. R. (2000). A review of chitin and chitosan applications. *Reactive and Functional Polymers*, 46: 1–27.
- [61] Geng, X. Y., Kwon, O. H., and Jang, J. H. (2005). Electrospinning of chitosan dissolved in concentrated acetic acid solution. *Biomaterials*, 26: 5427–5432.
- [62] De Vrieze, S., Westbroek, P., Van Camp, T., and Van Langenhove, L. (2007). Electrospinning of chitosan nanofibrous structures: feasibility study. *Journal of Materials Science*, 42: 8029–8034.
- [63] Duan, B., Dong, C., Yuan, X., and Yao, K. (2004). Electrospinning of chitosan solutions in acetic acid with poly(ethylene oxide). *Journal of Biomaterials Science Polymer Ed.*, 15(6): 797–811.
- [64] Klossner, R.R., Queen, H.A., Andrew, J., Coughlin, A.J., and Krause, W.E. (2008). Correlation of Chitosan's Rheological Properties and Its Ability to Electrospin. *Biomacromolecules*, 9: 2947–2953.
- [65] Desai, K., Kit, K., Li, J., and Zivanovic, S. (2008). Morphological and surface properties of electrospun chitosan nanofibers. *Biomacromolecules*, 9: 1000–1006.
- [66] Zhang, Y. Z., Su, B., Ramakrishna, S., and Lim, C. T. (2008). Chitosan Nanofibers from an Easily Electrospinnable UHMWPEO-Doped Chitosan Solution System. *Biomacromolecules*, 9: 136–141.
- [67] Kriegel, C., Kit, K. M., McClements, D. J., and Weiss, J. (2009). Electrospinning of chitosan-poly(ethylene oxide) blend nanofibers in the presence of micellar surfactant solutions. *Polymer*, 50: 189–200.
- [68] Jiang H., Fang D., Hsiao B., Chu B., and Chen W. (2004). Preparation and characterization of ibuprofen-loaded poly(lactide-co-glycolide)/poly(ethylene glycol)-g-chitosan electrospun membranes. *Journal of Biomaterials Science Polymer Ed.*, 15: 279–296.
- [69] Huang, X., Ge, D., and Xu, Z. (2007). Preparation and characterization of stable chitosan nanofibrous membrane for lipase immobilization. *European Polymer Journal*, 43: 3710–3718.
- [70] Jiang, H.L., Hu, Y.Q., Zhao, P.C., Li, Y., and Zhu, K.J. (2006). Modulation of protein release from biodegradable core-shell structured fibers prepared by coaxial electrospinning. *Journal of Biomedical Materials Research Part B: Applied Biomaterials*, 79B: 50–57.
- [71] Viswanathan, G., Murugesan, S., Pushparaj, V., Nalamasu, O., Ajayan, P. M., and Linhardt, R. J. (2007). Preparation of biopolymer fibers by electrospinning from room temperature ionic liquids. *Biomacromolecules*, 6: 415–418.

-
- [72] Luong-Van, E., Grondahl, L., Chua, K. N., Leong, K. W., Nurcombe, V., and Cool, S. M. (2006). Controlled release of heparin from poly(ϵ -caprolactone) electrospun fibers. *Biomaterials*, 27: 2042–2050.
- [73] Um, I. C., Fang, D., Hsiao, B. S., Okamoto, A., and Chu, B. (2004). Electro-spinning and electroblowing of hyaluronic acid. *Biomacromolecules*, 5: 1428–1436.
- [74] Tuzlakoglu, K., Bolgen, N., Salgado, A. J., Gomes, M. E., Piskin, E., and Reis, R. L. (2005). Nano- and micro-fiber combined scaffolds: a new architecture for bone tissue engineering. *Journal of Materials Science: Materials in Medicine*, 16: 1099–1104.
- [75] Chupa, J. M., Foster, A. M., Sumner, S. R., Madihally, S. V., and Matthew, H. W. (2000). Vascular cell responses to polysaccharide materials: in vitro and in vivo evaluations. *Biomaterials*, 21: 2315–2322.
- [76] Lahaye, M. and Robic, A. (2007). Structure and Functional Properties of Ulvan, a Polysaccharide from Green Seaweeds. *Biomacromolecules*, 8: 1765–1774.
- [77] Morelli, A. and Chiellini, F. (2010). Ulvan as a New Type of Biomaterial from Renewable Resources: Functionalization and Hydrogel Preparation. *Macromolecular Chemistry and Physics*, 211: 821–832.
- [78] Toskas, G., Hund, R. D., Laourine, E., Cherif, C., Smyrniotopoulos, V., and Roussis, V. (2011). Nanofibers Based on Polysaccharides from the Green Seaweed *Ulva Rigida*. *Carbohydrate Polymers*, 84: 1093–1102.
- [79] Langer, R. (2009). Perspectives and Challenges in tissue Engineering and Regenerative Medicine. *Advanced Materials*, 21: 3235–3236.
- [80] Freed, L. E., Engelmayer, G. C. Jr., Borenstein, J. T., Moutos, F. T., and Guilak, F. (2009). Advanced Material Strategies for Tissue Engineering Scaffolds. *Advanced Materials*, 21: 3410–3418.
- [81] Pham, Q. P., Sharma, U., and Mikos, A. G. (2006). Electrospun poly(ϵ -caprolactone)microfiber and multilayer nanofiber/microfiber scaffolds: characterization of scaffolds and measurement of cellular infiltration. *Biomacromolecules*, 7: 2796–2805.
- [82] Van Lieshout, M. I., Vaz, I. C. M., Rutten, M. C. M., and Peters, G. W. M. (2006). Electrospinning versus knitting: two scaffolds for tissue engineering of the aortic valve. *Journal of Biomaterials Science Polymer Ed.*, 17: 77–89.

Chapter 6

DEVELOPMENT OF TEXTILES CUSTOMIZED AS REINFORCEMENT TO CEMENTITIOUS MATRICES

S. W. Mumenya*

Department of Civil and Construction Engineering,
University of Nairobi, Nairobi, Kenya.

ABSTRACT

During the ancient Roman civilization, discrete fibers were used to reinforce brittle matrices such as mortar and clay in order to improve the tensile load carrying capacity of the brittle matrices. Natural fibers such as: horse hair, sisal, and grass were employed in their natural form. With the advent of cement and concrete construction at the beginning of the 19th century, the need for reinforcement, and the potential of fibers was well understood.

Since the early 19th century, asbestos fibers were known to be effective in reinforcing cement mortar to produce a composite referred to as “asbestos cement”. Indeed, during this period, asbestos-cement industry was most successful owing to the strong chemical bond that develops at the fiber/matrix interface. However, since mid 19th century exposure to asbestos was known to be a health hazard. Therefore, research has been on-going for a suitable replacement to “asbestos cement”. Over the years, there has been an increasing trend in general acceptance of fibers as reinforcement to brittle cementitious matrices.

The development of fiber reinforced cementitious composites can be traced back to the 1960's when straight short discrete steel fibers were mixed into mortar and concrete for construction of slabs on grade. Later, other fiber types were accepted for use in cementitious matrices. This insight was the driving force in innovations that occurred in mid 1970's involving new techniques of production of polypropylene fibers.

Since 1990's, the manufacture and processing of different fiber types has been customized for cement-based applications. Among these fibers are steel, Alkali Resistant (AR) glass, carbon, polymeric fibers, as well as naturally occurring fibers. Similarly, for textiles, the innovations in the individual fibers has led to new processing and

* E-mail: wsiphila@uonbi.ac.ke

manufacturing techniques aimed at making the textiles adaptable to cementitious composites.

To date, the use of fibers and textiles in cementitious composites have been adopted in many countries, for example, South Africa, India, United States of America, Germany, as well as in Kenya and other East African countries.

This chapter describes the development of the unique technology of manufacture of firstly the basic fibers, and secondly, textiles woven from the fibers for application in cementitious matrices. This Chapter is dealt with the advantages of treated sisal fibers and also discussed the manufacturing techniques of the fibers and textiles for adaptation in cementitious matrices.

ABBREVIATIONS, ACRONYMS AND SYMBOLS

AR	Alkali resistant
CMCs..	Ceramic Matrix Composites
CH ₃ ...	Methyl group
C=C..	Carbon to carbon double bond
°C	Degrees Centigrade
Denier	A unit of fiber fineness, equal to one gram per 9,000 meters of yarn
D'tex	Weight per kilometer of fiber in grams
d'tex.	10 kilometers of a d'tex of filament (weight=3 grams)
°F	Degrees Fahrenheit
f _{cu}	Concrete crushing strength
GFRP	Glass-Fiber Reinforced Plastic
G	gram
g cm ⁻³	gram per cubic centimeter
H ⁺	Hydrogen ion
LPDE	Low-density polyethylene
Km	Kilometer
m	Meter
kg m ⁻³	Kilograms per cubic meter
kN m ⁻²	Kilonewton per square meter
mm	Millimeter
MMCs	Metal Matrix Composites
MPa	Mega Pascal
N m ⁻²	Newton per square meter
OH ⁻	Hydroxide ion
PAN	Poly(acrylonitrile)
PE	Polyethylene
PETE (PET)	Polyethylene Terephthalate
PMCs	Polymer Matrix Composites
PP	Polypropylene
PVA	Poly Ethyl Alcohol
PVC	Poly Vinyl Chloride
SFRC	Steel Fiber Reinforced Concrete

SFRS	Steel Fiber Reinforced Shortcrete
TC	Textile concrete
TRC	Textile Reinforced Concrete
tex	1tex = g/km
W/mK	Watt per meter Kelvin
WWF	Welded Wire Fabric
E	Young's Modulus of Elasticity
ρ	Density
ε	Strain
σ	Stress
Mm	Micrometer

1. INTRODUCTION

1.1. Historical Use of Binder

The use of natural cement as a binding material for bricks can be traced back to well before the Roman times during the construction of the great pyramids of Giza [1]. This cement was composed of a mixture of pozzolanic ash and clay, which, if left in contact with the atmospheric air and water, was found to harden since it had a hydraulic property. This behavior aroused curiosity among the builders of the time who sought its deeper understanding. Over the years, the cement was used in the same natural state although the desire to understand its other properties and to experiment with it did not die off.

1.2. Concrete as a Traditional Building Material

Concrete is one of the most widely used construction material largely due to its rapid development during the 20th century. Concrete has the advantage that it can be delivered to site in a plastic state. This unique quality makes concrete desirable as a building material because it can be molded to virtually any form or shape. In addition, concrete provides a wide range of surface textures and colors and can be used to construct different types of structures, such as multi-storey buildings, highways, bridges, dams, airport runways, irrigation structures, breakwaters, piers and docks, sidewalks, silos and farm buildings, homes, and even barges and ships [1].

In its most basic form concrete is a composite material produced by mixing cement with ballast/stone, sand (aggregates) and water, which hardens as a result of hydraulic reaction between cement and water. Depending on the specified requirements during service, admixtures could be added to concrete mix to improve workability and strength.

Evidence of the use of concrete in buildings goes back to well before Roman times during the construction of the Great Pyramids of Giza in Egypt [2]. The Romans also left evidence of their skill in using an early form of concrete in the remains of buildings such as the Pantheon in Rome. The Pantheon, which is one of the most famous buildings in the world, was commissioned by Hadrian in A.D. 118, and was completed in A.D. 128. At one time it

had a colonnaded court leading to the portico. The dome of the rotunda behind the portico is 43.2 m in diameter. The oculus (a round opening) at the top is 8.5 m in diameter and provides the only source of light for the interior [3].

In the 1st century A.D., there was increase in the use of concrete by Romans architects, who molded arches, vaults, and even domes from concrete and faced them with bricks for added strength [4]. These early form structures were decorated with an exterior layer of marble or stucco.

After the death of a famous Roman Emperor Nero, his successor, Vespasian constructed a great amphitheater on the ruins of Nero's official residence in Rome as a palace for the masses. The construction of the amphitheatre went on between 70 A.D. and 82 A.D [5]. The amphitheatre is best known for its multilevel system of vaults made of concrete. It is called the Colosseum after a colossal statue of Nero that once stood nearby, but its real name is the Flavian Amphitheater. It was used for staged battles between lions and Christians, among other spectacles, and is one of the most famous pieces of architecture in the world [6].



Figure 1. Use of concrete in historical buildings.

Concrete enabled the architects of the great amphitheater to build tunnels that allowed easy access for spectators. This feature is still included in the design of modern football stadia. The use of concrete also allowed the Romans to enclose larger spaces for their baths and other rectangular structures called basilicas.

Mortar has historically been used for construction of buildings at the coastal towns of Kenya. For example, the historic site known as Gedi at the coastal towns of Kenya consists of the ruins of a fifteenth century Arab-African town, typical of a number of such towns up and down the coast of East Africa. The buildings have architectural features such as columns and arches built using traditional Islamic architecture. Figure 1 shows (a) part layout plan of a palace that was constructed in 1339, referred to as at Gedi Ruins and (b) Mihrab that is still standing on the North Wall of a Mosque at Gedi Ruins that was constructed at the palace using coral stones and mortar joints.

1.3. Portland Cement

The production of the world's first Portland cement dates back to 1824 when Joseph Aspdin of Leeds took out a patent on the cement he had produced [7]. This cement was formed by heating a mixture of finely divided clay and limestone or chalk in a furnace to a

temperature sufficiently high to drive off all the carbon dioxide. He called it Portland cement because he thought it resembled Portland stone in color. (Portland stone is a yellowish-white limestone quarried in the Isle of Portland, on the Dorset coast of southwest England). The properties of the cement could be pre-determined.

This artificial form of cement has gradually been improved over the years to the high quality Portland cement widely used today [7, 8]. There have been many developments in the manufacture of cement, and modern Portland cement is now made to high standards in most parts of the world [8]. Figure 2 shows Kilifi Bridge, an example of modern bridge structure over an estuary at the Kenyan coast. The bridge is built in lightweight and durable concrete which has been reinforced with steel bars and mesh.

1.4. Reinforced Concrete

Hardened cement paste itself is brittle when subjected to normal tensile stresses and impact loads. Therefore, on its own it is not ideal for many building applications, however, when combined with aggregates and used in compression, it is very hard and strong, and a high compressive strength (up to 100 MPa) is easily achievable [9]. This is ideal for compression members in structures but for bending and tension members, conventional concrete has a low tensile strength (1-4 MPa). As a result, in conventional concrete construction, other means have been used to compensate for this low tensile strength, including steel reinforcing in the form of bars (or mesh) or through various “small fiber” composite additions. It is this aspect of these fiber cement composites that is the focus of this chapter.



Figure 2. Use of concrete in modern structures.

Traditionally, steel reinforcement is cast in concrete to carry the bending tensile stresses, whilst relying on the concrete to carry the bending compressive stresses. The use of mild steel bars (commonly referred to as rebars) placed in the tension zone of a section in relatively small amounts provides the necessary tensile strength resistance. The bars are referred to as primary reinforcement. This technique provides a practical solution to the brittleness of concrete. Hence the term “reinforced concrete” that is in general use in construction [8]. Figure 3 illustrates schematically the flexural action in a reinforced concrete beam element and the role of primary reinforcement.

Rebars are available in various forms and sizes. They are either high yield square twisted bars, high yield ribbed bars, or round mild steel bars, with sizes ranging between 6 and 32 mm in diameter. Their application as primary reinforcement depends on the structural design of the concrete structure or element under consideration.

The second form of reinforcement in concrete is referred to as secondary reinforcement. This is non-structural in nature. Secondary reinforcement caters for the minimization and possible prevention of certain non-structural deformations in concrete such as the inhibition of cracking.

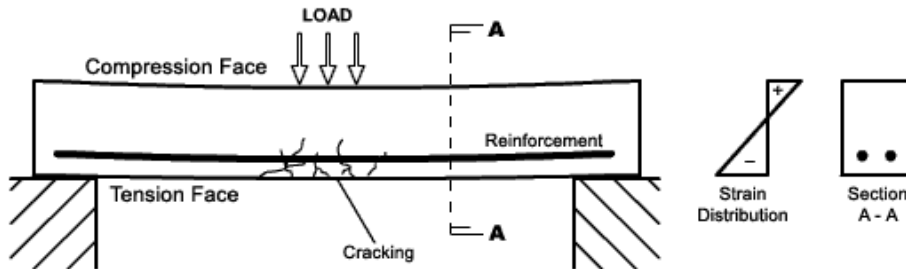


Figure 3. Flexural action in reinforced concrete.

Secondary reinforcement is mainly employed in different structural elements, for example ground floor slabs that do not require primary reinforcement for strength. A traditional form of secondary reinforcement is welded wire fabric (WWF), commonly known as wire mesh.

1.5. Composite Materials

A composite material is made up of a combination of two or more different materials. A composite material can provide superior and unique mechanical and physical properties because it combines the most desirable properties of its constituents. For example, a glass-fiber reinforced plastic (GFRP or fiberglass) combines the high strength of thin glass fibers with the ductility and chemical resistance of plastic; the brittleness that the glass fibers have when isolated is therefore not a characteristic of the composite.

Composites make up a very broad and important class of engineering materials and are used in a wide variety of applications. The world annual production of composites is over 10 million tons and the market has in recent years been growing at 5-10 per cent per annum [9]. The opportunity to develop superior products for aerospace, automotive, and recreational applications has sustained the interest in advanced composites.

Currently, composites are being considered for wider applications that include civil engineering structures such as bridges and freeway pillar reinforcement; and for biomedical products, such as prosthetic devices. Table 1 lists some typical applications of composites in modern industries [10].

1.5.1. Use of Composites in Ancient Civilizations

Although the development of composite materials is a modern concept, the use of high strength fibers to stiffen and strengthen cheap matrices is probably older than the wheel itself. Indeed, straw and horsehair have been used to reinforce mud bricks (by improving their fracture toughness) for at least 5000 years [11]. For example, in ancient Babylon, one of the lesser wonders of the ancient world was the route followed by cultic and political leaders for the New Year's festival ceremonies (the "Processional Way"). The route was built of bitumen which was reinforced with plaited straw.

The other common composite materials which have been known since the ancient Roman times are paper and concrete. Similarly, almost all natural materials such as wood, bone, muscle, teeth and hide are composites with complex internal structures designed to give mechanical properties that adapt to different applications. The manufactured of composite materials to be adaptable to different engineering applications requires input from the field of materials science.

1.5.2. Mechanics of Composite Action

Most of manufactured composite materials consist of synthetic fibers embedded in and tightly bound by the matrix [12]. Therefore, a composite can be visualized as being made up of three phases; matrix, the reinforcing phase (or reinforcement), and the fiber/matrix interface. The reinforcement is either fibrous or particulate [13].

Table 1. Applications of composites in modern industries

Industrial Sector	Examples of Composites
Aerospace	Wings, fuselage, antennae, tail-planes, helicopter blades, landing gears, seats, floors, interior panels, fuel tanks, rocket motor cases, nose cones, launch tubes.
Automobile	Body panels, cabs, spoilers, consoles, instrument panels, lamp housings, bumpers, leaf springs, drive shafts, rears, bearings.
Boats	Hulls, decks, masts, engine shrouds, interior panels.
Chemical	Pipes, tanks, pressure vessels, hoppers, valves, pumps, impellers.
Domestic	Interior and exterior panels, chairs, tables, baths, shower units, ladders.
Electrical	Panels, housings, switchgear, insulators, connectors.
Leisure	Motor homes, caravans, trailers, golf clubs, racquets, protective helmets, skis, archery bows, surfboards, fishing rods, canoes, pools, diving boards, playground equipment.

The reinforcing phase normally comprises of fibers or particles with at least one of the dimensions much smaller than the other, say less than 500 μ m and sometimes only in the order of a micron. This phase enhances the mechanical properties of the matrix. In some types of composites, the reinforcement is stronger and stiffer (more brittle) than the matrix. For example a ceramic matrix reinforced with metallic fibers. In other types of composites, the reinforcement is less stiff (more ductile) than the matrix, for example, rubber-like reinforcement embedded in a brittle polymer matrix.

The geometry of the reinforcing phase is a major parameter in determining the effectiveness of the reinforcement; thus, the mechanical properties of composites are a

function of the shape and dimensions of the reinforcement. Figure 4 represents a commonly employed classification scheme for composite materials [13].

Particulate reinforcements have dimensions that are approximately equal in all directions. The shape of the reinforcing particles may be spherical, cubic, platelet or any regular or irregular geometry. The arrangement of the particulate reinforcement may be random or with a preferred orientation. In the majority of particulate reinforced composites the orientation of the particles is considered, for practical purposes, to be random as illustrated in Figure 5 (a). The figure illustrates different types of composites as follows: (a) particulate, random; (b) discontinuous fibers, unidirectional; (c) discontinuous fibers, random; (d) continuous fibers, unidirectional. The arrows in the figure indicate the stronger direction.

A fibrous reinforcement is characterized by length that is much greater than the cross-sectional dimension. However, for different composites, the aspect ratio (the ratio of length to the cross-sectional dimension) can vary considerably. Single-layer composites with long fibers with high aspect ratios are referred to as continuous fiber reinforced composites, whereas discontinuous fiber composites are fabricated using short fibers of low aspect ratio.

The orientation of discontinuous fibers may be preferred or random as illustrated in Figure 5(b) and (c). The frequently encountered preferred orientation in the case of a continuous fiber composite is illustrated by Figure 5(d). This is referred to as unidirectional and the corresponding random situation is approximated to so-called bi-directional woven reinforcement.

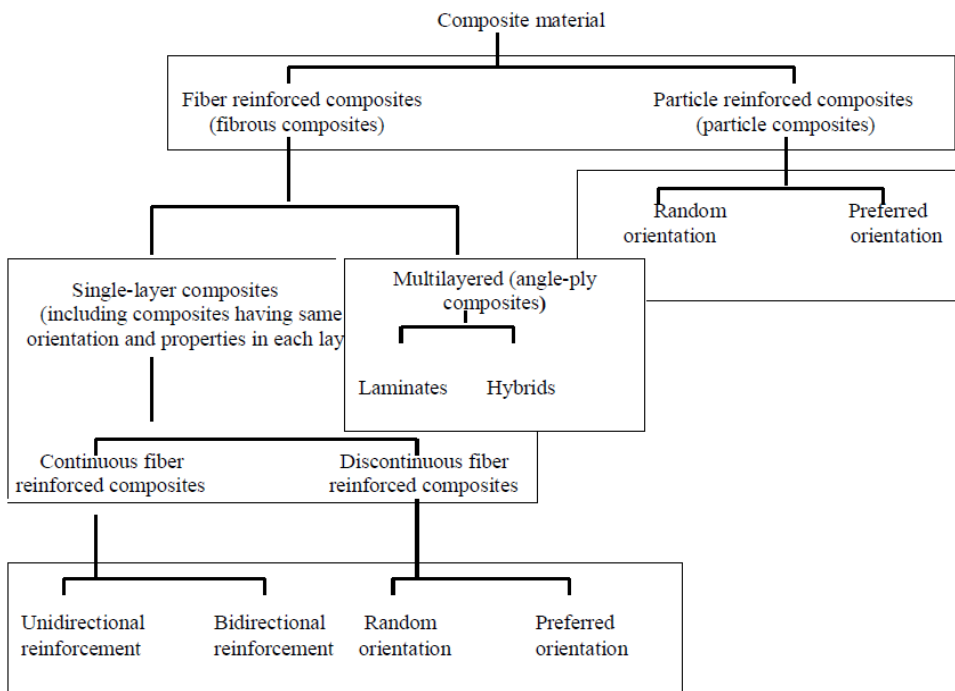


Figure 4. Classification of composite materials.

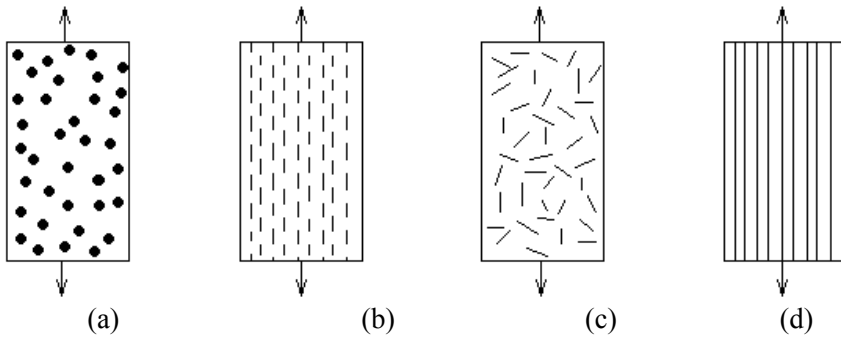


Figure 5. Examples of composite materials.

The other category of fiber reinforced composites is multilayered composites. These are classified as either laminates or hybrids. Laminates are sheet constructions, which are made by stacking layers (also called plies or laminates and they are usually unidirectional) in a specified sequence. Hybrids are multilayered composites with different types of fibers and they are becoming popular in the composites industry. The fibers may be mixed in a ply or placed layer by layer. These composites are designed to have the advantage of the properties of the different fibers [13].

The most widely used type of composite material is polymer matrix composites (PMCs). PMCs consist of fibers which are mostly made of carbon or alkali resistant (AR) glass that is embedded in a plastic matrix. Typically, the fibers make up about 60 percent of a polymer matrix composite by volume. Metallic or ceramic matrices can be substituted for the plastic matrix to provide more specialized composite systems, which are referred to as metal matrix composites (MMCs) and ceramic matrix composites (CMCs), respectively. These three main classes of composites, i.e. polymer, metal and ceramic matrix composites have different microstructures according to the nature of the matrix as shown in Figure 6 [10]. The composites in Figure 6 illustrate: (a) polymer composite of epoxy crossply laminate reinforced with carbon fiber (b) aluminum metal reinforced with silicon carbide and (c) glass ceramic reinforced with silicon carbide bars.

Fibers manufactured for composite production consist of thin continuous fibers or relatively short fiber segments. When using short fiber segments, however, fibers with a high aspect ratio are required. Continuous-fiber composites are generally required for high performance structural applications. The specific strength (strength to density ratio) and specific stiffness (elastic modulus-to-density ratio) of continuous carbon fiber PMCs, for example, can be vastly superior to conventional metal alloys. Composites can also have other attractive properties, such as high thermal or electrical conductivity, and a low coefficient of thermal expansion. Also, depending on how the fibers are oriented or interwoven within the matrix, composites can be fabricated such that they have structural properties specifically tailored for a particular structural use.

Despite composite materials having certain advantages over conventional materials, composites also have some disadvantages. For example, PMCs and other composite materials tend to be highly anisotropic, that is, their strength, stiffness, and other engineering properties are different depending on the orientation of the composite material.

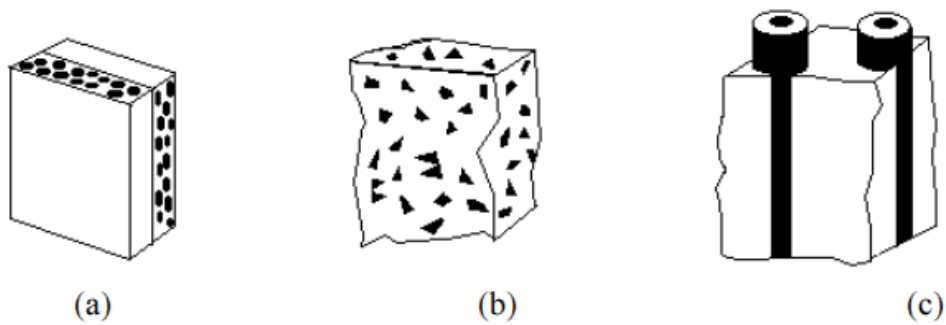


Figure 6. Schematic illustration of composites.

When PMC is fabricated so that all the fibers are lined up parallel to one another, then the PMC will be stiffer in the direction parallel to the fibers than in the perpendicular direction. These anisotropic properties pose a significant challenge to the designer who may require the composite materials to transfer multidirectional forces on a structural member. The other common shortcoming of composite materials is that bonding between separate composite material components is difficult [1].

Choosing the composition and structure of a composite material for a particular application requires knowledge of the mechanics of the composite. The introduction of reinforcement into a matrix alters all its properties. It is also necessary to take account of possible changes in the microstructure of the matrix resulting from the presence of the reinforcement. The generation of residual stresses from differential thermal contraction during manufacture may also be significant. A broad view of the property combinations offered by potential combinations obtainable from different composite systems can be visualized using “property maps” as illustrated in Figure 7. The “property map” shows a plot of Young's Modulus, E , against density, ρ . A particular material (or type of material) is associated with a point or a region. This is a conventional method of comparing the property combinations offered by potential matrices and reinforcements with those of alternative conventional materials [10].

1.5.3. Historical Evidence of Reinforcing Mortar with Fibers

The concept of reinforcing mortar and concrete using fibers is not a new concept. Historical records show that for centuries, man has attempted to reinforce mortar and concrete using different types of fibers. The early use of fibers in concrete to improve its physical properties was documented by in form of ancient Egyptian hieroglyphics [2].

These hieroglyphics illustrate that camel hair was applied in mortar which was thereafter used for plastering the outer surfaces of pyramids [2]. Similarly, Romans used fibers in form of horsehair in construction of various types of structures. In the United States of America, a dwelling that is located in New Mexico, which is reputed to be the oldest known structure in the United States depicts evidence of straw in its mortar [14].

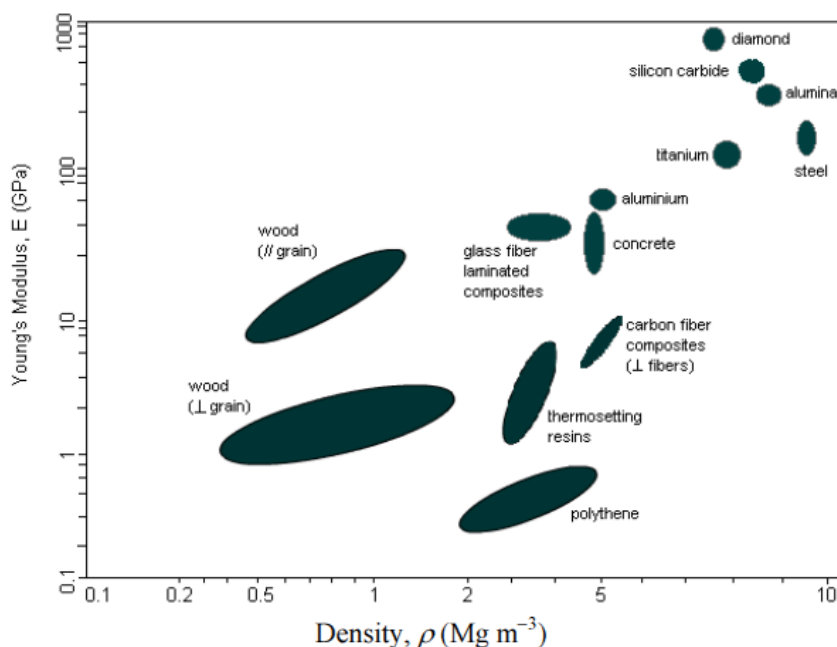


Figure 7. Data of common engineering materials.

2. REINFORCEMENT OF CONCRETE WITH FIBERS

2.1. Developments in Fiber Cement Composites

Like concrete, fiber cement composite technology is not a new development since fiber has been used to reinforce brittle materials since ancient times. Its use can be traced to as far back as 3,000 BC when the Chinese used cementitious materials to hold bamboo boats together and in building of the great wall. Similarly, the Egyptians also had developed this technology when they reinforced mud bricks with straw for use in wall construction [2].

This technology has not remained static. Just like any other technology, through innovation and research, a deeper understanding of the various types of fibers has been achieved. Among them was the natural mineral fiber asbestos, whose use with cement has been known since the mid-nineteenth century [10].

By the latter half of the twentieth century, new methods of physical and chemical analysis were uncovering the principles that govern the properties of natural polymers which resulted in chemists creating a new industry of manmade organic materials. This industry made thermoplastic products like polypropylene, polyethylene and nylon, which found a wide application in the motor, textile and building industries [11].

After the introduction of fibers as reinforcement to concrete, asbestos cement became the most successful fiber cement industry due to its extremely good bonding nature with cement [10]. However, research into the link between asbestos and respiratory diseases, including lung cancer, led to the demise of the widespread use of asbestos fibers. A great demand thus developed in the search for a suitable substitute. This demand was accelerated by the rising

awareness among workers, researchers and journalists of the hazardous effects of asbestos fibers which put a lot of pressure on the World Trade Organization to ban asbestos cement trading. In recent times, the concrete industry has adopted fibers which are obtained as a by-product of other industries.

2.2. Types of Reinforcement Fibers

The fibers used for reinforcement of concrete can be classified under three main categories as follows:

- a. Natural fibers
- b. Metallic fibers
- c. Synthetic fibers

These different fibers have varied properties and applications in concrete composites.

2.2.1. Natural fibers

With the exception of straw and various types of animal fibers, which were used to reinforce mortar in ancient times, few natural fibers are known to effectively reinforce concrete. Among the few fibers, sisal is the most common fiber that has been used as reinforcement to cement mortar and concrete. The sisal plant is abundant in Kenya and other East African countries.

Sisal, like many other agave plants, is a tropical freshly leaved plant cultivated for its fiber. The fiber is ordinarily used for the production of cordage, rope, twine, cloth, carpets and similar products. However, with the fast development of the concept of fiber reinforced concrete, the feasibility of using sisal fibers as reinforcement for concrete is attractive for various reasons:

- The mechanical and physical properties of sisal fiber are comparable with those of many fibers that are currently being used for reinforcement of brittle materials;
- Sisal fiber is a cheap and abundant locally available material in many tropical countries;
- Sisal is a renewable resource which requires comparatively little energy and simple technology to process;
- Sisal has acceptable environmental characteristics and can replace asbestos, which is a health hazard.

Sisal fiber can be used as reinforcement of both organic materials such as plastics and inorganic materials such as gypsum and concrete. Gypsum is perhaps the oldest matrix material that has been used with sisal fiber as its reinforcement [15]. Reinforcing of concrete with sisal fibers has in the recent past been investigated. A study carried out by Nilsson in 1975 demonstrated that there was great potential of using sisal fiber reinforced concrete, thus the keen interest in research on sisal fiber reinforced concrete [16].

2.2.1.1. Mechanical Properties of Sisal Fiber

The potential of sisal fiber as reinforcement for concrete has been investigated using information on the physical and mechanical properties [17,18]. The physical properties mostly relates to the textiles and cordage form of the fiber. The most important mechanical properties are density, tensile strength, and modulus of elasticity and stress-strain characteristics. These properties vary with moisture content and rate of stress application during the test. The following are the mechanical properties of sisal fiber [17-19].

- Density, ρ is 1230 kg m^{-3} when dry. The lowest value reported for the density is 715 kg/m^3 and the highest is 1530 kg m^{-3} .
- Tensile Strength, σ is $330 - 820 \times 10^6 \text{ N m}^{-2}$.
- Modulus of Elasticity, E is $2.6 \times 10^{10} \text{ N m}^{-2}$. The lowest value reported is $1.32 \times 10^{10} \text{ N m}^{-2}$.
- Ultimate Strain ε is 3.2 percent when dry and 3.4% when wet, with extreme values of 1.0 and 5.8%, respectively.
- The stress-strain relationship is linear up to failure. On unloading, linear relaxation occurs but the strain is not completely recovered. In subsequent loading cycles, hysteresis may be avoided by a slow rate of stress application.

The mechanical properties of sisal fiber which are reported here are based on tests that were carried out on the textiles and cordage forms of the fibers. When the fibrils themselves are tested instead of the whole fiber, there is a variation in the mechanical properties. For instance, Nutman [19] gives the tensile stress of sisal fibrils at failure as $820 \times 10^6 \text{ N m}^{-2}$. When the whole fiber is considered, a reduction of the tensile strength to $278 \times 10^6 \text{ N/m}^2$ is observed [20].

The important physical properties of sisal fiber are its absorption and the ability to withstand degradation due to alkaline cementitious environments and bacteriological decay. Sisal fiber has high water absorption. Percentage absorption of up to 105% relative to the weight of dry fibers has been observed to take place within a relatively short wetting time of 20 minutes [21]. This fast water absorption has important consequences in the manufacturing process of sisal fiber reinforced concrete.

Sisal fibers, like other vegetable fibers, may biologically deteriorate if not treated. On the other hand the alkalinity of the concrete matrix protects the fibers from biological deterioration. Thus the fibers, when embedded in concrete, will have a good durability against biological attack. However, the alkalinity of the concrete may affect the fibers chemically by decomposing the lignin that holds the constituent parts of the fiber together [22]. This process reduces the strength and ductility of the fibers. Nilsson [16] has reported results that indicated a significant reduction in strength (74% reduction) after the fibers were immersed in lime prior to casting them in concrete. However, Swift and Smith [20] argue that Nilsson's test conditions were probably too severe. They reported that when the fibers were removed from an 18-month-old mortar block that was stored dry after 28 days curing in a foggy room showed no reduction in strength.

In comparison with other fibers commonly used as reinforcement in brittle materials, sisal can be considered as a low modulus high elongation fiber. The price to strength ratio of sisal fibers is the lowest and is likely to remain low for a long time to come [23].

2.2.1.2. Production of Concrete Reinforced with Sisal Fibers

There are two main ways in which sisal fibers can be processed for use in a concrete matrix: (a) the sisal fibers can be used as discontinuous chopped short sisal fibers (15–75 mm in length) or (b) as continuous long fibers (greater than 75 mm in length). Sometimes both short and long fibers can be used together. The manners in which the fibers are incorporated into the matrix affect the properties of the composite both in its fresh state as well as in the hardened state.

The properties that affect sisal fiber reinforced concrete during mixing are workability of the mix, bleeding of concrete, the balling tendency of the fibers, and the rate of cement hydration. Not much research has been carried out to determine the influence of sisal fibers on these properties. However, reported results [24, 25] show that the incorporation of sisal fibers in the concrete matrix has the following effects on the fresh properties of the composite:

- Sisal fibers absorb water when introduced into the mix. This stiffens the mix (due to the reduction in water content) and thereby reduces the workability of the composite relative to that of the unreinforced matrix. To maintain good workability additional water is required.
- Sisal fibers reduce the bleeding tendencies of the concrete. This is advantageous as it results in a more stable material.
- Chopped sisal fibers tend to ball up if their volume content and length exceed certain limits. This results in the production of an unworkable and segregated mix, which in turn results in a highly porous and honeycombed composite.
- Sisal fibers retard the rate of cement hydration. This is a phenomenon which is peculiar to sisal fibers. More time is needed for complete hydration when the fibers are incorporated into the concrete matrix [26].

While recognizing the above drawbacks, many researchers have shown that a suitable composite can be achieved by adopting innovative mixing procedures. For instance, Nilsson [16] adopts a procedure of mixing the ingredients with about half the water before adding the dry fibers and the remaining water. Swift and Smith [20] pre-coated the fibers with cement paste and placed them in layers that alternated with the concrete mix.

The quantity of fibers that can be incorporated into the matrix depends on the usual factors, i.e. maximum aggregate size, cement content, type of mixer, fiber length, and method of fiber incorporation. In order to achieve the best results the concrete matrix should be of a reasonably high quality (say $f_{cu} \geq 30 \text{ N mm}^{-2}$) with a small maximum size aggregate (say $f_{cu} \leq 10 \text{ mm}$). Normally shorter lengths of chopped fibers give a better workability, and quite high fiber volume content can be achieved with such fibers. However, the most practical fiber volume content does not normally exceed 10 percent.

There exists information to prove that sisal fiber reinforced concrete is a viable alternative building material due to the following advantages:

- Sisal fibers have significant mechanical properties that make them eligible as reinforcement to concrete.
- The sisal fibers impart tensile strength, ductility and toughness to the concrete matrix. When the fibers are used as short discontinuous fibers (15–75 mm in length)

there is normally little improvement in the ultimate tensile strength, but the fibers inhibit early cracking and improve ductility. When continuous fibers are used there is very pronounced strengthening effect.

- There is strong indication that sisal fiber reinforced concrete, if properly protected, can achieve good resistance against normal environmental exposures.

2.2.1.3. Applications of Sisal Fiber Reinforced Concrete

There are many possibilities of utilizing sisal fiber reinforced concrete particularly in low cost housing schemes. The applications range from manufacture of roofing sheets, cladding mud-brick walls, production of light walling and cladding, plastering, and many other applications.

Roofing Sheets

There are not many feasible alternatives for roofing materials in many developing countries, especially in the rural areas where modern housing has to rely almost exclusively on the use of corrugated aluminum or asbestos sheets. Due to the high prices of these items, this makes roofing to be an expensive item in rural housing schemes. Current research shows that roofing sheets made from sisal fiber reinforced concrete can provide a cheap alternative to the conventional corrugated aluminum sheets. Sisal fiber reinforced concrete sheets are fire resistant and durable. They also have good thermal and sound insulating properties [27]. Sisal fiber reinforced concrete roofing sheets can be produced in small-scale industries, thereby offering opportunities for improving the quality of life in rural areas²⁸.

Light Walling and Cladding

Sun screens and cladding for multi-storey buildings can be manufactured from sisal fiber reinforced concrete, while hollow sisal fiber reinforced concrete blocks can be used for making light load bearing wall elements [26].

Plastering

Sisal fiber reinforced concrete surfacing can protect mud-brick walls and mud-and-pole constructions from destruction by rain [26].

Other Applications

Sisal fiber reinforced concrete can also be used for the manufacture of paving slabs and as surfacing for concrete bridge decks. There are also wide possibilities for semi-structural applications of sisal fiber reinforced concrete in the form of light beams, frames and trusses and as permanent formwork for cast-in-situ concrete [26, 29].

2.3. Metallic Fibers

Various types of fibers have been used in construction for the past 30 years. A common steel fiber that has been used for reinforcing concrete are steel fibers. When steel fibers entered mainstream construction, there was the issue of whether the use of steel fibers was more advantageous than the use of polypropylene fibers. Therefore, it was necessary to document the main benefits of steel fiber reinforced concrete. What followed was a large-

scale testing program to compare steel fiber reinforced concrete with unreinforced and conventionally reinforced concrete in various applications, in particular industrial slabs on grade.

Studies undertaken at Imperial College in London on simply supported slabs showed that steel fibers modify the cracking mechanism in concrete slab after loading [30]. This work paved the way for further research at Thames Polytechnic [31], (now the University of Greenwich). The investigations were useful in that they provided more insight into the behavior of steel fibers under loading in comparison with traditional reinforcing with fabric mesh, and unreinforced concrete in elements such as slabs on grade.

Steel fibers have been found to be a technically feasible option of fiber reinforced concrete applications. The main advantages of steel fibers over other fiber types are: crack width control, redistribution of stresses, enhanced load-bearing capacity, time savings, and added ductility. The reinforcing action of steel fibers depends on fiber geometry, aspect ratio and tensile strength [32]. There are practical advantages of using steel fibers in industrial floors such as: elimination of fabric mesh and other reinforcement accessories, reduced slab thickness, faster construction times and fewer joints [33].

Steel fibers are added either at the batching plant or on site. Figure 8 shows the addition of steel fibers to a concrete truck mixer at the batching plant before it leaves for site [49]. The arrival of laser screed machines in developed nations like the United States and the United Kingdom revolutionized industrial flooring, and this enhanced the performance capabilities of the flooring contractor, as they were able to pour ready-reinforced concrete floors out of the truck mixer. Figure 9 illustrates the way steel fibers look before and after they are added to the rest of the concrete ingredients in the mix.

Introduction of randomly distributed steel fibers into a concrete mix transforms the hardened concrete material into a more ductile composite. This is because the tensile stresses in concrete are not just compensated for in one or two locations but throughout the entire concrete section, and in multiple directions as shown in Figures 10-12. The resulting steel fiber reinforced concrete is able to withstand much greater stresses, both prior to and after cracking [33].

Homogeneously reinforced concrete has substantially greater fatigue and impact resistance than conventionally reinforced materials, greatly reducing the potential for fractures and spalling. Should a crack develop, a fiber immediately redistributes the load, maintaining a micro crack and resisting development into the macro crack phase. This mechanism is illustrated in Figure 12.



Figure 8. Addition of steel fibers to a concrete truck mixer.



Figure 9. Steel fibers (a) before and (b) after addition to concrete.

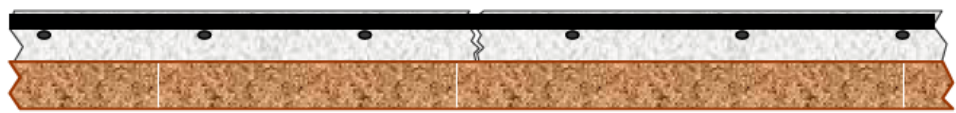


Figure 10. Conventional reinforcement showing a single point crack restraint.



Figure 11. Steel fibers providing continuous crack restraint.

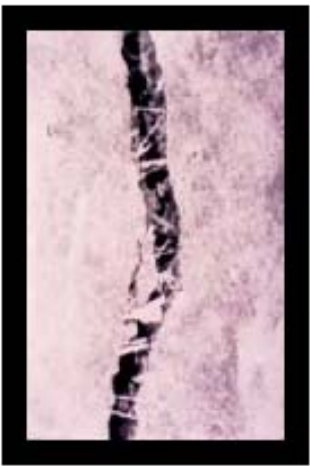


Figure 12. Close-up of steel fibers crossing a crack.

2.3.1. Difficulties in Mixing and Durability of Steel Fibers

One of the main problems with steel fibers is segregation, which varies with the fiber types and dosages but, as the blemishes were generally unacceptable, satisfactory remedial measures were devised, such as snipping the loose ends with wire cutters and filling surface blemishes with resin mortars. Surface fibers have now been minimized and, with careful use of fiber suppressants, can be eliminated [34]. Since then, contractors have gained more experience and the range of steel fibers has grown.

The long-term durability of steel fiber reinforced concrete is well documented and steel fiber concrete is generally much more resistant to impact than traditionally reinforced slabs. In addition to the inhibition of macro cracks, the potential spalling is minimal because the diameters of many types of steel fibers are generally small (0.5–1mm). There is also evidence of autogenous healing of cracks, which benefits long-term durability [35].

2.3.2. Types of Steel Fibers for Use as Reinforcement to Concrete

There exist several manufacturers of steel fibers which are specially engineered for concrete reinforcement. These are all based in either European or the United States' standards, which include manufacturers such as Novocon, a division of Synthetic Industries, based in Illinois, United States of America [49]. Out of all the different manufacturers of steel fibers,

Novocon steel fibers have proven to be the most widely used, mainly due to their high production standards as well as the many brands of steel fiber manufactured. The brand names of these Novocon steel fibers are: (a) XorexTM, (b) NovotexTM, (c) TwintexTM and (d) FortexTM [49].

2.3.2.1. XorexTM Steel Fibers

XorexTM steel fiber is a leading low carbon, cold drawn steel fiber for use in concrete reinforcement. It is evenly distributed in concrete mixtures to provide improved mechanical bonding capacity and enhancing the flexural and shear strength, fatigue, impact resistance and ductility of concrete. XorexTM is a reliable and cost efficient concrete reinforcement that is designed to be easy to mix, place and finish. Figure 13 illustrates the appearance and dimensions of an individual XorexTM steel fiber.

2.3.2.2. NovotexTM Steel Fibers

NovotexTM steel fiber is manufactured from high quality low carbon, and it is cold drawn steel that meets high toughness performance specifications [36]. It has a good bonding capacity with a wide range of concrete and shotcrete applications, at the same time it reduces the time and material costs associated with traditional rebar or wire mesh reinforcement. Figure 14 illustrates the appearance and dimensions of an individual NovotexTM steel fiber.

2.3.2.3. TwintexTM Steel Fibers

TwintexTM fiber offers better joint stability, reduces joint spalling and saves valuable maintenance costs in large, heavy traffic applications. It features a unique conical design and meets high toughness performance specifications [36] (level V and ISO 9002). TwintexTM fiber is specially designed to “yield” as opposed to pulling out, which provides exceptional load transfer stability, impact resistance and crack width control in concrete applications. Figure 15 illustrates the appearance and dimensions of an individual TwintexTM steel fiber.

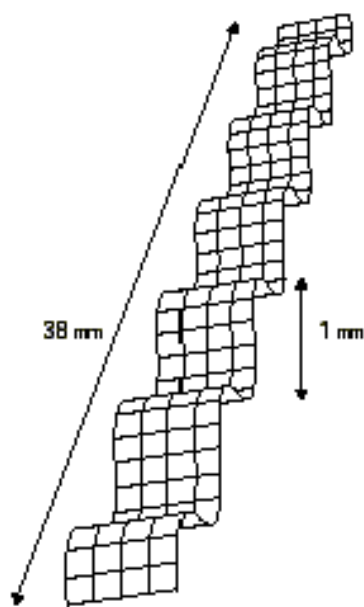


Figure 13. Xorex™ steel fiber showing the key dimensions.

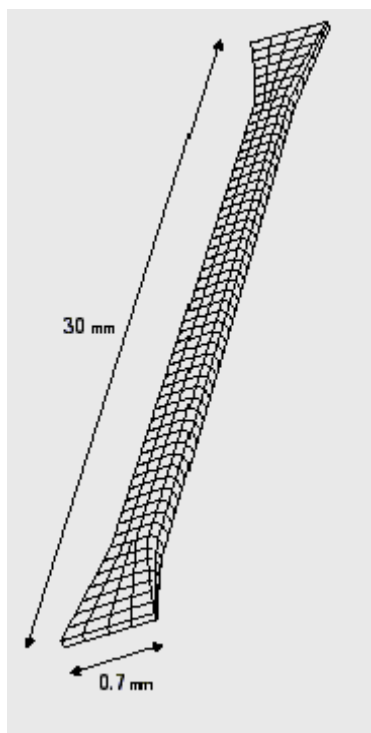


Figure 14. Novotex™ steel fiber showing the key dimensions.

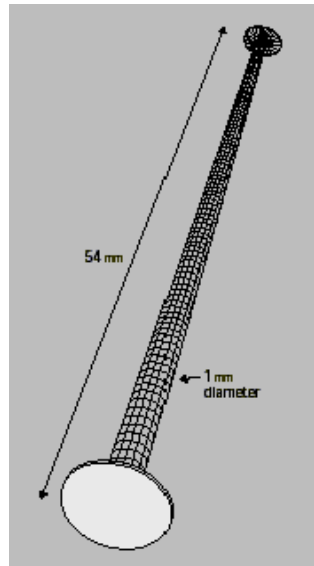


Figure 15. Twintex™ steel fiber showing key dimensions.

2.3.2.4. Fortex™ Steel Fibers

Fortex™ steel fiber offers a cost effective concrete reinforcement system with high strength and ease of handling. Fortex™ is easy to mix, place and finish and is manufactured to meet the specific performance and cost objectives of owners and concrete professionals worldwide. Figure 16 illustrates the main features and dimensions of a single Fortex™ steel fiber.

In general, the benefits of Novocon steel fibers include:

- The fibers comply with ASTM A820, Type I, cold drawn high tensile deformed steel wire [37].
- The fibers meet Toughness Performance Level III [36].
- Variable equivalent diameter and continuously deformed shapes provide superior reinforcement resulting in less cracking.
- High tensile strength fibers bridging joints or cracks to provide superior aggregate interlock resulting in increased load carrying capacity.
- Manufactured in different lengths to meet specific applications.
- Provide uniform, multi-directional concrete reinforcement.
- Require less labor to incorporate into concrete applications than rebar or wire mesh.
- Eliminate the need to bend and tie rebar or mesh in shotcrete applications.
- Require no special equipment to install reinforcement.
- Offer greater project scheduling accuracy.
- No special equipment is needed to mix, place or finish.
- Provide superior contraction joint stability and crack width control.
- Compatible with all types of cements and concrete mixtures.
- Are ideally suited for hand or vibratory screeds, laser guided screeds and all conventional finishing equipment.

- Are compatible with all curing compounds, super-plasticizers, mid and high range water reducers, hardeners and coatings.

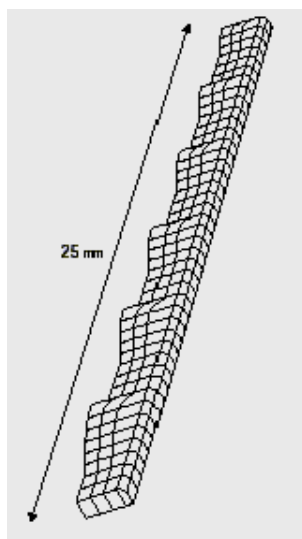


Figure 16. Fortex™ steel fiber with main dimension.

Novocon steel fibers also comply with several codes as outlined below:

- Comply with ASTM A820 [37], Type I, cold drawn high tensile deformed steel wire.
- Novocon steel fiber reinforced concrete and shotcrete (SFRC and SFRS) conforms to ASTM C94 [38] standard specifications for ready-mixed concrete uniformity requirements.
- Toughness and workability conforms to ASTM C1116 [39] and ASTM C1018 [36].

Some of the main applications of Novocon steel fibers are:

- Industrial slabs on grade
- Composite metal decks
- Precast units
- Shotcrete for shrinkage crack control
- Overlays
- Airport runways and taxiways
- Highway pavements
- Hydrodynamic structures
- Equipment foundations
- Blast resistant structures
- Joint free design
- Seismic design
- Structural design

Table 2 shows technical information of Novocon steel fibers. The ranges of values shown in the Table are due to the different brands of Novocon steel fibers (i.e. Xorex™, Novotex™, Twintex™ and Fortex™).

Table 2. Technical information for Novocon steel fibers

Property	Specifications
Tensile strength	$345 \times 10^6 - 1150 \times 10^6 \text{ N/m}^2$
lengths	25.4 - 63.5 mm (1.0 - 2.5 in.)
Average equivalent diameters	0.7 - 1 mm (0.0276 - 0.040 in.)
Average Widths	0.284 - 0.495 mm (0.0112 - 0.0195 in.)
Average Aspect Ratios	25 - 70
Deformations:	
Xorex™	Continuously deformed cut sheet steel
Novotex™	End deformed conical head;
Twintex™	Round shaft with flattened ends
Fortex™	Continuously deformed circular segment
Appearances	Bright and clean

2.3.3. Future of Steel Fiber Reinforced Concrete

The construction industry has steadily moved towards large-pour jointless floors and blended steel/polypropylene fiber-reinforced elements [42]. Manufacturers, engineers and contractors have pushed the boundaries of design and construction beyond slabs on grade where research in steel fiber reinforced concrete began [43].

Generally, steel fiber reinforced concrete for industrial ground floor slabs has pushed the industry to become efficient in terms of execution times. With higher quality and wide engineering knowledge through research, the future for steel fiber reinforced concrete seems bright. A typical example of such research initiative is the Association of Concrete Industrial Flooring Contractors, which has formed a working party of contractors, leading fiber suppliers and the ready-mixed concrete industry, and has produced a guide to steel-fiber-ground floor slab construction [34].

2.4. Synthetic Fibers

Synthetic fibers are artificially made under specific manufacturing conditions and factory environments by the chemical process of synthesis. There are several types of synthetic fibers, which include; glass fibers, carbon fibers as well as fibers derived from organic polymers.

2.4.1. Alkali resistant (AR) Glass Fibers

Alkali Resistant (AR) glass fibers are fine filaments of varying diameters in the order of $10\mu\text{m}$. An AR glass yarn is a bundle of thousands of fine filaments which act a single entity.

The bundle of filaments is visualized as being composed of outer and inner filaments which interact with each other through the mechanism of mechanical bonding. To improve the bond between the outer and inner filaments in the yarn, a polymer coating composed of styrene-butadiene is normally used. The content of the polymer in the yarn is often below 10 percent by weight.

2.4.2. Carbon Fibers

Despite the traditional and more widespread usage of carbon fibers in diverse industries such as: motor industry; electronics; telecommunications; entertainment; infrastructure and transportation, as well as a number of high-end niche market segments, carbon fibers are rapidly emerging as concrete reinforcement.

2.4.2.1. Highlights in Development of Carbon Fibers

Carbon fibers were discovered in the late 1800's when Thomas Edison was testing more than a thousand materials to use as a filament in the first incandescent light bulb [44]. In one of those experiments, he "baked" a piece of ordinary cotton thread to produce a pure carbon fiber. This was the breakthrough he needed to make electric lighting both practical and affordable.

A similar process was developed nearly a century later to produce carbon fibers from synthetic fibers. Commercial production of these "graphite" carbon fibers in the 1960s provided the high-strength and lightweight materials needed for military aircraft and the space program [44].

In recent decades, the high cost of these synthetic-based carbon fibers have limited their application in aircraft industry, sporting goods, and special products that require strength, stiffness, lower weight and good fatigue properties [44].

2.4.2.2. Properties of Carbon Fibers

The most successful carbon fiber has been Polyacrylonitrile (PAN). Typical values of certain properties of PAN fibers used in composites are outlined in Table 3. The properties listed in the Table are for PAN Grade T800 Toray (Japan) carbon fiber [45].

Table 3. Properties of PAN carbon fibers used in composites

Property	Quantity
Diameter	7 μm
Density	1810 kg/m^3
Tensile Strength	$5.6 \times 10^6 \text{ kN/m}^2$
Young's Modulus, E	$300 \times 10^6 \text{ kN/m}^2$
Elongation, δ	1.9 percent
Electrical resistivity	14 $\Omega \text{ m}$
Linear coefficient of thermal expansion, α	$0.75 \times 10^{-6} \text{ K}^{-1}$
Thermal conductivity	15 $\text{Wm}^{-1} \text{ K}^{-1}$

2.4.4. Advantages of Carbon Fibers as Concrete Reinforcement

From the value of mechanical properties of carbon fibers shown in Table 3, it is clear that by replacing conventional steel re-bar with carbon fibers in concrete, an equivalent finished

panel may only be 50mm thick. The carbon fiber reinforced panel would have a comparable strength and durability with conventional reinforced concrete panel, but at one-third the thickness and weight. Such a significant reduction in thickness and weight means that three times as many panels could be transported on a truck. At the same time, the labor required for placing and tying the steel re-bar would also be eliminated. Replacing the steel re-bar means that rusting would be eliminated, thus reducing building maintenance costs. In addition, lighter cladding translates into taller buildings for the same (or less) quantities of materials. Therefore, design options would be opened up to a whole new range of exciting possibilities [45].

There are several advantages of using carbon fiber reinforced concrete for offshore platforms, which are used as support structures for oilrigs. In conventional construction, the challenge has been how to build the elements quickly and economically, while at the same time providing a structure with sufficient durability, affordability and strength. Considering that sea water is salty and could thus accelerate corrosion of steel re-bars, replacing them with carbon fibers could be a viable solution to the challenges.

The biggest limitation to the application of carbon fibers as the primary reinforcement in concrete is cost. Carbon fibers are extremely expensive as compared with other forms of concrete reinforcement, which has limited their application particularly in developing countries such as Kenya.

2.5. Synthetic Polymeric Fibers

Synthetic fibers are derived from organic polymers. These are the most widely marketed and distributed concrete reinforcement fibers throughout the world. Most organic fibers are thermoplastic, that is, they are softened by heat. Chemical processes are the basis of the manufacturing process of thermoplastic synthetic fibers, and examples of the fibers include nylon, acrylic fibers, aramids/aromatic fibers, spandex fabrics, olefins, and polymers (which include polypropylene (PP)) [1].

Out of these thermoplastics, polypropylene has desirable properties, namely durability, and chemical resistance. In addition, polypropylene, has a low density, is impact and temperature resistant. Therefore, polypropylene has been widely used in concrete as reinforcement.

2.5.1. Historical Background of Polypropylene

Polypropylene was an innovative development that originally was in the form of fibers, films or molded pipes. The plastic polymer PP was discovered by Giulio Natta from Italy and Karl Ziegler from Germany [1], renowned chemists and academicians who combined efforts that led to being jointly awarded the 1963 Nobel Prize in chemistry [48].

In the 1930s Natta's attention shifted to organic, rather than inorganic, chemistry, and he pursued the study of polymers (large molecules). Natta used his knowledge of polymers to help develop methods of producing synthetic rubber. While visiting Frankfurt, Germany, in 1952, Natta heard a lecture by Karl Ziegler, whose own work in the field of the practical importance of polymers paralleled Natta's [48].

Karl Ziegler's work with substances that accelerate chemical reactions (catalysts) made valuable contributions to the field of plastics. After World War II (1939-1945), Ziegler

conducted research on organic aluminum compounds, work that eventually led to the discovery that the compounds tri-ethyl aluminum and titanium tetrachloride produced a type of plastic of a very high molecular weight. This mixture of compounds became known as the Ziegler catalyst, and its product, a tougher, more heat-resistant plastic, revolutionized the plastics industry and, consequently, provided Ziegler with abundant royalties. This plastic material was referred to as polypropylene (PP). The discovery of the catalyst that was used in production of polypropylene revolutionized the plastics industry, Ziegler was awarded the 1963 Nobel Prize in chemistry, which he shared with Italian chemist Giulio Natta [48].

Natta and Ziegler collaborated on the production of a plastic that was not only heat-resistant and hard, but also highly impact resistance and malleable. It could be spun into fibers, spread out as a film, or molded into pipes, for example, with strength and resilience comparable to the previously used materials such as nylon or metal.

2.5.2. Developments in Usage of Polypropylene Fibers

Polypropylene fiber products account for approximately 15% of polypropylene consumption. The products range from continuous filaments (for carpeting and rope), to melt-blown fibers for non-woven goods. Specific applications include outdoor carpets, yarns for upholstery and automobile seats, replacement for canvas in luggage and shoes, disposable goods (diapers, surgical gowns), ropes, cords and fibers for concrete reinforcement and additive purposes [46].

2.5.3. Chemistry of Synthetic Polypropylene Fibers

Polypropylene is a polymer material, which is formed by the chemical process of polymerization. A polymer is a large molecule containing hundreds or thousands of atoms formed by combining one, two or occasionally more kinds of small molecules (monomers) into chain or network structures [47].

These molecular structures are classified according to the various types of polymer materials that are available. The main categories of polymer materials used in civil engineering include the following:

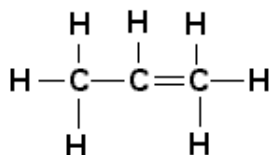
- Hydrocarbon polymers
- Other carbon chain polymers
- Hetero-chain polymers
- Network polymers
- Copolymers, alloys and hybrids [47].

PP is a hydrocarbon polymer, which is essentially a combination of monomers containing only hydrogen and carbon atoms, arranged in rows, rings or both, and connected by single, double or triple bonds. Since the monomer from which PP is formed is an alkene (propylene or simply propene), therefore it is a double bond. In addition, PP is a thermo-softening plastic, which become soft when heated and can therefore, be molded or remolded. Thermo-softening plastics are linear polymers of the general structure: $-X-X-X-X-X-X-$ where X represents the monomer [48].

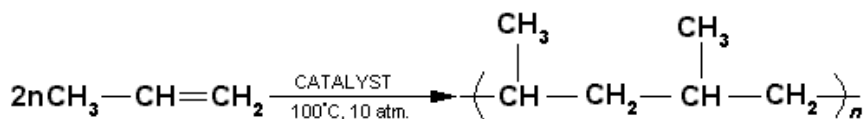
Polymerization of propene into polypropylene is carried out by addition polymerization, which is a characteristic of any compound having a $C=C$ bond. This process of addition polymerization requires the presence of an initiator. Examples of initiators include:

- An acid (H^+) – Cationic polymerization
- An anion (OH^-) – Anionic polymerization
- A free radical, e.g. a methyl group ($\bullet CH_3$) – Free radical polymerization

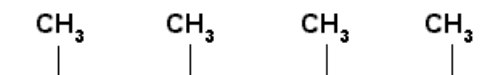
The monomer propene, C_3H_6 , whose formula can otherwise be shown as $CH_3-CH=CH_2$, has the following chemical structure:



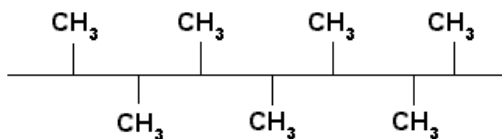
This propene monomer now undergoes addition polymerisation to form a polypropylene polymer as shown by the following chemical reaction:



where the value of $n \cong 2000$. This addition polymerization produces the polypropylene polymer in which the methyl groups (CH_3) on the alternate carbon atoms all have the same orientation, i.e. they lie on the same “side”. These types of polymers are described as “isotactic” or “syndiotactic”, and it is this regularity of structure (i.e. polymeric stereoregularity), which allows neighboring molecules of polypropylene to be closely packed together to give a crystalline structure [48].



In atactic polymers, the orientations of the side-chains are random and the compounds are non-crystalline [48].



The regularity or lack of regularity in polymers affects their properties in their abilities to crystallize. Atactic polymers are amorphous (non-crystalline), soft (“tacky”) materials with little or no physical strength. The corresponding isotactic or syndiotactic polymers, such as PP, are usually obtained as highly crystalline materials. Crystallinity leads to high physical

strength and increased solvent and chemical resistance as well as differences in other properties that depend on the crystalline nature [46].

2.5.4. Physical and Mechanical Properties of Polypropylene Fibers

Being a thermoplastic material, PP exhibits pronounced creep at normal service temperatures (approx. 20°C). For example, the strain (ϵ) under constant tensile load, or stress (σ) increases with time. In thermoplastics, most but not always all of the creep strain is progressively recovered on removal of the load [47].

An important mechanical property of PP is the impact performance. In general, polymer impact performance can be classified into three categories namely: (a) brittle, (b) notch brittle, and (c) tough. This classification is after experimental tests of the energy absorption of polymers during fracture. The following is a description of each of these three categories of polymer impact performance:

- a) Brittle: specimens break even when un-notched.
- b) Notch brittle: specimens do not break un-notched, but break when sharp-notched (notch tip radius $r = 0.25$ mm).
- c) Tough: specimens do not break completely even when sharp-notched ($r = 0.25$ mm).

PP has been identified as a “notch brittle” polymer [47]. Table 4 gives the main physical properties of the thermoplastic material PP [47]. Like other solid polymers, PP does not contain interconnected pores and may generally be regarded as impermeable. However, when used as very thin sheets or surface coatings, PP may transmit measurable amounts of gases, vapors and liquids by direct permeation through the solid [47]. A typical PP membrane has been found to be less permeable than other common polymers such as: low-density polyethylene (LPDE), unplasticised PVC, and natural rubber [47]. Being a thermoplastic, the dimensional and environmental stability of PP is an important property especially when its chemical resistance is to be relied on. This fiber stability directly affects the overall performance of fiber reinforced concrete when used in different environmental conditions. Table 5 shows the properties that affect the stability of PP in relation to other thermoplastics, namely, nylon and polyethylene terephthalate (PETE or PET) [10].

Table 4. Physical properties of polypropylene

Property	Units	Values
Density, ρ	kg m^{-3}	905
Young's Modulus, E	MNm^{-2}	1000 – 1400
Poisson's Ratio, ν	-	0.3
Tensile Strength, σ	MNm^{-2}	20 - 40
Failure Strain/Elongation to tensile breakage, ϵ	%	≥ 300
Thermal Expansivity, α	10^{-6} K^{-1}	110
Thermal Conductivity, K	$\text{W m}^{-1} \text{ K}^{-1}$	0.2
Specific Heat Capacity	$\text{kJ kg}^{-1} \text{ K}^{-1}$	1.9
Melting Point	$^{\circ}\text{C}$	175
Deflection Temperature under load at 1.82 MN m^{-2}	$^{\circ}\text{C}$	60 – 65

Table 5. Properties of different thermoplastic polymers

Property	Nylon 6.6	Polypropylene
Melting Temperature (°C)	256	164
Distortion Temperature (°C)	120 – 150	80 – 120
Shrinkage on curing (%)	-	-
Water absorption (24h @ 20°C) (%)	1.3	0.03
Chemical resistance	Good, attacked by strong acids	Excellent

2.5.4. Production of Polypropylene Fibers

While polyethene, (or polyethylene), has been manufactured since 1939, polypropylene (PP) is a comparatively new material. The production of PP did not begin in Great Britain until 1962, but the amounts produced since then have increased rapidly [48]. The reason behind this rapid increase in production of PP has been due to several advantages that it has over polyethylene. Some of these advantages are: (a) PP has greater tensile strength, (b) PP is relatively lighter (c) PP has a higher softening point and (d) PP has significant impact strength.

The manufacturing of PP fibers involves forming and shaping them through processes of extrusion and molding. During these processes, the PP polymer is processed in the molten state into fibers through the following five stages [48].

- a) Polymerization of propene to yield polypropylene (PP).
- b) The PP, which is now too finely divided, is melted.
- c) Strands are formed in a continuous process by extrusion of the PP homopolymer resin, into either a mono-axially coordinated sheet or film form, or monofilament yarn.
- d) The strands are then chopped into lengths of about 0.3 cm, known as moulding powder. This can now be used in injection mouldings and extruders.
- e) Fibrillated fibers are manufactured from the extruded sheet, which is subjected to molecular alignment, mechanical fibrillation, coating and cutting into appropriate lengths.

The final stage in the manufacturing of PP fibers includes quality assurance and controls which standardize the following physical properties [49]:

- Denier (this is a unit of measurement that specifies the fineness of the fiber)
- Surface finish
- Shrinkage
- Tensile strength
- Elongation
- Weight and length
- Visual appearance

2.6. Synthetic Polypropylene Fibers for Use as Concrete Reinforcement

There exist several types of fibers manufactured specifically for use as a form of reinforcement in concrete elements, depending on the intended applications and availability. These fibers include: carbon, graphite, steel, glass, polyester, nylon, and organic fibers, among others [50, 51]. In addition to these fibers, synthetic PP fibers have been widely used for concrete reinforcement.

Synthetic PP fibers engineered specifically for concrete emerged in 1983. Advancements in the use of synthetic PP fibers in concrete emanate from its application as a primary form of crack inhibition and prevention. Therefore, in choosing the type of fiber to use, it is essential to understand the nature of cracking in concrete, its various forms and types, and the traditional, and yet widespread methods of tackling this age-old problem of concrete cracking. It has been shown that the use of PP fibers is a viable solution to concrete cracking problem. Therefore, when synthetic PP fibers emerged in 1983, new levels of performance were achieved at affordable costs.

Their use has been very prevalent in developed countries, with a wide application in projects worldwide. PP fibers continue to gain popularity in the construction industry throughout the East African region as knowledge and exposure to its useful existence increases. In Kenya, synthetic PP fibers were introduced to the construction industry towards the latter part of the 1990s through local distributors.

The role of synthetic PP fibers in concrete can be categorized into three functions as follows:

- a. As non-structural secondary reinforcement in ground floor concrete slabs.
- b. As an admixture in several concrete applications with numerous benefits.
- c. To reduce segregation of the components of concrete during casting and settling processes.

One of the leading producers of synthetic fibers specifically engineered for reinforcement in concrete is Fibermesh, a division company of Synthetic Industries, Inc. based in the US. The PP fibers that Fibermesh manufactures are varied in both physical and chemical characteristics. The specifications depend on their application. Fibermesh manufactures different types of PP fibers which are marketed under different brands as follows: Fibermesh (MD) Multi-Design, Harbourite, Fibermix Stealth, Microban 'B', High Performance Polymer (HPP).

There are other manufacturers, for example MBT Middle East LLC based in United Arab Emirates (U.A.E.) in Dubai [52]. The Company produces Rheofiber, also a PP fiber. In addition, International Engineering Materials and Supplies, also based in U.A.E. [53] manufacture PP fibers by the brand name Fiberon. The different types of fibers are differentiated by their physical properties and manufacturing processes [52, 53].

2.6.1. Fibermesh (MD) Multi-Design

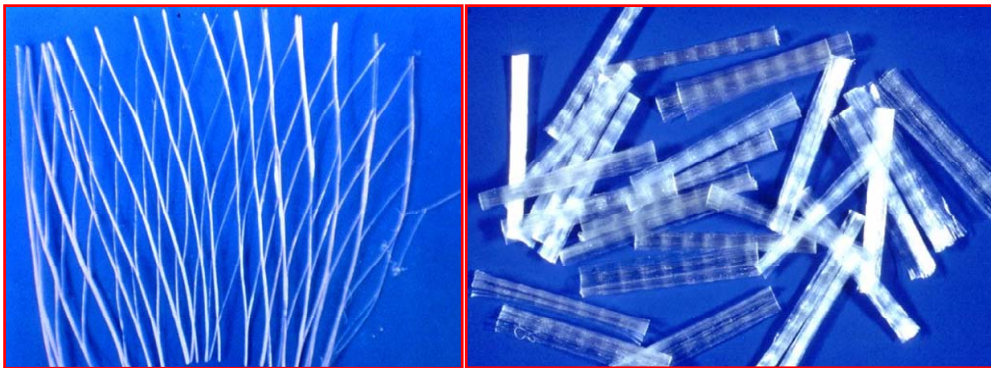
Fibermesh MD (Multi-Design) fibers are made from 100 percent homopolymer virgin polypropylene fibrillated fibers containing no olefin materials. They are specifically engineered and manufactured to an optimum gradation for use as fibrous secondary (non-structural) reinforcement for controlling plastic shrinkage cracks as well as settlement

cracking in plain concrete and shotcrete, which is a terms used to describe a mixture of cement and sand and water that is sprayed on a surface under pneumatic pressure.

The fact that these fibers are fibrillated, and not monofilament or multifilament (having single separated strands), enables the fibrillated bundle of fibers to open up during concrete mixing, thus enhancing their bondage with the rest of the concrete's components, Figure 17 shows fibrillated fibers which are deformed and shredded to form a net-like mesh in order to enhance bonding with cement paste.

2.6.2. *Harbourite*

Harbourite fibers are either fibrillated (Harbourite 340CP) or monofilament (Harbourite S/G). The family of Harbourite polypropylene fibers is engineered by the Fibermesh Company for the shotcrete and gunite concrete industry as well as for the precast concrete pipe industry. Thus, Harbourite fibers are mainly for use in Portland cement plastering, including proprietary exterior wall coatings and precast applications. The chemical and physical properties of Harbourite fibers are shown in Table 6.



(a)

(b)

Figure 17. Fibrillated Fibermesh MD bundle (a) before opening (b) after opening.

Table 6. Chemical and physical properties of Harbourite fibers

Property	Value	Property	Value
Absorption	Nil	Young's Modulus, E	$3.5 \times 10^6 \text{ kN m}^{-2}$
Fiber Length	12, 38 and 50 mm	Ignition Point	593°C (1100°F)
Melting Point (324°F)	162°C	Electrical Conductivity	Low
Thermal Conductivity	Low	Alkali Resistance	100%
Acid and Salt Resistance	High		
Specific Gravity	0.91		

Some of the advantages of Harbourite fibers are:

- Reduction of plastic crack formation
- Increase of cohesion

- Increase of weather resistance
- Enhancing freeze–thaw resistance
- Improvement of shatter resistance
- Improvement of blast resistance (using the longer fiber lengths, i.e. 38 and 50 mm)
- Reduction of water penetration
- Additional toughness
- Improvement of workability
- Increase of long-term durability

2.6.3. *Fibermix Stealth*

Fibermix Stealth fibers are 100% virgin polypropylene multifilament fibers specifically engineered for use in concrete as secondary reinforcement, help to reduce segregation, plastic settlement and shrinkage cracking. Fibermix Stealth PP fibers are also chemically inert and are unaffected by the long-term moist and alkaline environment of concrete. Therefore, they cannot rust or stain; they are non-magnetic, noncorrosive and alkali proof.

Fibermix Stealth fibers are especially used in architectural concrete where an aesthetic finish is of ultimate importance. Their suitability for this purpose is that they are very fine and numerous such that if compared with other PP fibers, they constitute the greatest number of fibers per unit volume of concrete. This gives the concrete a very high resistant to intrinsic cracking and thus an extremely smooth finish. The chemical and physical properties of Harbourite fibers are shown in Table 7.

Table 7. Chemical and physical properties of Fibermix Stealth fibers

Property	Value	Property	Value
Absorption	Nil	Young's Modulus, E	3.5×10^6 kN/m ²
Fiber Length	3, 12 and 19 mm	Ignition Point	590°C (1100°F)
Melting Point (324°F)	160°C-170°C (320°F – 340°F)	Electrical Conductivity	Low
Thermal Conductivity	Low	Alkali Resistance	100%
Acid and Salt Resistance	High		
Specific Gravity	0.91		

Fibermesh fibers with Microban 'B' thus provide a system of reducing and eliminating microbial and fungal growth in addition to the fiber's traditional role of secondary reinforcement in concrete.

Microban additives are sub-micron sized cell wall penetrants that disrupt the metabolic function of thin-walled microorganisms such as bacteria, yeast and fungi. Thick-walled cells of humans and red-blooded animals are unaffected [50].

2.6.5. *High Performance Polymer (HPP)*

High Performance Polymer (HPP) Fiber is extruded from 100 percent virgin polypropylene and mechanically deformed in a proprietary shape to maximize anchorage for reinforcement in cementitious composites. The fiber is collated in small bundles for rapid introduction into wet, cementitious mixtures. Chemical and physical properties of HPP fibers are shown in Table 8.

Some of its functions and uses of Fibermix Stealth include the following:

- Inhibits and controls the formation of intrinsic cracking in concrete
- Reinforces against impact forces
- Reinforces against abrasion
- Reinforces against the effect of shattering forces
- Reinforces against water migration
- Improves blast resistance (using the longer fiber length, i.e. 19 mm)
- Provides improved durability
- Reduces plastic shrinkage and settlement cracking
- Alternate system to welded wire fabric when used for secondary (crack control) reinforcing in concrete

Table 8. Chemical and physical properties of High Performance Polymer fibers

Property	Value	Property	Value
Nominal Filament Diameter	0.9mm	Young's Modulus, E	$3.5 \times 10^6 \text{ kN m}^{-2}$
Fiber Lengths	30; 40; 50 mm	Ignition Point	590°C (1100°F)
Deformation Spacing	3/cm	Electrical Conductivity	Very Low
Absorption	Nil	Acid/Alkali Resistance	High
Fiber Length	3, 12 and 19 mm	Ignition Temperature	360°C (680°F)
		Thermal Conductivity	0.2 W/mK @ 20°C
Melting Point	175°C (350° F)	Acid and Salt Resistance	High
		Specific Gravity	0.91

2.6.4. Microban 'B'

Concrete might seem hard and impervious, However, on the microscopic level, concrete is permeable and subject to microbial intrusion that can occur and cause problems. In some cases, this microbial attack shows up on concrete surfaces as bacteria and fungi, which can cause potential hygiene-related and aesthetic problems.

The synthetic polypropylene fibers manufactured by other companies throughout the world are outlined in the sections that follow.

2.6.6. Rheofiber

Rheofiber is a monofilament polypropylene fiber developed as a crack-controlling additive for concrete and mortar by MBT Middle East LLC based in Dubai, United Arab Emirates (UAE) [52]. Rheofiber is used to inhibit the formation of small cracks which can occur through plastic shrinkage and settlement, premature drying and early thermal changes. Rheofiber is specifically designed for crack control in cementitious materials and it is particularly effective in readymix concrete, precast concrete, conventional shotcrete and screed-rendering mortars. Chemical and physical properties of Rheofiber are shown in Table 9.

The specified advantages by the manufacturer include the following:

Table 9. Chemical and physical properties of Rheofiber

Property	Value
Fiber diameter	18 microns
Fiber length	12 mm
Surface area	230 m ² / kg
Alkali content	Nil
Tensile strength, σ	320 - 400 x 10 ³ kN/m ²
	590°C (1100°F)
Ignition Point	Very Low
Electrical Conductivity	High
Acid/Alkali Resistance	
Ignition Temperature	360°C (680° F)
Thermal Conductivity	0.2 W/mK @ 20°C High
Acid and Salt resistance	
Specific Gravity	0.9
Sulphate content	Nil
Chloride content	Nil
Increase in Air entrainment	Not significant
Constituents	Polymerized polypropylene

- Can replace anti-crack wire mesh in factory and warehouse floors
- Inhibits intrinsic cracking in concrete
- Disperse uniformly throughout the mix
- Improves finishing characteristics
- Improves concrete durability
- Increases impact and abrasion resistance
- Rustproof
- Impervious to alkali attack
- Decreases construction time and labor
- Reduced risk of subsequent damage
- Improves fire resistance – reduces the incidence of explosive spalling during heating.

A special manufacturer's note on the effects of overdosing Rheofiber indicates that overdosing of the fiber will generally produce a reduction in workability, and an increase in the cohesiveness of the mix [52].

2.6.7. Fiberon

Like Rheofiber and the rest of the synthetic fibers mentioned earlier, Fiberon is a micro polypropylene fiber developed as a crack controlling additive for cementitious materials. It is produced and distributed by International Engineering Materials and Supplies, also based in the United Arab Emirates (UAE) [53]. It is available as fibrillated monofilament in lengths of 12 mm and 10 mm for concrete mixes with aggregate size greater than 5 mm, and 6 mm fiber length for plaster and mortar mixes only. Chemical and physical properties of Fiberon are shown in Table 10.

Table 10. Chemical and physical properties of Fiberon fiber

Property	Value
Appearance	Polypropylene fiber
Specific Gravity	0.91
Alkali content	Nil
Sulphate content	Nil
Chloride content	Nil
Air entrainment	Air content of concrete will not be significantly increased
Constituents	Polymerized virgin polypropylene C ₃ H ₆
Fiber thickness	3 and 6 denier
Fiber length	12 mm
Shelf life	Maximum of 12 months from date of manufacture
Tensile strength, σ	$350 \times 10^6 \text{ N/m}^2$
Young's Modulus, E	$5.5 - 7 \times 10^6 \text{ kN/m}^2$
Melting point	160° C

2.7. Advantages of Textiles over Discrete Fibers

The advantages of Fiberon and Rheofiber are identical. The main advantages of using textile over the use of discrete fibers are that firstly, in a textile format, the fibers are oriented in the required plane and secondly, a textile format means that high fiber concentrations are achievable. As far as the type of fibers are concerned, several difficulties have been identified which justify the search for an alternative fiber to asbestos for use in cement based composites. These difficulties are conveniently categorized into four broad areas, which are summarized below:

- Handling difficulties in mortar cement paste when short, discrete fibers are added to concrete, referred to here as “workability” problems.
- Long term performance of the composite after deterioration of either the matrix, the fiber, or the failure of the desirable fiber/matrix interface characteristics.
- Economic considerations.
- Health and environment related issues [54].

The problems outlined above are also related to the use of discrete fiber in cement, mortar, and indeed concrete mixes. Each of the above problems will be briefly discussed, starting with the workability issue which is encountered at the onset of the material preparation.

2.7.1. Workability Problems

Both natural and synthetic fibers have common problems as far as workability of fresh concrete is concerned. The main difficulty encountered with the use of short, discrete

polypropylene fibers in cement-based mixes is that the presence of the fibers necessitates an increase in the ratio of water to cement in concrete resulting in a reduction in strength of the composite. This is due to the fact that as more water is added to make the concrete mix more workable, there is an increase in the risk of flaws from drying shrinkage cracking, which is associated with strength reduction. Similar difficulties in fresh concrete are encountered when other short fibers like nylon and polyethylene are used. Apart from the workability problem, it is also found that when there is limited control over the fiber orientation within the matrix, the strength of the composite cannot be pre-determined and hence the durability of the material cannot be reliably predicted [55, 56].

Closely associated with workability problems in fresh concrete are the handling problems common when steel fibers are used as the reinforcement. These fibers are sharp, so they tend to damage hands, and are stiff, so they tend to stick out on the element's surface after manufacture. Steel fiber reinforcement is therefore not the most appropriate option for use in thin building elements [55]. Fortunately, the technology of fibrillation that is employed in the manufacture of the polypropylene textile material offers a good solution to such workability problems.

2.7.2. Performance Problems

It is important to ensure that, even after overcoming workability problems, the long-term performance, or the behavior of the composites as a function of ageing can be understood and hence predicted, which has unfortunately not always been the case in the past. Natural fibers are an example of fibers which are known to degrade in mortar [57]. The implications of fiber decay are that the composite material loses the strength properties the fibers initially helped to create. Studies in the long-term behavior have been undertaken in the past with sisal, which is a natural fiber. In this sisal study, the fibers tended to clump in the mix, while setting was retarded by leaching, or from organic impurities from the pre-soaked cuttings. This delayed the setting of the concrete thus reducing the composite strength [58]. Textiles in a mesh format provide a reinforcing material without such difficulties and whose properties in the long run are therefore predictable.

Performance problems have not only been reported in natural fiber reinforced concrete, but also in composites of synthetic mineral fibers as well. A good example is in the case of glass fibers which deteriorate in cementitious matrices due to the latter's high alkalinity, (pH of 12 to 13). To overcome this difficulty, the glass can be coated (alkali resistant-AR glass) but this is expensive. Alternatively, polymeric fibers like polyvinyl alcohol (PVA), polyethylene (PE), and polypropylene (PP) among others, have been suggested in the past. They have however, not been able to fully satisfy the bonding problem [58].

The problems which have been outlined so far, can best be understood after the mechanism of bonding between the fibers and the matrix has been understood. From the foregoing, it is clear that short, discrete, polypropylene fibers do not offer the best solution to the long-term performance of the composite. With ordinary polypropylene fibers there is fiber pullout at relatively low stresses, and thus they are not capable of achieving closely spaced multiple cracking in the relatively brittle matrix, which is a desirable property of a tough material. Therefore, if the interface bond problem can be overcome, then there is great potential for composite action. However, before any recommendations are made, the economic viability of different fibers has to be justifiable.

2.7.3. Economic Considerations

Economics is becoming a significant factor, not only in terms of money, but also in energy terms. To be able to have a feel of the economic aspects of a composite material, there is need to examine for the matrix, and for each fiber type, the availability, global distribution of the materials, as well as the individual material's production costs. To start with, minerals which are the raw materials from which cement is made, are present on earth in almost limitless quantities and they are geographically very well distributed, hence the cost of cement is not the critical component of the composite material⁵⁸. It is however important to include in the composite cost, the cost of any pre-treatment on cement, which may be required in order to minimize mortar alkalinity which affects the durability of the composite [56].

The real costs of the reinforcing materials should include fiber pre-treatment to improve its durability in concrete. A good example where a potentially viable fiber was disqualified on economics ground was that of carbon fibers. These are fibers, which have a fibril structure, very similar to that of asbestos, and their surface properties can be modified by suitable treatments, which control the interfacial properties of the composite. However, their high costs would seem to rule them out for major civil engineering and cement composite applications [59]. A similar argument would apply for steel fibers, whose production energy requirement per cubic meter is many times higher than that of both cement and of common plastics production [56, 58]. These cost considerations have to be finally weighed against the issue of human health and the environment before the material can be formulated to produce a composite of acceptable engineering performance.

2.7.4. Health and the Environment

The hazardous effects associated with asbestos cement have already been outlined. It is emphasized that this has been the single major motivation in the search for alternative fiber reinforcement. This matter has been so serious that since the early 1920's, pressure has been steadily building up from various interested groups for a ban on the entire asbestos industry [54]. Closely associated with matters of human survival is the problem of environmental degradation and therefore the two issues are considered here side by side.

Over the years, as cities continue to grow, the inevitable effect has been that building activities have also increased. This has placed a severe stress on resources which sometimes, coupled with poor management, has led to a serious degradation of the natural environment. This calls for up to date technology whereby efficient use of the available resources has to be explored. The international guidelines on how this can be achieved are outlined in the resolutions drawn by the United Nations Conference on Environment and Development of June 1992 under Agenda number 21 [60]. The resolution spelled out the policies that needed to be put in place by Governments of the member states for efficient use of the available resources.

2.7.5. Polypropylene Fiber Cement Composites

As the asbestos cement industry was grappling with the mounting pressure to have the use of asbestos fibers banned, other industries found a ready opportunity and market for their new products. The properties and performance of these new products were, however, not quite the same as those of asbestos fibers. The products included steel, glass, carbon, boron and a number of polymeric fibers. An example of the polymeric group of fiber industries

developed was the use of polypropylene fibers which could be produced in different forms ranging from short fibers to long, continuous fibers [58]. Meanwhile, the reinforcing action of polypropylene fiber in concrete was being studied and indeed, David Hertz had by 1983 developed a lightweight, architectural composite made from cement, coal flyash (a waste product from coal-fired power plants), and waste polypropylene fiber from a carpet manufacturing plant [58]. This product which was known as “Syndecrete”, was meant to be an alternative to limited or non-renewable natural materials. It, therefore, found many applications in the manufacture such items as kitchen counter tops, sinks, tub surrounds, tile flooring, and furniture.

Research into the reinforcing properties of polypropylene fibers in concrete shows that the properties of the composite depend on: fiber type, fiber volume fraction, and strength of the bond between the fiber and the matrix [61]. High fiber volumes lower the workability of the plastic concrete. This is compensated for by the addition of more water to make the mix more workable. This addition of water increases the water/cement ratio which lowers the concrete strength and durability [62].

The rate of development of the use of concrete reinforced with polypropylene fibers as an industry has not however been as fast as that of the asbestos cement industry as shown by previous studies. This is mainly due to certain difficulties related to interface bonding and working with the material in short strand form [58]. Short polypropylene fibers have relatively low interfacial bond strengths and hence pull out at relatively low stresses [61]. Moreover, when these fibers are used as reinforcement to concrete in the short strand form, there is a lack of control over the fibers’ dispersion as well as location and orientation within the matrix. This is because the typical batch plant storage and weighing hoppers, as well as discharge systems employed in concrete mixing are generally unable to handle such fiber inclusions. Consequently, the difficulties in the use of short polypropylene fibers as reinforcement in concrete have led to a search for long-term solutions. In order to overcome these difficulties, and since polypropylene is still considered to be a satisfactory substitute for asbestos as reinforcement to concrete, a new technology has recently been introduced into the market, creating great enthusiasm among researchers, engineers and contractors, namely textile concrete technology [63-65].

2.8. Textiles for Use in Cement-Based Matrices

From as early as the ancient Roman times, textiles have been known to effectively reinforce brittle matrices subjected to limited tensile loading. The conventional textile production technology comprised of ginning, spinning, weaving, and knitting.

Adaptation of Textiles for use in Cement-base matrices takes place in the traditional textile mills. The first step in the manufacturing process has not changed significantly because it still comprises using the conventional technology of ginning, spinning, weaving, and knitting. However, differences exist in the processing of ordinary textiles for clothing industry, and textiles for use in cementitious composites. For example, for natural fibers, wet processing is an important step whereas for synthetic fibers (for example polypropylene), the manufacturing process includes polymerization prior to spinning, weaving, and finally knitting.

Textile concrete technology itself is a relatively new concept, but it is gradually gaining acceptance, not only in South Africa, but also in other parts of the world, notably, the United States of America and New Zealand [66].

2.8.1. Polypropylene Textiles

During the last decade or so, textiles have been customized for application in cementitious matrices [67, 68].

The development of the textiles owes much to the work of Hannant and co-workers [69, 70] in which continuous open fibrillated polypropylene films were employed as alternatives to asbestos fibers in thin sheet products. The developments were aimed at producing quasi-ductile cement-based composites capable of developing closely spaced cracks at failure [71], without the deleterious health aspects associated with asbestos.

In South Africa, the key developments in the process of manufacture of PP textiles for use in cement-based matrices was to go from a single strand tape or core, to (a) a multi fibril fine fiber core, with (b) the addition of a “hairy” or “fluffy” outer fibrous span component. To prevent segregation or separation of this outer fluffy layer from the inner multi fibril core, it was (c) ultrasonically welded intermittently (also referred to as bonded fiber) to the core at approximately 6 mm centers to ensure sufficient attachment of the “fluffs” to the “fiber”. The bonded fiber is also referred to as a “hybrid fiber”. Figure 18 illustrates the two PP “hybrid” fiber formats: (a) non-bonded and (b) bonded. Non-bonded refers to main fibers with a fluffy layer that has not been ultrasonically welded to the central core.

Polypropylene textile material used is open textured reinforcing (4mmx4mm)-mesh fabric, made of polypropylene strands and fibers. It is designed for use with cement matrices. It is also inert to the alkalinity of cement and has an extended fibrous interface area with which cement matrix can interact and mechanically bond. The textile material has a nominal strength of 2000 kg m^{-1} of width, has a mass of 125 g m^{-2} and moulds to a thickness of 1–2 mm. The polypropylene fiber content in a mix is therefore $6.25\text{--}12.5 \text{ kg m}^{-3}$ against typically 1 kg/m^3 loose fiber that could be mixed in.

The “hybrid fiber” is a unique feature of the yarn because it provides the basis for achieving not only sufficient strength, but controlled mechanical bond to the cementitious matrix and resists fiber pullout behavior, simulating asbestos fiber bonding with cement [72]. The ultrasonic welding of PP fibers illustrated in Figure 18 was developed by Textile Concrete Consultants in South Africa [66].

The PP “hybrid” fiber can provide a very strong mechanical bond to the cement paste (simulating asbestos fiber bonding). The “hybrid” fiber could then be fabricated into a fine or coarse woven textile fabric, further providing localized strength and high fiber volume fraction at the appropriate position and orientation within the cementitious matrix [63, 64]. The textile can be made in different mesh formats depending on the design that is desired. These different formats are either regular or irregular and the fibers themselves can vary from single to multiple strands as illustrated in Figures 19–22.



Figure 18. "Hybrid" fibers showing fluffy outer layer.



Figure 19. "Hybrid" fibers arranged in an irregular single fiber mesh.

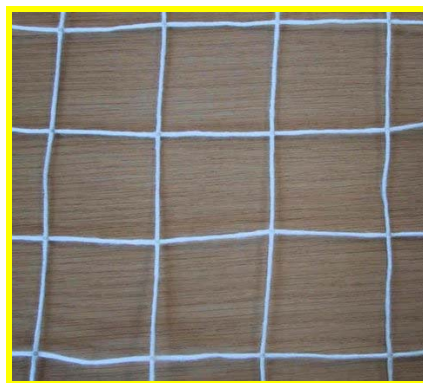


Figure 20. 'Hybrid' fibers arranged in single fiber regular mesh.



Figure 21. "Hybrid" fibers arranged in double fiber regular mesh.

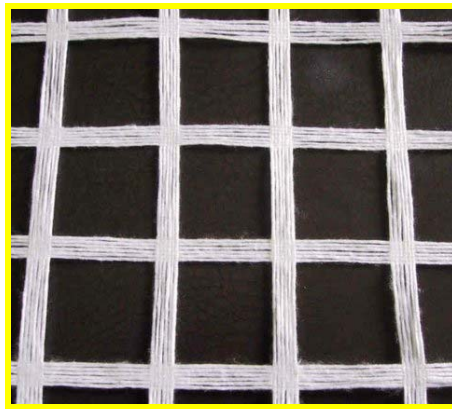


Figure 22. "Hybrid" fibers arranged in multiple fiber regular mesh.

In South Africa particularly, the “hybrid fibers” are woven into a fine or coarse two-dimensional woven polypropylene (PP) textile that is commercially known as Cemforce [66]. The weaving further provides localized strength. Cemforce can also be ultrasonically bonded to water-proof membranes to provide the desired properties.

2.8.2. Specifications of Cemforce

Polypropylene (PP) textiles for use in cementitious matrices are made in the conventional textile manufacturing technique of weaving special PP yarns in the weft direction and fibrillated PP strands (or other fiber types) in the weft direction.

Cemforce consists of two-dimensional woven polypropylene (PP) produced from 110 D'tex (weight in grams per kilometre of fiber) ‘hybrid fibers’ in the weft direction. The ‘hybrid fibers’ consisted of fluffy layers of PP fibrils spun around two strands of fibrillated tapes of polymeric fibers as the core. The inner core is made from two strands; each 110 D'Tex fibrillated polypropylene strands. The outer fluffy layers are spun from 3 d'tex fibers

(10 kilometres of a d'tex of filament weigh 3 grams) to form 100 D'Tex polypropylene filaments [66].

The spinning process arranges the fine fibers helically, at the same time extending them lengthwise along the inner core, with an overlap of approximately 40mm. Each of the fine fibrils in the sheath is 60 mm long. The density of the 'hybrid' (weft) yarns is approximately 0.94 g cm^{-3} and the cross-sectional area is 0.303 mm^3 . The tensile strength and stiffness of the fibers prior to any environmental exposure are approximately 77 N and 1077 MPa respectively [73]. The warp fibers consist of 110 D'tex strands of fibrillated polypropylene tapes. Cemforce (magnified eight times) showing fibers in the warp direction twisted over the weft "hybrid" yarns is shown in Figure 23. The figure shows CemForce at magnification of eight to reveal "hybrid" fibers in the weft direction. The variety of Cemforce shown in Figure 23 is single fiber regular mesh format that was developed by Textile Concrete Consultants in South Africa [66]. The quoted nominal strength of the textile shown in the figure is 20 kN per meter width, and the unit mass is 125 g m^{-2} .

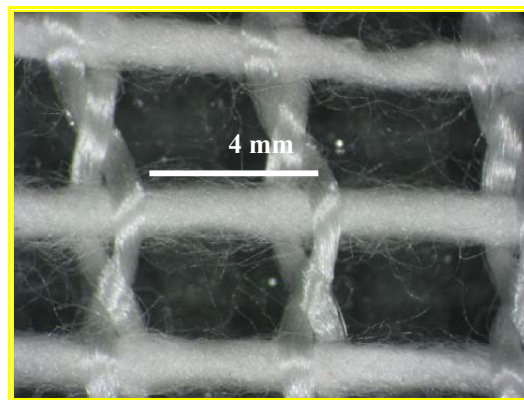


Figure 23. Eight times magnification of Cemforce.

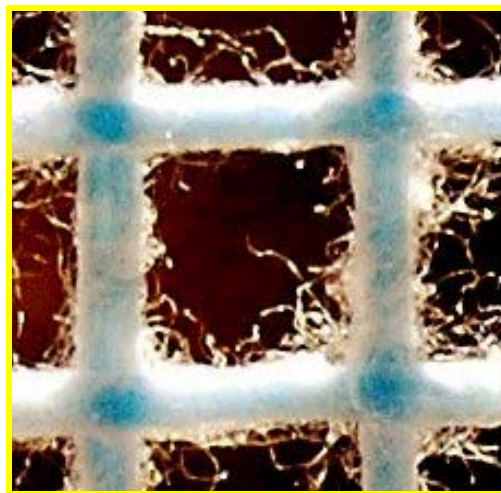


Figure 24. Welded two dimensional single fiber mesh.

A different variety of PP textile that is produced by ultrasonically welding the hybrid fibers in two directions is shown in Figure 24. The welding technique further enhances the performance of the textile in a cementitious matrix. The two types of textiles shown in Figures 23 and 24 clearly depict the extended fibrous interface of the “hybrid” fibers.

2.8.3. Alkali Resistant (AR) Glass Textiles for Use in Cementitious Matrices

AR glass textiles for use in cementitious matrices are woven fabrics of multi-filament yarns. The polymer coating of on the filaments enhances the bonding between the textile and the surrounding finely grained concrete matrix [74]. From civil engineering perspective, the fineness of the yarns used in the production of the textile indicates the degree of reinforcement that the textile will contribute to the composite, i.e. the higher the number of filaments in the particular yarn, the higher the reinforcement. The mass per unit area of AR glass textile ranges between 300 and 1000 g m⁻².

AR glass textiles are manufactured in different specifications, depending on the following variables:

- The reinforcement ratio and the yarns’ properties in both warp and weft directions.
- Fineness of the yarns and the presence or absence of a polymer coating.
- Filament diameter.
- Number of filaments per yarn.
- Yarn spacing.
- Percentage by mass of polymer coating

Figure 25 shows a schematic view of a biaxial textile made of alkali-resistant glass yarns. The figure illustrates the spacing of the yarns in the warp and weft directions. Alkali-resistant glass yarns are utilized in research work by the Institute of Construction Materials, Faculty of Civil Engineering, Technische Universität Dresden, in Germany [74]. A sample of biaxial AR glass textile is shown in Figure 26.

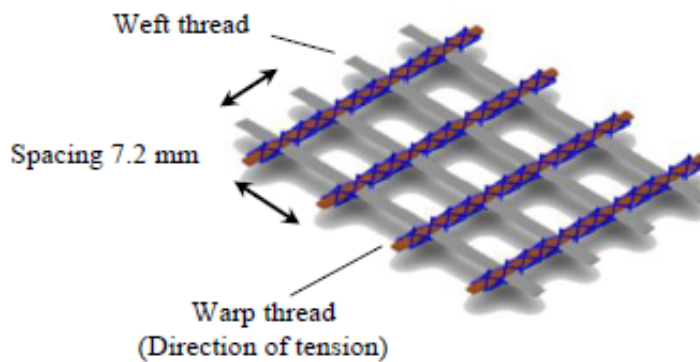


Figure 25. Biaxial textile made of alkali-resistant glass yarns.

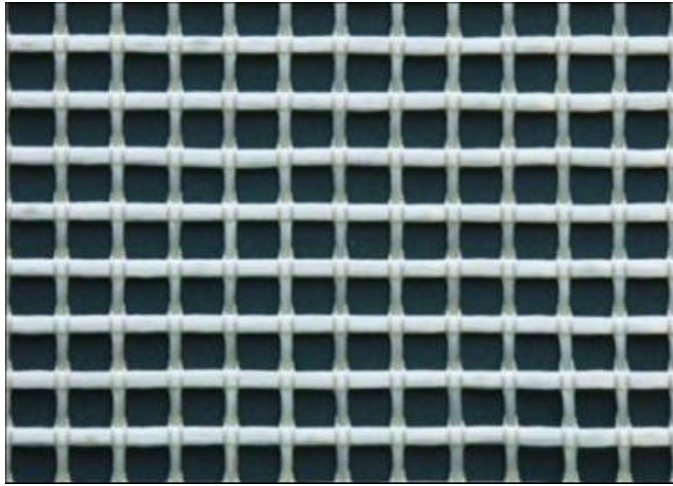


Figure 26. Biaxial textile reinforcement made of alkali-resistant glass textile.

2.8.4. Carbon Textiles

Carbon textiles for use in cementitious matrices are similar to AR glass textiles in that they are woven fabrics of multi-filament yarns. Diameters of carbon filaments are approximately $7\text{ }\mu\text{m}$, an order of magnitude lower than AR glass filaments. Carbon filaments are also polymer coated to enhance bonding. The mass per unit area of carbon glass textiles are lower than AR glass 257 g m^{-2} . Figure 27 shows a sample of carbon fiber textile. Varieties of carbon fiber textiles can be obtained in a similar manner to AR glass textiles i.e. by changing the specifications of the individual filaments, and the woven textile.



Figure 27. Carbon fiber textile.

The advantage of alkali-resistant (AR) glass or carbon fibers in comparison with steel reinforcement is that they are not susceptible to corrosion. In contrast to steel reinforcements, a concrete covering is not necessary. Therefore, slimmer and lighter construction elements and thinner reinforcement layers can be produced.

2.9. TEXTILE CONCRETE

Textile concrete (TC) is a composite that is produced from a woven textile by impregnating it with mortar or fine concrete. The cementitious matrix can be applied by dipping, spraying or block brushing onto the textile. The mortar or concrete can be mechanically pressed into the textile to increase the homogeneity and reduce water and void content. This method of application of concrete does not have the kind of handling problems that would be encountered if discrete fibers were to be used in a bulk mix. As the concrete flows around the fine fibers, it creates a bond and sets into a homogeneous, tough and strong material.

Due to the presence of a woven fabric, Textile Concrete (TC) production utilizes hand lay-up technique that involves compressing the textile in the cementitious matrix to a thickness of between one and two millimeters. The production of TC involves casting a number of textile layers in fine grained mortar. As illustrated in Figure 28(a), six layers were cast in mortar produced from fine grained sand to cast the sample shown in Figure 28(b) [73].



Figure 28. Textile concrete composite.

By using TC, there is better structural efficiency, firstly because the paste is often high quality, and secondly because there is a reduced cover in thin element applications.

In the South African Textile Concrete industry, layers of Cemforce are placed in cement paste, mortar or concrete in the appropriate location and orientation for optimum performance to produce a composite with very high fiber volume fraction (in excess of 10 percent). Because cracking in concrete depends on type and amount of fiber, a high fiber volume fraction results in significant reduction in cracking. The applications of TC are: thin elements; permanent forms; containers; signs and many more [66].

2.9.1. Textile Reinforced Concrete (TRC)

Textile Reinforced Concrete (TRC) is a new technique of placing a textile fabric on an existing concrete structural element, and thereafter impregnated the textile with mortar (or fine grained concrete) in order to strengthen the element. The composite acts as a reinforcement that is placed onto a damaged part of an existing structure [74]. Figure 29 shows an AR-glass fiber textile being placed at the bottom of a damaged concrete beam prior to impregnation with mortar.

TRC can be used in prefabrication for new construction. Two examples of TRC application are described in detail by Butler *et al* [75]. The examples are: a façade panel and a hybrid pipe system with an inner plastic layer. A different example of TRC application is seen from the work by Jesse [76] whereby segments made of TRC were used for construction of a pedestrian bridge with bondless pre-stressing. Another pedestrian bridge with a record length of 100 m was composed of six large precast TRC elements. Figure 30 shows application of mortar on a textile for repair of a top surface of a damaged part of a structure [77]. By embedding the textile reinforcement in mortar, the structure is strengthened.



Figure 29. Placing of textile to reinforce existing structure.



Figure 30. Strengthening of damaged structures.

CONCLUDING REMARKS

This Chapter has mainly dealt with the production techniques of four different classes of fibers which are used for reinforcing cementitious matrices. These classes are; natural, metallic, mineral, and synthetic fibers. Sisal has been discussed as the most common type of natural fibers. Within the class of metallic fibers, different types of steel fibers have been discussed. Glass and carbon fibers, which represent the class of mineral fibers, have been dealt with. Polypropylene (PP), which is an abundant and economical synthetic fiber, has been dealt with in as far as its industrial processing is concerned. The physical and mechanical properties of the different types of fibers have also been briefly reviewed.

The advantages of using textiles instead of discrete fibers have been highlighted. The production techniques of textiles from the different types of fibers have been dealt with.

Finally, the production of the composite: Textile Concrete (TC) has been dealt with together with the common applications of the composite. A special application that is referred to as Textile Reinforced Concrete (TRC) has been highlighted. The technique used in TRC in the repair of damaged concrete elements has been briefly discussed.

ACKNOWLEDGEMENTS

I am indeed indebted to various individuals who participated in one way or the other towards making this chapter possible.

I would like to extend my sincere gratitude in a special way to the Principal of the School of Engineering, and staff of the Department of Civil and Construction Engineering, University of Nairobi for the opportunity to provide their services and for the invaluable moral support they gave in the course of writing this chapter.

I would also like to extend my gratitude to the Director of Kenya Building Research Centre at the Ministry of Public Works in Nairobi and the staff who took time out of their busy schedules to provide the necessary information required in writing this chapter. The research team of the Forum for Women Engineers and Girl Scientists in Africa: (Forum WEGSA)-Kenya Chapter, who endured long hours going through the manuscript and ensuring accurate information was presented in this work. To my family who endured long hours of my absence deserve special mention. I thank you all for your contributions to this very special book Chapter.

REFERENCES

- [1] Moore, E. (1996). *Polypropylene Handbook*; Hunser Publishers.
- [2] Morel, V. (2001). “*The pyramid Builders*”, National Geographic magazine. pp 78-99 (ISBN 0027-9358)
- [3] World Wide Web page. www.sacred-destinations.com/italy/sacred-sites, The Pantheon
- [4] World Wide Web page. www.sacred-destinations.com/italy/sacred-sites, The Colosseum

-
- [5] World Wide Web page. www.livius.org/ei-er/emperors/emperors01.html, Emperor Nero
- [6] World Wide Web page. www.artres.com/c/htm/tree-flight.aspx?sca,Scala/Art Resource, NY
- [7] Hein, M. (2001). “*Historical Timeline of Concrete*”; Auburn University Building Science Department; BSCI 3450, 1-19.
- [8] McGovern, M. (2001). “*Concrete Technology Today*”; Portland Cement Association no. 3. 22: 1-5.
- [9] Neville, A.M. (1996). “*Properties of Concrete*”; Pitman Publishing Co: 1977.
- [10] Derek, H.; Clyne, T.W. *An Introduction to Composite Materials*; 2nd edition, Cambridge University Press.
- [11] The Second Book of Moses Called EXODUS. *The Holy Bible*; New King James Version; Thomas Nelson, Inc. Nashville, TN, USA, 1982; Ex. Ch 5, Vs. 7-16.
- [12] Microsoft® Encarta® Encyclopedia (2002). © 1993-2001 Microsoft Corporation.
- [13] Matthews, F.L.; Rawlings, R.D. (1994). *Composite Materials*; Engineering and Science; Chapman and Hall: London.
- [14] Dennis, J.H. (1991). “Synthetic Fibers Strengthen Concrete: History of Fibrous Concrete”; *Ready Mix*, p 26-27.
- [15] Brothie, J.E., Urbach, G. (1962). “*Flexural Behaviour of Fibrous Plastic Sheets*”. 14(1): 68-93.
- [16] Nilsson, L. (1975). “*Reinforcement of Concrete With Sisal and Other Vegetable Fibres*”; Swedish Council for Building research: Report D.14.
- [17] Mawenya, A.S., Mwamila, B.L.M. (1980). “Characteristics of Sisal as a Reinforcing Fibre”, *Uhandisi Journal*, 5(1): 24-34.
- [18] Lock, G.W. (1969). *Sisal*; 2nd Edition; Longman.
- [19] Nutman, F.J. (1936). “Agave Fibres”, *Empire journal of Experimental Agriculture*. 5: 7-111.
- [20] Swift, D.G.; Smith, R.B.L. (1978). “*Sisal Reinforcement of Cement Paste and Concrete*”. *Proceedings: Int’l. Conf. of Materials of Construction for Developing Countries*; Asian Institute of Technology, Bangkok, pp 221-234.
- [21] Castro, J.; Naaman, A.E. (1981). “Cement Mortar Reinforcement with Natural Fibres”. *ACI Journal Technical Paper*, 78 – 106.
- [22] Skarendhal, A. (1982). “*Natural Fibre Concrete for Roofing*”. 27-29th April 1982, paper Presented at the National Construction Council Seminar on Building Materials, Arusha, Tanzania.
- [23] Mutuli, S.M., Bessell, T.J., and Talitwala, E.S.J. (1982). The Potential of Sisal as a Reinforcing Fiber in Cement based materials. *African Journal of Science and Technology*, 1(1): 50 – 63.
- [24] Mawenya, A.S., and Mwamila, B.L.M. (1980). Rheological Properties of sisal reinforced concrete. *University Science Journal* (Dar es Salaam University), 6 (1), pp 177 – 189.
- [25] Persson, H., and Skarendahl, A. (1978). *Sisal fiber concrete for roofing sheets and other purposes*, SIDA Industrial Division.
- [26] Mawenya, A.S. (1983). “*Developments in Sisal Fiber Reinforced Concrete*”. 7 – 14th Nov. 1983, Proceedings: Symposium on Appropriate Building Materials for Low Cost Housing: Africa Region; Nairobi, Kenya, E. and F. Spon.

-
- [27] Mativo, M. “*Appropriate Technology Building Materials*”. (1990 – 1991), Final Year Project Report. Department of Civil Engineering, University of Nairobi. Chapter 2: Fibre Concrete Roofing Sheets.
 - [28] Mawenya, A.S., and Mwamila, B.L.M. (1981). “*Mechanics of Sisal Fibre Concrete*”. 1981, Internal Report, Department of Civil Engineering, University of Dar es Saalam, Tanzania.
 - [29] Theuri, S.M. “*Use of sisal fibres for concrete reinforcement*”. (1986 – 1987), Final Year Project Report. Department of Civil Engineering, University of Nairobi.
 - [30] Sir Fredrick, S. and Partners. The use of Dramix steel fibre reinforcement for concrete industrial ground floor slab. Imperial College. 1988, pp 24.
 - [31] Beckett, D., and Shah, S. (1989). Comparative tests on plain, fabric reinforced and steel fibre reinforced concrete ground slabs. *Thames Polytechnic*, 34 Ref: TP/B/1.
 - [32] Soroushian, P., and Baysai, Z. (1991). Fiber type effects on the performance of steel fiber reinforced concrete. March/April 1991, *ACI Materials Journal*, 88(2): 129 – 134.
 - [33] John, G. (2001). Ten years of steel-fiber concrete: A manufacturer’s view”, *Concrete*. September 2001.
 - [34] Association of Concrete Industrial Flooring Contractors, *Steel fiber reinforced concrete industrial ground floor slabs: an introductory guide*. 1999, The Concrete Society, pp 24 (ref: CS124).
 - [35] Gray, R. (1984). Autogenous healing of fiber/matrix interfacial bond in fiber-reinforced mortar, *Cement and Concrete Research*, No. 3, 14: 315 – 317.
 - [36] ASTM C1018: Standard Test Method for Flexural Toughness and First- Crack Strength of Fibre- Reinforced Concrete.
 - [37] ASTM A820: Standard Specification for Steel Fibres for Fibre- Reinforced Concrete.
 - [38] ASTM C94: Standard Specification for Ready- Mixed Concrete
 - [39] ASTM C1116: Standard Specification for Steel Fibers for Fiber- Reinforced Concrete and shotcrete.
 - [40] ACI 506: Guide for Shotcrete.
 - [41] ACI 544- 3R: Guide for Specifying, Proportioning, Mixing, Placing, and Finishing Steel Fiber Reinforced Concrete.
 - [42] Thoof, H. (2000). Structural behavior of steel fiber reinforced pile supported concrete floors. *Concrete*, 34(8): 50 – 54.
 - [43] Emmitt, K. (2000). The use of Durablend at the Port of Tyne, Fibrin UK/Bekaert internal report, Summer 2000.
 - [44] Carbon Solutions from Conoco, www, <http://carbonfiber.conoco.com/> Cevolution.
 - [45] Hill, J., Thomas, C.R., and Walker, E.J. (1974). Proceedings of the International Conference on “Carbon Fibres, Their Place in Modern Technology”, The Plastics Institute: London.
 - [46] Odian, G. (1991). *Principles of Polymerization*; Third Edition; John Wiley and Sons, Inc: 657-658.
 - [47] Jackson, N., and Dhir, R.K. (1984). *Civil Engineering Materials*; Fourth Edition; ELBS/Macmillan, 27: 351.
 - [48] Norman, R.O.C., and Waddington, D.J. (1983). *Modern Organic Chemistry*; Fourth edition; ELBS/Bell and Hyman: Ch. 21 pp. 327- 329.
 - [49] Fibermesh Division, Synthetic Industries Inc., “Fibermesh Micro-Reinforcement System. Advancing Concrete Technology The World Over”. 1989, Brochure Series.

-
- [50] Dennis, J.H. (1987). Fiber reinforcement comes of age. *Concrete*, April 1987,
- [51] Landau, A. (1987). Director of International Sales, Fibermesh Division, Synthetic Industries Inc., “*Breakthrough to increase the life of concrete structures*”; ISSN: 0217 – 5541; Building and Construction News: July 1987.
- [52] World Wide Web Page. [www.mbt-middle-east.com/MBT online](http://www.mbt-middle-east.com/MBT_online) (Master Builders Technologies), “Products”.
- [53] “Fiberon” Technical Information and Data Sheet. International Engineering Materials and Supplies Est., Abu Dhabi, United Arab Emirates.
- [54] Chaudri, M.A., Jamil, N.A., Shandila, Shamin, M. (1982). *Pakistani Journal of Scientific and Industrial Research*. 15: 405.
- [55] Evans, B. (1986). Understanding Natural Fiber Concrete: Its Application as a Building Material. *International Technical Publication*: 4 – 23.
- [56] Shah, S.P. (1972). *Mineral Organic and Metallic Fiber Reinforced Concrete*” Proc., New Materials in Concrete, Univ. of Illinois at Chicago Circle, pp 1 – 23.
- [57] Tait, R.B., and Guddye, C. (2002). “*Textile Concrete- Mechanical Characterization of a Unique Fiber System for Cement Composites*”. March 13 – 14, 2002, Concrete for 21st Century Conference, Johannesburg.
- [58] Hannant, D.J. (1978). *Fiber Cements and Fiber Concretes*, John Wiley.
- [59] Heger, F.J.; Simpson, G. “*Buildings: Plastics and Composites*”, The Encyclopaedia of Materials, Arlington, U.S.A.
- [60] World Wide Web Page. <http://www.un.org> (2003). United Nations, “*Promoting Sustainable Human Settlement Development*”, United Nations Division for Sustainable Development, Agenda 21.
- [61] Gray, B.H. (1972). “*Fibre Reinforced Concrete – A General Discussion of Field Problems and Applications*”, Proc., New Materials in Concrete, Univ. of Illinois at Chicago Circle, 1 – 14.
- [62] Neville, A.M. (1971). “*Hardened Concrete: Physical and Mechanical Aspects*”; Michigan, ACI.
- [63] Owens, G. (2002). Concrete Trends – Annual Cement and Concrete Review. *Journal of Cement and Concrete Institute*, 4 – 11.
- [64] Aspires, F.F., and Manalo, J.R.I. (1995). Utilisation of Textile Waste Cuttings as Building Material, *Journal of Materials Processing Technology*, 48: 379 – 384.
- [65] Callec, P., (2003). “*Textile reinforced Concrete*”, World Wide Web Page <http://www.rilem.net>, RILEM Publications.
- [66] Textile Concrete Consultants, World Wide Web Page <http://www.textileconcreteconsultants.com/reinforced.html>
- [67] Kenai, S., Refai, A., and Brooks, J. *The use of polymer grids as surface reinforcement to plain and reinforced concrete*, in ‘New Development in Concrete Science and Technology’; Southeast University, Nanjing; China.
- [68] Konrad, M., Chudoba, R., Butenweg, C., and Brukermann, O. (2003). Textile reinforced concrete part ii: Multilevel modeling concept, in ‘International Conference on the Applications of Computer Science and Mathematics in Architecture and Civil Engineering’, Weimer.
- [69] Hannant, D., Zonsveld, J., and Hughes, D. (1978). Polypropylene film in cement based materials, *Composites*, 83 – 87.
- [70] Hannant, D., and Zonsveld, J. (1978). *Polyolefin fibrous networks in cement*.

- [71] Hibbert, A., and Hannat, D. '*Toughness of cement composites containing polypropylene films compared with other fibre cements*', *Composites*, The International Journal of Science and Technology of Reinforced Materials, Plastics, Cement, Metals, Ceramics (Special Issue), 393 – 399.
- [72] Tait, R. (2002). Guddye, C. Textile concrete-mechanical characterization of a unique fibre system for cement composites, in 'Concrete for 21st Century Conference'; Johannesburg.
- [73] Mumanya, S.W. (2007). Evaluation of mechanical properties of Textile Concrete subjected to different environmental exposures. PhD Thesis, University of Cape Town, South Africa.
- [74] Bruckner, A., Ortlepp, R., and Curbach, M. (2006). Textile reinforced concrete for strengthening in bending and shear. *Mater Structures*, 39: 741 – 748.
- [75] Butler, M., Hempel, R., and Schorn, H. (2006). Bond behavior of polymer impregnated AR_Glass textile reinforcement in concrete. In: Proceedings of the International Symposium Polymers in Concrete. April 2-4, Guimares, Portugal, 173 – 183.
- [76] Jesse, D., and Jesse, F. (2010). *Textile Reinforced Concrete FOR Lightweight Segmental Bridges with Post-Tensioning*. In: Proceedings of 3rd International fib Congress. Washington D.C., USA, May 29 – June 2 2010; Paper 154.
- [77] Hegger, J., Kulas, C., and Goralski, C. (2010). Elegant foot – bridge of textile-reinforced concrete- Design and construction. *Concrete Plant + Precast technology; IBFT International*: 76 (2): 60 – 61.

Chapter 7

A REVIEW ON THERMAL ENGINEERING DESIGN OF CLOTHING

Luo Jie¹, Mao Aihua^{2,*} and Li Yi¹

¹ Institute of Textiles and Clothing,
Hong Kong Polytechnic University,
Hung Hom, Hong Kong.

² School of Computer Science and Engineering,
South China University of Technology,
Guangzhou, 510006, China.

ABSTRACT

Clothing thermal engineering design is an effective and economical solution of designing clothing with superior thermal performance for people to live in various environments with a feeling of comfort. To achieve desirable thermal functions, the clothing design process is not traditional trial and error but a functional engineering process which involves multi-disciplinary knowledge and computer-aided design (CAD) technologies to investigate, simulate and preview the physical thermal behaviors in the clothing. Clothing designers can thus scientifically evaluate with computer before the produce of real products that if their design concepts are achieved and suitable for the expected wearing environment. This chapter gives a systematical review on the related research and methods in clothing thermal engineering design. The accomplishment of clothing thermal engineering design is on the fundamentals of the computational simulation of the thermal behaviors and CAD technologies.

1. INTRODUCTION

Clothing plays a very important role in the daily lives of human beings, as it contributes to biological health and psychological happiness in our lives. More and more modern

* Corresponding author. E-mail address: ahmao@scut.edu.cn

consumers understand the importance of textiles and thus have come to prefer the apparel products with high added values in terms of functional performance [1]. Currently, clothing design focuses not only on the pattern and fashion design, but also pays more attention to the functional performance of the clothing, making the clothing more smart and satisfying human needs in various environments.

From the points of view of biology and physiology, people will be aware of discomfort in terms of warmth or coolness if the temperature of any part of the skin changes by more than 4.5°C , and will be fatal if the core body temperature rises or falls by more than 1.5°C [2]. Actually, there is a thermoregulatory system inside the human body to maintain the body thermal comfort or even being survived in various external environments. When the body temperature drops or rises, the human body must generate or dissipate heat to allow the body temperature to remain in the reasonable range. However, when people are exposed in an extremely hot or cold environment, the thermoregulatory system is not strong enough to maintain the balance between the rates of heat loss and heat generated inside the body. The clothing, as the barrier between the body and environment, needs to be sensitive enough to take the outside environment into consideration and generate a reasonable thermal microenvironment around the body to help it deal with/cope in extreme weather conditions. Recently, with the successful multidisciplinary teamwork, more and more innovative textile materials and structures are developed for the study of biology and health [2]. Heat generating/storing fiber/fabrics, micro and nano-composite materials, smart phase change material and intelligent coating/membrane are developed and available for clothing functional design [3]. The clothing with superior thermal performance is being known to consumers and regarded as an important concern in their buying decision.

Clothing thermal engineering design is a systematic solution of designing clothing with superior thermal performance for people to deal with various environments, which considers the whole wearing situations, including not only the clothing material, but also the biological behaviors of human body and the wearing environments. Figure 1- illustrates all the key issues to be considered in the clothing thermal engineering design. The final product of clothing is supposed to be achieved considering all the physical and physiological phenomena involved during the wearing process. For instance, the design of clothing worn in the hot environment or a certain activity situation should consider the hot sensitive parts of the body which easily accumulate sweat. The design of clothing worn in the cold environment should consider the cold sensitive parts of the body which need more thermal protection. The thermal performance of the designed cloth needs to be suitable for the wearing situations.

The computer plays a critical role in the clothing thermal engineering because it offers a virtual platform for the users to perform their design in the following ways: (i) the rapid provision of numerical and graphic representation to the traditional qualitative trial-and-error method of clothing design; (ii) detailed product design, which is manually practiced in design/workshop office in traditional way; (iii) and modeling the involved behaviors/mechanisms and visualizing product performance. This computerized engineering method makes a great advance in both the computer applications and functional clothing engineering design. However, it cannot be taken for granted that this method can be realized individually by computer technologies or engineering design or their simple combination. It is an engineering application of multi-disciplinary knowledge which makes effective communications and integration between the research studies in different areas.

In order to establish a theoretical understanding of the knowledge behind this computerized thermal engineering system, it is necessary to investigate the physical and physiological behaviors involved in the wearing system and their mathematical representations in the virtual environment. Also it is necessary to devise effective strategies to diffuse the computer technologies into the clothing thermal engineering design.

2. THERMAL BEHAVIORS IN THE CLOTHING WEARING SYSTEM

Clothing is one of the most intimate objects in people's daily life since it covers most of the human body most of the time. People may keep having subjective psychological feelings of the clothing and consciously judging the warm/cold/comfort sensation during the wearing time. On the basis of wearing experience, people can make a rough evaluation of the thermal function of clothing and choose suitable clothing for their daily activities. However, as projected in the thermoscopic world, the wearing situation of people can be regard as a complex and interactive multi-component system. Figure 1 shows the components of the clothing wearing system. The thermal behaviors involved in the wearing situation may be categorized as [4]:

- (i) Heat and moisture transfer in the textile materials. This is the physical behavior mainly deciding the thermal performance of clothing. It can be regarded as the following physical process:
 - The heat transfer process in the textile material in terms of conduction, convection and radiation;
 - The vapor moisture transfer process in the textile material in terms of diffusion and convection;
 - The liquid water transfer process in the textile material;
 - Phase change process in the textile material. It is an approach allowing the heat and moisture transfer in a coupled way, including moisture condensation/evaporation in the fabric air void volume, moisture absorption/desorption of fibers, and micro-encapsulated phase change materials;
 - Influence of functional treatments of textiles on the heat and moisture transfer process, such as waterproof fabric, moisture management treatment, PCM coating and heating fabrics.
- (ii) Thermoregulatory behaviors of the human body, such as sweating, shivering and biological metabolism, and heat and moisture exchange of body skin and environment.
- (iii) Interactions between the inner clothing and body skin.
- (iv) The climatic conditions of wearing situation in terms of temperature, relative humidity and wind velocity, which influence the heat and moisture behaviors of textile materials and the human body.

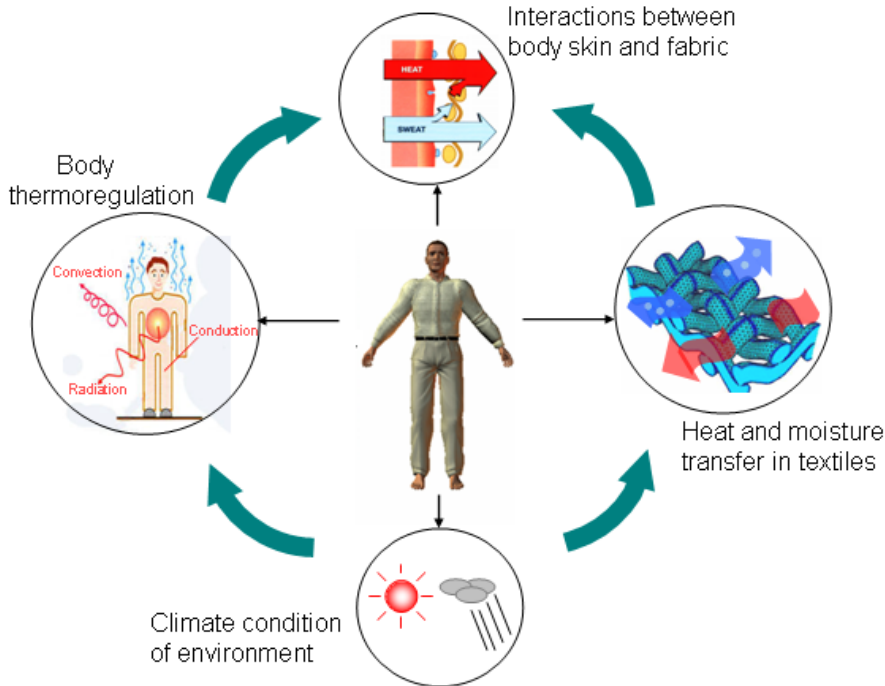


Figure 1. Components of the clothing wearing system.

3. THEORETICAL MODELING OF THE CLOTHING WEARING SYSTEM

3.1. Heat and Moisture Transfer in the Textile Materials

Normally, the heat and moisture transfer processes in the textile material occur when there are gradients of temperature and water vapor pressure across textile structures, and these two processes are often coupled accompanying with the appearance of phase change process.

3.1.1. Heat Transfer Process

The overall heat transfer in textile materials is the sum of contributions through the fiber and interstitial medium, which may involve multiple transfer mechanisms in terms of conduction, convection and radiation. Theoretically, conduction heat transfer always occurs in the solid fiber material and the medium trapped in the spaces between the fibers as long as a temperature gradient is presented. Convection heat transfer will be obviously observed if the medium is gaseous and if the space is large enough, that is to say, the more porous the textile material is, the more effectively convection takes place. Radiation heat transfer can be ignored when the temperature gradient is small. Consequently, the heat transfer via conduction is the most dominant transfer mechanism.

In the engineering applications, thermal conductivity is usually adopted to express the thermal properties of materials because thermal conduction is better documented and mathematically analyzed [5]. Unlike other porous materials, in textiles the air filled in the space between fibers has substantially bigger proportion than that of the fibers and the

thermal conductivity of fiber is much smaller than air [6]. The heat flow by thermal conduction at any position (x) inside the textile structure can be expressed by the Fourier's law:

$$Q_k(x)_c = -K \frac{dT(x)}{dx} \quad (1)$$

$$K = (1 - \varepsilon)K_f + K_a \quad (2)$$

where, Q_k is conductive heat flux, T is the temperature and K is the effective thermal conductivity of the textile structure, which is the combination of the conductivities of the air (K_a) and the solid fiber (K_f). ε is the porosity of textile material.

The radioactive heat transfers in the ways of emitting or absorbing electromagnetic waves when the standard temperature of the textile material is above zero. The intensity of radioactive is depended on the ratio between the radiation penetration depth and the thickness of textile material, besides the temperature difference between the two surfaces of textile material. Farnworth reported that when the radiation depth is similar to the thickness of fabric, the amount of radiation should be taken into account as it is comparable to the amount of the conduction heat flow, and the radiation heat flux in fabric can be expressed by [7]:

$$\frac{\partial F_R}{\partial x} = -\beta F_R + \beta \sigma T^4, \quad \frac{\partial F_L}{\partial x} = \beta F_L - \beta \sigma T^4 \quad (3)$$

$$\beta = \frac{(1 - \varepsilon)}{r} \varepsilon_r \quad (4)$$

where, β is the radiation absorption constant for textile materials, σ is the Boltzmann constant, F_R and F_L respectively is the total thermal radiation incident traveling to the right and left way.

3.1.2. Moisture Transfer Process

Thanks to the porosity of the fabric, the interstices between fibers provide the space for moisture to flow away. There are four ways of moisture (in the phase of water vapor or liquid) transfer occurring in textile materials as summarized by Mecheels [8]: (i) diffusion through the space between the fibers, (-ii) absorption/desorption by the fiber materials, (iii) transfer of liquid water through capillary interstices in yarns/fibers, and (iv) migration of liquid water on the fiber surface.

There are many similarities between heat conduction and moisture diffusion in the textile material. When the system scale, material properties and initial and boundary conditions are similar, the governing equations, analysis methods and results would be analogous for these two processes [9]. When there is a difference between the water vapor concentration on the fibers' surface and that of the air in the fiber interstices, there will be a net exchange of

moisture. The water vapor diffusion through the textile material can be described by the First Fick's law [9]:

$$Q_w = D_a \frac{\Delta C}{L} \quad (5)$$

where Q_w is the moisture transfer rate, D_a is the diffusion coefficient of water vapor through the textiles, L is the thickness of the fabric sample, and ΔC is the vapor concentration gradient of two fabric sides.

Since the fiber has a small proportion of volume in the fabric, the main contribution of moisture flux is from the diffusions process through the air in the fiber interstices. However, it was identified by Wenhner *et al.* [10] that absorption of moisture by the fiber also importantly affected the response of fabric to the moisture gradient. The water vapor concentration on the fiber surface, theoretically, depends on the amount of absorbed moisture onto the surface and the local temperature of the fiber. The fiber will keep absorbing as much moisture as it can until it reaches a saturated status with respect to the absorption rate. And when the fiber becomes saturated, additional vapor moisture may condense into liquid phase onto the fiber surface. With regard to the physic nature of fibrous materials, condensate water may be held on the surface of the fiber and be relative immobile, or may be transferred across the textile structure by capillary actions.

The moisture absorption capacity of fibers is described by the property of hygroscopicity (also called moisture regain), which means the amount of moisture that the fiber contains when placed in an environment at certain temperature and relative humidity. In 1967, Nordonb land David [11] proposed an exponential relationship to describe the change rate of water content of the fibers, and developed a numerical solution with computer technology at that time. Li and Holcombe, in 1992, devised a new absorption rate equation by analyzing the two-stage sorption kinetics of wool fibers and incorporating it with more realistic boundary condition [12]. They assumed the water vapor uptake rate of fiber is composed by two components associated with the two stages of sorption:

$$\frac{\partial C_f}{\partial t} = (1 - \alpha)R_1 + \alpha R_2 \quad 0 \leq \alpha \leq 1 \quad (6)$$

$$R_1 = \frac{\partial C_f}{\partial t} = \frac{1}{r} \frac{\partial}{\partial r} (r D_f \frac{\partial C_f}{\partial r})$$

where, R_1 and R_2 are the moisture sorption rates in the first and second stages respectively, α is the proportion of uptake occurring during the second stage. R_1 can be obtained by regarding the sorption/desorption process as Fickian diffusion. R_2 is identified by experimental data and related to the local temperature, humidity and sorption history of the fibers.

3.1.3. Liquid Transfer Process

When liquid water transfers across the textile material, it will experience wetting and wicking stages, in which wetting of textile is prerequisite for the wicking process [13]. Both wetting and wicking are determined by surface tensions between the solid-vapor-liquid interfaces. In view of the macroscopic world, these tensions are the energy that must be supplied to increase the surface/interface area by one unit. The liquid water put in touch with fibrous material comes to an equilibrium state with regard to minimization of interfacial free energy on the surface. The force involved in the equilibrium can be expressed with the well-known Young's equation:

$$\gamma_{LV} \cdot \cos \theta = \gamma_{SV} - \gamma_{SL} \quad (7)$$

where, γ_{sv} , γ_{sl} , γ_{lv} respectively represents the interfacial tensions that exists between the solid-vapor, solid-liquid and liquid-vapor interfaces. And the term γ_{lv} is also usually regarded as the surface tension of the liquid. θ is equilibrium contact angle, which is the consequence of wetting instead of the cause of it. The term $\gamma_{LV} \cdot \cos \theta$ is defined as adhesion tension or specific wettability of textile material. This equation shows that wettability increases with the decreased equilibrium contact angle θ . The equilibrium contact angle is an intrinsic value described by the Young equation for an ideal system. However, precise measurement of surface tension is not commonly possible. The experimentally measured contact angle between the fiber and the liquid can be observed on a macroscopic scale and is an apparent physical property.

When textiles surface is fully wet by the liquid, the wicking process will happen spontaneously, where the liquid water transports into the capillary space formed between fibers and yarns by capillary force. The fibrous textile assembly is a complex non-homogeneous capillary system due to irregular capillary spaces. These spaces have various dimensions and discontinuous radius distributions. The practical engineering field, an indirectly determined effective capillary radius, is adopted to represent the no-uniform capillary spaces in yarns and fabrics. If the penetration of liquid is limited to the capillary space and the fiber does not absorb the liquid, the wicking process is called capillary penetration, and the penetration is originally driven by the wettability of the fiber, which is decided by the chemical nature and geometry structure of its surface [13]. Ito and Muraoka pointed out that the wicking process will be suppressed with the decreased number of fibers in the textiles [14]. When the number of fibers becomes greater, water moves along the void spaces even between the untwisted fibers, which indicates that sufficient number of continuity of pores is very important to the wicking process.

3.1.4. Coupled Heat and Moisture Transfer

The research of the heat transfer and moisture diffusion in textile materials was initially regarded as independent under the assumption that the temperature and moisture concentration of the clothing is steady over a period of time. In this steady-state condition, there is no need to address the interactions between heat and moisture transfer process [15]. However, under some transient situations where some phase change processes happen, such

as moisture sorption/desorption and evaporation/condensation, these two processes are coupled and interact significantly.

The moisture absorption/desorption capability of the solid fiber depends on the relative humidity of the enclosed air in the microclimate around the fiber and the type of fiber material. When fibers absorb moisture, heat is generated and released. Consequently, the temperature of fiber will rise and thus results in an increase of dry heat flow and a decrease in latent heat flow across the fabric [16]. The absorbed/desorbed moisture of fibers and the water vapor in the enclosed microclimate in textiles compose the water content of the textile material, which can originate from the wicking process or result from condensation in case of the fully saturated water vapor in fibrous materials [17].

Similar to the phase change process of moisture sorption/desorption, liquid condensation/evaporation pose an impact on the flow of heat and moisture across the textiles by acting as a heat source or be merged into the heat transfer process. Condensation is a physical phenomenon which commonly takes place when the fibrous material is exposed to a large temperature gradient and high humid source, both of which cause the local relative humidity to attain 100% or full saturation. And provided that there is still extra moisture diffusing into the fibrous material, condensation continues. The condition of condensation is different from the transient process of moisture sorption/desorption. When the relative humidity of surrounding microclimate is less than 100%, evaporation occurs.

The first model describing the transient heat and moisture transfer process in porous textile material was developed by Henry (1939) in terms of two differential equations respectively for mass and heat governing formulation [18], as listed in the following. A simple linearity assumption was made in this model to describe the moisture absorption/desorption of fibers to obtain analytical solution. This modeling work established a basic framework of modeling the complicated coupled process of heat and moisture transfer through the textiles material.

$$\varepsilon \cdot \frac{\partial C_a}{\partial t} = \frac{D_a \cdot \varepsilon}{\tau_a} \cdot \frac{\partial^2 C_a}{\partial x^2} - (1 - \varepsilon) \cdot \Gamma_f \quad (8)$$

$$C_v \cdot \frac{\partial T}{\partial t} = K_{fab} \cdot \frac{\partial^2 T}{\partial x^2} + (1 - \varepsilon) \cdot \lambda_v \cdot \Gamma_f \quad (9)$$

$$\Gamma_f = \frac{\partial C_f}{\partial t} = const. + a_1 C_a + a_2 T \quad (10)$$

where, α_1 and α_2 are coefficients. Henry assumed the moisture sorption rate Γ_f to be a linear relationship between temperature and moisture concentration, allowing him to solve the equations analytically.

Ogniewicz and Tien [19] proposed a model considering the heat transport that happened by the ways of conduction, convection and condensation in a pendular state. That model ignored moisture sorption and was lack of a clear definition of the volumetric relationship between the gas phases and the liquid phase. Motakef [20] extended this analysis to describe

mobile condensates, in which the moisture condensation was taken into account with simultaneous mass and heat transfer process.

$$\frac{\partial C_a}{\partial t} = D_a \frac{\partial C_a}{\partial x} + \Gamma_{lg} \quad (11)$$

$$c_v \frac{\partial T}{\partial t} = K \frac{d^2 T}{dx^2} - \lambda_{lg} \Gamma_{lg} \quad (12)$$

$$\rho_c \varepsilon \frac{\partial \theta}{\partial t} = \rho_c \varepsilon \frac{\partial}{\partial x} \left(D_l(\theta) \frac{\partial \theta}{\partial x} \right) - \Gamma_{lg} \quad (13)$$

In Motakef's model, a concept of critical liquid content (CLC) was introduced to address the liquid diffusivity. When the liquid content θ is below the CLC, the liquid is in the pendular state and has no tendency to diffuse. When the liquid content θ is beyond the CLC, a liquid diffusivity $D_l(\theta)$ was introduced to describe the liquid transfer by surface tension force from regions of higher liquid content to the drier regions. $D_l(\theta)$ is a complicated function of the internal geometry and structure of the medium.

Fan and Luo [17] incorporated the new two-stage moisture sorption/desorption model of fibers into the dynamic heat and moisture transfer model for porous clothing assemblies. They considered the radiation heat transfer and the effect of water content of fibers on the thermal conductivity of fiber material. Further, Fan and his co-workers improved the model by introducing moisture bulk flow, which was caused by the vapor-pressure gradients and super-saturation state [17]. This improvement made up for the ignorance of liquid water diffusion in the porous textile material in previous models. The equations of the model are listed as follows:

$$\varepsilon \frac{\partial C_a}{\partial t} = -\varepsilon \mu \frac{\partial C_a}{\partial x} + \frac{D_a \varepsilon}{\tau} \frac{\partial^2 C_a}{\partial x^2} - \Gamma(x, t) \quad (14)$$

$$\rho(1 - \varepsilon) \frac{\partial (W - W_f)}{\partial t} = \rho(1 - \varepsilon) D_l \frac{\partial^2 (W - W_f)}{\partial x^2} + \Gamma(x, t) \quad (15)$$

$$C_v(x, t) \frac{\partial T}{\partial t} = -\varepsilon \mu C_{va}(x, t) \frac{\partial T}{\partial x} + \frac{\partial}{\partial x} \left(k(x, t) \frac{\partial T}{\partial x} \right) - \frac{\partial F_R}{\partial x} + \frac{\partial F_L}{\partial x} + \lambda(x, t) \Gamma(x, t) \quad (16)$$

where, $\Gamma(x, t)$ accounts for moisture change due to absorption/desorption of fibers and the water condensation/evaporation; $W - W_f$ is the free water content in the fibrous material; D_l is the diffusion coefficient of free water in the fibrous batting, which is assumed with a constant value with reference to some previous work. C_v is the effective volumetric heat capacity of fibrous material.

In 2002 year, Li and Zhu reported a new model for simulation of coupled heat and moisture transfer processes, considering the capillary liquid diffusion process in textile [21], which developed the liquid diffusion coefficient as a function of fiber surface energy, contact angle, and fabric pore size distribution. Based on this new model, Wang et al. considered more the radiative heat transfer and moisture sorption and condensation in the porous textile,

achieving more accurate simulation for the realistic situation [22]. The governing equations of the model are shown as follows:

$$\frac{\partial(C_a \varepsilon_a)}{\partial t} = \frac{1}{\tau_a} \frac{\partial}{\partial x} \left(D_a \frac{\partial(C_a \varepsilon_a)}{\partial x} \right) - \varepsilon_f \xi_1 \Gamma_f + \Gamma_{lg} \quad (17)$$

$$\frac{\partial(\rho_l \varepsilon_l)}{\partial t} = \frac{1}{\tau_l} \frac{\partial}{\partial x} \left(D_l(\varepsilon_l) \frac{\partial(\rho_l \varepsilon_l)}{\partial x} \right) - \varepsilon_f \xi_2 \Gamma_f - \Gamma_{lg} \quad (18)$$

$$c_v \frac{\partial T}{\partial t} = \frac{\partial}{\partial x} \left(K_{mix}(x) \frac{\partial T}{\partial x} \right) + \frac{\partial F_R}{\partial x} - \frac{\partial F_L}{\partial x} + \varepsilon_f \Gamma_f (\xi_1 \lambda_v + \xi_2 \lambda_l) - \lambda_{lg} \Gamma_{lg} \quad (19)$$

The previous research about the heat and moisture transfer in textile material limited their focus on a single layer of porous textiles. Li and Wang extended the model for coupled heat and moisture transfer to multilayer fabric assemblies [22]. They described the geometrical features, layer relationships and blend fibers of the multilayer fabric assemblies by the following definitions:

$$l_{(i-1)0} = l_{il} \quad (2 < i < n) \quad (20)$$

$$Contact_{in} = \begin{cases} 1 & l_{ij} = 0 \\ 0 & l_{ij} \neq 0 \end{cases} \quad (1 \leq i \leq n, j = 0, 1) \quad (21)$$

$$\bar{p} = \sum_{ti=1}^m f_{ti} p_{ti} \quad (tn \geq 2) \quad (22)$$

where, l_{i0} and l_{il} are defined as the thickness of the left and right gap between neighbored layers. Contact is defined to express the contact situation at boundaries between layers, which determines the heat and moisture transfer behavior at the layer boundary. The symbol of \bar{p} is the weighted mean property of all blend fibers in the fabric based on their fractions f_{ti} . In addition, they individually developed boundary conditions for different fabric layers to achieve the numerical solutions.

3.1.5. Waterproof Fabric

Waterproof fabric, which is laminated or coated with micro-porous or hydrophilic films, is frequently used in the design of functional clothing for the weather of low temperature, wind, rain, and even more extreme situations. With waterproof fabric, the clothing can effectively protect the body from the wind and water; as well as reduce the heat loss from the body to the environment. These functions of waterproof fabric, scientifically, are achieved by significantly affecting the processes of heat and moisture transfer through the textile products.

The term ‘water vapor permeability’ (WVP, $\text{g.m}^{-2}.\text{day}^{-1}$) is commonly used to measure the breathability of the fabric, which indicates the moisture transfer resistance in the heat and mass transfer processes. This property can be obtained by the experimental measurement with the Evaporation and Desiccant methods. The calculation formulation is expressed according to the first Fick’s law of diffusion [12]:

$$WVP = \frac{Q_w}{tA} = \frac{\Delta C}{W_n}, \quad (23)$$

where, Q_w is the weight loss/gain in grams over a period time t through an area A , W_n is the water vapor resistance and ΔC is the difference of water vapor concentration on the two surfaces of the fabric sample.

Meanwhile, R_n is employed to express the thermal resistance of the waterproof fabric. Thus, the simulation of the thermal effect of the waterproof fabric can be realized by specifying the heat and moisture transfer coefficients at the boundaries, as shown by the following formula [23]:

$$H_{mn} = \frac{1}{W_n + \frac{1}{h_{mn}}} \quad (24)$$

$$H_{cn} = \frac{1}{R_n + \frac{1}{h_{cn}}} \quad (25)$$

where, h_{mn} and h_{cn} are respectively the mass and heat transfer coefficients of the inner and outer fabric surface. When the fabric is laminated or coated with microporous or hydrophilic films as being waterproof, the combined mass and heat transfer coefficients H_{mn} and H_{cn} ($n = 0,1$) can be obtained by integrating the water vapor resistance W_n and the thermal resistance R_n of the waterproof fabric.

3.1.6. Phase Change Material (PCM) Fabric

The phase change material (PCM), which has the ability to change its phase state within a certain temperature range, such as from solid to liquid or from liquid to solid, is micro-encapsulated inside the textile fabrics in the functional clothing design in recent years to improve the thermal performance of clothing when subjected to heating or cooling by absorbing or releasing heat during a phase change at their melting and crystallization points. With PCM technology, the temperature of clothing is able to gain a change delay due to the energy released/absorbed from the PCM when exposed to a very hot/cold environment.

In the textile application, the PCM is enclosed in small plastic spheres with diameters of only a few micrometers. These microscopic spheres containing PCM are called PCM microcapsules, and are either embedded in the fibers or coated on the surface of the fabric. Research on qualifying the effect of the PCM fabric in clothing on the heat flow from the

body was experimentally conducted by Shim [24]. He measured the effect of PCM clothing on heat loss and gain from the manikin which moved from a warm environment to a cold environment and back again. Ghali *et al.* [25] analyzed the sensitivity of the amount of PCM inside the textile material on the fabric thermal performance. The percentage of PCM in the fabric was found to influence the length of time period during which the phase change occurs. Also, they drew a conclusion that under steady-state environmental conditions, PCM has no effect on the thermal performance; while when there is a sudden change in the ambient temperature, PCM can delay the transient response and decrease the heat loss from the human body.

In order to investigate the mechanisms of thermal regulation of the PCM on the heat and moisture transfer in textiles, Li and Zhu developed a mathematical model to describe the energy loss rate from the micro-spheres which is considered to be a sphere consisting of solid and liquid phases [26], as shown in the following equations:

$$\frac{\partial T_{ms}(x, r, t)}{\partial t} = a_{ms} \frac{1}{r^2} \frac{\partial}{\partial r} \left(r^2 \frac{\partial T_{ms}(x, r, t)}{\partial r} \right) \quad \text{spherical core} \quad (26)$$

$$\frac{\partial T_{ms}(x, r, t)}{\partial t} = a_{ms} \frac{1}{r^2} \frac{\partial}{\partial r} \left(r^2 \frac{\partial T_{ms}(x, r, t)}{\partial r} \right) \quad \text{spherical shell} \quad (27)$$

where, T_{ms} and T_{ml} respectively are the temperature distributions in a sphere containing solid and liquid PCM. These energy governing equations are developed on the radial coordinate. r denotes the radius of the latest phase interface in micro-PCM. The smaller is the radius of the micro-spheres, the more significant is the effect of the PCM.

3.2. Human Body Thermoregulatory System

To sustain life in various environments, the human body must have the ability to keep the temperature of core and skin at a reasonable range under a variety of external conditions, that is, the core body temperature should be maintained at $37.0 \pm 0.5^\circ\text{C}$, and the skin temperature should be managed at approximately 33°C . In the human body, the regulation of the body temperature is implemented by the thermoregulation system, which responds to produce/dissipate heat when the body core temperature drops/rises. The basic mechanism of the body thermoregulation system involves two processes: (i) when the body feels warm, the blood vessels react with vasodilatation and the glands begin to perform the sweating process; (ii) when the body feels cold, the blood vessels reduce the blood flow to the skin and increase the heating production by muscle shivering. The schematics of thermoregulatory system of the human body can be seen in Figure 2.

The thermal mathematical models for human body can be classified for a single part and/or for the entire body. The models for a single part of the body, which was usually developed by physiologists, most of them are too complicated to simulate the physiological and anatomical details of the specific parts. It seems that these partial models theoretically can be added together to form a complete representation of the thermal exchange of the whole

body. However, Fu [27] claimed that such methods were not practical due to the fact that the connection between these models is very difficult, and adding the models together would need a supercomputer even if the connection between models is feasible. The thermal models for the entire body, reviewed by Fu [27], can be characterized by the following classifications: (i) one-node models, (ii) two-node thermal models, (iii) multi-node models, and (iv) multi-element models.

Though most of these models are likely to produce acceptable simulation results under the condition that the temperature is relatively uniform throughout the body, the multi-node and multi-element models perform better when large temperature gradients exist within the body because of the greater amount of details provided about the body temperature fields.

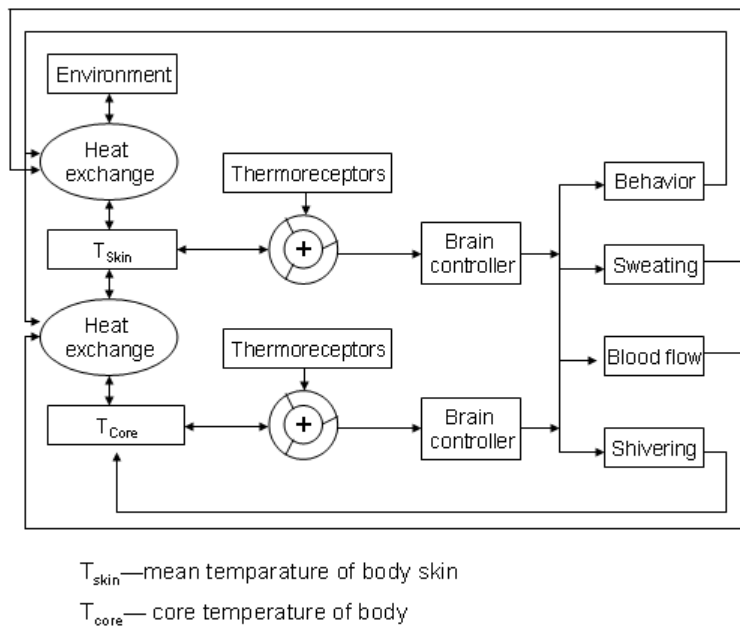


Figure 2. Schematic diagram of the thermoregulatory system of human body.

3.2.1. One-Node Thermal Models

One-node thermal models, in which the human body is represented by one node, are also called empirical models. They usually depend on experiments to determine the thermal response of the human body, and therefore, are not mathematical models in a phenomenological sense. A well-known empirical prediction model for the entire human body was reported by Givoni and Goldman [28]. It was derived by fitting curves to the experimental data obtained from the subjects exposed to various environments.

3.2.2. Two-Node Thermal Models

Two-node thermal models tend to divide the entire human body into two concentric shells of an outer skin layer and a central core representing internal organs, bone, muscle and tissue. The temperature of each node is assumed to be uniform. The energy balance equations are usually developed for each node and solved to produce the skin and core temperature and other thermal responses.

The early two-node models were not widely used by people due to the lack of sufficient consideration of the complicated physiological phenomena of the human body. Gagge *et al.* [29] introduced a more complete two-node model for the entire body, which includes the unsteady-state energy balance equation for the entire human body and two energy balance equations for the skin node and core node, as listed in the following:

$$S = M - E_{res} - C_{res} - E_{sk} - R - C - W \quad (28)$$

$$S_{cr} = M - E_{res} - C_{res} - W - (K_{min} + c_{pbl}V_{bl})(T_{cr} - T_{sk}) \quad (29)$$

$$S_{sk} = (K_{min} + c_{pbl}V_{bl})(T_{cr} - T_{sk}) - E_{sk} - R - C \quad (30)$$

where, S_{cr} and S_{sk} respectively are the heat storage of core and skin shell, M is the metabolic heat, E_{res} and C_{res} respectively is latent and dry respiration heat loss, W is moisture transfer resistance, R is radioactive heat loss, C is convective heat loss, V_{bl} is skin blood flow rate, and c_{pbl} is specific heat at constant pressure of blood.

Gagge *et al.* [29] later improved their two-node model by the development of the thermal control functions for the blood flow rate (V_{bl}), the sweat rate (RSW), and the shivering metabolic rate (M).

$$V_{bl} = [6.3 + 200(WARM_{cr})]/[1 + 0.1(COLD_{cr})] \quad (31)$$

$$RSW = 4.72 \times 10^{-5} \cdot WARM_{bm} \cdot e^{(WARM_{sk}/10.7)} \quad (32)$$

$$M = 58.2 + 19.4 \cdot COLD_{cr} \cdot COLD_{sk} \quad (33)$$

Due to the two-node nature of this model, it is able to be applied easily and simply with the straightforward numerical solution. Smith pointed out that Gagge's model was applicable for situations with moderate levels of activity and uniform environment conditions. However, due to the limitation imposed by only two nodes, Gagge's model can only be applied under uniform environmental circumstances.

3.2.3. The Multi-Node Models

Multi-node models divided the entire human body into more than two nodes and developed energy balance equation for each node as well the control functions for blood flow rate, shivering metabolic rate, and so on.

Stolwijk *et al.* [30] presented a more complex multi-node mathematical thermal model of the entire human body, in which many efforts are made to the statement of the thermal controller. This model firstly divided the body into six cylindrical parts of head, trunk, arm, hands, legs and feet and a spherical body part comprising the head. Each part is further divided into four concentric shells of core, muscle, fat and skin tissue layers. Specifically, in

this model all the blood circulation in the human body is regarded as a node called the central blood pool, which is the only communication connecting each body part. Therefore, Stolwijk's model is also called a 25-node model, and energy balance equations are developed for each node with the assumption of uniform temperature in each layer, which includes heat accumulation, blood convection, tissue conduction, metabolic generation, respiration and heat transfer to the environment. The descriptions for these equations are shown as follow:

$$\text{Core layer : } C(i,1) \frac{dT(i,1)}{dt} = Q(i,1) - B(i,1) - D(i,1) - RES(i,1) \quad (34)$$

$$\text{Muscle layer : } C(i,2) \frac{dT(i,2)}{dt} = Q(i,2) - B(i,2) + D(i,1) - D(i,2) \quad (35)$$

$$\text{Fat layer : } C(i,3) \frac{dT(i,3)}{dt} = Q(i,3) - B(i,3) + D(i,2) - D(i,3) \quad (36)$$

$$\text{Skin layer : } C(i,4) \frac{dT(i,4)}{dt} = Q(i,4) - B(i,4) + D(i,3) - E(i,4) - Q_i(i,4) \quad (37)$$

where, $C(i,j)$ is the heat capacity of each node, $T(i,j)$ is the node temperature, $Q(i,j)$ is the sum of the basic metabolic rate, $B(i,j)$ is the heat exchanged between each node and central blood compartment, $D(i,j)$ is the heat transmitted by conduction to the neighboring layer with the same segment. $E(i,j)$ is the evaporative heat loss at skin surface.

Similar to Gagge's model [29], Stolwijk *et al.* [29] also developed the thermal control functions in terms of tissue temperature signals, in which the warm signal (WARMS) and cold signal (COLDS) are corresponding to warm and cold receptors of the skin and are calculated by the error signal (ERROR). These controller equations produce the signals to drive the regulator, including total efferent sweat command (SWEAT), total efferent shivering command (CHILL), total efferent skin vasodilation command (DILAT), and total efferent skin vasoconstriction command (STRICT).

Stolwijk's model [29] has made much advancement compared to previous multi-node models as it is not only capable of calculating the spatial temperature distribution for each node, but also has improved the representation of the human's circulatory system since the blood circulation is the most important function of human body. This model has been validated with the good agreements between the experimental and predicted results of most cases. The limitation of this model is that it cannot be used for the highly non-uniform environmental situations caused from the negligence of spatial tissue temperature gradients.

3.2.4. Multi-Element Models

The greater difference between the multi-element thermal models and the two-node or multi-node models is that it divides the human body into several parts or elements without further division, and the temperature of each part or elements is no longer assumed as uniform. With the lifting of node uniform assumption, the mathematical descriptions of thermal functions, circulation, respiration etc. have also become more detailed to correspond with the detailed temperature field.

Wissler [15] developed a multi-element model for the entire body by dividing the human body into six elements: head, torso, two arms and two legs, which were connected by the heart and lung where venous streams were mixed. Later on, Wissler improved his model and divided the human body into 15 elements to represent the head, thorax, abdomen, and the proximal, medial, and distal segments of the arms and legs, which were connected by the vascular system composed of arteries, veins and capillaries. Energy balance equations for each element and the arterial and venous pools were developed with the assumption that the blood temperature of arteries and veins in each element were uniform, and the thermal control equations for blood flow rates, the shivering metabolic rate and the sweat rate were built up. The limitations of this model are that it is not applicable to the situations where a large internal temperature gradient or highly nonuniform environmental conditions exist. Additionally, the effect of the vasodilation and vasoconstriction was not included in the model. Finally, the parameters and constants used in the control equation are not easy to determine.

Smith [31] developed a 3-D, transient, multi-element thermal model for the entire human body with detailed control functions for the thermoregulation system. Compared to the previous models, the improvements were that he: (i) developed a 3-D temperature description of the human body; (ii) provided a detailed description of the circulatory system, the respiratory system and the control system; and (iii) employed the finite-element method to get the numerical solutions of the model, which made a 3-D transient model for the entire human body possible. The model divided the human body in 15 cylindrical body parts: head, neck, torso, upper arms, thighs, forearms, calves, hand and feet. Each body part is connected only by the blood flow and without tissue connection. The simulation results showed this model works well for situations of human thermal response during sedentary conditions in both uniform and non-uniform environments for either hot or cold stress conditions. However, the behaviors of the model during cold or hot exercising conditions were less satisfactory.

Fu [27] summarized the limitations of the previous models and developed a 3-D transient, mathematical thermal model for the clothed human to simulate the clothed human thermal response under different situations. The main improvement of this model is the addition of the subcutaneous fat layer, the accumulation of moisture on the skin, and the blood perfusion and blood pressure to Smith's model. The development of the human model includes the thermal governing equations of the passive and control systems. Fu's 3-D transient model has a good ability of simulating the human body thermoregulatory system in situations where there exists high temperature vibration and even in the extremely atrocious weather conditions.

Though the multi-elements models can predict the thermal status of the human body in more detail, however, it should be noticed that there are many difficulties in applying the multi-element models into clothing engineering design due to the following considerations: (i) the multi-element model requires the clothing to be 3-D meshed and modeled, which may cause great complexity in the integration of the models of clothing and human body, and the computation load is very intensive; (ii) the many parameters involved in the multi-element models have high demanding on the data availability in the engineering application.

3.3. Interfaces between the Body Skin and Clothing

In the daily life, the clothing acts as an important barrier for heat and vapor transfer between the skin and the environment, protecting against extreme heat and cold, but meanwhile hampering the loss of superfluous heat during physical effort. This barrier is formed by the clothing materials themselves and by the air they enclose as well as the still air bound to the outer surfaces of the clothing.

Some researchers [32] experimentally observed the phenomena of heat and moisture that exchange actively between the clothing and skin, and found the exchanged amount is considerable compared to the total increase/decrease volume. The maximum heat flow from the skin to clothing depends on the heat conductivity of the inner layer of clothing and covering area of skin. Also, the heat exchange between the human body and clothing is dependent on the external parameters, such as air temperature, air humidity, and wind speed. The clothing with the least porous, greatest thickness and lowest permeability will provide the greatest protection to heat and perspiration from the skin to environment provided with least porous and thickest thickness.

Li and Holcombe [33] reported a new model by interfacing the model for a naked body with a heat and moisture transfer model of a fabric. They developed the boundary condition between the body and clothing by quantifying the heat and mass flow.

At the fabric-skin interface

$$\text{Heat: } M_t = h_{ti}(T_{sk} - T_{fi}) \quad (38)$$

$$\text{Mass: } M_d = h_{ci}(C_{sk} - C_{fi}) + L_{sk} \frac{\partial C_{sk}}{\partial t} \quad (39)$$

At the interface between fabric and ambient air

$$\text{Heat: } K \frac{\partial T}{\partial x} \Big|_{x=L} = -h_t(T - T_{ab}) \quad (40)$$

$$\text{Heat: } D_a \frac{\partial C_a}{\partial x} \Big|_{x=L} = -h_c(C_a - C_{ab}) \quad (41)$$

where, M_d is the moisture flow from the skin and M_t is the heat flow from the skin.

Since the air spacing between the skin and the fabric continuously varies in time depending on the level of activity and the location, the thermal transfer processes are influenced by the ventilating motion of air through the fabric initiated from the relative motion between the body and surrounding environment, such as in the walking situations. Ghali *et al.* [34] developed a 1D model of the human body. The oscillating trapped air layer gap width and the periodically-ventilated fabric predict the effect of walking on exchanges of heat and mass. Murakami *et al.* [35] presented a numerical simulation of the combined radiation and moisture transport for heat release from a naked body in a house where continuous slight air flow exists by considering the thermal interaction between the human body and the environment and the intrinsic complex air situation in the real world.

Though much attention has been paid to the simulation of the thermal behaviors in the integrated system of human body, clothing and environment, and some numerical algorithms were reported for the simulation, these research studies put their focuses only on the scientific exploration and investigation. Few are developed systemically with a user-oriented purpose and used for clothing functional design.

4. CLOTHING THERMAL ENGINEERING DESIGN

4.1. Clothing Thermal Functional Design

The clothing thermal functional design, if following the traditional way of the clothing design and production, begins from the conception design and the prototypes making. As a result, a series of testing configured with experimental protocols will be performed by employing wearing subjects or by thermal manikins, and related thermal data will be measured using various equipments during the experiments. Based on the analysis of experimental data, designers attempt to find the difference of measured thermal functions of clothing and their design concepts to obtain feedback to improve their design. After the iterative trial and error process, the final products can be put on the market. This traditional design process is very expensive, time-consuming and tedious due to the real prototypes making, experimental testing and burdensome data analysis.

These shortcomings of the traditional design method make it difficult to satisfy the requirements of designers and manufacturers. People come to resort to the powerful capacity of the computer in the design process of thermal functional clothing. Antunano *et al.* [36] employed a computer model and heat-humidity index to evaluate the heat stress in protective clothing. Schewenzferier *et al.* [37] optimized thermal protective clothing by using a knowledge bank concept and a learning expert system. Computer has acted a role in the clothing thermal functional design. However, it still cannot directly help the designer to preview the thermal performance of clothing, which is a crucial function for clothing thermal functional design.

James *et al.* [38] applied the commercial software of computational fluid dynamics (CFD) in their strategy to simulate the heat and moisture diffusive and convective transport as well as effect of sweating to predict the performance of chemical and steam/fire protective clothing. Kothari *et al.* [39] simulated the convective heat transfer through textiles with the help of computational fluid dynamics (CFD) to observe the effects of convection on the total heat transfer of the fabric. The software tools like CFD provide a possible pathway for the user to simulate the heat and fluid distribution in the clothing. However, these tools do not take into account the structural features of the textile materials and the special features of the heat and moisture transfer process in textile materials that are related to the physical properties and chemical compositions of the textile materials. They cannot reflect the practical wearing situation and preview the true complex thermal behaviors in clothing.

In order to obtain scientific simulation of clothing thermal performance, some researchers have made efforts to apply the theoretical models describing the complex heat and moisture behaviors in clothing wearing system to the clothing thermal functional design. Parsonin [40] adopted thermal models for the clothed body including human thermoregulation and clothing to work as tools for evaluating clothing risks and controls. Prasad *et al.* in 2002 [41]

constructed a detail mathematical model to study transient heat and moisture transfer through wet thermal liners and evaluated the thermal performance of fire fighter protective clothing. Their research has made good exploration in clothing thermal functional design with the computer tools. Design and evaluation models, experts systems, applications of CFD software, and theoretical simulation models have been utilized to help to carry out clothing thermal functional designs. They either simply focus on evaluating certain thermal properties of clothing or need specialized knowledge to understand. They are very difficult to be applied as engineering tools for the general designers.

4.2. CAD Systems for Clothing Thermal Engineering Design

The application of CAD technologies for clothing design is a significant sign of revolutionary advancement in the development of computerization and automation in the clothing industry. Clothing designers/engineers are offered a number of flexibilities in their design with CAD systems, such as the usage of textile material, exploration of functional design and products display.

Currently many CAD packages are available, targeting at pattern design, garment construction, fashion design and physical fitting simulation, which have made many achievements in catering for different requirements of the clothing industry [42, 43]. They are helpful to shorten the design cycle and save time and money on the prototypes preparation as well as improve productivity considerably. Recently, 3D clothing design and visualizations have been developed to simulate and visualize the physical performance of the clothing wear on the body in 3D virtual ways [44, 45], which enable the designs to be more realistic and make detailed analysis and evaluation of the clothing mechanical performance. However, these pioneer achievements are mainly focused on the mechanical behaviors of clothing.

The newest interest in the CAD system for clothing functional design places the focus on the thermal behaviors of clothing. Clothing thermal engineering design with CAD systems and tools is an effective and economical solution of designing clothing with superior thermal performance for wearing in various environments with a feeling of comfort. The CAD system for clothing thermal engineering design aims to create a virtual platform, which offers designers the ability to conceive their products using the engineering method. Thermal engineering design of clothing is the application of a systematic and quantitative way of designing and engineering of clothing with the inter-disciplinary combination of physical, physiological, mathematical, computational and software science, and engineering principles to meet with the thermal biological needs of protection, survival and comfort of human body. The research in these fields discussed in the above sections lays substantial foundation to achieve this strategy. With this engineering design system, designers can simulate the thermal behaviors of the clothing, human body and environment system in specified scenarios, preview and analyze the thermal performance of the clothing, and iteratively improve their designs for desirable thermal functions of clothing.

In order to help the designers and manufacturers to quickly carry out clothing thermal functional design, Mao *et al.* [64, 47] have developed two software systems respectively for multi-layer and multi-style thermal functional design of clothing. With these tools, the designers and manufacturers may have a quick preview of the different thermal performance when using different textile materials to have a comparison and make decision; or they can

consider the different style (long, media or short) of the clothing and its thermal performance on the different body parts (Figure 3 shows the interface for clothing thermal design). The thermal performance of the sportswear can be quickly simulated and validated with the CAD system before the physical pattern making to reduce the design cycle and lower the design cost.

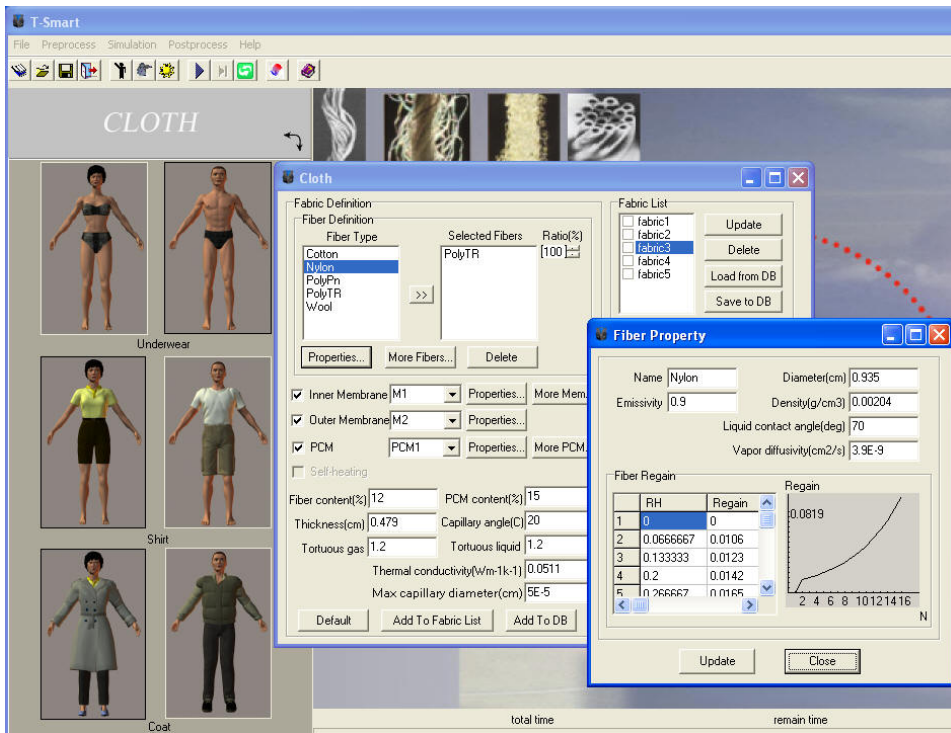


Figure 3. Interfaces for clothing thermal design.

This new application of CAD technologies demonstrates great potentials in the clothing thermal engineering design, because the capacity of simulating and predicting the thermal performance of clothing is indispensable for designing clothing for thermal protection and comfort. While physical fit and a good-looking fashion style are crucial aims of clothing design, the thermal performance of clothing is another critical aspect that relates to the survival, health and comfort of human beings living in various environmental conditions. As more and more consumers want to wear clothing with higher functional and comfort performance, there is an urgent need for a CAD system to design clothing and analyze its thermal performance effectively and efficiently.

CONCLUSION

The thermal engineering strategy for clothing design with desirable functions is to numerically design clothing and specify wearing scenarios, scientifically analyze the predicted thermal results, iteratively make decision and improve their designs to achieve

desirable functions, and then produce real products. The theoretical research of physics, chemistry related to textile and clothing, physiological thermoregulations of the human body, and the dynamic interactions between the clothing and body lead to thermal engineering design of clothing to achieve desirable thermal functions. The computational simulation can be enabled by related mathematical models, which is the substantial foundation for the engineering design, and the CAD systems provide a friendly tool for users through a series of functionalities to quickly carry out engineering design of clothing for desirable thermal functions. This strategy of thermal engineering design of clothing can hopefully speed up the design cycle and reduce the design cost.

ACKNOWLEDGEMENTS

The work of this paper is financially supported by the National Natural Science Foundations of China (Grant No. 61003173) and the Fundamental Research Funds for the Central Universities (Grant No. 2009ZM0128) and the Foundation for Distinguished Young Talents in Higher Education of Guangdong, China (LYM10018).

REFERENCES

- [1] Li, Y. (2007). Computational Textile Bioengineering Studies in *Computational Intelligence*, ed. Li, Y., Zeng, X., Ruan, D., and Keohl. L, 55: 203-221.
- [2] Angnew, B. (1998). NIH Plans Bioengineering Initiative. *Science*, 280(5369): 1516-1518.
- [3] Tao, X. M. (2001). *Smart fibers, fabric and clothing*. Wood Head Publishing Limited Cambridge England.
- [4] Pan, N. (2006). Thermal and moisture transport in fibrous materials. Cambridge: Woodhead Pub.
- [5] Martin, J. R., and Lamb, G. E. R. (1987). Measurement of Thermal Conductivity of Nonwovens using a Dynamic Method. *Textile Research Journal*, 57(12): 721-727.
- [6] Hatch, K. L. (1993). *Textile Science*, Minneapolis: West Publishing.
- [7] Farnworth, B. (1983). Mechanisms of heat flow through clothing insulation. *Textile Research Journal*, 53: 717-725.
- [8] Mecheels, J. (1971). Concomitant Heat and Moisture Transmission Properties of Clothing. Shirley Institute 3rd Seminar: *Textiles in Comfort*.
- [9] Crank, J. (1979). *The mathematics of diffusion*, Oxford: Clarendon press.
- [10] Wehner, J. A., and Miller, B. (1998). Dynamics of Water-vapor Transmission Through Fabrics Barriers. *Textile Research Journal*, 58(10): 581-592.
- [11] Nordon, P., and David, H. G. (1967). Coupled Diffusion of Moisture and Heat in Hygroscopic Textile Materials. *Textile Research Journal*. 37(10): 853-866.
- [12] Li, Y., and Holcombe, B. V. (1992). A Two-Stage Sorption Model of the Coupled Diffusion of Moisture and Heat in Wool Fabric. *Textile Research Journal*, 62: 211-217.
- [13] Kissa, E. (1996). Wetting and Wicking, *Textile Research Journal*, 66: 660-668.

-
- [14] Ito, H., and Muraoka, Y. (1993). Water transport along textile fibers as measured by an electrical capacitance technique. *Textile Research Journal*, 63(7): 414-420.
 - [15] Wissler, E. H. (1961). Steady-State Temperature Distribution in Man. *Journal of Applied Physiology*, 16(4): 734-740.
 - [16] Downes, J. G. (1958), Sorption Kinetics of Water Vapour in Wool Fibers. *Journal of Polymer Science*, 28: 45-67.
 - [17] Li, Y., and Luo, Z. X. (1999). An improved mathematical simulation of the coupled diffusion of moisture and heat in wool fabric. *Textile Research Journal*, 69(10): 760-768.
 - [18] Henry, P. S. H. (1939). Diffusion in Absorbing Media. *Proceedings of the Royal Society of London. Series A*, 171: 215-241.
 - [19] Ogniewicz, Y., and Tien, C.L. (1981). Analysis of Condensation in Porous Insulation. *International Journal of Heat and Mass Transfer*, 24: 421-429.
 - [20] Motakef, S., and El-Masri, M. A. (1986). Simultaneous Heat and Mass Transfer with Phase Change in A Porous Slab. *International Journal of Heat and Mass Transfer*, 29(10): 1503-1512.
 - [21] Li, Y., and Zhu, Q. Y. (2003). Simultaneous Heat and Moisture Transfer with Moisture Sorption, Condensation and Capillary Liquid Diffusion in Porous Textiles. *Textile Research Journal*, 73(6): 515-524
 - [22] Wang, Z., Li, Y., Zhu, Q. Y., and Luo, Z. X. (2003). Radiation and Conduction Heat Transfer Coupled with Liquid Water Transfer, Moisture Sorption and Condensation in Porous Polymer Materials. *Journal of Applied Polymer Science*, 89: 2780-2790.
 - [23] Wang, Z., Li, Y., Yeung, C. Y., and Kwok, Y. L. (2003). Influence of waterproof fabrics on coupled heat and moisture transfer in a clothing system. *Journal of the Society of Fiber Science and Technology*, 59(5): 187-195.
 - [24] Shim, H., and McCullough, E. A. (2000). The effectiveness of phase change materials in outdoor clothing, Proceedings of the International Conference on Safety and Protective Fabrics. in Industrial Fabrics Association International. Roseville.
 - [25] Ghali, K., Ghaddar, N., and Harathani, J. (2004). Experimental and numerical investigation of the effect of phase change materials on clothing during periodic ventilation, *Textile Research Journal*, 74(3): 205-214.
 - [26] Li, Y., and Zhu, Q. Y. (2004). A Model of Heat and Moisture Transfer in Porous Textiles with Phase Change Materials. *Textile Research Journal*. 74(5): 447-457.
 - [27] Fu, G. (1995). A transient 3-D Mathematical Thermal Model for the Clothed Human, *Kansas State University: Kansas*, p. 270.
 - [28] Givoni, B., and Goldman, R. F., (1972). Predicting Rectal Temperature Response to Work, Environment and Clothing. *Journal of Applied Polymer Science*, 32: 812-822.
 - [29] Gagge, A.P., Stolwijk, J.A.J., and Nishi, Y. (1971). An Effective Temperature Scale based on a Simple Model of Human Physiological Regulatory Response, *ASHRAE Transactions*, 77: 247-262.
 - [30] Stolwijk, J. A. J. (1971). A Mathematical Model of Physiological Temperature Regulation in Man, in *NASA Technical Report*, No. NASA CR-1855.
 - [31] Smith, C. E. (1991). A Transient, Three-Dimensional Model of the Human Thermal System, *Thesis*, Kansas State University.
 - [32] De Dear, R.J., Knudsen, H.N., and Fanger, P.O. (1989). Impact of Air Humidity on Thermal Comfort during Step-changes. *ASHRAE Transactions*, 95: 336-350.

-
- [33] Li, Y., and Holcombe, B.V. (1998). Mathematical Simulation of Heat and Mass Transfer in Human-Clothing-Environment System. *Textile Research Journal*, 67(5): 389-397.
- [34] Ghaddar, N., Ghali, K., and Jones, B. (2003). Integrated human-clothing system model for estimating the effect of walking on clothing insulation. *International Journal of Thermal Sciences*, 42: 605–619.
- [35] Murakami, S., Kato, S., and Zeng, J. (1998). Combined Simulation of Airflow, Radiation and Moisture Transport for Heat Release from Human body. *ROOMVENT*, 98b: 141-150.
- [36] Antunano, M. J., and Nunneley, S. A. (1992). Heat stress in protective clothing : validation of a computer model and the heat-humidity index (HHI). *Aviation, space, and environmental medicine*. 63(12): 1087-1092
- [37] Schwenzfeier, L., Warne-Janville, B., Delhomme, G., and Dittmar, A. (2001). Optimization of the thermal protective clothing using a knowledge bank concept and a learning expert system. In *The sixth biennial conference of the European Society for Engineering and Medicine*, Belfast, Northern Ireland.
- [38] Barry, J. J., and Hill. R. W. (2002). Computational Modeling of Protective Clothing In *International Nonwovens Technical Conference*. Atlanta, Georgia.
- [39] Kothari, V. K., and Bhattacharjee, D. (2008). Prediction of thermal resistance of woven fabrics. Part II: Heat transfer in natural and forced convective environments. *Journal of the Textile Institute*, 99(5): 433–449.
- [40] Parsons, K. C. (1995). Computer Models as Tools for Evaluating Clothing Risks and Controls. *Annals of Occupational Hygiene*, 39(6): 827-839.
- [41] Prasad, K., Twilley, W., and Randall Lawson, J. (2002). Thermal Performance of Fire Fighters Protective Clothing, *Technical Report NISTIR 6881*, National Institute of Standards and Technology, Gaithersburg, Maryland.
- [42] Breen, D. E., House, D. H., and Wozny, M. J. (1994). Predicting the drape of woven cloth using interacting particles. *Proceedings of SIGGRAPH 94*, annual conference series: 365-372.
- [43] Cordier, F., and Seo, H., Magnenat Thalmann, N. (2003). Made-to-measure technologies for an online clothing store. *IEEE Computer Graphic Applications*, 23(1): 38-48.
- [44] Choi, K. J., and Ko, H. S. (2005). Research problems in clothing simulation. *Computer-Aided Design*, 37: 585-592.
- [45] Editorial, (2005). CAD methods in garment design, *Computer-Aided Design*, 37: 583-584.
- [46] Mao, A. H., Li, Y., Luo, X. N., and Wang, R. M. (2008). A CAD system for multi-style thermal functional design of clothing. *Computer-Aided design*, 40: 916-930.
- [47] Li, Y., Mao, A. H., and Wang, R. M. (2006). P-smart—a virtual system for clothing thermal functional design. *Computer-Aided Design*, 38: 726-739.

Chapter 8

SURFACE MODIFICATION OF TEXTILES WITH NON-THERMAL PLASMAS

Nathalie De Geyter and Rino Morent*

Research Unit Plasma Technology (RUPT) – Department of Applied Physics
Ghent University – Faculty of Engineering
Jozef Plateaustraat 22 – 9000 Ghent – Belgium.

ABSTRACT

This chapter attempts to give an introduction on surface modifications of textiles with non-thermal plasmas. A non-thermal (or cold or low temperature) plasma is a partially ionized gas with electron temperatures much higher than ion temperatures. The high-energy electrons and low-energy molecular species can initiate reactions in the plasma volume without excessive heat causing substrate degradation. Non-thermal plasmas are particularly suited to apply to textile processing because most textile materials are heat sensitive polymers. In addition, it is a versatile technique, where a large variety of chemically active functional groups can be incorporated into the textile surface. Possible aims are improved wettability, adhesion of coatings, printability, induced hydro- and/or oleophobic properties, changing physical and/or electrical properties, cleaning or disinfection of fiber surfaces etc. Moreover, non-thermal plasma surface modifications can be achieved over large textile areas. After a general introduction, this chapter starts with a short overview of different plasma sources used for surface modification of textiles. Thereafter, different effects that can be induced on a textile product by a plasma treatment and ways to obtain these effects are reviewed.

1. INTRODUCTION

Pre-treatment and finishing of textiles by non-thermal plasmas gain popularity as surface modification technique [1, 2] due to numerous advantages over conventional chemical processes. It is far more economical and ecological because plasma-assisted surface

*Corresponding author: Rino.Morent@UGent.be

modification does not require the use of water and chemicals resulting in a drastic reduction in pollutants and a corresponding cost reduction for effluent treatment [3]. Non-thermal plasma is also referred to as cold or low temperature plasma and it is a partially ionized gas in which the temperature of the electrons is much higher than the temperature of the other species. High-energy electrons and low-energy molecular species initiate reactions in the plasma volume without excessive heat causing substrate degradation. Therefore, non-thermal plasmas are particularly suited to apply to textile processing because most textile materials are heat sensitive polymers. In addition, it has a wide range of applications due to the large variety of chemically active functional groups that can be incorporated into the textile surface layers: improved wettability, adhesion of coatings, printability, induced hydro- and/or oleophobic properties, changing physical and/or electrical properties, cleaning or disinfection of fibre surfaces etc.

In the first part of this chapter, a short introduction will be given on plasma sources used for surface modification of textiles. In the second part, the most important effects that can be induced on a textile product by a plasma treatment, and ways to obtain these effects will be reviewed. Due to the introductory level of this chapter, it should be noted that only the most occurring effects described in literature will be discussed here. The interested reader can find a more complete overview with other, less frequently described effects in [2].

2. NON-THERMAL PLASMAS FOR SURFACE MODIFICATION

Plasma is sometimes referred to as the fourth state of matter as introduced by Langmuir [4]. Plasma is a partly ionized, but quasi-neutral gas in the form of gaseous or fluid-like mixtures of free electrons, ions and radicals, generally also containing neutral particles (atoms, molecules). Some of these particles may be excited and can return to their ground state by emission of a photon. The latter process is at least partially responsible for the luminosity of a typical plasma. In plasma several electrons are not bound to molecules or atoms, but free. Therefore, positive and negative charges can move somewhat independently from each other.

Plasmas are frequently subdivided into equilibrium (or non-thermal/low-temperature/cold) and non-equilibrium (or thermal/high-temperature/hot) plasmas. Thermal equilibrium implies that the temperature of all particles (electrons, ions, neutrals and excited species) is the same. This is, for example true for stars, as well as for fusion plasmas. High temperatures are required to form these types of plasmas [5, 6]. In contrast, plasmas with strong deflection from kinetic equilibrium have electron temperatures that are a lot more elevated than the temperature of the ions and neutrals. Such plasmas are classified as non-equilibrium or non-thermal plasmas. It is clear that the high temperatures used in thermal plasmas are destructive for heat-sensitive polymers and most applications for surface modification of textiles will make use of non-thermal or cold plasmas. Therefore, this chapter will be limited to plasma sources for generating non-thermal plasmas.

In plasma technology, non-thermal plasmas are typically generated by an electrical gas discharge. When a strong electric field is applied to a neutral gas, ionization occurs in the gas volume. The created charged particles are affected by the applied electrical field and primarily the electrons are accelerated by the field due to their light mass and gain most

energy. They achieve high temperatures (10^5 - 10^6 K), while the heavy ions efficiently exchange their energy by collisions with the background gas and thus remain at low temperature. The gas temperature is typically below 473 K. When energetic electrons collide with neutral molecules, radicals are created which play an important role in the chemical activity of the plasma. Due to the low gas temperature, plasma surface treatment can be applied to heat-sensitive materials, such as textiles.

In the field of surface modification, different plasma sources operate at vacuum pressures (10^{-3} -1000 Pa). At these pressures the discharge is more stable and it is easier to control the plasma reactions. The particles have a long mean free path and only few collisions occur resulting in only a small reduction in the number of chemically active species. However, the application field of plasma technology is growing very fast and increasing demands from industry encourage the continuous development of more efficient and more flexible plasma techniques. Therefore, in recent plasma technology research, large efforts are made to develop atmospheric pressure technologies that overcome the disadvantages of low pressure discharges. Because there is no need for vacuum devices, investment costs are substantially lower and atmospheric plasma technology can easily be scaled up to industrial dimensions and integrated in in-line processes. The main problem of working at atmospheric pressure is that instabilities in the discharge rapidly arise, so that transition to a thermal arc discharge is likely to happen. The discharge constricts to a narrow current channel resulting in a loss of homogeneity. Moreover, the high current density causes an increase in gas temperature, which dispels the non-thermal character of the discharge. Preventing this transition is the major challenge for atmospheric pressure technology. One successful approach is limiting the discharge operating time by working in a pulsed regime in order to prevent that the instabilities have enough time to develop. In this way, for example pulsed corona and microwave discharges can be employed at atmospheric pressure [7]. In the case of a dielectric barrier discharge self-pulsation of the discharge anticipates on the transition to an arc discharge in an AC arrangement with a dielectric barrier covering one or both electrodes [8,9]. Applying a fast gas flow in transverse direction is another method to prevent accumulation of charges so that instabilities are “blown” away, for example in the DC glow discharge [10].

Surface treatment with atmospheric plasma technology can be divided into active and remote plasma treatment as shown in Figure 1 according to the location of the treated sample with respect to the gas discharge chamber. In active plasma treatment, the substrate to be treated will pass between the electrodes resulting in direct contact between the substrate surface and the active plasma. In remote plasma treatment, the substrate is located outside the plasma chamber, but passes in the gas stream that runs through the plasma chamber and that is loaded with radicals and other active species. Therefore, the sample is treated in the afterglow of the plasma. An active plasma treatment has the advantage of a higher concentration of active species near the surface of the substrate, while for remote plasma treatment, this concentration decreases as a function of distance to the plasma chamber and depends on the lifetime of the active species [11]. But then again, active plasma treatment risks backside treatment and pin-holing, while remote treatment prevents damages from the discharge as the discharge current does not flow through the sample. Moreover, remote treatment offers the possibility to treat the surface of substrates of any thickness and any geometry (3D objects). The active treatment is often limited to thin substrates due to limited space between the electrodes.

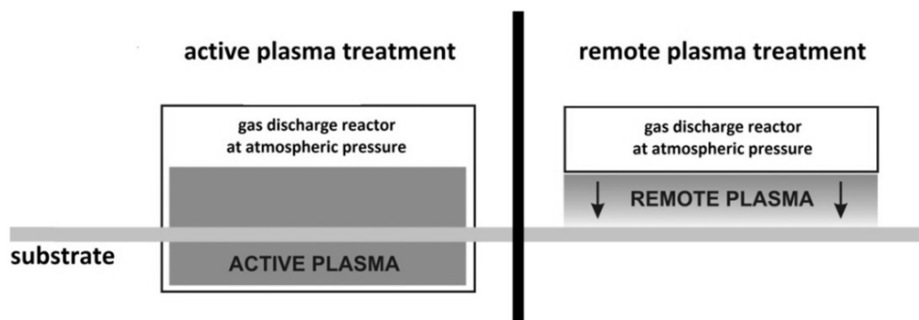


Figure 1. Active versus remote atmospheric plasma treatment.

In the following paragraphs, we will briefly review the most important properties of some typical non-thermal plasma sources used for surface modification. However, classifying plasma sources unambiguous in one or another category can be tricky because they can show features of different categories.

2.1. Corona Discharges

A corona discharge is a low current discharge caused by partial or local breakdown of a gas gap with a strongly inhomogeneous electric field at atmospheric pressure. To realise a non-uniform electric field distribution in the gap, the electric field near one or both electrodes must be stronger than in the rest of the discharge gap. This situation typically arises when the characteristic dimensions of at least one of the electrodes is much smaller than the distance between the electrodes, e.g. point-plane or wire-cylinder configurations. Around the sharp-edged electrode an inhomogeneous localised corona glow is detected with a small active volume. Despite this minor active volume, corona discharges are often applied for treatment of polymers.

2.2. Dielectric Barrier Discharges

Different configurations are able to realize a dielectric barrier discharge (DBD). There are three basic configurations for generating DBDs.

The first configuration is the volume discharge arrangement. A characteristic feature of such a DBD is that at least one of the electrodes is covered by a dielectric layer which is the essential part of the discharge. After ionization at a certain location in the discharge gap, the transported charge accumulates at the dielectric surface and generates an electrical field. This opposite field reduces the field in the gap and interrupts the current flow after a few nanoseconds. The exact duration depends on the pressure, gas composition and the dielectric properties. By applying an AC voltage (typical frequencies: 1-100 kHz) with an amplitude sufficient for breakdown, a large number of so-called microdischarges are induced, randomly distributed in time and space. The dielectric layer has two functions: 1) limiting the amount of charge transported by one single microdischarge and 2) distributing the microdischarges over the entire electrode area. Next to this filamentary type of volume discharge, several research

groups have reported on diffuse discharges in DBD configurations at atmospheric pressure and gap widths up to several centimetres [12-15]. However, this diffuse mode is often disturbed when a substrate is inserted in the discharge and the discharge undergoes the transition to a filamentary discharge.

The second and third arrangements for a DBD used for surface modification are the so-called surface discharge and coplanar discharge arrangement. A surface discharge arrangement consists of a plane dielectric with a thin or long electrode (or several in parallel) on one surface and an extended metallic cover as counter-electrode on its reverse side. The extension of the discharge depends on the amplitude of the voltage. In a coplanar discharge arrangement, pairs of long parallel electrodes with opposite polarity are close to the surface embedded within a dielectric bulk. The inter-electrode distance can be of the order of 100 μm . In literature, there are a large number of excellent reviews on DBDs [8, 9, 16-20].

Especially in literature on plasma treatment of textiles, it should be noted that occasionally also the term corona discharge or corona treatment is used in connection with DBDs, although most authors prefer to use this term only for discharges between bare metal electrodes without dielectric.

2.3. Radio Frequency Discharges

A plasma can also be excited and sustained by high-frequency electromagnetic waves. When the frequency of the electromagnetic field increases, the ions and subsequently the electrons can no longer reach the electrode surface during the acceleration phase of the exciting external field. At such radio frequencies (RFs), the interaction between the power supply and the plasma is now dominated by displacement currents rather than by real currents [21]. This is the reason why these discharges can be used with electrodes that are not in contact with the plasma. This can be a major advantage for applications because in this way impurities originating from the electrodes are avoided. In most cases these discharges are operated at low pressure, although some applications are operated outside this range and even at atmospheric pressure.

RF discharges operate in the frequency range of 1-100 MHz, most commonly at 13.56 MHz. Therefore, the wavelength of the electromagnetic field is much larger than the chamber dimensions. The power coupling in RF discharges can be accomplished in two ways: by oscillating electric fields (capacitive coupling) or by oscillating magnetic fields (inductive coupling).

2.4. Microwave Discharges

In the microwave (MW) region (0.3-10 GHz) the wavelength of the electromagnetic field becomes comparable to the dimensions of the discharge chamber resulting in other coupling mechanisms. Microwave ovens used in everyday life work at 2.45 GHz. Therefore, microwave sources are most available and least expensive at this frequency [21].

Different types of MW discharges are available, which ensures that MW plasmas can be sustained over a wide range of operating conditions, with pressures ranging from 0.1 Pa up to

atmospheric pressure. The majority of microwave induced plasmas (MIPs) are produced in a waveguide structure or a resonant cavity [22].

2.5. Recent Achievements in Non-Thermal Plasma Sources

As already mentioned before, it is often hard to unambiguously categorise different discharges. Inspired by the search for stable and homogeneous atmospheric pressure discharges, a lot of the described plasma sources in literature during the last two decades are combinations of the techniques described in sections 2.1-2.4. In this last section 2.5, we want to describe two general concepts using such combinations that are thoroughly studied for the moment:

(I) Microplasmas

To generate and sustain a stable glow discharge at atmospheric pressure, the discharge is often spatially confined to dimensions of 1 mm or smaller [23, 24]. These promising approaches to generate stable discharges are called microplasmas and represent a new and emerging field of plasma technology. Microplasmas show a remarkable stability towards arcing. The mechanisms that are responsible for this behaviour are still one of the frontiers of knowledge. One mechanism is the so-called “ pd ”-scaling. The breakdown voltage of a discharge depends on the product of pressure p and electrode separation d (Paschen curve) [23]. Therefore, the voltage necessary to ignite a discharge, can be kept low for essentially all gases even at atmospheric pressure if the distance between the electrodes is below 1 mm. High loss of charge carriers to the surrounding walls is another principle that contributes to the observed stability of microplasmas. Microplasmas are able to selectively generate chemical reactive species which could open the door to a wide range of applications in e.g. surface treatment [25].

(II) Plasma Jet

One can imagine that it is desirable for several applications to work with a remote plasma treatment and for this purpose several sources were developed. The plasmas produced are not spatially bound or confined by electrodes and are often referred to as cold plasma jets. Plasma needle, plasma plume or plasma pencil are other designations of plasma jets [26, 27]. Some authors even use the term plasma torch, but usually this name is reserved for thermal plasmas employed in industry for cutting and welding applications. Plasma jets typically operate at atmospheric pressure and are widely tested for biomedical applications [26]. Plasma jets are launched into the surrounding environment by devices that internally generate atmospheric pressure non-thermal plasmas [27]. The jets are blown outside the source by a gas flow, so that the surface treatment is performed by the afterglow of the discharge. Plasma jets are generated in different gases and mixtures and their power sources cover a wide spectrum of frequencies from direct current to microwaves [26, 27]. Figure 2 shows a picture of a DBD argon plasma jet sustained at atmospheric pressure.

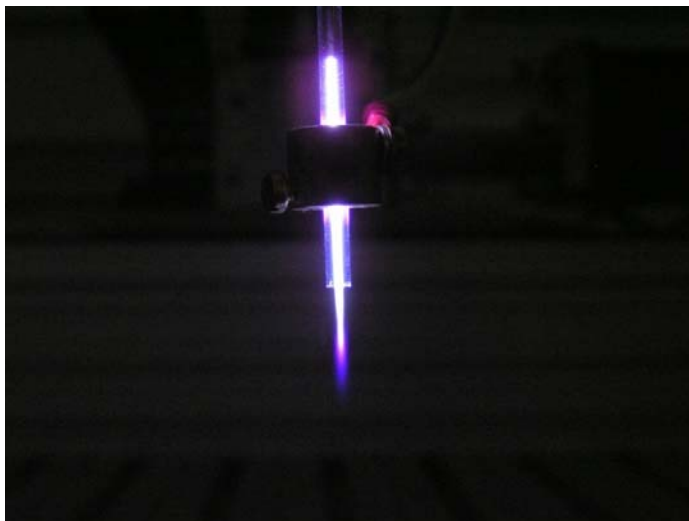


Figure 2. A DBD argon plasma jet at atmospheric pressure (2000 sccm Ar, 13 kV).

3. PLASMA TREATMENT EFFECTS

Because of the enormous amount of potential uses of non-thermal plasmas for the modification of textile products, categorizing the applications is difficult, and therefore a review is given on plasma treatment effects or results rather than on the textile applications that benefit from the treatment.

3.1. Hydrophilicity Enhancement of Fibres

Improving wettability by non-thermal plasma treatment has been done on all possible fibre types, with varying success. This treatment aims at the introduction of water compatible functional groups such as $-\text{COOH}$, $-\text{OH}$ and $-\text{NH}_2$. Of all plasma effects, this is without a doubt the most studied because it influences many plasma applications [2]. Next to an effective wettability enhancement, the permanence of the plasma treatment effect is another issue that has gained importance and attention over the last decade [28-30].

Polyethylene terephthalate (PET) and polypropylene(PP) non-wovens have been modified with a 10 kHz DBD in air, helium and argon at medium pressure (5.0 kPa) by Morent *et al.* [30, 31]. The helium and argon atmospheres contain a fraction of air smaller than 0.1%. The non-woven, modified in air, helium and argon, shows an enhancement in hydrophilicity due to the incorporation of oxygen-containing groups, such as C-O , O-C=O and C=O . It has been shown that an air plasma is more efficient in incorporating oxygen functionalities than an argon plasma, which is more efficient than plasma generated in helium. The air plasma treatment is the most efficient in incorporating oxygen on the surface due to the fast reaction between the radicals on the textile surface and the oxygen species, present in the discharge. Argon and helium plasmas contain some oxygen traces and plasma treatment leads to an oxidized cross-linked structure on the textile surface. Since the cross-

linking reaction inhibits the incorporation of oxygen and since only traces of oxygen are present, a helium and argon plasma are less efficient in oxidation of the textile surfaces. The difference between argon and helium plasma treatment can be explained as follows: the argon plasma used contains more ions than the helium plasma resulting in a higher degree of cross-linking and a faster incorporation of oxygen-containing groups. Scanning Electron Microscopy (SEM) pictures of the plasma-treated non-wovens show that the hydrophilicity of the non-wovens can be increased to a saturation value without causing physical degradation of the surface. The ageing behaviour of the plasma-treated textiles after storage in air is also studied in detail [30]. The smallest ageing effect is observed for the argon plasma-treated fabrics, followed by the helium plasma-treated fabrics. The air plasma-treated fabrics show a larger ageing effect. During the ageing process, the induced oxygen-containing groups re-orientate from the surface into the bulk of the material. A restriction of the polar group motion and therefore of the ageing process can be obtained by cross-linking of the polymer chains during plasma treatment. An air-plasma treated non-woven is not or less cross-linked and therefore shows a large ageing effect. A helium plasma treatment of the non-wovens leads to cross-linked textile surfaces resulting in a smaller ageing effect. Argon plasma-treated non-wovens had a higher degree of cross-linking resulting in an even less pronounced ageing effect.

Other approaches are also used. Negulescu *et al.* [32] have treated a PET fabric in a low pressure SiCl_4 plasma resulting in the implantation of SiCl_x groups at the PET fibre surface. These groups spontaneously hydrolyse by reaction with humidity present in the atmosphere, creating hydrophilic Si-OH groups in addition to the plasma created carbonyl groups. In this way, a hydrophilic fibre surface is created. Water contact angle measurements show a reduction from an original 86° for the untreated surface to 60° after a 30 s treatment and to 46° after a 10 min plasma treatment. Tsai *et al.* [33] have used a so-called one atmosphere uniform glow discharge plasma (OAUGDP) [34] to enhance the wettability of PP melt blown webs after a 1 to 4 min treatment in CO_2 or CO_2+O_2 plasmas. Addition of oxygen to CO_2 improves the effectiveness of the treatment. They report that in this configuration the wettability of the webs is determined by six critical parameters that are dependent on each other: power frequency, power voltage, electrode gap, working gas, treatment time and temperature of the working gas. This atmospheric pressure plasma source is competitive with low pressure plasma sources as observed by Dai *et al.* [35]. Different uses of this OAUGDP in industry are described and evaluated in more detail by Roth and Bonds [36].

Borcia *et al.* have studied a 80 kHzDBD in air for the treatment of PET and nylon fabrics [37, 38] and have shown that the wettability and wickability strongly increase within the first 0.1-0.2 s of treatment. Any subsequent surface modification following longer treatment (> 1.0 s) seems less important. They attribute the increased wettability to the enhanced level of oxidation where supplementary polar functionalities are created on the fabric fibre surface.

Two studies about penetration of plasma into textiles have been published by De Geyter *et al.* [39, 40] in which they have treated three layers of a 100% PET non-woven in the medium pressure range (0.3–7 kPa) with a 50 kHz dielectric barrier discharge in air and helium to study the influence of pressure and treatment time on the penetration depth. Current and voltage waveforms and Lichtenberg figures were used to characterize the discharge. Process pressure shows to be a crucial parameter to obtain the optimal plasma penetration. In the pressure range 0.3–1 kPa, increasing pressure results in an enhanced treatment of all three layers. In the pressure range 1–7 kPa, higher pressure demands longer treatment time to reach

a satisfying hydrophilicity for layer 1 and 2, in contrast with layer 3, which reaches this hydrophilicity faster with increasing pressure. This behaviour can be explained by two reasons. The first one is the diffusive transport of active species through the layers. If the mean free path of a textile modifying particle is close to or larger than the mean pore size of the textile, the loss of active species is low, resulting in a high diffusive transport. In contrast, smaller mean free paths cause substantial losses, which limit diffusive transport. The second reason is a different behaviour of the DBD. In the pressure range 0.3–1 kPa, the plasma burns above the textile layers using the upper textile layer as the dielectric surface. No microdischarges – typical for DBD discharges – were seen on a photographic film, placed under the textile layers. Therefore the change in hydrophilicity of layer 2 and 3 is solely a result of diffusive transport of the active species generated in the plasma above layer 1. In the pressure range 1–7 kPa the barrier discharge goes through the textile layers using the glass plate as dielectric surface, and individual microdischarges are observed on the Lichtenberg figures. Therefore, in this pressure range the generation of active species also occurs between the fibres and, together with the diffusive transport, this is responsible for the hydrophilicity. With increasing pressure, the number of microdischarges increases, while the diameter and the distance between them decrease. Poll *et al.* have also showed that pressure is a critical parameter in penetration of plasmas into textile structures and they have not been able to detect any penetration of the plasma effects at atmospheric pressure [41].

3.2. Enhancement of the Dyeing and Printing Properties of Fibres

Closely related to the wettability enhancement, this section focuses on the improvement of dyeing and printing properties of fibres. Plasma treatment modifies or removes the fibre's hydrophobic outer layer in order to improve the interaction dye-fibre and to increase the flux of dye molecules through the fibre surface into the fibre bulk. This dyeing enhancement has many aspects: (a) increase in dyeing rate, (b) increased dye bath exhaustion, and (c) improved dyeing homogeneity. Improvements in dyeing properties have been reported on all fibre types and two types of plasma processing can be distinguished for this purpose: coating plasmas or non-coating plasmas. In the former, the required functional groups are part of a coating that is plasma polymerised in situ at the fibre surface. Non-depositing plasmas (e.g. O₂ plasma) introduce functional groups that interact with an (ionic) dye molecule directly at the fibre polymer surface by chemical reaction, or alter the hydrophobic character of the fibre surface to improve diffusion of (ionic) dye molecules [2].

With a low pressure plasma source (RF) carboxylic acid groups are introduced by Öktem *et al.* [42] at PET fibre surfaces via two routes: 1) directly treated in an acrylic acid plasma, 2) first treated in an argon plasma and then immersed in an aqueous acrylic acid bath. The argon plasma creates a large amount of surface radicals that initiate the polymerisation reaction. Dyeing with a basic dye causes the dyeability to increase from 0.34 K/S for the untreated fabric to 0.82 K/S for a 5 min in situ plasma polymerization. A value of 1.48 K/S is obtained for 15 min plasma treatment in argon followed by a 5 min incubation time in an acrylic acid solution.

The influence of plasma polymerisation of acrylic acid on dyeability of PET, polyamide (PA) and PP woven fabric has also been tested by Ferrero *et al.* [43]. The overall colour strength is significantly enhanced. However, while the wash fastness is acceptable on PA, it is

not satisfactory on PET and PP fabrics, probably due to the lack of penetration of the acrylic acid monomer in the fibre. SEM and Fourier transform infrared spectroscopy (FTIR) confirms that grafting of polyacrylic acid is only effective on the surface of PET and PP, but in the case of PA the interior of the fibre is also modified.

The impact of a nitrogen plasma treatment on the dyeing properties of wool fabric is studied in detail by El-Zawahry [44]. Non-thermal plasma treatment results in etching of the fibre surface, enhancing the hydrophilicity and wettability of the treated wool along with creating and introducing new active sites onto the wool surface. The treatment also improves the dyeing rate and the time to reach dyeing equilibrium is shortened. The nitrogen plasma introduces new $-NH_2$ groups onto the wool surface, thereby enhancing the extent of dye exhaustion.

In a publication by Sarmadi *et al.* [45] the grafting of $SiCl_x^+$ cations from a 30 kHz low pressure $SiCl_4$ plasma onto additive-free acetone extracted PET fibres is described. As already described in section 3.1, the highly reactive $SiCl_x$ species implanted on the surface are hydrolysed to $Si(OH)_x$ in a post plasma reaction with atmospheric humidity. Untreated samples show a 0.4 K/S value, while after a one minute plasma treatment followed by 30 s of dyeing with a basic blue dye, K/S values of up to 1.6 are observed. This group of Sarmadi *et al.* [46, 47] has also studied other situations. Covalently bonded coatings are coated on CCl_4 and acetone extracted PP fabrics in an argon/acrylonitrile 13.56 MHz cold plasma [47]. The fabrics show both increased hydrophilicity and increased uptake of acid dye: K/S increases from 0.6 for the untreated fabric up to 4.25 for treated fabric. In [46] they have studied the O_2 and CF_4 plasma treatment of PET fabrics. The O_2 plasma again improves both the hydrophilicity and the surface dyeability, while CF_4 plasma results in excellent water repellency and unexpected improved surface dyeability. This behaviour can be attributed to intense fluorination reactions and simultaneous unsaturated bonds and trapped free radical formation.

Another possible explanation for the positive influence of a plasma treatment on the dyeing kinetics of PET fibres is suggested by Urbanczyk *et al.* [48]. The outer molecular layers of PET fibres are markedly more ordered than the bulk polymer, creating a barrier for molecules diffusing into the fibre. A plasma treatment alters or removes these outer layers, thus increasing diffusion rates of dye and solvent molecules.

3.3. Enhancing Adhesion

Adhesion enhancement aims at the introduction at the fibre surface of functional groups that show affinity for, or form chemical bonds with a product, such as a coating or a composite matrix. In the case of composite materials, the interface between fibre and matrix plays an important role in transferring the forces towards the fibres and determines the composite's mechanical and chemical properties to a large extent. Plasma treatments are known to improve interlaminar shear strength (ILSS) of composite materials as well as their resistance to fatigue, delamination and corrosion. These enhancements are due to enhanced interactions in the interphase, by a combination of a plasma induced increase in bonding surface and change in surface chemistry. Each combination of fibre and matrix requires a specific set of fibre surface properties. In many publications, the matrix is an epoxy resin; the functions introduced at the reinforcing fibre's surface ($-NH_2$, $-OH$, $-COOH$) are to react with

the epoxy function. Sun *et al.* [49] have showed an enhancement of ILSS of carbon fibre reinforced epoxy composites due to an oxygen plasma treatment. Gao and Zeng have studied the fibre/epoxy adhesion after plasma treatment of ultrahigh molecular weight polyethylene (UHMWPE) [50, 51]. Also Rostami *et al.* [52] treated UHMWPE with an inductively coupled plasma and show a fivefold enhancement in interfacial strength between the fibres and the epoxy matrix. Optimum conditions are reached with a 15s etch in argon plasma, followed by a 3 min allylamine plasma polymerization. Next to carbon and polyolefinic fibres, aramid (Kevlar 69) fibres are also modified by NH_3 , O_2 or H_2O plasmas in order to improve the adhesion to epoxy resin [53]. After plasma treatment, the interfacial shear strength (IFSS) of aramid/epoxy composites is substantially improved up to 83%, while the fibre strength is only little affected (less than 10% loss). This significant improvement in IFSS principally results from the formation of covalent bonds between the newly reactive functionalities at the modified fibre surfaces and the epoxides of the resin.

3.4. Enhancing Hydrophobicity and Oleophobicity of Fibres

In contrast to the three previous sections where textiles are treated to attract a certain liquid, this section describes properties induced by plasma treatment that repel liquids such as water and oil. Therefore, the plasma treatment introduces certain functional groups via a coating or a graft co-polymer, removes hydrophilic functional groups or changes hydrophilic groups into non-hydrophilic ones. The most straightforward way is the treatment of a fabric in a non-depositing gas which grafts (or exchanges) single fibre polymer atoms with hydrophobic groups such as fluorine groups. In another method the fabric is immersed in a fluid consisting of or containing the hydrophobic prepolymer with added initiators, after which the textile is plasma-treated leading to the grafting of the prepolymer on the fibre surface. The method with the highest potential is the deposition of a polymer structure at the fibre surface while the textile remains in the plasma reactor. The deposition can occur (a) while the plasma is ignited (plasma polymerization) or (b) in a two-step process: (b1) creation of radicals at the fibre surface in an inert plasma (e.g. argon) and (b2) reaction of these radicals with unsaturated monomers (plasma grafting) [2].

Lei *et al.* [54] have started from untreated PET with a contact angle of 71° and have subjected the PET surface to a corona discharge after which a hydrogen silicone fluid is grafted on the polyester fabric. This procedure results in a maximum contact angle of 127° after a 30 s treatment.

Although other cases are reported as exemplified in the above mentioned work, in most cases fluorine-containing gases are used to induce hydrophobicity on a textile fabric surface. Shen and Dai studied the treatment of silk and cotton fibres by a C_3F_6 vacuum plasma [55]. Table 1 shows the contact angles before treatment and after different treatment duration. After only a 1 min treatment, contact angles change from 0° to 120° . Longer treatment times do not result in a considerable increase in contact angle. Using XPS, the authors have observed on both fibre surfaces the incorporation of $-\text{CF}$, $-\text{CF}_2$, $-\text{CF}_3$ groups. After washing with water and alcohol extraction, partial loss of fluorine from the surface is observed, but contact angle measurements on the fibres still show largely improved hydrophobic properties. Chaivan *et al.* [56] have employed low pressure SF_6 plasma to improve the hydrophobic properties of silk. After a 3 min treatment the contact angles increase from $\pm 70^\circ$ for the untreated samples

to 130-140° for treated samples. Hochart *et al.* [57] have induced hydrophobicity with low pressure MW plasma on polyacrylonile (PAN) fibers by graft-polymerisation of fluorinated methacrylate. Vaswani *et al.* [58] have used CF_3CHF_2 and C_4F_8 as monomers for plasma polymerisation on cellulose fibres to enhance their hydrophobicity.

Table 1. Water contact angle of silk and cotton fabrics for various durations of C_3F_6 plasma treatment [55]

exposure time (min)	contact angle (°)	
	silk	cotton
0	0	0
1	119.4 ± 2.0	124.2 ± 0.9
3	123.9 ± 2.6	127.2 ± 1.6
5	122.1 ± 2.1	127.5 ± 1.6
10	122.0 ± 0.8	127.9 ± 1.7

3.5. Surface Cleaning: Desizing, Removal of Impurities

When using a plasma treatment for surface cleaning, selectivity of the plasma for the material to be removed from the fibre surface is required, since the fibre structure itself should not be damaged [2]. Cai *et al.* [59] have applied air/He and air/ O_2 /He atmospheric plasmas to desizepolyvinylalcohol (PVA) on cotton. The air/ O_2 /He treatment shows to have a greater effect on PVA than the air/He plasma. Both plasma treatments do not only serve to remove some PVA size, but also to significantly facilitate PVA removal by subsequent washing. They have attributed this effect to the enhanced swelling, dissolving and dispersing of PVA. The tensile strengths of the fabrics and yarns are not statistically significantly affected by the plasma treatment. The same authors have also applied both treatments for desizing PVA on rayon (viscose) fabrics [60]. Both treatments are able to remove some of the PVA on the rayon and increase PVA solubility in cold water, resulting in a higher weight loss in cold washing. Plasma treatment followed by one cold and one hot washing has the same effect as the conventional chemical treatments followed by two cycles of cold and hot washing. The plasma treatment has again no negative effect on rayon fabric tensile strength.

5 min O_2 plasma treatment of glass fibre fabrics containing originally 1.09% of paraffin size results in levels of only 0.3% paraffin [61]. Therefore plasma treatment can replace common desizing procedures for glass fibre fabrics that involve the lengthy heating of fabric rolls in a carefully controlled temperature regime and atmosphere, e.g. 48-72 h at 620 K in nitrogen.

3.6. Inactivation of Micro-Organisms: Disinfection/Sterilization

A plasma can be an efficient sterilising tool via vacuum pressure, highly energetic UV light and/or reactive plasma species [2]. Roth *et al.* have applied the same OAUGDP as described in section 3.1 for the decontamination of heating, ventilation and air conditioning

(HVAC) filters [62] and other non-wovens (e.g. PP melt blown webs) [63]. Figure 3 shows the survival curve for the micro-organism *E. coli* K12 on a PP sample [64]. Short treatments of about 25 s are sufficient to decrease the number by a factor 10^5 - 10^6 . Apart from the plasma parameters, the efficiency of decontamination depends on the micro-organism and the substrate on which it resides. Typically, 99.99% of captured micro-organisms are destroyed within 5 s (direct parallel plate OAUGDP, *E. coli*) to 10 min (afterglow OAUGDP, certain viruses).

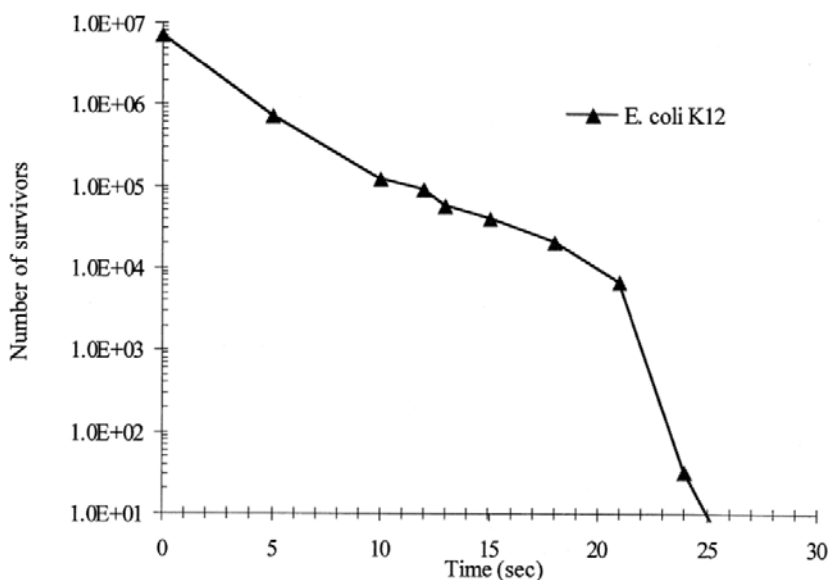


Figure 3. Typical survival curve for micro-organisms on a PP sample containing an initial loading of 6×10^6 *E. coli* K12 cells treated by an OAUGDP.

When medical textiles having specific surface properties are to be sterilized, a plasma treatment can change these surface properties and therefore render the medical device useless. Plasma sterilisation of textiles (aimed at destroying residing micro-organisms) seems therefore limited to non-medical applications, such as the applications mentioned above. Nevertheless plasma technology offers other biomedical applications for other purposes like described by Virk *et al.* [65]. The non-woven fabric Sontara®, commonly used for surgical gowns, is treated with antimicrobial finishes and a plasma containing fluorocarbon gas. The plasma treatment does not alter the weight, thickness, stiffness, air permeability, breaking strength and elongation. Plasma-treated and water repellent Sontara samples show higher blood and water resistance compared to other treatments. Plasma-treated samples also show a zone of inhibition for *Staphylococcus aureus*, thus providing a barrier against microbes. The beneficial antibacterial activity of silver grafted on textile fabrics by a RF plasma is studied by Yuranova *et al.* [66]. A minimum loading of silver is necessary to inhibit the bacterial growth, like *E. coli*. As is the case for many plasma-for-textiles applications, the effectiveness of a sterilisation process strongly depends on the ability of the effect to penetrate in a textile structure.

3.7. Wool Shrink-Proofing

The treatment requires physical and chemical etching process conditions that change the frictional properties of wool fibres. The occurrence of scales at the wool fibre surface is responsible for the shrinking of woollen textiles (a.k.a. felting) in the presence of water and mechanical agitation [2]. Both static and kinetic effects are involved. Statically, the hydrophilic character of the fibre surface is most important. Kinetically, the most important physical property is the differential friction, i.e. difference in frictional coefficients in the against-scale and with-scale directions [67]. Physically, shrink-proofing by plasma is caused by an increase in fibre-to-fibre friction and a decrease in differential friction. Chemically, it is caused by the increase in surface charging via the incorporation of hydrophilic groups at the fibre surface.

One of the oldest and most investigated plasma effects to date, shrink proofing of wool by plasma is initiated to replace wet chemical processes that cause various degrees of environmental stress. Thorsen has published a series of studies on the AC “corona” treatment of wool and mohair card webbing, top, yarn and fabric [68-70] at temperatures between 373 K and 413 K. These elevated temperatures are used to reduce formation of ozone. Usually, one of the large plate electrodes is covered by a dielectric material so that the discharge type is a DBD. Therefore, the term corona treatment is somewhat misleading. Shrink proofing proves to be successful for treatment times between 4 and 30 s, depending on the form in which the fibres are treated (loose fibres, card webbing or top). The increase in with-scale friction decays slowly with time after treatment, against-scale friction does not (up to at least 1000 h) [71]. Again penetration of the plasma effect is an issue. Fabric samples cannot be made shrink-proof because the gaseous reactants do not penetrate adequately, however, shrink-proof fabric can be made of yarns spun from treated card webbing. All treatments harshen the hand of the fibres, necessitating a subsequent treatment with softeners. However, shrink proofing is lost when using cationic softeners. In his publications, Thorsen gives complete information on the cost and the productivity of the treatment. The usefulness of corona treatment for various effects can be increased by multiple passing of the textile through the reactor [72]. For a desized and scoured cotton/wool fabric a single, double and threefold corona treatment lead to a laundry shrinkage of 27.1, 22.3 and 21.9% respectively, as compared to 29.7% for untreated wool/cotton fabric. However, treating the same fabric for 3 min in a low pressure oxygen glow discharge reduces the laundry shrinkage to only 3.9%. Shrink resistance is also obtained via a 3 kHz parallel plate glow discharge in 1:1 helium/argon and acetone/argon atmosphere at atmospheric pressure [73]. The laundering shrinkage of the non-treated fabric is 39.4% after 20 cycles. A treatment of 60 s in He/Ar or acetone/Ar plasma results in a shrinkage of 18.4%, while a treatment of 180 s results in a shrinkage of 9.1%.

CONCLUSION

The chapter’s main purpose is to offer the reader an introduction in non-thermal plasma treatment of textiles and to give some examples of the wide variety of obtainable effects. Taking into account this diversity of effects, it is therefore at least surprising that the impact

of plasma processing in the textile industry is rather low. Notwithstanding the advantages of plasma technology, from the relevant information gathered in literature, it is often difficult, sometimes impossible, to do an objective scientific or industrial comparison of different plasma processes and their effects. To overcome the scepticism from industry, it is necessary that researchers in plasma technology for textiles show an open-minded attitude to the work of their colleagues. If a researchers' own developed plasma source is incapable to reach the demands from industry for a certain application, referring the industrial partner to another research group is sometimes necessary and will not at all be unfavourable. On the contrary, when non-thermal plasma treatment for textiles reaches an accepted level for other processes in the textile industry, every researcher in plasma technology will benefit from this achievement.

REFERENCES

- [1] Shishoo, R. (2007). *Plasma technologies for textiles*, Cambridge, Woodhead Publishing Limited in association with The Textile Institute.
- [2] Morent, R., De Geyter, N., Verschuren, J., De Clerck, K., Kiekens, P. and Leys, C. (2008). Non-thermal plasma treatment of textiles. *Surface and Coatings Technology*, 202: 3427-3449.
- [3] Carneiro, N., Souto, A. P., Silva, E., Marimba, A., Tena, B., Ferreira, H. and Magalhaes, V. (2001). Dyeability of corona-treated fabrics. *Coloration Technology*, 117: 298-302.
- [4] Langmuir, I. (1928). Oscillations in ionized gases. *Proceedings of the National Academy of Sciences of the United States of America*, 14: 627-637.
- [5] Bogaerts, A., Neyts, E., Gijbels, R. and van der Mullen, J. (2002). Gas discharge plasmas and their applications. *Spectrochimica Acta Part B-Atomic Spectroscopy*, 57: 609-658.
- [6] Lieberman, M. A. and Lichtenberg, A. J. (2005). *Principles of plasma discharges and materials processing - Second edition*, Hoboken, New Jersey, John Wiley and Sons, Inc.
- [7] Fridman, A., Chirokov, A. and Gutsol, A. (2005). Non-thermal atmospheric pressure discharges. *Journal of Physics D-Applied Physics*, 38: R1-R24.
- [8] Kogelschatz, U. (2003). Dielectric-barrier discharges: Their history, discharge physics, and industrial applications. *Plasma Chemistry and Plasma Processing*, 23: 1-46.
- [9] Kogelschatz, U., Eliasson, B. and Egli, W. (1997). Dielectric-barrier discharges. Principle and applications. *Journal de Physique IV*, 7: 47-66.
- [10] Akishev, Y., Goossens, O., Callebaut, T., Leys, C., Napartovich, A. and Trushkin, N. (2001). The influence of electrode geometry and gas flow on corona-to-glow and glow-to-spark threshold currents in air. *Journal of Physics D-Applied Physics*, 34: 2875-2882.
- [11] Temmerman, E., Akishev, Y., Trushkin, N., Leys, C. and Verschuren, J. (2005). Surface modification with a remote atmospheric pressure plasma: dc glow discharge and surface streamer regime. *Journal of Physics D-Applied Physics*, 38: 505-509.

-
- [12] Massines, F. and Gouda, G. (1998). A comparison of polypropylene-surface treatment by filamentary, homogeneous and glow discharges in helium at atmospheric pressure. *Journal of Physics D-Applied Physics*, 31: 3411-3420.
 - [13] Roth, J. R., Sherman, D. M., Ben Gadri, R., Karakaya, F., Chen, Z. Y., Montie, T. C., Kelly-Wintenberg, K. and Tsai, P. P. Y. (2000). A remote exposure reactor (RER) for plasma processing and sterilization by plasma active species at one atmosphere. *IEEE Transactions on Plasma Science*, 28: 56-63.
 - [14] Roth, J. R., Rahel, J., Dai, X. and Sherman, D. M. (2005). The physics and phenomenology of one atmosphere uniform glow discharge plasma (OAUGDP (TM)) reactors for surface treatment applications. *Journal of Physics D-Applied Physics*, 38: 555-567.
 - [15] Okazaki, S., Kogoma, M., Uehara, M. and Kimura, Y. (1993). Appearance of Stable Glow-Discharge in Air, Argon, Oxygen and Nitrogen at Atmospheric-Pressure Using A 50-Hz Source. *Journal of Physics D-Applied Physics*, 26: 889-892.
 - [16] Kogelschatz, U. (2002). Filamentary, patterned, and diffuse barrier discharges. *IEEE Transactions on Plasma Science*, 30: 1400-1408.
 - [17] Wagner, H. E., Brandenburg, R., Kozlov, K. V., Sonnenfeld, A., Michel, P. and Behnke, J. F. (2003). The barrier discharge: basic properties and applications to surface treatment. *Vacuum*, 71: 417-436.
 - [18] Gibalov, V. I. and Pietsch, G. J. (2000). The development of dielectric barrier discharges in gas gaps and on surfaces. *Journal of Physics D-Applied Physics*, 33: 2618-2636.
 - [19] Pietsch, G. J. (2001). Peculiarities of dielectric barrier discharges. *Contributions to Plasma Physics*, 41: 620-628.
 - [20] Xu, X. J. (2001). Dielectric barrier discharge - properties and applications. *Thin Solid Films*, 390: 237-242.
 - [21] Roth, J. R. (1995). *Industrial Plasma Engineering - Volume 1: Principles*, Bristol and Philadelphia, Institute of Physics Publishing.
 - [22] Eliasson, B. and Kogelschatz, U. (1991). Nonequilibrium Volume Plasma Chemical-Processing. *IEEE Transactions on Plasma Science*, 19: 1063-1077.
 - [23] Foest, R., Schmidt, M. and Becker, K. (2006). Microplasmas, an emerging field of low-temperature plasma science and technology. *International Journal of Mass Spectrometry*, 248: 87-102.
 - [24] Becker, K. H., Schoenbach, K. H. and Eden, J. G. (2006). Microplasmas and applications. *Journal of Physics D-Applied Physics*, 39: R55-R70.
 - [25] Kogelschatz, U. (2007). Applications of microplasmas and microreactor technology. *Contributions to Plasma Physics*, 47: 80-88.
 - [26] Stoffels, E. (2007). "Tissue processing" with atmospheric plasmas. *Contributions to Plasma Physics*, 47: 40-48.
 - [27] Laroussi, M. and Akan, T. (2007). Arc-free atmospheric pressure cold plasma jets: A review. *Plasma Processes and Polymers*, 4: 777-788.
 - [28] De Geyter, N., Morent, R. and Leys, C. (2008). Influence of ambient conditions on the ageing behaviour of plasma-treated PET surfaces. *Nuclear Instruments and Methods in Physics Research Section B-Beam Interactions with Materials and Atoms*, 266: 3086-3090.

-
- [29] Morent, R., De Geyter, N., Leys, C., Gengembre, L. and Payen, E. (2007). Study of the ageing behaviour of polymer films treated with a dielectric barrier discharge in air, helium and argon at medium pressure. *Surface and Coatings Technology*, 201 : 7847-7854.
- [30] Morent, R., De Geyter, N., Leys, C., Gengembre, L. and Payen, E. (2007). Surface modification of non-woven textiles using a dielectric barrier discharge operating in air, helium and argon at medium pressure. *Textile Research Journal*, 77: 471-488.
- [31] De Geyter, N., Morent, R. and Leys, C. (2006). Surface modification of a polyester non-woven with a dielectric barrier discharge in air at medium pressure. *Surface and Coatings Technology*, 201: 2460-2466.
- [32] Negulescu, I. I., Despa, S., Chen, J., Collier, B. J., Despa, M., Denes, A., Sarmadi, M. and Denes, F. S. (2000). Characterizing polyester fabrics treated in electrical discharges of radio-frequency plasma. *Textile Research Journal*, 70: 1-7.
- [33] Tsai, P. P., Wadsworth, L. C. and Roth, J. R. (1997). Surface modification of fabrics using a one-atmosphere glow discharge plasma to improve fabric wettability. *Textile Research Journal*, 67: 359-369.
- [34] Reprinted from *Surface and Coatings Technology*, vol. 131, no. 1-3, R. Ben Gadri, J. R. Roth, T. C. Montie, K. Kelly-Wintenberg, P. P. Y. Tsai, D. J. Helfrich, P. Feldman, D. M. Sherman, F. Karakaya, and Z. Y. Chen, "Sterilization and plasma processing of room temperature surfaces with a one atmosphere uniform glow discharge plasma (OAUGDP)," pp. 528-542, Elsevier Limited (2000), with permission from Elsevier.
- [35] Dai, X. J. and Kviz, L. (2001). Study of Atmospheric and Low Pressure Plasma Modification on the Surface Properties of Synthetic and Natural Fibres. In: *Proc. of Textile Institute 81st World Conference*, Melbourne, Australia, 2001. 1-10.
- [36] Roth, J. R. and Bonds, T. A. (2006). The Application of a One Atmosphere Uniform Glow Discharge Plasma (OAUGDP®) to Roll-to-Roll Surface Energy Enhancement and Plasma Chemical Vapor Deposition (PCVD) on Films and Fabrics. In: *15th Annual TANDEC Nonwovens Conference*, Knoxville, Tennessee, USA, 2006. 1-11.
- [37] Borcia, G., Anderson, C. A. and Brown, N. M. D. (2003). Dielectric barrier discharge for surface treatment: application to selected polymers in film and fibre form. *Plasma Sources Science and Technology*, 12: 335-344.
- [38] Borcia, G., Anderson, C. A. and Brown, N. M. D. (2006). Surface treatment of natural and synthetic textiles using a dielectric barrier discharge. *Surface and Coatings Technology*, 201: 3074-3081.
- [39] De Geyter, N., Morent, R. and Leys, C. (2008). Pressure dependence of helium DBD plasma penetration into textile layers. *IEEE Transactions on Plasma Science*, 36: 1308-1309.
- [40] De Geyter, N., Morent, R. and Leys, C. (2006). Penetration of a dielectric barrier discharge plasma into textile structures at medium pressure. *Plasma Sources Science and Technology*, 15 : 78-84.
- [41] Poll, H. U., Schladitz, U. and Schreiter, S. (2001). Penetration of plasma effects into textile structures. *Surface and Coatings Technology*, 142: 489-493.
- [42] Oktem, T., Ayhan, H., Seventekin, N. and Piskin, E. (1999). Modification of polyester fabrics by in situ plasma or post-plasma polymerisation of acrylic acid. *Journal of the Society of Dyers and Colourists*, 115: 274-279.

-
- [43] Ferrero, F., Tonin, C., Peila, R. and Pollone, F. R. (2004). Improving the dyeability of synthetic fabrics with basic dyes using in situ plasma polymerisation of acrylic acid. *Coloration Technology*, 120: 30-34.
- [44] El-Zawahry, M. M., Ibrahim, N. A. and Eid, M. A. (2006). The impact of nitrogen plasma treatment upon the physical-chemical and dyeing properties of wool fabric. *Polymer-Plastics Technology and Engineering*, 45: 1123-1132.
- [45] Sarmadi, M., Denes, A. R. and Denes, F. (1996). Improved dyeing properties of SiCi(4) (ST)-plasma treated polyester fabrics. *Textile Chemist and Colorist*, 28: 17-22.
- [46] Fabrics by Plasma Treatment. *Textile Chemist and Colorist*, 25, 33-40.
- [47] Sarmadi, A. M., Ying, T. H. and Denes, F. (1993). Surface Modification of Polypropylene Fabrics by Acrylonitrile Cold-Plasma. *Textile Research Journal*, 63: 697-705.
- [48] Urbanczyk, G. W., Lippsymonowicz, B. and Kowalska, S. (1983). Influence of Low-Temperature Plasma on the Fine-Structure and Dyeability of Polyester Fibers. *Melliand Textilberichte International Textile Reports*, 64: 838-840.
- [49] Sun, M. J., Hu, B. R., Wu, Y. S., Tang, Y., Huang, W. Q. and Da, Y. X. (1989). The Surface of Carbon-Fibers Continuously Treated by Cold-Plasma. *Composites Science and Technology*, 34: 353-364.
- [50] Gao, S. L. and Zeng, Y. G. (1993). Surface Modification of Ultrahigh Molecular-Weight Polyethylene Fibers by Plasma Treatment .2. Mechanism of Surface Modification. *Journal of Applied Polymer Science*, 47: 2093-2101.
- [51] Gao, S. L. and Zeng, Y. G. (1993). Surface Modification of Ultrahigh Molecular-Weight Polyethylene Fibers by Plasma Treatment .1. Improving Surface-Adhesion. *Journal of Applied Polymer Science*, 47: 2065-2071.
- [52] Rostami, H., Iskandarani, B. and Kamel, I. (1992). Surface Modification of Spectra(Tm)-900 Polyethylene Fibers Using Rf-Plasma. *Polymer Composites*, 13: 207-212.
- [53] Sheu, G. S. and Shyu, S. S. (1994). Surface-Properties and Interfacial Adhesion Studies of Aramid Fibers Modified by Gas Plasmas. *Composites Science and Technology*, 52: 489-497.
- [54] Lei, J., Shi, M. and Zhang, J. (2000). Surface graft copolymerization of hydrogen silicone fluid onto fabric through corona discharge and water repellency of grafted fabric. *European Polymer Journal*, 36: 1277-1281.
- [55] Shen, L. and Dai, J. J. (2007). Improvement of hydrophobic properties of silk and cotton by hexafluoropropene plasma treatment. *Applied Surface Science*, 253: 5051-5055.
- [56] Chaivan, P., Pasaja, N., Boonyawan, D., Suanpoot, P. and Vilaithong, T. (2005). Low-temperature plasma treatment for hydrophobicity improvement of silk. *Surface and Coatings Technology*, 193: 356-360.
- [57] Hochart, F., De Jaeger, R. and Levalois-Grutzmacher, J. (2003). Graft-polymerization of a hydrophobic monomer onto PAN textile by low-pressure plasma treatments. *Surface and Coatings Technology*, 165: 201-210.
- [58] Vaswani, S., Koskinen, J. and Hess, D. W. (2005). Surface modification of paper and cellulose by plasma-assisted deposition of fluorocarbon films. *Surface and Coatings Technology*, 195: 121-129.

-
- [59] Cai, Z. S., Qiu, Y. P., Zhang, C. Y., Hwang, Y. J. and McCord, M. (2003). Effect of atmospheric plasma treatment on desizing of PVA on cotton. *Textile Research Journal*, 73: 670-674.
- [60] Cai, Z., Qiu, Y., Hwang, Y. J., Zhang, C. and McCord, M. (2003). The Use of Atmospheric Pressure Plasma Treatment in Desizing PVA on Viscose Fabrics. *Journal of Industrial Textiles*, 32: 223-232.
- [61] Rakowski, W., Okoniewski, M., Bartos, K. and Zawadzki, J. (1982). Plasma Treatment of Textiles - Potential Applications and Future-Prospects. *Melliand Textilberichte International Textile Reports*, 63: 307-313.
- [62] Kelly-Wintenberg, K., Sherman, D. M., Tsai, P. P. Y., Ben Gadri, R., Karakaya, F., Chen, Z. Y., Roth, J. R. and Montie, T. C. (2000). Air filter sterilization using a one atmosphere uniform glow discharge plasma (the Volfilter). *IEEE Transactions on Plasma Science*, 28: 64-71.
- [63] Kelly-Wintenberg, K., Montie, T. C., Brickman, C., Roth, J. R., Carr, A. K., Sorge, K., Wadsworth, L. C. and Tsai, P. P. Y. (1998). Room temperature sterilization of surfaces and fabrics with a One Atmosphere Uniform Glow Discharge Plasma. *Journal of Industrial Microbiology and Biotechnology*, 20: 69-74.
- [64] Ben Gadri, R., Roth, J. R., Montie, T. C., Kelly-Wintenberg, K., Tsai, P. P. Y., Helfritch, D. J., Feldman, P., Sherman, D. M., Karakaya, F. and Chen, Z. Y. (2000). Sterilization and plasma processing of room temperature surfaces with a one atmosphere uniform glow discharge plasma (OAUGDP). *Surface and Coatings Technology*, 131: 528-542.
- [65] Virk, R. K., Ramaswamy, G. N., Bourham, M. and Bures, B. L. (2004). Plasma and antimicrobial treatment of nonwoven fabrics for surgical gowns. *Textile Research Journal*, 74: 1073-1079.
- [66] Yuranova, T., Rincon, A. G., Bozzi, A., Parra, S., Pulgarin, C., Albers, P. and Kiwi, J. (2003). Antibacterial textiles prepared by RF-plasma and vacuum-UV mediated deposition of silver. *Journal of Photochemistry and Photobiology A-Chemistry*, 161: 27-34.
- [67] Kang, J. Y. and Sarmadi, M. (2004). Textile plasma treatment review - Natural polymer-based textiles. *Aatcc Review*, 4: 28-32.
- [68] Thorsen, W. J. (1968). A Corona Discharge Method of Producing Shrink-Resistant Wool and Mohair - Part II: Effects of Temperature, Chlorine Gas, and Moisture. *Textile Research Journal*, 38: 644-650.
- [69] Thorsen, W. J. and Koller, J. (1966). A Corona Discharge Method of Producing Shrink-Resistant Wool and Mohair. *Textile Research Journal*, 36: 651-661.
- [70] Thorsen, W. J. and Landwehr, R. C. (1970). A Corona Discharge Method of Producing Shrink-Resistant Wool and Mohair - Part III: A Pilot-Scale Top Treatment Reactor. *Textile Research Journal*, 40: 688-695.
- [71] Thorsen, W. J. (1971). Temporary and Permanent Fiber-Friction Increases Induced by Corona Treatment. *Textile Research Journal*, 41: 331-336.
- [72] Ryu, J., Wakida, T. and Takagishi, T. (1991). Effect of Corona Discharge on the Surface of Wool and Its Application to Printing. *Textile Research Journal*, 61: 595-601.
- [73] Tokino, S., Wakida, T., Uchiyama, H. and Lee, M. (1993). Laundering Shrinkage of Wool Fabric Treated with Low-Temperature Plasmas Under Atmospheric-Pressure. *Journal of the Society of Dyers and Colourists*, 109: 334-335.

Chapter 9

TECHNICAL TEXTILE YARNS CONTAINING METAL FILAMENTS/WIRES

Ayşe (Celik) Bedeloglu* and Yalcin Bozkurt

Dokuz Eylül University, Textile Engineering Department,
Tinaztepe Yerleskesi, 35160, Izmir, Turkey.

ABSTRACT

Textile industry is in progress in smart and multifunctional products containing high performance materials (fiber, yarn, fabrics and so on) in last decades. Various novel and practical products have been emerged by the rapid development in science and technology to meet human demands, in recent years. Textile products, which incorporate with different sciences, are taking part in different application areas including industry, military, space, medical to perform needing for health, protection, defense, communication and automation.

Conductive textiles also have interesting application areas due to their excellent properties that are provided by smart materials and a variety of manufacturing techniques. Conductive textile materials have a big role in production of sensors, electromechanical shielding, monitoring, static dissipation, anti-dust and anti-bacterial applications, data transfer and so on. Researchers focus on novel products, which have such smart and intelligent properties in applications for different requirements of humankind, over the last several years. Conductive fibers can be inherently conductive or gain conductive properties after some applications. Metal fibers can be obtained from metal plates or strips. Conductive yarns can be obtained from conductive filaments or wires, staple metal fibers or spinning traditional textile fibers with conductive filaments/wires. Metal filaments or wires also can be wrapped around the traditional textile yarns to develop conductive technical yarns.

This chapter aims to present novel designs, techniques and materials used for developing technical textile yarns containing metal filaments for smart textile applications. The review is organized as follows: In the first section, an overview of metal fibers, production methods and usage fields will be presented. In the second section, a general introduction to yarns containing metal filaments/wires and their

* E-mail: ayse.celik@deu.edu.tr

features in terms of materials and manufacturing techniques used will be given. In addition, advancements and application areas with recent studies will be recounted. Finally, suggestions on future studies and the conclusions will be given.

1. INTRODUCTION

Although there are many electrically conductive or semi-conductive textile products since the middle of 1980s [1], integration of electronics into textiles was performed in 1990s for the first time [2]. Conductive yarns are widespread used in military and medical areas (physiotherapy applications, sensors for body health and so on) [3]. In military clothes, yarns having metal wires or fibers are positioned in textile material to perform conduction of electricity, communication and other functional purposes [4]. The clothes giving response to environmental threats, garments in which mobile phones, portable music players and small controllers were integrated and sensor included shirts are some examples.

Today, there are smart textiles as complex conductive fabrics sensing stimulus such as pressure and temperature, actively. Development of different smart textile products is directly related to development of appropriate smart materials [5-6]. Initially, conductive fibers and yarns were mainly used in technical areas. Electrotexiles combined conductive textile structures with an electronic or computational function [7].

Conductive fiber or yarns can be naturally conductive or conductivity can be formed later by special treatments. Following techniques are used to produce conductive textile materials: fiber/wire manufacturing from metal plates, sliver or wires [5], fiber production by spinning and extrusion [8-9], coating fibers or yarns with metals [10-12], metal oxides, metal salts, conductive carbon or conductive polymers [13-15]. Different production processes also have importance to define metal fibers [16].

Most of the synthetic fibers used in the textile applications do not conduct enough electricity due to their high resistivity (order of $10^{15} \Omega \text{ cm}^{-2}$). However, for instance, $10^9 - 10^{13} \Omega \text{ cm}^{-2}$ is desired resistivity of an anti-electrostatic material [17]. "Conductive textile" term is used for wide variety of textiles (fiber, yarn, fabric and etc.) that possess varying degrees of conductivity [18-22]. In addition to metal fibres, stripes, tapes, foils, electrically conductive polymers and inks, conductive coatings are used to produce conductive yarns and fabrics for smart textiles. These conductive textiles can be used in communication, entertainment, health, security, heating, protection and so on [23]. Besides, metal-based textile materials present a wide variety of functions in electromagnetic shielding applications, antistatic applications, electronic applications as sensors and actuators, monitoring applications, defence and protection applications.

In this chapter, yarns having metal fibres, wires or filaments are described with recent studies and also, materials and techniques used and usage places of metal-based yarns are explained.

2. AN OVERVIEW OF METAL FIBERS, PRODUCTION METHODS AND USAGE FIELDS

Conductive fibers can be classified into two general categories: intrinsically conductive fibres and fibres that are specially treated to gain conductivity. Different production methods such as wire drawing, bundled wire drawing, cutting production method, melt spinning and melt extraction are utilized to produce electrically conductive fibres. Intrinsically conductive fibres can be pure metals, such as nickel, stainless steel, titanium, aluminium and copper, a metal alloy or carbon. Wire drawing is a well known mechanical process to manufacture metal fibers. Beside, intrinsically conductive fibres can be produced from polymers without adding any conductive substance [24].

Conductive metal fibers can be obtained from different metals and alloys such as ferrous alloys, nickel, stainless steel, titanium, aluminum, copper and so on. Metal fibers can be produced in the form of metal filaments or staple fibers with changing diameters [5]. Metal fibres and wires were characterized by Sprintmetal according to their diameter as following: while a fine wire has a diameter between 30 micrometers (μm) to 1.4 mm, a metal fibre have a diameter of 2 to 40 μm [25]. However, metal fibres were defined as very thin metal filaments with diameters ranging from 1 to 80 μm by Bekaert Fibre Technologies [26].

The fibres should be fine, as fabrics should have a low weight per unit area (usually not more than 300 g m^{-2}). However, there is a contrast between weight and geometries of metal fibres and yarns for effective electrical conductivity, and requested physical properties of produced textile materials, as metal elements (fibres, wires and filaments) increases rigidity and reduces elasticity of textile materials [24].

Metal-based fibers can be manufactured by shaving thin metal layers or by bundle drawing techniques. Since the high conductivity metallic fibers are heavier and more fragile to conventional textile fibers, it is troublesome that metallic fibers are mixed with other traditional fibers homogeneously. It is difficult to manufacture these yarns in traditional machines, as they damage to machine parts in spinning mills by abrasion. Therefore, manufacturing costs can be high [5].

Mixing of conductive metal slivers with traditional textile slivers in short staple manufacturing stages can form high conductivity ($10^5 \Omega \times \text{cm}$)⁻¹ blends. However, difference in strenghts of yarns with and without metal fibers influences performance of textile products, negatively. Conductive metal blend yarns can be used in electromagnetic shielding garments, static charge dissipation fabrics for furnitures and special textile filters for underground works. *Manufactured yarns from metal fibers should be flexible during usage and durable in washing steps by giving traditional textile appearance and comfort* [5].

There are some patent studies that explain metal fiber manufacturing techniques. *In a patent study*, Holvoet and Verstraeten from Bekaert company (2006) [20] manufactured bundle drawn metal fibers that have at least three concentric metal layers (a core, a surface and an intermediate layer) having radial cross-section area. Surface layer forms outer layer of metallic fibre drawn from bundle. For bundle drawing process, a chemical material is coated around the metal fibres formed with at least three layers. Then, drawing process is performed until desired diameter is obtained. After drawing process, layer and matrix that is around the composite wire is removed. Produced bundle fibers are twisted to obtain yarn. Thus, bundle drawn fibers are transformed into materials having thin and equivalent diameters [6].

De Bondt and Decrop [27], in their patent study, explained manufacturing of the stainless steel fibres by bundle drawing technique from stainless steel wires that are embedded in matrix. In fiber production stage, stainless steel wires are bunched and drawn at the same time. Single wires are separated from each other by coating a matrix material and put in an enveloping material. Bundle of coated wires are drawn to obtain the requested diameter. Matrix and enveloping materials are chemically removed. Mechanical features of metals such as iron and copper are similar to metals that are drawn, so these metals are generally utilized as matrix/envelope materials. However, when these metals are used as matrix material, the heating process can cause dissolution of drawn wires and metals together [27].

3. AN OVERVIEW OF METAL-BASED YARNS, PROPERTIES AND MANUFACTURING TECHNIQUES

The metal-based yarns were initially used to obtain aesthetic and decorative appearances in knitted and woven textile products. The first example for conductive metallic yarn that was used for embroidery and ornaments in clothes was formed by wrapping a thin metal foil around a conventional yarn made of natural fibers [24]. When thin strip of aluminium was entered to market, in the 1950s, it was highly demanded. In the 1990s, fabrics composed of silk and steel threads were used in fashion and interior applications [28-29].

Today, metallic yarns are used for different aims such as conductivity to fulfil functional expectations of smart textile products. The most commonly used metals in smart textiles are copper, aluminium and stainless steel. Other metals such as silver, titanium and gold are also used in special applications despite of their higher costs [30].

Conductive yarns can be produced from conductive filaments, staple conductive fiber or spinning conductive fibers and wires with traditional non-conductive textile fibers. Besides, conductive textiles can be manufactured by wrapping non-conductive yarns/slivers around the conductive metal (such as copper, stainless steel, silver and so on.) materials (foils, tapes, wires and stripes) [31-32]. Conductivity can be gained to fabrics by using conductive yarns and wires in its structure and by treating conductive materials onto fabric. Coatings are suitable for many textile types by giving good conductivity without significantly changing existing textile physical properties. However, adhesion between the metal and the textile results corrosion problems in further stages. Common textile coating processes include electroless plating, evaporative deposition, sputtering, and coating the textile with a conductive polymer.

Conductive metallic materials that are used in textile application should have some specific electrical and physical features such as being washable, not allergic and comfortable enough. Metallic yarns, which are thinner and have more strength, are utilized as sewing thread to sew electronics-integrated textiles. Places of the stitches determine the conductivity of the structure [31].

The metal-based yarn manufacturing (see Figure 1), generally, was implemented on modified ring spinning machine [33-38], open-end Dref-3 yarn manufacturing system [39] and fancy yarn manufacturing system.



Figure 1. Images of metal-based polyacrylic yarns produced by ring spinning (a), core-spun (b) and wrapping, (c) manufacturing methods.

A core spun yarn is commonly formed from two compounds: a core that can be monofilament, multifilament or staple fibers and is placed in the center of yarn, and a sheath that is staple fibers and wraps around the core and forms composite yarn structure [40]. Core or sheath can be metal-based materials to obtain conductive composite yarn. Conductive metals used should be appropriate to textile usage performance features such as thin, flexible or pliable. In friction core spun yarn manufacturing system, the filament in the core does not take twist during spinning process. Since perforated spinning cylinders provide air suck, sheath fibers are held on the surface of the spinning cylinder. Since friction was formed by turning of spinning cylinders, fibers in sheath take a stroll around the filament in the core and provide core spun yarn formation [39].

Bramley [41], in a patent study, used metal filament to obtain electrically conductive rope that is also lightweight and high strength. Produced rope can be used to control animal movement area or placed as a fence. Rope is formed from many yarns that are twisted together and have several filaments. Metallic filament is arranged on the surface of the yarn [41]. Douglas and Watson [42], explained a yarn that was formed by wrapping a metal filament around the core having twisted or untwisted fibers. Chiou *et al.* [43] wrapped two metal stripes (1-2 mm thickness) around a yarn.

Ueng and Cheng [44] manufactured conductive core-spun yarn in open-end friction spinning machine (see Figure 2) to develop fabrics that can be used for protection from static electricity and electromagnetic waves. In order to reduce production costs, stainless steel is used in the core and polyester and stainless steel staple fibers are used in the sheath. Single and ply yarns were woven on a semi-automatic loom. Fabric type, fabric density and conductive material quantity influenced the electromagnetic shielding effectiveness and static charge dissipation behaviour of woven fabrics.

Cheng *et al.* [45] produced metal-based open-end friction spun yarn from an open-end friction spun yarn and a core stainless steel wire combined within the yarn twisting zone of the friction drum. Stainless steel, Kevlar or rayon staple fibers were used as the sheath and stainless steel wire was used as the core. Different blend ratios for metal-based open-end friction core spun yarns were performed. Using these yarns, a woven fabric was produced on the semi-automatic weaving loom. When density of weft and warp yarns was increased, electromagnetic shielding effectiveness increased in all frequencies. Electromagnetic shielding effectiveness of rayon based fabrics was higher than kevlar based fabrics [45]. Lin and Lou [46] and Su and Chern [47] manufactured composite yarns made of stainless steel staple fibers and filaments to produce complex woven fabrics. Lin and Lou [46] produced

yarns containing stainless steel filaments, propylene nonwoven tapes and reinforcement filaments by using rotor-wrapping-twister.

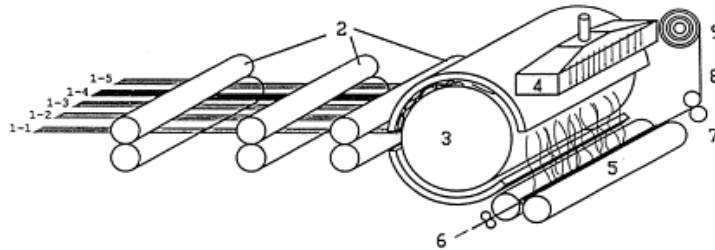


Figure 2. Schematic diagram of DREP III type open-end friction spinning machine [44]. 1-1, 1-2, 1-3, 1-5: sheath slivers with the staple fibers; 1-4: sheath slivers with the stainless steel staple fibers; 2: drafting drum; 3: carding drum; 4: compressed air; 5: friction drum; 6: core feed with the stainless steel wire; 7: draw-off roller; 8: open-end yarn; 9: take-up roller.

Conductive metal-based yarn, in ring frame (see Figure 3), was produced by using a metal wire in the yarn core. The copper and stainless steel materials were utilized as core and rovings made of 100% rayon and polyester/rayon were used as sheath of the yarn. Yarn manufacturing was carried such conventional ring yarn spinning that metal yarn was fed through yarn guide at three angles 50° , 70° and 90° and with the guide pulley of the guide mechanism in contact with the front roller. After the metal wire was covered by staple fibers, core spun yarn was fabricated by twisting and winding procedures. When the count of the cover material was Ne15, the core spun yarn, for all materials, exhibited the highest tenacity (11~22 cN/tex). The hairiness of the rayon hybrid yarn as cover material was approximately 50% greater than that of the polyester/rayon yarn cover. Anti-electrostatic, electromagnetic shielding and electrostatic dissipating textiles can be manufactured from these yarns by weaving or knitting techniques [48].

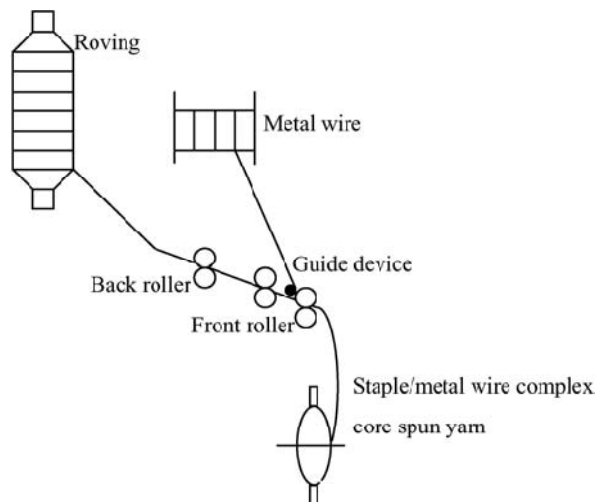


Figure 3. The diagram of roving and metal wire fabricated core spun yarn spinning mechanism [48].

Rattfalt and Linden [49] manufactured three different metal-based yarns and fabrics to investigate behaviours of textile electrodes due to their structures. In the study, three electrodes were tested in terms of electrode impedance and polarization potential. The first yarn was 100% stainless steel yarn and its electrode single jersey knitted fabric. The second yarn was made of 20% stainless steel wire as the core and 80% polyester staple fiber yarn as the sheath. The second electrode was a knitted fabric, third yarn was formed with polyester fibers in the core and silver coated copper monofilament was wrapped around it. Last electrode was a woven fabric. The first yarn that was formed from multiple filaments had lower yarn resistance compared to second yarn. However, when fabrics were manufactured using these yarns, second yarn showed better electrode impedance. The third yarn had high electrode impedance and varying mean polarization potentials. Production techniques for yarns and fabrics influenced the performances of textile electrodes.

Chen *et al.* [50] produced various conductive hybrid yarns to utilize the conductive co-woven-knitted fabrics. Loop yarns for knitting structure formed by using a copper wire and a polyamide filament as the core yarn and a stainless steel wire as wrapping yarn. Copper wire and stainless steel were used for their high conductivity and high permeability, respectively. The weft-inlaid yarn was manufactured by the nonwoven selvage as the core yarn and the conducting wire as the wrapping yarn. The conductive hybrid yarns were fabricated with rotor twister (see Figure 4) that provides frictionless and tensionless manufacturing process during the twisting and winding up progresses and which can fabricate with any types of yarn, selvages or tapes. Co-wovenknitted fabrics were laminated with various angles in several layers and then heat pressed to 2 and 3 mm in thickness. The surface resistivity, electromagnetic shielding effectiveness and electrostatic discharge attenuation percentage of the co-wovenknitted fabrics and co-wovenknitted fabrics reinforced composites were investigated.

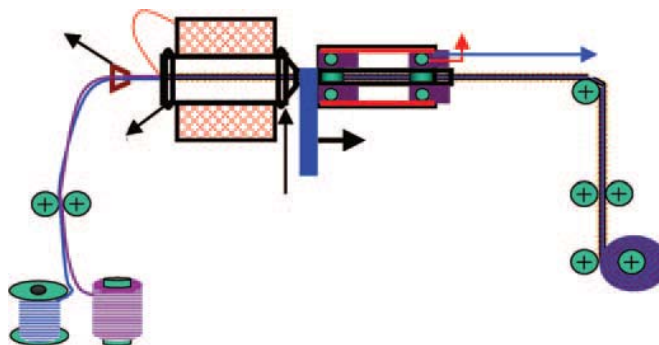


Figure 4. Diagram of rotor twister [66].

In another study, a low cost metal composite fabric with electromagnetic shielding effectiveness, flexibility, and processibility was designed and developed. Electrical properties including electromagnetic interference shielding and electrical conductivity, comfort and aesthetic properties of manufactured multifunctional fabrics were investigated. Metal composite yarns, which were used to manufacture metal composite fabrics, were produced with a polyester filament as a core, the fine metal filament (silver plated copper or stainless steel) covered the polyester filament in the Z-direction, and another polyester filament

covered the previous metal covered polyester yarn in the S-direction, using a hollow spindle spinning machine. Metal composite fabrics were produced in a plain weave using an automatic sample rapier loom. Metal-based yarns were inserted in certain intervals into the fabric to obtain different metal densities on the fabric. Metal content enhanced the overall electromagnetic shielding effectiveness. By modifying the metal grid size and geometry, electromagnetic shielding effectiveness can be increased [51].

Ramachandran and Vigneswaran [52] designed and developed core-sheath conductive yarns with copper filament as core and cotton carded slivers as sheath using Dref-3 friction spinning system by varying the draft in the second drafting unit. The special guide mechanism achieved a uniform yarn structure having three different core-sheath ratios such as 67/33, 80/20, and 90/10, respectively. The copper core conductive yarns having 328 tex nominal yarn linear density were used to develop the conductive fabrics. The electrical properties of yarns were studied at three different applied voltages of 6, 12, and 24 V. the core-sheath yarns showed very low resistance ranges of about 3–28 MΩ. The conductive fabric having core-sheath ratio of 67/33 copper core exhibited the highest shielding effect in the range 760–860 MHz. The electromagnetic shielding wearable textiles, mobile phone charging, and body temperature sensing garments can be developed using these fabrics.

Researchers investigated electromagnetic shielding effectiveness of knitted fabrics, which were produced by using copper core yarns; in the frequency range 20–18000 MHz using network analyzer equipment. For producing copper core yarn in ring spinning machine with core attachment, copper wires with different diameters (0.1, 0.11 and 0.12 mm) were used as core materials (conductive fillers) and cotton fiber was used as sheath material. Researchers observed that the shielding effectiveness increased with an increase in course density, wale density and tightness factors. The interlock knitted fabric had better electromagnetic shielding effectiveness at low frequency to higher frequency range than plain and rib knitted fabrics. Shielding effectiveness decreased generally with an increase in copper wire diameter [53].

Perumalraj and Dasaradhan [54] investigated the effects of the process variables on tensile properties of the copper core yarns as well as the effects on core and sheath components. The copper core yarns were produced by a Dref II friction spinning machine and a ring spinning machine with a core attachment device. Substantial proportion of yarn tenacity was generated by the interaction of copper core and polyester and cotton sheaths in the sheath core yarns produced from the two components.

Örtlek *et al.* [55] investigated the color and whiteness properties of fabrics knitted from different hybrid core-spun yarns (ring, siro and compact core-spun yarns) containing metal wire. Influence of ratio of metal wire, spinning method and dyeing and optical brightening processes was evaluated. An increase in the metal content of yarns caused a decrease in the whiteness and color strengths of fabrics. The siro spinning method, gave better results in terms of whiteness and color properties of knitted fabrics.

Metal-based sewing threads that are used to stitch smart electronic textiles are thinner and have more strength. Level of conductivity is controlled by the place of the stitches. Electroless coating, thermal evaporation, sputtering spray coating, coating with conductive polymers, filling with conductive materials and carbonization can be applied to sewing threads.

Sewing properties of metal wires were investigated by Orth [32] using a mathematical model. Electronics can be integrated into textile material (see Figure 5) by embroidery technique in a lightweight and low-cost way. A conductive yarn is used to achieve

interconnection between embroidered electronic modules and other required electronic parts. Linz *et al.* [56] performed measurements for conductivity and durability of contacts in flexible electrotextiles.

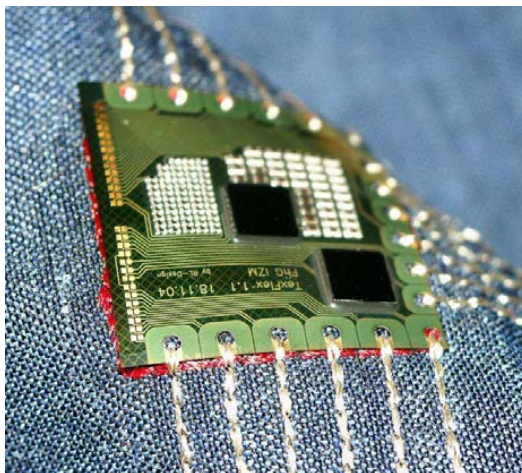


Figure 5. Flexible electronic module connected with conductive yarn by embroidery [56].

4. METAL-BASED CONDUCTIVE FABRICS

Electrically conductive metal-based fabrics are produced with different ways. For example, metal-based composite yarns, metal wires of filaments can be integrated into a fabric, a garment or a felt with specific intervals.

Besides traditional well known methods such as knitting and weaving to form a fabric structure is used commonly in applications that special features are desired. For any manufacturing method, produced fabric should be soft and comfortable enough to be worn. More rigid and compact fabric structures possessing metal wires/filaments can serve as electrical circuits for portable electronic devices on garments or as panels for heating or electrostatic dissipation applications. Besides, braiding and embroidering techniques are also used to produce metal-based conductive structures.

Bekaert company focus on producing metal-based textile yarns and fabrics for diverse applications such as anti-static textiles, cut-resistant gloves, heat resistant separation materials, filtration media, heatable pads and heating elements, electromagnetic shielding textiles, body armours [57].

Duru Baykal and Sığnak [58] investigated physical properties of woven fabrics including metallic yarns. Metal filament was plied with two cotton yarns to form metal-based weft yarns for weaving process. Kayacan *et al.* [59] used steel-based conductive yarns to manufacture heating panels by weaving for interactive electronic heated garments. Heating was achieved by portable power supplies integrated to fabric-based panels. Metal-based conductive fabrics can be used in electromagnetic shielding electrostatic and discharging applications in industry, military and health [51, 53].

CONCLUSIONS

While using metal fibers/wires or filaments, physical properties of produced fabrics or clothes such as flexibility, stretch, recovery, drape, shear and handle are prominent for further usage stages. Metal fibers (stainless steel, copper and etc.) resist to curve during textile manufacturing processes such as spinning, knitting and weaving, as they are rigid materials compared to polymer-based textile materials. The increase in diameter of metal fiber/wire causes difficulty in the bending of yarn. Therefore, metal wire and textile sliver as components of yarn are separated resulting spaces in the fabric structure. This situation decreases the efficiency of metal-based fabric in further applications.

Incorporation metal wires/filaments within textiles increases rigidity and reduce elastic quality. Thus, usage places of metal-based fabrics are influenced by situation of metal fiber content and separation. Therefore, coating or printing textiles with metal-based conductive solutions or materials can be alternative way to produce more flexible and comfortable conductive textiles.

This chapter aimed to present features, manufacturing methods and usage of metal-based conductive yarns in a wide variety application fields in textile products. Metal-based yarns and textiles have attracted attention in recent years. Metal-based conductive yarns brought a new dimension to ordinary textiles, as there is a possibility for low-cost and easy manufacturing in traditional textile mills. High value added conductive yarns and smart garments or industrial textiles produced from conductive composite yarns having metal elements are competitive materials in global market.

REFERENCES

- [1] Smith, W. (1988). Metallized Fabrics-Techniques and Applications. *Journal of Coated Fabrics*, 17: 242-253.
- [2] Langenhove, L. V. and Hertleer, C. (2011). Smart Clothing: a New Life. http://www.iafnet.com/files/iaf_03_presentations/Smart%20Clothing-%20a%20new%20life.pdf
- [3] Aniolczyk, H., Koprowska, J., Mamrot, P., and Lichawska, J. (2004). *Application of Electrically Conductive Textiles as Electromagnetic Shields* in Physiotherapy. *Fibres and Textiles in Eastern Europe*, 12: 47-50.
- [4] Saphotonics. (2010). Wearable Electronics.
- [5] http://www.saphotonics.com/technology/wearable_electronics.html.
- [6] Anderson, K., and Seyam, A. (2002). The Road To True Wearable Electronics. *JTATM*, 2: 1-7.
- [7] Maclaga, B., and Fisher, W.K. (2001). Static Dissipation Mechanism in Carpets Containing Conductive Fibers. *Textile Research Journal*, 71: 281-286.
- [8] Redström, M., Redström, J., and Mazé, R. (2005). *IT + Textiles*, IT Press.
- [9] Pomfret S.J., Adams P.N., Comfort N.P., and Monkman A.P. (1999). Advances in processing routes for conductive polyaniline fibres. *Synthetic Metals*. 101: 724-725.

-
- [10] Kim, B., Koncar, V., Devaux, E., Dufour, C., and Viallier, P. (2004). *Electrical and morphological properties of PP and PET conductive polymer fibers. Synthetic Metals.*, 146: 167–174.
- [11] Lu G., Li X., and Jiang H. (1996). *Electrical and shielding properties of ABS resin filled with nickel-coated carbon fibers. Composites Science and Technology.* 56: 193–200.
- [12] Tzeng S.S., and Chang F.Y. (2001). Electrical resistivity of electroless nickel coated carbon fibers. *Thin Solid Films.*, 388: 143–149.
- [13] De Rossi, D., Carpi, F., Lorussi, F., Paradiso, R., Scilingo, E.P., and Tognetti, A. (2005). Electroactive fabrics and wearable man–machine interfaces. In: *Wearable electronics and photonics*, Woodhead Publishing Co. UK.
- [14] Mazzoldi, A., De Rossi, D., Lorussi, F., Scilingo, E.P., and Paradiso, R. (2002). Smart textiles for wearable motion capture systems. *AUTEX Res J.* 2: 199–203.
- [15] Xue, P., and Tao, X.M. (2005). *Morphological and Electromechanical Studies Of Fibers Coated With Electrically Conductive Polymer. J Appl Polym Sci.*, 98:, 1844–1854.
- [16] De Rossi, D., Santa, A.D., and Mazzoldi, A. (1999). Dressware: wearable hardware. *Mater Sci Eng C.7*: 31–35.
- [17] Moehring, M., and Bittorf, B. Current Trends of Wearable Computing: State of the Art in Context-Awareness and Conductive Textiles, Bauhaus University Weimar /Germany, <http://scholar.google.com/scholar?hl=nlandlr=andie=UTF-8andq=cache:HdGnqjP9OJOJ:www.uniweimar.de/~bimber/Pub/AR/TP4.pdf+current+tr ends+of+wearable+computing+textile+>,
- [18] Chen, H.C., Lee, K.C., Lin, J.H., and Koche, M. (2007). *Comparison of electromagnetic shielding effectiveness properties of diverse conductive textile via various measurement techniques. Journal of Materials Processing Technology.*, 192–193: 549–554.
- [19] Lewin, M., and Preston, J. (1993). High Technology Fibers, Part C; Handbook of Fiber Science and Technology Series, Vol. III, Marcel Dekker Inc.: New York.
- [20] Okoniewski, M. (1994). *Intern. Techtextil Sympos.*, 2: 1–9.
- [21] Holvoet, J. and Verstraeten, S. (2006). Bundle Drawn Metal Fiber with Three Layers, WO/2006/120045.
- [22] Neudeck, A., Möhring, U., Müller, H., Gimpel, S., and Scheibner, W. (2004). Proceedings of the 4th International Conference on Textile Coating and Laminating, ENSITM Mulhouse,
- [23] Stegmaier, T., Schmeer-Lioe, G., Vogel, H.-P., and Planck, H. (2006). *Techn. Text*, 49: 57–60.
- [24] Xue, P., Tao, X.M., Leung, M.Y., and Zhang, H. (2005). *Electromechanical Properties Of Conductive Fibres, Yarns And Fabrics. In: Wearable Electronics And Photonics. Woodhead Textiles Series No. 46, ; Woodhead Publishing*, 81–104.
- [25] Clevertex, Report on Intelligent Textiles: State of the art, www.clevertex.net/Image/documents/State%20of%20the%20art.pdf
- [26] UGITECH S.A., www.sprintmetal.com,
- [27] Bekaert Fibre Technologies, www.bekaert.com,
- [28] De Bondt, S., and Decrop, J. (2007). Bundle Drawn Stainless Steel Fibers, United States Patent 7166174..

-
- [29] Jakob Schläpfer, www.jakob-schlaepfer.ch
 - [30] Braddock, S. E.; O'Mahony, M. (1999). *Techno textiles – revolutionary Fabrics for Fashion and Design*, Thames and Hudson Ltd.
 - [31] Post, E. R., and Orth, M. (1997). Digest of papers of the 1st IEEE International Symposium on Wearable Computers. Cambridge, Massachusetts, USA, pp. 167-171
 - [32] Post, E.R., Orth, M., Russo, P.R., and Gershenfeld, N. (2000). *Embroidery Design and Fabrication of Textile Based Computing IBM Systems Journal*. 39: 3-4.
 - [33] Orth, M., and Post, E.R. (1997). Smart Fabric, or Washable Computing. Digest of Papers of the First IEEE International Symposium on Wearable Computers. 10: 167-168.
 - [34] Sawhney, A.P.S., Harper, R. J., Ruppenicker, G. F, and Robert, K.Q. (1991). Comparison of Fabrics Made with Cotton Covered Polyester Staple-Core Yarn and 100% Cotton Yarn. *Textile Res. J.*, 61: 71-74.
 - [35] Sawhney, A.P.S., Robert, K.Q., Ruppenicker, G.F., and Kimmel, L.B. (1992). Improved Method of Producing Cotton Covered/Polyester Staple-Core Yarn on a Ring Spinning Frame. *Textile Res. J.* 62: 21-25.
 - [36] Sawhney, A.P.S., Ruppenicker, G.F., Kimmel, B., and Robert, K.Q. (1992). Comparison of Filament-Core Spun Yarn Produced by New and Conventional Methods. *Textile Res. J.* 62: 67-73.
 - [37] Sawhney, A.P.S., Robert, K.Q., and Ruppenicker, G.F. (1989). Device for Producing Staple- Core/Cotton-Wrap Ring Spun Yarns. *Textile Res. J.*, 59: 519-524.
 - [38] Merati, A. A., Konda, F., Okamura, M. and Marui, E. (1998). *Analysis of Yarn Tension in the Yarn-Forming Zone in Friction Spinning. Textile Research J.* 68, 254-264.
 - [39] Miao, M., How, Y.L. and Ho, S.Y. (1996). Influence of Spinning Parameters on Core Yarn Sheath Slippage and Other Properties. *Textile Res. J.* 66: 676-684.
 - [40] Aydogmus, Y. and Behery, H.M. (1999). Spinning Limits of the Friction Spinning System (DREF-III). *Textile Res. J.* 69: 925-930.
 - [41] Goswami, B.C., Martindale, J.G. and Scardino, F.L. (1977). *Textile Yarns Technology, Structure and Application*, New York: Wiley-Interscience Publication.
 - [42] Bramley, A. (1966). Electrically Conducting Rope, United States Patent 3291897.
 - [43] Watson, D.L. (1999). Electrically Conductive Yarn, United States Patent 5927060.
 - [44] Chiou, H.-H., Chiu, S.F, Liu, J.-K and Wu, C.-C. (1999). Conducting Yarn, United States Patent 5881547,
 - [45] Ueng, T.H. and Cheng, K.B. (2001). *Friction Core-Spun Yarns For Electrical Properties Of Woven Fabrics*. *Composites Part A: Applied Science and Manufacturing*, 32: 1491-1496.
 - [46] Cheng, K.B., Cheng, T.W., Lee, K.C., Ueng, T.H. and Hsing, W. H. (2003). *Effects of Yarn Constitutions and Fabric Specifications on Electrical Properties of Hybrid Woven Fabrics. Composites Part A: Applied Science and Manufacturing*, 34: 971-978.
 - [47] Lin, J.H. and Lou, C.W. (2003). Electrical Properties of Laminates Made from a New Fabric with PP/Stainless Steel Commingled Yarn. *Textile Research Journal*. 73: 322-326.
 - [48] Su, C.I. and Chern, J.T. (2004), Effect of Stainless Steelcontaining Fabrics on Electromagnetic Shielding Effectiveness. *Textile Res. J.* 74: 51–54.
 - [49] Lou,C.-W. (2005). Process of Complex Core Spun Yarn Containing a Metal Wire. *Textile Research Journal*, , 75: 466-473.

-
- [50] Rattfalt, L. and Linden, M. (2007), Electrical Properties of Textile Electrodes, Proceedings of the 29th Annual International Conference of the IEEE EMBS, 5735-5738.
- [51] Chen, H.C., Lin, J.H. and Lee, K.C. (2008). *Electromagnetic shielding effectiveness of copper/stainless steel/polyamide fiber co-woven-knitted fabric reinforced polypropylene composites*. Journal of Reinforced Plastics and Composites, 27: 187-204.
- [52] Roh, J.-S., Chi, Y.-S., Kang, T.J. and Nam, S.-W. (2008). *Electromagnetic Shielding Effectiveness of Multifunctional Metal Composite Fabrics*. Textile Research Journal, 78: 825-835.
- [53] Ramachandran, T. and Vigneswaran, C. (2009). Design and Development of Copper Core Conductive Fabrics for Smart Textiles. *Journal of Industrial Textiles*, 39: 81-93.
- [54] Perumalraj, R. and Dasaradan B.S. (2009). *Electromagnetic shielding effectiveness of copper core yarn knitted fabrics' shielding effectiveness of copper core yarn knitted fabrics*. Indian Journal of Fibre and Textile Research. 34: 149-154.
- [55] Perumalraj, R. and Dasaradhan, B.S. (2009). *Tensile Properties of Copper Core Yarns*. JTATM, 6: 1-23
- [56] Ortlek, H.G., Kilic, G., Yolacan, G. and Tutak, M. (2010). *Color and Whiteness Properties of Fabrics Knitted from Different Hybrid Core- Spun Yarns Containing Metal Wire*. Fibers and Polymers, 11: 1067-1074.
- [57] Linz, T.; Kallmayer, C., Aschenbrenner, R. and Reichl, H. (2005). *Embroidering Electrical Interconnects with Conductive Yarn for The Integration of Flexible Electronic Modules into Fabric*. Proceedings of the 2005 Ninth IEEE International Symposium on Wearable Computers (ISWC'05),
- [58] Bekaert textile,
- [59] <http://www.bekaert.com/en/Product%20Catalog/Application/Basic%20materials/Textile.aspx?Industry={F4EFD0BC-A1FB-4B5E-9923-B5241DCF01F7}&ProductCategory={2DDBEBF8-6AA8-4A2B-818F-E3712FFB524F}>
- [60] Duru Baykal, P. and Sıgnak, N. (2009). An Investigation of Performance Properties of Woven Fabrics Including Metallic Yarn. *Tekstil ve Konfeksiyon*, 1: 39-44.
- [61] Kayacan, O.; Bulgun E. and Sahin, O. (2009). Implementation of Steel-based Fabric Panels in a Heated Garment Design. *Textile Research Journal*, 79: 1427-1437.

Chapter 10

MESOSCOPIC MODELS OF WOVEN TEXTILES

*Jean-François Ganghoffer**

LEMTA – ENSEM, 2, Avenue de la Forêt de Haye,
BP 160, 54054 Vandoeuvre CEDEX, France.

ABSTRACT

Micromechanical schemes are elaborated for analyzing the mechanical behavior of woven structures at the scale of the weave pattern, which defines the repetitive unit cell for a quasi periodical textile at a mesoscopic scale. The mechanical behavior of the dry fabric before impregnation by the resin is the object of those analyses, with the general objective of calculating the overall effective mechanical properties versus the unit cell geometry and mechanical properties of the micro-constituents, namely the weft and warp yarns. Micromechanical analyses further provide a quantitative understanding of the deformation mechanisms of woven's, allowing relating the macroscopic overall response to the underlying microscopic behavior. Two parallel strategies are exposed in the present contribution, the first one basing on the minimization of the total potential energy of the woven structure, and the second one relying on discrete homogenization techniques specific to architected materials. Simulations of the overall tensile response of serge and fabric highlight the effect of geometrical nonlinearities for fabric, due to the crimp changes, leading to a J-shape tensile response; by contrast, serge exhibits a quasi linear response, as the initial yarn profile is flatter. The impact of the yarn mechanical properties on the overall mechanical behavior is assessed; especially, the Poisson's ratio of fabric is evaluated versus the applied load and the respective properties of both sets of yarns. Discrete homogenization techniques are developed in the last part of this contribution, basing on an analysis of a repetitive unit cell, representing the pattern in the case of textile. The equivalent behavior of a Cauchy or Cosserat type continuum is obtained in algorithmic format as an outcome. The simulation of the tensile response of the crimp changes of fabric by a perturbative approach reproduces the J-shape curve measured behavior. Those micromechanical analyses provide overall a guideline for the design and optimization of woven structures.

* E-mail: jean-francois.Ganghoffer@ensem.inpl-nancy.fr – Fax: (33) 383595551.

1. INTRODUCTION

The analysis of the deformations and shape forming of textiles is an important scientific and technological topic nowadays, due to the wide range of applications of these structures in many areas, such as composites with a woven reinforcement in aerospace industry or woven and braided structures for biomechanical applications (vascular prosthesis; scaffolds). The analysis of the motion and behaviour of the dry fabric (before being impregnated with a resin as in the RTM process) is very peculiar, due to the relative ease of motion of the yarns. This motion, in turn, determines the shape forming of the woven structure, thus calling for a separate analysis [1-3]. Three imbricated scales of the woven structure can be identified: the microscopic scale (scale of the yarn), the macroscopic scale of the woven structure, and an intermediate scale of a few intertwined yarns, which defines the unit cell reproducing the whole structure by a periodic translation, coined the mesoscopic scale. The organization of the yarns within the unit cell (that defines different armours, such as satin, serge) and the interactions between yarns (contact, friction) play an important role at both mesoscopic and macroscopic scales, as they respectively determine the constitutive law and the shape forming capacity of the initially flat structure. It is therefore important to develop reliable and accurate micromechanical models, in order to set up reliable constitutive models accounting for the geometrical nonlinearities due to crimp interchanges between yarns and to predict the 3D deformation of woven structures during real forming processes.

There is accordingly a need for reliable simulation tools for predicting the overall mechanical behavior of textile composites, accounting for informations relative to the fiber orientations and fibre density, which strongly determines how the composite part will behave, especially with regards to stiffness, damage, fatigue, and rupture [4-6]. Despite the great amount of existing works and modelling strategies and due to the multiscale aspects, no unitary model exists yet in the literature, as mentioned in Hamila and Boisse [7]; the existing families of models can be summarized as follows:

- I. The mechanical behavior of the meso structure can be homogenized assuming textile behaves as an anisotropic continuum [8-12]. Those models can next be incorporated into large strain finite element analysis at the structural scale using shell or membrane elements. The drawback of this first class of models lies in the fact that they largely ignore the discrete nature of textile (the continuity of the geometry is questionable, as well as the notion of continuum strain and stress; there are interactions between yarns, including sliding, which are not included). The evolving anisotropy due to the change of orientations of the material fibers and yarns during the service life of the structure is also not incorporated; hence the traditionally assumed fixed orthotropic behavior is no more a valid assumption.
- II. Discrete approaches accounting for the multi-scale nature of the woven textile in which each yarn or fibre is individually modelled constitute a second modelling strategy [13-15]. Due however to the very large number of fibers being generally present, the representation of the meso-structure is usually oversimplified, especially in view of simulations. Those simulations are most of the time restricted to a small domain, typically a representative unit cell, and involve simple rheological models (such as networks of springs or rods).

- III. The semi-discrete approach achieves a compromise between the two previous modeling strategies [7, 11]: the components at the micro or meso scale are here considered as part of finite elements. The kinematics of those discrete elements (yarns, fibers) is prescribed by the nodal displacements within the element, leading to the continuity between warp and weft fibers that remain in contact if this were the case in their initial state. These models usually retain only the significant mechanical properties of the yarns, such as fiber tension and in-plane shear rigidities.

The mechanical behavior of the dry fabric before the impregnation with a resin is very specific. In the case of yarns made of thousands of fibers, despite the relative sliding between fibers, the tensile stiffness in the yarn direction is still much larger compared to those in other directions. Due to the small diameter of the yarns, the flexional rigidity is at least one order of magnitude smaller than the tensile rigidity, as the quadratic moment is very small. This means that flexion of yarns and the induced crimp changes may be a dominant deformation mechanism, responsible for the large strains observed at the macroscopic scale. This geometrical non linearity (the geometry of the yarn changes, whereas it may still undergo small deformations due to the high tensile rigidity) at the mesoscopic scale of the armour is enhanced by the rather complex interactions between yarns, as a result of the contact between the warp and the weft, which involves yarn transverse compressibility and possible yarn-yarn sliding.

The assembly of yarns within the armour of woven textiles entails a specific overall mechanical behavior in terms of equivalent properties in different directions (tensile rigidities, Poisson's ratio). Very few models and analyses of the interactions between yarns at the mesoscopic scale have been performed in the literature; especially, the prediction of the effective mechanical behavior of textiles from the geometry and mechanical behavior of the yarns – including their mutual interactions - within the armour is still a challenging task. Recent contributions from the literature accounting for interactions between yarns include the model developed in King *et al.* [16], based on a representation of yarns as a network of trusses, with 'crossover springs' connecting the pin joints at the yarn crossover points, and the multiscale model in Ben Nadler *et al.* [17] describing overlapping crimped yarns as extensible elastica mutually coupled by a constraint of non-penetration. As underlined in King *et al.* [16], those interactions include the so-called *crimp interchange* (elongation of the fabric in one direction accompanied by a contraction in the transverse direction), *locking* (resistance to deformation), and *resistance to yarn relative rotation* when in-plane shear behavior becomes important.

Tracing back to the original works devoted to trellis approaches, Weissenberg [18] introduced the trellis model and treated the yarns as inextensible and inflexible rods; yarns are pinpointed at their nodal points with lines of zero elongation in the pattern by offering no resistance to the allowed changes in the lines orientations. The same author also stated that the Poisson's effect and sliding are observed under the action of external forces. In a contemporary period, Chadwick *et al.* [19] investigated the bias deformation of a woven fabric with the application of the trellis model submitted to a simple traction. Kilby [20] soon after developed a simple trellis model and analyzed the planar stress-strain relationship, based on the continuum mechanics for anisotropic elastic lamina. He admitted later the deficiency of this theoretical model for not including the Poisson effect. He was the first to derive the fabric tensile modulus in any direction other than the warp and weft directions. A good

summary of the analysis of the mechanical properties of woven fabrics prior to 1969 was included in the monograph by Hearle *et al.* [21], who derived the Poisson's ratio of a woven fabric assuming that the yarn extension and compression were negligible. De Jong and Postle [22] applied an energy analysis to the woven fabric structure, wherein the yarn extension was introduced. The general idea of this analysis is an organization of the yarns in an optimal manner, in the sense that the total energy of the structure is minimized. The majority of previous works concentrate on predictive modelling, and their drawback lies in the rather complicated mathematical relations between stresses and strains [23-26]; furthermore, the predictability of these models is not always satisfactory.

A mesoscopic model of fabric was initially developed in Ben Boubaker *et al.* [27-30], relying on a topological description of the yarns as an undulated beam modelled by analogical spring elements, in connection with a given kinematics of the analogical elements (extensional, flexional and torsional springs). We shall in the next section focus on the main improvements of this model and refer the reader to the referenced works for further details.

Regarding notations, vectors are represented by boldface symbols.

2. INTERNAL REACTION FORCES BETWEEN YARNS

The difficult point in the assembly of the woven potential energy is the evaluation of the reaction forces between both sets of yarns, for general armours, considering as a matter of simplicity monolayers. As a starting point, for a beam of length L submitted to a tensile effort P (horizontal) and a vertical punctual force R_{c1} due to a transverse yarn (Figure 1), the beam deflection is bounded over a finite interval, hence it may be written as the following Fourier series, with coefficients depending upon the exerted forces.

$$w = \sum_{k=1}^{\infty} a_k \sin\left(\frac{k\pi x}{L}\right) \quad (1)$$

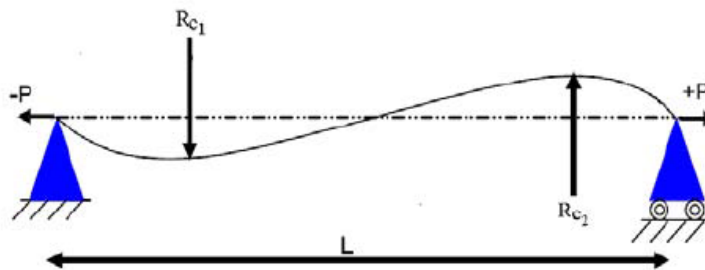


Figure 1. Beam element submitted to reaction forces.

The variable x is the curvilinear abscissa along the beam, and $w = w(x)$ is the deflection of the beam at the current position x .

2.1. Woven Equilibrium as Minimisers of the Potential Energy

Considering a beam undergoing mostly flexion as the dominant deformation mode (Figure 1), the internal energy resulting from the previous shape expression (1) is

$$U^* = \frac{EI}{2} \int_{x=0}^L \left(\frac{d^2 w}{dx^2} \right)^2 dx = \frac{\pi^4 EI}{4L^3} \sum_{k=1}^{\infty} k^4 a_k^2 \quad (2)$$

For a given yarn modelled as an undulated beam, the external work W_{ext}^* is further calculated, considering the work of the applied tensile and the work of the reaction forces due to the set of transverse yarns. The elementary displacement of a beam element is given by

$$d\lambda = ds - dx = dx \sqrt{1 + \left(\frac{dw}{dx} \right)^2} \approx \frac{1}{2} \left(\frac{dw}{dx} \right)^2 dx \quad (3)$$

which can be integrated using (1) to deliver

$$\lambda \approx \int_{x=0}^L \frac{1}{2} \left(\frac{dw}{dx} \right)^2 dx = \frac{\pi^2}{4L} \sum_{k=1}^{\infty} k^2 a_k^2 \quad (4)$$

The work of external forces is then given by

$$W_{\text{ext}}^* = \sum_{j=1}^{N_{\text{tr}}} \left(R_{c_j} \sum_{k=1}^{\infty} a_k \sin \left(\frac{k\pi c_j}{L} \right) \right) + P \frac{\pi^2}{4L} \sum_{k=1}^{\infty} k^2 a_k^2 \quad (5)$$

Hence, assembling (2) and (5), the total potential energy of the structure expresses as

$$V^* = \frac{\pi^4 EI}{4L^3} \sum_{k=1}^{\infty} k^4 a_k^2 - \sum_{j=1}^{N_{\text{tr}}} \left(R_{c_j} \sum_{k=1}^{\infty} a_k \sin \left(\frac{k\pi c_j}{L} \right) \right) - P \frac{\pi^2}{4L} \sum_{k=1}^{\infty} k^2 a_k^2 \quad (6)$$

in which the summation over all warp yarns has been performed. The equilibrium shape of the structure is given by the minimum of its total potential energy: minimizing V^* with respect to the Fourier coefficients $(a_k)_{-k}$ delivers

$$a_k = \frac{2L^3 \sum_{j=1}^{N_{\text{tr}}} R_{c_j} \sin \left(\frac{k\pi c_j}{L} \right)}{EI\pi^4 \left(k^2 \cdot \left(k^2 + \frac{PL^2}{\pi^2 EI} \right) \right)} \quad (7)$$

In order to incorporate the interactions between the warp and weft set of yarns, we consider to be more specific a weft submitted to the reactions forces of the N_{wa} warp. The deformed shape of this yarn is given as a particular case from (7) as

$$w_{we}(x) = K \sum_{p=1}^{\infty} \frac{\sum_{j=1}^{N_{wa}} R_{we/wa}(c_j) \sin\left(\frac{p\pi c_j}{L}\right)}{p^2 \cdot \left(p^2 + \frac{P_{wa} L^2}{\pi^2 EI}\right)} \sin\left(\frac{p\pi x}{L}\right) \quad (8)$$

with the constant coefficient $K := \frac{2L_{we}^3}{EI_{we}\pi^4}$, depending upon the yarn period and flexion modulus. Expression (8) is indeed in the form of a Fourier series, and will allow the evaluation of the reaction forces of the transverse yarns. The convergence of the series expressed in (8) can be assessed by calculating an upper bound of the general term

$$\left| K \frac{\sum_{j=1}^{N_{wa}} R_{we/wa}(c_j) \sin\left(\frac{p\pi c_j}{L}\right)}{p^2 \cdot \left(p^2 + \frac{P_{wa} L^2}{\pi^2 EI}\right)} \sin\left(\frac{p\pi x}{L}\right) \right| \leq K \frac{\sum_{j=1}^{N_{wa}} |R_{we/wa}(c_j)|}{p^4} \quad (9)$$

The right hand side is the term of a convergent Riemann series with remainder equivalent to

$\frac{B}{3p^3}$, with the (positive) amplitude coefficient $B = K \sum_{j=1}^{N_{wa}} |R_{we/wa}(c_j)|$; this is a classical result when comparing series to integrals of decreasing functions. It shows that the convergence of the series is fast, thus we shall retain 50 terms in the simulations (this gives a precision of the order of $\frac{1}{p^3} = 8 \cdot 10^{-6}$). Hence, inserting (8) into (1), the vertical displacement of the contact

points at the cross-over positions $x=c_i$ may be expressed in compact form versus the reactions forces of the transverse yarns R_{c_j} as

$$w_{we,ci} = w_{we}(x=c_i) = \sum_{j=1}^{N_{wa}} A_{i,j}^{we} R_{c_j} \quad (10)$$

wherein A_{we} is the interaction matrix with general coefficient

$$A_{i,j}^{we} = K_{we} \sum_{p=1}^{\infty} \frac{\sin\left(\frac{p\pi c_i}{L}\right) \sin\left(\frac{p\pi c_j}{L}\right)}{p^2 \cdot \left(p^2 + \frac{P_{wa} L_{we}^2}{\pi^2 EI_{we}}\right)} \quad (11)$$

In order to express the reaction force exerted by the weft onto the set of warp, we define the vector of reaction forces as

$$\mathbf{R} := (R_{ci})_{i=1..N_{wa}} \quad (12)$$

(the subscripts ‘wa’ and ‘we’ stand respectively for the warp and weft, here and in the sequel). The previous developments show that the reaction forces’ vector is given by

$$\mathbf{R} = (R_{wa/we}^i)_{i \in [1, N_{wa}]} = A_{we}^{-1} \cdot \mathbf{w}_{we} \quad (13)$$

with A_{we}^{-1} the inverse of the matrix A for the considered weft. Using the action-reaction principle, the reaction force of the warp onto the weft is opposite to the reaction force $R_{we/wa}(c_j)$ in (13), when evaluated at the contact point $x = c_j$, viz one can write

$$R_{we/wa}(c_i) = -R_{wa/we}(c_i) = -[A_{we}^{-1}]_{ij} w_{we}(c_j) \Leftrightarrow \mathbf{R}_{we/wa} = -A_{we}^{-1} \cdot \mathbf{w}_{we} \quad (14)$$

Considering a woven in the absence of sliding (the cohesion or static friction between yarns is strong enough to prevent relative motion of the warp and weft), the continuity of the displacement at the contact point between warp and weft at the position $x = c_j$, gives the vectorial condition valid for all contact nodes

$$\mathbf{w}_{we} = \mathbf{w}_{wa} + \mathbf{w}_{we,0} - \mathbf{w}_{wa,0} \quad (15)$$

with \mathbf{w}_{wa} the vector of displacements of the contact nodes

$$\mathbf{w}_{wa} = \{w_{wa}(c_j)\}_j$$

The initial positions (self-equilibrium in the absence of external load) of the warp and weft nodes on the common contact point are denoted successively $\mathbf{w}_{wa,0} = \{w_{wa,0}(c_j)\}_j$ and $\mathbf{w}_{we} = \{w_{we}(c_j)\}_j$, and are supposed to be known. Relations (14) and (15) give the reactions of the weft versus the displacements of the contact points, with the flexural rigidity of the weft as a parameter, according to (11). Hence, the vertical displacement of the contact points may be expressed in compact form versus the reactions forces of the transverse yarns R_{c_j} as

$$w_{ci} = K \cdot \sum_{j=1}^{N_{tr}} A_{ij} R_{cj} \quad (16)$$

with $K = \frac{2L^3}{EI\pi^4}$, and A a matrix with general term

$$A_{ij} = \sum_{k=1}^{\infty} \frac{\sin\left(\frac{k\pi c_i}{L}\right) \sin\left(\frac{k\pi c_j}{L}\right)}{k^2 \cdot \left(k^2 + \frac{PL^2}{\pi^2 EI}\right)} \quad (17)$$

Defining the vector of reduced deflections

$$\mathbf{b} := \left(\frac{1}{K} w_{ci} \right)_{i=1..N_{tr}} \quad (18)$$

$\mathbf{Q} := (R_{ci})_{i=1..N_{tr}}$ the vector of reaction forces, previous developments show that the deflection is given by

$$\mathbf{Q} = \mathbf{A}^{-1} \mathbf{b} \quad (19)$$

Hence, the work of the reaction forces writes

$$W_{\text{réaction}} = {}^t \mathbf{Q} \cdot \mathbf{K} \mathbf{b} = K \cdot ({}^t \mathbf{b} {}^t \mathbf{A}^{-1} \mathbf{b}) \quad (20)$$

Those equations are to be solved for a given woven structure submitted to applied tractions in warp and weft directions. The internal reaction forces are part of the solution of the structural problem. As an input of the mesoscopic model, it is required to know the yarns mechanical property, as well as the quadratic moment, itself dependent on the chosen model of the yarn section.

In the specific case of fabric, the reaction force of the transverse yarn only involves the deflection at the point of application of the force (and not all contact points along the yarn), given by

$$R_{we/wa} = \frac{\pi^4}{2} \frac{EI_{wa}}{(L_p^{wa})^3} \tilde{w}_{wa} \quad (21)$$

with $\frac{L_{wa}}{N_{we}} = L_p^{wa}$ the half-period length of a warp yarn. We find the same result as given by Timoshenko [31] for one half-period, viz $N_{we, wa} = 1$. As a matter of comparison, a similar analysis made by Euler gives a quite comparable value, $R = 48 \frac{EI}{(L_p)^3} \tilde{w}$.

The total potential energy V is then obtained as the difference between the internal deformation energy U (due to the flexion and extension of the yarn), and the external work W_{ext} defined by

$$W_{ext} = W_{traction} + W_{gr} + W_{reaction \text{ forces}} \quad (22)$$

with $W_{traction}$ the work of the traction loads P_{wa} and P_{we} applied respectively in the warp and weft directions (supposed to be uniformly distributed along the edge nodes), W_{gr} the work of the gravity load, and $W_{reaction \text{ forces}}$ the work of the reaction forces at the contact points. The total potential energy is expressed in terms of the coefficients $(a_n^{wa})_{n \in [1, N_{we}]}$ of the Fourier series (accounting for the deflection of the warp to weft contact point), together with the extensions $(u_2, u_3, \dots, u_{N_d+1})$ of the nodes of the discrete warp yarn (accounting for the clamped end condition $u_1 = 0$), hence $V = V(a_1^{wa}, \dots, a_2^{wa}, \dots, a_{N_{we}}^{wa}, u_2, \dots, u_i, \dots, u_{N_d+1})$. For a conservative structure (one excludes any dissipation due e.g. to relative sliding between yarns or to a viscous behavior of the yarn), the yarn equilibrium shape is then characterized by the minimum of the total potential energy with respect to the set of arguments $(a_1^{wa}, \dots, a_2^{wa}, \dots, a_{N_{we}}^{wa}, u_2, \dots, u_i, \dots, u_{N_d+1})$, i.e. by the following set of algebraic nonlinear equations:

$$\frac{\partial V}{\partial a_1^{wa}} = \dots = \frac{\partial V}{\partial a_i^{wa}} = \dots = \frac{\partial V}{\partial a_{N_{we}}^{wa}} = 0 \quad ; \quad \frac{\partial V}{\partial u_2} = \dots = \frac{\partial V}{\partial u_i} = \dots = \frac{\partial V}{\partial u_{N_d+1}} = 0 \quad (23)$$

This set of equations constitutes a necessary equilibrium condition, and one has to check that the energy level indeed corresponds to a true minimum; this testing together with the numerical solution strategy of the nonlinear coupled system of equations (23) is the object of specific algorithms to be described next.

2.2. Simulation Results: Effective Properties of Fabric and Serge

As the absolute minimum of the potential energy of a given woven structure cannot easily be reached using deterministic methods (gradient or conjugated gradient access to local minima), we combine an initial guess of the solution with a genetic algorithm. As their name indicates, those algorithms rely on techniques derived from genetics and natural evolution, namely crossings, mutations and selection. The principle consists in searching for the extremum of a function over a space of data. For this purpose, one has to rely on the following key elements:

- I. A coding principle of any population element, namely the translation of points of the state space into a data structure. The quality of this coding largely determines the success of genetic algorithms.
- II. A mechanism to generate the initial population. The velocity of convergence towards the global optimum is very dependent upon the choice of the initial population. The size of the initial state space is also important on the convergence velocity, as it allows exploring more or less rapidly a wider state space.
- III. A function to be optimized, presently the total potential energy.
- IV. Operators allowing to diversify the population across the generations and to explore the state space. For instance, the crossing operator recomposes the genes of individuals of the population and the mutation operator warrants to explore the whole state space.
- V. Sizing parameters, such as the population size, the total number of generations or an arrest criterion, the probabilities for the application of the crossing and mutation operators.

The state space is here defined as the set of all arguments of the potential energy (the Fourier coefficients are equivalently replaced by the discrete deflections),

$$V = V[u_1, u_2, u_3, \dots, u_{n+1}, w_2, w_3, \dots, w_n] \quad (24)$$

The initialisation vector is calculated as a prediction, using the linear beam theory: the axial displacement of the warp is then predicted for both armours as

$$u(x) = \frac{P}{EA} x \quad (25)$$

The vertical displacement can be predicted depending upon the armour, as a function of the yarns diameters, viz for fabric:

$$w_i = (-1)^k \cdot A_0 \quad (26)$$

with $A_0 = \frac{D_{\text{weft}}}{2}$ the radius of the weft. The change of sign in (26) accounts for the successive and alternate passages of the weft above and below the considered warp.



Figure 2. Armour of serge.

The initial amplitude for serge (Figure 2) can be deemed as the diameter of the weft (here chosen equal to the warp diameter as a matter of simplicity) regarding the curved part $w_i = A_0 = D_{\text{weft}} / 2$, and opposite this value for the straight part.

The main steps of the algorithms can be summarized as follows:

- 1) Input data: mechanical properties of the yarns. EI_{wa} ; EA_{wa} ; EI_{we} ; EA_{we} and external load.
- 2) Assemble the total potential energy V .
- 3) Calculate the work of reaction forces.
- 4) Determine woven structure at equilibrium using genetic algorithms for the minimum of V .
- 5) Output: kinematic variables for the woven.
- 6) Simulate the tensile response under uniaxial or biaxial loading.

Results of simulations are successively given for fabric and serge, chosen as two prototype armours. The mechanical properties of the yarns are chosen for both armours as:

$$EI_{\text{wa}} = 1.5e^{-6} \text{ N.m}; EA_{\text{wa}} = 130 \text{ N}$$

considering a balanced fabric (the mechanical properties of the weft are identical). Those values correspond to a typical tensile modulus of the order of 1GPa, representative of standard textile (Polyamide-Nylon 6) yarns.

The response of fabric exhibits the typical J-shape curve (Figure 3), characterized by low forces in the first regime (the crimp change is easy), followed by hardening due to an increase of the internal reaction forces. The main deformation mechanism at the yarn scale is the variation of the yarn geometry (crimp), responsible for the observed geometrical nonlinearity. As expected, the reaction forces are distributed in an antiperiodical manner.

The bottom curve is a fictive response when the yarn interactions are neglected. The uniaxial traction curve of fabric exhibits a nonlinear response, witnessing the geometrical nonlinearities due to the crimp changes. As the yarn becomes flatter, the reaction forces due to the transverse yarns increase, leading to a geometrical hardening (Figure 4). The local deformation mechanisms responsible for the overall behavior may be inferred from the extensional and flexional contributions of the displacement (Figure 4): the extensional displacement increases monotonously with the applied load, whereas the flexional displacement shows a two stages evolution: it first rapidly increases the crimp changes are easy with low internal reactions), and then reaches a plateau, with reaction forces reaching their maximum value (the structure is locked with respect to rotations).

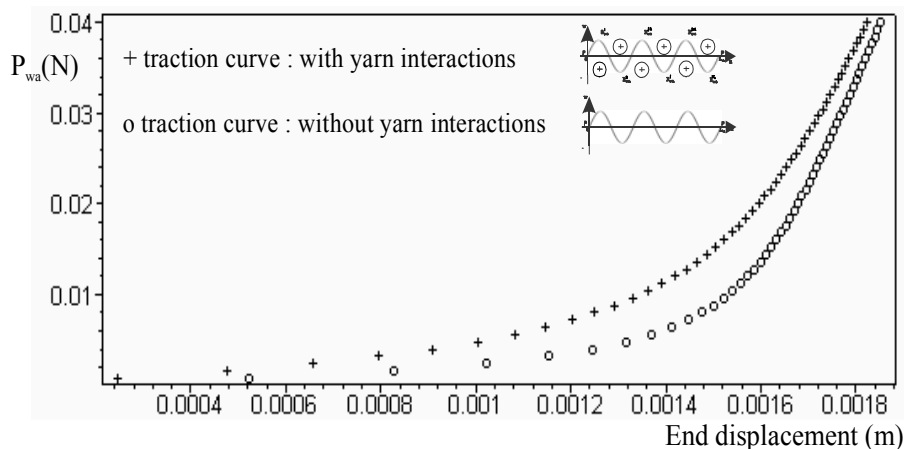


Figure 3. Uniaxial tensile of fabric. Effect of yarn-yarn interactions.

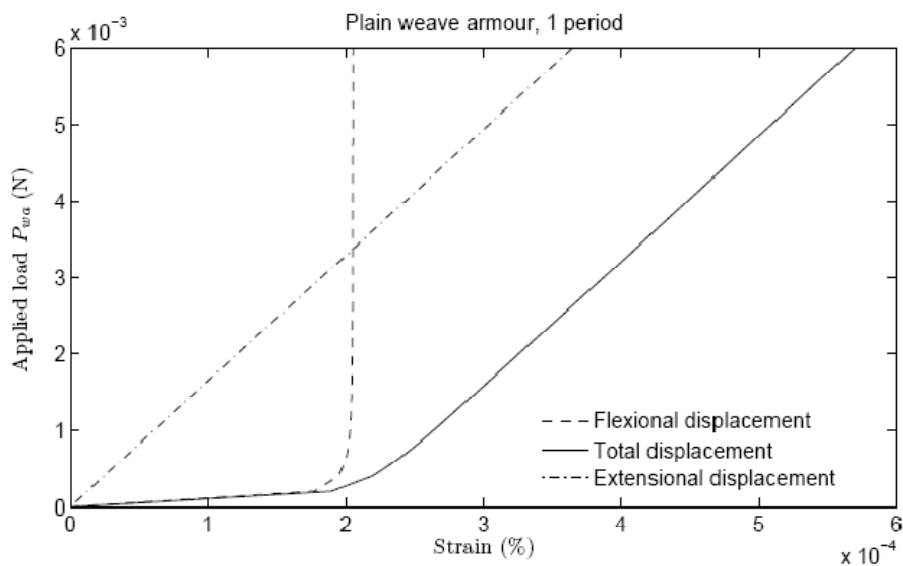


Figure 4. Tensile response of fabric. Evolution versus the applied load of the extensional and flexional contributions to the overall displacement.

In order to assess the effect of the mechanical and geometrical properties on the fabric traction behavior, simulations of the traction behavior of the fabric in the warp direction are performed for different values of the transverse yarns rigidity. Figure 5 shows that a stiffer transverse yarn increases the reaction forces, thus leads to a stiffer response of the warp. At the end of this stiffening, the reaction force tends toward a limit value, which indicates that the yarn has exhausted its possibilities of crimp changes. We further analyze the effect of the transverse extension load P_{we} on the fabric mechanical behavior, in the warp direction (x-direction); specialization of previous general equations in the case of fabric give the reaction force of the transverse yarn as

$$R_{we/wa}^{j,k} = -R_{wa/we}^{j,k} = -\frac{\pi^4 (EI)_{we}}{2 (L_p^{we})^3} \left(1 + \frac{\alpha_{we}}{N_{we}^2} \right) \left[(w_{so-we}^{j,k} - w_{so-wa}^{j,k}) + w_{s-wa}^{j,k} \right]; \quad \alpha_{we} = \frac{P_{we}}{P_{cr}^{we}} \quad (27)$$

with P_{cr}^{we} the first critical buckling load of the weft under compression; we deduce from (27) that the reaction force occurring at the interlacing points varies with P_{we} , thus leads to different fabric traction responses. The results (Figure 5) show that increasing the transverse extension load P_{we} leads to a stiffer response of the fabric: this is due to the decrease of the yarn-yarn undulation transfer capacity.

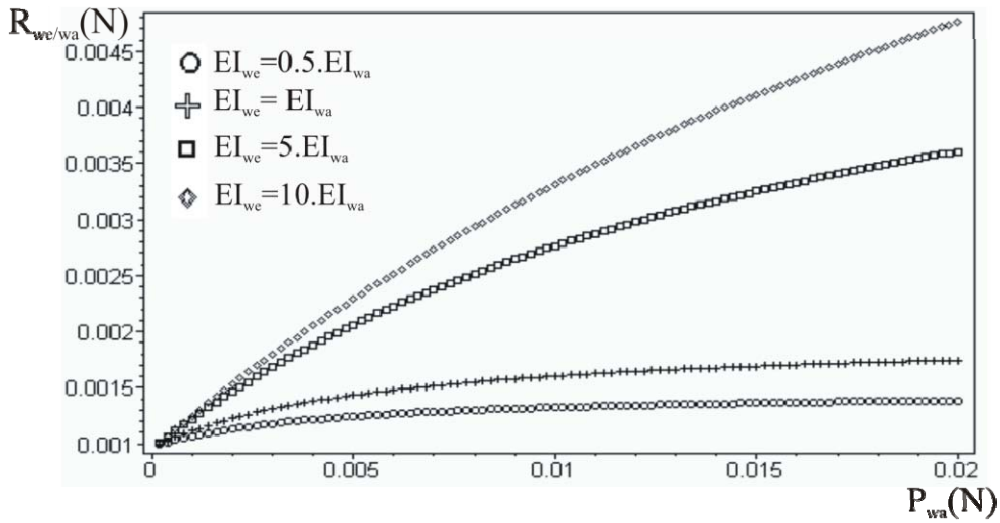


Figure 5. Variation of the reaction force. Effect of warp and weft modulus.

Indeed, from Eq. (27), we notice that the reaction load $R_{we/wa}$ increases with P_{we} , which affects the yarn-yarn undulation transfer, thus leading to a stiffer response (Figure 6).

Although the reaction load $R_{we/wa}$ tends toward a limit value in the case of a uni-axial extension ($P_{we} = 0$), we remark that, in the case of biaxial extension, it grows continuously without reaching a limit value: equation (27) shows that the reaction force $R_{we/wa}$ not only varies according to the position of the warp/weft yarns' summits, but also according to the transverse extension load P_{we} . In fact, when the yarn-yarn undulation transfer process is exhausted, the reaction force does not vary any more (since the positions of the contact points between yarns do not change any more); it solely varies vs. P_{we} , with a linear variation that explains the linear part observed on the biaxial tensile responses (Figure 7).

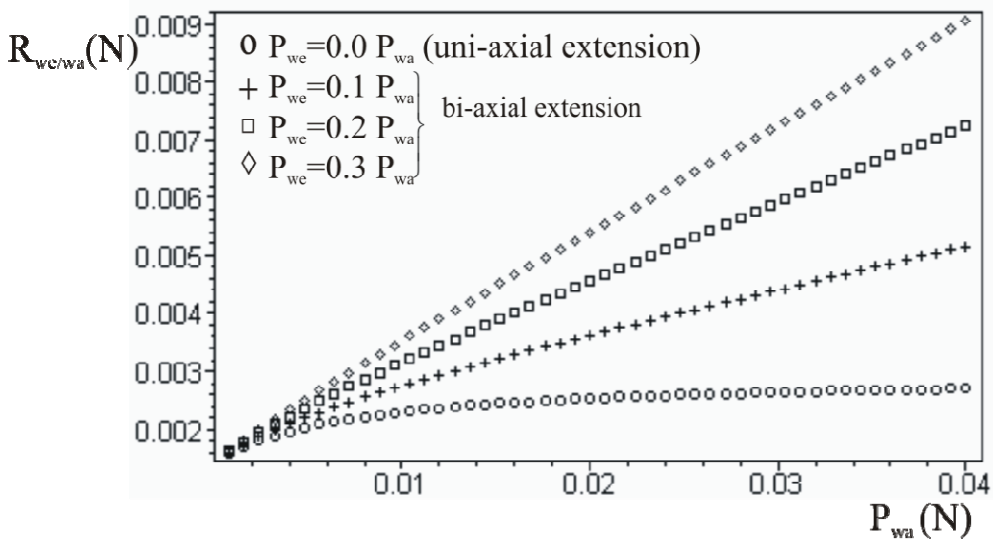


Figure 6. Variation of the reaction load $R_{we/wa}$: effect of the transverse load P_{we} .

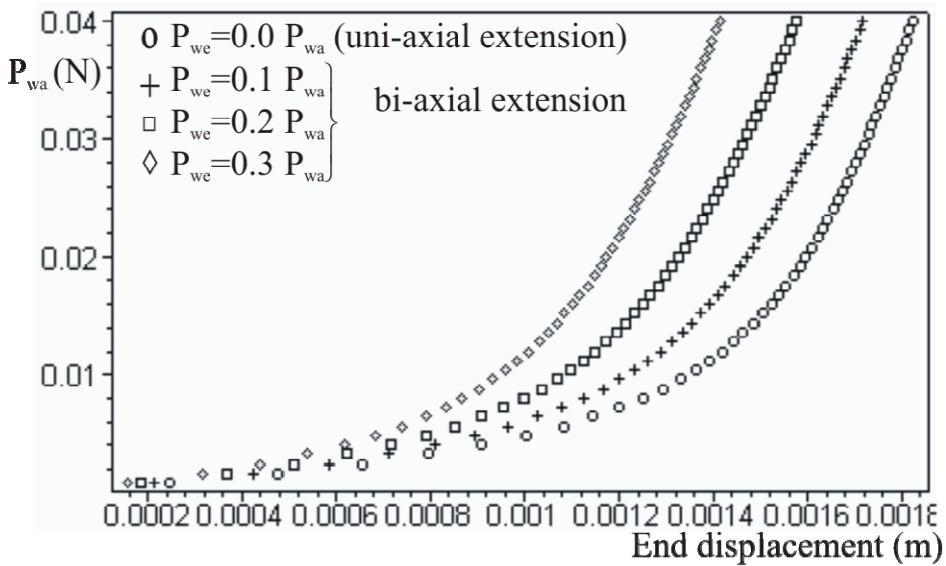


Figure 7. Tensile response of fabric: effect of the transverse extension load P_{we} .

Increasing the weft to warp flexion modulus leads to a stiffer overall tensile response, since the crimp changes become more and more limited by the stiffer transverse yarn (Figure 8).

Simulations results give relatively good agreement compared to tensile measurements on Polyethylene terephthalate weave fabric (Figure 9); the tensile moduli of the warp and weft are respectively $E_{warp} = 8.26 \cdot 10^9 \text{ Pa}$ and $E_{weft} = 7.94 \cdot 10^9 \text{ Pa}$.

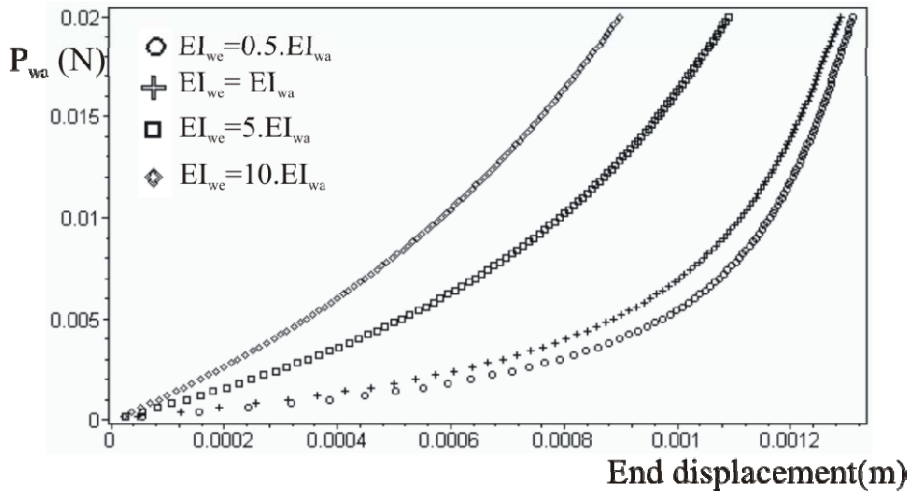


Figure 8. Fabric extension in the warp direction. Effect of the weft modulus.

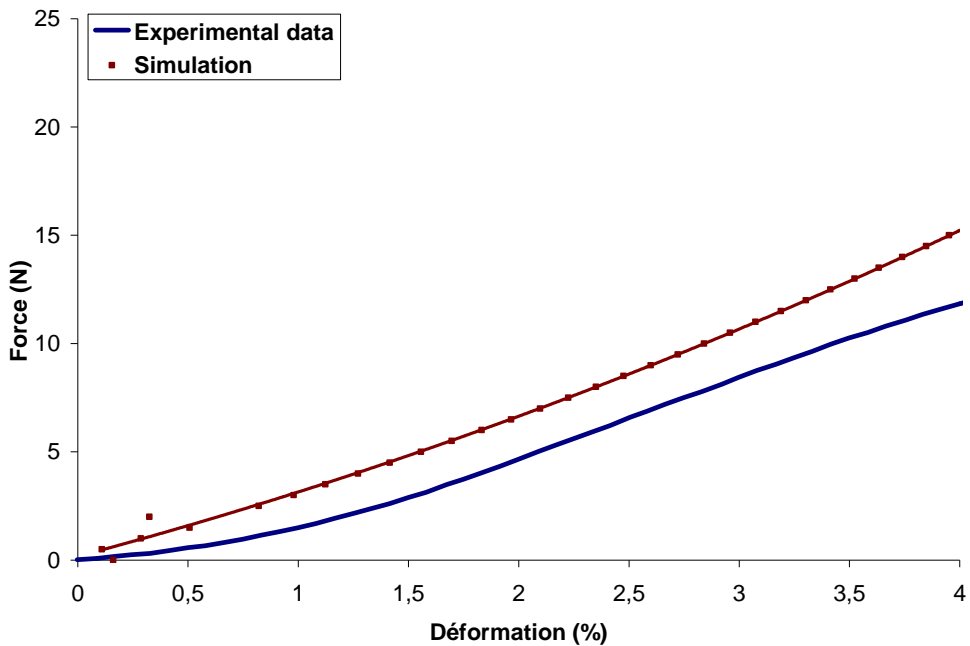


Figure 9. Measured and simulated tensile responses of Polyethylene terephthalate weave fabric.

The response of serge contrasts with that of fabric, and exhibits a linear feature (Figure 10), due to the dominant contribution of the straight part of the warp. Hence, the geometrical nonlinearities which could appear because of the curved part of the warp beam line are not present here. The horizontal error bars (Figure 10) are the variations due to the initial population size in the genetic algorithm.

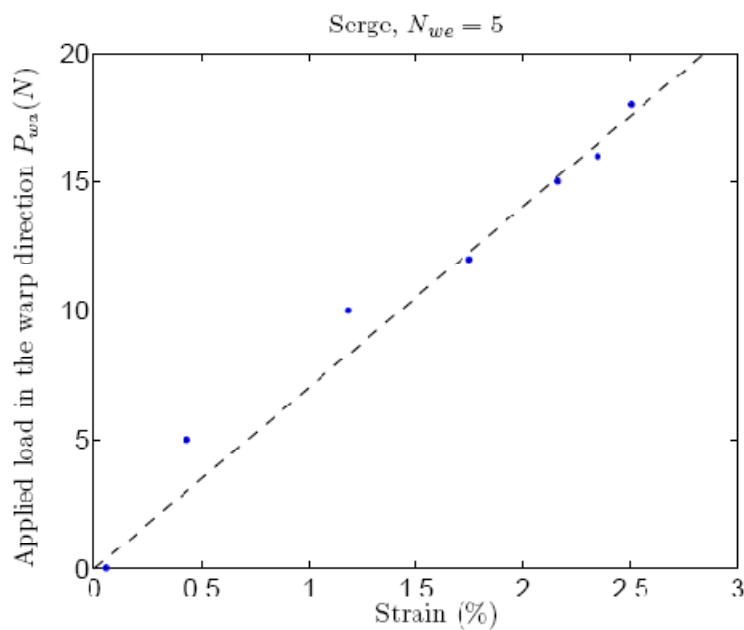


Figure 10. Uniaxial force-strain response of serge (5 transverse yarns) for one period.

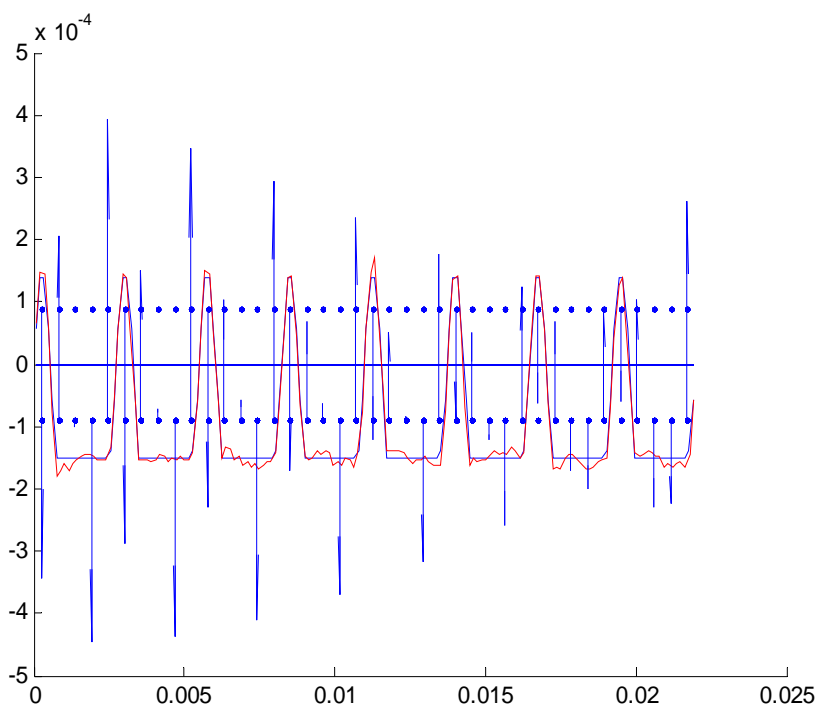


Figure 11. Deformation of serge. Arrows indicate the reaction forces. The initial shape is superposed on the deformed shape.

Due to the weave pattern, the reaction forces are distributed in a non symmetrical manner (Figure 11). The arrows drawn on the same figure indicate the reaction forces, with their length indicative of their intensity. Genetic algorithms allow finding the absolute minima of the structure potential energy, with however an important computational time. The calculation of general armours may be undertaken relying on the same methodology, with extension to multilayers.

2.3. Evaluation of Poisson's Ratio of Fabric

A peculiar feature of woven structures is the magnitudes of Poisson's ratios, which can attain some peculiar values, in contrast to conventional engineering materials, leading in turn to unusual stress-strain relationships. The Poisson's ratio is one of the fundamental mechanical characteristics for a woven fabric, as it is a structural parameter, consequence of the armour geometry, the yarn mechanical properties and the yarn-yarn interactions. The magnitudes of Poisson's ratios can attain values outside the range 0.1/2 for woven fabrics [9], very different from those for conventional engineering materials, leading to unusual stress-strain relationships. As for the other macroscopic properties of woven structures, the Poisson's ratio is the result of a multiscale imbricated process. Three imbricated scales of the woven structure can indeed be identified: the microscopic scale (scale of the yarn), the macroscopic scale of the woven structure, and an intermediate scale of a few intertwined yarns, which defines the unit cell reproducing the whole structure by a periodic translation, called the mesoscopic scale. Very few works in the literature are devoted to the quantitative evaluation of the Poisson coefficient of textiles, see [32] considering modeling approaches based on a geometrical description of the yarn within a unit cell, and the complete list of references therein; on the other hand, it is difficult to develop reliable measurements protocols. The effects of mechanical properties of yarns and structural parameters on the Poisson's ratio of a woven fabric are next investigated.

The in-plane Poisson's ratio of fabric is defined as the ratio of the transverse to the longitudinal strain:

$$\nu_{wa-we} = -\frac{\frac{u_N^{we}}{L_{we}}}{\frac{u_N^{wa}}{L_{wa}}}; \nu_{we-wa} = -\frac{\frac{u_N^{wa}}{L_{wa}}}{\frac{u_N^{we}}{L_{we}}} \quad (28)$$

with L_{wa}, L_{we} the length of the considered samples in the warp and weft directions respectively. The indices 'wa' and 'we' stand respectively for the warp and weft. Similarly, the equivalent traction moduli are defined by

$$E_{wa} = \frac{P_{wa}}{\frac{u_N^{wa}}{L_{wa}}}; E_{we} = \frac{P_{we}}{\frac{u_N^{we}}{L_{we}}} \quad (29)$$

Simulations show that $\frac{\nu_{we-wa}}{E_{we}}$ is very close to $\frac{\nu_{wa-we}}{E_{wa}}$, hence fabric behaves as an orthotropic structure, as confirmed by [32]. The evolution of both Poisson's ratio versus the applied loads is depicted in Figures 12 and 13.

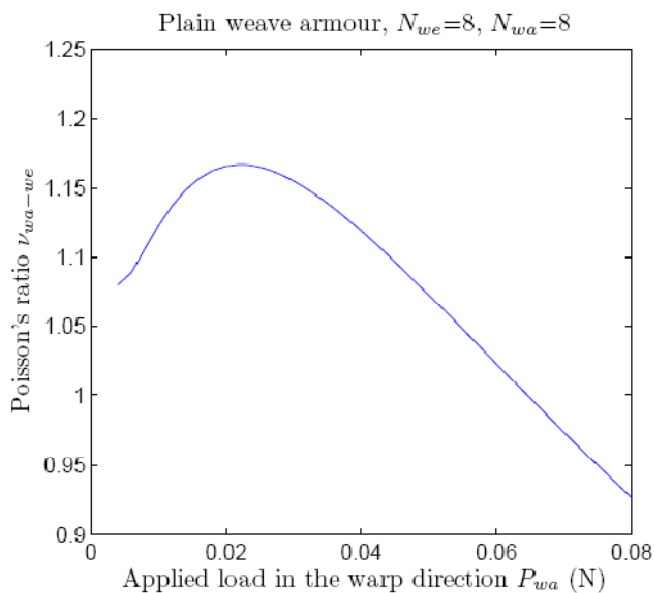


Figure 12. Poisson's ratio ν_{wa-we} of fabric vs. the applied load (N) in the warp direction.

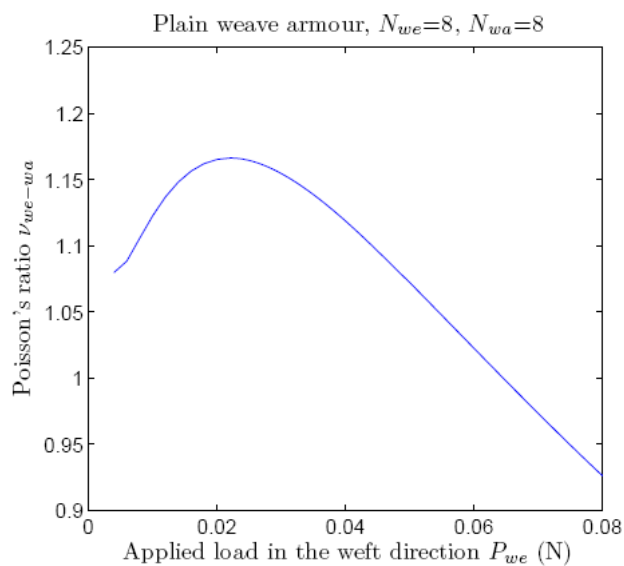


Figure 13. Poisson's ratio ν_{we-wa} of fabric versus the applied load (N) in the weft direction.

Both Poisson's ratios increase towards a maximum, corresponding to the increase of the structure's shrinkage in the transverse direction. The subsequent decrease is due to the monotonous increase of the axial load, with the transversal dimensions nearly constant. As the equivalent traction moduli determine the dimensional variations of the fabric structure, we next plot the evolution of the reduced Poisson's ratio $\frac{v_{wa-we}}{E_{wa}}$ (resp. $\frac{v_{we-wa}}{E_{we}}$) versus the applied load P_{wa} (resp. P_{we}).

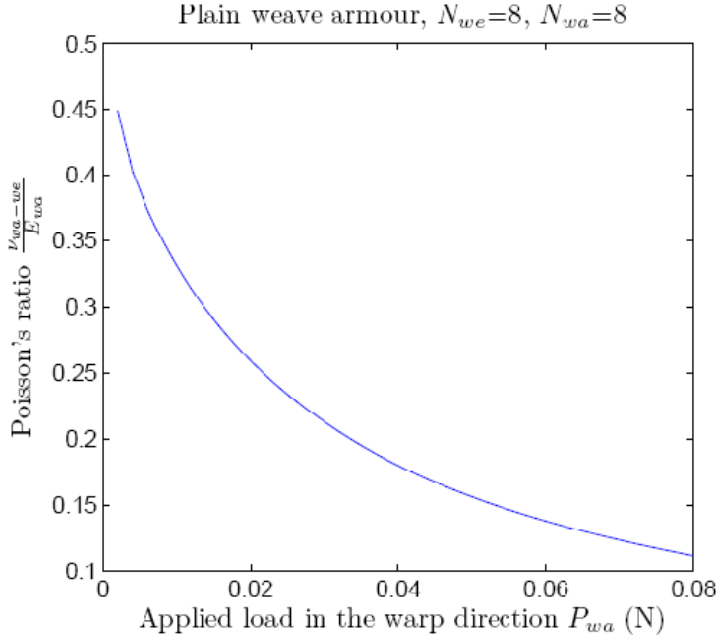


Figure 14. Evolution of the reduced Poisson's ratio $\frac{v_{wa-we}}{E_{wa}}$ versus the load applied in the warp direction.

The highest the applied load, the highest the reaction forces limiting the crimp changes, hence the transverse motion. Figure 6 shows indeed that the reaction force $R_{we/wa}$ plays a determinant role on the deformation mechanisms and overall response of fabric; although the reaction $R_{we/wa}$ tends to a horizontal asymptote for a uniaxial traction ($P_{we} = 0$), it continues to increase in the case of a biaxial traction. When the crimp variations for fabric are exhausted, the reaction force $R_{we/wa}$ does not change due to the position of the contact points between yarns (they are fixed), but solely due to P_{we} , which in turns linearly varies versus P_{wa} ($P_{we} = \alpha P_{wa}$). Accordingly, the linear variation of $R_{we/wa}$ versus P_{wa} explains why the important values reached by the reaction forces prohibit any undulation transfer.

The impact of a variation of the extensional and flexional yarn rigidities is assessed in Figures 16 and 17.

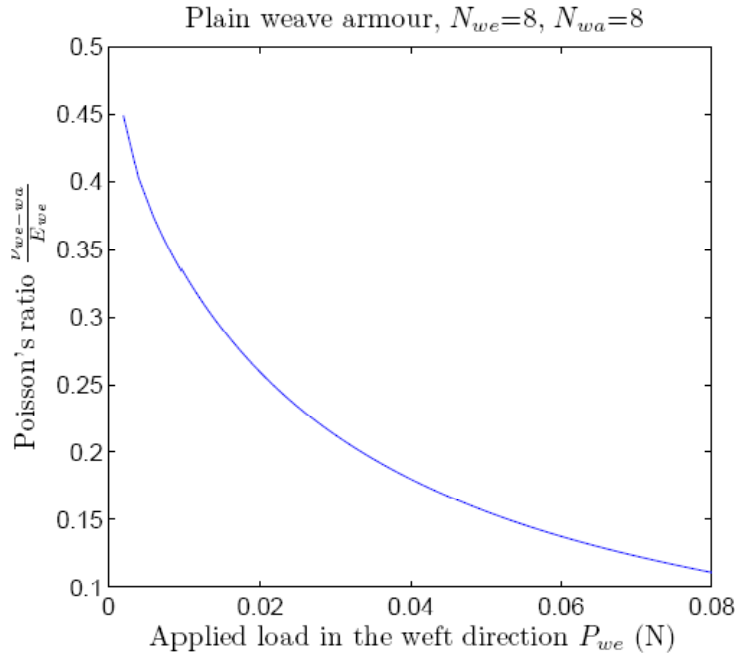


Figure 15. Evolution of the reduced Poisson's ratio $\frac{\nu_{we-wa}}{E_{we}}$ vs. the load applied in the weft direction.

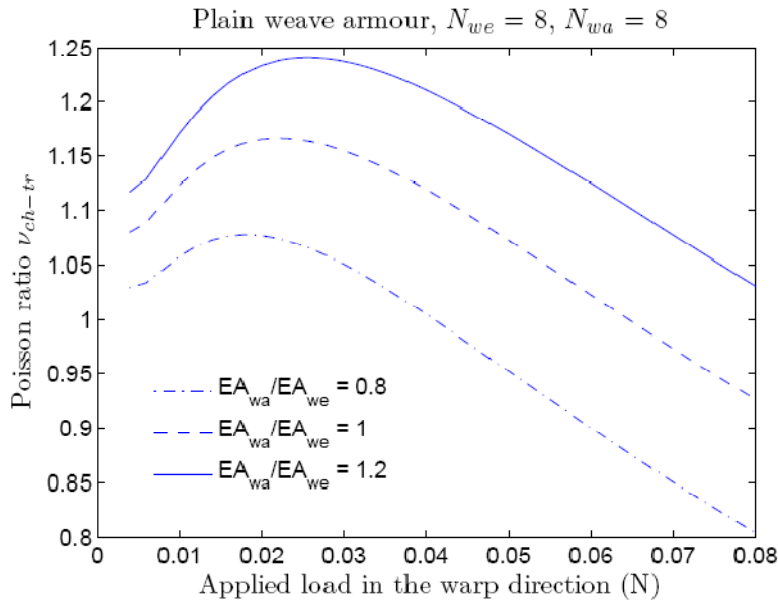


Figure 16. Poisson's ratio in the warp direction vs. the applied load. Effect of the yarn extensional rigidity.

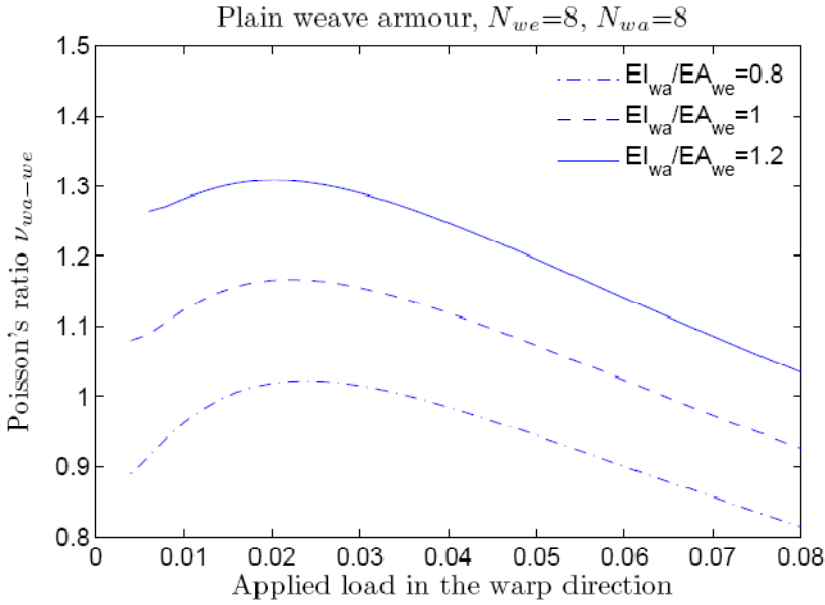


Figure 17. Poisson's ratio in warp direction vs. applied load. Effect of the yarn flexional rigidity.

In both cases, the highest the warp to weft rigidity ratio, the highest the transverse shrinkage. However, the difference between Figure 16 and 17 is the evolution of the maximum point, which occurs in opposite directions.

3. CONSIDERATION OF YARN-YARN INTERACTIONS: TRANSVERSE COMPRESSIBILITY AND FRICTION

The general framework laid down in previous section shall be involved in the sequel to incorporate the transverse compressibility and yarn-yarn friction as additional important features of the mechanics of textiles; the specific case of fabric will be considered, in order to be able to write down closed form expressions of the reaction forces, which would not be possible for more general armour. This will however not restrict the generality of the presented methodology.

Under the effect of the loads P_{wa} and P_{we} applied in the warp and weft directions respectively (supposed to be uniformly distributed along the edge nodes), a lateral compressive deformation of the yarns and an undulation transfer due to the yarn-yarn interaction occur at the contact points; thereby, the undulation transfer process is followed by a lateral displacement of the contact points. The displacement continuity occurring at the crossing points labeled by the set of indices (j, k) then expresses as (Figure 18a)

$$\delta_t^{wa} = \delta_t^{we} \Rightarrow w_{s-we}^{j,k} = w_{so-we}^{j,k} + w_{s-wa}^{j,k} - w_{so-wa}^{j,k} - (-1)^j (\delta_c^{wa} + \delta_c^{we}) \quad (30)$$

wherein δ_c^{we} and δ_c^{wa} respectively denote the vertical displacement of the weft and warp under compression (Figure 18a).

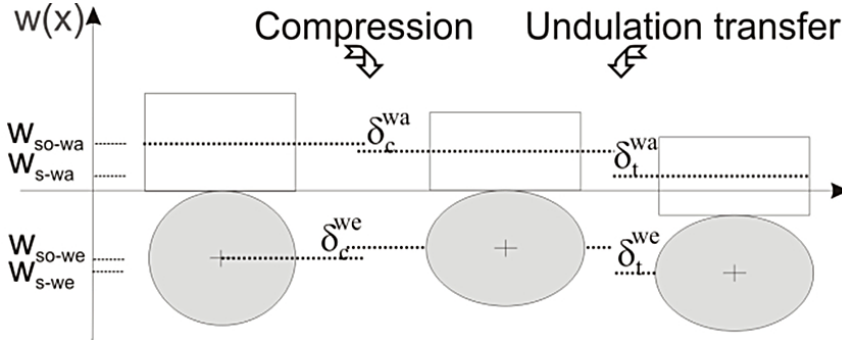


Figure 18a. Compression and undulation transfer between yarns.

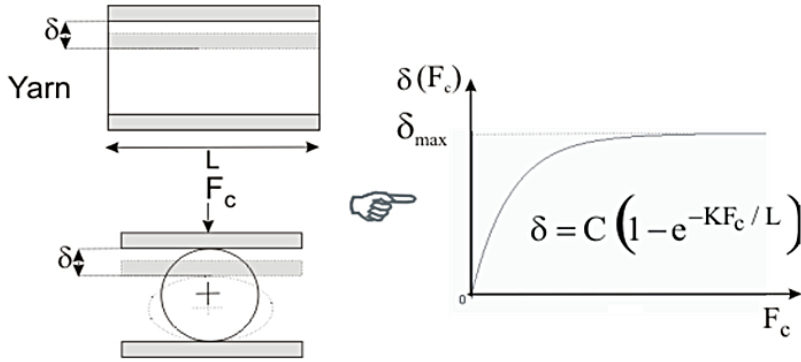


Figure 18b. Compression law for a yarn (Kawabata [3]).

The deformation under compression of a warp, δ_c^{wa} , varies vs. the contact force exerted by the transverse weft according to the (in inversed form) compression law of Kawabata [3], relying on measurements (Figure 18b):

$$\delta_c^{wa} = C_1 \left(1 - e^{-K_1 |R_{we/wa}| / L_c^{wa}} \right) \Leftrightarrow |R_{we/wa}| = -\frac{L_c^{wa}}{K_1} \ln \left(1 - \frac{\delta_c^{wa}}{C_1} \right) \quad (31)$$

with C_1 , K_1 the two Kawabata parameters for the warp and L_c the curvilinear length of a yarn portion defined within a half-period (Figure 18b). In the same way, the deformation under compression of a weft, variable δ_c^{we} , varies vs. the contact force exerted by the warp according to

$$\delta_c^{we} = C_2 \left(1 - e^{-K_2 |R_{wa/we}| / L_c^{we}} \right) \Leftrightarrow |R_{wa/we}| = -\frac{L_c^{we}}{K_2} \ln \left(1 - \frac{\delta_c^{we}}{C_2} \right) \quad (32)$$

with C_2 , K_2 the two Kawabata parameters of the weft. The parameter C can be interpreted as the limit value of the compressive deformation δ , when the compressive force increases. The parameter K therein provides information relative to the flexibility (inversely proportional to the rigidity) of the yarn response during the compression motion. Actually, from an experimental point of view, the value of K is shown to increase as the yarn compressive rigidity decreases.

According to the action / reaction principle valid at the contact points, viz $|R_{we/wa}| = |R_{wa/we}|$, the compression displacements of both yarns are further related by the following relationship

$$\delta_c^{we} = C_2 \left[1 - \left(1 - \frac{\delta_c^{wa}}{C_1} \right)^{\frac{K_2 L_c^{wa}}{K_1 L_c^{we}}} \right] \quad (33)$$

From the relations (27), (30) and (33) and using the action-reaction principle, the expression of the reaction force $R_{we/wa}$ is further elaborated as

$$R_{we/wa}^{j,k} = -R_{wa/we}^{j,k} = -\frac{\pi^4 (EI)_{we}}{2 (L_p^{we})^3} \left(1 + \frac{\alpha_{we}}{N_{wa}^2} \right) \left[w_{so-we}^{j,k} + w_{s-wa}^{j,k} - w_{so-wa}^{j,k} - (-1)^j \left(\delta_{c,k}^{wa} + C_2 \left[1 - \left(1 - \frac{\delta_{c,k}^{wa}}{C_1} \right)^{\frac{K_2 L_c^{wa}}{K_1 L_c^{we}}} \right] \right) \right] \quad (34)$$

Notwithstanding this modification, the finding of the equilibrium shape of the woven structure relies as previously on the minimization of the total potential energy, adding the set of variables $\{\delta_{c,k}^{wa}\}_k$ to the kinematic unknowns.

The incorporation of friction phenomena needs an enlargement of previous framework, as the woven structure becomes non conservative due to the appearance of non holonomic forces; this extension is presented next. Several models and empirical approaches of the friction phenomena in fabric have been developed in the literature, dating back to the early fifties [33-36]. We adopt in the sequel and as a matter of simplicity the Gralen model [37, 38], based on measurements made on Nylon and wool, that was established in the situation of two fibers in an elastoplastic contact, being twist, and submitted to a compression load W . It relies on the following linear relation between the static friction force and the reaction effort

$$F_T = \alpha R_{we/wa} + \beta \ell R \quad (35)$$

with α , β two material constants relative to the elastic and plastic properties of the material, which are evaluated from measurements, ℓ the effective contact length between the two yarns, and R the radius of the considered fiber. The friction forces F_T exerted at the contact

points vary versus the reaction force (normal force) exerted by the transverse yarns on the warp; a clarifying picture of the yarn-yarn interactions in terms of these forces is given in Figure 19 in the case of fabric.

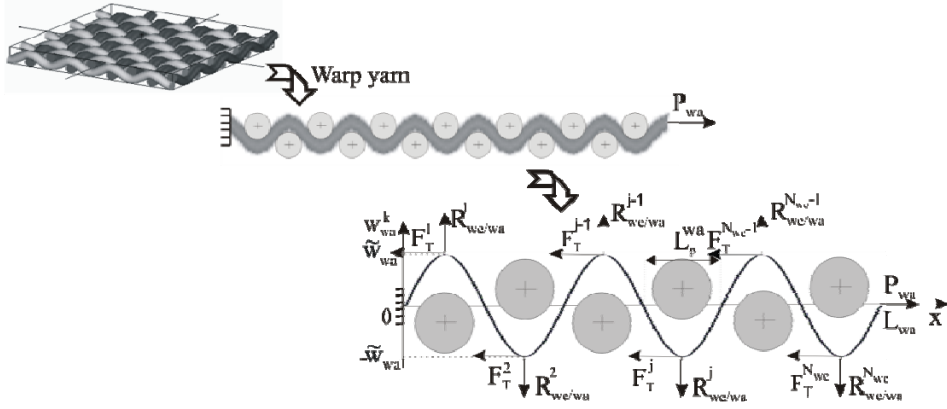


Figure 19. Warp submitted to an external traction. Reaction and friction forces.

Substituting next the expression (34) of the reaction force in the previous expression (35) delivers

$$F_T^{j,k} = -\alpha \frac{\pi^4 (EI)_{we}}{2 (L_p^{we})^3} \left[w_{so-we}^{j,k} + w_{s-wa}^{j,k} - w_{so-wa}^{j,k} - (-1)^j \left(\delta_{c,k}^{wa} + C_2 \left[1 - \left(1 - \frac{\delta_{c,k}^{wa}}{C_1} \right) \frac{K_2 L_c^{wa}}{K_1 L_c^{wc}} \right] \right) \right] + \beta \ell R \quad (36)$$

It appears from this expression that the friction forces vary not only versus the material constants, but also versus the vertical displacement of the summit nodes. During the traction process, the friction forces cause a loss of energy; this introduces an irreversible motion due to a slip of one family of yarn relative to the other one, which in turn modifies the equilibrium state of the structure. In the case of the yarn-on-yarn friction, one can remark that the friction force does not modify the previous expression of the total potential energy; the non holonomic forces have to be accounted for as an additional contribution on the right-hand side of the Euler-Lagrange equations resulting from the stationnarity of V in the specific case of a conservative structure.

A static model of friction is considered in the sequel. The generalization of d'Alembert postulate of static equilibrium of motion accounting for the presence of the non-holonomic forces [39] is formulated, using the decomposition of the generalized forces $\{Q_\alpha\}_\alpha$ that

intervene into the expression of the virtual work, $\delta W = \sum_{\alpha=1}^n Q_\alpha \delta q_\alpha$, as the sum of

conservative contributions $Q_\sigma^c = -\frac{\partial V}{\partial q_\sigma}$ - in which V does not depend on the rate of the generalized coordinates - and non-holonomic forces (generalized non conservative forces)

$$Q_{\sigma}^{nc} = \sum_{n=1}^{N_d} \mathbf{F}_T^n \cdot \frac{\partial \mathbf{r}_n}{\partial q_{\sigma}} \quad (37)$$

with \mathbf{r}_n and \mathbf{F}_T^n the displacement and the non-conservative force vectors of the node of index n , respectively. In (37), the generalized coordinates $(q_{\sigma})_{\sigma \in \langle 1, N_{we} + N_d + 1 \rangle}$ have been introduced, s.t.

$$q_{\sigma} = \begin{cases} a_{\sigma}^{wa} & \forall \sigma \in [1, N_{we}] \\ u_{\sigma - (N_{we} - 1)} & \forall \sigma \in [N_{we} + 1, N_{we} + N_d] \\ \delta_c^{wa} & \sigma = N_{we} + N_d + 1 \end{cases}$$

The following differential identity is then obtained

$$\frac{\partial V}{\partial q_{\sigma}} = Q_{\sigma}^{nc} \quad \sigma \in \langle 1, N_{we} + N_d + 1 \rangle \quad (38)$$

which characterizes the equilibrium shape of the yarn. This equation can be rewritten as

$$\frac{\partial V}{\partial q_{\sigma}} = Q_{\sigma}^{nc} = \sum_{n=1}^{N_d} \mathbf{F}_T^n \cdot \frac{\partial \mathbf{r}_n}{\partial q_{\sigma}} \quad \sigma \in [1, N_{we} + N_d + 1] \quad (39)$$

One obtains after projection in the Cartesian basis (\vec{e}_x, \vec{e}_y) :

$$Q_{\sigma}^{nc} = \sum_{n=1}^{N_d} \mathbf{F}_T^n \cdot \frac{\partial \mathbf{r}_n}{\partial q_{\sigma}} = \sum_{n=1}^{N_d} \left(-F_T^n \cdot \vec{e}_x \right) \cdot \left(\frac{\partial u_n}{\partial q_{\sigma}} \vec{e}_x + \frac{\partial w_n}{\partial q_{\sigma}} \vec{e}_y \right) = \sum_{n=1}^{N_d} -F_T^n \frac{\partial u_n}{\partial q_{\sigma}} \quad (40)$$

Assuming that the contact occurs only at the summit of the undulations, the friction forces are nil at other nodes, thus the previous expression simplifies to

$$Q_{\sigma}^{nc} = \sum_{n=1}^{N_d} -F_T^n \frac{\partial u_n}{\partial q_{\sigma}} = \begin{cases} \sum_{j=1}^{N_{we}} -F_T^j \frac{\partial u_j}{\partial a_{\sigma}^{wa}} = 0 & \text{if } \sigma \in [1, N_{we}] \\ \sum_{j=1}^{N_{we}} -F_T^j \frac{\partial u_j}{\partial u_{\sigma}} = \begin{cases} -F_T^j & \text{for summit nodes} \\ 0 & \text{otherwise} \end{cases} & \sigma \in [1, N_{we} + N_d + 1] \\ \sum_{j=1}^{N_{we}} -F_T^j \frac{\partial u_j}{\partial \delta_c^{wa}} = 0 & \text{if } \sigma = N_{we} + N_d + 1 \end{cases} \quad (41)$$

Accounting for the expressions (41), the equilibrium equations (38) then express as the following system of algebraic equations

$$\begin{cases} \frac{\partial V}{\partial a_1^{wa}} = \dots = \frac{\partial V}{\partial a_i^{wa}} = \dots = \frac{\partial V}{\partial a_{N_{we}}^{wa}} = 0 \\ \frac{\partial V}{\partial u_i} = \begin{cases} -F_T^j & \text{if } i = \frac{(2j-1)N_d}{2N_{we}} \text{ with } j \in [1, N_{we}] \text{ (index of summit nodes)} \\ 0 & \text{otherwise} \end{cases} \\ \frac{\partial V}{\partial \delta_c^{wa}} = 0 \end{cases} \quad (42)$$

The non nil tangential displacement u_i on a summit node (Figure 19) represents the local slip of the set of warp yarns, relative to that of the transverse weft. Note that it gives an effective representation of slip, without explicitly describing the relative slip (the nodes of both yarns are identified in the present model).

The effect of the friction on the fabric mechanical behavior is next assessed, from numerical simulations; a simulation without friction gives a reference comparison case to assess the importance of the yarn-yarn friction. For this purpose, the previous set of mechanical parameters of the warp and weft yarns is considered. In addition, the frictional parameters of the woven structure are taken as Lindberg and Gralen [37].

$$\alpha = 0.2 ; \ell = 2\text{mm} ; R = 1\text{mm} \text{ and } \beta = 10^3 \text{ N.m}^{-2}$$

Figure 20 shows that the consideration of the yarn-on-yarn friction leads to a stiffer response: this behavior can be explained by the loss of energy due to yarn-on-yarn friction. The importance of friction increases with ongoing extension during the first stage of deformation (up to 0.005 m), and remains thereafter constant (both curves are nearly parallel, Figure 20), as the reaction forces increase, thus also the friction force.

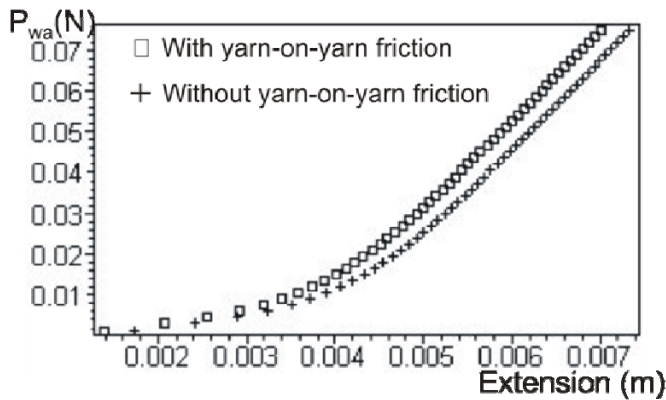


Figure 20. Uni-axial traction curve: effect of the yarn-yarn friction.

The results presented so far show that the friction and the compressibility effects are not negligible. Suitable experiments shall further be performed in order to identify the present set of model parameters. Future research in this field shall take into account the effective contact area between yarns, involving a distribution of friction forces within the contact zone. Furthermore, as the yarn is most of the time a complex structure made of fibers (except for monofilaments), friction is associated to complex phenomena occurring at a very microscopic scale, and involves instabilities such as stick-slip. The construction of mechanical models for complex yarns remains accordingly a challenging task for the future.

4. DISCRETE HOMOGENIZATION AND FIRST APPLICATIONS TO TEXTILES

The discrete homogenization method is a mathematical technique to derive the equivalent continuous medium behaviour of repetitive discrete structures. As textiles can be considered as periodic structures made of the repetition of a pattern consisting of intertwined yarns, they are good candidate for such a homogenization. The technique is inspired from the homogenization of periodic media developed thirties years ago by Sanchez-Hubert and Sanchez-Palencia [40]; Panasenko [41]; Bakhvalov and Panasenko [42] and more recently applied by Warren and Byskhov [43]; Mourad and Caillerie [44], although restricting to mechanics of bars in the last contribution. It has been also combined with the energy method by Pradel and Sab [45] and applied to discrete homogenization.

The discrete homogenization method consists in assuming asymptotic series expansions of both the node displacements, tension, moments and external forces versus a small parameter labelled ε , defined as the ratio of a characteristic length of the basic cell to a characteristic length of the lattice structure. Those expansions are then inserted into the equilibrium equation, conveniently expressed in weak form. The balance equation of the nodes, forces-displacement relations and the moment-rotation relations of the beams are developed by inserting those series expansions and by using Taylor's expansion of finite differences. The discrete sums are finally converted in the limit of a continuous density of beams into Riemann integrals, thereby highlighting continuous stress and strain measures. The calculations may be done for a quite general truss and closed form expressions of the effective (homogenized) properties are obtained from the effective compliance or rigidity matrix. The method has given rise to implementation into a dedicated software. More details about the method can be found in Tollenaere and Caillerie [46]; Mourad et al. [43]; Caillerie et al. [47]; Dos Reis and Ganghoffer [48], and only the main steps are exposed in the sequel.

4.1. Asymptotic Parameters and Description of the Lattice Geometry

The discrete asymptotic technique requires the development of all variables as Taylor series; the beam length l^{eb} , the beam width t^{eb} , thickness e^{eb} , the displacement u^{en} and the rotation of the lattice nodes ϕ^{en} (both constitute the kinematic variables) vs. the small parameter ε . A Bernoulli beam model is considered in this study. From the results of Mourad

et al. [43], one can express the beam length as follows (only the first order term needs to be considered in a small strain framework)

$$l^b = l_0^b + \varepsilon l_1^b + \varepsilon^2 l_2^b + \dots + \varepsilon^p l_p^b \quad (43)$$

The normal and transverse efforts, and the moment at the beam extremities can be successively expressed versus the kinematical nodal variables as in Dos Reis and Ganghoffer [48]:

$$\begin{aligned} N^\varepsilon &= \frac{E_s S}{l^b} (\Delta \mathbf{U}^{b\varepsilon} \cdot \mathbf{e}^b) \\ T_t^\varepsilon &= \frac{12 E_s I_z}{(l^b)^3} \left((\Delta \mathbf{U}^{b\varepsilon} \cdot \mathbf{e}^{b\perp}) - \varepsilon \frac{l^b}{2} (\phi^{O(b)\varepsilon} + \phi^{E(b)\varepsilon}) \right) \\ M^{O(b)\varepsilon} &= \frac{12 E_s I_z}{(l^b)^3} \left(\varepsilon^2 \frac{(l^b)^2}{6} (2\phi^{O(b)\varepsilon} + \phi^{E(b)\varepsilon}) - \frac{1}{2} \varepsilon l^b (\Delta \mathbf{U}^{b\varepsilon} \cdot \mathbf{e}^{b\perp}) \right) \\ M^{E(b)\varepsilon} &= \frac{12 E_s I_z}{(l^b)^3} \left(\varepsilon^2 \frac{(l^b)^2}{6} (\phi^{O(b)\varepsilon} + 2\phi^{E(b)\varepsilon}) - \frac{1}{2} \varepsilon l^b (\Delta \mathbf{U}^{b\varepsilon} \cdot \mathbf{e}^{b\perp}) \right) \end{aligned} \quad (44)$$

where I_z is the quadratic moment of the beam, \mathbf{e}^b the unit director for each beam and $\mathbf{e}^{b\perp}$ the transverse unit vector. $M^{O(b)\varepsilon}$ and $M^{E(b)\varepsilon}$ are the moment at the origin and end positions of a generic beam respectively. The truss under consideration is completely defined by the positions of the nodes and their connectivity. Each beam links two nodes and is oriented so that it has an origin node $O(\tilde{b})$ and an end node $E(\tilde{b})$. Although one can choose the origin node as part of the reference cell, this is not necessarily the case for the end node, which nevertheless belongs to the next neighbouring cell. Moreover, we associate to each beam a node defined as its centre denoted $C(b)$, Figure 3. Each extremity node has two displacements in the two principal directions \mathbf{e}^b (unit vector along the beam element) and $\mathbf{e}^{b\perp}$ (unit vector orthogonal to the beam element) and one rotation in the plane (i, j) (see Figure 21). The beam kinematic parameters together with the efforts and moments are shown on Figure 21.

The algebraic part of the moments $M^{O(b)\varepsilon}, M^{E(b)\varepsilon}$ has been written in (44); it is nevertheless clear that they are in fact vectors supported by the unit vector \mathbf{Y}_3 normal to the plane supported by the two basis vectors $\{\mathbf{e}^b, \mathbf{e}^{b\perp}\}$.

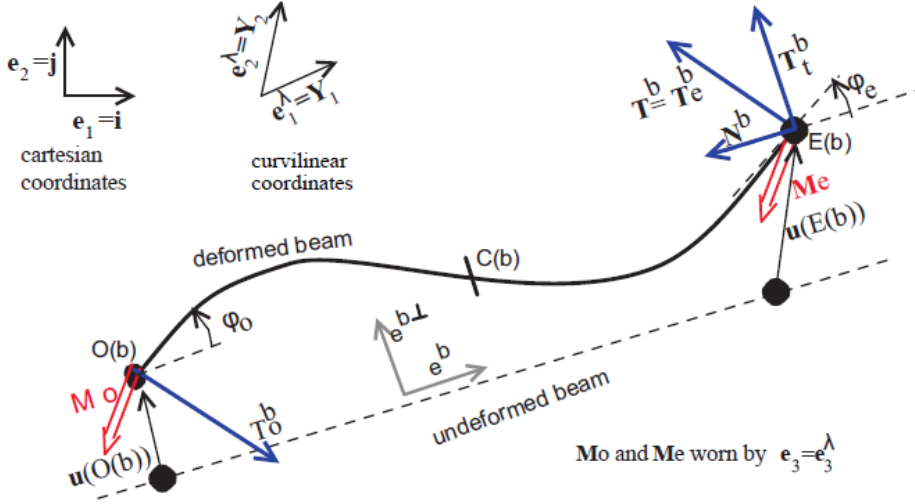


Figure 21. Kinematic and static parameters of a lattice beam.

4.2. A Survey of the Asymptotic Homogenization Technique

We give the essentials relative to the asymptotic homogenisation technique considering the micropolar framework, which is the more complete equivalent continuum, as it incorporates a microrotation in addition to the displacement as kinematic descriptors at the continuum level. The principal steps of the discrete homogenization method started by writing the equilibrium equations of the equivalent micropolar continuum in virtual power manner in order to proof the stress tensor σ and the micromoment m as internal dyadic products of the base vector within curvilinear coordinate system. Consequently, one can identify the Cauchy stress tensor and couple stress tensor respectively, written S^i and μ^i :

$$\int_{\Omega} \underbrace{(g\sigma \cdot e_{\lambda}^i)}_{S^i} \cdot \frac{\partial \mathbf{v}}{\partial \lambda_i} d\lambda + \int_{\Omega} \underbrace{(gm \cdot e_{\lambda}^i)}_{\mu^i} \cdot \frac{\partial \mathbf{w}}{\partial \lambda_i} d\lambda = 0 \quad (45)$$

In a second step, one shows anticipant forthcoming development that the discrete equilibrium takes the same form after homogenization

$$\sum_b \mathbf{T}^b \cdot \mathbf{v} + \sum_b \mathbf{M}^b \cdot \mathbf{w} = 0 \Rightarrow \int_{\Omega} \mathbf{S}^i \cdot \frac{\partial \mathbf{v}}{\partial \lambda_i} d\lambda + \int_{\Omega} \boldsymbol{\mu}^i \cdot \frac{\partial \mathbf{w}}{\partial \lambda_i} d\lambda = 0 \quad (46)$$

In order to identify the stress tensor S^i and the couple stress tensor μ^i , the comparison of the homogenized formulation with the micropolar equilibrium is done, which leads to the elaboration of the stress and the couple stress. The reader is referred to Dos Reis and

Ganghoffer [48] for more details. One can write the translational and the moment equilibrium as follows

$$\int_{\Omega} \mathbf{S}^i \cdot \frac{\partial \mathbf{v}}{\partial \lambda^i} d\lambda = 0; \int_{\Omega} \boldsymbol{\mu}^i \cdot \frac{\partial \mathbf{w}}{\partial \lambda^i} d\lambda = 0 \quad (47)$$

The following equations involve virtual velocities (\mathbf{v}, \mathbf{w}) , respectively equivalent to the rates $(\dot{\mathbf{u}}, \dot{\boldsymbol{\phi}})$. By expressing the curvilinear gradients of the virtual velocities versus those of the

nodal positions, $\frac{\partial \mathbf{v}}{\partial \lambda_i} = \nabla_x \mathbf{v} \cdot \frac{\partial \mathbf{R}}{\partial \lambda_i}$; $\frac{\partial \mathbf{w}}{\partial \lambda_i} = \nabla_x \mathbf{w} \cdot \frac{\partial \mathbf{R}}{\partial \lambda_i}$, with \mathbf{R} the position vector of the lattice node, the two last discrete equilibrium equations can then be transformed into a continuous formulations after homogenization. Those two equations can be written as the following dyadic products of the stress and couple stress vectors with the curvilinear gradient of the position vector:

$$\boldsymbol{\sigma} = \frac{1}{g} \mathbf{S}^i \otimes \frac{\partial \mathbf{R}}{\partial \lambda^i}; \quad \mathbf{m} = \frac{1}{g} \boldsymbol{\mu}^i \otimes \frac{\partial \mathbf{R}}{\partial \lambda^i} \quad (48)$$

The vectors \mathbf{S}^i and $\boldsymbol{\mu}^i$ are next expressed according to the unit cell topology and the mechanical properties of the beam; this constitutes the homogenization of the discrete equilibrium. The equilibrium of forces writes in virtual power form and after asymptotic development, for the whole lattice as

$$\sum_{\mathbf{v}^i \in \square^2} \sum_{\mathbf{b} \in B_R} \mathbf{T}^{eb} \cdot (\mathbf{v}^e(\mathbf{O}(\mathbf{b})) - \mathbf{v}^e(\mathbf{E}(\mathbf{b}))) = 0 \quad (49)$$

with $\mathbf{v}(\cdot)$ a virtual velocity field choosing to vanish on the edges. The vector of efforts \mathbf{T}^b decomposes into a normal and a transverse contribution as (see equation (44)):

$$\mathbf{T}^b = N^b \mathbf{e}^b + T_t^b \mathbf{e}^{b\perp} \quad (50)$$

In a second step, we write the discrete equilibrium of moments as the virtual power developed by all lattice nodes

$$\sum_{\mathbf{v}^i \in \square^2} \sum_{\mathbf{b} \in B_R} \mathbf{M}^{O(b)} \cdot \mathbf{w}(\mathbf{O}(\mathbf{b})) + \mathbf{M}^{E(b)} \cdot \mathbf{w}(\mathbf{E}(\mathbf{b})) = 0 \quad (51)$$

In this work, the vector director \mathbf{e}^b and the beam lengths remain fixed under the adopted small strain framework.

The asymptotic development of the virtual velocity and rotation rate are next expressed. For any virtual velocity field $\mathbf{v}^\varepsilon(\lambda)$, a Taylor series development leads to

$$\mathbf{v}^\varepsilon(\mathbf{O}(\mathbf{b})) - \mathbf{v}^\varepsilon(\mathbf{E}(\mathbf{b})) = \mathbf{v}^\varepsilon(\lambda^\varepsilon + \varepsilon \delta^{\text{ib}}) - \mathbf{v}^\varepsilon(\lambda^\varepsilon) = \varepsilon \frac{\partial \mathbf{v}(\lambda^\varepsilon)}{\partial \lambda^i} \delta^{\text{ib}} \quad (52)$$

The rotation rate field is similarly expanded taking into account the central node of the beam

$$\begin{aligned} \mathbf{w}^{\mathbf{C}(\mathbf{b})\varepsilon} &= \frac{1}{2} \left(\mathbf{w}^{\mathbf{O}(\mathbf{b})\varepsilon} + \mathbf{w}^{\mathbf{E}(\mathbf{b})\varepsilon} \right) \\ \mathbf{w}^{\mathbf{O}(\mathbf{b})\varepsilon}(\lambda) &= \mathbf{w}(\lambda); \quad \mathbf{w}^{\mathbf{E}(\mathbf{b})\varepsilon}(\lambda + \varepsilon \delta^i) = \mathbf{w}(\lambda) + \varepsilon \frac{\partial \mathbf{w}(\lambda)}{\partial \lambda^i} \delta^i \end{aligned} \quad (53)$$

In the forthcoming development, and for simplicity raison, a rectangular section of the beam will be considered with a constant thickness $e=1$ and a width t^b . Thus, we can simplify the expression of the bending and stretching stiffness by defining the slenderness parameter $\eta = \frac{t^b}{l^b}$. Inserting equation (44) and (52) into (49) and considering the aforementioned simplifications, leads after development and ordering following the successive power of ε to

$$\begin{aligned} &\sum_{\mathbf{v}^i \in \square^2} \sum_{\mathbf{b} \in \mathbf{B}_R} \left[\varepsilon^2 \left(E_s \eta (\Delta \mathbf{U}_1 \cdot \mathbf{e}^b) \mathbf{e}^b + \left(E_s \eta^3 \Delta \mathbf{U}_1 \cdot \mathbf{e}^{b\perp} - \frac{1}{2} E_s \eta^3 l^b (\phi_0^{\mathbf{O}_R(\mathbf{b})} + \phi_0^{\mathbf{E}_R(\mathbf{b})}) \right) \mathbf{e}^{b\perp} \right) \cdot \frac{\partial \mathbf{v}(\lambda^\varepsilon)}{\partial \lambda^i} \delta^{\text{ib}} \right] + \\ &\sum_{\mathbf{v}^i \in \square^2} \sum_{\mathbf{b} \in \mathbf{B}_R} \left[\varepsilon^3 \left(E_s \eta (\Delta \mathbf{U}_2 \cdot \mathbf{e}^b) \mathbf{e}^b + \left(E_s \eta^3 \Delta \mathbf{U}_2 \cdot \mathbf{e}^{b\perp} - \frac{1}{2} E_s \eta^3 l^b (\phi_1^{\mathbf{O}_R(\mathbf{b})} + \phi_1^{\mathbf{E}_R(\mathbf{b})} + \frac{\partial \phi_0}{\partial \lambda^i} \delta^{\text{ib}}) \right) \mathbf{e}^{b\perp} \right) \cdot \frac{\partial \mathbf{v}(\lambda^\varepsilon)}{\partial \lambda^i} \delta^{\text{ib}} \right] = 0 \end{aligned} \quad (54)$$

with $\Delta \mathbf{U}_1$ the first order difference of displacement obtained after asymptotic development vs. ε as

$$\Delta \mathbf{U}^{\text{b}\varepsilon} = \varepsilon \underbrace{\left(\mathbf{u}_1^{\mathbf{E}_R(\mathbf{b})} - \mathbf{u}_1^{\mathbf{O}_R(\mathbf{b})} + \frac{\partial \mathbf{u}_0}{\partial \lambda^i} \delta^{\text{ib}} \right)}_{\Delta \mathbf{U}_1} + \varepsilon^2 \underbrace{\left(\mathbf{u}_2^{\mathbf{E}_R(\mathbf{b})} - \mathbf{u}_2^{\mathbf{O}_R(\mathbf{b})} \right)}_{\Delta \mathbf{U}_2}$$

The previous discrete equation can be transformed into a continuum Riemann integral on the domain Ω when the small parameter ε tends to zero. For any enough regular function g , the quantity $\varepsilon^2 \sum_{\mathbf{v}^i \in \square^2} g(\varepsilon \mathbf{v}^i)$ can be interpreted as the Riemann sum of an integral over Ω ,

$\int_{\Omega} g(\lambda) d\lambda$, when $\varepsilon \rightarrow 0$. Thus, the equation (54) becomes after homogenization

$$\int_{\Omega} \mathbf{S}^i \cdot \frac{\partial \mathbf{v}}{\partial \lambda^i} d\lambda = 0$$

The stress vector splits into a first and a second order contribution, viz $\mathbf{S}^i = \mathbf{S}_1^i + \varepsilon \mathbf{S}_2^i$, with

$$\begin{aligned} \mathbf{S}_1^i &= \sum_{b \in B_R} \left(E_s \eta (\Delta \mathbf{U}_1 \cdot \mathbf{e}^b) \mathbf{e}^b + \left(E_s \eta^3 \Delta \mathbf{U}_1 \cdot \mathbf{e}^{b\perp} - \frac{1}{2} E_s \eta^3 l^b \left(\phi_0^{O_R(b)} + \phi_0^{E_R(b)} \right) \right) \mathbf{e}^{b\perp} \right) \delta^{ib} \\ \mathbf{S}_2^i &= \sum_{b \in B_R} \left(E_s \eta (\Delta \mathbf{U}_2 \cdot \mathbf{e}^b) \mathbf{e}^b + \left(E_s \eta^3 \Delta \mathbf{U}_2 \cdot \mathbf{e}^{b\perp} - \frac{1}{2} E_s \eta^3 l^b \left(\phi_1^{O_R(b)} + \phi_1^{E_R(b)} + \frac{\partial \phi_0}{\partial \lambda^i} \delta^{ib} \right) \right) \mathbf{e}^{b\perp} \right) \delta^{ib} \end{aligned} \quad (55)$$

The stress tensor is then reconstructed from \mathbf{S}^i as expressed in (48).

Similarly to the previous development, the equilibrium moment (51) is homogenized, inserting the asymptotic expansion (53) of the virtual rotation rate. After simplifications and passing to the limit $\varepsilon \rightarrow 0$ in the discrete sums, the moment equilibrium equation can be written as

$$\int_{\Omega} \boldsymbol{\mu}^i \cdot \frac{\partial \mathbf{w}}{\partial \lambda^i} d\lambda = 0 \quad (56)$$

with the couple stress vector (supported by \mathbf{Y}_3) identified on two orders $\boldsymbol{\mu}^i = \boldsymbol{\mu}_1^i + \varepsilon \boldsymbol{\mu}_2^i$, as

$$\boldsymbol{\mu}_1^i = \sum_{b \in B_R} E_s \eta^3 \frac{(l^b)^2}{12} \left(\phi_0^{E_R(b)} - \phi_0^{O_R(b)} \right) \delta^{ib} \mathbf{Y}_3; \quad \boldsymbol{\mu}_2^i = \sum_{b \in B_R} E_s \eta^3 \frac{(l^b)^2}{12} \left(\phi_1^{E_R(b)} - \phi_1^{O_R(b)} + \frac{\partial \phi_0}{\partial \lambda^i} \delta^{ib} \right) \delta^{ib} \mathbf{Y}_3 \quad (57)$$

This allows the reconstruction of the couple stress tensor \mathbf{m} from the vector $\boldsymbol{\mu}^i$ according to (48). Using the symmetries properties of the lattice, we can simplify the expressions of the vectors of effort \mathbf{S}^i and the couple stress $\boldsymbol{\mu}^i$. The general form of the constitutive equations of linear micropolar elasticity relating the stress and couple stress tensors to the strain and curvature tensors writes in matrix format as

$$\begin{aligned} \{\boldsymbol{\sigma}\} &= [\mathbf{A}]\{\boldsymbol{\varepsilon}\} + [\mathbf{B}]\{\boldsymbol{\kappa}\} \\ \{\mathbf{m}\} &= [\mathbf{C}]\{\boldsymbol{\varepsilon}\} + [\mathbf{D}]\{\boldsymbol{\kappa}\} \end{aligned}$$

This form of the continuum constitutive law can presently be identified from the expressions of the homogenised stress and couple stress tensors

$$\boldsymbol{\sigma} = \underbrace{\frac{1}{g} \mathbf{S}_1^i \otimes \frac{\partial \mathbf{R}}{\partial \lambda^i}}_{[\mathbf{A}]\{\boldsymbol{\varepsilon}\}} + \underbrace{\frac{1}{g} \varepsilon \mathbf{S}_2^i \otimes \frac{\partial \mathbf{R}}{\partial \lambda^i}}_{[\mathbf{B}]\{\boldsymbol{\kappa}\}}, \quad \mathbf{m} = \underbrace{\frac{1}{g} \boldsymbol{\mu}_1^i \otimes \frac{\partial \mathbf{R}}{\partial \lambda^i}}_{[\mathbf{C}]\{\boldsymbol{\varepsilon}\}} + \underbrace{\frac{1}{g} \varepsilon \boldsymbol{\mu}_2^i \otimes \frac{\partial \mathbf{R}}{\partial \lambda^i}}_{[\mathbf{D}]\{\boldsymbol{\kappa}\}} \quad (58)$$

We restrict ourselves to centro-symmetric medium in this study: this leads to the vanishing of the coupling matrices $[\mathbf{B}]$ and $[\mathbf{C}]$ as shown in (Trovalusci and Masiani [49]). The expression of the stress and couple stress vectors substantially simplifies as follows

$$\mathbf{S}^i = \mathbf{S}_1^i = \sum_{b \in B_R} \left(E_s \eta (\Delta \mathbf{U}_1 \cdot \mathbf{e}^b) \mathbf{e}^b + \left(E_s \eta^3 \Delta \mathbf{U}_1 \cdot \mathbf{e}^{b\perp} - \frac{1}{2} E_s \eta^3 l_0^b (\phi_0^{O_R(b)} + \phi_0^{E_R(b)}) \right) \mathbf{e}^{b\perp} \right) \delta^{ib} = \sum_{b \in B_R} \left(N_1^b \mathbf{e}^b + T_{11}^b \mathbf{e}^{b\perp} \right) \delta^{ib} \quad (59)$$

$$\boldsymbol{\mu}^i = \boldsymbol{\mu}_2^i = \sum_{b \in B_R} E_s \eta^3 \frac{(l^b)^2}{12} \left(\phi_1^{E_R(b)} - \phi_1^{O_R(b)} + \frac{\partial \phi_0}{\partial \lambda^i} \delta^{ib} \right) \delta^{ib} \mathbf{Y}_3 = \sum_{b \in B_R} \frac{1}{2} \left(M_2^{E_R(b)} - M_2^{O_R(b)} \right) \delta^{ib} \mathbf{Y}_3$$

with N_1^b , T_{11}^b and M_2^n , respectively, the first and second order according the power of ε homogenized continuous functions. Equations (54 bis) and (59) involve the unknown displacements u_1^n, u_2^n and rotations ϕ_0^n, ϕ_1^n , which are solved for (localization problem over the unit cell) using the equilibrium equations (49), (50) and (4.9).

4.3. Application to Plain Weave Fabric

The unit cell of fabric is pictured in a planar section (Figure 22); the geometry of the warp is discretized as a succession of straight segments, while the section of the transverse weft is modelled with a hexagonal shape, connected to the summit of the warp by vertical beams, endowed with specific properties, representing an equivalent transverse compressibility of both yarns.

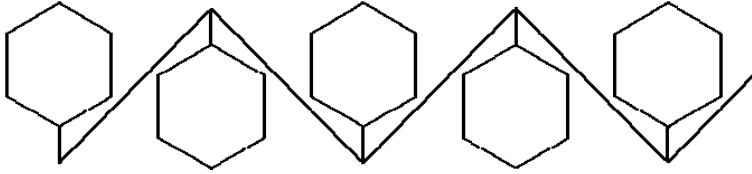


Figure 22. Repetitive unit cell in a section of the fabric armour.

The tensile behavior of fabric is simulated assuming inextensible yarns (this is a valid assumption in the first stage of the response, as shown in section 2), by increasing the angle between successive warp segments. The equivalent modulus is evaluated using a perturbative approach of the previously exposed homogenization technique, according to the following steps:

- I. Fix a reference network defined by one or a few geometrical descriptors; the equivalent moduli are known for this chosen reference configuration.
- II. Perturb the network geometry by allowing a small variation of the geometrical parameters chosen as descriptors, in a displacement control approach. Evaluate then the new updated equivalent moduli for this new geometry.
- III. Elaborate strain measures from the geometrical parameters and record the variation of the moduli versus those strain measures. The functional dependence of the updated moduli is deemed representative of the non-linear mechanical behavior of the membrane.

The equivalent tensile modulus increases in a monotonous manner versus the unit cell longitudinal strain measure (Figure 23); note that the tensile rigidity of the contact beam linking the warp and weft has a weak influence on the overall simulated response. Applications to more complex textile armours are envisaged.

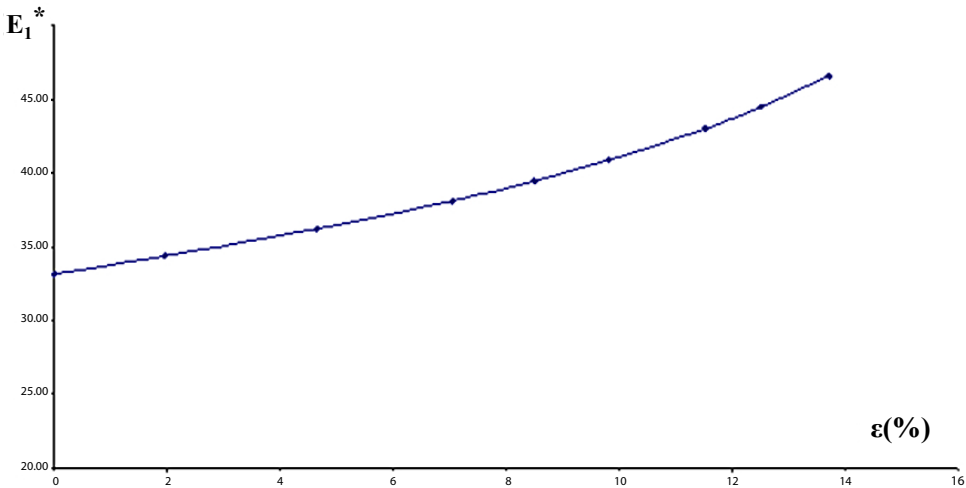


Figure 23. Evolution of the equivalent tensile modulus obtained by discrete homogenization.

Homogenization techniques prove a powerful technique to access the equivalent mechanical properties of discrete media such as textiles [50], and can be applied to a wide variety of discrete structures, including biological networks [51].

CONCLUDING REMARKS

Micromechanical analyses of textiles realize a good compromise between the computational cost and accuracy; they provide a quantitative assessment of the impact of the geometry of the armour within the unit cell and of the mechanical properties of the yarns on the macroscopic behavior. Their main advantage lies in a straightforward incorporation of the interactions between yarns, in comparison to the complexity and computational cost of finite element analyses. Nevertheless, as the yarn itself is a structure made of multiple filaments, it is clear that the physical mechanisms responsible for yarn-to-yarn contact and friction are very complex (strongly non linear, prone to instabilities) and occur at a finer scale of a few microns. Due to this heterogeneous structure, the setting up of a rheological model of a complex yarn accounting for the couplings between various modes of deformation remains a challenging task. The biggest challenge for the future of textile modeling is the understanding of the physics specific to those structures, starting from the microscopic scale and its transcription in terms of multiscale models.

ACKNOWLEDGMENTS

Amongst the co-workers who did directly or indirectly contribute to the methods and results exposed in this chapter, the contributions from M. Assidi, F. Dos Reis, B. Ben Boubaker are especially acknowledged.

REFERENCES

- [1] Gasser, A., Boisse, P. and Hanklar, S. (2000). Analysis of the mechanical behaviour of dry fabric reinforcements. 3D simulations versus biaxial tests. *Computational Material Science*, 17, 1: 7-2.
- [2] Kawabata, S., Niwa, M. and Kawai, H. (1973). *Journal of the Textile Institute*, 64: N° 21.
- [3] Kawabata, S. (1989). Nonlinear mechanics of woven and knitted materials, in: T.W. Chou, F.K. Ko (Eds.), *Textile Structural Composites*, 3, Elsevier, Amsterdam, 67-116.
- [4] Potluri P, Parlak I, Ramgulam R. and Sagar, T.V. (2006). Analysis of tow deformations in textile preforms subjected to forming forces. *Composites Science and Technology*, 66: 297–305.
- [5] Liu W, Drzal L, Mohanty A. and Misra M. (2007). Influence of processing methods and fiber length on physical properties of kenaf fiber reinforced soy based biocomposites. *Composites Part B*, 38: 352–9.
- [6] Mattsson, D., Joffe, R. and Varna, J. (2007). Methodology for characterization of internal structure parameters governing performance in NCF composites. *Composites Part B*. 38: 44–57.
- [7] Hamila, N. and Boisse, P. (2008). Simulations of textile composite reinforcement draping using a new semi-discrete three node finite element. *Composite Part B*, 39: 999-1010.
- [8] Peng X. and Cao, J. (2005). A continuum mechanics-based non-orthogonal constitutive model for woven composite fabrics. *Composites Part A*, 36: 859–74.
- [9] Boisse, P., Borr, M., Buet, K. and Cherouat, A. (1997). *Composites Part B* 28B : 453-464.
- [10] Boisse, P., Daniel, J.L., Gasser, A., Hivet, G. and Soulat, D. (2001). *Mech. Ind.*, 1, 303-311.
- [11] Boisse P, Gasser A, Hagege B. and Billoet J.L. (2005). Analysis of the mechanical behaviour of woven fibrous material using virtual tests at the unit cell level. *International journal of Materials Sciences*, 40, 5955–62.
- [12] Akkerman R and Lamers E.A.D. (2007). Constitutive modelling for composite forming. In: *Composite Forming Technologies*. Woodhead Publishing. 22–45, Chapter 2.
- [13] Durville D. (2005). Numerical simulation of entangled materials mechanical properties. *Journal of Materials Science*. 40: 5941–8.
- [14] Sze, K.Y. and Liu, X.H. (2005). A new skeletal model for fabric drapes. *International Journal of Mechanics and Materials in Design*, 2: 225–43.
- [15] Duhovic M. and Bhattacharyya D. (2006). Simulating the deformation mechanisms of knitted fabric composites. *Composites A*, 37(11): 1897–915.

-
- [16] King, M.J., Jearanaisilawong, P. and Socrate, S. (2005). A continuum constitutive model for the mechanical behavior of woven fabrics. *Int. J. Solids Struct.*, 42: 3867-3896.
 - [17] Nadler, B., Papadopoulos, P. and Steigmann, D.J. (2006). Multiscale constitutive modeling and numerical simulation of fabric material. *Int. J. Solids Struct.*, 43: 206-221.
 - [18] Weisseberg, K. (1949). The use of a trellis model in the mechanics of homogeneous materials. *Journal of Textile Industry*, 40: T89-110.
 - [19] Chadwick, G.E., Shorter, S.A. and Weisseberg, K. (1949). A trellis model for the application and study of simple pulls in textile materials. *J. Text. Inst.*, 40: 111-160.
 - [20] Kilby, W.F., 1963. Planar stress-strain relationships in woven fabrics. *J. Text. Inst.*, T9-27.
 - [21] Hearle, J.W.S., Grosberg, P. and Backer, S. (1969). Structural Mechanics of Fibers, Yarns and Fabrics. Vol. 1. New York, Wiley Interscience.
 - [22] De Jong, S. and Postle, R. (1977). An energy analysis of woven-fabric mechanics by means of optimal-control theory, Part I: tensile properties. *J. Textile Inst.*, 68(11): 350-61.
 - [23] Grosberg, P. and Kedia, S. (1966). The mechanical properties of woven fabrics. Part I: the initial load-extension modulus of woven fabrics. *Text. Res. J.*, 36: 71-79.
 - [24] Shanahan, W.J., Lloyd, D.W. and Hearle, J.W.S. (1978). Characterizing the elastic behavior of textile fabrics in complex deformations. *Text. Res. J.*, 48 (15): 495.
 - [25] Anandjiwala, R.D. and Leaf, G.A.V. (1991a). Large-scale extension and recovery of plain woven fabrics. Part I: theoretical. *Text. Res. J.*, 61: 619-634.
 - [26] Anandjiwala, R.D. and Leaf, G.A.V. (1991b). Large-scale extension and recovery of plain woven fabrics. Part II: experimental and discussion. *Text. Res. J.*, 61: 743-755.
 - [27] Ben Boubaker, B. Haussy, H. and Ganghoffer, J.F. (2007a). Consideration of the yarn-yarn interactions in meso/macro discrete model of fabric. Part I: single yarn behaviour. *Mech. Res. Comm.* 34, Issue 4: 359-370.
 - [28] Ben Boubaker, B. Haussy, H. and Ganghoffer, J.F. (2007b). Consideration of the yarn-yarn interactions in meso/macro discrete model of fabric. Part II: Woven fabric under uniaxial and biaxial extension. *Mech. Res. Comm.* 34, Issue 4: 371-379.
 - [29] Ben Boubaker, B., Haussy, H. and Ganghoffer, J.F. (2007c). Discrete woven structure model: yarn-on-yarn friction, *Comptes Rendus Mécanique*, 335, Issue 3: 150-158.
 - [30] Ben Boubaker, B., Haussy, H. and Ganghoffer, J.F. (2007d). Discrete models of woven structures considering yarn interactions. *Multidiscipline Modeling in Materials and Structures*. 3, N°2 : 141-173.
 - [31] Timoshenko, S. (1947). Théorie de la Stabilité Elastique, BERANGER, Paris and Liège.
 - [32] Sun, H., Pan, N. and Postle, R. (2005). On the Poisson's ratios of a woven fabric. *Composite Structures*, 68: 505-510.
 - [33] Gupta, B. S, and El Moghahzy, Y. E. (1991). Friction in Fibrous Materials. *Textile Res. J.*, 61, N°. 9: 547-555.
 - [34] Howell, H. G. (1953). The Laws of Static Friction. *Textile Res. J.*: 589-591.
 - [35] H.G. Howell, J. Mazur (1953). The laws of static friction. *J. Textile Inst.*, 23: 589-591.
 - [36] Lincoln B. (1952). Frictional and elastic properties of high polymeric materials. *British J. Applied Phys.*, 3: 260. doi: 10.1088/0508-3443/3/8/304.

-
- [37] Lindberg J. and Gralen N., "Measurement of Friction Between Single Fibers. II. Frictional Properties of Wool Fibers Measured by the Fiber-Twist Method. *Text. Res. J.* May 1948, 287-301.
 - [38] Olofsson, B. and Gralen, N. (1950). Measurement of Friction Between Single Fibers. V. Frictional Properties of Viscose Rayon Staple Fibers. *Text. Res. J.*, 20, no. 7: 467-80.
 - [39] Arczewski, K. and Pietrucha, J. (1993). Mathematical modelling of complex mechanical systems, Volume 1: Discrete models. Ellis Horwood.
 - [40] Sanchez-Hubert, J. and Sanchez-Palencia, E. (1992). Introduction aux méthodes asymptotiques et à l'homogénéisation - Application à la mécanique des milieux continus.
 - [41] Panasenko, G.P. (1983). Averaging processes in framework structures, *Mat. Sb. (N.S.)*, 122(164):2(10):220–231.
 - [42] Bakhvalov N.S. and Panasenko G.P. (1989). Homogenization: Averaging processes in periodic media. English transl. Kluwer, Dordrecht/Boston/London.
 - [43] Warren, W.E. and Byskov, E. (2002). Three-fold symmetry restrictions on two-dimensional micropolar materials. *European Journal of Mechanics A/Solids*, 21: 779-792.
 - [44] Mourad, A. Caillerie, D. and Raoult, A. (2003). A nonlinearly elastic homogenized constitutive law for the myocardium. *Computational Fluid and Solid Mechanics*: 1779-1781.
 - [45] Pradel, F., Sab, K. (1998). Cosserat modelling of elastic periodic lattice structures. *C. R. Acad. Sci. Paris*, t. 326, Serie II b, :p. 699-704.
 - [46] Tollenaere, H. and Caillerie, D. (1998). Continuous modeling of lattice structures by homogenization. *Advances in Engineering Software*, 29, Issues 7-9: 699-705.
 - [47] Caillerie, D., Mourad, A. and Raoult, A. (2006). Discrete Homogenization in Graphene Sheet Modeling. *Journal of Elasticity*, 84: 33-68.
 - [48] Dos Reis, F. and Ganghoffer, J.F. (2010). Discrete homogenization of architected materials: implementation of the method in a simulation tool for the systematic prediction of their effective elastic properties. *Technische Mechanik*, 30, 1-3: 85 – 109.
 - [49] Trovalusci, P. and Masiani, R. (1999). Material symmetries of micropolar continua equivalent to lattices. *International Journal of Solids and Structures*, 36, Issue 14, 1: 2091-2108.
 - [50] Assidi, M., Ben Boubaker, B. and Ganghoffer, J.F. (2011). Equivalent properties of monolayer fabric from mesoscopic modelling strategies. *Int. J. Solids Struct.* In print.
 - [51] Assidi, M., Dos Reis, F. and Ganghoffer, J.F. (2011). Equivalent mechanical properties of biological membranes from lattice homogenization. *Journal of the Mechanical Behavior of Biomedical Materials*. In print.

Chapter 11

A NOVEL METHOD FOR ANTIMICROBIAL FINISHING OF TEXTILE WITH INORGANIC NANOPARTICLES BY SONOCHEMISTRY

*Ilana Perelshtein, Nina Perkas, Guy Applerot and
Aharon Gedanken**

Department of Chemistry, Bar-Ilan University, Ramat-Gan 52900, Israel

ABSTRACT

This chapter reviews the research that has been done for the functionalization of textile with inorganic nanoparticles (Ag, CuO, ZnO, MgO, Al₂O₃) by sonochemical method. Sonochemistry is one of the most efficient techniques for creation of nanosized compounds. Ultrasonic waves in the frequency range of 20 kHz - 1 MHz are the driving force for chemical reaction. The sonochemical reaction is dependent on the acoustic cavitation, which means creation, growing and explosion collapse of a bubble in the solution. Extreme conditions (temperature >5000 K, pressure >1000 atm and cooling rates >10⁹ K/sec) are developed when this bubble collapses, and that is the reason of break and formation of chemical bonds.

The nanoparticles have been deposited on the surface of various fabrics (cotton, nylon, polyester) using ultrasound irradiation. This process produces a uniform coating of nanoparticles on surfaces with different functional groups. The coating can be performed by an in-situ process where the nanoparticles are formed and immediately thrown to the surface of the fabrics. This approach was used for Ag, ZnO and CuO. In addition, the sonochemical process can be used as a "throwing stone" technique, namely, previously synthesized nanoparticles will be placed in the sonication bath and sonicated in the presence of the fabric. This process has been shown with MgO and Al₂O₃ nanoparticles. The nanoparticles are thrown to the surface by the microjets and strongly adhered to the textile. This phenomenon was explained because of the local melting of the substrate due to the high rate and temperature of nanoparticles thrown at the solid surface by sonochemical microjets.

* E-mail: gedanken@mail.biu.ac.il

The antibacterial activities of the nanocoated fabric composites were tested against Gram negative and Gram positive cultures. A significant bactericidal effect, even with low concentration of the nanoparticles, less than 1wt%, was demonstrated.

1. NANOPARTICLES

Nanoparticles are of great scientific interest as they are effectively a bridge between bulk materials and atomic or molecular structures. A bulk material should have constant physical properties regardless of its size, but at the nano-scale ('nano' derives from the Greek word "nanos", which means dwarf or extremely small. It can be used as a prefix for any unit to mean a billionth (10^{-9}) of that unit) this is often not the case. Size-dependent properties are observed such as quantum confinement in semiconductor particles, surface plasmon resonance in some metal particles and superparamagnetism in magnetic materials.

The properties of materials change as their size approaches the nanoscale and as the percentage of atoms at the surface of a material becomes significant. For bulk materials larger than one micrometer the percentage of atoms at the surface is relative to the total number of atoms of the material. The interesting and sometimes unexpected properties of nanoparticles are partly due to the aspects of the surface of the material dominating the properties in lieu of the bulk properties.

Nanoparticles exhibit a number of special properties relative to bulk material. For example, the bending of bulk copper (wire, ribbon, etc.) occurs with movement of copper atoms/clusters at about the 50 nm scale. Copper nanoparticles smaller than 50 nm are considered super hard materials that do not exhibit the same malleability and ductility as bulk copper. The change in properties is not always desirable. Ferroelectric materials smaller than 10 nm can switch their magnetisation direction using room temperature thermal energy, thus making them useless for memory storage. Suspensions of nanoparticles in the solution are possible because the interaction of the particle surface with the solvent is strong enough to overcome differences in density, which usually result in a material either sinking or floating in a liquid. Nanoparticles often have unexpected visible properties because they are small enough to confine their electrons and produce quantum effects. For example, gold nanoparticles appear deep red to black in solution.

Nanoparticles have a very high surface area to volume ratio. This provides a tremendous driving force for diffusion, especially at elevated temperatures. Sintering can take place at lower temperatures, over shorter time scales than for larger particles. This theoretically does not affect the density of the final product, though flow difficulties and the tendency of nanoparticles to agglomerate complicates matters. The large surface area to volume ratio also reduces the incipient melting temperature of nanoparticles.

At the small end of the size range, nanoparticles are often referred to as clusters. Nanospheres, nanorods, and nanocups are just a few of the shapes that have been grown. Metal, dielectric, and semiconductor nanoparticles have been formed, as well as hybrid structures (e.g., core-shell nanoparticles). Nanoparticles made of semiconducting material may also be labeled quantum dots if they are small enough (typically sub. 10 nm). It is called size quantization and arises because the size of a nanoparticle is comparable to the "de Broglie wavelength" of its charge carriers (*i.e.* electrons and holes). Due to the spatial confinement of the charge carriers, the edge of the valence and conduction bands split into

discrete, quantized, electronic levels. These electronic levels are similar to those in atoms and molecules. The spacing of the electronic levels and the bandgap increases with decreasing particle size. This is because the electron hole pairs are now much closer together and the Coulombic interaction between them can no longer be neglected giving an overall higher kinetic energy. Such nanoscale particles are used in biomedical applications as drug carriers or imaging agents.

1.1. Nanosynthesis

To date, pioneering synthetic approaches have been invaluable in establishing the new field of scientific endeavor, i.e. that of nanostructured materials. There are a few widely known methods for producing nanomaterials, e.g. sol-gel, aerogels, aerosol spray pyrolysis, inverse micelle methods, reactive evaporation of metals, zintl salts, inert gas condensation, mechanical alloying or high-energy ball milling, plasmas synthesis, sonochemical, microwave, and electrodeposition etc. All these processes synthesize nanomaterials to varying degrees of commercially – viable quantities [1]. To date, only sol-gel synthesis is widely used since it is easy, economical, can form various homogeneous, bulk, purity nanoproducts at relatively low temperatures, and is comparatively more understood.

1.2. Classification of Nanomaterials

If we consider that the periodic table of the elements is a "puzzle" that contains a huge treasure of new materials (nanomaterials), every known substance and every material yet to be discovered will yield a new set of properties, depending on size. The thousands of substances that are solid under normal temperatures and pressures can be subdivided into metals, ceramics, semiconductors, composites, and polymers. These can be further divided into biomaterials, catalytic materials, coatings, magnetic and electronic materials [2]. All of these solid substances, with their widely variable properties, take on another subset of new properties when produced in nanoform. The possibilities are endless. Chemistry and chemists have a leadership role if this new field is to prosper. The field of nanostructured materials has evolved; many names and labels have been used. Their definitions [3] are briefly given below.

- I. Nanoparticle: A solid particle in the 1-100 nm range could be crystalline, amorphous, or an aggregate of crystallites. ii. Nanocrystal: A solid particle that is a single crystal in the nanometer size range.
- II. Nanostructured, nanoscale or nanophased material: Any solid material that has a nanometer dimension (<100 nm): three dimensions - particles; two dimensions – thin film; one dimension - thin wire.
- III. Quantum dots: A particle that exhibits a size quantization effect in at least one dimension.
- IV. Cluster: A collection of units (atoms or reactive molecules).
- V. Colloid: A stable liquid phase containing particles in the 1-100 nm range.

1.3. Application of Nanomaterials

Since nanomaterials possess unique and beneficial chemical, physical, and mechanical properties, they can be used for a wide variety of applications. These applications include [4], but are not limited, to the following: next-generation computer chips, better insulation materials, phosphors for high-definition TV, low-cost flat-panel displays, tougher and harder cutting tools, elimination of pollutants, high energy density batteries, high-power magnets, high-sensitivity sensors, longer-lasting medical implants, solar cells, self cleaning and unusual coloring in paints.

2. APPLICATION OF NANOTECHNOLOGY FOR "SMART" TEXTILES

Nanotechnology is an emerging interdisciplinary technology that has been booming in many areas during the recent decade, including materials science, mechanics, electronics, and aerospace. Its profound societal impact has been considered as the huge momentum to usher in a second industrial revolution.

The impact of nanotechnology in the textile finishing area has brought up innovative finishes as well as new application techniques. Particular attention has been paid in making chemical finishing more controllable and more thorough. Ideally, discrete molecules or nanoparticles of finishes can be brought individually to designated sites on textile materials in a specific orientation and trajectory through thermodynamic, electrostatic or other technical approaches.

“Nano functional” textiles are those designed and engineered on the nanoscale to create specific functions. These nano functions are very diverse and can be used for:

- UV protection
- Flame retardant
- Moisture management
- Antibacterial functions
- Antistatic
- Stain
- resistant

Nowadays, there are growing requirements for high quality textiles with antibacterial properties for hygienic clothing, active wear, and wound healing. The control on microorganisms extended from the hospital institutions to house holds. It is recognized that neither synthetic, nor natural fibers have resistance to bacteria and pathogenic fungi [5]. An explosive growth is expected in the wound care production. The wound care market of the US healthcare system was in excess of \$7 billion in 2007 [6]. The consumers' demands cause a significant growth in the production of the antibacterial textile. The worldwide industry reports estimate the wound care market to exceed \$ 11.8 billion by 2009 and project a yearly growth for all products (devices for wound closure such as sutures and staples, dressings, etc.) in excess of 7%. European markets have accounted for about half of the spending [7]. The

high demands encourage the intensive research and development of new methods for antimicrobial treatment of the textile fabrics and fibers. The recent achievements in the field of antibacterial textiles were briefly described in a review by Gao [8]. According to his data, the metal and metal salts are one of the major classes of antibacterial agents as well as quaternary ammonium compounds, triclosan, chitosan, chlorine-containing *N*-halamine compounds *etc.*

Nanoparticles such as metal oxides and ceramics are used in textile finishing altering surface properties and imparting textile functions. Nanosize particles have a larger surface area and higher efficiency than larger size particles. These unique properties have found a wide application in the textile industry, namely, in antibacterial treatment of textiles [9-11]. The market for textiles using nanotechnologies is predicted to climb dramatically from \$13.6 billion in 2007 to \$115 billion by 2012 [12].

Nanosilver is one of the most widely used as an effective antibacterial agent in general textiles and in wound dressing [13-15]. The antibacterial properties of silver have been known and used for centuries [16]. A unique and available source of silver has long been mineral salts. A new way for delivery of silver into the bacterial killing medium is the formation of organic-inorganic nanocomposites combining the properties of textile substrate with antibacterial activity [17, 18]. To achieve the optimum antibacterial effect of nanocomposite fibers, a high concentration of silver ions must be available in the solution. Despite the small number of silver ions released from metallic silver nanocrystals, about 30 times less than that from silver complexes (e.g., silver sulfadiazine), a more rapid microbe-killing curve has been observed with nanocrystals [19].

Different methods have been used for the deposition of silver NP on fabrics. For example, a poly(ethylene terephthalate) fabric (meadox double velour) was coated with metallic silver using a patented ion-beam-assisted deposition process developed by the Spire Corporation (Bedford, MA). *Antimicrobial fibers were produced by the implementation of nanoscaled silver particles into a solution of cellulose and N-methylmorpholine-N-oxide* [20]. Other methods were constant pressure padding, impregnation in the colloid silver solution [21], immersion of the fabric in the silver precursor solution in ethanol or propanol following the boiling procedure for reduction of silver ions [22], magnetron sputter technique [23] *etc.* Some of the methods are based on reactions in the liquid medium and require surfactants, reducing agents or templates for the synthesis of silver nanoparticles, resulting in the presence of toxic impurities in the final products. This method has some disadvantages with regard to the environment.

Nanosized particles of ZnO, CuO, MgO and Al₂O₃ possess photocatalytic ability, UV absorption, and photooxidizing capacity against chemical and biological species. In the last decade intensive research involving metal oxides NP was pushed forward focusing on the production of the textile with antibacterial, self-decontaminating and UV blocking functions [24-26]. Nylon fibers filled with ZnO nanoparticles can provide UV shielding function and reducing static electricity of nylon fiber. A composite fiber with nanoparticle of TiO₂/MgO can provide self-sterilizing function.

The nanostructured metals and inorganic oxides can be incorporated into the textile by various methods. Among the techniques are: high energy γ -radiation and thermal treatment assisted impregnation [27, 28]. In these works, cotton and cotton/polyester fabrics were immersed in antimicrobial formulation based on zinc oxide (ZnO), Impron MTP (binder), and Setamol WS (dispersing agent) and subjected to fixation by γ -radiation techniques. The effect

of this treatment on the growth of bacteria (*Bacillus subtilis*) was estimated. On the basis of microbial detection, it was found that the ZnO formulation causes a net reduction in the bacterial cells, which amounts to 78 and 62% in the case of treated cotton and cotton/polyester fabrics, respectively. However, it was found that the treatment with ZnO formulation caused a reduction in the thermal stability of the fabrics as indicated by thermogravimetric analysis.

One of the widely used techniques for coating the textile substrates is the combination of sol-gel synthetic procedure with the "pad-dry-cure" method [29, 30]. The synthesis process usually involved two main steps. For instance, the hexagonally ordered ZnO nanorod arrays might be grown onto fiber substrates in the same way as zero-gel ZnO [31]. The growing seeds were formed by coating ZnO nanosol using dip-coating, dip pad-curing or spraying methods by natural solvent evaporation. In order to stabilize the precursor solution, triethenamine, with the same molar ratio as zinc acetate was added to form a transparent homogeneous solution. The TiO₂ and TiO₂/SiO₂ nanocomposites prepared by the low temperature sol-gel synthesis were coated onto cotton fabrics by a dip-pad-dry-cure process [32, 33]. The sol-gel immobilization and controlled release of various bioactive liquids from modified silica coatings were investigated [34]. The deposition of nano-ZnO onto cotton fabric was performed by padding of the textile in the colloid formulation of zinc oxide-soluble starch nanocomposite to impart the material the antibacterial and UV-protection functions [35].

Very recently some new publications appeared for deposition of "in situ" formed metal oxide NP on the textile fabrics. A superhydrophobic ZnO nanorod array film on cotton substrate was fabricated via a wet chemical route and subsequent modification with a layer of *n*-dodecyltrimethoxysilane [36]. ZnO nanoparticles were in-situ grown on SiO₂ coated cotton fabric through hydrothermal method. After water treatment at 100°C or higher, the cotton fabric was covered with approximately 24 nm diameter needle-shaped ZnO nanorods, which had an excellent UV-blocking property [37]. ZnO particles were prepared by wet chemical method using zinc nitrate and sodium hydroxide as precursors and solubilized starch as stabilizing agent [38]. These NP were impregnated onto cotton fabrics by the "pad-dry-cure" method using acrylic binder.

Copper is one of a relatively small group of metallic elements, which are essential to human health. These elements, along with amino and fatty acids and vitamins, are required for normal metabolic processes. Copper is considered safe to humans as demonstrated by the widespread and prolonged use of copper intrauterine devices (IUDs) [39]. At the same time, there are not many publications on production and application of CuO-textile composite with the exception of Gabbay *et al.* [40, 41]. The copper containing fibers of cotton and polyester prepared by these authors demonstrated significant antifungal and antimicrobial properties. They inserted the preliminary synthesized copper oxide powder into the polymer fibers during the master-batch stage, and impregnated in the cotton by a multi-phase soaking procedure including treatment in formaldehyde.

To summarize, most of the methods employed for the deposition of nanostructured materials on the textile are based on the multistage procedure including the preliminary synthesis of the NP and the application of some templating agents for their anchoring to the substrates. This approach is rather complicated and can result in the release of some toxic compounds into the wastes. Therefore, the current research is focused on the fabrication of *in situ* coated fabrics via ultrasound irradiation. The sonochemical method prevents the use of

toxic binders and makes the coating procedure shorter, effective, and environmentally friendly.

3. A SONOCHEMICAL METHOD FOR THE SYNTHESIS OF NANOSTRUCTURED MATERIALS AND THEIR ADHERENCE TO SOLID SUBSTRATES

Sonochemistry has been proven as an efficient method for the synthesis of various kinds of nanoparticles [42, 43]. In this chapter, we will describe the unique properties that make ultrasound irradiation an excellent technique for the adherence of nanoparticles (NPs) to a large variety of substrates. Ultrasonic chemistry is a research field where waves in the frequency range of 20 kHz - 1 MHz are the driving force for chemical reactions. The reaction is dependent on the acoustic cavitation, i.e., the formation, growth, and implosive collapse of the bubbles in the solution. Extreme conditions (temperature >5000 K, pressure >1000 atm and cooling rates $>10^9$ K/sec) are developed when the bubble collapses, resulting in chemical reactions [44].

A theoretical explanation as to how 20 kHz ultrasonic radiation can break chemical bonds is given in several works [45, 46]. The question arising is how such a bubble can be formed, considering the fact that the forces required to separate water molecules to a distance of two Van-der-Waals radii would require a power of 10^5 W/cm. On the other hand, it is well known that in a sonication bath with a power of 0.3 W/cm, water is readily converted into hydrogen peroxide. The explanation of this phenomenon is based on the existence of unseen particles or gas bubbles that decrease the intermolecular forces, enabling the creation of the void. The experimental evidence for the importance of unseen particles in sonochemistry is that when the solution undergoes ultrafiltration before the application of ultrasonic power, there is no chemical reaction and chemical bonds are not ruptured. The second stage is the growth of the bubble, which occurs through the diffusion of the solvent and/or solute vapours into the volume of the bubble. The third stage is the collapse of the bubble, which occurs when the size of the bubble reaches its maximum value. From here on we will adopt the hot spot mechanism, one of the theories that explain why upon the collapse of a bubble, chemical bonds are broken. This theory claims that very high temperatures (5,000-25,000 K) [47] are obtained upon the collapse of the bubble. Since this collapse occurs in less than a nanosecond, very high cooling rates in excess of 10^{11} K/sec are obtained. These extreme conditions develop when the bubble's collapse causes the chemical reactions to occur. The high cooling rate prevents the crystallization of the products. This is the reason why amorphous nanoparticles are formed when volatile precursors are used and the gas phase reaction is predominant. However, from this explanation the reason for the formation of nanostructured material is not clear. Our explanation for the creation of nanoproducts is that the fast kinetics does not permit the growth of the nuclei, and in each collapsing bubble a few nucleation centres are formed whose growth is limited by the short collapse. If the precursor is a non-volatile compound, the reaction occurs in a liquid phase in a 200 nm ring surrounding the collapsing bubble [46]. The products are sometimes nano-amorphous particles and in other cases nanocrystalline, depending on the temperature in the ring region where the reaction

takes place. In fact, when the sonochemical reactions were used for the synthesis of inorganic products, nanomaterials were obtained.

Over the last 15 years we have reported on the ultrasound-assisted synthesis of about 100 nanomaterials and on the deposition/insertion of nanoparticles on/into ceramic and polymer bodies (see previous reviews) [43, 48]. Other review articles on similar topics have also been published [42, 49, 50].

In the current chapter we report on the development of a sonochemical technique for the doping of the produced nanoparticles into the textile materials. We benefit from a well-known property of the acoustic bubbles, i.e. when they collapse near a solid surface, microjets and shock waves are among the after effects of the bubbles' collapse. These microjets throw the newly-formed nanoparticles onto the textile at a very high speed, causing them to be embedded in the fabric.

Typically, the doping procedure is as follows. The textile substrate is introduced into the sonication cell containing the precursor solution, leading to the fabrication of nanoparticles under ultrasonic waves. The ultrasonic irradiation passes through the sonication slurry under an inert or oxidizing atmosphere for a specified time. This synthetic route is a single-step, effective procedure. The excellent adherence of the nanoparticles to the substrate is reflected, for example, in the lack of leaching of the nanoparticles from the substrate surfaces after many washing cycles. Another way of embedding the nanoparticles into the solids is the sonochemical irradiation of preliminary synthesized or commercial nanoparticles in the presence of the corresponding materials. This technique is called the “throwing stones” mechanism, because the ultrasonic waves cause the throwing of the already existing nanoparticles onto the fabric. In both cases the nanoparticles strongly adhere to the substrate and the coating/incorporation is stable.

This chapter will include the research on the sonochemical embedding of inorganic nanoparticles such as metal and of metal oxides, as well as sonochemically-prepared protein microspheres, into textiles, thus imparting them with the antibacterial activity. The advantages of sonochemistry as a one-step, environmentally-friendly method for the deposition of nanoparticles on different kinds of textiles such as cotton, wool, nylon, polyester, etc., will be demonstrated.

4. EMBEDDING OF NANOSILVER INTO DIFFERENT KINDS OF TEXTILES BY THE SONOCHEMICAL TECHNIQUES

We have demonstrated that sonochemistry is an effective method for the incorporation of silver nanoparticles into ceramic and polymer supports [51-53]. The Ag/nylon yarns were produced by an ultrasound-assisted technique [54]. The work was based on coating nylon chips (2-3 mm) with nanosilver. The silver–nylon nanocomposite was used as a master batch for the production of nylon yarns by a melting and spinning process. Antibacterial tests of the final silver–nylon fabrics showed very promising results. Our further aim was to avoid the fiber production stage and to develop a direct method for coating natural and synthetic fabrics with silver NPs.

The growing interest in the safety of natural yarns with antimicrobial properties stimulated an extensive search for new technologies for the modification of wool fibers [55,

56]. Different types of antimicrobial treatments were studied for the protection of wool products from the damage caused by pathogenic microorganisms. Among these treatments, there are the coating of wool with resin-bonded copper-8-quinolinolate, chlorinated phenol and its derivatives, sodium dichloroisocyanurate, quaternary ammonium compounds, metal ions, and organic tin compounds in finishing processes [57, 58]. A biotemplate redox technique was employed for the deposition of silver nanoclusters on another type of a natural fiber, silk fibroin [59].

We demonstrated the deposition of small silver nanoparticles on woolen fabrics by the coating of neat fibers with silver nanoparticles via ultrasound irradiation without the use of any special binding or templating agent [60]. The process is performed in a one-step, sonochemical procedure with the slurry-containing wool fibers, silver nitrate, and ammonia in an aqueous medium. The produced silver-coated wool fabrics maintained the high flexibility and elasticity typical of wool. The study of silver-coated wool fiber by physical and chemical methods demonstrated the presence of highly-dispersed silver nanoparticles (~5 nm) incorporated into the natural wool. Some of the silver particles were aggregated into clusters and located mainly at the fiber crossovers. X-ray photoelectron spectroscopy (XPS) studies demonstrated that silver nanoparticles are attached to the keratin fibers as a result of the interaction between both Ag^{1+} or Ag clusters and sulfur. The origin of these sulfur atoms is most likely the partial disconnection of the S-S bond in the keratin fibers. The stability of the coating is satisfactory: even after several cycles of thermal treatment and simulating laundering, no change in the silver concentration was detected.

Later on, we applied the sonochemical method for the incorporation of silver NPs into different fabrics (nylon, polyester and cotton) [61] to investigate the interaction between the fiber surface and the metallic silver as a result of the sonochemical irradiation. The options that can result from the sonication are the formation of a chemical bond between the silver and the functional groups of the substrate, and/or the physical adsorption of the silver nanoparticles on the surface of the fabric. We performed experiments on three types of fabrics, nylon, polyester and cotton. These fabrics differ in their functional groups, which are amide, ester and alcohol, respectively. All these fabrics were exposed to the same reaction conditions, i.e. reagent concentration, reaction time, temperature, and sonication power. The silver content in the fabrics was determined by volumetric titration and the results are presented in Table 1.

Table 1. Silver content in the fabrics

Type of fabric	Silver content (% wt)
Nylon	1.4
Polyester	1.2
Cotton	1.1

The amount of silver deposited on the three different fabrics is almost the same. This indicates that the amount of deposited silver is independent of the nature of the substrate. This also indicates that most probably the mechanism of coating by ultrasound irradiation is not involved in the creation of new bonds between the silver and the functional groups of the substrate. In addition, Raman spectroscopy has been applied for the characterization of a

silver-cotton composite and to provide knowledge about the structure, bonding nature, and changes in the material's state upon its sonochemical reaction. The spectrum of Ag-coated cotton closely resembles the spectrum of amorphous diamond-like carbon, and can be resolved into the G (graphitic) and D (disordered) Raman bands near 1600 and 1350 cm^{-1} , respectively, which are not found in the Raman spectrum of the pristine cotton. Obviously, here we observe the effect of surface-enhanced Raman scattering (SERS), typical for silver nanoparticles deposited on pure carbon and widely used for the characterization of the carbon containing material. Similar Raman spectra are observed for other fabrics (nylon, polyester) after silver deposition by ultrasound irradiation. From this data we can assume that the temperature and speed of the silver nanoparticles thrown to the fabric surface by sonochemical micro jets are high enough to cause melting and carbonization of the fibers at the place of their contact with the silver nuclei. These "hot spots" become the center of fusion of the silver nanoparticles and the fabric's substrate. As a result, the silver nanoparticles strongly adhered to the fabric surface, regardless of its properties, and the coated material stays on the fabric for at least 20 washing cycles without a reduction in the silver content.

The mechanism of Ag formation during ultrasound irradiation is as follows:

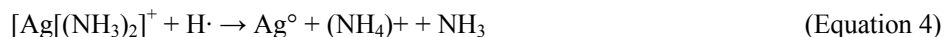
Ultrasound irradiation of aqueous solution generates free radicals:



The free radical of hydrogen from equation 1 reacts with silver ions:



Namely, the reduction of silver can occur by ultrasound irradiation without addition of any other reagents. However, it was found that addition of ammonia expedites the formation of Ag^0 . Ammonia works as a catalyst of the reduction process, and formation of silver takes place through the ammonium complex $[\text{Ag}(\text{NH}_3)_2]^+$.



The optimal molar ratio of ammonia to silver was found to be 2:1, and this ratio is matching for the formation of a $[\text{Ag}(\text{NH}_3)_2]^+$ complex.

The Ag nanoparticles produced by this reaction are thrown at the surface of the fabric by the sonochemical microjets resulting from the collapse of the sonochemical bubble. The coating process involves the in-situ generation of silver nanoparticles and their subsequent deposition on fabrics in a one-step reaction via ultrasound irradiation.

The XRD result indicates that sonochemically-deposited Ag nanoparticles on a cotton fabric are crystalline in nature, and the diffraction peaks match a face-centered cubic (fcc) phase of Ag (PDF: 4-783). The particles size estimated using the Debye-Scherrer (DS) equation was 80 nm.

The morphology of the fibers before and after deposition of Ag nanoparticles was studied by HRSEM (Figure 1). After the sonication, the homogeneous deposition of silver nanoparticles on the cotton yarn is obtained. The calculated average size of the silver nanoparticles deposited on the surface of the cotton fibers is 80 nm, and it matches well with the XRD results.

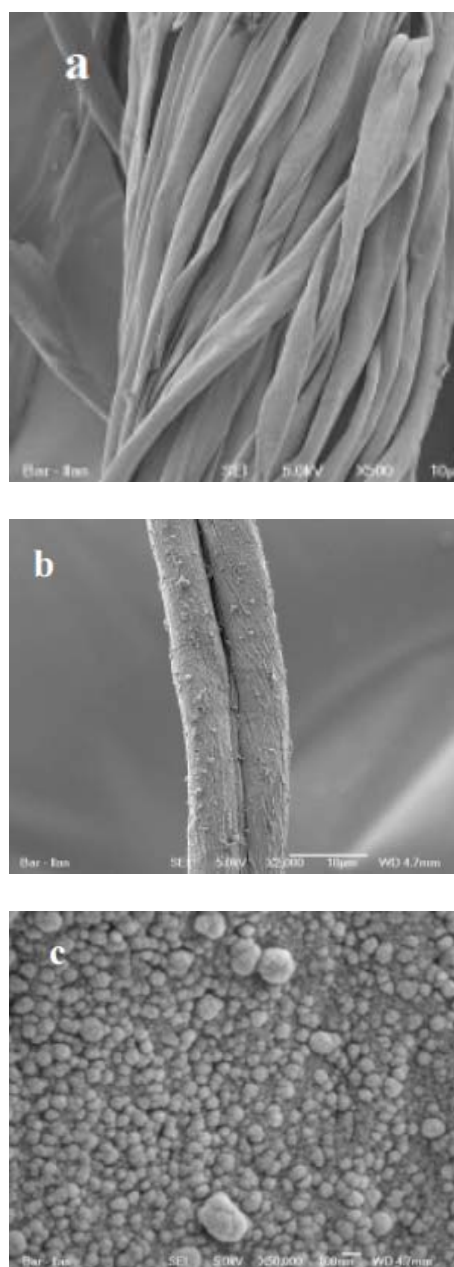


Figure 1. (a) HR-SEM images of pristine fibers, (b) fabrics coated with Ag nanoparticles at a low magnification (x20K), (c) fiber coated with Ag nanoparticles at a high magnification (x50K).

Rutherford backscattering spectroscopy (RBS) based on elastic collisions between ions the atomic nucleus, and particle-induced X-ray emission (PIXE) techniques based on ionization of the inner shells of atoms, were used to obtain the additional information. Scanning micro-PIXE–RBS analysis, where the ion probe is focused on a micrometer level and scanned over the sample, allows us to obtain the lateral distribution of elements. For an Ag thickness layer, it was found that whatever the region, an Ag coating layer was present, but some variations in the Ag thickness of approximately 30% were observed. Some traces of Ag (3–4 at.%) were detected locally in the fiber as deep as several hundred nanometers (Figure 2).

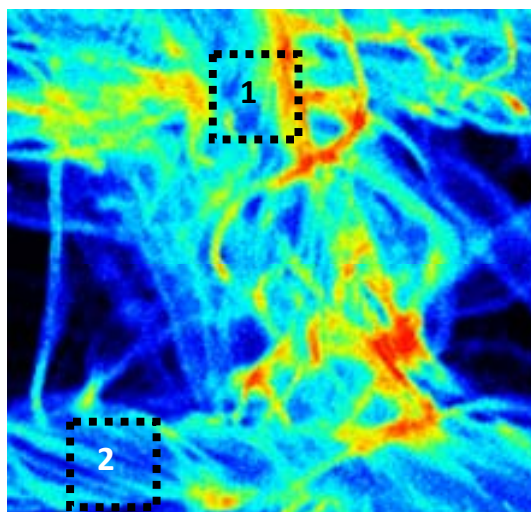


Figure 2. Distribution of Ag on the textile fibre in the selected regions 1 and 2 from PIXE cartography, 1 mm² area.

The tensile mechanical properties of a common impregnated fabric were studied on a universal testing machine, Zwick 1445. The silver-coated samples showed a rather more brittle behavior compared to the pristine fabric. Ultimately, the tensile force for the coated sample was ~10% less than that of the non-impregnated one. The observed change in the mechanical behavior of the yarn is in a range that is acceptable for standard cotton fabrics. According to this result, we conclude that the sonochemical treatment of the fabric did not cause any significant damage to the structure of the yarn.

The antibacterial activity of these Ag–fabric composites against *E. coli* (gram-negative) and *St. aureus* (gram-positive) cultures was estimated and traced at very low concentrations of coating. Cultures of both kinds of bacteria were eradicated completely after 1 h of treatment with the 6 wt% coated fabric, and after approximately 1.5 h with the sample containing 1 wt% Ag. The antimicrobial activity of the silver-coated cotton fabric containing 1 and 6 wt% of silver corresponds to the maximum possible Ag⁺ in the saline solution, as 130 and 780 ppm, respectively. However, the diffusion of silver ions from the deposited silver nanoclusters to the saline is very slow, and only a small part of the total amount of silver can participate in antibacterial activity. Nevertheless, even the total possible amount of silver is less than the minimum inhibitory concentration (MIC) in a solution that is commonly used in

commercial preparations, 800 - 1000 ppm [62, 63]. Thus, the excellent killing effect of bacteria was demonstrated.

The coating is stable on the fabric for at least 20 washing cycles in hot (40°C) water, and so the adherence of the silver NPs to the fabrics by a sonochemical method is very strong without the addition of any binding agents.

5. ULTRASOUND ASSISTED DEPOSITION OF METAL NANOOXIDES ON TEXTILES AND THEIR ANTIBACTERIAL PROPERTIES

5.1. Synthesis and Deposition of ZnO

The antibacterial activity of ZnO depends on the particle size: decreasing the particle size leads to an increase in the antibacterial activity [64]. We have developed a simple new method for the preparation of cotton bandages with antibacterial properties by immobilizing ZnO NPs into the fabrics via ultrasound irradiation [65]. The aim of this work was to obtain a homogeneous coating of small ZnO NPs on the fabric with a narrow size distribution and to reach a minimal effective ZnO concentration, which will still demonstrate antibacterial activity. This process involves *in situ* generation of ZnO under ultrasound irradiation and its deposition on fabrics in a one-step reaction.

We have found that the yield of product and particle size are strongly dependent on the rate of inter particles collisions and on the concentration of the reagents during the sonochemical synthesis. That is why the experimental parameters such as time and concentration of the precursor were selected as important factors for the optimization of the sonochemical reaction.

XRD demonstrated that the ZnO NPs on the coated bandage are crystalline, and the diffraction patterns matched the hexagonal phase of the ZnO structure. No peaks characteristic of any impurities were detected. The particle size estimated by the Debye-Scherrer equation is 30 nm.

The morphology of the coated bandage before and after the deposition of ZnO NPs studied by HR SEM is presented in Figure 2. Figure 2a demonstrates the smooth texture of the pristine cotton bandage. After sonication, the fibers of bandage are homogeneously coated with NPs (Figure 3b). The inset image in Figure 3b was taken at a higher magnification in order to obtain the particles' size distribution. The distribution of the particles is quite narrow, and primary particles are in a very low nanometric range (~30 nm) that matches well with the XRD results. The selected-area HR SEM image studied with the elemental dot-mapping technique is shown in Figure 3c. The distribution of zinc and oxygen in the mapped area is presented in parts d and e of Figure 3, respectively. These images verify a homogeneous coating of the fibers with ZnO NPs.

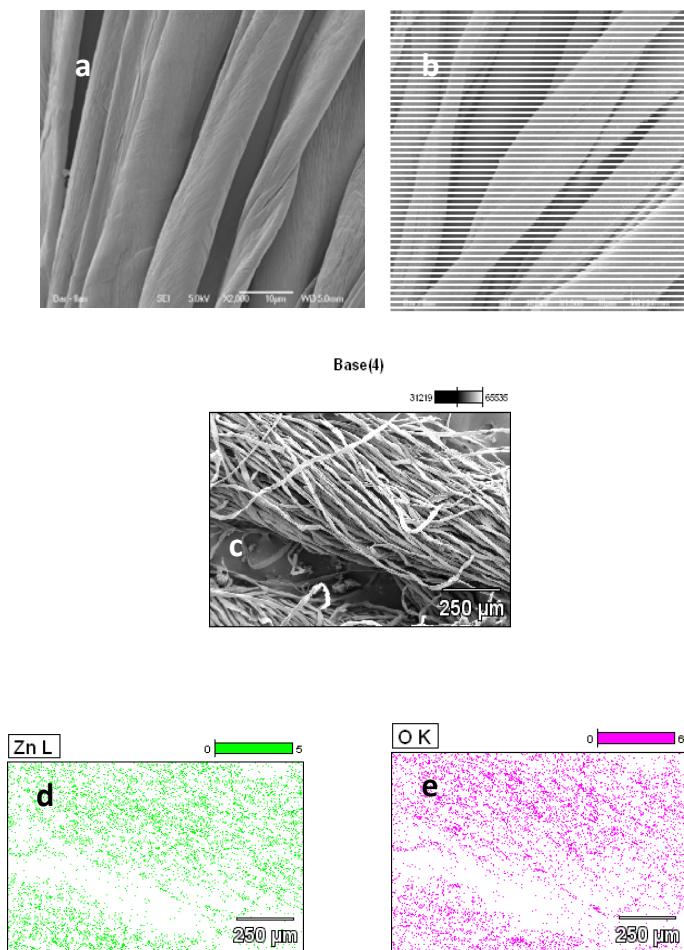
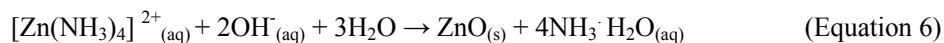
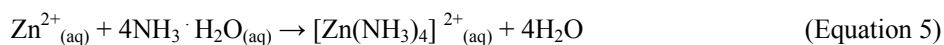


Figure 3. HRSEM images of (a) pristine bandages (magnification x2K), (b) bandage coated with ZnO NPs (magnification x1500; the inset shows a magnified image (x50K) of the ZnO NPs on the fabric), (c) selected image for X-ray dot mapping, (d) X-ray dot mapping for zinc, (e) X-ray dot mapping for oxygen.

We considered the coating mechanism as follows: it involves the *in situ* generation of ZnO NP and their subsequent deposition on fabrics in a one-step reaction via ultrasound irradiation. The zinc oxide is formed during the irradiation according to the following reactions:



Ammonia works as catalyst for the hydrolysis process, and the formation of zinc oxide takes place through the ammonium complex $[\text{Zn}(\text{NH}_3)_4]^{2+}$. The ZnO NPs produced by this reaction are thrown at the surface of the bandages by the sonochemical microjets resulting from the collapse of sonochemical bubbles.

The sonochemical irradiation of a liquid causes two primary effects, namely, cavitation (bubble formation, growth, and collapse) and heating. When the microscopic cavitation bubbles collapse near the surface of the solid substrate, they generate powerful shock waves and microjets that cause effective stirring/mixing of the adjusted layer of liquid. The after effects of the cavitation are several hundred times greater in heterogeneous systems than in homogeneous system. In our case, the ultrasonic waves promote the fast migration of the newly formed zinc oxide nanoparticles to the fabric's surface. This fact might cause a local melting of the fibers at the contact sites, which may be the reason why the particles strongly adhere to the fabric. To further support the coating mechanism, the FTIR spectra of the pristine cotton bandage and the ZnO coated bandage have been recorded. Both spectra show the characteristic bands of cellulose. The recorded spectrum of ZnO-coated bandages revealed an additional sharp single band at 464 cm^{-1} , which is attributed to a Zn-O vibrational band. The coating assisted by ultrasound irradiation is a physical phenomenon that occurs regardless of the surface properties, especially when there are chemical interacting groups on the surface.

In this aspect, the question rises if the sonication doesn't damage the fabric substrate. Thus, the tensile mechanical properties of a cotton impregnated fabric were studied on a universal testing machine, Zwick 1445. The tensile force for the zinc oxide-coated sample observed to be ~11% less than that of the pristine. The observed changes in the mechanical behavior of the yarn are in a range that is acceptable for standard cotton fabrics. According to this result, we conclude that the sonochemical treatment of the bandage doesn't cause any significant change in the structure of the yarns (Figure 4).

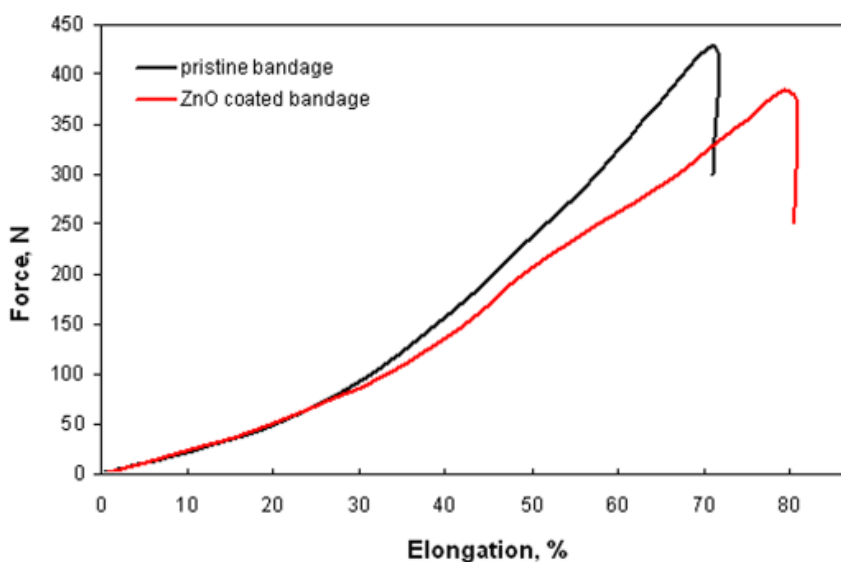


Figure 4. Mechanical properties of the cotton bandage before and after the deposition.

One of the factors influencing the commercial exploitation of the antibacterial fabrics is the release of NPs into the surrounding environment. In light of a recent paper that found that silver NP of 10 to 500 nm in diameter leach from sock textile, we attempted to find leached

ZnO NP in the washing solution. We have carried out the leaching experiments in 0.9% NaCl (pH~7) solution for 96 hours, checking the presence of nanoparticles/ions in the solution after each 24 hours.

Figure 5 presents the change of percentage of remained ZnO on fabric during the time. After 96 h, 30% of the initial concentration of Zn^{2+} have been found in the solution. The reason for presence of Zn^{2+} in the washing solution can be explained by the constant of solubility (K_{sp}) of the material that estimated to be $\sim 10^{-10}$.

DLS and TEM studies did not reveal the presence of any nanoparticle in the washing solution after 96 hours. That means that sonochemically deposited ZnO nanoparticles are strongly anchored to the textile substrate.

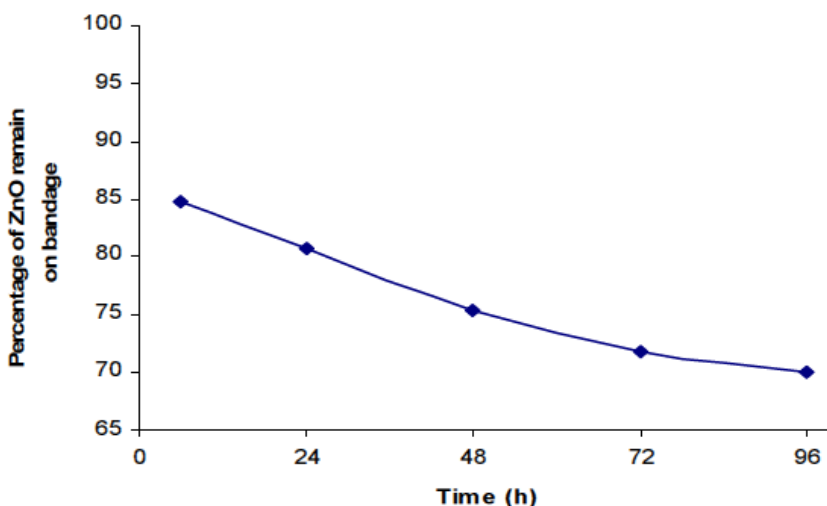


Figure 5. Change of percentage of remaining ZnO on bandages.

ZnO-coated bandages were taken one step further – for sterilization. 8 samples have been prepared, coated with ZnO nanoparticles, in two concentrations: 0.8% and 1.65% (%wt). The samples were tested by 4 different sterilization techniques: (1) gamma, (2) damp heat at 134°C, (3) steam at 121°C, and (4) Ethylene Oxide. After sterilization the samples were characterized for the quantity of ZnO coating, the morphology of the NP, and for their antibacterial activity. Table 1 summarizes the quantity results before and after sterilization. It can be seen that there is no significant change in the amount of coating after sterilization.

The morphology of the coating after sterilization was tested by SEM (Figure 6). All 8 samples were tested, and Figure 2 presents only 2 of the obtained results (a) sterilized by EO, and (b) sterilized by steam at 121°C. No significant damage such as aggregation of nanoparticles was observed after exposing of the ZnO-coated bandages for different types of sterilization.

The results indicate that the above-mentioned sterilization techniques don't influence the quantity and the morphology of the sonochemical coating. The nanoparticles strongly adhered to the fabric surface and remain stable after exposing to extreme conditions.

Table 1. Content of ZnO before/after sterilization

Sample number	Average content of ZnO before sterilization	Average content of ZnO after sterilization
1-1	0.80	0.81
1-2		
1-3		
1-4		
2-1	1.65	1.60
2-2		
2-3		
2-4		

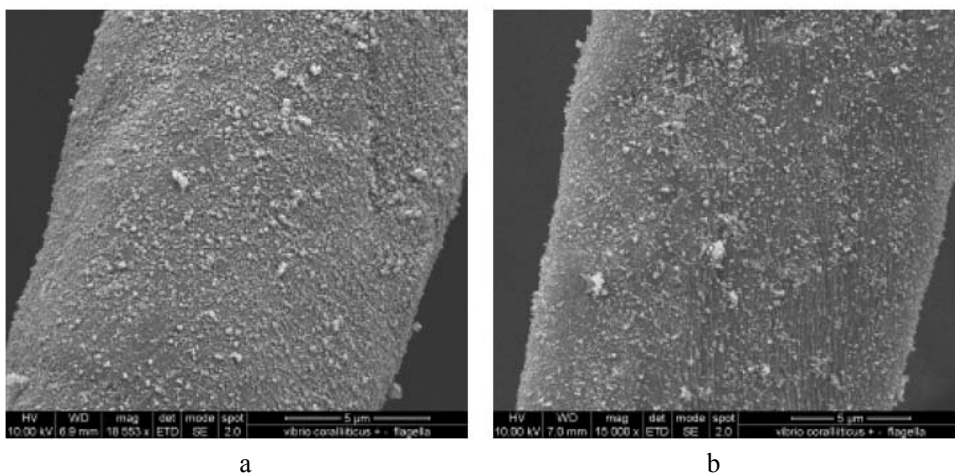


Figure 6. SEM image of (a) cotton bandage sterilized by EO, (b) cotton bandage sterilized by steam at 121°C.

The mechanism of the antibacterial activity of the metal nanooxides is poorly understood, and is still controversial. Suggested mechanisms in the literature include the role of reactive oxygen species (ROS) generated on the surface of the particles, ion release, membrane dysfunction, and nanoparticle internalization [66-68]. The generation of ROS is derived from the highly reactive nature of defect sites (such as oxygen vacancies) on a wet metal oxide surface.

Sawai *et al.* [69, 70] demonstrated that ROS concentration increased with the ZnO content of the slurries. Following the same paradigm, Applerot *et al.* [71], in an innovative study using electron spin resonance (ESR) coupled with the spin trapping probe technique, monitored ROS, namely, hydroxyl radicals produced in water suspensions of ZnO NPs. These findings showed that amount of hydroxyl radicals was closely related to the size of the ZnO particles, with smaller sizes having greater amounts of $\bullet\text{OH}$ on the basis of the equivalent ZnO mass content. These results were correlated with the increase in the antibacterial effect

of the small NPs. Thus, the small size and large specific surface area endow them with high chemical reactivity and intrinsic toxicity. Interestingly, combining gram-negative bacterium *E. coli* and ZnO NPs suspensions immediately enhanced the generation of $\bullet\text{OH}$ for up to an average of 142% (Figure 7).

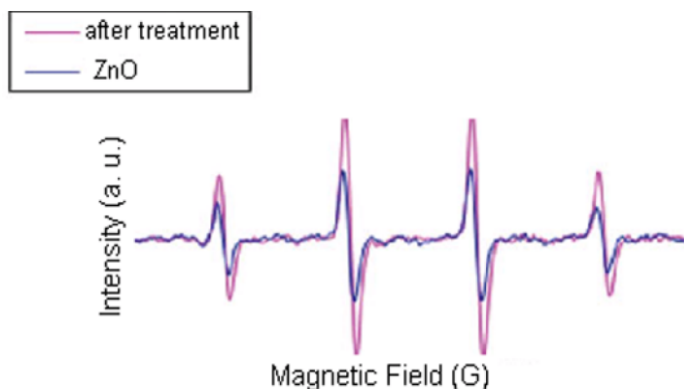


Figure 7. ESR spectra demonstrating changes in hydroxyl radical concentrations upon antibacterial treatment of *E. coli* with a water suspension of ZnO.

The antibacterial activity of the sonochemically-coated cotton fabrics [65] determined with 0.75 wt% ZnO against the gram-negative bacterium *E. coli* and the gram-positive bacterium *S. aureus* is shown in Table 2. The treatment for 1 h with the coated cotton leads to the complete inhibition of *E. coli* growth. Regarding *S. aureus*, a 100% reduction in viability was reached after 3 h, while after 1 h of treatment a reduction of 60% could be seen.

Table 2. Antibacterial activity test of ZnO-coated cotton*

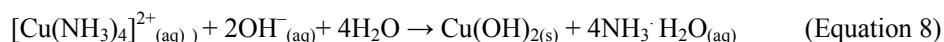
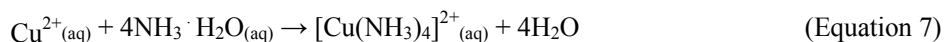
<i>E. coli</i>						
Sample	Duration of treatment					
	1h			2h		
	CFU (ml ⁻¹)	N/N ₀	viability reduction (%)	CFU (ml ⁻¹)	N/N ₀	viability reduction (%)
Pristine fabric	1.02·10 ⁻⁷	0.98	0.98	1.34·10 ⁻⁷	1.28	-28.23
No fabric	1.17·10 ⁻⁷	1.14	-28.57	1.23·10 ⁻⁷	1.35	-35.16
0.75wt%ZnO on fabric	1.71·10 ⁻⁷	1.58·10 ⁻³	99.84	0	0.9·10 ⁻⁸	100
<i>S. aureus</i>						
Sample	Duration of treatment					
	1h			3h		
	CFU (ml ⁻¹)	N/N ₀	viability reduction (%)	CFU (ml ⁻¹)	N/N ₀	viability reduction (%)
Pristine fabric	0.7·10 ⁻⁷	0.71	20.46	0.99·10 ⁻⁷	1.125	-12.5
No fabric	0.98·10 ⁻⁷	1.10	-10.11	0.67·10 ⁻⁷	0.75	24.72
0.75wt%ZnO on fabric	3.9·10 ⁻⁶	0.34	66.4	7.6·10 ⁻³	6.55·10 ⁻⁴	99.93

*The viable bacteria were monitored by counting the number of colony-forming units (CFU); N/N₀: survival fraction.

Zinc is an essential micronutrient for prokaryotic organisms. However, at super physiological levels, Zn^{2+} inhibits the growth of many bacteria [72]. According to our leaching experiment on the ZnO-embedded fabric with 0.9 wt% NaCl, the concentration of Zn^{2+} in solution corresponds to $36.7 \mu\text{M l}^{-1}$ [65]. Compared to the minimum inhibitory concentration reported in the literature of $4\text{--}8 \text{ mM l}^{-1}$ [73], the amount of zinc ions released from fabrics in our work is lower by at least a factor of 2. Therefore, we assume that the Zn^{2+} have a minor influence on the antibacterial activity. The major components responsible for the bactericidal effect are the ZnO nanoparticles. Although ZnO nanoparticles were not found in the solution, they can generate some species of oxyradicals as it was reported earlier [69, 74].

5.2. Synthesis and Deposition of CuO Nanoparticles

We extended the sonochemical approach for the deposition of CuO NPs on the textile fabrics [75], and, as in the case with ZnO NPs, the formation of copper oxide takes place through the ammonium complex. Copper ions react with a solution of ammonia to form a deep blue solution containing $[\text{Cu}(\text{NH}_3)_4]^{2+}$ complex ions. This complex is hydrolyzed and crystalline CuO NPs are obtained. The CuO NPs produced by these reactions are thrown at the surface of the fabric by sonochemical microjets and are deposited on the surface of the substrate.



The morphology of the fibers' surface area before and after the deposition of copper oxide was studied by XRD and HR SEM. The XRD revealed the monoclinic structure of CuO nanocrystals. The difference between pristine and coated cotton fabric is clearly demonstrated in Figure 8. The insert image in Figure 8b at higher magnification shows that the primary particles are in a very low nanometric range ($\sim 10\text{--}20 \text{ nm}$).

While Cu^{+2} is considered an environmentally-safe ion, a much more important and serious issue is the leaching of CuO NPs. DLS and TEM studies of the washing solution after treatment of the CuO-coated fabrics in 0.9 wt% NaCl didn't reveal the presence of any nanoparticles. This means that the sonochemically-deposited CuO NPs are strongly anchored to the textile substrate, probably due to the local melting of the fibers at the contact sites. Similar results were obtained for the coating of various types of textiles, such as nylon, polyester, and composite types of textiles with CuO NPs.

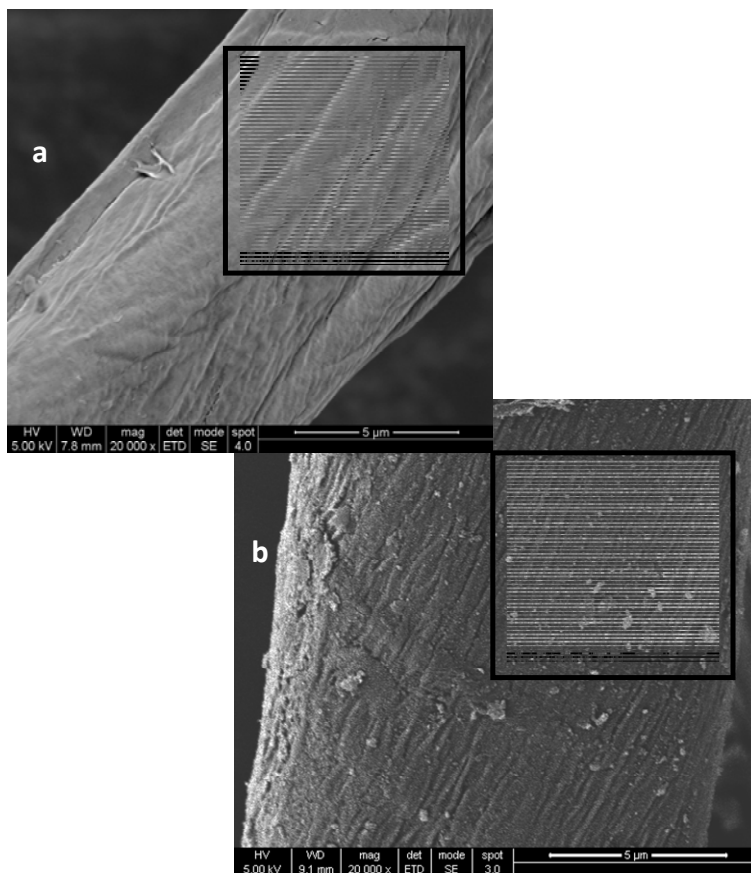


Figure 8. HR-SEM images of cotton fibers: a – pristine cotton; b – cotton coated with CuO NPs (magnification $\times 20000$, inset images - magnification $\times 100000$).

The antimicrobial activity of the cotton bandages coated with CuO *via* ultrasonic irradiation was tested against the *E. coli* and the *S. aureus*. Detailed investigations showed that after 1 h the growth of both strains was completely inhibited. One of the factors influencing the antibacterial activity of the developed coating is the release of the active phase into the surrounding medium, namely copper ions or/and copper oxide NPs. The examination of the leaching of the copper ions indicated that only a very low amount (namely $\sim 1.3\%$) of the deposited copper was removed by washing with a 0.9 wt% NaCl solution that corresponds to a concentration of Cu^{2+} 0.15 ppm. The slight solubility of copper oxide can be explained by the very low K_{sp} of CuO, which dictates that the very small concentration of Cu^{2+} appears in the solution. In order to examine the influence of copper ions on the antibacterial effect, a control antibacterial test was performed using a supernatant with the same concentration of Cu^{2+} instead of the coated cotton. After incubation for 24 h at 37 °C, no reduction in *E. coli* after 2 h was observed (Figure 9).

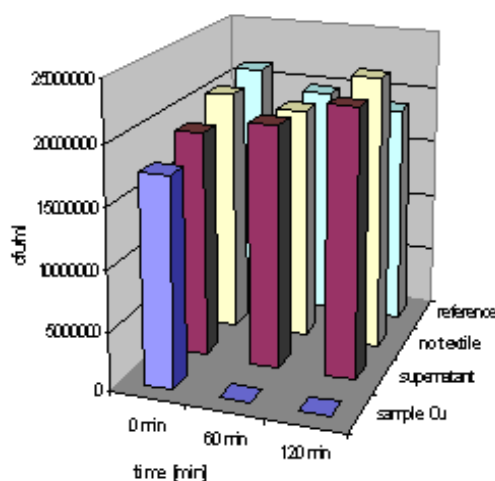


Figure 9. Antibacterial test of CuO-coated cotton against *E. coli*.

This result indicates that the Cu^{2+} ions have no influence on the antibacterial activity. Thus, the antibacterial effect can be attributed to the copper oxide NPs. Although CuO nanoparticles were not found in the solution, they can generate some active species that are responsible for damaging of the bacteria's cells. These active species were detected in ESR studies conducted with and without the bacteria present in the ESR tube.

5.3. Deposition of MgO and Al_2O_3 Nanoparticles

MgO is well known to have strong antibacterial activity [76, 77]. Different methods have been reported on the synthesis of magnesium oxide NPs, such as the controlled speed of formation following the heating procedure [76], microwave-assisted synthesis [78], formation of MgO from aqueous droplets in a flame spray pyrolysis reactor [79], sonochemically-enhanced hydrolysis followed by supercritical drying [80] etc. However, there is nothing in the literature related to the deposition of magnesium oxide on textiles.

The deposition of magnesium oxide and aluminum oxide nanoparticles on fabrics in a one-step sonochemical reaction is impossible. The sonication of M-acetate ($\text{M} = \text{Mg}, \text{Al}$) leads to amorphous phases of corresponding M – hydroxides. Antibacterial tests towards *S. aureus* and *E. coli* show that these M-hydroxides are not active as a bactericide. Only the heating of the amorphous product up to several hundreds degrees allows the formation of crystalline nanooxides. This action is not possible when the nanoparticles are deposited on textiles, because at such temperatures the textile will be destroyed. In the current study, we apply the ultrasound irradiation as a "throwing stones" technique for deposition of commercial MgO or Al_2O_3 NP on the textile. Namely, we used commercial nanopowders of MgO (< 50 nm), and Al_2O_3 (< 50 nm) and sonicated them in the presence of the cotton fabric.

One of the aims of this research was to reach a minimal effective concentration of the deposited metal oxide nanoparticles on the fabrics, which will still demonstrate an antibacterial activity. Optimal conditions such as: reaction times, type of the solvent, amount of the reagents were found in order to obtain the high quality coating.

When the suspension of the preliminary synthesized nanoparticles and the fabric is irradiated, the microjets formed after the collapse of the acoustic bubble throw the nanoparticles as a "stones" at a high speed to the cotton yarns. The "throwing stones" mechanism for the sonochemical deposition of nanoparticles is schematically presented in (Figure 10). This use of ultrasound irradiation for coating differs from our previous reports where the nanoparticles of CuO, ZnO were formed from the precursor's solution under the ultrasound irradiation and subsequently thrown to the solid surface by the microjets. The main distinction between the one and two-stages is the measured amount of the deposited material. The anchored amount for the commercial NPs was found to be smaller by a factor of 2-3 as compared to the one-stage deposition due to the fact that not all of particles are pushed by the microjets to the fabric surface. Nevertheless, using ultrasound as a "throwing stones" technique is an efficient process especially for nanoparticles that cannot be synthesized sonochemically.

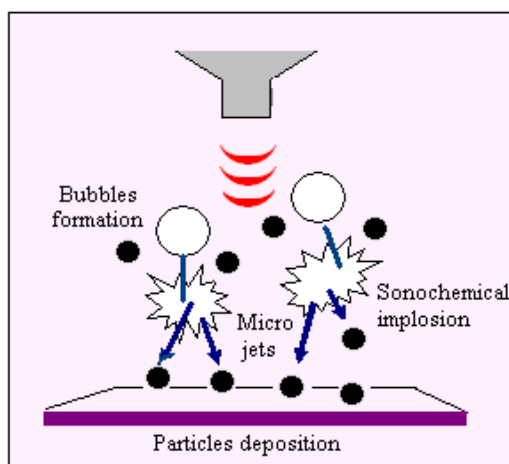


Figure 10. Scheme of the sonochemical deposition of nanoparticles on the solid substrate.

In order to study the morphology of the Al_2O_3 -coated fabric and the influence of the ultrasound on the structure of the nanoparticles, a high resolution transmission electron microscope (HRTEM) was used. The cotton fibers were embedded in the copper grid, using the epoxy embedding technique and ultramicrotome cutting.

Before the sonochemical coating reaction, the commercial aluminium oxide nanopowder was tested by XRD and a single crystalline phase of orthorhombic $\delta\text{-Al}_2\text{O}_3$ was detected (PDF No. 046-1215). After the reaction, HRTEM of the Al_2O_3 -coated fabric is depicted in Figure 11a and a uniform distribution of the particles along the fiber is observed. The red-marked particle in Figure 11a was taken under high magnification (Figure 11b), which provides further verification for the identification of the coating as Al_2O_3 . The measured distances between (131), (220) and (311) lattice planes are 0.25, 0.28 and 0.25 nm respectively, which match very well the distances reported in the literature for the orthorhombic lattice of the $\delta\text{-Al}_2\text{O}_3$ (PDF No. 046-1215). These results indicate that ultrasound irradiation can be used as an effective method for coating textiles without causing any damage to the crystalline structure of the commercial nanoparticles.

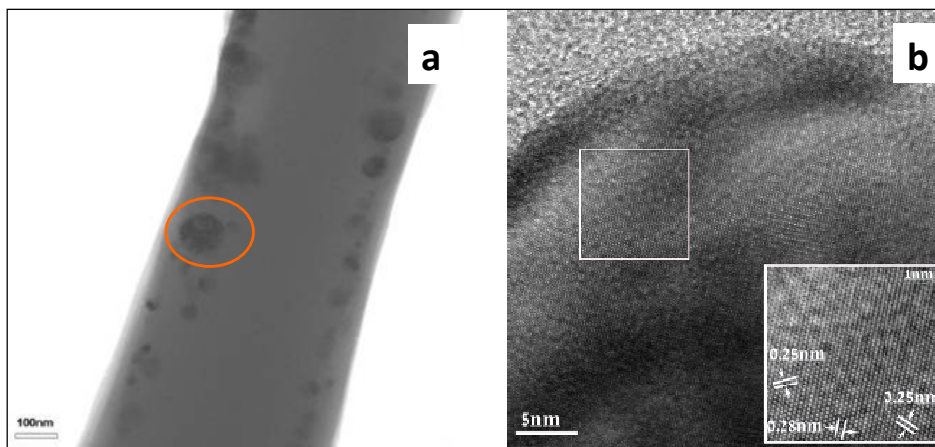


Figure 11. (a) HRTEM of Al_2O_3 -coated bandage; (b) high magnification (x1M) of the red-marked particle.

The morphology of the fiber surface before and after the deposition of magnesium oxide nanoparticles studied by HR SEM is presented in Figure 12. The image in Figure 12a demonstrates the smooth structure of the cotton fabric before coating with MgO nanoparticles. After the sonication, the homogeneous deposition of nanoparticles on the cotton yarn is observed (Figure 12b). The particle size is in the low nanometric range (~20-30 nm). The nanoparticles are well dispersed along the fibers, however some aggregation can be found.

In order to confirm that the structure of the MgO nanoparticles is not damaged during sonication, a control experiment was carried out, namely, the magnesium oxide nanopowder was sonicated under the same reaction conditions as experiment 7, and at the end of reaction the powder was centrifuged and dried. The XRD patterns of sonochemically-treated MgO nanoparticles demonstrate that the magnesium oxide is crystalline in nature, and the diffraction peaks match a cubic phase of MgO (PDF No. 004-0829). The peaks at $2\theta = 42.9, 62.3, 74.67, \text{ and } 78.61^\circ$ are assigned to the (200), (220), (311), and (222) reflection lines of cubic MgO particles, respectively. No peaks characteristic of any impurities were detected.

The antibacterial activity of cotton fabrics coated with 0.8% of MgO was determined using the Gram positive bacterium *Staphylococcus aureus* and the Gram negative bacterium *Escherichia coli*. As shown in Table 3, treatment for 1 hour with the MgO-coated cotton leads to a complete growth inhibition of *E. coli*. Regarding *S. aureus*, a 100% reduction in viability was reached after 3 hours, while after 1 hour of treatment a reduction of 90% could be seen. As for Al_2O_3 , it is evident from this study that alumina NPs possess milder antimicrobial properties. Treatment for 1 hour with the Al_2O_3 -coated cotton leads to about a 23% growth inhibition of *E. coli*, and an 84% growth after 3 hours. Regarding *S. aureus*, only an 11% growth inhibition was observed after 1 hour of treatment, and about 75% after 3 hours. Experiments of MgO and Al_2O_3 coated bandages toward *E. coli* and *S. aureus* were repeated 5 times: Statistical interpretation for MgO experiments- killing results (in percentage): mean values for *E. coli* after treatment for 60 min: 99.80 ± 0.2 ; 180 min: 99.96 ± 0.058 . The results for *E. coli* are reproducible; the same is true for *S. aureus*. The mean values for *Staph aureus* elimination: 60 min: 89.244 ± 0.8566 ; 180 min: 99.99512 ± 0.0068 . If we compare the results

for the two strains, the difference between the two strains after 60 minutes is highly significant $P < 0.005$. After 180 minutes, the difference is for sure not significant.

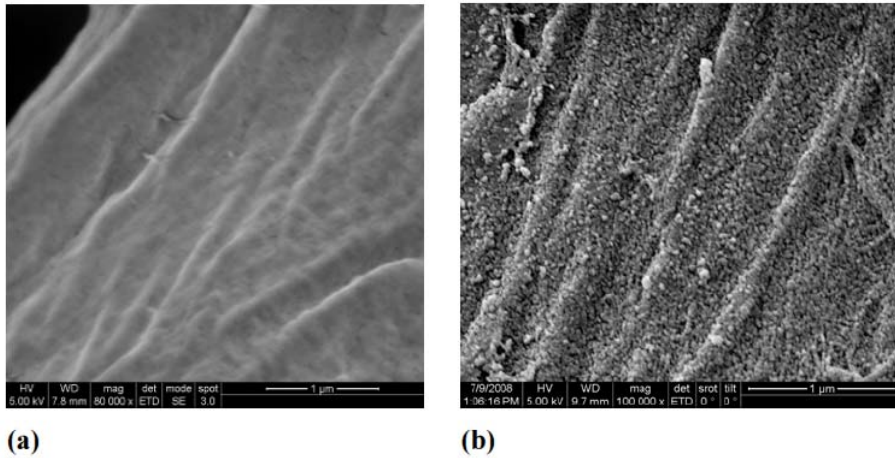


Figure 12. SEM images of a) pristine cotton bandage; b) MgO -coated bandage.

**Table 3. Antibacterial activity test using *E. coli* and *S. aureus*.
The viable bacteria were monitored by counting the number of
colony forming units (CFU); N/N₀: survival fraction**

Duration of treatment						
Treatment	1 h			3 h		
	CFU ml ⁻¹	N/N ₀	% reduction in viability	CFU ml ⁻¹	N/N ₀	% reduction in viability
<i>E. coli</i>						
Clean fabric	6.2×10^6	0.95	4.6	6.39×10^6	0.98	1.7
No fabric	5.8×10^6	1.05	-5.5	5.09×10^6	0.925	7.5
MgO	5.5×10^3	8.1×10^{-4}	99.9	260	$\sim 3.8 \times 10^{-5}$	100.00
Al ₂ O ₃	5.0×10^6	0.77	23.43	1.0×10^5	0.16	84.10
<i>S. aureus</i>						
Clean fabric	6.5×10^6	0.87	13.33	5.7×10^6	0.67	24
No fabric	6.7×10^6	0.94	5.63	6.5×10^6	0.92	13.33
MgO	6.3×10^5	9.5×10^{-2}	90.45	2.58×10^3	3.9×10^{-4}	99.96
Al ₂ O ₃	6.3×10^6	0.89	11.12	1.76×10^6	4.0×10^{-2}	74.95

Using the chemiluminescence method [81] showed that the dominant ROS generated on MgO surfaces were superoxide anions. As mentioned above, these ROS are not very reactive themselves to bacterial cells; however, these species are in equilibrium, as shown in the following reaction:



When $\bullet\text{O}_2^-$ species are generated near the bacterial membrane during the respiratory process, hydroperoxyl radicals ($\text{HO}_2\bullet$) are produced. The $\text{HO}_2\bullet$ is much more reactive than $\bullet\text{O}_2^-$ and is able to penetrate the cell's membrane. This concept will support the fact that contact between bacterial cells and MgO powders is important for MgO-induced bacterial death. Moreover, as a consequence of this contact, a local alkaline effect due to basic sites on MgO surfaces may also enhance the antibacterial activity of MgO [82].

These results obtained in the current work confirmed that the sonochemical method is effective for the production of antibacterial fabrics, irrespective of the mode of the nanoparticles deposition, i.e., the creation of NPs in the sonochemical reaction and their simultaneous deposition or sonochemical-assisted deposition of the preliminary synthesized NPs.

CONCLUSION

Nanoparticles with intrinsic antibacterial properties (Ag_2O , ZnO , CuO , MgO , Al_2O_3) can be synthesized and uniformly deposited onto the surface of different kinds of textiles by the sonochemical method. The coating was performed by a simple, efficient, one-step procedure using environmentally friendly reagents. The physical and chemical analyses demonstrated that nanocrystals are finely dispersed onto the fabric surfaces without any significant damage of the structure of yarns. The mechanism of nanoparticles formation and adhesion to the textile was discussed. It is based on the local melting of the substrate due to the high rate and temperature of nanoparticles thrown at the solid surface by sonochemical microjets. The strong adhesion of metal nanooxides to the substrate was demonstrated in terms of absence of leaching of the NP into the washing solution. The performance of fabrics coated with low content of active nanomaterial (<1 wt%) as an antibacterial agent was investigated and their excellent bactericidal effect was demonstrated.

Coated fabrics can have potential applications in wound dressing, bed lining and as bandages. They can be also recommended for the purification of medical and food equipment, domestic cleaning, etc.

REFERENCES

- [1] Srivasta, D.N., Perkash, N., Gedanken, A., and Felner, I. (2002). Sonochemical Synthesis of Mesoporous Iron Oxide and Accounts of Its Magnetic and Catalytic Properties *Journal of Physical Chemistry B*, 106: 1878-1883.
- [2] Mertl, M. (1999). AAAS Meeting: Neurobiologic Science, 283: 775-778.
- [3] Niu, H., Chen, Q., Zhu, H., Lin, Y., and Zhang, X. (2003). Magnetic field-induced growth and self assembly of cobalt nanocrystallites. *Journal of Material Chemistry*, 13: 1803-1805.
- [4] Wang, J., Chen, Q., Zheng, C., and Hou, B. (2004). Magnetic-Field-Induced Growth of Single-Crystalline Fe_3O_4 Nanowires *Advance Materials*, 16(2): 137-140.

- [5] Perkas, N., Amirian, G., Rottman, C., De La Vega, F., and Gedanken, A. (2009). Sonochemical deposition of magnetite on silver nanocrystals. *Ultrasonic Sonochemistry*, 16: 132-135.
- [6] Zalesky, T. (2008). "Active" products drive wound-care market. *GEN Biobusiness Biomarket Trends*; 9 (May 1):1-2, <http://genengnewa.com/articles/chitem>.
- [7] Petrulyte, S. (2008). Advanced textile materials and biopolymers in wound management. *Dan Med Bull*, 55: 72-77.
- [8] Gao, Y., and Cranston, R. (2008). Recent advances in antimicrobial treatments of Textiles. *Textile Research Journal*, 78: 60-72.
- [9] Craighead, H., Leong, K.M.C., Roco, R.S., and Alivisatos, P.(2000). *Netherlands: Kluwer Academic Publishers*,153-156.
- [10] Qian, L., and Hinestroza, J.P. (2004). Application of nanotechnology for high performance textile. *Journal of Textile Apparel Technology Management*, 4: 1-7.
- [11] Wong, Y.W.H., Yuen, C.W.M., Leung, M.Y.S., Ku, S.K.A., and Lam, H.L.I. (2006). Selected applications of nanotechnology in textiles. *AUTEX Research Jorنال*, 6: 1-8.
- [12] Coyle, S., Wu, Y., Lau, K.T., De Rossi, D., Wallace, G., and Diamond, D. (2007). Smart Nanotextiles. *MRS Bulletin*, 32: 434-437.
- [13] Klueh, U., Wagner, V., Kelly, S., Johnson, A., and Bryers, J.D. (2000). Efficacy of silver-coated Fabric to prevent bacterial colonization and subsequent device-based biofilm formation. *Journal of Biomedical Material Research*, 53: 621-631.
- [14] Lee, H.J., Yeo, S.Y., and Jeong, S.H. (2003). Antibacterial effect of nanosized silver colloidal solution on textile fabrics. *Journal of Material Science*, 38: 2199-2204.
- [15] Gorenšek, M., and Recelj, P. (2007). Nanosilver functionalized cotton fabric. *Textile Research Journal*, 77: 138-141.
- [16] Searle, A. (1919). The Use of Metal Colloids in Health and Diseases. *Sutton: N.Y.*
- [17] Birringer, R. Nanocrystalline materials *Mater. Sci. Eng. A* 1989, 117, 33-43.
- [18] Shukla, S., Seal, S., Schwartz, S., and Zhou, D. (2001). Synthesis and Characterization of Nanocrystalline Silver Coating of Fly Ash Cenosphere Particles by Electroless Process. *Journal of Nanoscience Nanotechnology*, 417-424.
- [19] Richard, P., LeFloch, R., Chamoux, C., Pannier, M., Espaze, E., and Richet, H. (1994). Pseudomonas aeruginosa outbreak in a burn unit: role of antimicrobials in the emergence of multiply resistant strains.. *Journal of Infectious Diseases*, 170: 377-383.
- [20] Wendler, F., Meister, F., Montigny, R., and Wagener, M. (2007). A new antimicrobial ALCERU fiber with silver nanoparticles. *Fibers and Textiles in East Europe A*, 15: 64-65.
- [21] Duran, N., Marcato, P.D., De Souza, G.I.H., Alves, O.L., and Espósito, E. (2007). Antibacterial effect of silver nanoparticles produced by fungal process on textile fabrics and their effluent treatment. *Journal of Biomedical Nanotechnology*, 13: 203-208.
- [22] Yuranova, T., Rincon, A.G., Pulgarin, C., Laub, D., Xantopoulos, N., Mathieu, H.J., and Kiwiet, J. (2006). Performance and characterization of Ag-cotton and Ag/TiO₂ loaded textiles During the abatement of *E. coli*. *Journal of Photochemistry and Photobiology A*, 181: 363-369.
- [23] Scholz, J., Nocke, G., Hollstein, F., and Weissbach, A. (2005). Investigations on fabrics coated with precious metals using the magnetron sputter technique with regard to their anti-microbial properties. *Surface and Coating Technology*, 192: 252-256.
- [24] Daoud, W.A., and Xin, J.H. (2004). Low temperature **sol-gel** processed photocatalytic titania coating. *Journal of Sol-Gel Science Technology*, 29: 25-29.

-
- [25] Uddin, F. (2008). *86th Textile-Institute World Conf., Conf. Proceed. 2:U291-307*. Hong Kong: Polytechnic University, Institute of Textiles and Clothing Press.
- [26] Sojka-Ledakowicz, J., Lewartowska, J., Kudzin, M., Jesionowski, T., Siwińska-Stefańska, K., and Krysztafkiewicz, A. (2008). Modification of textile materials with micro- and nano-structural metal oxides. *Fibers and Textiles in Eastern Europe A*, 16: 112-116.
- [27] Shi, L., Zhao, Y., Zhang, X., Su, H., and Tan, H. (2008). Antibacterial and anti-mildew behavior of chitosan/nano-TiO₂ composite emulsion. *Korean Journal of Chemical Engineering*, 25: 1434-1438.
- [28] El-Naggar, A.M., Zohdy, M.H., Hassan, M.S., and Khalil, E.M. (2003). Antimicrobial protection of cotton and cotton/polyester fabrics by radiation and thermal treatments. I. Effect of ZnO formulation on the mechanical and dyeing properties. *Journal of Applied Polymer Science*, 88: 1129-1137.
- [29] Zohdy, M.H., Kareem, H.A., El-Naggar, A.M., and Hassan, M.S. (2003). Microbial detection, surface morphology, and thermal stability of cotton and cotton/polyester fabrics treated with antimicrobial formulations by a radiation method. *Journal of Applied Polymer Science*, 89: 2604-2610.
- [30] Schollmeyer, E. (2007). *Tekstil*, 56: 75-78.
- [31] Xue, C.H., Jia, S.T., Chen, H.Z. and Wang, M. (2008). Preparation of superhydrophobic surfaces on cotton textiles *Science and Technology of Advance Materials*, 9: 035001-035007.
- [32] Wang, R., Xin, J.H., Tao, X.M. and Daoud, W. (2004). ZnO Nanorods grown on cotton fabrics at low temperature. *Chemical Physics Letter*, 398: 250-255.
- [33] Daoud, W.A., Xin, J.H., and Zhang, Y.H. (2005). Surface functionalization of cellulose fibers with titanium dioxide nanoparticles and their combined bactericidal activities. *Surface Science*, 599: 69-75.
- [34] Qi, K.H., Chen, X.Q., and Liu, Y.Y. Facile preparation of anatase/SiO₂ spherical nanocomposites and their application in self-cleaning textiles. (2007). *Journal of Material Chemistry*. 17: 3504-3508.
- [35] Haufe, H., Muschter, K., Siegert, J., and Bottcher, H. (2008). Bioactive textiles by sol-gel immobilised natural active agents. *Journal of Sol-Gel Science Technology*, 45: 97-101.
- [36] Vigneshwaran, N., Kumar, S., Kathe, A.A., Varadarajan, P.V., and Prasad, V. (2006). Functional finishing of cotton fabrics using zinc oxide-soluble starch nanocomposites. *Nanotechnology*, 17: 5087-5095.
- [37] Xu, B., Niu, M., Wei, L., Hou, W., and Liu, X. (2007). The structural analysis of biomacromolecular wool fiber with Ag-loading SiO₂ nano-antibacterial agent by UV radiation. *Journal of Photochemistry Photobiology A: Chemistry*, 188 (1): 98– 105.
- [38] Mao, Z., Shi, Q., Zhang, L., and Cao, H. (2006). The formation and UV-blocking property of needle-shaped ZnO nanorod on cotton fabric. *Thin Solid Films*, 517: 2681-2686.
- [39] Bilian, X. Intrauterine devices (2002). *Best Practice and Research Clinical Obstetrics and Gynaecology*. 16: 155-168.
- [40] Gabbay, J., Borkow, G., Mishal, J., Magen, E., Zatcoff, R., and Shemer-Avni, Y. (2006). Copper oxide impregnated textiles with potent biocidal activities. *Journal of Industrial Textiles*, 35: 323-335.

-
- [41] Borkow, G., and Gabbay, J. (2005). Copper as a Biocidal Tool. *Current Medical Chemistry*, 12: 2163-2175.
- [42] Suslick, K.S., and Price, G.J. (1999). Application of ultrasound to materials chemistry. *Annual Review of Materials Research*, 29: 295-326.
- [43] Gedanken, A. (2004). Using sonochemistry for the fabrication of nanomaterials. *Ultrasonic Sonochemistry*, 11: 47-55.
- [44] Suslick, K.S., Choe, S.B., Ciclowlas, A.A., and Grinstaff, M.W. (1991). Sonochemical synthesis of amorphous iron. *Nature*, 353: 414-416.
- [45] Mason, T.J. (1990). *Sonochemistry*. London: Royal Society of Chemistry Press.
- [46] Doktycz, S.J., and Suslick, K.S. (1990). Interparticle collisions driving by ultrasound. *Science*, 247: 1067-1069.
- [47] Suslick, K.S., Hammerton, D.A., and Cline, R.E. (1986). Sonochemical hot spot. *Journal of American Chemical Society*, 108: 5641-5642.
- [48] Gedanken, A. (2007). Doping nanoparticles into polymers and ceramics using ultrasound radiation. *Ultrasonic Sonochemistry*, 14: 418-430.
- [49] Mason, T.J. (2007). Development in ultrasound non-medical. *Progress in Biophysics and Molecular Biology*, 93: 166-175.
- [50] Vajnhandl, S., and Le Marechal, A.M. (2005). Ultrasound in textile dyeing and the decolouration/mineralization of textile dyes. *Dyes and Pigments*, 65: 89-101.
- [51] Pol, V.G., Srivastava, D.N., Palchik, O., Palchik, V., Slifkin, M.A., Weiss, A.M., and Gedanken, A. (2002). Sonochemical deposition of silver nanoparticles on silica spheres. *Langmuir*, 18: 3352-3357.
- [52] Kotlyar, A., Perkas, N., Amiryan, G., Meyer, M., Zimmermann, W., and Gedanken, A. (2007). Coating silver nanoparticles on poly(methyl methacrylate) chips and spheres via ultrasound irradiation. *Journal of Applied Polymer Science*, 104: 2868-2876.
- [53] Perkas, N., Shuster, M., Amirian, G., Koltypin, Y., and Gedanken, A. (2008). Sonochemical immobilization of silver nanoparticles on porous polypropylene. *Journal of Polymer Science, Part A: Polymer Chemistry*, 46: 1719-1729.
- [54] Perkas, N., Amirian, G., Dubinsky, S., Gazit, S., and Gedanken, A. (2007). Ultrasound-assisted coating of nylon 6,6 with silver nanoparticles and its antibacterial activity. *Journal of Applied Polymer Science*, 104: 1423-1430.
- [55] Sun, Y., and Sun, G. (2002). Durable and regenerable antimicrobial textile materials prepared by a continuous grafting process. *Journal of Applied Polymer Science*, 84: 1592-1599.
- [56] Takasima, M., Shirai, F., Sageshima, M., Ikeda, M., Okamoto, Y., and Dohi, Y. (2004). Distinctive bacteria-binding property of cloth materials. *American Journal of Infection Control*, 31: 27-30.
- [57] Freddi, G., Arai, T., Colonna, G.M., Boschi, A., and Tsukada, M. (2001). Binding of metal cations to chemically modified wool and antimicrobial properties of the wool-metal complexes. *Journal of Applied Polymer Science*, 82: 3513-3519.
- [58] Zhu, P., and Sun, G. (2004). Antimicrobial finishing of wool fabrics using quaternary ammonium salts. *Journal of Applied Polymer Science*, 93: 1037-1041.
- [59] Dong, Q., Su, H., and Zhang, D. (2005). In situ depositing silver nanoclusters on silk fibroin fibers supports by a novel biotemplate redox technique at room temperature. *Journal of Physical Chemistry B*, 109: 17429-17434.

-
- [60] Hadad, L., Perkas, N., Gofer, Y., Calderon-Moreno, J., Ghule, A., and Gedanken, A. (2007). Sonochemical deposition of silver nanoparticles on wool fibers. *Journal of Applied Polymer Science*, 104: 1732–1737.
- [61] Perelshtein, I., Applerot, G., Perkas, N., Guibert, G., Mikhailov, S., and Gedanken, A. (2008). Sonochemical coating of silver nanoparticles on textile fabrics (nylon, polyester and cotton) and their antibacterial activity. *Nanotechnology*, 19: 245705-245710.
- [62] Kawashita, M., Toda, S., Kim, H.M., Kokubo, T., and Masuda, N. (2003). Preparation of antibacterial silver-doped silica glass microspheres. *Journal of Biomedical Materials Research A*, 66A: 266-274.
- [63] Chun-Nam, L., Chi-Ming, H., Rong, C., Qing-Yu H., Wing-Yiu, Y., Hongzhe, S., Paul Kwong-Hang, T., Jen-Fu, C., and Chi-Ming, C. (2007). Silver nanoparticles: partial oxidation and antibacterial activities. *Journal of Biological Inorganic Chemistry*, 12: 527-534.
- [64] Yamamoto, O. (2001). Influence of particle size on the antibacterial activity of zinc oxide. *International Journal of Inorganic Materials*, 3: 643-646.
- [65] Perelshtein, I., Applerot, G., Perkas, N., Wehrschetz-Sigl, E., Hasmann, A., Guebitz, G.M., and Gedanken, A. (2009). Antibacterial properties of an in situ generated and Simultaneously deposited nanocrystalline ZnO on fabrics. *ACS Applied Materials and Interfaces*, 1: 361-366.
- [66] Li, N., Xia, T., and Nel, A. E. (2008). The role of oxidative stress in ambient particulate matter-induced lung diseases and its implications in the toxicity of engineered nanoparticles. *Free Radical Biology and Medicine*, 44: 1689-1699.
- [67] Neal, A.L. (2008). What can be inferred from bacterium–nanoparticle interactions about the potential consequences of environmental exposure to nanoparticles? *Ecotoxicology*, 17: 362-371.
- [68] Hu, X., Cook, S., Wang, P., and Hwang, H. (2009). In vitro evaluation of cytotoxicity of engineered metal oxide nanoparticles. *Science of the Total Environment*, 407: 3070-3072.
- [69] Sawai, J., Igarashi, H., Hashimoto, A., Kokugan, T., and Shimizu, M. (1996). Effect of particle size and heating temperature of ceramic powders on antibacterial activity of their slurries. *Journal of Chemical Engineering Japan*, 29: 251-256.
- [70] Sawai, J., Shoji, S., Igarashi, H., Hashimoto, A., Kokugan, T., Shimizu, M., and Kojima, H. (1998). Hydrogen peroxide as an antibacterial factor in zinc oxide powder slurry. *Journal of Fermentation and Bioengineering*, 86: 521-522.
- [71] Applerot, G., Lipovsky, A., Dror, R., Perkas, N., Nitzan, Y., Lubart R., and Gedanken, A. (2009). Enhanced antibacterial activity of nanocrystalline ZnO due to increased ROS-mediated cell injury. *Advanced Functional Materials*, 19: 842-852.
- [72] Soderberg, T., Agren, M., Tengrup, I., Hallmans, G., and Banck, G. (1989). The effects of an occlusive zinc medicated dressing on the bacterial flora in excised wounds in the rat. *Infection*, 17: 81–85.
- [73] Lansdown, A.B.G., Mirastschijski, U., Stubbs, N., Scanlon, E., and Agren, M.S. (2007). Zinc in wound healing: Theoretical, experimental, and clinical aspects. *Wound Repair Regeneration*, 5: 16-22.
- [74] Sengupta, G., Ahluwalia, H.S., Banerjee, S., and Sen, S.P. (1979). Chemisorption of water-vapor on zinc oxide. *Journal of Colloid and Interface Science*, 69: 217–224.

-
- [75] Perelshtein, I., Applerot, G., Perkas, N., Wehrschuetz-Sigl, E., Hasmann, A., Guebitz, G.M., and Gedanken A. (2009). CuO–cotton nanocomposite: Formation, morphology, and antibacterial activity. *Surface and Coating Technology*, 204, 54–57.
- [76] Huang, L., Li, D.Q., Lin, Y.J., Wei, M., Evans, D.G., and Duan, X. (2005). Controllable preparation of nano-MgO and investigation of its bactericidal properties. *Journal of Inorganic Biochemistry*, 99: 986-993.
- [77] Ohira, T., Kawamura, M., Iida, Y., Fukuda, M., and Yamamoto, O. (2008). Influence of the mixing ratio on antibacterial characteristics of MgO-ZnO solid solution in two phase coexistence region. *Journal of the Ceramic Society of Japan*, 116: 1234-1237.
- [78] Makhluף, S., Dror, R., Nitzan, Y., Abramovich, Y., Jelinek, R., and Gedanken, A. (2005). Microwave-assisted synthesis of nanocrystalline MgO and its use as a bactericide. *Advanced Functional Materials*, 15: 1708-1715.
- [79] Seo, D.J., Park, S.B., Kang, Y.C., and Choy, K.L. (2003). Formation of ZnO, MgO and NiO nanoparticles from aqueous droplets in flame reactor, *Journal of Nanoparticle Research*, 5: 199-210.
- [80] Stengl, V., Bakardjieva, S., Marikova, M., Bezdicka, P., and Subrt, J. (2003). Magnesium oxide nanoparticles prepared by ultrasound enhanced hydrolysis of Mg-alkoxides. *Materials Letters*, 57: 3998-4003.
- [81] Sawai, J., Kojima, H., Igarashi, H., Hashimoto, A., Shoji, S., Sawaki, T., Hakoda, A., Kawada, E., Kokugan, T., and Shimizu, M. (2000). Antibacterial characteristics of magnesium oxide powder. *World Journal of Microbiology and Biotechnology*, 16: 187-194.
- [82] Ardizzzone, S., Bianchi, C.L., and Vercelli, B. (1998). MgO powders: interplay between adsorbed species and localization of basic sites. *Applied Surface Science*, 126: 169-75.

Chapter 12

ADVANCED TEXTILES FOR MEDICAL USES

Anicuta Stoica-Guzun*

Chemical Engineering Department,
University Politehnica of Bucharest, Romania.

ABSTRACT

New technologies are emerging nowadays in industrial practices and the textile industry could not be omitted from this technical progress. From this industry, technical textiles are designed to satisfy particular needs in different fields of activity. Among these, one of the most important and rapidly expanding sectors is that of medical textiles. The use of textiles in medicine has a long tradition. Because there are a huge number of diverse applications of medical textiles, in this chapter only the new trends in this field will be attained.

First of all, the attention will be focused on biopolymers as alginate, collagen, chitin, chitosan, cellulose and bacterial cellulose, gelatine and others which have already their place in advanced biomedical applications. The use of fibers and textiles in medicine has increased exponentially as new types of fibers, new innovative structures and new therapies have been developed.

Secondly, the progress accomplished in the new emerging technologies like nanotechnology, electrospinning and biotechnology will be underlined.

There will be also presented the progress achieved in the advanced materials for regenerative medicine, wound healing and drug delivery. The development of wound dressing has changed from passive to active types, having some specific functions in order to enhance wound healing without trauma for the patient. Textile structures for wound dressing can contain specialized additives with various properties, such as antibacterial properties. Among these, silver in different forms is the most well known, being used in medical applications.

The future will select the best of the solutions proposed in our days, but it is sure that the era of smart textiles or even intelligent textiles has already begun.

* E-mail: stoica.anicuta@gmail.com

1. INTRODUCTION

The textile industry is rapidly moving from traditional textile products towards advanced and high value-added medical textiles. These materials can be classified into four areas of application: implantable medical textiles, non-implantable materials, extracorporeal devices and healthcare/hygiene products. A new generation of medical textiles is emerging and the new products are already created by adding modern functionalities to traditional textile materials and even transforming these materials using new technologies.

The aim of this chapter is to present some innovations in the medical textile field, starting from various biopolymers which can be used in regenerative medicine, wound dressing and drug delivery. These biopolymers belong to the classes of polysaccharides, proteins, biopolymers produced by microbial fermentation and biopolymers chemically synthesized from bio-based monomers.

Biotechnology, nanotechnology and electrospinning were chosen as representative techniques in order to illustrate the technological progress in the field of medical textiles.

Advanced biotechnology procedures or new processing methods have led to significantly improved properties of fibers like cotton, silk, flax and hemp, offering the possibility to obtain new materials by using genetic engineering. Nanotechnology can be used to create new nanofibers and yarns and to improve fabric finishing. It can produce textiles which are able, on the one hand, to prevent the growth of microorganisms, to remove unpleasant odor and to protect from UV radiation, and on the other hand to have properties of self cleaning surfaces, affording protection both for the user of the textile material and for the textile itself. Electrospinning is a broadly used technology for electrostatic fibers formation which offers unique capabilities for producing novel natural nanofibers and fabrics with controllable pore structure. It also seems to be a promising technology for tissue engineering and other related applications. Because there are a huge number of diverse applications of medical textiles, in this chapter only the new trends in this field will be attained, including wound dressings and tissue engineering scaffolds.

2. BIOPOLYMERS USED IN TEXTILE MEDICAL APPLICATIONS

Biopolymers are a versatile class of materials having a lot of applications in practically all sectors of economy. Many of their properties are superior to synthetic polymers, for example biodegradability, biocompatibility, and versatility. They can be produced from renewable resources, especially by-products of agricultural, forestry, seafood industry and other industrial activities. Yet, there are some drawbacks when it comes to their intensive industrial utilization. The most important is their price, commercially available biopolymers being more expensive than synthetic polymers. Nonetheless the good news is that the price of biopolymers has continued to fall over the past ten years. Their competitiveness over synthetic polymers will continue to increase, because many researchers from different companies or universities are involved in the innovation of this field. A lot of biopolymers can directly replace synthetically polymers in many traditional applications. In the mean time, there are new materials from this class, which have new properties that could be used in new applications, and such an opportunity should not be neglected. Table 1 presented a

comparison between the two classes of polymers: synthetic polymers obtained from fossil resources and biopolymers produced from renewable resources.

It is rather difficult to classify the biopolymers, because they are encountered not only in industry, but also in the cycle of our life as nucleic acids, for example. Figure 1 depicted a classification of biopolymers which emphasizes those which can be used as biomedical textiles.

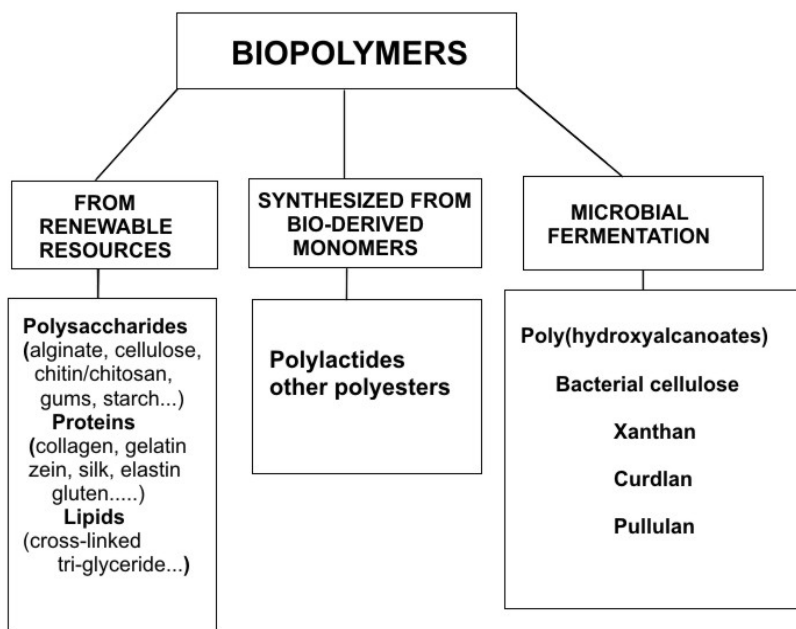


Figure 1. Biopolymer classification.

Table 1. Comparison between biopolymers from renewable resources and synthetic polymers obtained from fossil resources

Biopolymers from renewable resources	Synthetic polymers from fossil resources (crude oil or gas)
Advantages	
<ul style="list-style-type: none"> -Use renewable resources, especially by-products of others human activities -Could reduce the dependence on import of fossil resources -Are biodegradable -Their price continue to fall -Government programs exists to promote the market introduction of biopolymers -Some biopolymers can directly replace synthetic polymers -Can create new commercial opportunities 	<ul style="list-style-type: none"> -Are produced of very high scale -Are technically mature

Table 1. Continued

Biopolymers from renewable resources	Synthetic polymers from fossil resources (crude oil or gas)
Disadvantages	
<ul style="list-style-type: none"> -High production costs -High research and development costs -Are in an early stage of development -Interdisciplinary nature of the field which oblige at more cooperation 	<ul style="list-style-type: none"> -High fluctuations of fossils resources price -These resources are uneven distributed all over the world -Are not biodegradable -Are obtained from toxic compounds and could generate toxic by products

2.1. Polysaccharides

Polysaccharides are a class of biopolymers constituted by simple sugar monomers which can be obtained from different sources: microbial, vegetal and animal. Polysaccharides have been considered the most promising materials for medical textiles, because they present many positive attributes like good biocompatibility, high biodegradability, non-toxicity, potential bioactivity and, with few exceptions, have low costs in comparison with other biopolymers. These polysaccharidic polymers have been widely proposed as scaffold materials in tissue engineering applications, as well as carriers for drug delivery systems, providing ample opportunities for further development [1, 2].

2.1.1. Alginates

Alginates are polysaccharides that provide the main structural component of marine brown algae (*Phaeophyceae*), as well as capsular polysaccharides in some bacteria. Commercial alginates are at present still exclusively extracted from algal sources. These include *Laminaria hyperborean*, *Ascophyllum nodosum*, and *Macrocystis pyrifera* in which alginate comprises up to 40% of the dry weight [2]. Alginates are linear copolymers of (1 / 4) linked β -D-mannuronic acid (M) and α -L-guluronic acid (G). They are soluble in aqueous solution at room temperature and form stable gels in the presence of divalent cations, such as Ca^{2+} , Ba^{2+} , and Sr^{2+} . The viscosity of alginate solutions depends on the medium pH. Another characteristic of alginates, in addition to their gelling and stabilizing properties, is their ability to retain water. Because of their linear structure and high molecular weight, alginates also form strong films and good fibers in solid state [3]. Alginate as textile fiber is relatively expensive, and tends to dissolve in the alkali conditions of many textile processes such as bleaching, dyeing, and finishing. Since the 1980s, alginate fibers have been widely used in the manufacture of high-tech wound dressings and now are considered one of the most versatile wound dressing materials [4]. Alginates can also be used as excipients in drug delivery, as dental impression materials and in some formulations preventing gastric reflux [5, 6]. Here are some examples from the commercial forms of alginates as haemostatic materials and wound dressing: Sorbsan[®] which was launched in 1983, AlgiSite[®], AlgiDERM[®], Curasorb[®], Kaltostat[®], Kalginate[®], [1, 4, 6, 7]. The alginate within the dressing absorbs the exudate resulting in a hydrophilic gel over the wound which provides a good moist environment for

healing. Alginate scaffolds have potential application in the regeneration of many types of tissues [8]. Alginate composite with TiO₂ nano needles for tissue engineering application or with active substances from asiatic plants (*Centella asiatica*) for wound healing have been reported [8, 9]. Also, chitosan has been used to coat calcium alginate filaments (utilizing the cationic interaction of the chitosan with the anionic nature of the alginate to produce a tight interaction) in order to obtain chitosan/alginate fibers with potential use in wound dressings applications [1]. Composites of alginate with starch were used in drug release systems, salicylic acid being used as model drug [10].

2.1.2. Cellulose

Cellulose, the most abundant natural biopolymer, is found in the cell walls of higher plants, and has been widely used in biomedical applications due to its biodegradability, biocompatibility and nontoxicity. Cellulose, obtained as pulp from fibrous plant materials, consists of amorphous cellulose areas and, additionally, well-ordered crystalline regions. The degree of crystallinity of cellulose, usually in the range of 40–60%, depends on the origin and pre-treatment of the sample [11]. Cellulose is a cheap, raw material, but it is difficult to use because of its hydrophilic nature, its insolubility and high crystallinity. Cellulose fibers from cotton or wood pulp are the natural fibers most commonly used in the production of biomedical fabrics and related construction. From these two sources, cotton is preferred because it is characterized by excellent properties for medical applications and is almost pure cellulose (~98%) that can be found in nature. Wood is a lignocellulosic composite material consisting of ~50% cellulose. The cellulose isolation requires the removal of hemicelluloses and lignin from wood. Traditional technologies (i.e. alkaline or acid sulfite treatment) applied to delignify wood cause environmental pollution. For this reason, fibers from others crops, especially from by-products of these different plants, are rather interesting to be used as new cellulose or cellulose derivative sources. There are several good candidates which deserve to be mentioned: rice hulls, sunflowers seed hulls, sugarcane bagasse, sorghum, cornstalks, corn cob, wheat straw, sisal, barley, pineapple, bananas, coconut crops, soybean straw, hop stems and others [12–21]. Among the cellulose derivatives which are produced commercially, the most common are carboxy-methyl cellulose, methyl cellulose, ethyl cellulose, hydroxyethyl cellulose, hydroxypropyl cellulose and cellulose acetate. All of these cellulose derivatives have important industrial applications, some of them even for biomedical textiles, for example cellulose acetate fibers.

Cellulose fibers have the most diverse range of structures and properties, strongly influenced by many factors e.g., chemical composition, internal fiber structure, microfibril angle, cell dimensions and defects, which in return depend on cellulose sources and its technological processing. Strong interest has been devoted in recent years in cellulose nanoparticles, which can be used to obtain biocomposites with very large industrial applications. Even if the terminology for cellulose fibrils at nanoscale level is not consistent, tremendous efforts have been devoted to obtain different forms of crystalline cellulose, named in literature as microcrystalline cellulose, cellulose microfibrils, microcrystals, nanofibrils, nanocellulose and cellulose whiskers or nanowhiskers [22, 23].

Microcrystalline cellulose (MCC) is partially depolymerized cellulose with a degree of polymerization (DP) below 350. MCC is basically made of crystallites of colloidal size. The crystallites aggregate, forming particles of about 15±20 µm diameter. It consists in a fine, white, odorless, crystalline powder. Due to the crystalline parts of cellulose fibrils, they have

extraordinary mechanical properties, interesting for various applications, including biomedicine. In order to obtain MCC a necessary step is the hydrolysis of cellulose using mineral acid, enzymes or microorganisms, the conventional method being acid hydrolysis. Microcrystalline cellulose is now used in various fields such as pharmacy, cosmetics, food industry, and plastics processing industry [24-26]. The surface of the MFC can be also modified using different chemical treatments [27]. MFC can be encountered in drug released formulations and it is considered an ideal component of different composite materials, which could be used also for medical applications.

From the nanosized forms of cellulose, cellulose whiskers enjoy a great popularity. Cellulose nanowhiskers are manufactured from renewable materials: not only natural plants, but also bacteria, fungi, algae, and marine animals [28, 29]. Cellulose nanowhiskers, with excellent mechanical properties, are extracted from a purified cellulose source material by hydrolytic degradation, using strong mineral acid such as sulfuric acid. They are described as elongated rod-like nanoparticles and are also known as cellulose nanocrystals [22, 30, 31]. Cellulose nanowhiskers have been used as reinforcement in many synthetic polymers and biopolymers matrices (i.e. poly(vinyl alcohol), poly(3-hydroxybutyrate-co-3-hydroxyvalerate), starch, cellulose acetate butyrate, polylactic acid), and are considered to have a huge potential in obtaining bionanocomposites, out of which some can be used in medical applications, for example for wound dressing and tissue engineering [21, 23, 29, 32-40].

Another new field related to the use of cellulose or cellulose derivatives for high value-added materials concerns the incorporation of inorganic nanoparticles into a cellulose fiber assembly, especially for enhancing antibacterial properties, but also for obtaining auto-self cleaning materials [41, 42]. Silver and silver-based compounds are well-investigated antimicrobial agents. It has been shown that silver bound on a solid surface, as well as in solution, acts as a very effective biocide. It is biocompatible and non-toxic to human cells at concentrations which are effective against microorganisms. The antimicrobial efficiency of silver depends directly on its concentration, which should not drop under the limit value required for minimal inhibition [43-46]. From the new developed processes to obtain nano silver particles, there may be mentioned a “green process” using natural extracts of *Eucalyptus citriodora* and *Ficus bengalensis*. The size of silver nanoparticles was found to have 20 nm [47]. Silver was also incorporated by adsorption onto cotton microfibrils after what a chelating monomer (glycidyl methacrylate-*iminodiacetic acid* (GMA-IDA)) was grafted onto cotton fibers by UV-polymerisation [48].

Even though silver is the most well investigated antimicrobial agent for cellulose and its derivatives, other antimicrobial substances are also tested, for example miconazole nitrate, triazine derivatives and chlorhexidine [35,49-51].

Self-cleaning textiles containing cotton have been obtained, by modifying their surfaces, especially with TiO₂ using different techniques, as sol-gel process, RF (radio-frequency) or MW (microwave) plasma and UV (ultraviolet) irradiation. Another objective was to introduce not only TiO₂, but also silver, as antibacterial agent, in order to produce antibacterial and photochromic textiles [52-54].

2.1.3. Chitin/Chitosan

Chitin is one of the most abundant polysaccharide in the world, situating itself on the second place after cellulose. It is found in the exoskeleton or cuticles of arthropods and other invertebrates, but also in the cell walls of most fungi and some algae. The most important sources of chitin for industrial use are crustaceans shells (from crabs, shrimps and lobsters), which are waste products of food industry. Chitin, from a chemical point of view, is poly(β -(1-4)-*N*-acetyl-D-glucosamine [55]. Because of its intractability and insolubility, chitin was replaced, in many commercial applications, by chitosan (CS), which is a fully or partially deacetylated form of chitin. Chitosan is commercially produced by alkaline deacetylation of crustacean chitins, the degree of deacetylation of typical commercial chitosan being usually between 70% and 95%, and the molecular weight between 10 and 1000 kDa [2]. Chitosan is insoluble in organic solvents, in acids at high concentration and in alkali, but dissolves easily at low pH. It exhibits a pH-sensitive behavior as a weak poly-base due to the large quantities of amino groups on its chain [2]. Chitin and chitosan are non-toxic, antibacterial, biodegradable and biocompatible biopolymers. Taking these properties into account, they have a huge potential for biomedical applications.

Chitin and chitosan can be processed in many forms, the most encountered being: gels, membranes, fibers and nanofibers, micro and nanoparticles, scaffolds and sponges [56]. For example, chitin fibers were mentioned to be used in textile materials, chitin sutures having very good properties over other fibers used in surgery. There were also reported various attempts for chitin dissolution and spinning it into chitin fibers.

Blends of chitin, chitosan and its derivatives with various natural or synthetic polymers (i.e. cellulose, collagen, cornstarch, dextran, gelatine, poloxamer, PLLA (poly-L-lactic acid), PVA, poly(*N*-isopropyl acrylamide, polymethylmethacrylate (PMMA)) have been obtained, these materials presenting improved properties, for example higher antimicrobial capacity, and being used especially for wound dressings and as scaffold for tissue engineering [55,57-70]. The obtained blends exist in different forms, from hydrogel to membranes and sponges. Other recent examples are: a hydrogel sheet composed of a blended powder of alginate, chitin/chitosan and fucoidan [71], a composite nanofibrous membrane of type I collagen, chitosan, and polyethylene oxide fabricated by electrospinning, which could be further cross-linked by glutaraldehyde vapor [72], cross-linked hydrogel films prepared with polyvinyl alcohol (PVA) and chitosan using the freeze-thawing method [68]. A lot of research is focused on silver, especially silver nanoparticles, which are used as antibacterial agents in many composite materials along with chitin and chitosan [73-77].

Composite chitosan fibers with many biopolymers like sodium alginate, alginic acid, sodium alginate filaments, collagen, cellulose, viscose cellulose, silk fibroin and other polymers like poly(ethylene terephthalate) (PET), were obtained using different techniques, from which electrospinning is the most promising [78-80]. Some recent examples deserve to be mentioned: cellulose/*O*-hydroxyethyl chitosan fibers (CHCFs), with antimicrobial properties, which were manufactured by blending *O*-hydroxyethyl chitosan (HECS) xanthate with cellulose xanthate for spinning via the viscose process [81], fibers of poly(L-lactic acid) (PLLA) and chitosan (CHS), which were blend spun and then fabricated into PLLA/CHS fabrics [82]. To enhance antibacterial activity of chitosan and chitosan composite fibers, silver is intensively used [83-84].

Chitosan and its derivatives are currently being used as an antibacterial agent for alginate fiber, cellulose fiber, cotton fiber, polyester fiber, wool and others [1, 81, 85-87]. Chitosan

nanoparticles loaded with silver ions were used to improve bactericidal efficacy when applied on polyester fabrics [88]. Cotton fabrics were chemically modified using chitosan followed by incorporating silver nanoparticles in the fabrics, which exhibit excellent antibacterial action against model bacteria *E. coli*. [89]. Chitosan can be used as reducing agent for silver nitrate in order to obtain chitosan-based silver nanoparticles with antimicrobial activity [90]. A great deal of progress has been made in the understanding the antimicrobial effect of chitosan [91].

The biomedical applications, in regenerative medicine, of chitin and chitosan and their derivatives and composites are well known. These materials have a wide variety of applications in tissue engineering, wound dressing, drug delivery and targeting, gene therapy and in the area of nanobiotechnology. Biocompatible wound dressings and bandages derived from chitin and chitosan are already commercially available. The promise for these biomaterials in medical field is vast and will continue to extend to nerve guides, cartilage regeneration and as osteogenic bone substitutes [92-96]. In order to improve the bioactivity of chitosan in bone tissue engineering chitosan/HA composite scaffolds were reported, containing also carbon nanotubes [97-101]. For orthopedic applications there were obtained composite materials containing chitosan and calcium phosphate [97,102-105]. At present, chitosan and its derivatives and composites are among the most promising biopolymers for biomedical applications.

2.2. Proteins

Many natural polymers containing proteins were used in the production of medical textiles. Well known examples are: silk, wool, collagen, gelatin, casein, zein and elastin. These materials were darkled by the synthetic polymers derived from petroleum feedstock, even though they have properties which are superior to synthetic materials. The key to synthetic polymers' success was their price and the large scale production. Today, when we face major fluctuations of the price of fossils resources and we are concerned about the toxicity of the industrial products and environmental pollution, the natural polymers can offer a good guarantee for a sustainable development. At the same time, the large scale production of natural protein fibers requires either the development of large cultivation methods, or the discovery of alternative methods of production using, for example, genetic engineering.

2.2.1. Collagen/Gelatin

Collagen is a protein complex arranged in a fibrous form and is normally found in bone, skin, and various connective tissues of higher animals. Collagen fibrils are arranged in different ways, depending on the biological function of the particular type of connective tissue [106]. The main function of collagen is to provide structural support to the tissue in which it is present, but it is also known to sequester many factors required for tissue maintenance and regeneration. There are several different types of collagens, which can be isolated from a variety of sources. More than 80% of collagens in the body consist mainly of type I, II and III and share similar features in all species [107]. In human bodies, for example, 25 distinct collagen types have been identified up to date on the basis of protein and/or DNA sequence information [108]. Gelatin is also a natural polymer that is derived from collagen by means of controlled hydrolysis, and is commonly used for pharmaceutical and medical

applications. Generally, gelatin is of two types: Type A and Type B, depending on the hydrolysis condition of isolation from collagen. Today, these materials are obtained from animal sources, collagen being mainly extracted from bovine or porcine sources. Either because some animal diseases could be transmitted to human beings, or because of several religious interdictions, these sources cannot be used all over the world. As a consequence, the alternative sources of collagen, especially from aquatic animals including freshwater and marine fish and mollusks have been regarded more attentively. A recent paper reports a new fish source for collagen [109]. Because animal-derived collagens and gelatins can elicit immune responses in humans, recombinant collagens have been produced as an alternative [108].

For obtaining materials with mechanical enhanced properties starting from proteins, it is necessary to use different cross-linking methods, either physical or chemicals ones. As physical cross-linking agents there can be used gamma or UV radiations, the disadvantage being the possibility that the proteins be destroyed. Chemical cross-linking can lead to highly cross-linked materials in a very short time, but the unavoidable use of toxic cross-linkers or initiators causes a cytotoxicity problem. For this reason, new cross-linkings agents and new cross-linking methods are still studied [110].

Collagen-based devices have found themselves many biomedical applications such as implants, scaffolds for artificial organs, skin grafts and drug carrier systems [111]. Collagen can be used in many forms (e.g., porous matrices, films, gels, or monofilaments), alone or in composite materials. Collagen can form a variety of homogeneous composites with other biopolymers (e.g. chitosan, elastin), with synthetic polymers and also with inorganic materials. Collagen membranes can be produced by drying a collagen solution or a fibrillar collagen dispersion cast on a nonadhesive surface. Porous collagen matrices are generally obtained by freeze-drying an aqueous volume of collagen solution or dispersion. The freeze-dried porous matrix requires chemical cross-linking to stabilize the structure. Collagen gels may be formed by shifting the pH of dispersion away from its isoelectric point or by other techniques. Collagen filaments can be produced by extrusion techniques and by spinning and electrospinning [107, 112, 113].

The most important applications of collagen and gelatin concern regenerative medicine. Collagen matrices can be a major tool for cartilage, tendon or ligament repair, nerve and vascular repair [114-119].

At the same time, collagen and its composites could be used as wound dressings, for skin regeneration, especially for burns and for drug delivery systems [108, 120]. Here are some examples of medical applications of collagen or gelatin and of their composites as skin substitute.

Over the past 15 years, significant research has been focused on artificial epithelial, collagen being regarded as a promising material which can be used for dermal equivalents. Here are some examples of various dermal substitutes and materials which are currently used. Integra® is composed of a collagen/chondroitin sulfate porous scaffold and a silicone membrane, and has been widely applied for dermal regeneration. Apligraf® contains type I bovine collagen with cultured human fibroblasts and keratinocytes [121]. The dermal substitute Matriderm® is a collagen/elastin composite material which was found to be superior to other collagen sponges for wound healing [122]. A bilayer dermal equivalent (BDE) composed of a covalently cross-linked collagen chitosan sponge was tested to treat burn wounds in a pig model [121]. A new biological temporary skin cover Xe-Derma®,

derived from a cellular pig dermis, was tested for the treatment of superficial scald burns in children [123].

From the inorganic composites of collagen, those with hydroxyapatite are the most well known. They can be used for hard tissue repair or as drug delivery systems [124-125]. Collagen, which is the most prevalent structural protein in the human body, is a natural biomaterial which can be safely used in biomedical applications. In the future, tissue engineering will also benefit of collagen and its composites matrices.

2.2.2. Silk and Spider Silk

Silk fibers are typically composite materials formed of silk protein and other associated molecules such as glycoproteins and lipids. Many of their properties recommend them for biomedical applications. For example, silk proteins are biocompatible, biodegradable and can be processed from water solutions, which makes them much more attractive than other synthetic fibers like Kevlar.

Silk fibers produced by mulberry silkworms (*Bombyx mori*) are obtained at industrial scale and have already a variety of uses, including biomedical textiles. It would be hard to imagine better sources to obtain silk. And still, there is one, namely spiders. Approximately half of the 34,000 different species of spiders produce silk in order to catch their prey in webs. But to obtain this type of silk is a major provocation, because, in contrast to silkworms, there are new inherent problems. For example, it is impossible to farm spiders at large scale because of their cannibalistic nature [126, 127].

Therefore, the best option, for moving the application of spider silks forward, is to obtain genetically engineered analogues in sufficient yield and purity [128].

Silk proteins can be modified in order to obtain composite materials with new properties. Silkworm fibroin silk, for example, was modified using acid anhydride, and was also used to obtain graft copolymers with interesting properties [127]. In order to obtain composites with different other materials and different morphologies it is necessary to dissolve silk proteins in specific solvents. Processing techniques for silk composites are: dry/wet spinning, electrospinning for fiber obtaining, freeze-drying for hydrogels, electrospray drying for silk spheres and others [129]. Silk is a very versatile material which can be combined with synthetic polymers (nylon, poly(acrylamide), poly(acrilonitrile), poly(ethyleneoxide), poly(vinylalcohol), poly(aspartic acid), poly(ϵ -caprolactone, etc.), with biopolymers (collagen, gelatine, hyaluronic acid, alginate, cellulose, chitin, chitosan) to mention only the most known [129-134]. Silk protein and metal nanoparticles (as silver and gold) are also composite materials which have been obtained especially for their antimicrobial, electrical and magnetic properties [135, 136]. The possibility of biomineralization with calcium carbonate, calcium phosphate or silica was also demonstrated for tissue engineering applications [129].

The most important applications of silk fibers produced by silkworms are the following: first, they are used as suture in surgery, for wound dressings, tissue scaffolds and secondly, as drug delivery systems [137-146]. In all these applications silk proteins can be used as non-woven silk fibers, hydrogels, films, foams and even as nanoscale fibers [129].

Spider silk can be attractive for obtaining high-performance fibers and composites and has a large potential in medical textiles and biomedical applications.

2.3. Biopolymers Produced by Microbial Fermentation

Even if microbial fermentation is very well known, and if it has a wide range of applications, microbial biopolymers are not produced in high quantities, because of the high capital and energy costs. Two examples, with certain future application in medical textiles are given bellow.

2.3.1. Bacterial Cellulose

Cellulose can be produced by certain species of bacteria by fermentation, yielding a very pure cellulose product with unique properties. Bacterial cellulose (BC) is synthesized by several bacterial genera, like *Sarcina*, *Agrobacterium*, *Rhizobium* and *Acetobacter*. Among these, *Acetobacter xylinum* (reclassified as *Gluconacetobacter xylinum*) is the only species of bacteria known to be capable of producing cellulose in commercial quantities. BC is secreted as a ribbon-shaped fibril, less than 100 nm wide, which is composed of much finer 2–4 nm nanofibrils [147]. Bacterial cellulose is a water-insoluble material that has a very large surface area because of its large network of fibers. BC has an ultrafine, nanofibril network structure. BC microfibrils have a density of 1600 kg m^{-3} , Young's modulus of 138 GPa and tensile strength of at least 2 GPa, which are almost equal to those of aramid fibers [46]. It has also high water-holding capacity and a good biocompatibility. BC differs from plant cellulose in its higher purity, crystallinity (above 60%) and degree of polymerization (between 2000 and 6000), having a very good potential as biomedical material [148]. Bacterial cellulose can be obtained in static cultures or agitated cultures, the structure and properties of BC depending on the cultivation methods. For example, static culture is suitable on a small scale and agitated culture is more suitable for commercial scale production [149]. Figure 2 and Figure 3 present a BC pellicle obtained in a static culture and, respectively, a SEM image of a bacterial cellulose dry sheet.



Figure 2. BC pellicle obtained in a static culture (University Politehnica of Bucharest-Romania).

Because the production costs of bacterial cellulose are high, due to the low efficiency of the bacterial process, new cheap carbon sources are being tested, like fruit juices, konjac powder and waste from beer fermentation broth, to mention only the most recent contributions [150-152].

The physical properties of microbial cellulose can be controlled during synthesis. BC structure could be modified in combination with other substances, especially organic

polymers. A lot of composites have been obtained in situ, by modification of culture medium with water soluble polysaccharides as sodium alginate, chitosan, pectin gel, starch, xylocucan, Konjax glucomannan and other hemicellulosic polysaccharides, cellulose derivatives like carboxymethyl cellulose sodium salt, hydroxypropylmethylcellulose and even waste products like liginosulfonate [148, 149, 153-160]. From the synthetic polymers was tested a hydrophilic one, poly(vinyl alcohol), in order to obtain bio-nanocomposites [161]. Bacterial cellulose can also be used as raw material for composites manufacturing with organic and inorganic substances. For our purpose the most important are those with silver, for their antimicrobial properties, and with hidroxyapatite for the possibility to use them in bone healing applications [162-167].

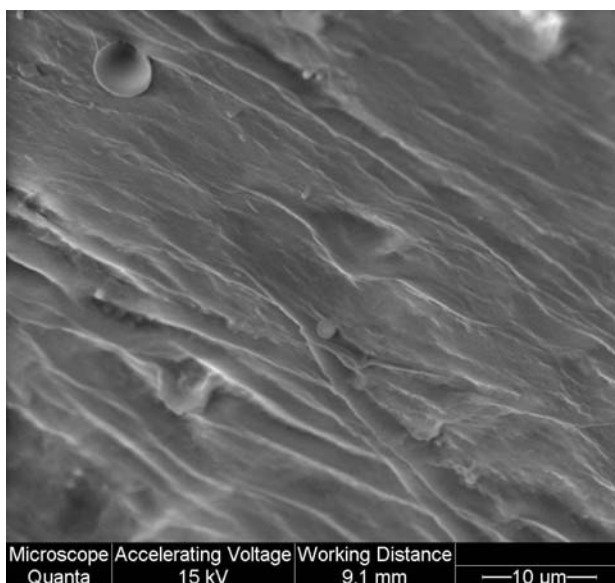


Figure 3. Scanning electron micrograph of a bacterial cellulose dry pellicle (courtesy of PhD Ghiurea Marius-ICECHIM Bucharest-Romania).

Bacterial cellulose with its distinctive nanofibrillar structure is considered a perfect matrix as an optimal wound healing environment and a temporary skin substitute in the therapy of difficult wounds, burns and ulcers [168]. BC is also a new scaffold material in tissue engineering cartilage, blood vessels and for bone replaces [169]. BASYC[®], a patented bacterial cellulose product, has been developed as microvessel for microsurgery [170]. Other commercial products from biocellulose already exist, such as Biofill[®], Bioprocess[®] and Xcell[®] used in the therapy of burns, ulcers as temporary artificial skin and Gengiflex[®] applied in treating periodontal diseases [168].

2.3.2. Polyhydroxyalkanoates

Polyhydroxyalkanoates (PHAs) are polyesters of various hydroxyalkanoates synthesized by many gram-positive and gram-negative bacteria, being accumulated as storage materials which allow microbial survival under stress conditions [171, 172]. They are biodegradable plastics having typical properties similar to those of thermoplastics. PHAs can be classified

into two groups depending on the number of carbon atoms in the monomer units: shortchain-length (SCL) PHAs, which consist of 3–5 carbon atoms, and medium chain length (MCL) PHAs, which consist of 6–14 carbon atoms [173]. PHAs are obtained by microbial fermentation using renewable resources such as sugars or plant oils as raw materials. Because the biggest drawback of mass production and applications of PHA is the cost of production, new routes are investigated to produce PHAs using recombinant microbes and transgenic plants in order to maximize the yield of PHA from a producer organism. These efforts are combined with the advances in fermentation and purification technology in order to reduce the production cost [174, 175]. The PHAs are non-toxic, biocompatible, biodegradable thermoplastics. They have a high degree of polymerization, are highly crystalline, optically active and isotactic (stereochemical regularity in repeating units), piezoelectric and insoluble in water [172]. Polyhydroxybutyrate (PHB) was the first PHA to be discovered and is also the most widely studied and best characterised. In this chapter there will be underlined only the biomedical uses of PHAs, even though their range of application is much wider. They can be used as cardiovascular products, for nerve and soft tissue repair, but also in drug delivery systems and wound managements, as surgical sutures and wound dressings [176]. Composite membranes between PHB and bacterial cellulose were recently reported [177]. The future of PHAs will be decided by economical considerations, and only when their prices will be close to that of other biodegradable plastic materials such as polylactide and aliphatic polyesters, they will go into competition with the other plastic materials.

2.4. Biopolymers Chemically Synthesized from Bio-Based Monomers

From this class, the most important biopolymers are polylactides, which belong to the family of aliphatic polyesters. Polylactides are characterized by biodegradability, biocompatibility and can, for this reason, be used in biomedical applications. A lot of effort is being made to tailor PLA with different architectural characteristics in order to enhance its uses in biomedical applications [178]. The monomeric precursor for obtaining PLA is lactic acid, which can be produced by carbohydrate fermentation; either using especially strains of *Lactobacillus* or via petrochemical feedstocks. The first route is commonly used and the market for fermentation lactic acid is growing every year, because lactic acid is used to obtain not only bio-based polymers like polylactides, but also other value added chemicals [179, 180]. Poly(lactic acid) can be manufactured by different polymerization routes as: polycondensation and ring-opening polymerization (ROP). Condensation polymerization is the least expensive one, but is difficult to obtain high molecular weights [178]. The advantages of ROP over polycondensation route are: milder reaction conditions, shorter reaction times, absence of reaction by-products. In this way it is easier to obtain high molecular weights [181]. A large number of copolymers based on lactic acid have been prepared by ring-opening copolymerization, modification by high energy radiation and peroxides or by graft polymerization. By ring-opening copolymerization, glycolide and ϵ -caprolactone are the most utilized comonomers which can be incorporated into lactic acid based polymer [182]. The transformation of PLA and its copolymers in textile structure for biomedical application is complicated. A brief enumeration of the processes which can be applied for polymers extrusion into monofilament and multifilament is: melt spinning, dry spinning, wet spinning and dry-jet-wet spinning. Commercially PLA fibres are generally

produced using the melt spinning technique [178, 183]. There is no doubt that properties of the fibres are influenced by the processing methods. Electrospinning is also used to obtain PLA fibres with a diameter varying from micrometer to nanometer. Electrospun fibres of PLA have been successfully used for tissue engineering and for biomedical applications [183].

The advantages and disadvantages of different methods are intensively discussed in many papers [178, 179]. For example, even electrospinning is intensively investigated in different research laboratories, though for the moment it is not a commercial technique, but there is no doubt that in the future electrospinning will be used to obtain PLA nano-fibers in pharmaceutical and biomedical applications [183].

PLA fibers are used in different textile applications as, for example, non-woven textile for clothes, and as resorbable surgical sutures and meshes. PLA can be used alone or also in composites with nanoclay and TiO_2 as potential reconstruction matrices in tissue engineering [183-185]. It can be fabricated in different shapes like filament, braided, knitted, nonwoven or film, as required by the organ construction [178]. PLA can be also used in micro and nanoparticles for delivery systems used in medicine [186]. Among its copolymers, PLGA (copolymer of PLA with glycolic acid) is an ideal biomaterial for temporary medical applications, such as controlled drug/protein delivery systems and as scaffolds for tissue engineering [179, 187, 188].

2.5. Emerging Techniques for Biomedical Textiles

2.5.1. Biotechnology

Before offering a definition of biotechnology in connection with textile industry, perhaps we should start with a question which gives the title of a recent paper: Is biotechnology a new alchemy? Even though it is difficult to find the correct answer, one argument is that both alchemy and biotechnology promise to provide a transformation of fundamental aspects of the human condition [189]. Biotechnology comprises three distinct fields of activity, namely genetic engineering, protein engineering and metabolic engineering. A fourth discipline, known variously as biochemical, bioprocess and biotechnology engineering, is required for commercial production of biotechnology products and delivery of its services [190]. For textile industry, biotechnology can act in the following directions: development of new types of textile fibers and other textile materials, application of enzyme technology in textile processing and treatment of textile effluents [191]. Only the first and the second directions will be discussed, these ones being related with medical textiles.

New materials with potential applications in the biomedical field could be obtained through fermentation. Microbial fermentation was already presented for bacterial cellulose and poly(hydroxyalkanoates) production. Even though they remain relatively expensive, their production and use are environmentally sustainable. Substantial effort is underway in developing improved production of poly(hydroxyalkanoates) (PHAs), bacterial cellulose and other biodegradable, renewable, biopolymers [190]. There are also plans to synthesize PHA in transgenic plants [192].

In view of the recent progress in molecular plant biology, it is expected that new textile plants varieties will be generated in the future, among these being flax and hemp [193].

Fibrous protein could also be obtained using genetic engineering, spider silk being the first in line [128, 194].

The most rapidly growing biotechnology sector for textile industry is by far the use of enzymes in textile processing. Advances in biotechnology have made it possible to tailor special enzyme mixtures for specific applications. The possibility of replacing alkaline scouring with the enzymatic decomposition of cotton impurities, using various types of enzyme—cellulases, pectinase, lipases and proteases under different applications, has been studied [195]. The uses of the enzymes have benefited both the textile industry and the environment [196]. The most well known enzymes used in textile industry are: cellulase, amylase, pectate lyase, catalase and laccase. The use of laccase in the textile industry is growing very fast, since laccase is used not only to decolourise textile effluents but also to bleach textiles and even to synthesize dyes. Two earlier commercial products can be mentioned: DeniLite®, the first industrial laccase and the first bleaching enzyme acting with the help of a mediator molecule from Novo Nordisk (Denmark) and Zylite, developed by Zytex company (Zytex Pvt. Ltd., Mumbai, India), capable of degrading indigo in a very specific way [197]. Cellulases have achieved their worldwide success in textile and laundry because of their ability to modify cellulosic fibers in a controlled and desired manner, in order to improve the quality of fabrics [198]. Today several commercial preparations are available for biostoning and biofinishing cotton fabrics [199, 200]. Even if the greatest number of enzyme applications is focused on cotton, wool fibers could also benefit from enzymatic treatment in order to improve their physical and mechanical properties [201, 202].

2.5.2. Nanotechnology

Nanotechnology is a revolutionary technology which has a multidisciplinary character, affecting many traditional technologies, scientific disciplines and industries. It represents a technology which changed the scale from micro to nano, having a huge potential in many areas of scientific research and technological applications. The unique properties of nanomaterials and structures on nanometer scale have sparked the attention of many researchers and materials developers. At nano-scale the properties of the materials are significantly different from those of the same materials in bulk or macroscopic form [203, 204]. Nanotechnology is considered the second industrial revolution of the world. It is no wonder that nanotechnology by its innovative character has spread in many fields of activity. Nanotechnology offers a large portfolio of products and textile industry can benefit of this offer. Using nanotechnology production techniques, one can obtain atomic clusters/compounds like carbon nanotubes, nanoparticles, nano-thin films (e.g. nanocoatings, self-assembling monolayers and nanowires), nanofibers (as carbon fibers, polymer fibers, textiles, nanoyarns) and nanostructured materials (nanocomposites which are in conjunction with all of above) [205].

In the medical textiles field, nanotechnology could be applied for obtaining nanofibers and nanocomposites with a great added value, for obtaining nanoparticles and nanocrystals which are very useful in drug delivery, for enhancement of mechanical, chemical and functional properties of fibers and yarns and for improving fabric finishing also by creating nanomaterials which are additives in textile production. There are two ways to approach the nanoscale: the ‘top-down’ approach, by reducing the size of the smallest structures towards the nanoscale and the ‘bottom-up’ techniques which involve manipulating individual atoms

and molecules. Bottom-up nano usually implies controlled or directed self assembly of atoms and molecules into nano structures [205].

Because the number of nanotechnology applications in medical textiles field is increasing, only the most important research directions will be emphasized: obtaining nanofibers, enhancing the mechanical and functional properties of fibers and yarns (e.g. nanocoating, developing antimicrobial properties, UV protecting, auto-self cleaning), producing nanostructures for drug delivery and nanoscaffolds for tissue engineering. Only a few words will be dedicated to nanocomposites, because this is another large field of nanotechnology.

Nanofibers and nanofiber matrix composites have been studied extensively for their use in drug delivery and tissue engineering applications. Several fabrication methods for nanofibers have been developed, these ones including drawing, tubes by fiber templates synthesis, membrane/ template-based synthesis, phase separation, electrochemical polymerization, self-assembly, co-electrospinning and electrospinning. These techniques are largely discussed in a comprehensive review from 2007 [206]. Because the most part of these nanofibers are synthesized by electrospinning polymers from their solutions, this technique will be described separately. Several materials which can be electrospun into nanofiber were already presented. A brief enumeration is: biodegradable polymers such as PLGA and poly(caprolactone) (PCL), water-soluble materials such as poly(ethylene oxide) (PEO), polyvinyl alcohol (PVA), and natural polymers such as collagen, silk protein and others.

Nanotechnology can also develop diverse fiber functionalities for special applications, including medical field. A first and very large class of functional textiles is that of antimicrobial textiles.

Several different types of antimicrobial agents, such as oxidizing agents, coagulants, diphenyl ether (bis-phenyl) derivatives, heavy metals and metallic compounds, chitosan and quaternary ammonium compounds (QACs) could be used in textile industry for obtaining antimicrobial textiles [207]. Two different routes were tested in order to produce antimicrobial fibers or fabric. The first one is the addition of an antimicrobial agent to the polymer melting or solution before extrusion or spinning [208]. The second one is the post treatment of the fiber or fabric during finishing stages. From the antibacterial agents already presented, the most investigated, until now, are inorganic nano-particles and their nano-composites. An excellent recent review discusses the advances of the application of inorganic nano-structured materials for textile modification [209]. The inorganic nano-structured materials include titanium dioxide, silver, zinc oxide, copper, gallium, gold nano-particles, carbon nanotubes, nano-layered clay and their nano-composites. The most widely used are silver and titanium dioxide nano-particles. Several methods have been developed for surface modification of fibers or fabrics such as sol-gel process, RF (radio-frequency) or MW (microwave) plasma, UV (ultraviolet) irradiation, ultrasound irradiation, pad-dry-cure method, and polyelectrolyte self-assembled multi-layers to quote only a few [209-212]. An innovative method to obtain nano-particles, method which concerns silver, is to use nanobiotechnology. Silver nanoparticles colloid was prepared by making use of biomass filtrate of fungus *Fusarium solani* [213].

Perhaps the greatest immediate impact of nanotechnology in medicine is drug delivery. Nanoparticles have been widely used to deliver drugs, polypeptides, proteins, vaccines, nucleic acids, genes and so on. As a drug delivery system, nanoparticles can entrap drugs or biomolecules into their interior structures and/or absorb drugs or biomolecules onto their

exterior surfaces. Though there are several drug systems available, the most of the research studies are focused on biopolymer materials, due to their biocompatibility and biodegradability. From the anorganic systems used in drug delivery, carbon nanotubes (after chemical modification) and silica nanorods could be mentioned [206]. Many polymeric materials have been tested with success for drug delivery, including poly(lactic acid), poly(glycolic acid), poly(caprolactone), polysaccharides (particularly chitosan), poly(acrylic acid) family, proteins or polypeptides (such as gelatin, collagen). Among them, polysaccharides are the most popular polymeric materials able to prepare nanoparticles for drug delivery [214, 215].

Nanotechnology, there is no doubt, has the potential for the development of new materials, including biomedical textiles, but it is necessary to discuss also the adverse effects of nanomaterials on biological systems. Recent research has proved that there may be significant unhealthy effects associated with exposure to carbon nanotubes, to give only one example [206, 216].

2.5.3. Electrospinning

The interest for electrospinning is increasing every year, because it is a very promising technique due to its versatility. A large variety of polymers and copolymers were transformed via electrospinning in fibers in the submicron range, a performance which is difficult to achieve by other spinning technologies. Very comprehensive review articles mentioning not only the fundamentals of electrospinning, but also the recent developments and applications of this technique, were already published [96, 107, 217, 218]. Briefly, in electrospinning, a high electric field is applied to create electrically charged jets of a polymer solution or melt. These jets are accelerated between the electrodes, leading to the formation of continuous fibres with diameters ranging from 2 nm to several micrometers [219]. This process offers unique possibilities for producing novel natural nanofibers and fabrics with controllable pore structure with many applications. Some selected examples related to biomedical field are: tissue engineering, wound dressings, drug delivery, and enzyme immobilization. The process of 'electrospinning' was first investigated by Zeleny in 1914 and regained attention in the 1990s partly due to an interest in nanotechnology, as the process allowed the easy fabrication of fibers with nanoscale diameters from various polymers [107]. The factors that significantly affect the process of electrospinning are numerous, being discussed in many papers [218, 220, 221]. A brief enumeration is: substrate and solution related parameters, process related parameters and environment related parameters. The principal parameters to control fibres characteristics are: the polymer solution properties, the applied field, the distance between electrodes and the flow rate of solution during electrospinning. It is thus very important to know as much as possible about the correlations between the parameters which are directly controlled in electrospinning and the secondary ones which define the performance of the nonwovens. The results obtained until now suggest that one is able to design electrospun nanofiber based nonwovens with predetermined properties and functions in a highly controlled way [218, 222]. The most important applications of electrospun fibers are in the field of regenerative medicine. They have been used to fabricate scaffolds for various tissues such as bone, cartilage and cardiac muscle [223, 224]. Electrospinning generates loosely connected 3D porous mats with high porosity and high surface area which can mimic extra cellular matrix structure, their aspect having a crucial importance for tissue engineering. Two main directions are now followed by the researchers which are working in this field:

formation of non-woven mats of different biomaterials to biomimic physical dimensions of native extracellular matrix and modification of the electrospinning process for the mimicking of extra cellular matrix [217]. A lot of synthetic and natural polymers have been electrospun for obtaining non-woven materials for biomedical applications. Typical natural polymers include collagen, chitosan, gelatin, casein, cellulose acetate, silk protein, chitin, fibrinogen, hyaluronic acid, etc. [107, 217, 225-229]. Some representative synthetic polymers electrospun for biomedical applications are the following: poly(lactide) (PLA), poly(glycolic acid) (PGA), poly(caprolactone) (PCL), polycarbonate, poly(ethylene glycol) (PEG), poly(ethyleneimine), poly(urethane) (PU), poly(vinyl alcohol) (PVA) [107, 217].

Despite the several advantages offered by electrospinning, some disadvantages should be also underlined. The scales up of nanofibers through single jet are not very feasible and for several of its applications require large quantities of fibers. Other disadvantages are: it is difficult to obtain fibers with the same diameter, the productivity is quite low, the range of the resulting fibers is usually limited to the upper range of natural extra cellular matrix and it is difficult to control the complex architecture of these matrices. But in spite of these drawbacks the conclusion is an optimistic one, electrospinning process being a promising candidate for tissue engineering and regenerative medicine [107].

2.5.4. Wound Dressings

Wound management products constitute a growing field, due to the fact that basic health care services have been improved in the last decade and more and more people all over the world became interested in healthcare. A wound can be defined as a trauma caused by physical means whose result is the disruption of normal continuity of tissues and structures. This tissue break can be produced by different injuries, surgical operations or chronic diseases. There are a wide-ranging amount of devices for wound care, and they continue to diversify, as the number of wound dressings and adhesives is rapidly increasing [230]. This multitude of wounds and wound care products complicates the dressing selection process. At present there are a great number of different dressings and techniques available for managing wounds. For this reason, a classification of wound dressings is rather difficult to be done. Because modern dressings are designed to help the healing wound process, a good criterion may be the interaction between wound and wound dressing. From this point of view, wound dressings could be divided into main groups: inert/passive and interactive which contain a dynamical subclass of bioactive dressings [231]. Inert dressing can be sub-classified into absorbing and non-absorbing dressings. The interactive dressings can be absorbing, non-absorbing and moisture donating [232].

Another classification was proposed by Food and Drug Administration of the United States of America (FDA) in 1999. After FDA there are 5 categories of wound dressings: (1) Non-resorbable gauze/sponge dressing for external use, (2) Hydrophilic wound dressing, (3) Occlusive wound dressing, (4) Hydrogel wound and burn dressing and (5) Interactive wound and burn dressings.

If one considers the dressing structure (one layer, multi-layer), the dressings may be classified in (1) primary dressing (it comes in physical contact with the wound), (2) multi-layer dressings with a very large subclass of bi-layers dressings and (3) island dressings (a dressing that is constructed with a central absorbent portion surrounded by an adhesive portion).

However, the most frequently used classification is based on the nature of the material used for wound dressings. Following this way, the wound dressing can be made of natural, synthetic or semi-synthetic materials. Modern wound dressings are increasingly demanding modern textile products. Textiles used for wound dressings include: fibers and nanofibers, filaments, yarns, woven, knitted, non-woven materials and other materials [233]. Fibers used in wound care can be grouped into two main classes: biopolymers and synthetic polymers. From the first class, the most important fibers are: cotton, silk, linen, cellulose, alginates, chitin/chitosan, hyaluronan, collagen, silk (spider, silkworm), polylactides and bacterial cellulose. From the second class, there can be mentioned: polyester, polyamide, polypropylene, polyurethane, etc. A brief review, especially of the advanced wound dressings, will be done in this chapter.

For many years, the dressings were passive or inert dressings. The traditional materials used were gauze (a woven fabric of absorbent cotton) and tulle. Now, these materials are not that common, because of some disadvantages as: inability to prevent microbial invasion, adherence to the wound surface, low absorption of wound exudates, not proper permeability of gases, dry environment for wound and usage only for minor wounds [230]. Even if they have very limited use as primary dressing, some of them can be helpful as secondary dressings. Gauze is now available in a large number of formats and materials, including cotton or synthetic, non-impregnated, and impregnated with different substances designed to help sterility or to speed healing process [230].

It was believed, at first, that one of the most important aspects in the process of wound healing was to keep the wound dry. But in a dry wound, the production of granulation tissue is reduced and the advancing epithelium must burrow beneath the eschar or scab. A revolutionary idea was the concept of moist wound healing, this changing the nature of wound dressing materials [234]. From a historical point of view it is necessary to mention the pioneering works of Winter (1962) [235] and of Hinman and Maibach (1963) [236], who enunciated for the first time the principles of moist wound healing. A moist environment encourages granulation, reduces tissue, and results in improved rates of healing. Today, the most modern wound dressings keep wound tissues moist. These types of dressings can be divided in three performance categories: dressings that absorb excessive wound exudate, dressings that maintain the existing level of tissue moisture and those that add moisture to the tissue [234].

The most important and growing class of wound dressings belong to the interactive/bioactive dressings. These interactive wound dressings play a major role in healing, because they interact with the biochemical environment of the wound. From the first generation of interactive dressings one can enumerate the following types: semi-permeable films, foams, alginates, hydrocolloids, hydrogels and hydroactive.

Semi-permeable films are thin transparent polyurethane or other synthetic polymer sheets, which are permeable to gas and water vapor, but are a barrier to bacteria and water. Onto these films there is a special adhesive, which does not come in physical contact with the moist surface of the wound. As dressing brand names, the following should be mentioned: Aqua protects film, Transeal, Tegaderm, Bioclusive, Opsite, Polyskin, etc. [232].

Foams dressings are highly absorbent synthetic foams, especially polyurethane foams, being an attempt to solve the problem of wound adherence encountered with perforated film dressing. Foams are available in sheet or cavity filling shapes. Their main application is to absorb excess exudates, reducing the risk of maceration and the need for dressing changes

[232]. They can be used in combination with a hydrogel for necrotic wounds which require debriding. Some examples of this product are: Allevyn, Cavi-care, Hydrosorb, Curafoam, Lyofoam, Optifoam, Soft-foam.

Alginate dressings (consisting of calcium alginate or of a combination of sodium and calcium alginate) are highly adsorbent and biodegradable. They are similar to hydrocolloid dressings because they interact with wound fluid to form a nonadherent gel. They are made of woven or nonwoven fibers. They are primary dressings, which need to be covered by a secondary dressing. The fibrous nature of most alginates can leave residual fibers in the wound if there is insufficient wound exudate to gel the fibers. They are not antimicrobial, but antibiotics and other antimicrobial substances can be incorporated in their structure [231, 232, 237]. Some examples of alginates dressings were already given, others being: Algosteril, Fybron, SeaSorb, Gentell, and the enumeration could continue.

Hydrocolloids dressings contain gel-forming agents such as sodium carboxymethylcellulose and gelatine, attached to a foam sheet or a thin polyurethane film. Hydrocolloids are also available in paste and powders for increased adsorption and for reducing dead space in the wound cavity. Hydrocolloids are used in multilayer structures, which consist of an outer layer to provide protection and a supporting material (film, foam or fabric). The hydrocolloids absorb exudates and help to debride the wound. Hydrocolloid dressings are used for leg ulcers, minor burns, pressure sores, and traumatic injuries. Because they are not painful to remove, hydrocolloid dressings are often employed in pediatric wound management. A few brand names could be mentioned: Comfeel, CombiDERM, DuoDerm CGF Hydrocoll, Tegaseb, etc. [230, 232].

Hydrogel dressings are insoluble polymers (e.g. 2-hydroxyethyl methacrylate (HEMA), polyethylene oxide, starch - grafted copolymer, polyvinyl alcohol copolymers) that expand in water and are able to absorb large amounts of wound fluid. Not only synthetic polymers have been used as hydrogels wound dressings. From natural polymers, chitin/chitosan and collagen are the most commonly used as wound dressings, along with textile materials. Even if chitin is insoluble in most of the organic solvents because of its rigid crystalline structure, it can be dissolved in a solvent system consisting in calcium chloride dehydrate saturated methanol (Ca solvent). The obtained hydrogels can be used for wound dressing [238]. Not only chitosan, but also its derivatives could form hydrogels with biomedical applications. A recent example is a complex between β -glucan and chitosan (CS), which is considered by the authors who proposed it to be superior to Beschitin[®] W, a commercial wound dressing made from CS [239]. Another example is polyelectrolyte complex (PEC), which consists of chitosan as a cationic polyelectrolyte and γ -poly (glutamic acid) (γ -PGA) and which can be used as wound dressing material [240].

Most hydrogel dressings require an outer bandage or wrap to secure them to the wound surface. Hydrogels are relatively easy to apply to flat wound surfaces. Hydrogels and hydrocolloids have been used to deliver antimicrobial agents. The main disadvantage of hydrogels is their poor mechanical strength [230, 232, 237]. Some examples could be mentioned: Purilon Gel, Curafil, Curagel, DuoDERM, Hypagel, Flexigel, Sterigel and many others.

A second generation of interactive/bioactive dressings is already proposed as an alternative to the first generation. From this class, the most important are antimicrobial dressings. The antimicrobial compounds that are used include traditional antibiotics as well as organic antimicrobials such as triclosan, and inorganic compounds such as silver and titanium

dioxide. Silver has been in use since ancient times in the form of metallic silver, silver nitrate, silver sulfadiazine for the treatment of burns, wounds and several bacterial infections. Afterwards it has been overshadowed by the discovery of antibiotics, but this did not last long: it came back along with the emergence of nanotechnologies, which rendered it available in the form of silver nanoparticles. Though silver in its metallic state is inert, it reacts with the moisture in the skin and the fluid of the wound and gets ionized. This ionized silver is highly reactive, leading to microbial death [241]. The antibacterial, antifungal and antiviral properties of silver ions, silver compounds and silver nanoparticles have been extensively studied. Even if silver impregnated dressings are commercially available, the researchers are still developing new dressings containing silver in different forms, testing their efficiency especially for burns [73, 242, 243]. Examples of silver-impregnated dressings include the following antimicrobial dressings: Silvercel, Algicell, Calgitrol, Seasorb - Ag, Sorbsan Silver, Silverlon CA (with alginate), Actisorb 220 (charcoal impregnated), Aquacel Ag (hydrofibers), Contreet-H (hydrocolloid) [232, 237]. Other examples of second generation interactive/bioactive dressings are: cadexomer iodine, hydrofibers, silicon and honey dressings [232]. Wound dressings will advance for the enhancement of wound healing using new materials and new technologies moving beyond tissue engineering. Some attempts have been already done by temporary skin substitutes.

2.6. Advanced Materials as Scaffolds for Tissue Engineering

Tissue engineering is a multidisciplinary field, the aim of which is to control and regulate the potential of natural tissue regeneration for defect repair or even organ regeneration [244]. Tissue engineering has also diagnostic applications, being used to test the interaction between different drugs and tissues. Tissue engineering is also used in connexion with regenerative medicine. The first is a more technical concept of tissue and organ reconstruction by use of cells, scaffolds and biomolecules, while the second is focused on the support of self healing capabilities and the use of stem cells [245]. The most important research areas in tissue engineering are in the field of: cell, tissue, and organ culture, scaffolds obtaining and bioreactors design and operation. A significant part of tissue engineering efforts has been devoted to obtain scaffolds (defined as cells placed on or within matrices). One specific design objective of a porous scaffold for tissue engineering is to fabricate a porous scaffold out of absorbable polymer that mimic the extracellular matrix in supporting cell proliferation and organization [244]. Scaffolds used in tissue engineering must be first of all biocompatible and biodegradable, and for this reason they can be obtained only by using biomaterials. From the large class of biomaterials, biocompatible and biodegradable polymers constitute the first option. Their function is to guide complex multicellular processes of tissue formation and regeneration by providing three-dimensional scaffolds. Polymers used for making scaffolds belong either to the class of biopolymers, or to the class of synthetic polymers. The former includes: polysaccharides (alginates, chitin, chitosan, cellulose, starch), proteins (collagen, gelatin, silk), biopolymers obtained by microbial fermentation (bacterial cellulose) and biopolymers synthesized from bio-based monomers and their co-polymers (poly(lactic acid) (PLA), poly(glycolic acid) (PGA), poly(lactic-coglycolic acid) (PLGA) [55,69,246,247]. The latter includes frequently: poly(ϵ -caprolactone)(PCL), polyurethane, polyanhydrides, polycarbonates, polydioxanone and co-polymers (e.g. poly(lactic-cocaprolactone) (PLA-CL),

poly(propylene fumarate)). Specific applications, like bone regeneration, demand composite materials containing polymers or copolymers and inorganic materials as hydroxyapatite or tricalcium phosphate [244, 248].

A number of techniques have been explored to fabricate biodegradable polymers into 3D porous scaffolds with different properties. One of the most common techniques is particulate - leaching, also named solvent-casting method. This technique implies that a porogen material (salt, sugars, or polymer spheres) be dispersed in a matrix consisting of the scaffold material dissolved in an organic solvent. After solvent evaporation, there remains a composite of the polymer and of porogen. The composite is then immersed in water until complete dissolution of the porogen occurs, resulting in a porous scaffold. To prepare scaffolds with well-controlled interconnected porous structures, there are used paraffin spheres or sugar spheres as alternative porogen materials to salt particles. In this case, a thermal treatment was applied to form a bound template. Other techniques are: emulsion freeze-drying, thermally induced phase separation, 3D printing, gas foaming, solid free-form [244, 248, 249]. Collagen is the primary structural protein of the native ECM and for this motive it was widely investigated as scaffold for cell attachment, proliferation and differentiation. Collagen is hard to process, the extent and rate of degradability is hard to control and it has weak mechanical properties. Because of these disadvantages researchers have enhanced their efforts to obtain scaffolds which mimic the physical architecture of natural collagen. In this way, a new generation of nanofibrous scaffolds for tissue engineering was born. As technologies for nanoporous scaffolds fabrication there can be mentioned: self-assembly, modified TIPS (thermally induced phase separation) and electrospinning [244, 249-251]. A chitosan nanoscaffold in the form of a colloidal solution was obtained from the deacetylation of chitin whiskers under alkaline conditions by using a microwave technique [252]. From the multitude of applications of tissue engineering, only the most important will be shortly described.

Tissue engineering bone is one of the areas that have gained considerable attention, because there are a lot of diseases and traumas which can affect bone structure and functionality. Bone is a composite material consisting of minerals, matrix, cells, and water. Type I collagen is the principal component of the organic matrix of the bone, accounting for approximately 30% of the dry non demineralized matrix. There have been significant advances in the development of bone scaffolds with various compositions and 3-dimensional configuration. Numerous artificial tissue substitutes containing biomaterials were used for bone repair. According to their composition they can be classified mainly in three categories: bioactive inorganics, degradable polymers and their composites/hybridized forms [250]. Among bioactive materials are inorganic compounds such as bioceramics, including selected compositions of silicate glasses and glass-ceramics, as well as hydroxyapatite (HA) and related amorphous or crystalline calcium phosphates. Properties of ceramic materials can be influenced by the fabrication process. Like most ceramic materials, the major disadvantage of bioactive ceramics is their low fracture toughness (i.e. brittleness) [253]. They are thus often used combined with other polymers and especially for tissue engineering applications with biodegradable polymers. From the class of polymers, the most widely used is collagen. Nevertheless, collagen is a poor bone graft material when used alone.

Since collagen extracted from natural sources is known to elicit immunogenic responses upon implantation, the direct use of natural collagen has become limited. Instead, purified collagen or reconstituted collagen, which causes relatively low immunogenic responses, can represent a solution [244]. Other polymers which can be used extensively for the preparation

of bone and cartilage scaffolds belong to the class of polyhydroxyacids-for example polylactides, polyglycolides and their copolymers [254]. On the lowest level, bone extracellular matrix (ECM) consists of a highly organized nanocomposite of collagen type I fibrils and mineral phase hydroxyapatite (HAP). For this reason, in order to mimic this matrix only composite materials are successful. The first choice was biomineralized collagen with hydroxyapatite. Using the mineralized collagen fibrils as a starting material, several types of 2D and 3D scaffolds have been developed over the past years [255]. Other biocomposites containing polymer and inorganic materials are: PDLA/Bioglass[®], PLGA/hydroxyapatite, poly(hydroxybutyrate-cohydroxyvalerate)/inorganic phase composite [253].

Skin plays a crucial role in protecting the human body against the environment, dehydration, and infectious agents, being the body's largest laminar organ. Loss of large portions of skin integrity from burns, wounds, or diseases may produce significant disabilities or even death. Tissue-engineered skins provide an option to treat skin loss in many different forms: autologous and allogenic keratinocyte grafts, acellular biological matrices and cellular matrices including biological substances [218]. Conceptually, skin substitutes may be classified as permanent or temporary; epidermal, dermal or composite; and biological or alloplastic (synthetic) [256]. To obtain skin substitutes the material choice is a serious challenge, because from the many natural and synthetic existing materials, only a small number have interesting properties. From the class of biological materials, collagen is widely investigated and commercial products containing collagen have been produced. For example, Integra Life Sciences developed Integra[®] which consists of a collagen layer in a matrix with a silicon overlay. Bilayered collagen gels seeded with human fibroblasts in the lower part and human keratinocytes in the upper layer have been used as the 'dermal' matrix of an artificial skin product, being commercialized by Organogenesis in USA under the name of Apligraf[®] [2]. Biobrane[®] consists in a nylon film and hydrophilic type I porcine collagen, which is covalently bound to the hydrophobic inert nylon [257].

It is obvious that even if a lot of commercial applications of tissue engineering are already on the market, being successfully used, the discoveries in the field of tissue engineering and regenerative medicine will continue.

CONCLUSION

The future of biomedical textiles is rising from the activities of research of our days, research which has permanently in view the fact that biomedical textiles are essential for human healthcare. New materials and new technologies are already available and they will transform medical textiles into innovative products. But there is no doubt that tremendous efforts are still necessary in the next years in order to transform scientific research in commercial products and in new therapies for healthcare. What matters the most is that the first steps were already done and the new generation of biomedical textiles is already born.

ACKNOWLEDGMENTS

Among many colleagues from Chemical Engineering Department (UPB) the author is especially grateful to PhD Marta Stroescu for helpful suggestions.

REFERENCES

- [1] Knill, C.J., Kennedy, J.F., Mistry, J., Miraftab, M., Smart, G., Groocock, M.R., and Williams, H.J. (2004). Alginate fibres modified with unhydrolysed and hydrolysed chitosans for wound dressings. *Carbohydrate Polymers*, 55: 65–76.
- [2] Malafaya, P.B., Silva, G.A., and Reis, R.L. (2007). Natural-origin polymers as carriers and scaffolds for biomolecules and cell delivery in tissue engineering applications. *Advanced Drug Delivery Reviews*, 59: 207–233.
- [3] Rinaudo, M. (2008). Polyelectrolytes derived from natural polysaccharides. In: *Monomers, polymers and composites from renewable resources*, Elsevier, p. 502–506.
- [4] Qin, Y. (2008). The gel swelling properties of alginate fibers and their applications in wound management. *Polymer Advanced Technology*, 19: 6–14.
- [5] Dettmar, P. W., Strugala, V., and Richardson, J. C. (2011). The key role alginates play in health. *Food Hydrocolloids*, 25: 263–266.
- [6] Draget, K. I., and Taylor, C. (2011). Chemical, physical and biological properties of alginates and their biomedical implications, *Food Hydrocolloids*, 25: 251–256.
- [7] Paul, W., and Sharma, C.P. (2004). Chitosan and alginate wound dressings: A short review. *Trends in Biomaterials and Artificial Organs*, 18: 18–23.
- [8] Divya Rani, V.V., Ramachandran, R., Chennazhi, K.P., Tamura, H., Nair, S.V., and Jayakumar, R. (2011). Fabrication of alginate/nanoTiO₂ needle composite scaffolds for tissue engineering applications. *Carbohydrate Polymers*, 83: 858–864.
- [9] Sikareepaisan, P., Ruktanonchai, U., and Supaphol, P. (2011). Preparation and characterization of asiaticoside-loaded alginate films and their potential for use as effectual wound dressings. *Carbohydrate Polymers*, 83: 1457–1469.
- [10] Wang, Q., Hu, X., Du, Y., and Kennedy, J.F. (2010). Alginate/starch blend fibers and their properties for drug controlled release. *Carbohydrate Polymers*, 82: 842–847.
- [11] Cunha, A.G., and Gandini, A. (2010). Turning polysaccharides into hydrophobic materials: a critical review. Part 1. Cellulose. *Cellulose*, 17: 875–889.
- [12] Sun, X.F., Sun, R.C., Fowler, P., and Baird, M.S. (2004). Isolation and characterization of cellulose obtained by a two-stage treatment with organosolv and cyanamide activated hydrogen peroxide from wheat straw. *Carbohydrate Polymers*, 55: 379–391.
- [13] Reddy, N., and Yang, Y., (2005). Structure and properties of high quality natural cellulose fibres from cornstalks. *Polymer*, 46: 5494–5500.
- [14] Biswas, A., Shah, B.C., Lawton, J.W., and Willett, J.L. (2006). Process for obtaining cellulose acetates from agricultural by-products. *Carbohydrate Polymers*, 64: 134–137.
- [15] Agblevor, F.A., Ibrahim, M.M., and El-Zawawy, W.K. (2007). Coupled acid and enzyme mediated production of microcrystalline cellulose from corn cob and cotton gin waste. *Cellulose*, 14: 247–256.

-
- [16] Cerqueira, D.A., Filho, G.R., and Meireles, C.S. (2007). Optimization of sugarcane bagasse cellulose acetylation. *Carbohydrate Polymers*, 69: 579–582.
- [17] Huda, S., Reddy, N., Karst, D., Xu, W., Yang, W., and Yang, Y. (2007). Nontraditional biofibers for a new textile industry. *Journal of Biobased Materials and Bioenergy*, 1: 177–190.
- [18] Reddy, N., and Yang, Y. (2009). Natural cellulose fibers from soybean straw. *Bioresource Technology*, 100: 3593–3598.
- [19] Reddy, N., and Yang, Y. (2009). Properties of natural cellulose fibers from hop stems. *Carbohydrate Polymers*, 77: 898–902.
- [20] Shaikh, H.M., Pandare, K.V., Nair, G., and Varma, A.J. (2009). Utilization of sugarcane bagasse cellulose for producing cellulose acetates: Novel use of residual hemicellulose as plasticizer. *Carbohydrate Polymers*, 76: 23–29.
- [21] Siró, I., and Plackett, D. (2010). Microfibrillated cellulose and new nanocomposite materials: a review. *Cellulose*, 17: 459–494.
- [22] Dufresne, A. (2008). Cellulose-based composites and nanocomposites. In: *Monomers, polymers and composites from renewable resources*, Elsevier, p. 402–416.
- [23] Siqueira, G., Bras, J., and Dufresne, A., (2010). Cellulosic Bionanocomposites: A Review of Preparation, Properties and Applications. *Polymers*, 2: 728–765.
- [24] Adel, A.M., El-Wahab, Z.H.A., Ibrahim, A.A., and Al-Shemy, M.T. (2011). Characterization of microcrystalline cellulose prepared from lignocellulosic materials. Part II: Physicochemical properties. *Carbohydrate Polymers*, 83: 676–687.
- [25] Das, K., Ray, D., Bandyopadhyay, N.R., and Sengupta, S. (2010). Study of the properties of microcrystalline cellulose particles from different renewable resources by XRD, FTIR, nanoindentation, TGA and SEM. *Journal of Polymers and the Environment*, 18: 355–363.
- [26] Zimmermann, T., Bordeanu, N., and Strub, E. (2010). Properties of nanofibrillated cellulose from different raw materials and its reinforcement potential. *Carbohydrate Polymers*, 79: 1086–1093.
- [27] Stenstad, P., Andresen, M., Tanem, B.S., and Stenius, P. (2008). Chemical surface modifications of microfibrillated cellulose. *Cellulose*, 15: 35–45.
- [28] Rosa, M.F., Medeiros, E.S., Malmonge, J.A., Gregorski, K.S., Wood, D.F., Mattoso, L.H.C., Glenn, G., Orts, W.J., and Imam, S.H., (2010). Cellulose nanowhiskers from coconut husk fibers: Effect of preparation conditions on their thermal and morphological behaviour. *Carbohydrate Polymers*, 81: 83–92.
- [29] Satyamurthy, P., Jain, P., Balasubramanya, R.H., and Vigneshwaran, N. (2011). Preparation and characterization of cellulose nanowhiskers from cotton fibres by controlled microbial hydrolysis. *Carbohydrate Polymers*, 83: 122–129.
- [30] Bondeson, D., Mathew, A., and Oksman, K. (2006). Optimization of the isolation of nanocrystals from microcrystalline cellulose by acid hydrolysis. *Cellulose*, 13: 171–180.
- [31] Li, D., Liu, Z., Al-Haik, M., Tehrani, M., Murray, F., Tannenbaum, R., and Garmestani, H. (2010). Magnetic alignment of cellulose nanowhiskers in an all-cellulose composite. *Polymer Bulletin*, 65: 635–642.
- [32] Bhatnagar, A., and Sair, M. (2005). Processing of cellulose nanofibers-reinforced composites. *Journal of Reinforced Plastics and Composites*, 24: 1259–1268.

-
- [33] Oksman, K., Mathew, A.P., Bondeson, D., and Kvien, I. (2006). Manufacturing process of cellulose whiskers/poly(lactic acid) nanocomposites. *Composites Science and Technology*, 66: 2776–2784.
- [34] Jiang, L., Morelius, E., Zhang, J., Wolcott, M., and Holbery, J. (2008). Study of the poly(3-hydroxybutyrate-co-3-hydroxyvalerate)/cellulose nanowhisker. Composites prepared by solution casting and melt processing. *Journal of Composite Materials*, 42: 2629–2645.
- [35] Chen, Y., Liu, C., Chang, P.R., Cao, X., and Anderson, D.P. (2009). Bionanocomposites based on pea starch and cellulose nanowhiskers hydrolyzed from pea hull fibre: Effect of hydrolysis time. *Carbohydrate Polymers*, 76: 607–615.
- [36] Petersson, L., Mathew, A.P., and Oksman, K. (2009). Dispersion and properties of cellulose nanowhiskers and layered silicates in cellulose acetate butyrate nanocomposites, *Journal of Applied Polymer Science*, 112: 2001–2009.
- [37] Ibrahim, M.M., El-Zawawy, W.K., and Nassar, M.A. (2010). Synthesis and characterization of poly(vinyl alcohol)/nanospherical cellulose particle films. *Carbohydrate Polymers*, 79: 694–699.
- [38] de Mesquita, J.P., Donnici, C.L., and Pereira, F.V. (2010). Biobased nanocomposites from layer-by-layer assembly of cellulose nanowhiskers with chitosan. *Biomacromolecules*, 11: 473–480.
- [39] Wang, Y., Chang, C., and Zhang, L. (2010). Effects of freezing/thawing cycles and cellulose nanowhiskers on structure and properties of biocompatible starch/PVA sponges. *Macromolecular Materials and Engineering*, 295: 137–145.
- [40] Eichhorn, S. J. (2011). Cellulose nanowhiskers: promising materials for advanced applications. *Soft Matter*, 7: 303–315.
- [41] Meilert, K.T., Laub, D., and Kiwi, J. (2005). Photocatalytic self-cleaning of modified cotton textiles by TiO₂ clusters attached by chemical spacers. *Journal of Molecular Catalysis A: Chemical*, 237: 101–108.
- [42] Belgacem, M.N., and Gandini, A. (2008). Surface modification of cellulose fibres. In: *Monomers, polymers and composites from renewable resources*, Elsevier, p. 385–399.
- [43] Klemenčič, D., Simončič, B., Tomšič, B., and Orel, B. (2010). Biodegradation of silver functionalised cellulose fibres. *Carbohydrate Polymers*, 80: 426–435.
- [44] Tomšič, B., Simončič, B., Orel, B., Žerjav, M., Schroers, H., Simončič, A., and Samardžija, Z. (2009). Antimicrobial activity of AgCl embedded in a silica matrix on cotton fabric. *Carbohydrate Polymers*, 75: 618–626.
- [45] Ilić, V., Šaponjić, Z., Vodnik, V., Potkonjak, B., Jovančić, P., Nedeljković, J., and Radetić, M. (2009). The influence of silver content on antimicrobial activity and color of cotton fabrics functionalized with Ag nanoparticles. *Carbohydrate Polymers*, 78: 564–569.
- [46] Pinto, R.J.B., Marques, P.A.A.P., Neto, C.P., Trindade, T., Daina, S., and Sadocco, P. (2009). Antibacterial activity of nanocomposites of silver and bacterial or vegetable cellulosic fibers. *Acta Biomaterialia*, 5: 2279–2289.
- [47] Ravindra, S., Mohan, Y.M., Reddy, N.N., and Raju, K.M. (2010). Fabrication of antibacterial cotton fibres loaded with silver nanoparticles via “Green Approach”. *Colloids and Surfaces A: Physicochemical Engineering Aspects*, 367: 31–40.
- [48] Chen, C.-Y., and Chiang, C.-L. (2008). Preparation of cotton fibers with antibacterial silver nanoparticles. *Materials Letters*, 62: 3607–3609.

-
- [49] Wang, J.-H., and Cai, Z. (2008). Incorporation of the antibacterial agent, miconazole nitrate into a cellulosic fabric grafted with β -cyclodextrin. *Carbohydrate Polymers*, 72: 695–700.
- [50] Chen, L., Bromberg, L., Hatton, T.A., and Rutledge, G.C. (2008). Electrospun cellulose acetate fibers containing chlorhexidine as a bactericide. *Polymer*, 49: 1266–1275.
- [51] Hou, A., Zhou, M., and Wang, X. (2009). Preparation and characterization of durable antibacterial cellulose biomaterials modified with triazine derivatives. *Carbohydrate Polymers*, 75: 328–332.
- [52] Bozzi, A., Yuranova, T., Guasaquillo, I., Laub, D., and Kiwi, J. (2005). Self-cleaning of cotton textiles modified with TiO₂ at low temperatures under daylight irradiation. *Journal of Photochemistry and Photobiology A: Chemistry*, 174: 156–164.
- [53] Uddin, M.J., Cesano, F., Scarano, D., Bonino, F., Agostini, G., Spoto, G., Bordiga, S., and Zecchina, A. (2008). Cotton textile fibres coated by Au/TiO₂ films: Synthesis, characterization and self cleaning properties, *Journal of Photochemistry and Photobiology A: Chemistry*, 199: 64–72.
- [54] Kiwi, J., and Pulgarin, C. (2010). Innovative self-cleaning and bactericide textiles. *Catalysis Today*, 151: 2–7.
- [55] Pillai, C.K.S., Paul, W., and Sharma, C.P. (2009). Chitin and chitosan polymers: Chemistry, solubility and fiber formation. *Progress in Polymer Science*, 34: 641–678.
- [56] Jayakumar, R., Prabakaran, M., Nair, S.V., and Tamura, H. (2010). Novel chitin and chitosan nanofibers in biomedical applications. *Biotechnology Advances*, 28: 142–150.
- [57] Wang, X.H., Cui, F.G.Z., Feng, Q.L., Li, J.C., and Zhang, Y.H. (2003). Preparation and characterization of collagen/chitosan matrices as potential biomaterials. *Journal of Bioactive and Compatible Polymers*, 18: 453–467.
- [58] Wu, Y.-B., Yu, S.-H., Mi, F.-L., Wu, C.-W., Shyu, S.-S., Peng, C.-K., and Chao, A.-C. (2004). Preparation and characterization on mechanical and antibacterial properties of chitosan/cellulose blends. *Carbohydrate Polymers*, 57: 435–440.
- [59] Wittaya-areekul, S., and Prahsarn, C. (2006). Development and in vitro evaluation of chitosan–polysaccharides composite wound dressings. *International Journal of Pharmaceutics*, 313: 123–128.
- [60] Liu, Y.-J., Han, H.-S., and Wang, Y.-N. (2007). Design of wool knitted fabrics with chitin fiber wool. *Wool Textile Journal*, 5: 49–51.
- [61] Deng, C.-M., He, L.-Z., Zhao, M., Yang, D., and Liu, Y. (2007). Biological properties of the chitosan-gelatin sponge wound dressing. *Carbohydrate Polymers*, 69: 583–589.
- [62] Kim, I.Y., Yoo, M.K., Seo, J.H., Park, S.S., Na, H.S., Lee, H.C., Kim, S.K., and Cho, C.S. (2007). Evaluation of semi-interpenetrating polymer networks composed of chitosan and poloxamer for wound dressing application. *International Journal of Pharmaceutics*, 341: 35–43.
- [63] Wang, W., Lin, S., Xiao, Y., Huang, Y., Tan, Y., Cai, L., and Li, X. (2008). Acceleration of diabetic wound healing with chitosan-crosslinked collagen sponge containing recombinant human acidic fibroblast growth factor in healing-impaired STZ diabetic rats. *Life Sciences*, 82: 190–204.
- [64] Chen, Z., Mo, X., He C., and Wang, H. (2008). Intermolecular interactions in electrospun collagen–chitosan complex nanofibers. *Carbohydrate Polymers*, 72: 410–418.

-
- [65] Yang, X., Liu, Q., Chen, X., Yu, F., and Zhu, Z. (2008). Investigation of PVA/ws-chitosan hydrogels prepared by combined γ -irradiation and freeze-thawing. *Carbohydrate Polymers*, 73: 401–408.
- [66] Costa-Júnior, E.S., Barbosa-Stancioli, E.F., Mansur, A.A.P., Vasconcelos, W.L., and Mansur, H.S. (2009). Preparation and characterization of chitosan/poly(vinyl alcohol) chemically crosslinked blends for biomedical applications. *Carbohydrate Polymers*, 76: 472–481.
- [67] Duarte, A.R.C., Mano, J.F., Reis R.L. (2010). Novel 3D scaffolds of chitosan–PLLA blends for tissue engineering applications: Preparation and characterization. *The Journal of Supercritical Fluids*, 54: 282–289.
- [68] Sung, J. H., Hwang, M.-R., Kim, J.O., Lee, J.H., Kim, Y.I., Kim, J.H., Chang, S.W., Jin, S.G., Kim, J.A., Lyoo, W.S., Han, S.S., Ku, S.K., Yong, C.S., and Choi, H.-G. (2010). Gel characterisation and *in vivo* evaluation of minocycline-loaded wound dressing with enhanced wound healing using polyvinyl alcohol and chitosan. *International Journal of Pharmaceutics*, 392: 232–240.
- [69] Huang, C., Chen, R., Ke, Q., Morsi, Y., Zhang, K., and Mo, X. (2011). Electrospun collagen–chitosan–TPU nanofibrous scaffolds for tissue engineered tubular grafts. *Colloids and Surfaces B: Biointerfaces*, 82: 307–315.
- [70] Radhakumary, C., Antonty, M., and Sreenivasan, K. (2011). Drug loaded thermoresponsive and cytocompatible chitosan based hydrogel as a potential wound dressing. *Carbohydrate Polymers*, 83: 705–713.
- [71] Murakami, K., Aoki, H., Nakamura, S., Nakamura, S.-I., Takikawa, M., Hanzawa, M., Kishimoto S., Hattori, H., Tanaka, Y., Kiyosawa, T., Sato, Y., and Ishihara, M. (2010). Hydrogel blends of chitin/chitosan, fucoidan and alginate as healing-impaired wound dressings. *Biomaterials*, 31: 83–90.
- [72] Chen, J-P., Chang, G.-Y., and Chen, J.-K. (2008). Electrospun collagen/chitosan nanofibrous membrane as wound dressing. *Colloids and Surfaces A: Physicochemical and Engineering Aspects*, 313-314: 183–188.
- [73] Lu, S., Gao, W., and Gu, H. Y. (2008). Construction, application and biosafety of silver nanocrystalline chitosan wound dressing. *Burns*, 34: 623 – 628.
- [74] Vimala, K, Mohan, Y.M., Sivudu, K.S., Varaprasad, K., Ravindra, S., Reddy, N.N., Padma, Y., Sreedhar, B., and MohanaRaju K. (2010). Fabrication of porous chitosan films impregnated with silver nanoparticles: a facile approach for superior antibacterial application. *Colloids and Surfaces B: Biointerfaces*, 76: 248–258.
- [75] Sudheesh Kumar, P.T., Abhilash, S., Manzoor, K., Nair, S.V., Tamura, H., and Jayakumar R. (2010). Preparation and characterization of novel β -chitin/nanosilver composite scaffolds for wound dressing applications. *Carbohydrate Polymers*, 80: 761–767.
- [76] Hang, A.T., Tae, B., and Park, J.S. (2010). Non-woven mats of poly(vinyl alcohol)/chitosan blends containing silver nanoparticles: Fabrication and characterization. *Carbohydrate Polymers*, 82: 472–479.
- [77] Yoksan, R., and Chirachancha, S. (2010). Silver nanoparticle-loaded chitosan–starch based films: Fabrication and evaluation of tensile, barrier and antimicrobial properties. *Materials Science and Engineering C*, 30: 891–897.
- [78] Jung, K.-H., Huh, M.-W., Meng, W., Yuan, J., Hyun, S.H., Bae, J.-S., Hudson, S.M., and Kang, I.-K. (2007). Preparation and antibacterial activity of PET/chitosan

- nanofibrous mats using an electrospinning technique. *Journal of Applied Polymer Science*, 105: 2816–2823.
- [79] Alonso, D., Gimeno, M., Olayo, R., Vázquez-Torres, H., Sepúlveda-Sánchez, J.D., and Shirai, K. (2009). Cross-linking chitosan into UV-irradiated cellulose fibres for the preparation of antimicrobial-finished textiles. *Carbohydrate Polymers*, 77: 536–543.
- [80] Chen, Z.G., Wang, P.W., Wei, B., Mo, X.M., and Cui, F.Z. (2010). Electrospun collagen–chitosan nanofiber: A biomimetic extracellular matrix for endothelial cell and smooth muscle cell. *Acta Biomaterialia*, 6: 372–382.
- [81] Xu, X., Zhuang, X., Cheng, B., Xu, J., Long, G., and Zhang, H. (2010). Manufacture and properties of cellulose/O-hydroxyethyl chitosan blend fibers. *Carbohydrate Polymers*, 81: 541–544.
- [82] Zhang, X., Hua, H., Shen, X., and Yang, Q. (2007). In vitro degradation and biocompatibility of poly(L-lactic acid)/chitosan fiber composites. *Polymer*, 48: 1005–1011.
- [83] Zhuang, X., Cheng, B., Kang, W., and Xu, X. (2010). Electrospun chitosan/gelatin nanofibers containing silver nanoparticles. *Carbohydrate Polymers*, 82: 524–527.
- [84] Penchev, H., Paneva, D., Manolova, N., and Rashkov, I. (2010). Hybrid nanofibrous yarns based on N-carboxyethylchitosan and silver nanoparticles with antibacterial activity prepared by self-bundling electrospinning. *Carbohydrate Research*, 345: 2374–2380.
- [85] Lim, S. H., and Hudson, S. M. (2004). Application of a fiber-reactive chitosan derivative to cotton fabric as an antimicrobial textile finish. *Carbohydrate Polymers*, 56: 227–234.
- [86] Fouda, M.M.G., Wittke, R., Knittel, D., and Schollmeyer, E. (2009). Use of chitosan/polyamine biopolymers based cotton as a model system to prepare antimicrobial wound dressing. *International Journal of Diabetes Mellitus*, 1: 61–64.
- [87] Giri Dev, V.R., Venugopal, J., Sudha, S., Deepika, G., and Ramakrishna, S. (2009). Dyeing and antimicrobial characteristics of chitosan treated wool fabrics with henna dye. *Carbohydrate Polymers*, 75: 646–650.
- [88] Wazed Ali, S., Rajendran, S., and Joshi, M. (2011). Synthesis and characterization of chitosan and silver loaded chitosan nanoparticles for bioactive polyester. *Carbohydrate Polymers*, 83: 438–446.
- [89] Thomas, V., Bajpai, M., and Bajpai, S.K. (2011). In situ formation of silver nanoparticles within chitosan-attached cotton fabric for antibacterial property. *Journal of Industrial Textiles*, 40: 229–245.
- [90] Wei, D., Sun, W., Qian, W., Ye, Y., and Ma, X. (2009). The synthesis of chitosan-based silver nanoparticles and their antibacterial activity. *Carbohydrate Research*, 344: 2375–2382.
- [91] Kong, M., Chen, X.G., Xing, K., and Park, H.J. (2010). Antimicrobial properties of chitosan and mode of action: A state of the art review. *International Journal of Food Microbiology*, 144: 51–63.
- [92] Majeti, N.V., and Kumar, R. (2000). A review of chitin and chitosan applications. *Reactive and Functional Polymers*, 46: 1–27.
- [93] Shi, C., Zhu, Y., Ran, X., Wang, M., Su, Y., and Cheng, T. (2006). Therapeutic potential of chitosan and its derivatives in regenerative medicine. *Journal of Surgical Research*, 133: 185–192.

-
- [94] Muzzarelli, R.A.A. (2009). Chitins and chitosans for the repair of wounded skin, nerve, cartilage and bone. *Carbohydrate Polymers*, 76: 167–182.
- [95] Dash, M., Chiellini, F., Ottenbrite, R.M., and Chiellini, E. (2011). Chitosan – A versatile semi-synthetic polymer in biomedical applications. *Progress in Polymer Science*, 36: 981–1014.
- [96] Jayakumar, R., Prabakaran, M., Sudheesh Kumar, P.T., Nair, S.V., and Tamura, H. (2011). Biomaterials based on chitin and chitosan in wound dressing applications. *Biotechnology Advances*, 29: 322–337.
- [97] Khor, E., and Lim, L.Y. (2003). Implantable applications of chitin and chitosan. *Biomaterials*, 24: 2339–2349.
- [98] Kong, L., Gao, Y., Lu, G., Gong, Y., Zhao, N., and Zhang, X. (2006). A study on the bioactivity of chitosan/nano-hydroxyapatite composite scaffolds for bone tissue engineering. *European Polymer Journal*, 42: 3171–3179.
- [99] Fraga, A.F., de Almeida Filho, E., da Silva Rigo, E.C., and Boschi, A.O. (2011). Synthesis of chitosan/hydroxyapatite membranes coated with hydroxycarbonate apatite for guided tissue regeneration purposes. *Applied Surface Science*, 257: 3888–3892.
- [100] Song, L., Gan, L., Xiao, Y.-F., Wu, Y., Wu F., and Gu, Z.-W. (2011). Antibacterial hydroxyapatite/chitosan complex coatings with superior osteoblastic cell response, *Materials Letters*, 65: 974–977.
- [101] Venkatesan, J., Qian, Z.-J., Ryu, B.-M., Kumar, N.A., and Kim, S.-K. (2011). Preparation and characterization of carbon nanotube-grafted-chitosan – Natural hydroxyapatite composite for bone tissue engineering. *Carbohydrate Polymers*, 83: 569–577.
- [102] Di Martino, A., Sittinger, M., and Risbud, M. V. (2005). Review, Chitosan: A versatile biopolymer for orthopaedic tissue engineering. *Biomaterials*, 26: 5983–5990.
- [103] Ding, S.J. (2006). Preparation and properties of chitosan/calcium phosphate composites for bone repair. *Dental Materials Journal*, 25: 706–712.
- [104] Chesnutt, B.M., Viano, A.M., Yuan, Y., Yang, Y., Guda, T., Appleford, M.R., Ong, J.L., Haggard, W.O., and Bumgardner, J.D. (2009). Design and characterization of a novel chitosan/nanocrystalline calcium phosphate composite scaffold for bone regeneration. *Journal of Biomedical Materials Research. Part A*, 88: 491–502.
- [105] Tanase, C.E., Popa, I.M., and Verestiuc, L. (2011). Biomimetic bone scaffolds based on chitosan and calcium phosphates. *Materials Letters*, 65: 1681–1683.
- [106] Grohman, K., and Himmel, M.E. (1991). Advances in protein-derived materials. In: *Polymers from biobased materials*, Noyes Data Corporation, p. 149–150.
- [107] Bhardwaj, N., and Kundu, S. C. (2010). Electrospinning: A fascinating fibre fabrication technique. *Biotechnology Advances*, 28: 325–347.
- [108] Olsen, D., Yang, C., Bodo, M., Chang, R., Leigh, S., Baez, J., Carmichael, D., Perälä, M., Hämäläinen, E.-R., Jarvinen, M., and Polarek, J. (2003). Recombinant collagen and gelatin for drug delivery. *Advanced Drug Delivery Reviews*, 55: 1547–1567.
- [109] Singh, P., Benjakul, S., Maqsood, S., and Kishimura, H. (2011). Isolation and characterisation of collagen extracted from the skin of striped catfish (*Pangasianodon hypophthalmus*). *Food Chemistry*, 124: 97–105.
- [110] Sionkowska, A., Skopinska-Wisniewska J., Gawron, M., Kozłowska, J., and Planecka, A. (2010). Chemical and thermal cross-linking of collagen and elastin hydrolysates. *International Journal of Biological Macromolecules*, 47: 570–577.

-
- [111] Shanmugasundaram, N., Ravikumar, T., and Babu, M. (2004). Comparative physico-chemical and in vitro properties of fibrillated collagen scaffolds from different sources. *Journal of Biomaterials Applications*, 18: 247–264.
- [112] Li, S.T. (2003). Biologic biomaterials: tissue-derived biomaterials (collagen). In: *Biomaterials, principles and applications*, CRC Press, p. 117–132.
- [113] Chen, Z., Wei, B., Mo, X., Lim, C.T., Ramakrishna, S., and Cui, F. (2009). Mechanical properties of electrospun collagen–chitosan complex single fibers and membrane. *Materials Science and Engineering C*, 29: 2428–2435.
- [114] Aigner, T., and Stöve, J. (2003). Collagens—major component of the physiological cartilage matrix, major target of cartilage degeneration, major tool in cartilage repair. *Advanced Drug Delivery Reviews*, 55: 1569–1593.
- [115] Patel, M., Vandevord, P.J., Matthew, H.W., De Silva, S., Wu, B., and Wooley, P.H. (2008). Collagen-Chitosan Nerve Guides for Peripheral Nerve Repair: A Histomorphometric Study. *Journal of Biomaterials Applications*, 23: 101–121.
- [116] Caves, J.M., Kumar, V.A., Martinez, A.W., Kim, J., Ripberger, C.M., Haller, C.A., and Chaikof, E.L. (2010). The use of microfiber composites of elastin-like protein matrix reinforced with synthetic collagen in the design of vascular grafts. *Biomaterials*, 31: 7175–7182.
- [117] Koens, M.J.W., Faraj, K.A., Wismans, R.G., van der Vliet, J.A., Krasznai, A.G., Cuijpers, V.M.J.I., Jansen, J.A., Daamen, W.F., and van Kuppevelt, T.H. (2010). Controlled fabrication of triple layered and molecularly defined collagen/elastin vascular grafts resembling the native blood vessel. *Acta Biomaterialia*, 6: 4666–4674.
- [118] McClure, M. J., Sell, S. A., Simpson, D.G., Walpoth, B.H., and Bowlin, G.L. (2010). A three-layered electrospun matrix to mimic native arterial architecture using polycaprolactone, elastin, and collagen: A preliminary study. *Acta Biomaterialia*, 6: 2422–2433.
- [119] Huang, Y.-C., Hsu, S.-H., Chen, M.-T., Hsieh, C.-H., Kuo, W.-C., Cheng, H., and Huang, Y.-Y. (2011). Controlled release of chondroitinase ABC in chitosan-based scaffolds and PDLA microspheres. *Carbohydrate Polymers*, 84: 788–793.
- [120] Ruszczak, Z., and Friess, W. (2003). Collagen as a carrier for on-site delivery of antibacterial drugs. *Advanced Drug Delivery Reviews*, 55: 1679–1698.
- [121] Guo, R., Xu, S., Ma, L., Huang, A., and Gao, C. (2011). The healing of full-thickness burns treated by using plasmid DNA encoding VEGF-165 activated collagen chitosan dermal equivalents. *Biomaterials*, 32: 1019–1031.
- [122] Ryssel, H., Germann, G., Kloeters, O., Gazykan, E., and Radu, C.A. (2010). Dermal substitution with Matriderm® in burns on the dorsum of the hand. *Burns*, 36: 1248–1253.
- [123] Zajicek, R., Matouskova, E., Broz, L., Kubok, R., Waldauf, P., and Königova, R. (2011). New biological temporary skin cover Xe-Derma® in the treatment of superficial scald burns in children. *Burns*, 37: 333–337.
- [124] Li, J., Yin, Y., Yao, F., Zhang, L., and Yao, K. (2008). Effect of nano- and micro-hydroxyapatite/chitosan-gelatin network film on human gastric cancer cells. *Materials Letters*, 62: 3220–3223.
- [125] Pelin, I. M., Maier, S. S., Chitanu, G. C., and Bulacovschi, V. (2009). Preparation and characterization of a hydroxyapatite–collagen composite as component for injectable bone substitute. *Materials Science and Engineering C*, 29: 2188–2194.

- [126] van Nimmen, E., Gellynck, K., van Langenhove, L., and Mertens, J. (2006). The tensile properties of cocoon silk of the Spider *Araneus diadematus*. *Textile Research Journal*, 76: 619–628.
- [127] Hardy, J.G., Römer, L.M., and Scheibel, T.R. (2008). Polymeric materials based on silk proteins. *Polymer*, 49: 4309–4327.
- [128] Kluge, J.A., Rabotyagova, O., Leisk, G.G., and Kaplan, D.L. (2008). Spider silks and their applications. *Trends in Biotechnology*, 26: 244–251.
- [129] Hardy, J.G., and Scheibel, T.R. (2010). Composite materials based on silk proteins. *Progress in Polymer Science*, 35: 1093–1115.
- [130] Davarpanah, S., Mahmoodi, N. M., Arami, M., Bahrami, H., and Mazaheri, F. (2009). Environmentally friendly surface modification of silk fiber: Chitosan grafting and dyeing. *Applied Surface Science*, 255: 4171–4176.
- [131] Jones, G. L., Motta, A., Marshall, M.J., El Haj, A.J., and Cartmell, S.H. (2009). Osteoblast: Osteoclast co-cultures on silk fibroin, chitosan and PLLA films. *Biomaterials*, 30: 5376–5384.
- [132] Niamsa, N., Srisuwan, Y., Baimark, Y., Phinyocheep, P., and Kittipoom, S. (2009). Preparation of nanocomposite chitosan/silk fibroin blend films containing nanopore structures. *Carbohydrate Polymers*, 78: 60–65.
- [133] Wang, X., Yucel, T., Lu, Q., Hu, X., and Kaplan, D.L. (2010). Silk nanospheres and microspheres from silk/pva blend films for drug delivery. *Biomaterials*, 31: 1025–1035.
- [134] Bhardwaj, N., and Kundu, S. C. (2011). Silk fibroin protein and chitosan polyelectrolyte complex porous scaffolds for tissue engineering applications, *Carbohydrate Polymers*, 85: 325–333.
- [135] Altman, G. H., Diaz, F., Jakuba, C., Calabro, T., Horan, R.L., Chen, J., Lu, H., Richmond, J., and Kaplan, D.L. (2003). Silk-based biomaterials. *Biomaterials*, 24: 401–416.
- [136] Potiyaraj, P., Kumlangdudsana, P., and Dubas, S.T. (2007). Synthesis of silver chloride nanocrystal on silk fibers. *Materials Letters*, 61: 2464–2466.
- [137] Choi, H.-M., Bide, M., Phaneuf, M., Quist, W., and Logerfo, F. (2004). Antibiotic Treatment of Silk to Produce Novel Infection-Resistant Biomaterials. *Textile Research Journal*, 74: 333–342.
- [138] Wang, X., Wenk, E., Hu, X., Castro, G.R., Meinel, L., Wang, X., Li, C., Merkle, H., and Kaplan, D.L. (2007). Silk coatings on PLGA and alginate microspheres for protein delivery. *Biomaterials*, 28: 4161–4169.
- [139] Wang, X., Wenk, E., Matsumoto, A., Meinel, L., Li, C., and Kaplan, D.L. (2007). Silk microspheres for encapsulation and controlled release. *Journal of Controlled Release*, 117: 360–370.
- [140] Schneider, A., Wang, X.Y., Kaplan, D.L., Garlick, J.A., and Egles, C. (2009). Biofunctionalized electrospun silk mats as a topical bioactive dressing for accelerated wound healing. *Acta Biomaterialia*, 5: 2570–2578.
- [141] Baoyong, L., Jian, Z., Denglong, C., and Min, L. (2010). Evaluation of a new type of wound dressing made from recombinant spider silk protein using rat models. *Burns*, 36: 891–896.
- [142] Chung, T.-W., and Chang, Y.-L. (2010). Silk fibroin/chitosan-hyaluronic acid versus silk fibroin scaffolds for tissue engineering: promoting cell proliferations in vitro. *Journal of Materials Science. Materials in Medicine*, 21: 1343–1351.

-
- [143] Numata, K., and Kaplan, D.L. (2010). Silk-based delivery systems of bioactive molecules. *Advanced Drug Delivery Reviews*, 62: 1497–1508.
- [144] Pritchard, E.M., Szybala, C., Boison, D., and Kaplan, D.L. (2010). Silk fibroin encapsulated powder reservoirs for sustained release of adenosine. *Journal of Controlled Release*, 144: 159–167.
- [145] Guziewicz, N., Best, A., Perez-Ramirez, B., and Kaplan, D.L. (2011). Lyophilized silk fibroin hydrogels for the sustained local delivery of therapeutic monoclonal antibodies. *Biomaterials*, 32: 2642–2650.
- [146] Pritchard, E.M., Valentin, T., Boison, D., and Kaplan, D.L. (2011). Incorporation of proteinase inhibitors into silk-based delivery devices for enhanced control of degradation and drug release. *Biomaterials*, 32: 909–918.
- [147] Iguchi, M., Yamanaka, S., and Budhino, A. (2000). Review Bacterial cellulose - a masterpiece of nature's arts. *Journal of Materials Science*, 35: 261–270.
- [148] Grande, C.J., Torres, F.G., Gomez, C.M., Troncoso, O.P., Canet-Ferrer, J., and Martínez-Pastor, J. (2009). Development of self-assembled bacterial cellulose–starch nanocomposites. *Materials Science and Engineering C*, 29: 1098–1104.
- [149] Zhou, L.L., Sun, D.P., Hu, L.Y., Li, Y.W., and Yang, J.Z. (2007). Effect of addition of sodium alginate on bacterial cellulose production by *Acetobacter xylinum*. *Journal of Industrial Microbiology and Biotechnology*, 34: 483–489.
- [150] Hong, F., and Qiu, K. (2008). An alternative carbon source from konjac powder for enhancing production of bacterial cellulose in static cultures by a model strain *Acetobacter aceti* subsp. *xylinus* ATCC 23770. *Carbohydrate Polymers*, 72: 545–549.
- [151] Kurosumi, A., Sasaki, C., Yamashita, Y., and Nakamura, Y. (2009). Utilization of various fruit juices as carbon source for production of bacterial cellulose by *Acetobacter xylinum* NBRC 13693. *Carbohydrate Polymers*, 76: 333–335.
- [152] Shezad, O., Khan, S., Khan, T., and Kon Park, J. (2010). Physicochemical and mechanical characterization of bacterial cellulose produced with an excellent productivity in static conditions using a simple fed-batch cultivation strategy. *Carbohydrate Polymers*, 82: 173–180.
- [153] Iwata, T., Indrarti, L., and Azuma, J. I. (1998). Affinity of hemicellulose for cellulose produced by *Acetobacter xylinum*. *Cellulose*, 5: 215–228.
- [154] Hirai, A., Tsuji, M., Yamamoto, H., and Horii, F. (1998). In situ crystallization of bacterial cellulose III. Influences of different polymeric additives on the formation of microfibrils as revealed by transmission electron microscopy. *Cellulose*, 5: 201–213.
- [155] Whitney, S.E.C., Brigham, J.E., Darke, A.H., Reid, G.J.S., and Gidley, M.J. (1998). Structural aspects of the interaction of mannan-based polysaccharides with bacterial cellulose. *Carbohydrate Research*, 307: 299–309.
- [156] Astley, O. M., Chanliaud, E., Donald, A.M., and Gidley, M. J. (2001). Structure of *Acetobacter* cellulose composites in the hydrated state. *International Journal of Biological Macromolecules*, 2: 193–202.
- [157] Keshk, S. (2006). Physical properties of bacterial cellulose sheets produced in presence of lignosulfonate. *Enzyme and Microbial Technology*, 40: 9–12.
- [158] Keshk, S., and Sameshima, K. (2006). Influence of lignosulfonate on crystal structure and productivity of bacterial cellulose in a static culture. *Enzyme and Microbial Technology*, 40: 4–8.

-
- [159] Phisalaphong, M., and Jatupaiboon, N. (2008). Biosynthesis and characterization of bacteria cellulose–chitosan film. *Carbohydrate Polymers*, 74: 482–488.
- [160] Huang, H.-C., Chen, L.-C., Lin, S.-B., and Chen, H.-H. (2011). Nano-biomaterials application: In situ modification of bacterial cellulose structure by adding HPMC during fermentation. *Carbohydrate Polymers*, 83: 979–987.
- [161] Gea, S., Bilotti, E., Reynolds, C.T., Soykeabkeaw, N., and Peijs, T. (2010). Bacterial cellulose–poly(vinyl alcohol) nanocomposites prepared by an in-situ process. *Materials Letters*, 64: 901–904.
- [162] Maneerung, T., Tokura, S., and Rujiravanit, R. (2008). Impregnation of silver nanoparticles into bacterial cellulose for antimicrobial wound dressing. *Carbohydrate Polymers*, 72: 43–51.
- [163] Hu, W., Chen, S., Li, X., Shi, S., Shen, W., Zhang, X. and Wang, H. (2009). In situ synthesis of silver chloride nanoparticles into bacterial cellulose membranes. *Materials Science and Engineering C*, 29: 1216–1219.
- [164] Hong, L., Wang, Y.L., Jia, S.R., Huang, Y., Gao, C., and Wan, Y.Z. (2006). Hydroxyapatite/bacterial cellulose composites synthesized via a biomimetic route. *Materials Letters*, 60: 1710–1713.
- [165] Wan, Y.Z., Huang, Y., Yuan, C.D., Raman, S., Zhu, Y., Jiang, H.J., He, F., and Gao, C. (2007). Biomimetic synthesis of hydroxyapatite/bacterial cellulose nanocomposites for biomedical applications. *Materials Science and Engineering C*, 27: 855–864.
- [166] Dobre, L.M., Stoica, A., Stroescu, M., Jinga, S., Jipa, I., and Dobre, T. (2010). Characterization of composites materials based on biocellulose membranes impregnated with silver particles as antimicrobial agent. *UPB Science Bulletin Series B*, 72: 55–64.
- [167] Zimmermann, K.A., LeBlanc, J.M., Sheets, K.T., Fox, R.W., and Gatenholm, P. (2011). Biomimetic design of a bacterial cellulose/hydroxyapatite nanocomposite for bone healing applications. *Materials Science and Engineering C*, 31: 43–49.
- [168] Czaja, W., Krystynowicz, A., Bielecka, S., and Brown Jr., R.M. (2006). Microbial cellulose—the natural power to heal wounds. *Biomaterials*, 27: 145–151.
- [169] Svensson, A., Nicklasson, E., Harrah, T., Panilaitis, B., Kaplan, D.L. Brittberg, M., and Gatenholm, P., (2005). Bacterial cellulose as a potential scaffold for tissue engineering of cartilage. *Biomaterials*, 26: 419–431.
- [170] Klemm, D., Schumann, D., Udhardt, U., and Marsch, S. (2001). Bacterial synthesized cellulose-artificial blood vessels for microsurgery. *Progress in Polymer Science*, 26: 1561–1603.
- [171] Luengo, J. M., García, B., Sandoval, A., Naharro, G., and Olivera, E. R. (2003). Bioplastics from microorganisms. *Current Opinion in Microbiology*, 6: 251–260.
- [172] Reddy, C.S.K., Ghai, R., Rashmi, Kalia, V.C. (2003). Polyhydroxyalkanoates: an overview, *Bioresource Technology*, 87: 137–146.
- [173] Kessler, B., and Witholt, B. (1999). Poly(3-hydroxyalkanoates). In: *Encyclopedia of bioprocess technology: fermentation, biocatalysis and bioseparation*, vol. 1-5, John Wiley and Sons. Inc., p. 2024–2040.
- [174] Tan, I.K.P. (2004). Polyhydroxyalkanoate production from renewable resources. In: *Concise encyclopedia of bioresources technology*, The Howorth Press Inc., p. 653–662.
- [175] Khanna, S., Srivastava, A.K. (2005). Recent advances in microbial polyhydroxyalkanoates. *Process Biochemistry*, 40: 607–619.

-
- [176] Keshavarz, T., Roy I. (2010). Polyhydroxyalkanoates: bioplastics with a green agenda. *Current Opinion in Microbiology*, 13: 321–326.
- [177] Barud, H.S., Souza, J.L., Santos, D.B., Crespi, M. S., Ribeiro, C.A., Messaddeq, Y., Ribeiro, S.J.L. (2011). Bacterial cellulose/poly(3-hydroxybutyrate) composite membranes. *Carbohydrate Polymers*, 83: 1279–1284.
- [178] Gupta, B., Revagade, N., Hilborn, J. (2007). Poly(lactic acid) fiber: An overview. *Progress in Polymer Science*, 32: 455–482.
- [179] Avérous L. (2008). Polylactic acid: Synthesis, properties and applications. In: *Monomers, polymers and composites from renewable resources*, Elsevier, p. 433–450.
- [180] Jain, M.K., and Zeikus, J.K. (1999). Anaerobes, Industrial uses. In: *Encyclopedia of bioprocess technology: fermentation, biocatalysis and bioseparation*, John Wiley and Sons, p. 159–160.
- [181] Nair, L.S., and Laurencin, C.T. (2007). Biodegradable polymers as biomaterials. *Progress in Polymer Science*, 32: 762–798.
- [182] Södergård, A., and Stolt, M. (2002). Properties of lactic acid based polymers and their correlation with composition. *Progress in Polymer Science*, 27: 1123–1163.
- [183] Lim, L.-T., Auras, R., and Rubino, M. (2008). Processing technologies for poly(lactic acid). *Progress in Polymer Science*, 33: 820–852.
- [184] Richardson, S.M., Curran, J.M., Chen, R., Vaughan-Thomas, A., Hunt, J.A., Freemont, A.J., and Hoyland, J.A. (2006). The differentiation of bone marrow mesenchymal stem cells into chondrocyte-like cells on poly-L-lactic acid (PLLA) scaffolds. *Biomaterials*, 27: 4069–4078.
- [185] Saito, N., and Takaoka, K. (2003). New synthetic biodegradable polymers as BMP carriers for bone tissue engineering. *Biomaterials*, 24: 2287–2293.
- [186] Kumari, A., Yadav, S. K., and Yadav, S. C. (2010). Biodegradable polymeric nanoparticles based drug delivery systems. *Colloids and Surfaces B: Biointerfaces*, 75: 1–18.
- [187] Kim, T.K., Yoon, J.J., Lee, D.S., and Park, T.G. (2006). Gas foamed open porous biodegradable polymeric microspheres, *Biomaterials*, 27: 152–159.
- [188] Acharya, S., and Sahoo, S. K. (2011). PLGA nanoparticles containing various anticancer agents and tumour delivery by EPR effect. *Advanced Drug Delivery Reviews*, 63: 170–183.
- [189] Kirkham, G. (2009). Is biotechnology the new alchemy?. *Studies in History and Philosophy of Science*, 40: 70–80.
- [190] Gavrilescu, M., and Christi, Y. (2005). Biotechnology—a sustainable alternative for chemical industry. *Biotechnology Advances*, 23: 471–499.
- [191] Chen, J., Wang, Q., Hua, Z., and Du, G. (2007). Research and application of biotechnology in textile industries in China. *Enzyme and Microbial Technology*, 40: 1651–1655.
- [192] Zechendorf, B. (1999). Sustainable development: how can biotechnology contribute?. *Trends in Biotechnology*, 17: 219–225.
- [193] Ebskamp, M.J.M. (2002). Engineering flax and hemp for an alternative to cotton. *Trends in Biotechnology*, 20: 229–230.
- [194] Hinman, M.B., Jones, J.A., and Lewis, R.V. (2000). Synthetic spider silk: a modular fiber. *Trends in Biotechnology*, 18: 374–379.

-
- [195] Aly, A.S., Moustafa, A.B., and Hebeish, A. (2004). Bio-technological treatment of cellulosic textiles. *Journal of Cleaner Production*, 12: 697–705.
- [196] Kirk, O., Borchert, T.V., and Fuglsang, C.C. (2002). Industrial enzyme applications. *Current Opinion in Biotechnology*, 13: 345–351.
- [197] Rodríguez Couto, S., and Toca Herrera, J.L. (2006). Industrial and biotechnological applications of laccases: A review. *Biotechnology Advances*, 24: 500–513.
- [198] Hebeish, A., Hashem, M., Shaker, N., Ramadan, M., El-Sadek, B., and Hady, M.A. (2009). Effect of post- and pre-crosslinking of cotton fabrics on the efficiency of biofinishing with cellulase enzyme. *Carbohydrate Polymers*, 78: 953–960.
- [199] Bhat, M.K. (2000). Cellulases and related enzymes in biotechnology. *Biotechnology Advances*, 18: 355–383.
- [200] Pere, J., Puolakka, A., Nousiainen, P., and Buchert, J. (2001). Action of purified *Trichoderma reesei* cellulases on cotton fibers and yarn. *Journal of Biotechnology*, 89: 247–255.
- [201] Cortez, J., Bonner, P.L.R., and Griffin, M. (2004). Application of transglutaminases in the modification of wool textiles. *Enzyme and Microbial Technology*, 34: 64–72.
- [202] Hossain, Kh.M.G., Díaz González, M., Riva Juan, A., and Tzanova, T. (2010). Enzyme-mediated coupling of a bi-functional phenolic compound onto wool to enhance its physical, mechanical and functional properties. *Enzyme and Microbial Technology*, 46: 326–330.
- [203] Miyazaki, K., and Islam, N. (2007). Nanotechnology systems of innovation—An analysis of industry and academia research activities. *Technovation*, 27: 661–675.
- [204] Lines, M.G. (2008). Nanomaterials for practical functional uses. *Journal of Alloys and Compounds*, 449: 242–245.
- [205] Jaworek, A., and Sobczyk, A.T. (2008). Electrospraying route to nanotechnology: An overview. *Journal of Electrostatics*, 66: 197–219.
- [206] Kuchibhatla, S.V.N.T., Karakoti, A.S., Bera, D., and Seal, S. (2007). One dimensional nanostructured materials. *Progress in Materials Science*, 52: 699–913.
- [207] Kim, H.W., Kim, B.R., and Rhee, Y.H., (2010). Imparting durable antimicrobial properties to cotton fabrics using alginate–quaternary ammonium complex nanoparticles. *Carbohydrate Polymers*, 79: 1057–1062.
- [208] Pant, H.R., Bajgai, M.P., Nam, K.T., Seo, Y.A., Pandeya, D.R., Hong, S.T., and Kim, H.Y. (2011). Electrospun nylon-6 spider-net like nanofiber mat containing TiO₂ nanoparticles: A multifunctional nanocomposite textile material. *Journal of Hazardous Materials*, 185: 124–130.
- [209] Dastjerdi, R., and Montazer, M. (2010). A review on the application of inorganic nano-structured materials in the modification of textiles: Focus on anti-microbial properties. *Colloids and Surfaces B: Biointerfaces*, 79: 5–18.
- [210] Dubas, S.T., Kumlangdudsana, P., and Potiyaraj, P. (2006). Layer-by-layer deposition of antimicrobial silver nanoparticles on textile fibers. *Colloids and Surfaces A: Physicochemical Engineering Aspects*, 289: 105–109.
- [211] Abramov, O.V., Gedanken, A., Koltypin, Y., Perkash, N., Perelshtein, I., Joyce, E., and Mason, T.J. (2009). Pilot scale sonochemical coating of nanoparticles onto textiles to produce biocidal fabrics. *Surface and Coatings Technology*, 204: 718–722.

-
- [212] Rajendran, R., Balakumar, C., Ahammed, H.A.M., Jayakumar, S., Vaideki, K., and Rajesh, E.M. (2010). Use of zinc oxide nano particles for production of antimicrobial textiles. *International Journal of Engineering, Science and Technology*, 2: 202–208.
- [213] El-Rafie, M.H., Mohamed, A.A., Shaheen, Th.I., and Hebeish, A. (2010). Antimicrobial effect of silver nanoparticles produced by fungal process on cotton fabrics. *Carbohydrate Polymers*, 80: 779–782.
- [214] Liu, Z., Jiao, Y., Wang, Y., Zhou, C., and Zhang, Z. (2008). Polysaccharides-based nanoparticles as drug delivery systems. *Advanced Drug Delivery Reviews*, 60: 1650–1662.
- [215] de la Fuente, M., Raviña, M., Paolicelli, P., Sanchez, A., Seijo, B., and Alonso, M.J. (2010). Chitosan-based nanostructures: A delivery platform for ocular therapeutics. *Advanced Drug Delivery Reviews*, 62: 100–117.
- [216] Ellenbecker, M., and Tsai, S. (2011). Engineered nanoparticles: safer substitutes for toxic materials, or a new hazard?. *Journal of Cleaner Production*, 19: 483–487.
- [217] Agarwal, S., Wendorff, J.H., and Greiner, A. (2008). Use of electrospinning technique for biomedical applications. *Polymer*, 49: 5603–5621.
- [218] Zhang, X., Reagan, M.R., and Kaplan, D.L. (2009). Electrospun silk biomaterial scaffolds for regenerative medicine. *Advanced Drug Delivery Reviews*, 61: 988–1006.
- [219] Sokolsky-Papkov, M., Agashi, K., Olaye, A., Shakesheff, K., and Domb, A.J. (2007). Polymer carriers for drug delivery in tissue engineering. *Advanced Drug Delivery Reviews*, 59: 187–206.
- [220] Deitzel, J.M., Kleinmeyer, J., Harris, D., and Beck Tan, N.C. (2001). The effect of processing variables on the morphology of electrospun nanofibers and textiles. *Polymer*, 42: 261–272.
- [221] Frenot, A., and Chronakis, I.S. (2003). Polymer nanofibers assembled by electrospinning. *Current Opinion in Colloid and Interface Science*, 8: 64–75.
- [222] Hussain, D., Loyal, F., Greiner, A., and Wendorff, J.H. (2010). Structure property correlations for electrospun nanofiber nonwovens. *Polymer*, 51: 3989–3997.
- [223] Barnes, C.P., Sell, S.A., Boland, E. D., Simpson, D.G., and Bowlin, G.L. (2007). Nanofiber technology: Designing the next generation of tissue engineering scaffolds. *Advanced Drug Delivery Reviews*, 59: 1413–1433.
- [224] Lee, K.Y., Jeong, L., Kang, Y.O., Lee, S.J., and Park, W.H. (2009). Electrospinning of polysaccharides for regenerative medicine. *Advanced Drug Delivery Reviews*, 61: 1020–1032.
- [225] Su, P., Wang, C., Yang, X., Chen, X., Gao, C., Feng, X.-X., Chen, J.-Y., Ye, J., and Gou, Z. (2011). Electrospinning of chitosan nanofibers: The favorable effect of metal ions. *Carbohydrate Polymers*, 84: 239–246.
- [226] Wang, S., Zhang, Y., Wang, H., and Dong, Z. (2011). Preparation, characterization and biocompatibility of electrospinning heparin-modified silk fibroin nanofibers. *International Journal of Biological Macromolecules*, 48: 345–353.
- [227] Awal, A., Sain, M., and Chowdhury, M. (2011). Preparation of cellulose-based nanocomposite fibers by electrospinning and understanding the effect of processing parameters. *Composites Part B: Engineering*, 42: 1220–1225.
- [228] Fang, D., Liu Y., Jiang, S., Nie, J., and Ma, G. (2011). Effect of intermolecular interaction on electrospinning of sodium alginate. *Carbohydrate Polymers*, 85: 276–279.

-
- [229] Bonino, C. A., Krebs, M.D., Saquing, C. D., Jeong, S. I., Shearer, K. L., Alsberg, E., and Khan, S. A. (2011). Electr spinning alginate-based nanofibers: From blends to crosslinked low molecular weight alginate-only systems. *Carbohydrate Polymers*, 85: 111–119.
- [230] Gupta, B., Agarwal, R., and Alan, M. S. (2010). Textile-based smart wound dressings. *Indian Journal of Fibre and Textile Reserach*, 35: 174–187.
- [231] Paul, W., and Sharma, C. P. (2004). Chitosan and Alginate Wound Dressings: A Short Review. *Trends in Biomaterials and Artificial Organs*, 18: 18–23.
- [232] Weller, C., and Sussman G. (2006). Wound dressings update. *Journal of Pharmacy Practice and Research*, 36: 318–324.
- [233] Petrulyte, S. (2008). Advanced textile materials and biopolymers in wound management. *Danish Medical Bulletin*, 55: 72–77.
- [234] Ovington, L. G. (2007). Advances in wound dressings. *Clinics in Dermatology*, 25: 33–38.
- [235] Winter, G. D. (1962). Formation of scab and the rate of epithelialization of superficial wounds in the skin of the young domestic pig. *Nature*, 193: 293–294.
- [236] Hinman, C. D., and Maibach, H. I. (1963). Effect of air exposure and occlusion on experimental human skin wounds, *Nature*, 200: 377–378.
- [237] Miller, C. W. (2003). Bandages and Drains. In: *Textbook of Small Animal Surgery*, Elsevier, p. 244–249.
- [238] Tamura, H., Furuike, T., Nair, S.V., and Jayakumar, R. (2011). Biomedical applications of chitin hydrogel membranes and scaffolds. *Carbohydrate Polymers*, 84: 820–824.
- [239] Kofuji, K., Huang, Y., Tsubaki, K., Kokido, F., Nishikawa, K., Isobe, T., and Murata, Y. (2010). Preparation and evaluation of a novel wound dressing sheet comprised of β -glucan–chitosan complex, *Reactive and Functional Polymers*, 70: 784–789.
- [240] Tsao, C. T., Chang, C. H., Lin, Y. Y., Wu, M. F., Wang, J. L., Young, T. H., Han, J. L., and Hsieh, K. H. (2011). Evaluation of chitosan/ γ -poly(glutamic acid) polyelectrolyte complex for wound dressing materials. *Carbohydrate Polymers*, 84, 812–819.
- [241] Rai, M., Yadav, A., and Gade, A. (2009). Silver nanoparticles as a new generation of antimicrobials. *Biotechnology Advances*, 27: 76–83.
- [242] Vlachou, E., Chipp, E., Shale, E., Wilson, Y. T., Papini, R., and Moiemmen, N. S. (2007). The safety of nanocrystalline silver dressings on burns: A study of systemic silver absorption. *Burns*, 33: 979–985.
- [243] Moiemmen, N. S., Shale, E., Drysdale, K. J., Smith, G., Wilson, Y. T., and Papini, R. (2011). Acticoat dressings and major burns: Systemic silver absorption. *Burns*, 37: 27–35.
- [244] Liao, S., Chan, C. K., and Ramakrishna, S. (2008). Stem cells and biomimetic materials strategies for tissue engineering. *Materials Science and Engineering C*, 28: 1189–1202.
- [245] Meyer, U., Meyer, T., Handschel, J., and Wiesmann, H. P. (2009). Preface. In: *Fundamentals of tissue engineering and regenerative medicine*, Springer-Verlag, p. V–VI.
- [246] Phongying, S., Aiba, S.-I., and Chirachanchai, S. (2007). Direct chitosan nanoscaffold formation via chitin whiskers. *Polymer*, 48: 393–400.
- [247] Pashkuleva, I., López-Pérez, P. M., Azevedo, H. S., and Reis, R. L. (2010). Highly porous and interconnected starch-based scaffolds: Production, characterization and surface modification. *Materials Science and Engineering C*, 30: 981–989.

-
- [248] Marra, K. G. (2005). Biodegradable polymers and microspheres. In: *Tissue engineering in bone tissue engineering*, CRC Press, p.150–165.
- [249] Wei, G., and Ma, P. X. (2007). Polymeric biomaterials, In: *Tissue engineering using ceramics and polymers*, Woodhead Publishing Limited and CRC Press, p. 32–47.
- [250] Jang, J.-H., Castano, O., and Kim, H.-W. (2009). Electrospun materials as potential platforms for bone tissue engineering. *Advanced Drug Delivery Reviews*, 61: 1065–1083.
- [251] Wan, A.C.A., and Ying, J.Y. (2010). Nanomaterials for in situ cell delivery and tissue regeneration. *Advanced Drug Delivery Reviews*, 62: 731–740.
- [252] Lertwattanaseri, T., Ichikawa, N., Mizoguchi, T., Tanaka, Y., and Chirachanchai, S. (2009). Microwave technique for efficient deacetylation of chitin nanowhiskers to a chitosan nanoscaffold. *Carbohydrate Research*, 344: 331–335.
- [253] Misra, S. K., and Boccaccini, A. (2007). Biodegradable and bioactive polymer/ceramic composite scaffolds. In: *Tissue engineering using ceramics and polymers*, Woodhead Publishing Limited and CRC Press, p. 72–89.
- [254] Wiesmann, H. P., and Meyer, U. (2009). Biomaterials. In: *Fundamentals of tissue engineering and regenerative medicine*, Springer-Verlag, p. 457–465.
- [255] Gelinsky, M. (2009). Mineralized collagen as biomaterial and matrix for bone tissue engineering, Biomaterials. In: *Fundamentals of tissue engineering and regenerative medicine*, Springer-Verlag, p. 485–493.
- [256] Horch, R. E. (2009). Tissue engineering of cultured skin substitutes. In: *Fundamentals of tissue engineering and regenerative medicine*, Springer-Verlag, (2009), p. 329–338.
- [257] Kane, J. B., Tompkins, G. R., Yarmush, M. L., and Burke, J. F. (1996). Burn dressings. In: *An introduction to materials in medicine*, Academic Press, p. 360–367.

Chapter 13

SOLVOTHERMALLY PREPARED COPPER MODIFIED TiO₂ COMPOSITE SOLS - A COATING AGENT FOR TEXTILES TO REALIZE PHOTOCATALYTIC ACTIVE AND ANTIMICROBIAL FABRICS

***Frank Schmidt¹, Anja Fischer¹, Helfried Haufe¹,
Tilmann Leisegang² and Boris Mahltig^{3,*}***

¹ Gesellschaft zur Förderung von Medizin-, Bio- und Umwelttechnologien e.V.,
GMBU e.V., Postfach 520165, D-01317 Dresden, Germany.

² Saxray, Helmholtz-Zentrum, Dresden-Rossendorf e.V.,
Bautzner Landstrasse 400, D-01328 Dresden, Germany.

³ University of Applied Sciences, Faculty of Textile and Clothing Technology,
Webschulstrasse 31, D-41065 Mönchengladbach, Germany.

ABSTRACT

Anatase containing TiO₂ sols are prepared by a solvothermal process and used as liquid coating agents for textiles. This solvothermal process is driven at temperatures of 140°C and 180°C, which are adequate process conditions for the formation of the crystalline TiO₂ species anatase out of an amorphous TiO₂ pre-compound. By using this liquid coating agent for textile treatment, functionalized textiles with photoactive and antimicrobial properties are realized. For these materials different potential applications are thinkable as for example the wastewater treatment in a process with photoactive functionalized textiles or medical applications with antimicrobial functionalized textiles.

In this chapter, the pure TiO₂ sol is modified by copper doping. To perform this modification, a copper containing precursor was added to the sol before the solvothermal process. Under the chosen solvothermal conditions the copper precursor is proposed to be transformed to antimicrobial active copper containing compounds, probably a Cu-Ti crystalline phase. The formation of the crystalline TiO₂ type anatase is clearly determined by XRD. Also by XRD at least one unidentified copper containing phase is determined which could be probably an intermetallic phase of Cu:Ti as oxide, nitride or carbide.

* To whom all correspondence should be addressed, E-mail: Boris.mahltig@hs-niederrhein.de

Additional hints for the formation of those species are also found by UV/VIS-spectroscopy. The modified TiO_2 -sols are applied as coating agent onto textile fabrics. The photoactivity of coated textile is determined by degradation of the organic dye stuff Acid Orange 7. The effect of photocatalytic dye degradation is also investigated in presence of H_2O_2 . The antimicrobial property of the coated textiles can be clearly verified and is mainly the result of the metal component added to the TiO_2 coating. The high photoactivity observed in presence of H_2O_2 could be of high interest for applications in oxidative wastewater treatment. The developed high antimicrobial active textiles should also be of great relevance for the application in the medical sector to avoid the spreading of harmful germs.

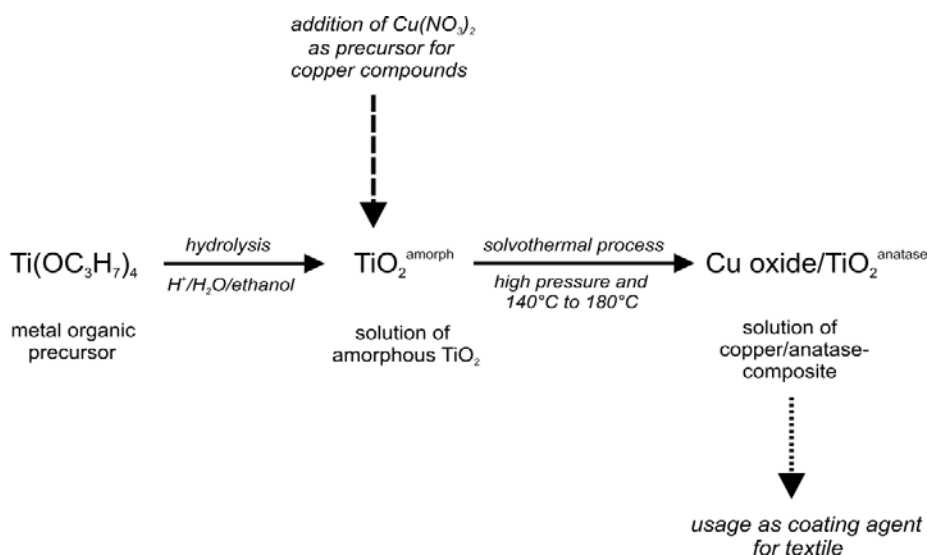
1. INTRODUCTION

As general definition, photocatalysts are materials which accelerate chemical reactions in case of illumination with light. In many cases reported in the literature or for practical applications, such photocatalytic processes are processes of photooxidation, which concern the oxidation by oxygen from air. As catalyst for photooxidation, mostly crystalline titanium oxide phases or modified titanium oxide is used in different arrangements [1-3]. TiO_2 is especially favored for this purpose for several reasons, it contains a high photoactivity, it is not toxic and the catalytic reaction works with light in the near UV range. Many different applications are suggested for TiO_2 used as photocatalyst, e.g. for degradation of organic dyes in wastewater [3], for degradation of chlorophenol [4, 5] or for the oxidation of gaseous benzene [6]. An interesting topic also is the application of TiO_2 as coating on fiber materials to reach self-cleaning fabrics, which eliminate dirt by photooxidative processes. Examples are given for different fiber materials like cotton [7], keratins [8] or polyester [9]. Beside the degradation of dye, toxic compounds or dirt, also bacteria can be degraded, and thus eliminated, by photooxidation. This degradation of bacteria is also named as the antimicrobial effect caused by a photooxidative process [10, 11]. In many cases, TiO_2 is modified by different types of materials to enhance the photocatalytic activity especially in view on the usage of visible light. Examples for materials for modification are phosphorous, nitrogen, molybdenum, iron oxide or aluminium oxide [12-13]. Aside, for the same reasons, titanium oxide is also modified in different preparation processes using elementary noble metals as platinum [15, 16] or gold [17-19]. However probably due to cost reasons more applications and examples are reported on composites of TiO_2 containing the less noble metals palladium [20-22] or silver [23-28] or even with copper [29-32]. The combination of TiO_2 and a noble metal in composites can be realized in different forms, as e.g. core-shell systems, combination of nanoparticles or the doping of TiO_2 with some metal atoms. TiO_2 composites combined with two different noble metals are also reported [33, 34].

Beside the optimization of the photocatalytic activity from TiO_2 containing composites, there is the practical challenge to incorporate the TiO_2 in the application as well. For applications like cleaning of dye containing wastewater from textile industry it is e.g. possible to use powders of TiO_2 -composites, which are homogenously dispersed into the wastewater. The disadvantage of this procedure is obviously that the dispersed TiO_2 has to be removed after the cleaning of the wastewater is finished. For this, it is most advantageous to use TiO_2 -composites coated on substrates, which can be easily removed after the task is fulfilled. An interesting point concerning the combination of TiO_2 with nanoparticles of copper oxide is

that nanoparticulate copper compounds can act as strong antimicrobial agents, as it is for example described with silver and copper containing SiO₂ coatings on textiles [35-37]. By using the combination of TiO₂ and copper it is therefore expected to realize strongly enhanced antimicrobial coatings onto textiles, which antimicrobial effect is independent from the photocatalytic effect of the TiO₂. These textile materials seem to be of high interest for applications where low light illumination is expected or in the medical section, where a strong antimicrobial effect is desired to avoid the spreading of harmful germs.

As substrates for such TiO₂ coating applications textiles or other fiber materials can be used - with several advantages [38-41]. Textiles, especially as carriers employed for wastewater treatment, have the advantages that they can be easily designed and cut as it is necessary for the particular application. Also liquids can flow through textiles which lead to an improved contact between the liquid and the photocatalytic coating due to the larger available surface of textiles. However, a significant disadvantage of using textiles for TiO₂ coatings is the low thermal stability of fiber materials in general. Anatase, the crystalline TiO₂ phase with high photoactivity, is formed from amorphous TiO₂ at temperatures usually higher than 350°C. For this, a subsequent transformation of an amorphous TiO₂ coating to crystalline anatase cannot be realized for most textile substrates. If the sol-gel technique is used for preparation of TiO₂ coatings onto textiles, the TiO₂ has to be present as anatase already in the coating solution. Such anatase containing coating solutions can be for example prepared by solvothermal processes or by addition of commercial anatase containing particles like P25 [40, 41]. For preparation of liquid coating agents containing composites of TiO₂ in anatase phase form together with particles of other metal compounds especially the solvothermal preparation method is of interest. The reason is, under solvothermal process conditions simultaneously anatase and metal compound particles can be formed from different precursors (see e.g. Scheme 1). Also the doping of TiO₂ by atoms of noble metals should be possible by using this method.



Scheme 1. Example for the preparation process of a copper/anatase-composite for the use as liquid coating agent for textile treatment.

With this background, the aim of the here presented work is the solvothermal preparation of copper containing TiO_2 composites for photocatalytic purposes as well as to investigate, if the addition of copper can enhance the photoactivity. The photoactivity is evaluated for related textile coatings. Because several publications as well as applications, report the utilization of H_2O_2 beside O_2 as oxidative agent for the photocatalysed reaction [43-50], the addition of hydrogen peroxide will be also taken into account in the presented work. The dye degradation in wastewater from textile industry is of high economic relevance. Therefore, the enhancement of oxidative degradation with H_2O_2 by using photocatalytic materials could have good chances for the implementation in industrial processes. A special attention is also paid in this chapter to the antimicrobial properties of these coated and functionalized textiles, which is determined in different testing arrangements with and without illumination with UV light.

2. EXPERIMENTAL PART

2.1. Materials and Preparation

TiO_2 sols are prepared starting from a mixture of 7 g $\text{Ti}(\text{OC}_3\text{H}_7)_4$, 113 ml ethanol, 1g of the triblock co-polymer P123 from BASF and (finally added) 0.9 mol of 1N HNO_3 . These mixed solutions are modified by addition of cupric nitrate trihydrate ($\text{Cu}(\text{NO}_3)_2 \cdot 3\text{H}_2\text{O}$ from Fluka), which is added in amounts up to 0.6 g. For reference, a TiO_2 -sol is also prepared without any addition of noble metal salt. 15 minutes after these solutions are prepared, they are treated in a solvothermal process at 180°C in a 500 ml steel autoclave with Teflon vessel (Berghof instruments GmbH, Germany; Hochdruck-Laborreaktor BR-500) (Figure 1).

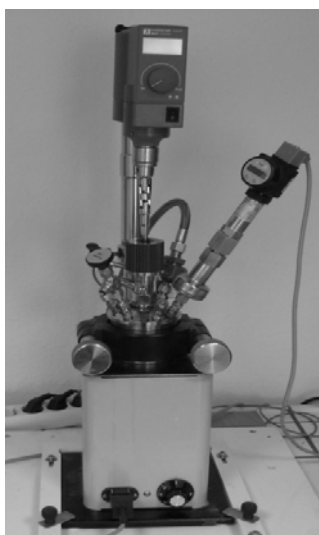


Figure 1. Steel autoclave system for preparation of TiO_2 sol coating solutions (supplied by Berghof, Germany). This autoclave is equipped with an electric oven, a mechanical stirrer and sensors for measurement of process parameters like temperature and pressure.

The process duration is set to 30 minutes. The annealing to reach the final process temperature takes 45 minutes, while for the subsequent cooling at least 2 hours are necessary. The process was also driven at temperatures of 140°C with process duration of 2 hours. This lower process temperature is usually faster reached after only 30 minutes of annealing. All TiO₂-sols are applied onto viscose fabrics by dip-coating. After application the fabrics are dried at room temperature and finally a thermal treatment of 120°C for 30 minutes is performed. The viscose fabric was made from multifilament yarn (supplied by KOB-Wolfstein, Germany) with a weight of 240 g m⁻² and was used for coatings as received. For X-Ray Diffraction (XRD) investigations and for UV/VIS-spectroscopy the coating solutions are also dried at room temperature and grinded to powders.

2.2. Analytical Methods

Powder X-ray diffraction measurements (XRD-measurements) are used to identify the crystalline phases in the solvothermally prepared materials. These measurements are performed on powders gained from the liquid coating solutions after drying for 48 hours at room temperature and an afterwards grinding. For the measurements these powders were regularly distributed onto a glass plate sample holder placed into X-ray diffractometer. The measurements were performed by using a D5005 diffractometer (Siemens/Bruker AXS), equipped with a Goebel-mirror and a scintillation detector. Monochromatic Cu-K α radiation was used. The diffraction patterns were collected in step-scan $\theta/2\theta$ mode in a 2θ range of 20 to 80°. The measurements were carried out under ambient conditions. The received diffraction patterns were evaluated by using the databases (PDF-2) [51] and ICSD [52]. The mean crystallite size of the coating materials is derived by a quantitative phase analysis (Rietveld refinement) of the diffraction patterns, as described in [42], using the program TOPAS [53].

Scanning electron microscopy (SEM) was used to determine topographical features on the coated textiles. These SEM investigations are performed using a commercially available device Gemini DSM982 (Zeiss, Germany). Before measurements the investigated textile samples are gold sputtered to enhance the surface conductivity. Reference measurements are performed on uncoated fabrics. The optical properties of coated textile fabrics are investigated by UV/Vis-spectroscopy in arrangement of diffuse reflectance. For this, a commercially available spectrometer MCS 400 (Zeiss) was used equipped with a set-up for measurement for diffuse reflectance.

The photocatalytic activity of the produced TiO₂ containing materials (as coatings on textile or as powder) was determined by degradation of the dyes Acid Orange 7 (Acros Organics, Great Britain; C.I.15510; M_w = 350 g mol⁻¹; C₁₆H₁₁N₂NaO₄S) and Rhodamin B (Merck KGaA, Germany; C.I.45170; M_w = 479 g mol⁻¹; C₂₈H₃₁ClN₂O₃) [41, 54] (see chemical structures in Scheme 2 and 3). For testing of coated textile samples, textile pieces of the size 1 cm × 5 cm were placed in 15 ml of a 0.025 mM aqueous dye solution and were shaken for 4 hours. During shaking the samples are illuminated by UV-lamps with a maximum intensity at the wavelength of 360 nm (OMNILUX 18Watt, 60 cm – supplier Eurolite). The spectral intensity of the lamp is shown in Figure 2. Altogether six lamps were used for illumination and are placed at a distance of 45 cm to the samples. To evaluate the

dye decomposition in presence of H_2O_2 the same arrangement was used. Solely to the 15 ml of dye solution an amount of 0.05 ml H_2O_2 solution (35%) is added, resulting in a H_2O_2 concentration of 0.1%. The concentration remaining organic dye is determined by UV/Vis-spectroscopy using a spectrometer MCS 400 (Zeiss) in arrangement of transmission by measurement of the absorption at the maximum in the visible area (see optical spectra of the used dyes in Figures 3a and 3b). Reference measurements are conducted with samples that have not been illuminated with any kind of light at all. To evaluate photoactivity the remaining dye concentration for treatments with and without UV light exposure are compared. From these values the photoactivity A can be calculated as percentage value using the relation $A (\%) = 100 \times (C - C_r)/C_r$ – with C as the final dye concentration in the UV illuminated arrangement and with C_r as dye concentration without light exposure. As reference the same procedures are performed with an uncoated textile and with a dye containing solution without any textile added.

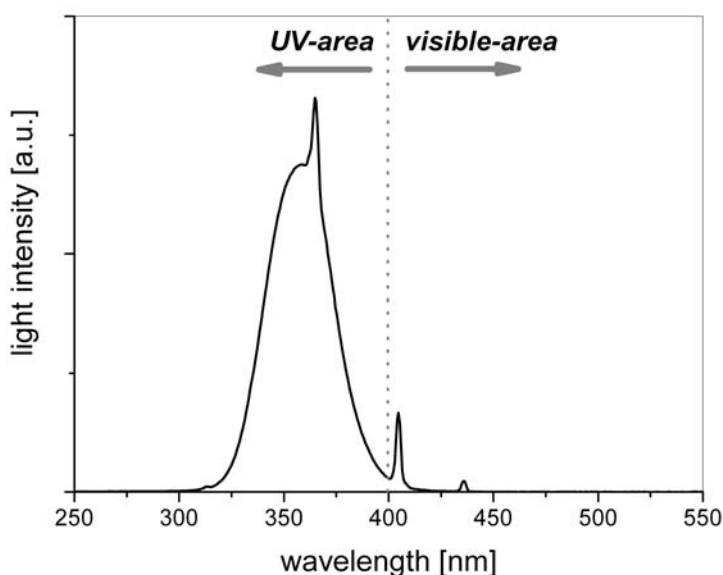
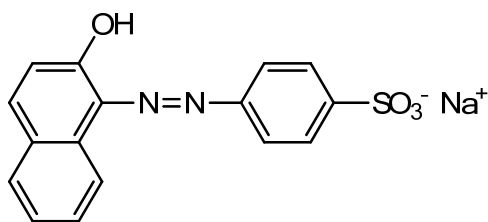
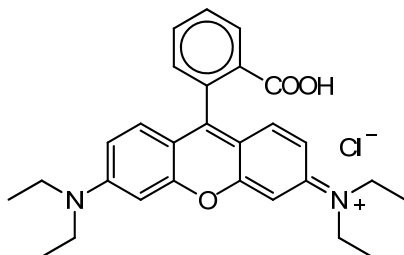


Figure 2. Intensity spectrum of the UV-lamp (OMNILUX 18Watt, Eurolite) used for measurements of photoactivity.



Scheme 2. Chemical structure of the dye Acid Orange 7.



Scheme 3. Chemical structure of the dye Rhodamin B.

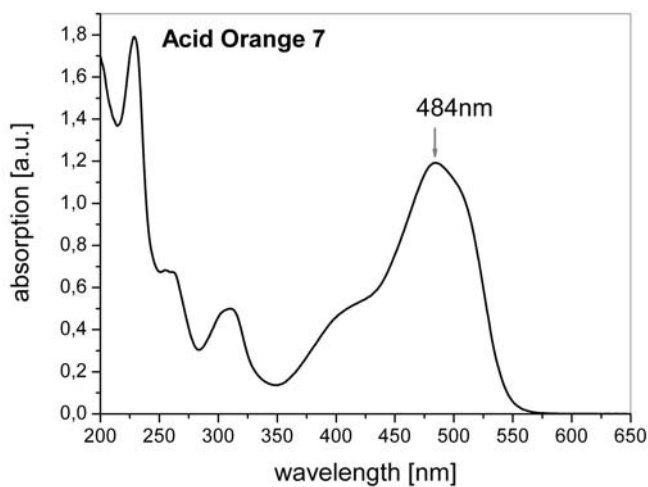


Figure 3a. UV/Vis-spectrum of the organic dye Acid Orange 7 ($2.5 \cdot 10^{-5}$ mol l⁻¹ solution in water) as used for measurements of photoactivity.

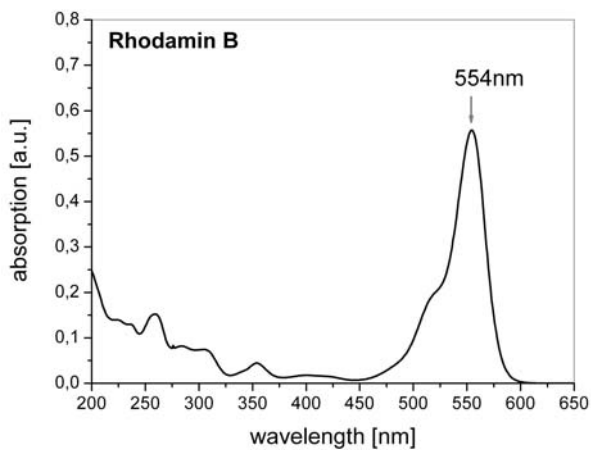


Figure 3b. UV/Vis-spectrum of the organic dye Rhodamin B ($5 \cdot 10^{-6}$ mol l⁻¹ solution in water) as used for measurements of photoactivity.

2.3. Antimicrobial Tests

To investigate the antimicrobial properties of the coated textile fabrics two different test regimes are used. With the first regime the antimicrobial properties are tested in absence of UV light. In the second regime the influence of UV-light is tested. Both tests are performed with *Escherichia coli* which is a gram-negative bacterium. In the first test regime, the coated viscose fabrics are shaken with bacteria suspension and inoculated for 24 hours at a temperature of 30°C. Afterwards the fabrics are leached in phosphate buffer (pH=7) and the buffer is inoculated on agar plates. After 24 hours the colony forming units CFU are counted. In the second test regime, the coated viscose fabrics are shaken with bacteria suspension and inoculated for 3.5 hours, 6 hours or 24 hours at a temperature of 30°C and under illumination with UV-light. The UV-light is gained from six UV-lamps with a maximum of intensity at 360 nm (OMNILUX 18Watt, 60 cm – supplier Eurolite). The UV lamps are placed in a distance of 45 cm from the textile sample. After this illumination the fabrics are leached in phosphate buffer (pH = 7) and the buffer is inoculated on agar plates. Finally, after 24 hours the colony forming units CFU are counted.

3. RESULTS AND DISCUSSION

The results for the copper modified TiO₂ composites and coatings on textiles are presented below. This presentation starts with a description on the material properties of the prepared composites and coatings, which are related to the optical properties, crystallinity and surface structure. These results are mainly obtained by UV/VIS-spectroscopy in arrangement of diffuse reflection, XRD measurements and scanning electron microscopy (SEM). After description of these basic material properties, the properties of the composite coatings adhered to the textiles are presented in respect to photocatalytic applications and antimicrobial activity.

3.1. Properties of Composite and Coatings

The application of copper containing TiO₂ coating agent lead to brown coloration of treated textile fabrics compared to a white/yellow coloration after coating with pure TiO₂ (Figure 4). The change to brown colored textiles increases with increasing the copper content in the applied coating. However with low copper content of smaller than 1% the change in coloration is small and should not influence the usability of the prepared coated fabric. This brown coloration gives a first hint that copper containing compounds are formed during the solvothermal preparation process of the coating agent. The complete reaction of Cu(NO₃)₂ to other copper compounds can be estimated, because the copper precursor Cu(NO₃)₂ exhibits a blue coloration and its application to the textile lead to a light blue coloration instead of a brown coloration, which is gained for example after deposition of copper oxide species [37]. The optical properties of the prepared coated textiles are more intensively investigated by UV/VIS-spectroscopy in arrangement of diffuse reflectance (Figures 5 and 6). For the pure TiO₂-coatings a drastic reduction of reflectance is observed for UV-light with wavelengths

smaller than 380 nm (Figure 5), which is probably caused by the optical properties of the applied TiO₂ [2]. With increasing the copper content in the TiO₂ coating the reflectance of the coated textiles decreases further over the whole range of visible light (Figure 5). These optical reflectance curves do not exhibit any maximum or minimum, so the formation of elementary copper is unlikely and the formation of copper oxide compounds or other copper compounds are more reasonable [55]. Compared to Figure 5, Figure 6 presents the results for the textiles coated with the TiO₂ prepared at 180°C. Here, besides a general decrease of the reflectance with increasing copper an increase for low copper contents is observed in the UV as well as in the near infrared region.

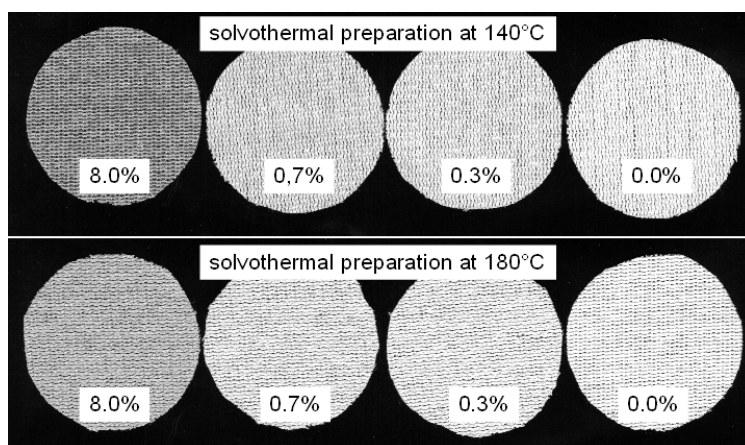


Figure 4. Viscose fabrics with coatings of copper containing TiO₂ composite, solvothermally prepared at 140°C or 180°C. The composites contain copper in amounts of 0% up to 8%.

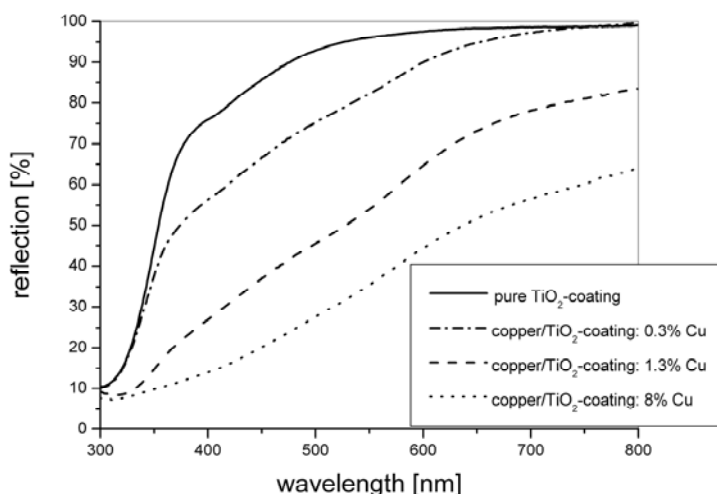


Figure 5. UV/Vis-reflectance spectra of TiO₂ and copper containing TiO₂-coatings on viscose. The coating agent is solvothermally prepared at 140°C.

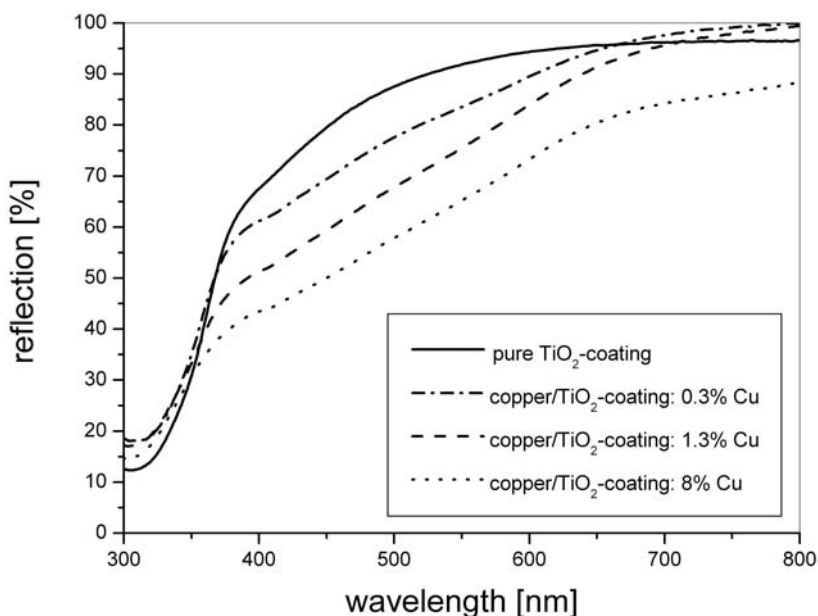


Figure 6. UV/Vis-reflectance spectra of TiO₂ and copper containing TiO₂-coatings on viscose. The coating agent is solvothermally prepared at 180°C.

However, by optical spectroscopy the copper-containing compound or copper oxide, which is formed during the solvothermal preparation process and is applied as coating component onto the textile fibers, cannot be clearly identified, so additionally XRD measurements are performed (Figures 7 and 8). Alternatively, with XRD measurements a phase analysis can be performed for the prepared materials. It can be stated, that beside the crystalline TiO₂ species anatase also crystalline Cu-Ti compounds are formed.

The formation of the crystalline TiO₂-type anatase is clearly verified by the XRD measurements (Figure 8). Under solvothermal preparation conditions at 140°C a beginning of anatase formation is observed. However, the individual reflections exhibit small intensities. This observation shows that only a minor part of the TiO₂ coating material is transformed into the anatase phase. In comparison, if the solvothermal preparation is performed at 180°C, the anatase reflections are more distinct and it can be concluded that the major part of the coating material is anatase-type TiO₂. The crystallite sizes of the anatase phase as well as the additional phase are summarised in Table 1.

As can be seen from Table 1, the size of formed anatase crystallites decreases with increasing the amount of copper compound added as additional precursor to the solvothermal reaction. For this, it can be suggested that the added copper inhibit the formation of crystalline anatase during the solvothermal process (cf. Figure 7). However, in case of the powders synthesized at 180°C, even for the highest copper content of 8%, the formation of anatase is clearly verified (Figure 8).

Table 1. Results of XRD measurements are summarized

Cu content (%)	Preparation temperature T (°C)	Crystallite size (nm)		Additional reflections, 2θ(°)
		Anatase	Add. Phase	
0	140	3.5(5)	—	—
0.3	140	3.1(4)	—	—
8.0	140	—*	—	—
0	180	7.8(2)	—	—
0.3	180	6.9(2)	—	—
2.7	180	6.3(2)	168(139)	32.24(2)
8.0	180	5.6(3)	88(44), 46(28), 49(86)	32.21(3), 46.15(12), 47.16(13)

*Could not be determined with statistical significance.

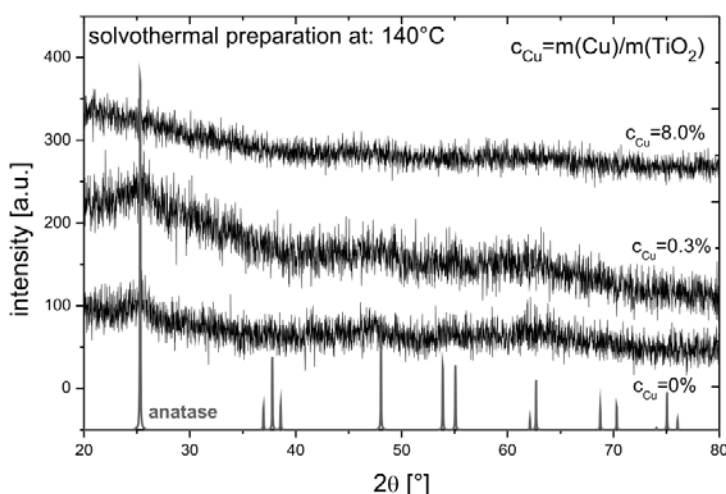


Figure 7. XRD measurements of powders obtained by solvent evaporation of Cu/TiO₂-composite coating solutions at 140°C. The copper content in the composite is set in the range of 0% up to 8.0%. Reflection positions of the anatase phase (ICSD [52]: coll. code 154601) are indicated by lines. The copper content c_{Cu} is calculated out of the amount m of Cu and TiO₂ used for preparation.

By comparison of the copper-containing powders synthesized at different temperatures it can be seen that a critical temperature, $140^{\circ}\text{C} < T \leq 180^{\circ}\text{C}$, for the formation of at least one additional phase exists. Their reflection positions 2θ , which can be clearly seen for copper amounts of $c_{\text{Cu}} \geq 2.7\%$, are summarized in Table 1. The crystallite size ranges from 46 to 168 nm (Table 1). Unfortunately, the few additional reflections could not be assigned to a known copper-including phase, e. g. Cu oxides, to elementary Cu or Ti or to gerhardtite which is a copper hydroxyl nitrate often formed under solvothermal conditions [56, 57]. In order to identify the unknown reflections a powder was synthesized without Ti containing precursors. Here, the gerhardtite as well as the cuprite phase were formed leading to a dark green-brown powder colour. However, for the Ti containing powders (light grey-brown colour) these phases have not been observed.

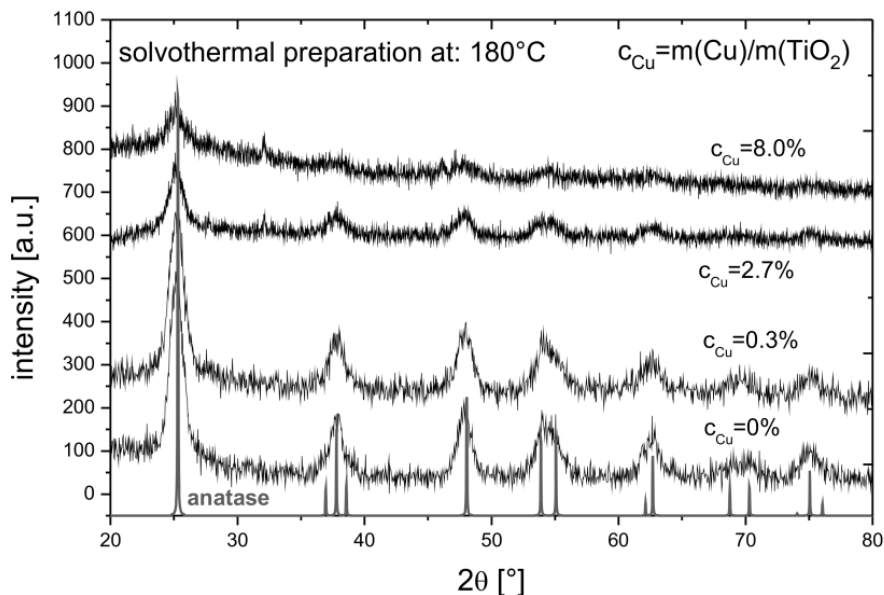


Figure 8. XRD measurements of powders obtained by solvent evaporation of Cu/TiO₂-composite coating solutions at 180°C. The copper content in the composite is set in the range of 0 % up to 8.0 %. Reflection positions of the anatase phase (ICSD [52]: coll. code 154601) are indicated by lines. The copper content c_{Cu} is calculated out of the amount m of Cu and TiO₂ used for preparation.

Regardless, an intermetallic phase with composition Cu-Ti (see for instance [58]) or Cu-Ti- X ($X = \text{O}, \text{N}, \text{C}$) seems probable. This is due to the following facts: (i) additional reflections firstly occur at high diffraction angles, typical for small, high-symmetric intermetallic compounds (organic materials usually generate high-intense Bragg reflections at low diffraction angles but is not observed), (ii) Cu-Ti compounds exhibit a diffraction pattern similar to the observed one (amount of reflections and intensity relations are comparable; scattering angles slightly differ), (iii) the additional reflections exhibit small full-width at half-maximum (FWHM) values and, in respect to the low amount of copper, high intensities, also typical for intermetallic compounds.

The evaluation of coated viscose textile, in respect to the morphology, is done by SEM (Figure 9, 10, 11). It can be seen that in addition to a smooth more regular coating also larger agglomerates occur and are fixed onto the fibers. The SEM images show viscose textiles coated by composites solvothermally prepared at 140°C (Figure 9) and 180°C (Figure 10). With both different process temperatures a regular coating and additional larger agglomerates are observed after coating on viscose. The presence and deposition of larger agglomerates seems, qualitatively, not to be significantly influenced by the process temperature.

Furthermore, as is indicated by SEM, the applied composite coating lead to a bridging between the fibers. Such a bridging/connection of fibers is typical for the application of a sol-gel coating agent [59, 60]. The extent of bridging is determined by the amount of applied sol-gel coating and can result, in case of application of high concentrated sols, in the formation of cracks in the coating [59]. For other applications, e. g. water repellent or soil repellent coatings of fibers, the formation of cracks in the protecting coating, will erase inhibit the wished desired effect of repellency. However, for purposes of antimicrobial or photoactive

applications the formation of cracks in the functional coating is not a disadvantage. A crack formation may lead to an increase of surface area and thus to distinct properties. In any case, a bridging of fibers cause a certain increase of the stiffness of the coated fabric, which may limit the usability of the coated textile for clothing purposes [61, 62]. However, for applications in the technical sector for wastewater treatment or filter materials this is not a disadvantage. For the development of antimicrobial wound bandages for use in the medical sector certain stiffness could also be helpful to reduce the sticking of the bandage to the healing wound [63].

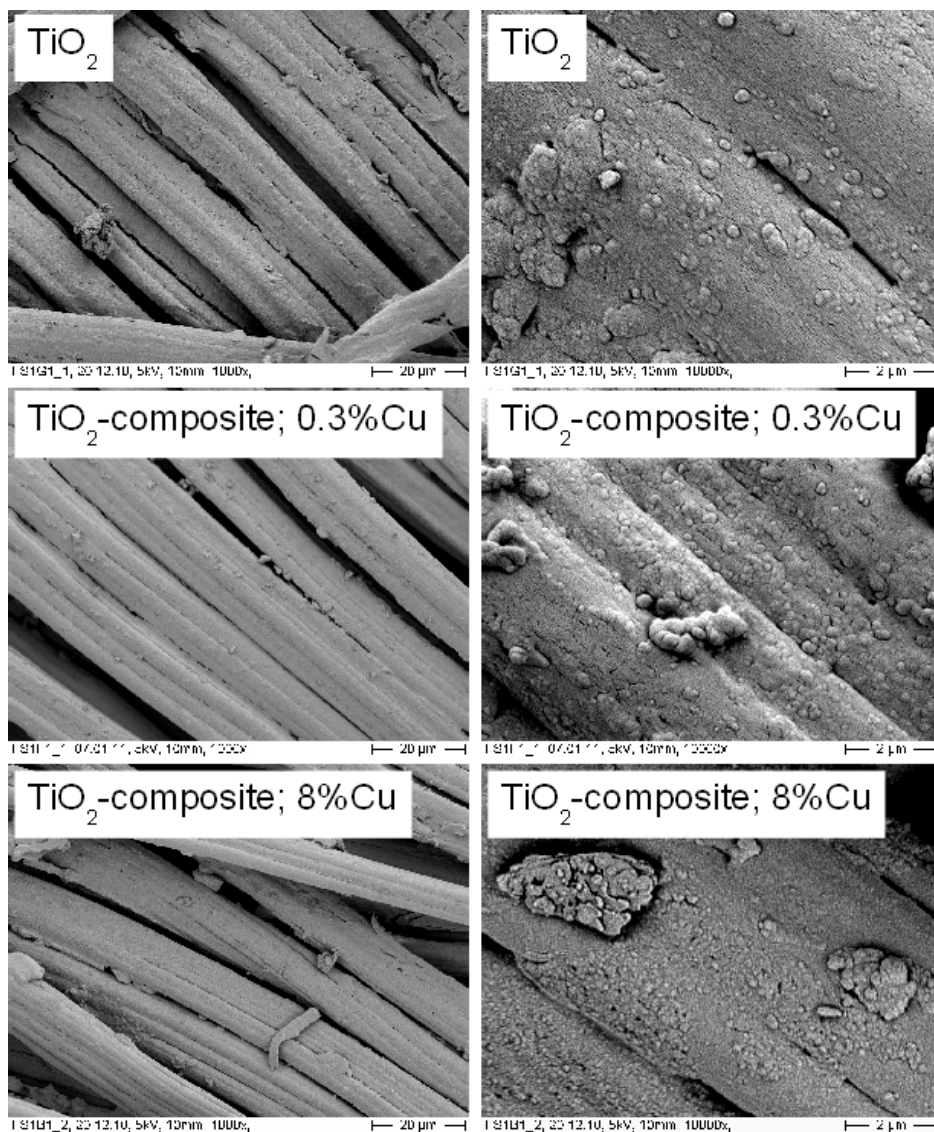


Figure 9. SEM-images of viscose fibers coated with TiO_2 with and without the copper component (solvothermal preparation of the coating agent at 140°C). Low resolution images are shown left, magnified ones right.

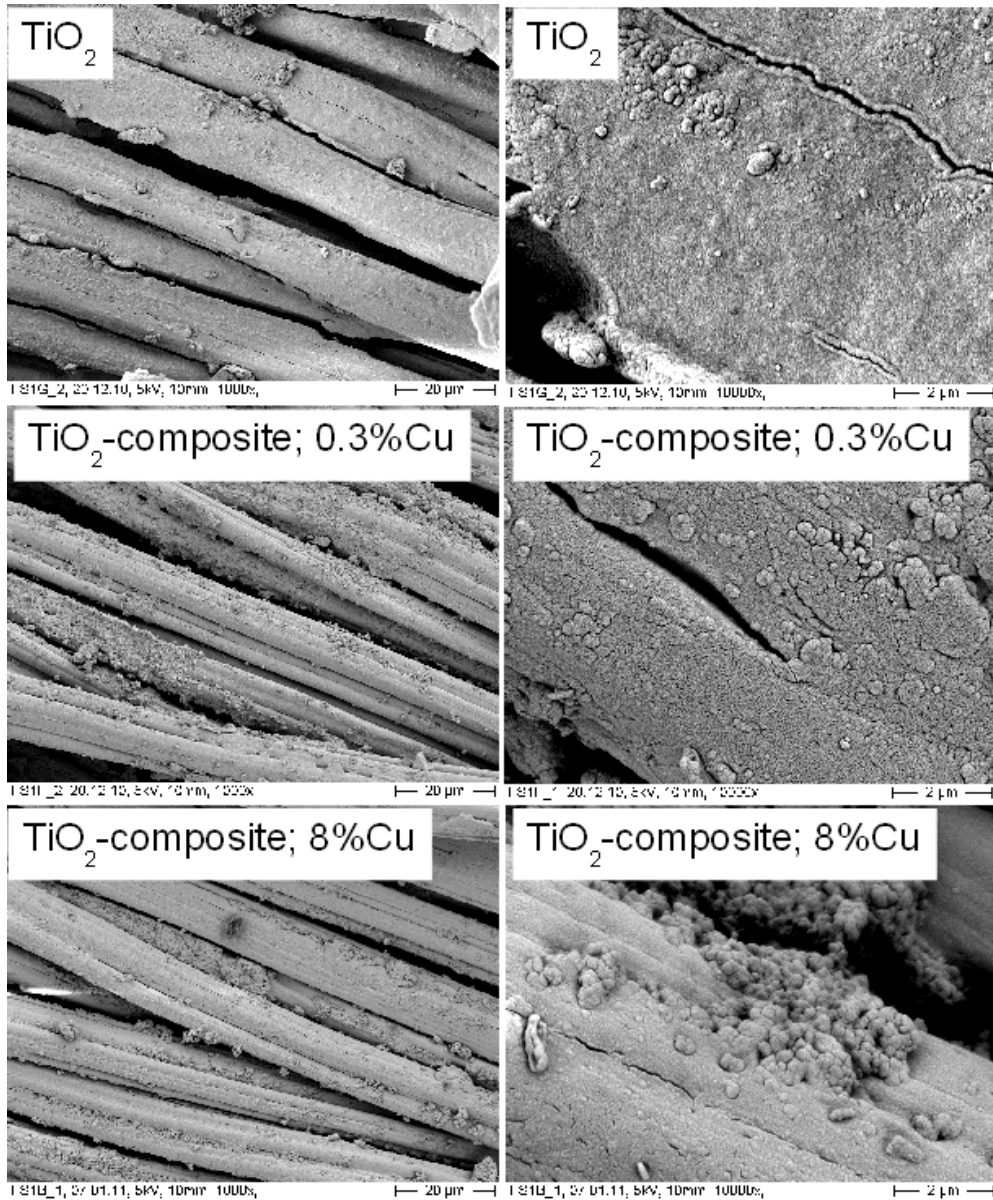


Figure 10. SEM-images of viscose fibers coated with TiO_2 with and without copper component (solvothormal preparation of the coating agent at 180°C). Low resolution images are shown left, magnified ones right.

From SEM images with higher resolution follows that the deposited TiO_2 composite contains a porous structure with typical dimension of less than 100 nm (Figure 11). A reference to an uncoated viscose fabric containing a smooth surface is also depicted in Figure 11. Such porosity may be an advantage to obtain certain photoactivity, again due to a larger surface area inherent to the porous structure and compared to analogous smooth coatings.

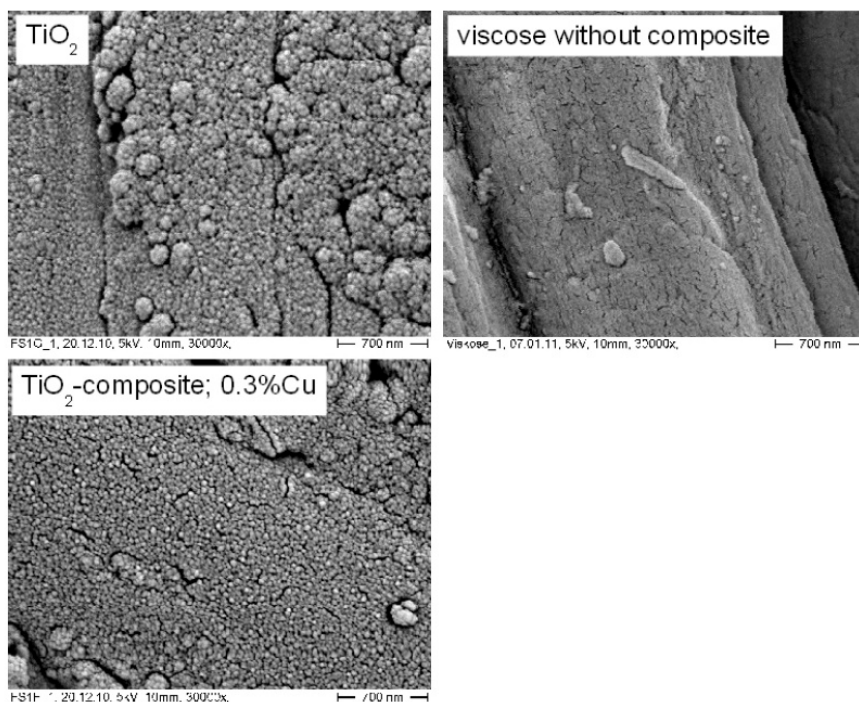


Figure 11. High-resolution SEM-images of viscose fabric with and without composite coating. Solvothermal preparation of the coating agent was done at 180°C.

3.2. Photocatalytic Activity of Coated Fabrics

The photocatalytic activity of the coated fabrics is determined as photodegradation of two organic dye stuffs in presence of oxygen and UV-light. Reference measurements are performed with the same testing procedure under dark conditions. In any case under dark conditions no significant reduction of dye concentration was detected. The tests were performed with the two dyes Acid Orange 7 and Rhodamin B. It is reported earlier that Rhodamin B is more sensitive for photodecomposition catalysed by TiO₂ as Acid Orange 7 [41]. This higher sensitivity probably explains the higher rate of photodecomposition of Rhodamin B compared to Acid Orange7 in presence of the viscose fabrics coated with TiO₂ (Figure 12).

It has to be noted, that the photodegradation of Rhodamin B in the chosen set-up lead to a shift of the absorption maximum of the dye solution and therefore to a change in coloration (Figure 13). This shift of the absorption spectrum is probably caused by deethylation reactions of the Rhodamin B during photodegradation [64-66]. In contrast by testing the photoactivity with Acid Orange 7 no shift of the absorption maximum at 484 nm is observed.

By testing with Acid Orange 7 a significant photodegradation is only observed for pure TiO₂ coatings and a solvothermal preparation of the TiO₂ coating agent at 180°C. If the solvothermal preparation is performed at the lower temperature of 140°C or only a small amount of copper are added to the TiO₂ composite, the photoactivity is drastically decreased to values smaller than 10%. Even if the testing is performed with the more sensitive dye

Rhodamin B, also for the composites prepared at 140°C no significant photodegradation was determined. In comparison, composites prepared at 180°C lead to certain photoactivity, even if copper is present in the TiO₂ coating. In this case, also the photoactivity decreases with increasing copper content in the composite coating (Figure 12).

The lower photoactivity of composite coatings prepared with the lower solvothermal process temperature of 140°C, can be easily explained. Under the chosen preparation conditions, the lower process temperature is insufficient for the formation of anatase, so mostly amorphous TiO₂ is deposited onto the viscose fabrics. However to gain a certain photoactivity the presence of TiO₂ in anatase modification is necessary. For the composites solvothermally prepared at higher temperature of 180°C, the situation is different. As could be shown by XRD, significant amounts of anatase are found in these composites and hence a significant photoactivity is observed for the pure TiO₂ coating.

By addition of copper to the composite the formation of anatase is hindered in the solvothermal process. Thus, the photoactivity decreases with increasing copper content in the composite. However, even with the highest copper content investigated, the formation of crystalline anatase can be clearly verified while the determined photoactivity is near zero. For this, it should be concluded that the addition of copper to the TiO₂ composite has two results. First, the formation of anatase is hindered. Second, even if crystalline anatase is formed, its photoactivity is low, so it could be concluded that the formed copper compounds inhibit the photoactivity of anatase. This observation, that the addition of copper to photoactive TiO₂ lead to a decrease of photoactivity is in contrast to several reports in literature which report an increase of the photoactivity in presence of copper component [29, 67]. However, in both references the active copper species is suggested to be in the oxidation state of Cu (I), e.g. as Cu₂O on the surface of TiO₂ particles. The solvothermally prepared Cu/TiO₂ composites are proposed to contain Cu in the oxidation state (II) and this as part of a Cu:Ti intermetallic phase and not as copper oxide. For this, it can be proposed that the formation of different Cu/TiO₂ composites is the reason for the inhibition of the photoactivity of TiO₂.

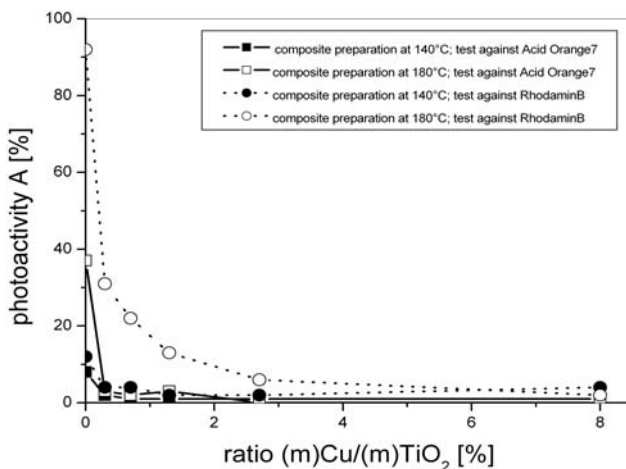


Figure 12. Photoactivity of Cu/TiO₂ composite coatings on viscose fabric as a function of increasing Cu content in the composite. The solvothermal preparation of the composites is performed at 140°C and 180°C. The photoactivity is tested as degradation of the dyes Acid Orange 7 and Rhodamin B.

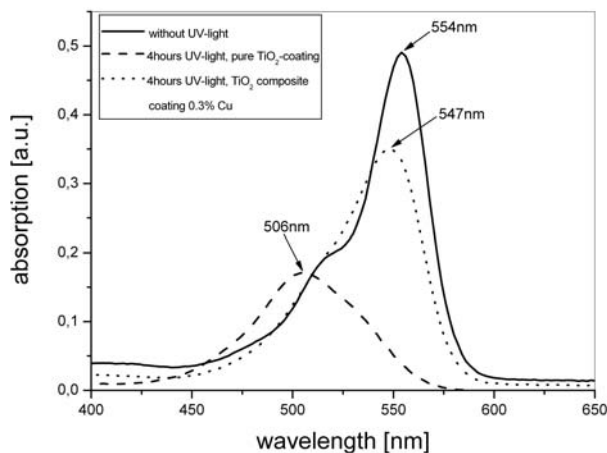


Figure 13. Optical spectra of solutions of Rhodamin B after photodegradation after 4 hours illumination with UV light. The changes of the absorption maxima are indicated.

Besides the testing of photoactivity in presence of oxygen, the photoactivity is tested additionally in the presence of the more reactive oxidative agent hydrogenperoxide. Without the presence of a photocatalyst the used dye solutions are stable in presence of H₂O₂ under dark conditions (Figure 14). For Acid Orange 7 also by illumination with UV-light only a small decomposition is observed. For Rhodamin B this decomposition is significant in presence of H₂O₂ and UV-light but without a photocatalyst (Figure 14). Also a nearly complete decolouration of Rhodamin B is observed in presence of the composite coated viscose and H₂O₂ in dark conditions. Due to this high sensitivity of Rhodamin B against decomposition with H₂O₂, the investigation of photoactivity of the prepared textile coatings in presence of H₂O₂ are only performed with the more stable dye Acid Orange 7.

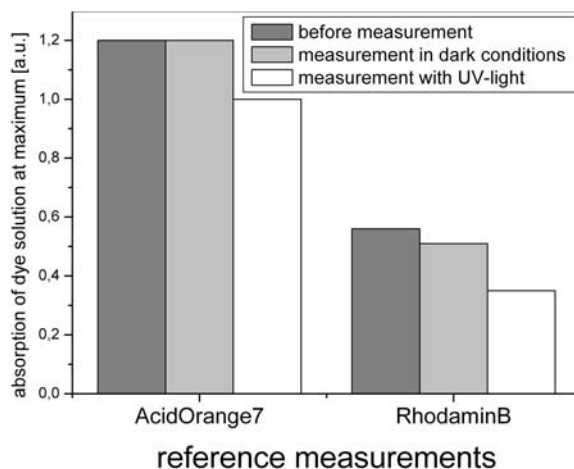


Figure 14. Reference measurements of dye decomposition in presence of H₂O₂ and UV light. The reference measurements are performed in presence of uncoated viscose fabrics and in absence of any TiO₂ composite. The absorption measurements are performed at the maximum absorption in the visible range – for Acid Orange 7 at 484 nm, for Rhodamin B at 554 nm.

If the photoactivity of the Cu/TiO₂ composite coated viscose is tested as photodecomposition of Acid Orange 7 in presence of H₂O₂, a totally different photoactive behaviour is observed (Figure 15). All TiO₂ composites solvothermally prepared at 140°C or 180°C contain a significant photoactivity. The photoactivity of the pure TiO₂ coatings is moderate between 20% and 30% and is increased drastically by addition of copper. The Cu/TiO₂ composites prepared at 140°C contain the highest photoactivity with photodecomposition rates of around 80%, which is nearly the plateau value between a Cu content of 1% up to 8%. The Cu/TiO₂ composites prepared at higher temperature of 180°C lead to less photoactive coatings onto viscose with a rate of photodecomposition of 70% which is reached with a copper content of 1% to 2.5%. The higher photoactivity of the composites prepared at lower temperature of 140°C surprises especially in the background, that under these preparation conditions nearly no anatase is observed by XRD measurements and the amorphous type of TiO₂ is not supposed to lead to strong photoactivity. A similar observation was made recently for SiO₂/TiO₂ composites prepared in a similar solvothermal process and used as coating agent for textile substrates [65].

The different behaviour of different TiO₂ modifications in presence of H₂O₂ is earlier described in the literature for a comparison between the modifications anatase and rutile [47]. It was observed that rutile does not cause a photoactive reaction with O₂ which has been explained by a higher stability of O₂⁻ species adsorbed on the rutile surface. When H₂O₂ is present next to rutile a reactive OH radical is formed leading to further photodecomposition reactions. Such a process may also be an explanation for the strong dye decomposition in presence of solvothermally prepared amorphous TiO₂ and H₂O₂. Additional to the stronger photoactivity of the prepared amorphous TiO₂ with H₂O₂, it should be proposed that this process is enhanced by copper doping of the TiO₂-composites.

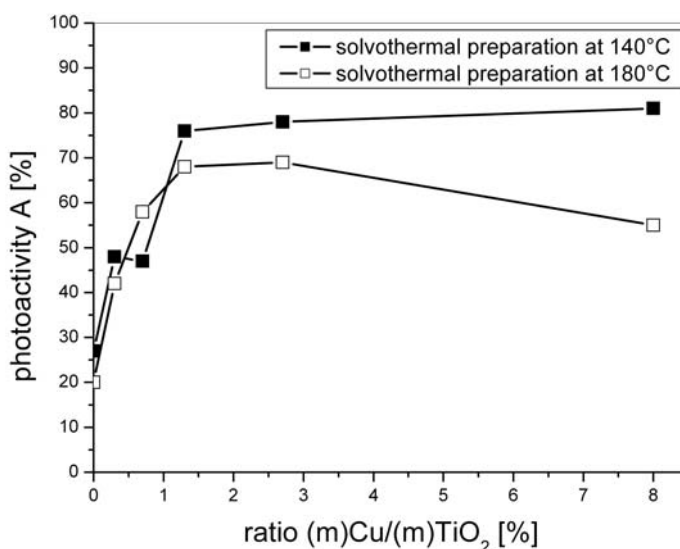


Figure 15. Photoactivity of Cu/TiO₂ composite coatings on viscose fabric as a function of increasing Cu content in the composite. The solvothermal preparation of the composites was done at 140°C and 180°C. The photoactivity is tested as degradation of the dye Acid Orange 7 by photooxidation with hydrogenperoxide H₂O₂.

The photoactivity of the coated fabrics is determined as the difference in dye decomposition measured after illumination with UV-light compared to the dye decomposition under dark conditions. If the photoactivity is determined without H₂O₂, under dark conditions nearly no decomposition of Acid Orange 7 is observed. In case of determining the photoactivity in presence of H₂O₂, a different behaviour with a certain decomposition of Acid Orange 7 under dark conditions is observed (Figure 16). Viscose fabrics coated with Cu/TiO₂-composites solvothermally prepared at 140°C lead to a dye decomposition under dark conditions which is enhanced with increasing copper content in the composite. In comparison the Cu/TiO₂-composites prepared at higher temperature of 180°C nearly exhibit no reaction under dark conditions. Also it has to be stated that after treatment in dark conditions the coated viscose fabrics nearly do not contain coloration after this dye exposition, so an adsorption of dye by Cu/TiO₂ coated textile can be excluded. For this reason the reduction of dye concentration is basically not a result of dye adsorption but should be attributed to dye decomposition. Since for this process of dye decomposition only the presence of Cu/TiO₂-composite but not the illumination with UV light is necessary, it could be suggested that in presence of H₂O₂ the here prepared Cu/TiO₂-composite coating acts additionally as a catalyst instead of a photocatalyst for dye decomposition. For practical application in wastewater treatment this property could be of high interest. A photoreactor for wastewater treatment based of textiles coated with this Cu/TiO₂-composite will keep a certain rate of decomposition even in case that the light source is not present. This is of particular interest for photoreactors using sunlight as light source, which light intensity varying depending on the daytime but also on the weather conditions.

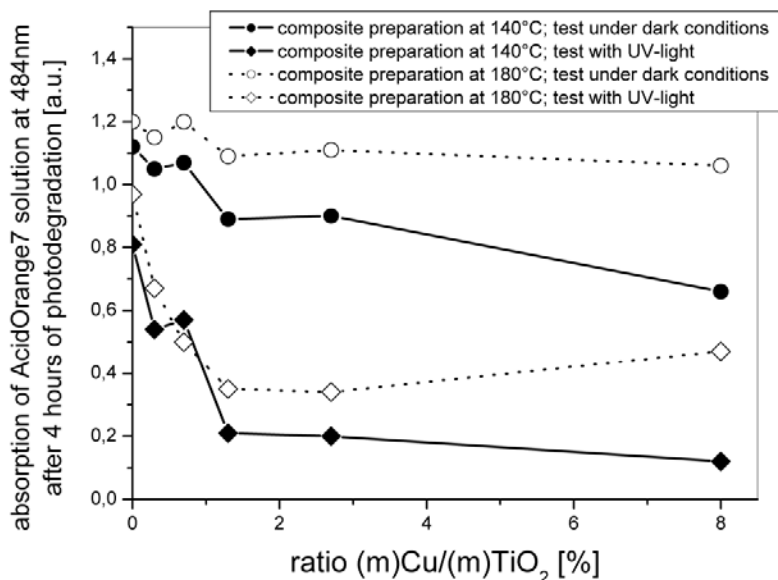


Figure 16. Decomposition of organic dye (Acid Orange 7) by H₂O₂ in presence of viscose fabrics coated with Cu/TiO₂-composites with increasing Cu content in the composite. The solvothermal preparation of the composites is performed at 140°C and 180°C. The decomposition is determined under dark conditions without light and under illumination with UV-light. Given is the absorption value at the absorption maximum at 484 nm.

3.3. Antimicrobial Activity of Coated Fabrics

The antimicrobial activity of fabrics coated with copper/TiO₂ composites is tested in two different test arrangements with and without illumination with UV-light. The composites used for coating preparation are solvothermally prepared at 140°C or 180°C and the antimicrobial activity is determined as function of increasing copper content in the composite (Tables 2 and 3).

Under conditions of no illumination with UV-light the antimicrobial effect is clearly related to the amount of copper in the composite (Table 2). The pure TiO₂ coating does not lead to an antimicrobial effect and the number of CFU counted is nearly the same as for the uncoated fabric used as reference. However even the addition of very small amounts of copper to the composite leads to a drastic decrease in CFU which indicates a strong antimicrobial effect. Even an amount of only 0.3 copper in the TiO₂ composite seems to be sufficient to inhibit the growth of *E.coli* bacterium after a contact time of 24 hours.

From these results it can be concluded that the pure TiO₂ do not contain any antimicrobial properties under dark conditions and that the copper containing composites in contrast exhibit a strong antimicrobial property. Because of measurements under dark conditions, it is clear that the antimicrobial effect of the copper component is not caused by a photocatalytic effect. Instead of antimicrobial properties caused by a photocatalytic effect it could be proposed that the antimicrobial effect of the copper containing composites is the result of the release of copper ions [37]. Copper belongs to a group of metals which inhibits the growth of microorganism. This antimicrobial effect of metals is often named oligodynamic effect and is observed for elementary metals but also with metal compounds [69]. This oligodynamic effect is not influenced by illumination and could explain the high antimicrobial activity of the coated textiles even if only small amounts of copper are present in the TiO₂ composite coating.

Table 2. Antimicrobial properties of viscose fabrics coated with copper/TiO₂ composites of increasing copper content. The composites are solvothermally prepared at 140°C and 180°C. The antimicrobial property is reflected by the amount of colony forming units CFU of the bacterium *E. coli* after 24 hours growing in dark conditions

Ratio Cu/TiO ₂ [%]	Colony forming units CFU; after 24 hours dark conditions	
	Solvothermal preparation at 140°C	Solvothermal preparation at 180°C
0	>500	>500
0.3	17	63
0.7	0	0
1.3	0	0
2.7	0	0
8.0	0	0
Uncoated reference	>500	

If the antimicrobial tests are performed in presence of UV-light the antimicrobial effect is related to the amount of copper in the composite, the temperature used during solvothermal preparation of the composite and the duration of UV-illumination (Table 3). Beside the values

given in table 3 also the photographs of the agar plates used for antimicrobial testing are depicted in Figure 17.

By using this test regime it is also clearly seen that with increasing copper content in the composite the antimicrobial effect of the composite coating increases. This can again be easily explained by the intrinsic high antimicrobial property of copper compounds. However, if the antimicrobial tests are performed under UV-illumination, also a significant germ reduction can be observed with the pure TiO₂ composite coatings or TiO₂ coatings with only small amounts of copper compound added.

This antimicrobial effect of the pure TiO₂ coating is only detectable with UV-illumination and increases also with increasing duration of UV-illumination. This is a significant hint, that the antimicrobial effect of the here used TiO₂ textile coatings is the result of a photocatalytic reaction. By this photocatalytic reaction the oxidation of germs by oxygen is driven and by this the germ spreading is inhibited. A further hint for the antimicrobial photoactive reaction is that TiO₂ composites solvothermally prepared at lower temperature of 140°C are less effective than the composites prepared at higher temperature of 180°C. Only the composites prepared at 180°C contains clearly the crystalline TiO₂ type anatase and lead also to a significant photodegradation of organic dye stuff. For this, these materials prepared at 180°C should contain a strong photocatalytic activity which also should lead to a more significant antimicrobial effect. However also a small antimicrobial effect based on the photoactivity could be estimated also for TiO₂ solvothermally prepared at 140°C, if the growth of *E. coli* on the agar plates is compared visually with the plates after testing the uncoated reference (Figure 17).

Table 3 Antimicrobial properties of viscose fabrics coated with Cu/TiO₂ composites with increasing copper content. The composites are solvothermally prepared at 140°C or 180°C. The antimicrobial property is reflected in the amount of colony forming units CFU of the bacterium *E.coli* after growing under illumination with UV light with increasing duration. For uncoated viscose a number of >200 CFU is counted under the chosen test conditions

Ratio Cu/TiO ₂ [%]	Solvothermal preparation at 140°C			Solvothermal preparation at 180°C		
	CFU; 3.5h UV light	CFU; after 6h UV light	CFU; after 24h UV light	CFU; 3.5h UV light	CFU; after 6h UV light	CFU; after 24h UV light
0	>200	>200	>200	>200	3	0
0.3	>200	>200	0	>200	19	0
0.7	>200	4	0	188	0	0
8.0	1	0	0	3	0	0

Altogether it can be stated, that the antimicrobial effect of the used composite coatings is the result of two effects, the photoactivity of the anatase and the oligodynamic effect of the copper compounds. The addition of copper lead to a decrease of photoactivity, determined by photodegradation of organic dyes, so it can be estimated that the influence of the photoactivity on the antimicrobial properties decreases with increasing copper content. The antimicrobial effect of those samples with higher copper content is probably only the result of the oligodynamic effect. In contrast the influence of the photoactivity on the antimicrobial

effect is higher, if no or only small amounts of copper compounds are present in the composite coating.

Both effects photoactive and oligodynamic are supposed to act contradictorily for the here used copper containing TiO_2 composites, because with increasing copper content the photoactivity of the composite decreases while the oligodynamic effect gets higher influence on the whole antimicrobial activity. With this background, the slightly increased number of CFU in case of low amount of 0.3% Cu/ TiO_2 compared to the pure TiO_2 composite is may be explainable. With addition of small amounts of copper the photoactivity of the TiO_2 composite is drastically decreased and this small amount of copper is not enough to compensate fully the loss in photoactivity by the oligodynamic effect.

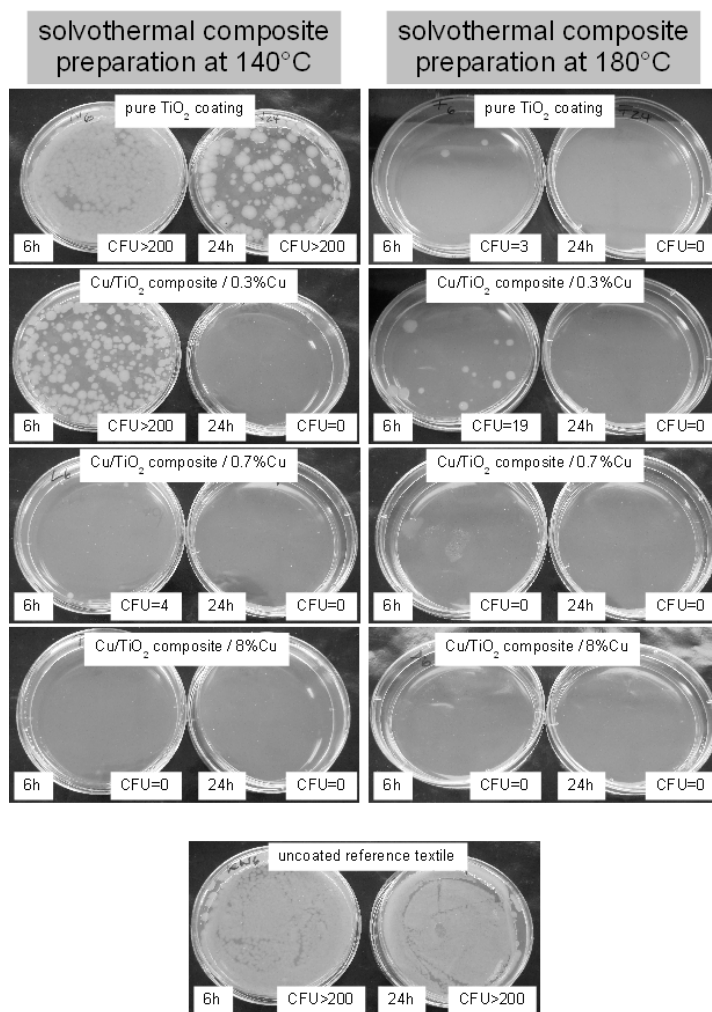


Figure 17. Agar plates after testing of antimicrobial properties of viscose fabrics coated with copper/ TiO_2 composites with increasing copper content. The composites are solvothermally prepared at 140°C and 180°C. The antimicrobial properties are reflected in the amount of colony forming units CFU of the bacterium *E. coli* after growing under illumination with UV light with duration of 6 hours and 24 hours. The agar plates for uncoated viscose as reference are given below.

CONCLUSION

It was demonstrated that a solvothermal preparation procedure can be used to prepare TiO₂ coating agents for the treatment of textiles. These TiO₂ coated textiles exhibit a certain photoactivity as determined by the decomposition of dye under UV light irradiation. TiO₂ particles in solution are modified by copper compounds leading to composite coating agents for textiles. The aim of this modification was to enhance the photoactivity of the coatings and to reach a significant antimicrobial property. However if the photoactivity is determined as dye decomposition in presence of O₂ as oxidative agent, the photoactivity is strongly decreased, if the TiO₂ is combined to a TiO₂/copper composite coating. A different behaviour is observed, if the photoactivity is determined with H₂O₂ as oxidative agent. In this case, textile fabrics coated with copper containing TiO₂ can be realized with high photoactivity. These composite coatings catalyse effectively the dye decomposition by oxidation with H₂O₂. Applications of these coated textiles can be found for example as filter material for wastewater treatment and decoloration of wastewater from textile dyeing industry.

By combination of TiO₂ coatings with copper compounds textile coatings with high antimicrobial activity can be realized. These coated textiles could be of interest for the medical sector, where a contamination with hazardous germs needs to be avoided. Also, applications for filter materials are of interest, if a biological contamination of the textile filter is not wanted.

For every type of mentioned application it is easily possible to optimize the Cu/TiO₂-composite used for textile coating by adjusting the copper content in the composite or the temperature of the solvothermal process for composite preparation.

ACKNOWLEDGEMENTS

This work was financial supported by: German Bundesministerium für Wirtschaft und Technologie within the research program „Industrielle Vorlaufforschung“ – project number: VF070012; German Bundesministerium für Bildung und Forschung (PT-DLR, Internationales Büro des BMBF) within the framework „Internationale Zusammenarbeit in Bildung und Forschung mit Korea“ – project number: KOR 08/025.

REFERENCES

- [1] Linsebigler, A.L., Lu, G., and Yates, J.T. (1995). Photocatalysis on TiO₂ Surfaces: Principles, Mechanisms, and Selected Results. *Chemical Reviews*, 95: 735-758.
- [2] Hoffmann, M.R., Martin, S.T., Choi, W., and Bahnemann, D.W. (1995). Environmental Applications of Semiconductor Photocatalysis. *Chemical Reviews*, 95: 69-96.
- [3] Han, F., Kambala, V.S.R., Srinivasan, M., Rajarathnam, D., and Naidu, R. (2009). Tailored titanium dioxide photocatalysts for the degradation of organic dyes in wastewater treatment. *Applied Catalysis A*, 359: 25-40.
- [4] Silva, A.M.T., Silva, C.G., Drazic, G., and Faria, J.L. (2009). Ce-doped TiO₂ for photocatalytic degradation of chlorophenol. *Catalysis Today*, 144: 13-18.

-
- [5] Theurich, J., Lindner, M., and Bahnemann, D.W. (1996). Photocatalytic Degradation of 4-Chlorophenol in Aerated Aqueous Titanium Dioxide Suspensions: A Kinetic and Mechanistic Study. *Langmuir*, 12: 6368-6376.
- [6] Zhong, J.B., Ma, D., He, X.Y., Li, J. Z., and Chen, Y.Q. (2009). Sol- gel preparation and photocatalytic performance of $\text{TiO}_2/\text{SrAl}_2\text{O}_4$: Eu^{2+} , Dy^{3+} toward the oxidation of gaseous benzene. *Journal of Sol-Gel Science and Technology*, 52: 140-145.
- [7] Qi, K., Daoud, W.A., Xin, J.H., Mak, C.L., Tang, W., and Cheung, W.P. (2006). Self-cleaning cotton. *Journal of Materials Chemistry*, 16: 4567-4574.
- [8] [8] Daoud, W.A., Leung, S.K., Tung, W.S., Xin, J.H., Cheuk, K., and Qi, K. (2008). Self-Cleaning Keratins. *Chemistry of Materials*, 20: 1242-1244.
- [9] Qi, K., Xin, J.H., Daoud, W.A., and Mak, C.L. (2007). Functionalizing Polyester Fiber with a Self-Cleaning Property Using Anatase TiO_2 and Low-Temperature Plasma Treatment. *International Journal of Applied Ceramic Technology*, 4: 554-563.
- [10] Chen, S.F., Li, J.P., Qian, K., Xu, W.P., Lu, Y., Huang, W.X., and Yu, S.H. (2010). Large scale photochemical synthesis of $\text{M}@\text{TiO}_2$ nanocomposites ($\text{M} = \text{Ag}, \text{Pd}, \text{Au}, \text{Pt}$) and their optical properties, CO oxidation performance, and antibacterial effect. *Nano Research*, 3: 244-255.
- [11] Mahltig, B., and Haufe, H. (2010). Wirkstoffe in der Matrix. *Farbe and Lack*, 116/3: 27-31.
- [12] Shen, Y., Xiong, T., Du, H., Jin, H., Shang, J., and Yang, K. (2009). Phosphorous, nitrogen, and molybdenum ternary co-doped TiO_2 : preparation and photocatalytic activities under visible light. *Journal of Sol-Gel Science and Technology*, 50 : 98-102.
- [13] Shen, X., Wang, Y.X., Lu, L.Q., Chen, Y.L., Xia, Y., and Li, Y.H. (2010). Preparation and optical properties of TiO_2 coreshell nanocatalyst from sol-gel-hydrothermal process. *Journal of Sol-Gel Science and Technology*, 54: 340-346.
- [14] Chen, D., and Jordan, E.H. (2009). Sol-gel synthesis and characterization of $\text{Al}_2\text{O}_3/\text{TiO}_2$ nanocrystalline powder. *Journal of Sol-Gel Science and Technology*, 50 : 44-47.
- [15] Neppolian, B., Jung, H., and Choi, H. (2007). Photocatalytic Degradation of 4-Chlorophenol Using TiO_2 and Pt-TiO_2 Nanoparticles Prepared by Sol-Gel Method. *Journal of advanced oxidation technologies*, 10: 369-374.
- [16] Wang, J.A., Cuan, A., Salmones, J., Nava, N., Castillo, S., Moran-Pineda, M., and Rojas, F. (2004). Studies of sol-gel TiO_2 and Pt/TiO_2 catalysts for NO reduction by CO in an oxygen-rich condition. *Applied Surface Science*, 230: 94-105.
- [17] Matsuoka, J., Yoshida, H., Nasu, H., and Kamiya, K. (1997). Preparation of Gold Microcrystal-Doped TiO_2 , ZrO_2 and Al_2O_3 Films Through Sol-Gel Process. *Journal of Sol-Gel Science and Technology*, 9: 145-156.
- [18] Sonawane, R.S., and Dongare, M.K. (2006). Sol-gel synthesis of Au/TiO_2 thin films for photocatalytic degradation of phenol in sunlight. *Journal of Molecular Catalysis A*, 243: 68-76.
- [19] Rodriguez-Gonzalez, V., Zanella, R., Angel del, G., and Gomez, R. (2008). MTBE visible-light photocatalytic decomposition over Au/TiO_2 and $\text{Au/TiO}_2\text{-Al}_2\text{O}_3$ sol-gel prepared catalysts. *Journal of Molecular Catalysis A*, 281: 93-98.
- [20] Crisan, D., Dragan, N., Crisan, M., Raileanu, M., Braileanu, A., Anastasescu, M., Ianculescu, A., Mardare, D., Luca, D., and Marinescu, V. (2008). Crystallization study of sol-gel un-doped and Pd-doped TiO_2 materials. *The Journal of Physics and Chemistry of Solids*, 69: 2548-2554.

-
- [21] Karakas, G., Mitome-Watson, J., and Ozkan, U.S. (2002). In situ DRIFTS characterization of wet-impregnated and sol-gel Pd/TiO₂ for NO reduction with CH₄. *Catalysis Communications*, 3: 199-206.
- [22] Sakthivel, S., Shankar, M.V., Palanichamy, M., Arabindoo, B., Bahnemann, D.W., and Murugesan, V. (2004). Enhancement of photocatalytic activity by metal deposition: characterisation and photonic efficiency of Pt, Au and Pd deposited on TiO₂ catalyst. *Water Research*, 38: 3001-3008.
- [23] Li, H., Zhao, G., Chen, Z., Song, B., and Han, G. (2010). TiO₂-Ag Nanocomposites by Low-Temperature Sol-Gel Processing. *Journal of the American Ceramic Society*, 93: 445-449.
- [24] Amin, S.A., Pazouki, M., and Hosseinnia, A. (2009). Synthesis of TiO₂-Ag nanocomposite with sol-gel method and investigation of its antibacterial activity against E. coli. *Powder technology*, 196: 241-245.
- [25] Zhang, H., and Chen, G. (2009). Potent Antibacterial Activities of Ag/TiO₂ Nanocomposite Powders Synthesized by a One-Pot Sol-Gel Method. *Environmental science and technology*, 43: 2905-2910.
- [26] Patil, S.R., Stangar, U.L., Gross, S., and Schubert, U. (2008). Super-Hydrophilic and Photocatalytic Properties of Ag-TiO₂ Thin Films Prepared by Sol-Gel Technique. *Journal of Advanced Oxidation Technologies*, 11: 327-337.
- [27] Lee, M.S., Hong, S.S., and Mohseni, M. (2005). Synthesis of photocatalytic nanosized TiO₂-Ag particles with sol-gel method using reduction agent. *Journal of molecular catalysis*, 242: 135-140.
- [28] Traversa, E., Di Vona, M.L., Nunziante, P., Licoccia, S., Sasaki, T., and Koshizaki, N. (2000). Sol-Gel Preparation and Characterization of Ag-TiO₂ Nanocomposite Thin Films. *Journal of Sol-Gel Science and Technology*, 19: 733-736.
- [29] Tseng, I.-H., Wu, J.C.S., and Chou, H.-Y. (2004). Effects of sol-gel procedures on the photocatalysis of Cu/TiO₂ in CO₂ photoreduction. *Journal of Catalysis*, 221: 432-440.
- [30] Celik, E., Gokcen, Z., Azem, N.F.A., Tanoglu, M., and Emrullahoglu, O.F. (2006). Processing, characterization and photocatalytic properties of Cu doped TiO₂ thin films on glass substrate by sol-gel technique. *Materials science and engineering*, 132: 258-265.
- [31] Bokhimi, X., Novaro, O., Gonzalez, R.D., Lopez, T., Chimal, O., Asomoza, A., and Gomez, R. (2009). Copper Precursor Effect on Reducibility and Titania Phases Concentration of Sol-Gel Cu/TiO₂ Catalyst. *Journal of Solid State Chemistry*, 144: 349-353.
- [32] Bokhimi, X., Morales, A., Novaro, O., Lopez, T., Chimal, O., Asomoza, M., and Gomez, R. (1997). Effect of Copper Precursor on the Stabilization of Titania Phases, and the Optical Properties of Cu/TiO₂ Prepared with the Sol-Gel Technique. *Chemistry of Materials*, 9: 2616-2620.
- [33] Epifani, M., Giannini, C., Tapfer, L., and Vasanelli, L. (2000). Sol-Gel Synthesis and Characterization of Ag and Au Nanoparticles in SiO₂, TiO₂, and ZrO₂ Thin Films. *Journal of the American Ceramic Society*, 83: 2385-2393.
- [34] Zhao, G., Kozuka, H., and Yoko, T. (1996). Photoelectrochemical properties of TiO₂ coating films prepared using different solvents by the sol-gel method. *Thin Solid Films*, 277: 147-154.

-
- [35] Mahltig, B., Fiedler, D., and Böttcher, H. (2004). Antimicrobial Sol-Gel Coatings. *Journal of Sol-Gel Science and Technology*, 32: 219-222.
- [36] Mahltig, B., Gutmann, E., Meyer, D.C., Reibold, M., Bund, A., and Böttcher, H. (2009). Thermal preparation and stabilization of crystalline silver particles in SiO₂-based coating solutions. *Journal of Sol-Gel Science and Technology*, 49: 202-208.
- [37] Mahltig, B., Fiedler, D., Fischer, A., and Simon, P. (2010). Antimicrobial coatings on textiles, modification of sol-gel layers with organic and inorganic biocides. *Journal of Sol-Gel Science and Technology*, 55: 269-277.
- [38] Mahltig, B. and Textor, T. (2008). *Nanosols and Textiles*, Singapore: World Scientific, p. 132-139.
- [39] Mahltig, B., Haufe, H., and Böttcher, H. (2005). Functionalisation of textiles by inorganic sol-gel coatings. *Journal of Materials Chemistry*, 15: 4385-4398.
- [40] Mahltig, B., Gutmann, E., Meyer, D.C., Reibold, M., Dresler, B., Günther, K., Faßler, D., and Böttcher, H. (2007). Solvothermal preparation of metallized titania sols for photocatalytic and antimicrobial coatings. *Journal of Materials Chemistry*, 17: 2367-2374.
- [41] Böttcher, H., Mahltig, B., Sarsour, J., and Stegmaier, T. (2010). Qualitative investigations of the photocatalytic dye destruction by TiO₂-coated polyester fabrics. *Journal of Sol-Gel Science and Technology*, 55: 177-185.
- [42] Mahltig, B., Gutmann, E., Reibold, M., Meyer, D.C., and Böttcher, H. (2009). Synthesis of Ag and Ag/SiO₂ sols by solvothermal method and their bactericidal activity. *Journal of Sol-Gel Science and Technology*, 51: 204-214.
- [43] Hirakawa, T., and Nosaka, Y. (2002). Properties of O₂⁻ and OH Formed in TiO₂ Aqueous Suspensions by Photocatalytic Reaction and the Influence of H₂O₂ and Some Ions. *Langmuir*, 18: 3247-3254.
- [44] Garcia, J. C., Oliveira, J.L., Silva, A.E.C., Oliveira, C.C., Nozaki, J., and Souza de, N.E. (2007). Comparative study of the degradation of real textile effluents by photocatalytic reactions involving UV/TiO₂/H₂O₂ and UV/Fe²⁺/H₂O₂ systems. *Journal of Hazardous Materials*, 147 : 105-110.
- [45] Dominguez, J.R., Beltran, J., and Rodriguez, O. (2005). Vis and UV photocatalytic detoxification methods (using TiO₂, TiO₂/H₂O₂, TiO₂/O₃, TiO₂/S₂O₈²⁻, O₃, H₂O₂, S₂O₈²⁻, Fe³⁺/H₂O₂ and Fe³⁺/H₂O₂/C₂O₄²⁻) for dyes treatment. *Catalysis Today*, 101: 389-395.
- [46] Saquib, M., Tariq, M.A., Haquea, M.M., and Muneer, M. (2008). Photocatalytic degradation of disperse blue 1 using UV/TiO₂/H₂O₂ process. *Journal of Environmental Management*, 88: 300-306.
- [47] Hirakawa, T., Yawata, K., and Nosaka, Y. (2007). Photocatalytic reactivity for O₂⁻ and OH radical formation in anatase and rutile TiO₂ suspension as the effect of H₂O₂ addition. *Applied Catalysis A*, 325: 105-111.
- [48] Harir, M., Gaspar, A., Kanawati, B., Fekete, A., Frommberger, M., Martens, D., Kettrup, A., El Azzouzi, M., and Schmitt-Kopplin, P. (2008). Photocatalytic reactions of imazamox at TiO₂, H₂O₂ and TiO₂/H₂O₂ in water interfaces: Kinetic and photoproducts study. *Applied Catalysis B*, 84: 524-532.
- [49] Elmolla, E.S., and Chaudhuri, M. (2010). Photocatalytic degradation of amoxicillin, ampicillin and cloxacillin antibiotics in aqueous solution using UV/TiO₂ and UV/H₂O₂/TiO₂ photocatalysis. *Desalination*, 252: 46-52.

-
- [50] Zhang, K., and Oh, W.-C. (2009). The Photocatalytic Decomposition of Different Organic Dyes under UV Irradiation with and without H₂O₂ on Fe-ACF/TiO₂ Photocatalysts. *Journal of the Korean Ceramic Society*, 46: 561-567.
- [51] Powder Diffraction File (PDF 2), release 2001 (2001) Joint Committee on Powder Diffraction Standards–International Centre for Diffraction Data (JCPDS–ICDD).
- [52] ICSD (2011). Inorganic Crystal Structure Database, <http://www.fiz-karlsruhe.de/icsd.html>
- [53] TOPAS (2000), General Profile and Structure Analysis Software for Powder Diffraction Data, V2.0, Bruker AXS GmbH, Karlsruhe, Germany.
- [54] Kryukova, G.N., Zenkovets, G.A., Shutilov, A.A., Wilde, M., Günther, K., Faßler, D., and Richter, K. (2007). Structural peculiarities of TiO₂ and Pt/TiO₂ catalysts for the photocatalytic oxidation of aqueous solution of Acid Orange 7 Dye upon ultraviolet light. *Applied Catalysis*, 71: 169-176.
- [55] Salz, D., Mahltig, B., Baalman, A., Wark, M., and Jaeger, N. (2000). Metal clusters in plasma polymer matrices. Part III. Optical properties and redox behaviour of Cu clusters. *Physical Chemistry Chemistry Physics*, 2: 3105-3110.
- [56] Oswald, H. R. (1961). Über natürlichen und künstlichen Gerhardtite. *Zeitschrift für Kristallographie*, 116: 210-219.
- [57] Effenberger, H. (1983). Verfeinerung der Kristallstruktur des monoklinen Dikupfer(II)-trihydroxi-nitrates Cu₂(NO₃)(OH)₃. *Zeitschrift für Kristallographie*, 165: 127-135.
- [58] Colinet, C., Pasturel, A., and Buschow, K.H.J. (1997). Enthalpies for formation of Ti-Cu intermetallic and amorphous phases. *Journal of Alloys and Compounds*, 247 :15-19.
- [59] Krüger, R., Bockmeyer, M.J., Dutschke, A., and Löbmann, P.C. (2006). Continuous Sol-Gel Coating of Ceramic Multifilaments: Evaluation of Fiber Bridging by Three-Point Bending Test. *Journal of the American Ceramic Society*, 89: 2080-2088.
- [60] Chapple, S.A., and Ferg, E. (2006). The influence of precursor ratios on the properties of cotton coated with sol-gel flame retardant. *American Association of Textile Chemists and Colorists : AATCC Review*, 6: 36-40.
- [61] Mahltig, B., and Fischer, A. (2010). Inorganic/organic polymer coatings for textiles to realize water repellent and antimicrobial properties-A study with respect to textile comfort. *Journal of Polymer Science B*, 48: 1562-1568.
- [62] Mahltig, B., and Textor, T. (2010). Silver Containing Sol-gel Coatings on Polyamide Fabrics as Antimicrobial Finish – Description of a Technical Application Process for Wash Permanent Antimicrobial Effect. *Fibers and Polymers*, 11: 1152-1158.
- [63] Mahltig, B., Böttcher, H., Langen, G., and Meister, M. (2002). Antiadhäsive Beschichtung zur Ausrüstung von Wundverbänden. German Patent DE1024987A1.
- [64] Yuan, S., Sheng, Q., Zhang, J., Yamashita, H., and He, D. (2008). Synthesis of thermally stable mesoporous TiO₂ and investigation of its photocatalytic activity. *Microporous and Mesoporous Materials*, 110: 501-507.
- [65] Wei, G., Zhang, Y., and Xiong, R. (2003). Controllable preparation of nanosized TiO₂ thin film and relationship between structure of film and its photocatalytic activity. *Science in China*, 46: 184-190.
- [66] Chen, F., Zhao, J., and Hidaka, H. (2003). Highly selective deethylation of rhodamine B : Adsorption and photooxidation pathways of the dye on the TiO₂ /SiO₂ composite photocatalyst. *International Journal of Photoenergy*, 5: 209-217.

- [67] Xu, Y., Liang, D., Lu, M., and Liu, D. (2008). Preparation and characterization of $\text{Cu}_2\text{O-TiO}_2$: Efficient photocatalytic degradation of methylene blue. *Materials Research Bulletin*, 43: 3474-3482.
- [68] Mahltig, B., Gutmann, E., and Meyer, D.C. (2011). Solvothermal preparation of nanocrystalline anatase containing TiO_2 and $\text{TiO}_2/\text{SiO}_2$ coating agents for application of photocatalytic treatments *Materials Chemistry and Physics*, 127: 285-291.
- [69] Wallhäußer, K. H. (1995). Praxis der Sterilisation Desinfektion – Konservierung, Stuttgart: Georg Thieme Verlag, p. 617-627.

Chapter 14

FUNCTIONAL CELLULOSE FIBRES FOR HYGIENIC AND MEDICAL APPLICATIONS

***Lidija Fras Zemljic^{*1}, Tatjana Kreže¹, Simona Strnad¹,
Olivera Šaupert¹ and Alenka Vesel²***

¹ Institute for Engineering Materials and Design, Faculty of Mechanical Engineering,
University of Maribor, Smetanova 17, SI-2000 Maribor, Slovenia.

Members of the European Polysaccharide Network of Excellence (EPNOE)

² Jožef Stefan Institute, Jamova 39, SI-1000 Ljubljana, Slovenia.

ABSTRACT

The presented research thematic focuses on cellulose fibres' functionalization by means of introducing new, naturally alternative polysaccharides as coatings for natural cellulose material. In this way, new advanced sanitary and medical cellulose materials could be developed *with* significant **absorption**, antiviral, and antimicrobial properties.

This chapter covers the physico-chemical and structural properties of cellulose fibres (natural and regenerated) and the influence of both properties on the adsorption of polysaccharides, in order to introduce new bioactive functionalities. It examines which properties predominately influence specific fibre functionality. Moreover, relevant methods are presented for revealing the structural and physico-chemical properties (with an emphasis on the charge determination) of non-functionalised, as well as functionalised, cellulose fibres (natural and regenerated). Finally, the applicability of these new materials for different hygiene and health care segments (skin and hygiene care, skin and gynaecological infections, wound treatment, etc.) are discussed.

* E-mail: lidija.zemljic@gmail.com

1. CELLULOSE FIBRES FOR TEXTILE APPLICATIONS - THE BEGINNING OF A NEW PROSPERITY

Textile fibres are broadly classified as natural fibres and man-made fibres, as shown in Figure 1. Natural fibres refer to fibres that occur within nature, and are found in vegetables (cellulose fibres), animals (protein fibres) and minerals (asbestos). Man-made fibres are those that are not present in nature, although they may be composed of naturally-occurring materials. They are classified into three main groups: those made by “transformation of natural polymers” (regenerated fibres), those made from synthetic polymers (synthetic fibres), and those made from inorganic materials (fibres made of metal, ceramics, and carbon or glass) [1].

NATURAL FIBRES	MAN-MADE FIBRES
VEGETABLE ORIGIN - CELLULOSE FIBRES	NATURAL POLYMER BASED
<ul style="list-style-type: none"> ● SEED FIBRES: COTTON ● BAST FIBRES: JUTE, FLAX, HEMP, KENAF ... ● LEAF FIBRES: ABACA, SISAL, MANILA ... 	<ul style="list-style-type: none"> ● REGENERATED CELLULOSE: VISCOSE, MODAL, LYOCCELL, CUPRO ● REGENERATED PROTEIN: CASEIN, ARACHIN ZEIN ● CELLULOSE ESTERS: ACETATES ● RUBBER: ELASTODIENE ● ALGINATE
ANIMAL ORIGIN – PROTEIN FIBRES	SYNTHETIC POLYMER BASED
<ul style="list-style-type: none"> ● WOOL ● HAIR FIBRES: ANGORA, MOHAIR, ALPACA ... ● SILK 	ACRYLIC, ARAMID, CHLOROFIBRE, FLUOROFIBRE, MODACRYLIC, POLYAMIDE, POLYESTER, POLYETHYLENE, POLYIMIDE, POLYPROPYLENE, VINYLAL, POLYLACTIDE ...
INORGANIC: ASBESTOS	INORGANIC: CARBON, CERAMIC, GLASS, METAL

Figure 1. Classification of textile fibres.

Currently, cellulose is the most common organic polymer, and is considered an almost inexhaustible source of raw material for the increasing demand for environmentally-friendly and biocompatible products. Wood pulp remains the most important raw material source for the processing of cellulose, most of which is used for the production of paper, cardboard, and for the production of cellulose-regenerated fibres and films.

Today, the use of cellulose fibres for the development of highly-innovative materials is recently gaining considerable attention, as emphasized by the numerous reviews on the topic. Moreover, cellulose fibres have a large active surface area and, due to their molecular structure, may be an ideal matrix for the design of bioactive, biocompatible, and intelligent materials [2-8]. Nowadays, the main goal regarding the surface treatments of cellulose fibres is to provide them with intelligent functions, such as the way they become: hydrophobic, which protect them from water uptake and release; to make them reactive towards polymeric matrices, in order to elaborate high-performance composite materials; to graft specific sensors at their surfaces to render them as photoluminescent, electrically-conductive materials, etc.

[9]. The trendiest is to incorporate a biofunctional product within the cellulose fibres [10]. Increasing world populations, aging population, better awareness and higher expectations regarding physical fitness, as well as improved hygiene and health-care standards, have had a great impact on the development of hygiene and health care products into highly-sophisticated smart devices. Diapers, sanitary-napkins, tampons, incontinence-products, panty-shields, wipes, etc. are designed to absorb and retain body fluids and solid wastes. A basic material, its chemical and supermolecular structure, as well as its composition and design as a hygiene product, have a major influence on its efficiency [2].

Thus, to clearly understand the functionality (physico-chemical and bioactive properties) of newly-processed cellulose fibres, it is extremely important to be able to analyse, in detail, fibre chemistry (fibre charge from among many others, is the most important), and the fibres' structure.

2. CELLULOSE STRUCTURAL AND PHYSICO-CHEMICAL CHARACTERISTICS

The molecular and supermolecular structures of natural and regenerated cellulose fibres have been thoroughly analysed over the last five decades [11-14]. The molecular structure of cellulose as a carbohydrate polymer is generated from repeating β -D-glucopyranose molecules that are covalently linked through acetal functions between the equatorial -OH group of C4 and the C1 carbon atom (β -1,4-glucan). As a result, cellulose is an extensive, linear-chain polymer with a large number of hydroxyl groups (three per anhydroglucose unit - AGU) present in the thermodynamically preferred 4C_1 conformation. In order to accommodate the preferred bond angles of the acetal oxygen bridges, every second AGU ring is rotated 180° within the plane. In this manner, two adjacent structural units define the disaccharide cellobiose.

The chain-length of cellulose, expressed as the number of constituent AGUs (degree of polymerization, DP), varies with the origin and treatment of the raw material. Cotton and other plant fibres have DP values within the 800-10000 range, and regenerate fibres from cellulose containing 250-500 repeating units per chain [15].

Its molecular structure imparts cellulose with its characteristic properties: hydrophilicity, chirality, degradability, and broad chemical variability, as initiated by the high donor reactivity of the OH groups. It is also the basis for extensive hydrogen bond networks, which give cellulose a multitude of partially crystalline fibrous structures and morphologies. The properties of cellulose are, therefore, determined by a defined hierarchical order within a supramolecular structure and organization.

The crystalline structure of native cellulose (cellulose I) can be described as a monoclinic unit cell. Apart from the thermodynamically less stable cellulose I, cellulose may occur within other crystal structures (cellulose II, III, and IV), of which cellulose II is the most stable structure of technical relevance (Figure 2). It can be formed from cellulose I after treatment with aqueous sodium hydroxide (mercerization) or by dissolution of the cellulose and subsequent precipitation/regeneration, as is done in the formation of fibre and film. The alkalization of cellulose is of considerable importance for commercial-scale cellulose

production as a method for increasing the reactivity (activation) of subsequent reactions, as well as for the mercerization of cotton [15].

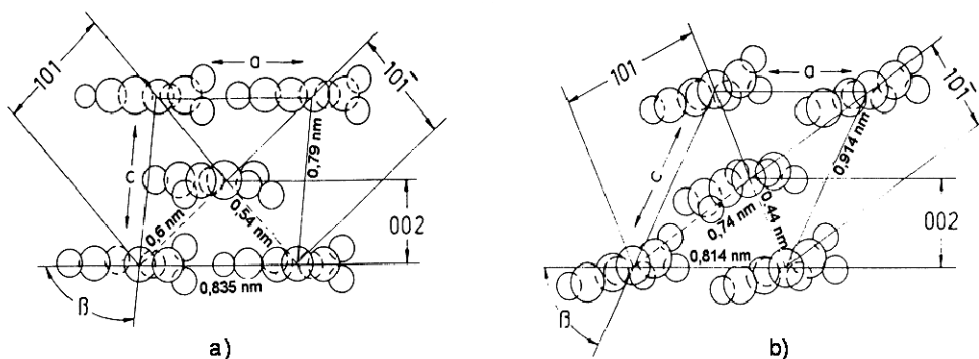


Figure 2. Crystalline structures of (a) native cellulose (cellulose I) and (b) regenerated cellulose (cellulose II) [16, 17].

It is well-known that cellulose fibres, natural as well as regenerated, have a crystalline/amorphous microfibrillar structure. The morphological hierarchy is defined by elementary fibrils, microfibrils, and microfibrillar bands. Elementary fibrils consist of a succession of crystallites and intermediate less-ordered amorphous regions. The lateral dimensions of these structural units are between 1.5 and 3.5 nm for elementary fibrils, between 10 and 30 nm for microfibrils, and in the order of 100 nm for microfibrillar bands. The length of the microfibrils is in the order of several hundred nm [11, 12].

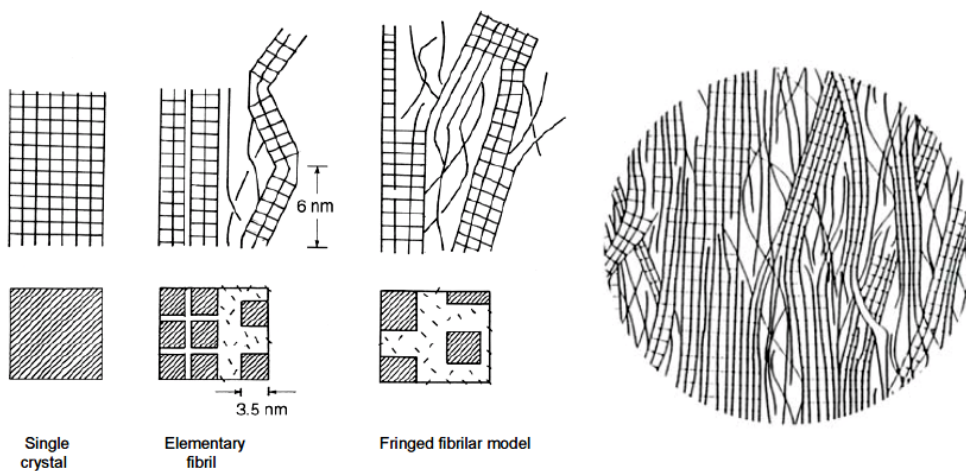


Figure 3. Supramolecular structural models of cellulose microfibrils [15, 18].

The fringed fibrillar model with crystalline regions and non-crystalline regions has proven successful for describing the structure of microfibrils and the partial crystalline structure of cellulose, in connection with the reactivity of this polymer (Figure 3). The void

structure can be considered the counterpart to the fibril morphology of cellulose and is considerably important for accessibility during chemical reactions.

The natural cellulose fibres are less reactive as the regenerated ones; the hydrophilicity of cotton can be improved by the mercerisation process, but not as highly as in the case of regenerated cellulose fibres [19]. As the skeletal component in all plants, cellulose is organized as a cellular hierarchical structure. In combination with the accompanying substances, hemicelluloses, lignin, and pectin, this structure leads to the extraordinary properties of native composite materials, such as wood, cotton, flax, and hemp. Figure 4 schematically illustrates the molecular, supramolecular structure and morphology of cotton fibre with differently structured layers, in which the secondary cell-wall layer contains the main quantity of cellulose [20].

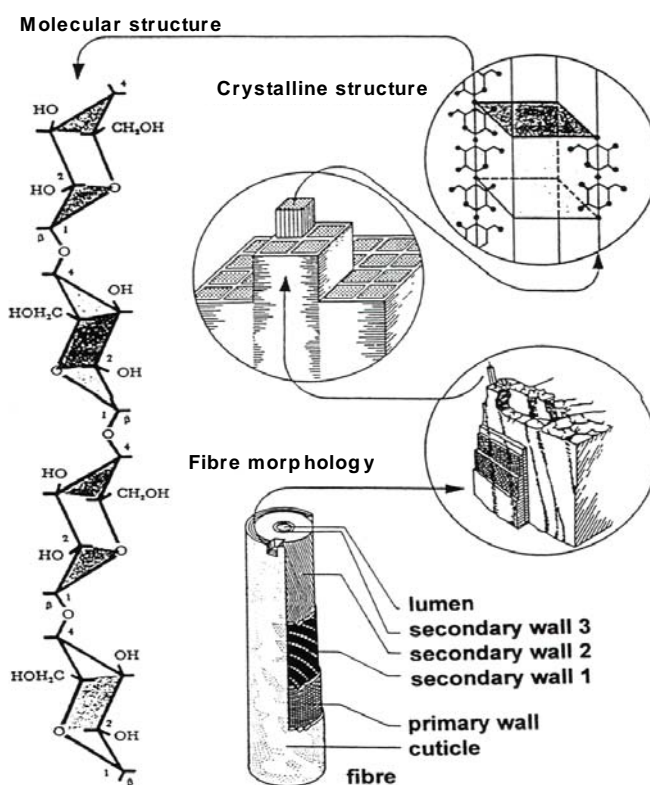


Figure 4. Schematic presentation of cotton fibre structure [20].

In the field of man-made fibres there are many commercial methods for manufacturing man-made cellulose fibres: the viscose, cuprammonium and several new alternative processes. Conventional regenerated cellulose fibres are generally produced by the indirect viscose process based on the derivatisation of cellulose using carbon bisulphide (viscose fibres), whilst high-tenacity modal fibres are produced using a modification of the basic procedure [21-23]. It is only recently that new processes have been developed, mainly due to considerable environmental problems in the viscose process. Lyocell fibres are produced by a more environmentally friendly procedure, from a solution of non derivated cellulose using a

solvent spinning process, whereby cellulose is regenerated from a solution of *N*-methylmorpholine-*N*-oxide (NMMO) monohydrate by spinning [24-27].

All regenerated cellulose fibres have the same chemical composition, yet they differ, regarding the average molecular mass, degree of polymerization and supermolecular arrangement but, above all, in their degree of crystallinity and orientation. Comparative investigations between lyocell and conventional viscose and modal fibres were made, during our previous research in order to explain the reasons for the differences in the molecular and fine structures of these fibres [21]. The differences between particular types of regenerated cellulose fibres are, above all, in the size of crystallites, and amorphous regions ; amorphous and crystalline orientation, size and shape of the voids and the number of interfibrillar lateral tie molecules (Figure 5).

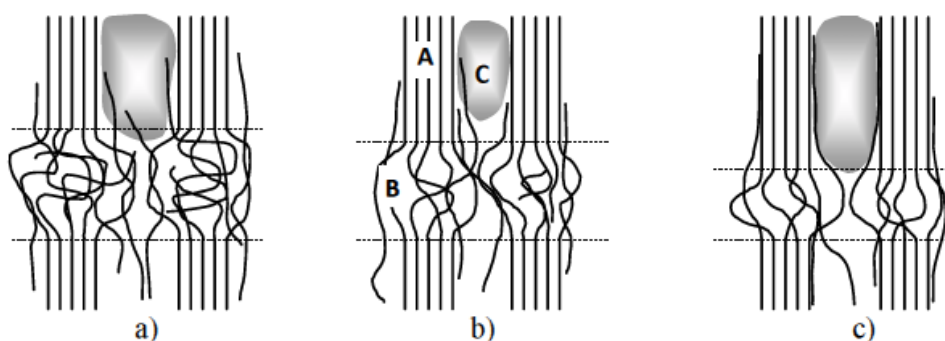


Figure 5. Fine structure of cellulose fibres – schematically: A - crystallites, B - amorphous regions, C – void; (a) viscose fibres, (b) modal fibres, (c) lyocell fibres [21].

According to our previous research on regenerated cellulose fibres [19, 21, 28-30] it is evident that a higher molecular weight, higher degree of crystallinity, and a higher orientation of the crystallites can be observed with lyocell fibres, the fibrillar structure being more strongly pronounced than in the case of “conventionally-regenerated” cellulose fibres (viscose, modal). Amorphous regions of lyocell fibres are smaller in comparison with modal and viscose fibres (Figure 5).

Nevertheless, the void parameters above all the void volume, is similar to that of viscose fibres (Figure 6). It becomes evident that the sorption ability of lyocell fibres is similar to viscose fibres and, contrary to expectations, does not conform to the basic structural data i.e. degree of crystallinity and molecular orientation (Figure 7). The volumes and inner-surface areas of voids are significant factors with regard to the accessibility, reactivity, and adsorption properties of fibres.

All of fibres’ structural characteristics have an influence on the fibres’ accessibility and, therefore, are of importance for the dissociation - adsorption character and reactivity of cellulose materials [29, 30].

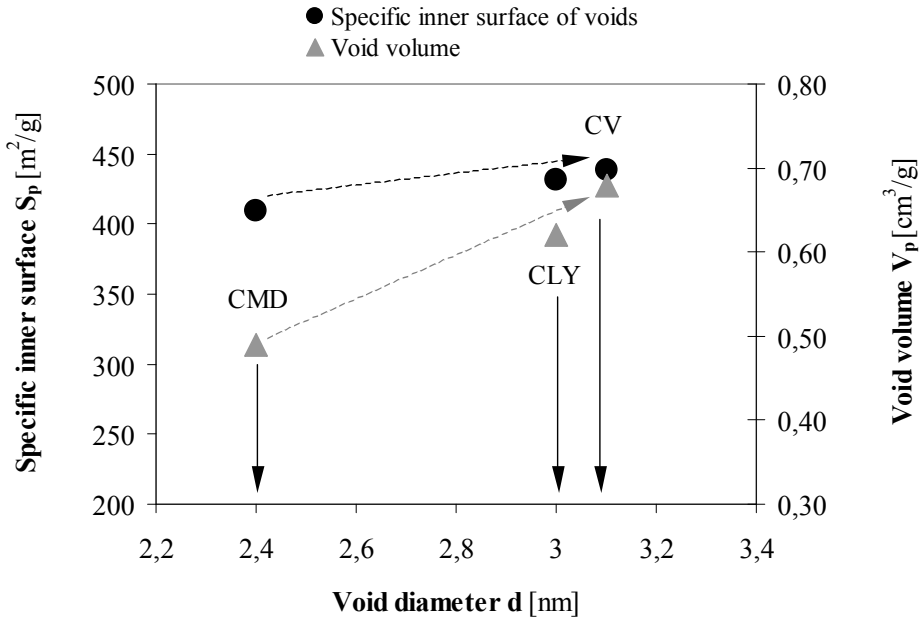


Figure 6. Voids diameter \bar{d} , voids volume V_p and specific inner surface S_p of voids in viscose, modal and lyocell fibres [30].

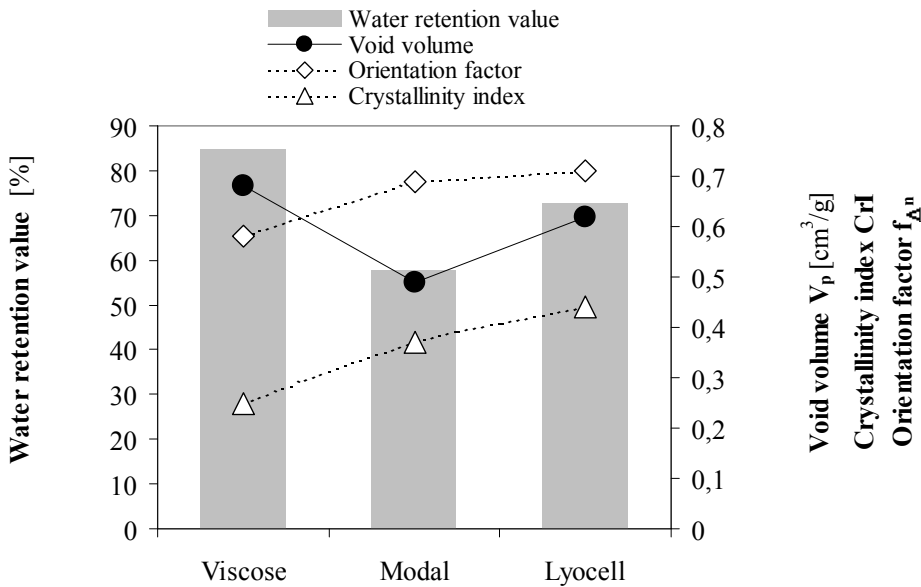


Figure 7. Correlation between the structural characteristics and the water adsorption of regenerated cellulose fibres [21].

It is well-known that the charge of cellulosic fibres is an essential feature of their chemical and physical properties and, hence, it is of great importance for the final properties and functionalization possibilities of cellulose fibres. It has been shown that fibre charges

strongly depend on cellulose fibre origin. In one of our previous researches [31, 32] potentiometric and conductometric titration were used to determine the amount of acidic groups in cellulose fibres. The surface, as well as the total charge, was obtained using polyelectrolyte adsorption. The origin of the charge was evaluated by determining the amount of carbon- and oxygen-containing groups on the fibre surfaces, by using X-ray Photoelectron Spectroscopy (XPS) and the pK values by using potentiometric titration. XPS is very surface sensitive method with detection depth of only few nanometers. Therefore, it is a very powerful technique for studying elemental composition and chemical state of the surfaces. In the case of cellulose materials different carbon-oxygen functional groups may be detected. Carbon peak (C1s) may have many side-peaks positioned at different binding energies due to different bonding of carbon atoms to oxygen [33]. This enables determination of surface functional groups (i.e. carboxylic groups) which can be associated with the surface charge.

It was found, that the average content of acidic groups in cotton fibres is higher than in regenerated cellulose fibres (viscose, modal, lyocell). The fibre charge of cotton is due to the dissociation of two types of acidic groups, one with $pK \approx 3.5$ and the other with $pK \approx 5.5$. In regenerated fibres there is only one type of acidic groups ($pK \approx 3.5$). The pK value of the stronger acid is typical for a carboxyl group in uronic acids.

The polyelectrolyte adsorption (ratio between surface and total charge) indicates that most of the carboxyl groups were located within the inner regions of all the cellulose samples (cotton and regenerated cellulose fibres) and not on their surfaces [31, 32, 34].

The titration methods, especially the surface-charge results, are very well supported by those obtained by XPS: decreasing of carbon compound values (O-C-O and O-C=O) from non-treated cotton to lyocell (Figure 8).

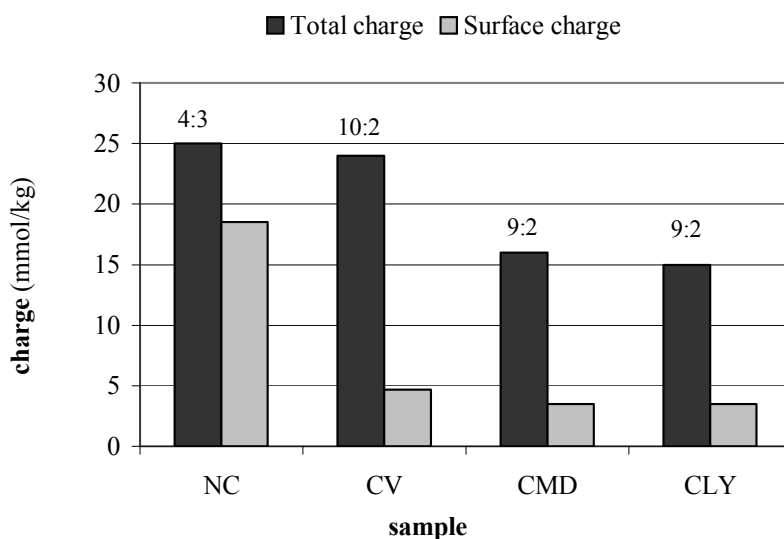


Figure 8. Amount of total and surface charge using polyelectrolyte adsorption; approximate ratios of the amounts are given for each sample: NC nontreated cotton, CV viscose, CMD modal, CLY lyocell [31, 32].

It has to be taken into account that cellulose fibre pre-treatment processes may also modify the fibres both structurally and chemically and, consequently, change the total charges [31, 32], which may clearly influence the fibre adsorption capacity and/or fibre reactivity.

In one of our previous researches a detailed study of the influences of bleaching and slack-mercerisation on dissociation properties of different types of regenerated cellulose fibres was performed [31, 32]. For all three types of fibres (viscose, modal, and lyocell) the content of accessible carboxyl groups is lowered by an increase in the degree of crystallinity, i.e. a reduction in the fraction of amorphous fibre domains. Bleaching with hydrogen peroxide causes some oxidative cellulose damage, thus obtaining, therefore, a larger amount of carboxyl groups (presumably formed at the ends of cellulose chains). Slack-mercerization does not significantly change the total amount of the acidic groups in the fibres, but their accessibility to cationic polyelectrolytes is substantially lowered, in particular to polymers with high molecular weight. It became clear that the amount of carboxyl groups within the regenerated cellulose fibres decreased throughout the pre-treatment processes, with the increase of fibres' crystallinity (Figure 9). The amount of carboxyl groups accessible to titration is reduced when the fraction of amorphous fibre regions is reduced. Assuming that there are no carboxyl groups within the crystalline regions, it can be concluded that crystallinity is of great importance for the amount of carboxyl groups formed during the different processing stages of the cellulose regenerated fibres.

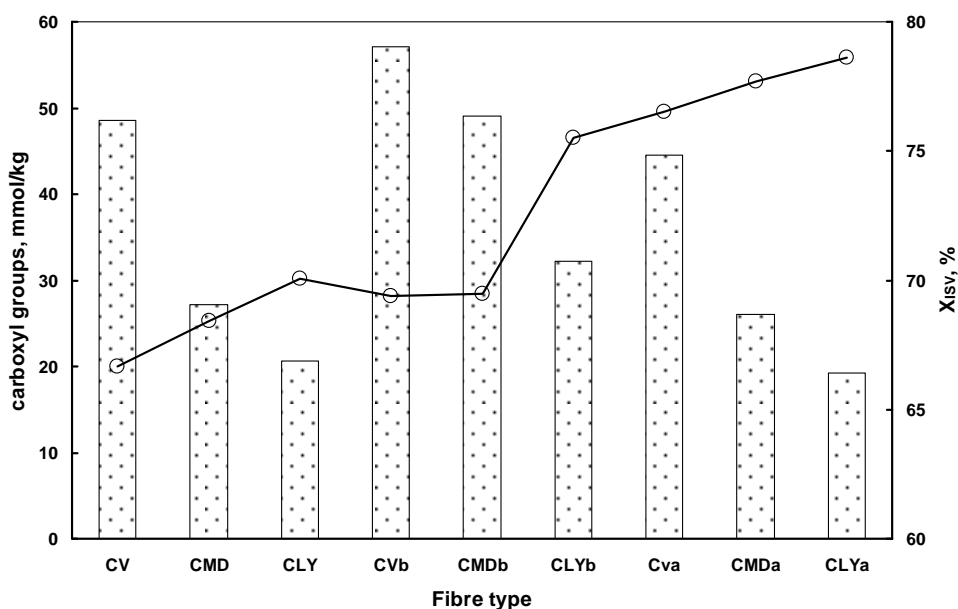


Figure 9. Comparison of -COOH groups amounts with the crystallinity degree determined by the Iodine sorption values (ISV) for non-treated and pre-treated (b-bleached, a-alkaline treated) regenerated cellulose fibres. Bars: carboxyl groups; Line: crystallinities [31].

Fras et al. [35] presented the selective oxidation of cotton fibres as a powerful treatment that causes the elimination of low molecular fractions (non-carbohydrate material), that cover the cotton cellulose fibres. This work indicates that the use of selective oxidation as pre-treatment results in cleaner fibre surfaces because non-carbohydrate material is removed

during this process. This is important for further treatment because a cleaner fibre surface leads to more effective interactions with substances such as dyes, and polyelectrolytes. In addition, the chemical analysis of fibres is much easier and precise in the cases of better-defined surfaces.

Information about oxidation progress (degree of oxidation as a function of new carboxyl group amount) was obtained, using titration methods whilst the results of XPS analysis showed some additional details regarding the surface chemistry of oxidised cotton. The fibre surface becomes much cleaner after selective oxidation. In the Figure 10 the comparison of the results obtained by those methods useful for the chemical analysis of fibre surface layers i.e. polyelectrolyte titration and XPS. Despite the fact, that the titration methods are performed in liquid media and cellulose fibres are in swollen state, their results are very well supported by those obtained by the XPS. In both cases, decreasing amount of COOH groups from sample A to D can be observed.

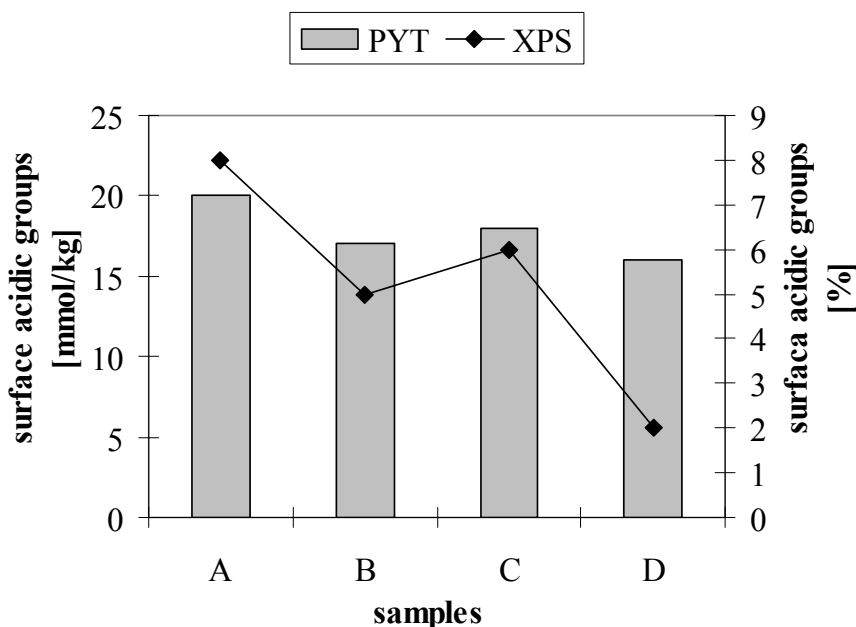


Figure 10. Comparison of surface acidic groups' amounts determined by polyelectrolyte titration - adsorption (PYT) and XPS for non-treated cotton (A) and oxidised cotton (B).

3. FUNCTIONALIZATION OF CELLULOSE FIBRES

It has become clear that it is essential to be able to modify the fibre chemistry as well as fibre structural parameters when creating advanced cellulose fibre properties. Our previous and other studies showed that the amount of carboxyl groups in cellulose fibres is, besides creating the most important fibre properties (dissociation capacity, hydrophilicity, etc.), also extremely important for binding of cationic substances. From among the latest, amino polysaccharides are extremely important due to their antimicrobial activity, where chitosan is ahead of all others [36-39].

Chitosan is a natural product gained from chitin. Chitin is a carbohydrate, similar to cellulose, which is the base component of the skeletons of crayfish, mussels, and other shellfish. Chitin is a polysaccharide, combined of 2-acetamino-2-deoksi- β -D-glucosic units, connected with β -1,4 linkages. It is the second more common biopolymer on earth, after cellulose [40].

Chitosan is a common name for a large group of chitins, deacetylated to different degrees. It is mainly combined of 2-amino-2-deoksi-D-glycol pyranose units, connected with β (1-4) linkages (Figure 11). The name chitosan is normally used for products with a degree of deacetylation higher than 70%. The reaction from the deacetylation of chitin in hot alkaline solutions mostly reaches only a deacetylation degree of 95%, even under very rigorous conditions. The methods for the deacetylation of chitin have been presented in detail already in 1973 by Muzzarelli [41].

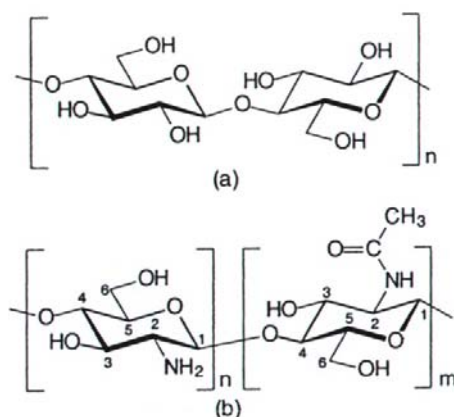


Figure 11. Chemical structures of cellulose (a), chitin and chitosan (b) – chitin mainly consists of monomers in the form of »m« (N-acetyl form), while chitosan, according to the degree of deacetylation, consists mainly of monomers in the »n« form (amine form) [42].

The chemical structures of chitin and chitosan are very similar. Both polymers include reactive hydroxyl groups; nevertheless the crystallinity degree of chitosan is usually lower in comparison to chitin, which makes it more sensitive to reagents and solvents. There are only a few solvents, which dissolve chitin but on the other hand, almost all the water solutions of acids dissolve chitosan. Formic and acetic acids are mostly used for dissolving of chitosan. Similar to celluloses, chitin and chitosan do not have a melting point, since in the process of heating both of them decompose before melting [43-46].

Chitin and chitosan are weak acids and, as such, they are subject to the reactions of neutralization in alkaline media. Chitosan is a potential nucleophilic, owing to free electron pairs on the primary amine group, which easily reacts with most aldehydes and forms imines. The molecules of chitosan have a highly-positive polarity and attract negative molecules.

Although most of the reactions with chitin and chitosan occur primarily on amino groups, there is also the possibility of a selective substitution of hydroxyl groups. The hydroxyl group on the C6 atom is more reactive than the group on the C3 atom [43].

The molecular mass of natural chitin is usually higher than one million, whilst the products of commercial chitosan have a molecular mass between 100000 and 1200000.

During the production of chitosan, rough conditions usually lead to the degradation of products. According to the Horowitz method of deacetylation [44], which assumes a 30 minutes treatment of chitosan at 180°C, it is possible to gain chitosan with a 95% degree of deacetylation, but such a kind of chitosan only has average chain lengths of about twenty units. Generally speaking, factors such as the presence of oxygen, high temperature, and shear-stress can cause a further degradation of the chitosan product.

The degree of deacetylation has a high effect on chitosan's dissolution in water media, since chitosan with a 40% degree deacetylation can be dissolved in water solutions with a pH up of to 9, whilst at a 85% degree of deacetylation, it can be only dissolved in solutions up to pH 6.5. Ethanoic and methanoic acids are the two most commonly-used acids when dissolving chitosan. Some diluted inorganic acids are also suitable, such as nitric acid, hydrochloric acid, perchloric acid and phosphoric acid, but only in the case of supplying enough energy in the form of a longer previous mixing and heating. In the case of chitosan dissolution in a water solution of nitric acid, there is the possibility of precipitations in the form of a white-coloured gel [44, 47].

There are many factors which affect the viscosities of chitosan solutions, such as the degree of deacetylation, average molecular masses, concentration, ionic strength, pH value, and the temperature. Any change in the pH value of the polymer solution influences the viscosity of the solution differently, depending on the acid used. The viscosity of the chitosan solution in an acidic medium of ethanoic acid generally increases with any decrease in the solutions' pH value, whilst the viscosity of the HCl solutions decreases with any reduction in the pH value [44, 48].

In those cases where acids as substances are unwelcome in products, such as in cosmetic preparations, drugs and food, the water solubility of chitosan is of great importance. It has been proven that chitosan with a 50% degree of deacetylation and produced by a homogeneous procedure, is water soluble [44]. Researchers have also analysed other methods for increasing the water solubility of chitosan. Kushino and Asano developed a procedure for the preparation of water soluble chitosan salt [47]. This method includes the dissolution of chitosan in water, adjusting of the solution's concentration to 10% and evaporating and drying to 175°C. The alternative for improving chitosan's water solubility presents different possibilities for its chemical modifications.

Due to the unique characteristics of chitosan, such as: biodegradability, non-toxicity, its cationic nature and antimicrobial activity, it is suitable for medical and hygienic applications. Owing to its structure being similar to cellulose, chitosan is ideal for the cellulose fibres' surface modification, in order to develop cellulose antimicrobial activity.

However, cellulose fibrous material has to be adequately activated for efficient irreversible chitosan adsorption; therefore, it is essential to obtain a well-cleaned basic material with an appropriate amount of binding sites. In regard to this, different standard chemical pre-treatments [49] are generally used that usually modify the fibres structurally and/or chemically [50].

In the case of chitosan binding onto fibrous materials in order to achieve permanent antimicrobial properties, there are two rather contradictory conditions, which have to be fulfilled: (i) a certain amount of anchoring sites on the fibres, onto which chitosan could permanently bind and, at the same time, (ii) as many as possible free amino groups of chitosan, which could act antimicrobially. The permanent wash-resistant antimicrobial activity of textile materials is a crucial property for hospital linen. As a natural renewable

resource, chitosan is a polycationic biopolymer that has well-documented antibacterial and antifungal activities. In addition to deacetylation degree and molecular weight, the amount and location of amino groups are the driving forces for chitosan's antimicrobial effectiveness [51].

Cellulose fibres treatment with chitosan is considered to be effective in the case of the optimal number of reductive cellulose groups onto which chitosan can bind permanently. It has also been demonstrated that the carboxyl groups within the cellulose, in comparison with aldehyde groups, have different effects on chitosan binding [52]. On the other hand, the introduction of adequate functional groups into cellulose fibres could have diverse influences on fibre properties [50].

In one earlier studies, the aim was to find out what kind of pre-treatment is more appropriate for later permanent chitosan binding, and the effective antimicrobial properties of the cellulose fibres.

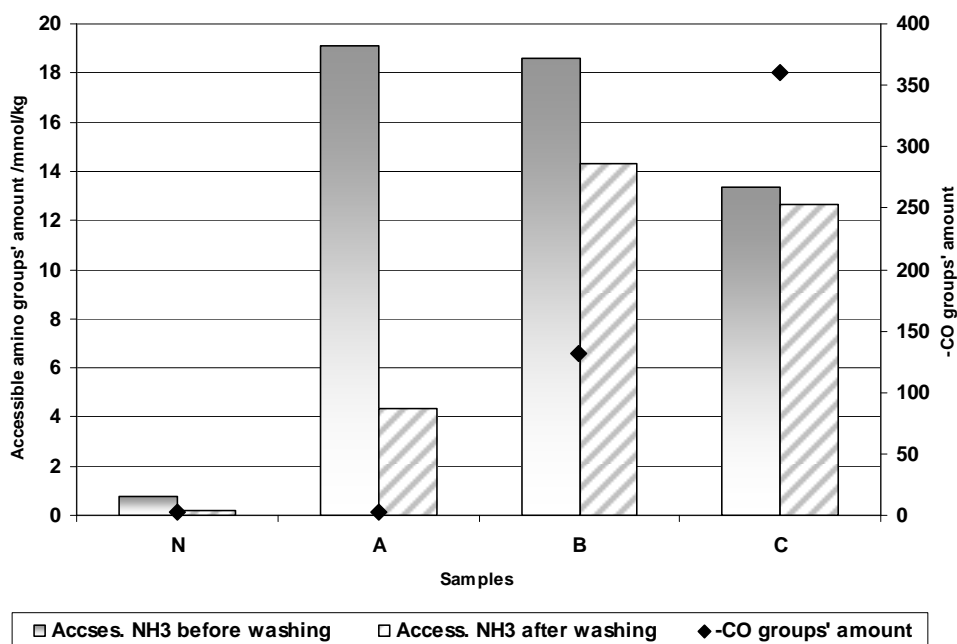


Figure 12. The influence of reducing groups' amount of KIO_4 (VII) oxidised samples (A, B, C) on the amount of accessible amino groups in chitosan treated samples before and after the washing procedure (N – nonoxidised cotton).

Different pre-treatments of cellulose fibres were applied in order to produce appropriate amounts of anchoring aldehyde or carboxyl groups, respectively. The fibres were oxidized by KIO_4 (VII) solutions in order to produce appropriate amounts of aldehyde groups, and an adequate amount of free carboxyl groups was achieved by the treatment of the fibres with BTCA. The amounts of accessible aldehyde, carboxyl and, after chitosan treatment the amino groups within the fibres, were evaluated using spectroscopic and titration techniques.

It was discovered that the amounts of aldehyde, as also the amounts of carboxyl groups within the fibre samples were inversely proportional to the amounts of accessible amino groups in the samples after chitosan treatments (Figures 12 and 13).

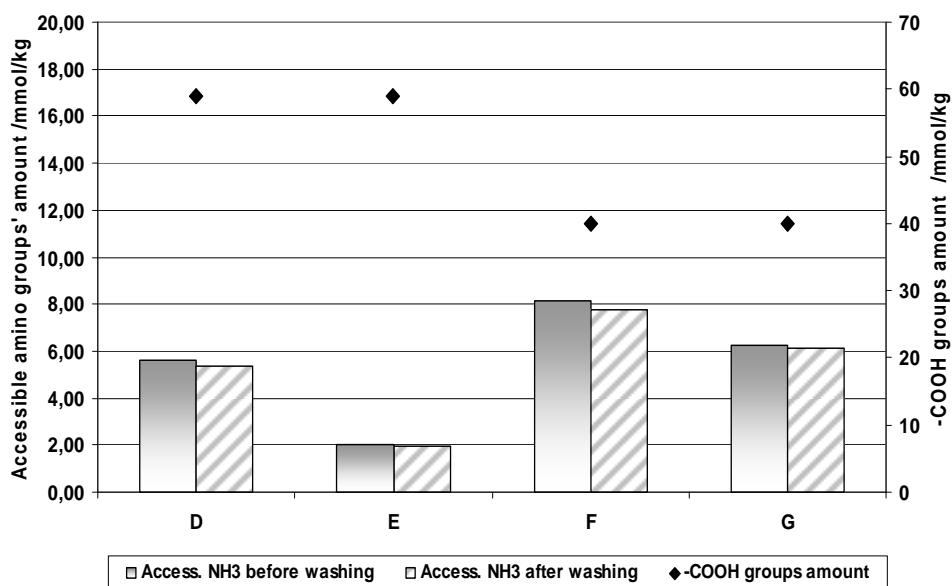


Figure 13. The influence of the carboxyle groups' amount after BTCA treatment of cotton fibres, on the accessible amino groups' amount in the chitosan treated fibres before and after the washing procedure.

The aldehyde and carboxyl groups introduced into the fibre samples by oxidation and BTCA treatment played an important role in chitosan fixation and chitosan treatment permanency after the washing procedure. The lowest resistance of chitosan treatment could be observed for the non-oxidised sample (sample N on the Figure 12). The strongly oxidised sample C (Figure 12) and all the BTCA treated samples (Figure 13) showed high degrees of chitosan treatment permanency. The amount of accessible amino groups after the washing procedure was practically unchanged in these samples. However, in order to achieve satisfactory results, it is extremely important to balance between the treatment resistance, the material's mechanical properties, and the amount of free amino groups (antimicrobial effect).

Among much more harmless surface activation procedures in comparison to chemical oxidation of cellulose fibres are plasma treatments. Plasma is created by passing a gas through an electric field where gas is ionized and transformed into a non-equilibrium state. Such gaseous discharge is a rich source of variety of chemical reactive species including positively and negatively charged ions, neutral atoms in the ground state as well as molecules and atoms in the excited states. Plasma particles readily interact with surfaces and cause their chemical modification (surface functionalization) [53]. Long duration of plasma treatment can also cause modification of surface morphology i.e. increasing of surface roughness of cellulose fibres [53]. Plasma does not just provide new functional groups on the surface but it can also causes removal of thin films of organic impurities from cellulose fibres (surface cleaning). For this reason, plasma represents an extremely powerful medium for modification of the surface properties of materials. Plasma can be created in different gases. The most popular is oxygen plasma which gives the best improvement of surface hydrophilicity (wettability) of cellulose fibres (Figure 14). Other oxidative plasmas can be used as well, including plasma created in air, carbon dioxide, water vapour, and mixtures of these gases with a noble gas. Such plasmas have been already successfully applied in an extremely wide

range of applications for the case of cellulose materials: e.g. enhancement of wettability and soaking capacity of fibres [50], enhancement of adhesion properties (e.g. adhesion of silver antibacterial coatings) [54, 55], improvement of dyeing, printing, for better impregnation etc. In the case of low pressure plasmas which are often used in laboratories, treatment of cellulose fibres can be performed in two different regions - either directly in glow region or in afterglow region. Afterglow region allows more gentle surface modification without damaging cellulose fibres which may happen during treatment in glow region when using more powerful plasmas.

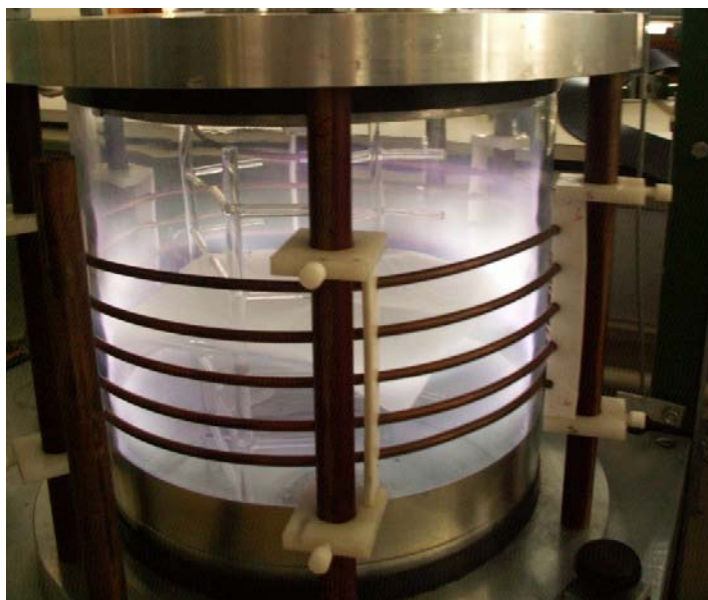


Figure 14. Apparatus for viscose fabric treatment by oxygen plasma.

From practical point of view are more popular atmospheric discharges (like dielectric barrier discharge – DBD) which do not require vacuum systems and are the only option for industry for batch processing in the case of large volume production.

Fras et al. concluded [49] that increasing the number of aldehyde and carboxyl groups due to plasma activation within the cellulose surface enabled more efficient chitosan adsorption (higher quantity) and consequently better antimicrobial properties.

In the latest study, different regenerated cellulose fibres that differed in charge behaviour, as well as in their structural parameters were used as a vehicle for irreversible chitosan adsorption. The following regenerated viscose fibres were used: viscose, lyocell, and modal. The aim of this research was: (i) to evaluate which type of tested regenerated cellulose fibres is the most appropriate for antimicrobial treatment; which means it is able to possess as much as higher amounts of accessible amino groups as a consequence of chitosan adsorption, and (ii) to analyze the influence of accessible amino group amounts on the final antimicrobial fibres' properties. The results were compared to those obtained for cotton cellulose, as the only representative of natural cellulose fibres about which plenty of similar research has been performed. The pre-treated viscose, modal and lyocell fibres were functionalised by 1% of chitosan solution using a classical impregnation procedure. When using chitosan as an

adsorbent for cellulose fibres, it is very important to determine the amount of accessible amino groups responsible for the antimicrobial character of fibres' surfaces.

Figure 15 represents the amino group amount of regenerated cellulose fibres determined by potentiometric titration, and by the Acid Orange VII method. The results were compared and it can be seen that the highest amount of amino groups possess viscose, followed by modal and lyocell, respectively. The amino group amount determined using the Acid Orange VII method is almost equal or smaller as that determined by potentiometric titration. A difference between these two methods is expected, namely the Acid Orange VII is indirect, whilst potentiometric method I the direct method for dissociated groups' determination. However, the Acid Orange VII method can be used as a good supporting technique for titration methods.

Differences in amino group amounts between all three samples are relatively small i.e. in the area of $\pm 20\%$ (Figure 15). The reason for the presented positive-charge within the fibre surface lies in different chitosan adsorption onto/into fibres, which was confirmed by Kjeldahl analysis [56]. The results indicated the occurrence of nitrogen (%) within those samples impregnated by chitosan solution. Chitosan adsorbed more extensively on viscose fibres: 15% increase of nitrogen content was observed when compared with the modal, and an 18% increase in comparison with the lyocell.

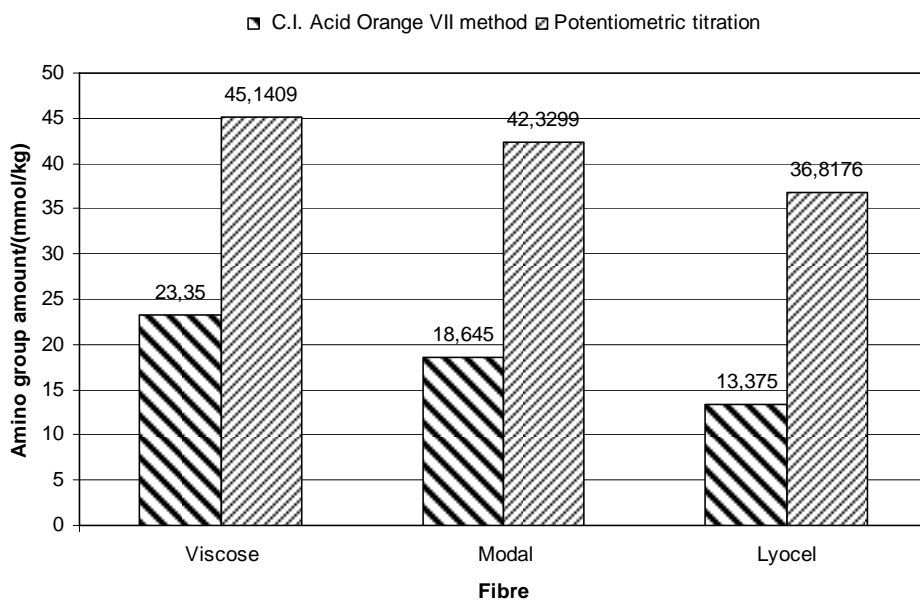


Figure 15. Amino group amount of regenerated cellulose fibres determined by potentiometric titration, and by the Acid Orange VII adsorption method.

So, it can be concluded that chitosan has the highest ability regarding the viscose and the lowest regarding the lyocell fibres. This may be attributed to the physical-chemical parameters, especially to the fibres' structural properties, like crystallinity degree and orientation factor (Figure 7). On the other hand, the amount of adsorbed chitosan and the accessibility of its amino groups could also be strongly associated with a fibre's surface

morphology. There are significant differences in the forms of cross-sections and accordingly also in surface morphologies of the three types of fibres. Viscose has, due to its so-called serrated cross-section, a significantly higher total surface area when compared to modal and lyocell, resulting in a higher chitosan adsorption and thus, higher range of amino groups' accessibility, which was determined by titration.

The relations between the amino groups' amounts and antimicrobial properties of functionalized regenerated fibres could be determined by different methods. The most appropriate for fibre samples among them is the microbiological testing according to ASTM E 2149-01. Pathogen micro-organism reduction (R in %) results of such a method for the regenerated cellulose and natural cotton fibres treated with 1% chitosan solution, are collected in Table 1. All the references i.e. the non-functionalized fibres show a positive reduction regarding pathogenic microorganisms. Sufficient reduction is only seen with the microorganism *Streptococcus agalactia*. In the examples of other tested microorganisms, the reduction is less than 75%, therefore, these fibres do not satisfy the condition required for antimicrobial efficiency. When comparing the reference regenerated cellulose fibres with the functionalized regenerated cellulose fibres, it can be seen that chitosan adsorption introduces satisfied antimicrobial activity ($R > 75\%$).

Table 1. Pathogenic bacteria and fungi reduction

Sample	Amino group amount - A_i mmol kg ⁻¹	Reduction R [%]				
		Pathogenic bacteria			Pathogenic fungi	
		<i>Staphylococcus aureus</i>	<i>Escherichia coli</i>	<i>Streptococcus agalactiae</i>	<i>Candida albicans</i>	<i>Candida glabrata</i>
Cotton 1%	20.09	84	98	93	73	59
Cotton NO		66	28	91	57	67
Viscose 1%	45.14	98	92	97	88	100
Viscose NO		65	55	85	9	45
Modal 1%	42.33	NH ₃ ⁺ 99	92	87	48	100
Modal NO		22	21	73	45	71
Lyocell 1%	36.82	97	90	63	74	90
Lyocell NO		57	21	45	36	50

NO – non-functionalized fibres.

1% - fibres functionalized with 1 % chitosan solution.

The most intensive inhibition for all the tested microorganisms (*Staphylococcus aureus*, *Escherichia coli*, *Streptococcus agalactiae*, *Candida albicans* and *Candida glabrata*) showed viscose, followed by modal, which was antimicrobially insufficient in the case of fungi *Candida albicans*, and by lyocell, which was relatively poor for the reduction of the Gram-positive bacteria *Streptococcus agalactiae*.

The bacteria *Staphylococcus aureus* is very similar in its inhibition with all the functionalized regenerated cellulose fibres used in this research. An analogue trend is obtained by the inhibition of Gram-negative bacteria *Escherichia coli*.

Results show that certain amino group's content influences antimicrobial properties. It is confirmed by the methods used in this presented work, that fibres with higher amino groups' content show a better total reduction of pathogen microorganisms.

4. COMPARING REGENERATED CELLULOSE ANTIMICROBIAL PROPERTIES WITH COTTON

When comparing the antimicrobial properties of regenerated cellulose to those achieved with cotton, it was clearly shown that, in general, viscose functionalized by chitosan showed better inhibition regarding pathogen bacteria and fungi, in comparison with identically-functionalized cotton. Viscose showed a better reduction in Gram-positive bacteria, such as *Staphylococcus aureus* and *Streptococcus agalactiae*, as well as fungi such as *Candida albicans* and *Candida glabrata*. When considering bacterial reduction, only the Gram-negative bacteria *Escherichia coli*, was reduced better by cotton functionalized with chitosan, when compared to functionalized viscose. The later showed bacteria and fungi reduction of over 75% and can, therefore, be considered as an efficient substrate for functionalizing with chitosan, resulting in good antibacterial properties. It can be seen that functionalized cotton insufficiently reduces both types of pathogen fungi used in this experiment. Microbiological activity was also evaluated for modal and lyocell. On the basis of the presented results, it can be seen that these two cellulose substrates functionalized with chitosan, show much worse antimicrobial activity when compared with the viscose and cotton fibres, respectively. It can be concluded that viscose is, from among all the examined cellulose fibres, the most perspective in the sense of antimicrobial efficiency.

5. OUTLOOK - POTENTIAL USE OF CELLULOSE FIBRES FUNCTIONALIZED WITH CHITOSAN

Cellulose fibres functionalized by polysaccharides for textile applications are at the beginning of regeneration. On the basis of our results, it can be concluded that all functionalized cellulose fibres used in our research could be explored for certain areas of applications. Among those medical materials that possess antimicrobial activity, there is substantial interest in producing materials for sanitary use, e. g. gauzes, patches, tampons, hygienic pads, etc. where cotton or viscose is usually used as a substrate. The role of modal and lyocell in the field of medical materials is insufficiently known, therefore, additional research for antimicrobial process optimization needs to be performed, together with an estimation of their possible usage in the medical area.

However, when we consider the high number of strategies for modifying fibre properties in polysaccharide-based textiles, we can recognise that only a few possibilities have been explored and commercialised up to date. We understand that an awareness of this future potential and its chances for the development of new materials would make researchers and producers enthusiastic about working within this particular field of research and technology.

REFERENCES

- [1] BISFA. (2006). *Terminology of man-made fibres*, 2006 Edition. Brussels: BISFA.
- [2] Anand, SC. (2006). Health care and hygiene Products: An overview. In: Anand, SC; Kennedy, JF; Mirafab, M; Rajendran, S. editors. *Medical Textiles and biomaterials for healthcare*. Cambridge England: Woodhead Publishing Ltd., CRC Press.
- [3] Muzzarelli, RAA; Guerrieri, M; Goteri, G; Muzzarelli, C; Armeni, T; Ghiselli, R; Cornelissen, M. (2005). The biocompatibility of dibutyl chitin in the context of wound dressings. *Biomaterials*, 26/29: 5844-5854.
- [4] Hoenich, AN. (2006). Cellulose for medical applications: past, present, and future. *BioResources*, 1/2: 270-280.
- [5] Ravi Kumar, MNV. (2000). A review of chitin and chitosan applications. *Reactive and Functional Polymers*, 46: 1-27.
- [6] Severiaon, D. (2002). *Polymeric Biomaterials*, Second Edition, New York: Marcel Dekker.
- [7] Jung, BO; Kim, CH; Choi, KS; Lee, YM; Kim, JJ. (1999). Preparation of amphiphilic chitosan and their antimicrobial activities. *Journal of Applied Polymer Science*, 72/13: 1713-1719.
- [8] Lim, SH; Hudson, SM. (2004). Synthesis and antimicrobial activity of a water soluble chitosan derivative with a fibre reactive group. *Carbohydrate Research*, 339: 313-319.
- [9] Kim, J; Yun, S; Ounaies, Z. (2006). Discovery of Cellulose as a Smart Material. *Macromolecules*, 39, 12: 4202-4206.
- [10] Gao, Y; Cranston R. (2008). Recent advances in antimicrobial treatments of textiles. *Textile research Journal*, 78, 1: 60-72.
- [11] Krässig, HA. (1993). *Cellulose, Structure, Accessibility and Reactivity*, Switzerland: Gordon and Breach Science Publishers, Y-Parc.
- [12] Klemm, D; Philipp, B; Heinze, T. (1998). *Comprehensive Cellulose Chemistry*, Vol.1, Fundamentals and Analytical Methods, Weinheim: Wiley-VCH Verlag.
- [13] Schurz, J. (1994). Was ist neu an den neuen Fasern der Gattung Lyocell. *Lenzinger Berichte*, 74: 37-40.
- [14] Schurz, J; Lenz, J. (1994). Investigations on the Structure of regenerated Cellulose Fibers. *Macromol. Symp.*, 83: 273-289.
- [15] Klemm, D; Heublein, B; Fink, H; Bohn, A. (2004). Cellulose: Fascinating Biopolymer / Sustainable Raw Material, *Ang. Chemie*, (Intl. Edn.), 44, 3358.
- [16] Krässig, H. (1984). Struktur und Reaktivität von Cellulosefasern. *Das Papier*, 38, 12: 571-582.
- [17] Krässig, H. (1979). Neuere Struktur auf dem gebiet der Cellulose. *Das Papier*, 33, 10A, 9-20.
- [18] Hearle, JWS. (1958). A fringed fibril theory of structure in crystalline polymers. *Journal of Polymer Science*, 28: 432-435.
- [19] Kreže, T; Stana-Kleinschek, K; Ribitsch, V. (2001). The sorption behaviour of cellulose fibres. *Lenzinger Berichte*, 80: 28-33.
- [20] Schurz, J. (1980). Die Struktur der Zellulose. *Lenzinger Berichte*, 49: 15-24.
- [21] Kreže, T; Malej-Kveder, S. (2003). Structural characteristics of new and conventional regenerated cellulosic fibres. *Textile research Journal*, 73, 8, 675-684.

-
- [22] Cook, G. (1984). *Handbook of Textile Fibres, Man-Made Fibres*, 5th ed., Shildon: Merrow Publishing.
 - [23] Moncrieff, RW. (1975). *Man-Made Fibres*, 6th Ed., London: Butterworths Scientific.
 - [24] Albrecht, W; Reintjes, M; Wulfhorst, B. (1997). Lyocell Fibers. *Chem. Fibres International*, 47: 289-304.
 - [25] Berger, W. (1994). Möglichkeiten und Grenzen alternativer Verfahren zur Celluloseauflösung und Verformung. *Chemiefasern/Textilindustrie*, 44/96: 747-750.
 - [26] Cole, DJ. (1994). Courtaulds Tencel Fibre in Apparel Fabrics. *Lenzinger Berichte*, 74: 45-48.
 - [27] Krüger, R. (1994). Cellulosic Filament Yarn Form the NMMO Process, *Lenzinger Berichte*, 74: 49-52.
 - [28] Kreže, T; Strnad, S; Stana-Kleinschek, K; Ribitsch, V. (2001). Influence of aqueous medium on mechanical properties of conventional and new environmentally friendly regenerated cellulose fibers. *Mat. Res. Innovat.*, 4: 107-114.
 - [29] Stana Kleinschek, K; Kreže, T; Strnad, S; Ribitsch, V. (2001). Reactivity and electrokinetical properties of different types of regenerated cellulose fibres. *Coll. Surf. A.*, 195: 275-284.
 - [30] Kreže, T; Jeler, S; Strnad, S. (2002). Correlation between structure characteristics and adsorption properties of regenerated cellulose fibers. *Mat. Res Innovat.*, 5: 277-283.
 - [31] Fras Zemljč, L; Peršin, Z; Stenius, P; Stana-Kleinschek, K. (2008). Carboxyl groups in pre-treated regenerated cellulose fibres. *Cellulose*, 15/5, 681-690.
 - [32] Fras Zemljč, L; Laine, J; Stenius, P; Stana-Kleinschek, K; Ribitsch, V; Doleček, V. (2004). Determination of dissociable groups in natural and regenerated cellulose fibres by different titration methods. *J. appl. polym. sci.*, 92/5: 3186-3195.
 - [33] Connors, TE; Banerjee, S. (1995). *Surface Analysis of Paper*. New York: CRC Press.
 - [34] Dumitriu, S. (2002). *Polymeric Biomaterials*. Second Edition, New York: Marcel Dekker, Inc.
 - [35] Fras Zemljč, L; Johansson, LS; Stenius, P; Laine, J; Stana-Kleinschek, K; Ribitsch, V. (2005). Analysis of the oxidation of cellulose fibres by titration and XPS. *Colloids surf., A Physicochem. eng. Asp*, 260, 1/3: 101-108.
 - [36] Strnad, S; Šauperl, O; Fras Zemljč, L; Jazbec, A. (2007). Chitosan – universally applicable polymer, *Tekstilec*, 50: 10-12.
 - [37] Strnad, S; Šauperl, O; Jazbec, A; Stana-Kleinschek, K. (2008). Influence of chemical modification on sorption and mechanical properties of cotton fibers treated with chitosan. *Textile Research Journal*, 78: 5, 390-398.
 - [38] Mesquita, JP; Donnici, LC; Pereira, FV. (2010). Biobased Nanocomposites from Layer by-Layer Assembly of Cellulose Nanowhiskers with Chitosan. *Biomacromolecule*, 11: 473-480.
 - [39] Pecse, A; Jordane, AA; Carluci, G; Cintio, A. (2005). Articles comprising caionic polysaccharides and acidic pH buffering means. *US Patent Application Publication*: 0124799 A1.
 - [40] Majeti, NV; Ravi Kumar, MNV. (2000). A review of chitin and chitosan applications. *Reactive and Functional Polymers*, 46/1: 1-27.
 - [41] Muzzarelli, RAA. (1973). *Natural Chelating polymers*, Toronto: Pergamon of Canada Ltd.

-
- [42] Lim, SH; Hudson, SM. (2003). Review of chitosan and its derivatives as antimicrobial agents and their uses as textile chemicals. *J. of macromolecular science*, C43/2: 223-269.
- [43] Tharanathan, RN; Kittur FS. (2003). Chitin – the undisputed Biomolecule of great potential. *Critical reviews in food science and nutrition*, 43/1, 61-87.
- [44] MFA. (1997). *Applications of Chitin and Chitosan*. Edited by MFA. Lancaster Pennsylvania: Goosen, Technomic publishing company Inc.
- [45] Domard, A; Roberts GAF; Varum KM. editors. (1997). *Advances in Chitin Science*. Lyon: Jacques Andre Publishers.
- [46] Domszy, JG; Roberts, GAF. (1986). Ionic interactions between Chitosan and oxidised Cellulose. In: Muzzarelli, RAA; Jeuniaux, C; Gooday, G. Editors. *Chitin in Nature and Technology*. New York: Plenum Press; 331.
- [47] Knittel, D; Schollmeyer, E. (1998). Chitosan und seine Derivate für die Textilveredlung. *Textilveredlung*, 33: 3-4, 67-71.
- [48] Domszy, JG; Moore, GK; Roberts, GAF. (1985). The Adsorption of Chitosan on Cellulose. In: Kennedy, JF; Phillips, GO; Wedlock, DJ; Williams, PA. Editors. *Cellulose and its derivatives: Chemistry, biochemistry and applications*. Chichester: Ellis Horwood Ltd; 463–473.
- [49] Fras Zemljič, L; Peršin, Z; Stenius, P. (2009). Improvement of chitosan adsorption onto cellulosic fabrics by plasma treatment. *Biomacromolecules*, 10, 5: 1181-1187.
- [50] Strnad, S; Stana-Kleinschek, K; Vesel, A; Mozetic, M; Persin, Z. (2008). *XPS and sorption measurements of plasma-treated regenerated cellulose fabrics and ageing effects*. Proceedings of the Polymer Processing Society, 24th Annual Meeting (PPS-24) June 15-19, Salerno, Italy.
- [51] Liu, J; Wang, Q; Wang, A. (2007). Synthesis and characterization of chitosan-g-poly(acrylic acid)/sodium humate superabsorbent. *Carbohydrate Polymers*, 70: 166-173.
- [52] Muzzarelli, RAA; Muzzarelli, C. (2005). *Chitosan Chemistry: Relevance to the Biomedical Sciences*. In: Heinze T, editor. *Polysaccharides I, Structure, Characterisation and Use*, Berlin Heidelberg: Springer-Verlag; 151-209.
- [53] Vesel, A; Mozetic, M; Strnad, S; Stana-Kleinschek, K; Hauptman, N; Persin, Z. (2010). Plasma modification of viscose textile. *Vacuum*, 84: 79-82.
- [54] Gorjanc, M; Bukosek, V; Gorenssek, M; Mozetic, M. (2010). CF₄ plasma and silver functionalized cotton. *Textile Research Journal*, 80: 2204-2213.
- [55] Gorjanc, M; Bukosek, V; Gorenssek, M; Vesel, A. (2010). The Influence of Water Vapor Plasma Treatment on Specific Properties of Bleached and Mercerized Cotton Fabric. *Textile Research Journal*, 80: 557-567.
- [56] Goyal, S; Dhull, SK; Kapoor, KK. (2005). Chemical and biological changes during composting of different organic wastes and assesment of composting maturity. *Bioresource Technology*, 96: 1584-1591.

Chapter 15

SKIN PROBLEMS ASSOCIATED WITH TEXTILES

***Araceli Sánchez-Gilo*, Enrique Gómez de la Fuente,
Marta Andreu Barasoain and Jose Luis López Estebaranz***
c/ Budapest, 1. 28922. Alcorcón, Madrid, Spain.

ABSTRACT

Clothing is composed by textile fibers, coupling and fixer agents, finish products, dyes and complements. Contact dermatitis is produced by the contact between these clothing components and the skin. Two types of textile contact dermatitis have been reported; irritant and allergic, being irritant contact dermatitis more frequent than allergic.

Dyes are the main cause of allergic contact dermatitis. Disperse dyes are the most frequent sensitizers among textile dyes, followed by the reactive dyes. Acid, direct and basic dyes are less common sensitizers. The use of the different dyes depends on the kind of fiber used in the fabric. Disperse dyes are more common in industrialized countries, because people from these countries usually wear clothes with nylon and polyester/cotton fibers.

Finish products are the second most common textile sensitizers; they are used in natural and mixed fibers. Resins belong to this group, being Kaurit and Fix the most allergenic formaldehyde resins.

Exact incidence of textile dermatitis is unknown because of the lack of controlled epidemiological studies. Textile dye sensitization has an estimated incidence rate from 1.4% to 5.8%. Women have a greater prevalence of allergic reactions to textile dyes and resins than men; this may be due to the use of tighter fitting synthetic and dark-colored clothing. Contact textile dermatitis is increasing, probably as a result of the wide use of new dyes in clothes production.

Many clinical manifestations of textile dermatitis have been described. Usually, patients are affected by an acute or chronic dermatitis, of localized or generalized distribution of lesions. Unusual forms can also be seen: purpuric lesions, hyperpigmented patches, papular rash, papulopustular lesions, urticaria, erythema multiforme-like lesions, nummular-like lesions, lichenification and erythroderma.

Topical or systemic corticosteroids can be used in the treatment of textile contact dermatitis. In addition, the patient should avoid the offending allergen or irritant source,

* E-mail: aracelisanchezg@hotmail.com

wearing 100% natural based fabrics, use loose fitting clothing, and avoid synthetic spandex, lycra, acetate, polyester fibers and nylon. It is recommended washing clothes three times before wearing them the first time.

Contact textile dermatitis may be undiagnosed because the atypical clinical manifestations do not give rise to suspicion of textile dermatitis. Clinical history, clinical findings and patch test are the best elements in the diagnosis. Therefore, the physician should suspect a contact dermatitis in patients showing suggestive clinical signs, which might lead to an early diagnosis and appropriate treatment.

1. INTRODUCTION

The use of clothes is a universal fact. They are used to protect individuals from external agents such as cold, but they are as well a beauty tool. Fashion is continuously changing, and this change depends on geographic region and cultural customs, for this reason, the industry uses many chemical agents such as resins and new dyes. This is causing an increasing frequency of contact dermatitis which can show different manifestations. Clothing is composed by different materials, which may cause skin problems. Contact dermatitis is produced by the contact between different components of clothes and the skin. Two types of textile contact dermatitis have been reported; irritant and allergic. Irritant is more frequent than allergic [1].

Exact incidence of textile dermatitis is unknown because of the lack of controlled epidemiological studies. Textile dye sensitization has an estimated incidence rate from 1.4% to 5.8% [2, 3]. Recent studies demonstrate that contact dermatitis produced by allergic or irritant reactions to clothes is more frequent than previously thought. It has also been shown that the frequency of textile-dye allergy is increasing [4]. Female patients had a greater prevalence of allergic reactions to textiles dyes and resins than men, perhaps due to thigh clothes [3].

Clothes are composed by textile fibers, coupling and fixer agents, finish products, dyes and complements. Dyes and finish products are the most frequent sensitizers [1].

2. TEXTILE FIBERS

Textile fibers are a rare cause of contact dermatitis. There are two kinds of textile fibers:

(i) *Natural fibers* are used less frequently than synthetic fibers in clothes. There are two kind of natural fibers: cellulosic fibers (cotton, flax, yuta, pitta, hemp) and protein fibers (silk, wool, angora, cashmere, mohair...) [1].

Wool, silk and nylon have all been known to cause allergic contact urticaria in textiles. However, allergic reactions to silk products are rare. Silk fiber consists of fibrous protein filaments, fibroin, glued together with sericin. The sericin is usually removed from silk during manufacture in the degumming process. In finished silk, there may be sericin in incompletely degummed silk fibers and contamination with material from silkworms, which can produce a contact dermatitis [5].

Wool fibers are frequently used in human clothes but can be irritant in direct contact with the skin. Wool fiber has frequently been shown to be irritant to the skin of atopic patients producing itching or burning sensation, and for this reason wool intolerance was included as a minor criterion in the diagnostic criteria of atopic dermatitis by Hanifin and Rajka in 1980. Wool fabric may produce an allergic or irritant contact dermatitis, being irritant dermatitis more frequent than allergic dermatitis. Usually, when a patient shows allergic dermatitis to wool fibers is due to additives [6, 7].

The occurrence of contact dermatitis to cotton is also rare. Cotton clothes occasionally cause itch or erythema, but this is usually an irritant dermatitis. However, a case of skin allergy to cotton has been described [8]. Traditionally, allergy to cotton has always been related to occupational asthma, exposure to airborne cotton dust that could lead to byssinosis, or airway obstruction.

(ii) *Synthetic fibers* are made by the polymerization of monomers obtained from petroleum and tar (polyester nylon acetate, polyethylene, vinyl resins). This kind of fiber causes irritant contact dermatitis more frequently than allergic contact dermatitis [1].

3. DYES

Allergic reactions to dyes are more frequent than allergic reactions to finish products. Two dyes classifications have been described:

- I. Dyes classification according to chemical structure; azo, anthraquinone and azine (Table 1). The most common dye sensitizers belong to azo and anthraquinone structures [9].
- II. Dyes classification according to their union with the fabric:
 - a) Disperse dyes are the most frequent sensitizers between dyes group. They are used for coloring synthetic and mixed fibers such as polyester, acrylic, acetate and polyamide. Disperse dyes link to the fiber through weak bonds. They are not water-soluble, however, their release from fibers can be increased by sweat, friction and pressure, promoting the contact between the dye and the skin, and consequently developing allergic contact reactions [10].
 - b) Reactive dyes have been used in the textile industry for the past 40 years. Currently, they are mainly used in natural fibers such as cotton (T shirts, polo sweaters, underwear), silk and wool (high-quality casual wear), in mixed fibers and polyamide. Reactive dyes consist of a direct colourant, with an azo or, more rarely, anthraquinone structure or phthalocyanine derivative group, connected to a reactive group, capable of linking through covalent bonds to fibers. This strong union does not allow the release of the reactive dye from the fibers; for this reason, the union of the dye to the skin is difficult. Therefore, reactive dyes have been considered potential sensitizers only at the beginning of the production stage [10]. However, some cases of textile reactive dye allergic contact dermatitis after wearing clothes have been reported [11].
 - c) Direct dyes: they are directly absorbed by the fibers in aqueous solutions [12]. Two types of direct dyes are differentiated: *acid dyes* are salts of sulfuric or

carboxylic acids which precipitate on the fiber. They are used in nylon, wool and animal fibers. *Basic dyes* are ammonium salts or complexes formed by zinc chloride and amines. They are used in natural fibers such as cotton [13].

Table 1. Dyes classification according to their chemical structure

Dyes chemical structure			
AZO		Anthraquinone	
	Disperse yellow 3		Disperse Blue 1
	Disperse yellow 4		Disperse Blue 3
	Disperse Red 1		Disperse Blue 7
	Disperse Red 17		Disperse Blue 26
	Disperse Red 19		
	Disperse Red 137		Disperse Blue 35
	Disperse Orange 1		Disperse Red 11
	Disperse Orange 3		Disperse Red 15
	Disperse Orange 76		
	Disperse Black 1		
	Disperse Black 2		Metilamino-4-(2-hidroximetilamino antraquinona)
	<i>p</i> -amino-acetianilida- <i>p</i> -cresol		
	Disperse Blue 106		Vat Green 1
	Disperse Blue 124		Acid Black 48
	Disperse Blue 102		
	Disperse Blue 85		
	Acid Yellow 23	Azine	Basic Black 1
	Supramide Yellow		
	Supramide Red		
	Basic Red 46		

Disperse dyes are the most frequent sensitizers among textile dyes (Disperse blue 106 and disperse blue 124), followed by the reactive dyes. Acid, direct and basic dyes are less common sensitizers [12].

Two concepts must be differentiated: staining action occurs when a coat of liquid dye or tint is used to penetrate the surface of a material and impart a rich color. In contrast, dyeing process gives color to materials by soaking in a coloring solution. Dyeing techniques usually ensure that the appropriate dye goes into the appropriate component of the blend, but if dyeing is carried out incorrectly, the dye may stain the fabric. This portion of the dye might have poor fastness on the fiber and would leach easily in washing or in wear, particularly in the presence of perspiration. Moreover, in dye-houses, unsuitable dyes may be used as a shading component for final color adjustments on any type of textile, this fact may induce releasing between the dye and the fabric, with an increased risk of dye allergic contact dermatitis [13].

Several dyes have a high percentage of cross-reactivity due to their close structural similarity [2]. There is cross-reactivity between multiple azo disperse dye sensitization and cross-sensitization between azo dyes and paraminophenylenediamine compounds [3, 11, 14]. Most dyes are used in combination; red, blue and yellow dyes are commonly combined. The

industry standard “best practice” for navy or black is to choose a dye close to the color required and then to add shading components to achieve the required match [13].

4. COUPLING AND FIXERS AGENTS

These agents are used to reduce the loss of dye from the dyed fabric during the washing process. Tinofix S ® and Naphtol AS belong to this group, however these agents rarely cause contact dermatitis, being Naphtol AS (3-hydroxy-2-naphthalinide, 3-hydroxy-2-naphthoic acid anilide) more sensitizer than Tinofix S [1]. Naphtol was first reported as a cause of pigmented contact dermatitis in textile worker in Mexico in the 1970s. It was identified as the cause of hand dermatitis in a needlewoman probably occupationally sensitized from clothes, and occasionally in other cases of textile dermatitis [15].

5. FINISH PRODUCTS

Finish products are used to impart wrinkle resistance during wear and laundering. They can also facilitate bleaching and dyeing, make fabrics waterproof, non-shrinkable, and moth-proof; they can ameliorate nylon and make it electrically antistatic. They give textile body, and improve their quality, touch, and appearance [16]. Finish products are the second most common textile sensitizers; they are used in natural and mixed fibers. Resins belong to this group, being Kaurit and Fix the most allergenic formaldehyde resins.¹ Formaldehyde resins are also named durable-press resins or permanent-press resins [17]. The cause of textile-resin dermatitis is usually free formaldehyde released from the resin which links to the skin, producing contact dermatitis. Formaldehyde resins rarely cause occupational disease; it has been scarcely documented in the literature in the past 30 years. However, cases of occupational allergy associated primarily with uniforms (water-resistant laboratory coats, zip-up greens worn by machinists and military wool garments) are still being described. There are also many individuals who own old clothes (including vintage clothes), which are expected to release higher levels of free formaldehyde. Finally, cotton upholstery may contain old textile resins that release higher amounts of free formaldehyde, and direct contact of skin with such furniture is an important source of potential contact allergy [16, 18].

The types of formaldehyde resins used in durable-press fabrics can be classified into high, medium and low formaldehyde releasers [16, 19, 20]. Based on this fact, two different chemical agents have been used:

- I. Urea-formaldehyde and melamine/formaldehyde products: urea-formaldehyde resins are derived from the polymerization of urea and formaldehyde with a curing agent and melamine/formaldehyde resins result from the condensation of formaldehyde and melamine. They were used until 1950s and they belong to high formaldehyde releaser resins group. Therefore, contact dermatitis due to formaldehyde present in textiles was commonly reported until that date, especially in Europe (1950 and 1960s), being the most frequent sensitizers in textile dermatitis at that time [16, 19].

- II. (ii)Cyclic urea derivatives: Formaldehyde-containing finishes. During the 1960s and 1970s, concern about formaldehyde encouraged development of cellulose cross-linking finishes with low free formaldehyde levels and later products completely formaldehyde free. The current textile finish resins are the cyclized urea derivatives, because they release small amount of formaldehyde, being less sensitizers than the other group [16].

Formaldehyde-free finishes. This group do not contain formaldehyde, the best known of them is 1,3-dimethyl-4,5-dihydroxyethylenurea. It has, however, a poor cost performance ratio, which is a reason for a relatively small market penetration. Another reason is that a completely formaldehyde-free finish is not so commercially important since the advent of the ultralow formaldehyde products [16].

Miscellaneous cross-linking agents: other chemical cross-linking agents used to provide durable press properties to cellulose include diglyoxal urea, carbamate derivatives, diepoxides, diisocyanates and polycarboxylic acid systems. However, due to either high cost or limited technical advantages, they are nowadays poorly used in the industry. Sometimes they are contained as minor components or mixtures for special effects [16].

Although, since 1960, textile industry began to use low formaldehyde releaser resins, clothing dermatitis cases continued increasing, perhaps in consequences to the widespread use of textile dyes, which are the most frequent textile sensitizers [16, 19].

Table 2. Examples of international limits for formaldehyde in clothing and other textiles (ppm)

Country	Infants and babies	Textiles in direct contact with the skin	Textiles not in direct contact with the skin
Australia	30	100	300
Austria	Textiles that contain 1500 ppm or above must be labeled		<300
China	<20	<75	<300
Finland	30	100	300
France	20	100	400
Germany	Textiles that contain 1500 ppm or above must be labeled		
Japan	Not detectable	75	
The Netherlands		120	
New Zealand	30	100	300
Norway	30	100	300

There are few studies of the prevalence of durable press chemical finishes. In North America, prevalence rates in the 1990s range from 5 to 7.2%. Since 2001, the rates are stable at a level slightly over 2% [20]. In Israel, the prevalence is around 6% [2]. The frequency of reports of formaldehyde textile dermatitis from Scandinavian countries is sharply contrasted to the scarcity of such reports from USA. Suggested explanations were the extensive use of formaldehyde antiperspirants in Scandinavia but not in the USA, lower amounts of free formaldehyde in clothes in the USA, and more thoroughly washing the clothes by American

manufacturers before they were sold (the potential for formaldehyde-release from resins usually decreases with the number of washes) [16, 19]. Some countries have legally limited the formaldehyde content of textile products to reduce the risk of contact dermatitis and other adverse effects among their populations. Japan was the first in 1973 (which led to a sharp decrease in the prevalence of sensitization to formaldehyde in the years thereafter), followed by Finland. Other countries with legal limitations include China, Norway, France, Japan and the Netherlands [16]. The regulations differ, but usually garments for babies and infants should contain < 20-30 ppm formaldehyde, for clothes in direct contact with the skin a maximum of 75-100 ppm, and for clothing and textiles without direct skin there are upper limits of 300-400 ppm formaldehyde in textiles (Table 2) [16].

6. COMPLEMENTS

Agents such as rubber, adhesives, nickel, chrome used in the manufactured of complements (buttons, zip, buckles...) may cause contact dermatitis.¹ Contact allergic reactions due to rubber components in textiles are exceptional, despite of their widespread use. However, some cases of contact dermatitis caused by different components of rubbers have been described, such as mercaptobenzothiazole contained in the rubber bands of the socks or bikinis. Moreover, water and sweat might have solved mercaptobenzothiazole molecules, prompting the link between the allergen and the skin, eliciting contact textile dermatitis [21].

7. DETERGENT

When fabrics are not properly rinsed after washing, detergent residues may remain in the fabric. However, biocides, bleaching agents and detergent residues are a rare cause of contact dermatitis [17]. Moreover, the exposure to fragrance allergens used in laundry products and associated with washed fabrics, even under exaggerated exposure conditions, seems highly unlikely to be a cause of the induction of sensitization [22].

Many clinical manifestations of textile dermatitis have been described. Typical clinical presentations are *acute or chronic dermatitis*, patients are usually affected by erythematous patches, associated or not with fine desquamation [2, 4] (Figure 1 and 2). No correlation has been found between specific clinical patterns or distribution of the lesions and the type of sensitizing allergen [2].

The distribution of the dermatitis is often widespread, usually corresponding to areas that come into contact with clothing. Often, the dermatitis is worse in areas with increased friction and sweating. In men, this is often the collar area on the neck. In women, this includes the axillary folds and suprapubic area. In both sexes the waistband area, buttocks and extremities mainly the inner, thighs or popliteal fossae, are commonly involved [12]. Less frequently, the lesions appear in hands, face, genital area and soles [2, 4]. Foot dermatitis is often assumed to be caused by shoes, and patch testing to dyes in socks is not always performed [13].



Figure 1. Acute dermatitis affecting the trunk.



Figure 2. Example of chronic dermatitis.

Unusual forms can also be seen:

(i) Purpuric lesions, extravasation of blood from cutaneous vessels into skin or mucous membranes results in reddish-purple lesions included under the term purpura [23]. Purpura related to hypersensitivity to textile dyes and resins has been described (Figure 3) [4].



Figure 3. Example of purpuric lesions in the legs.

(ii) *Papular lesions*: a papule is a solid, elevated lesion less than 0.5 cm in size in which a significant portion projects above the plane of the surrounding skin [23]. Papular lesions have been described due to hypersensitivity to formaldehyde and disperse blue dye (Figure 4) [4].



Figure 4. Example of rash papular.

(iii) *Pustulars lesions*: a pustule is a circumscribed, raised cavity in the epidermis or infundibulum containing pus [23]. Pustulars lesions may be due to dyes and resins (Figure 5) [4].



Figure 5. Pustulars lesions in the leg.

(iv) *Hyperpigmented patches*: are atypical manifestations of textile contact dermatitis occasionally described. They have been related to hypersensitivity to disperse dyes and to an azo dye coupling component agent, Naphtol AS (Figure 6) [4].



Figure 6. Hyperpigmented patches in the back.

(v) *Urticaria*: the lesions are due to swelling of the skin that is characteristically evanescent, disappearing within hours (Figure 7) [23].



Figure 7. Urticarial lesions in the abdomen.

(vi) *Erythema multiforme-like lesions*: it is a localized or widespread eruption formed by redness plaques. It may be an atypical manifestation of hypersensitivity to disperse dyes (Figure 8) [4].



Figure 8. Erythema multiforme lesions in a child.

(vii) Contact depigmentation from the textile dyes has been reported (Figure 9) [4].

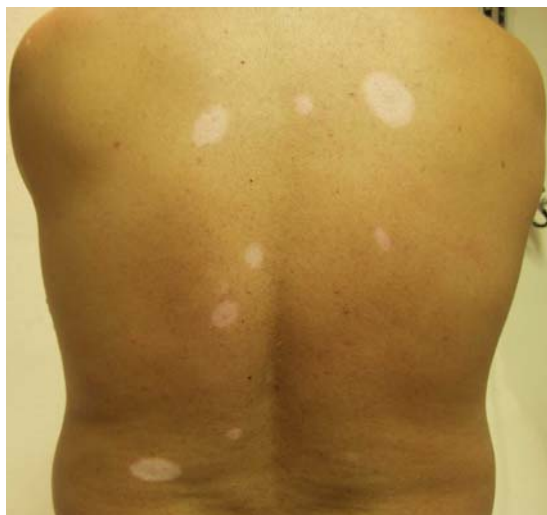


Figure 9. Example of depigmentation in the back.

(viii) *Pruritus and excoriations* are a rare form of hypersensitivity to textile dyes and resins [4]. Excoriations are surface excavations of epidermis that result from scratching and are frequent findings in patients experiencing pruritus (Figure 10) [23].



Figure 10. Excoriations and eczema patches in a patient.

(ix) *Nummular-like lesions*: these lesions are well-demarcated, coin-shaped plaques form from coalescing papules and papulovesicles (Figure 11) [23].



Figure 11. Nummular eczema in a patient.

(x) *Lichenification*: repeated rubbing of the skin may induce a reactive thickening of the epidermis, with accentuated markings, which may resemble tree bark. Lichenified plaques may also show signs of scratching, such as excoriations and crusts (Figure 12) [23].



Figure 12. Example of lichenification in a leg.

(xi) *Erythroderma* is a generalized deep redness of the skin involving more than 90% of the body surface within days to weeks (Figure 13) [2, 4, 23].



Figure 13. Example of erythroderma in the back.

Airborne contact dermatitis can have an allergic and irritant origin; chlorothalonil-treated fabrics should be used in open spaces or with sufficient ventilation and industrial vacuum cleaning at the source of the exposure [24]. Moreover, work related respiratory symptoms are not uncommon among dyehouse workers. Reactive and disperse dyes can cause rhinitis, asthma, bronchitis and conjunctivitis [14, 25].

When textile dermatitis assumes atypical appearance, the diagnosis may be delayed. Being familiar with textile contact dermatitis is important, because it allows a faster and precise diagnosis of clothing-related contact dermatitis [4].

The diagnosis is based on the clinical findings and confirmation with patch-test which is the gold standard method for the diagnosis of allergic contact dermatitis. The patch test determines if a specific substance causes allergic inflammation of the skin. It is intended to produce a local allergic reaction on a small area of the back where the diluted chemicals were applied. When the skin is exposed to an allergen, the triggered inflammatory response causes a reaction on the skin. The patch test is applied on the back of the patient for 48 hours, and the results are read in 96 hours. In order to avoid false negative reactions, late readings at day 7 are recommended, particularly if a special metal series is tested. The patch test is positive if we find an inflammation in the skin localized in the area where the allergen was applied (Figure 14). Between positive reactions, we may distinguish irritant from allergic reactions, the first ones usually improve between 48 and 72 hours after first reading, and allergic reactions worsen. However, it is very difficult to differentiate a mild allergic reaction from a mild irritant reaction. Negative results occur when we do not observe any lesions on the skin after 96 hours after allergen application. Relevance establishes the existence of the causal relationship between the positive test and the dermatitis and it is rated as definitive, probable, possible, past or unknown.



Figure 14. Positive result in patch test.

The chemicals included in the patch test kit are the offenders in approximately 85-90% of contact allergic eczema. The International Contact Dermatitis Research Group was formed in the late 1960s from an amalgamation of European organizations to coordinate and standardize patch testing worldwide. This organization inspired the formation of a domestic group, the North American Contact Dermatitis Group (NACDG), which became active in the validation and efficacy studies needed to gain Food and Drug Administration (FDA) approval for commercial patch testing. The most common test used for ACD screening today and the only

FDA-approved patch test is the Thin-Layer Rapid Use Epicutaneous (T.R.U.E.) Test (Table 3). Since the 1980s, the NACDG has worked to study and test new allergens suspected in eliciting ACD and now, it has 65 allergens. It has been demonstrated that NACDG series detects all the allergens in 65% of patients and at least one allergen in 90% of patients, so it is more effective than the commercially available T.R.U.E. Test. Moreover, it is possible to apply allergens from different specific batteries [26].

Table 3. Standard Spanish serie

1.	Nickel sulphate	16.	Black rubber mix
2.	Wool alcohols	17.	Kathon CG
3.	Neomycin sulphate	18.	Quaternium 15
4.	Potassium dichromate	19.	Mercaptobenzothiazole-kathon
5.	Caine mix	20.	<i>p</i> -Phenylenediamine
6.	Fragrance mix	21.	Formaldehyde
7.	Colophony	22.	Mercapto mix
8.	Epoxy resin	23.	Thiomersal
9.	Quinoline mix	24.	Thiuram mix
9.	Thiuram mix	25.	Diazolidinyl urea
10.	Balsam of Peru	26.	Imidazolidinyl urea
11.	Ethylenediamine dihydrochloride	27.	Budesonide
12.	Cobalt chloride	28.	Pivalate 21
13.	<i>p-t</i> - Butylphenol formaldehyde resin	29.	hydrocortisone butyrate 17
14.	Parabens	30.	Mercury
15.	Carba mix	31.	Lactones

We must consider that many allergens are not included in the different specific batteries, such as textile dye battery. For this reason, textile contact dermatitis may remain undiagnosed and underreported [27]. However, *p*-amino-phenylenediamine ($C_6H_4(NH_2)_2$), which historically has been considered to be a screening allergen for textile dye dermatitis, is included in most baseline patch test series. Despite we may observe cross-reactivity between multiple azo and *p*-amino-phenylenediamine compounds; it is not a good marker for textile dyes allergy [28]. Although studies are limited, disperse blue 106 and 124 may serve as good screening allergens for dye textile allergy, with positive reactions in approximately 80 and 57% of dye-related cases in two separate reports [12]. Several dyes have a high percentage of cross-reactivity due to their close structural similarity such as disperse blue 106 and 124 and azo compounds [2, 3, 11, 14]. One person may be sensitized for several dyes, because most dyes are used in combination with other dyes [13].

Formaldehyde and some resins are included in T.R.U.E. Test and in standard series. For example, the NACDG series includes three resins which may allow the diagnosis of contact dermatitis to finish products.

The treatment of contact dermatitis to textile consists of topical or systemic corticosteroids according to the seriousness of the lesions. Textile contact dermatitis can be generalized or localized; the generalized contact dermatitis to clothing is a severe condition,

which might require systemic corticosteroid treatment. The localized distribution includes areas of friction or contact with the sensitizer allergen, this form improves with topical corticosteroid treatment. The time of full recovery after discontinuing the exposure to the allergen is about 20 days [2].

In addition, the following procedures should be followed: preventing the offending allergen or irritant source, wearing 100% natural based fabrics, use of loose fitting clothing, and avoidance of synthetic spandex, lycra, acetate, polyester fibers and nylon. It is recommended washing clothes three times before wearing them the first time [2].

CONCLUSION

The use of clothing is a universal fact. They are composed by textile fibers, coupling and fixer agents, finish products, dyes and complements. These materials can cause a contact dermatitis and among them dyes are the most common sensitizers, being disperse dyes the most frequent, followed by reactive dyes. Finish products are the second most common textile sensitizers, although they were the most frequent sensitizers in the past.

Dyeing techniques usually ensure that the appropriate dye joins the adequate fiber. If unsuitable dyes are used on any type of textile, a release between the dye and the fabric is produced, which consequently increases the risk of dye allergic contact dermatitis [13]. Some cases of textile dye allergic contact dermatitis seem difficult to diagnose, due to the lack of up-to-date patch test series; this is further complicated by the continuous introduction to the market of new dyes, with chemical characteristics often inadequately specified for reasons of trade secrecy. A close relationship with the textile industry is necessary to obtain detailed and up-to-date information on newly introduced textile coloring agents [10].

The diagnosis of contact dermatitis caused by clothing may be difficult in some cases because of the wide spectrum of clinical presentations, including unusual clinical patterns and atypical localization, which could lead to a delayed diagnosis. Being familiar with the typical and unusual forms of textile contact dermatitis allows more rapid and precise diagnosis of clothing-related contact dermatitis, which is not uncommon [4].

Different textile components may cause respiratory and other general problems among dyehouse workers. Patients with work related symptoms probably have an increased tendency to change occupation or stop working and this fact may influence in the economy of the country [25].

Some countries have legally limited the formaldehyde content of textile products to reduce the risk of contact dermatitis and other adverse effects among their populations [16]. The European Union, through Directive (2002/61/EC) to restrict the marketing and use of certain dangerous substances and preparations (azo colorants) in textile and leather products, has taken the worldwide lead in restricting some dyes as a result of their carcinogenic nature. It is important to be vigilant for new and unexpected sources of allergens from textiles [29]. Because of the public health legislation in the European Union, the prevalence of textile dye dermatitis and durable-press finishes has probably decreased more quickly in the European Union than in the USA [18].

REFERENCES

- [1] Aguirre Martínez-Falero, A., and Vicente Calleja, J.M. (1999). Textile and shoes contact dermatitis. In: Giménez Camarasa JM. Contact Dermatitis. Ed. Grupo Aula Médica: Madrid. 99-224.
- [2] Lazarov, A. (2004). Textile dermatitis in patients with contact sensitization in Israel: a 4-year prospective study. *Journal of the European Academy of Dermatology and Venereology*, 8: 531-537.
- [3] Cordeiro, M.R., Gonçalo, M., Fernandes, B., Oliveira, H., Figueiredo, A. (2000). Positive lesional patch tests in fixed drug eruptions from nimesulide. *Contact Dermatitis*, 43(5): 307.
- [4] Lazarov, A., Cordoba, M., Plosk, N., Abraham, D. (2003). Atypical and unusual clinical manifestations of contact dermatitis to clothing (textile contact dermatitis): case presentation and review of the literature. *Dermatology Online Journal*, 9(3): 1.
- [5] Inoue, A., Ishido, I., Shoji, A., and Yamada, H. (1997). Textile dermatitis from silk. *Contact Dermatitis*, 37: 185.
- [6] Ricci, G., Patrizi, A., Bellini, F., and Medri, M. (2006). Use of textile in atopic dermatitis: care of atopic dermatitis. *Current Problems in Dermatology*, 33: 127-43.
- [7] Mason, R. (2008). Fabrics for atopic dermatitis. *Journal of Family Health Care*, 18(2): 63-65.
- [8] González de Olano, D., Subiza, J.L., and Civantos, E. (2009). Cutaneous allergy to cotton. *Annals of Allergy, Asthma and Immunology*, 102(3): 263-264.
- [9] Hatch, K.L., and Maibach, H.I. (1995). Textile dye dermatitis. *Journal of American Academy of Dermatology*, 32: 631-9.
- [10] Manzini, B.M., Motolese, A., Conti, A., Ferdani, G., and Seidenari, S. (1996). Sensitization to reactive textile dyes in patients with contact dermatitis. *Contact Dermatitis*, 34(3): 172-175.
- [11] Sánchez-Gilo, A., Gómez-De La Fuente, E., Calzado, L., and López-Estebanz, J.L. (2010). Textile contact dermatitis in a patient sensitized to Reactive Orange 107 dye. *Actas Dermosifiliográficas*, 101(3): 278-9.
- [12] Joe, E.K. (2001). Allergic contact dermatitis to textile dyes. *Dermatology Online Journal*, 7(1): 9.
- [13] Opie, J., Lee, A., Frowen, K., Fewings, J., and Nixon, R. (2004). Foot dermatitis caused by the textile dye Basic Red 46 in acrylic blend socks. *Contact Dermatitis*, 49: 297-303.
- [14] Anibarro, P.C., Breñosa, B.G., Madoz, S.E., Figueroa, B.E., Muruzabal, M.T., Bacaicoa, M.T., Sanchez, N.L., and Purroy, A.I. (2000). Occupational airborne allergic contact dermatitis from disperse dyes. *Contact Dermatitis*, 43(1): 44.
- [15] Le Coz, C.J., and Lepoittevin, J.P. (2001). Clothing dermatitis from Naphthol AS. *Contact Dermatitis*, 44: 366-375.
- [16] De Groot, A.C., Le Coz, C.J., Lensen, G.J., Flyvholm, M.A., Maibach, H.I., and Coenraads, P.J. (2010). Formaldehyde-releasers: relationship to formaldehyde contact allergy. Formaldehyde-releasers in clothes: durable press chemical finishes. Part 1. *Contact Dermatitis*, 62: 59-71.

- [17] Hatch, K.L., and Maibach, H.I. (1995). Textile dermatitis: an update (I). Resins, additives and fibers. *Contact Dermatitis*, 32: 319-926.
- [18] Nedorost, S., Warshaw, E., Jacob, S., Katta, R., Zirwas, M., and Scheman, A. (2010). Allergic contact dermatitis caused by durable-press finishes does exist in the USA. *Contact Dermatitis*, 63: 233-235.
- [19] Cockayne, S.E., McDonagh, A.J.G., Gawkrödger, D.J. (2001). Occupational allergic contact dermatitis from formaldehyde resin in clothing. *Contact Dermatitis*, 44: 109.
- [20] De Groot, A.C., Le Coz, C.J., Lensen, G.J., Flyvholm, M.A., and Maibach, H.I. (2010). Coenraads P-J. Formaldehyde-releasers: relationship to formaldehyde contact allergy. Part 2. Formaldehyde-releasers in clothes: durable press chemical finishes. *Contact Dermatitis*, 63:1-9.
- [21] Jung, P., Sesztak-Greinecker, G., Wantke, F., Götz, M., Jarisch, R., and Hemmer, W. (2006). Bikini dermatitis due to mercaptobenzothiazole. *Contact Dermatitis*, 54(6): 345-6.
- [22] Corea, N.V., Basketter, D.A., Clapp, C., Van Asten, A., Marty, J.P., Pons-Guiraud, A., and Laverdet, C. (2006). Fragrance allergy: assessing the risk from washed fabrics. *Contact Dermatitis*, 55(1): 48-53.
- [23] Garg, A., Levin, N.A., and Bernhard, J.D. (2008). Structure of skin lesions and fundamentals of clinical diagnosis. In: Fitzpatrick's. *Dermatology in general medicine*. Ed. McGraw-Hill. 7th ed: United States of America, 23-40.
- [24] Lensen, G., Jungbauer, F., Gonçalves, M., and Coenraads, P.J. (2007). Airborne irritant contact dermatitis and conjunctivitis after occupational exposure to chlorothalonil in textiles. *Contact Dermatitis*, 57: 181-186.
- [25] Nilsson, R., Nordlinder, R., Wass, U., Meding, B., Belin, L. (1993). Asthma, rhinitis, and dermatitis in workers exposed to reactive dyes. *British Journal of Industrial Medicine*, 50(1): 65-70.
- [26] Cohen, D.E., Rao, S., and Brancaccio, R.R. (2008). Use of the North American Contact Dermatitis Group Standard 65-Allergen Series Alone in the Evaluation of Allergic Contact Dermatitis: A Series of 794 Patients. *Dermatitis*, 19(3): 137-141.
- [27] Giusti, F., and Seidenari, S. (2003). Textile dyes sensitization: a study of 49 patients allergic to disperse dye alone. *Contact Dermatitis*, 48(1): 54-55.
- [28] Ryberg, K., Isaksson, M., Gruvberger, B., Hindsén, M., Zimerson, E., and Bruze, M. (2006). Contact allergy to textile dyes in southern Sweden. *Contact Dermatitis*, 54: 313-321.
- [29] Brookstein, D.S. (2009). Factors associated with textile pattern dermatitis caused by contact allergy to dyes, finishes, foams, and preservatives. *Dermatology Clinics*, 27(3): 309-322.

Chapter 16

APPLICATION OF LAYER-BY-LAYER METHOD FOR TEXTILES

Dawid Stawski*

Department of Physical Chemistry of Polymers,
Technical University of Lodz, Zeromskiego 116, 90-924 Lodz, Poland.

ABSTRACT

Textile materials have many advantages which make them useful for clothing and technical applications. They can be used in different forms, be permeable to air or fluids if needed, and additionally textiles have good mechanical parameters. They have a large surface in comparison to their mass. In many cases they offer a solution to problems, which are beneficial in terms of price and given application parameters. That is why surface modification, significantly increasing the range of textiles' applications, is an important research topic in textiles materials. Systematically grows a need to produce new materials or products with improved characteristics. In this chapter the latest methods which improve surface properties in a more effective way than conventional were described.

One of the newest methods of textile surface modification is the layer-by layer method. Initially this method has been used for different materials than textiles; however it is currently implemented in the textile industry. The use of multilayered polymeric films offers the possibility of creating new type of materials with great levels of reproducibility and controlled architectures. Fundamental and representative methods used for textile surface modification on the basis of layer-by-layer method were characterised. Theoretical assumptions, textile characteristic and practical conditions were discussed. Methods for specific applications were analysed as far as application and difficulties in their usage are concerned.

* E-mail: dawid.stawski@p.lodz.pl

1. LAYER-BY-LAYER METHOD

The synthesis of thin, mainly organic layers containing functional groups, designed for modifying the surface properties of different objects, is now the subject of a wide interest [1-15].

The most important principle of the layer-by-layer (lbl) method consists in alternately depositing oppositely charged layers of polyelectrolytes, which react between themselves owing to electrostatic forces. Nanolayer films are usually deposited using solution concentrations of several milligrams per milliliter. The adsorption step is followed by a rinsing or an excess removal procedure. The rinsing stage is used to avoid contamination with the next adsorption solution and to remove weakly adsorbed molecules. The coated material, which now possesses an outer layer of a polyelectrolyte, can now adsorb an opposite layer. The strong electrostatic attraction is the dominant factor in the adsorption of polyions. Multilayer structures may be composed of polyions, charged molecular substances or colloidal objects. Adsorption times per layer vary from minutes for polyelectrolytes to hours for some colloids. Operational factors such as: electrolyte concentration, ionic strength, temperature, adsorption time, rinsing and drying time may also influence the nanolayer structure and its thickness.

The creator and pioneer of this method was Gero Decher who published a series of works describing this technique in the nineties of the 20th century [1-6]. Since then such method has been investigated by different researchers [7-11] and by Decher himself [12-15]. By using such type of modification it is possible to obtain products that combine the properties of the main object with the superficial parameters of a new external layer. Through an appropriate selection of the layer to be deposited one can very precisely control the surface properties of the given product adjusting them to concrete requirements and needs.

Appropriate electrolyte or polyelectrolyte nanolayers can be deposited on various flat surfaces such as mica [16-17], glass [6, 13, 18-20], quartz [6], gold [21], titanium [22], silicon [15, 18, 23-25], pigment particles [26], polymeric membranes [25, 27-28], microspheres [29], or finally fibres and textiles.

The lbl method has greatly increased in popularity due to its simplicity and the fact that not only polyelectrolytes but also almost any type of charged nanoentities can be used to create the nanolayers in a controlled way. The adhesion of the layer to the base substrate is more dependent on the properties of the polymer than on those of the substrate.

There are no formal limitations with respect to substrate topology; nanolayers have been created on objects of various sizes.

In general the lbl technique exhibits several advantages over similar surface modification methods leading to the production of multilayered films. The main advantage is that a wide variety of different materials can be used to prepare a multilayer structure, hence creating really multicomposite films. Another advantage of the lbl adsorption is that film architecture is almost completely determined by the deposition conditions.

2. APPLICATION OF THE LAYER-BY-LAYER METHOD FOR TEXTILES

The surface of textile materials is much different in comparison with the standard materials used for lbl modification. In case of foil, mica, gold, glass, etc., the modified area

and the access of the liquid medium to such area are clear and well defined. In the textile modification the situation is different. The modified fibers surface is much bigger than textile area – the difference depends on the structure of textile material. The relation between fibers area (A_F) and textile fabric area (A_T) is ascribed by surface coefficient (e_u) (equation 1) [30]:

$$e_u = \frac{A_F}{A_T} = \frac{4ge_H}{\rho_s d_s} \quad (1)$$

where:

e_H – configuration factor, relation between real and theoretical fiber area, the factor is connected with not completely round fiber area;

d_s – average fiber diameter;

ρ_s – material density;

g – material number.

For instance for cotton fabric the fibers' area is about 50 times larger than fabric's area [30].

Additionally in textile fabrics there are spaces not available for liquid penetration, because of different types of weaves, compaction and fabric structure. This is characterized by the interspace factor e_v , which describes the relationship between summarized full fiber volume (V_T) and fiber volume available for penetration (V_Z) (equation 2) [30]:

$$e_v = \frac{V_Z}{V_T} = \frac{V_T - V_S}{V_T} = 1 - \frac{V_S}{V_T} = 1 - \frac{\rho_T}{\rho_s} \quad (2)$$

where:

V_S – volume not available for liquid penetration;

ρ_T – textile density.

Interspace factor is substantially connected with liquid factor (e_T) which can estimate the relation between the weight of the liquid which can fill up the material (G_F) and dry textile weight (G_T) (equation 3) [30].

$$e_T = \frac{G_F}{G_T} = \frac{\rho_F v_T}{\rho_s v_s} \quad (3)$$

In textile lbl application it is necessary to take into account a specific structure of the modified material and other such important factors as: type of flat material, its thickness, type of weaves, compaction, etc. Because of this, the application process is more complicated, and each measurement of properties is more difficult and requires special treatment and real attention.

The textile finishing industry increasingly makes use of functional nanoparticles in order to achieve new or improve properties of textile materials.

Every object interacts with surroundings through intervention of its surface. Therefore changes in its structure and character play a particular part in the modification process of structure and properties of a textile fabric. The lbl deposition process has no limitation on substrates, thus even textile substrates with nonplanar surfaces are suitable for this technique. The modification of fabric surface by the lbl method results in multi-component materials with complex structure and precisely selected properties. Initially, this method was used for other types of materials than textiles but now its implementation in the textile industry is in progress.

The first step of textile modification with the lbl method is activation, thus forming functional groups on the outer surface, whose purpose is to attach the first layer. The activation process may be carried out by a chemical reaction using appropriate reagents or surface grafting. These processes are usually carried out in a liquid environment, most often in an aqueous solution.

The process of layers deposition on fiber or fabric surface by the lbl method has been preliminary described in the scientific literature only in recent years [7, 24, 28, 31-39].

The deposition of layers on the surface of a single straight fiber from regenerated cellulose (rayon) placed on a silicon plate is reported in [24]. Partially acetylated poly(vinyl alcohol) and cationic partially acetylated poly(vinyl alcohol) were used as modifiers (Figure 1).

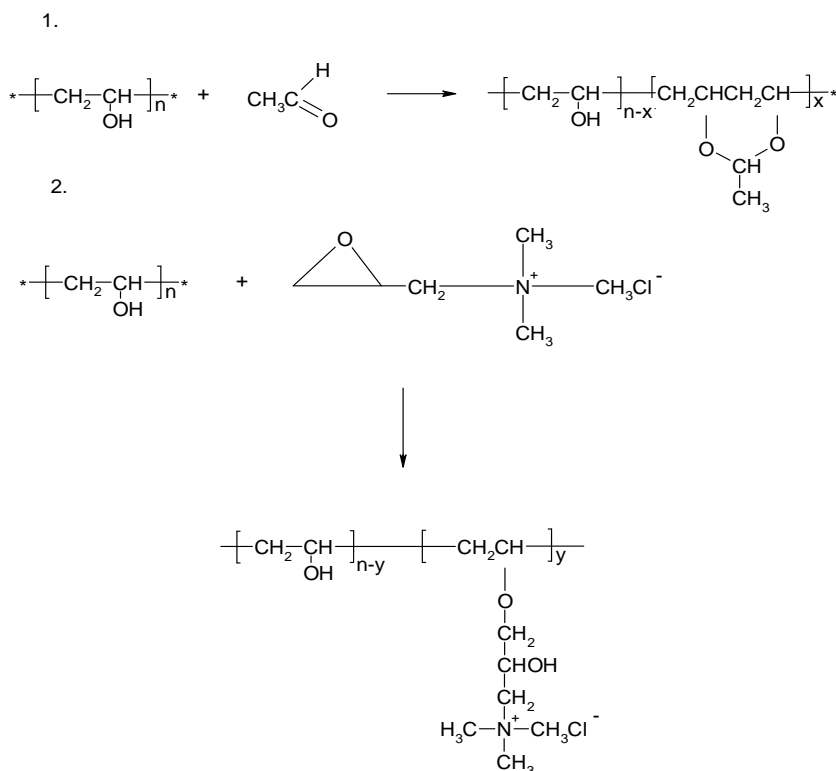


Figure 1. Synthesis of partially acetylated PVA and partially acetylated PVA: 1. Reaction PVA and acetaldehyde, 2. Cationisation of PVA [24].

A thermo-sensitive material was obtained and its topography was examined by the AFM technique. It has been observed that the lbl modification changes the roughness of fiber surface and the heating of modified samples at a temperature of 60°C causes the deposited particle to agglomerate. Depending on the type of the last layer, the fiber properties become more or less hydrophilic. Partially acetylated PVA shows small negative charges because of the residual hydroxyl group. Cationised derivative shows positive charges in neutral aqueous solution. The modified polymer can be used for a wide variety of applications such as sensors, switches, and recording materials.

Wang and Hauser [28] applied the lbl technique to modify the surface of cotton fabric using poly(4-styrene sulfonate) (PSS) and poly(diallyldimethylammonium chloride) (PDDA) (Figure 2).

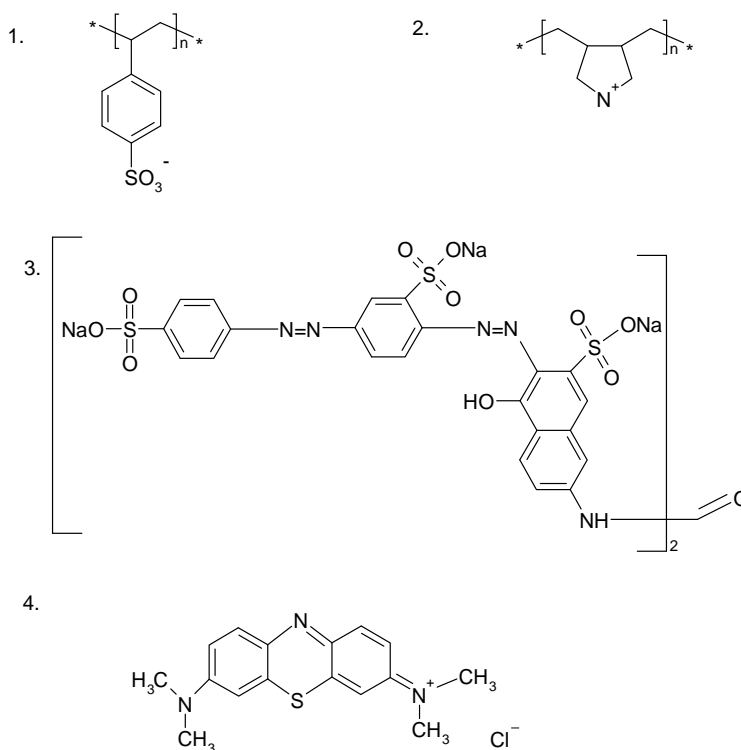


Figure 2. Chemical structures of: 1. PSS, 2. PDDA, 3. Direct Red 80 and 4. Methylene blue [28].

Dyeing tests of the fabrics after lbl deposition with anionic Direct Red 80 and cationic Methylene Blue (Figure 2) show regular and observable changes in terms of color depth (K/S value). Assessment of the variation of surface electric property of the cotton substrate depends on the alternate fabrication of PSS and PDDA on it. The authors observed a linear increase in UV absorbance at 226 and 261 nm of treated cotton fabrics. The layer-by-layer multilayers could be controlled by UV spectra monitoring of assembled cotton specimens. On the other hand attenuated total reflectance Fourier Transform Infrared Spectroscopy (ATR FT-IR) spectra did not show any identifiable differences between cotton substrates with and without polyelectrolyte deposition.

The modification of cotton fibers and fabrics is described in [31]. Their surface was activated with the use of 2,3-poly(propyltrimethyl ammonium chloride) to form the first layer with a positive charge (cationisation). Then PSS and poly(allylamine hydrochloride) (PAH) layers were alternatively deposited. The deposition process was confirmed by means of the XPS technique which gives similar results to those obtained for such a system on other surface. The thickness of one layer calculated on the basis of TEM photographs amount to 16 - 19 nm. The authors have not examined the changes in the characteristic properties of surface. The modification was analyzed by means of the IR reflection technique, XPS spectroscopy and TEM microscopy. Using the XPS analysis, authors have demonstrated that the ratio of nitrogen to sulfur present at the surface of the cotton fabric varies with successive deposition of either PAH or PSS layer.

Similar modification was made for wool [32, 33]. Wool fibers were functionalized [32] using 2,3-epoxypropyltrimethylammonium to prepare cationic layers. The cationic charges were successfully used to deposit layers of PAH and PSS [32].

Wang and Hauser [34] investigated the effects of self-assembled PSS and poly(diallyldimethylammonium chloride) (PDADA) deposition. The surface structure was confirmed using very similar methods as in earlier papers (dyeing tests and UV-Vis spectrometry). ATR FTIR spectra did not show any identifiable differences between cotton substrates with and without deposition of PSS/PDADA multilayers.

The conditions of grafting and the dyeability of modified polypropylene (PP) nonwovens with poly(acrylic acid) (PAA) and PAH are described by Połowiński [35]. It was found that the thickness of the deposited layers amounts to several nanometers (the mass increment was no higher than 0.01 g g^{-1}), and the dyeing technique allows the type of external layer deposited to be identified.

Polyamide nonwoven is modified by depositing a dye (scarlet red) and poly(diallyldimethylammonium chloride) (PDADMAC) by the lbl method. Dyed samples are subjected to measurements of light reemission [36]. The increase in K/S value at 510 nm was correlated with the dye deposition and was found to increase linearly with the number of layers. The conclusions show that increase in dye and PDADMAC concentrations (to 1 mM) enhance the deposition process, further increase in PDADMAC concentration led to a decrease in K/S value. The most advantageous salt concentration was found to be 0.5M and dipping times as short as 15 s to be sufficient for the deposition of the polyelectrolyte. Their results indicated that the growth of PDADA - scarlet dye multilayers on nylon fibers was highly dependent on various factors except the dipping time.

Natural dyed silk fibers have been modified by depositing alternative layers of a poly(diallyldimethylammonium chloride) and PSS (up to 30 layers) [37]. The surface structure was confirmed using ATR FTIR and the dye exhaustion from the silk fiber was monitored using UV-Vis spectroscopy. The aim of the modification was to improve the color fastness to washing of fibers dyed with scarlet dye. The ability of the polyelectrolyte layers to act as an electrostatic barrier against the release of the negatively charged dye was investigated as a function of the terminating top layer (negative layer is more efficient).

The deposition of polyelectrolytes on the surface of technical textile fabrics (nonwovens) has been described in [38]. The deposition of polyelectrolytes (PAA, poly(itaconic acid), poly(N-dimethylaminoethyl methacrylate) hydrochloride (PDAMA) and PAH) on polypropylene and polyester was confirmed with the use of a scanning electron microscope

(SEM) and light reemission of dyed samples. The deposition of subsequent layers to form polymer complexes modifies the properties of nonwovens (surface resistance and dyeability).

In turn, a polyester nonwoven is first treated with corona discharge (using laboratory prototyped device) followed by the deposition of polyelectrolyte layers [39] using lbl method and the effects obtained are assessed by means of the determination of the number of acidic groups, dyeing tests and reflective FTIR spectroscopy. The number of acidic groups, normalized activation energy, contact angle measurements and components of surface free energy on the surface were determined. The authors selected corona discharge treatment for the activation, which is a dry process and does not require the use of water or functional chemicals. This is the reason why authors decided to test the possibilities of applying corona discharge activation on polyester textiles. The presence of acid groups after activation process and lbl application was confirmed by test dyeing using Methylene Blue dye. The dyeing tests were also used for the reversible determination of deposited layer composition. The results obtained suggested that the discharge treatment is a better method for first layer deposition [39].

3. SPECIAL PROPERTIES OF TEXTILES MODIFIED USING LAYER-BY-LAYER METHOD

Colloidal particles possessing a negative potential (silver, gold and platinum) were adsorbed on external layers deposited on polypropylene (PP) nonwoven possessing a positive potential: PAH and PDAMA [7]. Deposition of such particles on the surface clearly increases the thermal stability of PP material. Additionally it was found, *that a significant increase in thermal resistance is observed when hydrogen saturated colloidal platinum has been incorporated.*

Lin *et al.* [40] investigated the effects of self-assembled PDDA - clay films on thermal properties of lignocellulosic fibers used for pulp fibers.

Antimicrobial silver nanoparticles were immobilized on polyamide and silk fibers (previously modified using PDADMAC and poly(methacrylic acid) (PMA)) by following the layer-by-layer deposition method [41]. The deposition of the nanoparticles on the material was controlled by the number of deposition cycles. The fibers coated with the nanoparticles exhibit antimicrobial activity against *Staphylococcus aureus* bacteria, which could offer them useful in applications such as water purification or antimicrobial fabrics. Additionally the preparation of the silver nanoparticles did not involve any toxic chemicals. The authors showed that the chemistry of the fibers surface plays an important role in the growth of the layer but pre-treatment could possibly improve the deposition process.

Polowiński and Jantas [42] *presented methods for the surface modification (using lbl method) of cotton woven fabric and polypropylene nonwoven in order to make them antibacterial. The surface of cotton fabric was functionalized with chloroacetate groups by means of chloroacetyl chloride, using pyridine as a catalyst, followed by the quaternalisation of the chloroacetate groups with poly(4-vinylpyridine). In the second case polypropylene nonwoven was firstly successfully impregnated with a multimonomer containing vinyl groups, which were then changed into tertiary amine groups by the addition of diethylamine. In next step these groups were quaternalised with propyl bromide. Additionally colloidal silver was incorporated into the nanolayers formed from polyelectrolytes on the polypropylene*

nonwoven. Authors made quantitative tests of bacteriological activity of the modified woven fabric and nonwoven showed both bacteriostatic and bactericidal activities. The most effective activity against Escherichia coli are the modifications leading to the formation of quaternary ammonium salts.

The electrokinetic properties of polypropylene nonwoven modified using lbl method were the main subject of paper [43]. Polyelectrolytes such as PAA and PAH with opposite charges have been deposited on a polypropylene surface previously grafted with acrylic acid. It has been found that there is a direct relation between the type of polyelectrolyte layer deposited on a nonwoven surface and the electrokinetic properties of this fabric. Based on the results obtained, it was concluded that the deposition of succeeding polyelectrolyte layers fails to provide a complete coverage of the modified surface. It was also concluded that the result of electrokinetic potential measurement is not affected by the molecular weight of polyelectrolyte and the value of Zeta potential depends exclusively on the type of the top layer rather than on the substrate, on which the layer is deposited.

Nonlinear polyelectrolyte structures of well defined comb polymers consisting of branched homo poly(ethylene imine), or poly(ethylene imine) with grafted poly(2-ethyl-2-oxazoline), having different degrees of polymerization and branches have been deposited using a layer-by-layer technique on a polypropylene nonwoven [44]. The surface properties of the materials have been analyzed by FTIR and XPS spectroscopy. Changes in the surface structure have been studied by employing electrokinetic and electrostatic measurements. The deposition of the polyelectrolytes increased the thermal stability of the nanomaterials and enabled the absorption of copper ions from solution.

The deposition of polyelectrolyte layers (PAA and PAH) by the lbl method significantly strengthens the thermal resistance of the modified fabric [45]. The effect is connected with the type and number of deposited layers. Thermal effects were also observed in both dynamic and isothermal analyses under air atmosphere. The authors suggest that these effects are due to the formation of a barrier by the deposited layers that insulates the main polymeric matter from oxygen access.

Additionally some papers recently published details new methods of lbl assembly with reduced deposition times and improved layer uniformity [46, 47]. Kim *et al.* [46] described a new technique for lbl deposition, which makes use of the standard lbl process and fluidic devices. In this procedure the multilayer structure can be produced in 90 s of processing time. In paper [47] the substrate is vertically oriented and polyelectrolytes are simultaneously sprayed on the surface. The new material position leads to continuous drainage and helps removing any substance that is not fixed on the surface. This technique does not include a drying step and can improve the uniformity of the film.

CONCLUSIONS

The use of multilayered polymeric films offers the possibility of creating new type of materials with great levels of reproducibility and controlled architectures.

To sum up the use of the lbl method for the modification of textiles, one should notice that according to the literature data this kind of modification has been just initiated. So far, only the basic methods for the confirmation of deposition on narrowly selected objects have

been published. Moreover, it was found that the deposited layers can be microreactors for different chemical processes. Layer-by-layer deposition of polyelectrolytes on textile materials might provide a new approach to create different functions to textiles. The surface functionality can be directly and flexibly altered by choosing appropriate polyelectrolytes. Therefore, the preparation of deposited multilayers on textiles is still easy, simple and energy-saving. Layer-by-layer deposition may offer many advantages as a surface modification technique for polymers.

The large number of different textile materials could possibly be used as substrates for the lbl deposition of nanolayers as far as they could hold charges on their surfaces.

Future development of the lbl technique on textile fiber is a very promising method for the development of a new range of application for the clothing and technical fiber industry.

REFERENCES

- [1] Decher, G., Hong, J., and Schmitt, J. (1992). Buildup of ultrathin multilayer films by a self-assembly process: III. Consecutively alternating adsorption of anionic and cationic polyelectrolytes on charged surfaces. *Thin Solid Films*, 210/211: 831-835.
- [2] Schmitt, J., Grünwald, T., Decher, G., Pershan, P., Kjaer, K., and Löschke, M. (1993). Internal structure of layer-by-layer adsorbed polyelectrolyte films: A neutron and X-ray reflectivity study. *Macromolecules*, 26: 7058-7063.
- [3] Hong, J., Lowack, K., Schmitt, J., and Decher, G. (1993). Layer-by-layer deposited multilayer assemblies of polyelectrolytes and proteins: from ultra thin films to protein arrays. *Progress in Colloid and Polymer Science*, 93: 98-102.
- [4] Lvov, Y., Haas, H., Decher, G., Möhwald, H., Michailov, A., Mchedlishvili, B., Morgunova, E., and Vainshtain, B. (1994). Successive deposition of alternate layers of polyelectrolytes and a charged virus. *Langmuir*, 10: 4232-4236.
- [5] Decher, G., Lehr, B., Lowack, K., Lvov, Y., and Schmitt, J. (1994). New nanocomposite films for biosensors: Layer-by-layer adsorbed films of polyelectrolytes, proteins or DNA. *Biosensors and Bioelectronics*, 9: 677-684.
- [6] Lehr, B., Seufert, M., Wenz, G., and Decher, G. (1995). Fabrication of poly(p-phenylene vinylene) (PPV) nanoheterocomposite films via layer-by-layer adsorption. *Journal of Supramolecular Science*, 2: 199-207.
- [7] Stawski, D., and Połowiński, S. Thermogravimetric measurements of poly(propylene) nonwovens containing deposited layers of polyelectrolytes and colloidal particles of noble metals. *Fibres and Textiles in Eastern Europe*, 15: 82-85.
- [8] Mao, G., Tsao, Y., Tirrel, M., Davis, H., Hessel, V., and Ringsdorf, H. (1993). Self-assembly of photopolymerizable bolaform amphiphile mono- and multilayers. *Langmuir*, 9: 3461-3470.
- [9] Saremi, F., Maassen, E., Tieke, B., Jordan, G., and Rammensee, W. (1995). Self-Assembled Alternating Multilayers Built-up from Diacetylene Bolaamphiphiles and Poly(allylamine hydrochloride): Polymerization Properties, Structure, and Morphology. *Langmuir*, 11: 1068-1071.

-
- [10] Kong, W., Zhang, X., Gao, M., Zhou, H., Li, W., and Shen, J. (1994). A new kind of immobilized enzyme multilayer based on cationic and anionic interaction. *Macromolecular Rapid Communication*, 15: 405-409.
- [11] Cheung, J., Fou, A., Rubner, M. (1994). Molecular self-assembly of conducting polymers. *Thin Solid Films*, 244: 985-989.
- [12] Decher, G., Lvov, Y., and Schmitt, J. (1994). Proof of multilayer structural organization in self-assembled polycation-polyanion molecular films. *Thin Solid Films*, 244: 727-777.
- [13] Sangrisub, S., Tangboriboonrat, P., Pith, T., and Decher, G. (2005). Adsorption of polystyrene-poly(4-vinylpyridine) diblock copolymer on the assembled latex film. *European Polymer Journal*, 41: 1531-1538.
- [14] Ladam, G., Gergely, C., Senger, B., Decher, G., Voegel, J., Schaaf, P., and Cuisinier, F. (2000). Protein interactions with polyelectrolyte multilayers: Interactions between human serum albumin and polystyrene sulfonate/polyallylamine multilayers. *Biomacromolecules*, 1: 674-687.
- [15] Ladam, G., Schaaf, P., Cuisinier, F., Decher, G., and Voegel, J. (2001). Protein adsorption onto auto-assembled polyelectrolyte films. *Langmuir*, 17: 878-882.
- [16] Adamczyk, Z., Zembala, M., and Michna, A. (2006). Polyelectrolyte adsorption layers studied by streaming potential and particle deposition. *Journal of Colloid and Interface Science*, 303: 353-364.
- [17] Adamczyk, Z., Zembala, M., Kolasińska, M., and Warszyński, P. (2007). Characterization of polyelectrolyte multilayers on mica and oxidized titanium by streaming potential and wetting angle measurements. *Colloids and Surfaces A: Physicochemical and Engineering Aspects*, 302: 455-460.
- [18] Kovacević, D., van der Burgh, S., de Keizer, A., Stuart, M. (2002). Kinetics of formation and dissolution of weak polyelectrolyte multilayers. Role of salt and free polyions. *Langmuir*, 18: 5607-5612.
- [19] Zucolotto, V., He, J., Constantino, C., Barbosa Neto, N., Rodrigues Jr, J., Mendonça, C., Zilio, S., Li, L., Aroca, R., Oliveira Jr, O., and Kumar, J. (2003). Mechanisms of surface-relief gratings formation in layer-by-layer films from azodyes. *Polymer*, 44: 6129-6133.
- [20] Shinbo, K., Baba, A., Kaneko, F., Kato, T., Kato, K., Advincula, R., Knoll, W. (2002). In situ investigations on the preparations of layer-by-layer films containing azobenzene and applications for LC display devices. *Materials Science and Engineering*, C22: 319-325.
- [21] Yoon, H., and Kim, H. (2000). Multilayered assembly of dendrimers with enzymes on gold: Thickness- controlled biosensing interface. *Analytical Chemistry*, 72: 922-926.
- [22] Sasaki, T., Ebina, Y., Watanabe, M., and Decher, G. (2000). Multilayer ultrathin films of molecular titania nanosheets showing highly efficient UV-light absorption. *Chemical Communications*, 21: 2163-2164.
- [23] Ngankam, P., Lavalley, P., Voegel, J., Szyk, L., Decher, G., Schaaf, P., and Cuisinier, F. (2000). Influence of polyelectrolyte multilayer films on calcium phosphate nucleation. *Journal of American Chemical Society*, 122: 8998-9005.
- [24] Lu, H., Zheng, A., and Xiao, H. (2007). Properties of a novel thermal sensitive polymer based on poly(vinyl alcohol) and its layer-by-layer assembly. *Polymers for Advanced Technologies*, 18: 335-345.

-
- [25] Seo, J., Lutkenhaus, J., Kim, J., Hammond, P., and Char, K. (2007). Development of surface morphology in multilayered films prepared by layer-by-layer deposition using poly(acrylic acid) and hydrophobically modified poly(ethylene oxide). *Macromolecules*, 40: 4028-4036.
- [26] Yuan, J., Xing, W., Gu, G., and Wu, L. The properties of organic pigment encapsulated with nano-silica via layer-by-layer assembly technique. *Dyes and Pigments*, 76: 463-469.
- [27] Yılmaztürk, S., Deligöz, H., Yılmazoğlu, M., Damyan, H., Öksüzömer, F., Naci Koç, S., Durmuş, A., and Gürkaynak, A. (2009). A novel approach for highly proton conductive electrolyte membranes with improved methanol barrier properties: Layer-by-Layer assembly of salt containing polyelectrolytes. *Journal of Membrane Science*, 343: 137-146.
- [28] Wang, Y., Wang, X., Guo, Y., Cui, Z., Lin, Q., Yu, W., Liu, L., Xu, L., Zhang, D., and Yang, B. (2004). Electric-field-induced layer-by-layer fabrication of second-order nonlinear optical films with high thermal stability. *Langmuir*, 20: 8952-8954.
- [29] Caruso, F., Lichtenfeld, H., Donath, E., and Möhwald, H. (1999). Investigation of electrostatic interactions in polyelectrolyte multilayer films: Binding of anionic fluorescent probes to layers assembled onto colloids. *Macromolecules*, 32: 2317-2328.
- [30] Kretschmer, A. (1989). Interesting Facts on Physical Fundamentals of Textile Finishing Process. *Wissenwertes von der Physik der Textilveredlung* 10 p.1098
- [31] Hyde, K., Russa, M., and Hinstroza, J. (2005). Layer-by-layer deposition of polyelectrolyte nanolayers on natural fibers: Cotton. *Nanotechnology*, 16: S422-S428.
- [32] Hyde, G., and Hinstroza, G. (2007). Electrostatic self-assembled nanolayer films for cotton fibers, In: Brown, P; Stevens, K. (ed) Nanofibers and nanotechnology in textiles, Woodhead Publishing Limited, Cambridge, England, ISBN-13: 978 1 84569 105 9.
- [33] Beknen, R., and Buschmann, H.J. (2010). Schollmeyer, E. Coating textile materials with polyelectrolytes: *Melliand Textilberichte*, 91: 43-45.
- [34] Wang, Q., and Hauser, P. (2009). New characterization of layer-by-layer self-assembly deposition of polyelectrolytes on cotton fabric. *Cellulose*, 16: 1123-1131.
- [35] Połowiński, S. (2005). Polyelectrolyte layer-by-layer processed coated textiles. *Fibres and Textiles in Eastern Europe*, 13: 50-52.
- [36] Dubas, S., Limsavarn, L., Iamsamai, C., and Potiyaray, P. (2006). Assembly of polyelectrolyte multilayers on nylon fibers. *Journal of Applied Polymer Science*, 101: 3286-3290.
- [37] Dubas, S., Chutchawalkulchai, E., Egkasit, S., Iamsamai, C., Potiyaray, P. (2007). Deposition of polyelectrolyte multilayers to improve the color fastness of silk. *Textile Research Journal*, 77: 427-441.
- [38] Połowiński, S. (2007). Deposition of polymer complex layers onto nonwoven textiles *Journal of Applied Polymer Science*, 103: 1700-1705.
- [39] Brzeziński, S., Kowalczyk, D., and Połowiński, S. (2009). Deposition of polymer complex nano-layers onto polyester fabrics activated with corona discharges. *Fibres and Textiles in Eastern Europe*, 17: 87-90.
- [40] Lin, Z., Renneckar, S., and Hindman, D. (2008). Nanocomposite-based lignocellulosic fibers 1. Thermal stability of modified fibers with clay-polyelectrolyte multilayers. *Cellulose*, 15: 333-346.

-
- [41] Dubas, S., Kumlangdudsana, P., and Potiyaraj, P. (2006). Layer-by-layer deposition of antimicrobial silver nanoparticles on textile fibers. *Colloids and Surfaces A: Physicochemical and Engineering Aspects*, 289: 105-109.
 - [42] Połowiński, S., and Jantas, R. (2008). Antibacterial and catalytic properties of textiles with modified surfaces. *Fibres and Textiles in Eastern Europe*, 16: 104-107.
 - [43] Stawski, D., and Bellmann, C. (2009). Electrokinetic properties of polypropylene textile fabrics containing deposited layers of polyelectrolytes. *Colloids and Surfaces A: Physicochemical and Engineering Aspects*, 345: 191-194.
 - [44] Stawski, D., Halacheva, S., Bellmann, C., Simon, F., Połowiński, S., and Price, G. (2011). Deposition of poly(ethylene imine)/poly(2-ethyl-2-oxazoline) based comb-branched polymers onto polypropylene nonwoven using the layer-by-layer technique. Selected properties of the modified materials. *Journal of Adhesion Science and Technology*, 25: 1481-1495.
 - [45] Stawski, D., Połowiński, S., Herczyńska, L., Sarna, E., and Rabiej, S. (2011). *Journal of Applied Polymer Science*, accepted DOI 10.1002/app.34616
 - [46] Kim, H.J., Lee, K., Kumar, S., and Kim, J. (2005). Dynamic sequential layer-by-layer deposition method for fast and region-selective multilayer thin film fabrication. *Langmuir*, 16: S422-S428.
 - [47] Porcel, C.H., Izquierdo, A., Ball, V., Decher, G., Vögel, G., and Schaaf, P. (2005). Ultrathin coatings and (poly(glutamic acid)/polyallylamine) films deposited by continuous and simultaneous spraying. *Langmuir*, 21, 800-802.

Chapter 17

CHALLENGES IN THE PRESERVATION OF CONTEMPORARY COUTURE – CONSOLIDATION AND PROTECTION OF TEXTILES WITH SOL-GEL SILICA COATINGS

***Marta Vieira^a, Márcia G. Ventura^b, Rita Macedo^{a,c},
Micaela M. Sousa^{a,b,*}, A. Jorge Parola^b and B. Coutinho^d***

^aDepartamento de Conservação e Restauro, Faculdade de Ciências e
Tecnologia, Universidade Nova de Lisboa,
2829-516 Monte da Caparica, Portugal.

^bREQUIMTE, Departamento de Química,
Faculdade de Ciências e Tecnologia,
Universidade Nova de Lisboa, Monte de Caparica, 2829-516, Portugal.

^cInstituto de História da Arte, Faculdade de Ciências Sociais e Humanas,
Universidade Nova de Lisboa, Av. De Berna, 26 C, 1069-061, Lisboa, Portugal.

^dMUDE, Museu da Moda e do Design,
Rua Augusta 24, 1100-053 Lisboa, Portugal.

ABSTRACT

Several haute couture contemporary textiles from museum collections exhibit serious conservation problems due to the high complexity of materials and production methods used in their conception. Conservation of contemporary textiles with new materials and production methods requires scientific research into the identification of materials and new conservation techniques. This was the case of the spectacular golden coat made by the French fashion designer Jean-Paul Gaultier, currently in MUDE (Museum of Fashion and Design), in Lisbon. The coat is an excellent example of Gaultier's eclectic selection of materials and technical versatility. It was created with a golden combined textile, with several attached golden polymeric and glass materials. Despite the importance of this piece, little information was available in the archives of MaisonGaultier. In order to

* E-mail: mmfs@fct.unl.pt

understand the creative processes and identify the coat's materials that could provide important information for the stabilization and treatment of the piece, an interdisciplinary research was carried out.

Characterization of the coat's materials with several analytical techniques revealed that the golden combined textile was apoly(ethylene terephthalate) canvas covered with apoly(dimethylsiloxane) (PDMS) layer and a yellow brass pigment hand-stitched to a yellow silk lining. The golden coat exhibits several pathologies, namely oxidation of the brass pigment and a significant deterioration of the PDMS layer due to humidity action. Indeed, the cohesion and adhesion properties of the PDMS layer are fragile inducing considerable material loss of the attached materials. The consolidation of the PDMS layer as well as its protection from a humidity environment was considered fundamental to stabilize the degradation of the golden coat.

With a similar PDMS chemical nature, sol-gel silica was considered a potential candidate for a coating application in order to enhance the PDMS properties. Silica sols were prepared by the sol-gel method with tetraetoxysilane using ethanol, water and an acid and/or a base as catalyzers. Different additives were used to improve the PDMS properties such as hydrofobicity, flexibility and adherence. The films containing SiO_2 were applied to test samples. Homogeneous thin films with few micro-cracks were obtained using spin coating and vapor-spraying on the film deposition. Moreover, minimal differences in pH and color were observed. The contact angle value improved slightly, indicating that the films exert in some extent a protection against the humidity. Further work is necessary to optimize the silica sol-gels process at room temperature and ensure that the film application will not change other coat properties.

2. INTRODUCTION

Currently, the conservation issues raised by contemporary haute couture from museum collections are quite challenging. Creators are eager to experiment with new materials and technologies in order to give form to their ideas. Their main interest is the expressive potential of these materials which are used to create ephemeral models to be shown in catwalks and not exactly to join a museum collection. Thus, despite their relatively young age, sometimes less than thirty years, these haute couture models, like what happens to other contemporary works of art, usually reveal substantial conservation problems. Many modern materials are quite unstable and will rapidly deteriorate [1]. On the other hand, the usual conservation materials and techniques that are used on traditional works of art are often inappropriate for contemporary haute couture. Therefore, in order to preserve these pieces along to future generations, it is essential to design a methodology in which art-historical and technical research can provide the information to develop a conservation project. When working with an object of a living artist, the research method should have specific features. First, it is crucial to identify and characterize the creative process that was in the origin of the work. A survey of the published material, including historical sources, criticism and interviews should be the first step. Departing from that, it is possible to identify technical training, main influences of the artist and general creative processes behind his/her oeuvre. This information also constitutes a starting point to develop a script to interview the artist as well as other persons involved in the materialization of the work, namely assistants, curators or other collaborators. This detailed art-historical and technical study should be accompanied by research into the materials, using analytical techniques. It is important to understand the

materials used in works of art and the way in which these materials react with one another, with environmental conditions, and with conservation treatment in order to understand as comprehensively as possible the factors that govern their behavior and stability, and those that could contribute to their deterioration[1].

After this thorough study, it is possible to design an adequate plan for preserving haute couture from museum's collections to next generations. This is an extremely complex task that requires expertise and experience in a wide range of disciplines, bringing together curators, art historians, conservators, designers, conservation scientists, chemists, etc.

The Design and Fashion Museum of Lisbon (MUDE, Portugal) holds a collection (Francisco Capelo collection) with more than 1,000 design and 1,200 fashion pieces, mostly haute couture. The collection portrays the history of design and fashion from 1930s until today, being one of the most important collections in Portugal and in the international scene from this period. This renowned collection range from furniture to small everyday objects, both unique and mass-produced. They reflect the 20th century's major design trends and movements, revealing the look of each decade. MUDE's collection is also a reflection of social developments, cultural transformations and outlooks in which the transformations in cutting techniques, research in new fabrics and materials, stylistic trends and the revolution of the silhouette may be observed. Most of the objects combine styles and materials, including handicrafts, luxury and minimalism, high-tech and recycling. In the fashion collection, it is noticeable the breakdown of the traditional barriers between ready-to-wear clothes, street clothes and haute couture as new stylists and design studios use elements from all these categories.

From this collection, a spectacular couture golden coat made by the French fashion designer Jean-Paul Gaultier, with several unstable pathologies, was selected to perform a detailed study and a conservation project. Jean Paul Gaultier (b. 1952) has been at the forefront of fashion for over twenty years. He is now considered one of the most significant designers of our time. Famous for having brought high fashion to the masses and street style to the catwalk, Jean Paul Gaultier has an unrivalled ability to create a harmonious balance between the radical and the traditional. Gaultier never received formal training as a designer but he worked in important couture houses like Pierre Cardin (1970 and 1974-75), Jacques Esterel (1971) and Jean Patou (1972-74) where he acquired skills and technical knowledge. Since his first collection, in 1976, Jean Paul Gaultier's have drawn inspiration from eclectic sources, from French cultural icons to the London street scene. His first Haute Couture is from 1997, the year he opened his own couture house, becoming the second designer in three decades to create couture under his own label [2].

The luxurious kimono style coat selected for this work (MUDE.M.D0040) was an important piece of 99/2000 Autumn/Winter Gaultier's collection (Figure 1). In fact, it was the last piece to be shown in the catwalk right before the wedding dress that usually closes the show. The coat is an excellent example of Gaultier's eclectic selection of materials and technical versatility. It is a large and heavy, $\frac{3}{4}$ length coat ($1.08 \times 0.68 \times 0.02$ m, circa 4 Kg), with kimono sleeves and two pendant flaps. It was created with a golden combined textile, *latex façond'or*, displaying a wide range of textures with several attached golden polymeric and glass materials.



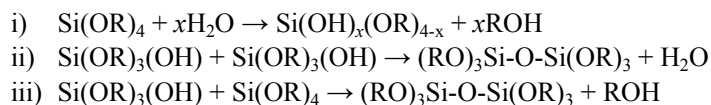
Figure 1. The golden coat of Jean Paul Gaultier's exhibited in the haute couture 99/2000 Autumn/Winter collection (MUDE.M.D0040).

Prior to the Gaultier's coat treatment proposal a detailed art-historical, technical and material research was conducted. Since little information about Gaultier's creative process has been found in literature, the study began with the identification of the museums in Europe and United States which have works of the designer in their collections. The aim was to understand if there were any unpublished studies about his creative processes, techniques and materials. The answer was surprisingly fast but unfortunately it was not possible to identify any thorough research about Gaultier's couture. The second step was the design of two questionnaires to be answered respectively by the archives of MaisonGaultier and by Jean Paul Gaultier himself. However, despite the importance of this piece, little information was available in the archives of MaisonGaultier and some of the persons involved in Kimono's creation process were no longer working at the atelier. MaisonGaultier could only describe the piece as a taffeta for the lining and latex with gold leaf for the external layer. Also, they had the information that the golden external layer was made by an outsourcing provider demanded at the request of the designer.

In order to confirm the information, understand the creative processes and identify the coat's materials that could provide important information for the stabilization and treatment of the piece, analysis with several techniques as micro Fourier transform infrared spectroscopy (μ -FTIR), micro energy dispersive X-ray fluorescence (μ -EDXRF), inductively coupled plasma with atomic emission spectrometry (ICP-AES), scanning electron microscopy-energy dispersive spectroscopy (SEM-EDS), high-performance liquid chromatography with diode array detector coupled to mass spectrometry (HPLC-DAD/MS), X-radiography, colorimetry and optical microscopy were performed. As the main unstable pathologies were identified in a polydimethylsiloxane (PDMS) golden layer of the Gaultier's coat, a treatment based on silica-gel coatings was considered.

Silica sol-gel coatings are produced through the sol-gel technique which is based on the hydrolysis of liquid precursors and formation of colloidal sols, which after condensation produce stable gels [3].

In this case silica alkoxides are used as precursors which in the presence of water molecules undergo hydrolysis (i) and then condensation (ii and iii):



These processes lead to the formation of a polymeric network of silica oxides yielding a wet gel. Films obtained by this method are associated to good mechanical stability and have good optical characteristics (transparency). Silica sol-gel coatings or silica-based modified coatings have been applied in several fields, among which the cultural heritage (μ) is included. The applications are diverse and involve materials such as glass, stone, wood, textiles and paper [4].

The modified silica coatings with organo-functional groups are considered of special interest since they own properties between those of the polymers and glasses [5]. Silica coatings can thus represent an option for maintenance or conservation purposes on works of art. In glass conservation, silica sol-gel coatings were used as an alternative to the silicon resins coatings, which tend to accumulate pollution, and revealed to have a good adhesion to the substrate contributing to the slowing down of the weathering phenomenon [6]. On the textiles field, sol-gel coatings are mainly used to functionalize tissues in order to improve their performance and to achieve new material properties. Examples of new materials that are being developed on this field are the textiles with water repellency [7-14] and with antimicrobial properties [12]. In textiles conservation, the traditional methods are still preferred to alternative methods but there are some studies in which polymeric materials such as acrylic products have been studied and applied for the effect [4]. On the present work, the consolidation of the PDMS layer as well as its protection from a humidity environment was considered fundamental to stabilize the degradation of the Gaultier's golden coat. Traditional textile consolidation treatments involving hand-stitch, water based adhesives, etc.[15] should not be applied to the golden coat due to the incompatibility with the PDMS layer. With a similar chemical nature and an affinity for the OH groups of the PDMS, silica sol-gel was considered a potential candidate for a coating application in order to increase the PDMS cohesion and adhesion, as well as prevent the coat from degradation due to the action of humidity.

The water repellency in textiles can be achieved by using modified silica sols. The modification is usually done through the introduction on the sol-gel system of fluorinated silanes or organo-alkoxysilanes for the enrichment at the coating surface on alkyl- or perfluoralkyl- functional groups, which promote the water repellency [8,12,14]. In this work, a non-modified water repellent silica sol-gel was obtained with a two-step catalysis which also allows the formation of large pores in the network, and hence, a higher textile flexibility[16]. Organo-alkoxysilane additives such as octyltriethoxysilane (OTEOS), 3-glycidoxypropyltrimetoxysilane (GPTS) were added to the sol-gel system in order to improve the hydrophobicity and porosity of the film [15]. Furthermore, the high polymeric character of these coatings could lead to an improvement on the mechanical affinity for the coat's

PDMS surface. A second approach to the sol-gel production was studied by preparing a sol-gel solution containing *n*-octylamine, a surfactant agent used as a porosity template [17,18]. The main purpose of this surfactant is to improve the flexibility of the coating and avoid the film cracking. Another different methodology developed in this work, was the application of silicone nanofilaments obtained from trichloromethylsilane to create super-hydrophobic coatings [7].

In order to assess the final quality of the coatings, as well as their feasibility and application in the golden coat, different methods of applying the sol-gel solutions and drying temperature of film (curing temperature) were investigated.

3. EXPERIMENTAL SECTION

3.1. Materials Identification

3.1.1. Samples

Analyses *in situ* and in micro samples of the golden coat were performed. The micro samples were preferably taken in several detached elements from the golden coat or non-visible areas under Leica KL 1500 LCD microscope, equipped with a 12x objective and a Leica Degilux 1 digital camera.

Circa 30 micro samples from the PDMS and three micro samples from the plain-weave support of the PDMS coating were collected for FT-IR analysis; three samples from the PDMS layer and the lining textile with circa 0.5-1mg were taken for ICP-AES analysis and two yellow fiber samples from the lining, with circa 0.2 mg each, were selected for dye analysis with HPLC-DAD/MS.

3.1.2. Instrumentation and Methods

A detailed characterization of the materials present in the Gaultier's golden coat using different analytical techniques was performed.

FTIR with a Nicolet Nexus spectrophotometer interfaced and a Continuum microscope was used to identify the organic materials of the golden coat. Spectra were obtained in transmission mode, using a diamond compression cell as described in [19]. Circa sixty *in situ* analyses of the coat and in some decorative elements were also performed using attenuated total reflectance [19] and μ -EDXRF. Mordant and metallic ions analyses were performed with a Horiba Jobin-Yvon Ultima ICP-AES [20] and using μ -EDXRF with an ArtTAX spectrometer of Intax GmbH, with a molybdenum (Mo) anode, Xflash detector refrigerated by the Peltier effect (Sidrift), with a mobile arm [19]. The experimental parameters used were: 40 kV of voltage, 300 μ A of intensity, for 200 s. Circa 20 areas of the golden coat were submitted to color coordinate measurements (CIELAB system), with three measurements in each area, using a portable Datacolor international spectrophotometer with D65 illuminant and 10° of observation angle, as described in [20]. The yellow synthetic dye present in the lining of the golden coat was extracted with the oxalic soft extraction method (oxalic acid (0.2M): acetone: water: methanol, 0.1:3:3:4, (v/v)) as reported in [21], prior to HPLC-DAD analysis. Dye characterization was performed with a Thermofinnigan Surveyor HPLC-DAD system, using a RP-18 Nucleosil 5 μ m particle size column (250 \times 4.6 mm), with a solvent gradient of

methanol and 0.3% aqueous perchloric acid (v/v), as described in [21]. A high resolution, *ArtXRay* X-ray digital system with the following conditions: maximum angle $4^\circ \times 80^\circ$, focus point 1.9 mm, X-Ray voltage of 40-160kV, X-Ray current 0.2-5.0 mA and maximum power of 480 W, was used to provide further information about the condition and construction of the Gaultier's coat.

3.2.Silica Sol Gels Tests

Replicas of the golden coat were performed to evaluate the effect of sol gels on PDMS layer. Plain-weave square polyester textiles of 3×3 cm were covered with the adhesive PDMS (Dow Corning, USA) containing the golden glitter. The coating texture was simulated through the creation of smooth and texturized areas with a small spatula as it is shown on Figure 2.

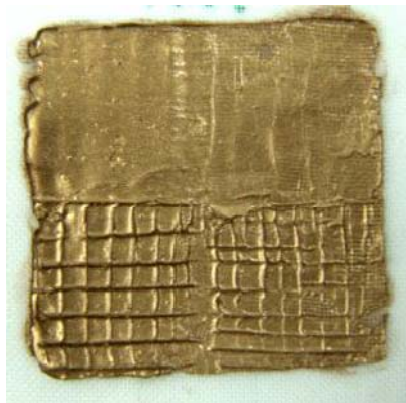


Figure 2. Plain-weave textile with the golden PDMS coating reproducing the golden coat before sol-gel film application.

3.2.1. Sol-Gel Silica Sols

Four different silica sols were prepared and applied as a coating to the golden PDMS replica samples. The preparation of the four sols was performed through the hydrolysis of alkoxysilanes in ethanol and water. The Sol I was prepared according to a two-step hydrolysis of tetraethoxysilane (TEOS) using acidic and basic catalysis as described in [22]; Sol II was prepared with TEOS and modified with octyltriethoxysilane (OTEOS) according to [14]; Sol III followed the same procedure of Sol II but using as modifier glycidoxypropyltrimethoxysilane (GPTS) [12, 23] and, Sol IV was prepared according to the procedure described in [15], through the addition of the surfactant *n*-octylamine.

An additional procedure using chemical vapor deposition (CVD) of trichloromethylsilane (TCMS) was also tested [6].

3.2.2. Application

The solutions were applied directly on the golden PDMS sample surface through the dip-coating, spin-coating or vapor-spraying methods. The dip-coating was performed by

immersing the sample in the silica sol solution for one minute, followed by the air drying of the sample. After the first immersion, three and five immersions were applied following the same procedure. The spin-coating was performed through the equipment Spincoat G3P-8 using 2000 rpm during one min according to [24]. On the vapor-spraying an ultrasonic humidifier PficoHealth was used to produce vapor of the silica sol. The spray tube was placed close to the sample surface at 5 mm of distance. The spraying time was of 2 min but 5, 10 and 20 min were also tested in order to check the effectiveness of film formation.

3.2.3. Thermal Treatment

Samples were thermal treated (cured) for two minutes at 100°C as described in literature [9,14]. A prior thermal treatment conducted at low temperatures to dry the sample [9,14] was not considered necessary as the surface of the silica sol dries very quickly. Nevertheless a thermal treatment test was also performed at 40°C for two minutes in order to obtain a less aggressive treatment.

3.2.4. Instrumentation and Methods

In order to assess the physical properties of the PDMS coating before and after the application of the sol gels, the contact angle, the pH and the color were measured on golden PDMS replica samples. The measurements were performed on the sample surface before silica sol application and after curing the silica film. The contact angle was measured on fifteen golden PDMS replicas using a Contact Angle Meter CAM100 using deionized water drop of 5 μ L. Three measurements were performed 0.5 min after the water drop has been deposited on the surface. The color coordinate measurements (CIELAB system) were performed as described previously. The pH measurements were performed on a Crimson pH meter Basic 2.0 at 20°C.

Samples were analyzed by optical microscopy (Zeiss Axioplan Z HAL100) and scanning electronic microscopy (SEM) with a Hitachi SU-70 microscope operating at 15kV and a 34 μ A. Samples for SEM analysis were introduced on the sample handler and coated with a thin layer of a gold-paladium alloy (SEM Polaron E5000).

4. RESULTS AND DISCUSSION

4.1. The Gaultier's Coat: A Jumble of Materials and Conservation Pathologies

The golden ($L^*=41.3\pm0.3$; $a^*=2.6\pm0.1$; $b^*=26.6\pm0.4$) coat with a geometrical structure, Figure 3, is composed by several layers as depicted in Figure 4.

All these layers and decorative elements are composed by diverse materials. The decorative motifs (sequins, tube beads, etc.), dispersed randomly in the PDMS layer are composed by different polymeric materials as the poly(ethylene-co-vinyl acetate) with a polyamide resin, poly(vinyl chloride) with phthalate additives or even other materials as glass, Table 1. The μ -FTIR spectra of the golden sequins exhibited the characteristic peaks of poly(ethylene-co-vinyl acetate) as the carbonyl group stretching 1736 cm^{-1} peak and the C-O-CO asymmetrical stretching 1254 cm^{-1} peak. Also significant were the C-H stretching

vibrations between 3000 and 2800 cm^{-1} . In the tube beads it were detected with μ -EDXRF analysis, elements from a glass composition as Si, Ca, K, Fe and other related compounds. The X-radiography confirmed also the presence of heavy elements as lead in the tube beads. Finally, in the golden appliques, it was possible to observe in the μ -FTIR spectra, the characteristic peaks of poly(vinyl chloride) as the bands at 1288 , 966 and 698 cm^{-1} from C-Cl groups.

All these decorative elements were attached to the PDMS coating perhaps before the silicon curing process as no evidence of glue medium was found.



Figure 3. Front-view of the golden coat, where it is possible to observe the external golden PDMS layer and several decorative elements.

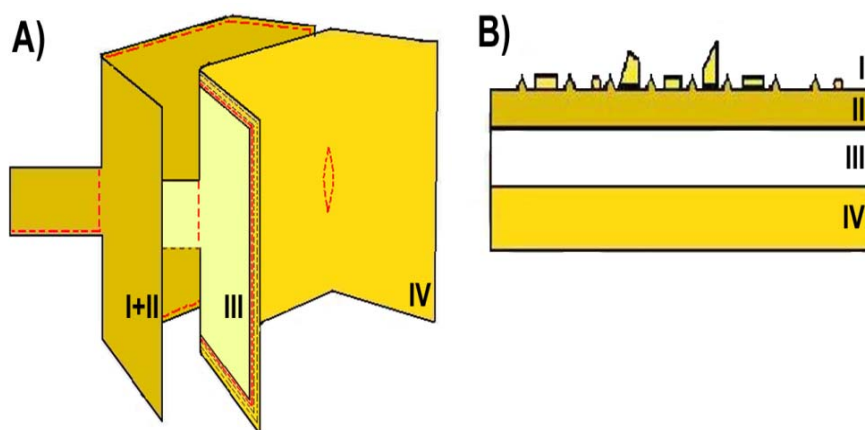
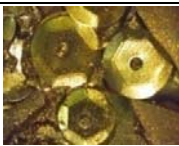
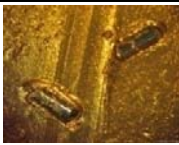


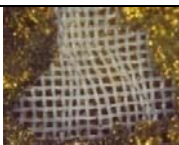
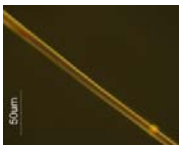
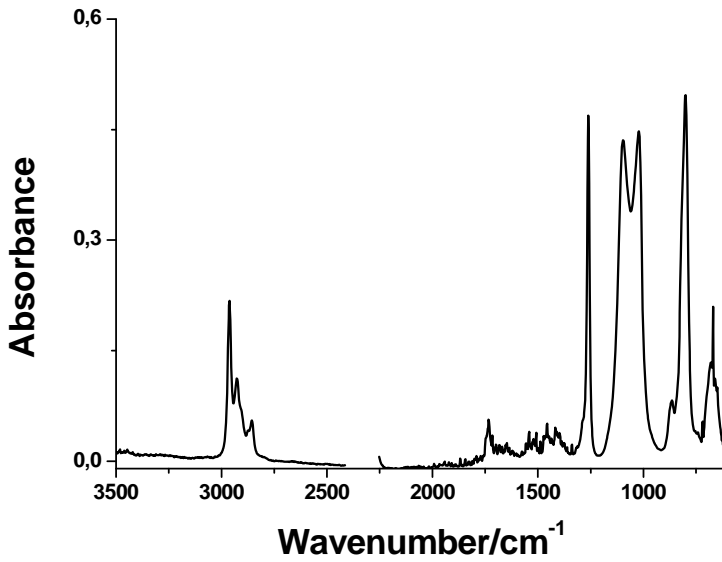


Figure 4. (A) Structure of the golden coat with different layers: I) Decorative elements, II) golden PDMS layer; III) canvas support of the PDMS layer; IV) golden lining. (B) General stratigraphy of the golden coat with the layers previously mentioned.

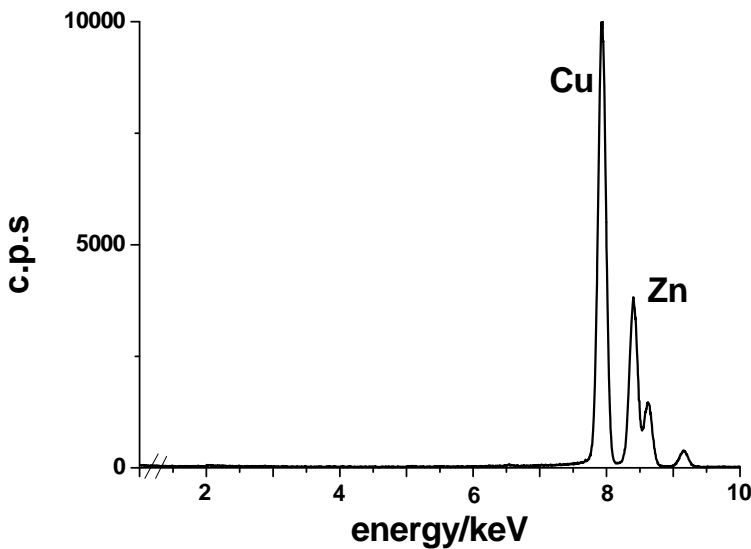
Table 1. Material results of the golden coat layers obtained with μ -FTIR, μ -EDXRF and HPLC-DAD/MS

Element/layer	Image	Materials
Decorative elements		
Golden sequins (Amplification 12x)		Poly(ethylene-co-vinyl acetate) with a polyamide resin
Blue tube beads (Amplification 10x)		Glass
Golden appliques (Amplification 7x)		Poly(vinyl chloride) with phthalate additives
Layer II -Golden PDMS coating		
(Amplification 25x)		Poly(dimethylsiloxane) with a golden brass pigment
Layer III –Canvas support of the PDMS coating		
(Amplification 25x)		Poly(ethylene terephthalate)
Layer IV - Lining		
(Amplification 500x)		Silk dyed with a yellow synthetic dye

The golden PDMS layer is a polydimethylsiloxane elastomer, with a golden brass pigment finely dispersed in the PDMS coating. As can be seen in Figure 5A the characteristic peaks of Si–O–Si in the μ -FTIR spectra from the golden PDMS coating are observed at 1094 cm^{-1} and at 1024 cm^{-1} . At 802 cm^{-1} , a strong absorption is observed. This could be assigned to Si–C stretching. The presence of polysiloxanes can also be assigned to the following O–Si–CH₃ group vibrations: the Si–CH₃ symmetrical bending at 1261 cm^{-1} , the C–H asymmetrical stretching at 2964 cm^{-1} and the weak C–H symmetrical stretching which appears at 2949 cm^{-1} [25,26]. In the X-ray fluorescence spectra, Figure 5B, the peaks of copper and zinc were detected with circa 74 and 26% respectively, indicating the presence of a brass pigment [27].



a



b

Figure 5. (A) μ -FTIR spectra of the golden PDMS coating, displaying a clear fingerprint of the polydimethylsiloxane elastomer. (B) X-ray fluorescence spectra of the golden PDMS coating.

The golden PDMS coating with the brass pigment was probably hand-applied to a support layer as the thickness of the silicon is very irregular. The support layer is a polyethylene terephthalate plain-weave canvas, as the FTIR spectra of this material exhibited the strong C=O stretching peak at 1726 cm^{-1} , C-O-CO asymmetrical stretching at 1255 cm^{-1} and symmetrical stretching at 1018 cm^{-1} . Also, the aromatic ring of PET can be assigned to 1581 , 1456 , and 1120 cm^{-1} peaks [25, 26].

The canvas support with the PDMS coating was stitched to a golden silk lining. The FTIR fingerprint for the silk protein was obtained, displaying the characteristic polyamide absorption pattern, namely the amide I (CO stretching, 1653 cm^{-1}), amide II (CN stretching and NH bending, 1550 cm^{-1}) and CN bending at 1450 cm^{-1} , as well as the OH and NH stretching at $3400\text{--}3000\text{ cm}^{-1}$ [28]. These results were also confirmed by the smooth longitudinal view of the lining fiber observed in optical microscopy, (see figure of the lining layer in Table 1). The silk was dyed with a synthetic yellow dye with a retention time of 28.8 min and a UV-visible spectrum maximum of 434 nm. The negative ESI mass spectrum for the principal yellow chromophore yielded a deprotonated ion $[M-H]^-$ at m/z 693.

The golden coat exhibits several serious pathologies, namely oxidation of the brass pigment and a loss of cohesion and adhesion of the PDMS layer. The deterioration of the PDMS coating is promoting the detachment of the decorative elements and a significant silicone loss material. Indeed, during the handling of the coat, several elements were detached. It is known that silicone rubbers are susceptible to hydrolytic degradation in high moisture conditions inducing the weakening and adhesion loss of the silicone matrix [29]. The presence of the brass pigment also might contribute further for PDMS layer deterioration, as metallic fillers on polymers usually induces their ageing, acting as degradation catalysts [30]. It was confirmed the migration of silicon based compounds [31] and the brass pigment to the golden lining with ICP-AES and FTIR analysis. Cu and Zn were detected in stained darker areas of the lining in considerable amounts (Cu = $1.89 \pm 0.05\text{ mg/g}$ silk, Zn = $0.99 \pm 0.02\text{ mg/g}$ silk). This migration of the silicon matrix to internal layers and the oxidation of the brass pigment are contributing simultaneously to the color change of the PDMS coating and silk lining, Table 2.

Table 2. Colorimetric measurements in deteriorated and non-deteriorated areas of the golden silk lining

Golden Lining (area)	L*	a*	b*	Observations
Non-deteriorated	60.3 ± 0.1	4.6 ± 0.4	44.1 ± 0.2	The luminosity (L*) of the sample and the yellow component (b*) has decreased significantly in stained areas.
Deteriorated	46.6 ± 0.2	8.3 ± 0.1	37.8 ± 0.1	

In order to stabilize these pathologies is fundamental to maintain the Gautier's coat in controlled environment conditions ($T = 18 \pm 2^\circ\text{C}$ and relative humidity between 45–55% [32]). It was also considered critical to consolidate the PDMS layer and promote its adhesion properties to stabilize the severe loss material as well as the other pathologies described previously.

It is not possible to maintain the relative humidity below the proposed levels, as the coat is composed by miscellaneous materials. However it could be advantageous for the PDMS coating and the oxidized brass pigment to reduce their contact with humidity. Therefore a consolidation treatment based on water repellent silica sol-gels with strong cohesion and adhesion properties was considered.

4.3. Trying to Regain the Gaultier's Coat Performance: Silica Sol-Gels Tests

4.3.1. Testing the Efficacy

The first step was to ascribe the sol-gels efficacy in obtaining films with good adhesion, cohesion and hydrophobic properties in which concerns the method of application and thermal treatment.

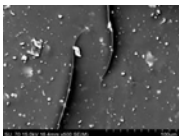
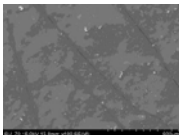
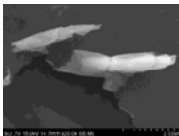
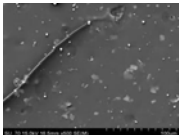
4.3.1.1. Silica Sol-Gel Sols

The different sol-gel solutions were all prepared using TEOS as silica precursor but containing different modifiers in their composition. The first solution contained only TEOS, the second and the third contained the TEOS and modifiers OTEOS and GPTS, respectively and, the fourth solution contained a surfactant (*n*-octylamine). The addition of the compounds OTEOS and GPTS to the sol-gel system is used to confer high water repellency. Furthermore, the existence of non-reactive organo-functional chains in these compounds are responsible for the enlargement of the pores and, thus for the improvement on the flexibility of the film. The addition of the surfactant *n*-octylamine to the sol-gel solution was also used to increase the flexibility of the film. The surfactant promotes a rearrangement of the pores of sol-gel network for a better adjustment to the substrate where it is applied [17].

The water repellency of the sol-gel is significantly influenced by the size of the carbon chain of alkoxysilane present in solution [14]. The introduction of OTEOS, an alkoxysilane with a larger chain than TEOS on the sol-gel solution could lead to an increase of the hydrophobicity of the film. However, this additive did not have a significant effect on this property when compared with the sol-gel without additive, for more details see next sections. The SEM image of the replica coated with this solution (Sol II, Table 3) by spraying application method, shows that the film is quite homogeneous with few micro-cracks, revealing a considerable cohesion and adhesion to the substrate. The addition of GPTS (Sol III, Table 3) to the silica solution also had no effect on the contact angle. From the SEM observation of the replicas applied by spin coating it is visible that the films cover the surface homogeneously. However a significant increase in the adhesion of the film was not observed. The results were similar to the previous one for the solution containing the surfactant *n*-octylamine (Sol IV, Table 3). Apparently, the films with surfactant are relatively homogeneous and adherent as demonstrated by SEM images. However, the increase of flexibility was not as high as expected, since the films still present micro cracks on the surface and grooves.

From the results obtained it may be conclude that it is possible to obtain sol-gels with a good adhesion to the PDMS surface and a reasonable cohesion. The flexibility of the films obtained need to be further improved probably with modifiers that contain larger alkyl chains. Indeed It were not noticed differences on the flexibility of films containing only TEOS (more glass nature) and those containing the modifiers with a polymer nature more close to the one of PDMS. Nevertheless, these properties are related with the method of application as it will be described below.

Table 3. The SEM images for the samples using the spraying method for the application of the silica coating. The temperature of cure was 100°C for all the tests

Silica sol-gel solutions	Micro-photography (SEM)	Observations
Sol I (TEOS)		Thin homogeneous film with superficial micro-fissures.
Sol II (OTEOS)		Homogeneous thin film with micro-cracks.
Sol III (GTPS)		Homogeneous thin film with micro-cracks that led to detachment of the film in some areas.
Sol IV (surfactant)		Homogeneous thin film with superficial micro-fissures.

4.3.1.2. Method of Application


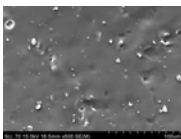

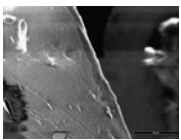

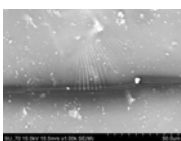


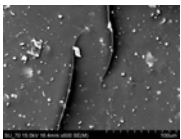
The four different sol-gels solutions mentioned previously were applied through different methods (dip, spin and spraying coating), exhibiting different characteristics when observed by optical microscopy and SEM, Table 4.

Films applied with dip coating were thick, brittle, and not homogeneous, revealing low cohesion and adhesion properties. It was found that the number of layers (one, two, three and five) applied through dip coating, increased the film thickness and affected negatively the adherence to substrate. In fact, the coatings were visibly fragile and less homogeneous on replicas coated with three and five layer films. In these replicas micro-fissures were observed at macroscopic scale. In the replica with only two layers the cracks were not visible at macroscopic scale, however through SEM observation, it was found that there were areas not covered with the sol-gel-film and therefore the film was not homogeneous.

Thinner and relatively homogeneous films almost free from cracks and with a considerable adherence to the substrate were obtained by applying the sol-gel solutions on the replica through spin-coating. In order to obtain a thinner film with higher capacity for impregnation and adherence to the replica surface than using spin-coating method, the spraying method was also tested. Different times of spraying were used. The time of 20 minutes was excessive because the replica surface, after the film deposition, was with a clear and matte appearance. This color alteration was visible at macroscopic scale, as evidenced by a high ΔE_{ab} (Table 6). The films produced with shorter spraying times (10, 5 and 2 min) had a reduced film thickness as detected only by SEM analysis. It was observed that with lower

times of spraying, fairly homogeneous films were formed and detected even at microscopic level. Spraying for 2 minutes was considered the best option, since it has returned good results and for longer times (5, 10, 20 min) the spraying solution is affected by the difficulty of maintaining a continuous stream flow due to the rapid solution solidification.

Table 4. Optical microscopy and SEM images for the replica samples before and after coating with sol-gels using different methods of application. The temperature of cure was 100°C for all the tests

Method of application	Micro-photography		Observations
	Optical Microscopy	SEM	
Before coating			Surface without cracks. White spots are dirt and the gray are pigments embedded in the PDMS
Dipcoating N=2 Sol I (TEOS)			Very thick and brittle film.
Spin coating Sol II (OTEOS), Sol III (GTPS) and Sol IV (surfactant)			Homogeneous thin film with micro-cracks. Stretch marks are visible on the PDMS surface. The film formed with Sol II was heterogeneous and brittle.
Spraying coating (20 min) Sol I (TEOS)		-	Homogeneous but thick film.
Spraying coating (2 min) Sol I (TEOS)			Thin homogeneous film with superficial micro fissures.

Films obtained through both spin coating and spraying methods present some micro-cracks formed during the cutting and handling the sample or by the thermal shock of the SEM electron beam. The presence of these micro-cracks indicates that perhaps the films have a reduced flexibility. In some areas near the cracks, the golden coat has stretched under the sol-gel film. Nevertheless, detachment or flaking of the silica coating was not observed indicating that reasonably good adhesion properties were obtained in the films using spraying methods.

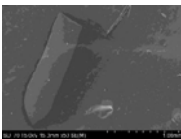
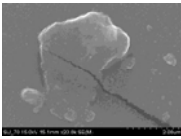
The results obtained, suggest that both application methods, spin-coating and spraying method, can be used for improving the adhesion and cohesion of the PDMS coating from the

Gaultier's coat. The spraying method is the best alternative since can be more easily applicable on a larger scale.

4.3.1.3. Thermal Treatment

A curing temperature of 100°C or above is usually used for textile treatment and functionalization, although some color changes might occur during the process [9,14]. As the curing temperature of 100°C applied in most of the tests in this study might lead to the degradation of other material present in the golden coat, the tests were repeated using the spraying method with a curing temperature of 40°C. From Table 5 it can be observed that the curing temperature does not influence the results of the evaluated parameters. Furthermore, SEM analysis shows that the temperature decrease did not affect the appearance of the films once the surface of the replicates was coated homogeneously. Also the physical behavior of the films cured at 40°C is similar to the films obtained in previous tests. Micro-cracks comparable to films cured at 100°C, were also obtained.

Table 5. The SEM images for the samples using the spraying method for the application of the silica coating. The used temperature of cure was 40°C for both samples

Silica sol-gel solutions	Micro-photography (SEM)	Observations
Sol I (TEOS)		Homogeneous thin film with micro-cracks.
Sol II (OTEOS)		Homogeneous thin film with micro-cracks.

4.3.1.4. Hydrophobicity

The hydrophobic properties were tested through the measurement of the contact angle. The PDMS layer of the golden coat has a high contact angle value ($\theta=112\pm3$). For this reason, it was not expected a great improvement on this value after the application of the silica coating (a material similar to PDMS). Nevertheless, it was observed a slight improvement of the contact angle value after the film deposition in all cases (in most of the cases the improvement is above 2.7% which corresponds to the standard error associated to the contact angle value on sample before the application of the film). This is an indication that the coat is effectively being formed over the replica surface and, that exerts in some extent a protection against the humidity, and thus pigment oxidation.

4.3.1.5. Mechanical Tests

Although mechanical tests were not conducted in order to ascertain the stress-strain behavior of the films obtained; the presence of minimal micro-fissures in several replicas can indicate that the mechanical properties were not severely altered during the treatment.

4.3.2. Testing the Harmfulness

Having tested the efficacy of the silica sol-gels, the next step was to ascribe its harmfulness in which concerns pH and color change, in both stages of film application and thermal treatment.

Minimal differences were found on color as well as on the pH value after the film application and thermal treatment. The values obtained were similar and it was difficult to define one major trend for the different sol-gel solutions and application methods used. A remarkable difference could be observed for the procedure involving the chemical vapor deposition of TCMS. Using this procedure, silicone nanofilaments were expected to be formed onto the surface of the tissue in order to render its surface super-hydrophobic [7]. However, during the hydrolysis of TCMS, the release of hydrochloric acid was responsible for the oxidation of the brass pigment. Despite this phenomenon, it was observed a minimal decrease of the pH replica surface. Nevertheless, the reaction led to a major change on the value of ΔE_{ab} inducing a brownish color in the sample surface.

CONCLUSION

The preservation of haute couture in museum collections is a challenging and complex task that requires a thorough research into the creative processes, art-historical details, materials and technical studies.

The analysis of the golden coats of Jean Paul Gaultier from MUDE with several analytical techniques as μ -FTIR, μ -EDXRF, ICP-AES, HPLC-DAD/MS and X-ray revealed that a complex mixture of polymeric and inorganic materials was used to obtain a luxurious golden effect. Although the coat was created less than thirty years ago, several serious unstable conservation pathologies were observed, being recommended its preservation in controlled environment conditions.

As the main pathologies identified in the coat were the loss of material and color alteration due to the degradation of a PDMS layer with a golden brass pigment, a treatment compatible with this layer to promote its cohesion, adhesion and water repellency was considered.

The results show that solutions produced by the silica sol-gel method can be a promising option for the consolidation of Gaultier's coat. Depending on the application method, the solutions produce homogeneous thin films, with a good adhesion to the surface of the coat material replicas. The films obtained also reveal good cohesion properties. Furthermore they are water repellent improving the coat's protection against moisture. Spraying the solutions resulted in very thin films, not visible under optical microscopy and containing only a few micro-cracks. The spraying method is very practical and could easily produce homogeneous sol-gel films over the surface of the coat. The use of curing temperatures around 100°C did not influence physical and optical properties of the coat, but once the cure has proved to be efficient at a lower temperature (40°C), the use of the latter would be preferable. After the application of the film significant changes were not observed on color and on pH of the samples. Although the films applied in coat's replicas, increased their adhesion, cohesion and water repellency properties without noticeable adverse effects, further tests are needed to ascertain the stability of the produced films and determine

if they can cause long term adverse consequences for the various elements present in the coat. It will be necessary to perform aging and resistance tests to ensure that the application of the protective film to the golden coat will not be detrimental to the work.

Table 6. Results obtained for the measurements of pH, color and contact angle. Values are given in % and reflect the difference before and after the application of the sol-gel film in the coated replica. Results are presented for the different prepared solutions and for two different temperatures

			pH	ΔpH (%)	ΔE_{ab}	$\Delta\Delta E_{ab}$ (%)	θ	$\Delta\theta$ (%)
Before application			6.7 ± 0.6	-	67.8 ± 0.2	-	112 ± 3	-
T=100°C	Dip coating (n appl.)							
	Sol I	1	6.9	2.2	68.8	1.5	-	-
		3	5.7	-15.1	73.3	8.2	-	-
		5	5.9	-12.6	72.9	7.5	-	-
		Spin coating (1 min)	6.7	-0.2	74.4	9.7	123	9.9
		Spraying (20min)	6.5	-3.9	73.8	8.9	112	0.2
		Spraying (10min)	7.3	8.4	69.8	3.1	121	7.8
		Spraying (5min)	6.8	0.7	69.5	2.6	124	10.1
		Spraying (2min)	7.0	4.4	69.1	1.9	128	14.4
	Sol II	Spraying (2min)	7.5	11.7	68.4	0.9	116	3.2
	Sol III	Spin coating (1 min)	7.4	9.9	71.0	4.9	121	7.4
		Spraying (2min)	7.4	10.5	69.0	1.9	115	2.3
	Sol IV	Spin coating (1 min)	7.4	9.6	69.0	1.8	121	7.6
		Spraying (2min)	7.4	9.5	69.0	1.8	117	4.5
	TCMS	CVD	5.7	-16.0	90.4	33.4	-	-
T=40°C	Sol I	Spraying (2min)	7.5	10.8	68.1	0.5	119	5.7
	Sol II	Spraying (2min)	7.5	11.7	68.4	0.9	116	3.5
	Sol III	Spraying (2min)	7.5	11.1	68.9	1.6	121	7.5

ACKNOWLEDGEMENTS

We would like to thank to Paula Cruz (Museum Conservation Institute, Portugal) and Pedro Teotónio (MUDE, Portugal) for the support in the condition coat report. We also thank Francisco Capelo (the collector, Portugal), Anne Marie and Milène Lajoix (Maison Gaultier, France) Mário Matos Ribeiro (designer, Portugal), Nicolas Giunta (Institut Mode Méditerranée, France) Kaye Spilker (LACMA, USA), for all the information related with the Gaultier's coat. We gratefully acknowledge Joaquim Vieira, Augusto Lopes, Ana Silva (Universidade de Aveiro, Portugal) and Nuno Leal (Universidade Nova de Lisboa, Portugal) for the SEM analysis.

REFERENCES

- [1] Hummelen, I., and Sillé, D. (Eds.) (2005). The project conservation of modern art. In: *Modern art: Who cares?* London: Archetype, p.14 -19.
- [2] McDowell, C. (2000). Polishing up the Polymath. In: *Jean Paul Gaultier*. London: Cassel Paperbacks, p.105-140.
- [3] Brinker, C.J., and Scherer, G.W. (1990). *Sol-gel science: the physics and chemistry of sol-gel processing*. Boston: Academic Press, p.1-18.
- [4] Princi, E., Vicini, S., Pedemonte, E., Arrighi, V., and McEwen, I. (2005). New polymeric materials for paper and textile conservation. I. Synthesis and characterization of acrylic copolymers. *Journal of applied polymer science*, 98: 1157-1164.
- [5] Pagliaro, M., Ciriminna, R., and Palmisano, G. (2009). Silica-based hybrid coatings. *Journal of materials chemistry*, 19: 3116-3126.
- [6] Dal Bianco, B., and Bertonecello, R. (2008). Sol-gel silica coatings for the protection of cultural heritage glass. *Nuclear instruments and methods in physics research B*, 266: 2358-2362.
- [7] Artus, G.R.J., Jung, S., Zimmermann, J., Gautschi, H.P., Marquardt, K., and Seeger, S. (2006). Silicone nanofilaments and their application as super hydrophobic coatings. *Advanced materials, Wiley-VCH Verlag GmbH and Co. KGaA*, 18: 2758-2762.
- [8] Mahltig, Bottcher, H. (2003). Modified silica sol coatings for water-repellent textiles. *Journal of sol-gel science and technology*, 27: 43-52.
- [9] Mahltig, B., Haufe, H., and Bottcher, H. (2005). Functionalisation of textiles by inorganic sol-gel coatings. *Journal of materials chemistry*, 15: 4385-4398.
- [10] Mahltig, B., Audenaert, F., and Bottcher, H. (2005). Hydrofobic silica sol coatings on textiles – the influence of solvent and sol concentration. *Journal of sol-gel science and technology*, 34: 103-109.
- [11] Textor, T., and Mahltig, B. (2010). A sol-gel based surface treatment for preparation of water repellent antistatic textiles. *Applied surface science*, 256: 1668-1674.
- [12] Mahltig, B., and Fisher, A. (2010). Inorganic/Organic polymer coatings for textiles to realize water repellent and antimicrobial properties – A study with respect to textile comfort. *Journal of polymer science: Part B: Polymer Physics*, 48: 1562-1568.
- [13] Messaoud, M., Houmard, M., Briche, S., Roussel, F., and Langlet, M. (2010) Hydrophobic functionalization of cotton-based textile fabrics through a non-fluorinated sol-gel route. *Journal of sol-gel science and technology*, 55: 243-254.
- [14] Wang, C., Li, M., Jiang, G., Fang, K., and Tian, A. (2007). Surface modification with silicon sol on cotton fabrics for water-repellent finishing. *Research journal of textile and apparel*, 11: 27-34.
- [15] Timar-Balazsy, A., and Eastop, D. (1998). Adhesives and consolidants. In: *Chemical principles of textile conservation*. Oxford: Butterworth – Heinemann, p. 304 – 324.
- [16] Mackenzie, J.D., Huang, Q., and Iwamoto, T. (1996). Mechanical properties of ormosils. *Journal of Sol-Gel Science and technology*, 7: 151-161.
- [17] Mosquera, M.J., Santos, D.M., Montes, M., and Valdez-Castro, L. (2008). New nanomaterials for consolidating. *Langmuir*, 24: 2772-2778.
- [18] Beck, J.S., Rartuli, J.C., Roth, W.J., Leonowicz, M.E., Kresge, C.T., Schmitt, K.D., Chu, C.T., Olson, D. H., Sheppard, E. W.; McCullen, S.B., Higgins, J. B., and

- Schenker, J. L. (1992). A new family of mesoporous molecular sieves prepared with liquid crystal templates. *Journal of American Chemical Society*, 114: 10834–10843.
- [19] Miguel, C., Claro, A., Gonçalves, A.P., Muralha, V.S.F., and Melo, M.J. (2009). A study on red lead degradation in the medieval manuscript, Lorrão Apocalypse (1189). *Journal of Raman Spectroscopy*, 40: 1966–1973.
- [20] Sousa, M. M., Melo, M., Aguiar-Ricardo, A., and Cruz, P. (2005). A green approach to antique textile cleaning. In: Paterakis, A.B. (Ed.) The 14th triennial ICOM meeting the Hague preprints, international council of museums, Amsterdam, p. 944–953.
- [21] Marques, R., Sousa, M.M., Oliveira, M.C., and Melo, M.J. (2009). Characterization of weld (*Reseda luteola* L.) and spurge flax (*Daphne gnidium* L.) by high-performance liquid chromatography–diode array detection–mass spectrometry in Arraiolos historical textiles. *Journal of chromatography A*, 1395–1402.
- [22] Fidalgo, A., Rosa, M.E., and Ilharco, L.M. (2003). Chemical control of highly porous silica xerogels: physical properties and morphology. *Chemical materials*, 15: 2186–2192.
- [23] Suyal, G., Mennig, M., and Schmidt, H. (2003). Synthesis of nanocomposite thin films containing Ag-Au alloy colloids for wavelength tunability. *Journal of Materials Science*, 38(8): 1645–1651.
- [24] Aegerter, M.A., and Mennig, M. (2004). Wet chemical coating technologies. In: *sol-gel technologies for glass producers and users*, New York: Kluwer Academic Publishers, p. 49–57.
- [25] Everall, N., Chalmers, J., Chalmers, M. and Griffiths, P. (2007). Measurements of the chemical characteristics of polymers and rubbers by vibrational spectroscopy. In: *Vibrational spectroscopy of polymers: principles and practices*. England: John Wiley and Sons, p. 113–142.
- [26] Hummel, D. (2002). FTIR spectral atlas of plastic additives. In: *Atlas of plastic additives - Analysis by spectrometric methods*, Berlin: Springer-Verlag, p. 131–519.
- [27] Duran, A., Perez-Rodriguez, J.L., Espejo, T., Franquelo, M.L., Castaing, J., and Walter, P. (2009). Characterization of illuminated manuscripts by laboratory-made portable XRD and micro-XRD systems. *Journal of Analytical and Bioanalytical Chemistry*, 395: 1997–2004.
- [28] Stuart, B. H. (1997). Applications: Proteins and peptides. In: *Biological applications of infrared spectroscopy*. West Sussex: John Wiley and Sons, p. 113 – 127.
- [29] Shashoua, Y. (2008). Degradation of Plastics. In: *Conservation of plastics: materials science, degradation and preservation*. United Kingdom: Butterworth Heinemann, p. 151 – 190.
- [30] Patel, M., Morrell, P., Cunningham, J., Khan, N., Maxwell, R.S. and Chinn, S.C., (2007). Complexities associated with moisture in foamed siloxane composites. *Polymer Degradation and Stability*, 93: 513 - 519.
- [31] Low molecular siloxanes can migrate from the elastomer matrix after polymerization as described in: Horie, C.V. (1987). Survey of polymers. In: *Materials for conservation*. United Kingdom: Butterworth Heinemann, p. 130 – 132.
- [32] Boersma, F. (2007). The museum environment. In: *Unraveling textiles – A handbook for the preservation of textile collections*. London: Archetype, p. 31–45.

Chapter 18

DEVELOPMENT OF POLYMER-DERIVED SiC FIBERS AND THEIR APPLICATIONS

Guohua Jiang^{a,b,*}

^a Department of Materials Engineering, College of Materials and Textile,
Zhejiang Sci-Tech University, Hangzhou 310018, P. R. China.

^b Key Laboratory of Advanced Textile Materials and Manufacturing Technology
(ATMT), Ministry of Education, Zhejiang Sci-Tech University,
Hangzhou 310018, P. R. China.

ABSTRACT

The polymer-derived SiC fiber is one of the most important reinforcing materials for high performance ceramic matrix composites (CMC). Three generation of SiC fibers have been developed over the past thirty years. The first generation fiber produced was an amorphous SiC fiber, next was a low-oxygen content SiC fiber, and nearly stoichiometric SiC fiber was developed. In this chapter, the preparation method, microstructure, and performance of three generation fibers are reviewed here. The representative properties of these fibrous materials and their expected applications are described.

1. INTRODUCTION

Regarding inorganic fibers, glass fibers and carbon fibers are well known all over the world. In addition, alumina-silica fibers, single crystalline oxide fibers and silicon carbide fibers, which show excellent oxidation resistance at high temperatures in air, have been developed and commercialized except for single crystalline oxide fibers [1]. Of these, silicon carbide (SiC) fibers have made a lot of progress over the past thirty years. SiC fibers exhibit an excellent high-elastic modulus, high-tensile strength, and high-temperature stability, excelling over carbon fibers, and are expected to be used as extreme materials in the space

* E-mail: polymer_jiang@hotmail.com

shuttle, aircraft, and nuclear fusion fields, including applications as clean environmental materials, such as for radiation gas burners and high power electrical cables [2]. Fundamentally, the fabrication of SiC fibers depends critically on the spinability of the polycarbosilane (PCS) precursor, including the pyrolysis process. Therefore, the synthesis of spinable PCS has been a key technique in the SiC fiber industry. Fine diameter SiC-based fibers are produced via polycarbosilane (PCS) route on the base of the method developed by Yajima *et al.* [3-6]. The processing includes the synthesis of PCS precursor, melt-spinning to obtain precursor fibers, curing to render the fibers infusible, and finally pyrolysis to give silicon carbide fibers. In the recently years, lots of advanced research on preparation of SiC fibers and to make the best use of their excellent heat-resistance and oxidation-resistance have been carried out. Furthermore, an excellent functional SiC fiber with a gradient surface layer was recently synthesized from an organosilicon polymer making full use of the technology of the aforementioned fiber production. In this case, a general process for in-situ formation of functional surface on ceramic fibers was proposed. This process is characterized by controlled phase separation (bleed out) of additives, analogous to the normally undesirable outward loss of low-molecular-mass components from some plastics; subsequent calcination stabilizes the compositionally changed surface region, generating a functional surface layer. This approach is applicable to a wide range of materials and morphologies, and should find use in catalysts (for example, photocatalysts), composites and environmental barrier coatings.

The objective of this chapter is to review the advance in these fibers and refer to the prospect for the future technology of inorganic fibers.

2. PREPARATION OF POLYCARBOSILANE (PCS) PRECURSORS

2.1. Overview

A silicon-carbide-based fiber is used as a fibrous reinforcement for plastics or ceramics owing to its excellent heat resistance and mechanical properties. As a silicon carbide fiber, there is widely known an amorphous or microcrystalline fiber (to be referred to as "amorphous silicon carbide fiber" hereinafter) produced from polycarbosilane by the thermal oxidation curing method at a relatively low temperature, e.g., a temperature of 1,300°C or lower, and the amorphous silicon carbide fiber has a high oxygen content and excess carbon [7]. It is practically used as a fibrous reinforcement for a variety of matrices. When the fiber is heated above 1573 K, the fiber crystallizes into β -SiC, which is accompanied by the release of CO and SiO gases. The fiber shows severe degradation caused by the release of these gases and growth of SiC grains [8-10]. The fiber has excellent strength and modulus properties for ceramic fibers, and retains its properties at high temperatures.

Concerning the above amorphous silicon carbide fiber and its production process, many proposals have been already made. Usually, the processing sequence of SiC fibers from polycarbosilane is shown in Figure 1 [11]. Polycarbosilane is called PCS in this chapter. The processing included the synthesis of PCS precursor, PCS fibers melt spinning to obtain precursor fibers, curing to render the fibers infusible, and finally heat treatment of the cured fiber at high temperature to give Si-C fibers.

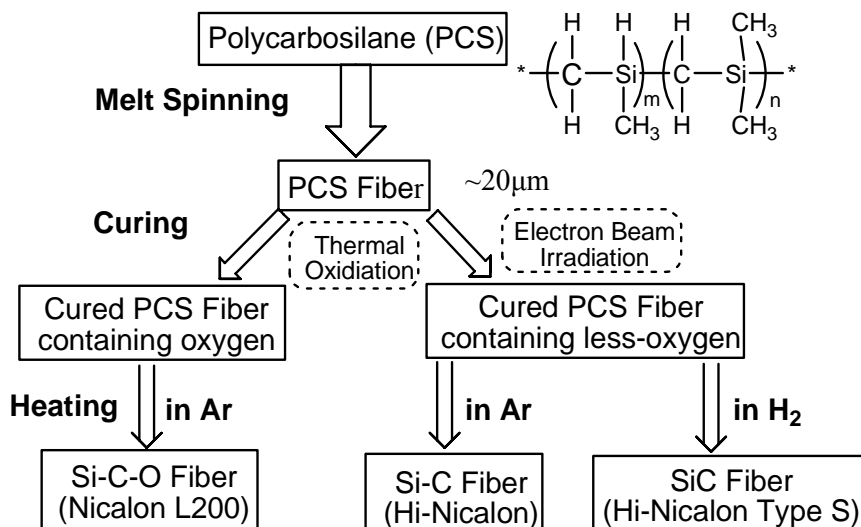


Figure 1. Preparation process of SiC-based ceramic fibers from polycarbosilane.

2.2. Preparation of Polycarbosilane (PCS)

Polycarbosilane (PCS) as a precursor polymer of SiC based ceramic fibers is synthesized by the thermal conversion of polydimethylsilane. The molecular structure of PCS is planar, consisting of ring-and chain structure. PCS consists of two units, $(\text{Si}(\text{CH}_3)_2\text{CH}_2)$ and $(\text{Si}(\text{CH}_3)\text{HCH}_2)$, and their unit ratio is almost the same. Its atomic ratio is $\text{SiC}_{1.93}\text{H}_{4.71}\text{O}_{0.01}$, oxygen being an impurity. Its number-average molecular weight is about 2000 and the melting point is 506 K. The preparation of polycarbosilane from polydimethylsilane is carried out by the "Kumada rearrangement" [12]. For the reaction, Si radicals have to be formed in the initial step of the reaction. The Kumada rearrangement of polydimethylsilane to polycarbosilane has been mostly studied by thermal decomposition at high temperature. However, this method poses significant operational problems such as generating gaseous by-products including CH_4 , Me_3SiH , SiH_4 , etc. The gaseous byproducts create extremely high pressure inside the autoclave, which renders the operation inconvenient and unsafe. To overcome these problems in the thermal decomposition process, Yajima *et al.* [5, 13] adopted a catalytic process in which polycarbosilane was synthesized at normal pressure by adding small amounts of polyborodimethylsiloxane to polydimethylsilane as a catalyst. Also, Hasegawa *et al.* [14] developed halide catalysts of MCl_3 for this reaction, such as AlCl_3 , MnCl_3 , CrCl_3 , VCl_3 , TiCl_3 and GaCl_3 etc. Duboudin *et al.* [15] reported monomeric boron catalysts like borane and $\text{B}(\text{OMe})_3$. However, these two catalytic methods provided low yields, and it is difficult to separate the catalysts from the finally formed PCS. Kim *et al.* [16] reported that the expensive ZSM-5 zeolite has good catalytic properties. Polycarbosilane was synthesized from polydimethylsilane in the presence of zeolite as a catalyst. The number average molecular weight (M_n) of the polycarbosilane was ranged between 300 and 2,500. They reported [16] the synthesis and characterization of polycarbosilane that is a suitable precursor for SiC fiber in the presence of a ZSM-5 catalyst ($\text{Si}/\text{Al}=30$). ZSM-5 can be a very effective catalyst for synthesizing polycarbosilane at 350°C under normal pressure. The

acidic strength of the hydroxyl group (Brønsted acid site), which is present on the surface of the ZSM-5 (Si/Al=30) crystallite, is adequate to catalyze the conversion of polydimethylsilane to polycarbosilane. However, with this method it is difficult to separate the powdery ZSM-5 from the produced PCS.

The filtering process for conventional powdery catalysts needs a dilution process to control the polymer viscosity for filtering and a drying process to remove the solvents. Therefore, the filtering process for powdery catalysts is undesirable in terms of cost, time, and yield for industrial mass production. Riu *et al.* [2] reported a very simple and good catalytic conversion process from PDMS to pure PCS using very cheap anodized aluminum oxide (AAO), which does not need a filtering process. The AAO surfaces comprise nanopores (high specific surface areas, as shown in Figure 2) with many Lewis acid sites. The AAO catalysts clearly show three important facts: (1) catalytic properties as good as ZSM-5, (2) reusability by a simple washing treatment, and (3) no need for a filtering process, which can simplify the complex steps of PCS synthesis.

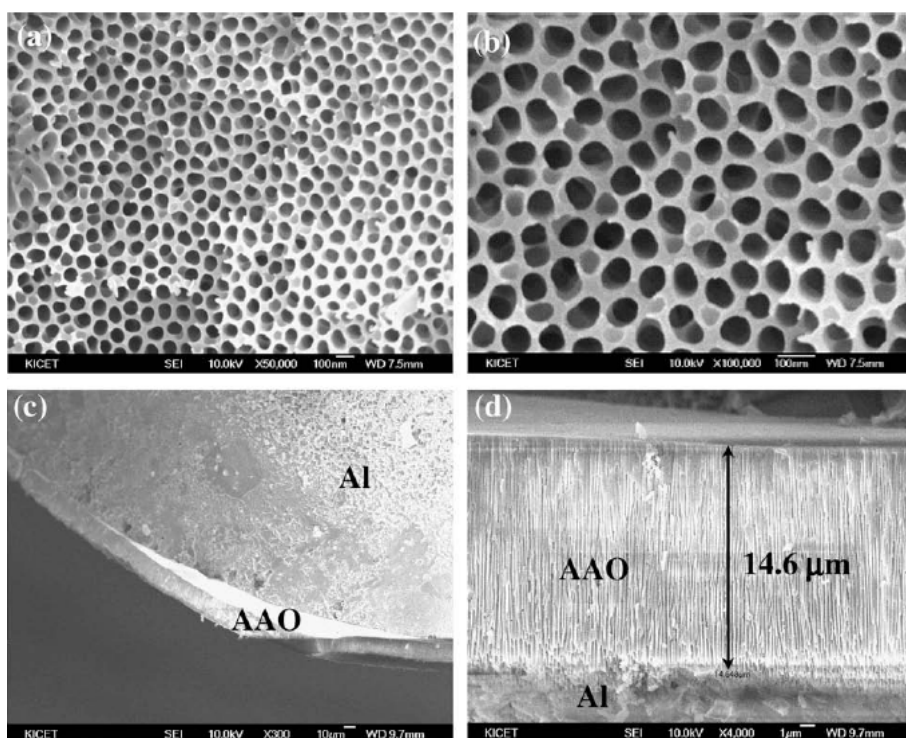


Figure 2. SEM images of surface morphologies of AAO catalysts (a and b) and cross-sectional views (c and d).

Recently, liquid hyperbranched hydridopolycarbosilanes (HBPCSs) have been regarded as excellent effective precursors for SiC ceramics because of their unique structures and favorable properties, such as lower viscosities, more favorable solubilities, and larger amounts of reactive end-functional groups [18-20]. The first HBPCS, derived from the Grignard reaction of chloromethyltrichlorosilane ($\text{Cl}_3\text{SiCH}_2\text{Cl}$) in ether, was reported in 1991, as shown in Figure 3 [21].

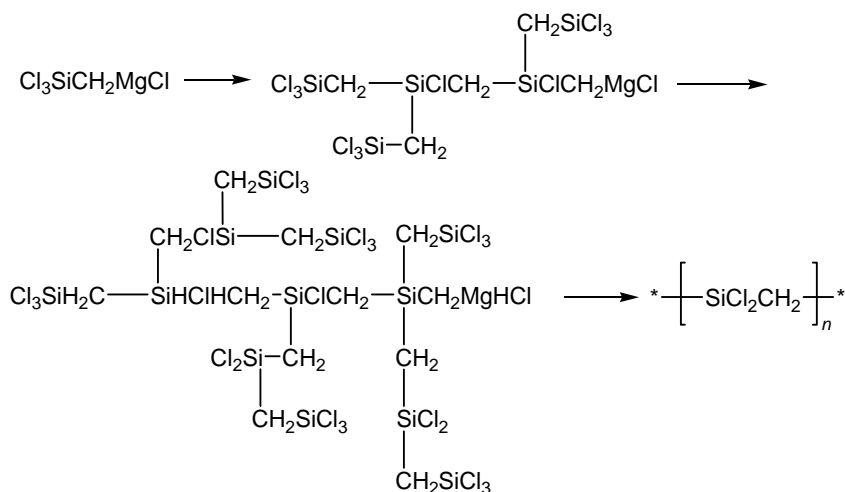


Figure 3. Proposed routes for formation of products based on methanol trapping experiment.

An improved preparation for allylhydridopolycarbosilane (AHPCS), an allyl-substituted HBPCS, was subsequently developed by Star-fire Systems, Inc. and sold under the trade name SMP-10 [22]; it is currently of strong interest as a precursor to a SiC matrix for making ceramic composites. Xia *et al* prepared a novel AHPCS by a one-pot synthesis with $\text{Cl}_3\text{SiCH}_2\text{Cl}$, $\text{Cl}_2\text{Si}(\text{CH}_3)\text{CH}_2\text{Cl}$ and allyl chloride ($\text{CH}_2\text{CH=CH}_2$) as the starting materials, and the compositions of this AHPCS could be tailored by controlling the amounts of the starting materials [23, 24].

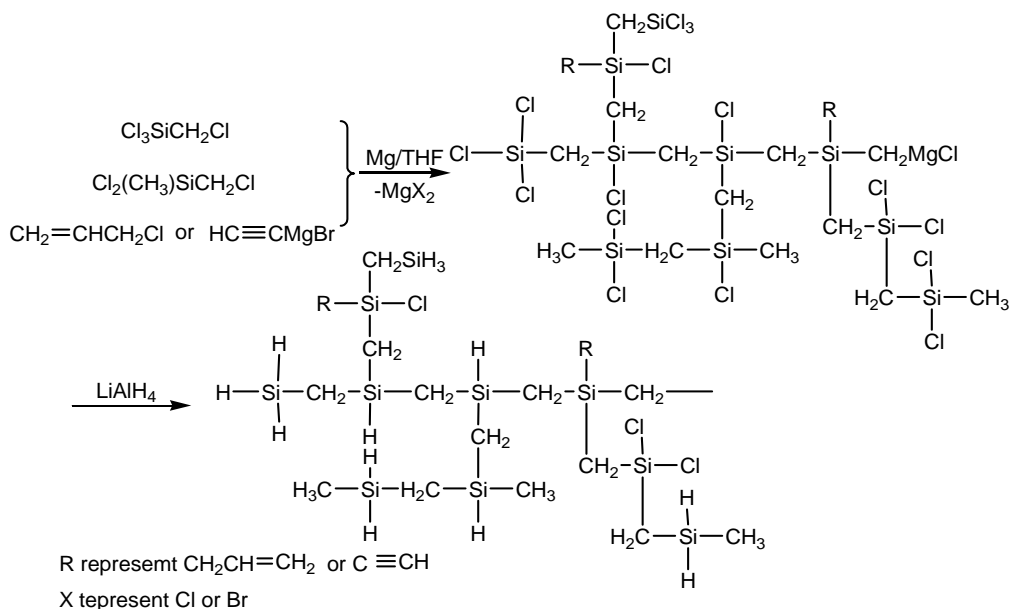


Figure 4. Reaction sequences of AHPCS and EHPCS.

They found that the AHPCS was partially modified with 9-BBN via a conventional hydroboration. The molecular weight of the as-synthesized B-AHPCSs significantly increased over that of the parent AHPCS. As expected, the B-AHPCS retained its hyperbranched structure after the 9-BBN modification. The thermal properties of B-AHPCS were investigated by TGA and FTIR. The TGA indicated that the 1000°C ceramic yield of B-AHPCS reached 75%, 15% higher than that of the parent AHPCS. The B-AHPCS underwent cross-linking, an organic-to-inorganic transition and a conversion of amorphous to crystalline SiC during the heat treatments. At high temperatures, the introduction of <1 wt. % boron significantly inhibited SiC crystallization. The 1800°C ceramics derived from B-AHPCS were found to be significantly denser than that from AHPCS [25].

Polymer cross-linking prior to pyrolysis, conventionally by heating the polymer in atmosphere, is required to increase the ceramic yield. Froehling [26] reported that the final ceramic yield of a branched polyhydridocarbosilane was significantly improved via a previous cross-linking treatment before pyrolysis. As aforementioned HPCS, due to its relatively high cross-linking temperature (ca. 300°C), loss of volatile oligomeric components occurs on unconfined pyrolysis in a flowing nitrogen atmosphere, leading to a ceramic yield of ca. 55%. Xia found the cross-linking process markedly reduced the evaporation of low-molecular weight oligomers, which accounted for the difference in the overall ceramic yields between non-cross-linked and cross-linked HPCS. For the HPCS/10 wt% divinylbenzene (DVB) system, the maximum of reaction degree of HBPCS was obtained, which might be responsible for the highest ceramic yield of 70.1 wt. % at 1000°C. However, the ceramic yield of the non-cross-linked HPCS was only 45 wt. % at 1000°C [27].

3. PREPARATION AND MICROSTRUCTURE OF SiC FIBERS

3.1. Conversion of PCS to SiC

The conversion of PCS to ceramic is generally attained by heating the precursor polymer to temperatures above 1000°C in an inert atmosphere. This pyrolytic conversion process of PCS and oxidation-cured PCS has been found to involve a number of stages. During pyrolysis up to ca. 800°C, degradation of low molecular weight molecules and decomposition of organic side groups occurs. Large weight losses and gaseous evolution of mainly H₂ and CH₄ are associated with these reactions. Si-H and C-H bonds are readily broken. With increasing temperature, connectivity of Si-C-Si bonds increases and a network structure can form via condensation reactions between CH₄ and CH₃ units [28]. In the pyrolysis residue after 700°C, the presence of C=C bonds has been confirmed, possibly arising from dehydrogenation in -CH-CH- fragments [29]. The increase in density is most rapid between ca. 550 and 800°C, when the organic PCS transforms into a more inorganic state. By 800°C, this transition is essentially complete and an amorphous residue is obtained. Soraru *et al.* [30] reported the presence of hydrogen as CH groups in this amorphous residue. Oxygen introduced in oxidation cured PCS is not eliminated by this stage of pyrolysis [29]. Absence of this oxygen is expected in uncured PCS, whereas none was mentioned by Soraru *et al.* [31]. Si-O bonds were reported by Hasegawa [32] and Okamura and Bouillon *et al.* [33]. Residual CH or CH₂ units in the amorphous residue decompose with increasing temperature but the structure

remains amorphous below 1000°C. In the pyrolysis of uncured PCS between 1000 and 1200°C, β -SiC microcrystals begin to nucleate from the amorphous matrix of Si, C, O and H accompanied by evolution of H₂ gas.

The presence of excessive hydrogen could delay this process [34]. Monthieux and Delverdier [35] found that carbon always nucleates first, as basic structural units (BSUs) which are small stacks of 2–3 polyaromatic layers about 1 nm in lateral extension. The presence of oxygen atoms would not favor this nucleation. The periphery of these carbon atoms is thought to be saturated with hydrogen atoms which, in the 1000 to 1200°C range, are removed mainly as H₂ gas. This release of H₂ induces an edge-to-edge association of BSUs into larger stacks. SiC was found to be the second phase to nucleate due to structural rearrangements at the solid state within the remaining Si-C-O phase. This was considered to occur concomitantly with the edge-to-edge association of the BSUs. The evolution from uncured PCS between 1000 and 1200°C did not occur in the pyrolysis of cured PCS, thus the oxygen introduced by the curing process is thought to suppress crystallization of the β -SiC [36]. Above 1200°C, crystallization of β -SiC continues with slow crystal growth for the uncured PCS, while it is the beginning of crystallization for the cured PCS. In the case of cured PCS, hydrogen evolution is not reported with the crystallization of β -SiC from the amorphous matrix [30, 32]. Instead, crystallization is accompanied by CO gas evolution. Thus, this CO gas could be due to carbothermal reduction of oxygen bonds which is linked to the oxidation curing process. Bouillon *et al* [37] reported the amorphous to crystalline transition for the cured PCS and suggested that the main gaseous product should be SiO with a lower proportion of CO. The production of SiO and CO should be the result of decomposition of the amorphous Si(C, O) phase. Crystal growth of the β -SiC is suggested to be the result of the reaction of the carbon and Si-O species at the β -SiC grain boundaries. The precipitation of carbon particles from the carbon-rich Si(C, O) phase may compete with the loss of carbon by reaction with Si-O species [38]. The precipitation rate is higher than the loss rate up to 1400°C. At ca. 1500°C, the loss rate of carbon is higher than the gain in carbon precipitation, and the amount of free carbon decreases with increasing temperature.

The conversion process of PCS to SiC ceramics could be characterized using infrared spectrum (IR), X-ray diffraction (XRD), thermogravimetry (TG), nuclear magnetic resonance (NMR), electron spin resonance (ESR), inelastic neutron scattering (INS), and X-ray absorption fine structure (XAFS) [11].

3.2. Microstructure of Amorphous SiC Fibers

The microstructure of the amorphous Si-O-C fibers have been studied by many researchers using XRD, neutron diffraction (ND), transmission electron microscopy (TEM), extended X-ray absorption fine structure (EXAFS), and Raman scattering. The amorphous Si-C fiber is homogeneously composed of ultra-fine β -SiC crystallites and an amorphous mixture of silicon, carbon, and oxygen.

Yu *et al.* [39] reported the SiC(OAl) fibers and the SiC(Al) fibers were fabricated by the use of aluminum-containing polycarbosilane (Al-PCS) precursor. The chemical formula of SiC(OAl) fibers is SiC_{1.31}O_{0.25}Al_{0.018} with C and O rich on the surface. The microstructure of SiC(OAl) fibers is a mixture of β -SiC nanocrystals, free carbon, and an amorphous silicon oxycarbide (Si-C-O phase), which have been confirmed by an amount of SiC₂O₂, SiCO₃,

SiO_4 and SiC_3O units in the ^{29}Si MAS NMR spectrum. A small quantity of aluminum is embedded uniformly in the Si–C–O amorphous continuous phase. For SiC(Al) fibers, nearly stoichiometric composition was confirmed as chemical composition of $\text{SiC}_{1.03}\text{O}_{0.013}\text{Al}_{0.024}$. The fiber is composed of a large number of β -SiC crystallites, a small amount of α -SiC crystalline and SiC amorphous phase. The aluminum in the SiC(Al) fibers mainly exists in two manners: Al–C bonds connected with the surfaces of the β -SiC grains and Al–O bonds, or Al_2O_3 , to the amorphous phase. Figure 5 shows schematic drawing of phase distribution in the SiC(OAl) and SiC(Al) fibers.

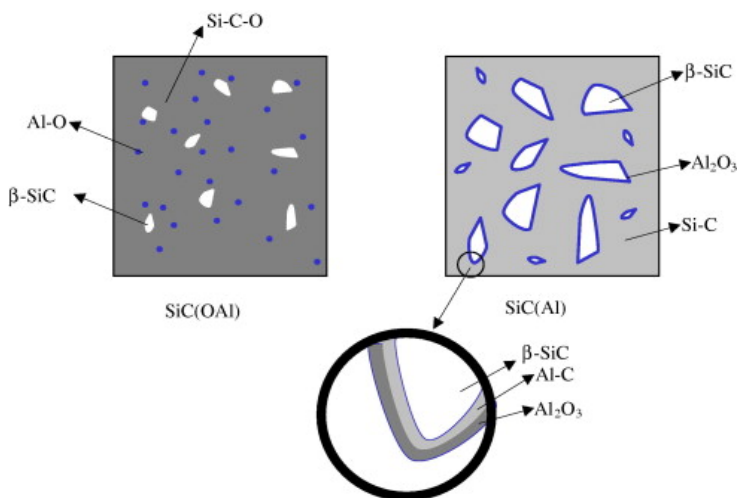


Figure 5. Schematic drawing of phase distribution in the SiC(OAl) and SiC(Al) fibers.

3.3. Microstructure of Low-Oxygen Content SiC Fibers

Hi-Nicalon® is the second generation SiC fibers. The precursor fibers are cured by electron-beam irradiation in inert atmosphere, so that the oxygen content in Hi-Nicalon® is reduced below 1 wt. %. However, Hi-Nicalon® contains about 20% excess carbon apart from silicon carbide. Therefore, its service temperature is only about 1300°C. To further improve the thermal stability, the excess carbon must be removed to give near stoichiometric silicon carbide fibers.

Feng *et al.* [40] reported the microstructural evolution of Hi-Nicalon Trade Mark SiC fibers annealed in O_2 – H_2O –Ar atmospheres. The dark field image of SiC fiber treated under different temperatures was shown in Figure 6, the bright parts in the image represented β -SiC crystal, the figure showed an evident grain growth with the increase of annealing temperature, the electron diffraction pattern of the fiber showed three main rings, corresponding to the 111, 220 and 311 β -SiC Bragg reflections. These rings got sharp and parted with the increase of temperature, which was consistent with the relatively larger size of the crystals.

The microstructure of β -SiC crystal was revealed in high resolution image. No obviously structural change was seen between the untreated fiber and fiber annealed in 1300°C, with the rise of temperature, structural defect such as dislocation and stacking faults appeared inside

the β -SiC crystals, as shown in, and their amounts increased with the rise of treating temperature, twin structure was also seen after annealing in 1600°C (Figure 7).

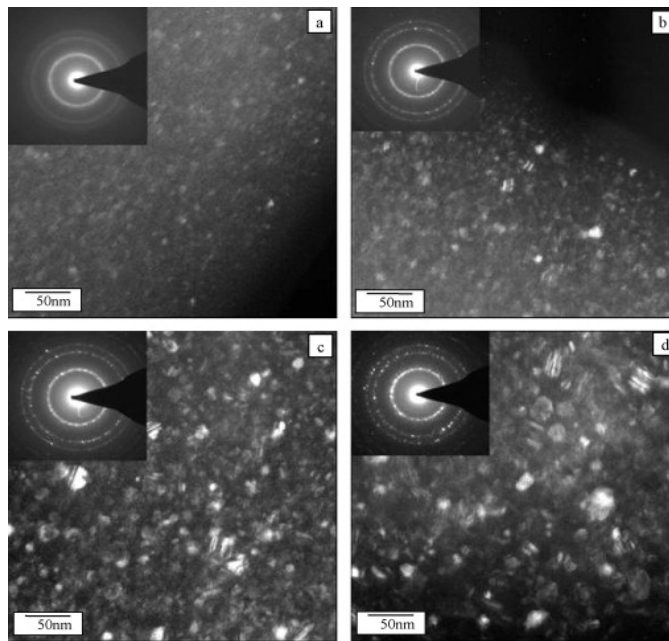


Figure 6. The dark field image of SiC fiber annealing in: (a) 1300°C; (b) 1400°C; (c) 1500°C; (d) 1600°C.

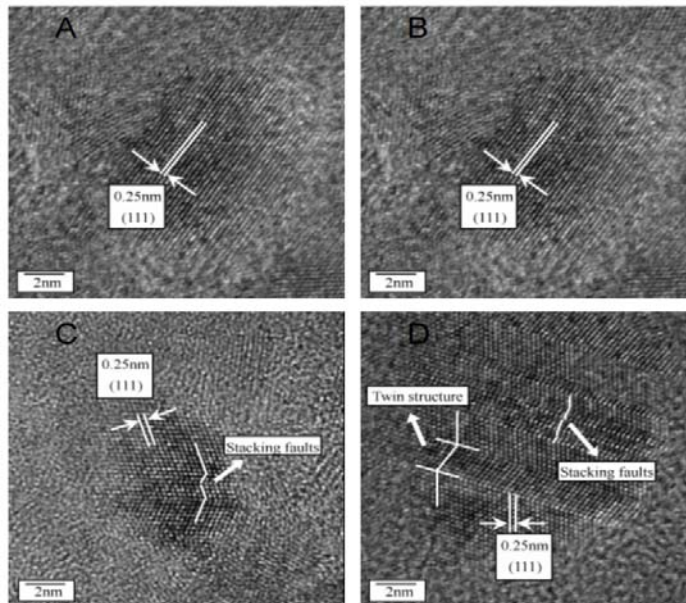


Figure 7. β -SiC in Hi-Nicalon fibers before annealing (A), after annealing in 1300°C (B), 1400°C (C) and 1600°C (D).

3.4. Microstructure of Nearly Stoichiometric SiC Fiber

Continuous silicon carbide (SiC) fiber fabricated by two-stage chemical vapor deposition on tungsten filament was developed by Zhang [41]. Microstructure of the fiber was investigated by means of scanning electron microscopy, X-ray diffraction, transmission electron microscopy and Raman spectrometry. The results showed that the fiber consists of tungsten core, a W/SiC interfacial reaction zone with the reaction products of W_5Si_3 and WC, and a predominant β -SiC layer (Figure 8). The W/SiC interface can be described as W/ W_5Si_3 /WC/SiC. The SiC originates at the surface of the WC with a buffer layer, in which β -SiC crystallites nucleate and grow with their preferred $\langle 111 \rangle$ orientation, exhibiting strong $\langle 111 \rangle$ fiber texture. Raman spectra revealed that the SiC in the fiber is stoichiometric, which is composed of β -SiC and amorphous SiC.

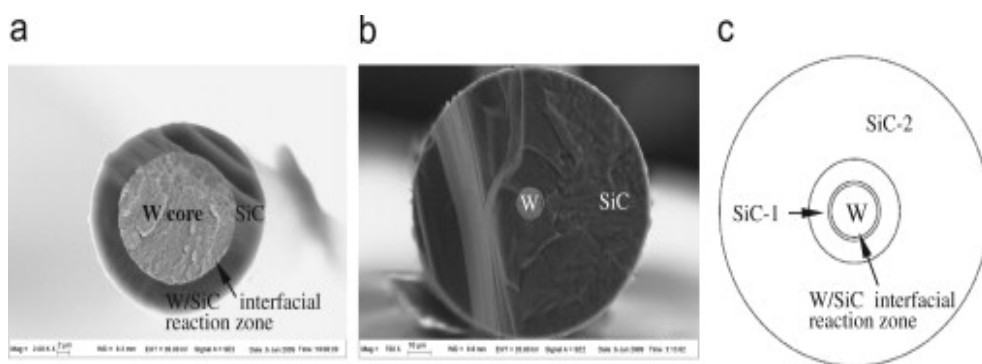


Figure 8. SEM images of the SiC fiber (a) after the first stage, (b) after the second stage and (c) schematic picture showing the structure of the fiber.

4. PERFORMANCE AND APPLICATIONS OF SiC FIBERS

4.1. Performance of SiC Fibers

Nicalon®, a trade name given by its manufacturer, Nippon Carbon, is the representative of the first generation Si-C fibers. This type of fiber was developed in Japan by Yajima and his colleagues and the first publications date from 1976 [42]. Usually, Nicalon® is produced from the commercial PCS, X9-6348. Due to the low molecular weight (MW) of this PCS, a curing process was necessary prior to pyrolysis. The curing is known to be performed oxidatively at 200°C in the air. It was reported that a blending of PCS with polyvinylsilane at 10 wt% level lowered the curing temperature, accompanied with a slightly increased ceramic yield upon pyrolysis [43]. In both cases, the oxidative curing of spun fibers led to high oxygen contents (10-20 wt.%) in Old-Nicalon fibers, which is closely related to their low thermomechanical stability, limiting its long-term service temperature below 1100°C. The typical properties of Si-C-O fibers are listed as shown in Table 1.

Table 1. Typical Properties of three generation Si-C fibers

● Excellent ○ Good ▲ Moderate	Nicalon Si-C-O fibers	Hi-Nicalon Si-C fiber	Hi-Nicalon Type S stoichiometric SiC fiber
Chemical C/Si Composition O	1.31 12 wt%	1.39 0.5 wt%	1.05 0.2 wt%
Tensile Strength Elastic Modulus Thermal Stability Oxidation Resistance Creep Resistance	● 3.0 GPa ○ 200 GPa ○ 1473 K ▲ ▲	○ 2.8GPa ○ 270 GPa ● 2073 K ▲ ○	○ 2.6 GPa ● 420GPa ● 2073 K ○ ●

Data from: <http://www.coicceramics.com>.

Nicalon™ ceramic fiber is available in two primary grades, namely, Ceramic Grade (CG) Nicalon™ and HVR (high volume resistivity) Grade NICALON™, differentiated by electrical properties. The typical properties of Nicalon (Si-C-O) fibers at room temperature are listed in Table 2.

Table 2. Typical Properties of Nicalon (Si-C-O) fibers at Room Temperature

	Ceramic Grade	HVR Grade
Fiber Denier	1800	1800
Density, g/cc	2.55	2.32
Composition, wt.% Si:C:O	57:32:12	57:32:12
Filaments per Tow	500	500
Filament Diameter, μm	14	14
Tensile Strength, GPa	3.0	2.8
Tensile Modulus, GPa	210	180
Vol. Resistivity, ohm-cm	10^3	$>10^6$
Dielectric Constant	9.2	6.4
Loss Factor	1.0	0.05
CTE, ppm/C, 0-900°C	3.9	3.9
Thermal Conductivity, W/m.K		
At 25°C	2.97	
At 500°C	2.20	
Specific Heat, J/g.K		
At 25°C	0.71	
At 500°C	1.17	

Data from: <http://www.coicceramics.com>.

4.2. Applications of SiC Fibers

Continuous SiC fibers with good high-temperature resistance, good oxidation resistance, high specific strength and high specific modulus are the basis and key of preparation of the ceramic matrix composites operated in high temperature environment. Presently the most SiC fibers are prepared by polymer-derived method and widely used in many fields such as aviation, astronavigation and military affairs.

The oxygen free SiC fiber (Hi-Nicalon) has been commercially produced by an electron beam curing process. And then the SiC fiber (Hi-Nicalon Type S) having stoichiometric SiC composition and high crystallinity has been developed. Hi-Nicalon fiber has higher elastic modulus and thermal stability than Nicalon fiber. The Type S fiber has the highest elastic modulus and thermal stability and excellent creep resistance in three types of Nicalon fibers. Recently, Type S fibers as industrial products have been developed and put on the market. The Type S fibers have a high tensile strength of 2.8 GPa, a high elastic modulus of 390 GPa. Against thermal exposure, Type S retains a tensile strength of 2.3 GPa and hardly changes its elastic modulus even at 1873 K. Moreover, Type S has outstanding creep resistance. Type S shows higher stress relaxation ratio than many other ceramic fibers after thermal exposure over 1673 K. Now, Hi-Nicalon Type S fiber/BN/SiC composites are being developed as the components of gas turbine for aerospace and land based power generation such as shrouds and combustors. Type Hi-Nicalon S can be supplied about 30 kg per a month at present [44].

Amorphous Si-B-C-N ceramic fibers prepared at 1000°C from a melt-processable boron-modified polysilazane $[B(C_2H_4SiCH_3NCH_3)_3]_n$ were annealed in the temperature range 1000-1800°C in a nitrogen atmosphere to identify the changes in the thermal and structural stability as well as in the related fiber strength. Fibers were shown to be extremely stable up to 1600°C without decomposition and measurable changes in their amorphous structure. At higher temperatures, X-ray diffraction and thermogravimetry analyses indicated that the structural and thermal properties of fibers were probably controlled by the carbothermal decomposition of a minor part of the silicon nitride phase providing Si_3N_4/SiC nanograins in the material at high temperature. The excellent strength retention after heat-treatment at 1600°C (1.3 GPa) is clearly related to the high structural and thermal stability of fibers. Between 1600 and 1700°C, the fiber strength decreased to 0.9 GPa then dropped to about one-quarter the original value at 1800°C while structural changes were evident. With an excellent stability in air at 1300°C, these Si-B-C-N fibers are potential candidates for continuous fiber-reinforced ceramic-matrix composites (CFCCs) [45].

Carbon fiber reinforced silicon carbide ceramic matrix composite materials (C/SiCs) are being tested for hot structures and thermal protection systems (TPS) of launch vehicles and spacecraft, and also for advanced friction system of aircraft and racing cars. A number of tribological and joining components are required in these applications, such as bushing and rolling contact bearings, nuts and bolts, which require excellent mechanical, physical and chemical properties at temperatures higher than 1650°C. Zhang reported that the room temperature tensile and shear strength of the bolts made of needled C/SiC are 139 MPa and 83 MPa, respectively. Even at 1800°C in a combustion environment, the strengths still retained about 116 MPa with a maximum decrease of 13%. More importantly, the bolts did not suffer significant mechanical degradation after tension-tension fatigue at 1 Hz for 24 h [46].

Recent progress toward development of irradiation resistant SiC/SiC composites has shown great promise for their application in nuclear systems. Takashi *et al.* [47] reported the results of a study on the evaluation of the mechanical properties of a nuclear grade SiC/SiC composite, which is being considered as a candidate control rod material for a very-high temperature gas-cooled reactor. Specifically, this study evaluates the anisotropy in tensile properties of the composites to provide a basis of the practical component design. The materials were satin woven or biaxially braided Hi-Nicalon (TM). Type-S fiber reinforced

chemical-vapor-infiltrated (CVI) SiC matrix composites with multilayered interphase. Results indicate excellent axial and off-axial tensile fracture behaviors for the satin woven composites. In contrast, the braided composites failed at unexpectedly lower stresses. The primary cause for this difference was the varied in-plane shear properties on which off-axial tensile properties significantly depend. Superior in-plane shear properties for the satin woven composites were achieved by increasing the volume fraction of transverse fibers normal to the fracture plane. Considering the failure modes depend on the off-axis angle the anisotropy of proportional limit tensile stress and fracture strength were preliminarily evaluated by a simple stress criterion model. It is worth noting that specimen size effect on axial and off axial tensile properties seems very minor for nuclear grade SiC/SiC composites with rigid CVI-SiC matrix.

CONCLUSION

Polymer-derived SiC fiber Nicalon has been produced commercially and widely used as a reinforcement of Polymer Matrix Composites (PMCs) and Ceramic Matrix Composites (CMCs). Main applications of Nicalon fibers are PMC for structural materials of aerospace and CMC for high temperature components of aerospace engine. In recent years, it has been increasing in demand for high performance CMC for high temperature application. CMCs are most promising materials for high temperature structural materials of gas turbines for aerospace and power generation. By reducing oxygen, this fiber has a higher elastic modulus and creep resistance, and thermal stability up to 1,600°C than those of Nicalon fiber. High temperature mechanical properties of CMCs using Hi-Nicalon have significantly improved. However, creep resistance of Hi-Nicalon CMC is not satisfactory as structural materials at high temperature, because Hi-Nicalon mainly consists of SiC micro-crystals and excess carbon. Recently, the SiC fiber (Hi-Nicalon type S) having stoichiometric SiC composition and high crystallinity have been developed by Nippon Carbon. By reducing excess carbon and putting C/Si ratio close to stoichiometric composition, Type S fiber has high elastic modulus of 420 GPa, high thermal conductivity, and excellent creep resistance. Hi-Nicalon Type S fibers should be the best candidates for the reinforcement of ceramic matrix composites. Hi-Nicalon Type S fiber/BN/SiC composites are being developed as the components of gas turbine for aerospace and power generation such as shrouds and combustor.

ACKNOWLEDGEMENTS

This work was financially supported by the Qianjiang Talents Project of Zhejiang Province (2010R10023), the Scientific Research Foundation for the Returned Overseas Chinese Scholars, the State Education Ministry (1001603-C), the Natural Science Foundation of Zhejiang Province (Y4100045), the Natural Science Foundation of China (20604024), and the Program for Changjiang Scholars and Innovative Research Team in University (PCSIRT: 0654).

REFERENCES

- [1] Ishikawa, T. (2005). Advances in inorganic fibers. *Advanced Polymer Science*, 178: 109-144.
- [2] Huh, S.H., Shin, D.G., Riu, D.H., Jin, E.J., Kong, E.B., Cho, K.Y., Kim, C.Y., and Kim, H.E. (2008). A simple synthetic route of polycarbosilane precursor using nanoporous anodized aluminum oxide. *Catalytic Communication*, 10: 208-212.
- [3] Yajima, S., Hayashi, J., Omori, M., and Okamura, K. (1976). Development of a silicon carbide fibre with high tensile strength. *Nature*, 261: 683-685.
- [4] Yajima, S., Hayashi, J., and Omori, M. (1975). Continuous silicon carbide fiber of high tensile strength. *Chemistry Letters*, 9: 931-934.
- [5] Yajima, S., Hasegawa, Y., Okamura, K., and Matsuzawa T. (1978). Development of high tensile strength silicon carbide fibre using an organosilicon polymer precursor. *Nature*, 273: 525-527.
- [6] Yajima, S., Hasegawa, Y., Hayashi, J., and Iiuma, M. (1978). Synthesis of continuous silicon carbide fibre with high tensile strength and high Young's modulus, part I. *Journal of Materials Science*, 13: 2569-2576.
- [7] Yajima, S., Okamura, K., Matsuzawa, T., Hasegawa, Y., and Shishido, T. (1979). Anomalous characteristics of the microcrystalline state of SiC fibres. *Nature*, 279: 706-707.
- [8] Yajima, S. (1983). Special heat-resisting materials from organometallic polymers. *American Ceramic Society Bulletin*, 62: 893-903.
- [9] Mah, T., Hecht, N.L., McCullum, D.E., Hoenigman, J.R., Kim, H.M., Katz, A.P., and Lipsitt, H.A. (1984). Thermal stability of SiC fibres (Nicalon®). *Journal of Materials Science*, 19: 1191-1201.
- [10] Laffon, C., Flank, A.M., Lagarde, P., Laridjani, M., Hagege, R., Olry, P., Cotteret, J., Dixmier, J., Miquel, J.L., Hommel H., and Legrand, A.P. (1989). Study of Nicalon-Based Ceramic Fibres and Powders by EXAFS Spectrometry, X-ray Diffractometry and some Additional Methods. *Journal of Materials Science*, 24: 1503-1512.
- [11] Okamura, K., Shimoo, T., Suzuya, K., and Suzuki, K. (2006). SiC-based ceramic fibers prepared via organic-to-inorganic conversion process-A review. *Journal of the Ceramic Society of Japan*, 114: 445-454.
- [12] Birot, M., Pillot, J. P., and Dunogues, J. (1995). Comprehensive chemistry of polycarbosilanes, Polysilazane, and Polycarbosilazanes as Precursors of Ceramics. *Chemical Review*, 95: 1443-1447.
- [13] Yajima, S., Okamura, K., Hayashi, J., and Omori, M. (1976). Synthesis of continuous silicon carbide fibers with high tensile strength. *Journal of the American Ceramic Society*, 59: 324-327.
- [14] Hasegawa, Y., Kobori, T., and Fukuda, K. (1986). Organosilicon polymer and process for production thereof, *U.S. Patents*, No. 4-590-253.
- [15] Duboudin, F., Birot, M., Babot, O., Dunogues, J., and Calas, R.J. (1988). Catalyseurs pour la transformation de polydomethylsilane en polycarbosilanes. *Journal of Organometallic Chemistry*, 341: 125-132.

-
- [16] Kim, Y.H., Jung, S.J., Kim, H.R., Kim, H.D., Shin, D.G., and Riu, D.H. (2004). Preparation of polycarbosilane using a catalytic process. *Advances in Technology of Materials and Materials Processing*, 6: 192-195.
- [17] Shin, D.G., Riu, D.H., and Kim, H.E. (2008). Web-type silicon carbide fiber prepared by the electrospinning of polycarbosilane. *Journal of Ceramic Processing Research*, 9: 209-214.
- [18] Interrante, L.V., and Shen, Q.H., Polycarbosilanes, in: *Siliconcontaining Polymers*, Netherlands: Kluwer Academic Publishers, p. 247-321.
- [19] Interrante, L.V., Moraes, K., MacDonald, L., and Sherwood, W. (2002). Echanical, thermochemical and microstructural characterization of AHPCS-derived SiC. *Ceramic Transactions*, 144: 125-140.
- [20] Interrante, L.V., Moraes, K., Liu, Q., Lu, N., Puerta, A., and Sneddon, L.G. (2002). Silicon-based ceramics from polymer precursors. *Pure and Applied Chemistry*, 74: 2111-2117.
- [21] Whitmarsh, C.K., and Interrante, L.V. (1991). Synthesis and structure of a highly branched polycarbosilane derived from (chloromethyl) trichlorosilane. *Organometallics*, 10: 1336-1344.
- [22] Interrante, L.V., and Shen, Q.H. (2009). Hyperbranched polycarbosilanes via nucleophilic substitution reactions (Chapter 12), In: *Silicon-containing Dendritic Polymers*, Netherlands: Springer Science + Business Media B.V., p. 315-343.
- [23] Huang, T.H., Yu, Z.J., He, X.M., Huang, M.H., Chen, L.F., Xia, H.P., and Zhang, L.T. (2007). One-pot synthesis and characterization of a new, branched polycarbosilane bearing allyl groups. *Chinese Chemical Letters*, 8: 754-757.
- [24] Huang, M.H., Fang, Y.H., Li, R., Huang, T.H., Yu, Z.J., and Xia, H.P. (2009). Synthesis and properties of liquid polycarbosilanes with hyperbranched structures. *Journal of Applied Polymer Science*, 113: 1611-1618.
- [25] Yu, Z., Huang, M., Fang, Y., Li, R., Zhan, J., Zeng, B., He, G., Xia, H., and Zhang, L. (2010). Modification of a liquid polycarbosilane with 9-BBN as a high-ceramic-yield precursor for SiC. *Reactive and Functional Polymers*, 70: 334-339.
- [26] Froehling, P.E. (1993). Synthesis and properties of a new, branched polyhydridocarbosilane as a precursor for silicon carbide. *Journal of Inorganic and Organometallic Polymers*, 3: 251-258.
- [27] Yu, Z., Zhan, J., Huang, M., Li, R., Zhou, C., He, G., and Xia, H. (2010). Preparation of a hyperbranched polycarbosilane precursor to SiC ceramics following an efficient room-temperature cross-linking process. *Journal of Materials Science*, 45: 6151-6158.
- [28] Hasegawa, Y., and Okamura, K. (1983). Synthesis of continuous silicon-carbide fiber. *Journal of Materials Science*, 18: 3633-3648.
- [29] Soraru, G.D., Babonneau, F., and Mackenzie, J.D. (1988). Structural Concepts on New Amorphous Covalent Solids. *Journal of Non-Crystalline Solids*, 106: 256-261.
- [30] Soraru, G.D., Babonneau, F., and Mackenzie, J.D. (1990). Polycarbosilane to SiC Ceramics. *Journal of Materials Science*, 25: 3886-3893.
- [31] Hasegawa, Y. (1989). Synthesis of continuous silicon carbide fiber, Part 6. *Journal of Materials Science*, 24: 1177-1190.
- [32] Hasegawa, Y., and Okamura, K. (1983). Synthesis of continuous silicon-carbide fiber. *Journal of Materials Science*, 18: 3633-3648.

-
- [33] Bouillon, E., Langlais, F., Pailler, R., Naslain, R., Cruege, F., Huong, P.V., Sarthou, J.C., Delpuech, A., Laffon, C., Lagarde, P., Monthieux, M., and Oberlin, A. (1991). Conversion mechanism of a polycarbosilane precursor into an SiC-based ceramic material. *Journal of Materials Science*, 26: 1333-1345.
- [34] Ly, H.Q., Taylor, R., Day, R.J., and Heatley, F. (2001). Conversion of polycarbosilane (PCS) to SiC-based ceramic Part II, pyrolysis and characterization. *Journal of Materials Science*, 36, 4045-4057.
- [35] Monthieux, M., and Delverdier, O. (1996). Thermal behavior of (organosilicon) polymer-derived ceramics. V: Main facts and trends. *Journal of the European Ceramic Society*, 16: 721-737.
- [36] Okamura, K., Sato, M., Matsuzawa, T., and Hasegawa, Y. (1988). In: *Ultrastructure processing of advanced ceramic*, New York: Wiley, p. 501-518.
- [37] Bouillon, E., Mocaer, D., Villeneuve, J.F., Pailler, R., Naslain, R., Monthieux, M., Oberlin, A., Guimon, C., and Pfister, G. (1991). Composition microstructure property relationships in ceramic monofilaments resulting from the pyrolysis of a polycarbosilane precursor at 800 to 400 °C. *Journal of Materials Science*, 26, 1517-1530.
- [38] Sasaki, Y., Nishina, Y., Sato, M., and Okamura, K. (1987). Raman study of SiC fibers made from polycarbosilane. *Journal of Materials Science*, 22: 443-449.
- [39] Yu, Y., Tang, X., and Li, X. (2008). Characterization and microstructural evolution of SiC(OAl) fibers to SiC(Al) fibers derived from aluminum-containing polycarbosilane. *Composites Science and Technology*, 68: 1697-1703.
- [40] Li, S., Feng, Z., Mei, H., and Zhang, L. (2008). Mechanical and microstructural evolution of Hi-Nicalon Trade Mark SiC fibers annealed in O₂-H₂O-Ar atmospheres. *Materials Science and Engineering A*, 487: 424-430.
- [41] Zhang, R.-J., Yang, Y.-Q., Shen, W.-T., Wang, C., and Luo, X. (2010). Microstructure of SiC fiber fabricated by two-stage chemical vapor deposition on tungsten filament. *Journal of Crystal Growth*, 313: 51-61.
- [42] Yajima, S., Omori, M., Hayashi, J., Okamura, K., Matsuzawa, T., and Liaw, C. (1976). Simple synthesis of the continuous SiC fiber with high tensile strength. *Chemistry Letters*, 6: 551-554.
- [43] Narisawa, M., Kitano, S., Okamura, K., and Itoh, M. (1995). Synthesis of silicon carbide fiber from blended precursor of organosilicon polymers. *Journal of the American Ceramic Society*, 78: 3405-3408.
- [44] Ichikawa, H. (2006). Advances in SiC fibers for high temperature applications. *Advances in Science and Technology*, 50: 17-23.
- [45] Bernard, S., Cornu, D., Miele, P., Weinmann, M., and Aldinger, F. (2005). Polyborosilazane-derived ceramic fibers in the Si-B-C-N quaternary system for high-temperature applications. *Ceramic Engineering and Science Proceedings*, 26: 35-42.
- [46] Zhang Y., Zhang, L., Cheng, L., Mei, H., Ke, Q., and Xu, Y. (2009). Fundamental issues of applications of C/SiC composites for re-entry vehicles. *Journal of Ceramic Processing Research*, 10: 248-256.
- [47] Nozawa, T., Lara-Curzio, E., Katoh, Y., and Shinavski, R.J. (2009). Tensile properties of advanced SiC/SiC composites for nuclear control rod applications. In: *Mechanical*

properties and performance of engineering ceramics and composites III. New York: Wiley, p. 223-234.

Chapter 19

PLASMA-ASSISTED MODIFICATION OF TEXTILE YARNS IN LIQUID ENVIRONMENT

***Sergey M. Kuzmin*, Natalya P. Prorokova
and Aleksey V. Khorev***

Institute of solution chemistry RAS,
Akademicheskaya St., 1 Ivanovo, 153045, Russia.

ABSTRACT

This chapter explores ways to improve the properties of polyester material in the processing of its surface temperature plasma at atmospheric pressure. The plasma discharge was generated in a sodium hydroxide solution. During the modification process a fiber was extend through the diaphragm which placed into electrolyte solution. Electric current was passed through the diaphragm which caused the appearance of the gas-vapor bubble. If the voltage applied to the diaphragm was 0.5 – 1.5 kV, a breakdown of the gas-vapor case is generated and discharge is allowed. The method of surface modification of polymers requires relatively low voltage, and allows concentrating zone of plasma near the surface of the sample. It is shown that plasma in the liquid environment is non-equilibrium and contains the components from the liquid substance. The influence of diaphragm size and broaching speed of polyester fiber through the plant for the plasma-chemical modification to the physical-mechanical characteristics of the finished polyester fibers was studied. The main criterion for successful modification of polyethylene terephthalate material was considered to be a formation the maximum possible number of active groups on its surface with the maximum preservation of strength parameters. It is shown that the use of such method of modification provides a formation of active hydroxyl and carboxyl groups on the surface of the polymeric material which are required for fixation of functional products. Their application on the surface of fibrous material can give it some new properties (hydrophobic, antimicrobial, deodorizing, etc.).

* E-mail: smk@isc-ras.ru

1. INTRODUCTION

Application of a polyester yarn is one of the most important trends in the textile industry. Polyester yarns have several advantages: high esthetic properties and high chemical, thermal and bio stability. Products from polyester have high wrinkle resistance and form stability. All of the above mentioned features of polyester yarns and yarns ensure the priority of their application in the production of consumer goods and industrial products. Along with valuable consumer properties the polyester textile materials have imperfections. The list of polyester yarn imperfections should include:

- Slight dye ability due to compact structure of polymer;
- A small number of functional groups capable to chemical interaction;
- Increased dirt retention of products from these yarns;
- Hard by touch;
- Glass glitter;
- High hydrophobic (water sorption at a relative humidity of 63% is only 0.4%), which makes products from polyester uncomfortable to wear [1-3].

Therefore, there is a problem of modification of polyester yarns and textile materials to improving their consumer properties. Currently part of the polyester yarns are manufactured with a modification leading to improve their functional (consumer) characteristics [4-6].

Modification of yarn is one of the simplest and most promising ways to control their properties. All methods of modification can be divided into three groups:

- a) Physical - without changing the chemical composition, but with a change in supramolecular structure and the outer surface of the yarn. Typically, this method is applied at the stage of spinning or subsequent processing of yarns;
- b) Chemical - with a change in chemical structure by copolymerization upon receipt of the initial polymer or introducing new functional groups by the processing of already squeezed yarns, as well as textile fabrics or materials;
- c) Compositional - by the introduction of additives in the initial melt (solution) before or simultaneously with process of the yarn forming.

One promising direction in giving the surface of textile materials new properties is to modify them by the low temperature plasma. The plasma surface modifications in low pressure conditions (<5 Torr) are well known. The gas breakdown results in non-equilibrium "cold" plasma [7, 8]; such ionized media, are powerful surface-modification tools in Material Science and Technology. Low-pressure plasmas allow modifying the surface composition and properties of materials compatible with low-medium vacuum, through the following three general classes of processes:

- a) Plasma Enhanced Chemical Vapor Deposition (PE-CVD), deposition of organic and inorganic thin films on the initial surface with composition and properties tune able with the deposition conditions;

- b) Plasma Treatments grafting of the very thin layers (1-3 nm) of polymers (or other materials) with chemical functionalities; plasma-induced cross-linking and branching;
- c) Plasma Etching Trough-mask ablation of materials for material patterning by means of reactive species generated in the plasma, with formation of gas products.

The technologies of polymer materials modification by low-pressure plasma and the equipment for industrial application of plasmas have been already created [9]. Technology developments of surface modification at atmospheric pressure have been done too [10]. As a rule the plasma surface modifications are attractive for the application of adhesion improvement because they avoid the use of toxic chemicals, only the surface is treated while the bulk properties remain unchanged, oxygen and/or nitrogen containing functional groups are easily introduced into the surfaces, surface cleaning and weak-layer elimination can be performed simultaneously with the surface modification [11]. Though the most of plasma-chemical modification of polymeric materials are non-selective or poorly selective, that is their major drawback, since the selectivity of process is a very important for modification of textile materials. Consequently, improving a selectivity of plasma action and simplifying technological approaches is essential. This chapter explores ways to improve the properties of polyester material in the processing of its surface temperature plasma at atmospheric pressure.

2. TYPES OF LOW-TEMPERATURE PLASMA AT ATMOSPHERIC PRESSURE

A non-equilibrium plasma that can be operated without the need for expensive vacuum apparatus, thus making large-scale cost-effective continuous plasma processing readily available. There are several types of discharge at atmospheric pressure and ways to organize the interaction of plasma and the polymer sample. Main parameters of the operating modes for different types of low-temperature plasma at atmospheric pressure are presented in Table 1.

It is supposed that the increasing of selectivity of plasma action is available under plasma-solution treatment conditions [53]. This opinion is based on the assumption that the active plasma particles entering the solution from a set of secondary particles which react with the surface of the polymer material in milder conditions and as a consequence, more selectively than in the case of “dry” plasma.

The additional reasons for selection of the diaphragm glow discharges for textile treatment application are also [54]:

- a) Relatively low voltage (0.5-1.5 kV) required for igniting the discharge;
- b) The possibility of concentrating the low-temperature plasma zone near the surface of the treated sample;
- c) High degree of non-equilibrium of the plasma, which allows treating the polymer samples without destruction by the thermal effect of the plasma;
- d) Transfer of the components of the solution into the gas phase, which allows operating by the plasma composition under treatment process.

Table 1. Electrical Characteristics and Technological Effects of Discharges at Atmospheric Pressure

type	Current, mA	Voltage, V	Technological effect
Corona discharges	0,02	20000	Disinfection and air purification [12,13]; Modification of polymers surface [14, 15]; Initiation of chemical processes in solutions [16,17]*
Dielectric Barrier Discharges	1	6000-10000	Disinfection and air purification [18 – 21]; Modification of polymers surface [21 – 28]
Glow discharges, stabilized by airflow	10	20000	Initiation of chemical processes in gases [29, 30]; Initiation of chemical processes in solutions [31]*; Modification of polymers surface [32, 33]
Electric pulse machining	-	30000-50000	Extracting plant material [34]* Disinfection of liquids [35]*
Glow discharges with electrolyte cathode	20-200	400-1500	Initiation of chemical processes in solutions [17, 36 – 40]*; Modification of polymers surface [41]*; Initiation of chemical processes in gases [42]*
“Gliding arc”	6	4000-6000	Initiation of chemical processes in gases [43 – 45]; Initiation of chemical processes in solutions [46]*; Disinfection of liquids [47]*
Contact glow discharges	200	600-800	Initiation of chemical processes in solutions [17, 48 – 50]*
Diaphragm glow discharges	100-300	700-1500	Initiation of chemical processes in solutions [51]*; Disinfection of liquids [52]*

* Indicates works devoted to investigation of plasma-solution systems.

It should be noted that the diaphragm glow discharge initiation does not reverse electrochemical process on a metal electrodes in the liquid. In particular, it is likely that the described [12-52] changes of the liquid phase are caused not only by the plasma. In general, changes induced by the electrochemical stage on a solid electrode have the same direction as the plasma action. For example, influence only of electrochemical process on wastewaters allows reducing the amount of heavy metal ions [55, 56], as well as decolorize and remove the dyes or phenolic compounds [57-63]. So, the development of a method of polymer surface modification has combined nature. Chemically active agents are formed directly during the processing both in plasma and at the solid electrode placed in solution. In this method, the prospect of using the small concentrations [53] of relatively safe chemical agents for surface modification of polymers is also very attractive from both economic and environmental positions [55-65].

3. CHARACTERISTICS OF THE PLASMA IN CONTACT WITH SOLUTIONS

The experimental set up for the diaphragm glow discharges ignition (Figure 1) consist of a cell filled with conductive liquid medium (1), separated by a dielectric baffle (2) with a hole - the diaphragm (3). Electric current was passed between stainless cathode (4) and anode (5) through the diaphragm. Sufficient current density in the diaphragm caused the appearance of the gas-vapor bubble due to the Joule heating and evaporating of the liquid media. If the voltage applied to the diaphragm reach to 0.5 – 1.5 kV, a breakdown of the gas-vapor create low temperature plasma into the bubble. The experiments are shown that the dc voltage leads to significant current pulsations during diaphragm glow discharge exist in liquids. It is may be explained by pulsations of the boundary position between liquid and gas which change the discharge gap. As a consequence - to change the voltage drop across the discharge gap and the change in current density.

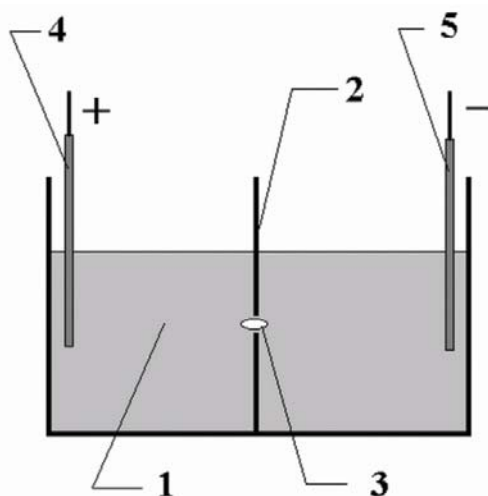


Figure 1. The experimental set up for the diaphragm glow discharges ignition.

The diaphragm glow discharges has the liquid anode on the one side, and the liquid cathode on the other side of the vapor-gas bubble. The liquid anode and liquid cathode are quite different in the electrical and chemical processes. Figure 2 shows an example of photographs of the discharge between electrolytic cathode ($0.025 \text{ mol l}^{-1} \text{ NaOH}$ solution) and copper anode obtained using differential filters. The emission of the N_2 molecular bands (filter 351 nm), H_β line (filter 652 nm) and Na doublet (filter 589 nm) are observed in the discharge radiation. Evidently, the following zones of plasma appear: 1 - cathode spot, 2 - anode spot, 3 - “dark” space, 4 - discharge channel and 5 - surrounding glow. Emission of the sodium lines arises due to the effective transfer of solute to the gas phase. High-speed mass transport through the interface associated with a high energy input in cathode area. The cathode fall consist of value 600-900 V [46, 66] and cathode current density close to 10^4 A m^{-2} [67] are approximately constant at variation of discharge current. The increasing of electrolyte concentration (in dilute solutions) result in decrease the cathode fall and increase

the cathode current density [66,67]. The spectral data demonstrate this form discharge is non equilibrium plasma with gas temperature in the range 900-2000 K, and electron temperature about 5000 - 8000 K, but estimates of temperatures near the liquid surface are quite different [66-69].

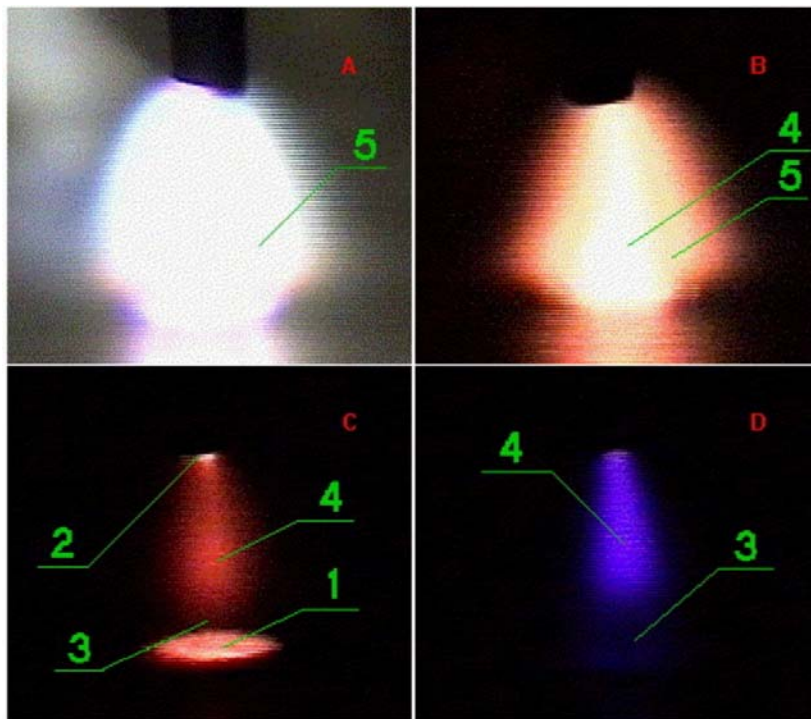


Figure 2. The images of DC discharge with 0.025 mol l⁻¹ NaOH solution as cathode. Current - 150 mA, gap - 7 mm. Different zone of discharge are shown: 1 - cathode spot; 2 - anode spot; 3 - dark space; 4 - plasma channel; 5 – surrounding glow.

If the electrolyte solution is used as anode the discharge is quite different: the dark space is near the liquid again, the discharge channel disappeared, and anode area looks like a lot of blue spots moved on the surface. The anode fall is around 200 V that evokes the much weaker velocity of evaporation than on the cathode border. The differences between the cathode and anode boundary leads to the fact that in the diaphragm discharge (Figure 3) the substance evaporating in the field of liquid cathode are condensed on the surface of liquid anode. So, if diaphragm glow discharge is ignited the plasma are a "pump" for the substance of the cathode to the anode moved ("Pumping" effect is highly dependent on the geometry of the diaphragm [70]). At the same time the gas-vapor bubble are displaced from anode to cathode if the shapes of diaphragm allow it. The accuracy measurements of the gas or electron temperature in the plasma of diaphragm glow discharges are difficult due to fast dynamic behavior. Though the estimation are shown that temperatures of plasma components are similar to plasma with electrolyte cathode under the same current.



Figure 3. The images of DC discharge with 0.025 mol l^{-1} NaOH solution as anode. Current - 150 mA, gap - 7 mm.

4. THE TREATMENT PROCESS

4.1. Technical Aspect

The device used to treat textiles by the diaphragm glow discharge is shown in Figure 4. The apparatus is a container consisting of discrete modules of metal (1) and (2) interconnected insulating septum (3). In the septum inserted diaphragm (4) special forms through which the stretch yarn (5). For plasma-chemical treatment process the yarn coiled on the slave cylinder (6), is passed through guide rollers and a diaphragm (4) and fixed on the head drum (7). Voltage are applied to the stainless steel electrodes (8,9), located in the modules (1) and (2) after broaching the thread is enabled to adjust the speed.

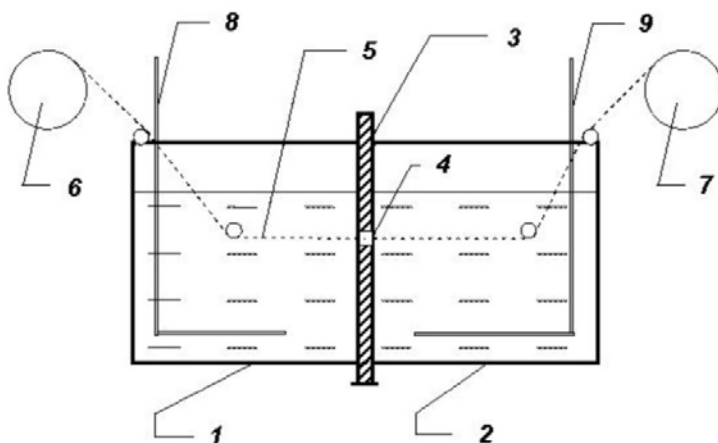


Figure 4. Schematic diagram of the processing of yarn into diaphragm discharge.

The treatment process using cylindrical aperture in the form presented in the photo (Figure 5). The shape of the diaphragm has a significant influence on the treatment process. First of all the changing the length and diameter or aperture leads to a change in average current density and voltage. Besides, the size and shape of the aperture affects the dynamics of gas-vapor bubble boundary and the hydrodynamics of the surrounding solution. More over, the mechanical loads exerted on the thread of the passage of the diaphragm at a given speed extremely depend on shape of aperture. In particular, during the process using the aperture of cylindrical shape at yarn feed speed more 20 m min^{-1} evokes disarranges of the yarns (Figure 6b) due to its mechanical contact with the diaphragm.



Figure 5. Photo of treatment process using diaphragm glow discharge with cylindrical aperture.

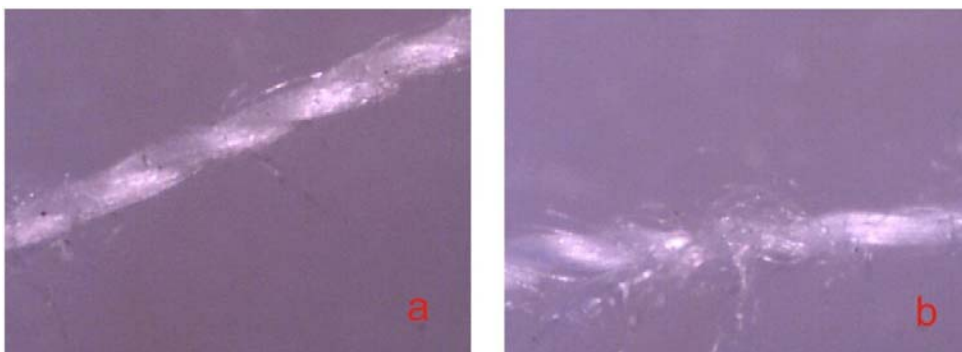


Figure 6. Photos original yarn (a); mechanically damaged by pulling the yarn through the diaphragm (b).

The nozzle tape diaphragm (Figure 7) allows avoiding mechanical damage of polyester yarns at high speed broaching the thread through the diaphragm. Additionally, high speed of

yarn in the discharge region leads to short time contact with a hot gas region, therefore the high temperature destruction of polymer are eliminated.

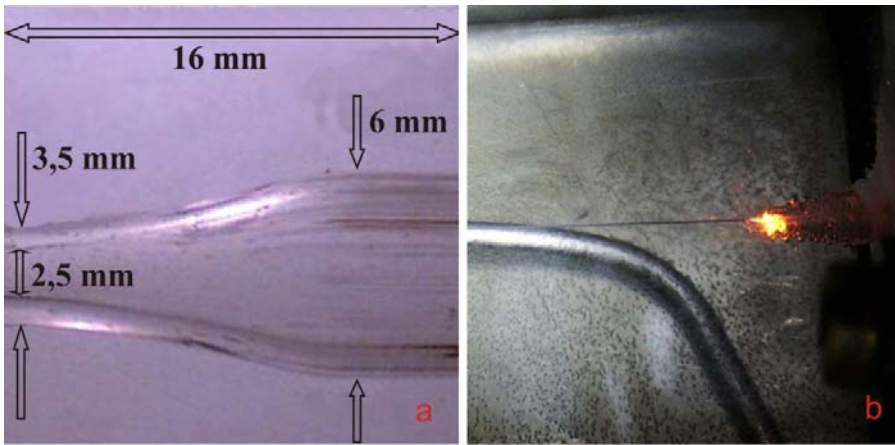


Figure 7. Aperture for high speed broaching (a) and process at high speed broaching of yarn (b).

The average voltage applied to the electrodes of the cell for the quasi stationary diaphragm glow discharge treatment increase if increase in speed broaching threads (Figure 8). (This is understandable, on the one hand, the stand with the yarns is heated, therefore, actively dissipates the energy deposited in the discharge. On the other hand, moving the thread deforms the vapor-gas shell, extending the discharge). This is understandable when one considers that extend a thread from one side, heats up, therefore, actively dissipates the energy deposited in the discharge. On the other hand, moving the thread deforms the vapor-gas shell, extending the discharge gap (Figure 5, 7).

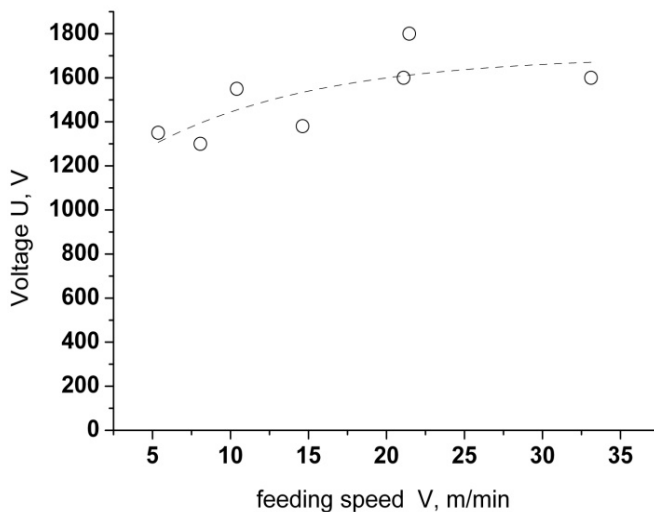


Figure 8. Effect of feeding speed of polyester yarns to the voltage necessary to maintain the discharge. Electrolyte - a solution of NaOH with a concentration of 0.075 mol l^{-1} , electrolyte temperature 25°C .

4.2. Fundamental

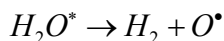
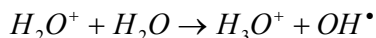
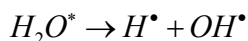
The treatment process has a combining effect that includes:

- impregnation of an electrolyte solution;
- plasma treatment when threading through the diaphragm;
- effect of activated electrolyte on the surface of yarn-activated plasma.

Sorbed liquid yarn, primarily is the yarn protection from harsh effects of high temperature and high reactivity of active species generated by plasma discharge orifice. The liquid retained on the yarn, primarily, is protecting the yarn from harsh effects of high temperature and high reactivity of active species generated by plasma diaphragm glow discharge. Nevertheless, the temperature gradient between the plasma and the solution, as well as between plasma and polymer material processed is significant. As a result, the surface layer of the material experiencing heat stroke, that leads to change in structure. Simultaneously, the plasma-chemical modification of the surface layer is going. The plasma-chemical processes are extremely depending on plasma composition. In our case, of course, the main component of the plasma is water vapor. It is well known that during treatment in such plasma formation of free radicals, crosslinking of macromolecules and oxidative chemical reactions are happened in the surface layer [11, 71, 72].

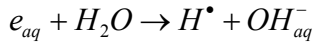
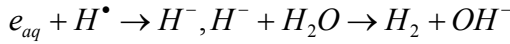
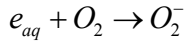
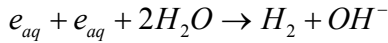
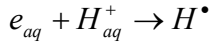
It should be noted that the area adjacent to the plasma solution is also an active reaction zone. This is especially pronounced when the electrolyte acts as a cathode for discharge, because the surface of the solution is bombarded with positive ions injected from the plasma zone. The energy of these ions, according to estimations of the cathode potential difference, should be several hundred electron-volts [46, 66-69]. We know that ion bombardment causes radiochemical effects. In drawing the analogy between radiochemical [73] and plasma initiation of a chemical process, we will hypothesize that the system examined has three stages of reaction of the bombarding ion with the solution: physical, physicochemical, and chemical. In the physical stage, excited molecules of water, H_2O^+ ions, and secondary electrons are formed in the water.

In the physicochemical stage, the excited molecules dissociate, and the primary molecular ion reacts with water molecules:

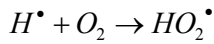
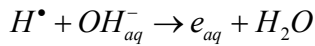


The electrons are the rmolyzed after $\sim 10^{-13}$ sec and are hydrated after $\sim 4 \cdot 10^{-13}$ sec. At the end of the physicochemical stage (approximately 10^{-12} sec), e_{aq}^- , H^\bullet , OH^\bullet , OH_{aq}^+ , O^\bullet , and H_2 exist in the water. However, due to high reactivity, the primary active particles are transformed, and the abbreviated list is given in the following list of reactions [74, 75]:

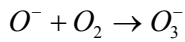
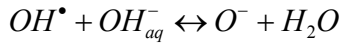
➤ solvated electrons



➤ H^\bullet atoms



➤ OH^\bullet and O^\bullet radicals



The effectiveness of activation processes in solution can obviously not be considered as the sum of the yields of the basic active particles H^\bullet , OH^\bullet , and e_{aq}^- , whose lifetime in solution is extremely short. Moreover, we should hypothesize that the primary active particles can only enter into bulk reactions directly at the cathode spot. More stable secondary active particles will participate in heterogeneous processes.

4.3. Application and Result

Treatment was realized with sodium hydroxide solutions with a concentration of 0.05, 0.075, and 0.125 M. The voltage on the electrodes necessary for igniting the discharge was determined experimentally for each of the thread drawing speeds. The residence time of the thread in the solution of the reagent was 0.15-2.3 sec, and the contact time with the plasma diaphragm discharge constituted 10^{-4} - 10^{-3} sec.

The formation of as large as possible a number of active groups on the surface with maximum preservation of strength indexes was the basic criterion of successful modification

of the polyester (poly(ethylene terephthalate)-PET) yarns. The appearance of active groups on the surface of the polymer material was demonstrated by IR spectroscopy (MFTIR) and they were identified in the same way. Due to the fact that the IR spectroscopy of yarn by the MFTIR method leads to large errors, we did the IR spectroscopy of PET film treated as a narrow band.

The number of surface-localized active groups was estimated by colorimetry [76] adapted by us for estimating the hydroxyl group content on the surface of polyester materials. It is based on the capacity of active dichlorotriazine dyes to form a covalent bond with the poly(ethylene terephthalate) hydroxyl group. The dye active dichlorotriazine bright blue KX was used in the study. The samples were dyed by standard technology for active dyes with index X [77]. The amount of dye fixed in the yarn was determined by the difference in the dye intensity of modified and unmodified polyester yarn. The dye intensity was evaluated with the color characteristics of samples of dyed polyester material, determined with the color-measuring complex in the Kolorist program (version 4.2.1994, 99, by V. S. Pobedinskii, F. Yu. Telegin, and I. A. Danilin). The strength of the treated thread was evaluated by the breaking load, measured with a RM-3-1 tensile testing machine according to GOST 6611.2-73.

The change in the chemical composition of the surface layer was judged with the IR spectra of the polyester film undergoing plasma-chemical treatment obtained by MFTIR (Figures 9, 10). The values of the relative intensity of the fundamental vibrations of the bands in the IR spectra are reported in Table 1.

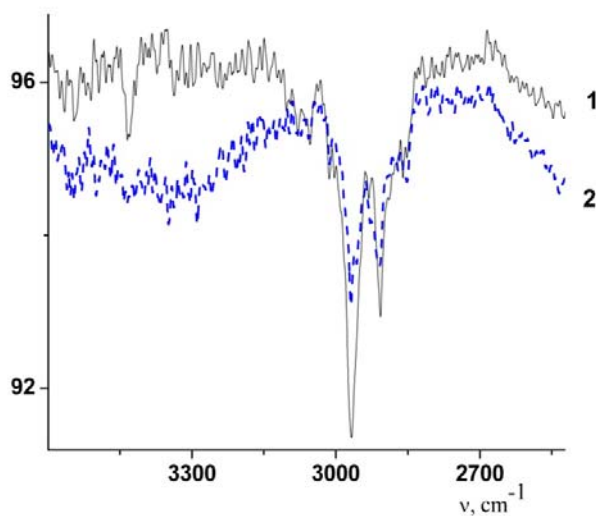


Figure 9. Vibration spectra (2600-3600 cm^{-1} range) of untreated polyester film (1) and film undergoing plasma-chemical modification (2).

The appearance of a band in the 3200-3500 cm^{-1} region (Figure 9) indicates the formation of OH groups. The spectra obtained are the basis for concluding that the processes that take place in poly(ethylene terephthalate) in combined treatment with sodium hydroxide and plasma are not limited to breaking of complex ester bonds. The increase in the intensity of the vibration bands characterizing C=O groups (1697 and 1712 cm^{-1} , Figure 10) is evidence of

the formation of carbonyl and/or carboxyl groups. Their formation can be considered an advantage of the plasma-chemical method in comparison to the chemical method [78], since many functional preparations are fixed on carboxyl groups. In addition, the intensity of the characteristic band of the $\text{CH}_2\text{—O—CH}_2$ oxygen bridge in the 1066 cm^{-1} region (indicated by the arrow in Figure 10) increases.

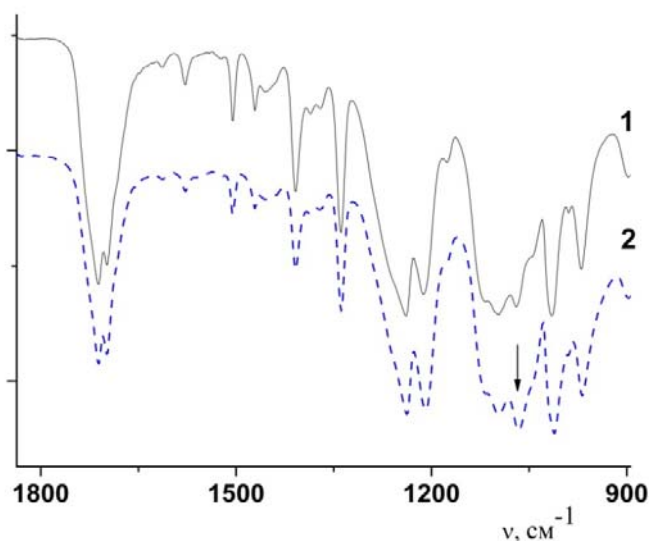


Figure 10. Vibration spectra ($900\text{--}1800\text{ cm}^{-1}$ range) of untreated polyester film (1) and film undergoing plasma-chemical modification (2).

The degree of ordering of the polymer can be judged by the ratio of the intensities of conformation-sensitive bands. The differences in the spectra of amorphous and partially crystallized obtained are the basis for concluding that the processes that take place in poly(ethylene terephthalate) are related to the predominant state of the $\text{—OCH}_2\text{—CH}_2\text{O—}$ group in the gauche conformation for the amorphous phase and in the trans conformation for the crystalline phase. According to this, the bands at 1473 , 1343 , 1120 , 937 , and 845 cm^{-1} characterize the ordered state of the polymer, while the bands at 1455 , 1370 , 1100 , 1042 , and 897 cm^{-1} characterize the disordered state. The bands are related to each other by pairs due to the possibility of conformational transitions: 1343 and 1370 , 973 and 1042 , 897 and 8435 cm^{-1} [79].

As the analysis of the ordering and disordering bands in the IR spectra showed, a tendency toward a slight increase in the amorphism of the surface layer of the polymer appears as a result of plasma-chemical modification.

The effect of the conditions of plasma-chemical treatment of poly(ethylene terephthalate) thread on the number of active groups formed was judged with the dependences in curves 1-3 in Figure 10. As we see, the maximum number of hydroxyl groups on the surface of the yarn is formed at a low (15-20 min) speed of drawing the thread through the plasma zone. This speed ensures a prolonged exposure time of the polymer material to the modifying factors. Changing the concentration of sodium hydroxide in the solution significantly affects the number of active groups formed. The formation of hydroxyl groups could be the result of

both hydrolytic degradation of the poly(ethylene terephthalate) macromolecules and destruction of ester bonds in the polymer in bombardment with the high-energy particles generated by the plasma. In both cases, the consequence of degradation of poly(ethylene terephthalate) molecules located on the surface should be a decrease in the strength of the treated polyester thread, which is confirmed by curves 1'-3' in Figure 11, characterizing the dependence of its breaking load on the drawing rate through the plasma zone. It follows from Figure 10 that in contrast to chemical modification, where the strength of the thread remains close to the initial value [78], the breaking load of the thread decreases significantly as a result of plasma-chemical treatment — to 55% (the breaking load of the initial thread is 1180 N). The maximum loss of strength is observed in drawing the thread through the plasma zone at a low speed (9-15 m min⁻¹) which provides for a contact time with the solution of 2-2.5 sec, of which the contact time with the plasma is approximately 2·10⁻³ sec. Thermal degradation of the thread due to local overheating in the plasma zone could play the decisive role in this case.

Table 2. Relative Intensity of Fundamental Vibration Bands in the IR Spectrum of Polyester Film

Wavelength, cm ⁻¹	Type of vibration*	Relative intensity	
		initial	after plasma-chemical modification
1712	ν (C=O)	2.04	2.5
1697	ν (C=O)	1.87	2.33
1473	δ (CH ₂) ordering	0.44	0.36
1455	δ (CH ₂) disordering	0.26	0.23
1410	Stretching vibrations of the chain as a whole (internal standard [68])	1	1
1120	ν (C–O) ordering	1.5	1.83
1100	ν (C–O) disordering	1.38	2.03
1066	ν (CH ₂ –O–CH ₂)	1.42	2.29
973	γ (O–C)	1.08	1.57
897	γ (CH ₂) disordering	0.37	0.39
875	Stretching vibrations of the chain as a whole	1.29	1.53
845	γ (CH ₂) ordering	1.04	1.31
793	γ (C=O) + δ (C–CO)	0.67	0.81

*The type of vibration is indicated by the Greek letters: ν- stretching, δ — deformation, γ — out-of-plane.

The breaking load of the thread also decreases with an increase in the concentration of sodium hydroxide in the solution. In passing the thread through the plasma zone at the rate of 50 m/min (0.18 sec treatment time), generation in a 0.05 M sodium hydroxide solution, the strength decreases by 3%, while it decreases by 18% in a 0.125 M solution. These data indicate the important contribution of alkaline hydrolysis of the poly(ethylene terephthalate) initiated by the plasma to degradation of the polymer material. At the same time, as the dependence of the breaking load of the thread on the increase in the hydroxyl group content in

Figure 12 shows, important formation of an additional number of active groups does not occur with a significant decrease in the breaking load. This is probably due to so-called “scouring” of the surface of the yarn forming the thread, whose essence consists of rapid and intense degradation of the surface layers of the polymer material with formation of low-molecular-weight products of hydrolysis that pass into the solution. As a result of this process, most of the active functional groups are removed from the surface. This same event can also explain why the conditions of maximum degradation of poly(ethylene terephthalate) and consequently the greatest decrease in the breaking load of the thread do not coincide with the conditions of formation of the maximum number of hydroxyl groups (see Figure 11) — the number decreases, in all probability, as a result of “scouring.” A similar event is observed in chemical activation of the surface of polyester materials made by treating them with solutions of bases of much higher concentration for 10–30 min [78]. However, in milder conditions of plasma-chemical treatment (high thread speed and low concentration of alkali), “scouring” does not take place, which preserves a relatively large number of active groups on the surface. The analysis of the data in Figs. 11 and 12 allows selecting the conditions of plasma-chemical modification of poly(ethylene terephthalate) thread that ensures an acceptable level of loss of strength (maximum of 15%) in formation of a larger number of active groups on the surface of the thread than in alkaline activation of the polyester material [78]: 0.75 M concentration of sodium hydroxide, 30–50 m min⁻¹ speed of passage of the sample through the plasma zone.

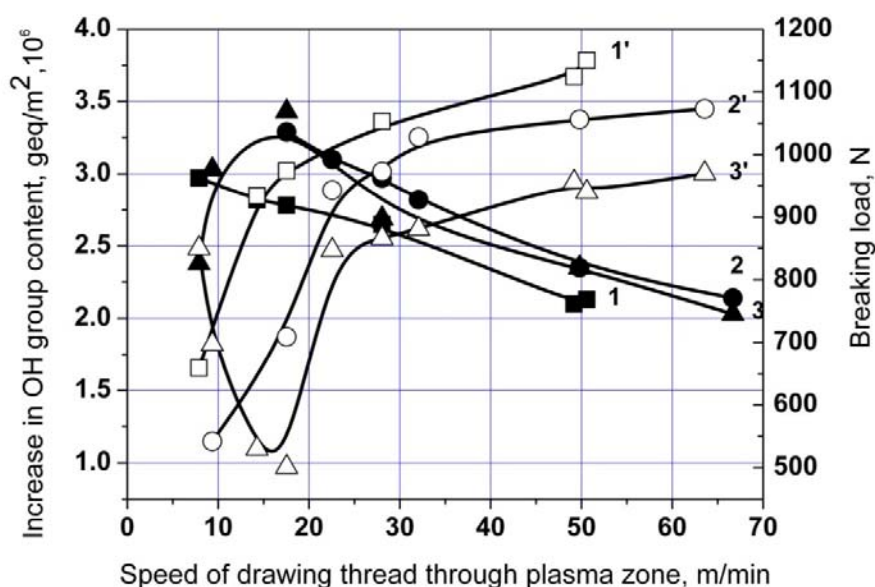


Figure 11. OH group content (1–3) and breaking load (1'–3') of poly(ethylene terephthalate) thread as a function of drawing speed through the plasma zone in sodium hydroxide solutions of different concentration (in M): 1, 1') 0.05; 2, 2') 0.075; 3, 3') 0.125.

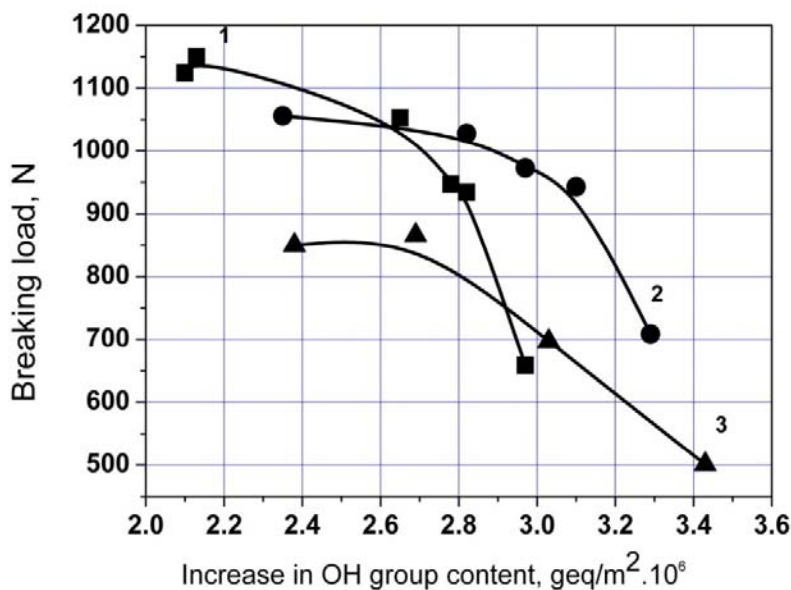


Figure 12. Breaking load of poly(ethylene terephthalate) thread as a function of its hydroxyl group content in treatment with diaphragm discharge in sodium hydroxide solution of varying concentration (in M): 1 - 0.05; 2 - 0.075; 3 - 0.125.

CONCLUSION

We have developed the plasma-chemical method of the polyester surface modification. The method like the chemical way of polyester modification is based on the controlled hydrolysis of poly(ethylene terephthalate) macromolecules in the surface layer of polymer yarns. As a result active functional groups are generated in the surface layer. The hydrolysis is initiated due to plasma treatment of the polymer surface. The atmospheric pressure discharge is generated in a diaphragm placed into electrolyte solution.

The suggested method was realized for the purpose of plasma-solution modification of the polyester yarns. The characteristics of the method are: (1) rather low voltage necessary for the discharge firing; (2) discharge localization which allows to concentrate low-temperature plasma zone near the polymeric surface; (3) high degree of non-equilibrium state of plasma that allows to treat yarns without thermal damage; (4) the possibility to form the composition of the orifice gas due to the transfer of solution components through the interphase boundary. The authors have studied the influence of the diaphragm size and treatment duration on the mechanical and chemical properties of yarns. The optimal treatment parameters for the effective formation of a new functional group and simultaneous minimization of mechanical properties degradation are obtained.

REFERENCES

- [1] Pakshver, A.B. (1976). Svoystva i osobennosti pererabotki khimicheskikh volokon *Khimiya*, Moscow, 496 s. (Rus.)
- [2] Krichevskiy G.E. (2000). Khimicheskaya tehnologiya tekstilnih materialov. *Uchebnik dlya vuzov v 3 tomah. RosZITLP*, Moscow, T. 1, 436 s. (Rus.)
- [3] McGregor, R., and Peters, R.H. (1968). Some Observations on the Relation between Dyeing Properties and Fibre Structure // *Journal Society. Dyers and Color*, 84(5): 267 – 276.
- [4] Ayzenshtayn, E.M. (2005). Fizichskaya i khimicheskaya modifikaciya poliefirnih volokon s cel'yu uluchsheniya svoystv gotovih izdeliy *Khimicheskiye volokna*, 6: 37 – 42. (Rus.)
- [5] Perepyeolkin, K.E. (2000). Khimicheskiye volokna. Nastoyashee i budushee. Vzgl'yad v sleduyushcheye stoletie. Chast' 1. *Khimicheskiye volokna*, 5: 3 – 16. (Rus.)
- [6] Perepyeolkin, K.E. (2000). Khimicheskiye volokna. Nastoyashee i budushee. Vzgl'yad v sleduyushcheye stoletie. Chast' 2. *Khimicheskiye volokna*, 6: 3 – 14. (Rus.)
- [7] [http://en.wikipedia.org/wiki/Plasma_\(physics\)](http://en.wikipedia.org/wiki/Plasma_(physics))
- [8] Paul, M. (2006). *Belland Fundamentals of Plasma Physics* Cambridge University Press: 628
- [9] <http://www.europlasma.be/pageview.aspx?id=130andmid=57>
- [10] <http://tri-star-technologies.com/about/industry.php>
- [11] *Plasma technologies for textiles* Ed. by R. SHISHOO//Woodhead Publishing Ltd. (Feb 2007) Pages: 360
- [12] Kurdel, M., and Morvova, M. (1997). Dc corona discharge influence on chemical composition in mixtures of natural gas with air and its combustion exhaust with air *Czechoslovak journal of physics*,. 47(2): 205 – 215.
- [13] Eichwald, O., Guntoro, N.A., Yousfi, M., and Benhenni, M. (2002). Chemical kinetics with electrical and gas dynamics modelization for NO_x removal in an air corona discharge, *Journal Physical D: Applied Physics*, 35(5): 439 – 450.
- [14] Lukin Yu. Obrabotka poverhnosti materialov koronnim pazpyadom Flexo Plus (2002). No. 3 (27), No. 4(28), http://www.flexoplus.ru/issues/f_iss33.html (Rus.)
- [15] Guimond, S., Radu, I., Czeremuszkina, G., Carlsson, D.J., and Wertheimer, M.R. (2002). Biaxially Oriented Polypropylene (BOPP) Surface Modification by Nitrogen Atmospheric Pressure Glow Discharge (APGD) and by Air Corona. *Plasmas and Polymers*, 7(1): 71 – 88.
- [16] Brisset, J.L. (1997). Air corona removal of phenols, *Journal Applied Electrochemistry*, 27(2): 179 – 183.
- [17] Kuzmin, S.M., Maximov, A.I., Sergeeva, I.N. (1997). Initiation of dye oxidation processes by non-equilibrium plasma on vacuum and plasma-solution systems. *Textile Chemistry*, 2(11): 68 – 70.
- [18] Bugaev, S.P., Kozyrev, A.V., Kuvshinov, V.A., Sochugov, N.S., and Khryapov, P.A. (1998). Plasma-Chemical Conversion of Lower Alkanes with Stimulated Condensation of Incomplete Oxidation Products, *Plasma Chemistry and Plasma Processing*, 18(2): 247 – 261.

-
- [19] Liu C.-J., Xue B., Eliasson B., He F., Li Y. and Xu G.-H. Methane Conversion to Higher Hydrocarbons in the Presence of Carbon Dioxide Using Dielectric-Barrier Discharge Plasmas // *Plasma Chemistry and Plasma Processing*, Vol. 21, No. 3, 2001, pp. 301-310
- [20] Lee H.M., Chang M.B. Gas-Phase Removal of Acetaldehyde via Packed-Bed Dielectric Barrier Discharge Reactor Plasma Chemistry and Plasma Processing (2001) Vol. 21, No. 3, pp. 329 – 343
- [21] Ma H., Chen P., Zhang M., Lin X., Ruan R. Study of SO₂ Removal Using Non-thermal Plasma Induced by Dielectric Barrier Discharge (DBD) Plasma Chemistry and Plasma Processing (2002) Vol. 22, No. 2, pp. 239 – 254
- [22] Massines, F., Messaoudi, R., and Mayoux, C. (1998). Comparison between Air Filamentary and Helium Glow Dielectric Barrier Discharges for the Polypropylene Surface Treatment. *Plasmas and Polymers*, 3(1): 43 – 59.
- [23] Borcia, G., Anderson C.A., and Brown N.M.D. (2004). The surface oxidation of selected polymers using an atmospheric pressure air dielectric barrier discharge Part I, *Applied Surface Science*, 221: 203 – 214.
- [24] Seebock, R., Esrom, H., Charbonnier, M., Romand, M. (2000). Modification of Polyimide in Barrier Discharge Air-Plasmas: Chemical and Morphological Effects. *Plasmas and Polymers*, 5(2): 103 – 118.
- [25] Massines, F., Gouda, G., Gherardi, N., Duran, M., and Croquesel, E. (2001). The Role of Dielectric Barrier Discharge Atmosphere and Physics on Polypropylene Surface Treatment. *Plasmas and Polymers*, 6(1-2): 35 – 48
- [26] Xu, X. (2001). Dielectric barrier discharge - properties and applications. *Thin Solid Films*, 390: 237 – 242.
- [27] Rehn, P., and Viol, W. (2003). Dielectric barrier discharge treatments at atmospheric pressure for wood surface modification. *Holz als Roh- und Werkstoff*, 61: 145 – 150
- [28] Bente, M., Avramidis, G., Forster, S., Rohwer, E.G., and Viol W. (2004). Wood surface modification in dielectric barrier discharges at atmospheric pressure for creating water repellent characteristics. *Holz als Roh- und Werkstoff*, 62: 157 – 163.
- [29] Akishev, Yu.S., Napartovich, A.P., Trushkin, N.I. (2003). Stacionarniy tleyuschiy pazryad atmosfernogo davleniya v vozduhe: fizika, tehnika, prilogenie XXX Zvenigorodskaya konferenciya po fizike plazmi i UTS, 24 – 28 Feb. 2003. (Rus.)
- [30] Castro, J.B., Guerra-Mutis, M.H., Dulce, H.J.M. (2003). Atmospheric Pressure RF (13.56 MHz) Glow Discharge: Characterization and Application to “In Line”. *Waste Water Treatment Plasma Chemistry and Plasma Processing*, 23(2): 297 – 307.
- [31] Kazuhiko, H., Takeru, O., Toshiro, K., Rikizo, H., and Hiroyuki, Y. (2005). Development of a Plasma Source Using Atmospheric-Pressure Glow Discharge in Contact with Solution. *Journal Plasma Fusion Research*, 81(6): 417 – 418.
- [32] Kelly-Wintenberg, K., Montie, T.C., Brickman, C., Roth, J.R., Carr, A.K., Sorge, K., Wadsworth, L.C., and Tsai, P.P.Y. (1998). Room temperature sterilization of surfaces and fabrics with a One Atmosphere Uniform Glow Discharge Plasma. *Journal of Industrial Microbiology and Biotechnology*, 20: 69 – 74.
- [33] Temmerman, E., Akishev, Yu, Trushkin, N., Leys, C., and Verschuren, J. (2005). Surface modification with a remote atmospheric pressure plasma: dc glow discharge and surface streamer regime. *Journal Physics. D: Applied Physics*, 38: 505 – 509.

-
- [34] Gorohova, V.G., Petrushenko, L.N., Shishko, A.A., Chernova, V.G., Ivanova, N.V., Kolamakina, O.A., Koshilev, N.A., Babakin, V.A., and Voronkov, M.G. (1995). Impulsnaya mekhanochivicheskaya obrabotka polimerov rastitel'nogo proishogdeniya. *Doklady Akademii Nauk*, 343(1): 62 – 64. (Rus.)
- [35] Goldaev, V.S. (1994). Obezrazagivanie gidkih materialov visokovol'nimi razryadami. *Elektonnaya Obrabotka Materialov*, 2 s: 70-73.
- [36] Gao, J., Liu, Y., Yang, W., Pu, L., Yu, J., and Lu, Q. (2005). Aqueous p-nitrotoluene oxidation induced with direct glow discharge plasma Central. *European Journal of Chemistry*, 3(3): 377 – 386.
- [37] Gao, J., Wang, X., Hu, Z., Deng, H., Hou, J., Lu, X., and Kang, J. (2003). Plasma degradation of dyes in water with contact glow discharge electrolysis. *Water Research*, 37(2): 267 – 272.
- [38] Harada, K., and Suzuki, S. (1997). Formation of amino acids from elemental carbon by contact glow discharge electrolysis. *Nature*, 266: 275 – 276.
- [39] Gao, J., Yu, J., Lu, Q., Yang, W., Li, Y., and Pu, L. (2004). Plasma Degradation of 1-Naphthylamine by Glow-discharge Electrolysis. *Pak. Journal Biological Science*, 7(10): 1715 – 1720.
- [40] Goodwin, A., Herbert, T., Leadley, S., and Swallow, F. Atmospheric pressure liquid deposition – a new route to high performance coatings www.sonotek.com/techdocs/atmospheric_pressure.pdf
- [41] Nikiforova, T.E., Bagrovskaya, N.A., Kozlov, V.A., Lilin, S.A., Maximov, A.I. and Sergeeva, I.N. (2003). Sposob izvlecheniya ionov tyagolih metalov iz vodnih rastvorov Pat. RF No. 2217389, B.I. No. 33, 2003
- [42] Suzuki, T., Ishihara, T., Shimosato, T., Yamazaki, T., and Wada, S. DC (1998). Plasma-assisted synthesis of diamond and alumina using liquid. *Journal European Ceramic Society*, 18(2): 141 – 145.
- [43] Czernichowski, A. (1994). Gliding arc. Applications to engineering and environment control. *Pure and Applied Chemistry*, 66(6): 1301 – 1310.
- [44] Czernichowski, A., and Ranaivosoloarimanana, A. (1996). Zapping VOCs with a discontinuous electric arc. *Chemistry and Technology*, 26(4): 45 – 49.
- [45] Kalra, C.S., Matveev, I., Gutsol, A., and Fridman, A. (2004). Transient Gliding Arc for Fuel Ignition and Combustion Control
- [46] www.plasmacombustion.com/publications/Combustion2004-TornadoGA.pdf
- [47] Janca, J., Kuzmin, S., Maximov, A., Titova, J., and Czernichowski, A. (1999). Investigation of the Chemical Action of the Gliding and "Point" Arcs Between Metallic Electrode and Aqueous Solution Plasma. *Chemistry and Plasma Processing*, 19(1): 53 – 67.
- [48] Moreau, M., Feuilloley, M.G.J., Orange, N., and Brisset, J.-L. (2005). Lethal effect of the gliding arc discharges on *Erwinia* spp. *Journal Applied Microbiology*, 98(5): 1039 – 1046.
- [49] Denaro, A.R., and Hickling, A. (1958). Glow discharge electrolysis in aqueous solution. *Journal of Electrochemical Society*, 105(5): 265-270.
- [50] Almubarak M.A., and Wood A. (1977). Chemical action of glow discharge electrolysis of ethanol in aqueous solution. *Journal of Electrochemical Society*, 124(9): 1356 – 1360.

-
- [51] Kravchenko, A.V., Berlizova, S.A., Nesterenko, A.F., and Kublanovskii, V.S. (2004). On the Change in Properties of Water Subjected to Low-Temperature Plasma Electrolysis. *High Energy Chemistry*, 38(5): 333 – 337.
- [52] Telyashov L.L. (1989). Osobennosti razvitiya “besproboynogo” razryada v gidkosti. *Elektonnaya Obrabotka Materialov*, 2s.: 38 – 41 (Rus.).
- [53] Sroykova, I.K. (2001). Khimichsraya aktivaciya vodnih rastvorov elektrolitov tleyuschim I diafragmennim gazovimi razryadami PhD Thesis, Ivanovo, 2001 (Rus.).
- [54] Kutepov, A.M., Zakharov, A.G., Maximov, A.I. (2004). Vakuumno-plazmennoe i plazmenno- rastvornoe modifitsirovanie polimernykh materialov. M.: *Nauka*, 496 s. (Rus.)
- [55] Kuzmin, S.M., Vavilova, S.Yu., Prorokova, N.P., Bagrovskaya, N.A. (2006). Maintenance of plasma chemical modifying of textile materials at atmospheric pressure Izvestiya VUZov. *Khimiya I Khimicheskaya tehnologiya* (2006) Vol.49, No. 8. pp. 66 – 70 (Rus.)
- [56] Abuzaid, N.S., Bukhari, A.A., and Al-Hamouz, Z.M. (2002). Ground water coagulation using soluble stainless steel electrodes. *Advances in Environmental Research*, 6: 325 – 333.
- [57] Adhoum, N., Monser, L., Bellakhal, N., and Belgaied, J.E. (2004). Treatment of electroplating wastewater containing Cu^{2+} , Zn^{2+} and Cr^{6+} by electrocoagulation. *Journal of Hazardous Material*, 112: 207 – 213.
- [58] Adhoum, N., and Monser, L. (2004). Decolorization and removal of phenolic compounds from olive mill wastewater by electrocoagulation. *Chemical Engineering Process*, 43: 1281 – 1287.
- [59] Aleboyeh, A., Daneshvar, N., and Kasiri, M.B. (2008). Optimization of C.I. Acid Red 14 azo dye removal by electrocoagulation batch process with response surface methodology. *Chemical Engineering and Processing*, 47: 827 – 832.
- [60] Alinsafi, A., Khemis, M., Pons, M.N., Leclerc, J.P., Yaacoubi, A., Benhammou, A., and Nejmeddine, A. (2005). Electrocoagulation of reactive textile dyes and textile wastewater. *Chemical Engineering and Processing: process intensification*, 44: 461 – 470.
- [61] Aoudj, S., Khelifa, A., Drouiche, N., Hecini, M., and Hamitouche, H. (2010). Electrocoagulation process applied to wastewater containing dyes from textile industry. *Chemical Engineering and Processing*, 49: 1176 – 1182.
- [62] Aouni, A., Fersi, C., Ali, M.B.S., and Dhahbi, M. (2009). Treatment of textile wastewater by a hybrid electrocoagulation/nanofiltration process. *Journal of Hazardous Materials*, 168: 868 – 874.
- [63] Clarke, E.A. and Anliker, R. (1980). Organic dyes and pigments In: Handbook of environmental chemistry, anthropogenic compounds, 3, part A. New York: Springer-Verlag, 181 – 215.
- [64] Holt, P.K., Barton, G.W., and Mitchell, C.A. (2001). The role of current in determining pollutant removal in a batch electrocoagulation reactor In: 6th World Congress of Chemical Engineering Conference Media CD, Melbourne, Australia.
- [65] Aksu, Z. (2005). Application of biosorption for the removal of organic pollutants: a review. *Process Biochemistry*, 40: 997 – 1026.

-
- [66] Aksu, Z., and Tezer, S. (2000). Equilibrium and kinetic modeling of biosorption of Remazol Black B by *R. arrhizus* in a batch system: effect of temperature. *Process Biochemistry*, 36: 431 – 439.
- [67] Titov, V.A., Rybkin, V.V., Maximov, A.I., Smirnov, S.A., Kulentsan, A.L., and Choi, H.S. (2005). Characteristics of atmospheric pressure air glow discharge with aqueous electrolyte cathode. *Plasma Chemistry and Plasma Processing*, 25: 503 – 518.
- [68] Kuzmin, S., and Janca, J. (1998). The characteristics of the DC discharge between metal electrode and water electrolyte solution as cathode at air under atmospheric pressure 11th Simp. On Elementary Processes and Chemical Reaction In Low Temperature Plasma, Low Tatras, June 22-26, pp.106 – 108
- [69] Kuzmin S., Janca J The interaction of water electrolyte solution as cathode and plasma of DC discharge in air under atmospheric pressure International symposium on high pressure low temperature plasma chemistry "HAKONE VI", Kork, Ireland, August 31-Sept. 2 1998, pp. 138 – 140
- [70] Mezei, P., and Cserfalvi, T. (2007). Electrolyte Cathode Atmospheric Glow Discharges for Direct Solution Analysis. *Applied Spectroscopy Reviews*, 42: 573 – 604.
- [71] De Baerdemaeker, F., Simek, M., Leys, C., and Verstraete, W. (2007). Pump Effect of a Capillary Discharge in Electrically Conductive Liquids Plasma. *Chemistry and Plasma Processing*, 27: 473 – 485.
- [72] Klomp, A.J.A., Terlingen, J.G.A, Takens, G.A.J., Strikker, A., Engbers, G.H.M., and Feijen, J. (2000). Treatment of PET Nonwoven with a Water Vapor or Carbon Dioxide Plasma. *Journal of Applied Polymer Science*, 75: 480 – 494.
- [73] Sophonvachiraporn, P., Rujiravanit, R., Sreethawong, T., Tokura, S., and Chavadej, S. (2011). Surface Characterization and Antimicrobial Activity of Chitosan-Deposited DBD Plasma-Modified Woven PET Surface Plasma. *Chemistry and Plasma Processing*, 31: 233 – 249.
- [74] Bugaenko, L.T., Kuz'min, M.G., and Polak, L.S. (1988). High-Energy. *Chemistry Khimiya*, Moscow: 368 (Rus).
- [75] Pikaev, A.K., and Kabakchi, S.A. (1982). Reakcionnaya sposobnost' pervichnih produktov radioliza vodi Energoatomizdat, Moscow (1982) Pages: 200 (Rus.)
- [76] Pikaev, A.K., Kabakchi, S.A., and Makarov, I.E. (1988). Vicsokotemperaturniy radioliz voidi i vodnih rastvorov Energoatomizdat, Moscow: 136 (Rus.).
- [77] Chegol, A.S., and Kvash, N.M. (eds.) (1982). Analytical Control in Production of Synthetic Fibres: *A Handbook Khimiya*, Moscow (1982), pp. 142 – 143(Rus.)
- [78] Byal'skii, A.L., and Karpov, V.V. (eds.) (1971). *Dyes for the Textile Industry: A Colorist's Handbook Khimiya*, Moscow (1971), p. 15 (Rus.).
- [79] Prorokova, N.P., Khorev, A.V., and Vavilova, S.Yu. (2009). Chemical method of surface activation of poly(ethylene terephthalate) fibre materials Part 1. Study of the Modifying Effect of Sodium Hydroxide Solutions and Products Made from Quaternary Ammonium Salts. *Fibre Chemistry*, 3: 164 – 168.
- [80] Dechant, J., Danz, R., Kimmer, W., and Schmolke, R. (1972). Infrarotspektroskopische Untersuchungen an Polymeren (Infrared Spectroscopy of Polymers) Akademie, Berlin (1972); (*Khimiya*, Moscow Pages: 471).

Chapter 20

APPLICATION OF ULTRASONIC ENERGY FOR WASHING TEXTILES

Juan A. Gallego-Juarez*

Power Ultrasonics Group, CSIC, Serrano 144, Madrid, Spain.

ABSTRACT

Cleaning of solid rigid materials is one of the older applications of high-intensity ultrasound. Nevertheless the use of ultrasonic energy for washing textiles was explored over several years without achieving successful development. Besides the specific problems related with softness of the fabric material, the strategies for ultrasonic washing of textiles were generally directed towards the production of washing machines to wash laundry by generating high-intensity ultrasonic waves in the entire volume of the basket containing the fabrics to be washed. Such strategies offer significant inconveniences because of the practical difficulties to achieve a homogeneous distribution of the ultrasonic energy in the entire washing volume. Then in the areas of low acoustic energy the cleaning effect is not reached and it causes the washing to be irregular.

During the last twenty years the use of ultrasonic technologies for cleaning textiles in domestic and industrial washing machines has been reinvestigated and new important advances in this area has been achieved. In fact, it has been found out that by diminishing the amount of dissolved air or removing the big bubbles in the wash liquor the application of ultrasonic energy improved wash results in comparison to conventional methods. It has been also shown that a high proportion of water with respect to the wash load is required to assure efficiency and homogeneity in the wash performance. The application of such requirements in domestic washing machines or even in large scale machines similar in design to them doesn't seem a realistic and economically viable option. However for specific industrial applications a new ultrasonic process has been developed in which the textiles are exposed to the ultrasonic field in flat format and within a thin layer of liquid by applying specific ultrasonic plate transducers. Such process has been implemented at laboratory and semi-industrial stage. This chapter deals with the progressive advances in the use of the ultrasonic energy for washing textiles and in particular with the new process and the structure and performance of the systems developed for its implementation.

* E-mail: jgallego@ia.cetef.csic.es, jgallego.ultrasonics@gmail.com

1. INTRODUCTION

The cleaning action of ultrasonic energy is mainly due to cavitation and acoustic streaming. Ultrasonic cavitation may be defined as the formation, pulsation and/or collapse of vapour or gas cavities inside a liquid under ultrasonic stresses [1]. Ultrasonic waves applied to a liquid may produce small cavities or bubbles because of the fluctuations of hydrostatic pressure they produce. Depending on the wave intensity two types of cavitation are generally produced: stable and transient cavitation. The stable cavitation is generated at moderate intensity levels and the bubbles inside the liquid oscillate around their equilibrium size. The second type of cavitation, which is known as transient or inertial cavitation and is the effective cavitation for cleaning, is generated under high-intensity ultrasonic waves. During the negative pressure of the ultrasonic cycle, the restoring force produced in the bubble/cavity by the gas becomes negligible with respect to the acoustic pressure and the bubble or cavity expands to several times its original size. Then during the compression half-cycle the bubble collapses violently. The collapsing bubbles develop very high localized pressures (thousands of atmospheres) and temperatures (thousands of degrees) which produce erosion on the surface of the solids submerged in the liquid and favour the cleaning effect by separation of the soiled material from the dirty solid. Such action may be done even in the small hidden parts of the solid material promoting a very effective and unique cleaning. The onset of inertial cavitation is only produced over a certain acoustic intensity threshold that mainly depends on the characteristics of the liquid and the frequency of the ultrasonic wave.

The application of high-intensity ultrasonic waves may produce other phenomena, such as acoustic streamings, that may contribute to the dispersion of the particles of contaminant removed from the soiled surface. Acoustic streaming [2] is a nonlinear acoustic effect in which steady fluid flows are induced by the high-intensity waves both in the free ultrasonic beam and near the obstacles. Microstreamings may also been produced by stable cavitation, that is, by the oscillation of bubbles without implosion during many cycles of the acoustic field. Such fluid flows play a determinant role in heat and mass transfer mechanisms, which help to remove impurities.

The application of high-intensity ultrasound for cleaning of solid rigid materials is very well known and it is already established as one of the most popular uses of ultrasonic energy. Nevertheless the extension of this technique for washing soft materials such as textiles offers specific problems to be solved. In fact, it has been explored for several years without achieving commercial development. The softness of the fabric material makes cavitation to produce small erosion effect on textiles. In addition, the reticulate structure of the fabric favours the formation of layers of big bubbles that obstruct the penetration of the ultrasonic waves.

The majority of the efforts developed for the application of ultrasonic energy in textile washing were generally directed towards wash laundry. The most common way explored was the production of cavitation in the entire volume of the bath in which the fabric load is submerged in the washing liquid [3-5]. Nevertheless such systems offer significant inconveniences. First of all, it is very difficult to achieve a homogeneous exposure of the wash load to the ultrasonic field. Another problem is the high attenuation of the ultrasonic wave when penetrating the multiple textile layers of the fabric load. Then in the areas of low acoustic energy the cavitation threshold is not reached and the washing effect results to be

very irregular. Therefore to overcome such difficulties in a wash system it would be needed to use a small wash load and a high water level. In addition, the fabric has to be continuously moved so that it passes through the areas of high acoustic intensity of the washing cavity to assure the production of "strong transient cavitation" on the fabric surface [6]. Such requirements made difficult the application of ultrasonics in conventional domestic washing machines.

From the investigations about the use of ultrasonic technologies for cleaning textiles in domestic washing machines we carried out at the beginning of the 90s, in the frame of an European project, it was found out that the detergency achieved by using ultrasound and partially degassing the wash liquor, was much better than the conventional washing [7- 9]. The same situation is for institutional cleaning where the washing process is carried out in large scale machines similar in design to domestic washing machines. Large commercial laundries use cleaning equipment of the tunnel-washer type which comprises a series of drum-type segments in which textiles undergo a sequence of wash steps.

However there exists a potential of the ultrasonic washing technique for industrial applications. This is, for example, the case of the textile manufacturing industry [10]. Fabric processing in textile manufacturing is a wet processing to improve the appearance and serviceability of the fabric. It includes several operations that usually require washing the fabric in a flat format. Another useful potential application is the process of cleaning roller-towels in large scale laundry. The use of ultrasonic energy in such operations may help in speeding up the process and in improving the quality of the final product. On the other hand, the development of an ultrasonic washing unit can be applied to improve the effectiveness of conventional industrial processes, such as the tunnel-washer type, by introducing a complementary ultrasonic pre- or post-treatment step. This would possibly result in less re-washing of unsatisfactory cleaned articles, and thus lower operating costs.

Looking for such industrial applications, a new process and system has been developed and patented [11] in which the textiles are successively exposed to the ultrasonic field in flat format and within a thin layer of liquid. Such process has been implemented at laboratory and semi-industrial stage [12].

2. THE WASHING PROCESS

The new process tries to overcome the problems regarding homogeneous exposure of the wash items to the ultrasonic energy as well as the attenuation of the ultrasonic waves, by successively exposing the textiles to the ultrasonic field. It is based on the application of the ultrasonic energy to the textiles to be washed by means of special vibrating plate radiators in direct contact or very close to them. The textiles are submerged in a shallow layer of liquid and conveyed in a flat format through the ultrasonic radiator by means of a roller-type system (Figure 1). The plate radiator is designed to vibrate with one of its simpler flexural vibration modes to avoid as much as possible great differences in the vibration amplitudes of the different areas of the plate.

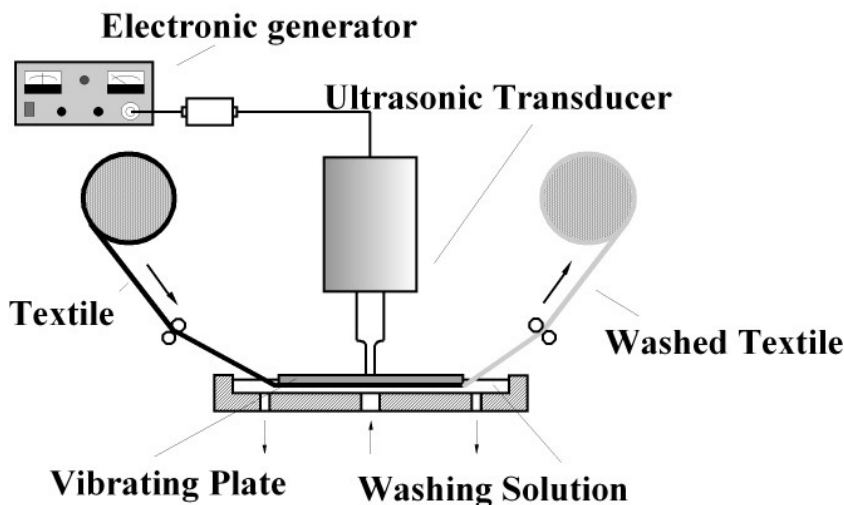


Figure 1. Basic scheme of the ultrasonic washing process.

The new procedure offers notable characteristics to be underlined. The cleaning effect is produced by the intense cavitation field generated by the plate radiator within the thin layer of liquid which is very favourable to produce high cavitation effect [13]. From the practical point of view, such liquid layer is very convenient for the low consumption of washing liquid required. The homogeneity of the washing effect is achieved by the fact that the fabric is passed along the surface of the plate radiator in such a way that all its parts are exposed during the same time to the areas of intense acoustic field. Finally, the radiation force produced by the high intensity ultrasonic beam directed over the surface of the textiles helps to remove the big bubbles formed within the reticulate structure of the fabric that impede the penetration of the ultrasonic wave.

The new washing process was initially implemented at laboratory stage by means of the simple set-up shown in Figure 2. The ultrasonic transducer developed for this laboratory set-up basically consisted of a rectangular aluminium plate radiator driven by a length expander piezoelectric vibrator (Figure 3a). The vibrator itself is constituted by a piezoelectric element of transduction in a sandwich configuration and a solid horn which acts as a vibration amplifier. The extensional vibration generated by the transducer element and amplified by the mechanical amplifier, drives the radiator which vibrates flexurally in one selected mode. The transducer was designed to operate at about 20 kHz with a vibration mode of the plate radiator with two nodal lines (black lines) almost parallel to the longer side of the plate (Figure 3b). The vibration of the plate clearly shows two zones at both sides of the nodal lines where the amplitude distribution is quite homogeneous. The maximum power capacity of this transducer was of about 200W which, according to the electroacoustic efficiency of the transducer (over 90% in water) and the surface area (110 cm²) of the radiator corresponds to an average acoustic intensity of about 1.5 W/cm². Such intensity is a little over the value of the cavitation threshold in tap water. For strong cavitation effect would be required to reach levels three or four times higher [6].

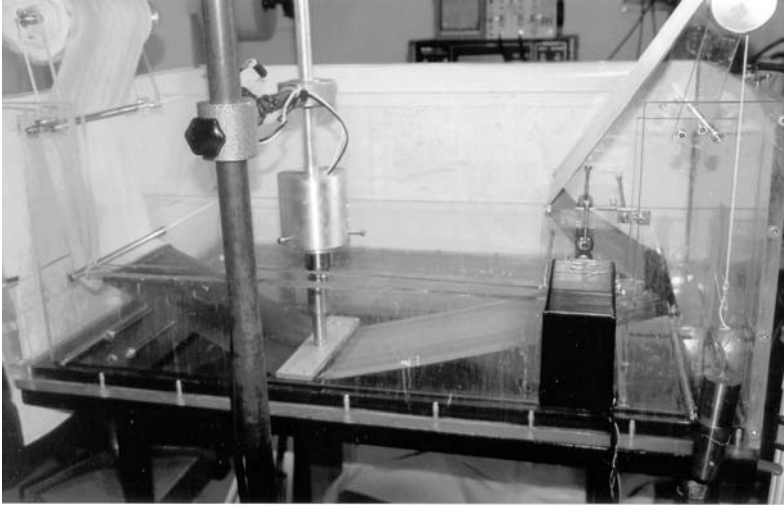


Figure 2. Laboratory set-up for the implementation of the washing process.

To increase the power capacity, a semi-industrial washing system was developed in a second stage. The basic objectives for the development of this system were: to improve the performance of the plate transducer aiming at industrial operation, to increase the number of transducers in order to speed up the washing process and to control and optimize the parameters of the process (liquid layer thickness, transducer-fabric distance, etc...).

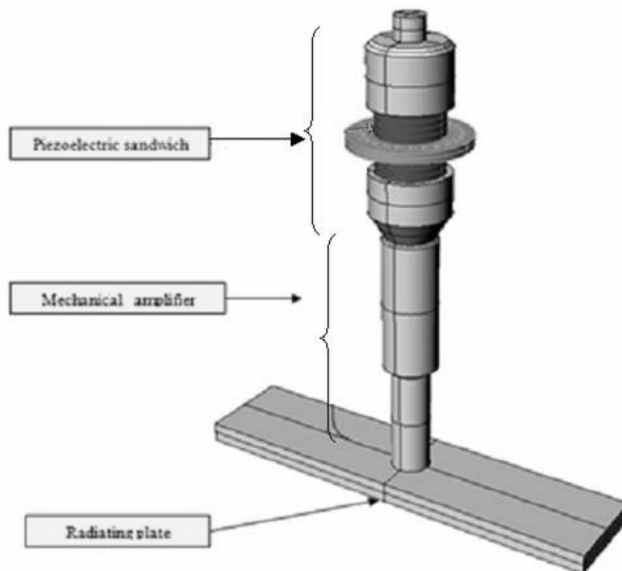


Figure 3. Basic scheme of the plate transducer (a) and operating vibration mode of the plate radiator (b).

The plate transducer constitutes the core of the system. Therefore, it requires to be provided with high power capacity to safely produce strong cavitation in the washing liquid. The main drawback of the flat plate transducer designed and constructed for the laboratory set-up was the significant number of vibration modes existing in the range of the operating frequency. This fact is particularly important at high excitation levels in liquids when the frequency band of the transducer becomes wider and, in addition, the driving signal may suffer distortion. In this case, undesired vibration modes easily interact with the operating mode causing serious disturbances and even damages in the transducer. To avoid this problem the design of the plate radiator was modified by using finite element methods (FEM) and following a procedure previously developed to control the vibration mode of stepped plate radiators [14]. Such procedure has been successfully applied for the development of the stepped-grooved plate transducers commercialized by the spin-off company PUSONICS for different power ultrasonics applications [15]. It basically consists of designing the plate radiator with a grooved profile on its back side. This profile is designed in such a way that the impedance of the operating vibration mode is diminished while the other modes are obstructed or moving away from the operation range. In fact, while in the flat plate radiator of the laboratory set-up appeared several modes within the range 19-22 kHz [12], in the grooved plate radiator (Figure 4a) only appear the operating mode (Figure 4b). The grooved-plate radiator was constructed in titanium alloy. The resulting transducer has a power capacity of about 600W with a radiating surface of about 110 cm². It means a capability for reaching acoustic intensities of up to about 4.5 W/cm².

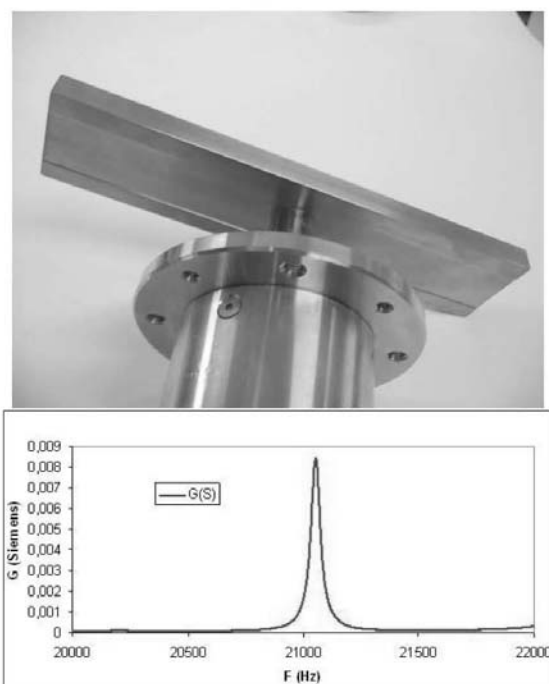


Figure 4. The grooved-plate transducer (a), and its frequency response(b).

Two of such transducers are installed in the washing section of the semi-industrial unit (Figure 5). Each transducer is driven by an electronic system consisting of an electronic controller to generate and control the driving signal, a power amplifier and a matching impedance circuit (Figure 6). The washing unit is mainly constituted by a soaking bath to previously wet the fabric and the washing section where the cleaning action is produced (Figure 7). The unit is provided of several rollers to convey the fabric in a flat format parallel to the radiator surface. The fabric is moved in a perpendicular direction to the nodal lines of the plate radiator (Figure 8). A motor is moving the whole system. The distance between the plate radiators and the fabric as well as between the plate radiators and the bottom of the container, which act as a reflector, may be adjusted by high-precision mechanical devices. Such distances are electrical and mechanically controlled and optimized by respectively measuring the transducer admittance at different distances, to adjust the resonance, and the cavitation activity, to maximize the cleaning effect.

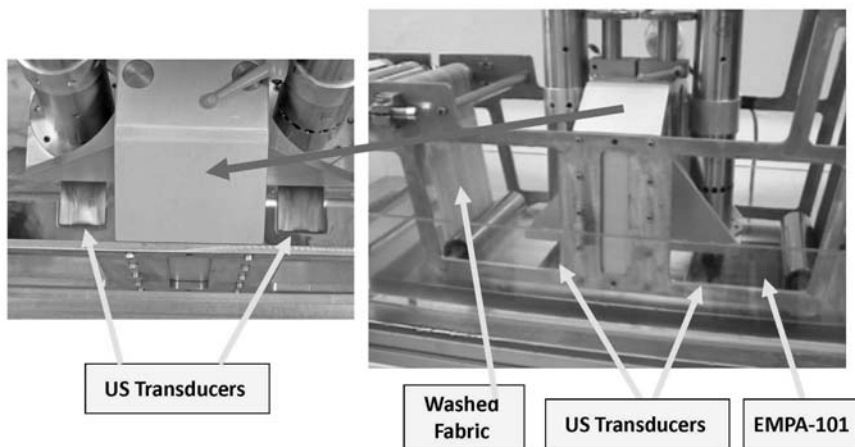


Figure 5. Washing section of the semi-industrial system.

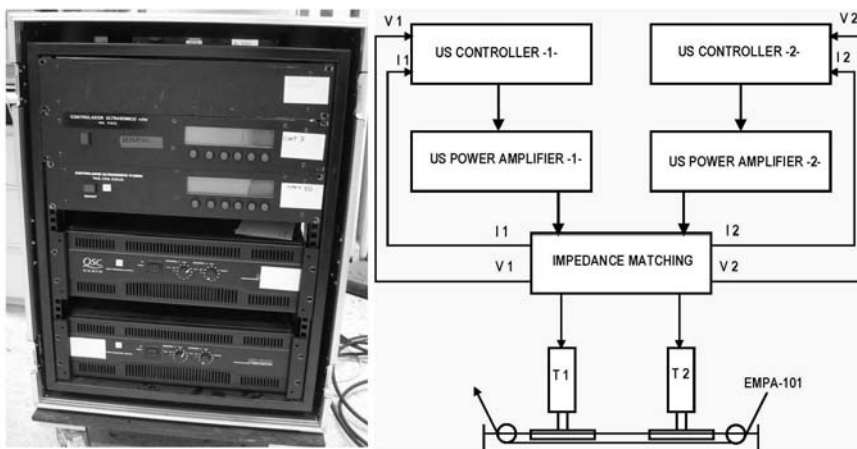


Figure 6. Electronic system to drive the ultrasonic transducers.

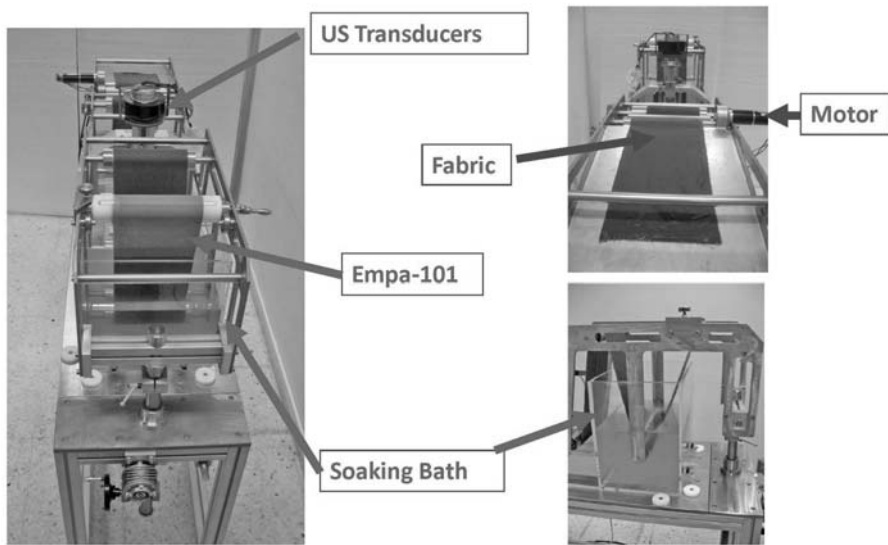


Figure 7. Semi-industrial washing unit.

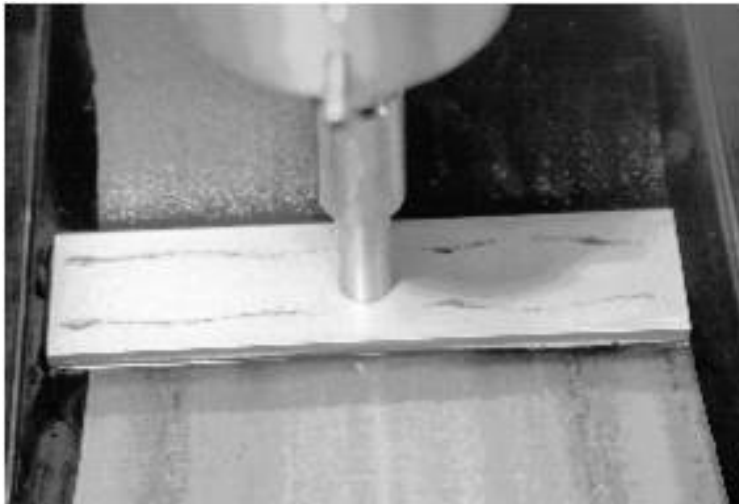


Figure 8. The fabric is conveyed perpendicularly to the nodal lines of the vibrating plate.

3. WASHING TESTS

By using both laboratory and semi-industrial set-ups the influence of the ultrasonic energy on the washing performance was studied for a number of representative standard test pieces: EMPA 101 (cotton soiled with carbon black and olive oil), AS9 (polyester/cotton soiled with fatty material and solid particles) and WFK30D (polyester soiled with skin fat and pigments). Figure 9 shows the cleaning results obtained by using the ultrasonic system

compared with those achieved with a conventional washing machine. For the WFK30D test piece probably a higher acoustic intensity was needed.

Even if the domestic washing machines generally work above 25°C there are some delicate synthetics with non-fast colours and woollen garments which must never be washed above 40°C and in certain cases the labels specify to wash under 30°C. Therefore the comparison of both conventional and ultrasonic washing at this temperature makes sense particularly if we bear in mind that the new process pretends to avoid heating or degassing the wash liquor. The influence of the temperature in the production of cavitation is controversial [16] and would require a specific study.

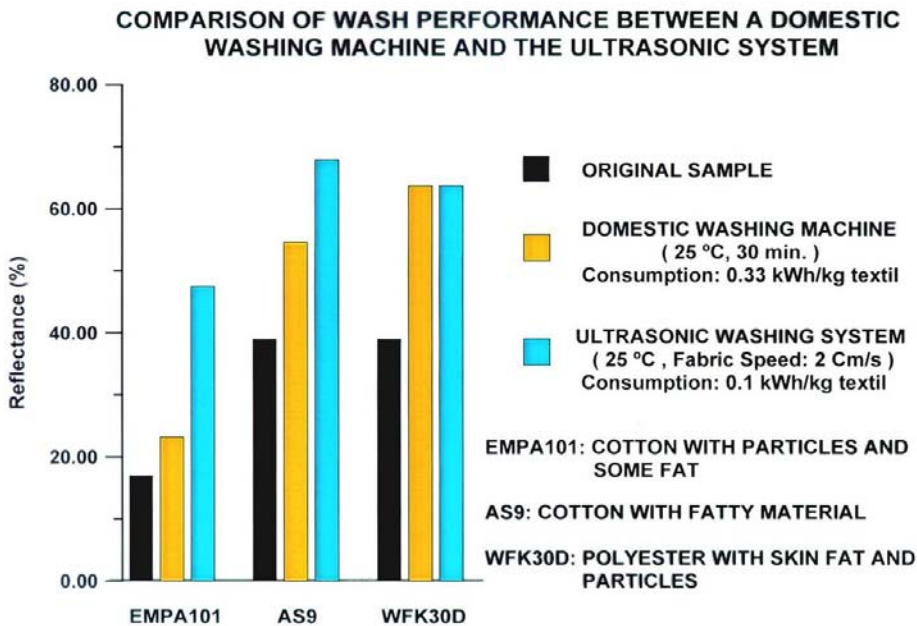


Figure 9. Comparison of wash performance between the ultrasonic system and domestic washing machines.

The washing solution used was a simple solution in standard tap water containing 1.75 g l^{-1} of SDBS (sodium dodecylbenzenesulphonate) surfactant and 3.5 g l^{-1} of STP (sodium triphosphate) a builder to enable surfactant to be more effective. The temperature of the washing solution was kept constant at about 25°C. Such temperature was chosen for practical reasons (the objective is a simple and low energy consumption process) and because according to our experience and the literature [16] this value is within a range (20–30°C) in which the cavitation intensity has not great variations. The layer of washing liquor was frequently refreshed. No chemical changes in the components of the washing solution due to the ultrasonic action were detected.

Washing tests carried out with typical EMPA-101 samples in the semi-industrial set-up confirmed the good cleaning effect previously obtained at the laboratory set-up. Such effect depends on the acoustic intensity and the treatment time. Figure 10 shows the reflectance of washed samples at 2 cm s^{-1} and different acoustic intensities. As it can be seen the cleaning performance, measured through the reflectance, increases almost linearly with the acoustic

intensity up to a certain value in which saturation starts. It means that for a certain washing time, which is controlled by the fabric speed, the ultrasonic intensity needed to produce a determinate cleaning effect can be fixed. The washing performance achieved even at relatively moderate acoustic intensities is clearly much higher than that obtained with a conventional washing machine. In fact, a typical reflectance value after washing an EMPA-101 sample in a conventional washing machine at 25°C programme is about 23%. The energy consumption of the ultrasonic washing process is very low: of the order of 0.1 kWh kg⁻¹ of textile.

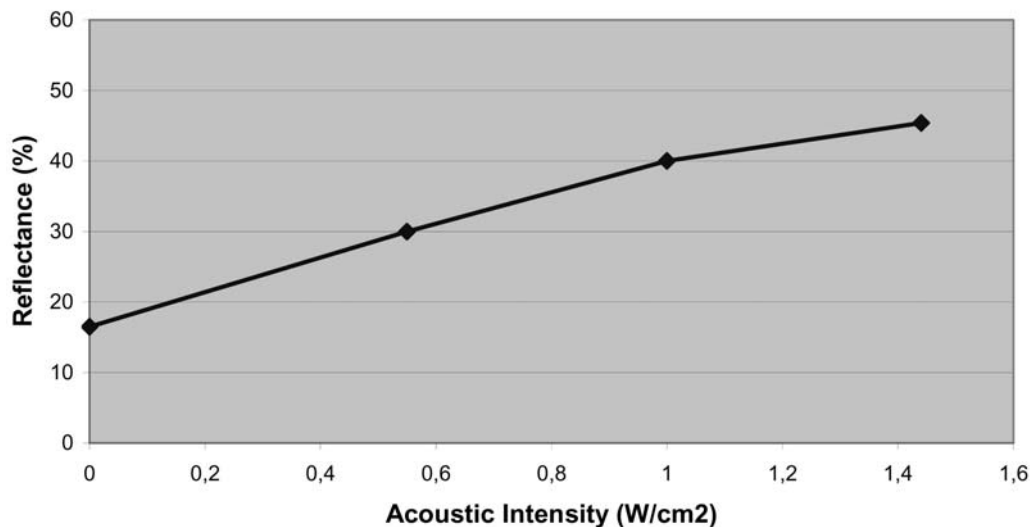


Figure 10. Ultrasonic washing performance versus acoustic intensity (EMPA-101 samples at 2 cm s⁻¹).

The evidence of the best washing performance achieved by the ultrasonic system is shown in Figure 11. The picture presents a visual comparison of the washing effect on EMPA-101 samples by using the ultrasonic system with two transducers at 400W and sample speed of 1 cm s⁻¹, with the washing result on the same kind of samples after two successive conventional washes in a domestic washing machine at 20°C and 50°C. In both cases the washing solution was a common commercial detergent in tap water.

The confirmation of the cleaning efficiency of the ultrasonic washing, have also been done by some tests on real stains like blood, chocolate, grass, etc. As the stains were difficult ones, and the detergent solution was a simple one, without enzymes, the time of exposition to ultrasonics was 60 seconds. For all the stains, the wash results achieved with an acoustic intensity of 1.4 W cm⁻² are better than those achieved in a domestic washing machine with the same detergent and temperature after 30 minutes (Figure 12). Some stains (Curry, Cherry, Cook oil, Gravy and Dirty Motor Oil) are washed better than the domestic machine after only 20 second ultrasonic washing [17].

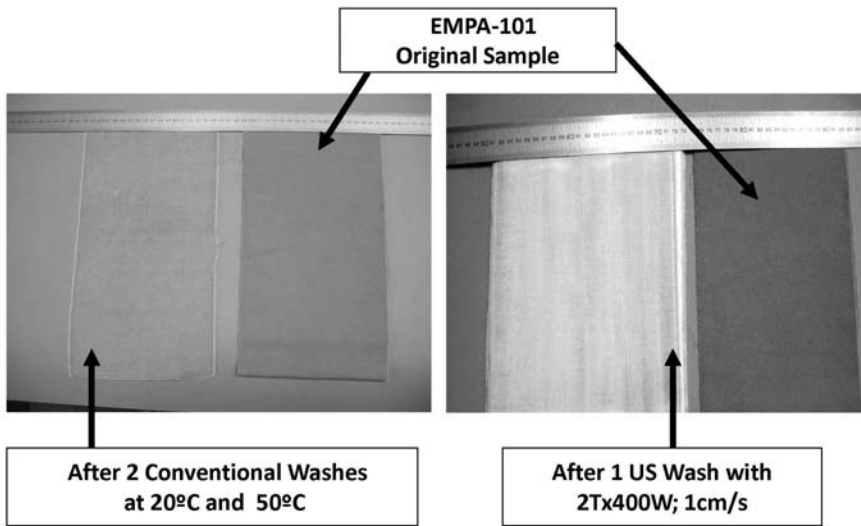


Figure 11. Visual comparison of the wash performance on EMPA-101 samples between the ultrasonic system (two transducers at 400W and sample speed of 1 cm s^{-1}), and a domestic washing machine (two successive washes at 20°C and 50°C).

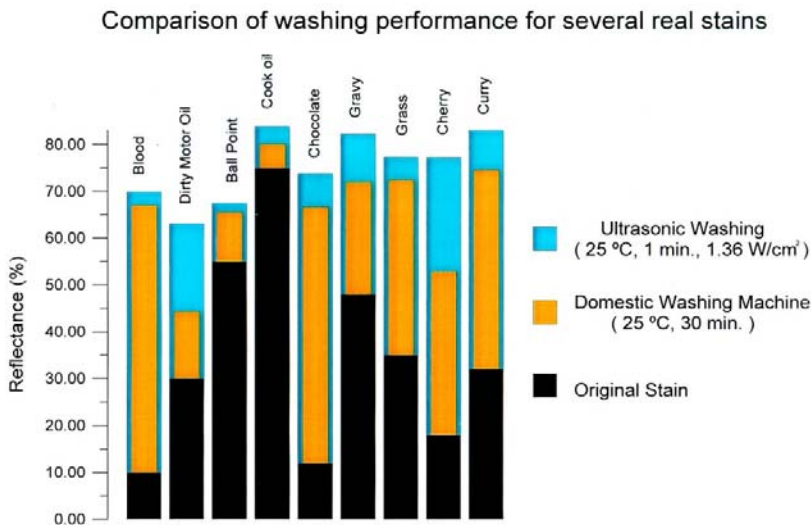


Figure 12. Cleaning efficiency of ultrasonic washing on different types of stains.

CONCLUSIONS

The ultrasonic energy for washing textiles represents a potential powerful tool for specific applications. It seems evident that the direct application of ultrasonics to the conventional existing washing devices doesn't result technically and economically viable. On

the contrary it is required to develop proper systems to efficiently use this source of energy. In this chapter a new ultrasonic washing procedure and specific developed systems for the continuous washing of textiles in liquid layers and flat format have been presented. The good washing performance obtained with very low energy consumption and short washing treatment times demonstrate the possibilities of the new technique. In addition, other important characteristics of the application of ultrasonic energy for the washing process are the use of low quantity of detergent solution of very simple composition and at low temperature. Such characteristics made the ultrasonic washing to be considered a green and sustainable process.

ACKNOWLEDGEMENTS

The experimental systems and results presented in this chapter were funded by the UE projects BRITE/EURAM (BREU-137), VALUE II (Project n° CTT-673) and STREP (Project NMP2-CT-2003-505892).

REFERENCES

- [1] Gallego-Juarez, J.A. (1999). "High-Power Ultrasound" In *"Wiley Encyclopedia Of Electrical And Electronics Engineering"* Vo.9, pp 49-59, New York.
- [2] "Nyborg W.L. (1965). "Acoustic Streaming", In *"Physical Acoustics, W. P. Mason (Ed), Vo II, New York, Academic Press.*
- [3] Wit, L.D.G. (1990). "Method For Ultrasonic Cleaning Of Textiles", *European Patent Application*, 0392586a1, 1990.
- [4] Lee, J.C. (1989). "Ultrasonic Washing Machine", *UK Patent Application*, Gb2233350a, 1989.
- [5] Frucco, G. (1987). "Ultrasonic Laundry Washing Machine", *European Patent Application*, 0261363a1, 1987.
- [6] Gaete-Garretón, L., Vargas-Hernández, Y., Vargas-Herrera, R., Gallego-Juárez, J.A., and Montoya Vitini, F. (1997). "On the Onset of Transient Cavitation in Gassy Liquids", *Journal of Acoustic Society of America*, 101 (5): 2536-2540.
- [7] Kubacsi, M., Kamarad, L., van der Vlist, P., Willemse, S., Gallego-Juárez, J.A., Warmoeskerken, M., and Rodríguez-Corral, G. (1993). "Procédé de lavage dans une machine à laver à ultrasons", *French Patent* 9304627, CIAPEM, April 1993.
- [8] Van der Vlist, P., Willemse, S., Gallego-Juárez, J.A., Warmoeskerken, M., Rodríguez-Corral, F., Kubacsi, M., and Kamarad, L. (1993). "Cleaning process", *European Patent* n° EP9320-1142.2, UNILEVER, April, 1993.
- [9] Gallego-Juárez, J.A., Rodríguez-Corral, G., Willemse, S., and Warmoeskerken, M. (1994). "Sistema ultrasónico para lavado de textiles" (Ultrasonic system for textile washing), *Spanish Patent* n° 9401960, 1994.
- [10] Vouters, M., Rumeau, P., Tierce, P., and Costes, S. (2004). "Ultrasounds: an industrial solution to optimise costs, environmental requests and quality for textile finishing", *Ultrasonics Sonochemistry*, 11: 33-388.

-
- [11] Gallego-Juárez, J.A., Nájera, G., Rodríguez, G., Vázquez, F., and Van der Vlist, P. (2001). "Process and device for continuous ultrasonic washing of textiles" *U.S. Patent*, nº 6,266,836 B1, 2001.
 - [12] Gallego-Juarez J.A., Riera E., Acosta V., Rodríguez G., and Blanco A. (2010). "Ultrasonic system for continuous washing of textiles in liquid layers", *Ultrasonics Sonochemistry*, 17: 234-238.
 - [13] Granger, C. and Dubus, B. (2005). "Ultrasonic cavitation in thin liquid layers", A. Moussatov, *Ultrasonics Sonochemistry*, 6: 415-422.
 - [14] Gallego-Juárez, J.A., Rodríguez-Corral, G., Montoya-Vitini, F., Acosta-Aparicio, V. M., Riera, E., and Blanco, A. (2005). "Macrosonic generator for the air-based industrial defoaming of liquids", International Patent PCT/ES2005/070113.
 - [15] www.pusonics.es
 - [16] Niemczewski, B. (2007). "Observations of water cavitation intensity under practical ultrasonic cleaning conditions", *Ultrasonics Sonochemistry*, 14: 13-18.
 - [17] Lammers, H., Van der Vlist, P., and Gallego-Juárez, J.A. (1995). Internal Report, VALUE II Project, (UE, CTT-673) 1995.

INDEX

A

- abatement, 394
- Abraham, 505
- access, 101, 125, 156, 157, 158, 163, 226, 340, 364, 509, 514
- accessibility, 141, 163, 471, 472, 475, 482
- accountability, 119
- accounting, 16, 119, 168, 332, 333, 339, 354, 364, 420
- acetaldehyde, 510
- acetic acid, 96, 115, 209, 211, 212, 219, 220, 477
- acetone, 211, 306, 310, 524
- acetylation, 423
- ACF, 128, 465
- acidic, 56, 75, 139, 214, 425, 474, 475, 476, 478, 486, 513, 525, 542
- acrylic acid, 305, 313, 314, 415, 487, 512, 514, 517
- acrylonitrile, 224, 306
- activated carbon, 186
- activation energy, 513
- active site, 306
- actuators, 318
- AD, 164
- adaptability, 53
- adaptation, ix, 40, 129, 224
- adaptations, 142, 198
- additives, xi, xiv, 75, 87, 101, 253, 399, 413, 431, 491, 506, 520, 523, 526, 528, 538, 540, 558
- adenosine, 431
- adhesion, ix, xiii, 279, 297, 298, 307, 320, 393, 481, 508, 520, 523, 530, 531, 532, 533, 535, 559
- adhesion properties, xiii, 481, 520, 530, 532, 533
- adhesives, 84, 85, 193, 416, 495, 523
- adjustment, 531
- adsorption, xii, 167, 168, 170, 171, 177, 180, 185, 186, 377, 404, 418, 457, 467, 472, 473, 474, 475, 476, 478, 481, 482, 483, 486, 487, 508, 515, 516
- adults, 13, 38, 56, 123, 134
- advancement, 5, 287, 291
- advancements, x, 318
- adverse effects, 415, 495, 504, 535
- aerogels, 371
- aerospace, 100, 228, 332, 372, 550, 551
- aesthetic, 253, 254, 320, 323
- AFM, 511
- Africa, 16, 17, 18, 20, 22, 23, 26, 40, 55, 62, 68, 71, 81, 89, 93, 119, 122, 132, 226, 268, 269
- agar, 446, 459, 460
- age, 61, 72, 76, 146, 251, 268, 269, 271, 520
- aggregation, 384, 391
- aging population, 469
- Agricultural Research Service, 128
- agricultural sector, 49, 52
- agriculture, vii, 30, 68, 133
- Agrobacterium, 130, 409
- Air Force, 145
- air temperature, 289
- Akan, 312
- albumin, 35
- alcohols, 503
- aldehydes, 477
- algae, 101, 214, 402, 404, 405
- Algeria, 68
- algorithm, 340, 345
- Alkali Resistant (AR), ix, 223, 244, 264
- alkaline hydrolysis, 570
- alkaline media, 477
- alkalinity, 235, 257, 258, 260
- alkaloids, 60
- allergens, 495, 503, 504
- allergic inflammation, 502
- allergic reaction, xii, 489, 490, 491, 495, 502

- allergy, 490, 491, 493, 503, 505, 506
allylamine, 307, 512, 515
alters, 127, 232, 306
aluminium, 3, 319, 320, 390, 440, 582
aluminum oxide, 389, 542, 552
ambient air, 289
amine, 96, 477, 513
amine group, 477, 513
amines, 492
amino, 2, 10, 11, 12, 26, 34, 35, 97, 133, 210, 211, 374, 405, 476, 477, 478, 479, 480, 481, 482, 483, 484, 492, 503, 575
amino acid, 2, 10, 11, 12, 26, 34, 35, 133, 210, 575
amino acids, 2, 10, 11, 26, 34, 575
amino groups, 97, 211, 405, 477, 478, 479, 480, 481, 482, 483, 484
ammonia, 52, 140, 377, 378, 387
ammonium, 4, 116, 121, 378, 382, 387, 492, 512
ammonium salts, 492
amoeboid, 207
amorphous phases, 109, 389, 465
amorphous polymers, 109
amplitude, 172, 300, 301, 336, 341, 582
amylase, 413
anatase, xi, 395, 439, 441, 448, 449, 450, 454, 456, 459, 464, 466
anatomy, 129
ancestors, 6
anchorage, 253
anchoring, 374, 478, 479
ancient world, 229
Angola, 18
animal disease, 407
animal diseases, 407
anisotropy, 71, 332, 550
annealing, 443, 546, 547
anticoagulant, 213, 214
antigenicity, 209
antimony, 197
antioxidant, 50, 214
antitumor, 214
aortic valve, 221
apoptosis, 127
apparel industry, 197
apparel products, 274
application techniques, 372
aqueous solutions, vii, 165, 186, 491
Arab countries, 47
architects, 226
Argentina, 4, 18, 37, 129
argon, 199, 302, 303, 305, 306, 307, 310, 313
Aristotle, 71
arrest, 340
arsenic, 132
arteries, 288
artery, 209
arthropods, 405
aryl hydrocarbon receptor, 132
asbestos, 3, 63, 92, 93, 94, 148, 192, 223, 233, 234, 237, 256, 258, 259, 260, 468
asbestosis, 94
ascorbic acid, 51
Asia, 6, 14, 20, 42, 45, 53, 62, 74, 80, 81
Asian countries, 40
aspartic acid, 408
Aspergillus terreus, 59
assessment, 23, 117, 119, 141, 154, 364
assimilation, 53
asthma, 502
atmosphere, 53, 304, 308, 310, 312, 313, 315, 376, 514, 544, 546, 550
atmospheric pressure, xiv, 299, 300, 301, 302, 303, 304, 305, 310, 311, 312, 557, 559, 572, 574, 576, 577
atomic emission spectrometry, 522
atomic nucleus, 380
atoms, 101, 102, 103, 107, 111, 247, 298, 307, 370, 371, 377, 380, 411, 413, 440, 441, 480, 545, 567
atopic dermatitis, 491, 505
atopic eczema, 118
attachment, 204, 215, 260, 324, 420
Austria, 4, 494
authorities, 50
automation, vii, 291, 317
Automobile, 229
automobile parts, 95
automobiles, 85
automotive sector, 111
avoidance, 504
awareness, 53, 199, 234, 469, 484

B

- Bacillus subtilis, 374
backscattering, 380
bacteria, 42, 44, 45, 59, 91, 92, 100, 101, 253, 254, 372, 374, 380, 386, 387, 389, 392, 396, 402, 404, 406, 409, 410, 417, 432, 440, 446, 483, 484, 513
bacterial cells, 374, 392, 393
bacterial infection, 419
bacteriostatic, 514
bacterium, 17, 386, 391, 397, 446, 458, 459, 460
ban, 234, 258

- bandgap, 371
Bangladesh, 46, 47, 52, 131
banks, 14, 59
Barbados, 16, 56
barriers, 199, 521
base, xiv, 39, 53, 62, 65, 67, 69, 70, 96, 259, 359, 405, 477, 508, 520, 540
baths, 226, 229
batteries, 372, 503
beams, 357, 363
bedding, 12, 34, 41, 49, 129, 212
beer, 55, 409
beetles, 7, 17
behaviors, ix, 273, 274, 275, 288, 289, 290, 291, 551
Belgium, 4, 37, 218, 297
bending, 45, 74, 205, 227, 272, 326, 361, 370, 528, 530
beneficial effect, 56, 185
benefits, 5, 40, 62, 67, 120, 182, 237, 240, 242, 251
benzene, 97, 103, 440, 462
beryllium, 111
beta-carotene, 50, 51
beverages, 55, 68
bias, 333
Bible, 47, 67, 269
binding energies, 474
bioactive materials, 420
biochemistry, 67, 487
biocompatibility, 100, 207, 209, 210, 214, 215, 400, 402, 403, 409, 411, 415, 427, 435, 485
biocompatible materials, 207, 215
biodegradability, 207, 209, 210, 211, 214, 400, 402, 403, 411, 415, 478
biodegradation, 100, 101
biodiversity, 21
biogas, 63
biological activities, 213
biological behavior, 274
biological control, 59, 120, 123, 124
biological markers, 127
biological processes, 101
biological systems, 216, 415
biomass, 101, 116, 129, 135, 146, 147, 214, 414
biomaterials, 204, 212, 216, 371, 406, 416, 419, 420, 425, 429, 430, 432, 433, 437, 485
biomedical applications, xi, 205, 215, 218, 302, 309, 371, 399, 403, 405, 406, 407, 408, 411, 412, 416, 418, 425, 426, 428, 432, 435
biomolecules, 206, 414, 419, 422
bionanocomposites, 404
biopolymer, 215, 220, 403, 415, 428, 477, 479
biopolymers, xi, 95, 204, 206, 207, 208, 216, 218, 394, 399, 400, 401, 402, 404, 405, 406, 407, 408, 409, 411, 412, 417, 419, 427, 436
biosafety, 426
biosciences, 147
biosensors, 515
bioseparation, 432, 433
biosynthesis, 80, 144
biotechnological applications, 434
biotechnology, xi, 120, 399, 400, 412, 413, 433, 434
birds, 1, 70
bisphenol, 79
blame, 94
bleaching, 70, 75, 402, 413, 475, 493, 495
bleeding, 236
blend films, 430
blends, 6, 63, 114, 208, 319, 405, 425, 426, 436
blood, 38, 56, 71, 113, 127, 134, 204, 208, 209, 213, 284, 286, 287, 288, 309, 410, 429, 432, 497, 588
blood circulation, 286, 287
blood clot, 71
blood flow, 284, 286, 288
blood pressure, 56, 113, 134, 288
blood vessels, 284, 410, 432
bloodstream, 209
body fluid, 469
boils, 55, 68, 70, 71
Bolivia, 81
Boltzmann constant, 277
bonding, 3, 74, 214, 232, 233, 240, 245, 252, 257, 259, 260, 264, 265, 306, 378, 474
bonds, 12, 73, 80, 94, 96, 101, 108, 111, 210, 214, 247, 306, 375, 377, 491, 544, 545, 546
bone, 37, 41, 157, 204, 210, 212, 219, 221, 229, 285, 406, 410, 415, 420, 421, 428, 429, 432, 433, 437
bone form, 212
bone marrow, 433
bones, 71, 157
bottom-up, 413
brain, 132, 149
branched polymers, 518
branching, 54, 214, 559
brass, xiii, 65, 520, 528, 529, 530, 535
Brazil, 4, 19, 42, 47, 62, 64, 68, 77, 80, 81, 131, 135, 165, 188
breakdown, xiv, 101, 300, 302, 521, 557, 558, 561
breast cancer, 127
breeding, 31, 40, 116, 134
Britain, 14, 47

brittle film, 533
 brittleness, 52, 58, 107, 112, 227, 228, 420
 bronchitis, 502
 budding, 91
 bulk materials, 370
 Burkina Faso, 23, 54, 56
 Burma, 54
 burn, 24, 26, 71, 196, 394, 407, 416
 burn dressings, 416
 business environment, 197, 201
 butadiene, 86, 87, 88, 99, 245
 buttons, 495
 buyers, 47
 by-products, 17, 67, 77, 400, 401, 403, 411, 422, 541
 byssinosis, 491

C

Ca²⁺, 402
 cables, 193, 540
 CAD, ix, 198, 273, 291, 292, 293, 295
 calcium, 3, 35, 50, 75, 91, 92, 159, 162, 403, 406, 408, 418, 420, 428, 516
 calcium carbonate, 91, 92, 408
 caliber, 146
 calyx, 53, 55
 CAM, 198
 cambium, 46, 72, 73
 Cameroon, 23, 115
 canals, 48, 66
 cancer, 55, 94, 148, 429
 cancer cells, 429
 cancer death, 94
 candidates, 207, 403, 550, 551
 cannabis, 126
 capillary, 151, 205, 277, 278, 279, 281
 caprolactam, 96
 capsule, 15, 36
 carbides, 112
 carbohydrate, 15, 50, 51, 60, 149, 214, 411, 469, 475, 477
 carbohydrates, 60, 76
 carbon atoms, 101, 102, 103, 247, 248, 411, 474, 545
 carbon dioxide, 48, 53, 99, 101, 133, 227, 480
 carbon nanotubes, viii, 112, 191, 406, 413, 414, 415
 carbonization, 324, 378
 carbonyl groups, 304
 carboxyl, xiv, 97, 474, 475, 476, 479, 480, 481, 557, 569
 carboxylic acid, 199, 305, 492
 carboxylic acids, 199, 492
 carboxylic groups, 474
 carboxymethyl cellulose, 410
 cardiac muscle, 210, 415
 cardiovascular disease, 218
 cardiovascular disease XE "cardiovascular disease" s, 218
 Caribbean, 20, 54, 55, 59, 62
 Caribbean countries, 59
 carnivores, 91
 carotene, 51
 cartel, 87
 cartilage, 204, 210, 219, 406, 407, 410, 415, 421, 428, 429, 432
 case studies, 154, 156, 157, 158, 159, 162
 case study, 131, 156, 157, 159, 162
 casein, 75, 98, 406, 416
 cash, 21
 cashmere, 2, 6, 116, 194, 490
 casting, 95, 235, 251, 266, 420, 424
 castor oil, 52
 catalysis, 204, 463, 523, 525
 catalyst, 97, 197, 247, 378, 382, 440, 457, 463, 513, 541
 catalytic properties, 518, 541, 542
 categorization, 142
 category a, 86
 catfish, 428
 cattle, 17, 24, 37, 122
 causal relationship, 502
 C-C, 444, 527, 570
 cell division, 72
 cell movement, 207
 cellulose derivatives, 2, 210, 403, 404, 410
 cellulose fibre, 308, 422, 424, 427, 467, 468, 469, 470, 471, 472, 473, 475, 476, 478, 479, 480, 481, 483, 484, 485, 486
 cellulose triacetate, 211
 cellulose xanthate, 76, 405
 cementitious matrices, ix, 136, 223, 224, 257, 260, 262, 264, 265, 268
 Census, 4
 Central Asia, 5
 ceramic, xiv, 67, 92, 99, 112, 154, 229, 231, 376, 397, 420, 437, 539, 540, 541, 543, 544, 548, 549, 550, 551, 552, 553, 554
 ceramic materials, 420
 Ceramics, 143, 272, 552, 553
 certification, 21, 84
 Chad, 22, 23
 challenges, 122, 213, 215, 216, 246
 charge density, 213
 charring, 154, 159, 162

- chemical bonds, xi, 306, 369, 375
chemical characteristics, 251, 504, 538
chemical etching, 149, 310
chemical industry, 433
chemical interaction, 558
chemical properties, vii, xii, 87, 153, 159, 207, 306, 467, 550, 572
chemical reactions, 207, 246, 375, 440, 471, 566
chemical reactivity, 386
chemical structures, 443, 477
chemical vapor deposition, 525, 535, 548, 554
chemicals, 8, 21, 22, 29, 33, 45, 71, 72, 87, 92, 93, 94, 121, 144, 193, 298, 407, 411, 487, 502, 513, 559
chemiluminescence, 392
Chicago, 271
children, 13, 47, 78, 99, 408, 429
Chile, 32
China, 1, 4, 8, 10, 13, 14, 15, 18, 20, 21, 22, 23, 29, 31, 32, 33, 37, 38, 40, 42, 43, 47, 54, 56, 61, 64, 74, 80, 81, 82, 83, 89, 118, 119, 120, 122, 124, 125, 127, 130, 144, 149, 195, 271, 273, 293, 433, 465, 494, 495, 539, 551
chirality, 469
Chitosan, 211, 212, 217, 219, 220, 405, 422, 428, 429, 430, 435, 436, 477, 482, 484, 486, 487, 577
chlorine, 75, 373
chlorophyll, 27, 35
cholesterol, 38, 55, 214
chondrocyte, 433
chondroitin sulfate, 407
Christians, 226
chromatography, 125, 538
chronic diseases, 416
circulation, 287
cities, 258
Civil War, 26
civilization, vii, ix, 1, 223
cladding, 237, 246
classes, 4, 52, 204, 205, 231, 268, 373, 400, 401, 417, 558
classification, 70, 230, 249, 401, 416, 417, 491, 492
clay minerals, 4, 115
cleaning, ix, xiv, 12, 45, 63, 74, 91, 92, 164, 195, 199, 200, 201, 297, 298, 308, 372, 393, 395, 400, 404, 414, 424, 425, 440, 462, 480, 502, 538, 559, 579, 580, 581, 582, 585, 586, 587, 588, 591
climate, 16, 43, 46, 47, 62, 71, 77, 90, 117, 119, 146
climate change, 117
climates, 6, 16, 41, 52, 53
clinical application, 206, 216
clinical diagnosis, 506
clinical presentation, 495, 504
clinical trials, 204
closure, 372
clusters, 200, 370, 377, 413, 424, 465
CMC, xiv, 539, 551
C-N, 550, 554
CO₂, 53, 76, 101, 304, 463
coal, 94, 259
coastal region, 59
coatings, ix, xii, 92, 99, 100, 199, 243, 249, 252, 297, 298, 306, 318, 371, 374, 428, 430, 441, 442, 443, 446, 447, 448, 450, 451, 453, 454, 455, 456, 459, 461, 464, 465, 467, 481, 518, 522, 523, 524, 532, 537, 540, 575
cobalt, 112, 393
cocoon, 10, 11, 13, 118, 193, 430
coding, 17, 340
coffee, 24, 46, 67, 68
collaboration, 121, 155, 156, 163, 216
collagen, viii, xi, 110, 203, 204, 208, 209, 211, 212, 216, 217, 218, 399, 405, 406, 407, 408, 414, 415, 416, 417, 418, 419, 420, 421, 425, 426, 427, 428, 429, 437
collagen sponges, 407
College Station, 41
collisions, 299, 380, 381, 396
Colombia, 68, 81
colon, 128
colon cancer, 128
colonisation, 121
colonization, 125, 394
color, iv, xiv, 5, 8, 9, 15, 28, 42, 43, 48, 53, 54, 57, 58, 66, 72, 75, 113, 195, 227, 324, 424, 492, 493, 511, 512, 517, 520, 524, 526, 530, 532, 534, 535, 536, 568
combustion, 110, 550, 573
combustion environment, 550
commodity, 49, 52, 118
Commonwealth of Independent States, 37, 40
communication, vii, 5, 286, 317, 318
communities, 50, 55
community, 32, 56, 204
compaction, 509
companion cell, 46
comparative advantage, 29
compatibility, viii, 146, 203, 207, 217
competition, 63, 79, 85, 98, 411
competitiveness, 29, 44, 400
competitors, 23
complement, 208

- complex interactions, 333
 complexity, xiii, 204, 288, 364, 519
 compliance, 209, 357
 compost, 54
 composting, 100, 101, 487
 compounds, x, xi, 59, 77, 85, 98, 101, 102, 122, 147, 211, 243, 247, 248, 321, 369, 373, 374, 377, 402, 404, 413, 414, 418, 420, 439, 440, 441, 446, 448, 450, 454, 458, 459, 461, 492, 503, 527, 530, 531, 576
 compressibility, 333, 351, 357, 363
 compression, 7, 73, 74, 79, 227, 334, 343, 352, 353, 524, 580
 computation, 288
 computational fluid dynamics, 290
 computer, ix, 67, 99, 111, 185, 273, 274, 275, 278, 290, 291, 295, 372
 computer technology, 278
 computer-aided design, ix, 273
 computer-aided design (CAD), ix, 273
 computerization, 291
 computing, 327
 conception, xiii, 290, 519
 Concise, 216, 432
 condensation, 96, 105, 275, 279, 280, 281, 371, 493, 523, 544
 conditioning, 308
 conduction, 48, 71, 112, 275, 276, 277, 280, 287, 318, 370
 conductivity, viii, 12, 52, 89, 110, 111, 118, 152, 191, 245, 276, 277, 281, 318, 319, 320, 323, 324, 325, 443, 551
 conductor, 12
 conductors, 110
 conference, 295
 configuration, 167, 300, 304, 363, 420, 509, 582
 confinement, 370
 conflict, 147
 Congo, 18, 54, 61
 CONGRESS, iv, 188, 200, 272, 576
 conjunctivitis, 502, 506
 connective tissue, 213, 217, 406
 connectivity, 358, 544
 conservation, vii, xiii, 67, 153, 155, 157, 164, 519, 520, 521, 523, 535, 537, 538
 conserving, 155, 164
 consolidation, xiii, 157, 520, 523, 530, 535
 constipation, 70
 constituent materials, 153
 constituents, x, 4, 60, 142, 228, 331
 construction, ix, 10, 12, 32, 49, 52, 68, 71, 85, 90, 92, 98, 156, 223, 225, 226, 227, 232, 233, 237, 238, 244, 246, 251, 255, 265, 267, 272, 291, 357, 403, 412, 525
 consumer goods, 82, 558
 consumers, 50, 56, 77, 83, 84, 274, 292, 372
 consumption, 5, 17, 23, 28, 29, 52, 55, 82, 83, 85, 88, 89, 119, 140, 247, 582
 contact dermatitis, xii, 489, 490, 491, 492, 493, 495, 498, 502, 503, 504, 505, 506
 contact time, 458, 567, 570
 containers, 39, 49, 77, 99, 106, 158, 266
 contaminant, 580
 contamination, 124, 132, 157, 158, 461, 490, 508
 continuous filaments, vii, 1, 247
 contraceptives, 86, 92
 controversial, 385, 587
 convention, 96
 conventional plastics, 98
 convergence, 336, 340
 COOH, 303, 306, 475, 476
 cooking, 34, 50, 70, 74
 cooling, 79, 97, 109, 110, 113, 283, 369, 375, 443
 cooperation, 402
 copolymer, 88, 95, 96, 110, 115, 210, 412, 418, 516
 copolymerization, 86, 219, 314, 411, 558
 copolymers, 88, 95, 96, 110, 210, 402, 408, 411, 412, 415, 418, 420, 421, 537
 copper, xi, 5, 35, 69, 154, 159, 162, 319, 320, 322, 323, 324, 326, 329, 370, 374, 377, 387, 388, 389, 390, 414, 439, 440, 441, 442, 446, 447, 448, 449, 450, 451, 452, 453, 454, 456, 457, 458, 459, 460, 461, 514, 528, 561
 copyright, iv
Copyright, iv
 corona discharge, 300, 301, 307, 314, 513, 517, 573
 correlation, 137, 433, 495
 correlations, 415, 435
 corrosion, 111, 157, 164, 246, 265, 306, 320
 cortex, 45, 46, 68, 72, 73
 corticosteroids, xii, 489, 503
 cosmetic, 25, 71, 478
 cosmetics, 50, 67, 404
 Cosserat type continuum, x, 331
 cost, 21, 29, 44, 50, 52, 63, 84, 87, 88, 99, 112, 200, 205, 209, 214, 237, 240, 242, 245, 246, 258, 292, 293, 298, 310, 323, 324, 326, 364, 372, 411, 440, 494, 542, 559
 Costa Rica, 68
 Côte d'Ivoire, 144
 coughing, 61
 coumarins, 142

covalent bond, 7, 101, 108, 110, 111, 113, 307, 491, 568
 covering, 63, 67, 265, 289, 299
 crabs, 211, 405
 cracks, xiv, 55, 111, 240, 242, 251, 254, 260, 450, 520, 531, 532, 533, 534, 535
 creative process, xiii, 520, 522, 535
 creep, 249, 550, 551
 criticism, 520
 crop, 16, 17, 20, 21, 26, 27, 28, 32, 37, 38, 40, 41, 42, 45, 47, 48, 55, 57, 64, 127, 134
 crop rotations, 27
 crops, 21, 32, 33, 36, 45, 50, 53, 54, 69, 80, 123, 131, 138, 144, 403
 cross-linked polymers, 107
 cross-linking reaction, 304
 crude oil, 193, 401, 402
 crystal growth, 545
 crystal structure, 94, 114, 431, 469
 crystalline, xi, 60, 73, 92, 95, 102, 107, 108, 109, 110, 215, 248, 371, 378, 381, 387, 389, 390, 391, 403, 411, 418, 420, 439, 441, 443, 448, 454, 459, 464, 469, 470, 472, 475, 485, 539, 544, 545, 546, 569
 crystalline lamellae, 110
 crystallinity, 43, 403, 409, 446, 475, 477, 550, 551
 crystallites, 107, 108, 109, 371, 403, 448, 470, 472, 545, 546, 548
 crystallization, 107, 283, 375, 431, 544, 545
 crystals, 546, 547, 551
 CT, 121, 166, 170, 171, 590
 CTA, 211
 Cu cluster, 465
 Cuba, 64
 cues, 215
 cultivars, 32, 40, 41, 70, 120, 124, 125, 130
 cultivation, 1, 10, 14, 15, 17, 20, 21, 22, 33, 34, 40, 47, 48, 53, 62, 80, 127, 131, 406, 409, 431
 cultural heritage, 523, 537
 cultural practices, 27
 cultural transformation, 521
 culture, 14, 16, 17, 46, 69, 142, 153, 409, 410, 419, 431
 culture medium, 410
 curcumin, 220
 cure, 374, 414, 532, 533, 534, 535
 curing process, 527, 545, 548, 550
 currency, 67, 95
 customers, 86
 cuticle, 138
 CV, 474
 CVD, 525, 558

cyanamide, 422
 cycles, 21, 235, 308, 310, 376, 377, 378, 381, 424, 513, 580
 cycling, 120
 cysteine, 35
 cytotoxicity, 397, 407

D

damages, iv, 69, 299, 584
 data analysis, 23, 290
 data availability, 288
 data structure, 340
 data transfer, x, 317
 database, 38
 deacetylation, 211, 219, 405, 420, 437, 477, 478
 debts, 78
 decay, 71, 235, 257
 decomposition, 7, 110, 354, 413, 444, 455, 456, 457, 461, 462, 541, 544, 545, 550
 decomposition temperature, 110
 decontamination, 308
 decortication, 40, 60, 63
 defect site, 385
 defects, 4, 110, 216, 403
 defence, 318
 deficiency, 27, 35, 112, 333
 deficit, 129
 deforestation, 49
 deformation, x, 12, 80, 108, 109, 114, 207, 331, 332, 333, 335, 339, 341, 349, 351, 352, 353, 356, 364, 365, 570
 degradation, ix, xii, xiii, 100, 101, 110, 112, 131, 137, 162, 186, 204, 207, 220, 235, 258, 297, 298, 304, 404, 427, 431, 440, 442, 443, 454, 456, 461, 462, 464, 466, 478, 520, 523, 530, 534, 535, 538, 540, 544, 570, 572, 575
 degradation process, 101
 degradation rate, 204
 degree of crystallinity, 403, 472, 475
 degumming, 45, 131, 490
 dehydrate, 418
 dehydration, 421
 Delta, 47, 50, 52, 56
 denaturation, 208
 denitrification, 97
 Denmark, 413
 deoxyribonucleic acid, 102
 Department of Agriculture, 41, 57, 128
 Department of Commerce, 4
 dependent variable, 174
 deposition, xiv, 73, 200, 201, 206, 217, 307, 314, 315, 320, 373, 374, 376, 377, 378, 379, 381,

- 382, 383, 387, 389, 390, 391, 393, 394, 396,
397, 434, 446, 450, 463, 508, 510, 511, 512,
513, 514, 515, 516, 517, 518, 520, 532, 534,
558, 575
- deposits, 161
- depth, 162, 177, 277, 304, 474, 511
- derivatives, 116, 174, 210, 213, 216, 377, 403,
404, 405, 406, 414, 418, 425, 427, 487, 494
- dermatitis, xii, 489, 490, 491, 493, 494, 495, 496,
502, 503, 504, 505, 506
- dermis, 408
- designers, ix, 273, 290, 291, 521
- desorption, 169, 275, 277, 278, 279, 280, 281
- destruction, 26, 49, 107, 155, 163, 237, 464, 559,
565, 570
- detachment, 530, 532, 533
- detectable, 159, 459, 494
- detection, 112, 154, 374, 395, 474, 538
- detergents, 195
- detoxification, 464
- developed countries, 17, 21, 29, 251
- developed nations, 238
- developing countries, 17, 21, 28, 62, 120, 237,
246
- dew, 29, 37, 39
- diabetes, 38, 134
- diabetic patients, 56
- diagnostic criteria, 491
- diallyldimethylammonium chloride, 511, 512
- diaphragm, xiv, 557, 559, 560, 561, 562, 563,
564, 565, 566, 567, 572
- dicotyledon, 4
- diet, 17, 134
- dietary fiber, 3, 35, 38
- differential equations, 175, 280
- diffraction, 378, 381, 391, 443, 450, 545
- diffuse reflectance, 443, 446
- diffusion, 118, 173, 185, 275, 277, 278, 279, 281,
283, 293, 294, 305, 306, 370, 375, 380
- diffusion process, 281
- diffusion rates, 306
- diffusivity, 281
- digestibility, 128
- diisocyanates, 494
- directionality, 95
- disaster, 80
- discharges, 299, 300, 301, 302, 305, 311, 312,
313, 481, 560, 562, 574, 575
- discomfort, 274
- discontinuity, 109
- discrete elongated pieces, vii, 1
- discrete fibers, ix, 223, 256, 266, 268
- discs, 99
- diseases, 27, 28, 40, 50, 53, 55, 56, 91, 124, 138,
148, 233, 420, 421
- disinfection, ix, 297, 298
- dislocation, 109, 546
- dispersion, viii, 115, 165, 166, 167, 168, 169,
170, 177, 179, 180, 181, 182, 184, 185, 186,
259, 407, 580
- displacement, 301, 335, 336, 337, 340, 341, 342,
351, 352, 354, 355, 356, 357, 359, 361, 363
- dissociation, 472, 474, 475, 476
- distillation, 167
- distilled water, 208
- distortions, 79
- distribution, viii, xii, xiv, 42, 85, 104, 129, 146,
165, 166, 167, 168, 171, 174, 177, 178, 179,
180, 181, 182, 184, 185, 219, 258, 281, 287,
290, 300, 357, 380, 381, 390, 489, 495, 504,
546, 579, 582
- diuretic, 55, 56
- diversity, 139, 310
- DMF, 213
- DNA, 130, 143, 206, 406, 515
- dogs, 3
- DOI, 114, 138, 141, 143, 144, 146, 147, 148,
150, 518
- doping, xi, 376, 439, 440, 441, 456
- double bonds, 87, 103
- draft, 195, 324
- drainage, 75, 99, 132, 145, 514
- drawing, 14, 196, 198, 205, 319, 320, 414, 546,
566, 567, 569, 571
- dressings, 71, 213, 219, 372, 400, 402, 405, 406,
407, 408, 411, 415, 416, 417, 418, 422, 425,
426, 436, 437, 485
- drinking water, 148
- drought, 32, 37, 43
- drug carriers, 371
- drug delivery, xi, 205, 211, 213, 214, 217, 399,
400, 402, 406, 407, 408, 411, 413, 414, 415,
428, 430, 433, 435
- drug release, 207, 212, 215, 216, 403, 404, 431
- drugs, viii, 32, 134, 147, 203, 204, 206, 211, 215,
219, 414, 419, 429, 478
- dry fabric before impregnation, x, 331
- drying, 34, 38, 45, 62, 66, 70, 74, 75, 77, 127,
132, 196, 198, 254, 257, 389, 407, 408, 420,
443, 478, 508, 514, 526, 542
- ductility, 228, 235, 236, 238, 240, 370
- durability, 5, 33, 52, 58, 63, 75, 84, 192, 235,
240, 246, 253, 254, 255, 257, 258, 259, 325
- dye distribution factor (DDF), viii, 165, 177, 179

dyeing, vii, 52, 70, 114, 157, 165, 166, 167, 168, 169, 170, 171, 172, 173, 177, 179, 180, 183, 185, 188, 189, 305, 306, 314, 324, 395, 396, 402, 430, 461, 481, 492, 493, 512, 513
 dyes, xii, 42, 52, 167, 185, 186, 314, 396, 413, 440, 443, 453, 454, 459, 461, 464, 476, 489, 490, 491, 492, 494, 495, 497, 498, 499, 500, 502, 503, 504, 505, 506, 560, 568, 575, 576
 dynamical systems, 176
 dynamism, 29
 dyspepsia, 55
 dysuria, 55

E

E.coli, 389, 458, 459
 early labor, 87
 earnings, 22, 46
 Eastern Europe, 30, 326, 395, 515, 517, 518
 ECM, viii, 203, 204, 205, 208, 213, 420, 421
 ecology, 17
 economic growth, 83
 economics, 258
 Ecuador, 66
 eczema, 13, 500, 501, 502
 editors, 485, 487
 effluent, 63, 298, 394
 effluents, 186, 412, 413, 464
 egg, 11
 Egypt, 1, 10, 14, 18, 21, 22, 26, 28, 36, 42, 50, 54, 56, 61, 74, 111, 125, 225
 El Salvador, 64
 elaboration, 359
 elastic deformation, 80, 108
 elasticity modulus, 207
 elastin, 208, 209, 218, 219, 406, 407, 428, 429
 elastomers, 80, 86, 98, 107, 108, 110
 electric field, 198, 205, 207, 298, 300, 301, 415, 480
 electrical conductivity, 112, 231, 319, 323
 electrical properties, ix, 298, 324, 549
 electrical resistance, 92, 151
 electricity, 12, 67, 93, 110, 318, 321, 373
 electrode surface, 301
 electrodeposition, 371
 electrodes, 299, 300, 301, 302, 310, 323, 415, 560, 563, 565, 567, 576
 electrolysis, 575
 electrolyte, xiv, 508, 517, 557, 560, 561, 562, 565, 566, 572, 577
 electromagnetic, 277, 301, 318, 319, 321, 322, 323, 324, 325, 327
 electromagnetic waves, 277, 301, 321

electron, ix, 7, 11, 103, 111, 143, 154, 159, 160, 161, 217, 298, 371, 385, 410, 443, 477, 512, 533, 545, 546, 550, 562, 566
 electron diffraction, 546
 electron microscopy, 154, 217, 443
 electron pairs, 477
 electronic materials, 371
 electronic systems, 113
 electrons, ix, 298, 301, 370, 566, 567
 electroplating, 576
 electrospinning, viii, xi, 198, 203, 205, 206, 207, 208, 211, 212, 213, 214, 215, 216, 217, 218, 219, 220, 399, 400, 405, 407, 408, 412, 414, 415, 416, 420, 427, 435, 553
 elephants, 98
 elongation, 43, 84, 96, 107, 109, 144, 205, 235, 309, 333
 embryogenesis, 216
 emission, 77, 131, 151, 298, 380, 561
 emulsions, 75
 encapsulation, 206, 430
 encoding, 117, 429
 endoskeleton, 91
 endothelial cells, 209
 endothermic, 79
 endurance, 75
 energy consumption, 587, 588, 590
 energy density, 372
 energy input, 561
 engineering, viii, ix, 5, 98, 167, 177, 197, 203, 204, 209, 215, 216, 217, 228, 229, 231, 233, 244, 247, 258, 264, 273, 274, 275, 276, 279, 288, 291, 292, 347, 400, 406, 412, 415, 419, 420, 421, 437, 463, 555, 575
 England, 14, 15, 21, 23, 76, 78, 87, 227, 293, 485, 517, 538
 enlargement, 353, 531
 entrepreneurs, 119
 entropy, 79
 entropy model, 79
 environment, ix, xiii, xiv, 49, 53, 101, 123, 131, 136, 154, 253, 256, 258, 273, 274, 275, 278, 282, 283, 286, 287, 288, 289, 291, 302, 373, 383, 402, 410, 413, 415, 417, 421, 510, 520, 523, 530, 535, 538, 549, 557, 575
 environment control, 575
 environmental characteristics, 234
 environmental conditions, 3, 28, 101, 249, 284, 288, 292, 521
 environmental degradation, 63, 100, 258
 environmental effects, 143
 environmental factors, 117
 environmental impact, viii, 128, 165

environmental management, 53
 environmental stress, 310
 environmental threats, 318
 environments, ix, 91, 235, 244, 273, 274, 284,
 285, 288, 291, 295
 enzyme, 52, 128, 137, 186, 211, 412, 413, 415,
 422, 434, 516
 enzyme immobilization, 211, 415
 enzymes, 6, 29, 59, 71, 100, 128, 206, 212, 404,
 413, 434, 516, 588
 epidermis, 30, 46, 72, 73, 498, 500, 501
 epithelium, 417
 epoxy polymer, 148
 epoxy resins, 111
 EPR, 433
 equilibrium, xiv, 79, 166, 167, 169, 170, 171,
 180, 279, 298, 306, 335, 337, 339, 341, 353,
 354, 355, 356, 357, 359, 360, 362, 363, 392,
 480, 557, 558, 559, 562, 572, 573, 580
 equipment, 85, 99, 167, 168, 169, 172, 189, 229,
 242, 324, 393, 526, 559, 581
 erosion, 33, 49, 59, 580
 erythema multiforme, xii, 489
 ESI, 530
 ESR, 385, 386, 389, 545
 ESR spectra, 386
 essential fatty acids, 34, 35
 ester, 105, 197, 377, 568, 570
 ester bonds, 568, 570
 etching, 306
 ethanol, xiv, 373, 442, 520, 525, 575
 ethics, 164
 ethylene, 88, 103, 104, 105, 115, 196, 200, 211,
 212, 220, 373, 414, 514, 517, 518, 520, 526,
 528, 570, 571
 ethylene glycol, 105, 197, 220
 ethylene oxide, 200, 211, 212, 220, 414, 517
 eucalyptus, 68
 Euler-Lagrange equations, 354
 Europe, 1, 10, 19, 20, 32, 33, 36, 37, 38, 40, 55,
 59, 61, 74, 77, 78, 87, 89, 138, 394, 493, 522
 European market, 372
 European Union, 94, 504
 evaporation, 205, 275, 279, 280, 281, 371, 374,
 420, 449, 450, 544, 562
 everyday life, 301
 evidence, 14, 56, 119, 157, 158, 225, 232, 240,
 375, 527, 568, 588
 evolution, 146, 168, 171, 178, 341, 348, 349,
 351, 544, 545, 546, 554
 EXAFS, 552
 excavations, 500
 excision, 127

excitation, 584
 execution, 244
 exoskeleton, 405
 expertise, 156, 521
 exploitation, 14, 133, 383
 explosives, 4
 exporters, 46
 exports, 62
 exposure, 7, 11, 16, 34, 45, 94, 100, 141, 148,
 196, 223, 251, 263, 308, 312, 397, 415, 436,
 444, 491, 495, 502, 504, 506, 550, 569, 580,
 581
 external environment, 274
 extinction, 92, 98
 extracellular matrices (ECM), viii, 203, 204
 extracellular matrix, 200, 204, 208, 210, 216,
 217, 419, 421, 427
 extraction, 3, 41, 45, 48, 58, 60, 63, 128, 198,
 307, 319, 524
 extracts, 123, 133, 404
 extravasation, 497
 extrusion, 95, 98, 139, 199, 250, 318, 407, 411,
 414
 exudate, 402, 417, 418

F

fabrication, 14, 68, 140, 198, 206, 211, 213, 216,
 374, 376, 396, 414, 415, 420, 428, 429, 511,
 517, 518, 540
 Fabrication, 198, 205, 328, 422, 424, 426, 515
 factories, 10, 77, 88, 194
 false negative, 502
 families, 332
 farmers, 8, 13, 20, 46, 50, 121
 farms, 50, 116, 119
 fat, 34, 38, 50, 51, 286, 288, 586
 fatty acids, 37, 38, 40, 77, 374
 FDA, 416, 502
 feedstock, 406
 feedstocks, 411
 feelings, 275
 FEM, 584
 fermentation, 100, 131, 400, 409, 411, 412, 419,
 432, 433
 fertility, 50, 53, 69, 133, 136
 fertilization, 16, 120
 fertilizers, 21, 38, 55, 63
 fiber bundles, 29, 112
 fiber content, 45, 49, 148, 260, 326
 fiber optics, 5, 116
 fibrillation, 250, 257
 fibrinogen, 209, 218, 416

- fibroblast growth factor, 425
fibroblasts, 220, 407, 421
fibrous tissue, 41
filament, 2, 10, 11, 13, 61, 141, 196, 199, 224, 245, 263, 264, 265, 321, 323, 324, 325, 412, 548, 554
fillers, 110, 324, 530
film formation, 526
film thickness, 532
films, xiv, 47, 98, 106, 111, 113, 149, 152, 196, 197, 246, 260, 272, 282, 283, 314, 402, 405, 407, 408, 417, 422, 424, 425, 426, 430, 463, 468, 508, 513, 515, 516, 517, 518, 520, 531, 532, 533, 534, 535
filters, 24, 63, 67, 92, 113, 210, 309, 319, 561
filtration, 75, 140, 197, 199, 204, 325
financial, 144, 461
financial support, 461
fine wool, 3
finite element method, 584
Finland, 74, 494, 495
fire resistance, 89, 255
first generation, xiv, 2, 417, 418, 539, 548
fish, 55, 71, 126, 407
fish oil, 71
fishing, 34, 40, 45, 57, 59, 70, 89, 92, 95, 99, 147, 229
fixation, xiv, 373, 480, 557
flame, 24, 52, 93, 110, 121, 122, 193, 196, 200, 389, 398, 465
flame retardants, 110
flammability, 76, 97, 98
flavonoids, 56
flavonol, 132
flavor, 55, 56, 63
flaws, 111, 257
flax fiber, 36, 39, 70
flexibility, viii, xiv, 191, 200, 207, 323, 326, 353, 377, 520, 523, 531, 533
flexural vibration modes, 581
flight, 269
flocculation, 186
flooring, 67, 84, 99, 238, 259
flora, 138, 397
flotation, 75
flour, 34, 68, 100
flowering period, 63
flowers, 35, 39, 53, 55, 56, 70
fluctuations, 87, 402, 406, 580
fluid, viii, 77, 80, 165, 166, 168, 169, 205, 290, 298, 307, 418, 419, 580
fluorescence, 154, 156, 522, 528, 529
fluorine, 307
foams, 85, 99, 100, 197, 408, 417, 506
foils, 318, 320
folic acid, 51
food, vii, 1, 17, 21, 32, 34, 50, 55, 67, 68, 70, 71, 73, 75, 90, 91, 92, 99, 101, 126, 393, 404, 405, 478, 487
Food and Drug Administration, 75, 416, 502
food industry, 404, 405
food products, 34
football, 226
footwear, 67, 86, 90
force, ix, xi, 12, 13, 79, 80, 98, 107, 108, 110, 167, 175, 178, 179, 181, 183, 223, 279, 281, 334, 337, 338, 342, 343, 346, 349, 352, 353, 354, 355, 356, 369, 370, 375, 380, 383, 580, 582
foreign exchange, 22, 46
formaldehyde, xii, 8, 61, 75, 98, 99, 100, 105, 106, 374, 489, 493, 494, 497, 503, 504, 505, 506
formula, 3, 60, 102, 248, 283, 545
fossils, 91, 402, 406
fouling, 199
foundations, 243
fracture toughness, 229, 420
fractures, 238
fragments, vii, 14, 91, 153, 157, 158, 544
France, 4, 14, 22, 32, 42, 54, 55, 76, 117, 331, 494, 495, 536
free energy, 205, 279, 513
free radicals, 378, 566
freezing, 16, 17, 198, 424
freshwater, 91, 407
freshwater species, 91
friction, 90, 92, 100, 132, 310, 321, 322, 324, 332, 337, 351, 353, 354, 355, 356, 357, 364, 366, 491, 495, 504, 550
frost, 32, 43
fructose, 99
fruits, 4, 34, 68
FTIR, 116, 154, 156, 159, 160, 162, 163, 306, 383, 423, 512, 513, 514, 522, 526, 528, 529, 530, 535, 538, 544, 568
FTIR spectroscopy, 513
functionalization, x, xii, 149, 206, 369, 395, 467, 473, 480, 534, 537
funding, 163
fungi, 26, 28, 45, 59, 92, 101, 125, 253, 254, 372, 404, 405, 483, 484
fungus, 27, 28, 59, 414
fusion, 298, 378, 540

G

Gabon, 137
gallbladder, 94
gallium, 414
gamma-tocopherol, 56, 134
gastrointestinal tract, 94
gel, xiv, 71, 210, 211, 371, 374, 395, 402, 410, 418, 422, 450, 462, 463, 465, 478, 520, 522, 523, 531, 535, 537
gelation, 198
gene therapy, 406
genes, 117, 124, 340, 414
genetic engineering, 400, 406, 412, 413
genetics, 340
genome, 143
genus, 15, 31, 35, 42, 45, 69, 80, 122
geographical origin, 14
geometrical parameters, 363
geometry, x, 229, 230, 238, 279, 281, 299, 311, 324, 331, 332, 333, 341, 347, 363, 364, 562
Georgia, 36, 40, 129, 295
Germany, ix, 32, 42, 47, 55, 76, 78, 79, 87, 98, 105, 121, 145, 200, 203, 218, 224, 246, 264, 327, 439, 442, 443, 465, 494
germination, 16, 55, 129
gibberellin, 138
gland, 11, 118
glass transition, 80, 109, 110
glass transition temperature, 80, 109, 110
glasses, 109, 420, 523
global scale, 22
glow discharge, 299, 302, 304, 310, 311, 312, 313, 315, 559, 560, 561, 562, 563, 564, 565, 566, 574, 575, 577
glucose, 60, 210, 211, 214
glue, 75, 527
glutamic acid, 418, 436, 518
glycerol, 210
glycine, 12
glycol, 477
glycoproteins, 408
glycosaminoglycans, 213, 214
gold nanoparticles, 370
google, 147, 327
grades, 4, 9, 37, 40, 59, 62, 68, 549
grading, 195
grain boundaries, 545
granules, 89, 146
graphite, 112, 245, 251
grass, ix, 1, 43, 45, 61, 130, 193, 223, 588
grasses, 49
grasslands, 6

gratings, 516
gravity, 339
Great Britain, 250, 443
Greece, vii, 19, 61, 129, 153, 154, 163, 203
Greeks, 9, 92
greenhouse, 53, 98, 123
greenhouse gas, 98
grids, 271
growth factor, 204, 213, 216
growth rate, 28, 88
growth rings, 73
Guangdong, 293
Guangzhou, 273
guidance, 217
guidelines, vii, 153, 158, 258
Guinea, 54
gunpowder, 13, 24
gutta-percha, 77, 78, 80, 142

H

H. sabdariffa, 53, 55
habitat, 71
habitats, 91
hair, ix, 2, 6, 29, 37, 40, 76, 93, 95, 114, 116, 117, 192, 223, 232
Haiti, 64, 77
Han dynasty, 10
handbags, 61, 68
HAP, 421
happiness, 273
hardener, 107
hardness, 110
hardwoods, 41, 71
harvesting, 17, 18, 44, 45, 58, 120, 146
hazards, 53, 94
HDPE, 99
healing, viii, xi, 67, 71, 98, 203, 204, 240, 270, 399, 403, 410, 416, 417, 419, 425, 426, 429, 432, 451
health, vii, xii, 32, 34, 40, 53, 55, 57, 70, 94, 199, 223, 234, 260, 273, 274, 292, 317, 318, 325, 416, 422, 467, 469
health care, xii, 416, 467, 469
heat capacity, 281, 287
heat conductivity, 289
heat loss, 274, 282, 283, 286, 287
heat release, 289
heat shield, 90
heat stroke, 566
heat transfer, 275, 276, 277, 279, 280, 281, 283, 287, 290
heavy metals, 214, 414

height, 16, 32, 35, 38, 40, 143, 166, 168, 170
helium, 303, 304, 310, 312, 313
hemicellulose, 116, 423, 431
hemp, 3, 4, 15, 29, 30, 31, 32, 33, 34, 35, 37, 42, 43, 61, 62, 66, 74, 76, 125, 126, 128, 193, 400, 412, 433, 471, 490
hemp fiber, 32, 33
herbal teas, 21, 55
herbicide, 20, 124
heritability, 116
heterogeneous systems, 383
hexane, 95
HFP, 208, 209
high recirculation flux values, viii, 165
high resolution transmission electron microscope, 390
high strength, 37, 71, 228, 229, 242, 321
highways, 225
history, vii, xiii, 1, 5, 9, 49, 69, 78, 105, 111, 114, 116, 121, 145, 148, 151, 152, 177, 180, 181, 192, 278, 311, 490, 521
HIV, 85
hobby, 8
homes, 10, 225, 229
homogeneity, xv, 211, 266, 299, 305, 579, 582
homopolymers, 210
honey bees, 63
Hong Kong, 15, 273, 395
hormones, 117
horses, 6, 60
host, 26, 28, 91, 125, 206
hot spots, 378
House, 295
housing, 70, 237
HPC, 211
HRTEM, 390, 391
human, vii, 1, 3, 34, 35, 36, 58, 110, 127, 197, 204, 208, 209, 220, 258, 273, 274, 275, 284, 285, 286, 287, 288, 289, 290, 291, 292, 295, 317, 374, 401, 404, 406, 407, 408, 412, 421, 425, 429, 436, 491, 516
human body, 204, 274, 275, 284, 285, 286, 287, 288, 289, 291, 292, 408, 421
human condition, 412
human health, 258, 374, 421
human skin, 110, 436
humidity, xiii, 27, 28, 42, 47, 63, 71, 73, 80, 275, 278, 279, 280, 289, 290, 295, 304, 306, 520, 523, 530, 534, 558
Hungary, 32
hybrid, 37, 65, 117, 130, 219, 260, 262, 263, 264, 267, 322, 323, 324, 370, 537, 576
hybridization, 80

hydrocortisone, 503
hydrogels, 210, 408, 417, 418, 426, 431
hydrogen, 2, 4, 7, 12, 95, 97, 101, 102, 103, 104, 127, 141, 167, 247, 307, 314, 375, 378, 422, 442, 469, 475, 513, 544, 545
hydrogen atoms, 101, 102, 103, 545
hydrogen bonds, 7, 12, 97
hydrogen peroxide, 103, 127, 375, 422, 442, 475
hydrogen sulfide, 141
hydrolysis, 211, 382, 389, 398, 404, 406, 423, 424, 523, 525, 535, 571, 572
hydrophilicity, 303, 305, 306, 469, 471, 476, 480
hydrophobic properties, 307, 314, 531, 534
hydrophobicity, 307, 314, 523, 531
hydrothermal process, 462
hydroxide, 570
hydroxyapatite, 408, 420, 421, 428, 429, 432
hydroxyethyl methacrylate, 418
hydroxyl, xiv, 97, 121, 211, 385, 386, 449, 469, 477, 511, 542, 557, 568, 569, 570, 572
hydroxyl groups, 97, 211, 469, 477, 569, 571
hydroxypropyl cellulose, 211, 403
hygiene, xii, 85, 199, 254, 400, 467, 469, 485
hypersensitivity, 497, 498, 499, 500
hypertension, 56, 134
hypothesis, 101
hysteresis, 235

I

ibuprofen, 211, 212, 220
ideal, 79, 81, 163, 179, 198, 227, 279, 404, 412, 468, 478
identification, vii, xiii, 9, 126, 143, 153, 154, 159, 161, 163, 390, 519, 522
identity, 49, 355
illumination, 440, 441, 442, 443, 446, 455, 457, 458, 459, 460
image, 161, 197, 215, 381, 382, 385, 387, 391, 409, 531, 546, 547
imagery, 125
images, 158, 212, 379, 381, 382, 388, 392, 450, 451, 452, 453, 531, 532, 533, 534, 542, 548, 562, 563
imitation, 49
immersion, 373, 526
immobilization, 212, 220, 374, 396
immune response, 407
immunogenicity, 210
impact strength, 95, 250
implants, 67, 92, 191, 372, 407
impregnation, x, 162, 266, 331, 333, 373, 481, 532, 566

- impression materials, 402
 improvements, viii, 165, 288, 334
 impurities, 87, 195, 257, 301, 373, 381, 391, 413, 480, 580
 in vitro, 212, 221, 425, 429, 430
 in vivo, 212, 216, 221, 426
 incidence, xii, 27, 28, 148, 255, 489, 490
 income, vii, 20, 21, 82
 incompatibility, 523
 incubation time, 305
 incubator, 11, 196
 India, ix, 1, 4, 10, 13, 14, 15, 18, 20, 22, 23, 26, 29, 36, 37, 38, 40, 42, 47, 49, 55, 59, 68, 81, 82, 83, 89, 118, 120, 121, 132, 133, 195, 224, 413
 Indians, 47, 134
 individuals, 38, 268, 340, 490, 493
 Indonesia, 47, 53, 54, 59, 82
 induction, 495
 industrial processing, 32, 268
 industrial revolution, 2, 10, 33, 372, 413
 industrialization, 49
 industrialized countries, xii, 489
 industries, viii, 30, 46, 47, 49, 56, 68, 84, 131, 191, 197, 228, 229, 233, 234, 237, 245, 258, 413, 433
 infants, 495
 infarction, 210
 infection, 124
 infectious agents, 421
 infestations, 26
 inflammation, 502
 information exchange, 105
 information technology, 198
 infrared spectroscopy, 154, 306, 522, 538
 infrastructure, 31, 245
 infundibulum, 498
 ingestion, 35
 ingredients, 236, 238
 inhibition, 228, 240, 251, 309, 386, 391, 404, 454, 483, 484
 inhibitor, 123
 initial state, 333, 340
 initiation, 205, 560, 566
 injure, 40
 injuries, 416, 418
 injury, iv, 55, 72, 148, 210, 397
 inoculum, 124
 INS, 545
 insecticide, 17, 20
 insects, 1, 10, 12, 17, 20, 26, 117, 196
 insertion, 111, 376
 institutions, 372
 insulation, 6, 9, 31, 33, 40, 48, 59, 67, 89, 92, 93, 99, 100, 293, 295, 372
 insulators, 106, 111, 229
 integration, 173, 175, 274, 288, 318
 integrity, 421
 interface, 132, 207, 223, 229, 256, 257, 259, 260, 264, 279, 284, 289, 291, 306, 516, 548, 561
 interference, 323
 intermetallic compounds, 450
 Internal structure, 515
 internalization, 385
 interphase, 306, 551, 572
 intervention, 153, 198, 510
 intrinsic value, 279
 inventors, 105, 106
 inversion, 172
 invertebrates, 405
 investment, 21, 299
 investments, 23, 26
 investors, 78
 iodine, 419
 ion bombardment, 566
 ionization, 298, 300, 380
 ions, 298, 299, 301, 304, 373, 378, 380, 384, 387, 388, 389, 406, 419, 458, 480, 514, 524, 566
 IR spectra, 568, 569
 IR spectroscopy, 568
 Iran, 18, 40, 54
 Iraq, 5
 Ireland, 577
 iron, 3, 5, 35, 50, 51, 61, 93, 111, 112, 159, 162, 320, 396, 440
 irradiation, xi, 143, 199, 201, 369, 374, 375, 376, 377, 378, 381, 382, 383, 388, 389, 390, 396, 404, 414, 425, 426, 461, 546, 550
 irrigation, 16, 22, 27, 28, 40, 129, 225
 Islam, 137, 434
 islands, 54, 62, 199
 isobutylene, 87
 isolation, 138, 403, 407, 423
 isophthalic acid, 96
 isoprene, 77, 86, 87
 Israel, 123, 369, 494, 505
 issues, 156, 157, 205, 216, 256, 258, 274, 520, 554, 573
 Italy, 10, 14, 40, 55, 89, 90, 129, 165, 246, 487
 Ivory Coast, 47

J

- Jamaica, 54, 56
 Japan, 10, 42, 49, 83, 116, 245, 397, 398, 494, 495, 548, 552

joints, 226, 238, 242, 333
 Jordan, 164, 462, 515
 journalists, 234
 J-shape tensile response, x, 331

K

Kazakhstan, 80
 Kenya, ix, 50, 62, 64, 223, 224, 226, 234, 246,
 251, 268, 269
 keratin, 6, 116, 159, 213, 377
 keratinocyte, 421
 keratinocytes, 220, 407, 421
 kidney, 94
 kill, 13, 16, 17, 113
 kinetic model, 577
 kinetics, vii, 115, 141, 165, 306, 375, 573
 knots, 71
 Korea, 4, 32, 461
 Kyrgyzstan, 80

L

labeling, 77
 labor market, 119
 labor markets, 119
 lack of control, xii, 259, 489, 490
 lactic acid, 100, 212, 405, 411, 415, 419, 427,
 433
Lactobacillus, 411
 lactose, 35
 lakes, 69, 75
 laminar, 112, 421
 larva, 10
 larvae, 10, 11, 17, 91, 122
 larynx, 94
 latency, 94
 lateral roots, 45
 Latin America, 54, 80
 lattices, 367
 laws, 366
 LDCs, 17, 20
 LDL, 214
 leaching, 257, 376, 384, 387, 388, 393, 420
 lead, viii, xiii, 5, 10, 29, 78, 95, 98, 100, 110,
 112, 165, 167, 177, 204, 206, 215, 293, 310,
 407, 441, 446, 450, 453, 454, 456, 457, 458,
 459, 478, 490, 491, 504, 523, 527, 531, 534,
 538
 leadership, 371
 LEAF, 468
 learning, 131, 290, 295
 Lebanon, 56

legislation, 504
 legs, 286, 287, 497
 legume, 55
 lending, vii
 lens, 67, 158
 Lepidoptera, 120, 122, 123
 lesions, xii, 489, 495, 497, 498, 499, 500, 502,
 503, 506
 lice, 68
 life cycle, 11, 117
 lifetime, 299, 567
 ligament, 209, 407
 light, 6, 7, 12, 32, 37, 44, 48, 57, 70, 75, 76, 93,
 97, 98, 100, 110, 111, 226, 237, 245, 298, 383,
 440, 441, 444, 446, 449, 453, 455, 457, 458,
 462, 465, 512, 513, 516
 light beam, 237
 light emitting diode, 98
 lignans, 38
 lignin, 3, 30, 33, 41, 46, 49, 57, 58, 66, 71, 74,
 111, 129, 130, 235, 403, 471
 limestone, 3, 226
 linear polymers, 107, 247
 linen, 4, 7, 14, 15, 30, 33, 36, 37, 42, 44, 61, 75,
 193, 417, 478
 linoleic acid, 35, 51, 134
 lipases, 413
 lipids, 126, 127, 408
 liquid chromatography, 154, 522, 538
 liquid interfaces, 279
 liquid phase, 167, 170, 178, 179, 278, 280, 284,
 371, 375, 560
 liquids, 97, 110, 220, 249, 307, 374, 441, 560,
 561, 584, 591
 liver, 209, 210, 215, 219
 liver failure, 215
 livestock, 17, 24, 40
 localization, 363, 398, 504, 572
 logging, 53
 Louisiana, 40
 low density polyethylene, 136
 low dispersion resistances, viii, 165
 low temperatures, 80, 109, 371, 425, 526
 low-density lipoprotein, 214
 lubricants, 52
 luggage, 247
 lumen, 73, 161
 luminosity, 298, 530
 lung cancer, 94, 233
 lung disease, 94, 397
 Luo, v, 54, 273, 281, 294, 295, 554
 lying, 70, 112
 lysozyme, 213

M

- machinery, 9, 33, 59, 85, 88, 194
 macromolecules, 2, 60, 102, 107, 204, 205, 213, 566, 570, 572
 magnesium, 3, 35, 92, 389, 391, 398
 magnetic field, 301
 magnetic field XE "magnetic field" s, 301
 magnetic materials, 370
 magnetic properties, 408
 magnets, 372
 magnitude, 166, 265, 333
 majority, 154, 230, 302, 334, 580
 Malaysia, 54, 55, 57, 77, 81, 82, 83, 134, 143
 mammals, 1
 man, 4, 5, 65, 97, 98, 115, 144, 232, 327, 468, 471, 485
 management, 9, 16, 17, 26, 27, 28, 123, 125, 129, 134, 144, 258, 275, 372, 394, 416, 418, 422, 436
 manganese, 3, 35, 124
 manifolds, 95
 manipulation, 130
 manpower, 198
 manufactured goods, 92
 manufactured housing, 31
 manufacturing, ix, x, 3, 10, 13, 22, 30, 36, 37, 46, 49, 50, 67, 84, 88, 111, 126, 141, 195, 199, 205, 224, 235, 244, 246, 250, 251, 259, 262, 317, 318, 319, 320, 321, 322, 323, 325, 326, 410, 471, 581
 manure, 55
 mapping, 125, 381, 382
 marijuana, 32, 126
 marine environment, 149
 marine fish, 407
 market penetration, 494
 market share, 23
 marketing, 86, 504
 marketplace, 22
 marsh, 14
 Maryland, 295
 MAS, 546
 mass spectrometry, 125, 522, 538
 materials science, 229, 372, 538
 mathematics, 293
 matter, iv, 25, 47, 86, 137, 197, 258, 298, 334, 339, 341, 353, 397, 514
 Mauritius, 68
 measurement, 9, 12, 132, 146, 151, 158, 197, 221, 250, 279, 282, 327, 442, 443, 444, 509, 514, 534
 measurements, 102, 116, 197, 304, 307, 325, 344, 347, 352, 353, 443, 444, 445, 446, 448, 449, 450, 453, 455, 456, 458, 487, 512, 513, 514, 515, 516, 524, 526, 530, 536, 562
 meat, 9, 35, 67, 117
 mechanical degradation, 550
 media, 59, 197, 210, 291, 325, 357, 364, 367, 476, 478, 558, 561
 medicine, ix, xi, 50, 55, 56, 92, 203, 204, 215, 295, 399, 412, 414, 437, 506
 Mediterranean, 14, 36, 89, 91
 Mediterranean countries, 14
 melon, 26, 124
 melt, 24, 78, 96, 97, 107, 210, 247, 304, 309, 319, 411, 415, 424, 540, 550, 558
 melting, xi, 96, 109, 110, 112, 151, 197, 283, 369, 370, 376, 378, 383, 387, 393, 414, 477, 541
 melting temperature, 109, 110, 151, 370
 membranes, 113, 199, 211, 212, 213, 214, 220, 262, 367, 405, 407, 411, 428, 432, 433, 436, 517
 memory, 370
 Mercury, 503
 mesenchymal stem cells, 433
 Mesopotamia, 14
 mesoscopic scale, x, 331, 332, 333, 347
 mesothelioma, 94
 metabolic syndrome, 134
 metabolism, 143, 275
 metal complexes, 396
 metal fibers, x, 317, 318, 319, 326
 metal ion, 377, 435, 560
 metal ions, 377, 435, 560
 metal nanoparticles, 408
 metal oxides, 318, 373, 376, 395
 metal salts, 101, 318, 373
 metals, vii, 1, 5, 71, 74, 79, 107, 108, 109, 111, 112, 157, 318, 319, 320, 321, 371, 373, 394, 440, 458
 metamorphosis, 10
 metastasis, 127
 meter, 224, 225, 258, 263, 526
 meth, 219
 methacrylic acid, 513
 methanol, 167, 189, 418, 517, 524, 543
 methodology, 58, 347, 351, 520, 524, 576
 methyl cellulose, 211, 403
 methyl group, 248
 methyl groups, 248
 methylation, 211
 methylene blue, 466

- Mexico, 8, 16, 40, 54, 56, 59, 61, 64, 68, 80, 81, 136, 232, 493
mice, 127, 128
microclimate, 279, 280
microcrystalline, 403, 422, 423, 540, 552
microcrystalline cellulose, 403, 422, 423
micrometer, 158, 370, 380, 412
micronutrients, 38, 53
microorganism, 458, 483
microorganisms, 58, 60, 101, 113, 253, 372, 377, 400, 404, 432, 483, 484
microscope, 3, 11, 115, 151, 160, 161, 162, 163, 512, 524, 526
microscopic behavior, x, 331
microscopy, 125, 154, 156, 163, 431, 512, 526, 533
Microsoft, 269
microspheres, 376, 397, 429, 430, 433, 437, 508
microstructure, xiv, 116, 137, 232, 539, 545, 546, 554
microstructures, 231
microwaves, 302
Middle East, 251, 254
migration, 207, 254, 277, 383, 530
mildew, 1, 7, 11, 42, 44, 123, 395
military, vii, 85, 95, 245, 317, 318, 325, 493, 549
milligrams, 508
mineralization, 396
Ministry of Education, 539
Minneapolis, 293
miscarriage, 24
mixing, viii, 89, 110, 165, 166, 167, 171, 172, 173, 177, 180, 181, 217, 225, 236, 252, 259, 383, 398, 478
MMCs, 224, 231
mobile phone, 99, 318, 324
model system, 134, 427
modelling, 332, 334, 365, 367
models, 167, 169, 173, 281, 284, 285, 286, 287, 288, 290, 293, 332, 333, 334, 353, 357, 364, 366, 367, 430, 470, 520
modern science, 192
modifications, vii, ix, 136, 206, 297, 456, 478, 514, 559
modules, 325, 563
modulus, 2, 74, 100, 107, 109, 113, 231, 235, 333, 336, 341, 343, 344, 345, 363, 364, 366, 409, 539, 540, 549, 550, 551, 552
moisture, 5, 7, 10, 12, 16, 27, 31, 32, 41, 50, 52, 58, 62, 73, 75, 110, 133, 196, 204, 235, 275, 276, 277, 278, 279, 280, 281, 282, 283, 284, 286, 288, 289, 290, 293, 294, 416, 417, 419, 530, 535, 538
moisture content, 62, 73, 75, 133, 235
moisture sorption, 278, 279, 280, 281
molasses, 55
mold, 98, 197
moldings, 99, 100
molds, 77
molecular mass, 97, 472, 477, 478
molecular orientation, 472
molecular structure, 12, 247, 370, 468, 469, 541
molecular weight, 77, 95, 102, 197, 211, 247, 307, 402, 405, 411, 436, 472, 475, 479, 514, 541, 544, 548
molecules, 101, 102, 103, 104, 113, 196, 204, 205, 206, 208, 214, 246, 247, 248, 298, 299, 305, 306, 371, 372, 375, 408, 414, 431, 469, 472, 477, 480, 495, 508, 523, 544, 566, 570
mollusks, 407
molybdenum, 95, 440, 462, 524
momentum, 372
Mongolia, 10
monks, 10
monolayer, 367
monomers, 86, 87, 88, 95, 96, 101, 102, 103, 105, 110, 247, 307, 308, 400, 402, 419, 477, 491
monopoly, 94
Montana, 38
Moon, 148
Morocco, 74
morphology, 107, 130, 198, 219, 379, 381, 384, 387, 390, 391, 395, 398, 435, 450, 471, 480, 483, 517, 538
Moscow, 142, 573, 577
Moses, 133, 269
motif, 208
motivation, 258
moulding, 250
Mozambique, 18, 64
MTBE, 462
mucosa, 211
mucous membrane, 497
mucous membranes, 497
multilayer films, 206, 515, 516, 517
multilayered structure, 107
multinational companies, 29
multiplication, 62
museum collections, xiii, 519, 520, 535
museums, 118, 522, 538
music, 318
mussels, 477
mutant, 134
mutation, 134, 340
mutations, 340
Myanmar, 18, 47, 55

myocardial infarction, 210
myocardium, 210, 367

N

NaCl, 212, 384, 387, 388
Namibia, 54
naming, 96
nanocomposites, 121, 201, 206, 373, 374, 395,
410, 413, 414, 423, 424, 431, 432, 462
nanocrystals, 373, 387, 393, 394, 404, 413, 423,
545
nanofibers, 198, 205, 206, 207, 208, 209, 210,
211, 212, 213, 214, 216, 217, 218, 219, 220,
400, 405, 413, 414, 415, 416, 417, 423, 425,
427, 435, 436
nanofibrous membranes, 213
nanoindentation, 423
nanolayers, 508, 513, 515, 517
nanomaterials, 371, 372, 376, 396, 413, 415, 514,
537
nanometer, viii, 102, 113, 197, 203, 207, 371,
412, 413
nanometer scale, viii, 203, 207, 413
nanometers, 205, 206, 380, 474, 512
nanometric range, 387, 391
nanoparticles, x, 200, 369, 370, 372, 373, 374,
375, 376, 377, 378, 379, 383, 384, 387, 389,
390, 391, 393, 394, 395, 396, 397, 398, 403,
404, 405, 406, 412, 413, 414, 419, 424, 426,
427, 432, 433, 434, 435, 436, 440, 509, 513,
518
nanorods, 370, 415
nanostructured materials, viii, 203, 205, 371, 374,
413, 434
nanostructures, 210, 414, 435
nanotechnologies, 373, 419
nanotechnology, viii, xi, 191, 197, 199, 200, 201,
372, 394, 399, 400, 413, 414, 415, 434, 517
nanotube, 428
nanowires, 413
NAP, 211
narcotic, 32
National Academy of Sciences, 114, 147, 311
national product, 55
Native Americans, 14
natural enemies, 123
natural evolution, 340
natural gas, 193, 573
natural polymers, 98, 205, 207, 208, 212, 215,
216, 233, 406, 414, 416, 418, 468
natural resources, 71, 215
neglect, 177

nematode, 27, 41, 55, 120, 128
Nepal, 47
nerve, 55, 406, 407, 411, 428
Netherlands, 4, 32, 37, 217, 394, 494, 495, 553
network polymers, 105, 107
neutral, 48, 298, 480, 511
New England, 98
New Zealand, 4, 6, 8, 9, 36, 69, 70, 71, 76, 116,
138, 139, 260, 494
next generation, 13, 435, 521
NH₂, 303, 306, 503
niacin, 51
niche market, 245
nickel, 5, 319, 327, 495
Nigeria, 40, 50, 54, 124
nitrates, 97, 149, 465
nitrification, 98
nitrogen, 2, 10, 27, 28, 40, 54, 69, 95, 120, 133,
306, 308, 314, 440, 462, 482, 512, 544, 550,
559
NMR, 118, 545, 546
Nobel Prize, 21, 102, 246, 247
noble metals, 440, 441, 515
nodes, 30, 185, 286, 337, 339, 351, 354, 355,
356, 357, 358, 360
non-destructive analysis of textiles, vii, 153
nontoxicity, 403
North Africa, 192
North America, 3, 18, 20, 31, 32, 33, 34, 36, 37,
41, 46, 61, 126, 164, 494, 502, 506
Northern Ireland, 295
Norway, 494, 495
NRCS, 81
nuclear magnetic resonance, 545
nucleation, 375, 516, 545
nuclei, 375, 378
nucleic acid, 401, 414
numerical analysis, 185
nutrient, 16, 33, 37, 117, 135
nutrients, 26, 27, 43, 53, 207
nutrition, 3, 36, 116, 487
nylons, 95, 96, 105

O

obstacles, 580
obstruction, 491
occlusion, 436
occupational asthma, 491
Oceania, 20
offenders, 502

-
- OH, 3, 224, 248, 303, 304, 306, 378, 385, 387, 456, 464, 465, 469, 523, 530, 566, 567, 568, 571
- oil, 3, 4, 14, 17, 24, 27, 34, 35, 36, 37, 38, 40, 46, 51, 55, 67, 71, 83, 84, 87, 89, 94, 99, 111, 126, 127, 128, 132, 134, 192, 199, 307, 588
- olefins, 246
- oleic acid, 51
- oligomers, 544
- olive oil, 50, 586
- omega-3, 35, 37, 38
- one dimension, 371
- opacity, 75
- open spaces, 502
- operating costs, 581
- operations, 168, 177, 416, 581
- opportunities, 53, 138, 206, 237, 401, 402
- optical fiber, 5
- optical microscopy, 522, 526, 530, 532, 535
- optical properties, 443, 446, 462, 535
- optimization, x, 219, 331, 381, 440, 484
- ordinary differential equations, 170, 174
- organ, 412, 419, 421, 552
- organic compounds, 60, 71, 97
- organic fibers, 33, 246, 251
- organic food, 21
- organic matter, 28, 38, 53, 120, 128, 157
- organic polymers, 244, 246, 410
- organic solvents, 209, 210, 405, 418
- organism, 208, 309, 411, 483
- organize, 198, 206, 559
- organs, 142, 215, 285, 407
- ornamental plants, 69
- orthogonality, 176
- oscillation, 580
- outsourcing, 522
- ovaries, 65
- overlap, 3, 263
- overlay, 49, 421
- oxidation, xiii, 110, 125, 135, 304, 397, 440, 454, 459, 461, 462, 465, 475, 476, 480, 486, 520, 530, 534, 535, 539, 544, 545, 549, 573, 574, 575
- oxidative stress, 132, 397
- oxide nanoparticles, 389, 391, 397, 398
- oxygen plasma, 307, 480, 481
- ozone, 310
- Pakistan, 4, 16, 18, 22, 23, 29, 46, 47
- palladium, 440
- PAN, 121, 224, 245, 308, 314
- Panama, 49, 54, 78, 81, 142
- pancreas, 204
- Paraguay, 19
- parallel, x, 3, 73, 109, 112, 195, 196, 232, 301, 309, 310, 331, 356, 582, 585
- parasite, 117
- parasites, 26, 27
- parenchyma, 45, 46, 48, 71, 73
- parents, 91
- partial differential equations, viii, 165, 168, 170, 173, 185
- pastures, 133
- pathogens, 85
- pathways, 465
- PCM, 275, 283, 284
- PCT, 591
- PDEs, 173
- pea starch, 424
- peat, 59, 128
- pellicle, 409, 410
- peptide, 96, 210
- peptides, 6, 126, 210, 219
- perfusion, 288
- pericardium, 94
- pericycle, 4
- periodontal, 410
- periodontal disease, 410
- peritoneum, 94
- permeability, 199, 282, 289, 309, 323, 417
- permeation, 116, 249
- permission, iv, 313
- permit, 113, 375
- peroxide, 79, 397
- personal hygiene, 111
- Peru, 77, 81, 138, 503
- PES, 99
- pesticide, 20
- pests, 17, 20, 26, 27, 40, 53, 55, 122, 123, 138
- PET, 99, 196, 224, 249, 303, 304, 305, 306, 307, 312, 327, 405, 426, 529, 568, 577
- petroleum, 8, 45, 50, 98, 149, 196, 406, 491
- pH, xiv, 29, 75, 257, 384, 402, 405, 407, 446, 478, 486, 520, 526, 535, 536
- pharmaceutical, 63, 210, 406, 412
- PHAs, 410, 412
- PHB, 411
- phenol, 100, 105, 377, 462
- phenolic compounds, 560, 576
- phenolic resins, 98
- phenomenology, 312
-
- P**
-
- PAA, 512, 514
- Pacific, 149
- paints, 34, 37, 40, 50, 67, 92, 100, 127, 372

- Philadelphia, 312
Philippines, 4, 42, 50, 61, 66
phloem, 4, 29, 30, 32, 46, 72, 73
phonons, 111
phosphate, 54, 121, 406, 408, 420, 428, 446, 516
phosphates, 420, 428
phospholipids, 124
phosphorous, 440
phosphorus, 35, 51, 121, 122
photocatalysis, 463, 464
photocatalysts, 440, 461, 540
photodegradation, 453, 455, 459
photographs, 459, 512, 561
photonics, 327
photooxidation, 440, 456, 465
photosynthesis, 26, 72, 76
phylum, 90
physical and mechanical properties, 235, 268, 413
physical chemistry, 167
physical environment, 119
physical features, 320
physical fitness, 469
physical mechanisms, 167, 364
physical properties, 58, 71, 73, 75, 133, 228, 232, 234, 235, 249, 250, 251, 252, 253, 254, 255, 256, 290, 319, 320, 325, 326, 365, 370, 409, 473, 526, 538
physical structure, 72
physicochemical properties, 215
physics, 180, 292, 311, 312, 364, 537, 573
Physiological, 124, 125, 294
physiology, 274
phytosterols, 142
piano, 9, 98
piezoelectric properties, 12
pigs, 128
pith, 46, 58, 73
placebo, 134
plant growth, 45
plants, vii, 1, 2, 3, 4, 14, 15, 16, 21, 27, 28, 29, 30, 31, 32, 33, 35, 36, 42, 43, 45, 48, 49, 53, 54, 56, 61, 62, 64, 66, 69, 76, 78, 80, 117, 118, 126, 130, 132, 133, 138, 139, 141, 142, 167, 214, 234, 403, 404, 411, 412, 471
plasmid, 429
plasmid DNA, 429
plastic deformation, 108
plasticity, 130
plasticizer, 116, 423
plastics, 32, 34, 45, 95, 97, 98, 99, 100, 101, 111, 139, 149, 196, 234, 246, 247, 258, 404, 410, 538, 540
plastics processing, 404
plastid, 143
platelets, 107, 108
platform, 274, 291, 435
platinum, 440, 513
playing, 77
PM, 100, 125
PMMA, 100, 405
Poland, 507
polar, 304
polarity, 301, 477
polarization, 323
political leaders, 229
pollen, 63, 113, 139
pollination, 70, 135
pollutants, 98, 298, 372, 576
pollution, 39, 59, 63, 167, 403, 406, 523
poly(3-hydroxybutyrate), 433
poly(ethylene terephthalate), xiii, 152, 405, 568, 569, 570, 571, 572, 577
poly(ethyleneoxide), 408
poly(methyl methacrylate), 396
poly(vinyl chloride), 527
polyamide fiber, 112, 329
polyamides, 96, 148
polyamine, 427
polyamines, 97
polybutadiene, 86
polycarbonate, 416
polycarbonates, 105, 419
polycondensation, 148, 411
polydimethylsiloxane, 522, 528, 529
polyelectrolyte complex, 418, 430, 436
polyesters, 95, 96, 98, 100, 105, 410, 411
polyhydroxyalkanoates, 432
polyisoprene, 77, 78, 86, 141, 142
polymer blends, 150
polymer chain, 79, 95, 206, 304
polymer chains, 79, 304
polymer composites, 152
polymer films, 313
polymer materials, 105, 247, 559
polymer matrix, 229, 231
polymer molecule, 205
polymer nanocomposites, 150
polymer networks, 425
polymer solutions, 217
polymer structure, 307
polymer systems, 150
polymer-based composites, 112
polymeric chains, 102, 107, 108
polymeric films, xiii, 507, 514

- polymeric materials, 97, 199, 366, 415, 523, 526, 537, 559
- polymeric matrices, 468
- polymeric membranes, 508
- polymerization, 86, 96, 101, 103, 104, 105, 111, 144, 247, 248, 259, 305, 307, 314, 403, 409, 411, 414, 469, 472, 491, 493, 514, 538
- polymerization process, 101
- polymethylmethacrylate, 405
- polyolefins, 74, 150
- polypeptide, 95
- polypeptides, viii, 203, 204, 414
- polypropylene, ix, 2, 63, 68, 104, 113, 136, 137, 206, 223, 233, 237, 244, 246, 247, 248, 249, 250, 251, 252, 253, 254, 255, 256, 257, 259, 260, 262, 263, 272, 303, 312, 329, 396, 417, 512, 513, 514, 518
- polysaccharide, 210, 211, 213, 214, 215, 221, 405, 477, 484
- polysaccharides, viii, xii, 60, 137, 203, 204, 210, 217, 400, 402, 410, 415, 419, 422, 425, 431, 435, 467, 476, 484, 486
- Polysaccharides, 126, 210, 221, 402, 435, 487
- polystyrene, 97, 99, 101, 104, 110, 516
- polythene, 46
- polyurethane, 11, 92, 118, 197, 417, 418, 419
- polyurethane foam, 92, 417
- polyurethanes, 95
- polyvinyl alcohol, 113, 208, 257, 405, 414, 418, 424, 426
- polyvinyl chloride, 97, 104, 110
- polyvinylchloride, 110
- ponds, 48
- pools, 229, 288
- population, 6, 57, 340, 345
- population size, 340, 345
- Porifera, 90, 147
- porosity, viii, 75, 170, 191, 207, 212, 216, 277, 415, 451, 523
- porous materials, 169, 276
- portfolio, 413
- Portugal, 89, 90, 145, 146, 272, 519, 521, 536
- potassium, 51
- poultry, 126
- power generation, 550, 551
- power plants, 259
- p-Phenylenediamine, 503
- precipitation, 145, 469, 545
- predators, 17, 91
- predictability, 334
- preservation, xiv, 154, 156, 157, 162, 163, 164, 535, 538, 557, 567
- pressure gradient, 281
- pressure sore, 418
- prevention, 228, 251
- principles, 103, 204, 233, 291, 417, 429, 537, 538
- probability, 100, 571
- probe, 380, 385
- process control, viii, 165
- process duration, 443
- processing stages, 475
- processing variables, 435
- producers, 22, 23, 42, 48, 56, 66, 82, 86, 89, 195, 251, 484, 538
- product design, 274
- product market, 85
- product performance, 274
- production costs, 29, 258, 321, 402, 409
- production technology, 259
- productivity rates, 31
- professionals, 155, 156, 242
- profit, 11, 20
- progenitor cells, 210
- prognosis, 94
- project, 169, 242, 372, 461, 520, 521, 537, 581
- proliferation, 204, 215, 419, 420
- propagation, 103
- propane, 167
- propylene, 167, 247, 322, 420, 515
- prosthesis, 332
- prosthetic device, 228
- protection, vii, xiii, 1, 5, 24, 48, 49, 72, 85, 113, 127, 274, 289, 291, 292, 317, 318, 321, 372, 374, 377, 395, 400, 418, 520, 523, 534, 535, 537, 550, 566
- protein engineering, 412
- proteinase, 142, 431
- proteins, viii, 2, 6, 11, 12, 35, 77, 95, 117, 118, 123, 144, 203, 204, 205, 206, 207, 208, 210, 213, 400, 406, 407, 408, 414, 419, 430, 515
- proteoglycans, 204, 205
- protoplasm, 71
- prototype, 341
- prototypes, 290, 291
- pruritus, 500
- Pseudomonas aeruginosa*, 394
- psychoactive drug, 32
- PTFE, 100
- public health, 504
- public policy, 148
- publishing, 200, 487
- pulp, 3, 4, 33, 37, 41, 49, 53, 65, 66, 67, 68, 71, 72, 74, 75, 76, 137, 140, 193, 403, 468, 513
- pumps, 229
- purification, 167, 393, 411, 560
- purity, 371, 408, 409

purpura, 497
 pus, 498
 PVA, 208, 212, 214, 215, 218, 224, 257, 308,
 315, 405, 414, 416, 424, 426, 510, 511
 PVC, 99, 104, 224, 249
 pyrolysis, 125, 371, 389, 540, 544, 545, 548, 554

Q

quality assurance, 250
 quality control, 56
 quality of life, 237
 quantification, 144
 quantization, 370, 371
 quantum confinement, 370
 quantum dot, 370
 quantum dots, 370
 quartz, 5, 508
 quaternary ammonium, 373, 377, 396, 414, 434,
 514

R

racing, 85, 550
 radar, 112
 radiation, 100, 112, 143, 200, 275, 276, 277, 281,
 289, 373, 375, 395, 396, 411, 443, 540, 561,
 582
 Radiation, 140, 143, 276, 294, 295
 radical formation, 306, 464
 radical polymerization, 248
 radicals, 298, 299, 303, 305, 307, 385, 393, 541,
 567
 radio, 301, 313, 404, 414
 radiography, 522, 527
 radius, 166, 168, 249, 279, 284, 340, 353
 rainfall, 17, 20, 43, 47, 53, 69, 80
 Ramadan, 134, 434
 Raman spectra, 378, 548
 Raman spectroscopy, 154, 377
 rash, xii, 489, 497
 raw material, vii, 5, 25, 37, 40, 52, 67, 74, 77, 98,
 99, 129, 131, 192, 197, 258, 403, 410, 411,
 423, 468, 469
 raw materials, 5, 52, 131, 192, 197, 258, 411, 423
 RE, 166
 reactants, 177, 310
 reaction time, 177, 377, 389, 411
 reaction zone, 548, 566
 reactions, ix, 115, 167, 297, 298, 299, 306, 336,
 337, 341, 373, 375, 376, 382, 387, 453, 456,
 464, 470, 477, 490, 491, 502, 503, 544, 566,
 567
 reactive oxygen, 385
 reactivity, 141, 142, 464, 469, 470, 472, 475,
 492, 503, 566
 reading, 113, 502
 reagents, 378, 381, 389, 393, 477, 510
 receptors, 123, 207, 216, 287
 recognition, 2, 21
 recommendations, iv, 257
 reconstruction, 362, 412, 419
 recovery, 11, 84, 136, 204, 326, 366, 504
 recreation, 71
 recreational, 32, 228
 recycling, 112, 117, 521
 redistribution, 238
 reflectance spectra, 160, 447, 448
 reflectivity, 515
 refractive index, 127
 regenerate, 210, 469
 regenerated cellulose, 4, 76, 469, 470, 471, 472,
 473, 474, 475, 481, 482, 483, 484, 486, 487,
 510
 regeneration, 207, 210, 211, 212, 215, 403, 406,
 407, 419, 428, 437, 469, 484
 regenerative medicine, viii, xi, 203, 204, 205,
 207, 208, 215, 216, 217, 218, 399, 400, 406,
 407, 415, 416, 419, 421, 427, 435, 436, 437
 regions of the world, 69
 regulations, 495
 reinforcement, 114, 135, 136, 139, 193, 223, 227,
 228, 229, 230, 232, 233, 234, 235, 236, 238,
 239, 240, 242, 245, 246, 247, 251, 253, 257,
 258, 259, 264, 265, 266, 267, 270, 271, 272,
 322, 332, 365, 404, 423, 540, 551
 relatives, 6, 91
 relaxation, 12, 79, 235, 550
 relevance, xii, 180, 440, 442, 469
 reliability, viii, 165
 relief, 516
 repair, 204, 215, 267, 268, 407, 408, 411, 419,
 420, 428, 429
 repellent, 309, 450, 465, 523, 530, 535, 537, 574
 repetitions, 206
 reproduction, 1, 128, 149
 reputation, 78
 requirements, x, xv, 5, 33, 35, 37, 40, 41, 101,
 120, 129, 225, 243, 290, 291, 317, 372, 508,
 579, 581
 research funding, 41
 researchers, 20, 88, 91, 99, 101, 105, 234, 236,
 259, 289, 290, 311, 400, 413, 415, 419, 420,
 484, 508, 545
 reserves, 99, 117
 residual error, 175

residuals, 174
 residues, 162, 495
 resilience, 58, 59, 79, 247
 resins, xii, 45, 60, 75, 77, 98, 106, 489, 490, 491, 493, 494, 495, 497, 498, 500, 503, 523
 resistance, 16, 20, 28, 33, 41, 44, 52, 53, 57, 58, 63, 75, 84, 85, 93, 94, 99, 110, 112, 120, 124, 130, 196, 207, 227, 228, 237, 238, 240, 246, 247, 249, 250, 253, 254, 255, 282, 283, 286, 306, 309, 310, 323, 324, 333, 372, 480, 493, 513, 536, 539, 540, 549, 550, 551, 558
 resolution, 162, 217, 258, 451, 452, 453, 525, 546
 resources, 120, 138, 258, 400, 401, 402, 406, 411, 422, 423, 424, 432, 433
 respiration, 286, 287
 respiratory problems, 61
 response, x, 23, 80, 114, 120, 124, 125, 146, 207, 220, 278, 284, 285, 288, 318, 331, 341, 342, 343, 344, 345, 346, 349, 353, 356, 363, 364, 428, 502, 576, 584
 restoration, 49, 67
 restrictions, 367
 reusability, 542
 reverse osmosis, 113
 rhinitis, 502, 506
 riboflavin, 51
 rights, iv
 rings, 72, 97, 102, 247, 546
 ringworm, 71
 risk, 78, 94, 255, 257, 417, 492, 495, 504, 506
 risks, 24, 290, 299
 rods, 229, 332, 333
 Roman civilization, ix, 223
 Romania, 399, 409, 410
 room temperature, 38, 79, 95, 109, 110, 212, 220, 313, 315, 370, 396, 402, 443, 520, 549, 550
 root, 16, 24, 27, 28, 55, 72, 125, 144
 root rot, 28, 125
 root system, 16, 28
 roots, vii, 1, 27, 49, 53, 55, 66, 70, 121, 142
 rotations, 341, 363
 roughness, 480, 511
 routes, 204, 305, 326, 411, 414, 543
 Royal Society, 294, 396
 rubber, 59, 72, 77, 78, 79, 80, 81, 82, 83, 84, 85, 86, 87, 88, 89, 98, 102, 106, 107, 112, 142, 143, 144, 145, 229, 246, 249, 495, 503
 rubber products, 78, 143
 rubbers, 82, 86, 88, 495, 530, 538
 rural areas, 237
 rural population, vii
 Russia, 4, 195, 557
 rutile, 201, 456, 464

S

safety, 197, 376, 436
 salinity, 53
 salmon, 27
Salmonella, 34, 133
 salt concentration, 512
 salts, 11, 12, 77, 113, 148, 154, 162, 371, 373, 396, 491, 514
 saltwater, 63
 saturation, 280, 281, 304, 588
 Saudi Arabia, 54
 savings, 238
 SAXS, 114
 scaling, 198, 302
 Scandinavia, 3, 494
 scanning electron microscopy, 154, 156, 446, 522, 548
 scanning process, 197
 scarcity, 494
 scattering, 378, 450, 545
 schema, 284
 school, 78
 science, 105, 127, 133, 205, 291, 312, 317, 463, 487, 537
 scope, viii, 131, 203
 scripts, 9
 seafood, 400
 second generation, 2, 418, 546
 Second World, 28, 78, 88, 95, 105
 secrete, 26, 204
 security, 75, 99, 318
 sedimentation, 75
 seed, 14, 17, 21, 22, 24, 25, 27, 28, 30, 34, 36, 37, 38, 39, 40, 49, 51, 53, 55, 58, 67, 68, 71, 76, 124, 126, 128, 129, 132, 134, 403
 seeding, 216, 219
 seedlings, 26, 27, 55, 124, 146
 segregation, 240, 251, 253, 260
 selectivity, 308, 559
 self-assembly, 116, 198, 205, 414, 420, 515, 516, 517
 self-repair, 204
 semiconductor, 370
 semiconductors, 371
 semicrystalline polymers, 109
 semi-crystalline polymers, 151
 sensation, 275, 491
 sensing, 318, 324
 sensitivity, 118, 283, 372, 453, 455
 sensitization, xii, 489, 490, 492, 495, 505, 506
 sensors, x, 197, 317, 318, 372, 442, 468, 511
 septum, 563

- serine, 142
serum, 126, 213, 516
serum albumin, 213, 516
services, iv, 134, 268, 412, 416
severe stress, 258
sewing thread, 22, 45, 320, 324
sexual reproduction, 91
shade, 146
shape, x, 11, 12, 13, 43, 44, 93, 97, 98, 102, 160, 176, 182, 183, 196, 198, 205, 212, 225, 230, 253, 331, 332, 335, 336, 339, 341, 346, 353, 355, 363, 472, 564
shear, 240, 272, 306, 326, 333, 478, 550, 551
shear strength, 240, 306, 550
sheep, 2, 5, 6, 8, 9, 60, 74, 114, 116, 117, 192
shellfish, 477
shelter, vii, 1, 31
shingles, 92
shock, 376, 383, 533
shock waves, 376, 383
shoot, 136
shortage, 63
shortfall, 98
showing, xiii, 41, 73, 180, 239, 241, 242, 261, 263, 490, 516, 548
Si₃N₄, 550
side chain, 12
sieve tube, 46
signals, viii, 203, 287
signs, xiii, 106, 266, 490, 501
silhouette, 521
silica, xiii, 3, 5, 91, 92, 122, 374, 396, 397, 408, 415, 424, 517, 520, 522, 523, 525, 526, 530, 531, 532, 533, 534, 535, 537, 538, 539
silicon, 4, 111, 112, 159, 231, 419, 421, 508, 510, 523, 527, 529, 530, 537, 539, 540, 545, 546, 548, 550, 552, 553, 554
silkworm, 10, 11, 12, 118, 193, 417
simulation, ix, x, 146, 173, 185, 273, 281, 283, 285, 288, 289, 290, 291, 293, 294, 295, 331, 332, 356, 365, 366, 367
simulations, 168, 173, 332, 336, 341, 342, 356, 365
Singapore, 464
single crystals, 112, 141
SiO₂, xiv, 201, 374, 395, 441, 456, 463, 464, 465, 466, 520
skeleton, 91, 92
slavery, 24
smart materials, x, 113, 317, 318
smoking, 94
smooth muscle, 209, 427
smooth muscle cells, 209
smoothness, 75
social development, 521
social upheaval, 10
society, 115
sodium, xiv, 5, 51, 75, 97, 208, 374, 377, 405, 410, 418, 431, 435, 469, 487, 557, 561, 567, 568, 569, 570, 571, 572, 587
sodium hydroxide, xiv, 374, 469, 557, 567, 568, 569, 570, 571, 572
software, 174, 290, 291, 357
softwoods, 71
soil erosion, 49
soil type, 53
solar cells, 372
sol-gel, xiii, 122, 199, 371, 374, 394, 404, 414, 441, 450, 462, 463, 464, 465, 520, 523, 524, 525, 530, 531, 532, 533, 534, 535, 536, 537, 538
solid phase, 170, 171, 178, 183
solid polymers, 249
solid state, 131, 402, 545
solid waste, 469
solidification, 112, 205, 533
solubility, 210, 216, 308, 384, 388, 425, 478
solvent molecules, 205, 306
solvents, 78, 98, 213, 408, 463, 477, 542
Sonochemistry, v, x, 369, 375, 394, 396, 590, 591
sorption, 136, 278, 280, 472, 475, 485, 486, 487
sorption kinetics, 278
South Africa, ix, 4, 18, 64, 81, 93, 120, 224, 260, 262, 263, 266, 272
South America, 6, 20, 77, 81
South Dakota, 37, 38
South Korea, 42
South Pacific, 69
Southeast Asia, 31, 77
Soviet Union, 81
sowing, 39, 47
SP, 188
space shuttle, 540
space technology, 199, 200
Spain, 6, 14, 47, 77, 89, 90, 145, 146, 579
spasticity, 114
specialists, 105
specialization, 29, 118, 342
specific gravity, 31, 37
specific heat, 286
specific surface, 199, 309, 386, 542
specifications, 86, 240, 243, 251, 264, 265
spectroscopy, xii, 137, 144, 154, 156, 380, 440, 443, 444, 446, 448, 512, 514, 522, 538, 568
spending, 372
sperm, 91, 117

- spiders, 1, 10, 117, 408
spin, xiv, 11, 47, 96, 118, 195, 196, 385, 520, 525, 531, 532, 533, 545, 584
spinal cord, 215
spindle, 324
spine, 64
sponge, 91, 92, 147, 219, 407, 416, 425
Sri Lanka, 68, 144
stability, 11, 98, 135, 174, 189, 218, 240, 242, 249, 302, 377, 456, 517, 521, 523, 535, 539, 548, 550, 552, 558
stabilization, xiii, 148, 464, 520, 522
standard error, 534
starch, viii, 67, 75, 100, 102, 201, 203, 204, 210, 214, 374, 395, 403, 404, 410, 418, 419, 422, 424, 426, 431, 436
stars, 298
state, 32, 47, 59, 78, 79, 101, 107, 109, 148, 167, 176, 177, 187, 216, 225, 236, 250, 279, 280, 281, 283, 284, 286, 298, 340, 354, 378, 419, 427, 431, 454, 474, 476, 480, 544, 552, 569, 572
state legislatures, 32
states, 26, 32, 38, 47, 174, 258, 480
steel, ix, 58, 109, 111, 112, 223, 227, 228, 237, 238, 239, 240, 241, 242, 243, 244, 245, 246, 251, 257, 258, 265, 268, 270, 319, 320, 321, 322, 323, 325, 326, 329, 442, 563, 576
stem cells, 419
stereomicroscope, 157, 158, 163
sterile, 62, 65
sterilisation, 309
steroids, 142
stimulus, 113, 318
stomach, 65
storage, 31, 113, 132, 136, 143, 153, 157, 259, 286, 304, 370, 410
stress, 27, 53, 80, 95, 107, 108, 113, 152, 178, 184, 235, 249, 288, 290, 295, 332, 333, 347, 357, 359, 360, 362, 366, 410, 478, 534, 550, 551
stretching, 7, 12, 74, 79, 107, 108, 361, 526, 528, 529, 530, 570
structural changes, 550
structural characteristics, 472, 473
structural defects, 111
structural protein, 408, 420
style, 9, 291, 292, 295, 521
styrene, 88, 99, 101, 103, 245, 511
subdomains, 174, 176
suberin, 89
substitutes, 46, 82, 92, 204, 213, 406, 407, 419, 420, 421, 435, 437
substitution, 82, 86, 89, 149, 429, 477, 553
substitution effect, 82
substitution reaction, 553
substrate, ix, xi, 49, 120, 297, 298, 299, 301, 309, 369, 373, 374, 376, 377, 383, 384, 387, 390, 393, 415, 463, 484, 508, 511, 514, 523, 531, 532
substrates, 217, 299, 374, 375, 440, 441, 456, 484, 510, 511, 512, 515
succession, 22, 363, 470
sucrose, 213
Sudan, 50, 54, 55, 56, 134
sugarcane, 116, 403, 423
sulfate, 52, 214
sulfur, 2, 52, 77, 78, 79, 107, 159, 377, 512
sulfuric acid, 12, 77, 97, 404
sulphur, 77, 143, 159
Sun, 120, 126, 130, 137, 151, 237, 307, 314, 366, 396, 422, 427, 431
supramolecular structures, 469
supplier, 443, 446
suppliers, 56, 121, 244
suprapubic, 495
surface area, viii, 191, 198, 199, 203, 205, 207, 216, 370, 373, 387, 409, 415, 450, 451, 468, 472, 483, 582
surface chemistry, 306, 476
surface energy, 281
surface layer, 99, 298, 476, 540, 566, 568, 569, 571, 572
surface modification, ix, xiii, xiv, 199, 297, 298, 299, 300, 301, 304, 414, 423, 430, 436, 478, 481, 507, 508, 513, 515, 557, 558, 559, 560, 572, 574
surface properties, xiii, 220, 258, 306, 309, 373, 383, 480, 507, 508, 514
surface region, 540
surface structure, 446, 512, 514
surface tension, 205, 212, 213, 279, 281
surface treatment, 137, 299, 302, 312, 313, 468, 537
surfactant, 220, 524, 525, 531, 532, 533, 587
surfactants, 212, 373
survival, 91, 146, 258, 291, 292, 309, 386, 392, 410
susceptibility, 41, 130
suspensions, 136, 385
sustainability, 47
sustainable development, 21, 406
Sustainable Development, 271
suture, 209, 408
sweat, 10, 274, 286, 287, 288, 491, 495
Sweden, 506

swelling, 37, 212, 308, 422, 498
 Switzerland, 97, 102, 485
 symmetry, 168, 367
 symptoms, 27, 28, 502, 504
 synthesis, 96, 110, 142, 167, 189, 198, 205, 216,
 218, 244, 371, 373, 374, 375, 376, 381, 389,
 396, 398, 409, 414, 427, 432, 462, 508, 540,
 541, 542, 543, 553, 554, 575
 synthetic fiber, vii, 2, 3, 4, 12, 22, 24, 44, 46,
 209, 229, 244, 245, 246, 251, 255, 256, 259,
 268, 318, 408, 490
 synthetic polymers, 109, 207, 212, 216, 400, 401,
 404, 405, 406, 407, 408, 410, 416, 417, 418,
 419, 468
 synthetic rubbers, 78, 81, 85, 87, 88, 89

T

tactics, 26
 taffeta, 522
 Taiwan, 4, 191
 talc, 94, 110
 tanks, 48, 95, 131, 136, 229
 tannins, 60
 Tanzania, 18, 56, 62, 63, 64, 136, 269, 270
 tar, 99, 149, 491
 target, viii, 130, 203, 205, 429
 tau, 78
 TCC, 163
 teams, 62
 technological advancement, 167
 technological change, 81
 technological progress, 400
 technologies, ix, xi, xiv, 29, 140, 150, 167, 197,
 273, 274, 275, 291, 292, 295, 299, 311, 376,
 399, 403, 419, 420, 421, 433, 520, 538, 559,
 573, 579, 581
 technology, ix, 1, 2, 5, 15, 30, 49, 59, 85, 98, 105,
 111, 114, 137, 140, 197, 198, 199, 200, 224,
 233, 234, 257, 258, 259, 260, 272, 283, 298,
 299, 302, 309, 311, 312, 317, 326, 372, 400,
 411, 412, 413, 432, 433, 435, 463, 484, 537,
 540, 568
 teeth, 62, 64, 71, 78, 195, 229
 telecommunications, 245
 telephones, 67
 TEM, 215, 384, 387, 512, 545
 temperature dependence, 109, 149
 tendon, 407
 tensile strength, 4, 12, 30, 33, 37, 42, 52, 70, 73,
 75, 108, 109, 130, 207, 209, 212, 227, 235,
 236, 238, 242, 250, 263, 308, 409, 539, 550,
 552, 554

tension, 73, 74, 227, 279, 333, 357, 550
 tensions, 279
 tenure, 144
 TEOS, 525, 531, 532, 533, 534
 testing, 174, 238, 245, 290, 339, 380, 383, 419,
 442, 443, 453, 455, 459, 460, 483, 495, 502,
 568
 testing program, 238
 tetraethoxysilane, 525
 textiles woven, ix, 224
 texture, 12, 46, 67, 69, 75, 193, 196, 381, 525,
 548
 TFE, 208, 209
 TGA, 423, 544
 Thailand, 40, 42, 47, 54, 55, 56, 82, 133
 therapeutic agents, 219
 therapeutics, 435
 therapy, 410
 thermal decomposition, 541
 thermal energy, 79, 370
 thermal evaporation, 324
 thermal expansion, 112, 231, 245
 thermal oxidation, 540
 thermal properties, 111, 276, 291, 513, 544, 550
 thermal resistance, 283, 295, 513, 514
 thermal stability, 374, 395, 441, 513, 514, 517,
 546, 550, 551
 thermal treatment, 373, 377, 395, 420, 443, 526,
 531, 535
 thermodynamic equilibrium, 180
 thermogravimetric analysis, 374
 thermogravimetry, 545, 550
 thermoplastic polyurethane, 197
 thermoplastics, 31, 33, 97, 107, 108, 110, 149,
 246, 249, 410
 thermoregulation, 284, 288, 290
 thermosets, 98, 105, 107
 thin films, xiv, 141, 413, 462, 463, 480, 515, 520,
 535, 538, 558
 thorax, 288
 threats, 138, 199
 three-dimensional model, 102
 time periods, 113
 time series, 168, 177, 178
 tin, 377
 tissue engineering, 204, 205, 206, 207, 208, 209,
 210, 211, 213, 214, 215, 216, 217, 218, 219,
 221, 400, 402, 403, 404, 405, 406, 408, 410,
 412, 414, 415, 416, 419, 420, 421, 422, 426,
 428, 430, 432, 433, 435, 436, 437
 titania, 394, 464, 516
 titanium, 75, 86, 247, 319, 320, 395, 414, 418,
 440, 461, 508, 516, 584

tobacco, 21
 tofu, 34
 Togo, 23
 tonic, 55
 top-down, 413
 topology, 360, 508
 total energy, 334
 toxicity, 134, 210, 386, 397, 402, 406, 478
 toxin, 17, 20, 120
 Toyota, 45
 toys, 106
 trade, 5, 14, 21, 37, 46, 93, 100, 504, 543, 548
 traditions, 50
 training, 520, 521
 traits, 4, 117
 trajectory, 372
 transcription, 364
 transducer, 582, 583, 584, 585
 transduction, 582
 transformation, 97, 130, 132, 177, 411, 412, 441, 468, 552
 transformations, 109, 521
 transient regime, viii, 166
 translation, 332, 340, 347
 transmission, 90, 92, 138, 147, 200, 215, 431, 444, 524, 545, 548
 transmission electron microscopy, 215, 545, 548
 transparency, 75, 523
 transpiration, 113
 transplantation, 212, 215
 transport, 166, 167, 168, 170, 171, 179, 181, 182, 184, 195, 280, 289, 290, 293, 305, 561
 transportation, 68, 245
 trauma, xi, 399, 416
 trial, ix, 56, 134, 273, 274, 290
 trifluoroacetic acid, 211
 Trinidad, 54, 55, 56
 Trinidad and Tobago, 54, 55, 56
 tropical forests, 71
 trypsin, 123
 tuberculosis, 139
 tumor, 127
 tumors, 38, 70, 92
 tungsten, 112, 548, 554
 tungsten carbide, 112
 Turkey, 6, 19, 74, 317
 twins, 17
 twist, 58, 195, 321, 353
 Tyrosine, 35

U

U.S. Department of Agriculture, 41

U.S. Department of Agriculture XE "Department of Agriculture" (USDA), 41
 U.S. Department of Commerce, 105
 UK, 4, 15, 25, 34, 42, 46, 56, 121, 147, 163, 270, 327, 590
 Ukraine, 17
 ultrasound, xi, xiv, 369, 374, 375, 376, 377, 378, 381, 382, 383, 389, 390, 396, 398, 414, 579, 580, 581
 ultrastructure, 125, 129
 uniform, xi, 4, 157, 170, 171, 178, 179, 180, 208, 214, 242, 279, 285, 286, 287, 288, 300, 304, 312, 313, 315, 324, 369, 390
 United, ix, 4, 8, 14, 17, 19, 21, 22, 23, 27, 28, 29, 32, 33, 36, 37, 38, 40, 46, 83, 87, 93, 118, 122, 127, 164, 195, 224, 232, 238, 240, 251, 254, 255, 258, 260, 271, 311, 327, 328, 416, 506, 522, 538
 United Kingdom, 32, 46, 164, 238, 538
 United Nations, 17, 118, 258, 271
 United States, ix, 4, 8, 14, 19, 21, 22, 23, 27, 28, 29, 32, 33, 36, 37, 38, 40, 83, 87, 122, 127, 195, 224, 232, 238, 240, 260, 311, 327, 328, 416, 506, 522
 universities, 400
 upholstery, 4, 9, 12, 45, 49, 57, 59, 193, 247, 493
 urea, 75, 493, 494, 503
 urethane, 416
 urinary bladder, 211, 219
 urinary tract, 56
 urinary tract infection, 56
 urticaria, xii, 489, 490
 USA, 4, 15, 22, 36, 38, 74, 78, 81, 83, 219, 269, 272, 313, 328, 421, 494, 504, 506, 525, 536
 USDA, 38, 81, 126
 USSR, 93
 UV, xii, 48, 103, 110, 199, 201, 308, 315, 372, 373, 374, 395, 400, 404, 407, 414, 427, 440, 442, 443, 444, 445, 446, 447, 448, 453, 455, 457, 458, 459, 460, 461, 464, 465, 511, 512, 516, 530
 UV light, 103, 199, 308, 442, 444, 446, 455, 457, 459, 460, 461
 UV radiation, 110, 201, 395, 400, 407
 Uzbekistan, 4, 18, 22, 23

V

vacancies, 385
 vacuum, 137, 158, 197, 199, 201, 299, 307, 308, 315, 481, 502, 558, 559, 573
 valence, 370
 validation, 295, 502

vapor, xiv, 110, 197, 275, 278, 279, 280, 281, 283, 288, 293, 397, 405, 520, 525, 551, 557, 561, 562, 564, 565
 variables, 174, 264, 324, 341, 353, 357, 358
 variations, viii, 12, 110, 146, 165, 174, 345, 349, 380, 587
 varieties, 17, 20, 27, 28, 30, 32, 37, 40, 57, 69, 70, 92, 123, 130, 412
 vascular system, 288
 vasculature, 213
 vasoconstriction, 287, 288
 vasodilation, 287, 288
 vector, 26, 176, 337, 338, 340, 358, 359, 360, 362
 vegetable oil, 17, 24, 38
 vegetables, 46, 51, 55, 68, 132, 468
 vegetation, 49
 vehicles, 83, 85, 87, 100, 193, 550, 554
 velocity, 166, 170, 173, 179, 275, 340, 360, 361, 562
 velvet, 76, 194
 Venezuela, 64, 68
 ventilation, 141, 294, 308, 502
 versatility, xiii, 67, 400, 415, 519, 521
 vessels, 92, 229, 284, 497
 vibration, 84, 288, 568, 570, 581, 582, 583, 584
 Vietnam, 59, 82
 vinyl chloride, 526, 528
 viruses, 26, 92, 309
 viscose, 2, 76, 77, 140, 141, 308, 405, 443, 446, 447, 448, 450, 451, 452, 453, 454, 455, 456, 457, 458, 459, 460, 471, 472, 473, 474, 475, 481, 482, 483, 484, 487
 viscose process, 140, 141, 405, 471
 viscosity, 76, 102, 108, 109, 207, 211, 213, 402, 478, 542
 vision, 78
 vitamin A, 219
 vitamin C, 55
 Vitamin C, 34, 38, 50, 51
 vitamin E, 219
 vitamins, 374
 Volunteers, 127
 vulcanization, 78, 79, 143, 144

W

wage level, 29
 walking, 289, 295
 war, 87, 88, 105
 Washington, 149, 164, 272
 waste, 45, 62, 63, 74, 75, 117, 135, 139, 259, 405, 409, 410, 422
 waste water, 75
 wastewater, xi, 439, 440, 441, 442, 451, 457, 461, 576
 water absorption, 7, 37, 235
 water diffusion, 281
 water purification, 113, 513
 water resources, 119
 water sorption, 558
 water vapor, 113, 276, 277, 278, 280, 282, 283, 417, 566
 wavelengths, 446
 weapons, 71, 197
 wear, xii, 12, 44, 47, 62, 76, 112, 115, 194, 196, 291, 292, 372, 489, 491, 492, 493, 521, 558
 wearing apparel, 23
 web, 8, 10, 195
 weeping, 77
 weight loss, 52, 283, 308, 544
 weight ratio, 31, 212
 welding, 260, 264, 302
 welfare, 156
 West Africa, 15, 22, 50, 53, 77, 81
 West Indies, 53
 Western Europe, 32
 wettability, ix, 279, 297, 298, 303, 304, 305, 306, 313, 480
 wetting, 75, 195, 235, 278, 279, 516
 wind speed, 289
 windows, 99
 wires, x, 15, 317, 318, 319, 320, 324, 325, 326
 Wisconsin, 99, 129
 wood, 3, 4, 30, 31, 33, 39, 40, 45, 46, 47, 48, 49, 50, 58, 60, 71, 72, 73, 74, 76, 77, 100, 111, 112, 126, 129, 140, 146, 193, 229, 403, 471, 523, 574
 wood density, 73, 146
 wood products, 3, 146
 wood species, 72, 73
 woodland, 145
 wool, 2, 5, 6, 7, 8, 9, 11, 23, 25, 33, 36, 40, 42, 43, 45, 46, 52, 63, 114, 116, 117, 118, 159, 160, 192, 195, 199, 201, 278, 294, 306, 310, 314, 353, 376, 377, 395, 396, 397, 405, 406, 413, 425, 427, 434, 490, 491, 492, 493, 512
 workers, 47, 65, 94, 141, 194, 195, 234, 260, 281, 365, 502, 504, 506
 World Bank, 131
 World Trade Organization, 234
 World War I, 145, 246
 World Wide Web, 268, 269, 271
 worldwide, 20, 21, 26, 53, 66, 70, 90, 119, 242, 251, 372, 413, 502, 504
 worms, 70

wound healing, xi, 205, 211, 214, 372, 397, 399,
403, 407, 410, 417, 419, 425, 426, 430

X

XPS, 307, 474, 476, 486, 487, 512, 514
X-ray diffraction, 146, 154, 443, 545, 548, 550
X-ray diffraction (XRD), 154, 545
X-ray photoelectron spectroscopy (XPS), 377
XRD, xi, 378, 379, 381, 387, 390, 391, 423, 439,
443, 446, 448, 449, 450, 454, 456, 538, 545
xylem, 30, 46, 72, 73

Y

Yale University, 121
yeast, 253

yield, 8, 11, 17, 21, 22, 23, 26, 27, 32, 37, 40, 41,
81, 101, 108, 128, 129, 130, 143, 144, 209,
228, 240, 250, 371, 381, 408, 411, 542, 544,
548, 553
yolk, 195

Z

Zimbabwe, 18
zinc, 35, 75, 78, 201, 373, 374, 381, 382, 383,
387, 395, 397, 414, 435, 492, 528
zinc oxide, 201, 373, 374, 382, 383, 395, 397,
414, 435
ZnO, xi, 200, 369, 373, 374, 381, 382, 383, 384,
385, 386, 387, 390, 393, 395, 397, 398
ZnO nanorods, 374